Atlas of Head and Neck Imaging

The Extracranial Head and Neck

Suresh K. Mukherji
Vincent Chong

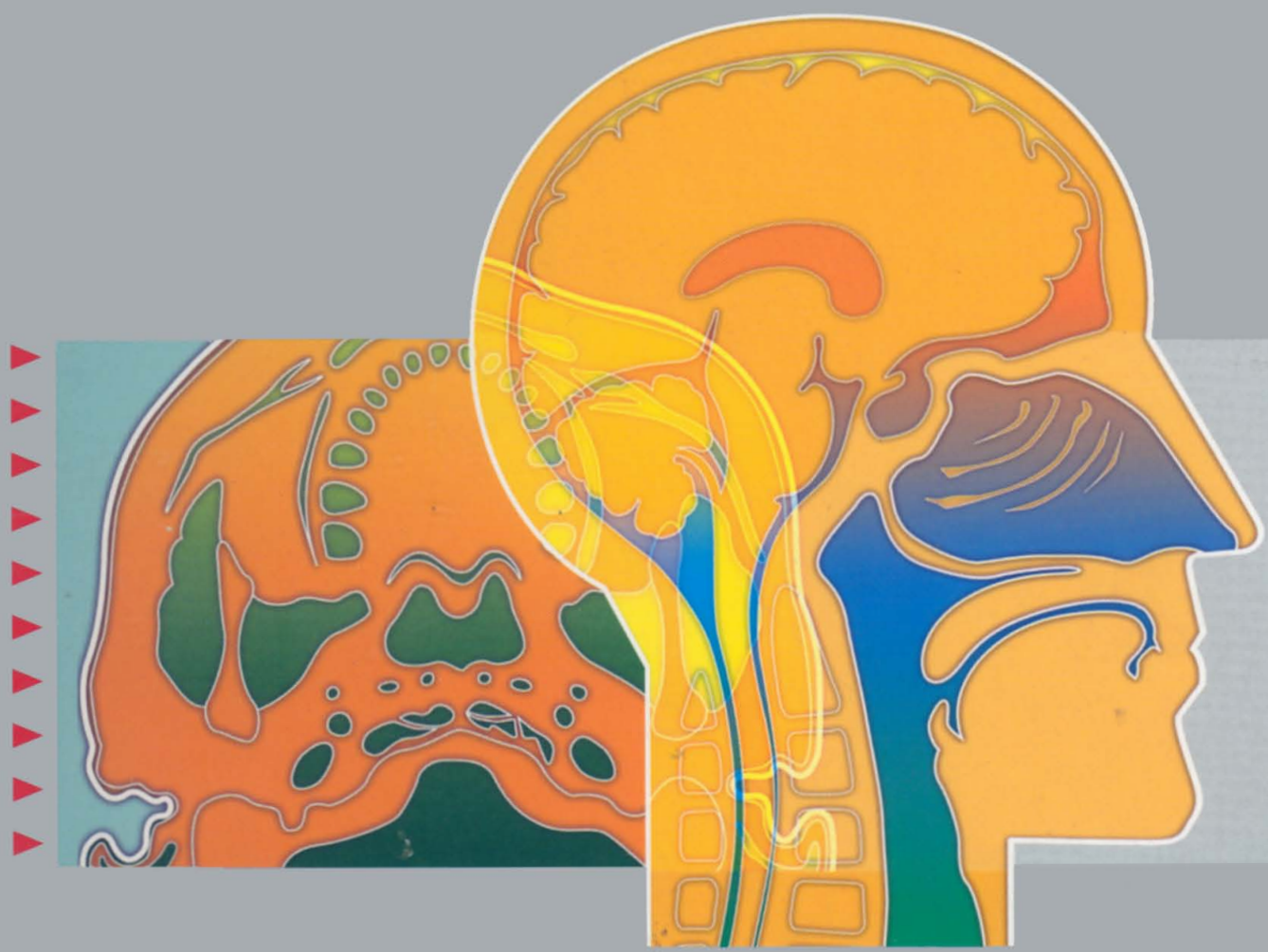

Thieme

Atlas of Head and Neck Imaging

The Extracranial Head and Neck

Atlas of Head and Neck Imaging

The Extracranial Head and Neck

Suresh K. Mukherji, M.D.
Division Director of Neuroradiology
and Head & Neck Radiology
Neuroradiology Fellowship Program Director
University of Michigan
Ann Arbor, Michigan

Vincent Chong, M.D.
Program Director for the Department
of Diagnostic Radiology
Singapore General Hospital
Singapore

Thieme
New York · Stuttgart

Thieme Medical Publishers, Inc.
333 Seventh Ave.
New York, NY 10001

Editorial Assistant: Kerry Wheeler
Director, Production and Manufacturing: Anne Vinnicombe
Production Editor: Becky Dille
Marketing Director: Phyllis Gold
Sales Manager: Ross Lumpkin
Chief Financial Officer: Peter van Woerden
President: Brian D. Scanlan
Compositor: Primustype Hurler
Printer: Druckhaus Goetz

Library of Congress Cataloging-in-Publication Data
Mukherji, Suresh K.
Head and neck radiology : text and atlas/Suresh K. Mukherji, Vincent Chong.
p. ; cm.
Includes bibliographical references and index.
ISBN 1-58890-178-5 (hardcover : alk. paper) - ISBN 3-13-136071-2 (hardcover : alk. paper)
1. Head-Radiography. 2. Head-Radiography-Atlases. 3. Neck-Radiography. 4. Neck-Radiography-Atlases.
[DNLM: 1. Head--rediography. 2. Head--radiography--Atlases. 3. Neck--radiography--Atlases. 4. Neck--radiography. 5. Radiology--methods--Atlases. 6. Radiology--methods. WE 705 M953h 2004] I. Chong, Vincent. II. Title.
RC936.M85 2004
617.5'107572-dc21

Important note: Medical knowledge is ever-changing. As new research and clinical experience broaden our knowledge, changes in treatment and drug therapy may be required. The authors and editors of the material herein have consulted sources believed to be reliable in their efforts to provide information that is complete and in accord with the standards accepted at the time of publication. However, in the view of the possibility of human error by the authors, editors, or publisher, of the work herein, or changes in medical knowledge, neither the authors, editors, or publisher, nor any other party who has been involved in the preparation of this work, warrants that the information contained herein is in every respect accurate or complete, and they are not responsible for any errors or omissions or for the results obtained from use of such information. Readers are encouraged to confirm the information contained herein with other sources. For example, readers are advised to check the product information sheet included in the package of each drug they plan to administer to be certain that the information contained in this publication is accurate and that changes have not been made in the recommended dose or in the contraindications for administration. This recommendation is of particular importance in connection with new or infrequently used drugs.
Some of the product names, patents, and registered designs referred to in this book are in fact registered trademarks or proprietary names even though specific reference to this fact is not always made in the text. Therefore, the appearance of a name without designation as proprietary is not to be construed as a representation by the publisher that it is in the public domain.

Printed in Germany

5 4 3 2 1

TMP ISBN 1-58890-178-5
GTV ISBN 3 13 136071 2

To my wife Rita and our children, Anika and Janak.
To my mother Chandra Mukherji, M.D. for her strength through difficult times, I love you!
In loving memory of my father, Phatick K. Mukherji, M.D. who instilled in me the belief that no hard work goes unrewarded.

Suresh K. Mukherji

To my wife FYF for all her patience and understanding
To my daughters Kitty and Jane for enriching our lives
To my parents CMY and WSM for their love

Vincent Chong

Acknowledgment

This book was five years in the making but represents a much greater experience. I would like to thank the many excellent neuroradiologists with whom I have worked throughout my career, especially Tony Mancuso and Mauricio Castillo. We gain much knowledge from our fellow radiologists. However, as a head & neck radiologist, some of the most valuable information we learn comes from our otolaryngology head and neck surgery colleagues. I would like to acknowledge all of these individuals who have added to my education over the past 11 years. A great deal of thanks and respect goes to the many individuals at Thieme who made the production of this textbook possible. It was a pleasure to work with all of you.

Suresh K. Mukherji

Table of Contents

Preface

Why write another book on head and neck radiology? A very reasonable question that we should try to answer. We have tried to create a text that can be easily and effectively used at the viewbox (or PACS station).

Once a lesion is identified, there are two questions that next need to be answered: (1) Where is it located? and (2) What could it be? In this book, each space has its own section that contains examples of the common pathology that arise in that area.

We have used a standard format consisting of Epidemiology, Clinical Presentation, Pathology, Treatment, and Imaging Findings. The imaging findings consist primarily of CT and MR because these are the most commonly used modalities for evaluating the extracranial head and neck. We discuss ultrasound and angiography findings when appropriate. Each chapter also includes a section entitled Imaging Pearls—information that may not be found in standard texts but that we have found from our experience to be occasionally helpful when evaluating the disease entity under discussion.

We have tried to be thorough while being concise and to the point. Although there are well over 200 different pathologies discussed in the text, this book is not intended to be an all-inclusive text on head and neck imaging; we have focused instead on the suprahyoid and infrahyoid neck. We did not include the orbits, sinuses, or temporal bone. We refer the reader to the excellent textbooks by Som and Curtin, and Swartz and Harnsbarger as well as the superb pathology text by Batsakis for more detailed information on diseases not covered in this text.

It was both a pleasure and a challenge to write this book. We hope you will find it readable, informative, and useful in your practice.

Suresh K. Mukherji, M.D.
Vincent Chong, M.D.

Introduction

The concept of dividing the extracranial head and neck into different spaces is an old notion that dates back to the 1800s. Anatomists and surgeons prior to the development of antibiotics and radiography identified and characterized the anatomy. Their mission was to explain the extension of infections of the extracranial head and neck to other areas in the neck, chest, and abdomen that seemed initially unrelated to the site of the primary infection. Their studies led to detailed descriptions of the cervical fascia and the numerous soft tissue spaces that were contained within the fascial layers. Over the years, this categorization was adapted and used by anatomists and otolaryngologists but was not commonly employed by radiologists, due primarily to our inability to adequately visualize these compartments.

The development and acceptance of CT and MR enabled radiologists to directly visualize the complex anatomy and pathology of the neck in ways not previously possible. In the late 1980s and early 1990s, Ric Hansberger reintroduced and popularized the space as a method of helping radiologists grasp the complexity of this region.

A good knowledge of the spaces allows one to generate a concise and accurate differential diagnosis based on the anatomic components of the individual spaces. However, the names and locations of the individual spaces are often difficult to learn. This is especially true for radiologists in training or for those not routinely performing a significant amount of head and neck imaging.

By remembering a few concepts, the majority of masses in the suprahyoid neck can be easily localized to their correct space. Various methods have been used to identify and localize neck masses. We use a very simplistic approach for helping to localize neck masses. This approach is based on the suprahyoid neck being a symmetric anatomic structure with the right half being a relative mirror image of the left. For large lesions that distort the normal anatomy of the involved side, one must first identify the location of the center of the mass. Once identified, this location should be approximated to the corresponding area on the uninvolved contralateral side. Although not a perfect method, this approach helps to localize the majority of large, transspatial lesions in the suprahyoid head and neck.

Another concept that aids in understanding the spaces is some knowledge of the fascia. If you think the fascial spaces of the extracranial head and neck are confusing, you're not alone! Consider what the French anatomist Malgaigne wrote in 1838: "[T]he cervical fascia appear in a new form under the pen of each author who attempts to describe them." Unfortunately, some understanding of the fascial layers is necessary. However, a detailed knowledge of the numerous fascial layers is not required for an understanding of the spaces of the suprahyoid neck.

There are two main fascial layers of the suprahyoid neck: (1) the superficial cervical fascia, and (2) the deep cervical fascia. The superficial cervical fascia consists of the subcutaneous tissues of the head and neck. The deep cervical fascia (DCF) has three separate components: (1) the superficial layer, (2) the middle layer (visceral or pharyngomucosal), and (3) the deep layer (prevertebral).

For purposes of understanding the spaces, a good knowledge of only the middle and deep layers of the DCF is necessary. Just remember that in the suprahyoid neck, the visceral fascia encloses the pharynx. Thus, using the spaces nomenclature, the oropharynx and nasopharynx are known collectively as the visceral space. The prevertebral fascia is just posterior to the visceral fascia. It defines the contents of the prevertebral space. Now, by understanding the location of the visceral and prevetebral fascias (components of the DCF), we are ready to embark on a detailed review of the various spaces.

Section I

Masticator Space

The masticator space (MS) primarily consists of the muscles of mastication (hence the name "*masticator space*"). These muscles are the medial and lateral pterygoid, masseter, and temporalis (Fig. I-1). Anatomically, the superficial layer of the deep cervical fascia splits to enclose the muscles of mastication to enclose this space (Figs. I-2 through I-4). The contents of the MS also include the additional structures encompassed within these fascial boundaries, which include the ramus of the mandible and the third division of the fifth cranial nerve (CN V) as it passes through the foramen ovale into the suprahyoid neck. These latter structures are important to remember because they expand the differential diagnosis of MS masses.

The MS is easy to identify because, by definition, any of the muscles of mastication are within the MS (Fig. I-5). The MS extends inferiorly to the attachment of the medial pterygoid and masseter muscles to the mandible. The superior extent of the MS varies. The superomedial margin of the MS is the skull base. This portion of the MS has been previously referred to as the "infratemporal fossa" or the "nasopharyngeal masticator space." This portion of the MS includes the soft tissues inferior to the foramen ovale. Thus any malignancy involving the MS has the potential to extend into the cavernous sinus via retrograde perineural spread along V_3. The superolateral margin of the MS is formed by the attachment of the temporalis muscle along the outer table of the skull. This has been previously referred to as the "temporal fossa" and the "suprazygomatic masticator space" because it is superior to the zygomatic arch.

The differential diagnosis of MS masses is centered on the anatomic components of the space. This includes lesions that may arise from muscle, nerve, bone, or extension from an adjacent space. Lesions that arise primarily within the muscles are likely to be of mesenchymal origin. The imaging findings of the various sarcomas are usually nonspecific.

Rhabdomyosarcoma is the most likely diagnosis of a primary MS arising in a muscle in a child. In adults, the most common lesions arising in a muscle are leiomyosarcoma and malignant fibrous histiocytoma. Metastases must also be considered in the differential diagnosis of a primary MS mass.

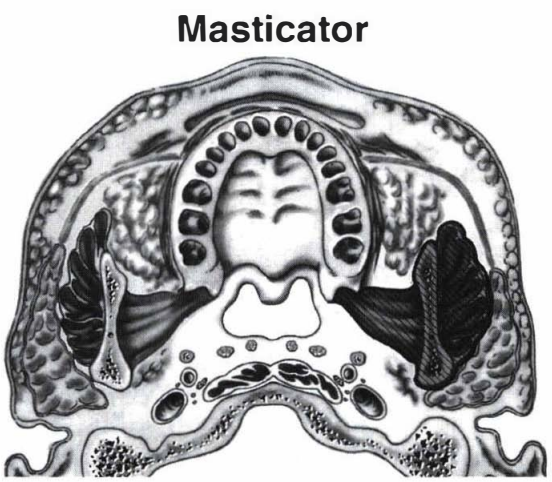

Figure I-1. Schematic illustration of the masticator space (see Color Plate I-1). (Figure reproduced with permission from Mukherji SK, Castillo M. A simplified approach to the spaces of the suprahyoid neck. Rad. Clin N Am *1998;36:761-780.)*

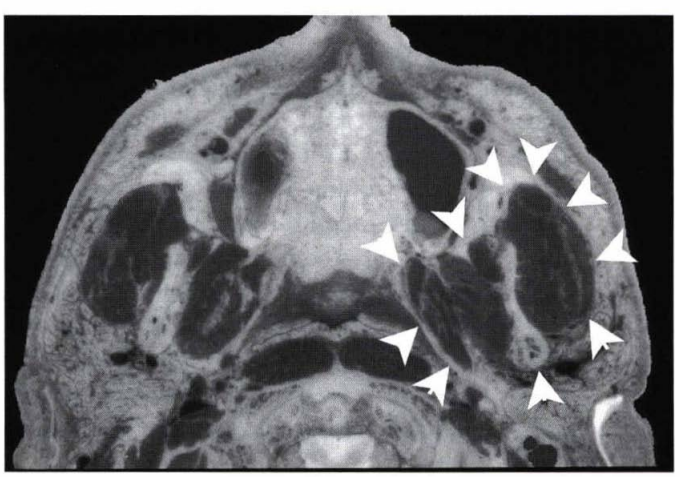

Figure I-2. Axial anatomic image illustrates the confines of the masticator space (arrowheads)

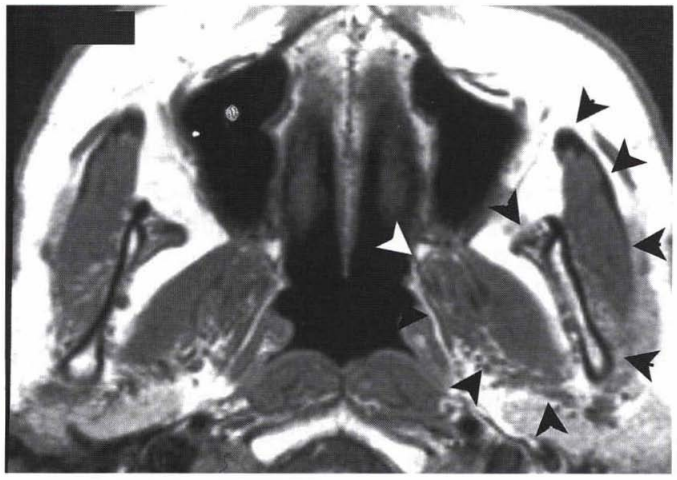

Figure 1–3. Arrowheads define the margins of the axial noncontrast T1-weighted image.

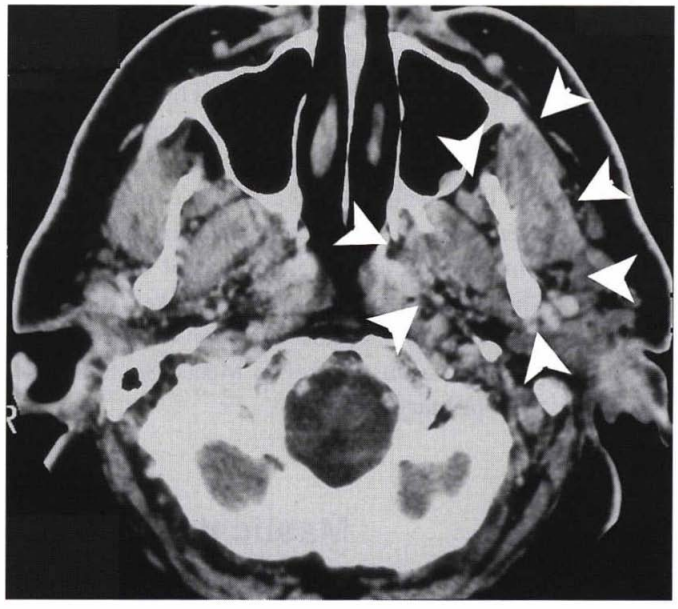

Figure 1–4. The margins of the masticator space are outlined on the axial CT.

Primary neurogenic lesions may involve either the proximal portion of the mandibular division of CN V or any of its distal branches. The most common primary neurogenic tumor is a schwannoma. This lesion may be suggested if the lesion displaces the lateral pterygoid muscle outwardly and the lateral wall of the pharynx medially. Coronal images may demonstrate the characteristic "dumbbell" appearance if the mass extends through the foramen ovale into the region of Meckel's cave. Retrograde spread along V_3 is also an important pathway for tumors that invade the MS. Because V_3 courses medial to the lateral pterygoid muscle, tumors may extend in a retrograde manner into the cavernous sinus. This potential pathway into the cavernous sinus needs to be examined for all malignancies located in the superomedial portion of the MS.

A variety of pathological processes may arise from the mandibular component of the MS. The most common lesion is an odontogenic infection that may present as an MS mass. The infection is usually due to infected second premolar or molar teeth. Infection of more anterior teeth usually results in a sublingual-space infection. Various bone lesions may involve the ramus of the mandible and present as primary MS masses.

The MS may also be involved by processes spreading from adjacent spaces. The most common is invasion of the MS from deep spread of a primary pharyngeal or retromolar trigone carcinoma. Intracranial and skull-base lesions may extend inferiorly into the MS. Meningiomas and skull-base chondrosarcomas may occasionally present as primary MS masses. Metastases may involve any of the components of the MS. The imaging findings of most malignancies are nonspecific and the diagnosis is usually made by clinical history and biopsy.

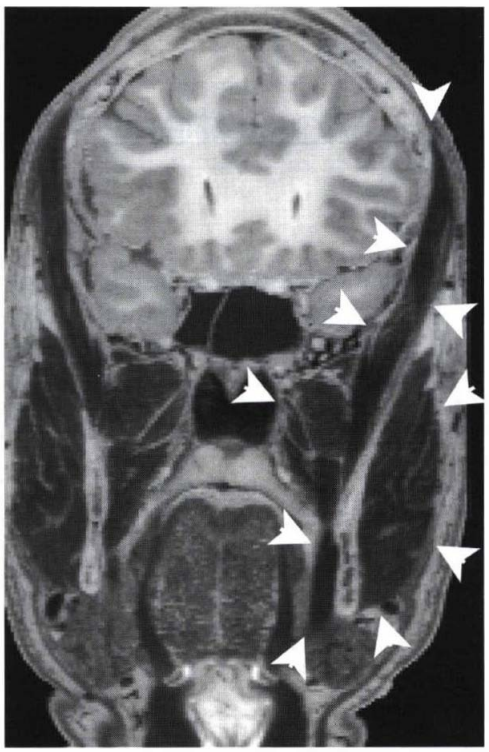

Figure 1-5. The masticator space is primarily defined by the extent of the muscle of mastication. The coronal anatomic image shows the large area covered by the masticator space (arrowheads).

Although the ramus of the mandible is included in the MS, the body of the mandible is not categorized under the commonly listed head and neck spaces. Localizing a lesion to the body of the mandible and differentiating this from a primary sublingual- or submandibular-space mass is important because the anatomically based differential diagnosis is significantly different for these regions. In their study of infections of the lip and face, Collier and Ygelesias showed that infections that arose within the body of the mandible rarely spread deeply or superficially. The reason for this containment was felt to be due to reinforcement of the periosteum by the overlying fascia and muscular insertions. Because of this spread pattern (or lack of one!), they coined the term *"space of the body of the mandible"* ("mandibular space") to identify this specific region. Because the "mandibular space" is an extension of the bony component of the MS, the differential diagnosis for these regions is similar.

Suggested Readings

1. Harnsberger HR, Osborn AG. Differential diagnosis of head and neck lesions based on their space of origin: the suprahyoid part of the neck. *AJR Am J Roentgenol* 1991;157:147-154.
2. Mukherji SK, Castillo M. A simplified approach to the spaces of the extracranial head and neck. *Radiol Clin North Am* 1998;36:761-780.
3. Harnsberger HR.: *Handbook of Head and Neck Imaging.* 2nd ed. St. Louis: Mosby-Year Book; 1995.
4. Braun IF, Hoffman JC. Computed tomography of the buccomaseteric region. *AJNR Am J Neuroradiol* 1984;5:605-610.

Chapter 1

Benign Masseteric Muscle Hypertrophy

Epidemiology

This is an uncommon entity that begins in adolescence or early adulthood and demonstrates slowly progressive enlargement of the affected muscles. Masseteric muscle hypertrophy is usually bilateral but may be seen as a unilateral lesion. The etiology is uncertain but is thought to be related to bruxism or excessive chewing. This has also been described in patients with acquired immune deficiency syndrome.

Clinical Findings

This condition may be discovered incidentally, or the affected individuals may complain of facial fullness. The masslike hypertrophy is not painful or tender to palpation. It hardens and enlarges when the teeth are clenched.

Pathology

Histologic examination shows normal skeletal muscle tissues.

Treatment

No treatment is required. However, surgical intervention may be elected for treatment of cosmetic deformities.

Imaging Findings

CT

CT shows enlargement of the masseteric muscle. The most commonly involved muscles include the masseter and temporalis muscles. The attenuation value of the affected muscles is normal. An exostosis at the angle of the jaw may also be demonstrated (Fig. 1-1).

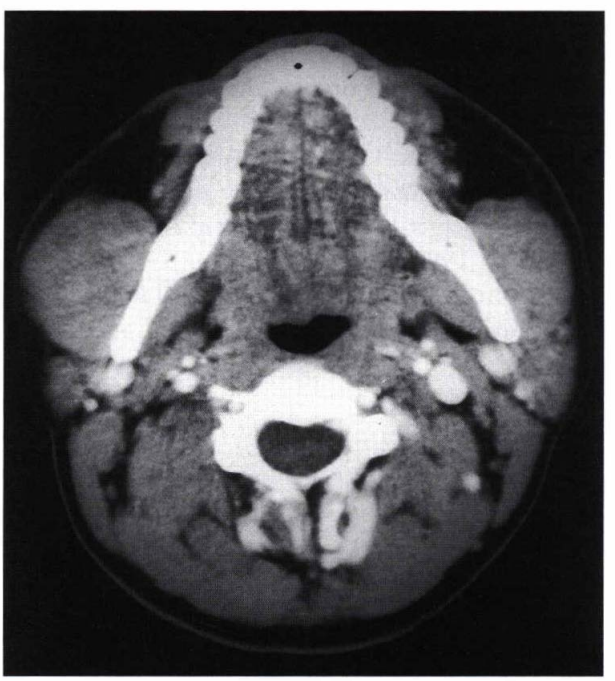

Figure 1-1. Benign masseteric hypertrophy. Axial contrast-enhanced CT shows bilateral enlargement of the masseter muscles. The muscles show no abnormal enhancement. Note that the medial pterygoid muscles are normal in size.

MR

The signal intensity of the enlarged muscles is similar to normal skeletal muscle of different pulse sequences. No abnormal enhancement is present in affected muscles.

Imaging Pearls

- Unilateral masseteric muscle enlargement may simulate a neoplasm. The lesion, however, maintains a smooth outline and shows normal attenuation or signal intensity on imaging. This diagnosis is confirmed upon the detection of associated enlargement of the other muscles of mastication.
- Unilateral masseteric muscle atrophy may give the impression of atrophy of the normal contralateral muscle. However, the atrophic muscle may show fatty infiltration or abnormal signals on MR imaging
- Bilateral mild to moderate masseteric muscle hypertrophy may not be easily recognizable on imaging and radiological findings should be correlated with clinical history.

Suggested Readings

1. Som PM, Brandwein M. Salivary glands. In: Som PM, Curtin HD, eds. *Head and Neck Imaging*. St. Louis: Mosby; 1996:823–891.
2. Waldhart E, Lynch JB. Benign hypertrophy of the masseter muscles and mandibular angles. *Arch Surg* 1971;102:115–118.

Chapter 2

Denervation Atrophy

Epidemiology

Adenocystic and squamous cell carcinoma of the head and neck have a propensity for perineural infiltration. Because the masticator space has no mucosal surface, malignant spread along the mandibular nerve is seen in tumors that have invaded this space. These tumors usually originate in the adjacent visceral spaces such as in nasopharyngeal and oropharyngeal cancers.

Clinical Findings

The primary disease usually overshadows symptoms and signs of early perineural spread along the mandibular nerve. Perineural infiltration of the mandibular nerve results in denervation atrophy of the masticator muscles resulting in trismus. Atrophy of the temporalis and masseter muscles is often visible on inspection. Trigeminal neuralgia, however, may be a prominent symptom when perineural infiltration of the mandibular nerve extends to the trigeminal nerve.

Pathology

Changes in the skeletal muscles following denervation can be divided into three phases: acute, subacute, and chronic. Animal models show that in the first 4 weeks, there is a decrease in the caliber of muscle fibers but no change in the total amount of tissue water. There is, however, a relative decrease in intracellular water associated with a relative increase in extracellular water. In the chronic phase, muscular atrophy associated with fatty infiltration takes place. A mixture of features seen in the acute and chronic stages characterizes the subacute phase. In addition, there is a relative increase in the perfusion of muscles following denervation.

Treatment

Involvement of the cranial nerves in nasopharyngeal carcinoma is T4 disease. All head and neck tumors showing perineural infiltration with intracranial extension carry a grave prognosis. Hence the identification of perineural infiltration is crucial so that appropriate therapy can be instituted. Surgical treatment is directed at excising the primary tumor along with adjacent structures affected by tumor infiltration. Postsurgical radiation therapy may be given depending on the status of surgical margins and proximal intracranial extension. The mainstay of treatment for nasopharyngeal carcinoma is radiation therapy.

Imaging Findings

CT

In the acute to subacute phases, CT may be unremarkable compared with MR findings. However, in the subacute to chronic phases, the muscles of mastication (medial and lateral pterygoids, masseter, and temporalis muscles) show a decrease in bulk in association with low attenuation as a result of fatty infiltration.

MR

In the acute to subacute phases, T2-weighted images show high signals thus producing an edema-like appearance. This is because the T2 of extracellular water is longer than the T2 of intracellular water. In addition, there is a relative increase in perfusion and increased accumulation of contrast in the extracellular spaces in denervated muscles resulting in increased contrast enhancement. The chronic phase is characterized by muscle atrophy and increased signals on T1 and fast spin echo T2-weighted images due to fat accumulation (Fig. 2–1).

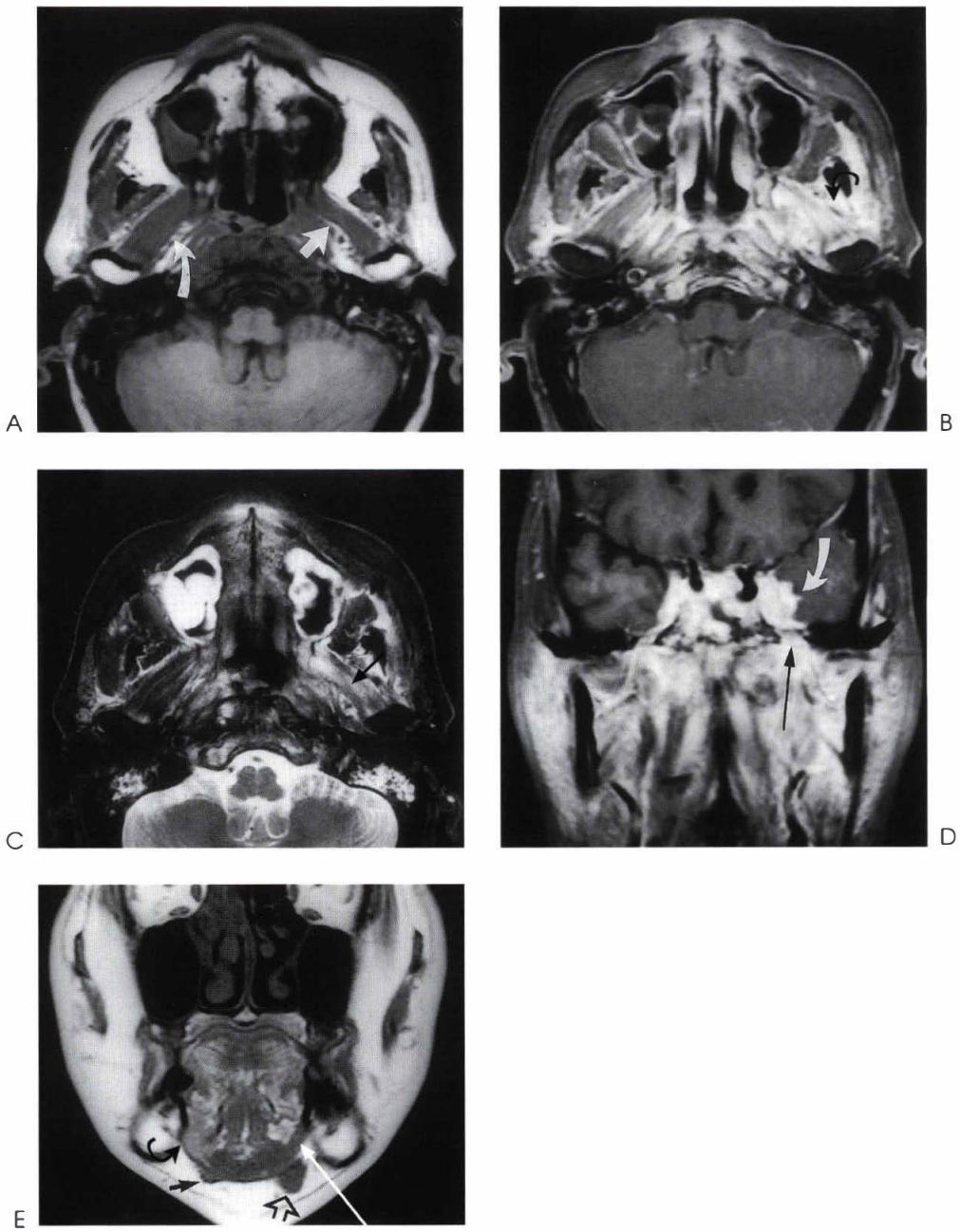

Figure 2–1. Denervation atrophy of muscles of mastication.
(A) Axial T1-weighted MR image shows atrophy of the left lateral pterygoid muscle (arrow). Note the normal right lateral pterygoid muscle (curved arrow).
(B) Axial contrast-enhanced MR image shows intense enhancement of the left lateral pterygoid muscle.
(C) Axial T2-weighted MR image shows high signals in the lateral pterygoid muscle. There are inflammatory changes in the maxillary sinuses and mastoid cells bilaterally.
(D) Coronal contrast-enhanced MR image shows enlargement and enhancement of the right foramen ovale (straight arrow) and cavernous sinus (curved arrow).
(E) Coronal T1-weighted MR image (different patient) shows atrophy of the anterior belly of the right digastric muscle (short black arrow) and the mylohyoid (curved arrow) muscle. Note the normal left anterior belly of the digastric muscle (hollow arrow) and the mylohyoid muscle (long white arrow).

Imaging Pearls

- The mylohyoid nerve, a branch of the mandibular nerve, supplies motor fibers to the mylohyoid muscle and the anterior belly of the digastric muscles. Atrophy of these muscles in the floor of the mouth is best seen on coronal MR images.
- Contrast enhancement of the muscles of mastication may be confused with tumor infiltration. Tumor infiltration is associated with the presence of mass effect. Denervated muscles either are normal in caliber or show atrophy.
- It is important to examine the entire course of the trigeminal nerve. Tumor may extend proximally to the route entry zone of the trigeminal nerve.

Suggested Readings

1. Caldemeyer KS, Mathews VP, Righi PD, Smith RR. Imaging features and clinical significance of perineural spread or extensions of head and neck tumors. *Radiographics* 1998;18:97–110.
2. Russo CP, Smoker WRK, Weissman JL. MR appearance of trigeminal and hypoglossal motor denervation. *AJNR Am J Neuroradiol* 1997;18:1375–1383.
3. Chong VFH. Trigeminal neuralgia in nasopharyngeal carcinoma. *J Laryngol Otol* 1996;110:394–396.
4. Davis SB, Mathews VP, Williams DW III. Masticator muscle enhancement in subacute denervation atrophy. *AJNR Am J Neuroradiol* 1995;16:1292–1294.

Chapter 3

Infection

Epidemiology

The majority of masticator space infections are secondary to odontogenic infections. These patients are typically adolescents or adults with poor oral hygiene. Occasionally, masticator space infection is secondary to malignant otitis externa often seen in diabetics or immunologically compromised patients.

Clinical Findings

Patients with masticator space abscess typically present with pain, fever, and trismus. The diagnosis of dental abscess or malignant otitis externa is usually evident from the clinical history and associated signs and symptoms. Trismus associated with masticator space infection often hampers the examination of the oral cavity or oropharynx. In addition, malignant otitis externa with temporomandibular joint extension may further aggravate trismus.

Pathology

The vast majority of masticator space abscesses due to odontogenic disease consist of mixed infection. Masticator space abscess may also be due to malignant otitis externa with the most common organism being *Pseudomonas*.

Treatment

The treatment for masticator space infection involves controlling the infection of the primary site. Spreading cellulitis requires only antibiotic therapy, and surgery is indicated only when pus formation ensues. If mandibular or external auditory canal osteomyelitis is present, subperiosteal drainage will be required. Multiple abscesses in multiple spaces may necessitate complex drainage procedures.

Imaging Findings

CT

Inflammation of the masticator space causes swelling of one or a combination of the following muscles: medial and lateral pterygoids and temporalis and masseter muscles. There is usually moderate to good contrast enhancement. Mandibular or temporal bone erosion is best seen on CT images acquired with bone algorithm. A masticator space abscess is characterized by a well-defined low attenuation mass that may have an enhancing rim (Fig. 3-1A).

MR

On fat suppressed, contrast-enhanced MR images, there is strong contrast enhancement of the involved muscles. A diagnosis of abscess formation is made when a mass with areas of no enhancement is noted. T2-weighted MR images typically show high signal intensities (Fig. 3-1B-D).

Imaging Pearls

- Bone algorithms need to be evaluated for evidence of odontogenic disease in all cases of abscesses involving the masticator space.
- When a masticator space abscess is secondary to malignant otitis externa, it is important to document the full extent of the skull base and temporal bone involvement. This may require thin sections in both axial and coronal planes using bone algorithms.

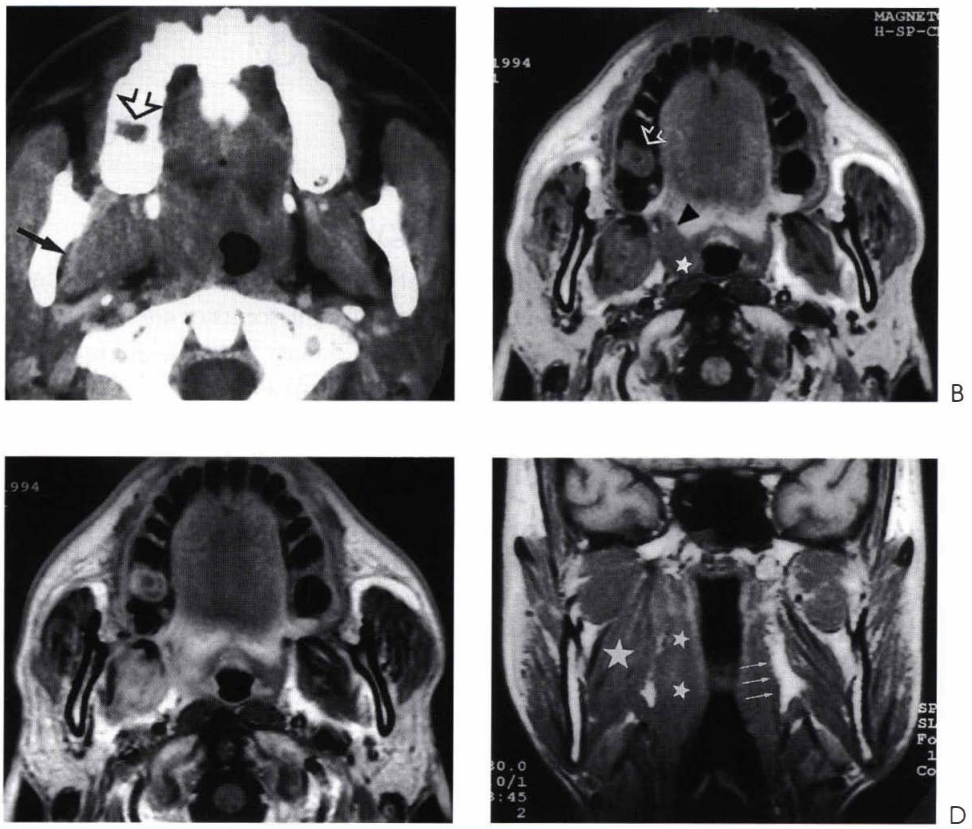

Figure 3–1. Masticator space infection secondary to dental abscess.
(A) Axial contrast-enhanced CT shows a right dental cavity (open arrow) and swelling of the right medial pterygoid muscle (arrow).
(B) Axial T1-weighted MR image shows an intermediate signal dental cavity involving the right mandible (arrow). There is also thickening of the right pharyngeal wall (star) and the tensor palatini muscle (arrowhead).
(C) Axial contrast-enhanced MR image shows enhancement of the odontogenic abscess, right medial pterygoid muscle, right pharyngeal wall, and tensor palatini muscle.
(D) Coronal T1-weighted MR image shows inflammation involving the right pharyngeal wall (small stars) and the medial pterygoid muscle (large star). The right parapharyngeal space is almost effaced. Note the normal high-signal intensity in the left parapharyngeal space (arrows). (With permission from Chong VFH, Fan YF. Radiology of the masticator space. Clin Radiol 1996;51:457–465.)

Suggested Readings

1. Jahn AF, Hawke M. Infections of the external ear. In: Cummings CW, ed. *Otolaryngology—Head and Neck Surgery.* St. Louis: Mosby; 1993:2787–2794.
2. Gherini SG, Brackmann DE, Bradley WG. Magnetic resonance imaging and computerized tomography in malignant otitis externa. *Laryngoscope* 1986;96:542–548.
3. Chong VFH, Fan YF. Radiology of the masticator space. *Clin Radiol* 1996;51:457–465.

Chapter 4

Abscess Associated with Odontogenic Infection

Epidemiology

Dental infection and periodontal inflammation are common infections. They may result in mandibular osteomyelitis if appropriate therapy is delayed. Septicemia with resultant osteomyelitis is uncommon but may be encountered in the pediatric age group. Mandibular osteomyelitis may spread into the adjacent medial pterygoid or masseter muscles resulting in masticator space infection.

Clinical Findings

Osteomyelitis is associated with pain and fever. In addition, patients with masticator space abscess will have varying degrees of trismus. Clinical examination will reveal redness and swelling over the face. A discharging sinus may also be evident on inspection. Masticator space abscess usually occurs from an infected premolar or molar tooth from either the mandibular or the maxillary alveolar ridge.

Pathology

Patients with dental and periodontal disease usually have a history of poor oral hygiene. In some patients the underlying cause is previous irradiation for head and neck malignancy. The immune system may be further compromised by the institution of chemotherapy. The most commonly cultured microorganism is *Staphylococcus.* However, a wide variety of anaerobes may also be found.

Treatment

The treatment consists of appropriate antibiotic coverage, removal of the infected tooth, and drainage of the masticator space abscess.

Imaging Findings

CT

Mandibular osteomyelitis is characterized by osteolysis and erosion of the involved mandible. This is associated with adjacent soft tissue swelling in the masseter or medial pterygoid muscle. Infections of the mandible may extend deeply into the sublingual space or superficially into the buccal space. Phlegmon is characterized by diffuse enhancement of the soft tissues. An abscess will have a low attenuation center with enhancement of the surrounding soft tissues. Air in the soft tissues may be present if the infection is due to gas-forming organisms (Fig. 4–1).

MR

On T1-weighted MR imaging, the high signal intensity of the mandibular marrow is replaced with intermediate signal intensity in inflammatory tissue. On T2-weighted images high signals can be seen in the marrow space and soft tissues of the masticator space. There is diffuse enhancement of the soft tissue with infections due to phlegmon. Abscess will show the characteristic enhancement.

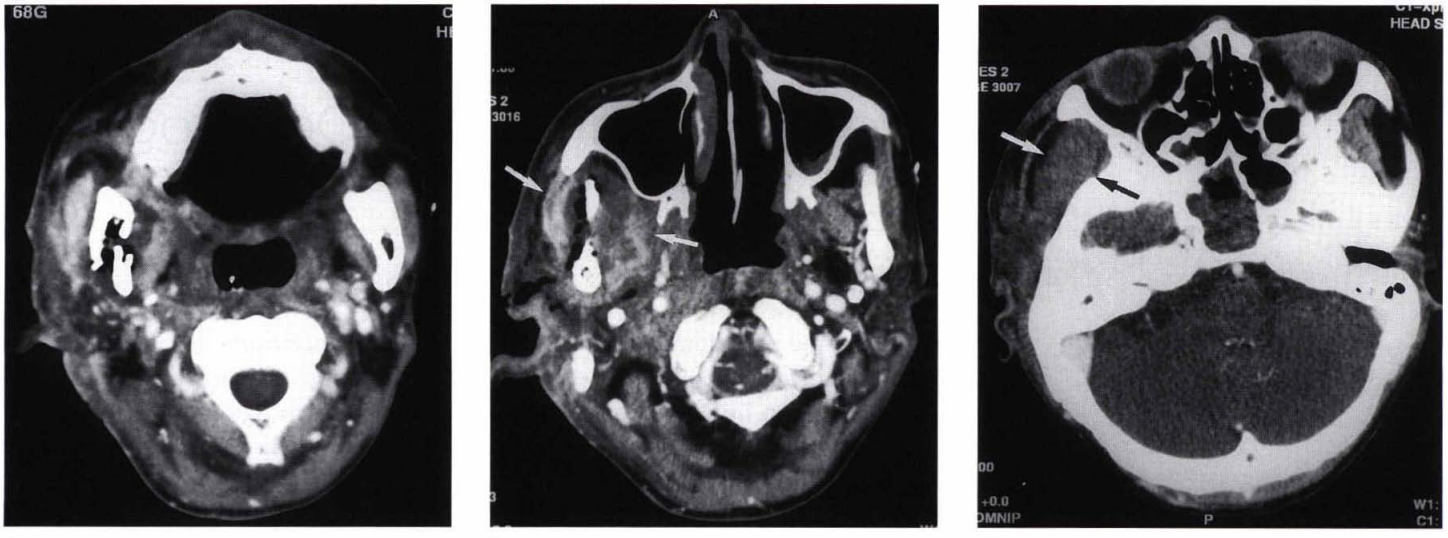

Figure 4-1. Mandibular osteomyelitis with masticator space abscess. (A) Axial contrast-enhanced CT shows fragmentation of the right mandibular ramus associated with pockets of gas. (B) Axial contrast-enhanced CT [superior to (A)] shows abscess formation with rim enhancement medial and lateral (arrows) to the right mandibular ramus. (C) Axial contrast-enhanced MR shows suprazygomatic extension and a thickened right temporalis muscle (opposing arrows).

Imaging Pearls

- In the evaluation of patients with a masticator space infection, bone algorithm must be obtained to evaluate for osteomyelitis of the mandibular or maxillary alveolar ridge from an infected tooth.

Suggested Readings

1. Rosai J. Maxilla and mandible. In: Rosai J, ed. *Ackerman's Surgical Pathology.* 8th ed. St. Louis: Mosby; 1996:257–288.
2. Chong VFH, Fan YF. Radiology of the masticator space. *Clin Radiol* 1996;51:457–465.

Chapter 5

Tuberculosis

Epidemiology

There is an increase in the number of tuberculosis cases in the United States as a result of the epidemic of acquired immune deficiency syndrome (AIDS). This increase also includes an increase in the number of extrapulmonary manifestations. It is believed that about 30% of patients with tuberculosis in the United States have AIDS. Conversely, 5 to 9% of patients with AIDS have tuberculosis. Tuberculosis with primary involvement of the masticator space is very rare. The masticator space may be affected by lesions originating from adjacent structures.

Clinical Findings

Tuberculosis of the masticator space may be overshadowed by the manifestations of AIDS or disseminated tuberculosis. Signs and symptoms of secondary masticator space involvement depend on the site of the lesion.

Pathology

Tuberculosis is caused by *Mycobacterium tuberculosis,* which can either be seen microscopically as acid-fast bacilli or demonstrated by culture. In adults, tuberculosis is most often a postprimary infection, whereas in children it is usually a primary event. In the head and neck, tuberculosis typically produces noncaseating granulomas in the lymph nodes, larynx, bones, or muscles.

Treatment

Tuberculosis can be effectively treated with antibiotic combinations that include streptomycin, isoniazid, rifampin, and ethambutol.

Imaging Findings

CT

CT findings depend on the site of involvement. Tuberculous lymphadenitis of facial nodes or abscess with masticator space involvement shows the same features as infections due to other pyogenic organisms. Contrast-enhanced CT shows an enhancing mass with or without areas of low density. The adjacent bones may show erosions or increased marrow density.

MR

Contrast-enhanced MR imaging may show necrotic facial nodes (for example, the malar group) with associated osteomyelitis of the zygoma and involvement of the suprazygomatic or infrazygomatic masticator space. T2-weighted MR images with fat suppression can also reveal high signal intensity lesions involving nodes, bones, and muscles (Fig. 5–1).

Imaging Pearls

- The facial nodes are usually divided into four groups: mandibular nodes, buccinator nodes, infraorbital nodes, and malar nodes. Tuberculosis or metastasis may involve these facial nodes with extension to the adjacent bones or spaces.
- There is an increase in incidence of extrapulmonary tuberculosis in AIDS. Therefore, a lesion involving bones and soft tissues should have tuberculosis included in the differential diagnosis.

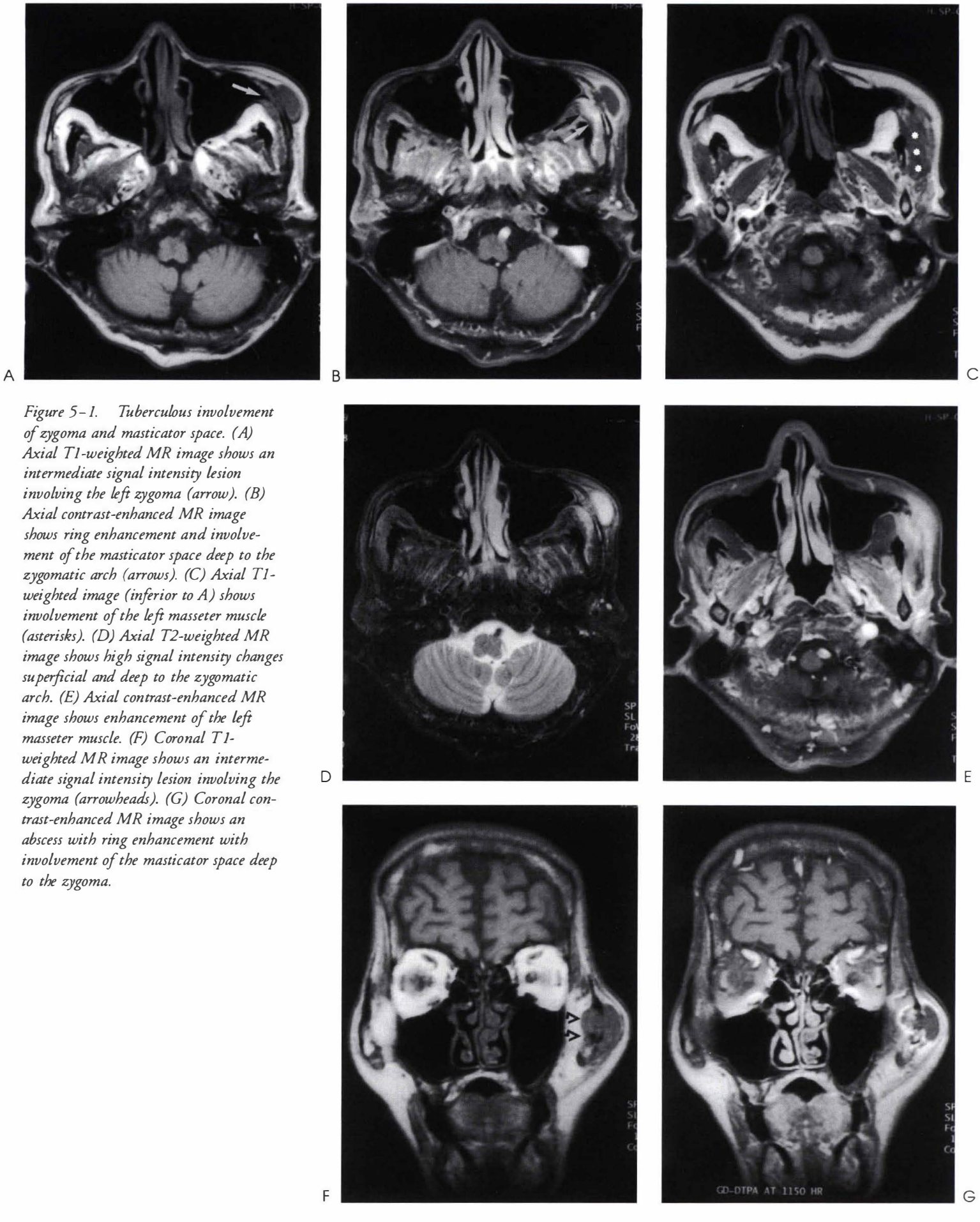

Figure 5–1. Tuberculous involvement of zygoma and masticator space. (A) Axial T1-weighted MR image shows an intermediate signal intensity lesion involving the left zygoma (arrow). (B) Axial contrast-enhanced MR image shows ring enhancement and involvement of the masticator space deep to the zygomatic arch (arrows). (C) Axial T1-weighted image (inferior to A) shows involvement of the left masseter muscle (asterisks). (D) Axial T2-weighted MR image shows high signal intensity changes superficial and deep to the zygomatic arch. (E) Axial contrast-enhanced MR image shows enhancement of the left masseter muscle. (F) Coronal T1-weighted MR image shows an intermediate signal intensity lesion involving the zygoma (arrowheads). (G) Coronal contrast-enhanced MR image shows an abscess with ring enhancement with involvement of the masticator space deep to the zygoma.

Suggested Readings

1. Tart RP, Mukherji SK, Avino AJ, Stringer SP, Mancuso AA. Facial lymph nodes: normal and abnormal CT appearances. *Radiology* 1993;188:695–700.
2. Chong VFH, Fan YF. Facial lymphadenopathy in nasopharyngeal carcinoma. *Clin Radiol* 2000;55:363–367.
3. Moon WK, Han MH, Chang KH, et al. CT and MR imaging of head and neck tuberculosis. *Radiographics* 1997;17:391–402.

Chapter 6

Retromolar SCCA with MS Spread

Epidemiology

Oral and oropharyngeal carcinomas are usually seen in patients over 60 years old. In recent years these tumors have been increasingly encountered in patients who are in the 30's, 40's and 50's. With the increased use of tobacco and alcohol by females, the male to female ratio of the incidence of oral and oropharyngeal tumors has changed from 10:1 to 4:1.

Clinical Findings

Retromolar trigone carcinoma may present with pain or bleeding in the oral cavity. On examination, a mass in the retromolar trigone/anterior tonsillar pillar area may be evident. This lesion may be associated with dysplastic mucosal changes in the oral cavity. Patients with deep involvement of the muscles of mastication may also complain of trismus.

Pathology

The retromolar trigone is located over the anterior aspect of the mandible behind the third molar. Laterally it is bounded by the buccal mucosa, and medially it is continuous with the anterior tonsillar pillar. Although the retromolar trigone is anatomically located within the oral cavity, it behaves like an oropharyngeal malignancy. The tumor is usually poorly to moderately differentiated squamous cell carcinoma. It may erode the ramus of the mandible posteriorly; invade the tonsillar fossa, tongue base, and muscles of mastication medially; and extend to the back of the maxilla and pterygopalatine fossa superiorly.

Treatment

Tumors that are small to moderate in size can be treated entirely with radiation therapy. However, invasion of the adjacent mandible requires surgical resection. Postsurgical radiation therapy may also be given.

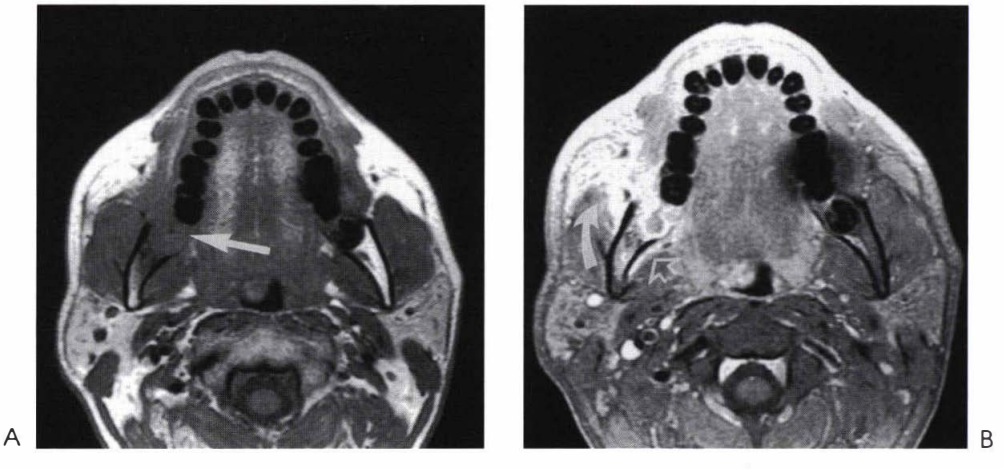

Figure 6-1. Retromolar carcinoma with masticator space spread. (A) Axial T1-weighted MR image shows a diffusely infiltrative right retromolar carcinoma (arrow). Note the infiltrated mandibular cortex and marrow replacement. (B) Axial fat-suppressed T1-weighted contrast-enhanced image shows infiltration of the right masseter muscle (curved arrow) and spread beneath the right lateral pterygoid muscle (open arrow).

Imaging Findings

CT

Like mucosal malignancies elsewhere, both CT and MR imaging underestimate the extent of mucosal involvement. The tumor shows moderate contrast enhancement. Early cortical erosion of the mandible is best identified with CT. Tumor can infiltrate the medial pterygoid muscle, spread superiorly to the pterygoid fossa, and continue to spread along the lateral pterygoid muscle.

MR

Deep infiltration of the masticator muscles shows good contrast enhancement. T2-weighted images typically demonstrate high signals. The high signal intensity mandibular marrow when replaced with tumor is readily seen on T1-weighted images (Fig. 6–1).

Imaging Pearls

- Perineural spread may take place when tumor invades the mandible and spreads along the inferior alveolar nerve to the pterygopalatine fossa and intracranially along cranial nerve V_2. Alternatively, tumor may spread directly to the pterygopalatine fossa and subsequently through the foramen rotundum.
- Perineural spread can also take place along cranial nerve V_3. Because the muscles of mastication are innervated by cranial nerve V_3, masticator space involvement may be followed by spread through the foramen ovale. It is therefore important to examine the course of both cranial nerve V_2 and V_3.

Suggested Readings

1. Shah JP, Lydiatt WM. Buccal mucosa, alveolus, floor of mouth and tongue tumors. In: Thawley SE, Panje WR, Batsakis JG, Lindberg RD, eds. *Comprehensive Management of Head and Neck Tumors*. 2nd ed. Philadelphia: WB Saunders; 1999:686–694.
2. Rosai J. Oral cavity and oropharynx. In: Rosai J, ed. *Ackerman's Surgical Pathology*. 8th ed. St. Louis: Mosby; 1996:223–255.

Chapter 7

Masticator Muscle Tumor Infiltration

Epidemiology

Malignancies originating in spaces and structures adjacent to the masticator space can involve the masticator muscles. Nasopharyngeal carcinoma frequently spreads into the masticator space to involve principally the medial pterygoid muscle. Tonsillar carcinoma or neoplasms arising from the mandible can also infiltrate the medial pterygoid muscle.

Clinical Findings

At presentation, the symptoms and signs of masticator muscle infiltration are frequently overshadowed by the primary tumor. However, on questioning, a history of trismus can be elicited. Clinical examination may also show varying degrees of limited mandibular excursion.

Pathology

In most cases, malignant infiltration is confined to the muscle adjacent to the primary tumor. However, neoplastic infiltrates may spread farther afield to involve the muscle in a permeative way. In some patients, involvement of muscle bundles leads to tumor spread along the mandibular nerve resulting in proximal extension through the foramen ovale. Squamous cell carcinomas and adenocystic carcinomas have a propensity to spread in this manner.

Treatment

The primary tumor is treated using established surgical principles of wide excision. This is supplemented with radiation therapy especially when there is doubt concerning completeness of extirpation. Some tumors such as nasopharyngeal carcinoma can be treated entirely with radiation therapy.

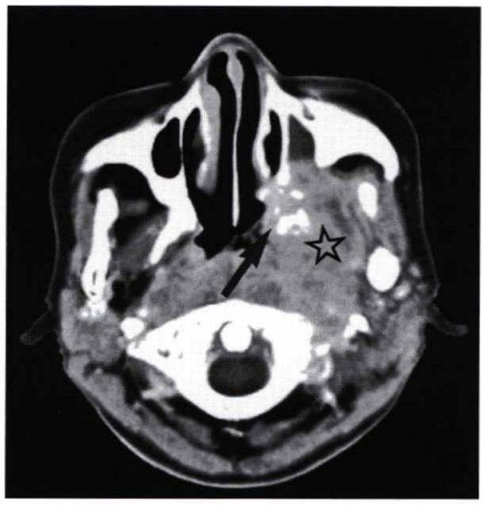

Figure 7-1. Nasopharyngeal carcinoma with masticator muscle invasion. Axial contrast-enhanced CT shows a large nasopharyngeal carcinoma invading the left masticator space (star). No normal masticator muscle could be seen. Note the destruction of the pterygoid process (arrow), which forms the origin of the pterygoid muscles.

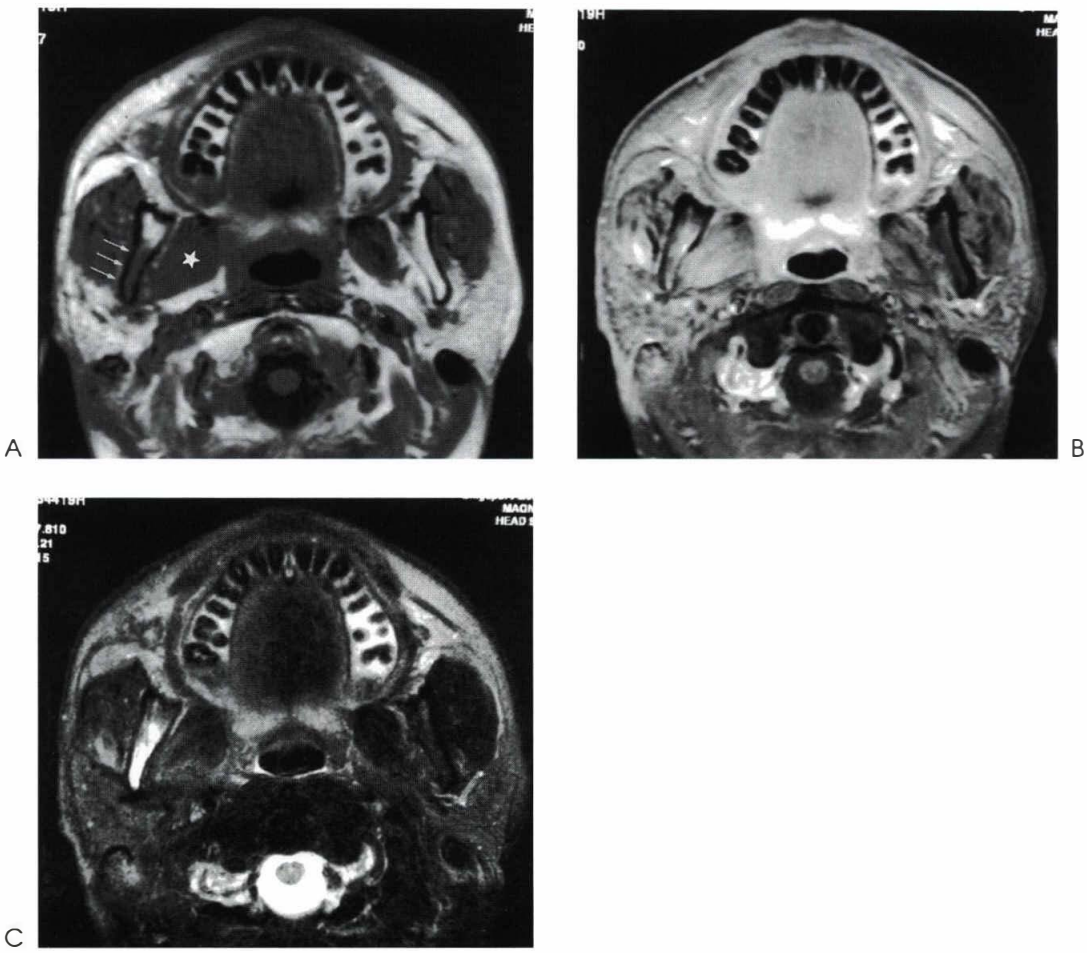

Figure 7-2. Nasopharyngeal carcinoma with infiltration of the medial pterygoid muscle. (A) Axial noncontrast, T1-weighted MR image shows an enlarged right medial pterygoid muscle (star). Note the infiltration of the mandibular marrow (arrows). (B) Axial contrast-enhanced MR image shows enhancement in the right pterygoid muscle and the mandibular marrow space. (C) Axial T2-weighted MR image shows high signals in the involved marrow. The right medial pterygoid muscle shows only a slight increase in signals. Denervation atrophy usually shows much higher signals on T2-weighted images in the subacute phase.

Imaging Findings

CT

Contrast-enhanced CT shows tumor within the involved muscle (usually the medial pterygoid muscle). The demarcation between muscle and tumor may be well defined. However, in some patients, there may be a diffuse increase in muscle bulk indicating permeative spread. Involvement of the medial pterygoid muscle may lead to the involvement of the lateral pterygoid muscle via the common insertion to the pterygoid process (Fig. 7-1).

MR

Contrast-enhanced MR imaging shows increased signals of the tumor tissue within the affected muscle bundle. The tumor-muscle demarcation is usually well defined. On T2-weighted images, there is good separation between high signal intensity tumor and low signal intensity normal muscle (Fig. 7-2).

Imaging Pearls

- Perineural infiltration of the mandibular nerve frequently results in enhancement of the muscles of mastication. This may be associated with high signal intensity on T2-weighted images involving the entire muscle bundle. Denervation atrophy, as the name suggests, results in a decrease in muscle bulk, whereas malignant infiltration results in increased muscle bundle size.

Suggested Readings

1. Russo CP, Smoker WRK, Weissman JL. MR appearance of trigeminal and hypoglossal motor denervation. *AJNR Am J Neuroradiol* 1997;18:1375–1383.
2. Chong VFH. The masticator space in nasopharyngeal carcinoma. *Ann Oto Rhinol Laryngol* 1997;106:979–982.
3. Chong VFH, Fan YF, Mukherji SK. Nasopharyngeal carcinoma. *Semin Ultrasound CT MR* 1998;19:449–462.

Chapter 8

Non-Hodgkin's Lymphoma

Epidemiology

There are two basic categories of lymphoma: Hodgkin's disease (HD) and non-Hodgkin's lymphoma (NHL). Together they account for approximately 3 to 5% of all newly diagnosed malignancies and deaths in developed countries. NHL is more common than HD and represents 60 to 70% of all lymphomas. These tumors affect all age groups. The distribution is, however, bimodal with a peak in young adulthood followed by a plateau in middle age and a steep rise in old age.

Clinical Findings

NHL can present either with lymph node enlargement, an extranodal mass, or both. Patients with masticator space NHL may have trismus or pain that may be associated with or without cervical lymphadenopathy. The incidence of systemic signs such as fever is 10 to 15%.

Pathology

Histologic classification of NHL is notoriously difficult but newer techniques for classification such as immunologic phenotyping, nucleic acid analysis with flow cytometry, and molecular genetics may help to explain the apparent diversity of morphological appearances. One of the most popular classifications is the Rappaport system, which is based on pattern of involvement and cellular appearance. In general, nodular lymphomas have a more indolent course compared with the diffuse variety. HD is almost always confined to lymph nodes, whereas 40 to 60% of NHL present have extranodal involvement. Approximately, one third to two thirds of extranodal involvement is found in the head and neck. The most common head and neck sites are the orbits and Waldeyer's ring. Masticator space NHL is rare.

Treatment

For treatment purposes, NHL is divided into favorable and nonfavorable treatment outcome categories. The favorable group comprises patients with nodular lymphocytic and well-differentiated lymphocytic subtypes. The rest of the subtypes belong to the unfavorable outcome group. They include four histologic patterns: diffuse poorly differentiated lymphocytic, diffuse histiocytic, diffuse undifferentiated, and nodular histiocytic. Patients with stage I favorable group can be treated with radiation therapy alone, whereas higher stages of the favorable group and all nonfavorable histologic subtypes are treated with a combination of radiation therapy and chemotherapy.

Imaging Findings

CT

NHL involving the masticator space shows nonspecific CT findings. There is a soft tissue mass that obliterates the normal fat planes of the masticator space. It enhances mildly to moderately after contrast injection. This may be associated cervical lymphadenopathy. The bones that make up the zygomatic arch and posterior wall of the maxillary sinus are often expanded and thinned suggesting a more slow-growing and indolent process (Fig. 8–1).

MR

MR imaging findings in the masticator space show an intermediate signal mass that involves the masticator space. This tumor diffusely enhances following contrast administration. The tumor may be intermediate to high signal on T2-weighted sequences.

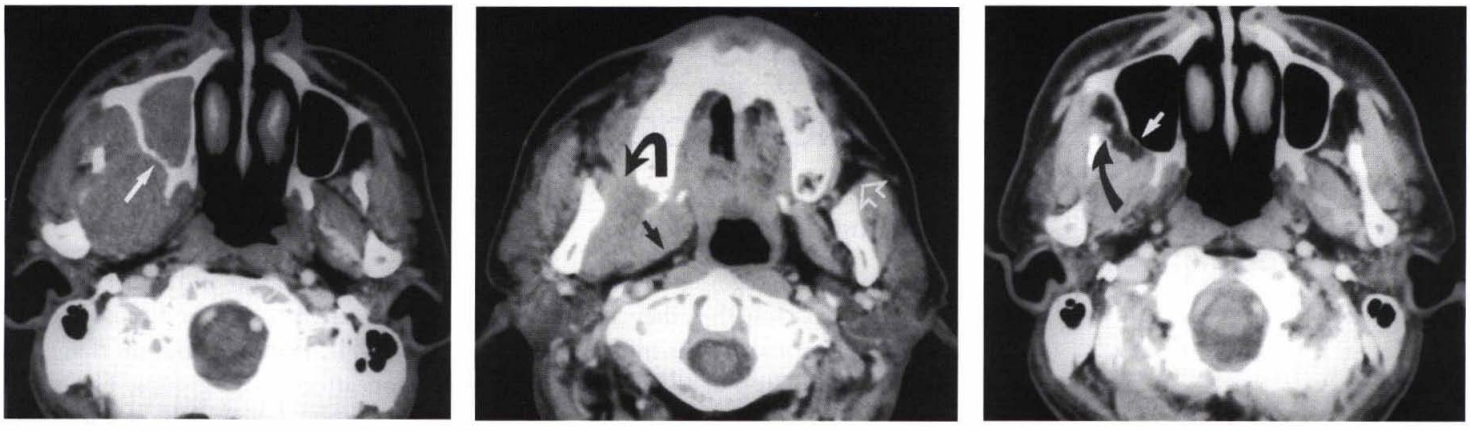

A B C

Figure 8–1. Lymphoma of the masticator space. (A) Axial contrast-enhanced CT shows a homogeneous mass involves the right masticator space. (B) Axial contrast-enhanced CT further inferiorly shows extension of the tumor into the buccal space (curved arrow) and displacement of the right parapharyngeal fat medially (straight arrow). Note the normal, fat-filled left buccal space (hollow arrow). (C) Axial contrast-enhanced CT shows resolution of the mass after radiation therapy. There is restoration of the normal posterior to the right maxillary sinus (curved arrow) and the curvature of the posterior sinus wall (arrow).

Imaging Pearls

- The diagnosis of NHL can be suggested in an elderly adult with soft tissue mass in the masticator space that regressively remodels bone.
- Special attention should be given to the mandibular branch of the trigeminal nerve and foramen ovale in all tumors that involve the masticator space.
- Although extranodal disease is common in NHL fewer than 10% of patients have NHL confined to an extranodal site. Therefore, the presence of a masticator space lesion in association with lymphadenopathy should alert one to the possibility of NHL.

Suggested Readings

1. American Joint Committee on Cancer. *Manual for Staging of Cancer*. 5th ed. Philadelphia: Lippincott; 1997.
2. Mendenhall NP. Lymphomas and related diseases presenting in the head and neck. In: Million RR, Cassisi NJ, eds. *Management of Head and Neck Cancer*. Philadelphia: Lippincott; 1994:857–878.
3. Linberg RD, Paris KJ, Fletcher GH. Radiation therapy of tumors of the neck. In: Thawley SE, Panje WR, Batsakis JG, Lindberg RD, eds. *Comprehensive Management of Head and Neck Tumors*. 2nd ed. Philadelphia: WB Saunders; 1999:1450–1477.

Chapter 9

Osteosarcoma

Epidemiology

Osteosarcomas usually involve the long bones and are most commonly diagnosed during childhood. However, head and neck osteosarcomas are mostly found in adults and these tumors account for 7 to 16% of all osteosarcomas. The most common site in the head and neck is the mandible. Skull base tumors are rare. There is a known relationship between the development of osteosarcoma with Paget's disease, fibrous dysplasia, bilateral retinoblastoma, and irradiation.

Clinical Findings

Patients with osteosarcoma usually present with a mass with or without pain. Most of these tumors are large at presentation. Clinically, the mass is rock hard. Lesions located in the skull base or deep face may have less obvious mass effect or facial deformity.

Pathology

The cell of origin is the osteoblast. Osteosarcomas are very pleomorphic. If they are well differentiated, osteoid formation is evident. Osteoids may show variable calcification or ossification. When these lesions breach the bone cortex, they lift the periosteum. New bone with the typical sunray appearance may form beneath the periosteum. The tumor frequently metastasizes and the most common site for secondaries is the lung.

Treatment

Treatment usually involves a combination of surgery, radiation therapy, and chemotherapy. The tumor shows very high frequencies of local recurrence if only surgery is performed.

Imaging Findings

CT

The CT appearances are variable depending on the degree of calcification and ossification of tumor osteoid. CT may show a tumor comprising mainly dense bone or a large soft tissue mass with associated bone destruction. The presence of sunray spiculation is characteristic (Fig. 9-1).

MR

Like CT, the MR appearances depend on the degree of calcification and ossification. Densely mineralized lesions appear as signal void areas. The soft tissue component enhances well and T2-weighted images show high signals. Associated marrow infiltration is best delineated with T1-weighted images where high signal intensity marrow is replaced by intermediate signal intensity neoplastic tissue.

Imaging Pearls

- When an osteosarcoma is suspected, it may be useful to find out if there is a history of previous radiation therapy. There are several criteria for the diagnosis of radiation-associated sarcoma: (a) there is a history of radiation therapy, (b) the second neoplasm must occur within the field of radiation, (c) the histology of the second neoplasm must be distinctly different from that of the primary tumor, (d) a latency period of many years, arbitrarily taken to be at least 5 years, must have lapsed between radiation therapy and the occurrence of the second tumor.

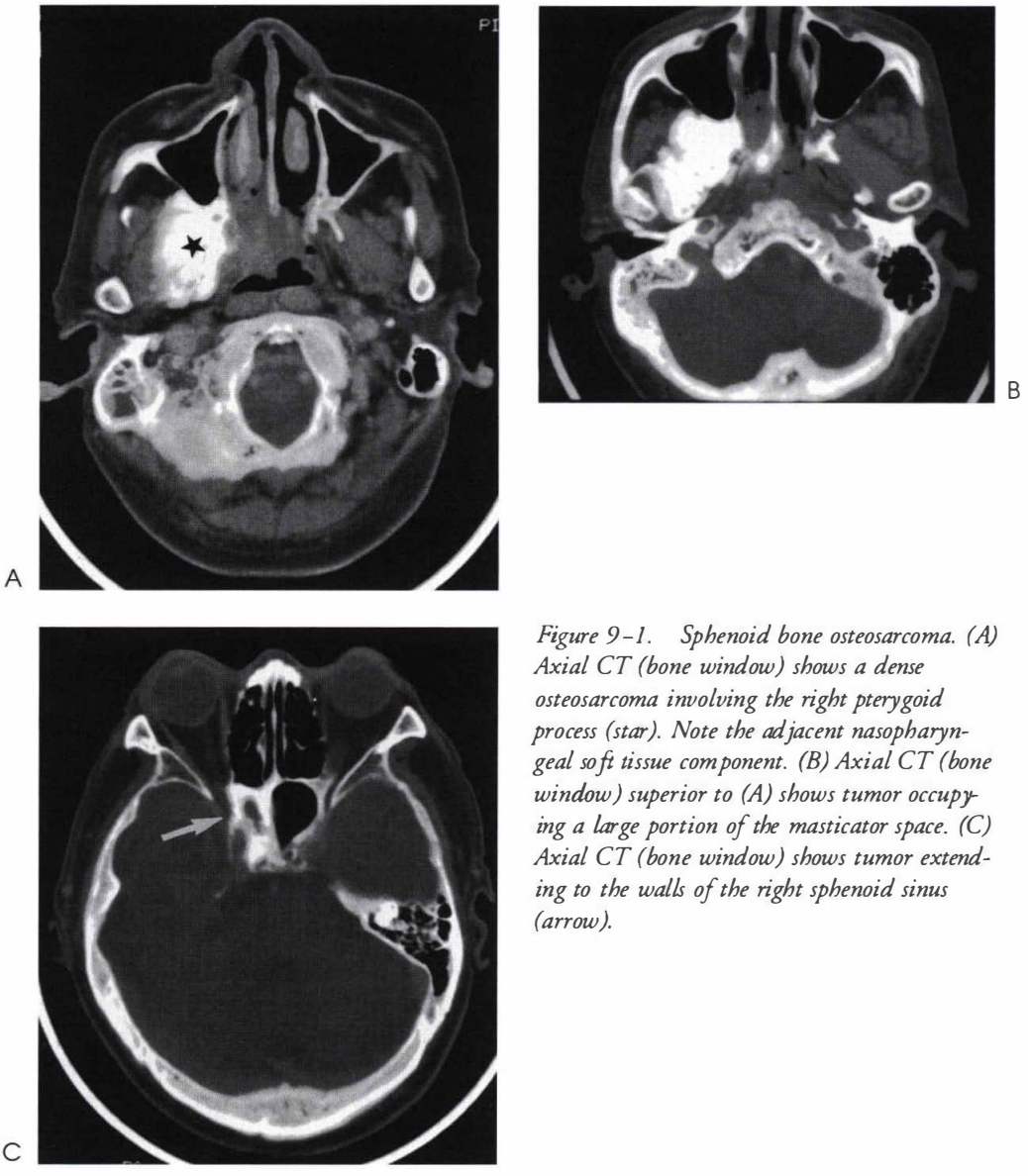

Figure 9-1. Sphenoid bone osteosarcoma. (A) Axial CT (bone window) shows a dense osteosarcoma involving the right pterygoid process (star). Note the adjacent nasopharyngeal soft tissue component. (B) Axial CT (bone window) superior to (A) shows tumor occupying a large portion of the masticator space. (C) Axial CT (bone window) shows tumor extending to the walls of the right sphenoid sinus (arrow).

Suggested Readings

1. Cahan WG, Woodward HG, Higinbotham NL, Stewart FW, Coley L. Sarcoma arising in irradiated bone: report of eleven cases. *Cancer* 1948;1:3-29.
2. Marcus RB, Post C, Mancusso AA. Pediatric tumors of the head and neck. In: Million RR, Cassisi NJ, eds. *Management of Head and Neck Cancer*. Philadelphia: Lippincott; 1994:811-839.
3. Chong VFH, Fan YF. Radiology of the masticator space. *Clin Radiol* 1996;51:457-465.

Chapter 10

Fibrosarcoma

Epidemiology

This tumor was formerly considered the most common soft tissue sarcoma. However, with better definition of tumors such as fibromatosis and malignant fibrous histiocytoma (which were previously lumped together with fibrosarcoma), fibrosarcoma now accounts for only 5 to 10% of all sarcomas. This tumor may be seen in all ages, but most of them occur in adults between 40 and 70 years of age. In children, most tumors are diagnosed in the first year. Males account for 60% of cases. These tumors tend to occur in the lower extremities, whereas head and neck lesions account for up to 20% of cases.

Clinical Findings

Patients usually present with a history of a slow-growing mass ranging from months to several years. The lesion is usually superficially located and feels firm or hard.

Pathology

Grossly, the tumor appears grayish white, firm, and well circumscribed. Poorly differentiated tumors and tumors in children appear more friable. In adults fibrosarcomas lend themselves to histologic grading because such grading (well, moderately, and poorly differentiated) correlates with recurrence rate, metastasis, and survival. However, in children, tumor behavior cannot be predicted from histology.

Treatment

If the tumor is deemed resectable, wide surgical margins should be obtained. The recurrence rate varies between 25 and 75%. Distant metastasis is present in 50% of patients and they are mainly hematogenous. Tumors that initially present as cervical nodal metastases account for < 10% of cases. This tumor is not particularly sensitive to irradiation although some patients may benefit from a course of radiation therapy following surgery. The overall 5- and 10-year survival rate is 50 to 60% and the prognosis is more favorable in children.

Imaging Findings

CT

On contrast-enhanced CT the tumor shows intermediate density and is usually well circumscribed. These tumors moderately enhance following contrast administration. These tumors are usually slow growing and rarely aggressively erode. The bony changes that are present are often due to regressive remodeling. Intratumoral calcifications are rare (Fig. 10–1).

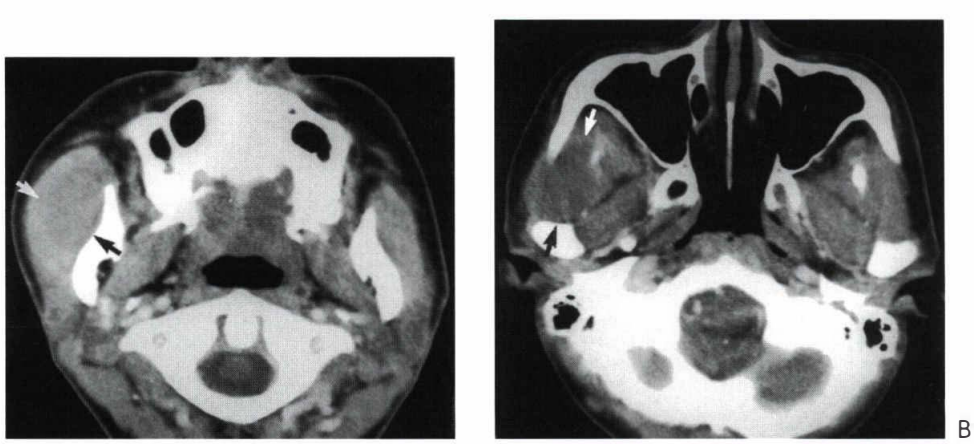

Figure 10–1. Fibrosarcoma involving the masseter muscle. (A) Axial contrast-enhanced CT shows a homogeneously low attenuation mass (relative to muscle) involving the right masseter muscle (arrows). (B) Axial contrast-enhanced CT [superior to (A)] shows the tumor (arrows) extending to the origin in the zygomatic arch and beyond into the suprazygomatic of the masticator space.

MR

The tumor shows variable signal intensity on both T1- and T2-weighted images. It diffusely enhances following contrast administration. In some patients T2-weighted images may be hypointense in signal intensity.

Imaging Pearls

- The tumor should be accurately delineated to facilitate wide surgical excision. Tumor affecting the masseter muscle may extend to the suprazygomatic portion of the masticator space.
- The diagnosis in an adult can be suggested by a primary masticator space mass that does not demonstrate aggressive bone destruction. The differential diagnosis would include non-Hodgkin's lymphoma, malignant fibrous histiocytoma, liposarcoma, and inferior extension of a skull base meningioma.

Suggested Reading

1. Kyriakos M, El-Mofty S. Pathology of selected soft tissue of head and neck. In: Thawley SE, Panje WR, Batsakis JG, Lindberg RD, eds. *Comprehensive Management of Head and Neck Tumors*. 2nd ed. Philadelphia, WB Saunders 1999.

Chapter 11

Malignant Fibrous Histiocytoma

Epidemiology

Malignant fibrous histiocytoma was uncommonly reported before the 1970s. Since then, this tumor has become the most frequently reported soft tissue sarcoma in most major institutions. About 3 to 10% of all malignant fibrous histiocytoma occur in the head and neck. There is no sex predilection and the tumor occurs most frequently in adults 50 to 60 years of age.

Clinical Findings

Patients usually present with a large mass, with or without pain. Symptoms and signs depend on the location of the tumor and compression of surrounding structures.

Pathology

These tumors arise from tissue histiocytes. They grow and invade along fascial planes. They usually have well-defined margins but are not encapsulated. The verifying histologic picture is the storiform pattern of fibroblastic and histiocytic cells. Most tumors show cellular pleomorphism with multiple giant cells.

Treatment

The prognosis is poor. There is a very high recurrence rate following surgery. The tumor is radioresistant and does not respond significantly to chemotherapy. Tumors also show a high propensity to metastasize.

Imaging Findings

CT

Malignant fibrous histiocytoma appears as a well-defined soft tissue mass with moderate contrast enhancement (Figs. 11-1 and 11-2). It may cause erosion of adjacent bony structures and may spread intracranially via neural foramina.

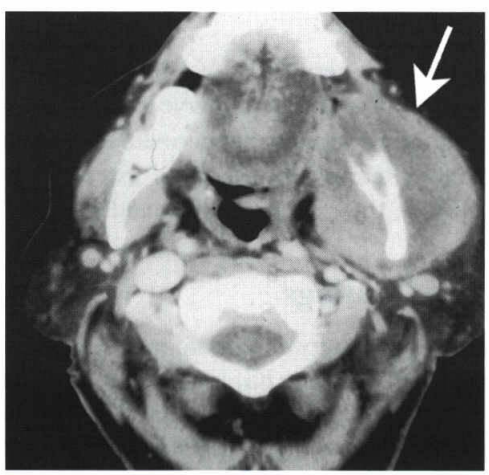

Figure 11-1. Axial contrast-enhanced CT shows a large mass centered in the left masticator space (arrow). Biopsy showed malignant fibrous histiocytoma.

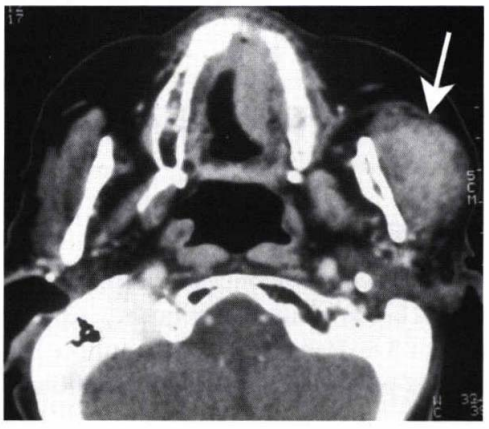

Figure 11-2. Axial contrast-enhanced CT shows a large mass situated in the masseter muscle (arrow) within the masticator space. Pathology revealed metastatic malignant fibrous histiocytoma from a distant primary site.

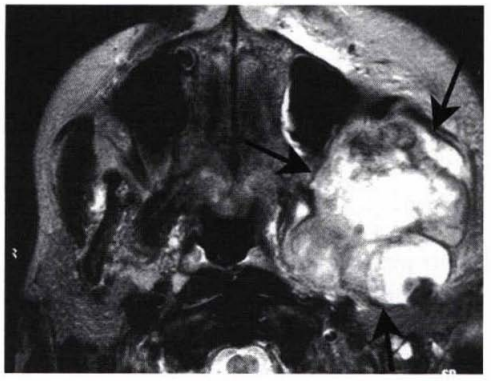

A

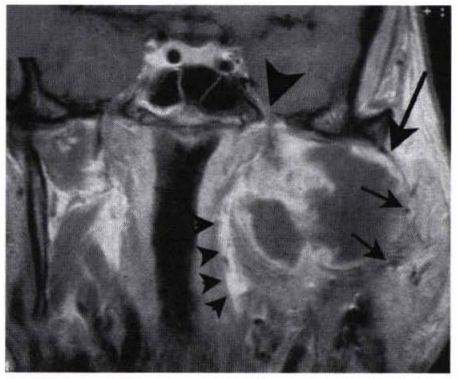

B

Figure 11-3. MR of malignant fibrous histiocytoma. (A) Axial T2-weighted image demonstrates a mass composed of heterogeneous, increased T2 signal located in the left masticator space (arrows). (B) Coronal contrast-enhanced T1-weighted image shows a heterogeneously enhancing mass located in the left masticator space (large arrows). The lateral displacement of the intact parotid gland (small arrows) and the medial displacement of the intact fat within the parapharyngeal space (small arrowheads) place the mass within the masticator space. The mandibular branch of the trigeminal nerve as it courses through the foramen ovale appears normal (large arrowhead) indicating that there is a very low likelihood of retrograde perineural spread along V_3.

MR

The tumor shows well-defined margins on both T1- and T2-weighted MR images (Fig. 11-3). Malignant fibrous histiocytomas normally enhance following contrast administration. These tumors usually have moderately increased signal on T2-weighted imaging. Intracranial spread is best demonstrated on coronal images following the administration of contrast.

Imaging Pearls

- Malignant fibrous histiocytoma must be considered in the differential diagnosis of any soft tissue mass involving the masticator space.
- The primary treatment is often based on the extent of disease identified on cross-sectional imaging because the full extent of masticator space masses is difficult to determine on clinical examination.
- The mandibular nerve (CN V_3) innervates the muscles of mastication. Because of the proximity of the mandibular nerve to the masticator space, it is important to examine the trigeminal nerve for possible perineural tumor spread in patients with masticator space malignancy. Retrograde perineural extension may extend through foramen ovale and may infiltrate the cavernous sinus and the gasserian ganglion

Suggested Readings

1. Kyriakos M, El-Mofty S. Pathology of selected soft tissue of head and neck. In: Thawley SE, Panje WR, Batsakis JG, Lindberg RD, eds. *Comprehensive Management of Head and Neck Tumors*. 2nd ed. Philadelphia: WB Saunders; 1999:1322-1394.
2. Marcus RB, Post JC, Mancuso AA. Pediatric tumors of the head and neck. In: Million RR, Cassisi NJ, eds. *Management of Head and Neck Cancer*. Philadelphia: Lippincott; 1994:811-839.
3. Eskey CJ, Robson CD, Weber AL. Imaging of benign and malignant soft tissue tumors of the neck. *Radiol Clin North Am* 2000;38:1091-1104.

Chapter 12

Rhabdomyosarcoma

Epidemiology

Rhabdomyosarcomas are most commonly seen in the pediatric age group. This malignant neoplasm is also the most common soft tissue tumor in childhood. It accounts for about 50 to 70% of all childhood sarcomas. Approximately 30 to 40% occur in the head and neck. About half of patients present before the age of 5 years. There is no sex predilection.

Clinical Findings

Signs and symptoms depend on the size and location of the lesion. Large tumors often cause trismus as a result of masticator muscle dysfunction or involvement of the temporomandibular joint. Pain may be related to bone erosion or nerve involvement. Physical examination reveals medial displacement of the pharyngeal mucosa. Patients may also present with nasal stuffiness if the tumor extends into the maxillary sinus or nasal cavity. These complaints may be similar to those of a juvenile angiofibroma.

Pathology

There are four histologic subtypes. The well-differentiated pleomorphic type is most commonly seen in adults. The alveolar type predominates in the adolescent age group. The embryonal and botryoid types are typically encountered in childhood. Besides the masticator space, other common sites include the orbit, nasopharynx, mastoid and middle ear, and the sinonasal area. The tumor spreads by both lymphatic and hematogenous routes. Metastasis to the lungs, bones, and marrow is common. In 8% of patients regional nodal spread can be seen.

Treatment

Rhabdomyosarcoma is best treated using a multimodality approach including surgery, radiation therapy, and chemotherapy. The best prognosis is seen in orbital rhabdomyosarcomas. Tumors that involve the nasopharynx and sinonasal regions have a propensity to extend intracranially and tend to have the worst prognosis. However, the prognosis has improved over the years with an overall 3-year survival of 85% and a 5-year disease free rate approaching 73%.

Imaging Findings

CT

The tumor is usually large at presentation. Contrast-enhanced CT usually shows mild enhancement. These tumors may extend anteriorly into the maxillary sinus and demonstrate aggressive destruction of the posterior wall of the sinus. Advanced lesions may also demonstrate aggressive bone destruction of the mandible and skull base.

MR

These locally aggressive tumors are an intermediate signal on T1-weighted sequences and a high signal on T2W (Fig. 12–1). The tumors homogeneously enhance following intravenous contrast. The internal characteristics tend to be homogeneous without internal flow voids.

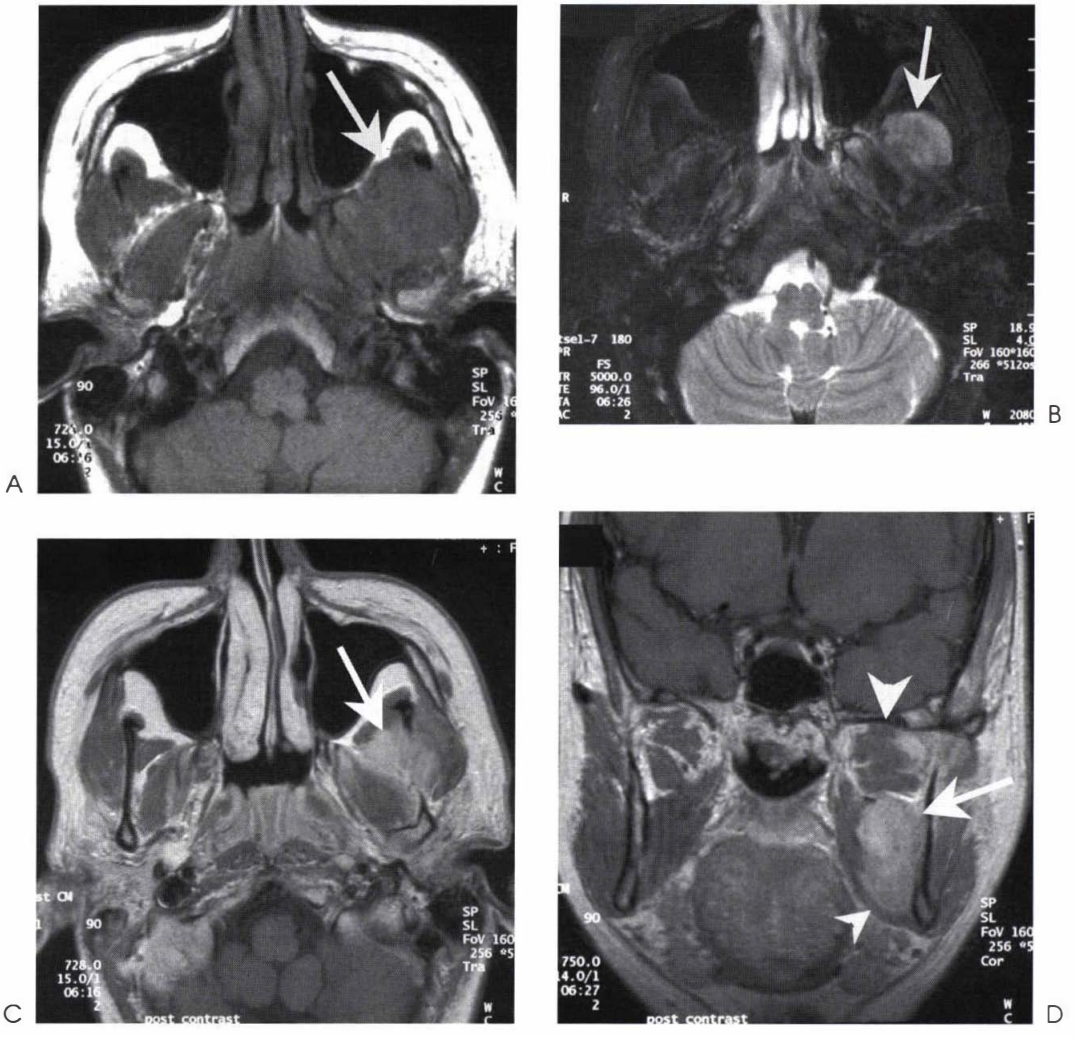

Figure 12–1. (A) Axial noncontrast T1-weighted image shows an intermediate signal mass involving the left masticator space (arrow). (B) Axial fat-suppressed T2W image shows the mass to contain high signal compared with surrounding muscle (arrow). (C) Axial contrast-enhanced T1-weighted image demonstrates that the lesion homogeneously enhances (arrow). (D) Contrast-enhanced coronal T1-weighted image shows the mass (arrow) to be inferior to the lateral pterygoid muscle (large arrowhead) and medial to the medial pterygoid muscle (small arrowhead).

Imaging Pearls

- A rhabdomyosarcoma should be the initial consideration for a primary tumor arising within the masticator space in a child.
- The lack of flow voids and the presence of aggressive bone destruction help differentiate a rhabdomyosarcoma from a juvenile angiofibroma in an adolescent male that extends into the sinonasal region.

Suggested Readings

1. Cunningham MJ, McGuirt WF, Meyers EN. Cancer of the head and neck in pediatric population. In: Myers EN, Suen JY, eds. *Cancer of Head and Neck*. 3rd ed. Philadelphia: WB Saunders; 1996:598–624.
2. Hudgins PA, Jacobs IA, Castillo M. Pediatric airway disease: malignant tumors and tumor-like conditions. In: Som PM, Curtin HD, eds. *Head and Neck Imaging*. 3rd ed. St. Louis: Mosby; 1996:604–611.

Chapter 13

Desmoid Fibromatosis

Epidemiology

Desmoid fibromatosis is arbitrarily divided into two types: anterior abdominal wall and extra-abdominal wall. The extra-abdominal variety, which is more common, is also known as musculoaponeurotic or aggressive fibromatosis. The histologic appearances of these varieties are the same. Approximately 10 to 30% of all extra-abdominal desmoids are found in the head and neck. Desmoid fibromatosis affects a wide age group ranging from infants to the eighth decade. Most patients, however, are in the third and fourth decades. There is no sex predilection for the extra-abdominal variety although there is a female preponderance in the abdominal type.

Clinical Findings

The lesion is firm to hard and is characteristically slow growing. Most lesions are nontender and painless. They may be noted to develop in previously irradiated fields or surgical scars. Some lesions are multicentric. Lesions resemble scar and may be impossible to distinguish from proliferating scar tissue both clinically and pathologically.

Pathology

The lesions are variable in size and may grow beyond 20 cm. They develop within muscles, aponeurosis, or fascia and typically infiltrate the muscles along the long axis. Microscopically, the muscles and aponeurosis are invaded by mature, uniform, spindle-shaped cells. The infiltrative process separates the muscle bundles and these muscles eventually show atrophy. In some patients these lesions turn sarcomatous.

Treatment

Lesions of head and neck desmoid fibromatosis appear more aggressive than lesions elsewhere. They should be treated by wide surgical resections. Because of the infiltrative behavior, surgical clear margins are difficult to achieve. Hence, recurrences are common (20–77%), and most lesions recur within the first 2 years. Patients may die from aggressive local disease, and some patients may also have distant metastasis. Chemotherapy may also be successful in some patients using nonsteroidal anti-inflammatory agents, tamoxifen, and colchicine.

Imaging Findings

CT

The CT findings of desmoid fibromatosis are nonspecific. These tumors show variable enhancement and cannot be distinguished from malignant infiltrative lesions (Fig. 13–1).

MR

The MR findings are also nonspecific. Lesions show intermediate signal intensity on T1-weighted images and high signal intensity on T2-weighted images. They enhance strongly after the injection of contrast (Fig. 13–2).

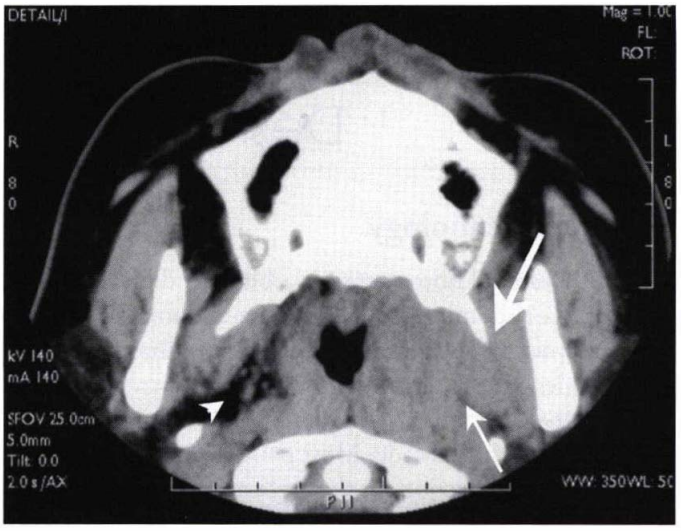

Figure 13–1. Axial CT shows a soft tissue mass involving the left masticator space (large arrow). The mass also extends into the adjacent parapharyngeal space (small arrow). Compare this with the normal fat of the parapharyngeal space on the uninvolved side (arrowhead). Pathology revealed fibromatosis.

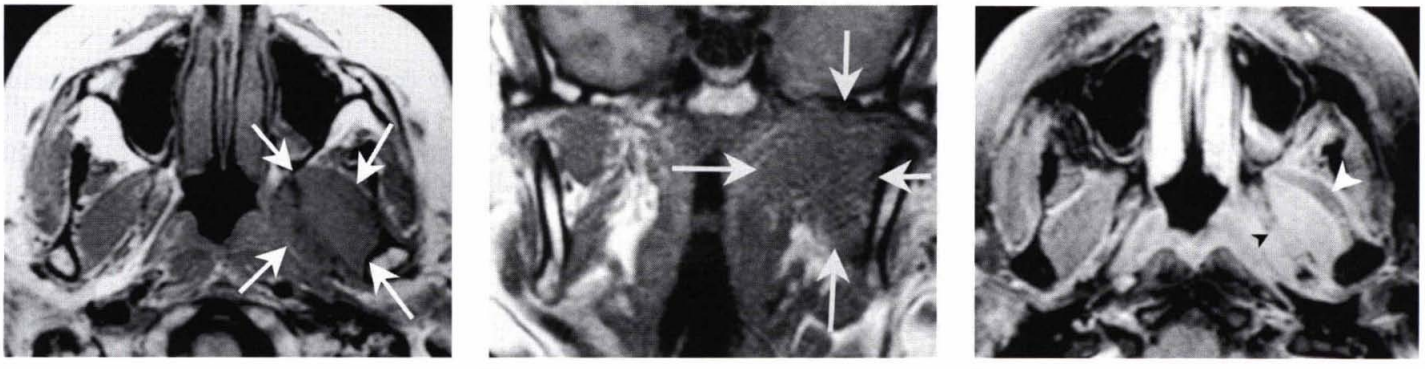

A B C

Figure 13–2. (A) Noncontrast T1-weighted image shows an intermediate signal mass located in the left masticator space (arrows). (B) Coronal noncontrast T1-weighted confirms that the mass is located in the masticator space (arrows). (C) Axial contrast-enhanced, fat-suppressed T1-weighted image shows the mass to laterally displace the lateral pterygoid muscle (large arrowhead) and medially displace the levator and tensor veli palatini muscles (small arrowhead). Pathology revealed fibromatosis.

Imaging Pearls

- CT and MR imaging findings cannot distinguish desmoid fibromatosis from other malignant lesions. However, because of the slow growing process, bones tend to be remodeled rather than infiltrated.
- Desmoid fibromatosis may be multicentric. Hence, separate masses in the head and neck may point toward this diagnostic possibility.

Suggested Readings

1. Conley J, Healey WV, Stout AP. Fibromatosis of head and neck. *Am J Surg* 1966;112:609–614.
2. Cole NM, Guiss LW. Extra-abdominal desmoid tumors. *Arch Surg* 1969;98:530–533.
3. Kyriakos M, El-Mofty S. Pathology of selected soft tissue of head and neck. In: Thawley SE, Panje WR, Batsakis JG, Lindberg RD, eds. *Comprehensive Management of Head and Neck Tumors*. 2nd ed. Philadelphia: WB Saunders; 1999:1322–1394.
4. Mukherji SK, Holliday RA. Pharynx. In: Som PM, Curtin HD, eds. *Head and Neck Imaging*. St. Louis: Mosby; 1996:437–472.

Chapter 14

Hemangiosarcoma

Epidemiology

Hemangiosarcomas can arise from endothelial cells in almost any organ. The head and neck represent the most common sites for these tumors, and they are predominantly located in the scalp. This malignancy is found mainly in the older age group but is also reported in the pediatric age group. Males are more commonly affected, with a sex ratio of M:F of 4:1.

Clinical Findings

Most patients present with a mass. The lesions appear blue with a peripheral zone of erythema.

Pathology

Hemangiosarcomas can be classified into two groups. Low-grade malignancy shows better tumor differentiation, whereas the high-grade variety exhibits poorly or undifferentiated tumor tissues. High-grade tumors tend to show wide and deep tissue infiltration, and the adjacent bony structures may be eroded. Hemangiosarcomas show cervical nodal or pulmonary metastasis in about one third of patients.

Treatment

Treatment depends on the site and size of the tumor. Surgical excision is the primary form of treatment. Radiation therapy can also be used. The most important reason for treatment failure is the underestimation of tumor volume. The prognosis is generally poor with more than 50% of patients dying within 5 years.

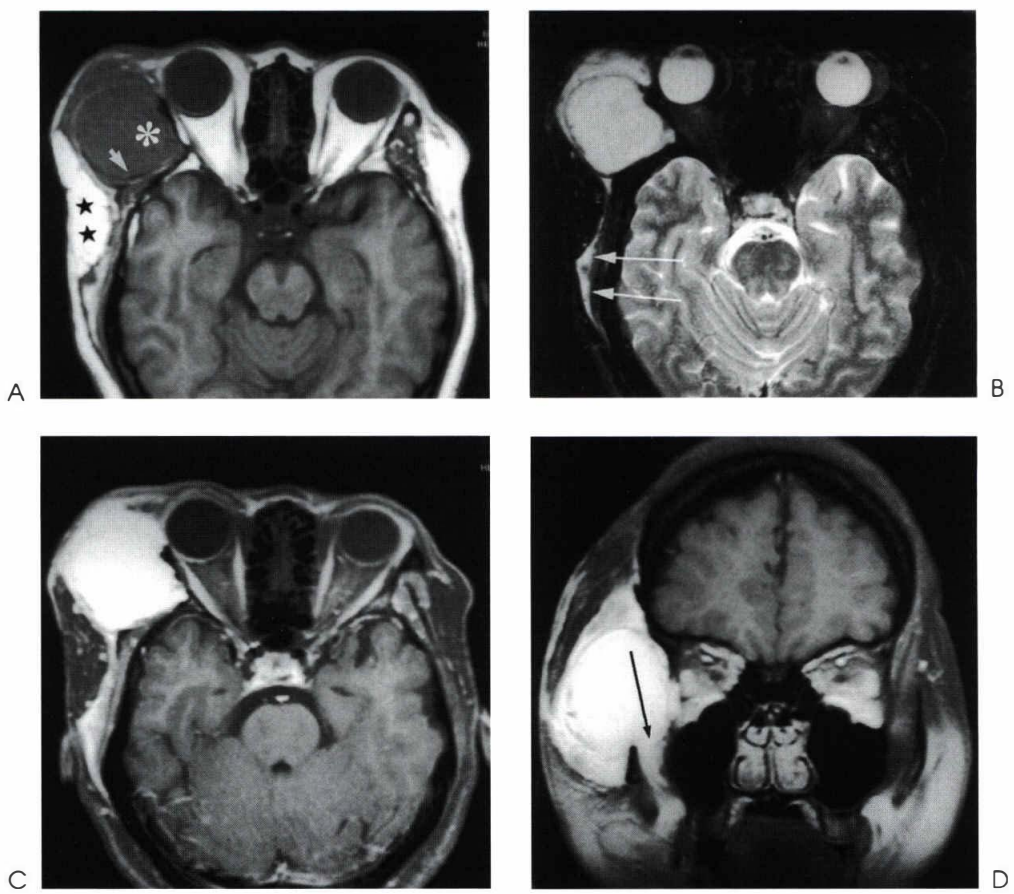

Figure 14–1. Suprazygomatic masticator space hemangiosarcoma. (A) Axial T1-weighted MR image shows an intermediate signal intensity right suprazygomatic hemangiosarcoma (asterisk). Note flap from previous operation (stars). There is a peculiar rim of high and low signal intensity probably related to hemoglobin degeneration products (arrow). (B) Axial T2-weighted MR image shows high signal intensity lesion with deep infiltration (arrows) not suspected clinically. (C) Axial contrast-enhanced MR shows intense enhancement. Note the contiguous, deep, and extensive tumor spread. (D) Coronal contrast-enhanced MR image shows tumor extending to the infrazygomatic portion of the masticator space (arrow).

Imaging Findings

CT

Contrast-enhanced CT shows an enhancing mass. There may be associated bony erosion. The presence of tumor bleeding may be masked following contrast enhancement.

MR

Hemangiosarcomas are often hemorrhagic and on T1- and T2-weighted images, high signals may be detected. The neoplasm shows intense enhancement following the injection of contrast. On T2-weighted images, the tumor shows high signals (Fig. 14–1).

Imaging Pearls

- The MR and CT findings of hemangiosarcomas are nonspecific but this diagnosis may be suggested if tumor hemorrhage is detected. Hemorrhage on CT may be missed when only contrast-enhanced examinations are performed.
- Tumor size estimation is frequently underestimated clinically and this may result in treatment failure. It is therefore important to delineate the full tumor extent.

Suggested Readings

1. Marcus RB, Brant TA, Mancuso AA. Adult mesenchymal tumor presenting in the head and neck. In: Million RR, Cassisi NJ, eds. *Management of Head and Neck Cancer*. Philadelphia: Lippincott; 1994:841–856.
2. Som PM, Brandwein M. Tumor and tumor-like conditions. In: Som PM, Curtin HD, eds. *Head and Neck Imaging*. St. Louis: Mosby; 1996:185–262.

Chapter 15

Neurofibromatosis Type 2

Epidemiology

Neurofibromatosis (NF) type 2 is characterized by multiple cranial nerve schwannomas, but associated peripheral and cutaneous neurofibromas are uncommon. These lesions may be associated with multiple meningiomas or ependymomas. The most common site for schwannomas involves the eighth cranial nerve. The reported incidence is about 1:210,000, which is 10 times less frequent than NF type 1. This entity has an autosomal dominant pattern of inheritance and shows no predilection based on race or sex.

Clinical Findings

Patients with vestibular schwannomas typically present with symptoms of hearing loss in the second and third decades and 30s. Young patients with meningiomas may present with symptoms related to raised intracranial pressure. These patients should be suspected to have NF2. In addition, patients may present with juvenile subcapsular lens opacity.

Pathology

Unlike neurofibromas, which are made up of all neural elements, schwannomas are composed of only Schwann's cells. Schwannomas are encapsulated tumors and they typically show a dense component (Antoni A tissue) and a looser component (Antoni B tissue). Schwannomas tend to undergo cystic changes and show hemorrhagic areas as they enlarge.

Treatment

Because NF type 2 may involve multiple sites and structures, surgery is warranted only if there are symptoms and significant compression of vital structures.

Imaging Findings

CT

When the mandibular nerve is thickened, it causes smooth enlargement of the foramen ovale. Contrast-enhanced CT shows an enhancing tumor with sharp outline.

MR

On T1-weighted images, schwannomas are isointense with skeletal muscles. Mandibular nerve schwannomas may obliterate the fat just below the opening of the foramen ovale. They show high signals on T2-weighted images and strong contrast enhancement (Fig. 15-1).

Imaging Pearls

- A fusiform mass in the expected course of the mandibular nerve should raise the possibility of a schwannoma or a neurofibroma. The rest of the trigeminal nerve should be examined for neurofibromata. This diagnosis of NF type 2 can easily be made in the presence of associated meningiomas or schwannomas involving the other cranial nerves, especially the eighth cranial nerve.

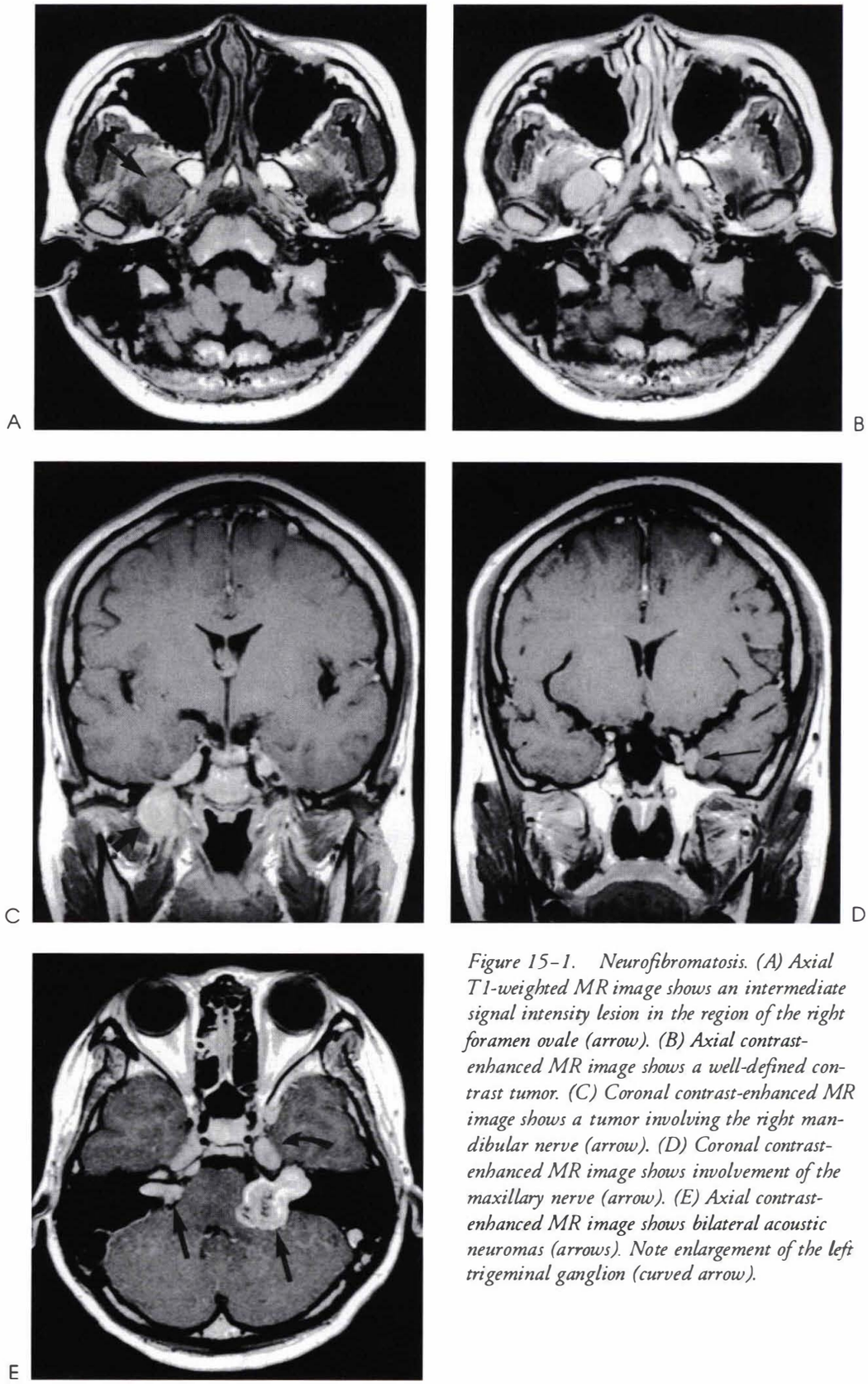

Figure 15–1. Neurofibromatosis. (A) Axial T1-weighted MR image shows an intermediate signal intensity lesion in the region of the right foramen ovale (arrow). (B) Axial contrast-enhanced MR image shows a well-defined contrast tumor. (C) Coronal contrast-enhanced MR image shows a tumor involving the right mandibular nerve (arrow). (D) Coronal contrast-enhanced MR image shows involvement of the maxillary nerve (arrow). (E) Axial contrast-enhanced MR image shows bilateral acoustic neuromas (arrows). Note enlargement of the left trigeminal ganglion (curved arrow).

Suggested Readings

1. Smirniotopoulos JG, Murphy FM. Central nervous system manifestations of the phakomatoses and other inherited syndromes. In: Atlas SW, ed. *Magnetic Resonance Imaging of the Brain and Spine*. 2nd ed. Philadelphia: Lippincott-Raven; 1996:773–802.
2. Kyriakos M, El-Mofty S. Pathology of selected soft tissue of head and neck. In: Thawley SE, Panje WR, Batsakis JG, Lindberg RD, eds. *Comprehensive Management of Head and Neck Tumors*. 2nd ed. Philadelphia: WB Saunders; 1999:1322–1394.
3. Weber AL, Montandon C, Robson CD. Neurogenic tumors of the neck. *Radiol Clin North Am* 2000;38:1077–1090.

Chapter 16

Benign Minor Salivary Gland Tumors (Pleomorphic Adenoma, Monomorphic Adenoma, Warthin's Tumor)

Epidemiology

A minor salivary gland consists of cellular constituents of the major salivary glands (parotid, submandibular, sublingual) that are located within the mucosa of the upper aerodigestive tract. It has been estimated that there are between 500 and 1000 minor salivary glands located throughout the oral cavity and oropharynx. They may be found within the hard and soft palate, uvula, lips, retromolar trigone, tongue base, floor of mouth, and tonsil. The same malignancies that arise in the major salivary glands occur in the minor salivary glands. Depending on the series, approximately one half of minor salivary gland tumors are benign as compared with approximately 70 to 80% of parotid tumors that are benign.

Clinical Findings

Patients often present with asymptomatic masses that have been present for several months. Pain and ulceration may be present; however, these are not consistent findings.

Pathology

The benign tumors that constitute minor salivary gland tumors include pleomorphic adenoma, monomorphic adenomas, and Warthin's tumor. The pathology of these lesions has been reviewed in other sections of this book.

Treatment

The exact treatment depends on the pathology. For most benign tumors complete local resection is adequate.

Imaging Findings

CT

The CT findings are not specific. The presence of regressive remodeling of the surrounding bone for lesions that arise in the hard palate is suggestive of a benign minor salivary gland tumor (Fig. 16-1).

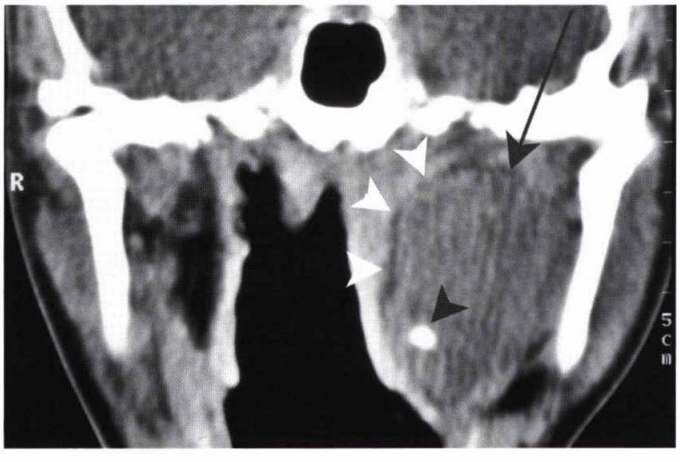

Figure 16-1. Coronal CT shows a round mass (large arrow) involving the masticator space with medial displacement of the fat in the parapharyngeal space (white arrowheads). Note the foci of calcification within the mass (black arrowhead) suggesting a benign process. Pathology revealed pleomorphic adenoma.

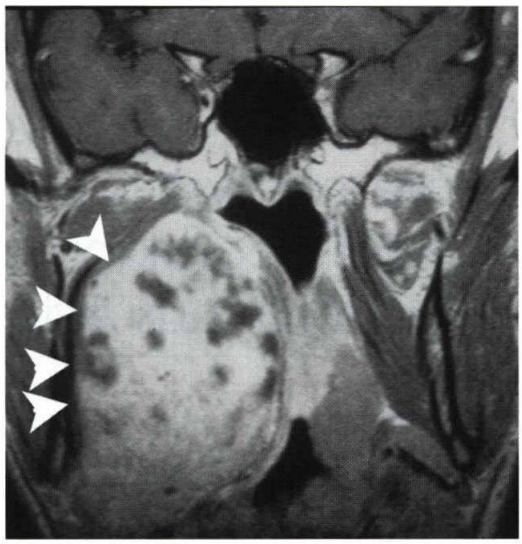

Figure 16–2. Coronal contrast-enhanced T1-weighted MR shows benign minor salivary gland tumor involving both the parapharyngeal and masticator spaces. The arrowheads denote the involvement of the masticator space.

MR

In general, the imaging findings are nonspecific. However, oral cavity or oropharyngeal lesions that are low to intermediate signal on T1-weighted and increased signal on T2-weighted sequences is suggestive of pleomorphic adenoma (Fig. 16–2).

Imaging Pearls

- In general, these are uncommon lesions with diagnosis usually at histology following initial biopsy. The intent of imaging is to provide information that cannot be detected on clinical examination. CT is helpful to evaluate the extent of bone erosion. MR should be performed to determine the presence of submucosal spread and deep invasion.

Suggested Readings

1. Batsakis JG. Neoplasms of the minor and lesser major salivary glands. In: Batsakis JG, ed. *Tumors of the Head and Neck.* Baltimore: William and Wilkins; 1979:76–99.
2. Smoker WRK. Oral cavity. In: Som PM, Curtin H, eds. *Head and Neck Imaging.* 3rd ed. New York: Mosby; 1996:488–544.
3. Shockley WM. Parotid tumors. In: Shockley WM, Pillsbury HC, eds. *The Neck: Diagnosis and Surgery.* New York: Mosby; 1994:265–294.

Chapter 17

Malignant Minor Salivary Gland Tumors (Adenoidcystic, Mucoepidermoid, Adenocarcinoma, Low-Grade Polymorphous Adenocarcinoma)

Epidemiology

The same malignancies that arise in the major salivary glands occur in the minor salivary glands. Depending on the series, approximately half of all tumors of minor salivary gland origin are malignant. The most common location is the palate. An interesting paradox is that the smaller the salivary gland, the greater the likelihood that a tumor originating from that gland will be malignant. The incidence of a salivary gland tumor being malignant is substantially greater in the palate than in the parotid.

Clinical Findings

Patients often present with asymptomatic masses that have been present for several months. Pain and ulceration may be present; however, these are not consistent findings.

Pathology

It has been estimated that there are between 500 and 1000 minor salivary glands located throughout the oral cavity and oropharynx. They may be found within the hard and soft palate, uvula, lips, retromolar trigone, tongue base, floor of mouth, and tonsil. The malignancies that constitute minor salivary gland tumors include adenoidcystic carcinoma, mucoepidermoid carcinoma, and adenocarcinoma. Many investigators now include low-grade polymorphous adenocarcinoma as a tumor of minor salivary gland origin. The most common malignancy of the minor salivary glands is adenoidcystic carcinoma.

Treatment

The treatment of malignant salivary gland tumors depends on the exact histologic type. In general, complete surgical resection offers the best chance for cure. Postoperative radiation therapy is required in the majority of cases. The role of neutron beam therapy for unresectable adenoidcystic carcinomas is currently being evaluated.

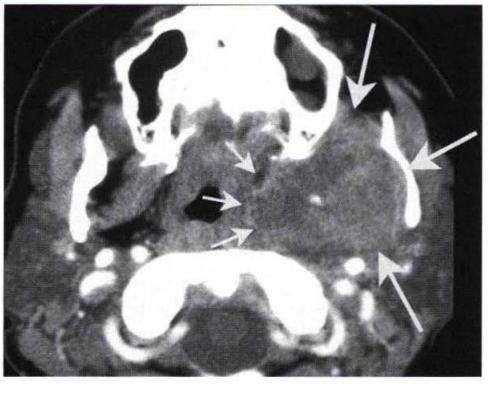

Figure 17–1. Axial contrast-enhanced CT shows an aggressive soft tissue mass situated in the masticator space (large arrows). There is medial extension into the parapharyngeal space (small arrows). Pathology revealed carcinoma expleomorphic adenoma.

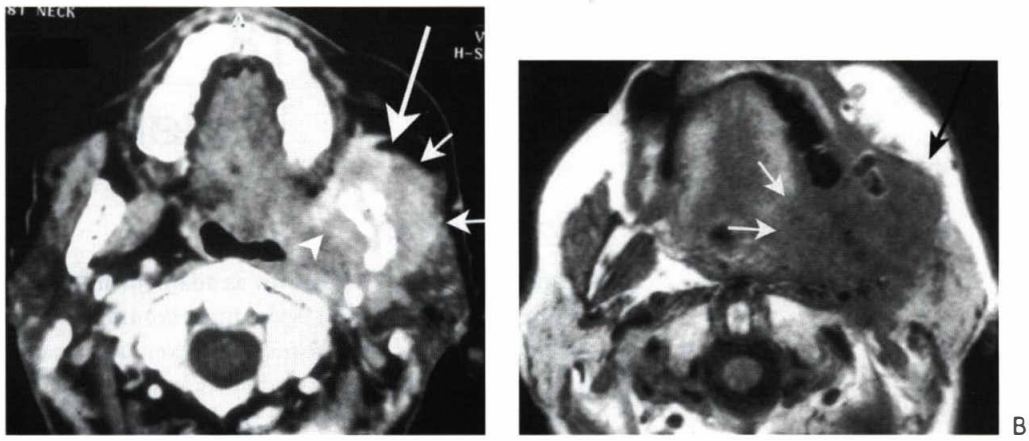

Figure 17-2. Mucoepidermoid carcinoma. (A) Axial contrast-enhanced CT shows an aggressive mass invading the masticator space (large arrow). There is involvement of masseter muscle (small arrows) and medial pterygoid muscle (arrowhead). (B) Axial noncontrast T1-weighted image shows the tumor to have intermediate signal (long arrow). The mass extends into the lateral aspect of the tongue base (short arrows). Primary malignant minor salivary gland tumors rarely arise from the masticator space. The involvement is typically due to extension from an adjacent primary site. This tumor probably arose from the submandibular gland or the tongue base.

Imaging Findings

CT

The CT findings are nonspecific (Fig. 17-1). These are usually soft tissue masses that enhance following contrast. The presence of aggressive bone erosion is suggestive of a high-grade malignancy (Fig. 17-2A).

MR

These tumors are usually intermediate signal on T1-weighted sequences and enhance following contrast administration (Fig. 17-2B). The T2-weighted signal is variable.

Imaging Pearls

- For adenoidcystic carcinoma involving the hard palate, CT should be performed to evaluate for bone erosion in the regions of the incisive canal and greater and lesser palatine foramen. MR should be performed to evaluate for extension into the pterygopalatine fossa and possible retrograde perineural spread along the maxillary division of cranial nerve V or along the nerve of the vidian canal. These are potential pathways of spread in the cavernous sinus. These potential spread patterns should be evaluated in all patients because this may preclude primary surgical resection at many institutions.
- Patients who present with infraorbital numbness and paresthesias should undergo a high-resolution MR of the palate and trigeminal nerve to evaluate for the presence of clinically occult adenoid cystic carcinoma of the hard or soft palate that has invaded the infraorbital nerve.
- We recommend performing MR imaging in patients with polymorphous adenocarcinoma arising in the oral cavity because, based on our experience, it appears this tumor has a propensity for marrow invasion.

Suggested Readings

1. Batsakis JG. Neoplasms of the minor and lesser major salivary glands. In: Batsakis JG, ed. *Tumors of the Head and Neck*. Baltimore: William and Wilkins; 1979:76-79.
2. Smoker WRK. Oral cavity. In: Som PM, Curtin H, eds. *Head and Neck Imaging*. 3rd ed. New York: Mosby; 1996:488-544.
3. Shockley WM. Parotid tumors. In: Shockley WM, Pillsbury HC, eds. *The Neck: Diagnosis and Surgery*. New York: Mosby; 1994:265-294.

Chapter 18

Ameloblastoma

Epidemiology

Ameloblastoma (also known as adamantinoma, adamantoblastoma, basaloma, and epithelioma ameloblastoides) is the most common odontogenic tumor and accounts for 11% of all odontogenic neoplasms. However, it remains an uncommon lesion, accounting for about 1% of all tumors and cysts arising in the jaw. Two thirds of all patients are between the ages of 20 and 49 years, with a mean age of 39 years. There is no known sex or ethnic predilection.

Clinical Findings

Ameloblastomas are slow-growing neoplasms. Seventy-five percent of patients have swelling as the main complaint, whereas 25% present with pain. Other manifestations include mobile teeth, ill-fitting dentures, ulcerations, draining sinuses, and nasal obstruction. Patients may complain of gradual facial deformity that may be painful. Perineural infiltration of the inferior alveolar nerve may present with pain and paresthesia over the lower lip. A history of prior tooth extraction or root canal treatment may also be encountered. Associated soft tissue masses are unusual and are more commonly seen in recurrent tumors. Metastases are uncommon but have been reported in recurrent lesions. The location of metastases includes the lungs, liver, and bones.

Pathology

Eighty percent of ameloblastomas originate in the mandible, of which 70% are located in the posterior aspect of the ramus. Ameloblastomas may arise from epithelial lining of dentigerous cysts, remnants of dental lamina or enamel organ, and the basal layer of the oral mucosa. The majority of ameloblastomas are benign with < 1% showing aggressive beha-

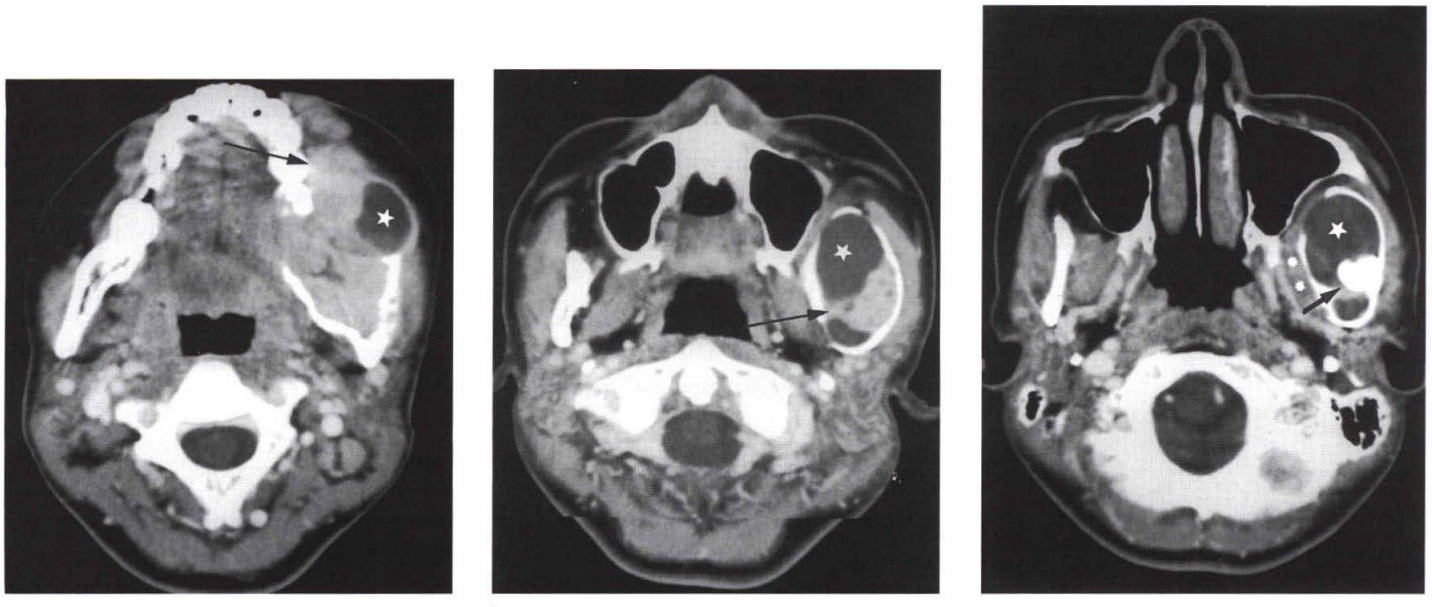

A B C

Figure 18–1. Ameloblastoma involving the left mandible. (A) Axial contrast-enhanced CT shows a grossly expanded mandible with destruction of the anterior cortex. Note the enhancing extraosseous solid (arrow) and cystic components (star). (B) Axial contrast-enhanced CT shows intraosseous lesion with cystic (star) and enhancing solid tissue (arrow). (C) Axial contrast-enhanced CT [superior to (A)] shows a tooth element (arrow) and a cystic component (star). There is encroachment of the left masticator space with compression of the medial pterygoid muscle (asterisks).

vior such as rapid growth, bone destruction, and distant metastases. Ameloblastomas infiltrate between bone trabeculae, but involvement of cortical bone is limited only to superficial erosion. Traditionally, these lesions are classified as solid or cystic. However, most ameloblastomas show cystic changes. They can also be divided into several gross morphological types. The tumor may be intraosseous solid, well-circumscribed unicystic, multicystic, and peripheral (extraosseous). Well-circumscribed unicystic lesions mimic dentigerous cysts in appearance and show less aggressive behavior compared with the other gross morphological types. Diagnosis can be made by aspiration biopsy.

Treatment

The preferred treatment is surgical resection, usually by a partial mandibulectomy or maxillectomy. Radiation therapy is usually not required following surgery. Curettage or enucleation (which may be sufficient for small unilocular lesions) is not recommended because it is associated with a high recurrence rate of up to 59%.

Imaging Findings

CT

This is a cystic expansile mass arising within the mandible surrounded by smoothly thinned bone. Advanced lesions may result in complete cortical loss of the involved mandible or maxilla. The neoplasm may appear unilocular or multilocular. The unilocular variety is usually associated with well-defined bony margins, and tooth displacement can also be frequently seen. The multilocular variety has a soap bubble–like appearance. Both cystic and solid components can be identified on CT. The cysts show nonenhancing low attenuation values, whereas solid components show moderate enhancement (Fig. 18–1).

MR

The MR imaging features depend on the relative size of the cystic and solid tumor components of the neoplasms. On T1-weighted images, the lesion shows intermediate signal intensity, but cysts with high protein content may demonstrate high signals. The cystic and solid areas show typical high signal intensities on T2-weighted images. The solid regions enhance following contrast administration.

Imaging Pearls

- CT is recommended for the demonstration of the bony abnormality. The expansile appearance is characteristic of ameloblastoma. However, small unilocular cysts cannot be distinguished from dentigerous cysts.
- The presence of a surrounding soft tissue mass should raise the possibility of a recurrent lesion or another disease entity.

Suggested Readings

1. McDaniel RK. Odontogenic cysts and tumors. In: Thawley SE, Panje WR, Batsakis JG, Lindberg RD. eds. *Comprehensive Management of Head and Neck Tumors.* 2nd ed. Philadelphia: WB Saunders; 1999:1566–1610.
2. Stewart JCB, Betts JB, Barber HD, Ellis E, Fonseca RJ. In: Thawley SE, Panje WR, Batsakis JG, Lindberg RD, eds. *Comprehensive Management of Head and Neck Tumors.* 2nd ed. Philadelphia: WB Saunders; 1999:1611–1636.
3. Delbalso AM. An approach to the diagnostic imaging of jaw lesions, dental implants, and the temporomandibular joint. *Radiol Clin North Am* 1998;36:855–890.

Chapter 19

Mandibular Osteoradionecrosis

Epidemiology

Radiation therapy is used extensively for the treatment of head and neck malignancies. The mandible is often included within the treatment portal, especially in the treatment of tongue or floor of mouth tumors. Although the mandible can withstand high doses of irradiation, osteoradionecrosis may be seen in up to 6% of patients following external beam irradiation. The frequency increases to 21% when radium implants are given in addition to external beam irradiation.

Clinical Findings

Patients with osteoradionecrosis usually present with associated mucosal ulceration, bone exposure, and pain. Osteoradionecrosis in the absence of bone exposure is uncommon. Soft tissue swelling and superimposed infection may be present. Most patients present with signs or symptoms 3 to 12 months following irradiation, but some patients present many years later.

Pathology

Histology shows damaged cellular elements of bone and vascular changes. Microorganisms may be seen on the surface of the affected bone in contrast to osteomyelitis where the pathogenic organisms are found deep within bone. The most common sites of mandibular osteoradionecrosis are the mylohyoid line and the anterior arch of the mandible.

Treatment

Small lesions may heal spontaneously. Most lesions (85–90%) can be managed conservatively. Hyperbaric oxygen therapy may be of value in more severe cases. In patients with advanced or extensive lesions, mandibulectomy is indicated. The frequency of osteoradionecrosis can be reduced by selective dental extractions prior to the commencement of irradiation.

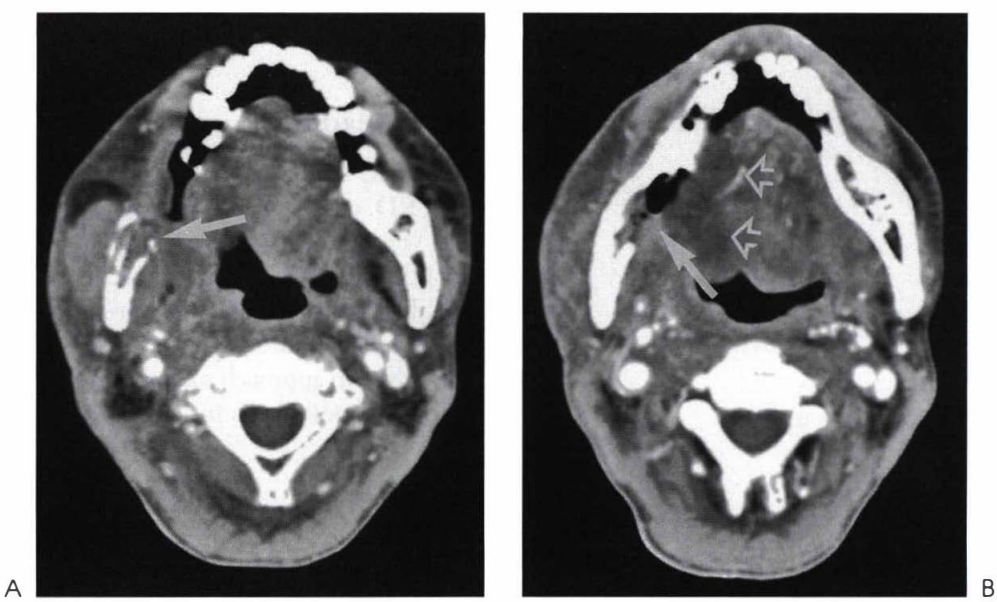

Figure 19-1. Mandibular osteonecrosis following treatment for nasopharyngeal carcinoma. (A) Contrast-enhanced CT shows fragmentation of the right mandibular ramus (arrow) with associated soft tissue swelling. Biopsy showed osteonecrosis associated with superimposed infection. (B) Contrast-enhanced CT shows a large bony defect in the mandible (solid arrow) with minimally associated soft tissue swelling. Note the atrophic right hemitongue (open arrows) and associated fatty infiltration due to hypoglossal nerve involvement in the skull base.

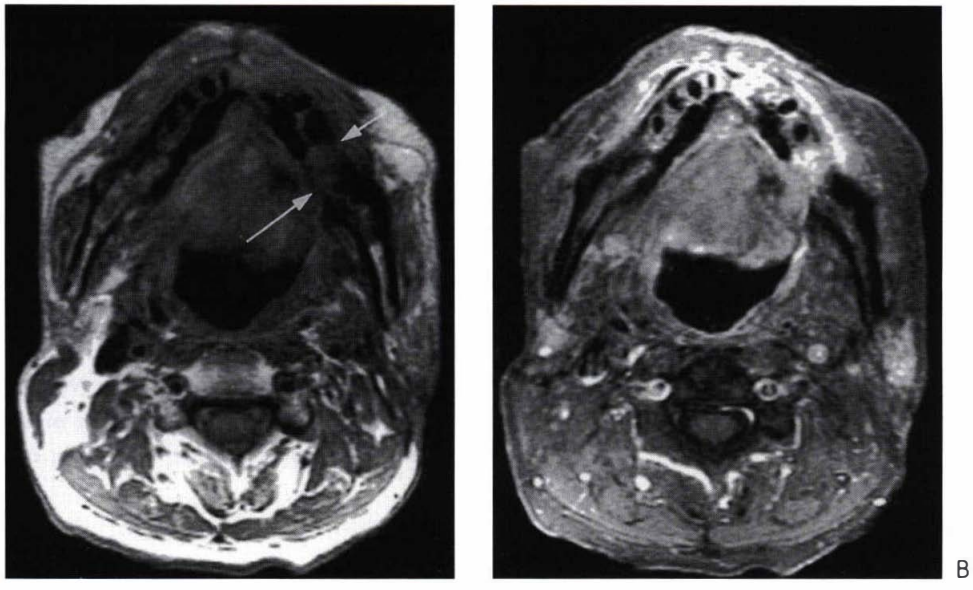

Figure 19–2. Mandibular osteonecrosis following treatment for floor of mouth carcinoma. (A) Axial T1-weighted MR image shows discontinuity in the left mandibular body (arrows) and replacement of high signal marrow. There is relatively mild soft tissue swelling. (B) Axial fat-suppressed, contrast-enhanced T1-weighted image shows contrast enhancement in the bone and mild soft tissue changes.

Imaging Findings

CT

On CT, there is osteolysis in association with an increase in density of the marrow space. There is often mild soft tissue swelling in the adjacent soft tissues. Sometimes gas translucencies may be seen but they do not invariably indicate infection by gas-forming organisms. In the chronic stage, bone fragmentation and sclerosis become evident (Fig. 19–1).

MR

The MR findings parallel that of CT. There is replacement of the high signal intensity marrow. On T2-weighted images, granulation tissues show high signal intensities, but mature scar will exhibit low signals. Immature granulation tissues show good contrast enhancement (Fig. 19–2).

Imaging Pearls

- The presence of bone erosions may indicate tumor recurrence with bone involvement. Osteoradionecrosis is usually not associated with a soft tissue mass. Because most cases of osteoradionecrosis are associated with bone exposure, clinical input is important in differentiating these diagnostic possibilities.
- Osteolysis may also indicate the presence of osteomyelitis. Again, clinical information is crucial in making the correct diagnosis. Osteoradionecrosis is usually not accompanied by gross or overt inflammatory changes in the adjacent soft tissues, but superimposed infection may complicate the diagnostic picture.

Suggested Readings

1. Parsons T. The effect of radiation on normal tissues of the head and neck. In: Million RR, Cassisi NJ, eds. *Management of Head and Neck Cancer.* Philadelphia: Lippincott; 1994:245–289.
2. Parsons JT, Bova FJ, Million RR. A reevaluation of split-course technique for squamous cell carcinoma of the head and neck. *Int J Radiat Oncol Biol Phys* 1980;6:1645–1652.
3. Chong J, Hinckley K, Ginsberg LE. Masticator space abnormalities associated with mandibular osteonecrosis: MR and CT findings in five patients. *AJNR Am J Neuroradiol* 2000;21:175–178.

Chapter 20

Masticator Muscle Fibrosis

Epidemiology

Radiation therapy for head and neck cancers may induce fibrosis in the muscles of mastication (masseter, temporalis, medial and lateral pterygoid muscles), resulting in trismus. This complication, which may be seen in 5 to 15% of patients, is most commonly encountered following treatment for malignancies involving the nasopharynx, tonsil, retromolar trigone, and paranasal sinuses. The frequency of masticator muscle fibrosis and trismus is higher if there is also a history of surgical treatment or malignant infiltration of the masticator muscles.

Clinical Findings

Patients with radiation-induced masticator muscle fibrosis typically present with increasing trismus a few years following treatment. Some patients may initially have trismus as a result of tumor involvement of the masticator muscles. Following successful tumor treatment, trismus subsides but may return later because of masticator muscle fibrosis. Clinical evaluation shows varying degrees of atrophy of masseter and temporalis muscles with associated limited excursion of the temporomandibular joint.

Pathology

Ionizing radiation damages deoxyribonucleic acid, and the injured cells perish only after failed attempts at mitosis. The rate at which injury develops is related to the tissue proliferative activity. Muscles, with slow cellular turnover, typically show delayed changes as a result of late somatic and vascular damage. Fibrous tissues eventually replace the damaged muscle fibers, causing dysfunction and muscle atrophy.

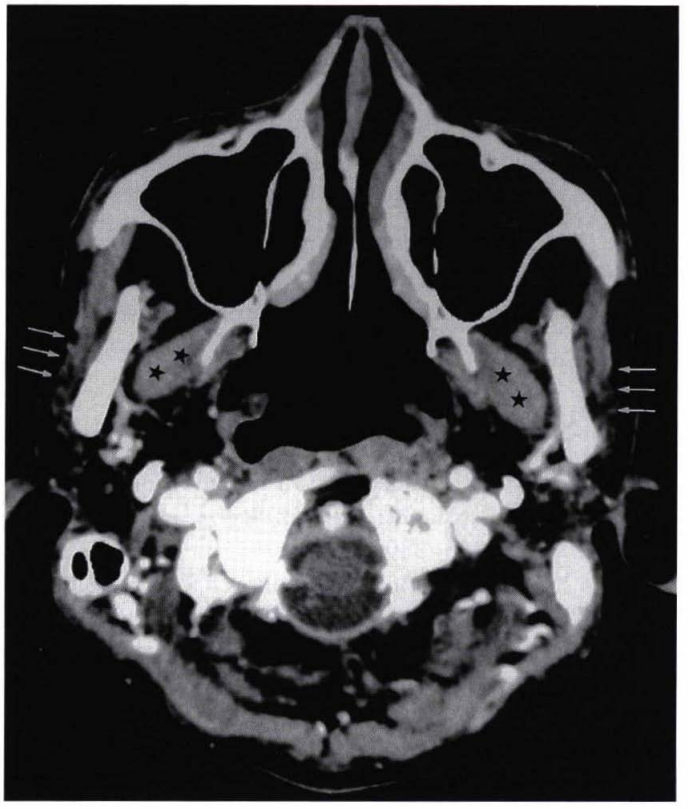

Figure 20–1. Masticator muscle fibrosis resulting in trismus as a result of radiation therapy. Axial contrast-enhanced CT shows a decrease in the bulk of the medial pterygoid muscles (stars) and the masseter muscles (arrows). Note the increase in size of the adjacent planes.

Treatment

The best treatment is to reduce the severity of fibrosis by limiting the radiation dosage to the muscles of mastication. This can be achieved by using high-energy x-rays (> 18 MeV) and by appropriately planned portals. Patients who have combined surgical and radiation treatment should have regular posttreatment jaw exercises. In severe cases, dental extraction may be necessary to facilitate the introduction of food into the mouth.

Imaging Findings

CT

Contrast-enhanced CT shows a decrease in mastication muscle bulk. The muscles may have a streaky and strandlike appearance. There may be an increase in the thickness of fat planes surrounding the muscles of mastication. There are, frequently, associated signs of atrophy in the salivary glands and the pharynx (Fig. 20–1).

MR

Signal changes in denervation atrophy of the muscles of mastication are well documented. However, there is a paucity of literature on radiation-induced fibrosis in the muscles of mastication. MR findings parallel those of CT showing a decrease in muscle bulk. The signal changes on T1- and T2-weighted images are usually similar to those of normal muscle.

Imaging Pearls

- Patients may have trismus as a result of denervation atrophy as a result of perineural infiltration. It is therefore important to trace the entire course of the mandibular nerve for evidence of neoplastic involvement.
- Radiation-induced masticator muscle fibrosis is frequently a bilateral affliction, whereas denervation atrophy is usually a unilateral lesion.
- The degree of trismus is often disproportional to the decrease in muscle bulk seen on imaging.

Suggested Readings

1. Perez CA. Nasopharynx. In: Perez CA, ed. *Principles and Practice of Radiation Oncology*. 2nd ed. Philadelphia: Lippincott; 1992:617–643.
2. Parsons T. The effect of radiation on normal tissues of the head and neck. In: Million RR, Cassisi NJ, eds. *Management of Head and Neck Cancer*. Philadelphia: Lippincott; 1994:245–289.

Chapter 21

Nodular Fascitis and Other Benign Fibroblastic Lesions

Epidemiology

Nodular fascitis is a benign soft tissue mass that results from fibroblastic proliferation. This entity is also referred to as subcutaneous pseudosarcomatous fibromatosis, infiltrative fascitis, and proliferative fascitis. Nodular fascitis represents a separate entity among a spectrum of lesions of fibroblastic origin. The benign entities include congenital generalized fibromatosis, fibrous hamartoma of infancy, palmar and plantar fibromatosis, and musculoaponeurotic fibromatosis. The malignant disorders that fall under this spectrum include aggressive fibromatosis and poorly differentiated fibrosarcoma. The pathogenesis of nodular fascitis is not exactly known but is generally felt to be a reactive nonneoplastic response to trauma. Nodular fascitis most commonly occurs in the upper extremities and trunk. Head and neck involvement is reported in about 15% of all cases of nodular fascitis. The disease most commonly presents between the ages of 30 and 40, but has been reported in all age groups.

Clinical Features

Patients often present with an enlarging palpable, firm, and mildly tender mass. The mass is usually fixed to the underlying structures and is not fixed to the skin. The specific symptoms depend on the location of the lesions. Lesions in the masticator space may present with trismus.

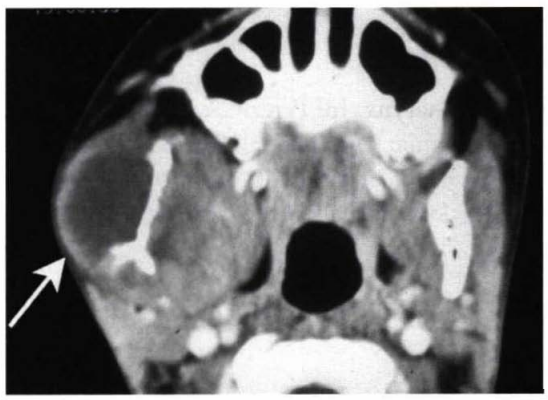

A

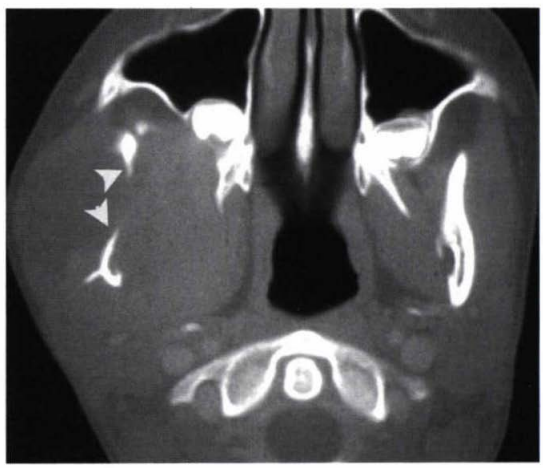

B

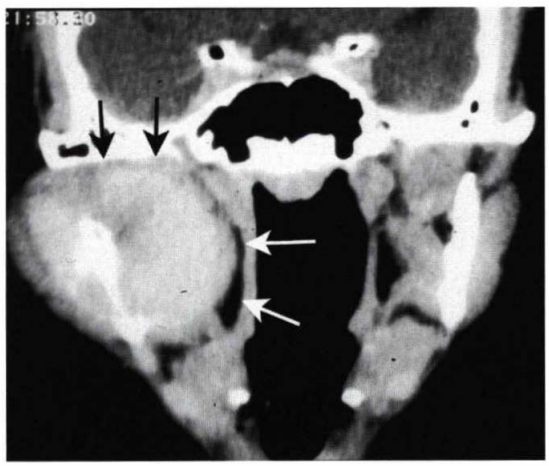

C

Figure 21–1. Nodular fascitis. (A) Axial contrast CT demonstrates an enhancing mass arising from the right masticator space (arrow). (B) Axial bone algorithm shows regressive remodeling with scalloping of the mandible (arrowhead). (C) Coronal CT shows the mass extends superiorly to the skull base (black arrows). Note the medial displacement of the parapharyngeal space that confirms that the mass is situated in the masticator space (white arrows).

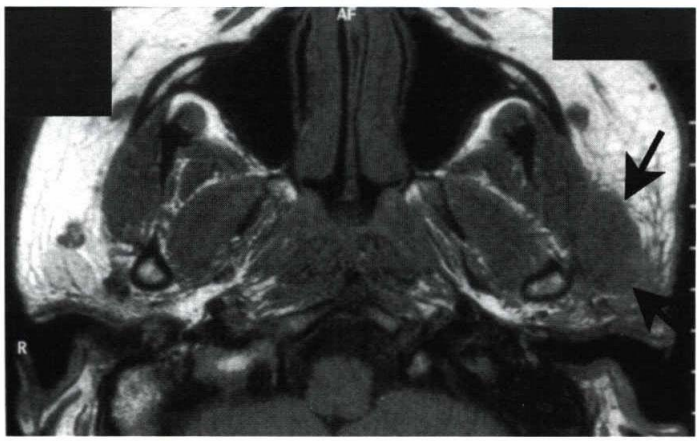

Figure 21-2. Axial T1-weighted MR shows an intermediate signal mass involving the posterolateral aspect of the left masseter muscle. Pathology revealed nodular fascitis.

Pathology

Nodular fascitis is characterized by four criteria: (1) spindle-shaped fibroblasts that tend to be arranged in long fascicles which are slightly curved, (2) small clefts or slitlike spaces that often separate the fibroblasts, (3) a few extravasated erythrocytes, and (4) mucoid interstitial ground substance.

Treatment

The preferred treatment of nodular fascitis and other benign fibroblastic lesions is complete surgical excision. The prognosis is excellent with distal metastases being very rare.

Imaging Findings

CT

The CT findings in benign fibrous lesions are of an enhancing smoothly marginated mass. They are often located in the masticator space or in the subcutaneous tissues. The adjacent bone may be disrupted but not in an aggressive manner as is typically seen in high grade malignancies (Fig. 21-1).

MR

These tumors are typically isointense to muscle on noncontrast T1-weighted images and homogeneously enhance following contrast administration. These lesions typically have demonstrated heterogenously increased signal on T2-weighted sequences (Fig. 21-2).

Imaging Pearls

- The diagnosis of benign fibrous lesions is nonspecific but may be suggested by an enhancing soft tissue mass with well-defined borders located in the subcutaneous tissue or masticator space that lacks aggressive bone destruction.

Suggested Readings

1. Koenigsberg RA, Faro S, Chen X, Marlowe F. Nodular fascitis as a vasculr neck mass. *AJNR Am J Neuroradiol* 1996;17:567-569.
2. Meyer CA, Kransdorf MJ, Jelinek JS, Moser RP. MR and CT appearance of nodular fascitis. *J Comput Assist Tomogr* 1991;15:276-279.
3. Batsakis JG. Fibrous lesions of the head and neck. In: Batsakis JG, ed. *Tumors of the Head and Neck*. Baltimore: William and Wilkins; 1979:252-279.

Chapter 22

Synovial Chondromatosis

Epidemiology

Synovial chondromatosis is a benign disorder in which foci of cartilage develop in a joint due to chondrometaplasia of the synovial membrane. The cartilaginous nodules may remain attached to the synovial membrane or dislodge into the joint space to form loose bodies. Synovial chondromatosis is more common in large diarthrodial joints (knee, hip, elbow, etc.) with involvement of the temporomandibular joint (TMJ) being less common. Involvement of the TMJ is slightly more common in females, has a predilection for the right, and typically presents between the fourth and fifth decades of life. This is in contradistinction to involvement of the larger joints, which is more common in males between the second and third decades of life. The etiology is unknown and may be due to trauma to the synovium, degenerative joint disease, or abnormal loading due to malocclusion or a displaced disc. This is a benign disease with malignant transformation being exceedingly rare.

Clinical Features

Patients present with preauricular swelling, pain, trismus, clicking, and jaw deviation with mouth opening.

Pathology

Synovial chondromatosis typically progresses through three distinct histologic phases: (1) synovial membrane metaplasia without detached nodules in the joint space, (2) coexistence of synovial chondrometaplasia with detached nodules in the joint space, and (3) loose bodies in the joint without active synovial chondrometaplasia. The cartilaginous nodules are composed of cellular clusters of chondrocytes that are arranged in lobules and show cytologic atypia. Pathologists may mistake this benign disorder for chondrosarcoma due to the chondrocyte atypia in the chondrometaplastic lesions.

Treatment

The standard treatment is resection of the loose bodies in addition to a complete synovectomy of the involved joint. The likelihood of recurrence has been reported as high as 30% due to residual metaplasia in unresected synovial tissue.

Imaging Findings

CT

There is typically irregularity and erosion of the TMJ. There is often a soft tissue mass associated with irregular and amorphous calcifications in and around the joint (Fig. 22–1).

MR

Three distinct MR patterns have been described in synovial chondromatosis: Pattern A is associated with homogeneous iso- to slightly hyperintense T1-weighted signal. This pattern is not associated with calcifications and occurs in about 15% of cases. Focal areas of signal loss that correspond to calcifications characterize pattern B (75%). Pattern C (10%) is described as heterogeneous T1-weighted intra-articular signal that enhances with contrast. This pattern is associated with calcifications (Fig. 22–2).

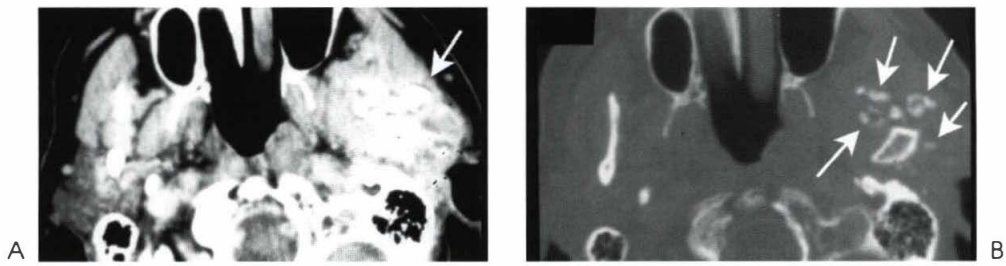

Figure 22–1. CT Findings of synovial chondromatosis. (A) Axial contrast-enhanced study shows a large mass situated in the left masticator space (arrow). (B) Bone windows demonstrate multiple calcific masses within the lesion (arrows). These benign-appearing ossified masses are characteristic of synovial chondromatosis.

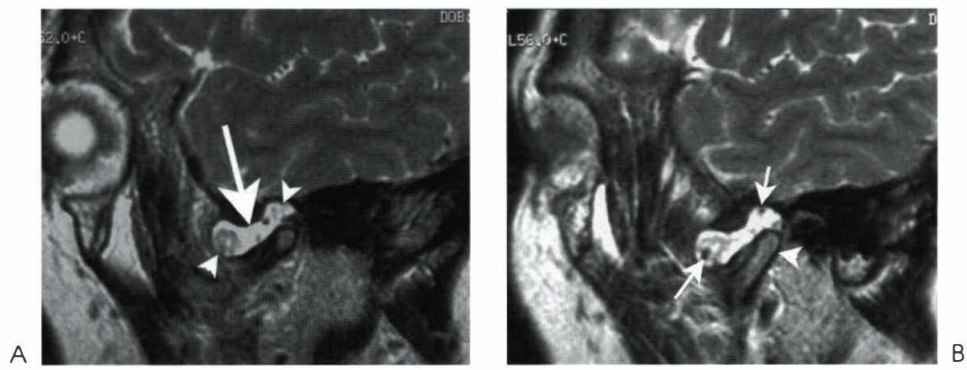

Figure 22–2. MR of synovial chondromatosis. (A) Sagittal T2-weighted image shows a large joint effusion within the temporomandibular joint (TMJ) (large arrow). There are multiple intermediate signal masses with the joint (arrowheads). (B) Some of the masses within the TMJ have low T2-weighted signal (arrows). This indicates calcified masses within the joint space and is strongly suggestive of the diagnosis of synovial chondromatosis of the TMJ. (Arrowhead connotes mandibular condyle.)

Imaging Pearls

- The imaging findings are characteristic and may help prevent the pathologist from misinterpreting this benign disorder from chondrosarcoma.

Suggested Readings

1. Tominaga K, Fujiki T, Mizuno A, Sato H, Izumi M, Uetani M. Synovial chondromatosis of the temporomandibular joint. *Dentomaxillofac Radiol* 1995;24:59–62.
2. Jiang W, Mishra S, Francis HW. Pathology forum: quiz case 4. Diagnosis: synovial chondromatosis of the TMJ. *Arch Otolaryngol Head Neck Surg* 2000;126:907–908.
3. Herzog S, Mafee M. Synovial chondromatosis of the TMJ. *AJNR Am J Neuroradiol* 1990;11:742–745.
4. Kramer J, Recht M, Deely DM, et al. MR appearance of idiopathic synovial osteochondromatosis. *J Comput Assist Tomogr* 1993;17:772–776.

Chapter 23

Lipoma

Epidemiology

The muscles of mastication make up the bulk of the masticator space. Most of the fat in the masticator space is posterior to the infratemporal wall of the maxillary sinus and the tissue planes between the muscle bundles. Lipomas may be seen occasionally in the masticator space and these lesions may involve both the suprazygomatic and nasopharyngeal portions. Lipomas appear more frequently in overweight individuals.

Clinical Findings

Small- to moderate-size lipomas in the nasopharyngeal portion of the masticator space may be asymptomatic. However, lipomas in the suprazygomatic region may be large enough to present as a painless mass. The patients often give a long history of a slowly growing mass that may show rapid increase in size during periods of weight gain. Clinically these lesions feel soft and mobile and often appear fluctuant.

Pathology

Lipomas are well-encapsulated tumors and consist of normal adult lipocytes. They may be mistaken for normal fatty tissue but there is always a fibrous capsule separating the lesion from the surrounding normal tissue. These tumors rarely undergo malignant transformation. Liposarcomas originate from lipoblasts within fascia rather than from ordinary lipocytes.

Treatment

Lipomas are benign lesions and no treatment is required if there are no symptoms or the lesion does not adversely affect the facial appearance. Lipomas are easily enucleated because they are well-encapsulated tumors.

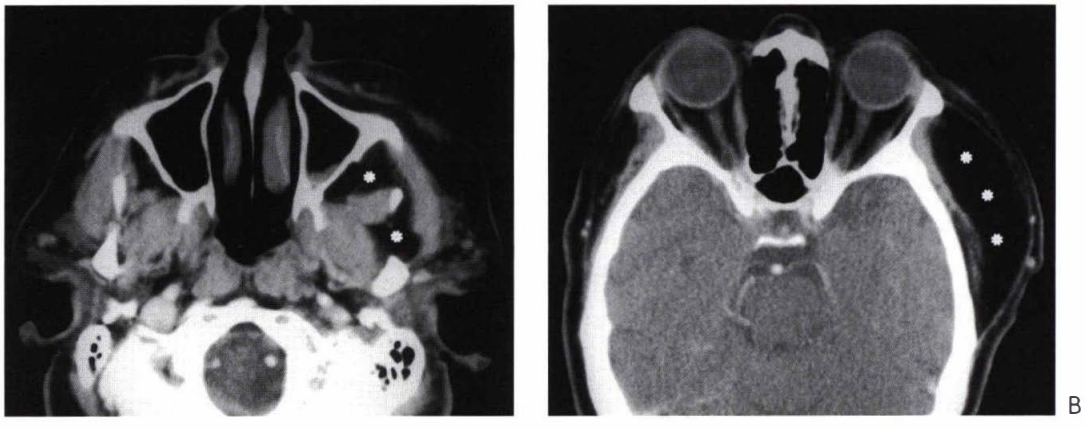

Figure 23-1. Masticator space lipoma. (A) Axial contrast-enhanced CT shows a left masticator space lipoma (asterisks). (B) Axial contrast-enhanced CT shows a large suprazygomatic extension (asterisks).

Imaging Findings

CT

Classic lipomas are homogeneously low attenuation and have Housefield that are characteristic of fat. They do not enhance following contrast administration. Occasionally lipomas will contain linear areas of intermediate attenuation. In such cases, the diagnosis of a liposarcoma cannot be excluded. Lipomas have low attenuation but the tumor margin adjacent to subcutaneous tissue may not be visible. However, when the tumor abuts the adjacent masticator muscles and bony structures the tumor outline is smooth (Fig. 23-1).

MR

The MR imaging features of a masticator space lipoma are also distinctive. The signal intensity of lipoma parallels that of normal fat. On T1-weighted images, lipomas show high signal intensity. On T2-weighted MR images, the fat shows relatively lower signals but on fast spinecho T2-weighted images, the signal intensity lipomas remain high. With fat suppression lipomas reveal a low signal intensity pattern. Lipomas do not show significant contrast enhancement.

Imaging Pearls

- Lipomas may show extensive spread into the nasopharyngeal or suprazygomatic portions of the masticator space. They may extend superiorly beneath the scalp or inferiorly to the buccal space. Sometimes the communication between the spaces may not be apparent.
- The diagnosis of a liposarcoma cannot be excluded if a presumed lipoma contains internal areas of soft tissue.

Suggested Readings

1. Harnsberger HR. *Handbook of Head and Neck Imaging.* 2nd ed. St Louis: Mosby; 1995:199-223.
2. Smoker RK. Oral cavity. In: Som PM, Curtin HD, eds. *Head and Neck Imaging.* 2nd ed. St. Louis: Mosby; 1996:488-544.

Chapter 24

Aneurysmal Bone Cyst

Epidemiology

The etiology of aneurysmal bone cysts (ABCs) is controversial. Lichtenstein suggests that ABCs result from a persistent local alteration in hemodynamics leading to increased pressure and subsequent transformation of the area into a dilated and engorged vascular bed. Some authors feel that ABCs represent an unorganized or canalized portion of a hematoma or false aneurysm. Still others suggest that ABCs are secondary lesions that result from a vascular response initiated by a separate primary bone lesion. These masses are more common in females and individuals under the age of 20. They are more likely to involve the mandible as opposed to the maxilla or zygoma. These lesions are often associated with a prior history of trauma to the site of origin.

Clinical Features

ABCs usually present with a rapidly increasing swelling in the absence of pain or paresthesias that results in facial deformity and malocclusion. There may be spontaneous bleeding around the teeth or from mucosal trauma.

Pathology

Grossly, the lesions are characterized by a spongy appearance with blood-filled spaces. Histologically, these are epithelial-lined lesions consisting of numerous cavernous blood-filled cavities located in a honeycombed meshwork of connective tissue. These lesions also contain multinucleated giant cells, areas of osteoid, inflammatory cells, and hemosiderin.

Treatment

These lesions are benign and complete local excision is curative.

Imaging Findings

Plain Films

Large multiloculated expansile radiolucent masses are most often centered in the mandible. There is often a thin rim of bone resulting from expansion of the mandibular and buccal cortex of the mandible. Fluid–fluid levels that likely indicate blood products at various stages of maturation characterize these lesions. There is typically no surrounding soft tissue mass in lesions that have not undergone prior treatment.

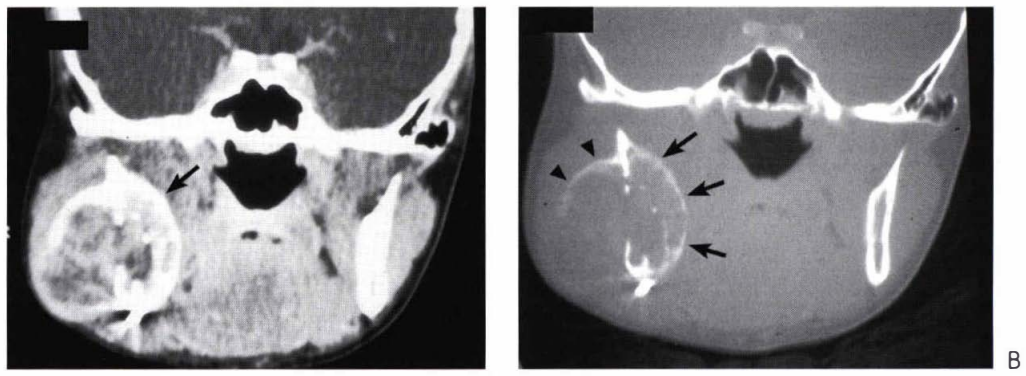

Figure 24-1. (A) Coronal contrast-enhanced CT shows an expansile mass (arrow) that appears to be centered in the mandible. (B) Bone algorithm shows expansion of the lingual (arrows) and buccal cortex (arrowhead) indicating a slowly growing indolent as opposed to an aggressive malignant process. Pathology revealed an aneurysmal bone cyst.

CT

These are typically an expansile cystic mass situated in the mandible. The inner and outer cortex of the mandible are displaced and thinned (Fig. 24–1).

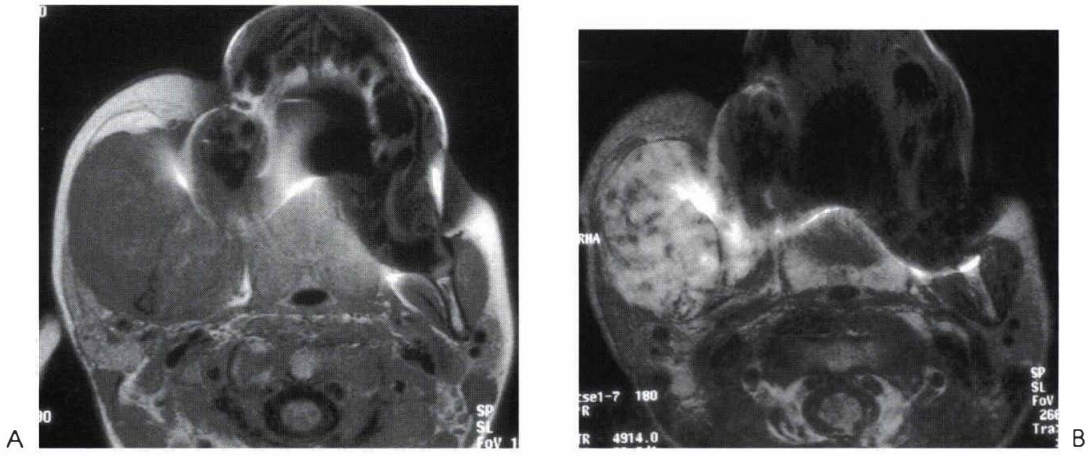

Figure 24–2. (A) Axial noncontrast T1-weighted MR shows an expansile mass located in the right masticator space. (B) There is dense enhancement of the aneurysmal bone cyst following administration of contrast.

MR

These lesions are characterized by a soft tissue mass replacing the mandible that contains numerous fluid–fluid levels. The margin of the lesion may enhance following contrast. However, untreated lesions typically lack a surrounding soft tissue mass that invades adjacent spaces (Figs. 24–2 and 24–3).

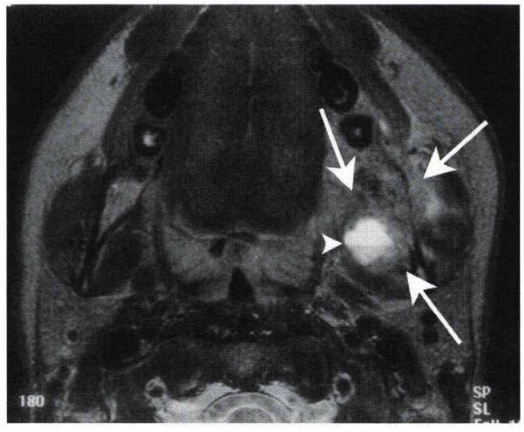

Figure 24–3. Axial T2-weighted image of an aneurysmal bone cyst in the masticator space shows a characteristic air–fluid level. This finding is suggestive but not pathognomonic of ABC. (Arrows designate ABC; arrowhead shows fluid–fluid level.)

Imaging Pearls

- The diagnosis may be suggested by the presence of an expansile cystic mass with multiple fluid–fluid levels.
- The differential diagnosis for tumors with these findings includes giant cell tumor and osteosarcoma.
- ABCs that have undergone prior treatment have an atypical appearance and may present as a solid enhancing soft tissue mass without internal fluid–fluid levels.

Suggested Readings

1. Batsakis JG. Nonodontogenic tumors of the jaw. In: Batsakis JG, ed. *Tumors of the Head and Neck.* Baltimore: Williams and Wilkins; 1979:381–419.
2. Weber AL, Scrivani SJ. Mandible: anatomy, cysts, tumors, and nontumorous lesions. In: Som PM, Curtin H, eds. *Head and Neck Imaging.* 3rd ed. New York: Mosby; 1996:319–349.
3. Lichtenstein L. Aneurysmal bone cyst: observations of fifty cases. *J Bone Joint Surg* 1957;39A:873–882.

Chapter 25

Vascular Malformations

Epidemiology

The classification of vascular lesions of the extracranial head and neck developed by Mulliken and Glowacki is based on their biological and clinical characteristics. In the past, different terms have been used by different specialties to describe the same lesions. This classification system attempts to unify the nomenclature and improve the understanding of these complex lesions. Vascular lesions are classified as malformations and hemangiomas. Malformations are further divided based on their histology and include capillary, venous, arteriovenous (arterial, fistulae), lymphatic, and mixed. Hemangiomas are further subdivided based on their growth phase, which consists of a proliferating and involuting phase.

Clinical Findings

Vascular malformations are always present at birth. Enlargement of these lesions is due to growth of the child rather than proliferation of the endothelial cells that compose the lesion. These lesions do not undergo spontaneous involution. The incidence in males is equal to that in females.

Hemangiomas typically present in neonates or in early infancy. These lesions enlarge by endothelial proliferation and begin to undergo spontaneous involution after the first year of life. Hemangiomas are more common in females (M:F ratio = 1:5).

Pathology

All vascular lesions are composed of endothelial cells. Vascular malformations consist of flat endothelial cells that have a normal rate of mitosis and cell growth. The types of malformed endothelial cells that may be seen include venule, veins, capillaries, and lymphatic vessels. The histology determines the specific type of vascular malformation. Mixed vascular malformations such as venous–lymphatic malformations may occur due to close association in the embryogenesis of the lymphatic and venous systems.

The histologic features of hemangiomas are based on the growth phase. Plump proliferating endothelial cells characterize the proliferating phase. Apoptosis and progressive flattening of endothelial cells characterize the involutional phase. There is a progressive reduction in vascular channels and an increase in the surrounding fibrofatty matrix.

Treatment

Because of their spontaneous regression, most hemangiomas are observed. More aggressive therapy is reserved for lesions that result in functional impairment. The treatment of vascular malformations is based on the specific type of malformation and is discussed in this text under the appropriate section.

Imaging Findings

The specific CT and MR imaging findings are discussed in detail in the appropriate sections of this text (Figs. 25–1 through 25–3).

Imaging Pearls

- The purpose of imaging is to (1) attempt to identify the specific type of vascular lesion, (2) determine the extent of the lesion, and (3) characterize the lesion as high flow or low flow. On MR imaging, the presence of flow voids or enhanced signal on flow-sensitive sequences within the lesion is indicative of a high-flow state. On Doppler ultrasound, high-flow lesions show arterial waveforms.

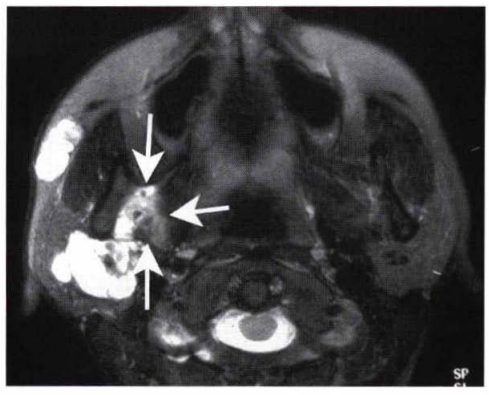

Figure 25–1. Axial T2-weighted images demonstrate a heterogeneous mass situated in the right masticator space (arrows). This was felt to most likely represent a mixed vascular malformation.

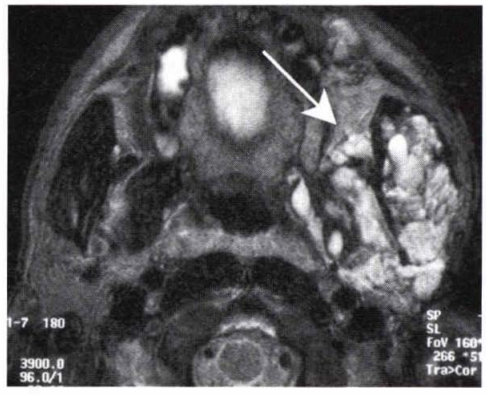

Figure 25–2. Axial T2-weighted images show a transspatial mass that extends into the masticator space (arrow). The lack of flow voids suggests a low-flow vascular malformation. Pathology revealed a lymphatic malformation.

Figure 25–3. Sonography of a lymphatic malformation demonstrates the multiple dilated cystic spaces (arrows) that constitute a lymphatic malformation. (Courtesy of Anil Ahuja, M.D.)

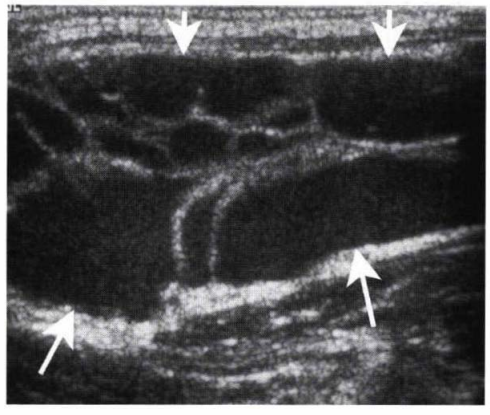

Suggested Readings

1. Mulliken JB, Glowacki J. Hemangiomas and vascular malformations in infants and children: a classification based on endothelial characteristics. *Plast Reconstr Surg* 1982;69:412–422.
2. Meyer JS, Hoffer FA, Barnes PD, Mulliken JB. Biological classification of soft-tissue vascular anomalies: MR correlation. *AJR Am J Roentgenol* 1991;157:559–564.
3. Waner M, Suen JY. A classification of congenital vascular malformations. In: Warner M, Suen JY, eds. *Hemangiomas and Vascular Malformations of the Head and Neck*. New York: Wiley-Liss; 1999:1–12.

Chapter 26

Hemangiomas

Epidemiology

Hemangiomas are proliferative endothelial vascular lesions that are identified by their characteristic clinical appearance and course. Forty percent of hemangiomas are present at birth and 60% appear within the first few months of life. Hemangiomas are more common in females than in males (5:1). Common sites of occurrence include skin, face, orbits, larynx, nasal cavity, and deep neck spaces.

The classification proposed by Mulliken and Glowacki distinctly separates hemangiomas from vascular malformations based on biological and clinical characteristics. Previous descriptive terms such as *strawberry, capillary, juvenile,* or *cellular* are not currently used to describe hemangiomas. These older names are now encompassed by the term *hemangioma.* Most authors now feel that "cavernous" hemangiomas are venous malformations. "Port-wine" hemangiomas are now considered capillary malformations.

Clinical Findings

Superficial hemangiomas are bright red papular lesions. Subcutaneous hemangiomas often present as a bluish mass that may be difficult to differentiate from a venous malformation or arteriovenous malformation.

Hemangiomas rapidly grow during the first 12 to 18 months of life (proliferative phase). This is followed by gradual regression (involuting phase) over the next 6 to 10 years. Approximately half of all lesions will completely involute, whereas the remainder will partially involute. Incomplete involution may result in residual telangiectasias, hypoplastic patches, or scarring.

Hemangiomas usually arise in the superficial layers of the skin and mucosa. The majority of hemangiomas have an uneventful course with spontaneous and complete involution. More advanced lesions, depending on their location, may cause severe facial disfigurement, impaired vision, or respiratory stridor.

In the past, hemangiomas have been associated with a variety of syndromes that include Dandy–Walker, Klippel–Trenaunay, Sturge–Weber, Beckwith–Wiedeman, von Hippel–Lindau, and Rendu–Osler–Weber. There is also an association with Kasabach–Merritt syndrome; a consumptive coagulopathy complicated by platelet trapping, hemorrhage, or high-output congestive heart failure that may occur with large hemangiomas. These associations were identified prior to the Mulliken and Glowacky classification system. Further investigations will be needed to determine whether these associations are still valid using the currently accepted classification scheme.

Pathology

The proliferative phase consists of proliferating plump endothelial cells with frequent mitoses. The end of the proliferative phase is characterized by a reduction in the mitotic activity, progressive flattening of the cells, and an abundance of mast cells. Apoptosis and progressive endothelial cells encompassed by large ectatic vascular channels in a matrix of fibrofatty tissue characterize the involuting phase.

Treatment

Because most hemangiomas undergo complete or near-complete spontaneous involution, the treatment is conservative and consists of observation and parental reassurance. More aggressive options such as steroid therapy and compression therapy are reserved for enlarging lesions that result in functional compromise. Surgery is reserved as a secondary procedure following initial therapy or incomplete involution. The role of antiangiogenesis agents is currently under investigation.

Imaging Findings

CT

These are densely enhancing soft tissue masses that may be localized or extend deeply along the fascial planes. Phleboliths are uncommon in true hemangiomas.

MR

These lesions are soft tissue masses that are intermediate signal on T1-weighted sequences and bright on T2-weighted sequences. These lesions densely enhance following contrast administration. The presence of internal flow voids suggests that these lesions are in the proliferative phase and can be characterized as high-flow lesions. The absence of flow voids suggests that the tumor is involuting and is a low-flow lesion (Figs. 26–1 and 26–2).

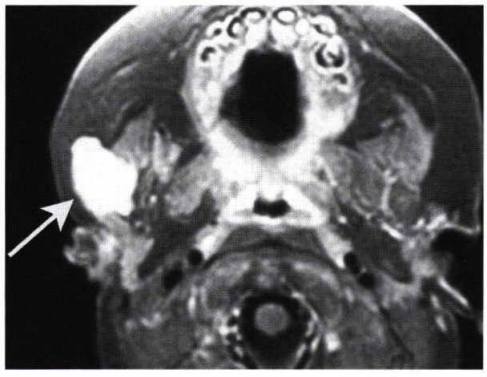

Figure 26–1. Axial contrast-enhanced T1-weighted fat suppressed image shows an enhancing hemangioma that lacks flow voids. This suggests that the hemangioma is involuting.

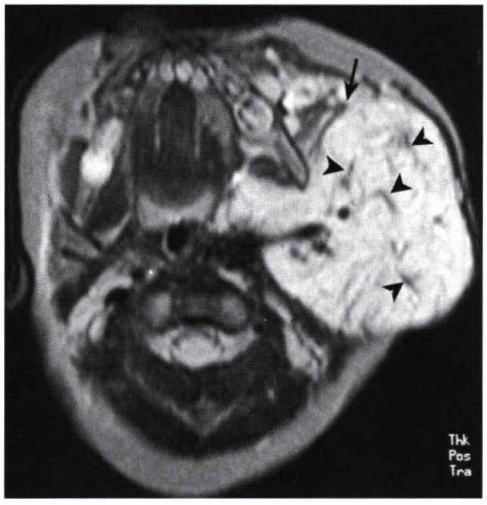

Figure 26–2. Axial T2-weighted images demonstrates a large hemangioma involving the parotid gland with extension into the adjacent masticator space (arrow). Arrowheads indicate decrease signal secondary to blood flow (flow voids).

Angiography

There is an organized pattern of arterial supply from the enlarged feeding arteries in high-flow lesions. Hemangiomas show an intense parenchymal enhancement with pooling of contrast material. Arteriovenous shunting is uncommon.

Doppler Ultrasound

This technique may be useful in attempting to differentiate between high-flow and low-flow lesions. High-flow hemangiomas in the proliferative phase will demonstrate an arterial waveform whereas involuting low-flow lesions will have a venous waveform (Fig. 26–3).

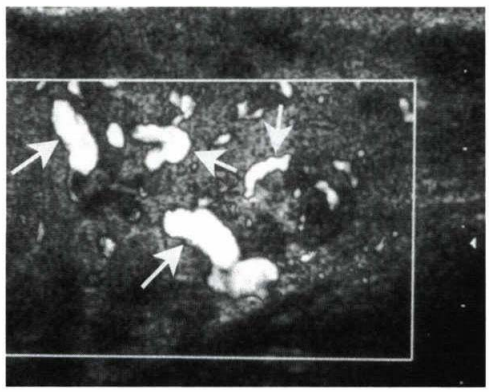

Figure 26-3. Color Doppler ultrasound demonstrates multiple serpiginous areas of signal (arrows) indicative of increased flow in a hemangioma. The increased flow is indicative of the proliferating phase of the hemangioma (see Color Plate 26-3). (Case courtesy of Anil Ahuja, Chinese University of Hong Kong.)

Imaging Pearls

- Flow-sensitive MR sequences may be helpful to confirm that a mass is a high-flow lesion.
  - The role of endovascular therapy for hemangiomas is currently under investigation. This approach may be best suited for high-flow hemangiomas in the proliferative phase.
- High-flow hemangiomas can be differentiated from high-flow arteriovenous malformations based on the findings that hemangiomas are associated with a soft tissue mass, whereas there is no parenchymal component associated with an arteriovenous malformation.
- Late-involuting (low-flow) hemangiomas may be difficult to differentiate from low-flow venous malformations.

Suggested Readings

1. Mulliken JB, Glowacki J. Hemangiomas and vascular malformations in infants and children: a classification based on endothelial characteristics. *Plast Reconstr Surg* 1982; 69:412-422.
2. Meyer JS, Hoffer FA, Barnes PD, Mulliken JB. Biological classification of soft-tissue vascular anomalies: MR correlation. *AJR Am J Roentgenol* 1991;157:559-564.
3. Waner M, Suen JY. A classification of congenital vascular malformations. In: Warner M, Suen JY, eds. *Hemangiomas and Vascular Malformations of the Head and Neck*. New York: Wiley-Liss; 1999:1-12.
4. James CA. Diagnostic imaging of congenital vascular lesions. In: Warner M, Suen JY, eds. *Hemangiomas and Vascular Malformations of the Head and Neck*. New York: Wiley-Liss; 1999:171-215.

Chapter 27

Arteriovenous Malformations

Epidemiology

Arteriovenous malformations (AVMs) are congenital lesions with multiple arterial and venous communications. This is in contrast to acquired AV fistulae (usually as a result of trauma), which show only one or two communications. These lesions, although congenital, may present at any age. Curiously, they may appear suddenly following puberty or pregnancy. These lesions are more commonly seen in females.

Clinical Findings

The skin over the lesion appears pink and warm, and the affected side is noticeably enlarged. AVMs may be painful, especially lesions with a mucosal surface, which are prone to bleed or ulcerate. Pulsations are usually evident on inspection or palpation.

Pathology

Clinical correlation is important during microscopic evaluation. AVMs have features of hemangiomas. The diagnosis of AVM is established when arteriovenous connections are detected on serial sections or the presence of intimal thickening in veins is noted.

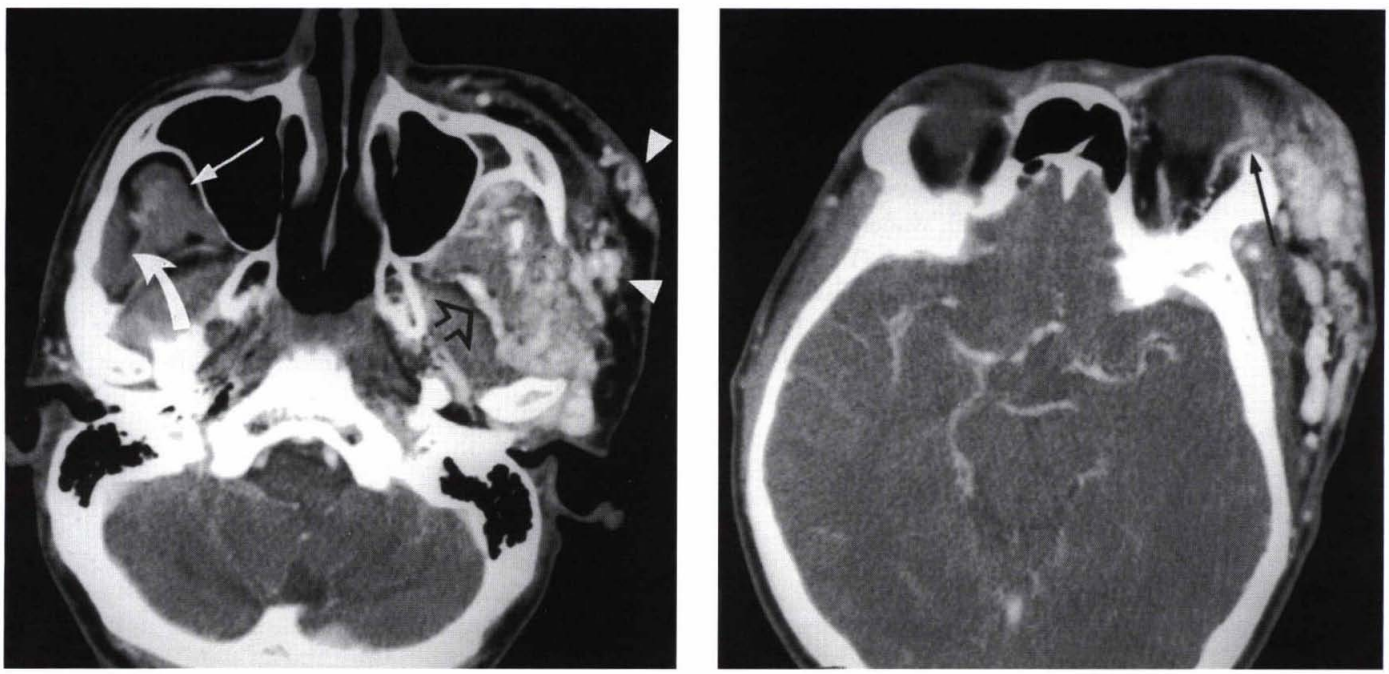

A B

Figure 27–1. Masticator space AVM. (A) Axial contrast-enhanced CT shows an AVM in the left masticator space involving the left temporalis muscle and the left masseter muscle. Note the normal right masseter muscle (curved arrow) and right temporalis muscle (straight arrow) for comparison. Note also the distended left parapharyngeal veins (open arrow) and subcutaneous draining veins (arrowheads). (B) Axial contrast-enhanced CT shows suprazygomatic involvement and slight extension into the orbit (arrow).

Treatment

Treatment of AVMs is difficult and almost never straightforward. They are usually treated with a combination of embolization followed by surgery. Surgical resection is often incomplete because there are no surgical planes to dissect. Furthermore, these lesions may involve several spaces in the face and neck. Ligation and embolization of proximal feeding arteries often produce only temporary results. Lasers can be used for superficial lesions, whereas steroids are ineffective.

Imaging Findings

CT

Contrast-enhanced CT multiple dilated serpentine vessels are situated in the masticator space. There is no associated soft tissue mass. Dilated veins draining into the pterygoid plexus, parapharyngeal, retromandibular, or facial veins can easily be identified (Fig. 27–1).

MR

The typical finding of multiple flow voids indicates the presence of an AVM. These lesions are not associated with an enhancing soft tissue mass. Flow-sensitive sequences will show increased signal in the dilated vessels.

Imaging Pearls

- AVMs are not difficult to diagnose clinically and radiologically. However, it is of crucial importance to identify the extent of the malformation.
- AVMs are often not isolated to a single space and may involve multiple adjacent spaces including the parapharyngeal, parotid, and buccal spaces. They may also extend into the orbit and involve the pharynx.

Suggested Readings

1. Calcattera T, Wang MB, Sercarz JA. Unusual tumors. In: Myers EN, Suen JY, eds. *Cancer of the Head and Neck*. 2nd ed. Philadelphia: WB Saunders; 1996:644–669.
2. Smoker WRK. Oral cavity. In: Som PM, Curtin H, eds. *Head and Neck Imaging*. 3rd ed. New York: Mosby; 1996:488–544.

Chapter 28

Masseter Muscle Venous Malformation

Epidemiology

It is now believed that cavernous hemangiomas represent venous malformations. They usually present at birth but may present in late childhood or early adulthood. These lesions grow slowly in proportion to body growth and they do not involute. They may also undergo spontaneous growth spurts in response to changes in hormonal environment such as puberty and pregnancy. Venous malformations are most commonly detected in the tongue, buccal space, and neck. They are usually superficially located but deep intramuscular involvement may also be seen.

Clinical Findings

Venous malformations are soft, compressible, and nontender lesions. If they are located superficially, they appear bluish. Masseter muscle venous malformations may mimic a parotid mass or enlargement of the masseter muscle. They are not associated with bruit or thrills.

Pathology

Venous malformations are characterized by cystic dilatation of venous lumen, and thrombosis may be seen in some large vessels. These vessel walls are thin and lined with matured endothelium. Large malformations may be associated with thrombocytopenia or intravascular coagulopathy. Small lesions are well circumscribed but some larger lesions may show an infiltrative pattern. Phleboliths are commonly detected in adults.

Treatment

Small lesions can be completely excised but infiltrative malformations are more difficult to excise completely. It is important to note that these lesions progress if left untreated, which makes them even more difficult to resect subsequently. Surgical excision is indicated when these lesions are associated with thrombocytopenia or coagulopathy. Steroids are ineffective and laser treatment may be useful in superficial lesions.

Imaging Findings

CT

Small intramuscular venous malformations may not be detected on CT. Phleboliths, which are hallmarks of this entity, are easily identified on CT. The muscles affected by venous malformation show good contrast enhancement. There may be associated contrast-enhanced venous channels in the adjacent subcutaneous tissues. However, multiple serpentine vessels are suggestive of an arteriovenous malformation rather than a venous malformation (Fig 28–1).

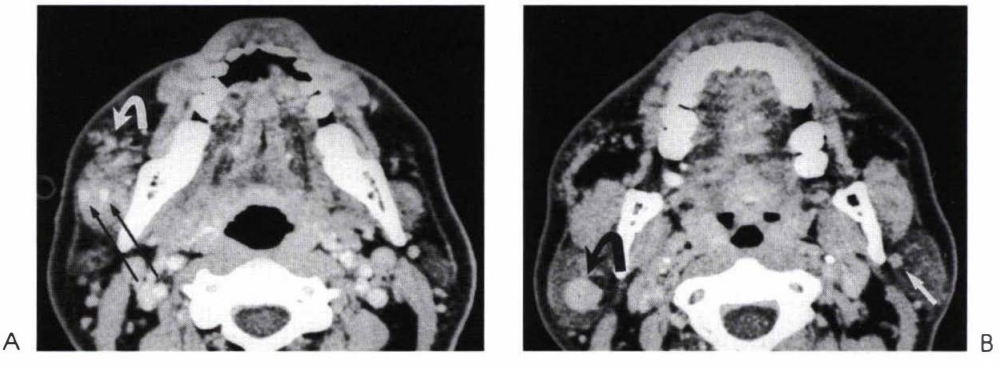

Figure 28–1. Venous malformation of masseter muscle. (A) Axial contrast-enhanced CT shows enlargement of the right masseter muscle and the presence of phleboliths (black arrows). Note the venous malformation in the subcutaneous tissue anterior to the muscle (curved arrow). (B) Axial contrast-enhanced CT shows dilatation of the right retromandibular vein (curved arrow), which drains the malformation. The left retromandibular vein is normal (straight arrow).

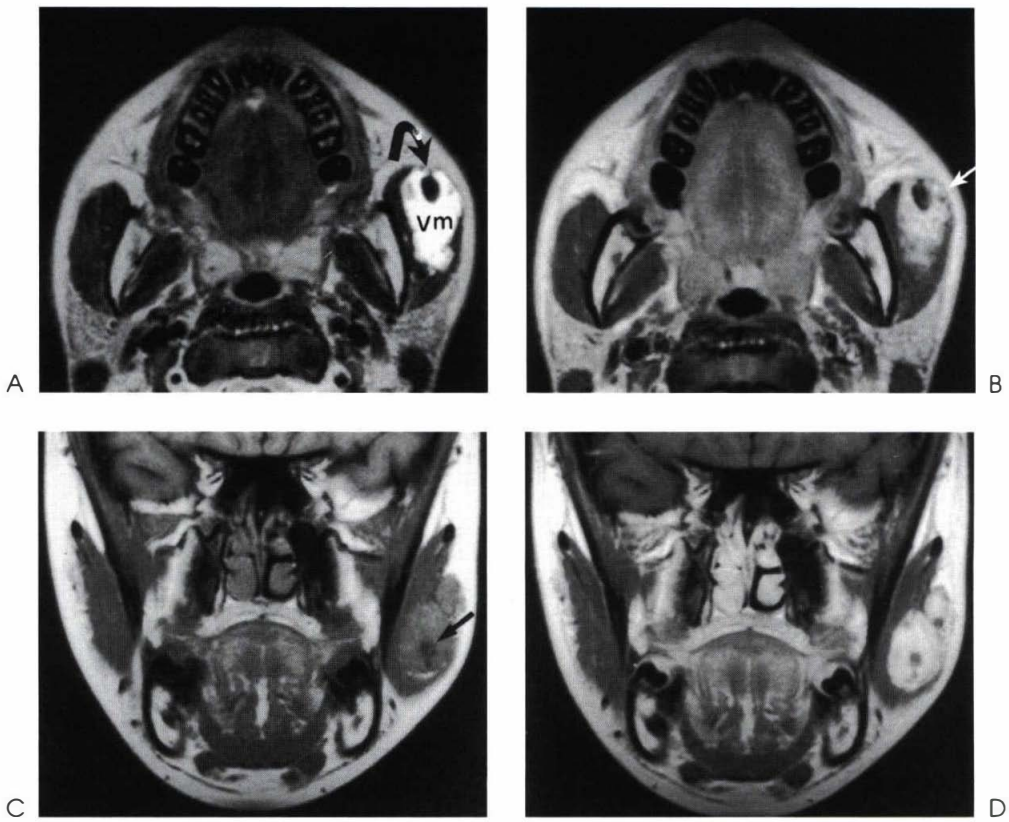

Figure 28–2. Venous malformation of masseter muscle. (A) Axial T2-weighted MR image shows a high signal intensity venous malformation (VM) in the left masseter muscle. Note the signal void phlebolith (curved arrow). (B) Axial contrast-enhanced MR image shows enhancement of the lesion in the left masseter muscle (arrow). There is a rim of slight enhancement in relation to the phlebolith that could represent the wall of a vein. (C) Coronal T1-weighted MR image shows a left masseter muscle venous malformation with an intermediate signal intensity that is higher than muscle. Note the low signal intensity phlebolith (arrow). (D) Coronal contrast-enhanced MR image shows strong enhancement of the lesion.

MR

On T1-weighted images, venous malformations are intermediate to high signal intensity compared with surrounding muscle. These lesions show high signal intensity on T2-weighted images. They show moderately intense enhancement. Focal areas of low signal may represent calcification due to phleboliths rather than flow voids. The margins of intramuscular small venous malformations are usually well defined. Larger lesions may have irregular margins and extend to adjacent spaces (Fig. 28–2).

Imaging Pearls

- MR imaging should be performed in patients who have a clinical suspicion of a venous malformation which cannot be seen on CT.
- Calcifications seen on CT are characteristic of venous malformation. These calcifications show low signals on all MR sequences and must not be mistaken for flow voids of AVMs. However, AVMs are usually clinically evident because they often have bruit or thrills. Clinical correlation is therefore important.

Suggested Readings

1. Mulliken JB, Glowacki J. Hemangiomas and vascular malformations in infants and children: a classification based on endothelial characteristics. *Plast Reconstr Surg* 1982;69:412–422.
2. Meyer JS, Hoffer FA, Barnes PD, Mulliken JB. Biological classification of soft tissue vascular anomalies: MR correlation. *AJR Am J Roentgenol* 1991;157:559–564.
3. James CA. Diagnostic imaging of congenital vascular lesions. In: Warner M, Suen JY, eds. *Hemangiomas and Vascular Malformations of the Head and Neck*. New York: Wiley-Liss; 1999:171–215.

Section II

Parotid Space

The parotid space (PS) is familiar to all of us and is a simple space to remember because it contains just the parotid gland. The parotid gland is divided into superficial and deep lobes by the plane of the facial nerve. The intraparotid facial nerve is difficult to see on routine imaging studies. However, the location of the facial nerve can be suggested because it is situated just lateral to the retromandibular vein (Figs. II-1 to II-4). Thus the retromandibular vein is a good landmark for distinguishing between the superficial and deep lobes of the parotid gland.

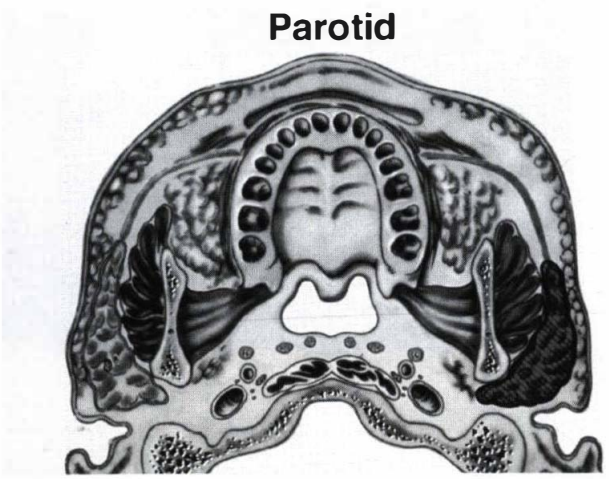

Figure II-1. Schematic illustration shows the location of the parotid gland (see Color Plate II-1). (Figure reproduced with permission from Mukherji SK, Castillo M. A simplified approach to the spaces of the suprahyoid neck. Rad. Clin N Am *1998;36:761-780.)*

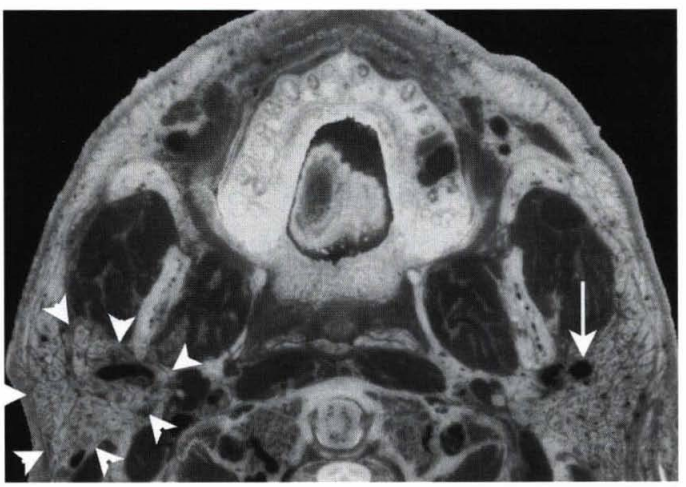

Figure II-2. Axial anatomic image shows the location of the parotid gland (arrowheads) and the retromandibular vein (arrow). The retromandibular vein separates the parotid gland into a superficial and a deep lobe.

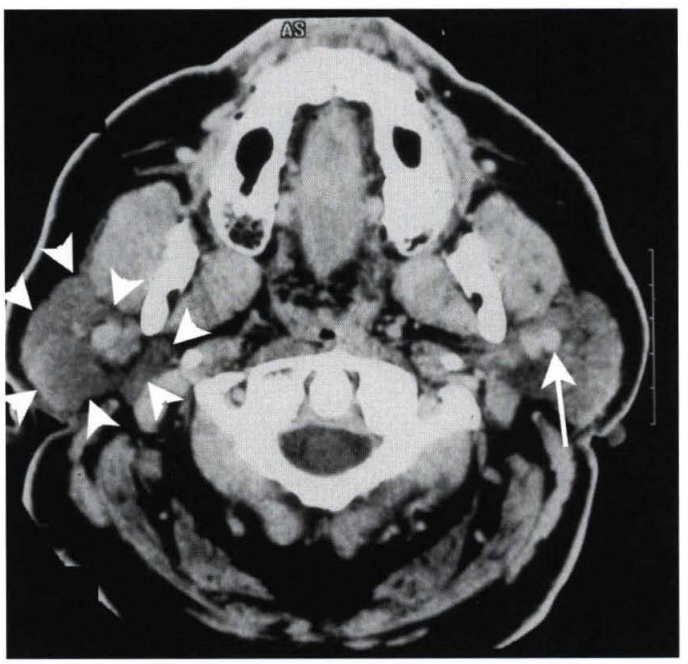

Figure II-3. Axial contrast-enhanced CT demonstrates the location of the parotid gland (arrowheads) and the retromandibular vein (arrow).

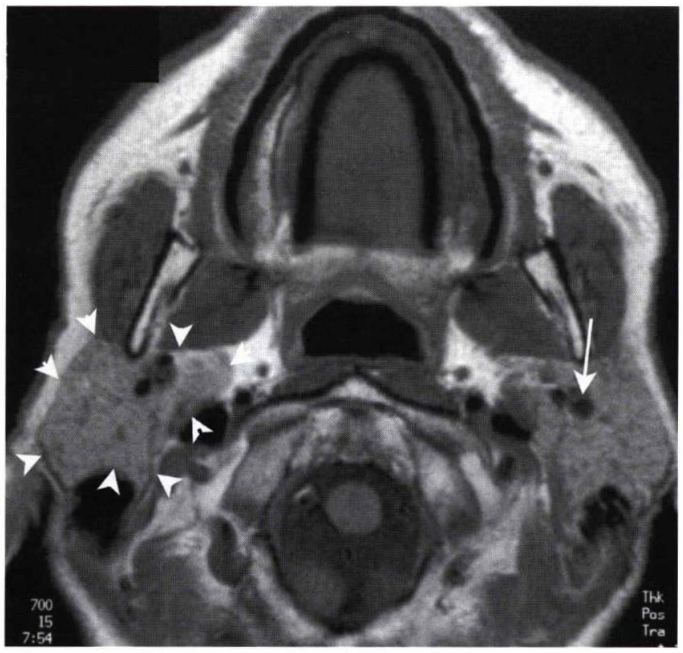

Figure 11–4. Axial noncontrast T1-weighted image shows the normal high signal within the parotid gland (arrowheads). The arrow denotes the retromandibular vein.

The PS consists of the gland parenchyma, facial nerve, retromandibular vein, external carotid artery, and intraparotid lymph nodes. The intraparotid lymph nodes are typically located in four locations: pretragal, below the capsule of the parotid gland, along the facial nerve, and in the tail of the parotid. The following chapters illustrate common pathologies of the parotid space.

Suggested Readings

1. Mukherji SK, Castillo M. A simplified approach to the spaces of the extracranial head and neck. *Radiol Clin North Am* 1998;36:761–780.
2. Harnsberger HR. *Handbook of Head and Neck Imaging*. 2nd ed. St. Louis: Mosby-Year Book; 1995.
3. Grodinsky M, Holyoke EA. The fasciae and fascial spaces of the head, neck and adjacent regions. *Am J Anat* 1938;63:367–408.

Chapter 29

Parotid Sialolithiasis

Epidemiology

Parotid sialoliths usually occur between 30 and 50 years of age and are slightly more common in men. Salivary gland calculi in children are rare, and when present, usually involves the submandibular gland. Between 10 and 20% of salivary gland stones occur within the parotid gland. Two thirds of parotid stones are single, whereas one third are multiple. Bilateral stones are unusual unless associated with an autoimmune sialadenitis. Multiple punctate calculi are indicative of sialadenitis.

Clinical Findings

Patients often present with recurrent episodes of pain and swelling of the parotid region, usually associated with eating. The symptoms usually last between 2 and 3 hours and gradually subside. Larger stones may completely obstruct the gland resulting in secondary infection and chronic atrophy if left untreated.

Symptomatic stones are usually found in Stensen's duct. A patient may have multiple intraparotid stones but only become symptomatic when a stone migrates and obstructs Stensen's duct. Strictures may result from calculi with or without an underlying infection.

Pathology

Parotid sialoliths consist of calcium phosphate in the form of hydroxyapatite with small amounts of magnesium, carbonate, and ammonium. The matrix consists of carbohydrates and amino acids.

Treatment

Small stones located at the opening of Stensen's duct may be treated by local excision or removal through an endoluminal approach. Parotidectomy may be required for patients with severe painful swelling or recurrent infections.

Imaging Findings

Plain Films

Plain films are still the initial study of choice for evaluating patients with parotid sialolithiasis. Sixty percent of submandibular stones are radiopaque on plain films.

Conventional Sialography

Sialography is still commonly performed for detection of intraductal stones. These are identified by intraluminal filling defects following installation of contrast into the cannulated duct.

CT

CT has a 10-fold increase over plain films in the ability to detect stones and is able to detect most stones that cannot be seen with plain films. A recently obstructed gland is enlarged and has intense contrast enhancement. A chronically obstructed gland is atrophic with only mild contrast enhancement (Figs. 29-1 to 29-3).

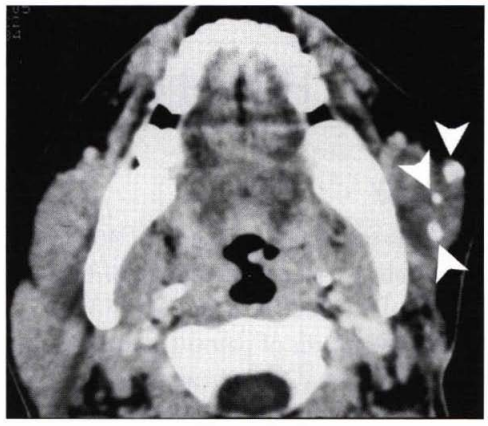

Figure 29–1. Contrast-enhanced CT demonstrates multiple large calculi located in the left parotid gland (arrowheads).

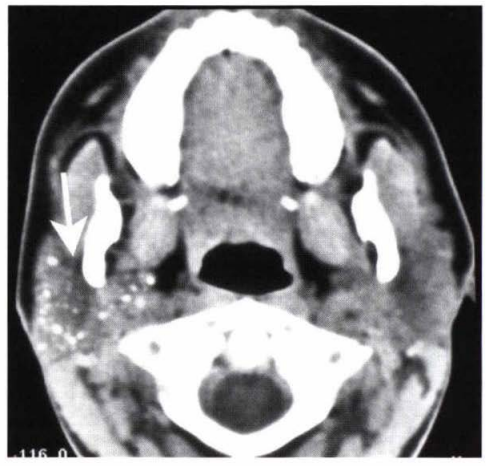

Figure 29–2. Noncontrast-enhanced CT shows multiple parotid calculi in the left parotid gland in a patient with chronic sialadenitis (arrow).

Figure 29–3. Noncontrast CT shows multiple parotid calculi situated within both parotid glands (arrows) in this patient with Sjögren's disease.

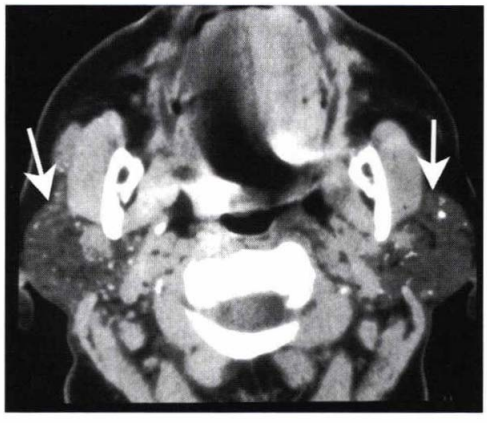

Imaging Pearls

- Either sialography or CT can be used to detect nonradiopaque stones.
- Noncontrast CT is required for detection of intraparotid stones.
- MR sialography is an excellent technique for identifying extraglandular and intraglandular ductal dilation. However, this technique may miss small intraductal calculi.

Suggested Readings

1. Batsakis JG. Nonneoplastic diseases of the salivary glands. In: Batsakis JG, ed. *Tumors of the Head and Neck.* 2nd ed. Baltimore: Williams and Wilkins; 1979:100–120.
2. Som PM, Brandwen M. Salivary glands. In: Som PM, Curtin H, eds. *Head and Neck Imaging.* 3rd ed. New York: Mosby; 1996:823–914.
3. Rabinov K, Weber AL. *Radiology of the salivary glands.* Boston: GK Hall; 1985:1–221.
4. Varghese JC, Thornton F, Lucey BC, Walsh M, Farrel MA, Lee MJ. A prospective comparative study of MR sialography and conventional sialography of salivary duct disease. *AJR Am J Roentgenol* 1999;173:1497–1503.

Chapter 30

Acute Infective Parotitis

Epidemiology

As a group, viral and bacterial infection forms the most common group of salivary gland disease. Mumps is caused by a ribonucleic acid paramyxovirus, and it predominantly affects the parotid glands. Unilateral parotid involvement may be seen in 20 to 30% of patients. Other viruses that may infect the parotid glands include influenza, parainfluenza, herpesvirus, and echovirus. Acute bacterial infection is usually due to ascending infection from the oral cavity. Most patients with ascending bacterial infection have predisposing factors such as dehydration, trauma, stones, and previous irradiation.

Clinical Findings

Mumps produces painful swelling of the parotid glands. The viral infection may be confined to the salivary tissues but may also cause epididymo-orchitis, meningoencephalitis, pancreatitis, and thyroiditis. Acute bacterial infection also produces a diffuse painful swelling, and pus may be seen in the opening of the parotid duct. Bacterial parotitis is usually a disease seen in debilitated patients. It is a known complication of dehydration following major surgery. Uncontrolled bacterial infection leads to abscess formation.

Pathology

The salivary glands have a combined daily output of 1.0 to 1.5 L. A normal flow of saliva is important in the maintenance of good oral hygiene. A decrease or stagnation in the flow of saliva increases the risk of ascending bacterial infection. The common pathogens include *Staphylococcus aureus, Hemophilus influenzae,* and *Streptococcus viridans.*

Treatment

Mumps is usually a self-limiting disease and treatment is directed at symptomatic relief. Bacterial infections should be treated by rehydration, improvement of oral hygiene, and the use of appropriate antibiotics. Abscesses should be surgically drained.

Imaging Findings

CT

Acute viral infection does not require imaging studies. Bacterial parotitis should be evaluated with CT because stones or gas formations are better demonstrated. Contrast-enhanced CT shows enhancement and enlargement of the parotid gland. A rim of variable thickness may be seen if abscess formation takes place. Subcutaneous streaking is also a prominent feature.

MR

T1-weighted images show diffuse intermediate signal replacing the high-fat signals in the parotid glands. High signal is detected following the injection of contrast and on T2-weighted images. Abscesses typically show a central zone of relatively low signals surrounded by a rim of contrast enhancement (Fig. 30–1).

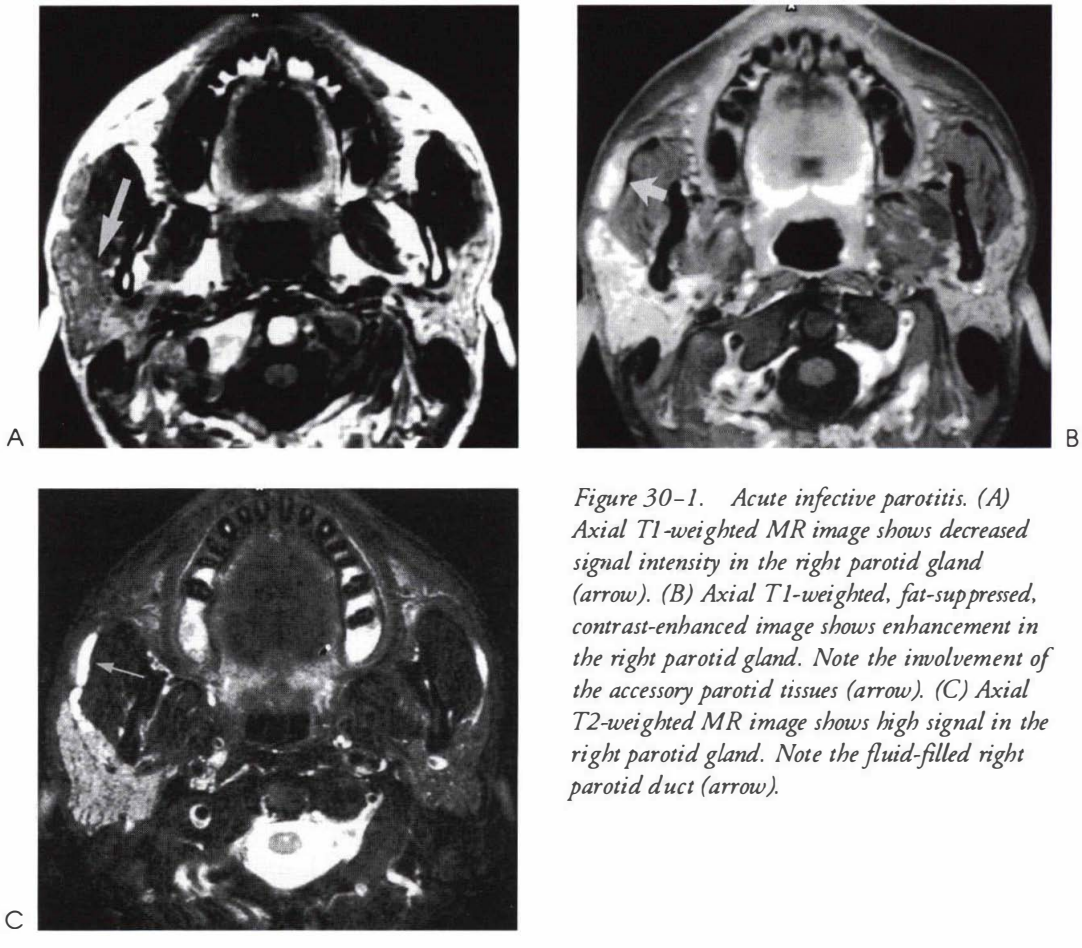

Figure 30–1. Acute infective parotitis. (A) Axial T1-weighted MR image shows decreased signal intensity in the right parotid gland (arrow). (B) Axial T1-weighted, fat-suppressed, contrast-enhanced image shows enhancement in the right parotid gland. Note the involvement of the accessory parotid tissues (arrow). (C) Axial T2-weighted MR image shows high signal in the right parotid gland. Note the fluid-filled right parotid duct (arrow).

Imaging Pearls

- If an abscess is present, it is important to demonstrate the extent of the deep parotid lobe involvement prior to surgery.
- The tail of the parotid gland may extend below the mandible. An abscess in this region can decompress inferiorly into the submandibular space.

Suggested Readings

1. Som PM, Brandwein M. Salivary glands. In: Som PM, Curtin HD, eds. *Head and Neck Imaging*. St. Louis: Mosby; 1996:823–877.
2. Harnsberger HR. *Handbook of Head and Neck Imaging*. 2nd ed. Mosby: Chicago; 1995.

Chapter 31

Pneumoparotitis

Epidemiology

Pneumoparotitis is the presence or retention of air within the parotid parenchyma or the ductal system. It is usually seen in children and in adults with occupations related to frequent and prolonged increase in intrabuccal pressures such as trumpet playing and glass blowing.

Clinical Findings

The patients usually present with recurrent painless cheek swelling. The swelling is typically nontender and soft in consistency.

Pathology

This condition may be unilateral or bilateral. The degree of parenchymal or ductal distension is variable.

Treatment

This is a benign condition and no treatment is required.

Imaging Findings

CT

The presence of air in the parotid duct is characteristic. The degree of ductal distension can appear dramatic. The parotid duct may show a sausage appearance (Fig. 31-1).

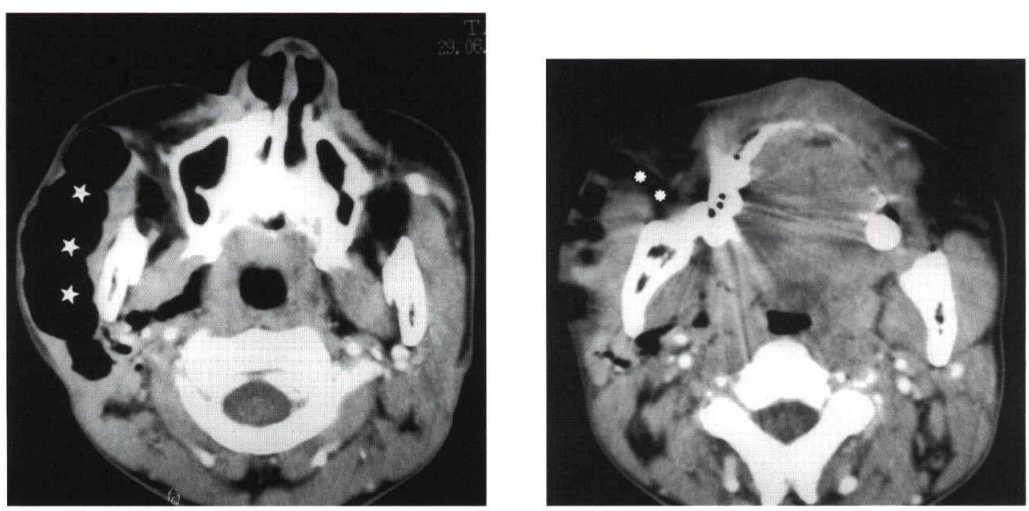

Figure 31-1. Pneumoparotitis. (A) Axial contrast-enhanced CT shows a grossly dilated right parotid duct with a slightly lobulated outline (stars). (B) Axial contrast-enhanced CT shows distended, air-filled parotid duct in the right buccal space (asterisks).

MR

The diagnosis of pneumoparotitis is straightforward. Air within the parotid on MR imaging also shows the typical signal void appearance on all imaging sequences.

Imaging Pearls

- The outline of the parotid duct may be difficult to define on CT because of the adjacent, low-attenuation subcutaneous fat or the buccal fat pad. The window level and width should be adjusted accordingly.
- On MR imaging, air stands out as signal void areas against a background of high-intensity fat in the parotid gland, buccal fat pad, and subcutaneous fat.

Suggested Reading

1. Som PM, Brandwein M. Salivary glands. In: Som PM, Curtin HD, eds. *Head and Neck Imaging.* St. Louis: Mosby; 1996:823–914.

Chapter 32

Sjögren's Syndrome

Epidemiology

Sjögren's syndrome is a systemic autoimmune disorder that affects the exocrine along with other organs. The disease is most common in women (9:1) between 40 and 60 years of age. The reported incidence is 1 in 225 individuals. The nomenclature associated with Sjögren's syndrome is often confusing; we will attempt to clarify this terminology.

Sjögren's syndrome is a specific clinical entity that consists of three major components: (1) keratoconjunctivitis sicca caused by lesions in the lacrimal glands, (2) xerostomia with or without salivary gland enlargement that results from damage to the salivary and mucous glands of the oral cavity, and (3) connective tissue disease of which the most common is rheumatoid arthritis. *Sicca complex* specifically represents a patient with xerophthalmia, xerostomia, and painless parotid gland enlargement. (Some authors also refer to the latter isolated involvement of the lacrimal and parotid glands without systemic involvement as primary Sjögren's syndrome.) Mikulicz's disease was described in 1892 as a patient with nonspecific bilateral enlargement of the lacrimal, parotid, and submandibular glands. This term may be used to describe patients who present with these clinical findings, which may be due to leukemia, lymphoma, tuberculosis, sarcoidosis, or other associated disorders.

Clinical Findings

Patients present with dry mouth, difficulty swallowing, oral pain, intraoral ulcers, loss of taste, dry eyes, and inability to cry. Parotid symptoms vary from nontender enlargement to recurrent episodes of tender glandular swelling. The diagnosis is suggested by identifying antinuclear antibodies SS-A or SS-B in the blood. A labial biopsy identifying $CD4^+$ T cell lymphocytes is positive in 60% of cases. Other collagen vascular diseases besides rheumatoid arthritis that can be associated with Sjögren's syndrome include systemic lupus erythematosus, progressive systemic sclerosis, polymyositis, polyarteritis nodosa, and mixed connective tissue disease. There is also an association with Waldenström's macroglobulinemia. Patients with Sjögren's syndrome are at substantially increased risk for developing lymphoma that may be either intra- or extraparotid.

Pathology

The initial stage of the parotid involvement is characterized by lymphocytic infiltrate that results in lymphoreticular hyperplasia. This eventually results in chronic inflammation characterized by atrophy of the acinar parenchyma and a variety of ductal changes ending in an "epimyoepithelial island."

Treatment

The treatment is usually supportive. Rarely, a parotidectomy may be performed in cases of recurrent infectious parotitis. Recent developments have focused on medications that enhance salivary production and flow. The long-term benefits of this approach are currently under investigation.

Imaging Findings

Sialography

Sjögren's syndrome is characterized by uniform multiple globular collections of contrast that are indicative of dilated ducts due to sialectasis. Enlargement of these collections suggest parenchymal destruction.

CT

The gland appears normal in the early stages of disease. In more advanced stages, there is progressive enlargement and enhancement of the gland, which contains tiny multiple cysts. This finding is not specific to Sjögren's syndrome but is consistent with a chronic sialadenitis (Fig. 32-1).

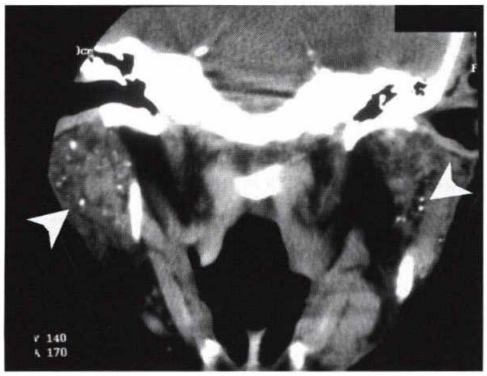

Figure 32-1. Coronal noncontrast CT shows multiple punctate intraparotid calcifications in a patient with Sjögren's disease (arrowheads).

MR

As with CT, the gland appears normal in the early stages of disease. As the disease progresses, there is bilateral enlargement of the parotid glands with heterogeneous signal. The parotid gland may develop multiple tiny intraparotid cysts that are indicative of a chronic sialadenitis (Figs. 32-2 and 32-3).

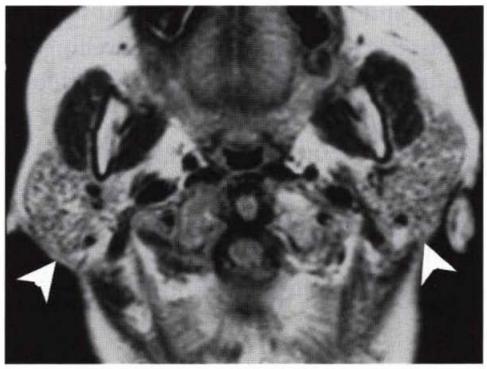

A

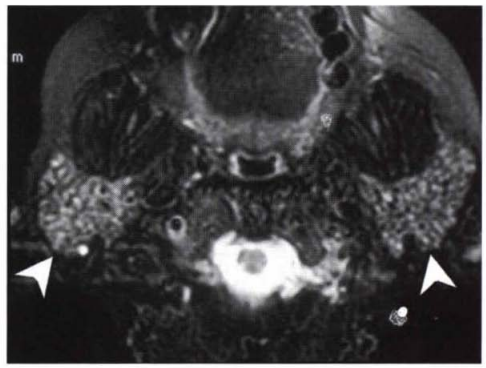

B

Figure 32-2. (A) Noncontrast T1-weighted image demonstrates a heterogeneous appearance to both parotid glands (arrowheads) due to chronic sialadenitis in a patient with Sjögren's disease. (B) Axial fat-suppressed T2-weighted image obtained in the same patient shows diffuse increased heterogeneous signal within both parotid glands (arrowheads).

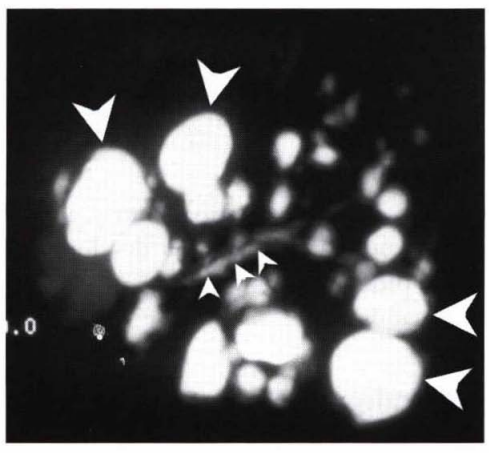

Figure 32-3. MR sialography obtained from maximum intensity projections of thin sections of fast spin echo imaging shows the "grapelike" appearance of chronic sialadenitis. A dilated main parotid duct is identified ("stem"-small arrowheads) along with massive cystic enlargement of terminal salivary ducts ("grapes"-large arrowheads).

Imaging Pearls

- The imaging findings of the parotid gland associated with Sjögren's syndrome are indicative of a chronic sialadenitis. Sjögren's disease is a clinical diagnosis that may be suggested based on imaging findings.
- MR sialography may be useful as a noninvasive technique for identifying sialectasis.

Suggested Readings

1. Batsakis JG. Nonneoplastic diseases of the salivary glands. In: Batsakis JG, ed. *Tumors of the Head and Neck.* Baltimore: Williams and Wilkins; 1979:100–120.
2. Sjögren's syndrome: comparison of assessments with MR sialography and conventional sialography. *Radiology* 1998;209:683–688.
3. Som PM, Brandwen M. Salivary glands. In: Som PM, Curtin H, eds. *Head and Neck Imaging.* 3rd ed. New York: Mosby; 1996:823–914.

Chapter 33

Radiation-Induced Parotitis

Epidemiology

Radiation therapy is frequently used for the treatment of head and neck cancers. Irradiating the parotid glands produces a spectrum of findings ranging from transient to permanent changes. Transient parotid swelling and pain may be seen in 5% of patients after the first few treatments. Acute radiation-induced parotitis is a rare clinical entity and appears during the course of radiation therapy. Almost all patients have subchronic or chronic changes after the delivery of 3500 cGy. In addition, there is a higher risk of ascending bacterial infection because of xerostomia.

Clinical Findings

Acute radiation-induced parotitis presents with gross facial swelling and pain. Xerostomia and increased risk of dental or salivary gland infection characterize chronic changes in the parotid glands.

Pathology

The pathogenesis and morphology of acute parotitis are poorly understood because biopsies are not obtained for obvious reasons. Radiation damages the glandular DNA and endothelial cells of the salivary glands. These damaged cells fail to replicate resulting in glandular fibrosis and subsequent atrophy.

Treatment

Mouth dryness is a very common side effect of radiation therapy. To combat this distressing symptom, the patients are encouraged to have frequent saline and soda mouth rinsing. Commercial preparations of artificial saliva may also produce some relief. It is important to keep the irradiated volume of salivary gland to a minimum.

Imaging Findings

CT

Acute parotitis shows gross glandular swelling with moderate enhancement following the injection of contrast. In the subchronic phase, there is glandular atrophy associated with increased enhancement. This phenomenon is related to leakage from the damaged endothelial lining. In the chronic phase, there is atrophy and fibrosis. Hence the irradiated glands have higher attenuation values compared with the fatlike attenuation values of normal glands (Fig. 33–1).

MR

In the subchronic and chronic phases, T1-weighted MR images show a decrease in signals as a result of fat replacement and fibrosis. However, contrast-enhanced images may show strong enhancement due to damages in the vessel walls. T2-weighted images show variable intensities depending on the presence or degree of edema and fibrosis.

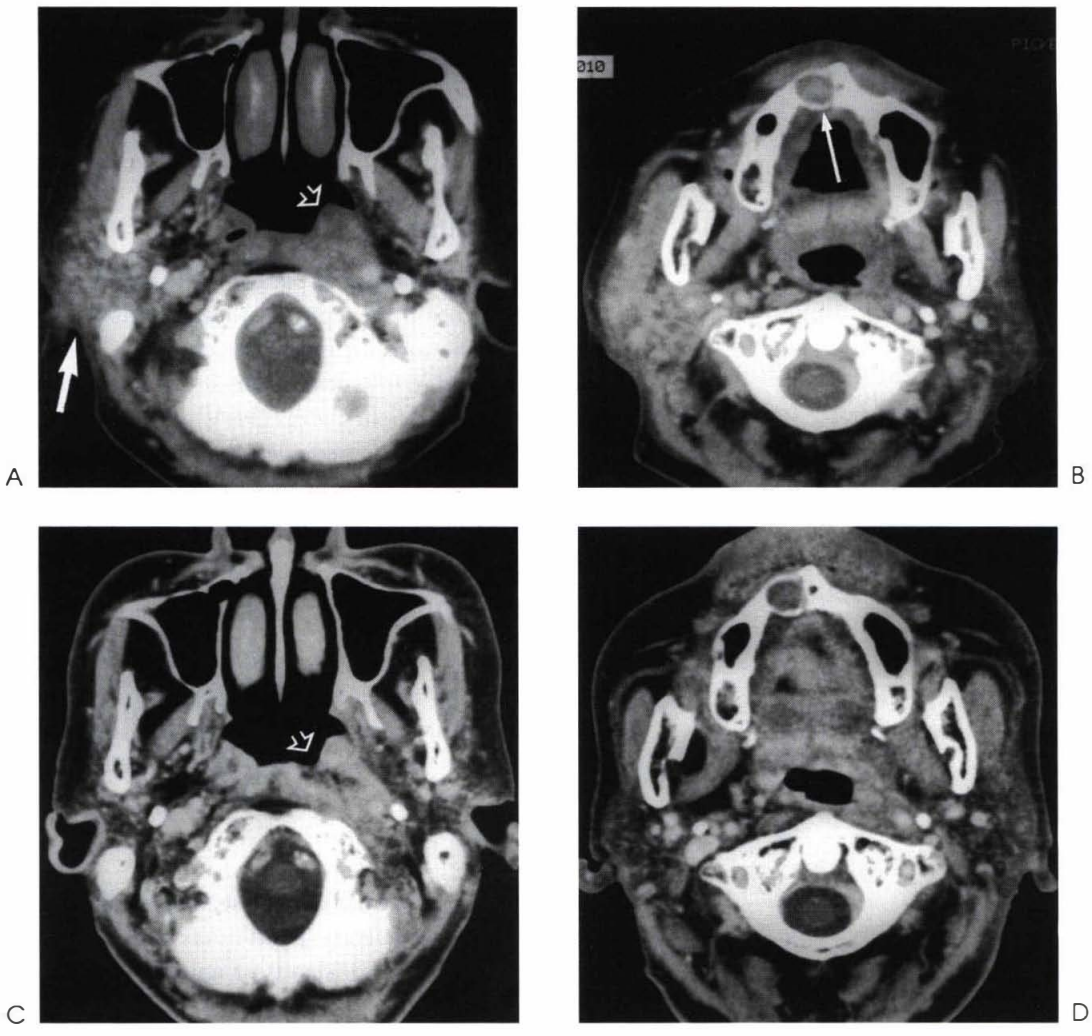

Figure 33–1. Acute radiation-induced parotitis during radiation therapy. (A) Axial contrast-enhanced CT shows enlargement of the right parotid gland with heterogeneous enhancement (solid arrow). Note a left nasopharyngeal carcinoma (hollow arrow). (B) Axial contrast-enhanced CT in the same patient shows diffuse enhancement and enlargement of the right parotid gland. Note the presence of an incidental radicular cyst in the maxilla (arrow). (C) Axial contrast-enhanced CT (6-month follow-up) at level similar to (A) shows sloughing in the left fossa of Rosenmüller (arrow) and resolution of right parotid swelling. (D) Axial contrast-enhanced CT (6-month follow-up) at level similar to (B) shows disappearance of right parotid swelling. Both parotid glands show mild radiation-induced atrophy.

Imaging Pearls

- Acute radiation-induced parotitis should be differentiated from acute bacterial parotitis. The former occurs during treatment and has a self-limiting course. The latter takes place after the completion of irradiation and is related to the increased risk of infection because of a decreased flow of saliva.
- The intense enhancement seen on CT or MR imaging should not be mistaken for infection. Radiation-induced changes are usually bilateral, whereas infection is usually unilateral.

Suggested Readings

1. Rabin BM, Meyer JR, Berlin JW, Marymount MH, Palka PS, Russell EJ. Radiation-induced changes in the central nervous system and head and neck. *RadioGraphics* 1996;16:1055–1072.
2. Parsons TT. Effects of irradiation on normal head and neck tissues. In: Million RR, Cassisi NJ, eds. *Management of Head and Neck Cancer*. Philadelphia: Lippincott; 1994:245–290.

Chapter 34

Lymphoepithelial Cysts

Epidemiology

Head and neck findings in patients with acquired immune deficiency syndrome (AIDS) are common. It has been reported that over 40% of patients with AIDS will have head and neck manifestations on initial presentation. Lymphoepithelial cysts (LECs) are associated with AIDS and represent the "classic" triad of head findings that occur in patients with human immunodeficiency virus (HIV) disease. The other two findings are enlarged cervical lymph nodes and enlarged adenoidal tissue in Waldeyer's ring. The pathogenesis of benign LECs has not been completely determined. These lesions probably represent a reactive phenomenon that results in intranodal inclusions within intraparotid lymph nodes.

Clinical Findings

LEC typically occurs in patients who are HIV positive. The cysts may be unilateral or bilateral and may be associated with diffuse cervical adenopathy. These patients usually present with a nonpainful enlarging neck mass. It may be difficult to differentiate an intraparotid LEC from an enlarging cervical lymph node based on palpation.

Pathology

Grossly, there is nodular or diffuse salivary gland enlargement. Histologic examination reveals dilatation of salivary gland ducts with extensive lymphocytic infiltration and replacement of ducts by solid islands of epithelial and myoepithelial cells.

Treatment

Because these are benign lesions, no immediate treatment is necessary. Surgical resection may be considered if the lesions are associated with an extensive cosmetic deformity.

Imaging Findings

CT

These cystic lesions may be single or multiple. They may be unilateral or bilateral. When multiple, these lesions are complex cystic lesions with internal septations that replace the normal parotid tissue. The cyst wall and septations enhance minimally. There may be additional solid enhancing lesions situated with the parotid gland associated with LECs. It is unclear as to whether these represent early LECs that have not undergone cyst formation, or enlarged intraparotid lymph nodes (Fig. 34-1).

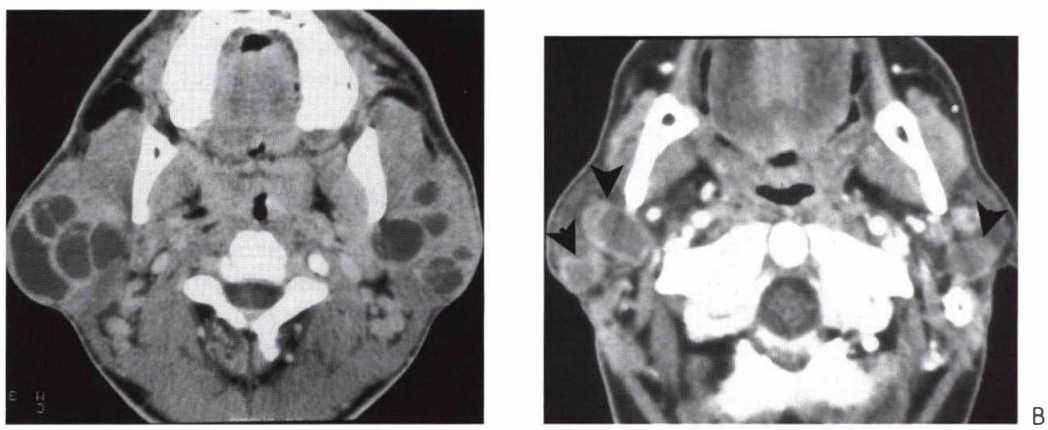

Figure 34-1. CT of lymphoepithelial cysts. (A) Axial contrast-enhanced CT shows multiple low-attenuation cysts scattered throughout both parotid glands. (B) Another example of lymphoepithelial cysts shows the cysts to be higher attenuation (arrowheads) than the cysts seen in (A). This is likely due to the presence of proteinaceous material within the cysts illustrated in this current example.

MR

These cystic lesions are low to intermediate signal on T1-weighted and high signal on T2-weighted sequences. The typical cyst signal characteristics may vary based on the protein content of the cysts. There may be mild enhancement along the cyst wall or internal septations. The cysts may involve the deep lobe of the parotid gland. The parapharyngeal space is not involved (Fig. 34-2).

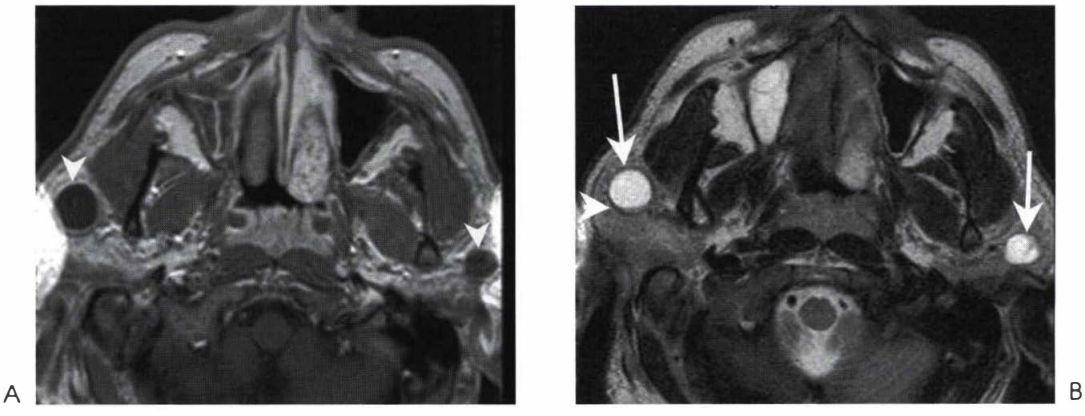

A B

Figure 34-2. MRI of lymphoepithelial cysts. (A) Axial contrast-enhanced T1-weighted image shows bilateral, low-signal, cystic masses with a thin rim of enhancement (arrowheads). (B) Axial T2-weighted image shows the typical appearance of these multiple cysts. The masses are typically well-circumscribed, high-signal masses (arrows). Note the fluid debris level in the cyst located in the right parotid gland (arrowhead). (Courtesy of Todd Smith, M.D.)

Imaging Pearls

- Histologically, it may be difficult to distinguish between a branchial cleft cyst and an LEC. The histologic findings should be taken into consideration with the imaging before rendering a final diagnosis.
- In our experience, it is not unusual to suggest the initial diagnosis of AIDS based on the findings of LECs in the parotid gland.

Suggested Readings

1. Kirshenbaum KJ, Nadimpalli SR, Friedman M, Kirshenbaum GL, Cavallino RP. Benign lymphoepithelial parotid tumors in AIDS patents: CT and MR findings in nine cases. *AJNR AM J Neuroradiol* 1991;12:271-274.
2. Holliday RA, Cohen WA, Schinella RA, et al. Benign lymphoepithelial parotid cysts and hyperplastic cervical adenopathy in AIDS-risk patients: a new CT appearance. *Radiology* 1988;168:439-441.
3. Som PM, Brandwen M. Salivary glands. In: Som PM, Curtin H, eds. *Head and Neck Imaging*. 3rd ed. New York: Mosby; 1996:823-914.

Chapter 35

Kimura's Disease

Epidemiology

Kimura's disease is an inflammatory disorder reported in Asian subjects. The disease usually affects the major salivary glands and neck nodes. Approximately 80% of cases occur in the second and third decades but the age range is wide (30 to 70 years). This disease has a male preponderance of > 80%.

Clinical Findings

Kimura's disease occurs mainly in the head and neck and the most common clinical presentation is that of a painless mass or lymphadenopathy. Other regions involved include axilla, groin, popliteal region, and forearm. Kimura's disease may therefore be mistaken clinically as a malignant lesion.

Pathology

The histologic features are dense infiltration of eosinophils and proliferation of follicular structures. Varying degrees of small vessel proliferation and fibrosis can also be seen. Peripheral blood eosinophilia (10–70%) is an invariable feature of this entity. Increased IGE concentrations have also been observed.

Treatment

Kimura's disease is a benign disorder but the clinical course is usually progressive with relapses. Complete surgical resection is difficult because of the diffusely infiltrative nature of this lesion. Most clinicians are hesitant to use radiation therapy because the patients are usually young. The initial response to corticosteroids, hydroxyurea, or oxyphenbutazone is often encouraging. However, to patients who are refractory to such treatment can benefit from low-dose radiation therapy.

Imaging Findings

CT

The findings on enhanced CT are nonspecific. There is diffuse enlargement of the parotid gland showing moderate to strong enhancement. On CT sialography, Kimura's disease shows diffuse glandular enlargement with ill-defined borders but a normal acinar appearance.

MR

The signal intensity of the lesions is variable and depends on the degree of fibrosis or vascular proliferation. Hence, T2-weighted images may show moderate to high signal intensities. Similarly, lesions may show high to intense enhancement following the injection of contrast (Fig. 35–1).

Imaging Pearls

- The imaging appearances of Kimura's disease are nonspecific. This entity should be suspected in patients with enlarged major salivary glands with or without lymphadenopathy, or in Asian subjects showing peripheral eosinophilia.

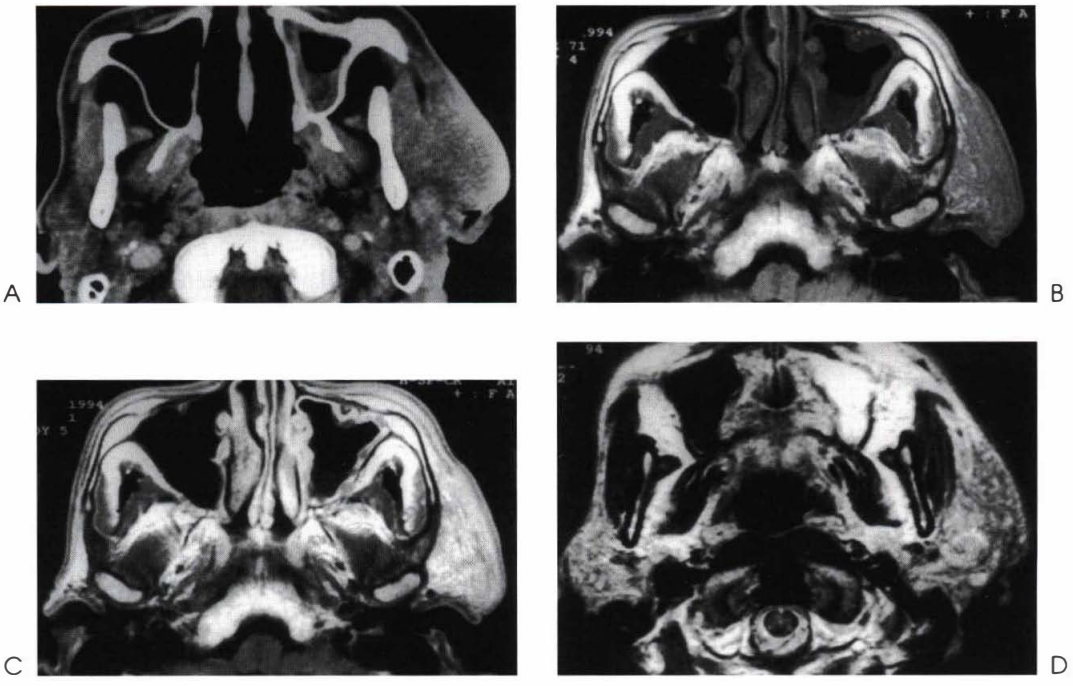

Figure 35-1. Kimura's disease of the parotid gland. (A) Axial contrast-enhanced CT shows a diffuse mass involving the left parotid gland. (B) Axial T1-weighted MR image shows an intermediate signal intensity left parotid mass. Note the diffusely infiltrative nature of the lesion. (C) Axial contrast-enhanced MR image shows diffuse enhancement. (D) Axial T2-weighted MR image shows intermediate heterogeneous signals in the mass. (Courtesy of WEH Lim, M.D., Singapore General Hospital, Singapore.)

Suggested Readings

1. Takahashi S, Ueda J, Furukawa T, et al. Kimura's disease: CT and MR findings. *AJNR Am J Neuroradiol* 1996;17:382–385.
2. Nyrop M. Kimura's disease: case report and brief review of the literature. *J Laryngol Otol* 1994;108:1005–1007.
3. Chong VFH, Balakrishnan A, Fong KW. Kimura's disease of the pharynx. *Clin Radiol* 2000;55:649–652.
4. Smith JRG, Hadgis C, Van Hasselt A, Metriweli C. CT of Kimura's disease. *AJNR Am J Neuroradiol* 1989;10:S34–S36.

Chapter 36

Warthin's Tumor

Epidemiology

Warthin's tumor (papillary cystadenoma lymphomatosum, cystadenolymphoma, lymphomatous adenoma) is the second most common parotid neoplasm. These tumors account for 10% of all benign parotid tumors. There is a strong male predominance, with the male to female ratio ranging from 5 to 7:1. The peak incidence appears to be between the fifth and sixth decades of life.

Clinical Findings

These lesions are usually asymptomatic. They may occasionally present as a painless mass in the parotid region. The facial nerve is almost always uninvolved.

Embryology

Warthin's tumors are interesting lesions whose pathophysiology is directly linked to embryology. The most commonly accepted theory regarding the origin of Warthin's tumors is that they arise from heterotopic salivary gland tissue situated within intraparotid lymph nodes. The parotid gland is the first salivary gland to develop, and initially appears between the fourth and sixth gestational weeks. The gland develops as a loose mesenchyma that contains aggregates of lymphoid tissue. The developing gland, like the other salivary glands, becomes encapsulated. However, the parotid gland is the last salivary to become encapsulated. The encapsulation of the parotid gland occurs after the development of the lymphatic system. As a result, the developing lymphoid aggregates form lymph nodes within the parotid gland. In contrast, the submandibular glands become encapsulated before the development of the lymphatic system and do not contain intraglandular lymph nodes. The intraparotid lymph nodes contain salivary ducts and acini. Warthin's tumors arise from these ductal elements, which are located within intraparotid lymph nodes. This explains the propensity for Warthin's tumors to be multicentric and bilateral (2–6%).

Pathology

On gross examination, Warthin's tumor appears as an encapsulated round or oval mass. Two histologic components must be present to make the diagnosis of Warthin's tumor. One component is an epithelial layer with a tubulopapillary-cystic pattern. The layer is contained within lymphoid tissue or is within an identifiable lymph node. Ultrastructural examination of the epithelial cell cytoplasm demonstrates numerous mitochondria that appear to be proliferating (oncocytes). As a result, Warthin's tumor may show uptake of technetium 99m pertechnetate. Histologically, about 30% of Warthin's tumor contains peripheral cysts. This would account for the peripheral areas of decreased attenuation seen on CT and increased T2-weighted signal occasionally identified on MR imaging.

Treatment

The treatment of choice is surgical resection. The type of surgical procedure depends on the number and the extent of the lesions. Because smaller lesions may not be palpable, imaging plays an important role for presurgical planning by determining whether tumors are multiple or bilateral or both. The likelihood of malignant transformation is extremely low.

Imaging Findings

CT

Warthin's tumor occurs in the expected distribution of intraparotid lymph nodes. The most common location of Warthin's tumor is in the parotid tail. Other sites are beneath the parotid capsule, the pretragal region, and adjacent to the main trunk of the facial nerve. The most common CT findings of Warthin's tumors are round, soft tissue masses situated within the parotid tail. These tumors may show mild contrast enhancement. The presence of peripheral lucencies may help suggest the diagnosis. These peripheral lucencies correspond to peripheral cystic regions occasionally seen on histologic examination.

MR

On MR imaging, these lesions are low to intermediate signal on T1-weighted sequences that enhance with contrast. On T2-weighted sequences, most tumors contain intermediate signal. Some lesions will have scattered foci of increased T2-weighted signal along the periphery. These areas are also likely due to the cystic changes occasionally seen on histologic examination (Figs. 36-1 through 36-3).

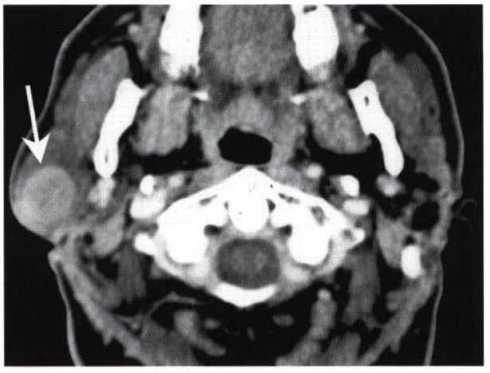

Figure 36-1. Axial contrast-enhanced CT shows a well-defined soft tissue mass located in the right parotid gland (arrow). Pathology revealed Warthin's tumor.

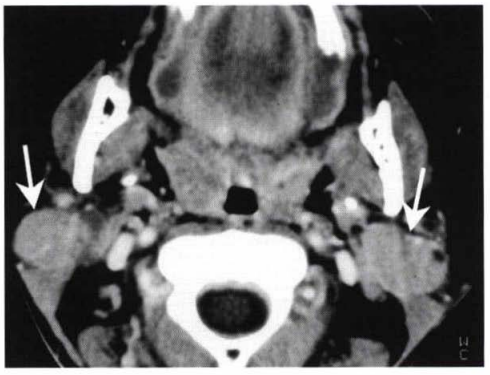

Figure 36-2. Contrast-enhanced CT demonstrates bilateral Warthin's tumors arising within both parotid glands (arrows).

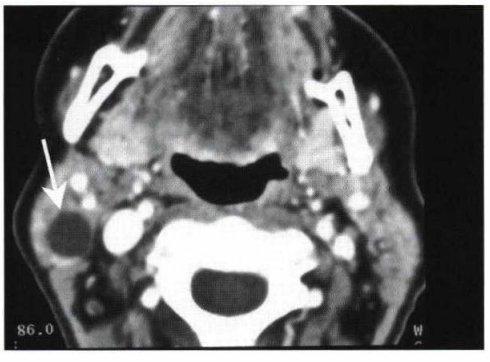

Figure 36-3. Axial CT shows an atypical homogeneously low attenuation appearance of a Warthin's tumor (arrow).

Imaging Pearls

- Upon encountering a mass in the parotid tail, one must examine the contralateral parotid gland for other lesions. Warthin's tumor should be considered when there are multiple or bilateral intraparotid masses in patients that have no other systemic disorder. The differential diagnosis for bilateral, intraparotid masses includes lymphoma, sarcoidosis, metastases, and rheumatologic disorders such as psoriasis.
- Although Warthin's tumors demonstrate uptake of technetium 99m pertechnetate, we have not found this modality to be clinically useful in our experience.

Suggested Readings

1. Batsakis JG. Tumors of the major salivary glands. In: Batsakis JG, ed. *Tumors of the Head and Neck*. Baltimore: Williams and Wilkins; 1979:1–76.
2. Som PM, Brandwen M. Salivary glands. In: Som PM, Curtin H, eds. *Head and Neck Imaging*. 3rd ed. New York: Mosby; 1996:823–914.
3. Shockley WM. Parotid tumors. In: Shockley WM, Pillsbury HC. *The Neck: Diagnosis and Surgery*. New York: Mosby; 1994:265–294.
4. Yoo GH, Eisele DW, Askin FB, Driben JS, Johns ME. Warthin's tumor: a 40-year experience at the Johns Hopkins Hospital. *Laryngoscope* 1994;104:799–803.
5. Minami M, Tanioka H, Oyama K. Warthin tumor of the parotid gland: MR–pathologic correlation. *AJNR Am J Neuroradiol* 1993;14:209–214.

Chapter 37

Pleomorphic Adenoma (Benign Mixed Tumor)

Epidemiology

Pleomorphic adenoma is the most common salivary gland tumor and the most common tumor to arise within the parotid gland. These tumors constitute 60% of all parotid neoplasms and 75% of benign parotid tumors. Eighty-four percent of pleomorphic adenomas arise within the parotid gland, 8% occur in the submandibular gland, 0.5% occur in the sublingual gland, and 6.5% arise in the minor salivary glands of the respiratory and upper digestive tracts. Pleomorphic adenomas are more common in females. They may occur in any age group; however, they most often present between 40 and 50 years of age.

Clinical Findings

The typical history is a painless mass that may be stable or slowly growing. On physical examination, the mass is smooth, firm, and nontender. The facial nerve is usually functioning normally.

Pathology

On gross pathological examination, these tumors are encapsulated, smooth, round or oval masses. The terms *"pleomorphic"* and *"benign mixed"* refer to the histologic appearance of this neoplasm. The tumor consists of both epithelial and mesenchymal elements. The epithelial component consists of an inner layer of epithelial cells, whereas the outer layer consists of myoepithelial cells that constitute the mesenchymal component. Both elements must be present for the diagnosis of pleomorphic adenoma to be made. These tissue elements may be arranged in a variety of patterns and associated with a variable amount of stroma. The stroma can consist of variable amounts of mucoid, fibroid, chondroid, vascular, or myxochondroid elements. The mucoid stroma is thought to be responsible for the signal characteristics present on T2-weighted imaging.

There are several malignancies associated with pleomorphic adenomas. These include carcinoma-expleomorphic adenoma, carcinosarcoma, and metastasizing benign mixed tumor. These will be discussed in separate chapters. It is felt that the incidence of an associated malignancy is related to longstanding tumors and those that have had multiple recurrences.

Treatment

The treatment of pleomorphic adenomas is surgical resection with a surrounding cuff of normal tissue. This may require a superficial parotidectomy for larger lesions located in the superficial lobe. Total parotidectomy may be required for masses that extend into the deep lobe. This important surgical decision is based on imaging findings and cannot usually be determined on physical examination alone. Simple enucleation has been abandoned due to the increased risk of facial nerve injury and the unacceptably high risk of recurrence associated with this procedure. The incidence of recurrence following surgical resection is 5%. Most cases of recurrence are thought to be due to incomplete tumor removal or disruption of the surrounding capsule with subsequent tumor spillage into the surgical bed.

Imaging Findings

CT

The typical CT appearance of a pleomorphic adenoma is a smoothly marginated, low-attenuation mass. Larger masses may contain areas of higher attenuation that represent areas of hemorrhage or calcification which arise within the stromal matrix. These tumors usually do not enhance immediately following contrast administration. However, these lesions do enhance on delayed imaging. A homogeneously low-attenuation intraparotid mass on CT is suggestive of a pleomorphic adenoma. However, a heterogeneous appearance is nonspecific and can be seen in both benign and malignant lesions (Fig. 37–1).

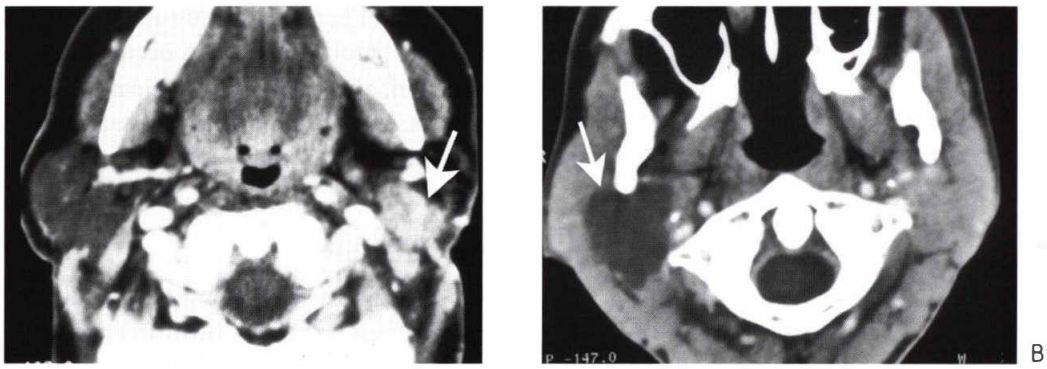

Figure 37–1. CT findings of pleomorphic adenoma. (A) Axial contrast-enhanced CT shows an enhancing well-defined mass located in the region of the deep lobe and tail of the parotid gland (arrow). (B) This enhanced image shows another appearance of a pleomorphic adenoma. This mass is low attenuation with very little enhancement and is located in the deep lobe of the parotid gland (arrow).

MR

On MR imaging, these lesions are low attenuation on T1-weighted imaging and enhance following contrast administration. These tumors are characteristically high signal on T2-weighted sequences. This is felt to be due to the high mucoid content of the stroma present in these tumors. When present, this finding is suggestive for pleomorphic adenoma (Fig. 37–2).

Imaging Pearls

- Imaging is used to determine whether a clinically palpable "parotid region" mass is located in the parotid gland. If the mass is intraparotid, then the relationship with the facial nerve needs to be determined.
- We prefer MR imaging for initial evaluation due to its superior tissue characterization. MR is the preferred imaging modality for evaluating recurrent pleomorphic adenoma. T2-weighted images are the sequence of choice for evaluating the extent of recurrent disease.

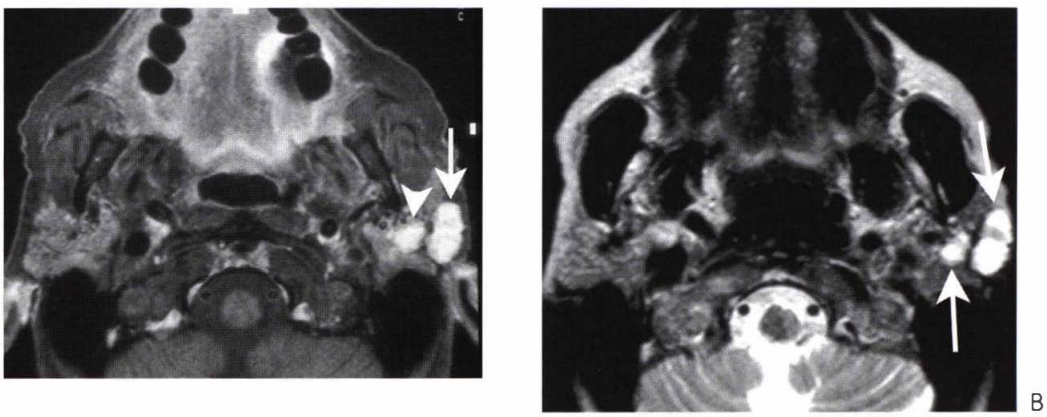

Figure 37–2. MR findings of pleomorphic adenoma. (A) Axial fat-suppressed, postcontrast T1-weighted image shows diffuse enhancement of a pleomorphic adenoma in the superficial lobe of the left parotid gland (arrow). There is a component of the mass that extends into the deep lobe (arrowhead). (B) Axial T2-weighted image of the same patient demonstrates the characteristic increased T2 signal in the left parotid gland (arrows).
(continues)

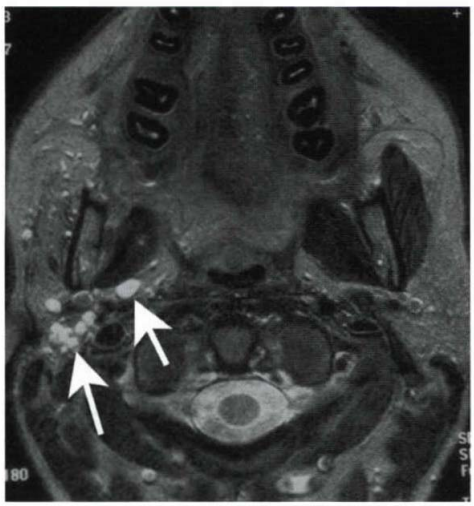

Figure 37-2. (C) Axial T2-weighted image obtained in a patient who had undergone a previous superficial parotidectomy for a pleomorphic adenoma. The multiple focal, increased signal masses are indicative of recurrent/residual disease (arrows). In our experience, this sequence is the most reliable for detecting recurrent pleomorphic adenoma.

Suggested Readings

1. Batsakis JG. Tumors of the major salivary glands. In: Batsakis JG, ed. *Tumors of the Head and Neck*. Baltimore: Williams and Wilkins; 1979:1-76.
2. Som PM, Brandwen M. Salivary glands. In: Som PM, Curtin H, eds. *Head and Neck Imaging*. 3rd ed. New York: Mosby; 1996:823-914.
3. Shockley WM. Parotid tumors. In: Shockley WM, Pillsbury HC. *The Neck: Diagnosis and Surgery*. New York: Mosby; 1994:265-294.
4. Ikeda K, Katoh T, Ha-Kawa SK, Iwai H, Yamashita T, Tanaka Y. The usefulness of MR in establishing the diagnosis of parotid pleomorphic adenoma. *AJNR Am J Neuroradiol* 1996;17:555-559.
5. Lev MH, Khanduja K, Morris PP, Curtin HD. Parotid pleomorphic adenomas: delayed CT enhancement. *AJNR Am J Neuroradiol* 1998;19:1835-1839.

Chapter 38

Carcinoma Expleomorphic Adenoma, Carcinosarcoma, Metastasizing Mixed Tumor

Epidemiology

Carcinoma ex-pleomorphic adenoma (CEPA) is an epithelial malignancy that is thought to arise from a preexisting pleomorphic adenoma. These lesions are believed to represent malignant degeneration of a pleomorphic adenoma. Some estimates suggest that nearly 25% of all pleomorphic adenomas may undergo malignant change if left untreated. CEPA may also occur in the setting of multiple recurrent pleomorphic adenomas. CEPA constitutes between 7 and 17% of all parotid malignancies and represents 2 to 5% of all salivary gland tumors. Other sites of occurrence include the submandibular gland, the palate, lip, paranasal sinuses, nasopharynx, tonsil, and minor salivary glands of the palate.

CEPA should be differentiated from other malignancies associated with pleomorphic adenomas. Carcinosarcoma is a true malignant pleomorphic adenoma with malignant epithelial and stromal elements. Metastasizing mixed tumor is the rarest of the malignancies associated with pleomorphic adenomas. These latter lesions are thought to arise from multiple procedures that have allowed cells to enter the lymphatic and venous system.

Clinical Findings

Patients usually present between the sixth and seventh decades of life. Patients usually complain of a mass that has often been present for 10 to 15 years which has suddenly increased in size. Patients may also present with pain and facial nerve palsy.

Pathology

The gross appearance of CEPA is a firm nodular mass that is partially encapsulated or unencapsulated. The lesions may occasionally be cystic and contain central hemorrhage or necrosis.

Histologically, these tumors are characterized by an infiltrative-growth malignant neoplasm. The malignant component may consist of adenocarcinoma, squamous cell carcinoma, or undifferentiated carcinoma. These features occur amidst the background of a preexisting neoplasm with features of a pleomorphic adenoma.

All the malignancies associated with pleomorphic adenomas can have nodal or systemic metastases. CEPA metastases show only the malignant epithelial component of the tumor. Nodal metastases from carcinosarcoma contain both malignant epithelial and stromal components. The metastases from metastasizing mixed tumor contain nonmalignant cells of pleomorphic adenoma.

Treatment

Total parotidectomy is the recommended surgical procedure due to the aggressive biological behavior associated with CEPA. The facial nerve may have to be sacrificed in patients with advanced disease. Perineural neural invasion has been identified in nearly 50% of patients. The 5-, 10-, and 15-year survival rates have been reported to be 40%, 24%, and 19%, respectively.

Imaging Findings

CT

The CT appearance of CEPA is variable. Early lesions may present as low-attenuation masses and mimic the appearance of a pleomorphic adenoma. CEPA may also appear as a pleomorphic adenoma with a focal area of low attenuation that may represent necrosis. Advanced lesions may have a very malignant appearance with aggressive margins that infiltrate the parenchyma of the parotid gland (Figs. 38–1 and 38–2).

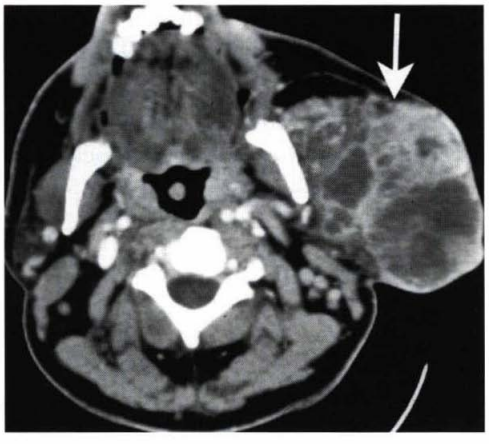

Figure 38–1. Axial contrast-enhanced CT of a carcinoma expleomorphic adenoma demonstrates a very large aggressive heterogeneous mass (arrow) arising from the left parotid gland.

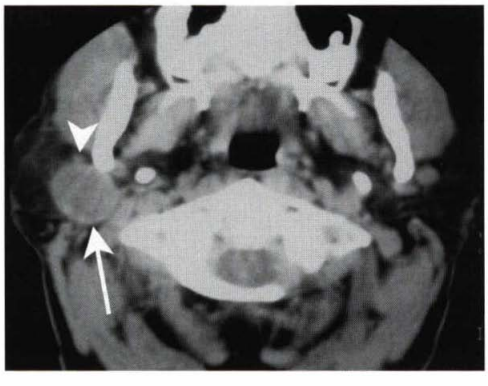

Figure 38–2. Axial contrast-enhanced CT shows a carcinoma expleomorphic adenoma arising from the deep lobe of the parotid gland with less aggressive features (arrow). A portion of the mass extends superficial to the retromandibular vein (arrowhead).

MR

The MR appearance may occasionally mimic a pleomorphic adenoma. However, these masses are often intermediate signal on T1- and T2-weighted signal due to their high cellularity. The presence of necrosis will result in areas of low T1-weighted signal and increased T2-weighted signal. The walls of advanced tumors are thick and irregular and enhance with contrast. Advanced tumors may completely replace the parenchyma of the parotid gland (Fig. 38–3).

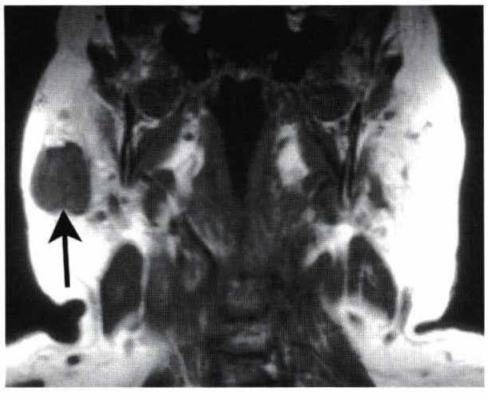

A

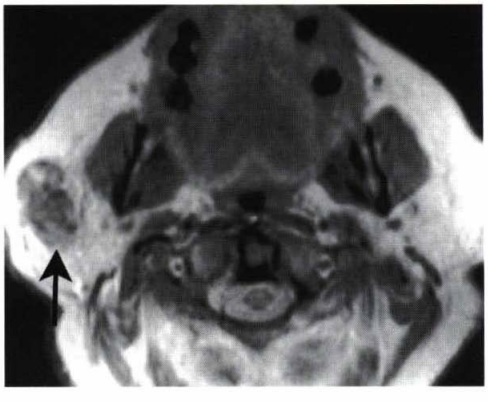

B

Figure 38–3. MR of carcinoma expleomorphic adenoma. (A) Axial contrast-enhanced T1-weighted image shows an intermediate signal mass situated in the right parotid gland (arrow). (B) The heterogeneous enhancement of the mass following administration of contrast (arrow). These findings are nonspecific and can be seen in a variety of solid parotid neoplasms.

Imaging Pearls

- Early CEPA may be indistinguishable from pleomorphic adenomas.
- In our experience, most CEPAs have been very advanced at presentation.
- CEPA should be considered in the differential diagnosis for any aggressive parotid mass that occurs in patients between 50 and 70 years of age.

Suggested Readings

1. Batsakis JG. Tumors of the major salivary glands. In: Batsakis JG, ed. *Tumors of the Head and Neck*. Baltimore: Williams and Wilkins; 1979:1–76.
2. Som PM, Brandwen M. Salivary glands. In: Som PM, Curtin H, eds. *Head and Neck Imaging*. 3rd ed. New York: Mosby; 1996:823–914.
3. Shockley WM. Parotid tumors. In: Shockley WM, Pillsbury HC. *The Neck: Diagnosis and Surgery*. New York: Mosby; 1994:265–294.

Chapter 39

Mucoepidermoid Carcinoma

Epidemiology

Mucoepidermoid carcinoma (MC) is the most common malignant tumor of the parotid gland and accounts for 44% of all parotid gland malignancies. The parotid gland (50%) is the most common location for MC followed by the palate (45%) and submandibular gland. MC is the second most common malignancy of the submandibular gland. MCs may present at any age but are most commonly diagnosed between the fourth and fifth decades of life. These tumors may be slightly more common in females. MC is the most common salivary gland malignancy in children.

Clinical Findings

Patients may present with a parotid region mass. Patients with more advanced tumors will present with pain and facial nerve paralysis.

Pathology

MC appears to arise from the epithelium of the large ducts of the major and minor salivary glands. As the name implies, MCs are composed of two major cell types: epidermoid (squamous) and mucous cells. Batsakis has identified six cell types that are seen in MC: maternal, intermediate, epidermoid, clear, columnar, and mucous. MCs are classified as high-, intermediate-, or low-grade tumors. Low-grade lesions are primarily composed of columnar and mucin-forming cells. Intermediate-grade tumors tend to be more cellular and are dominated by epidermoid and intermediate cells. High-grade MC is highly infiltrative and has a predominance of squamous cells. As a result, high-grade MC may be misdiagnosed as primary squamous cell carcinoma of the parotid gland. Perineural spread can be seen with MC. However, this type of spread pattern is not as common as adenoid cystic carcinoma.

Treatment

The recommended treatment is based on histologic grade. Low-grade tumors may be treated with surgical resection. The recurrence rate for low-grade tumor with negative margins is 6%. The 10-year survival rate for low-grade lesions is 90%. High-grade lesions often require surgery followed by adjuvant radiation therapy. The 10-year survival rate is $< 50\%$.

Imaging Findings

CT

The imaging appearance of MC is variable. Some investigators suggest that the variability is due to the histologic grade of the tumor. Low-grade lesions are often well-circumscribed, round, soft tissue masses. Small cysts may occasionally be present. High-grade lesions often appear as infiltrating masses that invade and replace the parenchyma of the parotid gland (Fig. 39–1).

MR

MCs may appear as round masses with smooth margins that are often low to intermediate signal on T1- and T2-weighted sequences. These lesions enhance with contrast and are often indistinguishable from solitary Warthin's tumor or low-grade adenoid cystic carcinoma. High-grade lesions have indistinct margins and tend to replace the normal high T1-weighted signal of the parotid gland (Fig. 39–2).

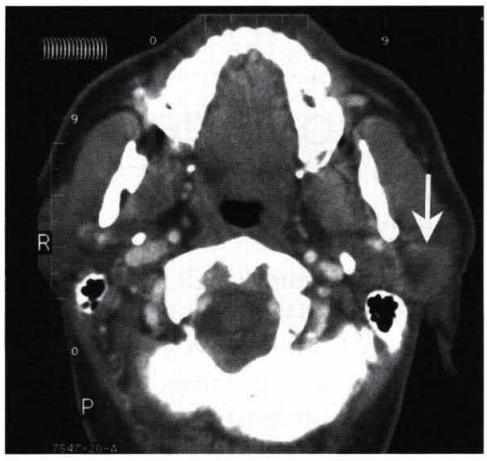

Figure 39-1. CT findings of mucoepidermoid carcinoma. Axial contrast-enhanced CT shows an enhancing soft tissue mass situated in the left parotid gland (arrow).

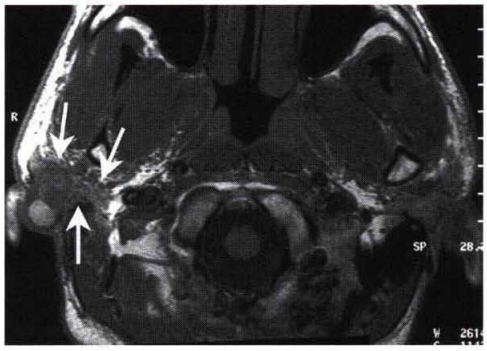

A

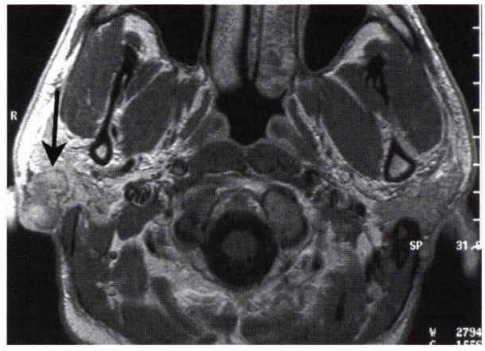

B

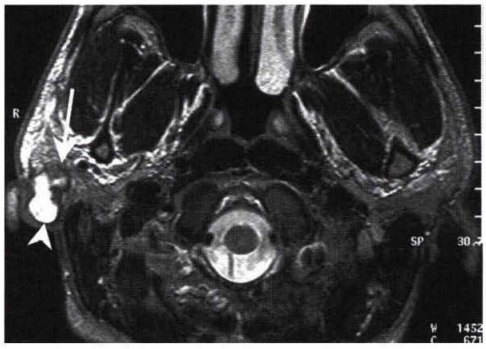

C

Figure 39-2. MR findings of mucoepidermoid carcinoma. (A) Noncontrast axial T1-weighted image shows an intermediate signal mass with poorly defined margins involving both the superficial and the deep lobes of the parotid gland (arrow). (B) The mass enhances following contrast administration (arrow). (C) Axial T2-weighted image shows that the mass appears to have both solid (arrow) and cystic (arrowhead) components. The cystic component is an atypical feature of mucoepidermoid carcinomas because the majority of these lesions tend to be solid.

Imaging Pearls

- There are no findings on CT and MR imaging that are specific for MC. The lack of increased T2-weighted signal indicates that a lesion is not a typical pleomorphic adenoma and should raise the possibility of a parotid malignancy.
- Detailed evaluation of the skull base should be performed to evaluate for retrograde perineural spread along the facial nerve in patients with MC. The presence of perineural extension into the skull base precludes surgical resection at many institutions.

Suggested Readings

1. Batsakis JG. Teratomas of the head and neck. In: Batsakis JG, ed. *Tumors of the Head and Neck*. 2nd ed. Baltimore: Williams and Wilkins; 1979:1–76.
2. Som PM, Brandwen M. Salivary glands. In: Som PM, Curtin H, eds. *Head and Neck Imaging*. 3rd ed. New York: Mosby; 1996:823–914.
3. Shockley WM. Parotid tumors. In: Shockley WM, Pillsbury HC. *The Neck: Diagnosis and Surgery*. New York: Mosby; 1994:265–294.

Chapter 40

Adenoid Cystic Carcinoma

Epidemiology

Adenoid cystic carcinoma (ACC) is a malignant epithelial tumor that can arise from major or minor salivary glands. These are uncommon tumors that constitute about 4% of all parotid tumors and approximately 15% of parotid malignancies. They most commonly present between 40 and 60 years of age. Males and females are equally affected.

Clinical Findings

These tumors typically present as a slow-growing mass in the parotid region that may occasionally be painful. Perineural invasion is the hallmark of this malignancy. ACC is the most common malignancy of the parotid gland to be associated with facial nerve weakness. This is due to the propensity of this tumor to invade nerves.

Pathology

These tumors probably arise from the canaliculi and intercalated ducts of the peripheral duct system of the salivary glands. On gross examination, these tumors are typically unilobular and appear grayish white or yellowish white on cut section. The tumors are relatively circumscribed with little or no encapsulation. There are four main histologic patterns of ACC: cribriform (classic), tubuloglandular, solid, and cylindromatous (hyaline). Neural invasion is a constant histologic finding. Skip lesions where uninvolved segments of nerve may be interspersed between involved segments also characterize these tumors. As a result, "clear" surgical margins play a less important prognostic role when compared with other malignancies.

Treatment

The treatment depends on the stage of disease and the extent of facial nerve involvement. Total parotidectomy is felt to be appropriate surgery if the facial nerve is uninvolved. Involvement of the peripheral branches of the facial nerve necessitates sacrificing the involved branches. Retrograde perineural extension through the stylomastoid foramen along the descending portion of the facial nerve may be a contraindication for surgical resection at many institutions. Postoperative radiation therapy is necessary for parotid malignancies. The 5-year survival rate is not indicative of overall prognosis. Survivorship may be affected up to 20 years after treatment. The greatest likelihood of cure appears to be associated with complete eradication of disease at the time of initial treatment. The high recurrence rate may be due to incomplete surgical resection due to inability to detect perineural extension.

Imaging Findings

CT

The CT findings are nonspecific. ACCs are usually soft tissue masses that enhance following contrast administration. The margin may either be smooth or irregular (Fig. 40–1).

MR

ACCs are often low to intermediate signal on T1- and T2-weighted sequences. These lesions enhance with contrast. High-grade lesions have indistinct margins and tend to replace the normal high T1-weighted signal of the parotid gland (Fig. 40–2).

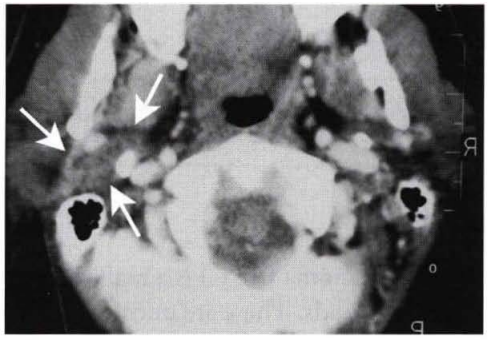

Figure 40–1. CT of adenoid cystic carcinoma. Axial contrast-enhanced CT demonstrates a focal soft tissue mass situated in the deep lobe of the parotid gland (arrows).

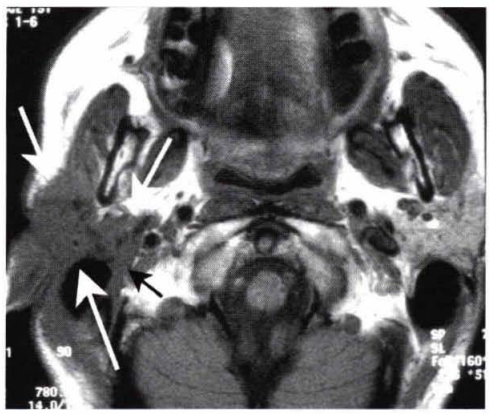

A

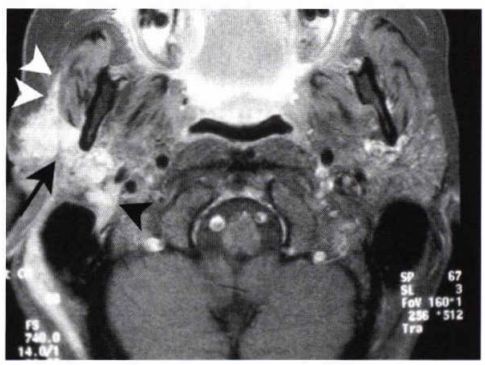

B

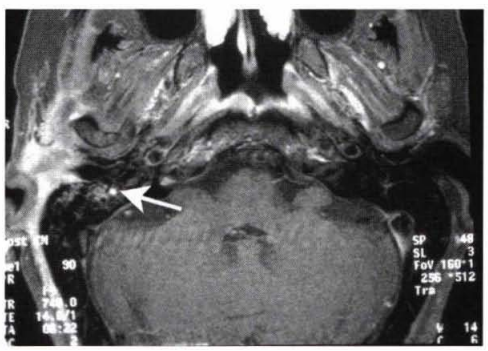

C

Figure 40–2. MR of adenoid cystic carcinoma. (A) Axial noncontrast T1-weighted image shows an aggressive tumor replacing the right parotid gland (large arrows). The tumor extends deep and medial to the mastoid tip. (B) T1-weighted postcontrast image performed with fat saturation shows the tumor to be densely enhancing (arrow). Note the extension medial to the mastoid tip into the expected location where the facial nerve exits the stylomastoid foramen (black arrowhead). The linear enhancement in the buccal space most likely represents perineural spread along the buccal branch of the facial nerve (white arrowheads). (C) Axial T1-weighted postcontrast image performed with fat saturation obtained 10 mm cephalad to Figure 40–2B shows dense enhancement of the descending portion of the facial nerve (arrow). This is characteristic of retrograde perineural spread along the descending portion of the facial nerve in the mastoid canal.

Imaging Pearls

- There are no CT or MR imaging findings that are specific for ACC. The lack of increased T2-weighted signal indicates that a lesion is not a typical pleomorphic adenoma and should raise the possibility of a parotid malignancy.
- MR should be performed in all patients with ACC to specifically evaluate the descending portion of the facial nerve. The presence of retrograde perineural extension involving the descending portion of the facial nerve may preclude surgical resection at many institutions.
- Identifying the extent of disease including perineural involvement is essential for radiation therapy planning.

Suggested Readings

1. Batsakis JG. Teratomas of the head and neck. In: Batsakis JG, ed. *Tumors of the Head and Neck*. 2nd ed. Baltimore: Williams and Wilkins; 1979:1–76.
2. Som PM, Brandwen M. Salivary glands. In: Som PM, Curtin H, eds. *Head and Neck Imaging*. 3rd ed. New York: Mosby; 1996:823–914.
3. Shockley WM. Parotid tumors. In: Shockley WM, Pillsbury HC. *The Neck: Diagnosis and Surgery*. New York: Mosby; 1994:265–294.

Chapter 41

Adenocarcinoma

Epidemiology

Adenocarcinomas can be considered glandular malignancies of the major salivary gland that cannot be placed in the other more definable malignant categories. It is possible that some lesions may arise from longstanding pleomorphic adenomas or adenoid cystic carcinomas. Adenocarcinoma of the parotid gland has distinct histologic features that separate these tumors from adenoid cystic carcinoma and mucoepidermoid carcinoma. Adenocarcinoma constitutes up to 15% of parotid malignancies. There is no gender predilection.

Clinical Findings

Adenocarcinoma is more common in older patients; however, these tumors have been re-Aported as early as the second decade of life. These neoplasms may have a variety of clinical presentations that may be associated with the grade of the tumor. Some tumors will present as painless, slow-growing masses. Other lesions are painful masses that are rapidly enlarging.

Pathology

On gross examination, these tumors are firm, hard masses that are often attached to the surrounding tissue. Histologically, these tumors are similar to adenocarcinomas that arise in the gastrointestinal tract. Adenocarcinoma arising from the major salivary gland tends to have a cystic papillary growth pattern. Most tumors produce mucin. High-grade adenocarcinomas tend to behave clinically like low-grade mucoepidermoid carcinomas.

Adenocarcinoma may be classified according to its architectural and cytologic appearance. Grade I tumors are circumscribed and minimally invasive with mild pleomorphism. Grade III lesions are pleomorphic solid tumors with a higher mitotic rate. Grade II tumors are between Grades I and III.

Treatment

The treatment of choice is parotidectomy with postoperative radiation therapy. The risk of nodal metastases is higher than that associated with adenoid cystic carcinoma, with rates ranging between 24 and 36%. As a result, elective neck dissection may be beneficial.

Imaging Findings

CT

The CT appearance is that of an aggressive infiltrative mass that has infiltrative margins. There may be areas of low attenuation indicative of necrosis in high-grade tumors

MR

The aggressive lesions have low to intermediate T1- and T2-weighted signal. These tumors often replace the substance of the parotid gland (Fig. 41-1).

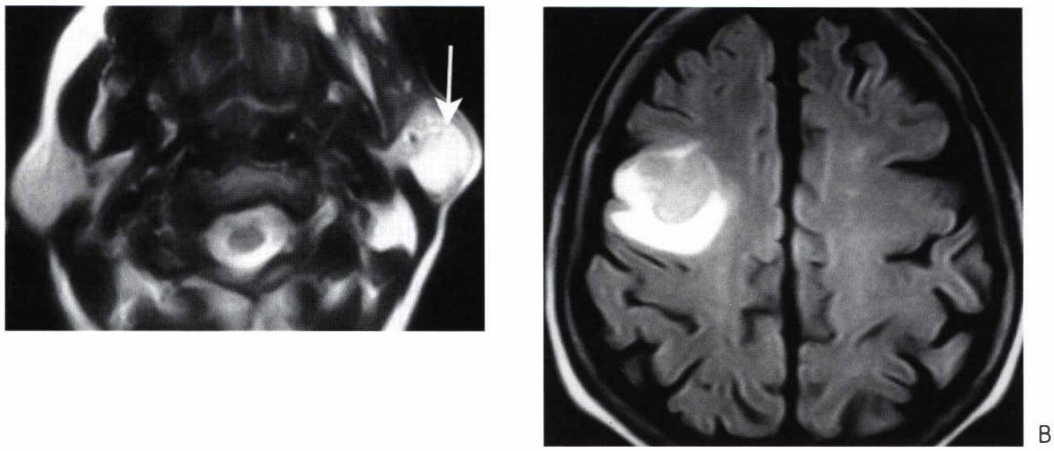

Figure 41-1. Primary adenocarcinoma of the parotid gland. (A) Axial T2-weighted image shows a high signal mass located in the parotid gland. The high signal may be due to a high mucin content within the mass. (B) Axial fluid attenuated inversion recovery (FLAIR) shows a mass in the left frontal lobe. The biopsy revealed adenocarcinoma that was thought to be metastatic from the primary parotid gland tumor.

Imaging Pearls

- These tumors may occasionally be confused with adenoid cystic carcinoma because of their histologic similarities. One needs to evaluate the facial nerve along its descending segment for retrograde perineural spread. This finding would favor adenoid cystic carcinoma and may preclude surgical resection.

Suggested Readings

1. Batsakis JG. Tumors of the major salivary glands. In: Batsakis JG, ed. *Tumors of the Head and Neck*. Baltimore: Williams and Wilkins; 1979:1–76.
2. Som PM, Brandwen M. Salivary glands. In: Som PM, Curtin H, eds. *Head and Neck Imaging*. 3rd ed. New York: Mosby; 1996:823–914.
3. Shockley WM. Parotid tumors. In: Shockley WM, Pillsbury HC. *The Neck: Diagnosis and Surgery*. New York: Mosby; 1994:265–294.
4. Eisele DW, Johns ME. Salivary gland neoplasms. In: Bailey BJ, ed. *Head and Neck Surgery: Otolaryngology*. 2nd ed. Philadelphia: Lippincott-Raven; 1998:1485–1508.

Chapter 42

Squamous Cell Carcinoma

Epidemiology

Primary squamous cell carcinoma (SCCA) of the parotid gland is a rare tumor and accounts for 1% of parotid tumors. SCCA comprises 3% of submandibular gland neoplasms and 4% of submandibular carcinomas. These tumors are more common in men.

Primary parotid SCCA should be considered a diagnosis of exclusion and should be made only after excluding the other neoplasms that could mimic its appearance. SCCA of the parotid gland can be confused with high-grade mucoepidermoid carcinoma or may occur from direct spread of SCCA arising from the external ear. In our experience, SCCA identified in the parotid gland is due to lymphatic drainage to intraparotid lymph nodes from skin cancer. The most common primary site locations for the cutaneous lesions include the temporal region, lateral face, eyelid, and scalp. These areas must be thoroughly examined in patients who are diagnosed with primary parotid SCCA.

Clinical Findings

These tumors usually present in the sixth or seventh decade as a rapidly enlarging mass. On clinical examination, these lesions are usually fixed to adjacent structures and often invade the overlying skin. Approximately 20% of patients complain of pain, with about 10% of patients having facial nerve palsy.

Pathology

The etiology of these tumors is unknown. Squamous epithelium is not normally found within the salivary gland. It is possible that squamous metaplasia may arise secondary to chronic inflammation. The site of origin is thought to be the salivary ducts. However, these tumors are often very advanced at presentation, making it difficult to identify a site of origin.

The gross appearance is that of an unencapsulated, infiltrative, grayish-white mass. Cavitation and necrosis are often present. Histologically, these tumors demonstrate intracellular keratinization, intracellular bridges, and keratin pearl formation. The majority of tumors are moderately differentiated.

There are no distinguishing microscopic features that allow primary SCCA of the parotid gland to be differentiated from advanced parotid metastases. The presence of SCCA within an intraparotid lymph node would suggest that the tumor arose from metastases rather than a primary parotid SCCA. The presence of mucin would help differentiate a high-grade mucoepidermoid carcinoma from SCCA of the parotid gland. Mucin-producing cells can be identified with special stains such as mucicarmine. The histologic diagnosis of primary parotid SCCA should only be arrived at after complete evaluation with special stains, histochemical studies, and electron microscopy.

Treatment

The treatment of primary parotid SCCA is resection with clear margins followed by radiation therapy. Neck dissection should be performed for patients with positive neck nodes as determined by palpation or imaging.

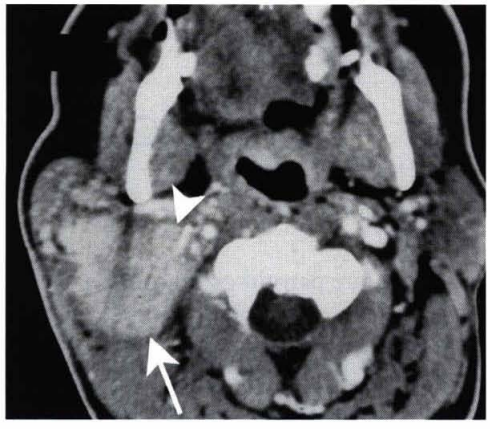

Figure 42–1. Contrast-enhanced CT shows a large, enhancing, soft tissue mass (SCCA) located in the right parotid gland (arrow), which extends into the deep lobe (arrowhead).

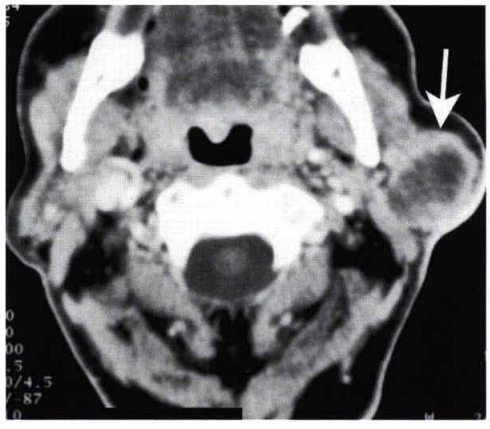

Figure 42–2. Contrast CT shows the necrotic appearance of SCCA situated in the left parotid gland (arrow). Compare this appearance with that shown in Figure 42–1.

Imaging Findings

CT

These tumors present as solid heterogeneous masses that have a thick enhancing rim and central low-attenuation center. There is often infiltration of the surrounding parotid parenchyma and fat of the skin overlying the parotid gland (Figs. 42–1 and 42–2).

MR

The imaging appearance is that of an aggressive parotid malignancy. The lesions are of low to intermediate T1 and T2 signal. The central necrosis may result in areas of increased T2-weighted signal within the mass.

Imaging Pearls

- Patients with SCCA are at risk for perineural spread. MR should be performed to evaluate for retrograde perineural spread along the auriculotemporal and facial nerves.
- SCCA may have retrograde perineural spread along the auriculotemporal nerve to the mandibular division of the trigeminal nerve (V_3). Tumors with this spread pattern which is similar to adenoid costic carcinoma may invade the cavernous sinus via retrograde spread along V_3.
- SCCA may also demonstrate retrograde spread along the descending portion of the facial nerve.
- Identification of retrograde perineural spread along V_3 or the descending portion of the facial nerve may preclude surgical resection.

Suggested Readings

1. Batsakis JG. Tumors of the major salivary glands. In: Batsakis JG, ed. *Tumors of the Head and Neck.* Baltimore: Williams and Wilkins; 1979:1–76.
2. Som PM, Brandwen M. Salivary glands. In: Som PM, Curtin H, eds. *Head and Neck Imaging.* 3rd ed. New York: Mosby; 1996:823–914.
3. Shockley WM. Parotid tumors. In: Shockley WM, Pillsbury HC. *The Neck: Diagnosis and Surgery.* New York: Mosby; 1994:265–294.

Chapter 43

Oncocytoma

Epidemiology

Oncocytomas are rare parotid gland tumors. These neoplasms are thought to represent parenchymal elements of acini or intralobular ducts that have been transformed by unknown etiologies. The majority of lesions are benign; however, malignant oncocytomas have been reported. The parotid gland is the most common site in the head and neck. The submandibular gland is rarely involved. Oncocytomas constitute < 1% of salivary gland tumors and account for about 1% of benign parotid gland neoplasms.

Clinical Findings

Patients usually present with a painless, parotid-region mass between the fifth and sixth decades of life. Oncocytomas appear to occur in males and females with equal incidence. Multiple bilateral tumors have been reported in 7% of cases.

Pathology

Batsakis (1979) suggests that the cellular transformation resulting in the formation of oncocytomas should be considered a compensatory rather than a degenerative process due to abnormal mitochondrial function. Oncocyte mitochondria produce relatively less adenosine tri-phospate than mitochondria in normal cells. It is thought that oncocytes try to compensate for the "mitochondriopathy" by increasing the amount of intracellular mitochondria. As a result, electron microscopy shows oncocytes to have an excess accumulation of normal- and abnormal-appearing mitochondria. Due to the high concentration of mitochondria, these tumors demonstrate uptake of technetium 99m pertechnetate.

Gross examination shows that oncocytomas are usually ovoid or round and may be coarsely granular. They are usually noncystic, firm, and rubbery. A thin capsule usually surrounds the lesions.

Histologically, oncocytomas consist of cells with a high nuclear to cytoplasmic ratio and a prominent nucleolus. Oncocytomas do not contain lymphoid tissue. This helps differentiate these lesions from Warthin's tumors.

Treatment

The treatment of choice is parotidectomy with preservation of the facial nerve. However, the type of parotidectomy will depend on the extent of lesion identified on imaging and at surgery.

Imaging Findings

CT

The CT findings are nonspecific. These lesions are usually round soft tissue masses that may enhance with contrast (Fig. 43–1).

MR

These lesions are usually low to intermediate on T1-weighted sequences. Most tumors are located in the superficial lobe. The T2-weighted appearance is variable. The lesions often have low to intermediate T2-weighted signal. They may occasionally contain increased T2-weighted signal. However, the signal is not as homogeneously increased as that seen in pleomorphic adenomas (Fig. 43–2).

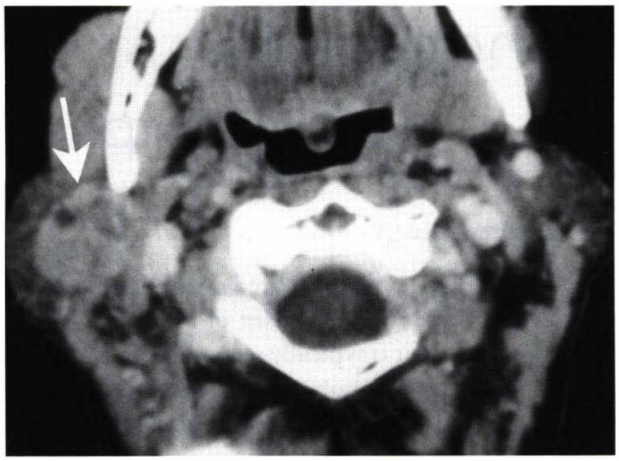

Figure 43-1. Axial contrast-enhanced CT shows the nonspecific imaging findings of a deep lobe oncocytoma (arrow).

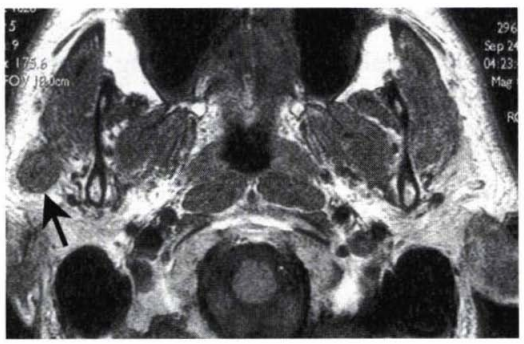

A

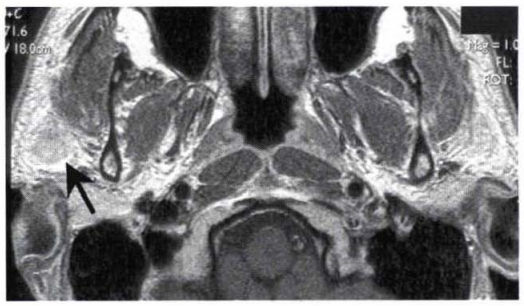

B

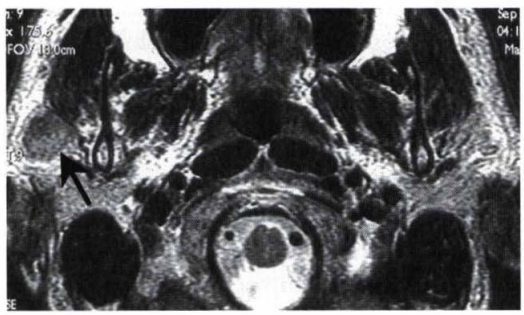

C

Figure 43-2. MR findings of oncocytoma. (A) Axial T1-weighted image of the parotid gland shows an intermediate signal mass in the right parotid gland (arrow). (B) Contrast-enhanced T1-weighted image shows the mass to diffusely enhance (arrow). (C) Axial T2-weighted image shows the mass to be intermediate to low signal (arrow). The lack of high signal indicates that the mass is likely not a pleomorphic adenoma.

Imaging Pearls

- Because of the relatively high concentration of intracellular mitochondria, oncocytomas and Warthin's tumors are the two parotid tumors that show uptake of technetium 99m pertechnetate.
- Careful attention must be given to both parotid glands due to the possibility of bilateral involvement.

Suggested Readings

1. Batsakis JG. Tumors of the major salivary glands. In: Batsakis JG, ed. *Tumors of the Head and Neck*. Baltimore: Williams and Wilkins; 1979:1-76.
2. Som PM, Brandwen M. Salivary glands. In: Som PM, Curtin H, eds. *Head and Neck Imaging*. 3rd ed. New York: Mosby; 1996:823-914.
3. Shockley WM. Parotid tumors. In: Shockley WM, Pillsbury HC. *The Neck: Diagnosis and Surgery*. New York: Mosby; 1994:265-294.

Chapter 44

Monomorphic Adenoma

Epidemiology

Monomorphic adenomas are benign parotid tumors that constitute 2% of all parotid neoplasms. These tumors consist of a very regular epithelial component and a mesenchymal component that is typically seen in pleomorphic adenoma. These lesions can arise in any of the salivary glands but are most common in the superficial lobe of the parotid gland. The majority (80%) of the minor salivary gland tumors occur near the upper lip. Monomorphic adenomas may be slightly more common in females.

Clinical Findings

Patients usually complain of a slow-growing mass in the parotid region and are otherwise asymptomatic. Patients with the classic basal cell type of monomorphic adenoma usually present between 60 and 70 years of age. The membranous form usually presents a decade earlier.

Pathology

Monomorphic adenomas are thought to arise from cells that compose the intercalated duct of the salivary gland. These tumors derive their name from the histology. These tumors are composed of uniformly differentiated cells of one type. There are various histologic types of monomorphic adenomas. These types include basal cell adenoma, membranous adenoma, myoepithelioma, and intermediate to mixed tumors and adenoid cystic carcinoma (hybrid forms). The basal cell adenoma pattern is the most common minor salivary gland pattern and is often found in lesions involving the upper lip. Membranous adenomas most commonly occur in the parotid gland. Myoepitheliomas are thought by Batsakis to represent a monomorphic variant of a pleomorphic adenoma. These tumors rarely exhibit a pure monomorphic pattern. These unusual tumors comprise less than 1% of salivary mixed tumors that have a predominance of myoepithelial cells. Hybrid forms must be differentiated from adenoid cystic carcinoma. A cannicular pattern is characteristic of the hybrid type and helps distinguish this lesion from adenoid cystic carcinoma. Some authors feel that monomorphic adenomas may evolve into pleomorphic adenomas if left untreated.

Treatment

These lesions are considered nonaggressive with the recommended treatment being parotidectomy. The recurrence rate is low for lesions that are completely resected.

Imaging Findings

CT

There is very little information on the imaging appearance of monomorphic adenomas. These tumors are well-defined lesions located in the superficial lobe of the parotid gland (Figs. 44-1 and 44-2).

MR

The lesions usually have low to intermediate T1-weighted signal and variable T2-weighted signal. The margins of these tumors are usually well defined.

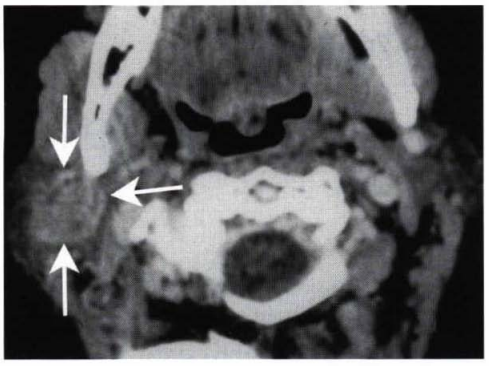

Figure 44-1. Axial contrast-enhanced CT shows a soft tissue mass situated in the deep lobe of the parotid gland (arrows). These imaging findings are nonspecific and can be seen in a variety of primary parotid tumors.

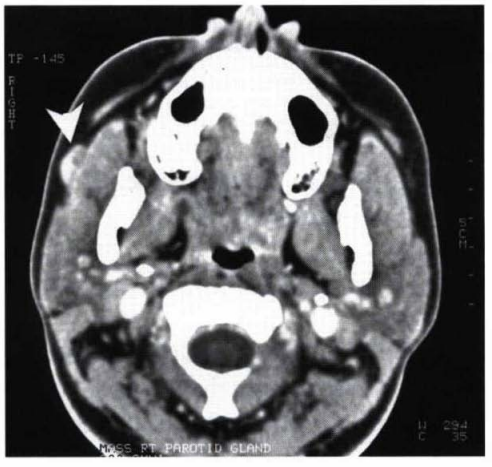

A

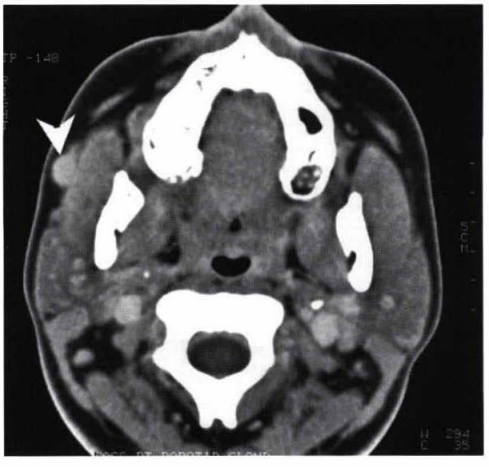

B

Figure 44-2. (A) Axial contrast-enhanced CT shows accessory parotid tissue overlying the masseter muscle (arrowhead). (B) Axial image obtained 6 mm superior to (A) shows a densely enhancing mass arising within the accessory parotid tissue (arrowhead). Pathology revealed monomorphic adenoma.

Imaging Pearls

- The imaging appearance of monomorphic adenomas is nonspecific. The tumor may be suggested by a well-defined mass located in the superficial lobe in an elderly patient.

Suggested Readings

1. Batsakis JG. Tumors of the major salivary glands. In: Batsakis JG, ed. *Tumors of the Head and Neck.* Baltimore: Williams and Wilkins; 1979:1-76.
2. Som PM, Brandwen M. Salivary glands. In: Som PM, Curtin H, eds. *Head and Neck Imaging.* 3rd ed. New York: Mosby; 1996:823-914.
3. Shockley WM. Parotid tumors. In: Shockley WM, Pillsbury HC. *The Neck: Diagnosis and Surgery.* New York: Mosby; 1994:265-294.

Chapter 45

Acinous Cell Carcinoma

Epidemiology

Acinous cell carcinoma (ACC) constitutes between 15 and 17% of all parotid malignancies. Eighty percent of ACCs arise in the parotid gland, 4% occur in the submandibular gland, and 10% are situated in the oral cavity. They most commonly present in adults in the fifth decade of life. However, they may be seen in all age groups and are the second most common salivary gland malignancy of childhood. ACCs may be multiple, bilateral, or both, and rank next to Warthin's tumors in their frequency of bilateral parotid gland involvement (3%). The tumors appear to have female predominance.

Clinical Findings

The clinical presentation is nonspecific. Patients typically present with an asymptomatic mass in the parotid region.

Pathology

ACCs are composed of serous cells that are found predominantly within the parotid gland. They are believed to arise from the terminal portions of the salivary duct system (intercalated ducts and terminal tubules). ACCs are generally considered low-grade malignancies. On gross pathological examination, these masses are well-defined firm masses that have a grayish-white appearance. A thin capsule may be present. Histologically, uniformly round or polygonal cells that have abundant cytoplasm and eccentric nuclei characterize these tumors. The cytoplasm is basophilic and contains zymogen granules. The cellular architecture is variable and may consist of the following: acinar–lobular, papillary–cystic, follicular, medullary, ductuloglandular, primitive tubular, and microcystic.

Treatment

Treatment is surgical resection. Total parotidectomy has been suggested due to the propensity of these lesions to be multicentric. The recurrence rate is low because the tumor is completely resected following the initial surgery. The likelihood of cervical nodal metastases is 10 to 20%.

Imaging Findings

CT

The CT findings are nonspecific and are usually those of a round soft tissue mass that may enhance with contrast.

MR

These masses are usually low to intermediate signal on T1-weighted sequences and enhance with contrast. Because the lesions are characterized histologically by abundant cytoplasm, these lesions may have increased signal on T2-weighted sequence (Figs. 45–1 and 45–2).

Imaging Pearls

- The increased T2-weighted signal may cause these lesions to mimic the MR imaging appearance of pleomorphic adenomas.

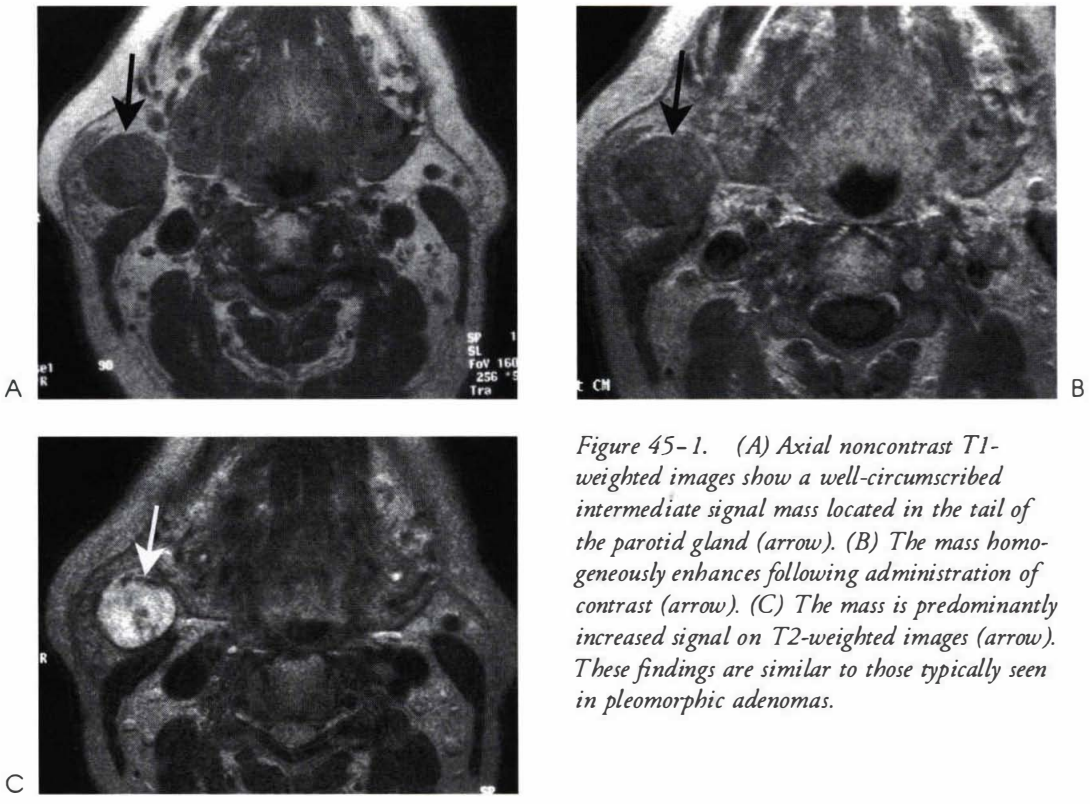

Figure 45–1. (A) Axial noncontrast T1-weighted images show a well-circumscribed intermediate signal mass located in the tail of the parotid gland (arrow). (B) The mass homogeneously enhances following administration of contrast (arrow). (C) The mass is predominantly increased signal on T2-weighted images (arrow). These findings are similar to those typically seen in pleomorphic adenomas.

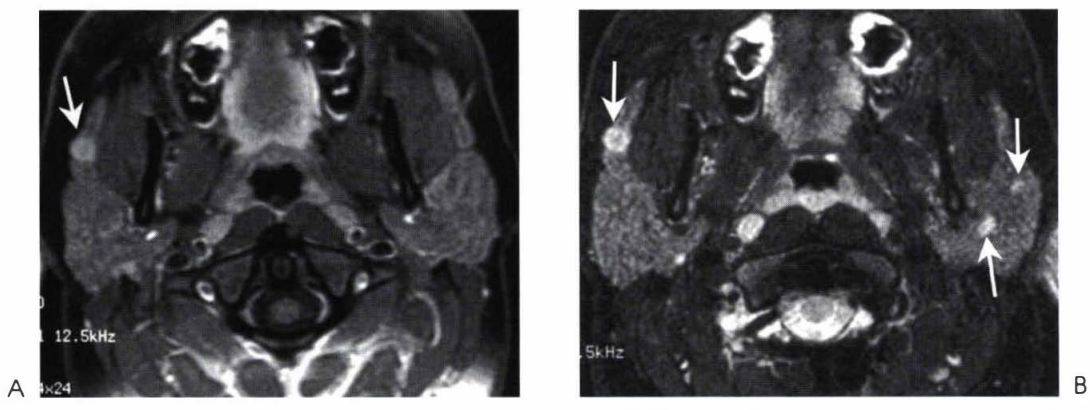

Figure 45–2. (A) Axial fat-suppressed, contrast-enhanced T1-weighted image shows a mass situated in an anterior portion of the right parotid gland (arrow). (B) Axial T2-weighted image with fat suppression obtained in the same patient and at the same level as shown in (A) demonstrates bilateral (arrows) acinous cell carcinomas that are high signal on T2-weighted sequences. These lesions appear more conspicuous on the T2-weighted images as opposed to the contrast-enhanced study illustrated in (A).

Suggested Readings

1. Batsakis JG. Tumors of the major salivary glands. In: Batsakis JG, ed. *Tumors of the Head and Neck*. Baltimore: Williams and Wilkins; 1979:1–76.
2. Som PM, Brandwen M. Salivary glands. In: Som PM, Curtin H, eds. *Head and Neck Imaging*. 3rd ed. New York: Mosby; 1996:823–914.
3. Shockley WM. Parotid tumors. In: Shockley WM, Pillsbury HC. *The Neck: Diagnosis and Surgery*. New York: Mosby; 1994:265–294.
4. Spiro RH, Huvos AG, Berk R, Strong EW. Acinic cell carcinoma of salivary gland origin. *Cancer* 1978;41:924–935.

Chapter 46

Lymphoma

Epidemiology

Lymphoma of the parotid gland may arise within the parotid parenchyma (primary) or within the intraparotid lymph nodes (secondary). Primary lymphoma of the parotid gland is very rare and accounts for < 5% of parotid tumors. Primary parotid lymphoma is felt to be part of mucosal associated lymphoid tissue lymphomas (MALT-omas). These lesions may involve any portion of the gastrointestinal tract where lymphoid tissue is part of the mucosal defense system. Lymphoid tissue is normally present in the parotid gland and absent in adult submandibular and sublingual glands. As a result, 80% of reported salivary gland involvement of primary lymphoma occurs in the parotid gland and 20% involves the submandibular glands.

Secondary lymphoma is also rare, with the reported incidence ranging between 1 and 8% of the cases of lymphoma. There is an association between both Sjögren's syndrome and Waldenström's macroglobulinemia and secondary parotid lymphoma.

Clinical Findings

Women are at slightly greater risk with the majority of patients presenting after the age of 50. Patients typically present with a painless parotid-region mass. The facial nerve is usually normally functioning.

Pathology

The criteria necessary to establish the diagnosis of primary parotid lymphoma are architectural and cytologic confirmation of involvement of the salivary parenchyma by lymphoma without evidence of systemic disease. Involvement of multiple intraparotid lymph nodes with preservation of the intervening parenchyma is indicative of secondary involvement from systemic disease. Primary lymphoma is usually due to non-Hodgkin's lymphoma. Secondary lymphoma may be caused by either Hodgkin's or non-Hodgkin's lymphoma. Large cell is felt to be the most common form of secondary lymphoma.

Treatment

The treatment of primary parotid lymphoma is variable. In general, isolated primary lymphoma is considered stage I disease and is associated with a good prognosis with 5-year disease-free survival rates ranging between 33 and 55%. The treatment of secondary lymphoma should be determined by the extent of systemic involvement and subsequent stage.

Imaging Findings

CT

Primary lymphoma is characterized by replacement of the parotid gland by an infiltrating soft tissue mass. Multiple discrete, round, intraparotid soft tissue masses are suggestive of secondary lymphoma. These masses are usually homogeneous without internal areas of decreased attenuation. There may be some thin peripheral-rim enhancement of the involved lymph nodes (Fig. 46–1).

MR

Primary and secondary lymphoma is characterized by intermediate signal on both T1- and T2-weighted sequences (Fig. 46–2).

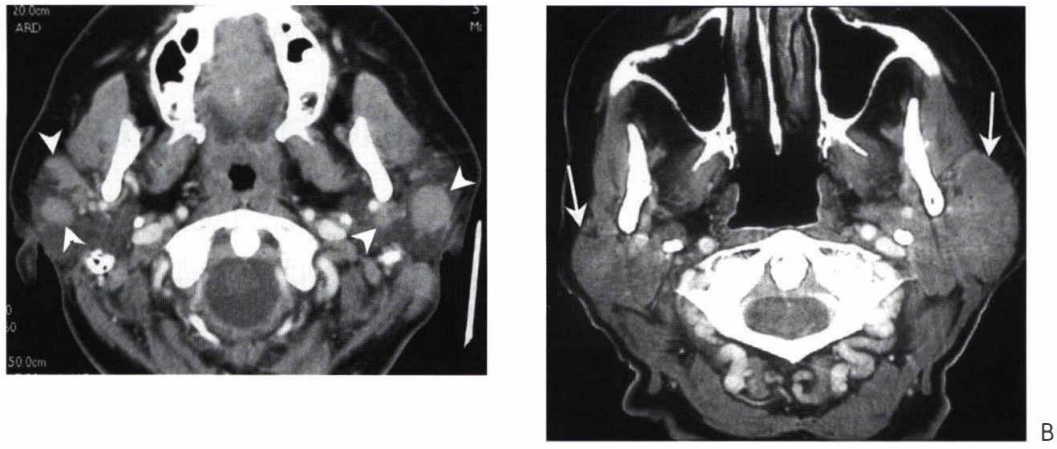

Figure 46–1. CT findings of intraparotid lymphoma. (A) Contrast-enhanced CT of the parotid glands shows multiple masses within both parotid glands (arrowheads) that likely represent enlarged intraparotid lymph nodes due to lymphomatous involvement. (B) Axial image shows a different appearance of parotid lymphoma (arrows). There is replacement of the entire normal parotid gland parenchyma by lymphoma in both parotid glands.

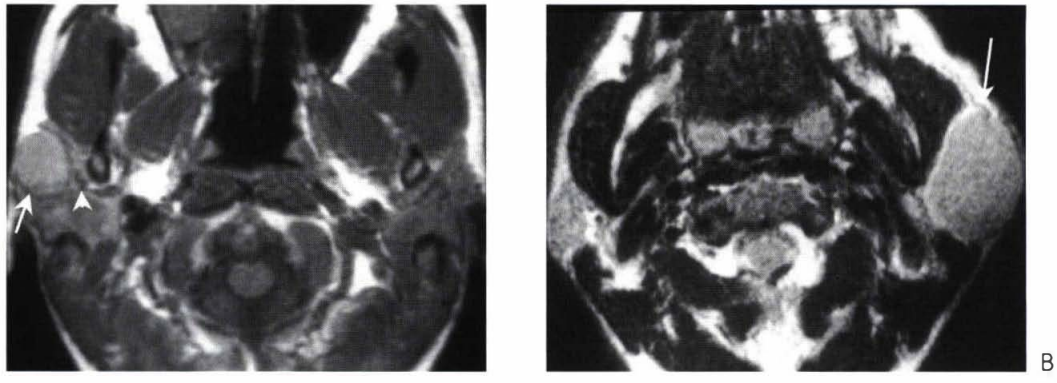

Figure 46–2. MR imaging findings of lymphoma. (A) Noncontrast T1-weighted image shows an intermediate signal mass located in the superficial lobe of the parotid gland (arrow). The mass is superficial to the retromandibular vein (arrowhead). (B) Axial T2-weighted image in a different patient shows the signal characteristics of diffuse lymphomatous involvement of the left parotid gland (arrow).

Imaging Pearls

- In our experience, secondary involvement of multiple intraparotid lymph nodes is much more common than primary parotid lymphoma.
- Lymphoma should be included in the differential diagnosis of elderly patients with multiple intraparotid masses. Based on our experience, the other most likely lesions to be considered in the differential diagnosis in elderly patients include Warthin's tumors and intraparotid metastases from squamous cell carcinoma of the skin for unilateral involvement, and Warthin's tumor and melanoma for bilateral involvement.

Suggested Readings

1. Batsakis JG. Tumors of the major salivary glands. In: Batsakis JG, ed. *Tumors of the Head and Neck.* Baltimore: Williams and Wilkins; 1979:1–76.
2. Som PM, Brandwen M. Salivary glands. In: Som PM, Curtin H, eds. *Head and Neck Imaging.* 3rd ed. New York: Mosby; 1996:823–914.
3. Eisele DW, Johns ME. Salivary gland neoplasms. In: Bailey BJ, ed. *Head and Neck Surgery: Otolaryngology.* 2nd ed. Philadelphia: Lippincott-Raven; 1998:1485–1508.
4. Kapadia SB. Hematologic diseases: malignant lymphomas, leukemias, plasma cell dyscrasias, histiocytosis X, and reactive lymph node lesions. In: Barnes L, ed. *Surgical Pathology of the Head and Neck.* Vol 2. New York: Marcel Dekker, Inc.; 1985:1045–1207.

Chapter 47

Facial Nerve Schwannoma

Epidemiology

Schwannomas can arise from motor, sensory, sympathetic, and cranial nerves (with the exception of the olfactory and optic nerves, which are not covered by Schwann cells). Approximately 25 to 40% of all schwannomas are found in the head and neck. In the head and neck more than half the lesions are located in the lateral cervical region. Schwannomas are typically seen during the third and fourth decades of life and are more common in females (female to male ratio of 2:1).

Clinical Findings

Most schwannomas present as a painless mass. A facial nerve schwannoma, like most other schwannomas, is rarely diagnosed clinically. Facial nerve palsy is uncommon in tumors arising from the parotid gland. This is because schwannomas grow around the nerve axons.

Pathology

Schwannomas are sharply circumscribed and encapsulated tumors. In only about 20% of patients can the nerve of exact origin be determined. Grossly they appear gray and possess a watery or slimy consistency. These tumors may show areas of cystic changes or hemorrhage. They are moderately vascular and show a mixture of compact cells (Antoni A) and loosely packed areas (Antoni B). They stain strongly with antibodies to S-100 proteins; this feature may be used to distinguish them from smooth muscle tumors, with which they may be confused.

Treatment

A facial schwannoma in a patient with no facial nerve palsy is often a management dilemma. The tumor is benign, and surgical extirpation may produce facial nerve palsy. The decision to resect the tumor is easier if facial nerve palsy is already present. Recurrence following resection is uncommon. This benign tumor rarely undergoes malignant degeneration.

Imaging Findings

CT

The tumor shows nonspecific findings. Parotid schwannomas show intermediate attenuation and good contrast enhancement (Fig. 47-1).

MR

On T1-weighted images, schwannomas demonstrate intermediate signal intensity. These tumors show high signal intensity on T2-weighted images and also exhibit enhancement following contrast administration.

Imaging Pearls

- Schwannomas are associated with neurofibromatosis (NF) type 2. It is therefore important to demonstrate the presence or absence of other cranial nerve schwannomas, meningiomas, or ependymomas.

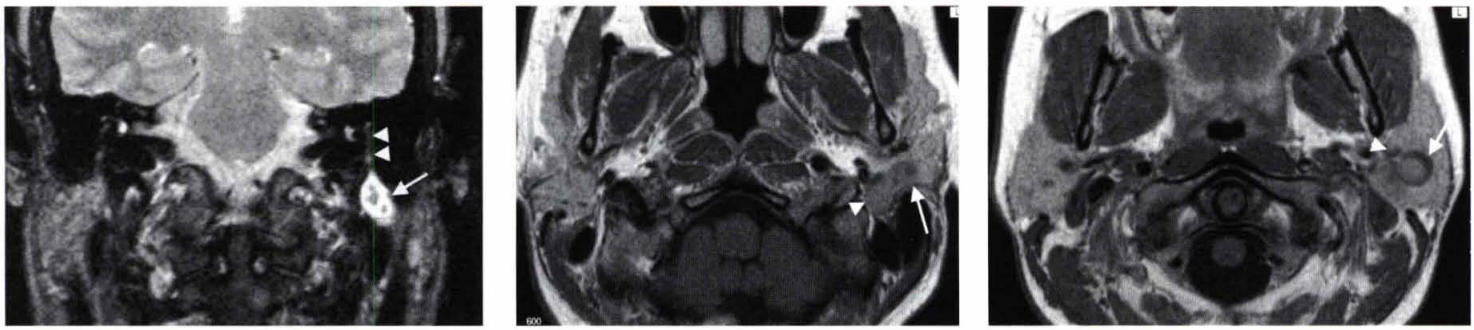

A B C

Figure 47-1. MR imaging findings of the facial nerve schwannoma. (A) Coronal T2-weighted image shows a well-circumscribed soft tissue mass that is located inferior to the skull base at the level of the stylomastoid foramen (arrow). Note that the distal aspect of the descending position of the facial nerve (arrowheads) exits into this mass. (B) Axial contrast-enhanced T1-weighted image shows the lesion to extend from the region of the stylomastoid foramen (arrowhead) into the superior aspect of the parotid gland (arrow) an approximate course of the facial nerve. (C) Axial contrast-enhanced CT obtained through the mid-portion of the parotid gland shows the mass (arrow) to be just lateral to the retromandibular vein (arrowhead) in the expected location of the in traparotid facial nerve.

Suggested Readings

1. Kyriakos M, El-Mofty S. Pathology of selected soft tissue of head and neck. In: Thawley SE, Panje WR, Batsakis JG, Lindberg RD, eds. *Comprehensive Management of Head and Neck Tumors*. 2nd ed. Philadelphia: WB Saunders; 1999:1322–1394.
2. May M. *The Facial Nerve*. New York: Thieme; 1986.

Chapter 48

Congenital Anomalies of the First Branchial Apparatus

Epidemiology

First branchial anomalies (FBA) are an uncommon group of lesions that result from abnormal embryogenesis of the first branchial apparatus. FBA account for approximately 8% of all branchial complex anomalies. The spectrum of abnormal development includes cysts, sinuses, and fistulae, or various combinations of these entities. FBA are seen more in children than adults and usually present before 10 years of age. These lesions appear more often on the left than on the right. Females are involved twice as often as males. Associated abnormalities may involve any other structure that arises from the first branchial apparatus. These include congenital craniofacial malformations and syndromes [Crouzon's disease (craniofacial dysostosis), Goldenhar's syndrome (oculo-auricular-vertebral syndrome), Treacher Collins–Franceschetti syndrome (mandibulofacial dysostosis), Nager's syndrome (preaxial acrofacial dysostosis), and Pierre Robin syndrome (Robin sequence)] and malformations of the external auditory canal, middle ear cavity, and ossicles.

Embryology

Due to the complex nature of these lesions, several classification systems have been developed to aid in the diagnosis and surgical management of these lesions.

Type I

Type I lesions are cysts or sinuses that are located in the parotid gland. These lesions are thought to represent either a duplication anomaly of the external auditory canal or buried cell rests of the first branchial cleft.

Type II

Type II defects are thought to arise from incomplete closure of the branchial cleft. They extend from the angle of the mandible to the vicinity of the membranous external auditory canal. These lesions typically communicate with the external auditory canal at the bony-cartilaginous junction.

Pathology

Type I

These lesions are ectodermally derived cysts lined by squamous epithelium with subepithelial lymphoid tissue.

Type II

These anomalies consist of both ectodermal and mesodermal elements with subepithelial lymphoid tissue.

Clinical Findings

Type I

Type I lesions often present as an asymptomatic parotid-region mass. Occasionally, these lesions may present as a painful mass or a discharging sinus in the region of the parotid gland. They are often located anterior or inferior to the pinna.

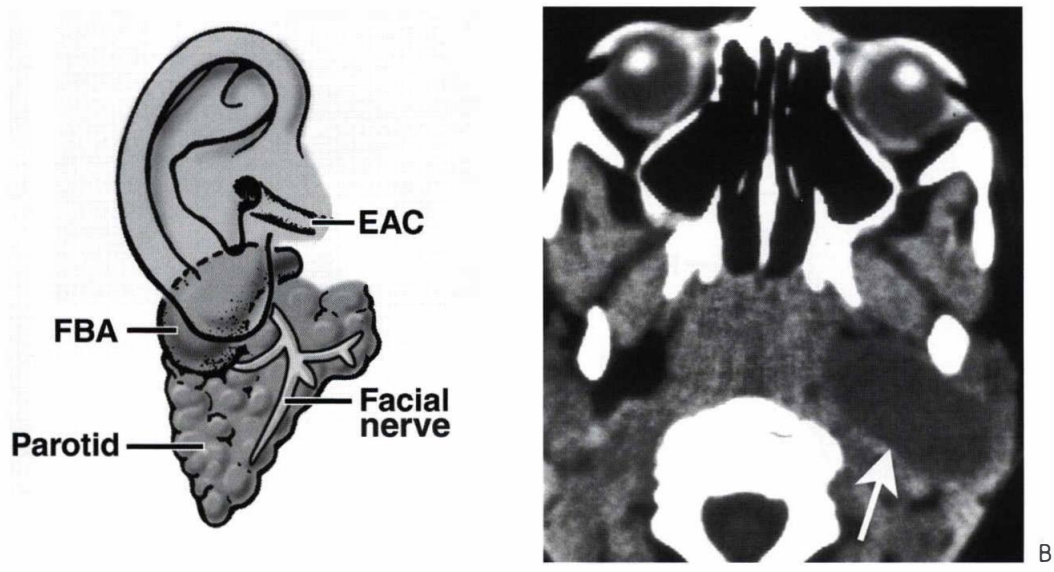

Figure 48-1. Type I first branchial anomaly. (A) Schematic illustration of a Type I first branchial anomaly. (B) Axial contrast-enhanced CT shows a low attenuation mass in the left parotid space (arrow) without an enhancing rim. EAC, external auditory canal. (A from Mukherji SK, Falterpekar G, Castillo M, Stone JA, Chung CJ. Imaging of congential anomalies of the branchial apparatus. Neuroimaging Clin N Am *2000;10:75-93. B from Mukherji SK, Tart RP, Slattery WH, Stringer SP, Mancuso AA. Evaluation of first branchial anomalies by CT and MR.* J Comput Assist Tomogr *1993;17:576-581. Used with permission).*

Type II

These anomalies present in childhood as a cyst or sinus located in the anterior triangle of the neck that may communicate with the external auditory canal. Type II lesions have a greater likelihood of being symptomatic and often present as a painful enlarging mass in the region of the parotid tail. They may be associated with a draining sinus tract that is typically located below the angle of the mandible. Occasionally, patients may present with otalgia or recurrent otitis media that is refractory to medical therapy. This may be due to the presence of a fistulous tract communicating between the cyst and the external auditory canal.

Imaging Findings

Type I

These are typically thin-walled unilocular cystic intraparotid masses. There is usually no significant enhancement of the cyst wall. The pretragal region of the parotid gland is the most common location (Fig. 48-1).

Type II

These are elongated, multilobular, cystic lesions that extend from the undersurface of the external auditory canal, course through the deep lobe of the parotid gland, and end in the submandibular space. Occasionally, these lesions may involve the parapharyngeal space (Fig. 48-2).

Imaging Pearls

- Type I lesions have a characteristic appearance. However, the appearance of the cystic component can vary with the protein content of the fluid. Pure cystic lesions are low attenuation on CT and are hypointense on T1-weighted and hyperintense on T2-weighted sequences. Lesions that have been infected often have a thick enhancing wall and have a higher protein content within the cystic component of the lesion. The result is increased attenuation on CT and increased signal on T1-weighted sequences.
- The location with respect to the facial nerve needs to be determined because damage to the nerve is a potential complication during resection.

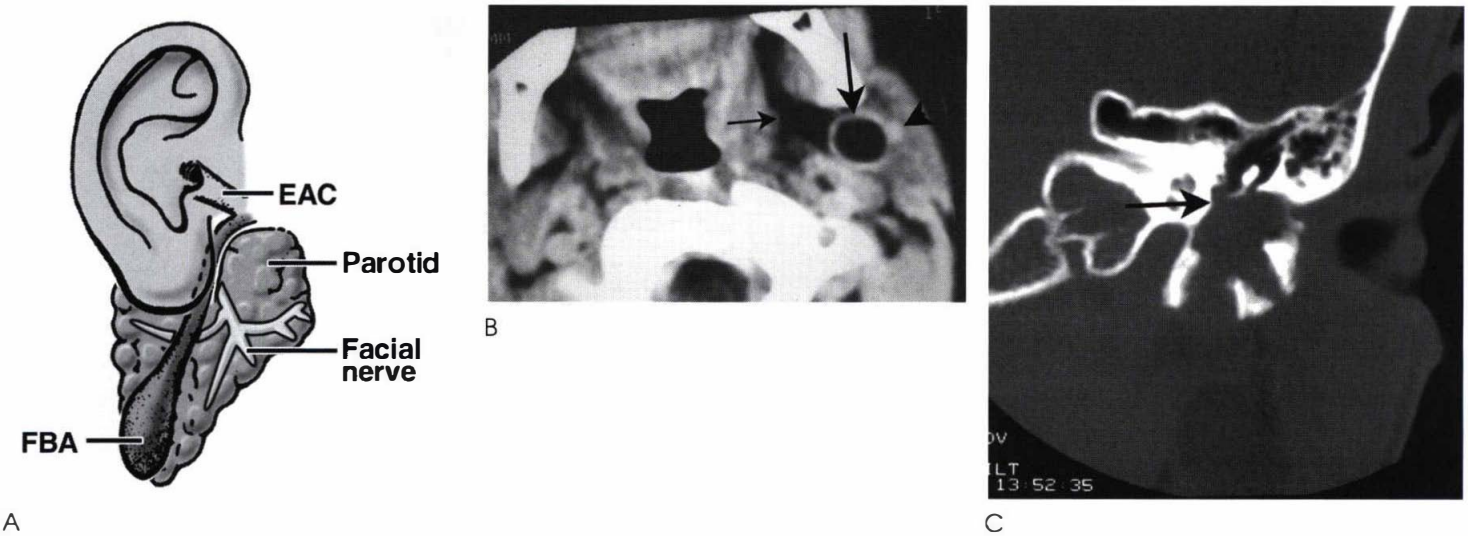

Figure 48-2. Type II first branchial anomaly (FBA). (A) Schematic illustration of a Type II FBA. EAC, external auditory canal. (B) Axial contrast-enhanced CT shows a Type II FBA involving the deep lobe of the parotid gland (large arrow). Note that the mass is deep to the retromandibular vein (arrowhead) and is lateral to the parapharyngeal space (small arrow). These findings isolate the mass to the deep lobe of the parotid gland. (C) Coronal CT of a Type II FBA shows a large communication with the external auditory canal. This is an unusual example because this Type II FBA was associated with an epidermoid that eroded the base of the temporal bone and enlarged the communication (arrow) (A from Mukherji SK, Falterpekar G, Castillo M, Stone JA, Chung CJ. Imaging of congential anomalies of the branchial apparatus. Neuroimaging Clin N Am *2000;10:75-93. Band C from Mukherji SK, Tart RP, Slattery WH, Stringer SP, Mancuso AA. Evaluation of first branchial anomalies by CT and MRI.* J Comput Assist Tomogr *1993;17:576-581. Used with permission.)*

- The bony sinus tract that communicates with the external auditory canal in Type II lesions can be demonstrated with coronal, contiguous, 1 mm thick sections reconstructed with bone algorithms.

Suggested Readings

1. Mukherji SK, Tart RP, Slattery WH, Stringer SP, Mancuso AA. Evaluation of first branchial anomalies by CT and MR. *J Comput Assist Tomogr* 1993;17:576–581.
2. Arnot JS. Defects of the first branchial cleft. *S Afr J Surg* 1971;9:93–98.
3. Work WP. Newer concepts of first branchial cleft defects. *Laryngoscope* 1972;82:1581–1593.
4. Mukherji SK, Falterpekar G, Castillo M, Stone JA, Chung CJ. Imaging of congenital anomalies of the branchial apparatus. *Imaging Clin N Am* 2000;10:75–93.

Chapter 49

Vascular Lesions

Epidemiology

The classification of vascular lesions of the extracranial head and neck developed by Mulliken and Glowacki is based on their biological and clinical characteristics. In the past, different terms have been used by different specialties to describe the same lesions. This classification system attempts to unify the nomenclature and improve the understanding of these complex lesions. Vascular lesions are classified as malformations and hemangiomas. Malformations are further divided based on their histology and include capillary, venous, arteriovenous (arterial, fistulae), lymphatic, and mixed. Hemangiomas are further subdivided based on their growth phase, which consists of a proliferating and an involuting phase.

Clinical Findings

Vascular malformations are always present at birth. Enlargement of these lesions is due to growth of the child rather than proliferation of the endothelial cells that constitute the lesion. Unlike hemangiomas, these lesions do not undergo spontaneous involution. The incidence in males is equal to that in females.

Pathology

All vascular lesions are composed of endothelial cells. Vascular malformations consist of flat endothelial cells that have a normal rate of mitosis and cell growth. The types of malformed endothelial cells that may be seen include venule, veins, capillaries, and lymphatic vessels. The histology determines the specific type of vascular malformation. Mixed vascular malformations such as venous-lymphatic malformations may occur due to close association in the embryogenesis of the lymphatic and venous systems.

Treatment

The treatment of vascular malformations of the parotid gland is based on the specific type of malformation, the extent of the lesion, and the lesion's location as it relates to important neural structures, especially the facial nerve. Because these lesions are benign, there is a general tendency to observe intraparotid malformations as opposed to surgical resection or sclerotherapy due to potential for damaging the facial nerve.

Imaging Findings

The specific CT and MR imaging findings are discussed elsewhere in this text (Figs. 49-1 and 49-2).

Imaging Pearls

- The purpose of imaging is to (1) attempt to identify the specific type of vascular lesion, (2) determine the extent of the lesion, and (3) characterize the lesion as "high flow" or "low flow." On MR imaging, the presence of flow voids or enhanced signal on flow-sensitive sequences within the lesion is indicative of a high-flow state. On Doppler ultrasound, high-flow lesions show arterial wave forms.

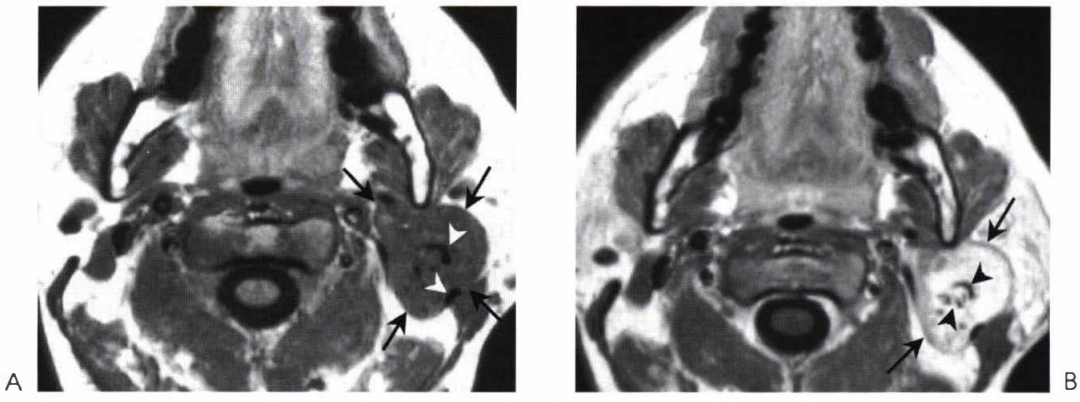

Figure 49–1. High-flow vascular malformation. (A) Noncontrast T1-weighted image shows an intermediate signal mass involving the deep lobe of the parotid gland (arrows). There are multiple flow voids (arrowheads) within the mass indicating this is a "high-flow" vascular malformation. (B) There is diffuse enhancement of the mass following contrast administration (arrows). The enhancement appears to increase the conspicuity of the internal flow voids (arrowheads). This lesion was embolized and the pathology was reported as "vascular malformation."

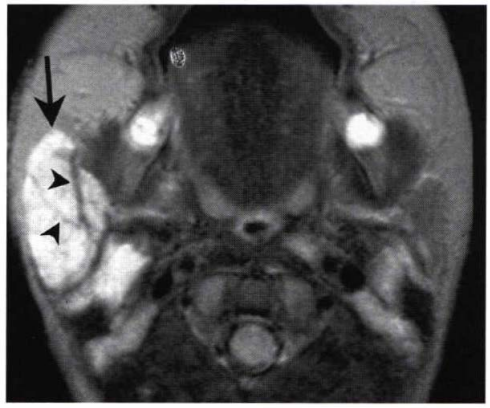

Figure 49–2. Low-flow vascular malformation. Axial T2-weighted image shows a high signal vascular malformation situated in the right parotid gland (arrow). There appear to be internal septations (arrowheads) but there are no distinct flow voids. These findings represent a "low-flow" vascular malformation, probably due to a lymphatic malformation.

Suggested Readings

1. Mulliken JB, Glowacki J. Hemangiomas and vascular malformations in infants and children: a classification based on endothelial characteristics. *Plast Reconstr Surg* 1982;69:412–422.
2. Meyer JS, Hoffer FA, Barnes PD, Mulliken JB. Biological classification of soft tissue vascular anomalies: MR correlation. *AJR Am J Roentgenol* 1991;157:559–564.
3. Waner M, Suen JY. A classification of congenital vascular malformations. In: Warner M, Suen JY, eds. *Hemangiomas and Vascular Malformations of the Head and Neck.* New York: Wiley-Liss; 1999:1–12.

Chapter 50

Lymphatic Malformations

Epidemiology

Lymphatic malformation (*LM*) is the current term used to describe lymphangiomas. Mulliken and Glowacki recommend that the suffix *oma* only be used in lesions that exhibit cellular proliferation, such as a hemangioma. LM is a congenital lesion that results from a defect in embryogenesis of the lymphatic system. Such lesions occur in equal frequency in males and females. They most commonly present in newborn children, with 65% of lesions noted at birth, 80% present at 1 year, and 90% present by 2 years of age. Ten percent of LMs may initially present in adulthood. LMs may be localized or associated with a generalized malformation of the lymphatic system. Advanced generalized disorders may be seen as diffuse lymphangiectasis in utero and are incompatible with life. LM has been associated with a number of syndromes, the most common being Turner's syndrome. Other syndromes include Noonan's syndrome, fetal alcohol syndrome, familial pterygium syndrome, distichiasis–lymphedema syndrome, and various chromosomal aneuploidies.

Embryology

LM is thought to arise from a defect in the normal drainage of the lymphatic channels into the venous system. The result is a progressive enlargement of the isolated lymphatic spaces due to the continued secretion of lymph. There are several proposed explanations for this malformation. The malformation may be due to a portion of the lymphatic network that fails to reestablish a communication with the venous system and is sequestered early in embryogenesis. Early malformations involving the more primitive jugular, subclavian, and axillary sac are thought to result in the formation of the larger cystic hygromas. These lesions occur in soft areolar tissues in areas with wide fascial planes, with the result being sharply demarcated round or oval lesions. Lesions that have smaller cystic spaces and are more diffuse and infiltrative are felt to occur later in embryogenesis. These malformations have time to grow distally along narrower fascial planes and insinuate themselves along vessels and nerve trunks. This probably results in the mixed malformations described by Mulliken and Glowacki such as lymphaticovenous and lymphaticocapillary malformations. Thus LMs that occur in the cheeks, lips, and tongue tend to contain more of an angiomatous component.

Pathology

Pathologically, LMs have been categorized in the past based on the size of the anomalous lymphatic space. It should be noted that *lymphatic malformation* has replaced terms such as *cavernous lymphangioma* and *capillary lymphangioma,* which probably refer to the "mixed" lymphatic malformations described by Mulliken and Glowacki. We present the older terminology below for historical consistency.

Cystic hygroma is the most common form and consists of a honeycomb of very large dilated lymphatic spaces lined by a single layer of flat endothelium. These lesions are often solitary and occur in the presence of an otherwise normal lymphatic system. Seventy-five percent of these lesions occur in the neck. These lesions have a predilection for the posterior compartment of the neck.

A cavernous lymphangioma is composed of mild to moderately dilated lymphatic spaces, the size of which is between the cystic spaces seen in cystic hygromas and capillary hemangiomas. These lesions tend to be situated in the oral cavity or salivary glands. Cavernous LMs tend to be subcutaneous lesions which have penetrated adjacent muscular and neurovascular structures without destroying them. The peripheral location and subcutaneous spread are suggestive of a defect in embryogenesis during a later phase of lymphatic development (9–10 weeks).

Capillary lymphangioma (simple, lymphangioma simplex) is composed of a network of small lymph, thin-walled channels that are the size of capillaries and is the least common form of lymphangioma. These lesions are located predominantly within the epidermis and can occur anywhere throughout the body. Because of their superficial location, capillary lymphangiomas are thought to form the latest in development.

Clinical Findings

The extracranial head and neck is the most common site of LMs (75%). They typically present as a soft, painless neck mass. Lesions that occur in the face are more likely to be mixed LMs. LMs tend to enlarge commensurate with the growth of the child and not by endothelial proliferation. Potential complications include disfigurement, respiratory compromise, and recurrent infections. Rapid enlargement may be due to infection or spontaneous hemorrhage within the lesion.

Treatment

Surgical resection is the treatment of choice for LMs with distinct margins. However, this is difficult for LMs that involve the parotid gland due to their infiltrating nature. It may be difficult to separate the margins of the tumor from the branches of the facial nerve for tumors that involve both the superficial and the deep lobes of the parotid gland. The role of interferon therapy for very advanced and infiltrative lesions is currently under investigation.

Imaging Findings

CT

The classic appearance of an LM is a sharply demarcated, low-attenuation mass that does not contain a visible wall. Large lesions may be multilobular and have considerable mass effect and may displace or replace the parenchyma of the parotid gland. Lesions that have been partially resected or have been repeatedly infected may demonstrate an enhancing wall or contain internal septations. Mixed LMs are heterogeneous and infiltrative. These lesions have a tendency to involve multiple spaces and may extend deeply to involve the parapharyngeal space. Because of the angiomatous components, mixed lesions may enhance with contrast (Fig. 50–1).

MR

A pure LM is low signal on T1-weighted sequences and high signal on T2-weighted sequences. There is no perceptible wall or enhancement following contrast administration. Pure LMs are low-flow lesions and lack flow voids. Mixed malformations are infiltrative heterogeneous lesions that enhance following contrast. The degree of the enhancement is likely due to the angiomatous component of the mixed lesion (Fig. 50–2).

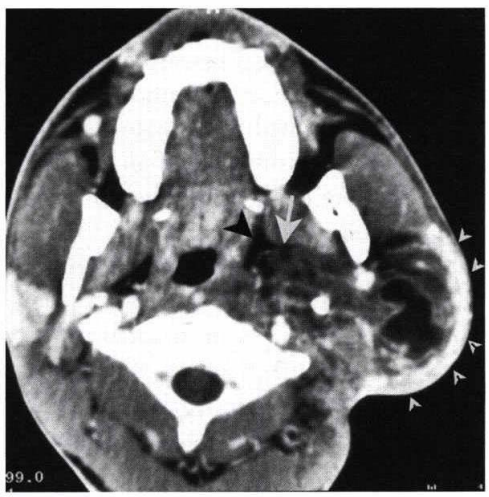

Figure 50–1. CT findings of lymphatic malformations. Axial contrast-enhanced CT demonstrates a heterogeneous lesion replacing the left parotid gland. The mass is predominantly low attenuation with areas of internal linear enhancement. The mass extends into the deep lobe of the parotid gland (arrow) and is distinct from the parapharyngeal space (large arrowhead). The superficial rim of enhancement surrounding the parotid gland is likely due to parotid tissue that is displaced by the deeper lymphatic malformation.

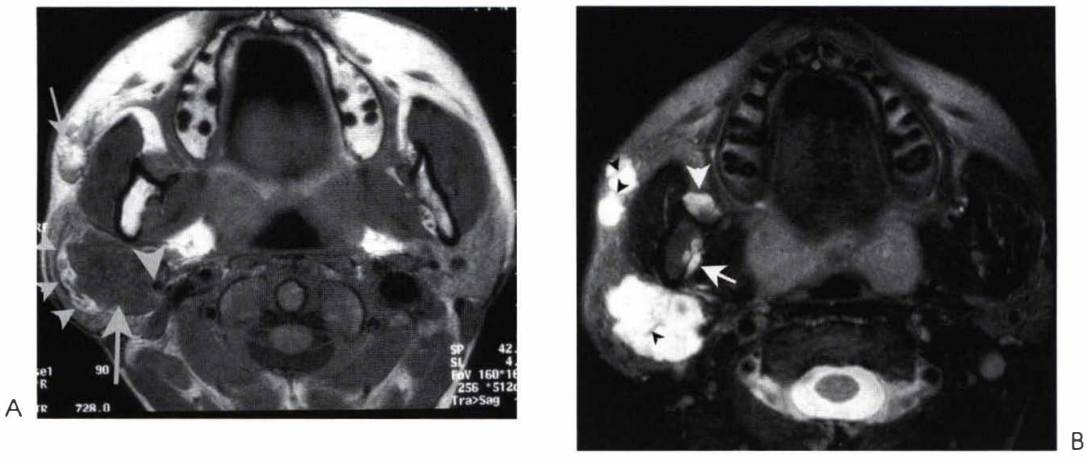

Figure 50-2. MR findings of lymphatic malformation. (A) Noncontrast T1-weighted image shows an intermediate signal mass situated in the superficial lobe of the parotid gland (large arrow). The retromandibular vein is displaced medially conforming the location of the mass (large arrowhead). There is a rim of increased T1-weighted signal along the superficial rim of the mass that could represent blood products or proteinaceous material (small arrowheads). There is an additional component located in the buccal space that may be arising from accessory salivary tissue (small arrow). (B) Axial T2-weighted image shows scattered internal septations (black arrowheads). This sequence also shows areas of lymphatic malformation situated in the masticator space (arrow) and deep buccal space (white arrowhead), which are present on the T1-weighted images shown in (A) but are more readily seen on the T2-weighted images.

Ultrasound

Pure LMs are hypoechoic masses that may occasionally contain internal septations or debris. Doppler analysis may be helpful in identifying and characterizing mixed LMs by identifying and characterizing the presence of intralesional blood flow.

Angiography

Pure LMs are avascular low-flow lesions. However, mixed LMs that have a substantial angiomatous component are hypervascular and have enlarged feeding vessels. Arteriovenous shunting is rare.

Imaging Pearls

- The relationship of a lymphatic malformation with the expected course of the facial nerve must be identified if surgical resection is contemplated.
- A predominantly cystic mass that is transspatial is the characteristic imaging of an LM.

Suggested Readings

1. Zadvinski DP, Benson MT, Kerr HH, et al. Congenital malformations of the cervicothoracic lymphatic system: embryology and pathogenesis. *Radiographics* 1992;1175–1189.
2. Batsakis JG. Vasoformative tumors. In: *Tumors of the Head and Neck*. 2nd ed. Baltimore: Williams and Wilkins; 1979:518–520.
3. Mulliken JB, Glowacki J. Hemangiomas and vascular malformations in infants and children: a classification based on endothelial characteristics. *Plast Reconstr Surg* 1982;69:412–422.
4. Mulliken JB. Vascular malformations of the head and neck. In: Mulliken JB, Young AE, eds. *Vascular Birthmarks: Hemangiomas and Malformations*. Philadelphia: WB Saunders; 1988:301–307.

Chapter 51

Hemangiomas

Epidemiology

Hemangiomas are proliferative endothelial vascular lesions that are identified by their characteristic clinical appearance and course. Forty percent of hemangiomas are present at birth and 60% appear within the first few months of life. Hemangiomas are more common in females than in males (5:1). Common sites of occurrence include skin, face, orbits, larynx, nasal cavity, and deep neck spaces.

The classification proposed by Mulliken and Glowacki distinctly separates hemangiomas from vascular malformations based on biological and clinical characteristics. Previous descriptive terms such as *strawberry, capillary, juvenile,* or *cellular* are not currently used to describe hemangiomas. These older names are now encompassed by the term *hemangioma.* Most authors now feel that cavernous hemangiomas are venous malformations. Port-wine hemangiomas are now considered capillary malformations.

Clinical Findings

Superficial hemangiomas are bright red papular lesions. Subcutaneous hemangiomas often present as a bluish mass that may be difficult to differentiate from a venous malformation or an arteriovenous malformation.

Hemangiomas rapidly grow during the first 12 to 18 months of life (proliferative phase). This is followed by gradual regression (involuting phase) over the next 6 to 10 years. Approximately half of all lesions will completely involute, whereas the remainder will partially involute. Incomplete involution may result in residual telangiectasias, hypoplastic patches, or scarring.

Hemangiomas usually arise in the superficial layers of the skin and mucosa. The majority of hemangiomas have an uneventful course with spontaneous and complete involution. More advanced lesions, depending on their location, may cause severe facial disfigurement, impaired vision, or respiratory stridor.

In the past, hemangiomas have been associated with a variety of syndromes that include Dandy–Walker, Klippel–Trenaunay, Sturge–Weber, Beckwith–Wiedemann, Hippel–Lindau, and Rendu–Osler–Weber. There is also an association with Kasabach–Merritt syndrome; a consumptive coagulopathy complicated by platelet trapping, hemorrhage, or high-output congestive heart failure that may occur with large hemangiomas. These associations were identified prior to the Mulliken and Glowacki classification system. Further investigations will be needed to determine whether these associations are still valid using the currently accepted classification scheme.

Pathology

The proliferative phase consists of proliferating plump endothelial cells with frequent mitoses. The end of the proliferative phase is characterized, by a reduction in the mitotic activity, progressive flattening of the cells, and an abundance of mast cells. Apoptosis and progressive loss of endothelial cells encompassed by large ectatic vascular channels in a matrix of fibrofatty tissue characterize the involuting phase.

Treatment

Because most hemangiomas undergo complete or near-complete spontaneous involution, the treatment is conservative and consists of observation and parental reassurance. More aggressive options such as steroid therapy and compression therapy are reserved for enlarging lesions that result in functional compromise. Surgery is reserved as a secondary procedure following initial therapy or incomplete involution. The role of antiangiogenesis agents is currently under investigation.

Imaging Findings

CT

These are densely enhancing soft tissue masses that may be localized or extend deeply along the fascial planes. Phleboliths are uncommon in true hemangiomas (Fig. 51-1).

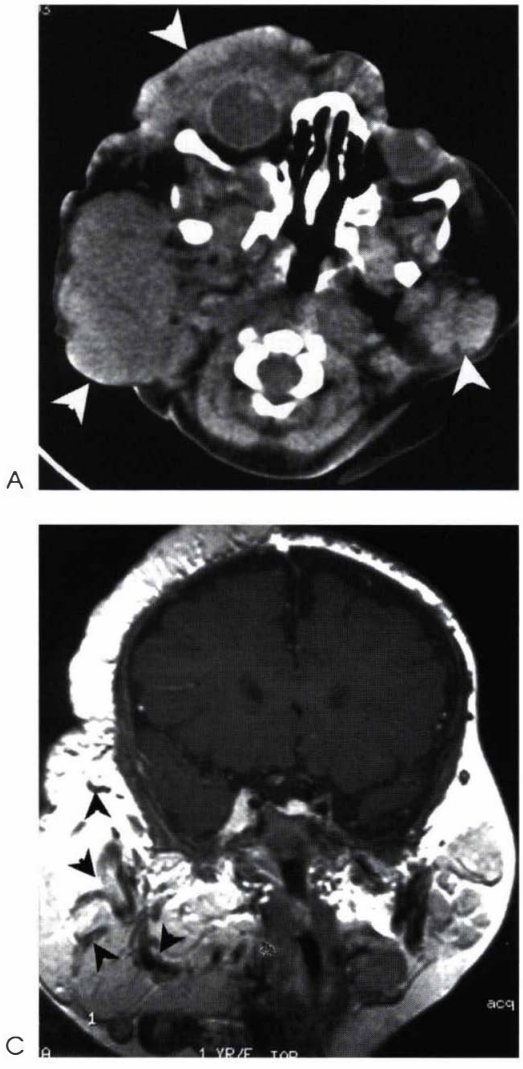

A

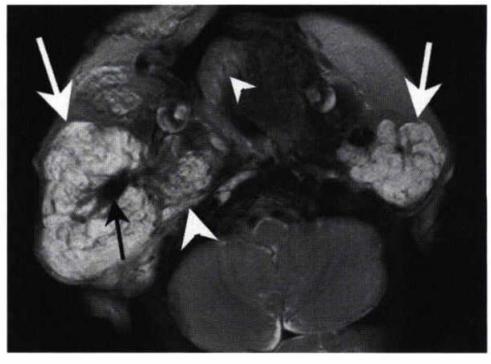

B

C

Figure 51-1. Proliferative phase of a parotid hemangioma.
(A) Noncontrast CT of the face in an infant shows multiple soft tissue masses involving both parotid glands and the right periorbital region (arrowheads). (B) Axial T2-weighted image shows the masses to be high signal (white arrows). Hemangioma is also present in the right parapharyngeal space (large arrowhead) and the right half of the oral tongue (small arrowhead). Note the marked enlargement of the right retromandibular vein (black arrow). (C) Coronal contrast-enhanced T1-weighted image shows multiple enlarged flow voids within the hemangioma (arrowheads). This indicates a high-flow vascular lesion and is characteristic of the proliferative phase of a hemangioma (see Fig. 26-1 for another example of a parotid hemangioma in the proliferating phase.) (A courtesy of Sammy Noujaim, M.D.).

MR

These lesions are soft tissue masses that are intermediate signal on T1-weighted sequences and bright on T2-weighted sequences. These lesions densely enhance following contrast administration. The presence of internal flow voids suggests that these lesions are in the proliferative phase and can be characterized as high-flow lesions. The absence of flow voids suggests that the tumor is involuting and is a low-flow lesion (Fig. 51-2).

Angiography

There is an organized pattern of arterial supply from the enlarged feeding arteries in high-flow lesions. Hemangiomas show an intense parenchymal enhancement with pooling of contrast material. Arteriovenous shunting is uncommon.

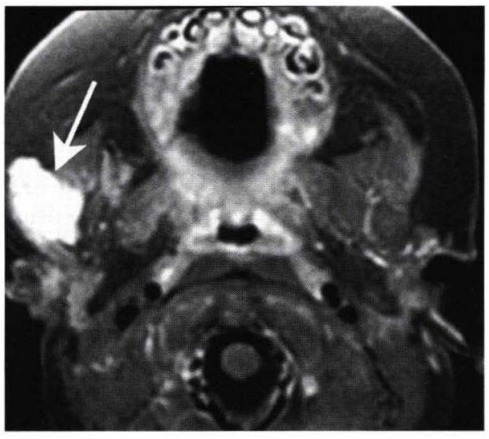

Figure 51-2. Involuting phase of a parotid hemangioma. Axial fat-suppressed, contrast-enhanced, T1-weighted image shows an enhancing hemangioma in the right parotid gland (arrow). The absence of flow voids suggests that the mass is in the involuting phase.

Doppler Ultrasound (see Fig. 26-2)

This technique may be useful in attempting to differentiate between high-flow and low-flow lesions. High-flow hemangiomas in the proliferative phase will demonstrate an arterial waveform whereas involuting low-flow lesions will have a venous waveform.

Imaging Pearls

- Flow-sensitive MR sequences may be helpful to confirm that a mass is a high-flow lesion.
- It is important to try to identify the facial nerve for hemangiomas that involve the parotid gland. However, this may be difficult to identify the retromandibular vein due to multiple dilated vessels that often occur in these high-flow lesions.
- The role of endovascular therapy for hemangiomas is currently under investigation. This approach may be best suited for high-flow hemangiomas in the proliferative phase.
- High-flow hemangiomas can be differentiated from high-flow arteriovenous malformations based on the findings that hemangiomas are associated with a soft tissue mass, whereas there is no parenchymal component associated with an arteriovenous malformation.
- Late involuting (low-flow) hemangiomas may be difficult to differentiate from low-flow venous malformations.

Suggested Readings

1. Mulliken JB, Glowacki J. Hemangiomas and vascular malformations in infants and children: a classification based on endothelial characteristics. *Plast Reconstr Surg* 1982;69:412-422.
2. Meyer JS, Hoffer FA, Barnes PD, Mulliken JB. Biological classification of soft tissue vascular anomalies: MR correlation. *AJR Am J Roentgenol* 1991;157:559-564.
3. Waner M, Suen JY. A classification of congenital vascular malformations. In: Warner M, Suen JY, eds. *Hemangiomas and Vascular Malformations of the Head and Neck*. New York: Wiley-Liss; 1999:1-12.
4. James CA. Diagnostic imaging of congenital vascular lesions. In: Warner M, Suen JY, eds. *Hemangiomas and Vascular Malformations of the Head and Neck*. New York: Wiley-Liss; 1999:171-215.

Section III

Visceral Space

The visceral space is the space that is surrounded by the visceral fascia (Fig. III-1A). Everything you see when you look into someone's mouth or the mucosal surface that the otolaryngologist visualizes during endoscopy is, by definition, in the visceral space (Figs. III-1B, C). The contents of the visceral space in the suprahyoid neck are the nasopharynx and the oropharynx. Therefore, the most common pathologies of the visceral space are processes involving the epithelial lining of the pharynx. The most common malignancy in this space is squamous cell carcinoma. Because the primary component of the visceral space is the pharynx and mucosa, some authors use the term *"pharyngealmucosal" space* as an alternate term for the visceral space. In the infrahyoid neck, the visceral fascia also encircles the hypopharynx, larynx, and thyroid gland. Thus, these structures are also components of the visceral space. Various pathologies of these various areas will be discussed in the following chapters.

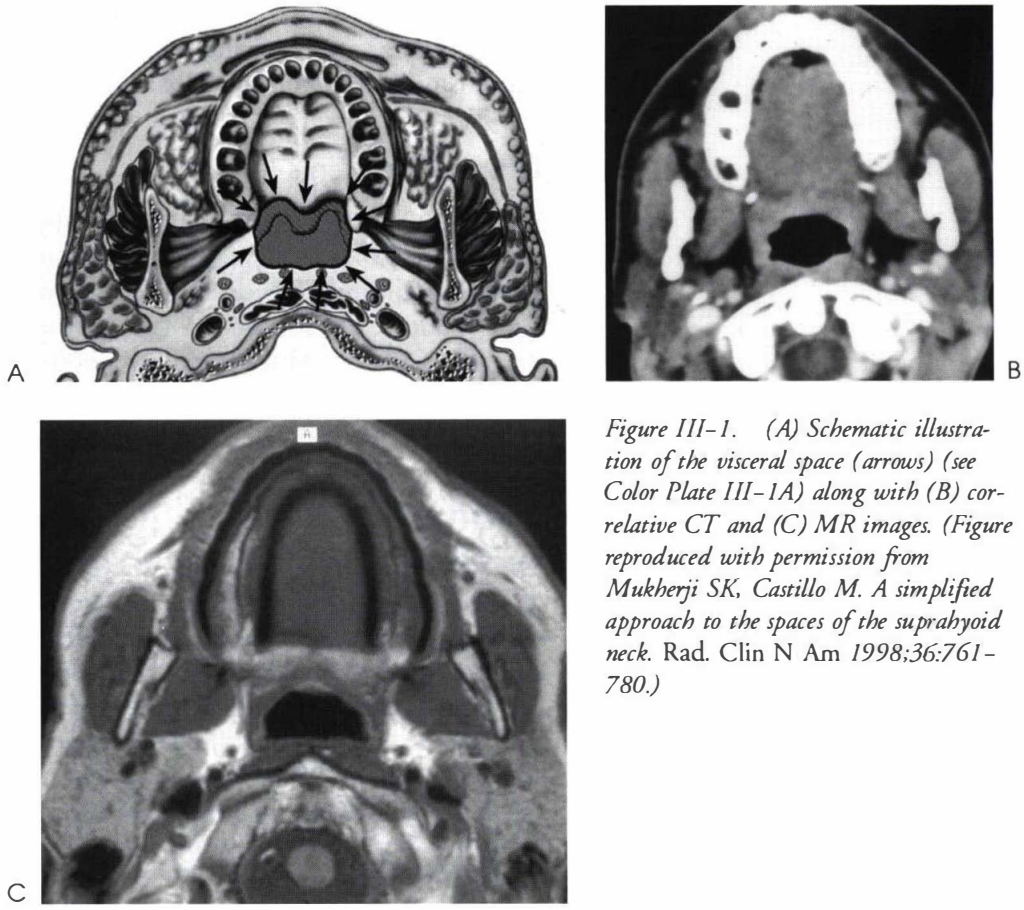

Figure III-1. (A) Schematic illustration of the visceral space (arrows) (see Color Plate III-1A) along with (B) correlative CT and (C) MR images. (Figure reproduced with permission from Mukherji SK, Castillo M. A simplified approach to the spaces of the suprahyoid neck. Rad. Clin N Am *1998;36:761-780.)*

Suggested Readings

1. Harnsberger HR. In: *Handbook of Head and Neck Imaging.* 2nd ed. St. Louis: Mosby Year Book; 1995.
2. Grodinsky M, Holyoke EA. The fasciae and fascial spaces of the head, neck and adjacent regions. *Am J Anat* 1938;63:367-408.
3. Mukherji SK, Castillo M. A simplified approach to the spaces of the extracranial head and neck. *Radiol Clin North Am* 1998;36:761-780.
4. Parker GD, Harnsberger HR, Jacobs JM. The pharyngealmucosal space. *Semin Ultrasound CT MR* 1990;11:460-475.

Chapter 52

Nasopharyngeal Carcinoma

Epidemiology

Nasopharyngeal carcinoma (NPC) is a unique malignancy. The etiology is based on the outcome of the interaction among genetic susceptibility environmental factors including chemical carcinogens and the Epstein-Barr virus (EBV). The high antibody titers to EBV antigens are useful diagnostic markers. The highest incidence rates are found in southern China, and this pattern persists in those who have emigrated. The highest incidence rates are found in Hong Kong followed by Singapore and the United States (Chinese Americans). The incidence rates in whites are very low but a relatively higher incidence is found in African Americans. NPC affects children, adolescents, and the middle-aged. This malignancy is more common in males, with a male to female ratio of 2.5:1.

Clinical Findings

The stages of NPC have been classified by the American Joint Committee on Cancer (AJCC) (Table 52–1). Enlargement of the upper cervical nodes is the most common presenting complaint followed by nasal symptoms such as blood-stained nasal discharge or frank epistaxis. The patients may also have unilateral hearing loss due to a tumor obstructing the eustachian tube leading to serous otitis media (Fig 52–1). Tinnitus occurs in approximately one third of patients. Endoscopically, a mass is easily identified usually originating in the fossa of Rosenmüller.

Pathology

The World Health Organization (WHO) classification recognizes two major types of NPC; namely, squamous cell carcinoma (SCCA) and nonkeratinizing carcinoma, with the latter subdivided into differentiated and undifferentiated subtypes. Undifferentiated carcinoma has in the past been alluded to as lymphoepithelioma (Schmincke's tumor) because of the intimate admixture of undifferentiated carcinoma and the nonmalignant lymphoid cells on light microscopy. Typical well-differentiated SCCA in the nasopharynx is rare, with reported frequencies of $< 2\%$. There is a strong association between EBV and undifferentiated carcinoma. Differentiated nonkeratinizing carcinoma also exhibits significant EBV associations, but they are not as strong and consistent as those of undifferentiated carcinoma. NPC–EBV associations are also present but are relatively weak in well-differentiated SCCA.

Table 52–1
Sixth American Joint Committee on Cancer Staging Classification for Oropharynx Cancer

Tis	Carcinoma in situ
T1	Tumor $\leq$ 2 cm in greatest diameter
T2	Tumor $>$ 2 cm but $\leq$ 4 cm in greatest diameter
T3	Tumor $>$ 4 cm in greatest diameter
T4a	Tumor invades larynx, deep/extrinsic muscle of tongue, medial pterygoid, hard palate, or mandible
T4b	Tumor invades lateral pterygoid muscle, pterygoid plates, lateral nasopharynx, or skull base, or encases carotid artery

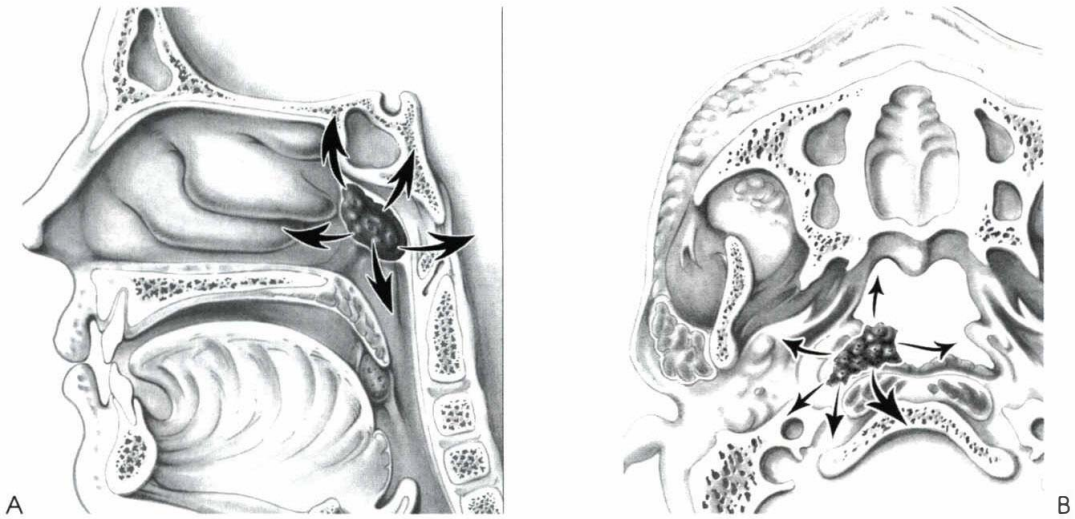

Figure 52-1. Early nasopharyngeal carcinoma. Axial contrast-enhanced MR image shows an enhanced tumor (arrow) originating from the right fossa of Rosenmüller. The tumor is entirely confined to the mucosal space.

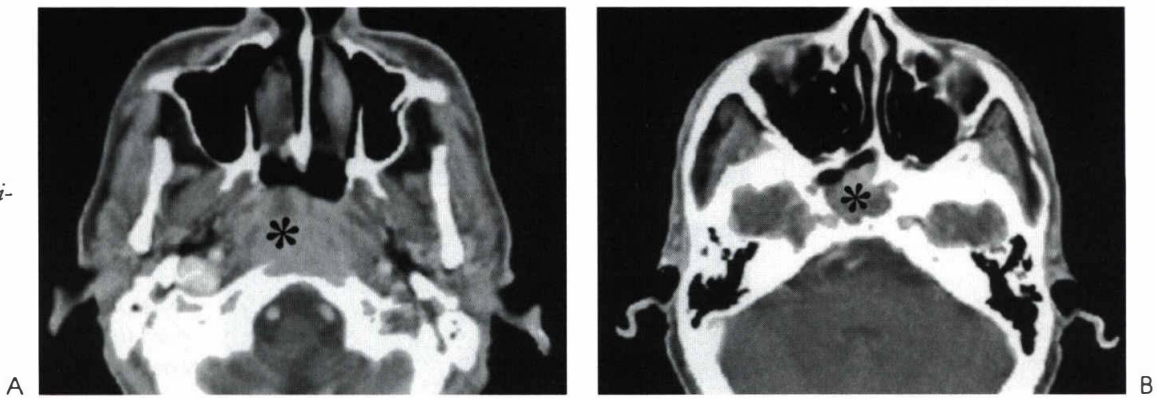

Figure 52-2. Nasopharyngeal carcinoma with skull base erosion. (A) Axial contrast-enhanced CT shows a large tumor in the nasopharynx (asterisk). (B) Axial contrast-enhanced CT shows superior tumor extension into the sphenoid sinus (asterisk).

Treatment

NPC is vety sensitive to irradiation, and the mainstay of treatment is radiation therapy. The role of surgery is restricted to patients with small tumor recurrences. However, surgery is the treatment of choice for cervical nodal recurrence. Previously, chemotherapy was reserved for use in patients with tumor recurrence or metastatic disease. It is now rarely used in combination with radiation therapy for advanced stage disease.

Imaging Findings

CT

NPC is an aggressive tumor. Superiorly, it may invade the skull base and extend intracranially. Inferiorly, it spreads to the oropharynx. It may spread anteriorly to the nasal cavity, laterally to the masticator space, and posteriorly to invade the retropharyngeal structures and the carotid sheath. Retropharyngeal and cervical lymphadenopathy are frequently encountered (Fig. 52-2).

MR

MR is the study of choice for evaluating NPC. It is superior to CT for detecting perineural spread along the mandibular nerve, intracranial tumor extent, and skull base marrow involvement (Fig. 52-3).

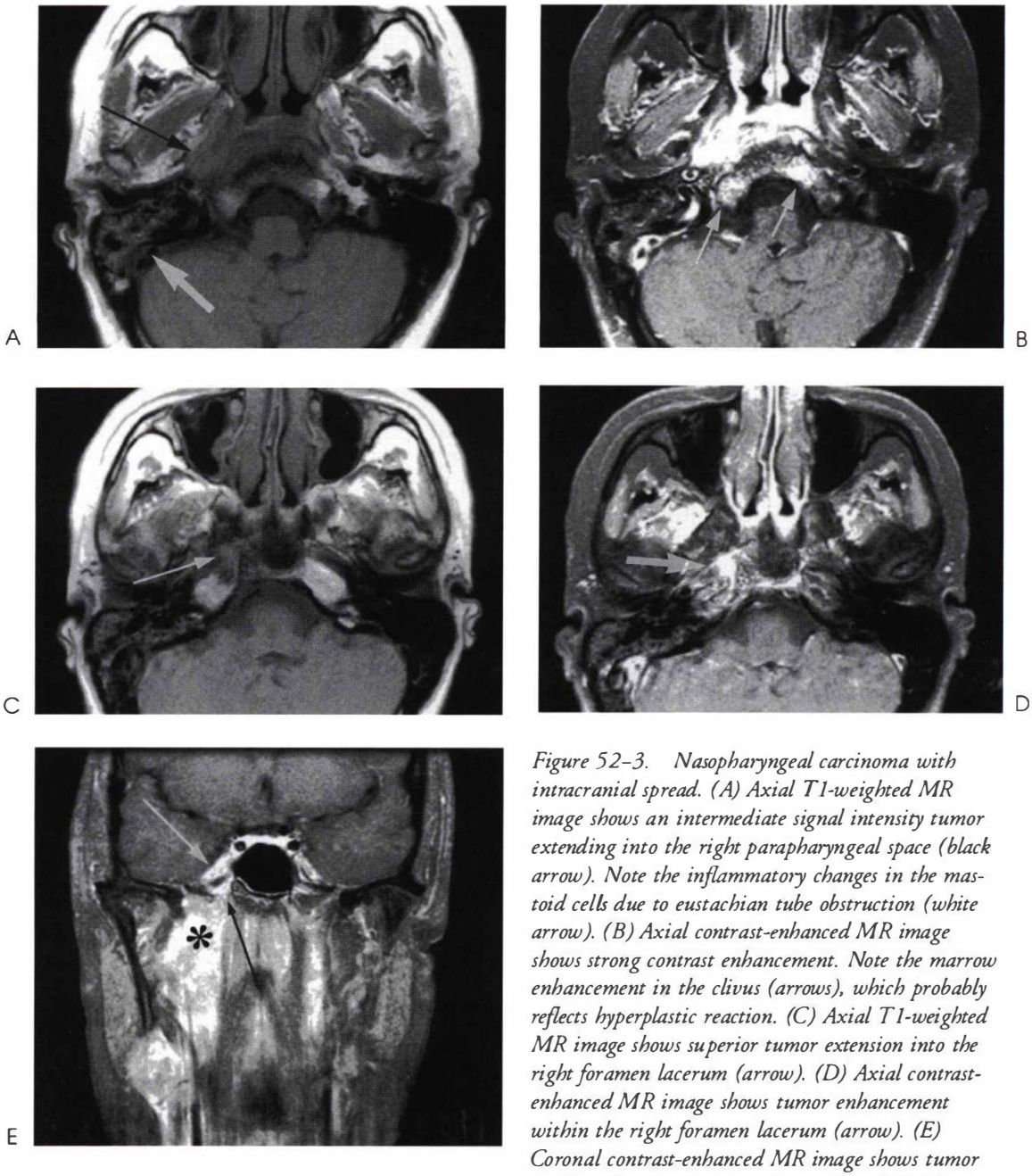

Figure 52–3. Nasopharyngeal carcinoma with intracranial spread. (A) Axial T1-weighted MR image shows an intermediate signal intensity tumor extending into the right parapharyngeal space (black arrow). Note the inflammatory changes in the mastoid cells due to eustachian tube obstruction (white arrow). (B) Axial contrast-enhanced MR image shows strong contrast enhancement. Note the marrow enhancement in the clivus (arrows), which probably reflects hyperplastic reaction. (C) Axial T1-weighted MR image shows superior tumor extension into the right foramen lacerum (arrow). (D) Axial contrast-enhanced MR image shows tumor enhancement within the right foramen lacerum (arrow). (E) Coronal contrast-enhanced MR image shows tumor in the right parapharyngeal space (asterisk). Note tumor extension through the right foramen lacerum (black arrow) and enlargement of the right cavernous sinus (white arrow).

Imaging Pearls

- The most common route of intracranial spread is via the foramen ovale. Fat is normally present beneath the foramen ovale. The obliteration of fat in this region signifies early perineural involvement of V_3 and spread through the foramen ovale.
- In patients with metastatic cervical lymphadenopathy involving level V of unknown origin, a histological diagnosis of undifferentiated carcinoma should prompt a search in the nasopharynx. Similarly, a significant increase in antibodies to the EBV should also alert the clinician to the possibility of a nasopharyngeal tumor.
- NPC has a propensity to spread submucosally, especially in patients with recurrent tumors. MR imaging is recommended in this group of patients.

Suggested Readings

1. Chong VFH, Fan YF. Skull base erosion in nasopharyngeal carcinoma. *Clin Radiol* 1996;51:625–631.
2. Chong VFH, Fan YF. Detection of recurrent nasopharyngeal carcinoma: MRI vs CT. *Radiology* 1997;202:463–470.
3. Chong VFH, Fan YF, Mukherji SK. Nasopharyngeal carcinoma. *Semin Ultrasound CT MR* 1998;19:449–462.

Chapter 53

Nasopharyngeal Carcinoma with Eustachian Tube Extension

Epidemiology

Nasopharyngeal carcinoma (NPC) usually originates in the lateral pharyngeal recess (fossa of Rosenmüller). The tumor can easily invade the opening of the eustachian tube, which is located immediately anterior and inferior to the fossa of Rosenmüller. Patients in the high-risk group who present with tinnitus or serous otitis media should be carefully evaluated. Risk factors include several factors: age (> 30 years), sex (male > female), ethnic group (especially ethnic Chinese), and a family history of NPC in a first-degree relative.

Clinical Findings

The most common ear symptom is unilateral hearing loss. This symptom is related to tumor obstructing the eustachian tube resulting in serous otitis media. Eustachian tube dysfunction can also be caused by tumor infiltration of the muscles of deglutination. In the absence of any infection or allergic nasal symptoms, a nasopharyngeal biopsy is indicated in all high-risk patients with unilateral serous otitis media. Epstein-Barr virus (EBV) serology may provide further useful information, especially in patients with a clinically occult primary.

Pathology

The EBV expresses several antigens. The viral capsid antigen (VCA) and the early antigen (EA) have diagnostic roles in NPC. An elevated anti-VCA titer is a highly sensitive indicator but is not very specific (sensitivity ≤ 95%, specificity 80–95%). On the other hand, anti-EA is more specific (> 95%) for NPC than anti-VCA but is less sensitive (90%). The two assays should be done together because they are clearly complementary. Significantly elevated EBV antibodies suggest the possibility of NPC. The value of serial EBV titers in the detection of tumor recurrence is controversial. In many patients with no clinical evidence for persistent or recurrent disease, the titers of antibodies may remain elevated. When persistently raised titers fall, relapse can still be detected by biopsies.

Treatment

The mainstay of treatment is radiation therapy. Previously, chemotherapy was reserved for use in patients with tumor recurrence or metastatic disease. It is now gaining acceptance for use together with radiation therapy as initial treatment. Serous otitis media has a self-limiting course and will resolve following successful treatment of the primary lesion. Follow-up evaluation usually shows progressive improvement in conductive hearing loss. However, long-term follow up may show progressive sensorineural hearing loss due to radiation damage to the inner ear structures and cochlear nerve.

Imaging Findings

CT

CT shows intermediate density fluid in the mastoid cells or the middle ear cleft either unilaterally or bilaterally, depending on the size of the tumor. It is usually difficult to identify the continuity of the tumor from the nasopharynx to the middle ear cleft on contrast-enhanced CT (Fig. 53–1A).

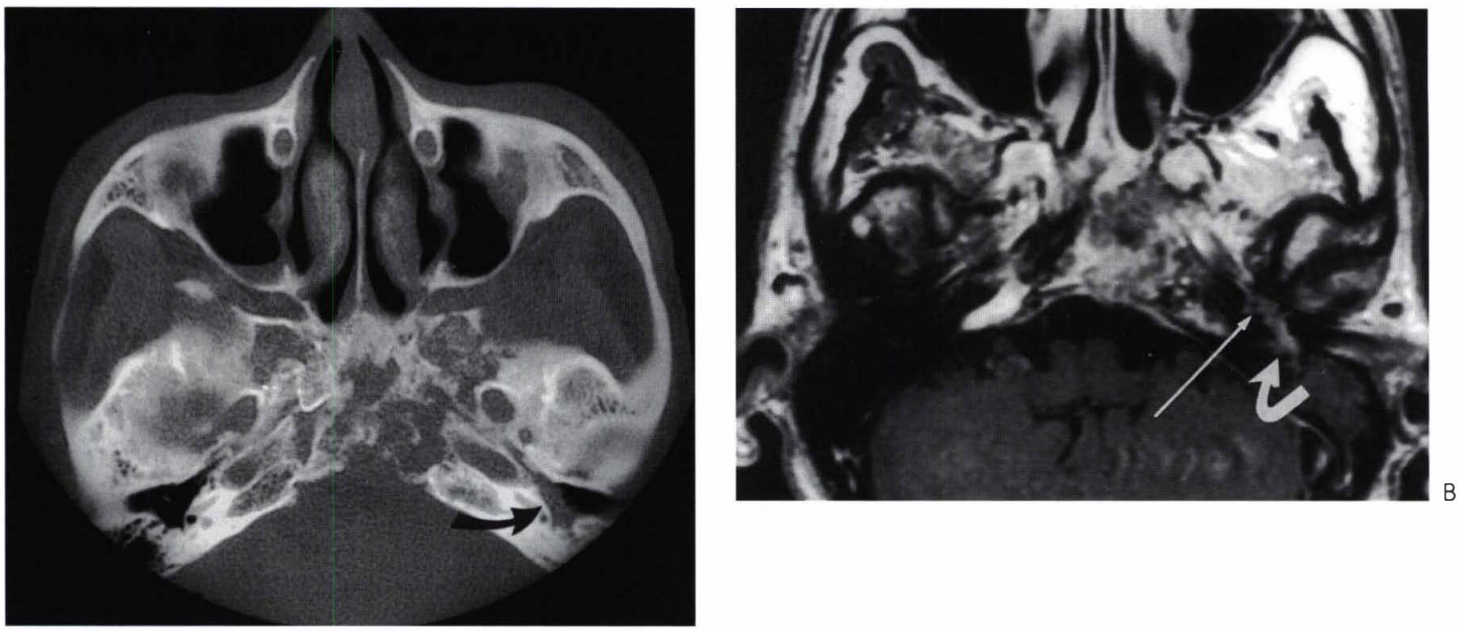

A B

Figure 53-1. Nasopharyngeal carcinoma with involvement of the eustachian tube. (A) Axial CT shows nasopharyngeal recurrence with extensive skull-base erosions. Note the soft tissue density in the left middle ear (curved arrow). (B) Axial contrast-enhanced MR image shows tumor extension along the left eustachian tube (long straight arrow) and enhancing tissues in the left middle ear cleft (curved arrow).

MR

Fluid in the middle ear cleft and the mastoid cells shows an intermediate signal intensity on T1-weighted images and high signal intensity on T2-weighted images. Following the injection of contrast enhancement, the tumor within the nasopharynx, eustachian tube, and middle ear cavity may be demonstrated (Fig. 53-1B).

Imaging Pearls

- The fossa of Rosenmüller may show normal asymmetry. This is due to the variable amount of lymphoid tissues or unequal distension by air within the pharyngeal recess. In contrast, the openings of the eustachian tube are usually symmetrical. A small lesion here may give rise to serous otitis media.
- The eustachian tube runs from the anteromedial portion of the middle ear cleft to the nasopharynx in an anteromedial direction. The nasopharyngeal end is lower than the middle ear portion. The eustachian tube can therefore be traced from the nasopharyngeal end to the middle ear opening by examining serial sections. A useful landmark is the horizontal portion of the carotid artery in the petrous temporal bone. The eustachian tube runs in an orientation anterior and parallel to the artery.

Suggested Readings

1. de Vathaire F, Sancho-Garnier H, de The H, et al. Prognostic value of EBV markers in the clinical management of nasopharyngeal carcinoma: a multicenter follow-up study. *Int J Cancer* 1988;42:176–181.
2. Wyatt DE, Brooker DS, Connoly JH, Coyle DV. Prognostic value of Epstein-Barr virus serology in patients with nasopharyngeal carcinoma. *J Infection* 1993;26:171–175.
3. Hsu MM, Young YH, Lin KL. Eustachian tube function of patients with nasopharyngeal carcinoma. *Ann Otol Rhinol Laryngol* 1995;104:453–455.
4. Sham JST, Wei WI, Lau SK, et al. Serous otitis media and paranasopharyngeal extension of nasopharyngeal carcinoma. *Head Neck* 1992;14:19–23.

Chapter 54

Nasopharyngeal Carcinoma with Pterygopalatine Fossa and Orbital Extension

Epidemiology

Nasopharyngeal carcinoma (NPC) often spreads anteriorly into the nasal fossa. This tumor may infiltrate the sphenopalatine foramen and extend through the pterygopalatine fossa in 15% of patients. In advanced cases, tumor may continue to spread into the orbital apex and subsequently through the superior orbital fissure into the intracranial cavity. NPC with intracranial extension may be seen in 31% of patients, but the most common route of spread is through the foramen ovale followed by direct tumor erosion through the skull base.

Clinical Findings

Involvement of the pterygopalatine fossa causes hypoesthesia or pain over the cheeks and this can be readily verified clinically by examining the cutaneous sensation over the distribution of the infraorbital nerve. The patient may also have concomitant weakness of the ocular muscles and diplopia.

Pathology

Tumor within the pterygopalatine fossa often usually widens the fossa, invades the pterygopalatine ganglion, or infiltrates the infraorbital nerve. Tumor may also spread intracranially via perineural involvement of the maxillary nerve and the nerve of the Vidian canal. Tumor in the orbital apex can cause dysfunction of the extraocular muscles. This is because Zinn's ring (attachment of the extraocular muscles) is located in the orbital apex.

Treatment

NPC is treated with radiation therapy, and the radiation portals should include the orbital apex. Because of this requirement, almost all patients will subsequently become visually impaired or blind. Symptoms of decreased vision set in slowly and gradually over a few years.

Imaging Findings

CT

The pterygopalatine fossa is filled with low-density fat. Early tumor invasion obliterates the fat density and subsequently widens the fossa. These features can be readily identified on CT. Enhanced tumor can also be easily identified in the orbital apex by noting the effacement of the normal fat density. Diagnosis of superior orbital fissure erosion or widening is usually straightforward (Fig. 54–1).

MR

On T1-weighted images the normal fat-filled pterygopalatine fossa shows high signal intensities. On T1-weighted images, the high fat signal intensity is replaced by intermediate signal intensity tumor. Contrast-enhanced studies should be performed with an added fat suppression pulse to prevent a decrease in tumor conspicuity, especially in the orbital apex.

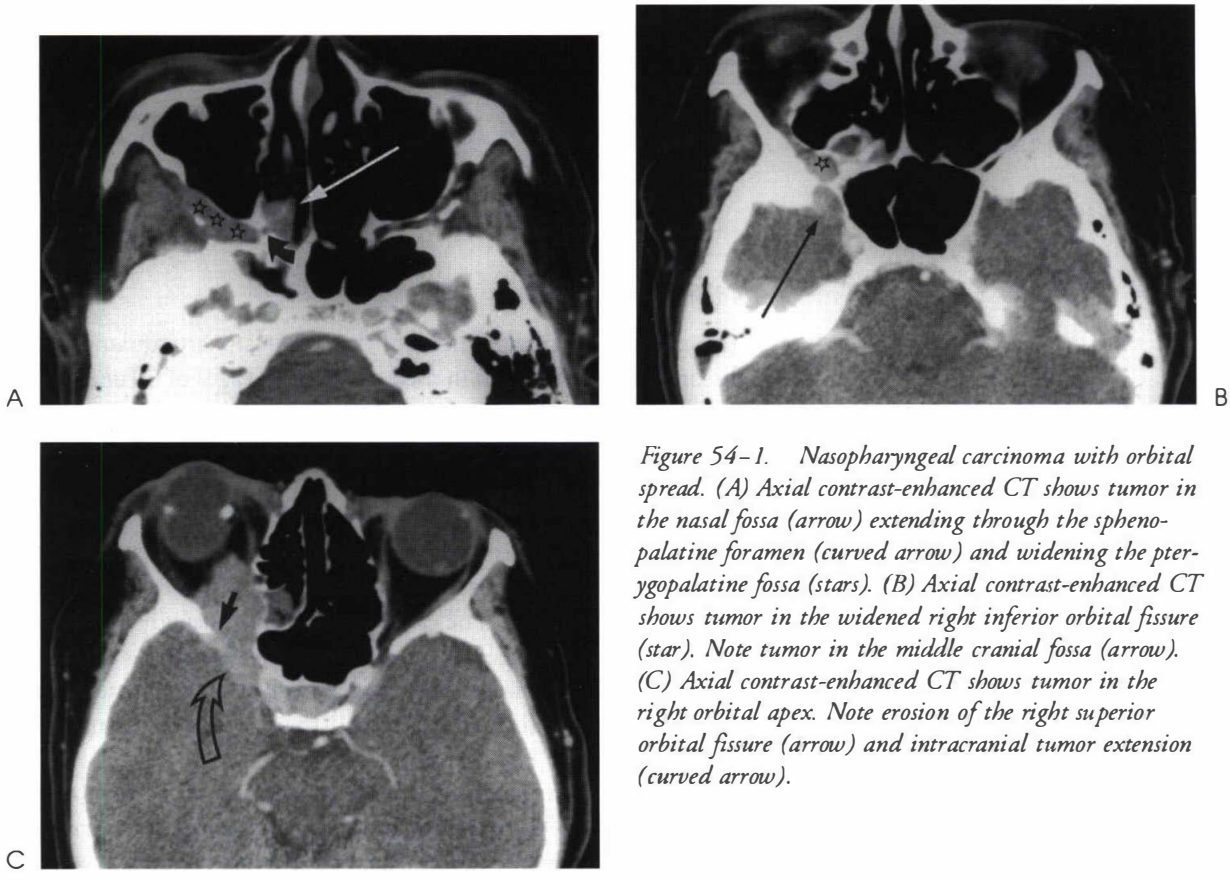

Figure 54–1. Nasopharyngeal carcinoma with orbital spread. (A) Axial contrast-enhanced CT shows tumor in the nasal fossa (arrow) extending through the sphenopalatine foramen (curved arrow) and widening the pterygopalatine fossa (stars). (B) Axial contrast-enhanced CT shows tumor in the widened right inferior orbital fissure (star). Note tumor in the middle cranial fossa (arrow). (C) Axial contrast-enhanced CT shows tumor in the right orbital apex. Note erosion of the right superior orbital fissure (arrow) and intracranial tumor extension (curved arrow).

Imaging Pearls

- Involvement of the maxillary nerve (V_2) can be demonstrated on contrast-enhanced MR images. The thickened maxillary nerve shows uniform enhancement and can be identified adjacent to lateral walls of the sphenoid sinus. Further retrograde spread to the cavernous sinus, trigeminal ganglion, and trigeminal nerve may be demonstrated.
- Extension into the pterygopalatine fossa also places the patient at risk for retrograde spread along the nerve of the vidian canal. Tumor may course along this nerve, which extends along the floor of the cavernous sinus. The tumor may continue to extend posteriorly along the greater superficial petrosal nerve, which communicates with the geniculate ganglion associated with cranial nerve VII. This spread pattern should be evaluated for in all patients with tumor extension in the pterygopalatine fossa, especially if the patient's symptoms are associated with the trigeminal and facial nerves.

Suggested Readings

1. Chong VFH, Fan YF, Khoo JBK. Nasopharyngeal carcinoma with intracranial spread: CT and MR characteristics. *J Comput Assist Tomogr* 1996;20:563–569.
2. Chong VFH, Fan YF. Pterygopalatine fossa and maxillary nerve infiltration in nasopharyngeal carcinoma. *Head Neck* 1997;19:121–125.
3. Chong VFH, Fan YF, Mukherji SK. Nasopharyngeal Carcinoma. *Semin Ultrasound CT MR* 1998;19:449–462.

Chapter 55

Squamous Cell Carcinoma of the Soft Palate

Epidemiology

The majority of malignancies of the soft palate are squamous cell carcinoma (SCCA). The disease is most common in men between the ages of 60 and 70. The most common risk factors are tobacco and excessive alcohol use.

Clinical Findings

Most cases of SCCA of the soft palate occur on the oropharyngeal side of the soft palate. The stages of SCCA have been classified by the American Joint Committee on Cancer (AJCC) (Table 55-1). The earliest symptom is usually a sore throat that can be exacerbated by eating or drinking. Advanced lesions that spread to adjacent areas may cause otalgia in addition to a sore throat. Very aggressive tumors will extend into the masticator space and cause trismus or temporal headaches. Extension into the nasopharynx may result in ipsilateral otitis media (Fig. 55-1).

There is a high incidence of neck metastases at the time of initial presentation, with between 40 and 45% of patients presenting with palpable cervical metastases. The lymphatic drainage is complex. Three separate drainage pathways for the soft palate—anterior, middle, and posterior—are described. Of these three, the middle is the most constant pathway. The lymphatic vessels of the middle path drain into Group II nodes and have crossed lymphatic drainage.

The lymphatics that constitute the posterior pathways are present in 60% of cases. These vessels drain posteriorly into the lateral retropharyngeal lymph nodes. Crossed drainage of the posterior pathways has been shown to be present in 50% of individuals. The anterior pathway is present in half of individuals and drains into the Group I lymph nodes and has crossed lymphatics in 50% of cases.

Pathology

The tumors are often reddish with ill-defined borders. They may be associated with a background of leukoplakia. The majority of SCCA of the soft palate are well-differentiated, unlike the other subsites of the oropharynx, which tend to be undifferentiated and anaplastic.

Table 55-1
Sixth American Joint Committee on Cancer Staging Classification for Oropharynx Cancer

Tis	Carcinoma in situ
T1	Tumor ≤ 2 cm in greatest diameter
T2	Tumor > 2 cm but ≤ 4 cm in greatest diameter
T3	Tumor > 4 cm in greatest diameter
T4 a	Tumor invades larynx, deep/extrinsic muscle of tongue, medial pterygoid, hard palate, or mandible
T4 b	Tumor invades lateral pterygoid muscle, pterygoid plates, lateral nasopharynx, or skull base, or encases carotid artery

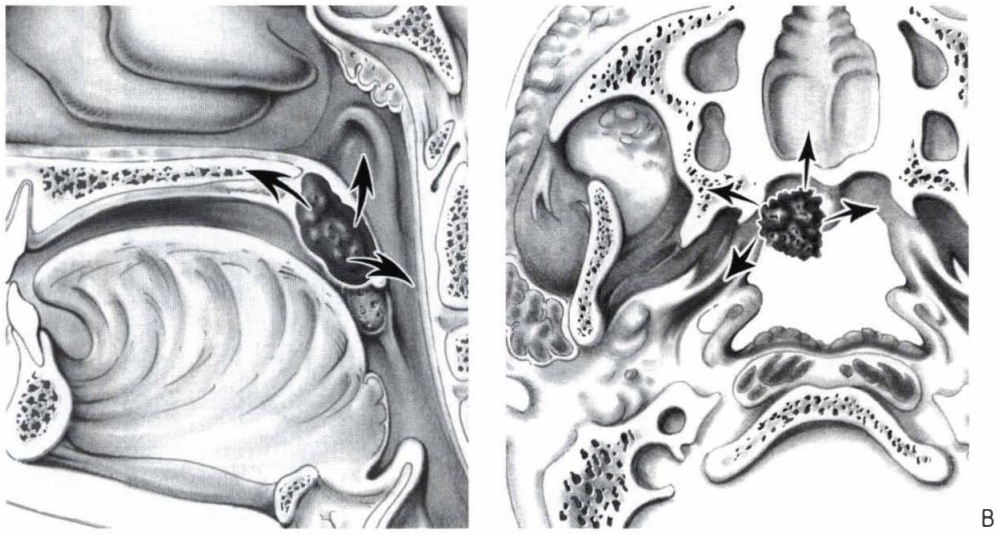

Figure 55-1. (A) Sagittal and (B) axial schematic illustrations demonstrate the potential spread patterns of soft palate carcinoma (Reprinted with permission from Mukherji SK, Pillsbury H, Castillo M. Imaging squamous cell carcinomas of the upper aerodigestive tract: what the clinicians need to know. Radiology *1997;205:629-646.)*

Treatment

The treatment of soft palate carcinomas depends on the size of the primary tumor and institutional preference. Another factor that will directly affect treatment is the presence of enlarged retropharyngeal lymph nodes. Early lesions may be treated with definitive radiation therapy or surgical resection. The presence of an enlarged retropharyngeal lymph node warrants specifically including these nodes in RT ports or exploring this area if the patient chooses to be treated surgically. Combined chemotherapy and radiation therapy is gaining acceptance for advanced tumors. Superior extension into the nasopharynx precludes surgical resection at many institutions.

Imaging Findings

CT

These tumors manifest as abnormal enhancement and soft tissue thickening within the soft palate. The involvement is often midline. The tumors are best evaluated by coronal imaging. Bone erosion is rare. Advanced tumors invade the pterygoid or buccinator muscles. It is common for these tumors to extend superiorly to invade the nasopharynx either mucosally or submucosally. Involvement of the nasopharynx will result in distortion of the normal surface anatomy of the nasopharynx (opening of the eustachian tube, torus tubarius, fossa of Rosenmüller) (Fig. 55-2).

MR

These tumors are intermediate signal on T1-weighted sequences and intermediate to high signal on T2-weighted sequences. These aggressive lesions diffusely enhance with contrast. MR is the study of choice for evaluating the extent of SCCA of the soft palate and involvement of retropharyngeal lymph nodes. The multiplanar capabilities are also useful for accurately assessing the margins of the tumor (Fig. 55-3).

Imaging Pearls

- Special attention must be given to evaluate the presence of metastases to the retropharyngeal lymph nodes. This lymphnode group is clinically occult and despite its proximity to the soft palate is not explored during standard resection of soft palate carcinomas. These lymph nodes may also be underdosed in standard RT treatment ports for soft palate carcinomas. These lymph nodes are considered as cervical lymph nodes for staging purposes.

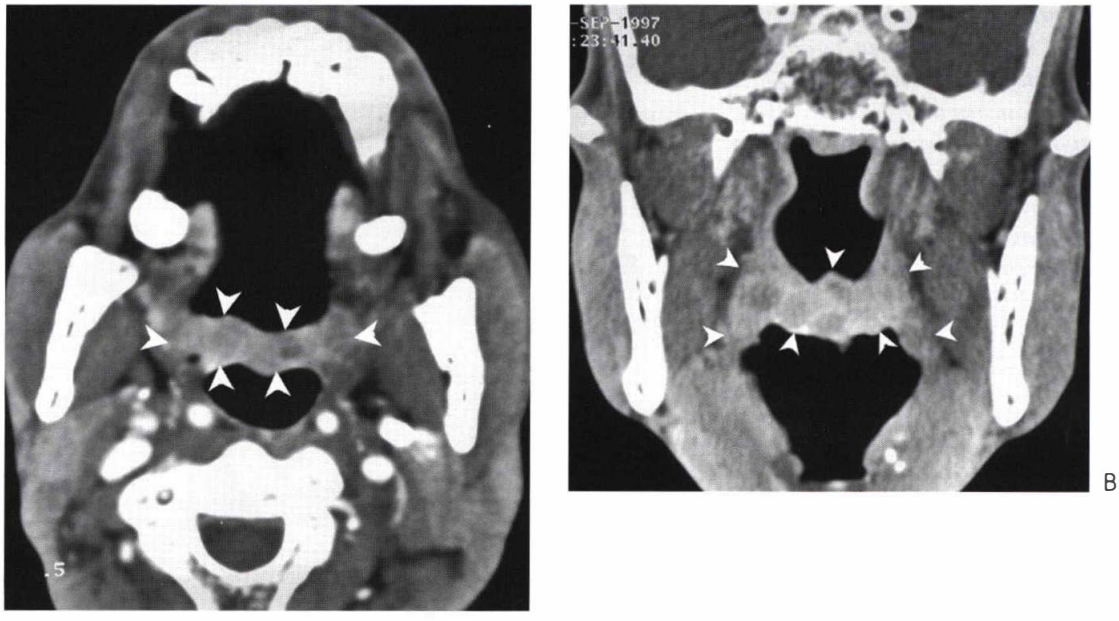

Figure 55-2. (A) Axial contrast-enhanced CT demonstrates a midline soft tissue mass involving the soft palate (arrowheads). (B) Coronal image demonstrates the full extent of the tumor (arrowheads).

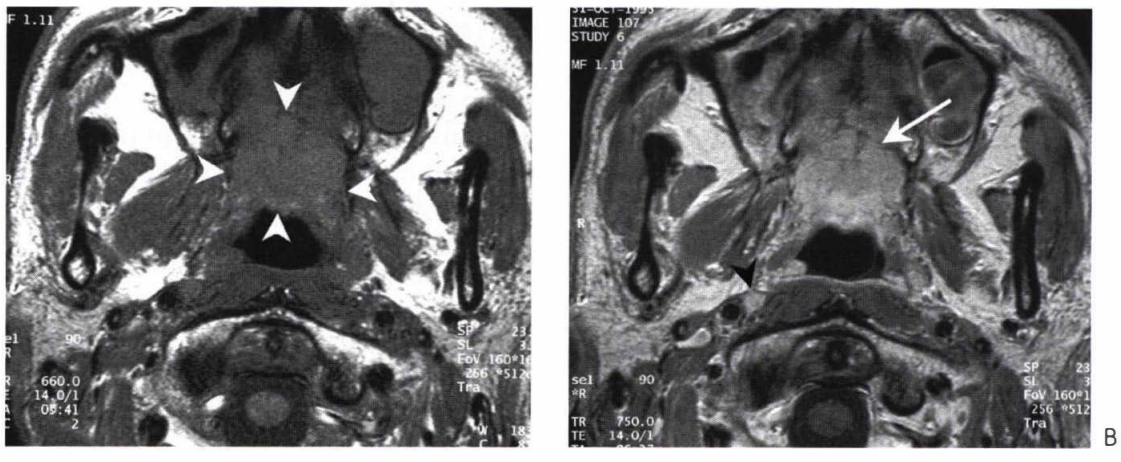

Figure 55-3. (A) Noncontrast axial T1-weighted image demonstrates a squamous cell carcinoma of the soft palate (arrowheads). The mass is intermediate signal and crosses the midline. (B) The tumor homogeneously enhances following contrast administration (arrowhead). There is an enlarged right retropharyngeal lymph node that is suspicious for early metastases (arrowhead). Because retropharyngeal lymph nodes are a primary echelon drainage site for the soft palate, it is important to include these lymph nodes in the radiation field if the patient elects to be treated with radiation therapy.

- The following information will directly affect treatment of a soft palate carcinoma and must be conveyed:
  - Detailed evaluation of submucosal extension into the soft tissues of the neck (pre- and poststyloid parapharyngeal space, nasopharynx)
  - Tongue base invasion
  - Encasement of the carotid artery
  - Bone erosion
  - Prevertebral muscle invasion

Suggested Readings

1. Mukherji SK, Pillsbury H, Castillo M. Imaging squamous cell carcinomas of the upper aerodigestive tract: what the clinicians need to know. *Radiology* 1997;205:629–646.
2. Million RR, Cassisi NJ, Mancuso AA. Oropharynx. In: Million RR, Cassisi NJ, eds. *Management of Head and Neck Cancer: A Multidisciniplinary Approach.* Philadelphia: JB Lippincott; 1994:401–430.
3. Batsakis JG. Squamous cell carcinoma of the oral cavity and oropharynx. In: Batsakis JG, ed. *Tumors of the Head and Neck.* Baltimore: Williams and Wilkins; 1979:144–176.

Chapter 56

Squamous Cell Carcinoma of the Palatine (Faucial) Tonsil

Epidemiology

Squamous cell carcinoma (SCCA) of the palatine tonsil accounts for between 1.5 and 3.0% of all cancers of the upper aerodigestive tract. This is second only in incidence to laryngeal carcinomas in this region. Men are affected more than women. The peak incidence is in the seventh decade in men and the sixth decade in women. The most common risk factors are excessive tobacco and alcohol use.

Clinical Features

The clinical findings are nonspecific and may often be subtle. The stages of SCCA have been classified by the American Joint Committee on Cancer (Table 56-1). The initial symptom may only be a sore throat. However, the presence of a sore throat plus otalgia should increase the suspicion of an underlying malignancy. Many patients will initially present with a neck mass. The palatine tonsil is a common location for patients that have neck metastases but no visible lesion (Fig. 56-1). This is referred to as an unknown primary tumor. Many institutions perform a tonsillectomy on the side of the nodal metastases due to the high likelihood of metastases from early tonsillar carcinomas. In fact, > 70% of patients with tonsillar carcinomas will present with neck metastases at initial examination. The primary echelon lymph nodes are to the ipsilateral jugular chain and the retropharyngeal lymph nodes. The spinal accessory and submandibular groups are also at risk. Tumors that extend inferiorly to the tongue base or superiorly to the soft palate attain the lymphatic drainage of these subsites. Contralateral involvement is less common, occurs in approximately 10% of cases, and is usually associated with spread to these areas.

Pathology

The majority (> 90%) of epithelial neoplasms of the tonsil are squamous cell carcinoma. These tend to be undifferentiated or anaplastic tumors that metastasize early.

Treatment

Early T1 and T2 lesions that do no extend through the visceral fascia into the parapharyngeal space can be treated with definitive RT or a wide local excision using a transoral approach. The surgical treatment for advanced tumors may be resected using a mandibular swing approach for tumors that are not adjacent to the mandible. The surgical resection for larger tu-

Table 56-1
Sixth American Joint Committee on Cancer Staging Classification for Oropharynx Cancer

Tis	Carcinoma in situ
T1	Tumor ≤ 2 cm in greatest diameter
T2	Tumor > 2 cm but ≤ = 4 cm in greatest diameter
T3	Tumor > 4 cm in greatest diameter
T4a	Tumor invades larynx, deep/extrinsic muscle of tongue, medial pterygoid „ hard palate, or mandible
T4b	Tumor invades lateral pterygoid muscle, pterygoid plates, lateral nasopharynx, or skull base, or encases carotid artery

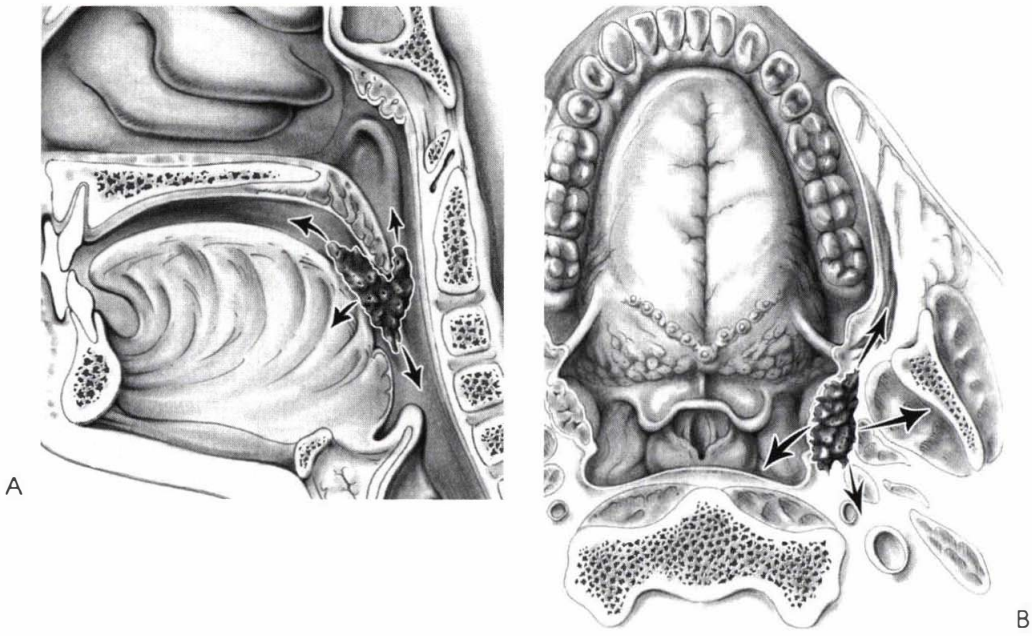

Figure 56-1. (A) Sagittal and (B) axial schematic illustrations demonstrate the potential spread patterns of tonsillar carcinoma involving the palatine tonsil (arrows). (Reprinted with permission from Mukherji SK, Pillsbury H, Castillo M. Imaging squamous cell carcinomas of the upper aerodigestive tract: what the clinicians need to know. Radiology. *1997;205:629-646.)*

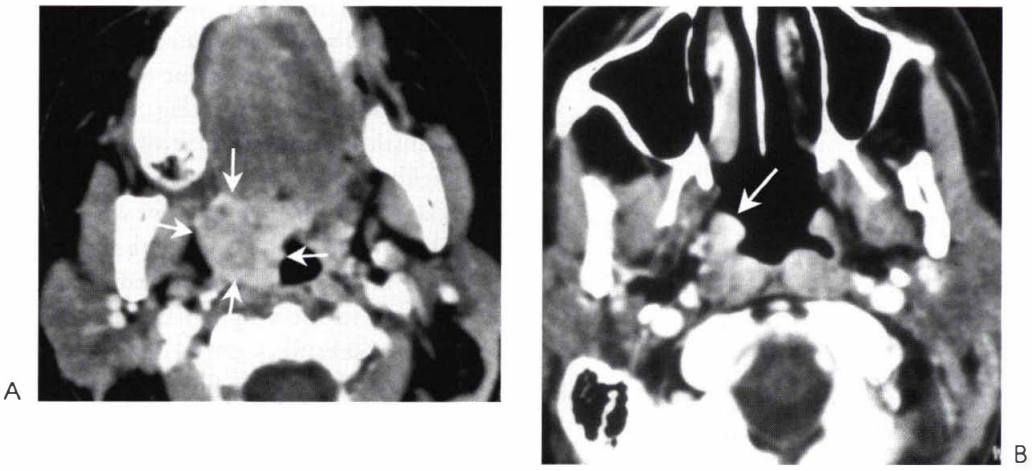

Figure 56-2. (A) Axial contrast-enhanced T1-weighted image demonstrates the characteristic appearance of a palatine (faucial) tonsil carcinoma (arrows). (B) Axial image performed at the level of the nasopharynx shows the asymmetrical enlargement of the ipsilateral torus tubarius (arrow). This indicates that the tonsillar carcinoma has extended superiorly to the nasopharynx. This precludes surgical resection of the tonsillar carcinoma at many institutions.

mors that are adjacent to the mandible require a segmental mandibulectomy and partial glossectomy followed by reconstruction. The primary treatment option for nonsurgical organ preservation for advanced tumors is combined chemotherapy and radiation therapy.

Imaging Findings

CT

SCCA of the palatine tonsils is localized to the tonsillar fossa. Early tumors may be indistinguishable from lymphoid tissue in the tonsillar bed. Asymmetric enhancing soft tissue in the tonsillar fossa should be carefully evaluated in patients with an ipsilateral neck mass. Advanced tumors are aggressive enhancing masses that can extend inferiorly to the lower pole of the tonsil and glossotonsillar sulcus. Superiorly, the tumor may invade the soft palate and extend to the skull base. The lesions may extend deeply to involve the parapharyngeal space. In fact, the most common lesion to involve the parapharyngeal space is deep invasion of a tonsillar carcinoma (Fig. 56-2).

MR

These tumors are intermediate signal on T1-weighted sequences and intermediate to high signal on T2-weighted sequences. These aggressive lesions diffusely enhance with contrast. MR is often superior to CT for detecting superior spread to the skull base and involvement of the retropharyngeal lymph nodes. MR is also superior to CT for detecting skull base involvement (Fig. 56-3).

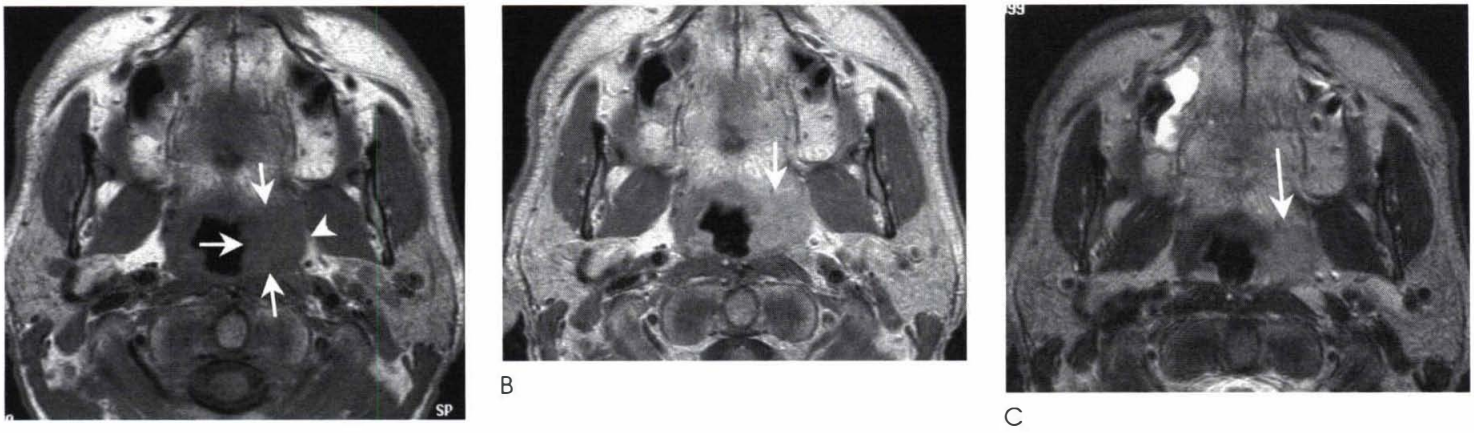

Figure 56-3. (A) Axial noncontrast T1-weighted image of a squamous cell carcinoma of the palatine demonstrates an intermediate signal mass centered in the left tonsillar fossa (arrows). There is early extension of the mass into the parapharyngeal space (arrowhead). This finding, which is clinically occult, precludes resection via an intraoral approach. (B) The mass homogeneously enhances following contrast administration (arrow). (C) The mass has intermediate signal on the T2-weighted sequences (arrow).

Imaging Pearls

The following will directly affect treatment of a palatine tonsil carcinoma and must be conveyed:

- Detailed evaluation of submucosal extension into the soft tissues of the neck (pre- and poststyloid parapharyngeal space, nasopharynx)
- Tongue base invasion
- Encasement of carotid artery
- Bone erosion
- Preveterbral muscle invasion

Suggested Readings

1. Mukherji SK, Pillsbury H, Castillo M. Imaging squamous cell carcinomas of the upper aerodigestive tract: what the clinicians need to know. *Radiology* 1997;205:629–646.
2. Million RR, Cassisi NJ, Mancuso AA. Larynx. In: Million RR, Cassisi NJ, eds. *Management of Head and Neck Cancer: A Multidisciplinary Approach.* Philadelphia: JB Lippincott; 1994.
3. Batsakis JG. Squamous cell carcinoma of the oral cavity and oropharynx. In: Batsakis JG, ed. *Tumors of the Head and Neck.* Baltimore: Williams and Wilkins; 1979:144–176.

Chapter 57

Squamous Cell Carcinoma of the Tongue Base/Valleculae

Epidemiology

The tongue base is located posterior to the oral tongue. The circumvallate papilla separates the oral tongue anteriorly (oral cavity) from the tongue base (oropharynx) posteriorly. It is important to differentiate the tongue base from the oral tongue because the anatomic subsite, lymphatic drainage, treatment, and prognosis are distinctly different. The posterior portion of the tongue base becomes continuous with the vallecula. Therefore, the squamous cell carcinomas (SCCAs) of the tongue or valleculae are often considered together and classified as a subsite of the oropharynx.

SCCA comprises over 95% of all malignancies of the tongue. The disease is more common in men between the ages of 50 and 70. The most common risk factors are smoking and excessive alcohol abuse.

Clinical Findings

The stages of SCCA have been classified by the American Joint Committee on Cancer (Table 57–1). The most common presenting symptoms include a visible or palpable mass, local pain, dysphagia, or a palpable neck mass. These tumors are often clinically silent and are often quite advanced at presentation. SCCAs of the tongue base are usually exophytic ulcerative tumors that tend to infiltrate beneath the mucosa. Early lesions are usually lateralized; however, advanced lesions often cross the midline. These tumors may also extend to the anterior tonsillar pillar, pharyngeal wall, submucosally under the valleculae into the supraglottic larynx, or anteriorly into the sublingual space. Lesions may also grow inferiorly and laterally to spread into the deep soft tissues of the neck, eventually involving the styloid musculature and the internal carotid artery (Fig. 57–1). As with all oropharyngeal carcinomas, bone erosion is unusual.

The lymphatic drainage of the tongue base consists of a superficial and deep muscular lymphatic network. The superficial network is continuous with the superficial plexus that covers the oral tongue. The primary drainage is to Groups II and III. The deep lymphatic drainage may drain ipsilaterally or have direct branches that drain to the contralateral neck. There is a high likelihood for nodal metastases from tongue base carcinoma. Approximately 70% of patients will have either unilateral or bilateral cervical metastases at initial presentation.

Table 57–1
Sixth American Joint Committee on Cancer Staging Classification for Oropharynx Cancer

Tis	Carcinoma in situ
T1	Tumor ≤ 2 cm in greatest diameter
T2	Tumor > 2 cm but ≤ 4 cm in greatest diameter
T3	Tumor > 4 cm in greatest diameter
T4a	Tumor invades larynx, deep/extrinsic muscle of tongue, medial pterygoid, hard palate, or mandible
T4b	Tumor invades lateral pterygoid muscle, pterygoid plates, lateral nasopharynx, or skull base, or encases carotid artery

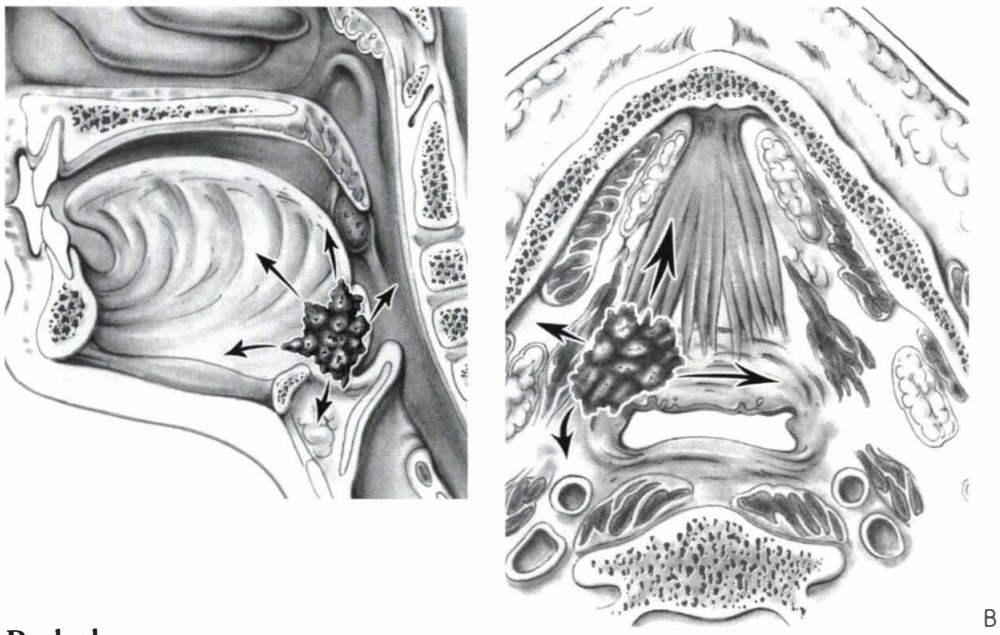

Figure 57-1. (A) Sagittal and (B) axial schematic illustrations demonstrate the potential spread patterns of tonsillar carcinoma involving the tongue base. (Reprinted with permission from Mukherji SK, Pillsbury H, Castillo M. Imaging squamous cell carcinomas of the upper aerodigestive tract: what the clinicians need to know. Radiology. 1997;205:629–646.)

Pathology

Tongue base cancers tend to be poorly differentiated tumors. This is in distinction from SCCAs of the oral tongue, which are usually moderately or well differentiated.

Treatment

The treatment for SCCA of the tongue base depends on the extent of disease. Wide local excision is performed for early lesions located along the lateral aspect of the tongue base. Tumors that cross the midline or extend posteriorly into the tongue base require a total or near-total glossectomy. This procedure would also require a supraglottic laryngectomy to prevent the aspiration that results following the glossectomy. Because of the substantial morbidity associated with this procedure, combined chemotherapy and radiation therapy is gaining acceptance for tumors that require total glossectomy and laryngectomy for surgical cure.

Imaging Findings

CT

These tumors present initially as enhancing masses located posterior to the circumvallate papilla. Advanced tumor may extend laterally across the midline, anteriorly to involve the oral tongue, or inferiorly to invade the vallecula and preepiglottic space. Bone erosion is unusual and typically occurs if the tumors extend into adjacent areas that have a higher likelihood of bone invasion such as the floor of the mouth (Figs. 57–2 and 57–3).

MR

The normal tongue base has an appearance that is distinct from the oral tongue and floor of the mouth. The muscle fibers are interspersed with the intrinsic fat of the tongue base and have an anterior to posterior alignment, whereas the muscle fibers of the oral tongue have a transverse orientation. SCCA is intermediate signal on T1-weighted images and replaces the normal striated appearance of the tongue base. SCCA is usually intermediate to high signal on T2-weighted images compared with normal muscle. SCCAs usually enhance following contrast administration (Fig. 57–4).

Imaging Pearls

- In our experience, overall MR is superior to CT for identifying the margins of tongue base SCCA. However, a substantial number of studies (10–30%) are often degraded by motion artifact due to pooling of secretions or dyspnea that results from the obstructing tumor. The patient's ability to cooperate while lying supine must be considered when one is determining which imaging study to perform.

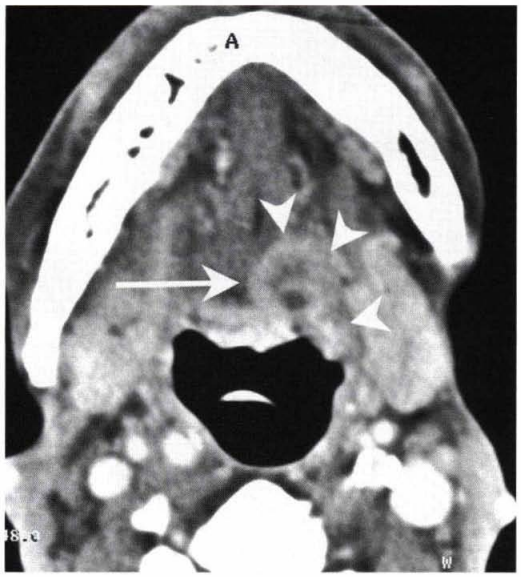

Figure 57–2. Axial contrast-enhanced CT shows a left tongue base carcinoma (arrowheads), which extends to the midline (arrow).

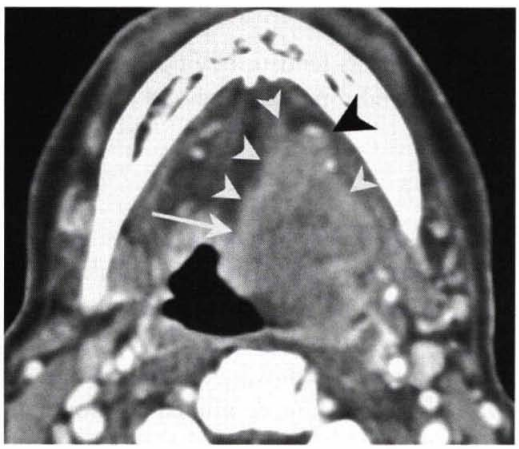

Figure 57–3. Axial contrast-enhanced CT shows a more advanced left tongue base that extends into the floor of the mouth (white arrowheads) and the crosses midline (arrow). The obliteration of fat surrounding the lingual artery is strongly suggestive of invasion of the lingual neurovascular bundle by the tumor (black arrowhead).

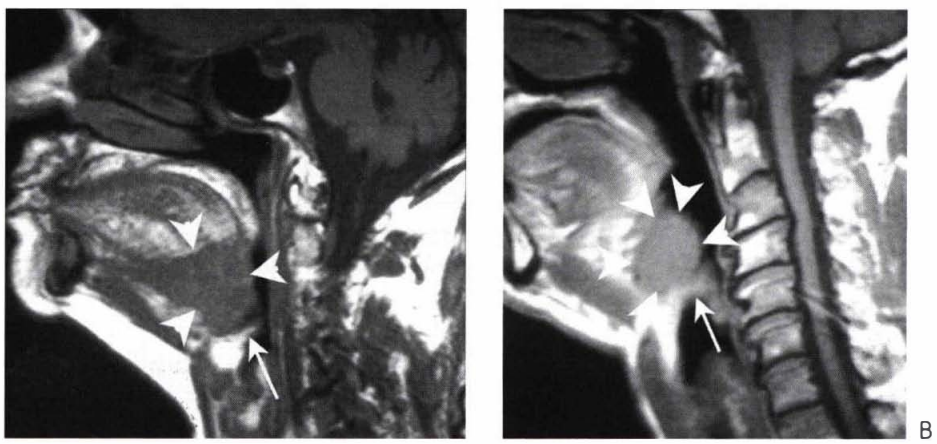

Figure 57–4. Noncontrast sagittal T1-weighted images performed in different patients illustrate the locations of (A) a tongue base cancer (arrowheads) and (B) a vallecular cancer (arrowheads). The arrows in (A) and (B) indicate the epiglottis.

- In our experience in patients with tongue base cancer, the shorter the study, the better the images. The MR sequences that best identify the extent of disease at the primary site are noncontrast, T1-weighted and dynamic, enhanced, two-dimentional gradient echo sequences with fat saturation.
- The following must be described in the reports and will directly affect the treatment and management of patients with tongue base carcinoma:
  - Extension to floor of mouth and surrounding structures
  - Relationship to ipsilateral lingual neurovascular bundle
  - Extension across midline and relationship to contralateral neurovascular bundle

Suggested Readings

1. Mukherji SK, Pillsbury H, Castillo M. Imaging squamous cell carcinomas of the upper aerodigestive tract: what the clinicians need to know. *Radiology* 1997;205:629–646.
2. Million RR, Cassisi NJ, Mancuso AA. Oropharynx. In: Million RR, Cassisi NJ, eds. *Management of Head and Neck Cancer: A Multidisciniplinary Approach*. Philadelphia: JB Lippincott; 1994:401–430.
3. Batsakis JG. Squamous cell carcinoma of the oral cavity and oropharynx. In: Batsakis JG, ed. *Tumors of the Head and Neck*. Baltimore: Williams and Wilkins; 1979:144–176.

Chapter 58

Squamous Cell Carcinoma of the Anterior and Posterior Tonsillar Pillar

Epidemiology

The tonsillar region is divided into three separate areas: the anterior tonsillar pillar, posterior tonsillar pillar, and palatine (faucial) tonsil. The palatine tonsil is covered in a separate chapter. This section focuses on the anterior and posterior tonsillar pillars.

The anterior tonsillar pillar (ATP) is formed by the mucosal fold that encompasses the palatoglossus muscle. The palatoglossus muscle extends from the lateral portion of the tongue base to the anterolateral aspect of the soft palate. Some authors group the ATP with the retromolar trigone. However, others feel (as we do) that the retromolar trigone should be considered part of the oral cavity, and the ATP as part of the oropharynx. The posterior tonsillar pillar (PTP) is formed by the mucosal fold that encompasses the palatopharyngeus muscle. This muscle extends from the pharyngeal wall to the posterolateral portion of the tonsil. ATP lesions are more common than PTP carcinomas. However, both are rare and are less common than squamous cell carcinoma (SCCA) that arises in the palatine tonsil. Men are affected more often than women. The peak incidence is in the seventh decade in men and the sixth decade in women. The most common risk factors are excessive tobacco and alcohol use.

Clinical Findings

Many early ATP and PTP lesions are asymptomatic. The stages of SCCA have been classified by American Joint Committee on Cancer (Table 58-1). The clinical findings are nonspecific and may often be subtle. The initial symptom may be only a sore throat. However, the presence of a sore throat plus otalgia should increase the suspicion of an underlying malignancy. Many patients will initially present with a neck mass. ATP lesions have a lower likelihood of clinically positive metastases at presentation when compared with tonsillar fossa tumors (45 vs 76%). Nodal groups I to III are at greatest risk.

PTP tumors are rare, however the nodal spread should be similar to palatine tonsil and nasopharynx tumors with a propensity for spread to the retropharyngeal and spinal accessory lymph nodes.

Table 58-1
Sixth American Joint Committee on Cancer Staging Classification for Oropharynx Cancer

Tis	Carcinoma in situ
T1	Tumor ≤ 2 cm in greatest diameter
T2	Tumor > 2 cm but ≤ 4 cm in greatest diameter
T3	Tumor > 4 cm in greatest diameter
T4a	Tumor invades larynx, deep/extrinsic muscle of tongue, medial pterygoid, hard palate, or mandible
T4b	Tumor invades lateral pterygoid muscle, pterygoid plates, lateral nasopharynx, or skull base, or encases carotid artery

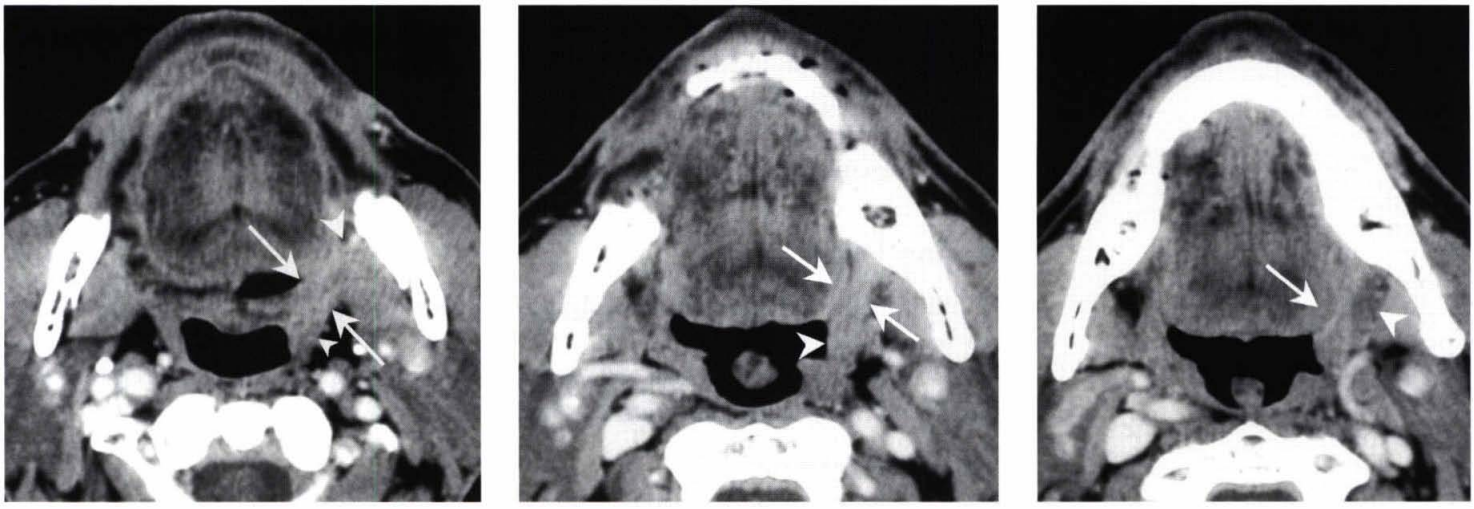

A B C

Figure 58–1. (A) Axial contrast-enhanced CT obtained at the level of the junction of the soft palate and tonsil demonstrates a mass involving the anterior portion of the tonsil (arrows). The lesion courses anteriorly along the superior constrictor muscle to the region of the pterygomandibular raphe (large arrowhead). The mass does extend posteriorly along the superior constrictor muscle (small arrowhead); however, the bulk of the mass is anterior. (B) The tumor extends inferiorly along the expected course of the palatoglossus muscle (arrows). The lack of the bulk disease involving the tonsillar fossa (arrowhead) indicates that the tumor is not a typical palatine tonsillar tumor. (C) The tumor courses inferiorly and invades the tongue base at the expected insertion of the palatoglossus muscle with the tongue base (arrow). Note the obliteration of the fat between the posterior border of the mylohyoid muscle, medial pterygoid muscle, and lingual cortex of the mandible (arrowhead) ["pterygomandibular space"]. This likely represents deep extension of this anteriorly located tumor.

Pathology

The majority (> 90%) of epithelial neoplasms of the tonsil are squamous cell carcinoma. These tend to be undifferentiated or anaplastic tumors that metastasize early. Early ATP lesions tend to be red or white flat mucosal lesions. More advanced lesions tend to ulcerate and infiltrate the palatoglossus muscle. Advanced tumors are bulky and infiltrate adjacent areas.

Treatment

Early T1 and T2 lesions that do no extend through the visceral fascia into the parapharyngeal space can be treated with definitive radiation therapy or a wide local excision using a transoral approach. The surgical treatment for advanced tumors may be resection using a mandibular swing approach for tumors that are not adjacent to the mandible. Larger tumors that are adjacent to the mandible require a segmental mandibulectomy and partial glossectomy followed by reconstruction. The primary treatment option for nonsurgical organ preservation for advanced tumors is combined chemotherapy and radiation therapy.

Imaging Findings

CT

SCCA of the ATP can be identified by a tumor involving the anterior portion of the tonsillar region in the expected location of the palatoglossus muscle. These tumors extend along the expected course of the palatoglossus muscle. Tumors may spread superiorly to involve the soft palate and inferiorly to involve the tongue base. The tumors may involve the retromolar trigone and gain access to the buccal space and gingivobuccal sulcus.

PTP tumors are very rare. They will involve the expected course of the palatopharyngeus muscle and often extend onto the posterior pharyngeal wall and pharyngoepiglottic fold (Fig. 58–1).

MR

These tumors are intermediate signal on T1-weighted sequences and intermediate to high signal on T2-weighted sequences. These aggressive lesions diffusely enhance with contrast. MR is often superior to CT for detecting extension into the adjacent areas and also for potential involvement of the retropharyngeal lymph nodes.

Imaging Pearls

The following information will directly affect treatment of ATP and PTP carcinoma and must be conveyed:

- Detailed evaluation of submucosal extension into the soft tissues of the neck (pre- and poststyloid parapharyngeal space, nasopharynx)
- Tongue base invasion
- Encasement of the carotid artery
- Bone erosion
- Preveterbral muscle invasion

Suggested Readings

1. Mukherji SK, Pillsbury H, Castillo M. Imaging squamous cell carcinomas of the upper aerodigestive tract: what the clinicians need to know. *Radiology* 1997;205:629–646.
2. Million RR, Cassisi NJ, Mancuso AA. Larynx. In: Million RR, Cassisi NJ, eds. *Management of Head and Neck Cancer: A Multidisciplinary Approach.* Philadelphia: JB Lippincott; 1994.
3. Batsakis JG. Squamous cell carcinoma of the oral cavity and oropharynx. In: Batsakis JG, ed. *Tumors of the Head and Neck.* Baltimore: Williams and Wilkins; 1979:144–176.

Chapter 59

Squamous Cell Carcinoma of the Retromolar Trigone

Epidemiology

The retromolar trigone (RMT) is a triangular area situated behind the molars between the posterior portion of the maxillary and mandibular alveolar ridges. Overall, the RMT is the least common site of squamous cell carcinoma (SCCA) of the oral cavity. However, it is one of the most frequently encountered oral cavity tumors associated with chewing betel nut. RMT SCCA is more common in men between the ages of 40 and 60.

Clinical Findings

In our experience, RMT SCCA is one of the most difficult lesions to accurately stage by clinical examination. The stages of SCCA have been classified by AJCC (Table 59–1). A tumor that is felt to be early stage disease is often only "the tip of the iceberg." These tumors commonly spread deeply to the pterygomandibular raphe and may continue to spread laterally along the buccinator muscle (Fig. 59–1). The RMT is located in close proximity to the anterior tonsillar pillar (palatoglossus muscle). As a result, these tumors may invade the palatoglossus muscle and extend superiorly to the soft palate or inferiorly to the tongue base. Early bone erosion is common and is often present without trismus. A common complaint is local and referred pain to the external auditory canal. Trismus is usually caused by extension into the masticator space. RMT SCCA may demonstrate perineural spread. The most common pathways are antegrade along the inferior alveolar nerve into the mandible, or retrograde along the inferior alveolar nerve to the main trunk of V_3.

The ipsilateral Group I lymph nodes are the primary echelon drainage for RMT SCCA. The incidence of clinically positive lymph nodes at presentation is between 35 and 40%.

Table 59–1
Sixth American Joint Committee on Cancer Staging Classification of Oral Cavity Carcinoma

TX	Primary tumor cannot be assessed
T0	No evidence of primary tumor
Tis	Carcinoma in situ
T1	Tumor $<$ 2 cm in greatest dimension
T2	Tumor $>$ 2 but $\leq$ 4 cm in greatest diameter
T3	Tumor $>$ 4 cm
T4 (lip)	Tumor invades through cortical bone, inferior alveolar nerve, floor of the mouth, or skin of the face (i.e., chin or nose)
T4a (oral cavity)	Tumor invades adjacent structures [e.g., through cortical bone, into deep (extrinsic) muscle of tongue (genioglossus, hyoglossus, palatoglossus, and styloglossus), maxillary sinus, or skin of the face]
T4b (oral cavity)	Tumor invades masticator space, pterygoid plates, or skull base and/or encases the internal carotid artery

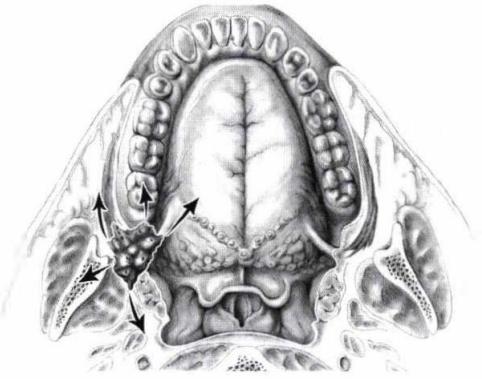

Figure 59–1. Axial schematic illustration of the potential spread patterns of a retromolar trigone carcinoma (arrows). (Reprinted with permission from Mukherji SK, Pillsbury H, Castillo M. Imaging squamous cell carcinomas of the upper aerodigestive tract: what the clinicians need to know. Radiology, *1997;205:629–646.)*

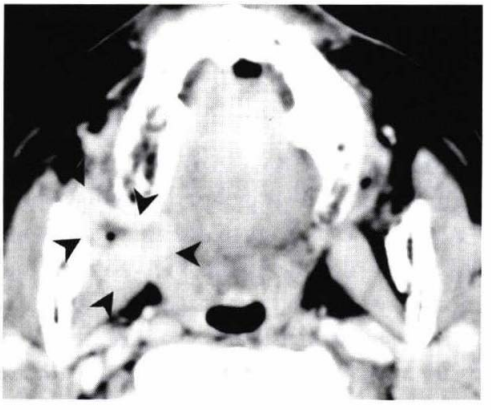

Figure 59–2. Axial contrast-enhanced CT demonstrates a squamous cell carcinoma arising from the right retromolar trigone (arrowheads). (Reprinted with permission from Mukherji SK, Pillsbury H, Castillo M. Imaging squamous cell carcinomas of the upper aerodigestive tract: what the clinicians need to know. Radiology, *1997;205:629–646.)*

Pathology

Histologically, SCCA is classified as well, moderately, and poorly differentiated. On microscopic examination, SCCA is seen as anaplastic-appearing cells found below the basement membrane with a variable degree of keratin production and intracellular bridges. RMT SCCA tends to be well differentiated.

Treatment

The most common treatment for RMT SCCA is surgical resection. Wide local excision is performed for superficial lesions without invasion of the periosteum. A marginal mandibulectomy is performed for tumors that are fixed to but do not invade the mandible. A segmental mandibulectomy is performed for tumors that erode the mandible. Combined chemotherapy and radiation therapy is gaining acceptance for advanced tumors that cross the midline or invade the tongue base.

Imaging Findings

CT

These tumors present as enhancing masses located posteriorly to the last molar. They may often extend laterally to the pterygomandibular raphe and may continue to extend to the buccinator muscle. These tumors may also spread superiorly to the soft palate or inferiorly to the tongue base. They have a propensity for early invasion along the posterior portion of the alveolar ridge or anterior aspect of the ramus of the mandible (Figs. 59–2 and 59–3).

MR

SCCA is usually intermediate signal on T1-weighted images and slightly increased signal on T2-weighted images. The tumors usually enhance following contrast administration. Mandibular involvement may be suspected if there is replacement of the normal high signal of the marrow by intermediate signal.

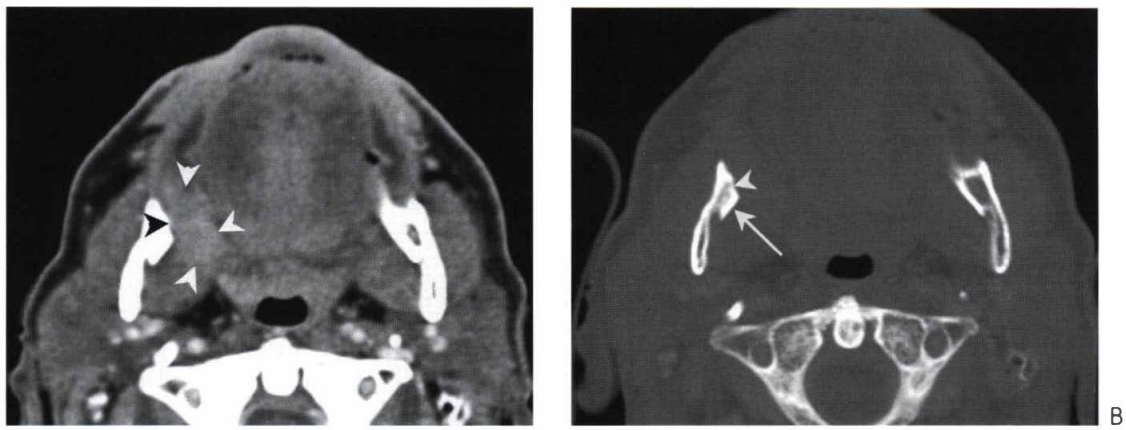

Figure 59–3. (A) Axial contrast-enhanced CT demonstrates a squamous cell carcinoma involving the right retromolar trigone (arrowheads). (B) Bone algorithm demonstrates erosion of the adjacent cortex (arrowhead) and sclerosis of the underlying mandible (arrow). Compare this with the normal appearance on the uninvolved contralateral side. These findings upstage the lesion to T4.

Imaging Pearls

- MR is superior to CT for defining the extent of RMT carcinomas and is recommended for all tumors arising in this location.
- The following specific information needs to be described in the reports and will directly affect the treatment and management of patients with RMT carcinoma:
  - Bone erosion
  - Submucosal spread
  - Perineural invasion

Suggested Readings

1. Mukherji SK, Pillsbury H, Castillo M. Imaging squamous cell carcinomas of the upper aerodigestive tract: what the clinicians need to know. *Radiology* 1997;205:629–646.
2. Million RR, Cassisi NJ, Mancuso AA. Oral cavity. In: Million RR, Cassisi NJ, eds. *Management of Head and Neck Cancer: A Multidiscini plinary Approach.* Philadelphia: JB Lippincott; 1994:321–400.
3. Batsakis JG. Squamous cell carcinoma of the oral cavity and oropharynx. In: Batsakis JG, ed. *Tumors of the Head and Neck.* Baltimore: Williams and Wilkins; 1979:144–176.

Chapter 60

Squamous Cell Carcinoma of the Gingiva and Hard Palate

Epidemiology

Squamous cell carcinoma (SCCA) of the gingiva and the mucosa covering the maxillary and mandibular ridges constitutes about 10% of all malignant neoplasms of the oral cavity. The incidence rate is lower than that of SCCA of the tongue. The incidence is more common in men (4:1) between the ages of 60 and 70. There is geographic predominance and the tumor has an increased incidence in women in the southeastern United States. This may be due to the use of chewing tobacco or snuff. SCCA of the hard palate does occur; however, it is unusual because the majority of hard palate neoplasms are minor salivary gland tumors.

Clinical Findings

The staging of oral cavity carcinoma is presented in Table 60–1. Gingival carcinomas occur most commonly in edentulous areas, and patients with SCCA of the gingiva may present first to the dentist and complain of loose teeth, ill-fitting dentures, tooth pain, or a nonhealing sore. These tumors may also appear at the free gingival margin close to the surface of a tooth. Advanced tumors may invade the underlying bone and the inferior alveor nerve and result in paresthesias. The most common site of invasion is along the occlusal surface of the maxillary and mandibular ridge (Fig. 60–1). The primary echelon lymphatic drainage is to the Group I lymph nodes. The primary drainage is usually ipsilateral to the side to the primary tumor. Contralateral involvement is unusual. The incidence of positive lymph nodes at initial presentation varies between 15 and 30%.

Pathology

Gingival carcinomas tend to be well differentiated. The tumors tend to be papillary exophytic lesions in edentulous patients. These tumors may also present as ulcerating plaques. Many gingival squamous cell carcinomas arise on a background of leukoplakia.

Table 60–1
Sixth American Joint Committee on Cancer Staging Classification of Oral Cavity Carcinoma

TX	Primary tumor cannot be assessed
T0	No evidence of primary tumor
Tis	Carcinoma in situ
T1	Tumor < 2 cm in greatest dimension
T2	Tumor more than 2 > 4 cm in greatest diameter
T3	Tumor > 4 cm
T4 (lip)	Tumor invades through cortical bone, inferior alveolar nerve, floor of mouth, or skin of face (i.e., chin or nose)
T4a (oral cavity)	Tumor invades adjacent structures [e.g., through cortical bone, into deep (extrinsic) muscle of tongue (genioglossus, hyoglossus, palatoglossus, and styloglossus), maxillary sinus, or skin of face]
T4b (oral cavity)	Tumor invades masticator space, pterygoid plates, or skull base and/or encases internal carotid artery

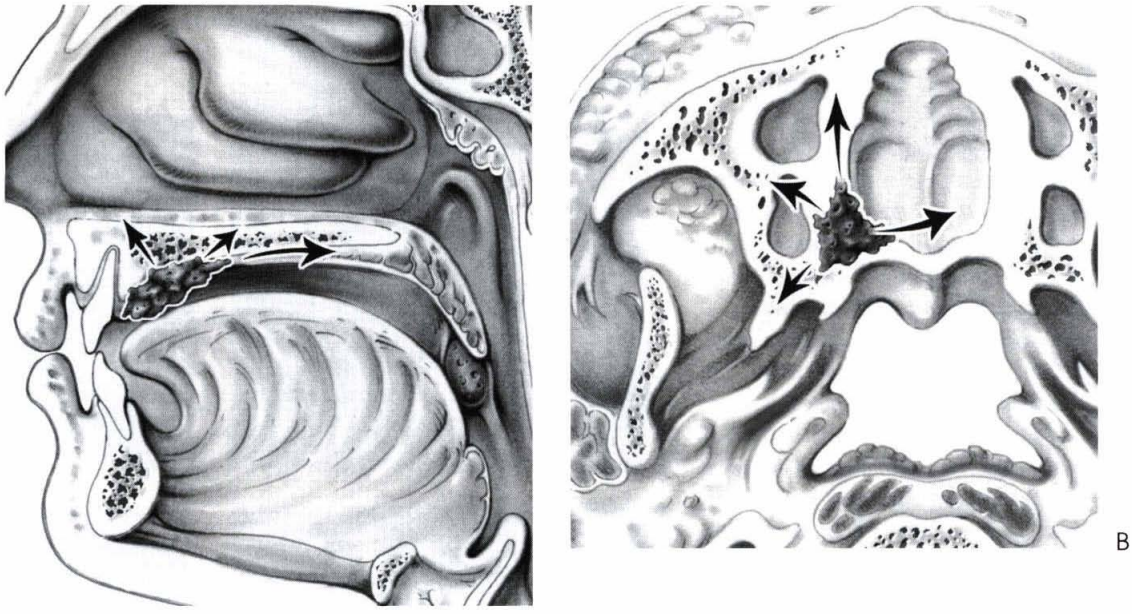

Figure 60-1. (A) Sagittal and (B) axial schematic illustrations of the spread patterns of a hard palate carcinoma (arrows). (Reprinted with permission from Mukherji SK, Pillsbury H, Castillo M. Imaging squamous cell carcinomas of the upper aerodigestive tract: what the clinicians need to know. Radiology, *1997;205:629-646.)*

Treatment

Wide local excision or radiation therapy is often performed for early superficial lesions that are mobile. A wide local excision may also be performed for tumors that are fixed to the mandible but do not invade the periosteum of the mandible. A marginal mandibulectomy is performed for tumors that involve the periosteum but do not invade bone. Segmental mandibulectomy is reserved for tumors that erode the mandible. Hard palate tumors that erode bone are treated with a partial maxillectomy. Combined chemotherapy and radiation therapy is gaining acceptance for advanced tumors in which surgical resection would result in a severe functional deformity that requires major reconstructive surgery.

Imaging Findings

CT

Early superficial lesions may not be identified on CT or MR imaging. Larger lesions often present as enhancing masses. Gingival tumors are best seen along the buccal cortex of the mandible. Alveolar ridge carcinomas occur along the occlusal surface of the alveolar ridge. Both alveolar ridge and hard palate tumors are best visualized on coronal studies reconstructed at soft tissue and bone algorithm. Hard palate cancers should be specifically evaluated for erosion of the incisive canal and greater and lesser palatine foramen (Figs. 60–2 and 60–3).

MR

SCCAs of gingiva and hard palate are usually intermediate signal on T1-weighted and slightly increased signal on T2-weighted images. They usually enhance following contrast administration. MR should be performed for hard palate carcinomas to evaluate for posterior extension into the pterygopalatine fossa and potential retrograde perineural spread along the nerve of the vidian canal or the maxillary division of the trigeminal nerve.

Imaging Pearls

- Certain specific information must be described in the reports and will directly affect the treatment and management of patients with buccal carcinoma:
  - Bone erosion
  - Perineural invasion of the incisive canal and greater and lesser palantine foramen

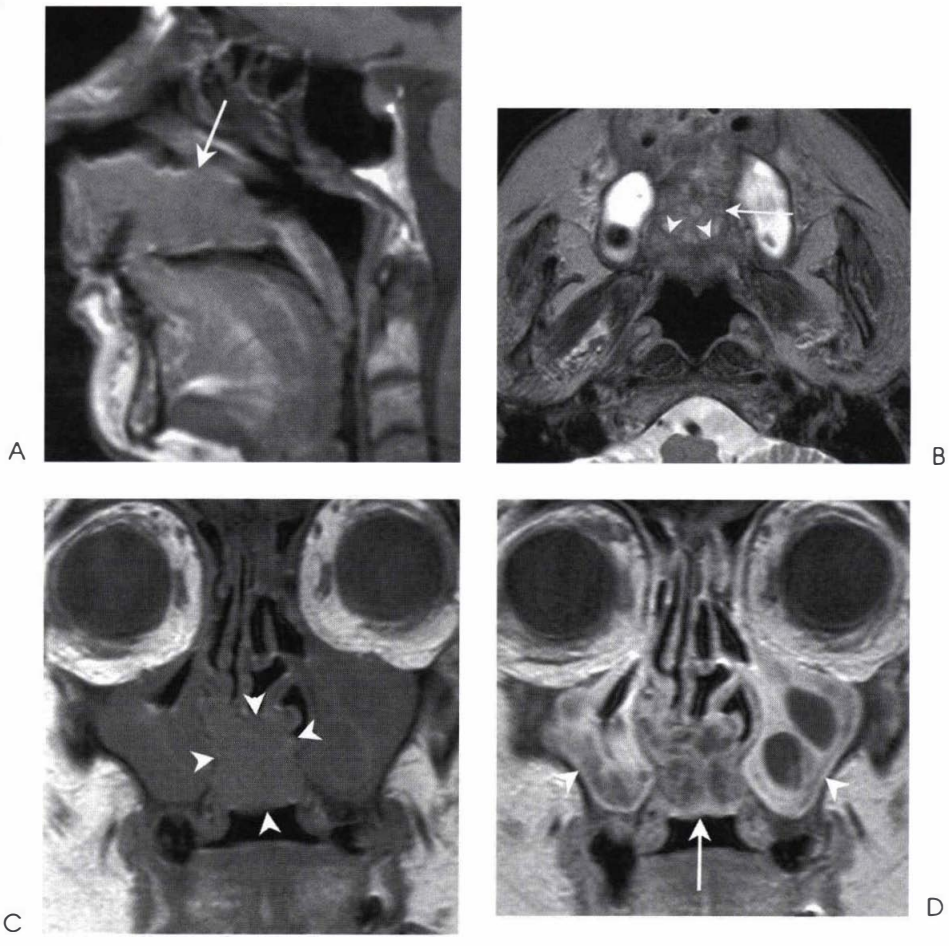

Figure 60–2. (A) Noncontrast sagittal T1-weighted image demonstrates a squamous cell carcinoma invading the hard palate (arrow). (B) Axial T2-weighted image demonstrates the mass to be intermediate signal (arrow). Note the transition between the tumor and the normal hard palate (arrowheads). (C) Coronal noncontrast T1-weighted image demonstrates the mass to involve the hard palate and extend superiorly into the inferior half of the nasal cavity (arrowheads). (D) The tumor homogeneously enhances following contrast (arrow). Note the difference in enhancement between the mass and maxillary sinuses (arrowheads). The enhancement in the sinuses is due to obstructed mucosal thickening.

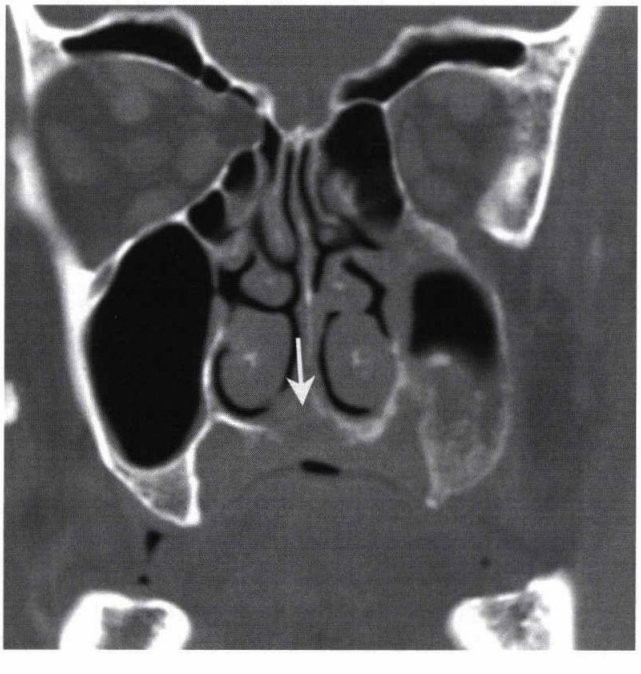

Figure 60–3. Coronal CT of a hard palate carcinoma reconstructed in bone algorithm shows erosion of the hard palate (arrow). This finding was clinically occult and "upsatged" the tumor to T4.

Suggested Readings

1. Mukherji SK, Pillsbury H, Castillo M. Imaging squamous cell carcinomas of the upper aerodigestive tract: what the clinicians need to know. *Radiology* 1997;205:629–646.
2. Million RR, Cassisi NJ, Mancuso AA. Oral cavity. In: Million RR, Cassisi NJ, eds. *Management of Head and Neck Cancer: A Multidisciplinary Approach.* Philadelphia: JB Lippincott; 1994:321–400.
3. Batsakis JG. Squamous cell carcinoma of the oral cavity and oropharynx. In: Batsakis JG, ed. *Tumors of the Head and Neck.* Baltimore: Williams and Wilkins; 1979:144–176.

Chapter 61

Squamous Cell Carcinoma of the Buccal Mucosa

Epidemiology

The cheek is formed by the buccinator muscle, overlying fibroadipose tissue, and skin, and constitutes the lateral margin of the oral cavity. The mucosal surfaces of the cheek extend laterally and are continuous with the mucosa of the mandibular and maxillary alveolar ridges. This occurs laterally at a commissure known as the gingivobuccal sulcus. The parotid duct empties into the buccal mucosa at the level of the second molar.

Buccal carcinoma is primarily associated with snuff dipping and chewing tobacco. As a result, these tumors have unique geographic and demographic characteristics. These tumors present later in life than other oral carcinomas, with the average age of presentation between 60 and 70 years. Overall, the incidence in men is greater than in women (4–10:1). However in the southeastern United States, the buccal carcinomas are more common in elderly women than in men (3:1). This may be due to a relative's high incidence of the use of non-chewing tobacco in women.

Clinical Findings

Stages of oral cavity carcinoma are presented in Table 61–1. Early tumors are often asymptomatic and may be discovered by a dentist at a routine checkup. These tumors typically occur on a background of leukoplakia. Small tumors may present as a mass. Large lesions may present as a painful bleeding mass. Advanced tumors may erode the underlying bone and/or extend posteriorly to the masticator space causing trismus (Fig. 61–1).

The primary echelon lymphatic drainage is to the Group I lymph nodes. The primary drainage is usually ipsilateral to the side to the primary tumor. Contralateral involvement is unusual. The incidence of positive lymph nodes at initial presentation varies between 10 and 30%.

Table 61–1
Sixth American Joint Committee on Cancer Staging Classification of Oral Cavity Carcinoma

TX	Primary tumor cannot be assessed
T0	No evidence of primary tumor
Tis	Carcinoma in situ
T1	Tumor < 2 cm in greatest dimension
T2	Tumor more than 2 > 4 cm in greatest diameter
T3	Tumor > 4 cm
T4 (lip)	Tumor invades through cortical bone, inferior alveolar nerve, floor of mouth, or skin of face (i.e., chin or nose)
T4 a (oral cavity)	Tumor invades adjacent structures [e.g., through cortical bone, into deep (extrinsic) muscle of tongue (genioglossus, hyoglossus, palatoglossus, and styloglossus), maxillary sinus, or skin of face].
T 4b (oral cavity)	Tumor invades masticator space, pterygoid plates, or skull base and/or encases internal carotid artery

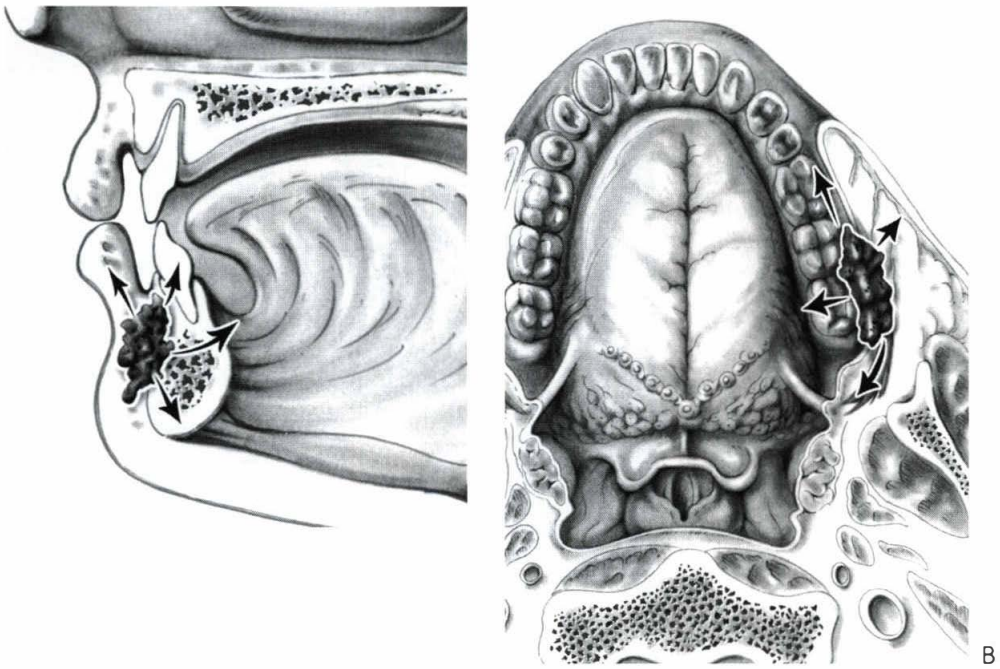

Figure 61-1. (A) Sagittal schematic illustration demonstrates the spread pattern (arrows) of an anterior buccal carcinoma. (B) Axial schematic illustration demonstrates the spread pattern (arrows) of carcinoma arising from the posterior aspect of the buccal cortex of the alveolar ridge. (Reprinted with permission from Mukherji SK, Pillsbury H, Castillo M. Imaging squamous cell carcinomas of the upper aerodigestive tract: what the clinicians need to know. Radiology, *1997;205:629-646).*

A

B

Pathology

There are three distinctive clinicopathologic types of buccal carcinoma: (1) exophytic, (2) ulceroinfiltrative, and (3) verrucous. The majority of buccal squamous cell carcinomas are low-grade exophytic lesions and usually occur on a background of leukoplakia.

Treatment

Wide local excision or radiation therapy is often performed for early superficial lesions that are mobile. A marginal mandibulectomy is performed for tumors that are fixed to but do not invade the mandible. A segmental mandibulectomy is performed for tumors that erode the mandible. Combined chemotherapy and radiation therapy is gaining acceptance for advanced tumors in which surgical resection would result in a severe functional deformity that would require major reconstructive surgery.

Imaging Findings

CT

Early superficial lesions may not be identified on CT or MR imaging. Having patients "puff" their cheeks during image acquisition may identify some early lesions. Larger lesions present as enhancing masses located along the lateral buccal surface of the maxillary or mandibular alveolar ridge. Advanced tumors may erode the alveolar ridge. Advanced tumors may also extend posteriorly along the buccinator muscle to pterygomandibular raphe and invade the masticator space (Figs. 61-2 and 61-3).

MR

Squamous cell carcinomas of buccal carcinomas are usually intermediate signal on T1-weighted and slightly increased signal on T2-weighted images. They usually enhance following contrast administration. Mandibular involvement may be suspected if there is replacement of the normal high signal of the marrow by intermediate signal. T1-weighted postgadolinium fat saturation sequences may be helpful for evaluating the full extent of the primary site on MR.

Imaging Pearls

- Coronal CT imaging or sagittal reconstructions may be helpful for identifying early cortical erosion along the alveolar ridge.

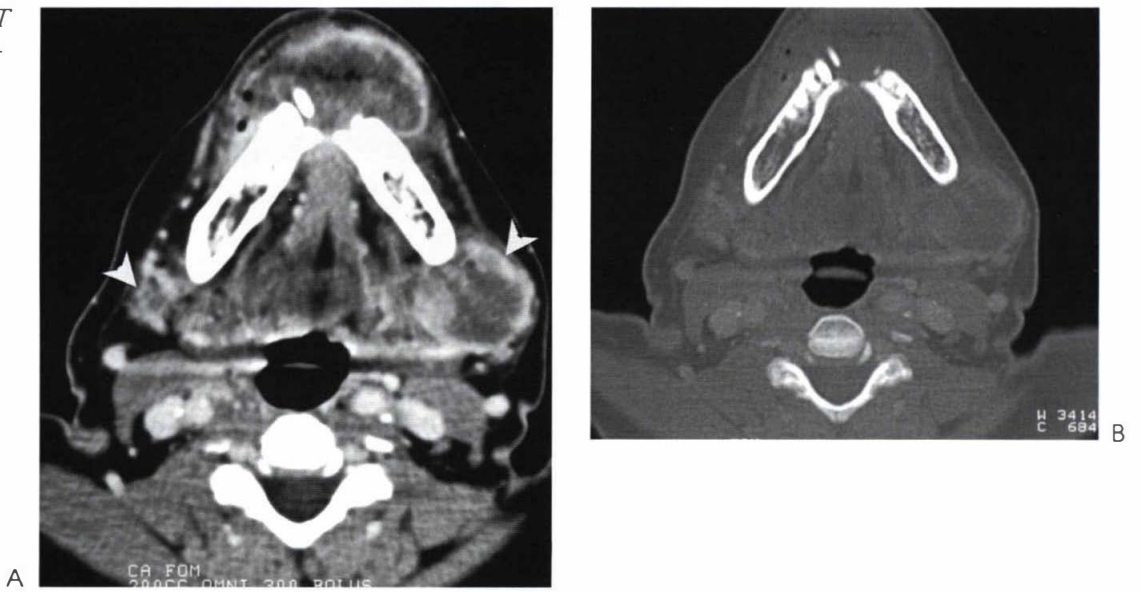

Figure 61-2. (A) Axial contrast CT of an advanced buccal cancer demonstrates an aggressive mass involving the anterior portion of the mandible. Note the metastatic bilateral level I lymph nodes (arrowheads). (B) Bone algorithm demonstrates the extensive degree of bone erosion.

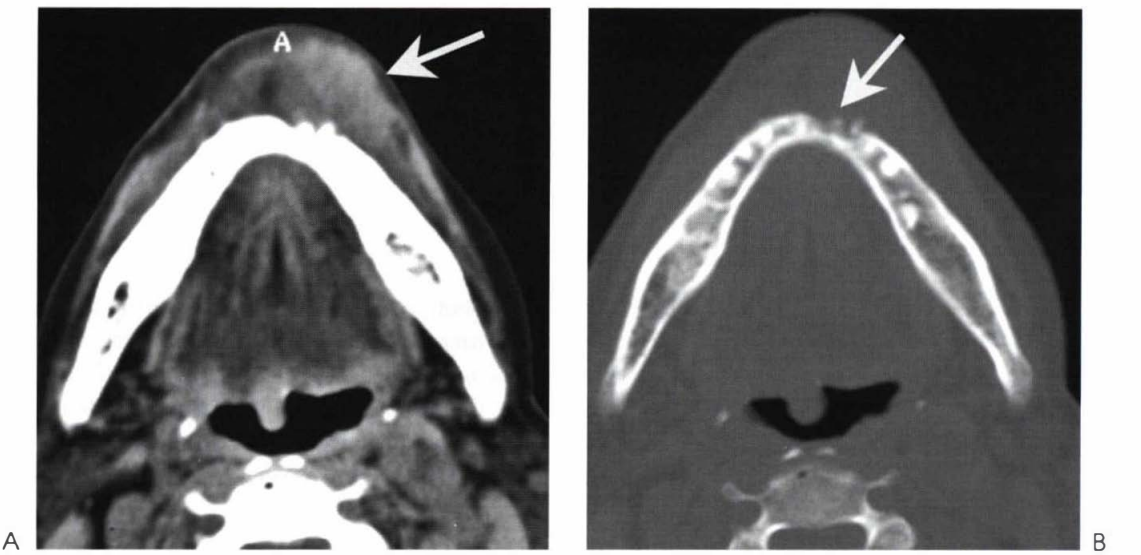

Figure 61-3. (A) Axial contrast-enhanced CT shows a squamous cell carcinoma arising from the buccal cortex of the mandible (arrow). (B) Bone algorithm demonstrates that the mass is eroding the buccal cortex of the mandible (arrow).

- Certain specific information must be described in the reports and will directly affect the treatment and management of patients with buccal carcinoma:
  - Submucosal extension posteriorly to the pterygomandibular raphe
  - Bone erosion

Suggested Readings

1. Mukherji SK, Pillsbury H, Castillo M. Imaging squamous cell carcinomas of the upper aerodigestive tract: what the clinicians need to know. *Radiology* 1997;205:629–646.
2. Million RR, Cassisi NJ, Mancuso AA. Oral cavity. In: Million RR, Cassisi NJ, eds. *Management of Head and Neck Cancer: A Multidisciplinary Approach.* Philadelphia: JB Lippincott; 1994:321–400.
3. Batsakis JG. Squamous cell carcinoma of the oral cavity and oropharynx. In: Batsakis JG, ed. *Tumors of the Head and Neck.* Baltimore: Williams and Wilkins; 1979:144–176.

Chapter 62

Squamous Cell Carcinoma of the Oral Tongue

Epidemiology

Squamous cell carcinoma (SCCA) of the oral tongue is the second most common site of SCCA of the oral cavity. SCCA comprises > 95% of all malignancies of the oral tongue. The disease is more common in men between the ages of 50 and 70. The most common risk factors are smoking and excessive alcohol abuse.

Clinical Findings

The staging of oral cavity carcinoma are presented in Table 62–1. The most common location is along the lateral border of the middle third of the oral tongue (Fig. 62–1). The common presenting symptoms include the sensation of a mass, a visible or palpable mass, local pain, dysphagia, or a palpable neck mass. Advanced tumors may extend posteriorly to invade the tongue base or inferiorly along the hyoglossus muscle and involve the floor of the mouth. This spread is often clinically occult. Bone erosion is unusual.

Group I to II lymph nodes are at greatest risk for metastases. About 40% of patients will have palpable nodal disease and 20% will have bilateral involvement.

Pathology

Oral tongue lesions are usually ulcerative and infiltrative. SCCA of the oral tongue are usually moderately or well differentiated. They may arise in apparently normal epithelium; however, it is common to see these tumors associated with leukoplakia or chronic glossitis.

Treatment

The treatment for SCCA depends on the extent of disease. Wide local excision is performed for early lesions located along the lateral aspect of the oral tongue. Tumors that extend in-

Table 62–1
Sixth American Joint Committee on Cancer Staging Classification of Oral Cavity Carcinoma

TX	Primary tumor cannot be assessed
T0	No evidence of primary tumor
Tis	Carcinoma in situ
T1	Tumor < 2 cm in greatest dimension
T2	Tumor more than 2 > 4 cm in greatest diameter
T3	Tumor > 4 cm
T4 (lip)	Tumor invades through cortical bone, inferior alveolar nerve, floor of mouth, or skin of face (i.e., chin or nose)
T4a (oral cavity)	Tumor invades adjacent structures [e.g., through cortical bone, into deep (extrinsic) muscle of tongue (genioglossus, hyoglossus, palatoglossus, and styloglossus), maxillary sinus, or skin of face].
T4b (oral cavity)	Tumor invades masticator space, pterygoid plates, or skull base and/or encases internal carotid artery

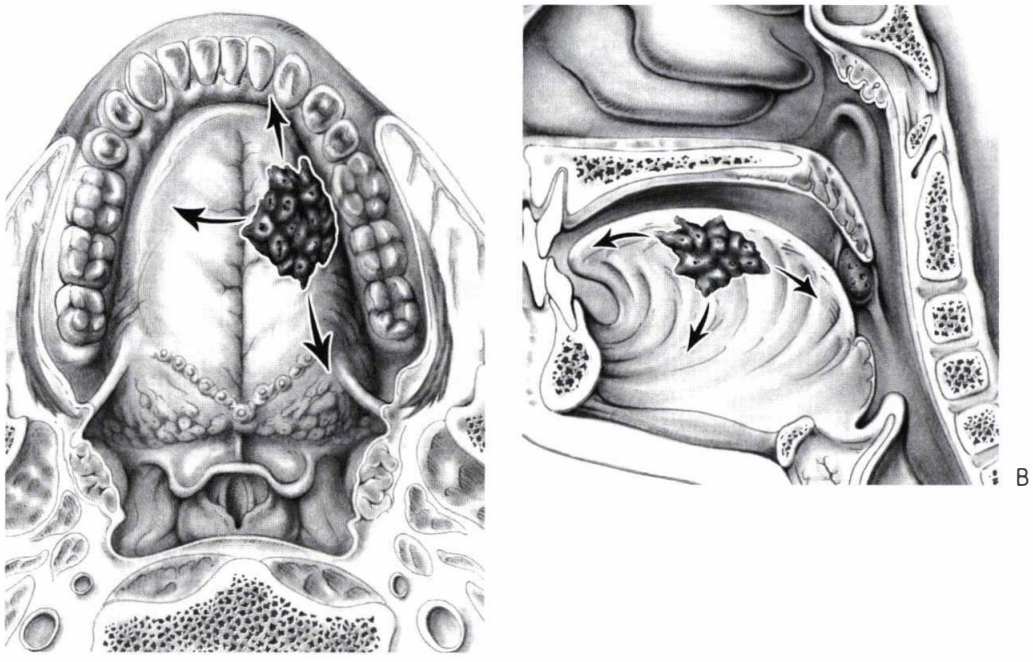

Figure 62–1. (A) Sagittal and (B) axial schematic illustrations of the spread patterns (arrows) of an oral tongue carcinoma. (Reprinted with permission from Mukherji SK, Pillsbury H, Castillo M. Imaging squamous cell carcinomas of the upper aerodigestive tract: what the clinicians need to know. Radiology, *1997;205:629–646.)*

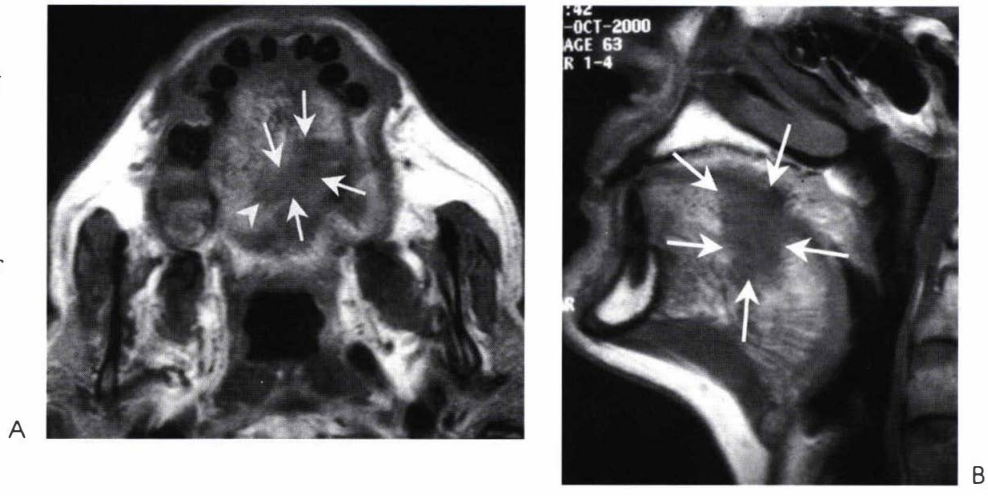

Figure 62–2. (A) Axial noncontrast T1-weighted image shows an intermediate squamous cell carcinoma involving the left side of the oral tongue (arrows). The mass does appear to cross the midline (arrowhead). (B) Sagittal noncontrast T1-weighted image shows the mass to be localized to the oral tongue (arrows) with no invasion of the floor of the mouth.

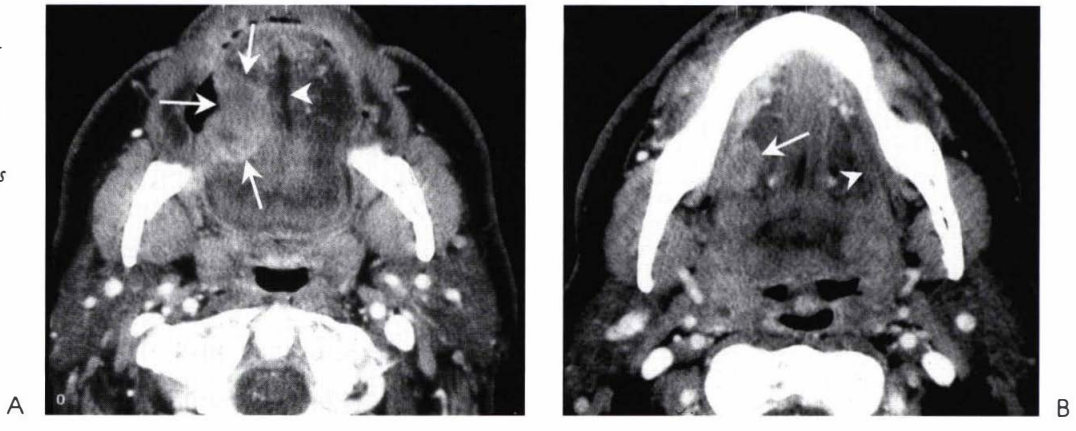

Figure 62–3. (A) Axial contrast-enhanced CT shows a squamous cell carcinoma involving the right oral tongue (arrows). The fat indicating the location of the lingual septum is midline (arrowhead). This indicates that the tumor does not cross the midline. (B) Axial image obtained in the floor of the mouth demonstrates the tumor to be extending inferiorly along the hyoglossus muscle (arrow). This extension was clinically occult but confirmed at surgery. This finding "upstages" the lesion to T4 because the tumor is involving the hyoglossus muscle, an extrinsic tongue muscle.Note the normal appearance of the hyoglossus muscle on the uninvolved contralateral side (arrowhead).

feriorly into the floor of the mouth may require a marginal mandibulectomy. Tumors that cross the midline or extend posteriorly into the tongue base require a total or near-total glossectomy. The latter would also require a supraglottic laryngectomy to prevent the aspiration following the glossectomy. Because of the substantial morbidity associated with this procedure, combined chemotherapy and radiation therapy is gaining acceptance for advanced tumors that cross the midline or invade the tongue base.

Imaging Findings

CT

These tumors present initially as an enhancing mass along the lateral margin of the oral tongue. Advanced tumor may extend laterally across the midline, posteriorly to involve the tongue base or inferiorly to invade the floor of the mouth. Bone erosion is unusual and typically occurs if the tumors extend into areas adjacent to bone and therefore, have a higher likelihood of bone invasion such as the floor of mouth (Figs. 62–2 and 62–3).

MR

The normal signal of the oral tongue consists of a meshwork of intermediate and increased T1-weighted signal. This represents a combination of the muscle and fat. SCCA is usually intermediate signal on T1-weighted and slightly increased signal on T2-weighted images. These tumors "replace" the normal expected signal of the oral tongue and enhance following contrast.

Imaging Pearls

- MR is superior to CT for identifying the full extent of tumor, especially for determining if the tumor crosses the midline or invades the tongue base.
- In our experience, the sequences that best identify the extent of disease at the primary site on MR are noncontrast T1-weighted and dynamic enhanced two-dimensional gradient echo sequences with fat saturation.
- Certain specific information must be described in the reports and will directly affect the treatment and management of patients with oral tongue carcinoma:
  - Invasion of ipsilateral lingual neurovascular bundle
  - Extension across the midline and relationship to the contralateral neurovascular bundle
  - Invasion of the floor of the mouth along the extrinsic tongue musculature
  - Secondary mandibular involvement following extension into the floor of mouth

Suggested Readings

1. Mukherji SK, Pillsbury H, Castillo M. Imaging squamous cell carcinomas of the upper aerodigestive tract: what the clinicians need to know. *Radiology* 1997;205:629–646.
2. Million RR, Cassisi NJ, Mancuso AA. Oral cavity. In: Million RR, Cassisi NJ, eds. *Management of Head and Neck Cancer: A Multidisciplinary Approach.* Philadelphia: JB Lippincott; 1994:321–400.
3. Batsakis JG. Squamous cell carcinoma of the oral cavity and oropharynx. In: Batsakis JG, ed. *Tumors of the Head and Neck.* Baltimore: Williams and Wilkins; 1979:144–176.

Chapter 63

Squamous Cell Carcinoma of the Epiglottis

Epidemiology

Cancer of the larynx is the most common head and cancer and accounts for about 2% of all carcinomas. Laryngeal cancer is more common in men (5–10:1). Patients typically present between the ages of 50 and 80. The supraglottic larynx is the second most common site of squamous cell carcinoma (SCCA) next to the true vocal cords. SCCA accounts for > 90% of cancers of the supraglottic larynx. The epiglottis is a subsite of the supraglottic larynx and is a common site for supraglottic carcinoma. Epiglottic carcinoma is directly related to cigarette smoking. Fortunately, the risk of tobacco-related cancers appears to be reversible; the risks for ex-smokers who have abstained from smoking for > 10 years are nearly equal to those for nonsmokers. Other forms of smoking, including cigar, pipe, and marijuana, are also felt to increase the likelihood of developing SCCA. Alcohol is the other major risk factor. Occupational exposure to oil, grease, and cement dust has also been associated with SCCA of the supraglottic larynx.

Clinical Findings

The staging of supraglottic carcinoma are presented in Table 63-1. Patients usually present with hoarseness and weight loss. Epiglottic carcinomas tend to be larger at presentation than glottic carcinomas because bulkier lesions are necessary to compromise the larger airway that is present at this level. Patients with advanced lesions may present with difficulty breathing and may require tracheotomy. Epiglottic carcinomas, especially at the level of the hyoid bone, often extend deeply into the preepiglottic space, upstaging these lesions to T3 (Fig. 63-1). This deep extension is often understaged clinically and is best identified on cross-sectional imaging.

The primary echelon lymphatic drainage is to levels II and III. The supraglottic larynx is rich in lymphatics, and nearly half of all patients will present with clinically positive neck metastases. Bilateral metastases will occur in up to 25% of all cases. Thus it is important to evaluate the lymph nodes on both the ipsilateral and the contralateral sides in patients with supraglottic carcinoma.

Pathology

Histologically, squamous cell carcinoma is classified as well, moderately, and poorly differentiated. On microscopic examination, SCCA appears as anaplastic cells found below the

Table 63-1
American Joint Committee on Cancer Staging Classification for Supraglottic Carcinoma

Tis	Carcinoma in situ
T1	Tumor confined to site of origin with normal mobility
T2	Tumor involving adjacent supraglottic site(s) or glottis without fixation
T3	Tumor limited to larynx with fixation and/or extension to involve postcricoid area, medial wall of pyriform sinus, or preepiglottic space
T4 a	Tumor invades through thyroid cartilage and/or tissues beyond the larynx
T4 b	Tumor invades prevertebral space, encases carotid artery, or invades mediastinal structures

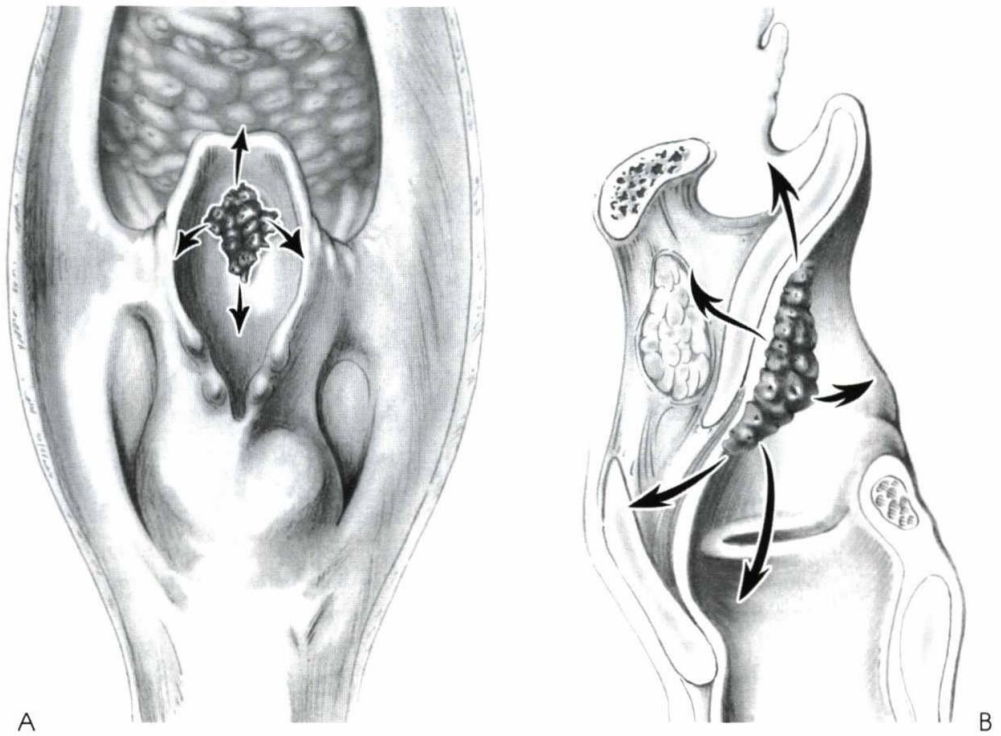

Figure 63-1. Schematic illustrations demonstrate the potential spread patterns (arrows) of an epiglottic carcinoma. (Reprinted with permission from Mukherji SK, Pillsbury H, Castillo M. Imaging squamous cell carcinomas of the upper aerodigestive tract: what the clinicians need to know. Radiology. *1997;205:629-646.)*

basement membrane with a variable degree of keratin production and intracellular bridges. Besides SCCA, other squamous cell aberrations that may arise in the larynx include the following categories: benign hyperplasia, benign keratosis, atypical hyperplasia, keratosis with epithelial atypia, intraepithelial carcinoma, and microinvasive squamous cell carcinoma. These lesions cannot be distinguished by cross-sectional imaging. SCCAs of the suprahyoid epiglottis tend to be bulky lesions that may extend deeply into the preepiglottic space or involve the aryepiglottic folds. Tumors of the infrahyoid epiglottis tend to grow circumferentially to involve the aryepiglottic folds, false vocal cords, and eventually the medial walls of the pyriform sinuses. Cartilage invasion may be present but is usually a late finding.

Treatment

The treatment for epiglottic carcinoma depends on the extent of disease and institutional preference. Very early lesions may be treated with radiation therapy or laser excision. More advanced tumors that do not cross the laryngeal ventricle (transglottic spread) may be treated with a supraglottic laryngectomy. Tumors that cross the laryngeal ventricle but have < 7 mm of anterior subglottic extension may be resected with supracricoid laryngectomy with cricohyoidopexy.

Recent studies have suggested pretreatment CT-derived tumor volume can be an important predictor of local control. It appears that CT can identify patients who have a high likelihood of cure with definitive radiation therapy as well as those patients who may require adjuvant chemotherapy or surgery.

Imaging Findings

CT

SCCA of the epiglottis presents as a midline bulky soft tissue mass. The tumor may extend anteriorly into the preepiglottic space or laterally to involve the aryepiglottic fold ("marginal lesion") (Fig. 63-2).

MR

SCCA is usually intermediate signal on T1-weighted images and slightly increased signal on T2-weighted images. These are typically bulky midline masses that diffusely enhance

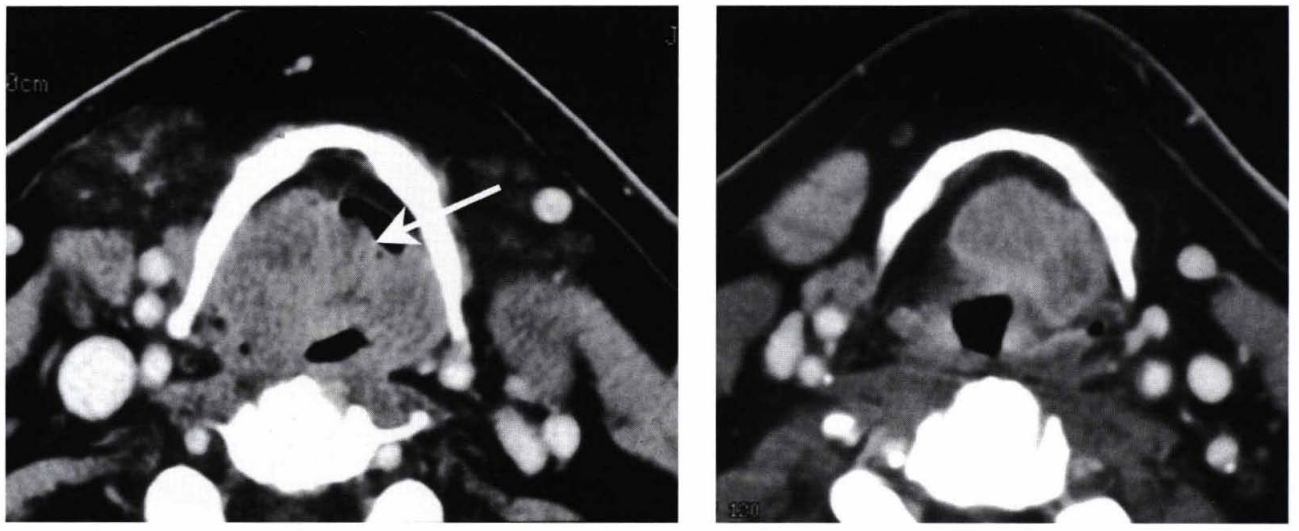

Figure 63–2. (A) Axial contrast-enhanced CT shows an aggressive lesion involving the epiglottis with involvement of the preepiglottic space. The tumor must be involving the epiglottis because the mass is involving the anterior portion of the larynx and is midline (arrow). The epiglottis is an anterior and midline structure, so the location of this tumor localizes it to the epiglottis. (B) Axial image in a different patient shows another example of an aggressive midline mass (primary epiglottic carcinoma) with less involvement of the preepiglottic space compared with the tumor illustrated in (A).

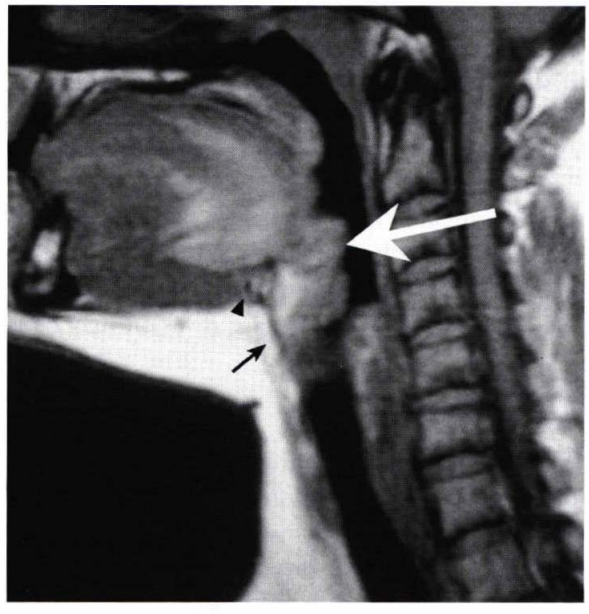

Figure 63–3. Sagittal contrast-enhanced T1-weighted image shows an aggressive enhancing tumor involving the suprahyoid (arrow) and infrahyoid (small arrow) portions of the epiglottis (arrowhead = hyoid bone).

with contrast. Cartilage invasion is detected by replacement of the increased T1-weighted signal on the noncontrast T1-weighted sequences (Fig. 63–3).

Imaging Pearls

- Certain specific information must be described in the reports and will directly affect the treatment and management of patients with epiglottic carcinoma:
  - Cartilage invasion
  - Exolaryngeal spread
  - Transglottic extension
  - Pyrifrom sinus invasion
  - Preepiglottic invasion

Suggested Readings

1. Mukherji SK, Pillsbury H, Castillo M. Imaging squamous cell carcinomas of the upper aerodigestive tract: what the clinicians need to know. *Radiology* 1997;205:629–646.
2. Million RR, Cassisi NJ, Mancuso AA. Larynx. In: Million RR, Cassisi NJ, eds. *Management of Head and Neck Cancer: A Multidisciplinary Approach*. Philadelphia: JB Lippincott; 1994.
3. Mancuso AA, Hanafee WN. Larynx and hypopharynx. In: *Computed Tomography and Magnetic Resonance Imaging of the Head and Neck*. 2nd ed. Baltimore: Williams and Wilkins; 1985.

Chapter 64

Squamous Cell Carcinoma of the Aryepiglottic Fold

Epidemiology

Cancer of the larynx is the most common head cancer and accounts for about 2% of all carcinomas. The supraglottic larynx is the second most common site of squamous cell carcinoma (SCCA) next to the true vocal cords. SCCA accounts for > 90% of cancers of the supraglottic larynx. Laryngeal cancer is more common in men (5–10:1). Patients typically present between the ages of 50 and 80. The aryepiglottic folds extend from the lateral margin of the epiglottis to the arytenoid cartilages. This is a subsite of the supraglottic larynx and is a common site for supraglottic carcinoma. All supraglottic carcinomas, including those that arise from the aryepiglottic folds, are directly related to cigarette smoking. Fortunately, the risk of tobacco-related cancers appears to be reversible; the risks for ex-smokers who have abstained from smoking for > 10 years are nearly equal to those for nonsmokers. Other forms of smoking, including cigar, pipe, and marijuana, are also felt to increase the likelihood of developing SCCA. Alcohol is the other major risk factor. Occupational exposure to oil, grease, and cement dust has also been associated with SCCA of the supraglottic larynx.

Clinical Findings

The staging of supraglottic carcinoma are presented in Table 64–1. Patients usually present with hoarseness and weight loss. Aryepiglottic fold carcinomas are usually exophytic lesions. Advanced lesions may extend to adjacent sites and lead to vocal cord fixation. The paretic cord is usually due to involvement of the cricoarytenoid joint or muscle rather than involvement of the recurrent laryngeal nerve. Patients with advanced lesions may present with difficulty breathing and may require tracheotomy. Advanced tumors may invade the thyroid and cricoid cartilages.

The primary echelon lymphatic drainage for aryepiglottic fold carcinomas is to nodal Groups II and III. The supraglottic larynx is rich in lymphatics, and nearly half of all patients will present with clinically positive neck metastases. Bilateral metastases will occur in up to 25% of all cases. However, in my experience, lateralized aryepiglottic fold carcinomas that do not extend to the epiglottis have a low likelihood of metastases to the contralateral neck. Thus it is important to define the full extent of disease because this may affect treatment of not only the primary site but also the neck.

Table 64–1
Sixth American Joint Committee on Cancer Staging Classification for Supraglottic Carcinoma

Tis	Carcinoma in situ
T1	Tumor confined to site of origin with normal mobility
T2	Tumor involving adjacent supraglottic site(s) or glottis without fixation
T3	Tumor limited to larynx with fixation and/or extension to involve postcricoid area, medial wall of pyriform sinus, or preepiglottic space
T4a	Tumor invades through thyroid cartilage and/or tissues beyond the larynx
T4b	Tumor invades prevertebral space, encases carotid artery, or invades mediastinal structures

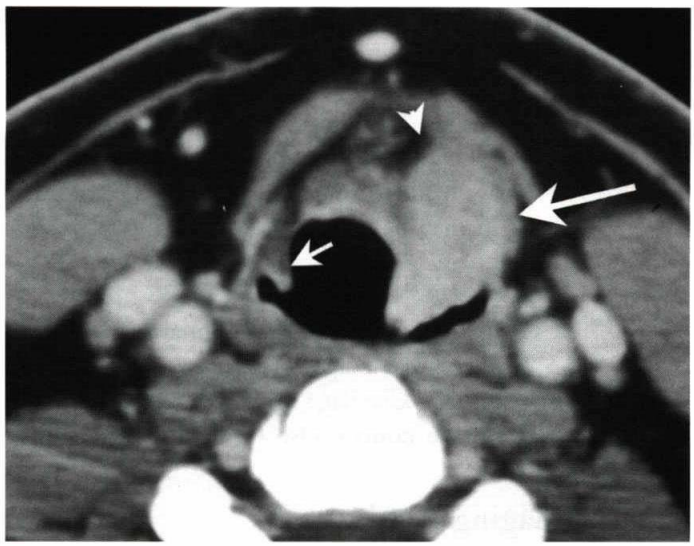

Figure 64–1. Axial contrast-enhanced CT shows an aggressive mass involving the left aryepiglottic fold (large arrow). The mass extends anteriorly into the preepiglottic space (arrowhead). Note the appearance of the normal aryepiglottic fold on the contralateral side (small arrow).

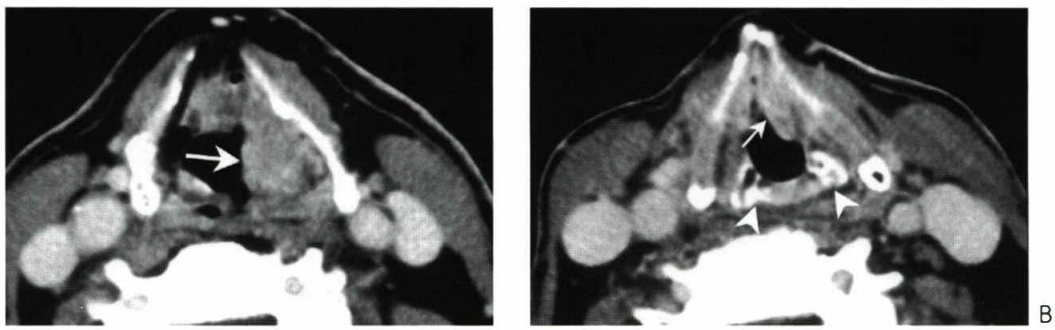

A B

Figure 64–2. Aryepiglottic fold carcinoma with transglottic spread. (A) Axial contrast-enhanced CT shows a left aryepiglottic fold carcinoma (arrow). Clinically, this patient had a muffled voice but was felt to be a candidate for a supraglottic laryngectomy. (B) However, this image obtained at the level of the true vocal cords (cricoarytenoid joints–arrowheads) shows tumor involving the anterior portion of the left true vocal cord (arrow). Thus the tumor extends inferiorly and has crossed the false vocal cord and laryngeal ventricle to involve the true vocal cord. This "transglottic spread" prevented this patient from undergoing a supraglottic laryngectomy.

Pathology

Histologically, squamous cell carcinoma is classified as well, moderately, and poorly differentiated. On microscopic examination, SCCA appears as anaplastic-appearing cells found below the basement membrane with a variable degree of keratin production and intracellular bridges. Besides SCCA, other squamous cell aberrations that may arise in the larynx include the following categories: benign hyperplasia, benign keratosis, atypical hyperplasia, keratosis with epithelial atypia, intraepithelial carcinoma, and microinvasive squamous cell carcinoma. These lesions cannot be distinguished by cross-sectional imaging. SCCAs of the aryepiglottic folds are exophytic but will involve important adjacent structures as the tumor enlarges. Cartilage invasion may be present but is usually a late finding.

Treatment

The treatment for SCCA of the aryepiglottic fold depends on the extent of disease and institutional preference. Very early lesions may be treated with radiation therapy. More advanced tumors that do not cross the laryngeal ventricle may be treated with a supraglottic laryngectomy. Tumors that cross the laryngeal ventricle (transglottic spread) but have < 7 mm of anterior subglottic extension may be resected with supracricoid laryngectomy with cricohyoidopexy.

Recent studies have suggested that pretreatment CT-derived tumor volume can be an important predictor of local control. It appears that CT can identify patients who have a high likelihood of cure with definitive radiation therapy as well as those patients who may require adjuvant chemotherapy or surgery.

Imaging Findings

CT

SCCA of the aryepiglottic fold presents as a paramedian bulky soft tissue mass. The tumor may extend anteriorly into the paralaryngeal space or medially to involve the epiglottic fold. Very advanced lesions may extend to the contralateral aryepiglottic fold, and the exact site of origin may be difficult to determine (Figs. 64–1 and 64–2).

MR

SCCA is usually intermediate signal on T1-weighted images and slightly increased signal on T2-weighted images. These are typically bulky midline masses that diffusely enhance with contrast. Cartilage invasion is detected by replacement of the increased T1-weighted signal on the noncontrast T1-weighted sequences.

Imaging Pearls

- Certain specific information must be described in the reports and will directly affect the treatment and management of patients with aryepiglottoc fold carcinoma:
  - Cartilage invasion
  - Exolaryngeal spread
  - Transglottic extension
  - Pyriform sinus invasion
  - Preepiglottic invasion

Suggested Readings

1. Mukherji SK, Pillsbury H, Castillo M. Imaging squamous cell carcinomas of the upper aerodigestive tract: what the clinicians need to know. *Radiology* 1997;205:629–646.
2. Million RR, Cassisi NJ, Mancuso AA. Larynx. In: Million RR, Cassisi NJ, eds. *Management of Head and Neck Cancer: A Multidiscinıplinary Approach.* Philadelphia: JB Lippincott; 1994.
3. Mancuso AA, Hanafee WN. Larynx and hypopharynx. In: *Computed Tomography and Magnetic Resonance Imaging of the Head and Neck.* 2nd ed. Baltimore: Williams and Wilkins; 1985.

Chapter 65

Squamous Cell Carcinoma of the False Vocal Cord

Epidemiology

Laryngeal carcinoma is the most common head cancer and accounts for about 2% of all carcinomas. The false vocal cord (FVC) are a subsite of the supraglottic larynx. However, this is an unusual primary site for a supraglottic carcinoma. The major risk factors are tobacco and alcohol. Other reported findings are occupational exposure to oil, grease, and cement dust. Supraglottic carcinoma is more common in men (5–10:1) and usually presents between the ages of 50 and 80.

Clinical Findings

The staging of supraglottic carcinoma are presented in Table 65–1. Patients usually present with hoarseness. Patients with advanced lesions may present with difficulty breathing and weight loss. FVC tumors may extend inferiorly to involve the true vocal cords. Such submucosal spread is often clinically occult and may lead to understaging of the lesion if this extension is undetected prior to surgery. FVC tumors may extend laterally to involve the medial wall of the pyriform sinus and medially to the inferior portion of the epiglottis, thereby, increasing the likelihood of invasion of the preepiglottic space. Cartilage invasion by FVC carcinoma is less common when compared to glottic carcinoma, and when present is typically seen with advanced lesions.

Pathology

Histologically, squamous cell carcinoma (SCCA) is classified as well, moderately, and poorly differentiated. On microscopic examination, SCCA appears as anaplastic cells found below the basement membrane with a variable degree of keratin production and intracellular bridges. Besides SCCA, other squamous cell aberrations that may arise in the larynx include the following categories: benign hyperplasia, benign keratosis, atypical hyperplasia, keratosis with epithelial atypia, intraepithelial carcinoma, and microinvasive squamous cell carcinoma. SCCAs that arise from the false vocal cord tend to be ulcerative and infiltrative with little exophytic component. Deep invasion by such tumors results in access of these tumors to the paraglottic space and may lead to fixation of the supraglottic larynx.

Table 65–1
American Joint Committee on Cancer Staging Classification for Supraglottic Carcinoma

Tis	Carcinoma in situ
T1	Tumor confined to site of origin with normal mobility
T2	Tumor involving adjacent supraglottic site(s) or glottis without fixation
T3	Tumor limited to larynx with fixation and/or extension to involve postcricoid area, medial wall of pyriform sinus, or preepiglottic space
T4a	Tumor invades through thyroid cartilage and/or tissues beyond the larynx
T4b	Tumor invades prevertebral space, encases carotid artery, or invades mediastinal structures

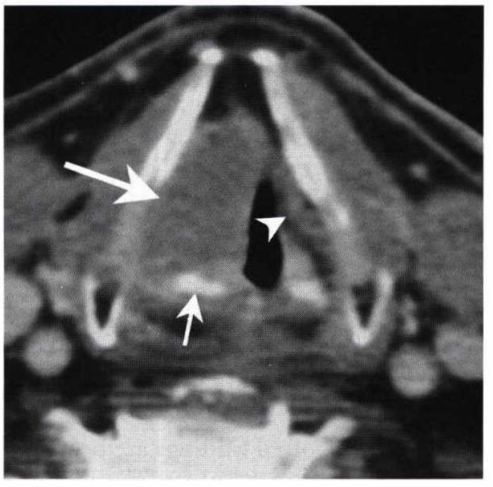

Figure 65-1. Axial CT demonstrates an aggressive lesion involving the right false vocal cord (large arrow). The radiographic landmarks that help localize the tumor to the false vocal cord are visualization of the superior portion of the arytenoid cartilage (small arrow) and the lateral thyroarytenoid muscle (arrowhead). Identification of both of these important landmarks indicates that the false vocal cord is involved by tumor. Compare this with the expected radiographic appearance of a tumor involving the aryepiglottic fold (Fig. 64-1).

Treatment

Early lesions can be treated successfully with radiation therapy or partial laryngectomy. Advanced lesions require total laryngectomy or some form of combined therapy. Combined radiation therapy and chemotherapy is gaining acceptance as a nonsurgical treatment alternative for advanced tumors.

Imaging Findings

CT

The imaging findings are nonspecific. A tumor that is primarily arising from the FVC can be suggested by a mass that is located at the level of the arytenoid cartilage and lateral thyroarytenoid muscle. This is approximately 6 to 9 mm superior to the level of the cricoarytenoid joint. These lesions have a propensity to extend inferiorly and posteriorly into the interarytenoid space and erode the arytenoid cartilage. Thyroid cartilage invasion is usually a late finding (Fig. 65-1).

MR

SCCA is usually intermediate signal on T1-weighted images and slightly increased signal on T2-weighted images. The lesions usually enhance with contrast. Cartilage invasion is detected by replacement of the increased T1-weighted signal on the noncontrast T1-weighted sequences.

Imaging Pearls

- Certain specific information must be described in the reports and will directly affect the treatment and management of patients with true vocal cord carcinoma:
  - Cartilage invasion
  - Exolaryngeal spread
  - Transglottic extension
  - Pyriform sinus invasion
  - Preepiglottic invasion

Suggested Readings

1. Mukherji SK, Pillsbury H, Castillo M. Imaging squamous cell carcinomas of the upper aerodigestive tract: what the clinicians need to know. *Radiology* 1997;205:629-646.
2. Million RR, Cassisi NJ, Mancuso AA. Larynx. In: Million RR, Cassisi NJ, eds. *Management of Head and Neck Cancer: A Multidisciplinary Approach.* Philadelphia: JB Lippincott; 1994.
3. Mancuso AA, Hanafee WN. Larynx and hypopharynx. In: *Computed Tomography and Magnetic Resonance Imaging of the Head and Neck.* 2nd ed. Baltimore: Williams and Wilkins; 1985.

Chapter 66

Squamous Cell Carcinoma of the True Vocal Cord (Glottis)

Epidemiology

Laryngeal carcinoma is the most common head cancer and accounts for about 2% of all carcinomas. The true vocal cords are the most common site of laryngeal carcinomas, with the ratio of glottic carcinomas to supraglottic carcinomas being approximately 3:1. These tumors involve the right and left true vocal cords with equal incidence. True vocal cord carcinoma is directly associated with cigarette smoking. Fortunately, the risk of tobacco-related cancers appears to be reversible; the risks of ex-smokers who have abstained from smoking for > 10 years are nearly equal to those for nonsmokers. Other forms of smoking, including cigar, pipe, and marijuana, are also believed to increase the risk of developing squamous cell carcinoma (SCCA). Other risk factors include alcohol, prior irradiation, and viruses (herpes simplex, papilloma virus). Laryngeal cancer is more common in men (5–10:1) between the ages of 50 and 80.

Clinical Findings

The staging of glottic carcinoma are presented in Table 66–1. Patients usually present with hoarseness. Those with advanced lesions may present with difficulty breathing and weight loss. A subset of glottic tumors are localized to the anterior commissure and are termed anterior commissure tumors. These tumors may spread along Broyle's ligament to the laryngeal surface of the thyroid cartilage and result in early cartilage invasion (Fig. 66–1).

The likelihood of nodal involvement associated with glottic carcinomas is dependent on the stage of the tumor. The incidence of nodal metastases in early T1 lesions is low (< 5%). This figure increases to approximately 20% for T3 and T4 lesions. The nodes most at risk of metastases are the internal jugular chain. Paratracheal nodes may be involved in glottic tumors that have a significant amount of subglottic spread.

Table 66–1
Sixth American Joint Committee on Cancer Staging Classification for Glottic Carcinoma

T1	Tumor limited to vocal cord (may involve anterior or posterior commissures) with normal mobility
T1a	Tumor limited to one vocal cord
T1b	Tumor involves both vocal cords
T2	Tumor extends to supraglottis and/or subglottis, and/or with impaired vocal cord mobility
T3	Tumor limited to the larynx with vocal cord fixation and/or invades paraglottic space, and/or minor cartilage erosion (e.g., inner cortex)
T4a	Tumor invades through thyroid cartilage and/or to other tissues beyond the larynx (e.g., trachea, soft tissues of neck, including thyroid, pharynx)
T4b	Tumor invades prevertebral space, encases carotid artery, or invades mediastinal structures

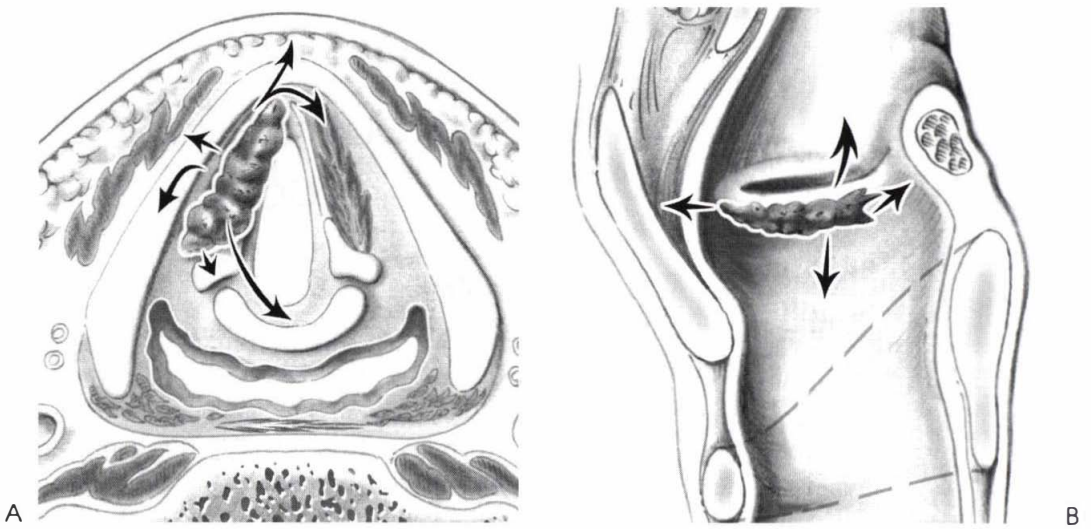

Figure 66–1. Schematic illustrations demonstrating the spread patterns (arrows) of a true vocal cord carcinoma.

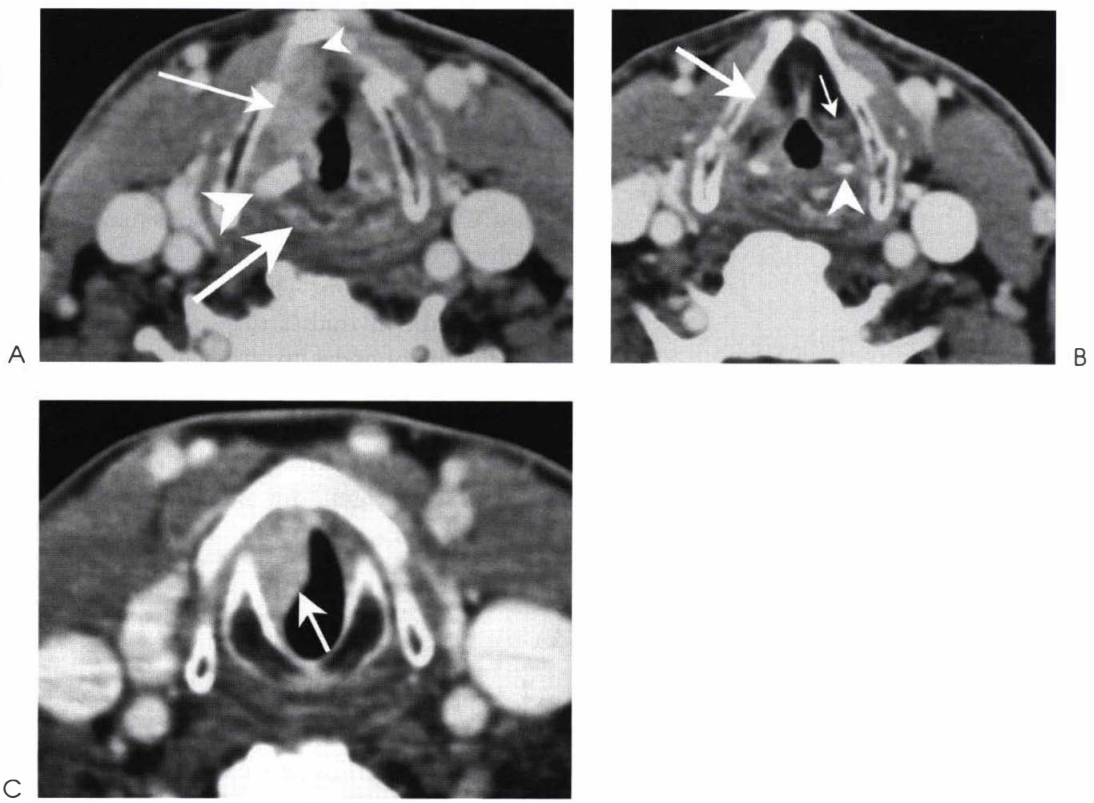

Figure 66–2. (A) Axial contrast-enhanced CT shows an aggressive lesion involving the right true vocal cord (small arrow). The tumor extends anteriorly to involve the anterior commissure (small arrowhead). The radiographic landmark that localizes the tumor to the true vocal cord is the cricoarytenoid joint, which consists of the arytenoid cartilage (large arrowhead) and the cricoid cartilage (large arrow). (B) The tumor extends superiorly to the level of the false vocal cord (large arrow). Therefore, the tumor has superior "transglottic" spread. The radiographic landmarks that localize the tumor to the level of the false vocal cord are visualization of the superior portion of the arytenoid cartilage (arrowhead) and lateral thyroarytenoid muscle (arrow). These findings preclude the patient from undergoing a standard hemilaryngectomy. (C) The tumor extends to the subglottis and therefore has "subglottic" spread (arrow). These findings prevent the patient from undergoing a standard supracricoid laryngectomy.

Pathology

Histologically, SCCA is classified as well, moderately poorly differentiated. On microscopic examination, SCCA appears as anaplastic cells found below the basement membrane with a variable degree of keratin production and intracellular bridges. Besides SCCA, other squamous cell aberrations that may arise in the larynx include the following categories: benign hyperplasia, benign keratosis, atypical hyperplasia, keratosis with epithelial atypia, intraepithelial carcinoma, and microinvasive squamous cell carcinoma. These lesions are unable to be distinguished by cross-sectional imaging.

Treatment

The treatment for true vocal cord carcinomas depends on the size of the lesion and institutional preference. Very early lesions may be treated with cordectomy, hemilaryngectomy, vertical partial laryngectomy with laryngoplasty, or radiation therapy. More advanced lesions may be treated with supracricoid laryngectomy, total laryngectomy, or combined chemotherapy and radiation therapy.

Imaging Findings

CT

SCCA of the glottis is usually smaller than lesions that present elsewhere in the upper aerodigestive tract. This is because patients present earlier due to hoarseness because the airway is narrower and the tumors need not be as large to significantly impinge on the airway. The CT findings are enhancing paramedian soft tissue masses that are located at the cricoarytenoid joint. Early superficial mucosal lesions may not be detected on imaging (Fig. 66–2).

MR

SCCA is usually intermediate signal on T1-weighted and slightly increased signal on T2-weighted images. The lesions usually enhance with contrast. Cartilage invasion is detected by replacement of the increased T1-weighted signal on the noncontrast T1-weighted sequences.

Imaging Pearls

- Certain specific information must be described in the reports and will directly affect the treatment and management of patients with true vocal cord carcinoma:
  - Transglottic extension
  - Subglottic extension and relationship to cricoid cartilage
  - Cartilage invasion
  - Cartilage sclerosis
  - Involvement of the anterior commissure
  - Involvement of the cricoarytenoid joint
  - Extension to the posterior commissure
  - Deep invasion of the paraglottic fat

Suggested Readings

1. Mukherji SK, Pillsbury H, Castillo M. Imaging squamous cell carcinomas of the upper aerodigestive tract: what the clinicians need to know. *Radiology* 1997;205:629–646.
2. Million RR, Cassisi NJ, Mancuso AA. Larynx. In: Million RR, Cassisi NJ, eds. *Management of Head and Neck Cancer: A Multidisciplinary Approach.* Philadelphia: JB Lippincott; 1994.
3. Mancuso AA, Hanafee WN. Larynx and hypopharynx. In: *Computed Tomography and Magnetic Resonance Imaging of the Head and Neck.* 2nd ed. Baltimore: Williams and Wilkins; 1985.

Chapter 67

Squamous Cell Carcinoma of the Subglottis

Epidemiology

The subglottic larynx extends from the inferior border of the true vocal cords to the inferior margin of the cricoid cartilage. Another commonly used definition to identify the proximal margin of the subglottis is that it begins mucosally at about 5 mm below the level of the free margin of the true vocal cords.

Primary squamous cell carcinomas (SCCAs) of the subglottis are rare and constitute between 4 and 6% of all laryngeal carcinomas. Because of this rarity, it is difficult to determine the specific population at risk. However, it is probably similar to the patient population at risk for other types of SCCA of the larynx.

Clinical Findings

The staging of subglottic carcinoma is presented in Table 67-1. Stridor and dyspnea are the most common symptoms. Hoarseness is also a common presenting complaint because many primary subglottic carcinomas are advanced at initial presentation and will involve the true vocal cords. Advanced lesions often extend inferiorly into the proximal trachea. Invasion of the cricoid cartilage and anterior extension through the cricothyroid membrane into the soft tissues of the neck are common (Fig. 67-1). The primary echelon lymph nodes for the subglottic larynx differ from other subsites of the larynx. The nodes at greatest risk of metastases from a primary SCCA of the subglottic larynx are the prelaryngeal (Delphian), pretracheal, paratracheal, and supraclavicular lymph nodes. The risk of nodal metastases is approximately 10%.

Pathology

Histologically, SCCA is classified as well, moderately, and poorly differentiated. On microscopic examination, SCCA appears as anaplastic cells found below the basement membrane with a variable degree of keratin production and intracellular bridges. Besides SCCA, other squamous cell aberrations that may arise in the larynx include the following categories: be-

Table 67-1
Sixth American Joint Committee on Cancer Staging Classification for Subglottic Carcinoma

Primary tumor cannot be assessed	
T0	No evidence of primary tumor
Tis	Carcinoma in situ
T1	Tumor limited to the subglottis
T2	Tumor extension to vocal cord(s) with normal or impaired cord mobility
T3	Tumor confined to larynx with cord fixation
T4a	Tumor invades through thyroid cartilage and/or to other tissues beyond the larynx (e.g., trachea, soft tissues of neck, including deep extrinsic muscles of the tongue, strap muscles, thyroid or esophagus)
T4b	Tumor invades prevertebral space, encases carotid artery, or invades mediastinal structures

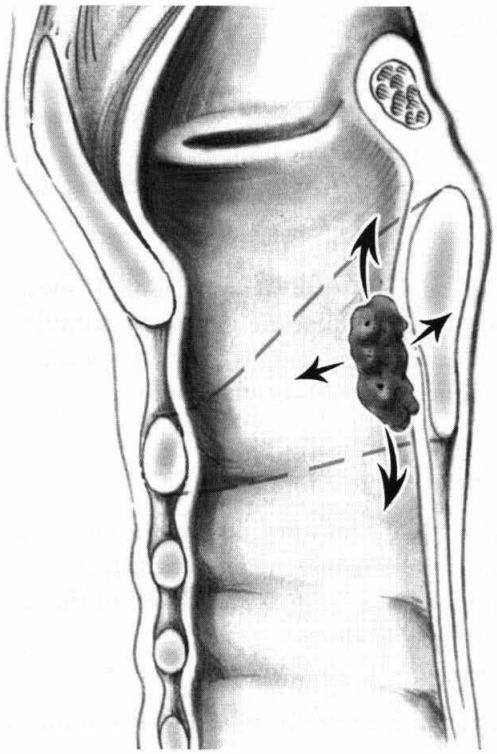

Figure 67–1. Schematic illustration of the spread patterns (arrows) of a primary subglottic carcinoma.

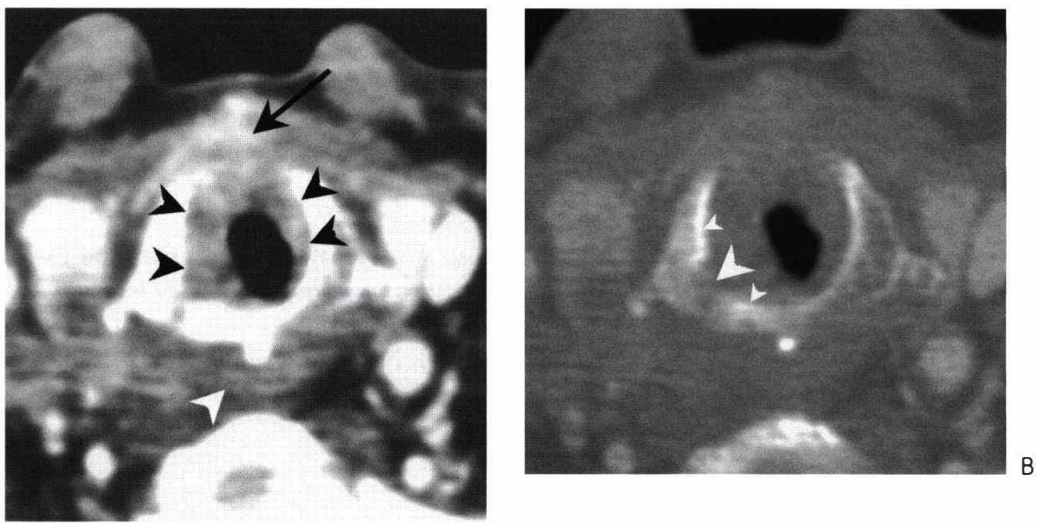

Figure 67–2. (A) Axial contrast-enhanced CT demonstrates a circumferential squamous cell carcinoma located in the subglottis (arrowheads). The mass extends anteriorly through the cricoid cartilage into the soft tissues of the neck (T4) (arrow). The presence of a soft tissue mass in the airway lumen at the level of the cricoid cartilage indicates the mass is involving the subglottis. The white arrowhead indicates the location of the "postcricoid" region. (B) Bone algorithm obtained at the same level as in (A) shows cartilage erosion of the inner cortex of the cricoid cartilage (large arrowhead) and areas of cartilage sclerosis (small arrowheads).

nign hyperplasia, benign keratosis, atypical hyperplasia, keratosis with epithelial atypia, intraepithelial carcinoma, and microinvasive squamous cell carcinoma. These lesions are unable to be distinguished by cross-sectional imaging. SCCA of the subglottis tend to be circumferential lesions that may extend superiorly to involve the true vocal cords and inferiorly to involve the proximal trachea. Advanced tumors may extend into the anterior soft tissues of the neck. Invasion of the cricoid cartilage is common.

Treatment

The most common treatment for SCCA of the subglottis is total laryngectomy. Tumors that involve the proximal portion of the trachea require resection of the involved area. The reported 5-year survival rates vary between 40 and 80%. Primary treatment with radiation therapy is not commonly performed. Combined treatment with radiation therapy and chemotherapy is currently under investigation.

Imaging Findings

CT

SCCA of the subglottis presents as a circumferential soft tissue mass located at the level of the cricoid cartilage. The tumors may extend superiorly to involve the true vocal cords and extend inferiorly to involve the trachea (Fig. 67-2).

MR

SCCA is usually intermediate signal on T1-weighted and slightly increased signal on T2-weighted images. These are typically circumferential masses that diffusely enhance with contrast. Cartilage invasion is detected by replacement of the increased T1-weighted signal on the noncontrast T1-weighted sequences.

Imaging Pearls

- Certain specific information must be described in the reports and will directly affect the treatment and management of patients with epiglottic carcinoma:
  - Inferior extent with identification of the levels of tracheal involvement
  - Cartilage invasion
  - Anterior soft tissue invasion
- Special attention needs to be directed to the presence of metastases to the paratracheal, Group IV, and supraclavicular lymph nodes.

Suggested Readings

1. Mukherji SK, Pillsbury H, Castillo M. Imaging squamous cell carcinomas of the upper aerodigestive tract: what the clinicians need to know. *Radiology* 1997;205:629-646.
2. Million RR, Cassisi NJ, Mancuso AA. Larynx. In: Million RR, Cassisi NJ, eds. *Management of Head and Neck Cancer: A Multidisciplinary Approach.* Philadelphia: JB Lippincott; 1994:431-497.
3. Mancuso AA, Hanafee WN. Larynx and hypopharynx. In: *Computed Tomography and Magnetic Resonance Imaging of the Head and Neck.* 2nd ed. Baltimore: Williams and Wilkins; 1985:241-357.
4. Batsakis JG. Neoplasms of the larynx. In: Batsakis JG, ed. *Tumors of the Head and Neck.* Baltimore: Williams and Wilkins; 1979:200-225.

Chapter 68

Squamous Cell Carcinoma of the Pyriform Sinus

Epidemiology

The pyriform sinus is a subsite of the hypopharynx and is the most common location for squamous cell carcinoma (SCCA) that originates in the hypopharynx. The superior margin of the pyriform sinus is the pharyngoepiglottic fold, which is at the level of the base of the vallecula. The pyriform sinus tapers to an apex, which is located at the top of the cricoid cartilage. On cross-sectional imaging, the apex of the pyriform sinus is located at the level of the cricoarytenoid joint.

The incidence of SCCA of the pyriform sinus cancer is lower than that of SCCA of the larynx. Risk factors include excessive tobacco and alcohol use, prior radiation therapy, and Plummer-Vinson syndrome (Paterson–Brown Kelly syndrome). This syndrome is thought to be precancerous and is characterized by iron-deficiency anemia; achlorhydria; generalized atrophy of the mucous membranes of the mouth, pharynx, and esophagus; webs in the hypopharynx and cervical esophagus; and weight loss. SCCA most commonly arises in middle-aged males. Plummer-Vinson syndrome is more common in women and should be considered in women with pyriform sinus or other types of hypopharyngeal carcinoma.

Clinical Findings

The staging of hypopharyngeal carcinoma is presented in Table 68–1. The hypopharynx is often a clinically silent area for early tumors. As a result, many of these tumors are advanced at initial presentation. Symptoms associated with early tumors include persistent sore throat, or pain after swallowing hot foods or liquids. Advanced lesions often present with dysphagia, change in voice, enlarging neck mass, and weight loss. Referred ear pain (otalgia) may occur and is due to invasion of the superior laryngeal nerve (Fig. 68–1). It is important to note that up to 15% of patients will have a synchronous or metachronous second tumor.

Table 68–1
Sixth American Joint Committee on Cancer Staging Classification for Hypopharyngeal Carcinoma

Primary tumor cannot be assessed	
T0	No evidence of primary tumor
Tis	Carcinoma in situ
T1	Tumor limited to one subsite of hypopharynx and < 2 cm in greatest dimension
T2	Tumor invades more than one subsite of hypopharynx or an adjacent site, or 2–4 cm in greatest diameter without fixation of hemilarynx
T3	Tumor > 4 cm in greatest diameter with fixation of hemilarynx
T4 a	Tumor invades thyroid/cricoid cartilage, hyoid bone, thyroid gland, esophagus, or central compartment soft tissue (prelaryngeal strap muscles and subcutaneous fat)
T4 b	Tumor invades prevertebral fascia, encases carotid artery, or involves mediastinal structures

The hypopharynx is rich in lymphatics. Up to 75% of patients will have nodal metastases at initial presentation. The primary echelon lymphatic drainage for pyriform sinus carcinomas is the retropharyngeal lymph nodes and Groups II through V. Early lesions limited to the pyriform sinus usually have ipsilateral drainage. However, lesions that involve the posterior pharyngeal wall place both sides of the neck at risk for metastases. Retropharyngeal lymph nodes are an important group to evaluate because this nodal group cannot be evaluated on clinical examination. They should be classified as cervical nodes for staging.

Pathology

Over 95% of tumors of the hypopharynx and pyriform sinus are SCCA. Histologically, SCCA is classified as well, moderately, and poorly differentiated. On microscopic examination, SCCA appears as anaplastic cells found below the basement membrane with a variable degree of keratin production and intracellular bridges. Besides SCCA, other squamous cell aberrations that may arise in the larynx include the following categories: benign hyperplasia, benign keratosis, atypical hyperplasia, keratosis with epithelial atypia, intraepithelial carcinoma, and microinvasive squamous cell carcinoma. Pyriform sinus carcinoma may erode the cartilage. This most commonly occurs when tumors wrap around the lateral margin of the ala of the thyroid cartilage.

Treatment

The preferred treatment for pyriform sinus carcinoma depends on institutional preference and the desires of the patient. Pyriform sinus carcinoma can be successfully treated with surgery, with the exact procedure depending on the extent of disease. A partial laryngopharyngectomy removes the false vocal cords, epiglottis, and pyriform sinus. This is usually performed for early (T1, T2) lesions confined to the pyriform sinus. A total laryngopharyngectomy is performed for advanced lesions and involves resection of the larynx and varying amounts of the pharyngeal wall.

Pyriform sinus carcinoma may also be treated with definitive radiation therapy (RT). Recent investigations have suggested that a pretreatment "imaging profile" based on tumor volume and involvement of the apex can be used to select patients that may be candidates for treatment with definitive RT. Pyriform sinus carcinomas with a tumor volume < 6.5 cc and minimal apical involvement have over 85% of local control when treated with RT alone. The role of combined chemotherapy and RT is currently under investigation.

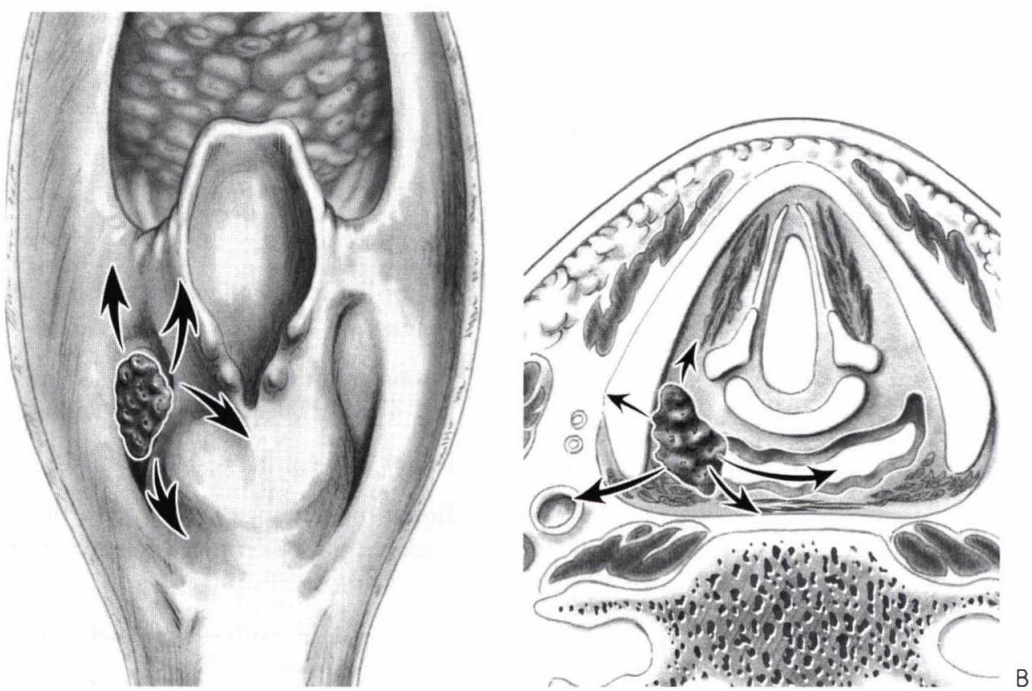

Figure 68–1. (A,B) The potential spread patterns (arrows) of pyriform sinus carcinoma. (Reprinted with permission from Mukherji SK, Pillsbury H, Castillo M. Imaging squamous cell carcinomas of the upper aerodigestive tract: what the clinicians need to know. Radiology, *1997;205:629–646.)*

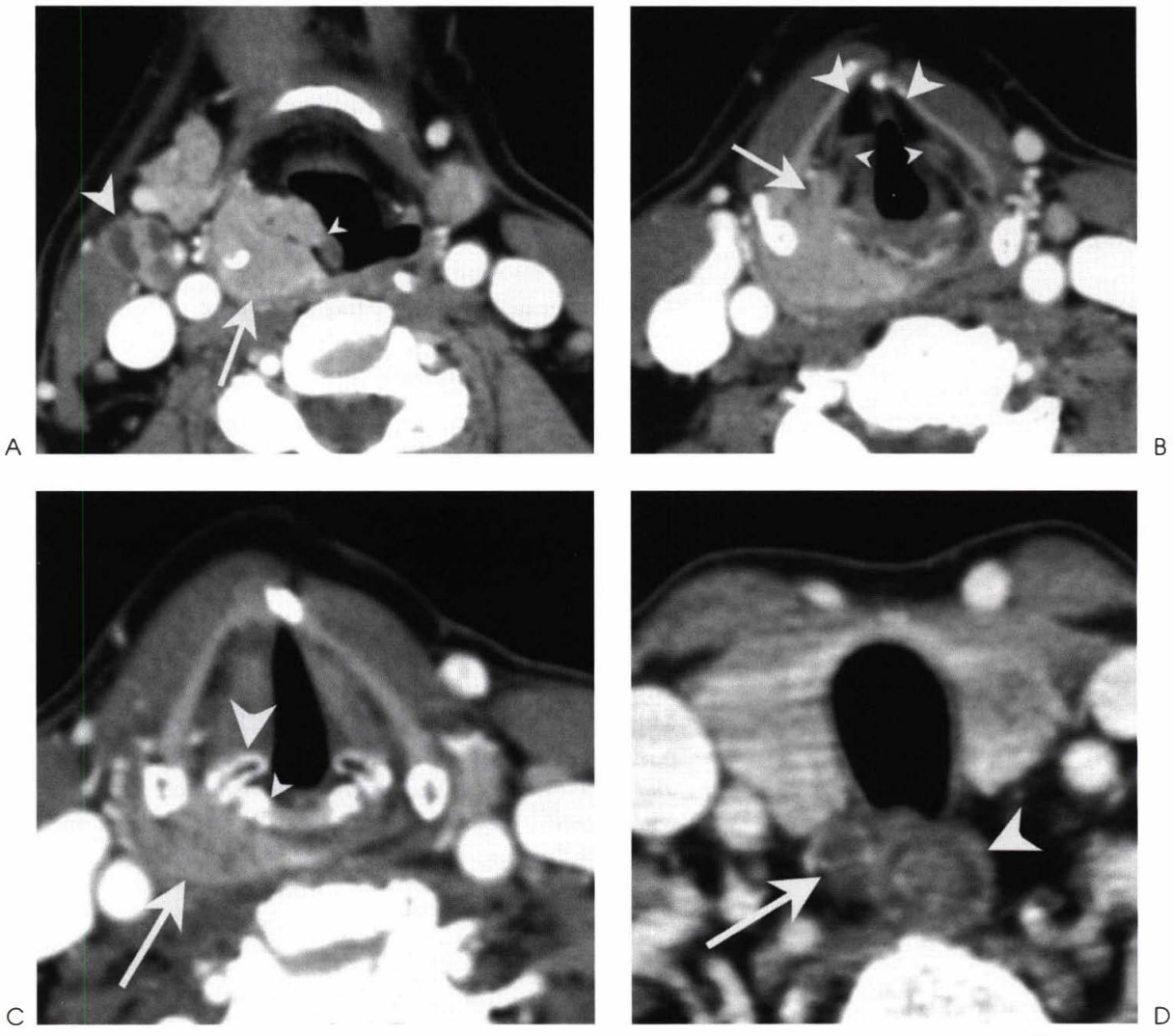

Figure 68–2. (A) Axial contrast-enhanced CT obtained at the level of the inferior margin of the hyoid bone demonstrates a squamous cell carcinoma of the right pyriform sinus (arrow). The tumor extends along the medial wall of the aryepiglottic fold, which is formed by the ipsilateral aryepiglottic fold (small arrowhead). The large arrowhead identifies a positive metastatic lymph node. (B) Axial image performed at the level of the thyroid cartilage shows the tumor to extend anteriorly into the right paraglottic space (arrow). The large arrowheads indicate the laryngeal ventricle; the small arrowheads, the lateral thyroarytenoid muscles. (C) There is "bulk apical disease" (> 1 cm diameter) at the level of the apex of the pyriform sinus. The radiologic landmarks that identify the apex of the pyriform are the arytenoid cartilage (large arrowhead) and the cricoid cartilage (small arrowhead), which together constitute the cricoarytenoid joint. (D) There is a metastatic tracheoesophageal lymph node (arrow) located adjacent to the esophagus (arrowhead). Large volume pyriform sinus tumors that extend to the apex of the pyriform sinus are at risk for metastases to this nodal group ("visceral group," level VI). This group is not routinely resected in a "radical," "modified radical," or "selective" neck dissection and requires a "central" neck dissection for resection.

Imaging Findings

CT

SCCA of the pyriform sinus presents as a soft tissue mass centered in the pyriform sinus and lateral to the aryepiglottic fold. The tumor may extend anteriorly into the paralaryngeal space or medially to involve the aryepiglottic fold. Very advanced lesions may cross the midline and involve the contralateral aryepiglottic fold. The tumors may extend inferiorly to involve the apex of the pyriform sinus and involve the postcricoid region (Fig. 68–2).

MR

SCCA of the pyriform sinus is usually intermediate signal on T1-weighted and slightly increased signal on T2-weighted images. These are typically bulky lateralized masses that diffusely enhance with contrast. Cartilage invasion is detected by replacement of the increased T1-weighted signal on the noncontrast T1-weighted sequences.

Imaging Pearls

Certain specific information must be described in the reports and will directly affect the treatment and management of patients with aryepiglottoc fold carcinoma:

- Surgery
  - Midline extension
  - Apical involvement
  - Extension into the esophageal inlet
  - Cartilage invasion
  - Anterior extension into paraglottic space
  - Exolaryngeal spread
  - Prevertebral muscle invasion
- Radiation therapy
  - Apical involvement
  - Cartilage invasion
  - Tumor volume

Suggested Readings

1. Mukherji SK, Pillsbury H, Castillo M. Imaging squamous cell carcinomas of the upper aerodigestive tract: what the clinicians need to know. *Radiology* 1997;205:629–646.
2. Million RR, Cassisi NJ, Mancuso AA. Hypopharynx: pharyngeal walls, pyriform sinus, postcricoid pharynx. In: Million RR, Cassisi NJ, Mancuso AA, eds. *Management of Head and Neck Cancer: A Multidisciplinary Approach.* Philadelphia: JB Lippincott; 1994.
3. Mukherji SK, Weissman JL, Holliday R. The pharynx. In: Som PM, Curtin H, eds. *Head and Neck Imaging.* 3rd ed. New York: Mosby; 1996.

Chapter 69

Squamous Cell Carcinoma of the Postcricoid Region

Epidemiology

The hypopharynx is the most caudad portion of the pharynx. The superior margin of the hypopharynx is at the level of the pharyngoepiglottic fold. This location can be approximated by the vallecula and the hyoid bone. The inferior border of the hypopharynx is at the cricopharyngeus muscle, which forms the "esophageal verge." On cross-sectional imaging, this is located at the inferior margin of the cricoid cartilage. The postcricoid region permits passage of food into the esophagus. There is no defined superior margin, however it may be considered to begin just below the arytenoids. The anterior wall of the postcricoid region is the mucosa on the posterior aspect of the cricoid cartilage. This is a common wall shared with the posterior wall of the subglottis and is often referred to as the "party wall." The inferior aspect of the postcricoid region is the esophageal verge formed by the cricopharyngeus muscle.

These are rare lesions. They are more common in elderly males. Specific risk factors have not been thoroughly investigated due to the rarity of these tumors but are probably similar to other subsites of squamous cell carcinoma (SCCA).

Clinical Findings

The staging of hypopharyngeal carcinoma is presented in Table 69-1. The symptoms are nonspecific and similar to other subsites in the hypopharynx. These include sore throat, difficulty swallowing, dysphagia, and weight loss. The majority of postcricoid region tumors are SCCA. Tumors arising from the posterior wall tend to remain on the posterior wall. Lesions originating from the anterior wall may invade the posterior cricoarytenoid muscle and arytenoid cartilages. Advanced lesions may encircle the lumen. The prognosis tends to be poor due to advanced stage at presentation and rich lymphatics. Up to 75% of patients will have nodal metastases at initial presentation. The apex of the pyriform sinus exits into the postcricoid region. Therefore, postcricoid carcinomas may extend superiorly to involve the apex of the pyriform sinus and its lymphatic drainage.

Table 69-1
Sixth American Joint Committee on Cancer Staging Classification for Hypopharyngeal Carcinoma

TX	Primary tumor cannot be assessed
T0	No evidence of primary tumor
Tis	Carcinoma in situ
T1	Tumor limited to one subsite of hypopharynx and < 2 cm in greatest dimension
T2	Tumor invades more than one subsite of hypopharynx or an adjacent site, or 2–4 cm in greatest diameter without fixation of hemilarynx
T3	Tumor > 4 cm in greatest diameter with fixation of hemilarynx
T4a	Tumor invades thyroid/cricoid cartilage, hyoid bone, thyroid gland, esophagus, or central compartment soft tissue (prelaryngeal strap muscles and subcutaneous fat)
T4b	Tumor invades prevertebral fascia, encases carotid artery, or involves mediastinal structures

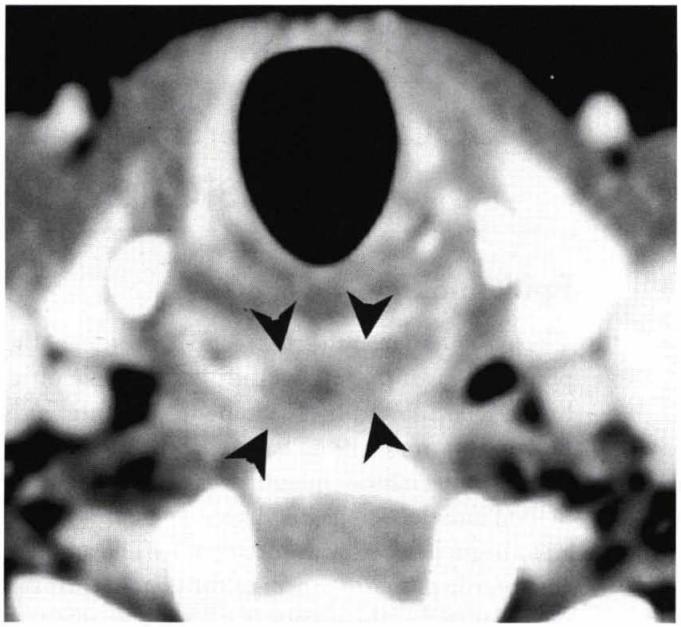

Figure 69–1. Axial contrast-enhanced CT demonstrates an aggressive enhancing tumor involving the postcricoid region (arrowheads). Note that the tumor is involving the hypopharynx at the level of the cricoid cartilage. The cricoid is the radiologic landmark for identifying the postcricoid region of the hypopharynx.

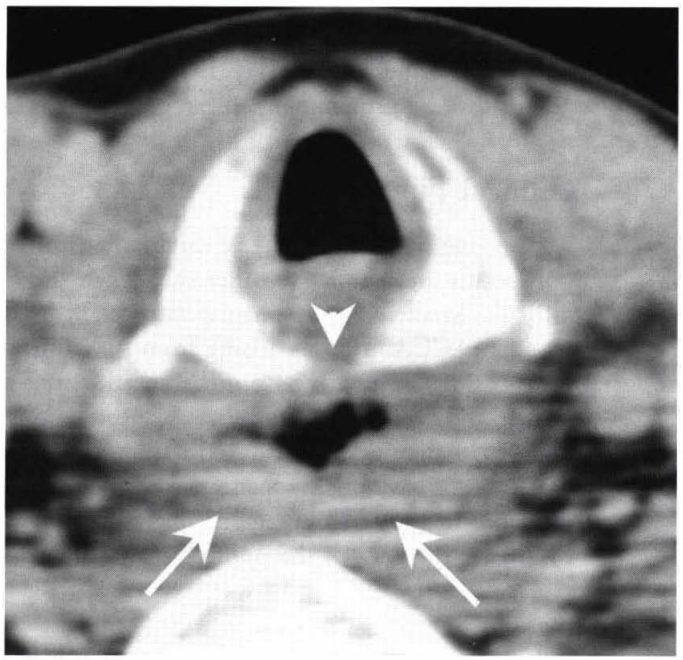

Figure 69–2. Axial contrast-enhanced CT demonstrates an aggressive tumor involving the postcricoid region (arrows). The arrowhead identifies erosion of the posterior portion of the cricoid cartilage.

Pathology

Histologically, SCCA is classified as well, moderately, and poorly differentiated. On microscopic examination, SCCA appears as anaplastic cells found below the basement membrane with a variable degree of keratin production and intracellular bridges. Besides SCCA, other squamous cell aberrations that may arise in the larynx include the following categories: benign hyperplasia, benign keratosis, atypical hyperplasia, keratosis with epithelial atypia, intraepithelial carcinoma, and microinvasive squamous cell carcinoma.

Treatment

Historically, the treatment of choice for postcricoid carcinomas is total laryngopharyngectomy with reconstruction. However, initial results suggest reasonable local control and survival rates for nonsurgical organ preservation therapy using combined chemotherapy and radiation therapy.

Imaging Findings

CT

SCCA of the postcricoid can be identified by bulky tumors that are limited to the pharynx at the level of the cricoid cartilage. These tumors may extend superiorly to involve the apex of the pyriform sinus or inferiorly to involve the esophageal verge and proximal cervical esophagus (Figs. 69-1 and 69-2).

MR

These tumors, as with the majority of SCCAs, are usually intermediate signal on T1-weighted and slightly increased signal on T2-weighted images. To be properly identified as a postcricoid tumor, they must be predominantly located in the pharynx at the level of the cricoid cartilage.

Imaging Pearls

- These tumors are rare.
- The specific information regarding the primary site that will affect treatment is the inferior extent of the tumor. This will often impact the specific type of reconstructive procedure.

Suggested Readings

1. Schmalfuss IM, Mancuso AA, Tart RP. Postcricoid region and cervical esophagus: normal appearance at CT and MR imaging. *Radiology* 2000;214:237-246.
2. Million RR, Cassisi NJ, Mancuso AA. Hypopharynx: pharyngeal walls, pyriform sinus, postcricoid pharynx. In: Million RR, Cassisi NJ, Mancuso AA, eds. *Management of Head and Neck Cancer: A Multidisciplinary Approach.* Philadelphia: JB Lippincott; 1994.
3. Mukherji SK, Weissman JL, Holliday R. The pharynx. In: Som PM, Curtin H, eds. *Head and Neck Imaging.* 3rd ed. New York: Mosby; 1996.

Chapter 70

Squamous Cell Carcinoma of the Posterior Pharyngeal Wall

Epidemiology

The pharyngeal wall consists of the posterior and lateral pharyngeal mucosa that extends to the nasopharynx, superiorly, esophageal inlet, inferiorly, and tonsils laterally. The incidence is more common in males with the peak incidence between 60 and 70 years of age. The most common risk factors are excessive tobacco and alcohol use.

Clinical Findings

Stages of oropharyngeal and hypopharyngeal cancer are presented in Tables 70–1 and 70–2, respectively. The most common complaint is sore throat. As these tumors progress (Fig. 70–1), patients may complain of dysphagia, foreign sensation, ear pain, blood-tinged saliva, aspiration, and change in voice quality. Patients with advanced disease may present with weight loss or a palpable neck mass indicative of a nodal metastasis.

Table 70–1
Sixth American Joint Committee on Cancer Staging Classification for Oropharyngeal Carcinoma (Involving the Posterior Pharyngeal Wall)

TIS	Carcinoma in situ
T1	Tumor ≤ 2 cm in greatest diameter
T2	Tumor > 2 cm but ≤ 4 cm in greatest diameter
T3	Tumor > 4 cm in greatest diameter
T4 a	Tumor invades larynx, deep/extrinsic muscle of tongue, medial pterygoid, hard palate, or mandible
T4 b	Tumor invades lateral pterygoid muscle, pterygoid plates, lateral nasopharynx, or skull base or encases carotid artery

Table 70–2
Sixth American Joint Committee on Cancer Staging Classification for Hypopharyngeal (Involving the Posterior Pharyngeal Wall)

T1	Tumor limited to one subsite of hypopharynx and < 2 cm in greatest dimension
T2	Tumor invades more than one subsite of hypopharynx or an adjacent site, or measures 2–4 cm in greatest diameter without fixation of hemilarynx
T3	Tumor > 4 cm in greatest dimension or with fixation of hemilarynx
T4 a	Tumor invades thyroid/cricoid cartilage, hyoid bone, thyroid gland, esophagus, or central compartment soft tissue
T4 b	Tumor invades prevertebral fascia, encases carotid artery, or involves mediastinal structures

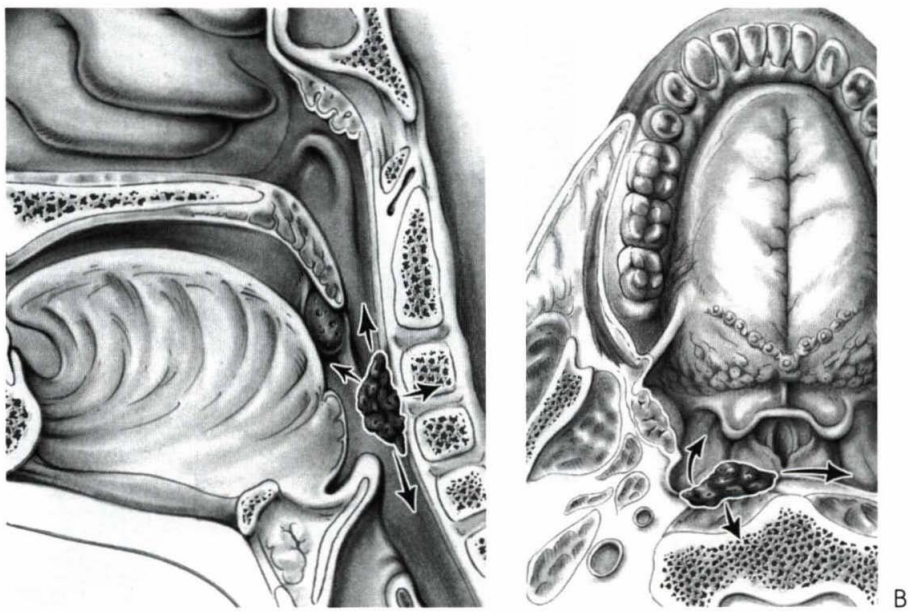

Figure 70–1. (A) Sagittal and (B) axial schematic illustrations demonstrate the spread pattern (arrows) of a posterior pharyngeal wall carcinoma.

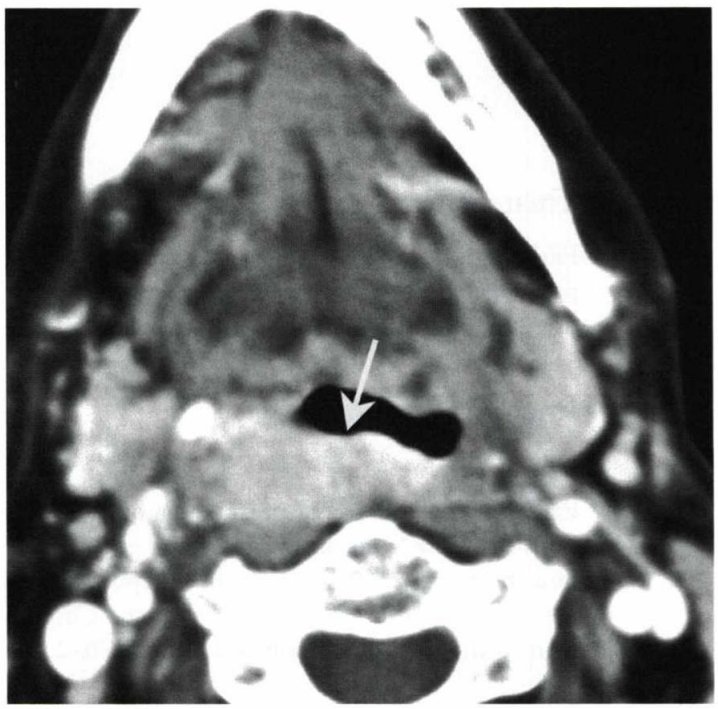

Figure 70–2. Axial contrast-enhanced CT obtained at the level of the tongue base shows an aggressive tumor arising from the posterior pharyngeal wall (arrow).

The prognosis of pharyngeal wall carcinomas is worse than carcinomas of the pyriform sinus due to the advanced stage of disease at presentation and high likelihood of metastases. The primary lymphatic drainage is to levels II through V and the retropharyngeal lymph nodes. Squamous cell carcinomas (SCCAs) of the lateral and posterior walls tend to metastasize early. Over half of patients have metastases at the time of presentation, with about 20% of patients having bilateral metastases. About 25% of patients will initially present with a palpable neck mass.

Pathology

The majority (> 95%) of malignant tumors of the pharyngeal wall are SCCA. On endoscopic examination, these tumors are typically large, exophytic, fungating masses. Histologically, SCCA of the pharyngeal wall tends to be undifferentiated or anaplastic tumors.

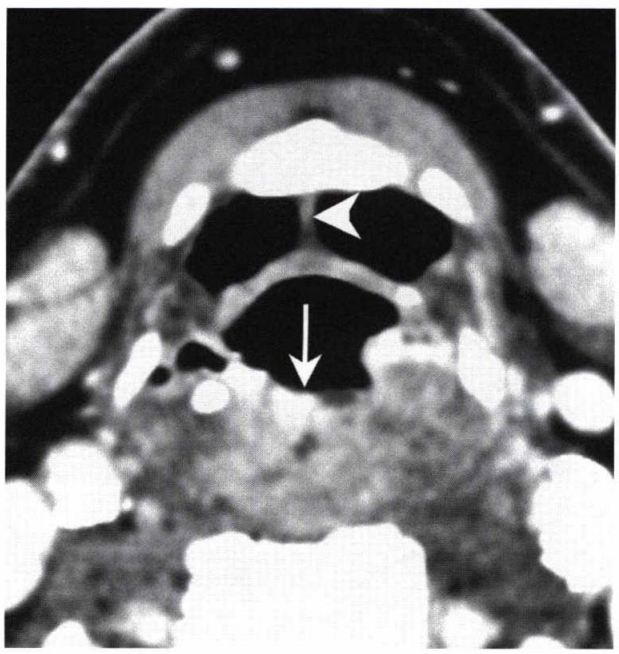

Figure 70–3. Axial contrast-enhanced CT performed at the level of the median glossoepiglottic fold (arrowhead) illustrates another example of a primary posterior pharyngeal wall carcinoma.

Treatment

Early tumors may be treated with either radiation therapy or partial pharyngectomy. In the past, advanced tumors were treated with either partial or total laryngopharyngectomy. The use of combined chemotherapy and radiation is gaining acceptance for advanced tumors.

Imaging Findings

CT

Early mucosal lesions may not be seen on CT. These lesions are usually aggressive, bulky lesions that arise from the posterior wall of the pharynx and extend into the airway. Invasion into the prevertebral fascia has been reported but is rare. The tumors heterogeneously enhance with contrast. Bone erosion is rare. Cartilage erosion may occur if these tumors extend to the level of the subglottis (Figs. 70–2 and 70–3).

MR

These tumors are intermediate signal on T1-weighted sequences and intermediate to high signal on T2-weighted sequences. These aggressive lesions diffusely enhance with contrast. MR is often superior to CT for detecting superior spread to the skull base and involvement of the retropharyngeal lymph nodes.

Imaging Pearls

- The retropharyngeal lymph nodes need to be specifically evaluated for metastases. This may have a direct affect on the surgical procedure and the placement of the treatment ports.
- Certain specific information must be mentioned in the reports and will directly affect treatment.
  - Detailed evaluation of submucosal extension into the soft tissues of the neck (pre- and poststyloid parapharyngeal space)
  - Superior extension to the tonsil or nasopharynx
  - Prevertebral muscle invasion
  - Midline extension

Suggested Readings

1. Mukherji SK, Pillsbury H, Castillo M. Imaging squamous cell carcinomas of the upper aerodigestive tract: what the clinicians need to know. *Radiology* 1997;205:629–646.
2. Million RR, Cassisi NJ, Mancuso AA. Hypopharynx: pharyngeal walls, pyriform sinus, postcricoid pharynx. In: Million RR, Cassisi NJ, Mancuso AA, eds. *Management of Head and Neck Cancer: A Multidisciplinary Approach.* Philadelphia: JB Lippincott; 1994.
3. Mukherji SK, Weissman JL, Holliday R. The pharynx. In: Som PM, Curtin H, eds. *Head and Neck Imaging.* 3rd ed. New York: Mosby; 1996.
4. Batsakis JG. Squamous cell carcinoma of the oral cavity and oropharynx. In: Batsakis JG, ed. *Tumors of the Head and Neck.* Baltimore: Williams and Wilkins; 1979:144–176.

Chapter 71

Rhabdomyosarcoma

Epidemiology

Rhabdomyosarcoma is the most common sarcoma in children (84%) and the second most frequent soft tissue tumor arising in the pediatric head and neck (35–45%). The orbit (36%) and nasopharynx (15%) are the most commonly involved sites, followed by middle ear (14%), paranasal sinuses (8%), and paraspinal regions. There is a bimodal peak for age of onset, 2 to 6 years and 14 to 18 years. Boys are affected more commonly, with a male to female ratio of 2:1. The incidence of metastatic cervical adenopathy at the time of presentation ranges from 3 to 25%.

Clinical Findings

Affected children present with a palpable neck mass and neck pain. The orbital tumor produces a rapidly developing unilateral proptosis. Large nasopharyngeal, oropharyngeal, or laryngeal lesions may cause airway obstruction. Nasopharyngeal rhabdomyosarcomas present with rhinorrhea, sore throat, and serous otitis media secondary to eustachian tube obstruction. Intraspinal extension may cause varying neurological deficits.

Pathology

Rhabdomyosarcoma is divided into four separate types: embryonal, botryoid, alveolar, and pleomorphic varieties. The less differentiated embryonal and botryoid types are seen in infants and children. The embryonal rhabdomyosarcoma is the most common (75%) histologic type. The alveolar type is seen in adolescents (20%) and has the worst prognosis. The well-differentiated pleomorphic type occurs in adults and accounts for 5% of the cases. Histologically, small, dark, spindle-shaped cells and small, round, blue cells within a loose myxoid background characterize rhabdomyosarcoma.

Treatment

Surgery is the initial treatment of choice followed by radiotherapy and chemotherapy.

Imaging Findings

CT

On CT, rhabdomyosarcomas appear as isodense to hypodense masses that enhance heterogeneously following contrast administration. They are usually associated with bone destruction and have poorly defined infiltrating borders. Nasopharyngeal rhabdomyosarcoma appears as an infiltrating soft tissue mass that may produce destruction of the skull base. In the masticator space, the tumor may cause destruction of the mandible. The superomedial quadrant of the orbit is the most commonly affected region in cases of orbital rhabdomyosarcomas. Paraspinal masses are associated with lytic or sclerotic vertebral destruction (Figs. 71–1 and 71–2).

MRI

The mass is isointense to muscle on T1-weighted images and hyperintense on T2-weighted images and may show areas of hemorrhage within. MRI accurately delineates the entire extent of the soft tissue mass and also shows early bone marrow infiltration. Paraspinal masses are associated with destruction of the vertebrae and intraspinal extension of the soft tissue mass that may cause cord compression. Rhabdomyosarcomas typically enhance heterogeneously following contrast administration.

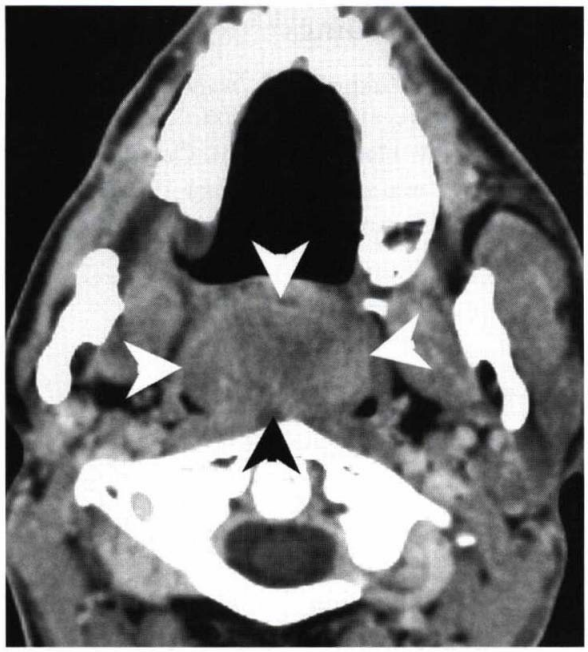

Figure 71-1. Axial contrast enhanced CT shows a mildly enhancing soft tissue mass located in the oropharynx (arrowheads). Pathology revealed rhabdomyosarcoma.

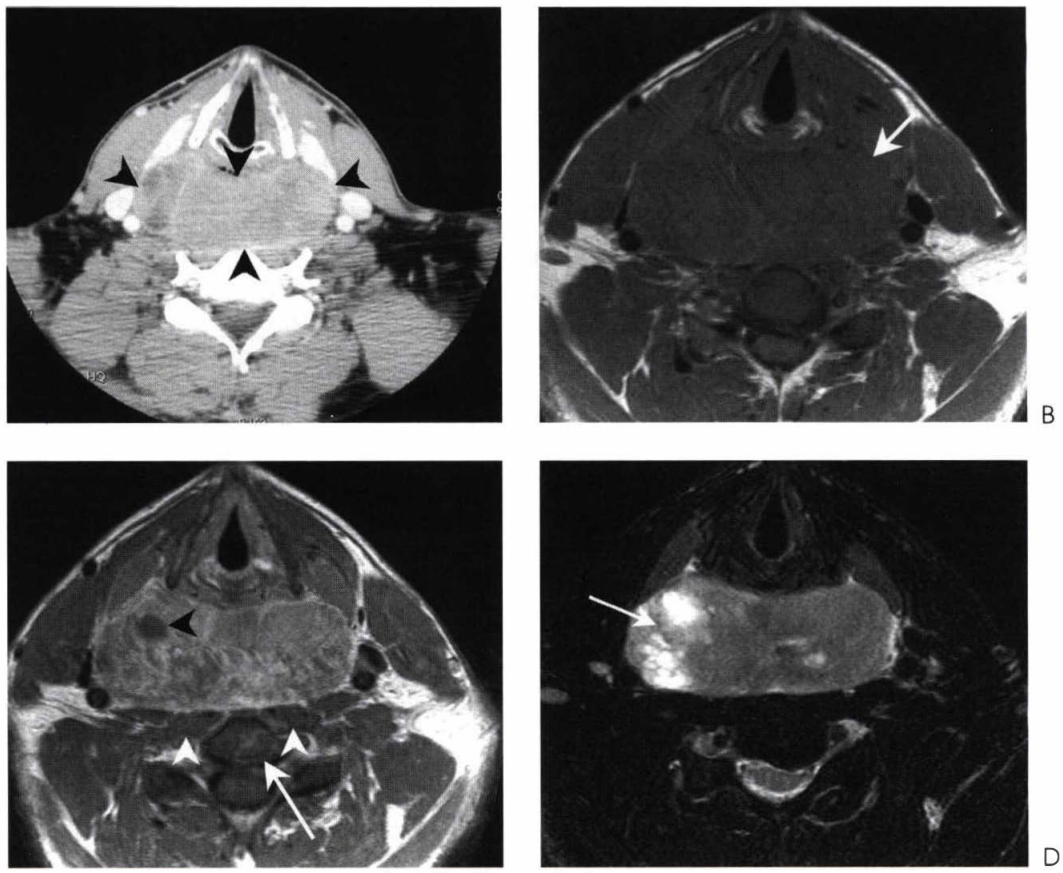

Figure 71-2. (A) Contrast-enhanced CT performed in a patient with dysphagia demonstrates a mildly enhancing homogeneous mass arising from the posterior wall of the hypopharynx (arrowheads). The mass was entirely submucosal. (B) Axial noncontrast T1-weighted image demonstrates the mass is isointense to muscle (arrow). (C) The majority of the mass homogeneously enhances following contrast except for one focal area of decreased enhancement (black arrowhead). The mass extends posteriorly into the retropharyngeal space. Note that the longus coli muscles (white arrowheads) and vertebral body (arrow) are not involved. This indicates that the mass is not arising from or involving the prevertebral space. (D) Axial T2-weighted image demonstrates the majority of the mass to be moderately high signal with focal areas of higher signal involving the right side of the lesion (arrow). CT-guided biopsy of the submucosal mass revealed rhabdomyosarcoma.

Imaging Pearls

- Rhabdomyosarcomas should be the primary consideration for a primary masticator space mass in a child.
- This diagnosis should be considered for aggressive masses that destroy bone and lack flow voids arising in children.

Suggested Readings

1. Castillo M, Mukherji SK. *Imaging of Pediatric Head, Neck and Spine*. Philadelphia: Lippincott-Raven; 1996:606–607.
2. Hardin CW, Harnsberger HR, Osborn AG, et al. Infection and tumor of the masticator space: CT evaluation. *Radiology* 1985;157:413–417.
3. Som PM, Curtin HD. *Head and Neck Imaging*. 3rd ed. St. Louis: Mosby; 1996:605–609.

Chapter 72

Nasopharyngeal Meningioma

Epidemiology

Meningiomas make up approximately 20% of all central nervous system tumors. They are benign tumors arising from arachnoid cells. However, 15 to 20% of all meningiomas extend outside the cranial cavity or spine. Extracranial tumors may be found in the temporal bone, orbit, sinonasal cavity, nasopharynx, and parotid gland. Meningiomas are most commonly found in the fifth decade of older patients and show a predilection for females. Meningiomas are rare in children.

Clinical Findings

The clinical signs and symptoms depend on the manner in which the meningioma reaches the nasopharynx. Tumor spreading through the superior orbital fissure and extending along the pterygopalatine fossa into the anterior nasopharynx may produce diplopia, maxillary nerve compression, and nasal symptoms. Large meningiomas reaching the nasopharynx from the jugular foramen may have lower cranial nerve palsies.

Pathology

Intracranial and extracranial meningiomas have identical histologic features. However, extracranial tumors tend to be less well circumscribed and show a greater propensity to invade surrounding structures. Malignant degeneration is rare. Immunochemistry tests that are typically positive include S-100 protein antigen, vimentin, and epithelial membrane antigen (EMD).

Treatment

The treatment of choice is complete surgical excision. However, multiple surgical approaches may be needed to tackle multiple lesions in the skull base. Radiation therapy rarely produces a cure but may extend disease-free periods. It should be noted that radiation itself could induce meningiomas after a latency period of 10 to 20 years.

Imaging Findings

CT

Unenhanced CT may detect a variable amount of calcification. However, there tend to be fewer psammoma bodies in extracranial meningiomas. The tumor typically enhances strongly with contrast, and these tumors may induce hyperostosis of the adjacent bones.

MR

On T1-weighted images meningiomas typically have intermediate signal intensity. On T2-weighted images, meningiomas appear hyperintense and show a heterogeneous pattern. Following the injection of contrast, these lesions enhance intensely (Fig. 72-1).

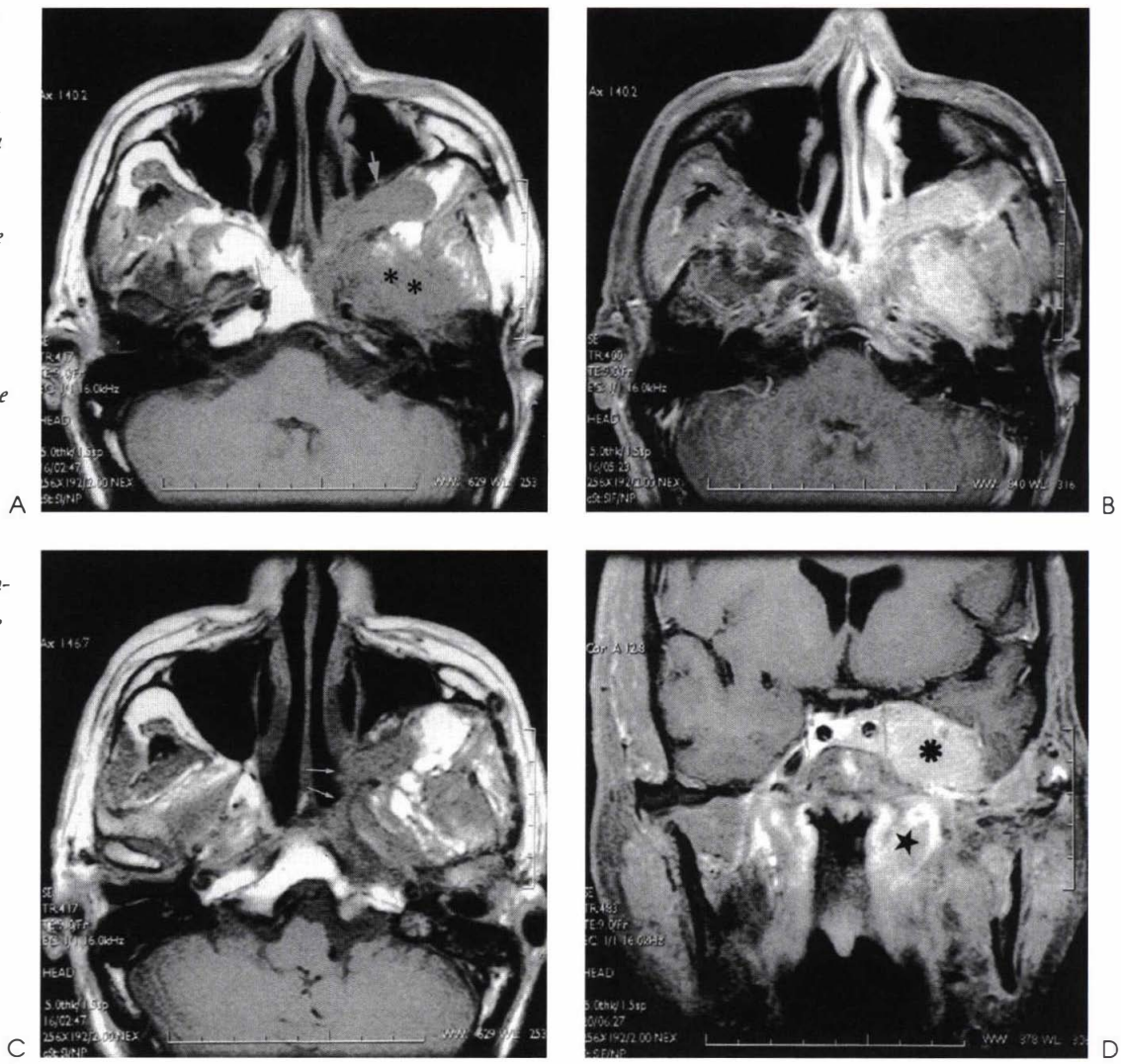

Figure 72–1. Middle cranial fossa meningioma with extension to nasopharynx. (A) Axial noncontrast T1-weighted MR image shows intermediate signal intensity meningioma in the left middle cranial fossa (asterisks). Note the component within the ipsilateral pterygopalatine fossa (arrow). (B) Axial contrast-enhanced MR image shows intense tumor enhancement. (C) Axial T1-weighted MR image shows tumor extending through the sphenopalatine foramen into the nasopharynx (arrows). (D) Coronal contrast-enhanced MR image shows middle cranial fossa meningioma with involvement of the cavernous sinus (asterisk) and extracranial component (star). (Courtesy of LL Chan, M.D., Singapore General Hospital.)

Imaging Pearls

- The diagnosis of a meningioma with extracranial extension is usually straightforward when an intracranial tumor can be demonstrated to be in contiguity with an extracranial component. However, the diagnosis may be difficult in patients with meningiomas arising from ectopic arachnoid granulation cells in the skull base. The presence of tumor calcification or hyperostosis induced in an adjacent bone may help in making the correct diagnosis.

Suggested Readings

1. Farr HW, Gray GF, Vrana M. Extracranial meningiomas. *J Surg Oncol* 1973; 5:411–420.
2. Calcaterra TC, Wang MB, Sercarz JA. In: Myers EN, Suen JY, eds. *Cancer of the Head and Neck*. 2nd ed. Philadelphia: WB Saunders; 1996:644–699.
3. Nuss DW, Janecka IP. Cranial base tumors. In: Myers EN, Suen JY, eds. *Cancer of the Head and Neck*. 2nd ed. Philadelphia: WB Saunders; 1996:234–275.

Chapter 73

Nasopharyngeal Hemangiopericytoma

Epidemiology

Hemangiopericytomas are unusual vascular tumors that occur mainly in adults. They represent 1% of all vasoformative tumors, most of which occur in the lower extremity, retroperitoneum, and pelvis. Approximately 15 to 20% occur in the head and neck region. They may be found in the sinonasal area, orbit, lacrimal sac, or jugular foramen. About 50% of cases are malignant, and distant metastasis, although rare, may occur, especially to the lungs. Differentiation between malignant and benign tumors may be a difficult pathological task and clinical correlation is required. Electron microscopy and immunohistochemical techniques may be necessary to differentiate hemangiopericytomas from other sarcomatous tumors.

Clinical Findings

Patients usually present with a history of epistaxis, nasal obstruction, or discharge. Facial pain may be related to associated paranasal sinusitis secondary to tumor obstructing the drainage pathways.

Pathology

Hemangiopericytomas typically show a tumor stroma abundant in spindle cells. Throughout the tumor, there were gaping, thin-walled vascular channels lined with flattened endothelium. A histologic diagnosis of hemangiopericytoma is based on a characteristic immunostaining pattern.

Treatment

Sinonasal hemangiopericytomas are thought to behave less aggressively than those occurring elsewhere in the body. Lymph node metastasis is rare and elective neck dissection is not indicated. The accepted treatment of these tumors is wide surgical excision. However, adequate surgical margins are usually difficult in the sinonasal region. As a result, hemangiopericytomas can exhibit a high recurrence rate in this area. Careful follow-up is therefore important with these patients.

Imaging Findings

CT

On contrast-enhanced CT, hemangiopericytomas appear as bulky or lobulated tumors showing moderate to marked enhancement. They may show tumoral calcification and bone erosion.

MR

On MR imaging the tumors show intermediate signal intensity on T1-weighted images and a cystic enhancement pattern following the injection of contrast material. The tumor may show areas of high signal intensity on both T1- and T2-weighted images, suggesting tumoral hemorrhage (Fig. 73–1).

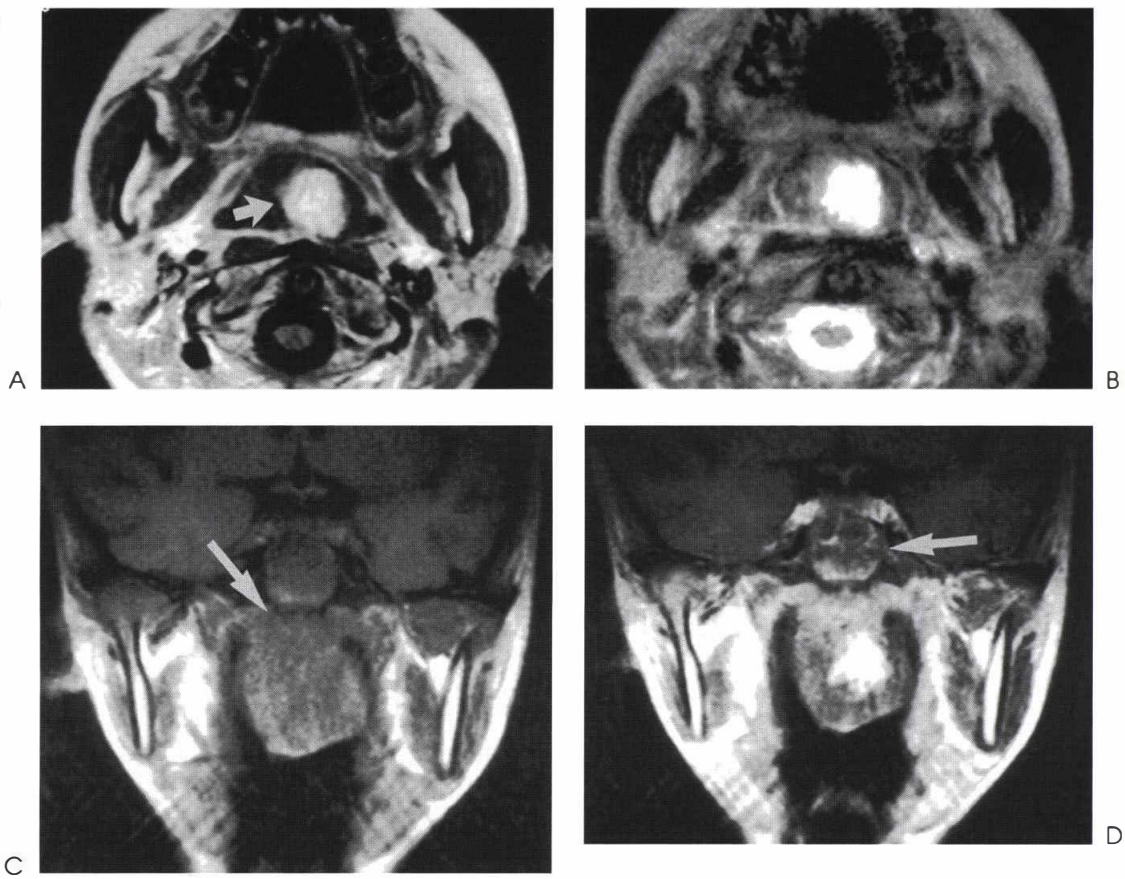

Figure 73-1. Hemangiopericytoma arising from the roof of the nasopharynx. (A) Axial contrast-enhanced T1-weighted MR image shows an enhancing hemangiopericytoma in the nasopharynx (arrow). (B) Axial T2-weighted MR image shows high signals corresponding to the region of contrast enhancement. (C) Coronal T1-weighted MR image shows the intermediate signal intensity lesion attached to the roof of the nasopharynx (arrow). (D) Coronal contrast-enhanced MR image shows tumor enhancement that is particularly dense in the central portion. Note the inflammatory changes in the sphenoid sinus (arrow).

Imaging Pearls

- Nasal or nasopharyngeal hemangiopericytomas are rare tumors. They may show a combination of calcification and cystic changes that may separate them from the more common squamous cell carcinoma or lymphoma.

Suggested Readings

1. Batsakis JG, Rice DH. The pathology of head and neck tumors: vasoformative tumors. *Head Neck* 1981;3:326-339.
2. Mafee MF, Carter BL. Nasal cavity and paranasal sinuses. In: Valvassori GE, Mafee MF, Carter BL, eds. *Imaging of the Head and Neck.* New York: Thieme; 1995:321-322.
3. Eichhorn JH, Dickersin GR, Bhan AK, Goodman ML. Sinonasal hemangiopericytoma: a reassessment with electron microscopy, immunohistochemistry and long-term follow-up. *Am J Surg Pathol* 1990;14:856-866.

Chapter 74

Nasopharyngeal Adenocystic Carcinoma

Epidemiology

In comparison with nasopharyngeal carcinoma (NPC), adenocystic carcinoma in the nasopharynx is rare. The vast majority of adenocystic carcinomas are found in the salivary glands, the mucosa of the oral cavity, the nasal fossa, and the paranasal sinuses. Lesions in the nasopharynx may arise from minor salivary gland rests in the hard palate or nasal cavity. This tumor affects patients in the their middle age and there is no reported sex predilection.

Clinical Findings

Adenocystic carcinoma of the nasopharynx usually presents with nasal symptoms such as epistaxis, nasal stuffiness, obstruction, or discharge. Unlike nasopharyngeal carcinoma, patients rarely present with cervical lymphadenopathy.

Pathology

The gross in situ size of the tumor is always deceptive and difficult to determine because of the insidious infiltration of bone, soft tissues, and nerves. On gross examination, these tumors are typically unilobular and appear grayish white or yellowish white on cut section. The tumors are relatively circumscribed with little or no encapsulation. There are four main histologic patterns of adenocystic carcinoma: cribriform (classic), tubuloglandular, solid, and cylindromatous (hyaline). Perineural infiltration is the hallmark of this tumor histologic finding. Branches of the mandibular nerve are particular at risk in tumors arising in the nasopharynx. Extension into the pterygopalantine fossa places the maxillary division of the trigeminal nerve and the nerve of the vidian canal at risk for retrograde perineural spread. These tumors are also characterized by skip lesions, where uninvolved segments of nerve may be interspersed between involved segments. As a result, "clear" surgical margins play a less important prognostic role when compared with other malignancies.

Treatment

Because of the high recurrence rate (75% over 15 to 20 years), both surgical and radiation therapy borders should be wide so as to decrease the recurrence rate. Tumors in the nasopharynx can be treated by a combination of surgery and postoperative radiation therapy. Because the incidence of nodal metastasis is low (14%), elective neck dissection for adenocystic carcinoma is not warranted. In contrast, hematogenous metastasis (usually to lungs and bones) may be seen in 40% of patients.

Imaging Findings

CT

Adenocystic carcinoma cannot be differentiated from NPC. The tumor shows moderate enhancement. Early tumors may be limited to the nasopharynx, whereas advanced tumors show aggressive margins and extend deeply into the nasopharynx.

MR

Adenocystic carcinoma shows intermediate signal intensity on T1-weighted images and enhances strongly after the injection of contrast. It also shows moderately high signals on T2-weighted images (Fig. 74–1).

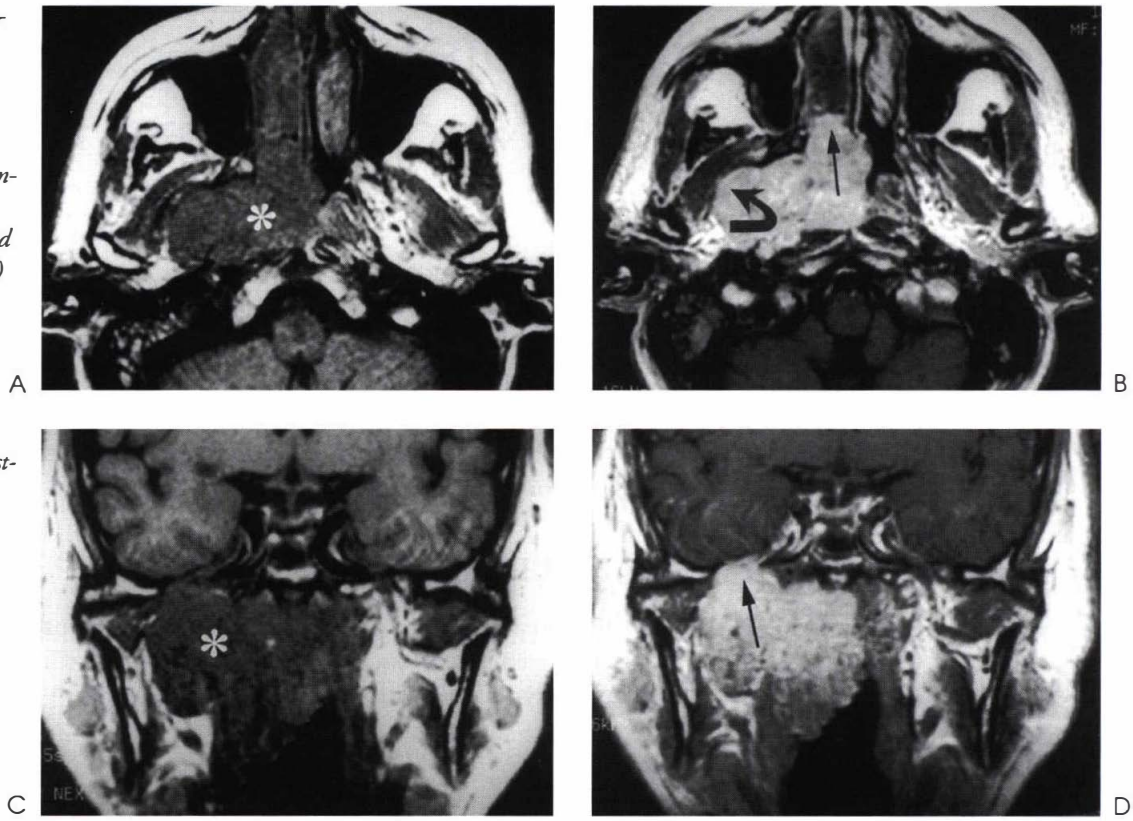

Figure 74-1. Nasopharyngeal adenocystic carcinoma. (A) Axial T1-weighted MR image shows a lobulated intermediate signal intensity lesion on the right side of the nasopharynx (asterisk). (B) Axial contrast-enhanced MR image shows intense enhancement. Note the spread into the nasal cavity (straight arrow) and the masticator space (curved arrow). (C) Coronal T1-weighted MR image shows a large lobulated nasopharyngeal mass with infiltration of the right masticator space (asterisk). (D) Coronal contrast-enhanced MR image shows enlargement and tumor extension through the right foramen ovale (arrow).

Imaging Pearls

- The frequency of lymphatic spread in adenocystic carcinoma is very low compared with NPC. More than 80% of patients with NPC have nodal metastasis at presentation.
- Perineural spread is common in both adenocystic carcinoma and NPC. A focus search for foramen ovale involvement should always be conducted in tumors arising from the nasopharyngeal mucosa. An early sign of perineural spread is the obliteration of fat density just below the foramen ovale.

Suggested Readings

1. Moss WT. Radiation therapy for tumors of the nasal cavity and paranasal sinuses. In: Thawley SE, Panje WR, Batsakis JG, Lindberg RD, eds. *Comprehensive Management of Head and Neck Tumors*. 2nd ed. Philadelphia: WB Saunders; 1999:601-607.
2. Batsakis JG. Pathology of tumors of the nasal cavity and paranasal sinuses. In: Thawley SE, Panje WR, Batsakis JG, Lindberg RD, eds. *Comprehensive Management of Head and Neck Tumors*. 2nd ed. Philadelphia: WB Saunders; 1999:522-539.
3. Chong VFH, Fan YF. Radiology of the nasopharynx. *Australas Radiol*. 2000;44:5-13.

Chapter 75

Plasmacytoma

Epidemiology

Plasma cell neoplasms can be grouped into three categories: multiple myeloma, plasmacytoma of bone, and extramedullary plasmacytoma. Extramedullary plasmacytomas account for approximately 20% of all plasma cell neoplasms, and 80% of these lesions are found in the head and neck. Plasmacytomas are most frequently seen in the upper airways such as the epiglottis, larynx, and nasopharynx but they have also been reported in the sinonasal cavity, clivus, and petrous apex. Plasmacytomas are most commonly seen in the sixth and seventh decades (mean age 60 years, range 28–74). These neoplasms have an 80% male preponderance. Approximately 30% of patients with extramedullary plasmacytoma will have systemic disease after 20 years.

Clinical Findings

Clinical findings depend on the size and site of the neoplasm. Upper airway involvement such as sinonasal lesions may produce nasal obstruction or bloody nasal discharge whereas laryngeal lesions produce hoarseness of voice. Diagnostic evaluation should include bone marrow biopsy, skeletal survey, measurement of urinary Bence Jones proteins, and quantitative measurements for κ and λ light chains.

Pathology

Plasmacytomas usually originate in the mucosa or submucosa lining the upper airway. These lesions may be polypoid or sessile. They are vascular tumors and often bleed easily or profusely. Histologically, plasmacytomas are composed of sheets of poorly differentiated plasma cells against a vascular background.

Treatment

Plasmacytomas are radiosensitive. The treatment of choice is local radiation therapy. The prognosis is good, with a 5-year survival rate of approximately 87%.

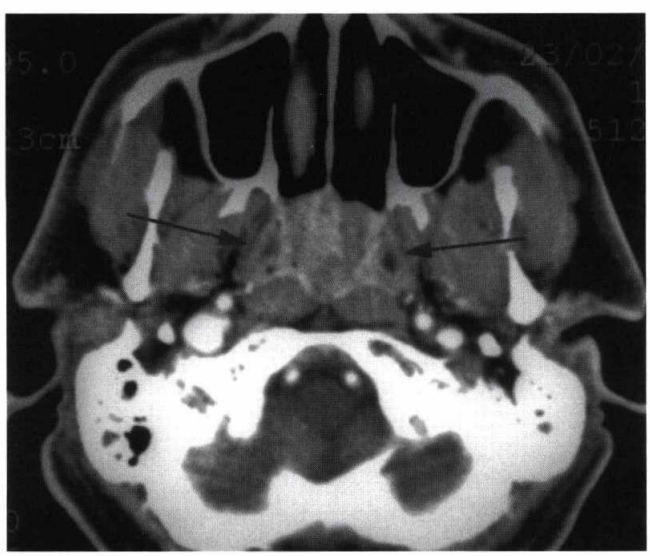

Figure 75–1. Nasopharyngeal plasmacytoma. Axial contrast-enhanced CT shows an enhancing mass in the nasopharynx (arrows). Note the superficial mucosal location with no submucosal or parapharyngeal infiltration.

Imaging Findings

CT

In the nasopharynx, plasmacytomas are homogeneous masses that diffusely enhance following contrast administration. These lesions may be confined to the soft tissues or show associated bone erosion. Central necrosis is rare (Fig. 75-1).

MR

On T1-weighted images, plasmacytomas show an intermediate signal intensity and diffusely enhance after contrast administration. These tumors are moderately high signal on T2-weighted sequences.

Imaging Pearls

- The imaging characteristics of nasopharyngeal plasmacytomas are nonspecific. These tumors may be associated with cervical lymphadenopathy in 10 to 20% of patients. This frequency is much lower compared with nasopharyngeal carcinoma (> 80%). It is not certain whether nodal disease represents true metastatic disease.

Suggested Readings

1. Mafee MF, Carter BL. Tumor and tumor-like lesions of the nasal cavity and paranasal sinuses. In: Valvassori GE, Mafee MF, Carter BL, eds. *Imaging of the Head and Neck*. New York: Thieme; 1995:302–328.
2. Mendenhall NP. Lymphomas and related diseases presenting in the head and neck. In: Million RR, Cassisi NJ, eds. *Management of Head and Neck Cancer*. Philadelphia: JB Lippincott; 1994:857–878.
3. O'Hare TJ. Granulomatous and lymphoproliferative diseases of the head and neck. In: Thawley SE, Panje WR, Batsakis JG, Lindberg RD, eds. *Comprehensive Management of Head and Neck Tumors*. 2nd ed. Philadelphia: WB Saunders; 1999:1931–1981.

Chapter 76

Nasopharyngeal Lymphoma

Epidemiology

Primary lymphoma of the nasopharynx is uncommon and is more commonly seen in conjunction with systemic disease. Nasopharyngeal lymphoma affects all age groups but is more commonly encountered in middle-aged and older individuals. The majority of these tumors belong to the non-Hodgkin's group.

Clinical Findings

Patients with primary nasopharyngeal lymphoma may present with nasal stuffiness, obstruction, headaches, or fever of unknown origin.

Pathology

Histologic classification of non-Hodgkin's lymphoma (NHL) is notoriously difficult but newer techniques for classification such as immunologic phenotyping, nucleic acid analysis with flow cytometry, and molecular genetics. These techniques may help explain the diversity of the morphological appearances. One of the most popular classifications is the Rappaport system, which is based on pattern of involvement and cellular appearance. In general, nodular lymphomas have a more indolent course compared with the diffuse variety.

Treatment

For treatment purposes, NHL is divided into favorable and nonfavorable treatment outcome categories. The favorable group comprises patients with nodular lymphocytic and well-differentiated lymphocytic subtypes. The rest of the subtypes belong to the unfavorable outcome group. These include diffuse poorly differentiated lymphocytic, diffuse histiocytic, diffuse undifferentiated, and nodular histiocytic. Patients with stage I favorable group can be treated with radiation therapy alone, whereas higher stages of the favorable group and all nonfavorable histologic subtypes are treated with a combination of radiation therapy and chemotherapy.

Imaging Findings

CT

Contrast-enhanced CT shows two morphological types: a circumscribed mass or diffuse thickening of the superficial tissues. The tumor is homogeneous and may be indistinguishable from nasopharyngeal carcinoma (Fig. 76–1).

MR

MR imaging findings are nonspecific and present as a homogeneous aggressive mass. Lymphoma is usually intermediate signal on T1-weighted sequences and intermediate signal to high signal on T2-weighted sequences. The mass usually homogeneously enhances following contrast administration.

Imaging Pearls

- Nasopharyngeal lymphoid tissue is prominent in children and adolescents. Such tissue should not be mistaken as an abnormal mass. Normal lymphoid tissues show typical high signal intensities following the injection of contrast and on T2-weighted images. Although prominent or large, normal lymphoid tissues do not invade adjacent structures.

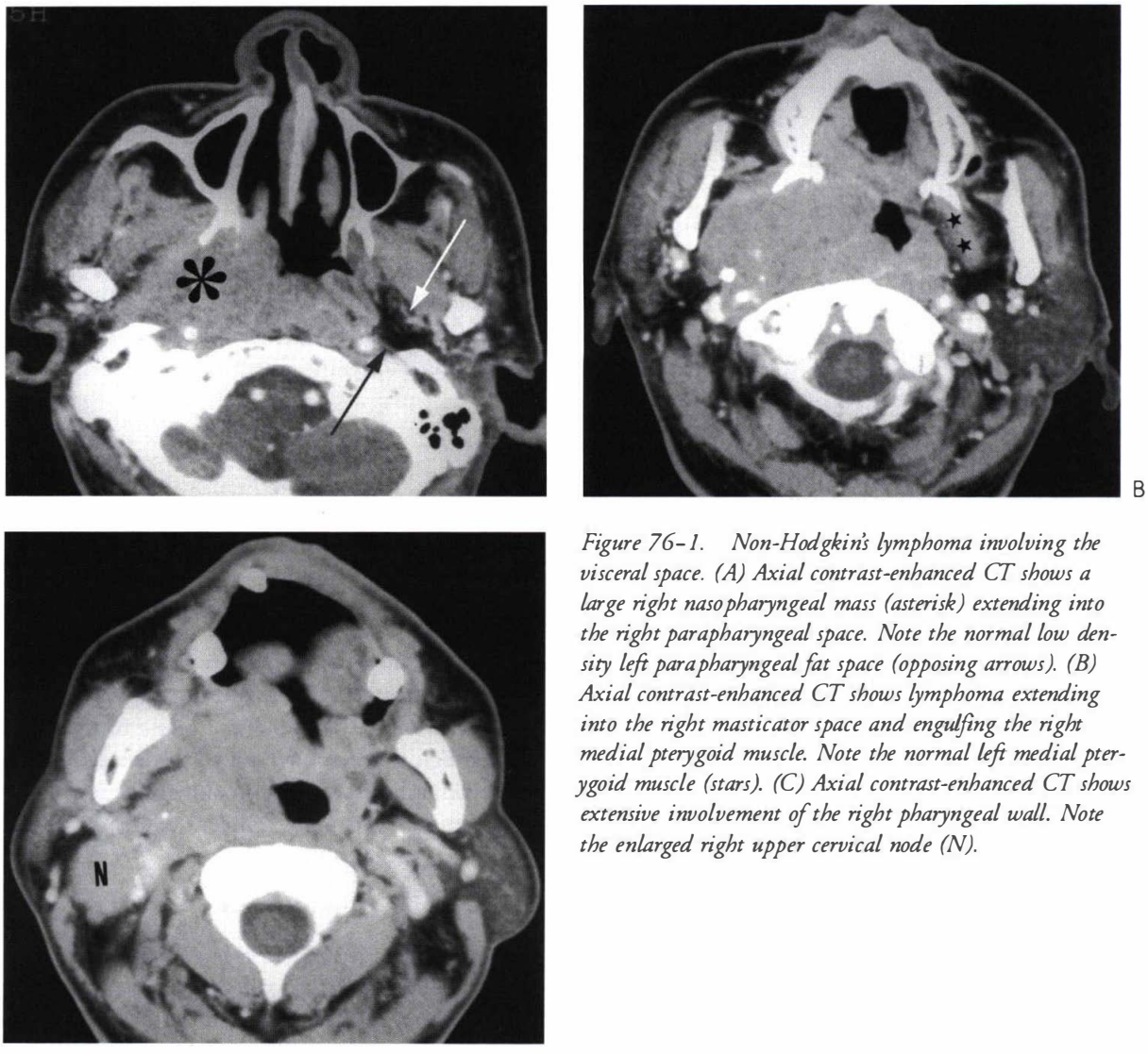

Figure 76-1. Non-Hodgkin's lymphoma involving the visceral space. (A) Axial contrast-enhanced CT shows a large right nasopharyngeal mass (asterisk) extending into the right parapharyngeal space. Note the normal low density left parapharyngeal fat space (opposing arrows). (B) Axial contrast-enhanced CT shows lymphoma extending into the right masticator space and engulfing the right medial pterygoid muscle. Note the normal left medial pterygoid muscle (stars). (C) Axial contrast-enhanced CT shows extensive involvement of the right pharyngeal wall. Note the enlarged right upper cervical node (N).

- It is often difficult to differentiate nasopharyngeal lymphoma and nasopharyngeal carcinoma on the basis of radiological features. Both these lesions are commonly associated with cervical lymphadenopathy. However, aggressive local spread, bone destruction, and perineural infiltration favor carcinoma over lymphoma.

Suggested Readings

1. Mendenhall NP. Lymphomas and related diseases presenting in the head and neck. In: Million RR, Cassisi NJ, eds. *Management of Head and Neck Cancer*. Philadelphia: JB Lippincott; 1994:857-878.
2. Linberg RD, Paris KJ, Fletcher GH. Radiation therapy of tumors of the neck. In: Thawley SE, Panje WR, Batsakis JG, Lindberg RD, eds. *Comprehensive Management of Head and Neck Tumors*. 2nd ed. Philadelphia: WB Saunders; 1999:1450-1477.
3. Chong VFH, Fan YF. Radiology of the nasopharynx. *Australas Radiol* 2000;44:5-13.

Chapter 77

Juvenile Angiofibroma

Epidemiology

Juvenile angiofibroma (JNA) accounts for < 0.5% of head and neck neoplasms. These benign but locally aggressive tumors are found almost exclusively in adolescent males. It is believed that the lesion originates in the region of the sphenopalatine foramen at the junction between the posterior nasal fossa and the nasopharynx.

Clinical Findings

The vast majority of patients are diagnosed relatively late in the course of the disease. Symptoms are usually present for at least 6 to 12 months before diagnosis. Nasal obstruction is the most common symptom followed by epistaxis. Other signs and symptoms include facial swelling, proptosis, and visual disturbance such as diplopia. These lesions are well circumscribed and appear deceptively avascular on clinical inspection.

Pathology

The tumor consists of a fibrous stroma of spindle-shaped cells and a rich network of irregular vascular channels. These vascular channels are lined by endothelium but they lack surrounding smooth muscle support. This phenomenon appears to contribute to the capacity for massive hemorrhage following manipulation.

Treatment

The most widely accepted treatment is embolization followed by resection. Very advanced lesions that have aggressive skull base erosion may be treated with radiation therapy. Residual tumor may regress after puberty because the growth of the tumor is felt to be hormonally based.

Imaging Findings

CT

These are characteristically hypervascular tumors. The classic tumor is centered in the sphenopalatine foramen and widens this foramen. The tumors extend laterally into the pterygopalatine fossa and widen the fossa. The posterior wall is often thinned and displaced anteriorly. Continued spread through the pterygopalatine fossa may result in extension into the masticator space or may follow the infraorbital fissure into the orbital apex. Medial spread from the sphenopalatine foramen will result in extension into the posterior nasal cavity and nasopharynx. Advanced disease may result in intracranial extension via the superior orbital fissure or aggressive skull base erosion. Occasionally, JNA may be primarily centered in the posterior nasal cavity and nasopharynx without significant extension into the pterygopalatine fossa (Figs. 77–1, 77–2, and 77–4).

MR

The tumors have intermediate signal on T1-weighted sequences and moderate to high signal on T2-weighted sequences. These tumors enhance intensely following the injection of contrast. Flow voids are a characteristic finding and may be seen on both T1- and T2-weighted images. They are best seen on postcontrast T1-weighted sequences (Figs. 77–1B–D and 77–3).

Angiography

JNAs are very vascular and the arterial supply is principally from the terminal branches of the internal maxillary artery. Large tumors may obtain supply from other branches of the external carotid artery (Fig. 77–5).

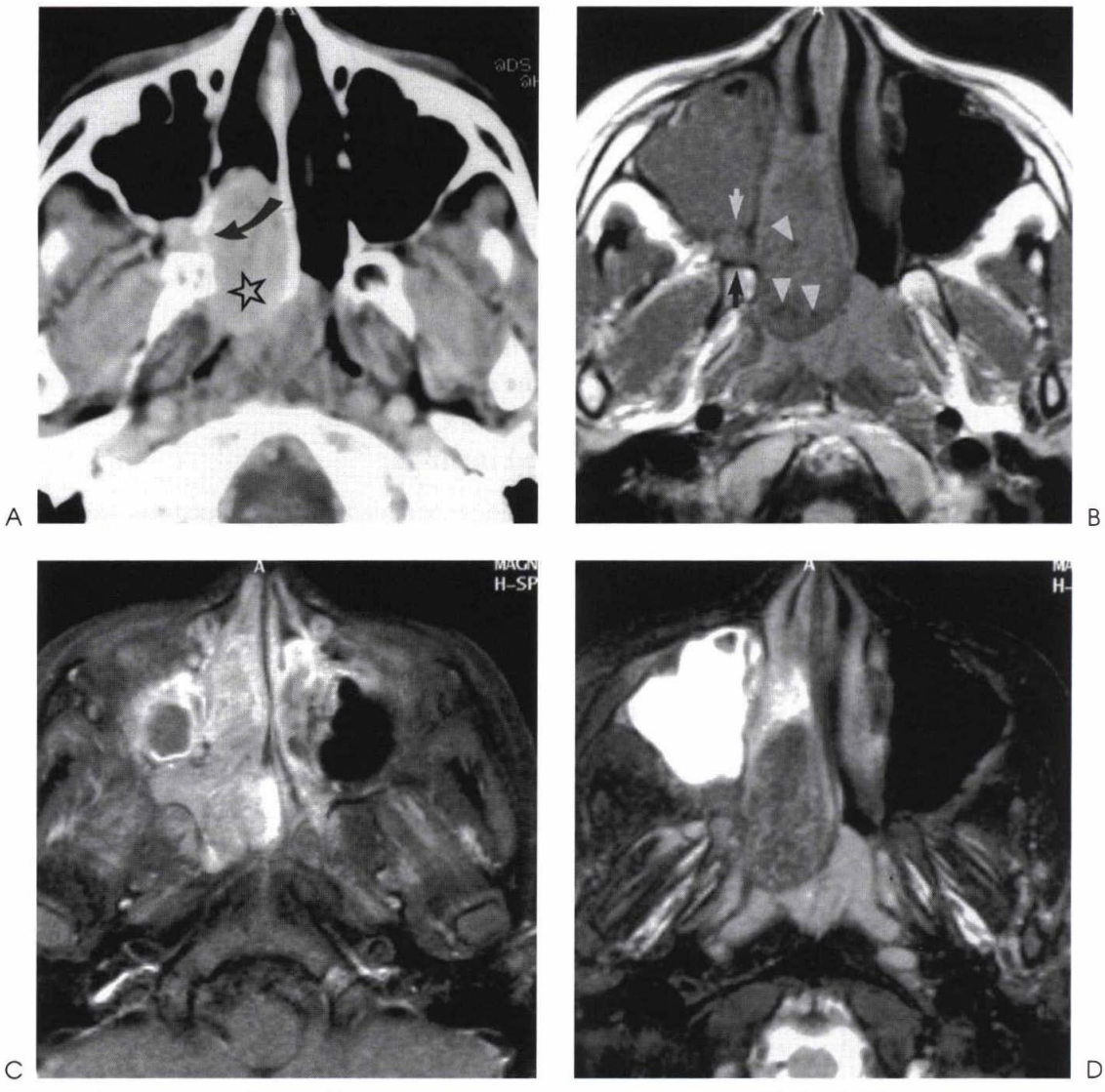

Figure 77–1. Juvenile angiofibroma involving the pterygopalatine fossa. (A) Axial CT shows an enhancing mass centered at the junction between the right nasal fossa and nasopharynx (star). Note the tumor tissue extending through the sphenopalatine foramen into the pterygopalatine fossa (arrow). (B) Axial T1-weighted MR image shows the intermediate signal intensity juvenile angiofibroma obstructing the right maxillary sinus. Note the widened right pterygopalatine fossa and early erosion of the maxillary sinus (opposing arrows) and multiple flow voids (arrowheads). (C) Axial contrast-enhanced MR image [slightly superior to (B)] shows tumor signal intensity slightly lower than enhanced mucosa. (D) Axial T2-weighted MR image shows heterogeneous moderate signals in the tumor.
(Courtesy of SH Ng, M.D., Chang Gung Memorial Hospital, Taoyuan, Taiwan)

Figure 77–2. Juvenile angiofibroma with sphenoid sinus extension. (A) Coronal contrast-enhanced CT shows an enhanced tumor (star) in the nasopharynx effacing the right torus tubarius and fossa of Rosenmüller. (B) Coronal contrast-enhanced CT shows tumor in the right nasal cavity and the right sphenoid sinus (star). Note the eroded floor of the right sphenoid sinus.

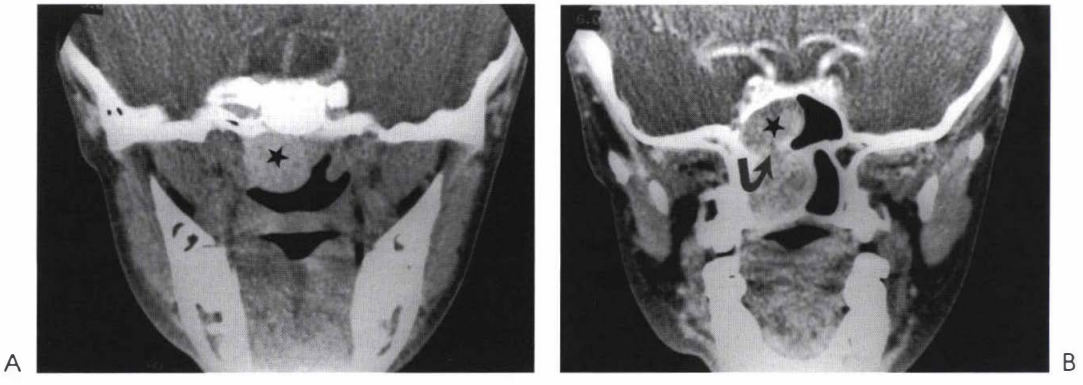

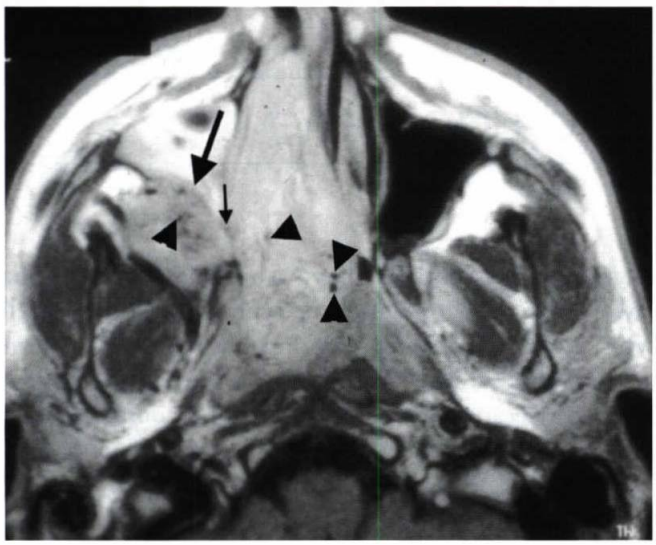

Figure 77-3. Axial contrast-enhanced T1-weighted image shows an enhancing mass centered in the nasal cavity. The tumor extends through the sphenopalantine foramen into the pterygopalantine fossa. The multiple flow voids are indicative of a juvenile angiofibroma.

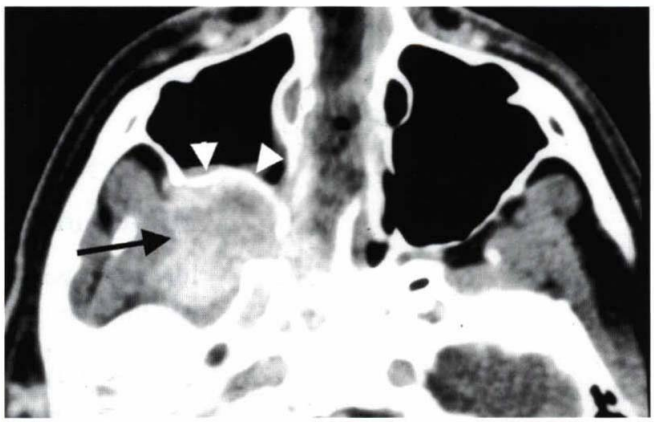

Figure 77-4. Contrast-enhanced CT shows a juvenile angiofibroma centered in the ptrygopalantine fossa (arrow). The posterior wall of the maxillary sinus is in tact but is anteriorly displaced (arrowheads) indicative of a slow-growing mass and is characteristic of a juvenile angiofibroma in an adolescent male. The CT correlate of the plain film finding of anterior displacement of the posterior wall of the maxillary sinus (Holman-Miller) sign that is characteristic of juvenile angiofibroma. It should be noted that advanced juvenile fibromas can erode bone and invade the skull base. In our experience, this is most common in males who present between the ages of 5 and10 years of age.

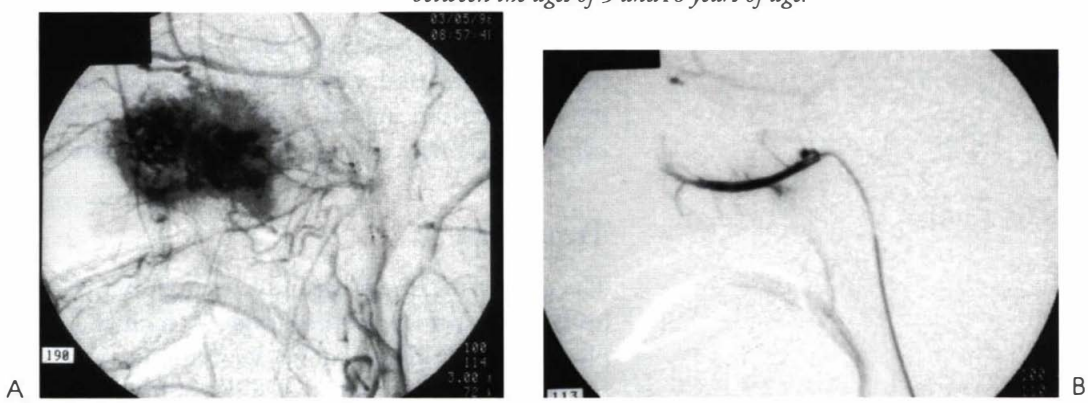

A B

Figure 77-5. (A) Lateral view from a selective injection of the external carotid artery in a patient with a JNA shows a large hypervascular lesion being that is predominantly supplied from the internal maxillary artery. (B) Lateral view of aselective internal maxillary artery angiogram shows no flow within the tumor following embolization of the internal maxillary artery.

Imaging Pearls

- A diagnosis of JNA should initially be considered on the basis of age, sex, and the typical sites of involvement demonstrated on imaging studies.
- It is important to differentiate a JNA from a rhabdomyosarcoma. Both tumors can occur in this location. The presence of flow voids and anterior displacement and regressive remodeling of the posterior wall of the maxillary sinus are suggestive of JNA. Lack of flow voids and aggressive bone erosion of the posterior wall of the maxillary sinus are suggestive of rhabdomyosarcoma.

Suggested Readings

1. Gullane PJ, Davidson J, O'Dwyer T, Forte V. Juvenile angiofibroma: a review of the literature and a case series report. *Laryngoscope* 1992;102:928–933.
2. Radkowski D, McGill T, Healy GB, Ohlms L, Jones DT. Angiofibroma: changes in staging and treatment. *Arch Otolaryngol Head Neck Surg* 1996;122:122–129.
3. Curtin HD, Som PM, Braun IF, Nadel L. Skull base. In: Som PM, Curtin HD, eds. *Head and Neck Imaging.* St. Louis: Mosby; 1996:1233–1299.

Chapter 78

Inverted Papilloma

Epidemiology

Inverted papillomas are uncommon tumors constituting 0.5 to 4% of all nasal tumors. The lesion, although benign, is associated with a synchronous or metachronous squamous cell carcinoma in 15 to 27% of patients. Inverted papillomas are notably more common in males (3–4:1)to 1. Whites are more commonly affected than blacks or Asians, and most patients are diagnosed in the fifth to seventh decades. These tumors are most commonly seen in the lateral nasal wall but they may be seen occasionally in the oropharynx, posterior pharyngeal wall, lacrimal sac, and nasopharynx, and within the paranasal sinuses.

Clinical Findings

Depending on the location of the papillomas, patients may present with nasal obstruction, epistaxis, rhinorrhea, or headache. Grossly, these tumors tend to be bulky and firm and show frondlike extensions.

Pathology

Inverted papillomas are thought to arise from the schneiderian respiratory membrane that lines the lateral nasal wall, turbinates, and paranasal sinuses. The name of the tumor reflects the characteristic inward endophytic growth of the hyperplastic respiratory epithelium. Large tumors may extend intracranially or into adjacent paranasal sinuses.

Treatment

The goal of treatment is complete surgical excision. Aggressive resection is recommended because the incidence of recurrence is high and dependent on the surgical techniques employed. Because of the known association of inverted papilloma with metachronous malignancy, patients should be carefully monitored on a long-term basis after surgery.

Imaging Findings

CT

Inverted papillomas appear as superficial lesions arising from the nasopharyngeal mucosa. These tumors cannot be differentiated from the more common undifferentiated carcinoma. They enhance moderately on CT.

MR

On T1-weighted MR images, the tumor shows intermediate signal intensity. They enhance strongly following the injection of contrast and show moderate to high signal intensities on T2-weighted images (Fig. 78–1).

Imaging Pearls

- Inverted papillomas do not show deep tissue invasions. If invasion is seen the tumor is most likely to be a nasopharyngeal carcinoma. It is however possible that the deep invasion represents an associated squamous cell carcinoma.
- Most nasopharyngeal carcinomas originate in the fossa of Rosenmüller. An exophytic mass arising in other parts of the nasopharynx should raise the possibility of other tumors such as an inverted papilloma.

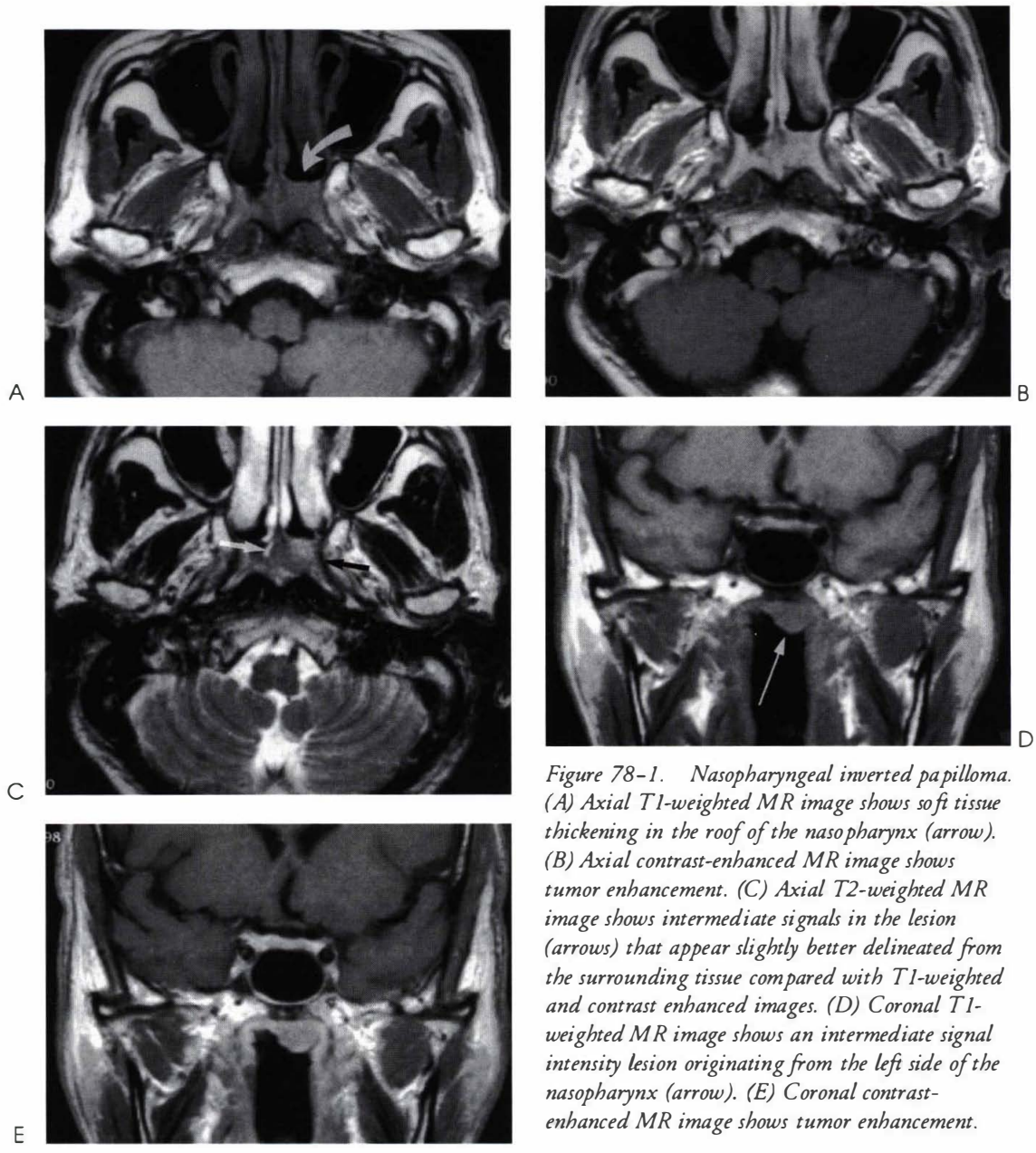

Figure 78-1. Nasopharyngeal inverted papilloma. (A) Axial T1-weighted MR image shows soft tissue thickening in the roof of the nasopharynx (arrow). (B) Axial contrast-enhanced MR image shows tumor enhancement. (C) Axial T2-weighted MR image shows intermediate signals in the lesion (arrows) that appear slightly better delineated from the surrounding tissue compared with T1-weighted and contrast enhanced images. (D) Coronal T1-weighted MR image shows an intermediate signal intensity lesion originating from the left side of the nasopharynx (arrow). (E) Coronal contrast-enhanced MR image shows tumor enhancement.

Suggested Readings

1. Calcaterra T, Thompson J, Paglia D. Inverted papilloma of the nose and paranasal sinuses. *Laryngoscope* 1980;90:53-60.
2. Lesperance MM, Esclamado RM. Squamous cell carcinoma arising in inverted papilloma. *Laryngoscope* 1995;105:178-183.
3. Allbery SM, Chaljub G, Cho NL, Rassekh CH, John SD, Guinto FC. MR imaging of nasal masses. *Radiographics* 1995;15:1311-1327.

Chapter 79

Benign Minor Salivary Gland Tumors (Pleomorphic Adenoma, Monomorphic Adenoma, Warthin's Tumor)

Epidemiology

A minor salivary gland consists of cellular constituents of the major salivary glands (parotid, submandibular, sublingual) that are located within the mucosa of the upper aerodigestive tract. It has been estimated that there are between 500 and 1000 minor salivary glands located throughout the oral cavity and oropharynx. They may be found within the hard and soft palate, uvula, lips, retromolar trigone, tongue base, floor of mouth, and tonsil. The same malignancies that arise in the major salivary glands occur in the minor salivary glands. Depending on the series, approximately 50% of minor salivary gland tumors are benign as compared with approximately 70 to 80% of parotid tumors that are benign.

Clinical Findings

Patients often present with asymptomatic masses that have been present for several months. Pain and ulceration may be present; however, these are not consistent findings. Patients with tumors arising in the larynx may present with symptoms of airway obstruction.

Pathology

The benign lesions that constitute minor salivary gland tumors include pleomorphic adenoma, monomorphic adenoma, and Warthin's tumor. The pathology of these lesions has been reviewed in other sections of this textbook.

Treatment

The exact treatment depends on the pathology. For most benign tumors complete local resection is adequate.

Imaging Findings

CT

The CT findings are not specific. The presence of regressive remodeling of the surrounding bone for lesions that arise in the hard palate is suggestive of a benign minor salivary gland tumor (Figs. 79-1 and 79-2C).

MR

In general, the imaging findings are nonspecific. However, oral cavity or oropharyngeal lesions that are low to intermediate signal on T1-weighted and increased signal on T2-weighted sequences are suggestive of pleomorphic adenoma (Figs. 79-2 A, B).

Imaging Pearls

- In general, these are uncommon lesions, with diagnosis usually at histology following initial biopsy. The intent of imaging is to provide information that cannot be detected on clinical examination. CT is helpful to evaluate the extent of bone erosion. MR should be performed to determine the presence of submucosal spread and deep invasion.

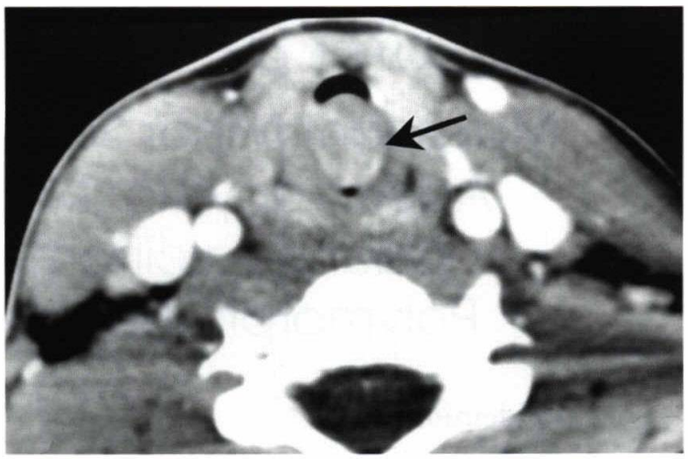

Figure 79–1. Axial contrast-enhanced CT shows a well-defined soft tissue mass located in the laryngeal airway (arrow). The mass is markedly narrowing the airway. There is no evidence of invasion of the adjacent soft tissues. Pathology revealed pleomorphic adenoma.

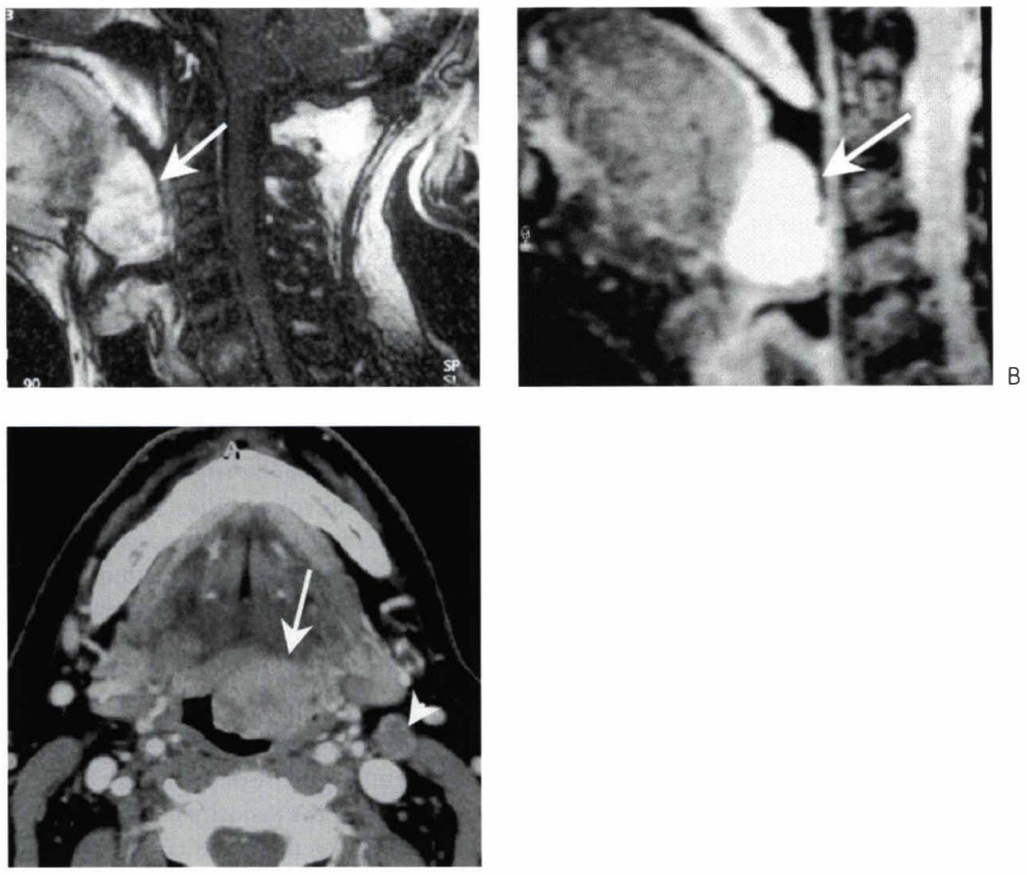

Figure 79–2. (A) Sagittal contrast-enhanced T1-weighted image shows an enhancing mass arising from the vallecula (arrow). (B) Sagittal T2-weighted image shows the mass to be high signal (arrow). (C) Axial contrast-enhanced CT shows the enhancing mass extending into the oropharyngeal airway (arrow). Note the abnormal left Group II lymph nodes with a low attenuation center (arrowhead). Pathology revealed pleomorphic adenoma both at the primary site and in the Group II lymph node. The nodal involvement was likely due to lymphatic spread from the rich lymphatic supply that is present in the tongue base and vallecula.

Suggested Readings

1. Batsakis JG. Neoplasms of the minor and lesser major salivary glands. In: Batsakis JG, ed. *Tumors of the Head and Neck.* Baltimore: Williams and Wilkins; 1979:76–99.
2. Smoker WRK. Oral cavity. In: Som PM, Curtin H, eds. *Head and Neck Imaging.* 3rd ed. New York: Mosby; 1996:488–544.
3. Shockley WM. Parotid tumors. In: Shockley WM, Pillsbury HC, eds. *The Neck: Diagnosis and Surgery.* New York: Mosby; 1994:265–294.

Chapter 80

Malignant Minor Salivary Gland Tumors Adenoidcystic, Mucoepidermoid, Adenocarcinoma, Low-Grade Polymorphous Adenocarcinoma

Epidemiology

The same malignancies that arise in the major salivary glands occur in the minor salivary glands. Depending on the series, approximately half of all tumors of minor salivary gland origin are malignant. The most common location is the palate. An interesting paradox is that the smaller the salivary gland, the greater the likelihood that a tumor originating from it will be malignant. The incidence of a salivary gland tumor being malignant is substantially greater in the palate than in the parotid.

Clinical Findings

Patients often present with asymptomatic masses that have been present for several months. Pain and ulceration may be present; however, these are not consistent findings.

Pathology

It has been estimated that there are between 500 and 1000 minor salivary glands located throughout the oral cavity and oropharynx. They may be found within the hard and soft palate, uvula, lips, retromolar trigone, tongue base, floor of mouth, and tonsil. The malignancies that constitute minor salivary gland tumors include adenoid cystic carcinoma, mucoepidermoid carcinoma, and adenocarcinoma. Many investigators now include low-grade polymorphous adenocarcinoma as a tumor of minor salivary gland origin. The most common malignancy of the minor salivary glands is adenoid cystic carcinoma.

Treatment

The treatment of malignant salivary gland tumors depends on the exact histologic type. In general, complete surgical resection offers the best chance for cure. Postoperative radiation therapy is required in the majority of cases. The role of neutron beam therapy for unresectable adenoid cystic carcinomas is currently being evaluated.

Imaging Findings

CT

The CT findings are nonspecific. These are usually soft tissue masses that enhance following contrast. The presence of aggressive bone erosion is suggestive of a high-grade malignancy (Fig. 80–1).

MR

These tumors are usually intermediate signal on T1-weighted sequences and enhance following contrast administration. The T2-weighted signal is variable (Fig. 80–2).

Imaging Pearls

- For adenoid cystic carcinoma involving the hard palate, CT should be performed to evaluate for bone erosion in the regions of the incisive canal and greater and lesser palatine foramen. MR should be performed to evaluate for extension into the pterygopalatine fossa

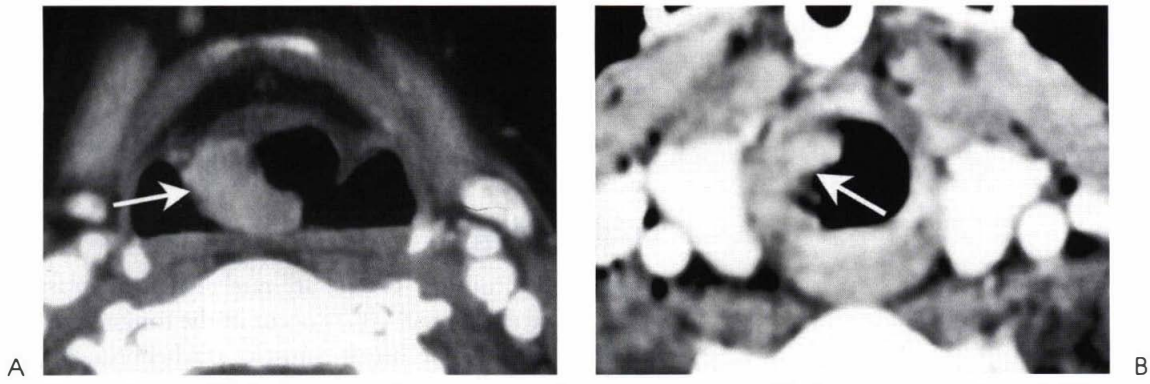

Figure 80–1. CT findings of malignant minor salivary gland tumors. (A) Axial contrast-enhanced CT demonstrates an aggressive mass involving the right aryepiglottic fold (arrow). Biopsy revealed adenoid cystic carcinoma. (B) Axial contrast-enhanced CT in a different patient shows an irregular mass involving the right side of the subglottis (arrow). Pathology revealed adenoid cystic carcinoma.

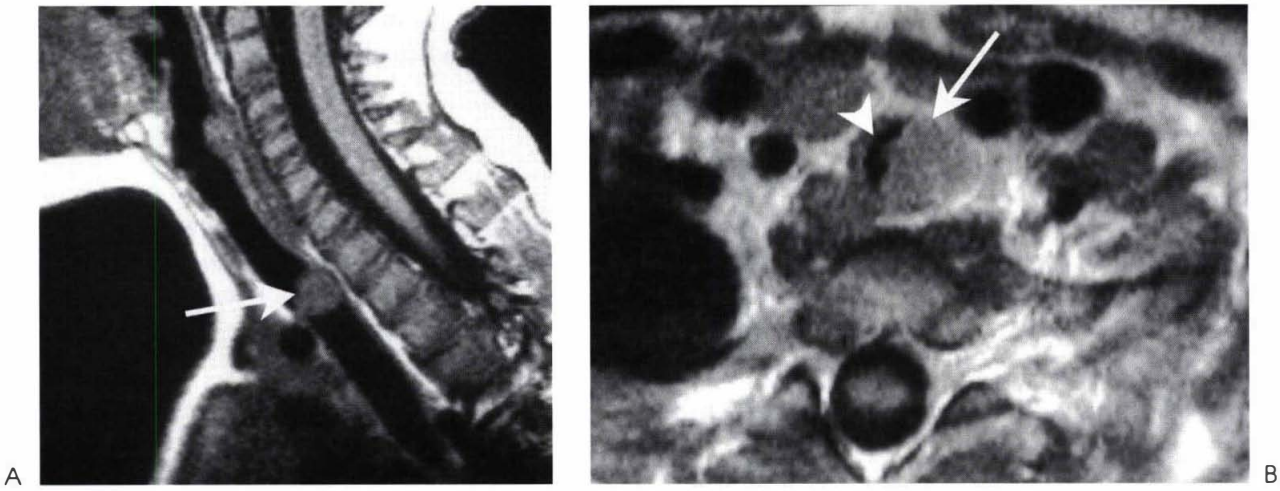

Figure 80–2. MR of malignant minor salivary gland tumor. (A) Sagittal noncontrast T1-weighted image shows a round mass located in the trachea (arrow). (B) Axial contrast-enhanced T1-weighted image shows the mass enhances (arrow) and is substantially narrowing the airway (arrowhead). Biopsy revealed mucoepidermoid carcinoma.

and possible retrograde perineural spread along the maxillary division of cranial nerve V or along the nerve of the vidian canal. These are potential pathways of spread in the cavernous sinus. These potential spread patterns should be evaluated in all patients because this may preclude primary surgical resection at many institutions.

- Patients who present with infraorbital numbness and paresthesias should undergo a high resolution MR of the palate and trigeminal nerve to evaluate for the presence of clinically occult adenoid cystic carcinoma of the hard or soft palate that has invaded the infraorbital nerve.
- We recommend performing MR imaging in patients with polymorphous adenocarcinoma arising in the oral cavity because, based on our experience, it appears this tumor has a propensity for marrow invasion.

Suggested Readings

1. Batsakis JG. Neoplasms of the minor and lesser major salivary glands. In: Batsakis JG, ed. *Tumors of the Head and Neck*. Baltimore: Williams and Wilkins; 1979:76–99.
2. Smoker WRK. Oral cavity. In: Som PM, Curtin H, eds. *Head and Neck Imaging*. 3rd ed. New York: Mosby; 1996:488–544.
3. Shockley WM. Parotid tumors. In: Shockley WM, Pillsbury HC, eds. *The Neck: Diagnosis and Surgery*. New York: Mosby; 1994:265–294.

Chapter 81

Granular Cell Tumors

Epidemiology

Granular cell tumors (GCTs) are rare benign neoplasms that can occur anywhere in the body. About 50% of all GCTs occur in the tongue and 30% involve the skin. The remaining areas include the breast, muscle, tracheobronchial tree, larynx, and temporal bone. Multiple lesions have been reported in 5 to 10% of involved patients. GCTs typically present in the fourth decade of life and are more common in women (2:1) and in African Americans than Caucasians (5:1).

In the past, the histogenesis of GCTs was controversial and has led to the use of various terms to describe the same tumor (Abrikosov's tumor, congenital epulis, nonchromaffin paraganglioma, granular cell myoblastoma, granular cell neurofibroma, myoblastic myoma, uniform myoblastoma, embryonal rhabdomyoblastoma). It is now believed that GCTs are felt to be of primitive neuroectodermal origin and the term *granular cell tumor* is the appropriate descriptor.

Clinical Findings

The presenting findings are nonspecific and vary with the primary location of the tumor. Patients with GCT involving the tongue often present with a visible or palpable mass, local pain, or dysphagia. Patients with GCT of the larynx complain of progressive hoarseness, shortness of breath, and dyspnea on exertion.

Pathology

These tumors have a characteristic histologic appearance. The cells are polymorphic ranging from a polyhedral to bizarre spindle forms. The tumors are embedded in variable amounts of connective or reticular tissue and may interdigitate into the adjacent fibrous stroma. Mitoses are uncommon.

Treatment

Because these are benign tumors and arise in relatively young patients, local excision is felt to be the preferred treatment. Recurrence is extremely rare in lesions that are completely excised. However, a progressively enlarging mass can be expected in tumors that are incompletely excised. Nodal metastases are very unusual.

Imaging Findings

CT

These are heterogeneously enhancing soft tissue masses. The margins are often identifiable but irregular. They may invade adjacent musculature (Fig. 81–1).

MR

The tumors are low signal on T1-weighted and increased signal on T2-weighted images. The tumors typically homogeneously enhance following contrast (Fig. 81–2).

Imaging Pearls

- The imaging findings of granular cell tumor are nonspecific and the diagnosis is made by histologic examination.
- An enhancing mass in the tongue or larynx in a relatively young patient may suggest the diagnosis.

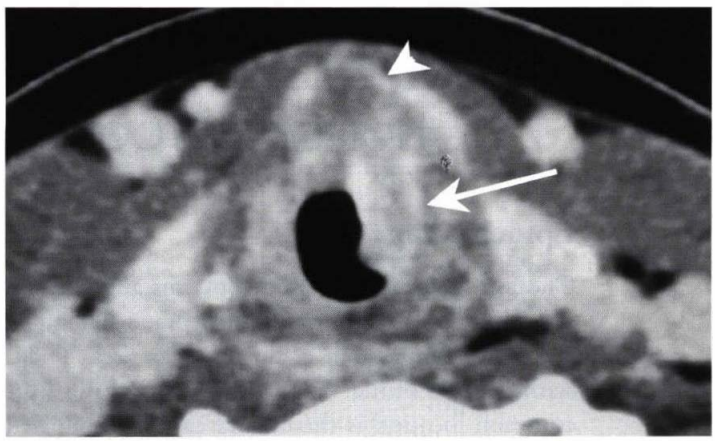

Figure 81-1. CT of granular cell tumor. Axial contrast-enhanced CT demonstrates an aggressive enhancing tumor (arrow) involving the subglottic larynx. The tumor extends through the anterior portion of the cricoid cartilage into the soft tissues of the neck (arrowhead).

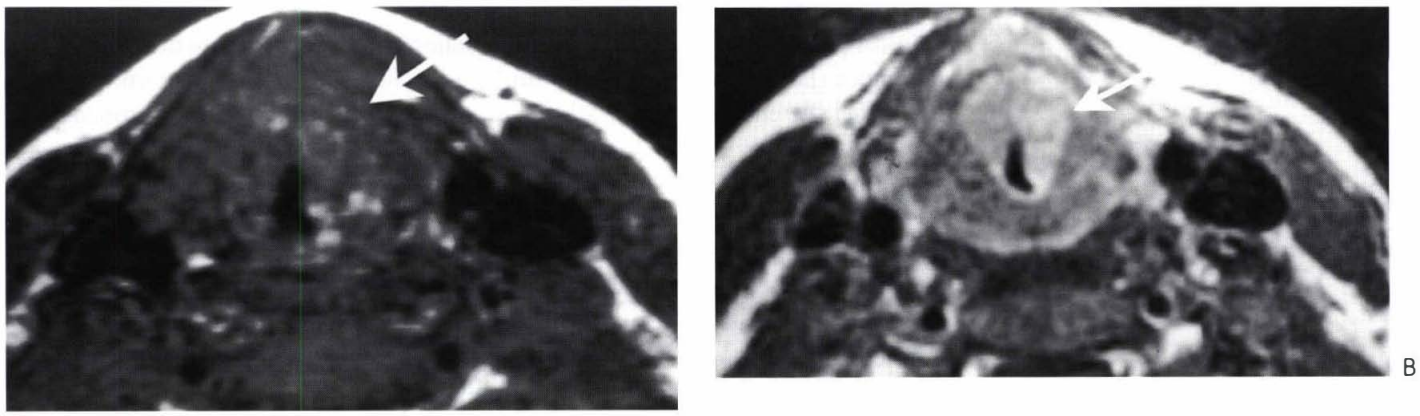

A B

Figure 81-2. MR of granular cell tumor: (A) Axial noncontrast T1-weighted image shows an intermediate signal mass involving the larynx (arrow). (B) The mass homogeneously enhances following contrast administration (arrow). These findings are nonspecific. However, the diagnosis can be suggested in a young patient.

Suggested Readings

1. Mukherji SK, Castillo M, Rao V, Weissler M. Granular cell tumors of the subglottic region of the larynx: CT and MR findings. *AJR Am J Roentgenol* 1995;164:1492–1494.
2. Dunaway CL, Brogdon BG, Robinson AE. Granular cell myoblastoma of the trachea. *Pediatr Radiol* 1981;11:210–211.
3. Batsakis JF. *Tumors of the Head and Neck: Clinical and Pathologic Considerations.* 2nd ed. Baltimore: Williams and Wilkins; 1979:313–333.

Chapter 82

Chondrosarcoma of the Larynx

Epidemiology

Chondrosarcomas are rare neoplasms and account for < 1% of all laryngeal tumors. Laryngeal chondrosarcomas are low grade malignancies and tend to be less aggressive than chondrosarcomas that occur in other sites. They usually present between the fourth and sixth decades of life. The incidence is greater in men than in women (5–10:1). The most common location is the cricoid cartilage followed by the thyroid cartilage.

Clinical Findings

Clinical presentation is nonspecific. The majority of symptoms are due to progressive narrowing of the airway. Presenting complaints include hoarseness, poor voice, dyspnea, and dysphagia. At endoscopy, laryngeal chondrosarcomas are very firm submucoid masses.

Pathology

The majority of chondrosarcomas are felt to arise from hyaline cartilage and have no evidence of elastic tissue. The pathologic criteria are as follows: (1) pronounced irregularity in size of the cells and their nuclei, (2) presence of numerous cells and their nuclei, (3) pronounced hyperchromatism of their nuclei, (4) any large or giant cartilage cells with single or multiple nuclei with clumps of chromatin.

Treatment

Surgical resection is the treatment of choice. Partial laryngectomy is preferred because these tumors tend to be less aggressive. Cricoid involvement is an important factor for surgical planning. Total laryngectomy is often required if greater than half of the cricoid lamina is involved.

Imaging Findings

CT

The typical appearance is an expansile mass arising with the laryngeal cartilages. The most commonly involved cartilage is the cricoid. These lesions are predominantly increased attenuation and contain an intratumoral matrix consisting of coarse or stippled calcifications. The majority of lesion are solid; however, chondrosarcomas with a cystic component have been described (Fig. 82–1).

MR

These lesions have intermediate T1-weighted signal and increased T2-weighted signal. They characteristically enhance following contrast administration. MR may not be able to reliably identify the chondroid matrix.

Imaging Pearls

- CT is the preferred cross-sectional modality to evaluate laryngeal chondrosarcoma because the diagnosis can be made based on the characteristic CT findings.
- Imaging plays an important role in evaluating this neoplasm because it may be very difficult to biopsy the tumor due to the hardness of the mass.

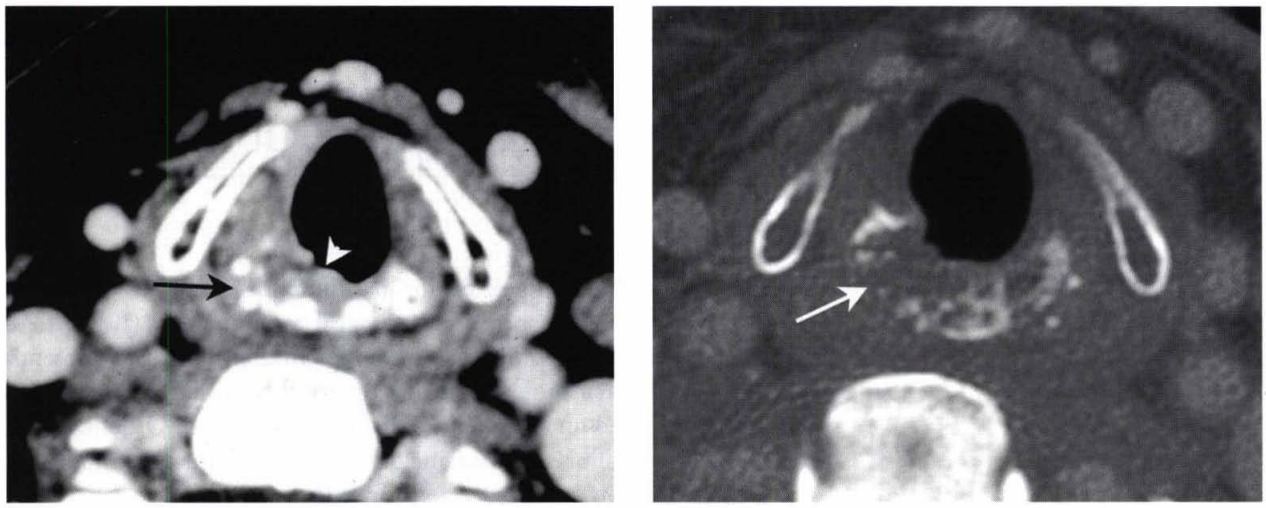

Figure 82–1. Chondrosarcoma of the cricoid cartilage. (A) Axial contrast-enhanced CT shows a lytic lesion of the cricoid cartilage (black arrow) associated with a soft tissue component extending into the airway (arrowhead). (B) Bone algorithm shows the lesion is centered in the cricoid cartilage and is composed of a chondroid matrix (arrow).

- It is important to identify the extent of disease involving the cricoid cartilage because this may directly affect surgical planning.
- It is very difficult to differentiate between benign and malignant chondroid lesions on CT.

Suggested Readings

1. Wippold FJ, Smirniotopoulos JG, Moran CJ, Glazer HS. Chondrosarcoma of the larynx: CT features. *AJNR Am J Neuroradiol* 1993;14:453–459.
2. Batsakis JG. Neoplasms of the larynx. In: Batsakis JG, ed. *Tumors of the Head and Neck.* Baltimore: Williams and Wilkins; 1979:200–225.
3. Sakai O, Curtin HD, Faquin WC, Fabian RL. Differentiated chondrosarcoma of the larynx. *AJNR Am J Neuroradiol* 2000;21:584–586.

Chapter 83

Juvenile Laryngeal Papillomatosis

Epidemiology

The most common laryngeal tumor in children is squamous papilloma. Multiple papillomas are often referred to as juvenile laryngeal papillomatosis (JLP). JLP may be seen in both children and adults but is more common in children. It usually presents before the age of 3 and may become symptomatic during the first year of life. The exact age of presentation is thought to be based on the extent of disease and location. Other factors that may also be associated with age of presentation include hormonal influence, and incubation time. No sexual predilection has been described for JLP.

Clinical Findings

Patients with JLP most commonly present with signs of airway obstruction. The most common symptoms are hoarseness, stridor, recurrent croup, or change in voice quality. Although histologically benign, JLP may be a potentially life-threatening disease due to obstruction of the airway. However, acute respiratory distress is unusual because JLP characteristically results in gradual airway narrowing.

JLP most commonly involves the true vocal cords, although supraglottic or subglottic extension is common. The tracheobronchial tree is often involved with tracheal involvement is reported to be as high as 26%. The cause of such involvement is felt by some to be the result of "seeding" of viral particles during airway manipulation. Many authors believe tracheotomy increases the likelihood of distal spread and recommend not performing this procedure if at all possible. Distal spread may result in the formation of multiple lung nodules that may cavitate. Esophageal papillomas that are believed to result from JLP have also been reported.

Etiology

JLP is believed to be caused by the human papilloma virus (HPV). The HPV is a DNA virus that results in epithelial proliferation. HPV-6 and HPV-11 have been identified as the viral subtypes in JLP. HPV-6C has been identified as the most common viral subtype and tends to be associated with more extensive and severe disease. JLP is also thought to be associated with condylomata acuminatum (maternal genital warts). This association is strengthened by the fact that HPV-6 and HPV-11 are believed to be responsible for 90% of genital warts. The DNA sequences of HPV isolated from JLP and condylomata acuminatum are indistinguishable. Additionally, JLP is rare in patients delivered by cesarean section, suggesting that delivery by cesarean section may play a protective role in cases of mothers with genital warts.

Pathology

At endoscopy, JLP appear as pink or red irregular, pedunculated, exophytic masses. These masses may be nodular and vary in size. Histologically, they consist of a very vascular core of connective tissue covered by stratified squamous epithelium with abnormal keratinization.

Treatment

JLP has an unpredictable clinical course and may spontaneously regress, respond to treatment, or progress. Malignant transformation occurring in chronic disease has been described but is the exception rather than the rule. The treatment of JLP has included medical therapy (antibiotics, hormones, interferon, steroids, antiviral agents, and various antimetabolities), radiation therapy, and surgery. Many authors currently favor the use of carbon dioxide laser for resection.

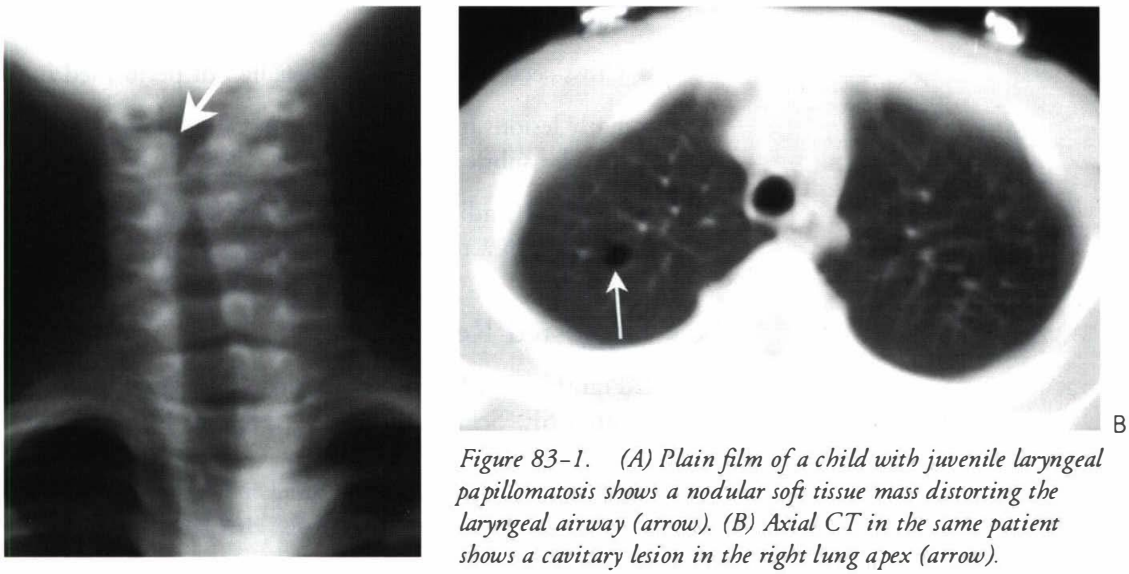

Figure 83-1. (A) Plain film of a child with juvenile laryngeal papillomatosis shows a nodular soft tissue mass distorting the laryngeal airway (arrow). (B) Axial CT in the same patient shows a cavitary lesion in the right lung apex (arrow).

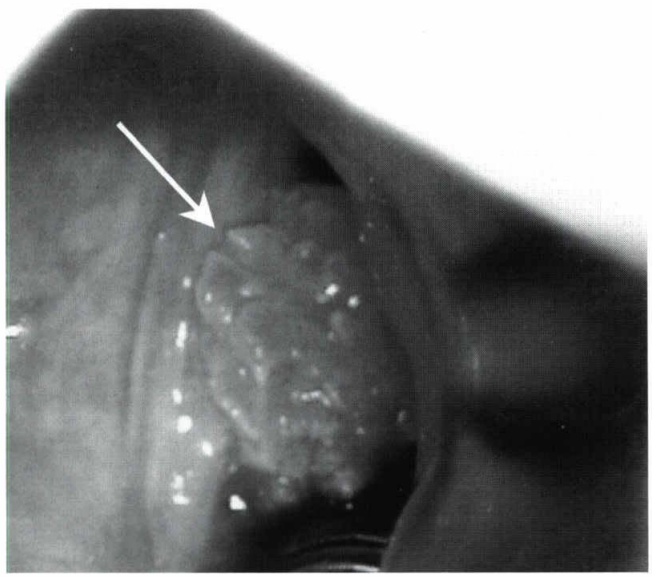

Figure 83-2. Endoscopic view of a laryngeal papilloma shows a reddish nodular exophytic mass at the level of true vocal cords (arrow). The mass is obstructing the laryngeal airway.

Imaging Findings

Plain Films

JLP is characterized on plain films by nodular soft tissue masses involving the tracheal air column. There may be distension of the air in the oropharynx above the soft tissue masses (Fig. 83-1A).

CT

The laryngeal findings are multiple endophytic nodular soft tissue masses that narrow the airway. Often, these lesions will appear as asymmetric thickening of the true vocal cords. These lesions may enhance with contrast.

The pulmonary findings consist of multiple bilateral parenchymal nodules that may be solid or cavitary (Fig. 83-1B). These lesions may gradually enlarge resulting in areas of consolidation or distal atelectasis. Solid lesions may eventually cavitate over time. The cavities are typically thin walled and may contain air-fluid levels and are prone to recurrent infections. An enlarging solid lesions is suggestive for malignant transformation (Fig. 83-2).

Imaging Pearls

- Cross-sectional imaging is usually not performed in most patients with JLP.
- Early lesions may not be seen on CT. Thin-section (< 2 mm thick) is necessary to identify the subtle changes.
- The MR findings have not to our knowledge been described because performing MR imaging in a toddler with airway obstruction is usually avoided.

Suggested Readings

1. Pransky SM, Seid AB. Tumors of the larynx, trachea and bronchi. In: Bluestone CD, Stool SE, Scheetz MD, eds. *Pediatric Otolaryngology*, Vol. 2. Philadelphia: Saunders; 1990:1215–1218.
2. Kramer SS, Wehnut WD, Stocker JT, Kashima H. Pulmonary manifestations of juvenile laryngotracheal papillomatosis. *AJR Am J Roentgenol* 1985;144:687–694.

Chapter 84

Laryngeal Paraganglioma

Epidemiology

Laryngeal paraganglia are rare lesions. They are thought to be more common in males. The average age at presentation is 45 (range: 15–67 years). Two pairs of the paraganglia have been identified in the larynx. These sites may give rise to laryngeal paraganglioma. One site is located beneath the epithelium above the anterior end of the vocal cord and near the internal branch of the superior laryngeal nerve. The second site is adjacent to the recurrent laryngeal nerve between the thyroid and cricoid cartilages. Additional rests of paraganglionic tissue have been found directly adjacent to the cricoid cartilage.

Clinical Features

These are rare lesions and the clinical findings have not been well described. These lesions may present as pulsatile submucosal masses, with the most common location being the posterior aspect of the aryepiglottic fold in the supraglottic larynx. The symptoms are felt to be directly proportional to size. Biopsy of the lesions may be associated with substantial hemorrhage from the biopsy site.

Pathology

These are benign tumors. Both light and electron microscopy demonstrate a biphasic or biphenotypic pattern identical to that seen in pheochromocytoma (adrenal paraganglioma). These lesions are composed of chief (type 1) cells and sustentacular cells (type 2) surrounded by a fibrovascular stroma. The chief cells are arranged into compact cell nests or balls of cells ("zellballen") and typically exhibit a whorled architecture. The chief cells are polygonal, round, or oval, with large, rounded nuclei and prominent nucleoli. They are more numerous than the sustentacular cells and are centrally distributed within the cell clusters. The sustentacular cells are located peripherally and are spindle-shaped with long cytoplasmic processes that may mimic vascular pericytes. These long cytoplasmic processes typically confer a characteristic whorled configuration. The likelihood of local recurrence or metastases after excision is rare.

Treatment

No specific surgical procedure is recommended for these lesions. In general, because they are benign lesions, total laryngectomy should be avoided if possible.

Imaging Findings

CT

These are well-defined submucosal enhancing masses located most commonly in the supraglottic larynx. Transglottic extension and cartilage invasion are rare (Fig. 84-1).

MR

The MR findings of these lesions have, to our knowledge, not been reported. The findings would likely be a diffusely enhancing mass in the supraglottic larynx. Flow voids may be present in larger lesions but may be absent in early tumors.

Imaging Pearls

- The diagnosis of laryngeal paraganglioma may be suggested for diffusely enhancing submucosal masses situated in the supraglottic larynx.

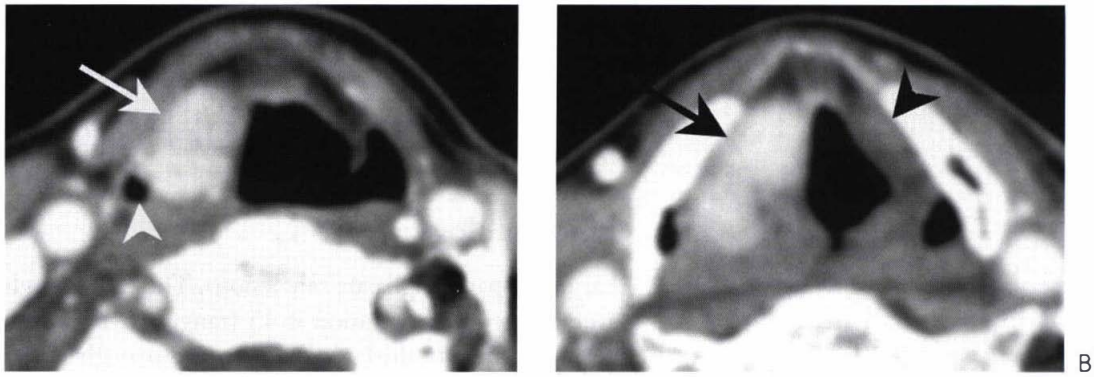

Figure 84–1. (A) Axial contrast-enhanced CT obtained at the level of the thyrohyoid membrane shows a densely enhancing mass (arrow) located in the right paralaryngeal space that extends anteriorly into the preepiglottic space. There is partial effacement of the right pyriform sinus (arrowhead). (B) Axial image performed at the level of the thyroid cartilage shows that the mass extends inferiorly along the paraglottic space (arrow). The arrowhead demonstrates the appearance of the normal paraglottic space on the contralateral side (arrowhead). Pathology revealed benign paraganglioma. (Case courtesy of Larry Ginsberg, M.D.)

Suggested Readings

1. Rao AB, Koeller KK, Adair CF. From the archives of the AFIP: paragangliomas of the head and neck—radiologic-pathologic correlation. *RadioGraphics* 1999;19:1605–1632.
2. Batsakis JG. *Tumors of the Head and Neck: Clinical and Pathological Considerations.* Baltimore: Williams and Wilkins; 1979.
3. Lack EE, Cubilla AL, Woodruff JM. Paragangliomas of the head and neck region: a pathologic study of tumors from 71 patients. *Hum Pathol* 1979;10:191–218.

Chapter 85

Posttransplant Lymphoproliferative Disorder

Epidemiology

Posttransplantation lymphoproliferative disorder (PTLD) is a lymphoproliferative disorder that occurs in patients who are chronically immunosuppressed after solid tissue organ transplantation. PTLD consists of a variety of disorders that include lymphoid hyperplasia and lymphoid neoplasia. The reported frequency range (1–10%) depends on the transplanted organ and may be related to specific immunosuppressive regimens. PTLD is believed to arise from unregulated B cell proliferation. There is a strong association between Epstein-Barr virus (EBV) and PTLD. A T cell variant of PTLD has been described that is not associated with EBV. The sites most commonly involved include Waldeyer's ring, larynx, and lymph nodes.

Clinical Findings

The patients have all undergone solid tissue organ transplantation and typically present at least 3 months after transplant. The clinical symptoms for head and neck involvement are nonspecific and include an enlarging neck mass, otalgia, facial numbness or paresthesia, or a "mononucleosis-like syndrome."

Pathology

There are a wide range of histopathologic findings included within the heading of PTLD. These range from B cell hyperplasia to lymphoma. The diagnostic criteria for PTLD are the presence of atypical lymphocytic infiltrates or destruction of normal parenchymal architecture. PTLD can be classified into three distinct categories: monomorphic, polymorphic, and hyperplastic.

Treatment

The specific treatment of PTLD is based on the specific histologic findings of the disease. The treatment modalities include a reduction in immunosuppressive therapy and treatment with chemotherapy, radiation therapy, antiviral therapy, or surgical resection. The prognosis is variable. In general, disease that occurs within the first year after transplant is associated with a lower mortality rate (36%) prognosis than late onset disease (70%). Patients with a more aggressive immunosuppressive regimen will likely have a worse prognosis than patients with a less potent regimen.

Imaging Findings

CT

Precontrast studies show the attenuation to be similar to muscle. These masses enhance and often have central areas of decreased attenuation. The most common location is in the region of Waldeyer's ring (Fig. 85–1).

MRI

This demonstrates thick intermediate T1-weighted signal that enhances following contrast. The masses are typically intermediate to high signal on T2-weighted sequences.

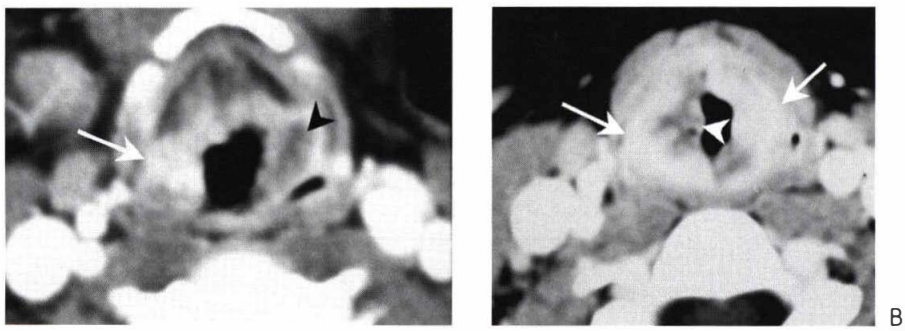

Figure 85-1. (A) Axial contrast-enhanced CT shows a diffusely enhancing mass involving the supraglottic larynx (arrow). Note the central area of decreased attenuation located in the left side of the supraglottis (arrowhead). (B) Axial image obtained in the same patient illustrated in (A) shows a diffusely enhancing mass involving the infrahyoid epiglottis (arrows). The arrowhead demonstrates an area of decreased attenuation within the mass.

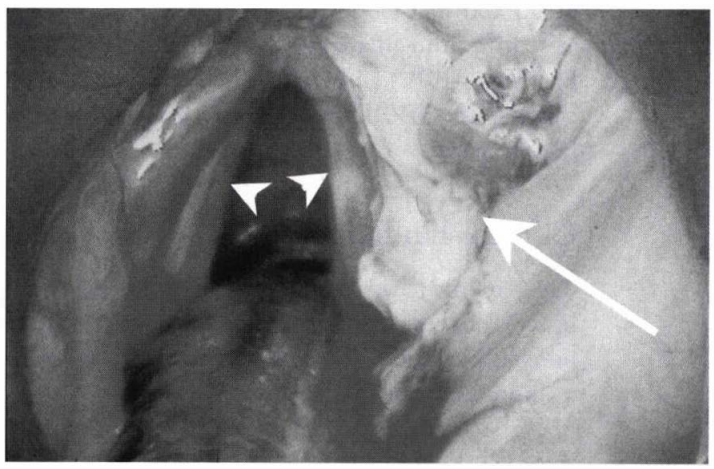

Figure 85-2. Endoscopic image of posttransplantation lymphoproliferative disorder shows an irregular white mass involving the supraglottis (arrow). The arrowheads demonstrate the true vocal cords.

Imaging Pearls

- The imaging findings are nonspecific and include lymphoma and fungal infections. PTLD tends to enhance more than lymphoma.
- The diagnosis can be suggested by the characteristic imaging findings in an immunosuppressed patient typically presenting 6 months following transplantation (Fig. 85-2).

Suggested Readings

1. Loevner LA, Karpati RL, Kumar P, Yousem DM, Hsu W, Montone KT. Posttransplant lymphoproliferative disorder of the head and neck: imaging features in seven patients. *Radiology* 2000;216:363-369.
2. Carigan S, Staples CA, Muller NL. Intrathoracic lymphoproliferative disorders in the immunocompromised patient: CT findings. *Radiology* 1995;197:53-58.
3. Donnellyly LF, Frush DP, Marshall KW, White KS. Lymphoproliferative disorders: CT findings in immunocompromised children. *AJR Am J Roentgenol* 1998;171:725-731.

Chapter 86

Kaposi's Sarcoma

Epidemiology

Kaposi's sarcoma is a vascular neoplastic disorder characterized by multiple violaceous nodules on the skin of the upper and lower extremities. The disease has become more common due to its strong association with acquired immunodeficiency syndrome (AIDS). There are three forms of Kaposi's sarcoma. The most common form in the United States is the AIDs-related type. A second type is the classic form that is most common in elderly men (3:1) of Jewish or Mediterranean descent. There is also a third type of the disease seen in Central Africa. This latter form has a striking male predominance (10–15:1); often affects younger individuals, including children and adolescents, and has a poor prognosis.

Clinical Findingss

Most patients with laryngeal involvement often present with the classic skin lesions. The most common laryngeal location of Kaposi's sarcoma is the epiglottis. The presenting symptoms include dysphonia, dyspnea, and dysphagia.

Pathology

On gross examination, the neoplasm is often bluish-red and may be nodular or pedunculated. The overlying epithelium may be intact or ulcerated. The tumor is characterized histologically by spindle cells with considerable pleomorphism and vascular channels of variable size. The stroma is infiltrated by chronic inflammation.

Treatment

Older patients with the Mediterranean form of Kaposi's sarcoma may not succumb to the disease. The prognosis in patients with laryngeal involvement by AIDS-related or central African Kaposi's sarcoma is usually poor. Localized lesions may be treated with surgery or radiotherapy. Chemotherapy may be used as a palliative treatment. Response rates up to 40% have been reported with high-dose alpha-2 interferon therapy.

Imaging Findings

CT

Kaposi's sarcoma may present as a focal or concentric laryngeal mass that enhances following contrast administration (Figs. 86–1 and 86–2).

MR

The MR findings have not been well described. The lesion is intermediate on T1-weighted images and diffusely enhances following contrast administration. The T2 signal is variable and may be iso- to hyperintense compared with surrounding mucosa. Exolaryngeal spread is unusual.

Imaging Pearls

- The imaging findings are nonspecific. The diagnosis may be suggested by the presence of the characteristic skin lesions or in the presence of other head and neck abnormalities associated with HIV disease (enlarged adenoidal tissue, enlarged lymph nodes, lymphoepithelial cysts in the parotid gland).

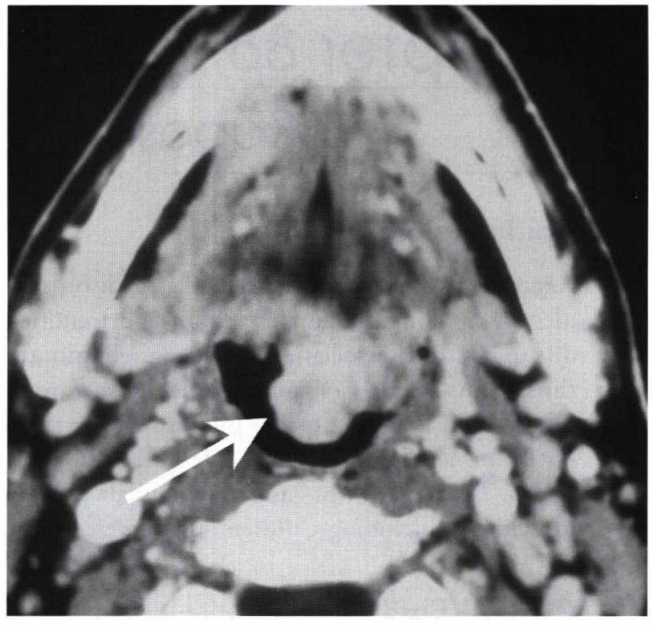

Figure 86-1. Axial contrast-enhanced CT shows a nodular enhancing mass involving the free margin of the epiglottis (arrow). Biopsy revealed Kaposi's sarcoma.

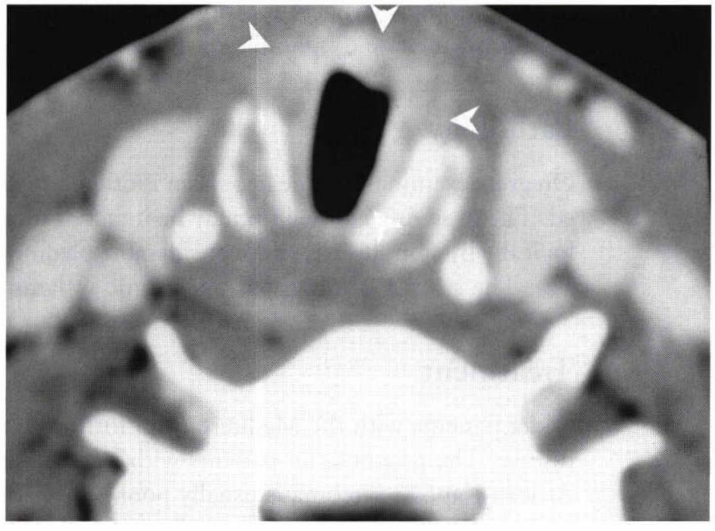

Figure 86-2. Axial image obtained through the subglottis shows eccentric enhancing soft tissue in the subglottis (arrowheads). The mass distorts the normal appearance of the airway. The patient was not known to be HIV positive prior to this imaging study and subsequent biopsy. Biopsy revealed Kaposi's sarcoma and the patient was found to be HIVG.

Suggested Readings

1. Becker M, Moulin G, Kurt AM, et al. Non-squamous cell neoplasms of the larynx: radiologic-pathologic correlation. *Radiographics* 1998;181:1189-1209.
2. Gridelli C, Palmiere G, Airoma G. Complete regression of laryngeal involvement by classic Kaposi's sarcoma with low dose alpha-2b interferon. *Tumori* 1990;76:292-293.
3. Gnepp DR, Chandler W, Hyams V. Primary Kaposi's sarcoma of the head and neck. *Annof Intern Med* 1984;100:107-114.

Chapter 87

Teratoma

Epidemiology

Teratomas are true neoplasms of germ cell origin that consist of elements derived from all three germ cell layers. The incidence is 1 in 4000 births. Teratomas may occur in numerous locations in the extracranial head and neck, including the neck, paranasal sinuses, nasopharynx, orbit, and pharynx. Seven to nine percent of teratomas occur in the cervical region. There is no reported gender predilection for cervical teratomas. However, nasopharyngeal teratomas have been reported to have a strong female predilection (6:1).

Clinical Findings

Cervical teratomas usually present in the first year of life and are often detected at birth. These lesions are often identified on prenatal ultrasound. They may be seen in full-term, premature, and stillborn infants. Cervical teratomas present as a bulky neck mass that may cross the midline. The symptoms of the mass are usually due to compression of adjacent structures. Tracheal compression may result in stridor, apnea, or cyanosis. Compression of the esophagus may result in dysphagia. About 20% of affected infants are associated with maternal polyhydramnios. This may be due to the inability of the infant to swallow amniotic fluid in utero due to esophageal compression.

Embryology

The embryogenesis of cervical teratomas is controversial. Historically, these lesions were felt to arise from anomalous development of the thyroid gland because they contained thyroid tissue. However, the explanation of the origin of cervical teratomas arising from the thyroglossal duct or the pharyngeal pouches (ultimobranchial anlage) is debatable.

Pathology

The majority of teratomas are benign lesions that contain histologically identifiable tissue from all three germ layers. Neural tissue is identified in 75 to 85% of cervical teratomas. These lesions typically have a well-defined capsule. The presence of fat and calcification allows easy diagnosis on imaging studies. Approximately one third of cases will have foci of normal thyroid tissue within the teratoma wall.

The risk of malignant change in cervical teratomas is low. The cause of the malignant degeneration is controversial. Some investigators feel malignant changes arise from de-differentiation of the teratomatous elements. Thyroid carcinoma can occur in lesions that contain residual thyroid tissue. This is rare and has been reported in $< 1\%$ of cases. Immature tissue components may suggest malignant change to the pathologist. However, these change may be reflective of the immaturity of the host.

Treatment

The treatment of cervical teratomas is surgical excision. Early and complete resection is essential for proper management of these patients. Respiratory obstruction is the leading cause of mortality in patients with large cervical teratomas. Delay in resection may result in progression of respiratory symptoms and may lead to atelectasis and pneumonia. Following treatment, careful follow-up is required of all patients who have undergone previous treatment due to increased risk of malignancy regardless of the location of the lesion and the histologic findings.

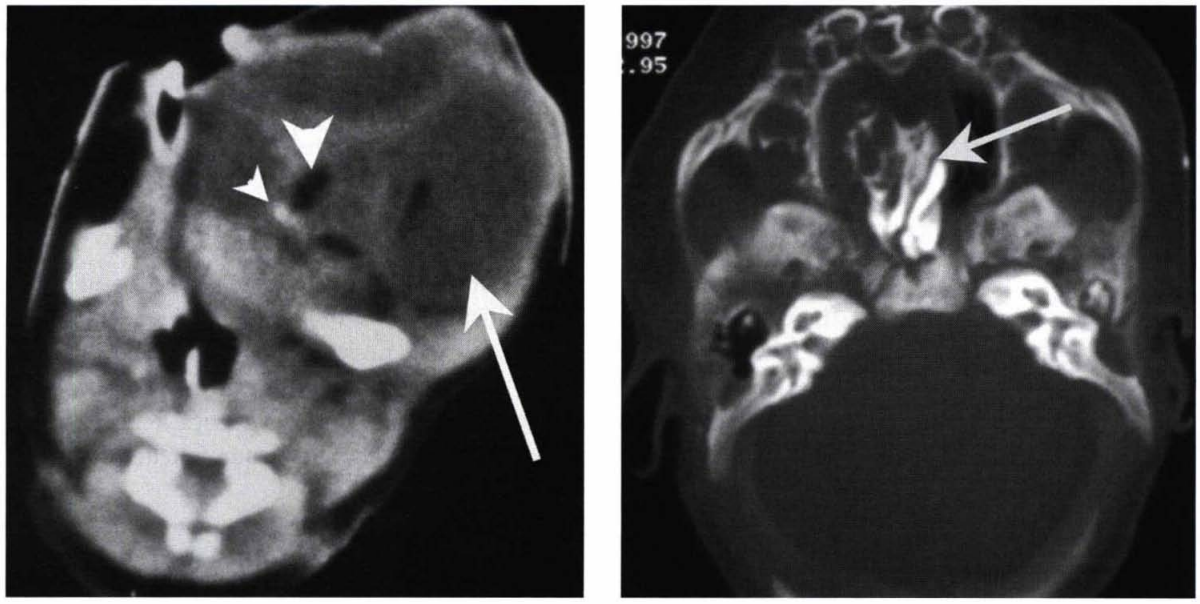

A B

Figure 87–1. CT findings of teratoma. (A) Axial noncontrast demonstrates a large oral teratoma involving the oral cavity and extending into the soft tissues of the neck. The mass contains fluid (arrow), fat (large arrowhead), and calcium (small arrowhead). (B) Axial CT obtained in bone algorithm in a different patient with an oral teratoma shows a large calcified mass (arrow) located in the oral cavity.

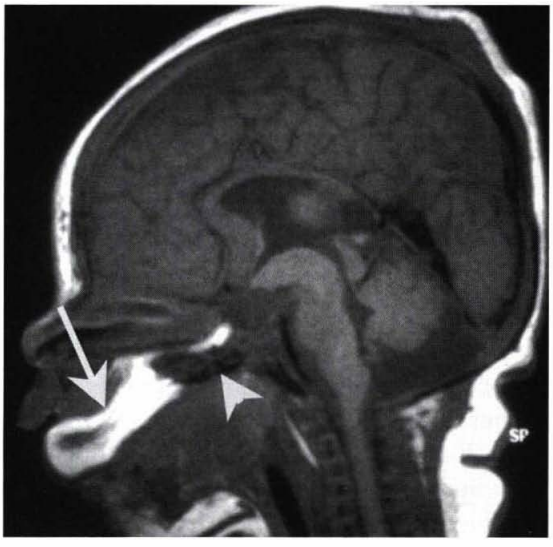

A

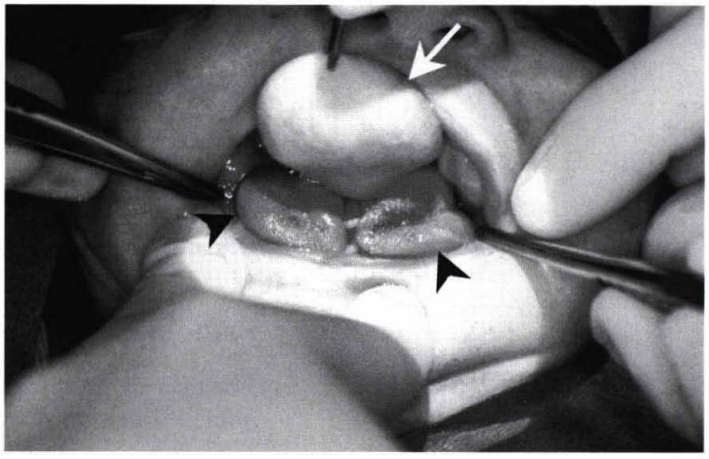

B

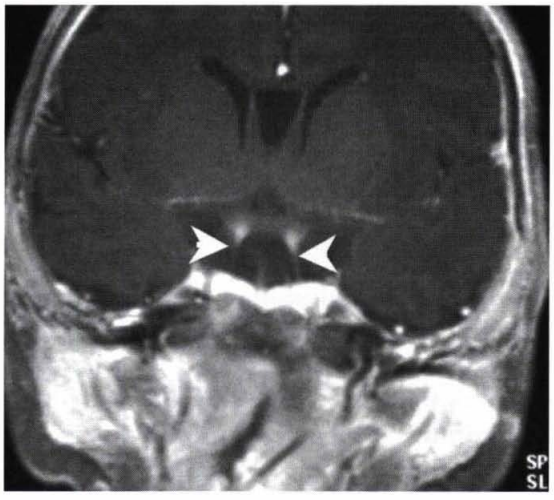

C

Figure 87–2. MR findings of teratoma. (A) Sagittal noncontrast MR performed in the same patient as in Figure 87–1B. The arrowhead denotes a low-signal mass that corresponds to the calcified mass illustrated in Figure 87–1B. The arrow identifies a high signal mass that corresponds to the fat component of the teratoma. (B) Intraoperative view performed in the same patient illustrated in Figure 87–2A shows the teratoma (arrow) associated with a bifid tongue (arrowheads). (C) Coronal postcontrast T1-weighted MR obtained in the patient illustrated in Figure 87–2A demonstrates two pituitary stalks (arrowheads), which indicates duplication of the pituitary gland.

Imaging Findings

CT

The CT appearance is characterized by a large, bulky, heterogeneous mass consisting of both solid and cystic components. There may be an enhancing rim. Teratomas centered in the neck are usually located adjacent to the thyroid gland. Teratomas are unilateral masses that may cross the midline or extend into the thoracic inlet. The presence of fat and calcification is the diagnostic hallmark. The attenuation of fluid component is variable depending on the amount of protein and fat within the lesion (Fig. 87-1).

MR

The MR imaging findings demonstrate a large heterogeneous mass. The signal characteristics vary with the amount of fat and protein present within the lesion. The chunky calcification located within teratomas will be seen as a focal area of signal loss (Fig. 87-2).

Imaging Pearls

- We prefer CT for imaging patients suspected of having a cervical teratoma. The substantially shorter imaging time may preclude the need for sedation. This is extremely important for patients with underlying respiratory compromise.
- The presence of a fatty mass with calcification could be due to either a dermoid or a teratoma. Teratomas tend to be more bulky and heterogeneous than dermoids.
- Calcifications are more easily detected on CT than with MR imaging.
- The multiplanar capabilities of MR imaging are helpful for large tumors that extend superiorly to the skull or inferiorly into the thoracic inlet.
- Oral cavity dermoids and teratomas are associated with other midline anomalies, including medial cleft syndrome and duplicated pituitary gland.

Suggested Readings

1. Myers EN, Cunningham MJ. Tumors of the neck. In: Bluestone CD, Stool SE, Scheetz MD, eds. *Pediatric Otolaryngology*, Vol 2. Philadelphia: WB Saunders; 1990:1359.
2. Batsakis JG. Teratomas of the head and neck. In: Batsakis JG, ed. *Tumors of the Head and Neck*. Baltimore: Williams and Wilkins; 1979:230-231.
3. Som PM, Sacher M, Lanzieri CF, et al. Parenchymal cysts of the lower neck. *Radiology* 1985; 157:399-406.
4. Smirniotopoulos JG, Chiechi MV. Teratomas, dermoids, and epidermoids of the head and neck. *Radiographics* 1995;15:1437-1455.

Chapter 88

Adenoidal Enlargement in HIV+ Patients

Epidemiology

Enlargement of the nasopharyngeal adenoidal tissue is well established. Adenoidal tissue is normally enlarged in children and young adults. This tissue usually regresses by the fourth to fifth decades of life. Hypertrophy of the adenoidal tissue has been reported in up to 60% of patients who are HIV+. The enlargement is believed to be due to reactive lymphoid hyperplasia and may even occur in HIV+ patients who have undergone prior adenoidectomy. There does not appear to be any substantial relationship between adenoidal width in HIV+ patients and CD4 count, hematocrit, or white blood count.

Clinical Findings

Patients with nasopharyngeal adenoidal hypertrophy typically present with nasal stuffiness, ear congestion, nasal bleeding, and hearing loss. Patients may also have palpable cervical lymph nodes.

Pathology

Histologically, there is follicular hyperplasia with an enlarged and irregular germinal center and thinning of the mantle zones. The germinal centers and mucosal surface may contain particles of HIV, HIV antigens, or markers for the RNA.

Treatment

There is no specific treatment for the adenoidal hypertrophy in HIV disease. The treatment is directed toward the disease itself.

Imaging Findings

CT

There is increased soft tissue isolated to the nasopharynx without deep extension through the visceral fascia. There is only mild enhancement following intravenous contrast administration (Fig. 88-1).

MR

The enlarged adenoidal tissue is iso- to slightly hyperintense to muscle on noncontrast T1-weighted sequences and increased signal on T2-weighted sequences. There is mild to moderate enhancement following contrast administration. The adenoidal width is measured on sagittal images. The mean width was found to be 6.76 + 5.82 mm in HIV+ patients and 3.36 + 2.48 mm in control subjects. Enlarged adenoidal tissue is limited to the nasopharynx and does not extend through the visceral fascia to invade the adjacent deep structures (Figs. 88-2 and 88-3).

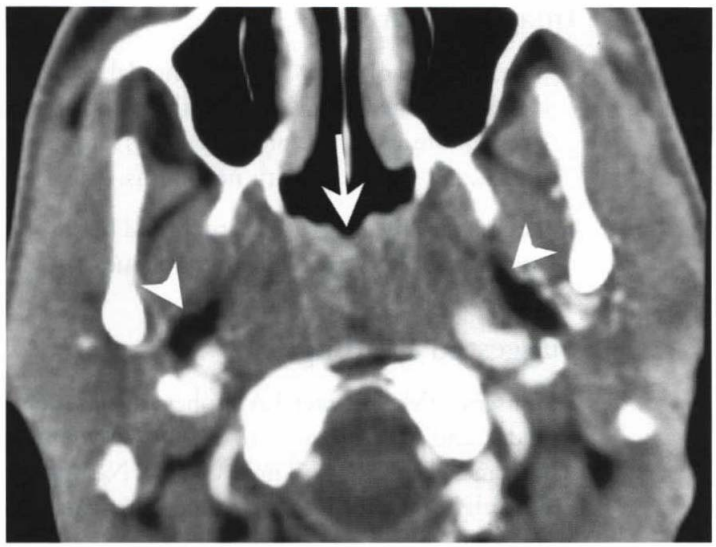

Figure 88–1. Axial contrast-enhanced CT performed in an HIV+ patient demonstrates abnormally enlarged nasopharyngeal adenoidal tissue in an adult (arrow). The attenuation is similar to that of muscle. However, there is no deep invasion into either parapharyngeal space (arrowheads) to suggest an aggressive process.

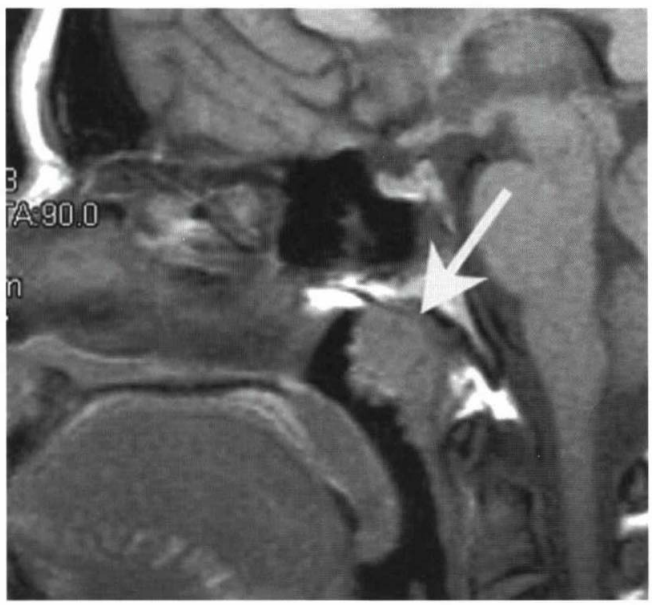

Figure 88–2. Sagittal noncontrast T1-weighted image obtained in a 40-year-old HIV+ male demonstrates abnormal enlargement of the adenoid tissue situated in the nasopharynx (arrow).

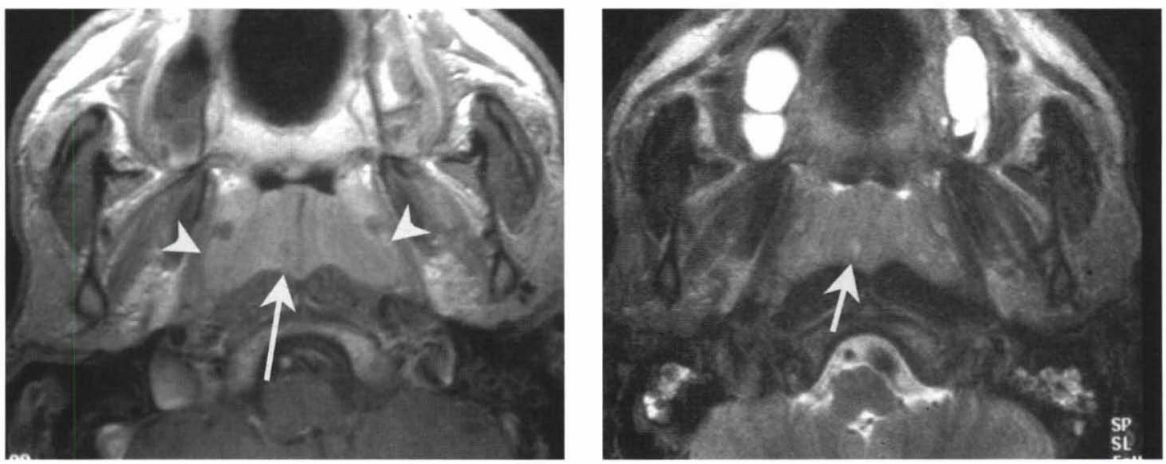

Figure 88–3. (A) Contrast-enhanced axial T1-weighted image shows diffuse enhancement of enlarged adenoidal tissue (arrow) in an HIV+ patient. Note how the adenoidal tissue is confined to the visceral space and does not invade deep to the expected location of the visceral fascia (arrowheads). (B) Axial T2-weighted image shows the adenoidal tissue (arrow) to be higher signal than the surrounding muscle and similar in signal to the gray matter of the posterior fossa in this example.

Imaging Pearls

- The hallmark of the enlarged adenoidal tissue is the lack of invasion into the fat and muscles deep to the visceral fascia in the nasopharynx. Invasion of the adjacent structures suggests a more aggressive process such as lymphoma, Kaposi's sarcoma, squamous cell carcinoma, and minor salivary neoplasms.
- The possibility of HIV disease should be suspected in patients over age 30 who have enlarged nasopharyngeal adenoidal tissue.

Suggested Readings

1. Yousem DM, Loevner LA, Tobey JD, Geckle RJ, Bilker WB, Chalian AA. Adenoidal width and HIV factors. *AJNR Am J Neuroradiol* 1997;18:1721–1725.
2. Barzan L, Carbone A, Tirelli U, et al. Nasopharyngeal lymphatic tissue in patients infected with human immunodeficiency virus: a prospective clinicopathologic study. *Arch Otolaryngol Head Neck Surg* 1990;116:928–931.
3. Stern JC, Lin PT, Lucente FE. Benign nasopharyngeal masses and human immunodeficiency virus infection. *Arch Otolaryngol Head Neck Surg* 1990;116:206–208.

Chapter 89

Nasopharyngeal Inflammation from Middle Ear Infection

Epidemiology

Middle ear infection is commonly associated with cholesteatoma. Fulminanting infection involving the middle ear may be seen as a complication in patients with immunosuppression, diabetes mellitus, and malignant otitis externa.

Clinical Findings

Clinical recognition of soft tissue swelling around the external ear associated with ear discharge is indicative of the diagnosis. These patients are also frequently septic. Radiologic evaluation is requested for demonstrating the disease extent prior to treatment.

Pathology

The offending organism is usually *Pseudomonas aeruginosa.* The infection causes an acute osteomyelitis of the temporal bone and is termed "malignant otitis externa." Infection involving the middle ear cleft can spread via the eustachian tube to the nasopharynx.

Treatment

Patients are treated with a combination of antibiotics, excision of infected bone, and abscess drainage.

Imaging Findings

CT

A soft tissue mass involving the external auditory canal and middle ear is usually evident. There is often associated erosion of the external auditory canal and obliteration of the mastoid cells. There may be erosion of the external auditory canal and skull base in cases of advanced malignant otitis externa. A swollen torus tubarius or a large mass involving the ipsilateral nasopharynx can be readily appreciated. There may be further spread of inflammation to the parapharyngeal or masticator spaces (Fig. 89–1).

MR

There is diffuse soft tissue swelling and enhancement. The extent of the soft tissue abnormality, especially superficial extension into the masticator space and deep extension to the stylomastoid foramen, is best identified on MR.

Imaging Pearls

- It is very important to get accurate clinical information. The CT findings may be indistinguishable from an extensive nasopharyngeal tumor. The soft tissue densities in the middle ear or the external auditory canal may be mistaken as tumor spread or serous otitis media. However erosion of the external auditory canal is rarely seen in tumors originating in the nasopharynx.
- Infection can erode the thin plate of bone separating the middle ear from the jugular foramen resulting in venous thrombosis or cranial nerve X, XI, or XII palsies. It is therefore important to examine the jugular foramen if there is a history of lower cranial nerve palsies.

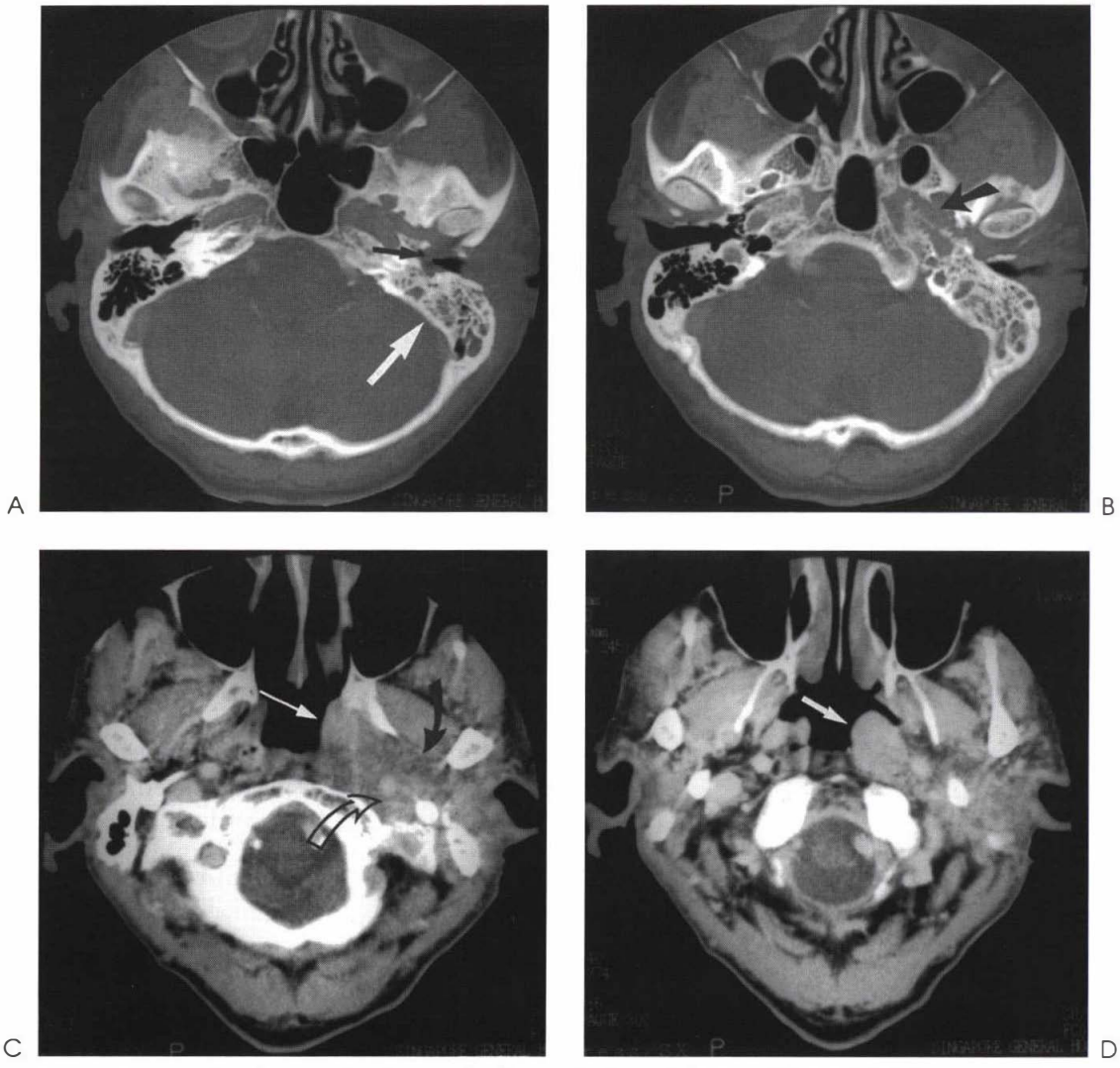

Figure 89-1. Nasopharyngeal inflammation from middle ear infection. (A) Axial CT (bone window) shows soft tissues within the left external acoustic canal and middle ear (arrow). Note the inflammatory changes in the ipsilateral mastoid cells. (B) Axial CT (bone window) inferior to (A) shows erosion along the eustachian tube, the anterior wall of the left carotid canal, and the petrous apex (arrow). (C) Axial contrast-enhanced CT shows a mass involving the left parapharyngeal space (black arrow), the left carotid space (curved hollow arrow), and the left nasopharyngeal wall (white arrow). (D) Axial contrast-enhanced CT shows a grossly swollen torus tubarius (arrow).

Suggested Readings

1. Valvassori GE, Buckingham RA. Acute otitis media, mastoiditis, and malignant necrotizing externa otitis. In: Valvassori GE, Mafee MF, Carter BL, eds. *Imaging of the Head and Neck*. New York: Thieme; 1995:67–104.
2. Chong VFH, Fan YF. Radiology of the jugular foramen. *Clin Radiol* 1998;53:405–416.

Chapter 90

Kimura's Disease

Epidemiology

Kimura's disease is a chronic inflammatory disorder of unknown etiology but thought to be immunologically mediated. Most cases have been reported in the parotid and submandibular glands and were described predominantly in Chinese and Japanese people. Kimura's disease has been reported in the external ear, epiglottis, salivary glands, and lymph nodes. The disease rarely involves the pharynx. This disorder occurs mainly in the second and third decades and is more common in males with a male to female ratio of 3:1.

Clinical Findings

The most common mode of presentation is painless neck swelling. Patients with pharyngeal involvement may present with neck pain and dysphagia. Peripheral blood eosinophilia is an invariable feature of this entity.

Pathology

Histology shows dense infiltration of eosinophils in the submucosa with formation of eosinophilic abscesses. Proliferation of small vessels lined by prominent endothelial cells has been noted with interspersed plasma cells and lymphocytes between aggregates of eosinophils.

Treatment

Kimura's disease is a benign disorder. The clinical course is typically progressive with relapses after the cessation of therapy. The initial response to corticosteroid and hydroxyurea treatment is often encouraging but patients usually benefit from low dose radiation therapy.

Imaging Findings

CT

Contrast-enhanced CT features of Kimura's disease in the nasopharynx or the salivary glands are nonspecific. The enhancement pattern is variable and may be related to the degree of fibrosis and vascular proliferation (Fig. 90-1).

MR

On T1-weighted MR images, the lesion shows low to intermediate signal intensity whereas the lesion is high signal on T2-weighted imaging. Kimura's disease shows intense enhancement following the injection of gadolinium.

Imaging Pearls

- Because Kimura's disease occurs in ethnic groups and geographic areas with high frequencies of nasopharyngeal carcinoma (NPC), the first consideration should be a nasopharyngeal cancer. Although NPC often spreads inferiorly into the oropharynx, hypopharyngeal involvement is rare. Furthermore, NPC occurs in middle-aged or older patients.
- Another radiologic differential diagnosis is lymphoma. Lymphoma with Waldeyer's ring involvement may show similar findings to nasopharyngeal carcinoma or Kimura's disease. The presence of peripheral eosinophilia should suggest the diagnosis of Kimura's disease.

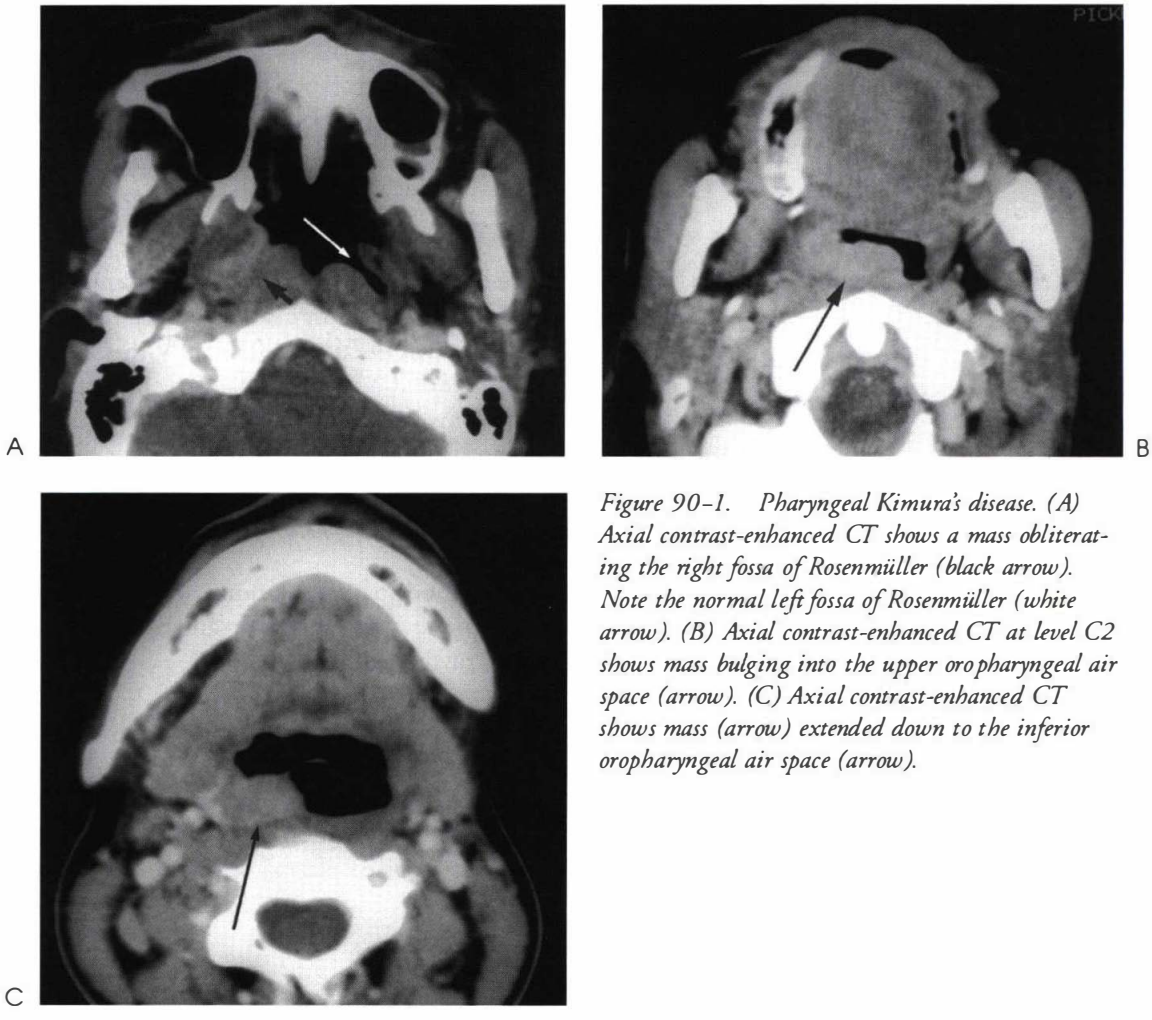

Figure 90–1. Pharyngeal Kimura's disease. (A) Axial contrast-enhanced CT shows a mass obliterating the right fossa of Rosenmüller (black arrow). Note the normal left fossa of Rosenmüller (white arrow). (B) Axial contrast-enhanced CT at level C2 shows mass bulging into the upper oropharyngeal air space (arrow). (C) Axial contrast-enhanced CT shows mass (arrow) extended down to the inferior oropharyngeal air space (arrow).

Suggested Readings

1. Chong VF, Balakrishnan A, Fong KW. Kimura's disease of the pharynx. *Clin Radiol.* 2000;55:649–651.
2. Som PM, Biller HF. Kimura disease involving parotid gland and cervical nodes: CT and MR findings. *J Comput Assist Tomogr* 1992;16:320–322.
3. Nyrop M. Kimura's disease: case report and brief review of the literature. *J Laryngol Otol* 1994;108:1005–1007.
4. Takahashi S, Ueda J, Furukawa T, et al. Kimura's disease: CT and MR findings. *AJNR Am J Neuroradiol* 1996;17:382–385.

Chapter 91

Sphenoethmoidal Polyps

Epidemiology

Isolated sphenoethmoidal recess polyps are rare. These polyps represent a group of lesions of various histologic types. When these lesions extend inferiorly, they present as a mass in the nasopharynx. Sphenoethmoidal recess polyps are mainly found in adults, and they constitute 28% of all isolated sphenoid sinus disease.

Clinical Findings

The most common presenting symptom is nasal obstruction followed by headache. Patients may be asymptomatic and the lesion discovered only incidentally. These lesions can be easily evaluated with nasal endoscopy and biopsy.

Pathology

The majority of sphenoethmoidal recess polyps are inflammatory in origin. The etiology of these polyps is unknown but is certainly related to retention cysts, chronic infection, or allergy. Inflammatory polyps can be classified as edematous, glandular, cystic, and fibrotic. Sphenoethmoidal polyps may also represent neoplastic disease such as inverted papillomas.

Treatment

Inflammatory polyps or retention cysts can be readily resected by endoscopic sphenoidotomy. If the polyps are neoplastic, surgical excision may entail partial excision of the middle turbinate and sphenoethmoidectomy. This approach is particularly important in reducing the recurrence rate of inverted papillomas.

Imaging Findings

CT

Polyps are low attenuation masses that have smooth, well-defined margins. They rarely erode bone. Large chronic masses may remodel adjacent bony structures (Fig. 91-1).

MR

Polyps show a variety of signal intensities reflecting the various stages of polyp development (edematous, glandular, cystic, and fibrotic). Most polyps show high signal intensities on T2-weighted images and enhance to varying extent.

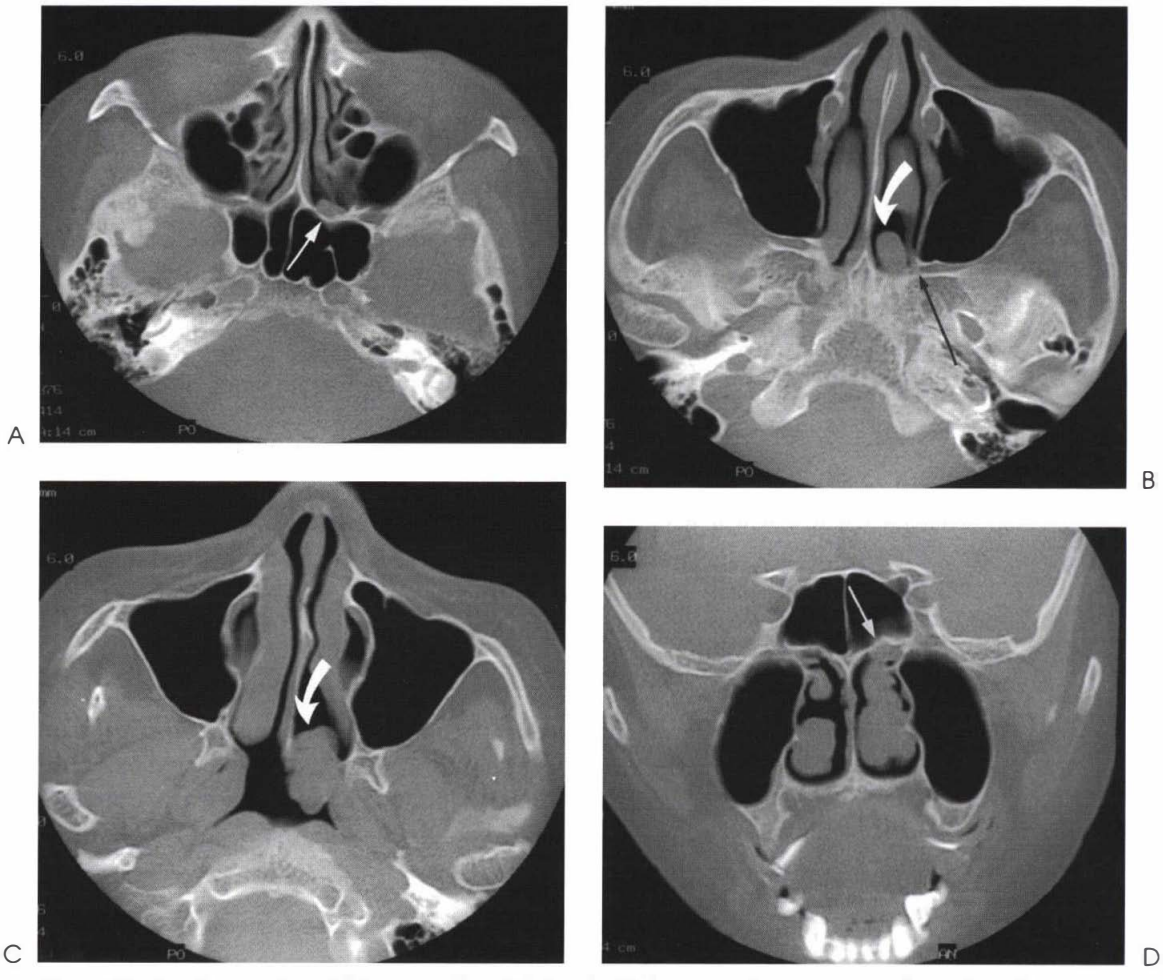

Figure 91–1. Sphenoethmoidal recess polyp. (A) Axial CT shows a polyp originating from the inferior aspect of the left sphenoethmoidal recess (arrow). (B) Axial CT shows polyp (curved arrow) at the level of the sphenopalatine foramen (straight arrow). (C) Axial CT shows the polyp as a mass within the nasopharynx (curved arrow). (D) Coronal CT shows origin of the polyp at the level of the left superior meatus (arrow).

Imaging Pearls

- When a smooth mass is present in the nasopharynx, it may be a lesion originating not from the visceral space but from the adjacent sinonasal mucosa. The mass should be traced to determine the site of origin.

Suggested Readings

1. Sethi DS, Lau DCP, Chee LWJ, Chong VFH. Isolated sphenoethmoid recess polyps. *J Laryngol Otol* 1998;112:660–663.
2. Mafee MF. Nasal cavity and paranasal sinuses. In: Valvassori GE, Mafee MF, Carter BL, eds. *Imaging of the Head and Neck*. New York: Thieme; 1995:288–292.
3. Chong VFH, Fan YF. Radiology of the nasopharynx. *Australas Radiol* 2000;44:5–13.

Chapter 92

Antrochoanal Polyp

Epidemiology

Antrochoanal polyp (ACP) is a polyp that originates from the maxillary antrum and extends into the nasal fossa usually through the secondary ostium of the maxillary sinus. ACP comprises about 5% of all polyps and most often presents in adolescents and young adults. These lesions are typically unilateral, but bilateral lesions have been reported in up to 30 to 40% of cases. The pressure of ACP are associated with allergies, systemic disorders which include multiple nasal polyposis, and cystic fibrosis.

Clinical Features

The most commonly presenting symptoms are nasal congestion and difficulty breathing. Patients may also present with sinus infection and drainage.

Pathology

A polyp is due to infiltration and expansion of the lamina propria of the schneiderian mucosa of the lining of the sinus or nasal cavity. Histologically, polyps are characterized by edema, proliferation of the connective tissue fibroblasts, and an inflammatory cellular infiltrate. An antrochoanal polyp is histologically indistinguishable from other forms of sinus or nasal polyps. In general, ACP tends to contain fewer eosinophils and mucous glands than nasal polyps.

Treatment

The treatment of choice is complete resection using a Caldwell-Luc or endoscopic intraantral approach. It is important that the stalk be resected. Incomplete removal of the stalk results in recurrent disease in 20 to 30% of cases.

Imaging Findings

Plain Films

There is typically unilateral opacification of the involved sinus without evidence of bone erosion.

CT

ACP presents as a soft tissue mass that completely opacifies the maxillary sinus and extends medially into the nasal cavity. The mass may extend posteriorly through the posterior choana into the nasopharynx. The internal attenuation varies depending on the protein content of the polyp. Polyps that contain a substantial amount of edema are low attenuation, whereas desiccated polyps with a high protein content are intermediate to high attenuation. The posterior wall of the maxillary sinus remains intact and may be thickened, indicating a chronic inflammatory process rather than an aggressive neoplasm (Fig. 92-1).

MR

ACPs are homogeneously high signal on T2-weighted sequences. They tend to be low signal on T1-weighted sequences and may have a thin enhancing rim following contrast administration (Fig. 92-2).

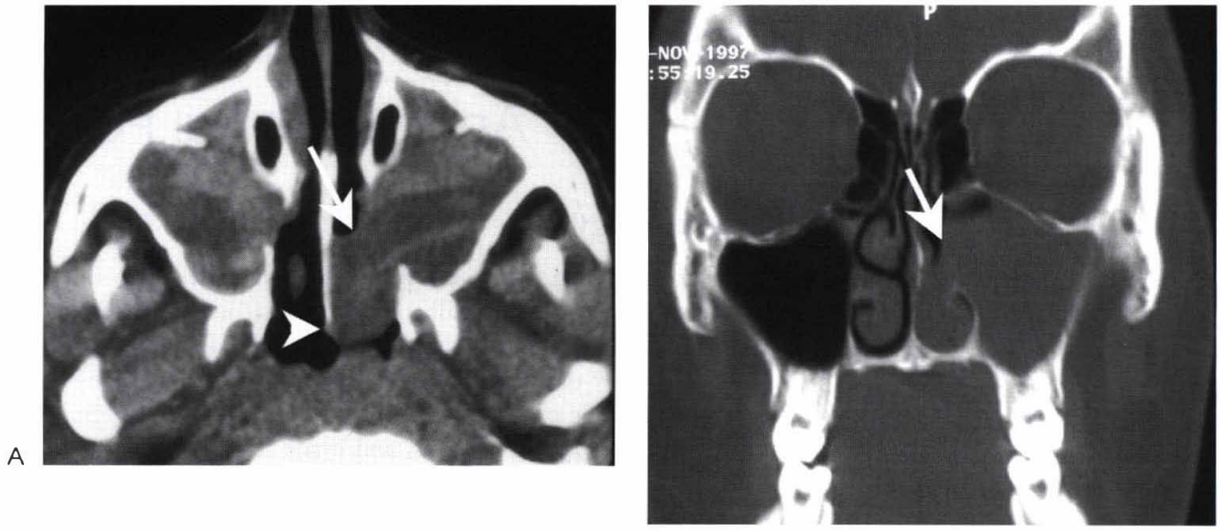

Figure 92–1. CT findings of antrochoanal polyp. (A) Noncontrast axial CT reconstructed in soft tissue algorithm demonstrates heterogeneous opacification of both maxillary sinuses. The areas of increased attenuation within the mucosal thickening may be due to desiccated secretions or fungal colonization. There is direct extension of the mucosal thickening through the secondary ostium of the maxillary sinus (arrow). The mass extends to the posterior choana (arrowhead). (B) Coronal CT in a different patient demonstrates partial opacification of the left maxillary sinus. The mass extends through the medial wall of the sinus and extends into the left nasal cavity (arrow).

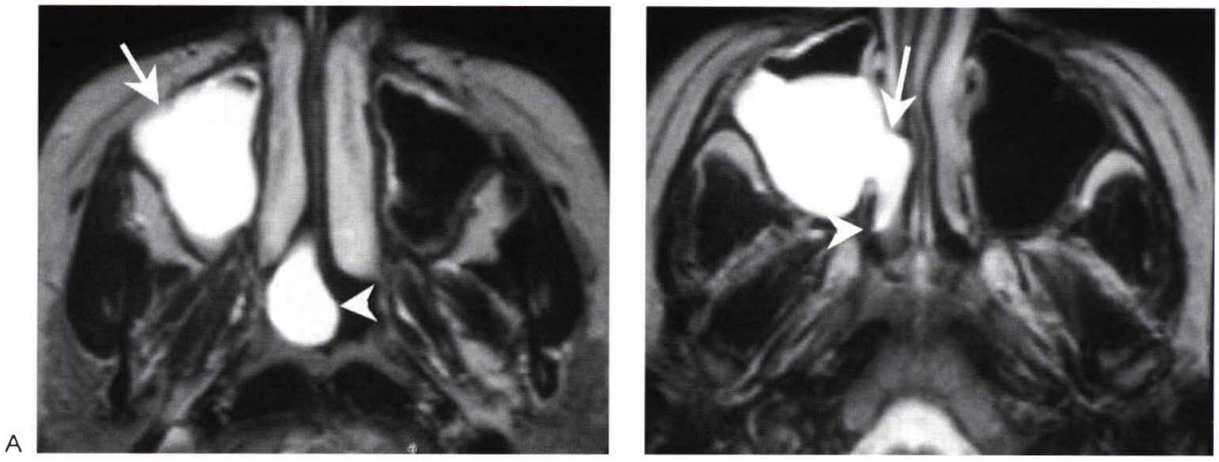

Figure 92–2. MR findings of antrochoanal polyp. (A) Axial T2-weighted image shows a high signal mass in the nasopharynx (arrow) and diffusely increased signal in the right maxillary sinus (arrowhead). (B) T2-weighted image obtained at a higher level from the same patient illustrated in (A). The mucosal thickening extends through the expected location of the secondary ostium of the maxillary sinus (arrow) into the posterior choana (arrowhead). This was directly attached to the nasopharyngeal mass shown in (A).

Imaging Pearls

- The maxillary sinus should be evaluated in all patients who present with a homogeneously high T2-weighted signal mass in the nasopharynx. A similar-appearing process in the maxillary sinus is suggestive of an ACP.
- A sphenochoanal polyp arises from the sphenoid sinus and extends into the posterior nasal cavity and pharynx via the sphenoethmoidal recess.
- The differential diagnosis for a unilateral maxillary sinus mass that completely opacifies the involved sinus includes ACP, mucocele, inverting papilloma, and tumor. The ACP, by definition, extends into the nasal cavity, is associated with a nonexpanded sinus, and is often associated with thickening of the posterior wall of the maxillary sinus. A mucocele is limited to the sinus and expands the involved sinus. An inverting papilloma is usually

higher attenuation and is limited to the maxillary sinus. This may be indistinguishable from a low-grade malignancy. Aggressive neoplasms typically erode the adjacent sinus walls.

Suggested Readings

1. Batsakis JF. *Tumors of the Head and Neck: Clinical and Pathologic Considerations.* 2nd ed. Baltimore: Williams and Wilkins; 1979:121–143.
2. Som PM, Brandwen M. Sinonasal cavities: inflammatory diseases, tumors, fractures, and postoperative findings. In: Som PM, Curtin H, eds. *Head and Neck Imaging.* 3rd ed. New York: Mosby; 1996:126–314.
3. Allbery SM, Chaljub G, Cho NL, Rassekh CH, John SD, Guinto FC. MR imaging of nasal masses. *Radiographics* 1995;15:1311–1327.

Chapter 93

Peritonsillar Abscess

Epidemiology

In contrast to acute tonsillitis, which is more common in children, peritonsillar abscess is more common in young adults. The average age is 25 years with more than 65% of patients falling between the ages of 20 and 40. This infection affects males and females equally.

Clinical Findings

The most common symptoms are sore throat, dysphagia, fever, and trismus. Almost all patients have a history of recurrent pharyngitis. Physical examinations show an inflamed oropharyngeal mass involving the soft palate and supratonsillar space. Patients express great anxiety and distress when the abscess begins to compromise the airway.

Pathology

Traditional textbook accounts state that peritonsillar abscesses are due to progression from acute tonsillitis. However, recent reviews indicate that a group of salivary glands (glands of Weber), located in the supratonsillar space, are the original site of infection. This explains why the tonsils (which seldom show acute exudation) are displaced inferiorly and anteriorly in patients with peritonsillar abscesses. Furthermore, the mean age of patients with acute tonsillitis differs from that of patients with peritonsillar abscesses. Cultures show no predominant type of bacteria.

Treatment

If an abscess has already formed, incision and drainage is the treatment of choice, followed by intravenous antibiotic therapy. This treatment should bring about rapid clinical improvement. It remains controversial whether tonsillectomy should be performed at the same time as the incision and drainage procedure. Tonsillectomy is recommended following the documentation of recurrent tonsillitis.

Imaging Findings

CT

CT shows an enhancing mass in the tonsillar fossa that may or may not show pus formation. Extension into the parapharyngeal space may involve the medial pterygoid muscles (leading to trismus). In extensive disease, the inflammatory process may spread posterolaterally to involve the carotid sheath (Fig. 93–1).

Imaging Pearls

- CT should be used to evaluate suspected peritonsillar abscess because it is quicker and cheaper than MR imaging. Gas-forming infections are much easier to identify on CT.
- When inflammation spreads beyond the oropharyngeal wall, it is important to determine the extent of disease tracking along the parapharyngeal space. Mapping the extent of the abscess will aid in surgical drainage.
- In the preantibiotic era, abscess involvement of the carotid sheath often led to serious or fatal consequences. It is important to evaluate the carotid sheath for possible jugular vein thrombosis or carotid artery erosion.

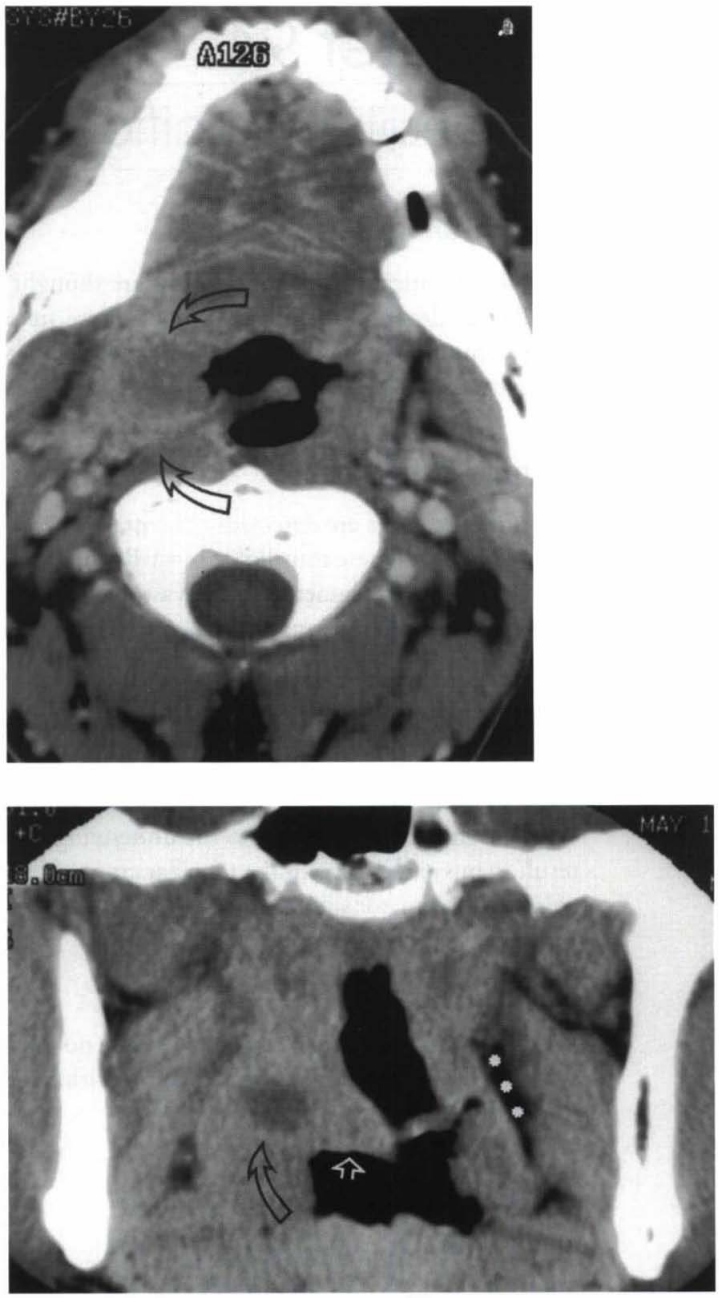

Figure 93-1. Peritonsillar abscess. (A) Axial contrast-enhanced CT shows swelling of the right tonsillar region (arrows). (B) Coronal contrast-enhanced CT shows thickening of the tonsillar fossa and an area of low attenuation indicating abscess formation (curved arrow). There is resultant effacement of the right parapharyngeal space. Note the normal left parapharyngeal space (asterisks). Inflammation has spread to the ipsilateral soft palate (hollow white arrow). (Courtesy of SH Ng, M.D., Chang Gung Memorial Hospital, Taoyuan, Taiwan)

Suggested Readings

1. Passy V. Pathogenesis of peritonsillar abscess. *Laryngoscope* 1994;104:185–190.
2. Gale DR. CT and MRI of the oral cavity and oral pharynx. In: Valvassori GE, Mafee MF, Carter BL, eds. *Imaging of the Head and Neck*. New York: Thieme; 1995:445–474.
3. Harnsberger HR. *Handbook of Head and Neck Imaging*. 2nd ed. Chicago: Mosby; 1995.

Chapter 94

Tonsillar Calcifications (Tonsilloliths)

Epidemiology

Tonsillar calcifications or tonsilloliths are thought to be secondary to previous episodes of tonsillitis. Although tonsillitis is much more frequently seen in children, tonsilloliths are more commonly detected in adults. These calcifications are seen in up to 10% of the adult population.

Clinical Findings

Most calcifications are detected incidentally in patients undergoing CT for unrelated clinical indications. These tonsilloliths usually measure a few millimeters but some may be up to one centimeter in diameter. In the vast majority of patients, tonsilloliths are asymptomatic. However, large lesions may produce sore throat or dysphagia.

Pathology

The tonsils are masses of lymphoid tissues covered by nonkeratinizing squamous epithelium. The exposed medial surface of the tonsils contains 15 to 20 narrow channels (tonsillar crypts) that penetrate deep into the underlying lymphoid tissues. Acute attacks of tonsillitis result in pus exuding from the tonsillar crypts. These exudates may subsequently calcify and enlarge to form tonsilloliths.

Treatment

Tonsilloliths are benign lesions that require no treatment and should be recognized for what they are. However, symptomatic patients with large tonsilloliths may require surgical removal of the lesions.

Imaging Findings

Tonsilloliths are usually detected on CT (Fig. 94–1). They vary in size and may be single or multiple. They are not usually demonstrated on plain radiographs or MR imaging. The calcifications are typically located within the tonsillar fossa in the medial aspect of the oropharyngeal wall. Associated soft tissue swelling is not a feature of this entity (Fig. 94–2).

Imaging Pearls

- An ingested radiopaque foreign body may be lodged in the tonsillar fossa mimicking a tonsillolith. It is therefore important to have an accurate clinical history of foreign body ingestion. On CT, a foreign body may have soft tissue swelling associated with trauma or infection. A calcified stylohyoid ligament may mimic a tonsillolith. The stylohyoid ligament connects the tip of the styloid process to the lesser cornua of the hyoid bone and gives attachment to the highest fibers of the middle pharyngeal constrictor muscles. It is thus intimately related to the lateral aspect of the oropharyngeal wall. A calcified ligament can be identified by recognizing the contiguity of the lesion through several sections. In addition, tonsilloliths may be multiple, a point of differentiation from a calcified stylohyoid ligament. It is rather unusual to have multiple foreign bodies lodged in the tonsillar fossae.

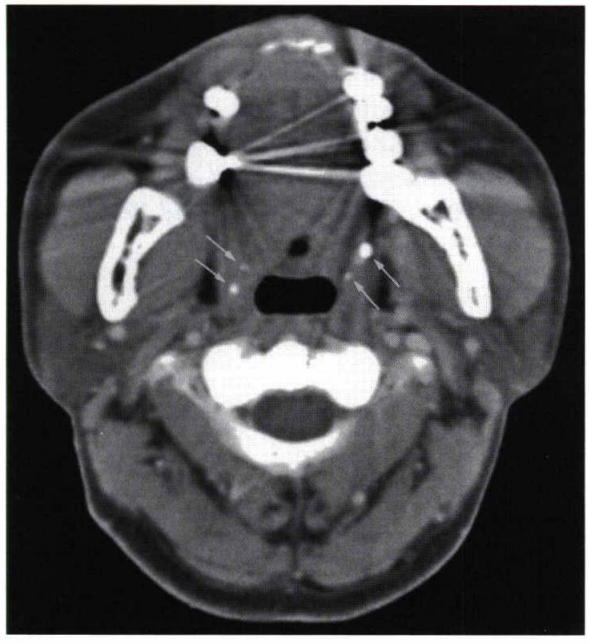

Figure 94–1. Tonsilloliths. Axial CT shows bilateral calcifications (arrows) in the tonsillar fossae. There is no associated soft tissue swelling.

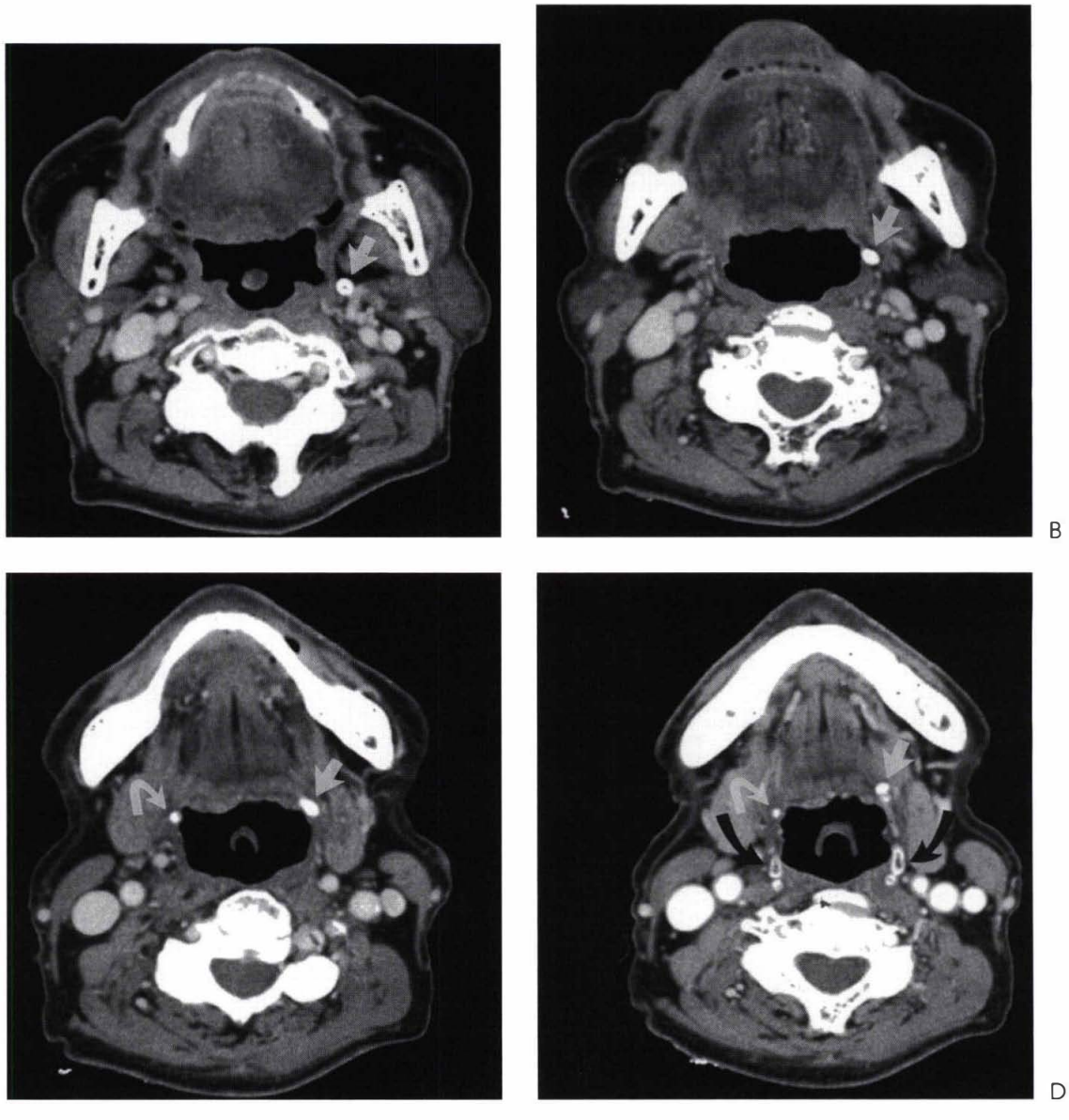

Figure 94–2. Calcified stylohyoid ligament. (A) Axial contrast-enhanced CT shows a prominently calcified left styloid process in the parapharyngeal space (arrow). (B) Axial contrast-enhanced CT shows the calcified stylohyoid ligament adjacent to the oropharyngeal wall (arrow). (C) Axial contrast-enhanced CT shows the stylohyoid ligament in a more anteriorly located position (arrow). Note the calcified contralateral stylohyoid ligament (curved arrow). Stylohyoid ligament calcification is frequently discontinuous. (D) Axial contrast-enhanced CT shows the insertion of the left (arrow) and right (curved arrow) stylohyoid ligaments into the hyoid bone (black arrows).

Suggested Readings

1. Ramsay AD. Palatine tonsils. In: McGee JO, Isaacson PG, Wright NA, eds. *Oxford Textbook of Pathology*. Oxford: Oxford University Press; 1992:1122–1123.
2. Gale DR. CT and MRI of the oral cavity and oral pharynx. In: Valvassori GE, Mafee MF, Carter BL, eds. *Imaging of the Head and Neck*. New York: Thieme; 1995:445–474.
3. Harnsberger HR. *Handbook of Head and Neck Imaging*. 2nd ed. Chicago: Mosby; 1995.

Chapter 95

Croup (Laryngotracheitis)

Epidemiology

Croup is a viral upper respiratory tract infection most often due to parainfluenzae 1 and 2 and influenza A. It is most common in children between the ages of 1 and 3. This disease frequently occurs in winter and is more common in males.

Clinical Findings

Patients characteristically present with a characteristic barking cough and stridor. Croup usually lasts between 3 and 7 days. Croup may be called atypical if it lasts more than 7 days, occurs in infants < 1 year of age, or is unresponsive to antibiotics. Severe cases of croup may progress to complete laryngeal obstruction. The importance and severity of the disease is emphasized by the fact that stridor at rest does not occur unless > 80% of the lumen is narrowed. Thus a small amount of edema occurring in a compromised subglottis may lead to complete laryngeal obstruction.

Pathology

Croup results in diffuse edema of the mucosa of the subglottis and trachea. Two characteristics of the subglottis predispose this region to croup. The subglottis is the narrowest portion of the respiratory tract in children < 3 years of age. The subglottis is the only portion of the upper respiratory tract to be surrounded by a complete cartilaginous ring. Therefore, the lumen is easily compromised by resultant mucosal edema.

Treatment

Humidification is felt by many to be the primary treatment for the majority of cases. Some authors advocate the use of racemic epinephrine or steroids for more sever cases. Tracheostomy is reserved for patients who are unresponsive to medical management with increasing carbon dioxide levels and decreasing neurological status.

Imaging Findings

Plain Films

The characteristic plain film findings are loss of the normal subglottic angles resulting in a "steeple-shaped" or "wine-bottle" appearance of the subglottis on the anteroposterior projection. The lateral films reveal loss of the normal appearance of the glottic region. Instead of the distinct soft tissue–air interphase between the glottic and subglottic regions, there is an ill-defined haziness between these structures in croup. There is often dilation of the pyriform sinuses and ballooning of the pharynx resulting from airway obstruction below the level of the glottis (Fig. 95–1).

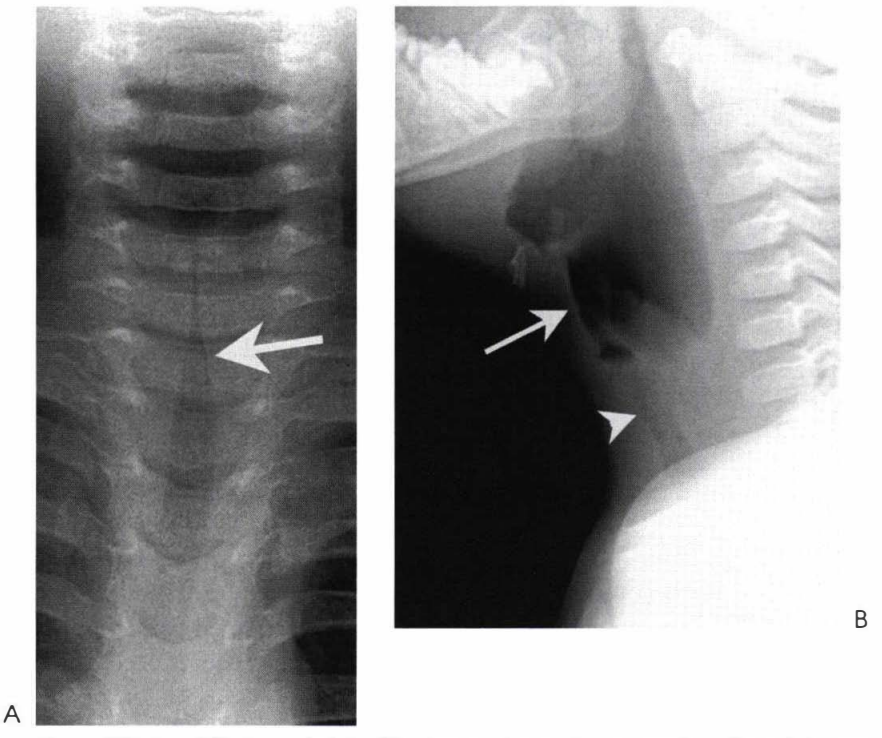

Figure 95–1. (A) Frontal plain film in a patient with croup shows loss of the normal subglottic angles resulting in characteristic "steeple-shaped" or "wine-bottle" appearance of the airway (arrow). (B) Lateral film reveals dilatation of the oropharyngeal airway (arrow) and an ill-defined haziness in the glottic and subglottic airway (arrowhead). (Case courtesy of Peter Strouse, M.D.)

Imaging Pearls

- CT and MR have little role in the initial diagnosis. The role of cross-sectional imaging is to exclude other causes of stridor such as a foreign body.

Suggested Readings

1. Jones KR, Pillsbury HC. Infections and manifestations of systemic disease of the larynx. In: Cummings CW, Frerickson JM, Harker LA, Krause CJ, Schuller DE, eds. *Otolaryngology and Head and Neck Surgery*, Vol 3. St. Louis: Mosby Year Book; 1993:1854–1857.
2. Curtin HD. The larynx. In: Som PM, Bergeron RT, eds. *Head and Neck Imaging*. 2nd ed. St. Louis: Mosby Year Book; 1991:664.

Chapter 96

Epiglottitis

Epidemiology

Epiglottitis is a systemic disease that involves the supraglottis, especially the epiglottis. This disease usually occurs in children between the ages of 2 and 4, although recent reports suggest that its incidence is increasing in patients < 2 years of age. There is no reported gender predilection.

Clinical Findings

Epiglottitis is a systemic infection that results in generalized septicemia. Patients often present with high fever and signs of respiratory obstruction. Blood cultures are often postive in these patients. Affected children are characteristically sitting upright and drooling at presentation. These individuals have greater inspiratory than expiratory stridor. The onset of symptoms is often acute and may occur over a 2- to 6-hour period.

On examination, the epiglottis is swollen and cherry red in appearance. The aryepiglottic folds are usually swollen with resultant narrowing of the supraglottic airway. The secretions in patients with epiglottitis are often thick and tenacious, and sudden respiratory arrest may be caused by mucous plugging of an already compromised airway.

Pathology

The most common organism causing epiglottitis is *Haemophilus influenzae* type B. The newborn is believed to be protected from this disease because of immunity to the capsular antigen acquired from the mother. This passive immunity is thought to resolve by 3 months of age. The child's own immune system does not appear to produce a significant amount of similar antibody until 3 to 4 years after birth. Many believe this window of diminished antibody levels is partly to blame for the high incidence of *H. influenzae* in this age group.

Treatment

On initial presentaion, the anesthesiologist and otolaryngologist should be immediately notified. Because the airway in these individuals is susceptible to acute laryngospasm and prone to obstruction during forced inspiration, every attempt should be made not to excite the child during initial evaluation. Initial examination should be kept to a minimum. Initial radiographic evaluation should be a lateral plain film of the neck and should be performed in the emergency room. Affected children will require nasotracheal or orotracheal intubation under anesthesia. Tracheostomy is not currently recommended for achieving airway control. The treatment of epiglottitis is aggressive antibiotic therapy.

Imaging Findings

Plain Films

A lateral plain film of the soft tissues of the neck should be performed in patients suspected of having epiglottitis. These studies should be performed in the emergency department. Patients must be accompanied by the otolaryngologist or anesthesiologist if imaging has to be performed in the radiology department. The findings on plain radiography are those of a diffusely thickened epiglottis, which is often two to three times the size of a normal epiglottis. The aryepiglottic folds of the false vocal cord are also thickened. There may be dilatation of the oropharynx if the supraglottic larynx is narrowed as a result of diffuse edema caused by infection (Fig. 96–1).

CT

There is no role for CT and MR in imaging children at initial presentation and in fact these studies may be life threatening because placing the patient in the supine position will further reduce the caliber of an already narrowed airway (Fig. 96–2).

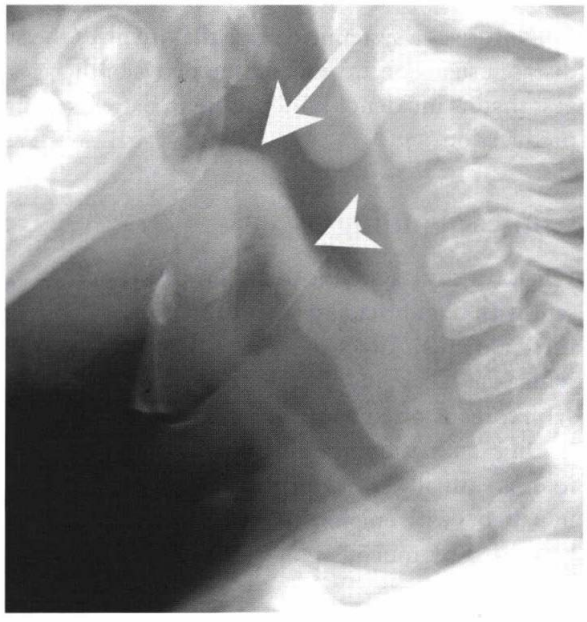

Figure 96–1. Lateral plain film of a patient with epiglottitis shows diffuse thickening of the epiglottis (arrow) and aryepiglottic folds (arrowhead).

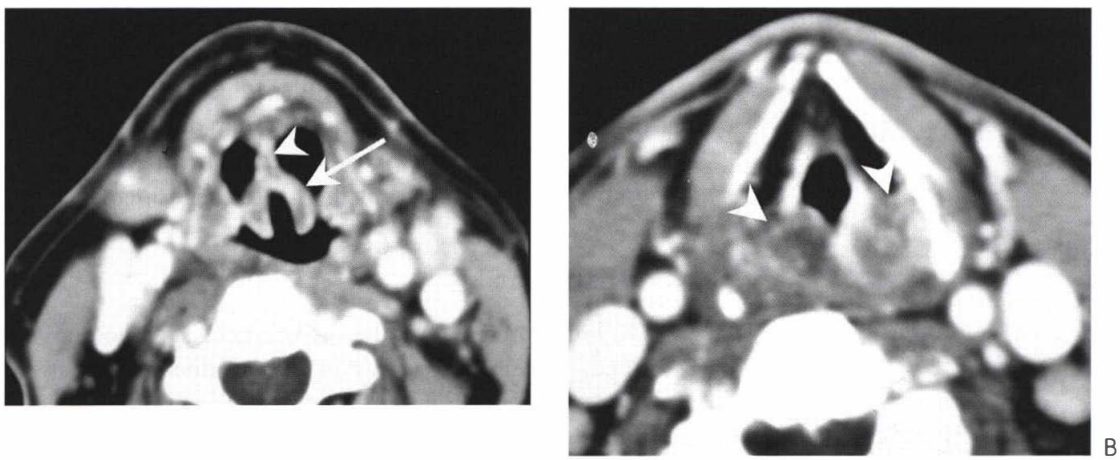

Figure 96–2. (A) This patient initially underwent CT for excluding a neck abscess and was not believed to have epiglottitis. Following the CT, the patient was diagnosed as having epiglottitis. Contrast-enhanced CT obtained at the level of the suprahyoid epiglottis shows diffuse thickening of the epiglottis (arrow) and median glossoepiglottic fold (arrowhead). (B) Axial image obtained at the level of the thyroid cartilage shows diffuse thickening of the aryepiglottic folds (arrowheads). It should be emphasized that this illustration should not be interpreted as support for the use of CT imaging for evaluation of epiglottitis.

Suggested Readings

1. Jones KR, Pillsbury HC. Infections and manifestations of systemic disease of the larynx. In: Cummings CW, Fredrickson JM, Harker LA, Krause CJ, Schuller DE, eds. *Otolaryngology and Head and Neck Surgery.* Vol. 3. St. Louis: Mosby Year Book; 1993:1854–1857.
2. Curtin HD. The larynx. In: Som PM, Bergeron RT, eds. *Head and Neck Imaging.* 2nd ed. St. Louis: Mosby Year Book; 1991:664.

Chapter 97

Laryngeal Infection: Supraglottitis

Epidemiology

Laryngitis specifically refers to inflammation of the laryngeal mucosa and vocal cords resulting in hoarseness. Supraglottitis can be considered an adult form of epiglottitis. It indicates diffuse swelling of the supraglottis that is indicative of a much more severe condition than laryngitis and may be life threatening. In addition to the larynx, the disease involves the valleculae, uvula, base of the tongue, soft palate, and prevertebral soft tissues. The incidence of supraglottitis is 1.8 cases per 1 million adults. However, this may underestimate the true prevalence of this disease because endoscopy is necessary to confirm it. Supraglottitis is associated with acquired immune deficiency syndrome.

Clinical Findings

The most common presenting symptoms include fever, sore throat, and dysphagia. Other symptoms include odynophagia, stridor, muffled voice, and drooling. The course of the disease is more indolent in adults than in children. In the majority of adults, the symptoms do not result in airway obstruction. This may be due to the larger diameter and greater rigidity of the adult airway.

Pathology

The organisms that are believed to cause supraglottitis include *Haemophilus influenzae,* group A, and group F beta-hemolytic *Streptococcus pyogenes* and *Staphylococcus aureus.*

Treatment

The treatment is appropriate medical therapy and airway management. Medical treatment consists of humidification, hydration, and intravenous antibiotics. Some authors have advocated the use of intravenous steroids to reduce the degree of inflammation. Most cases of supraglottitis resolve quickly with medical management and require a short hospital stay.

Imaging Findings

Plain Films

There is massive enlargement of the epiglottis, enlarged aryepiglottic folds, and false vocal cords. The prevertebral soft tissues are swollen and there is ballooning of the hypopharynx.

CT

CT demonstrates diffuse swelling of the epiglottis, aryepiglottic folds, and false vocal cords along with diffuse enhancement of the overlying mucosa. There is obliteration of the preepiglottic and paralaryngeal fat and thickening of the prevertebral fascia associated with edema in the retropharyngeal space. There may also be thickening of the platysma muscle with reticulation of the adjacent fat (Fig. 97–1).

MR

The MR findings have not been well defined. The imaging findings would likely be similar to the CT findings. These findings include diffuse thickening and edema of the supraglottis and adjacent fat planes, and thickening and infiltration of the platysma and adjacent fat.

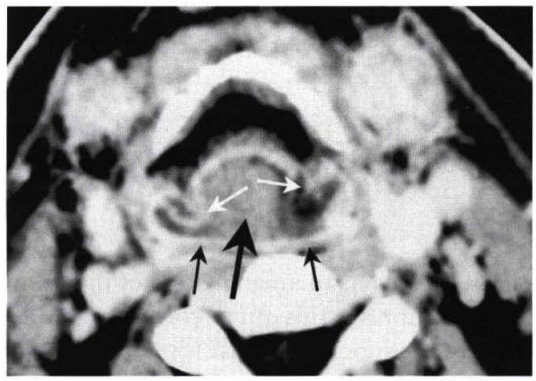

A

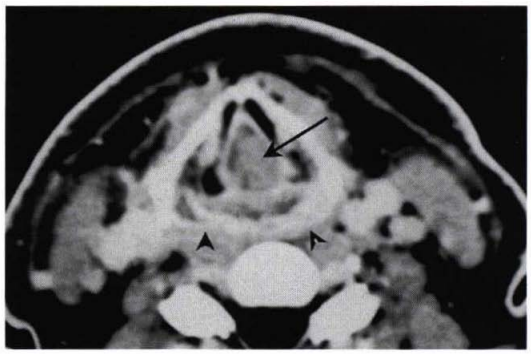

B

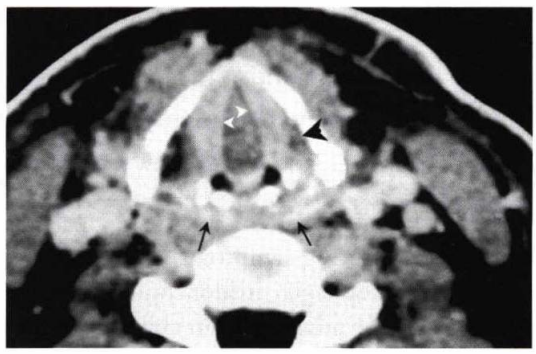

C

Figure 97-1. CT of supraglottitis. (A) Contrast-enhanced axial image obtained at the level of the hyoid bone shows diffuse inflammatory changes of the supraglottis. There is diffuse thickening of the aryepiglottic folds (white arrows) and thickening and enhancement of the pharyngeal mucosa (small arrows). The airway is filled with fluid (large arrow). (B) At the level of the infrahyoid epiglottis, there is diffuse enhancement of the mucosa (arrowheads) and fluid within the airway (arrow). (C) Axial image obtained at the inferior margin of the false vocal cords shows diffuse thickening of the false vocal cords (white arrowheads), obliteration of the paraglottic space (black arrowhead), and diffuse enhancement of the pharyngeal mucosa (arrows).

Imaging Pearls

- Supraglottitis is a clinical diagnosis and is treated medically. The role of imaging is to confirm the endoscopic findings and exclude an abscess that would require surgical drainage.
- If a cross-sectional study is felt to be clinically indicated, we prefer CT as the cross-sectional modality of choice for imaging due to the substantially reduced imaging time, thereby placing the patient at less risk for airway compromise.

Suggested Readings

1. Smith MM, Mukherji SK, Thompson JE, Castillo M. CT in adult supraglottitis. *AJNR Am J Neuroradiol* 1996;17:1355–1358.
2. Shih L, Hawkins DB, Stanley RB. Acute epiglottitis in adults: a review of 48 cases. *Ann Otol Rhinol Laryngol* 1988;97:527–529.
3. Nemzek WR, Katzberg RW, Van Slyke MA, et al. A reappraisal of the radiologic findings of acute inflammation of the epiglottis and supraglottic structures in adults. *AJNR Am J Neuroradiol* 1995;16:495–502.
4. Barrow HN, Vastola AP, Wang RC. Adult supraglottitis. *Otolaryngol Head Neck Surg* 1993;109:474–477.

Chapter 98

Herpes Pharyngitis

Epidemiology

The cause of herpes pharyngitis is a group of herpesviruses including herpes simplex virus types 1 (HSV-1) and 2 (HSV-2). Infection with herpes simplex virus is a common ailment; approximately 65% of adults in the general U.S. population carry antibodies to HSV-1. Approximately 25% carry antibodies to HSV-2. The latter behaves as a sexually transmitted disease, and seroprevalence is increased in postpubescent adults. Homosexual and bisexual men with human immunodeficiency virus (HIV) infection harbor the rate of seropositivity of approximately 75%. Heterosexual men and women with HIV infection also have high rates of carriage of HSV-2.

Clinical Findings

The hallmarks of the herpetic lesions are vesicles and ulcers with an erythematous base occurring at a mucocutaneous site. HSV-1 most commonly causes lesions on the mouth or lips; HSV-2 generally infects genital and perianal regions. During primary exposure, the initial episode lasts for approximately 2.5 weeks, whereas recurrent episodes usually resolve within 10 days. Frequently there is a prodromal syndrome involving paresthesias at the site of the developing lesion. The patients classically present with throat pain, erythema, and changes occasionally associated with lymphadenopathy.

Pathology

HSV is transmitted by direct contact between mucous membranes. After viral replication, a latent stage is established in which the HSV genome is maintained in the ganglia (sensory nerve cells). The reactivation that causes flare-ups of HSV is poorly understood, but it is assumed that HSV virions travel from the cell body along the axon of the original infection site. In case of herpetic pharyngitis this represents the pharyngeal mucosa. Infected tissue is characterized by multinucleated giant cells and cells that contain intranuclear viral inclusions. The herpesvirus may also be grown in a viral culture.

Treatment

Nucleoside analogues such as acyclovir remain the mainstay of HSV treatment and prophylaxis. Effective control of HSV infections is now possible with potent antiviral agents such as nucleoside analogues (famciclovir), pyrophosphate analogues (foscarnet), and phosphonate analogues (cidofovir).

Imaging Findings

CT

The most common imaging finding for a mucosal lesions in the visceral space is a normal study. Advanced lesions may result in thickening of the mucosa or underlying muscle. Deep extension may result in soft tissue phlegmon or abscess involving the parapharyngeal space.

MR

Herpes pharyngitis may result in diffuse thickening and enhancement of the mucosa and underlying muscle. The involved area may be thickened and have increased signal on T2-weighted sequences (Fig. 98–1).

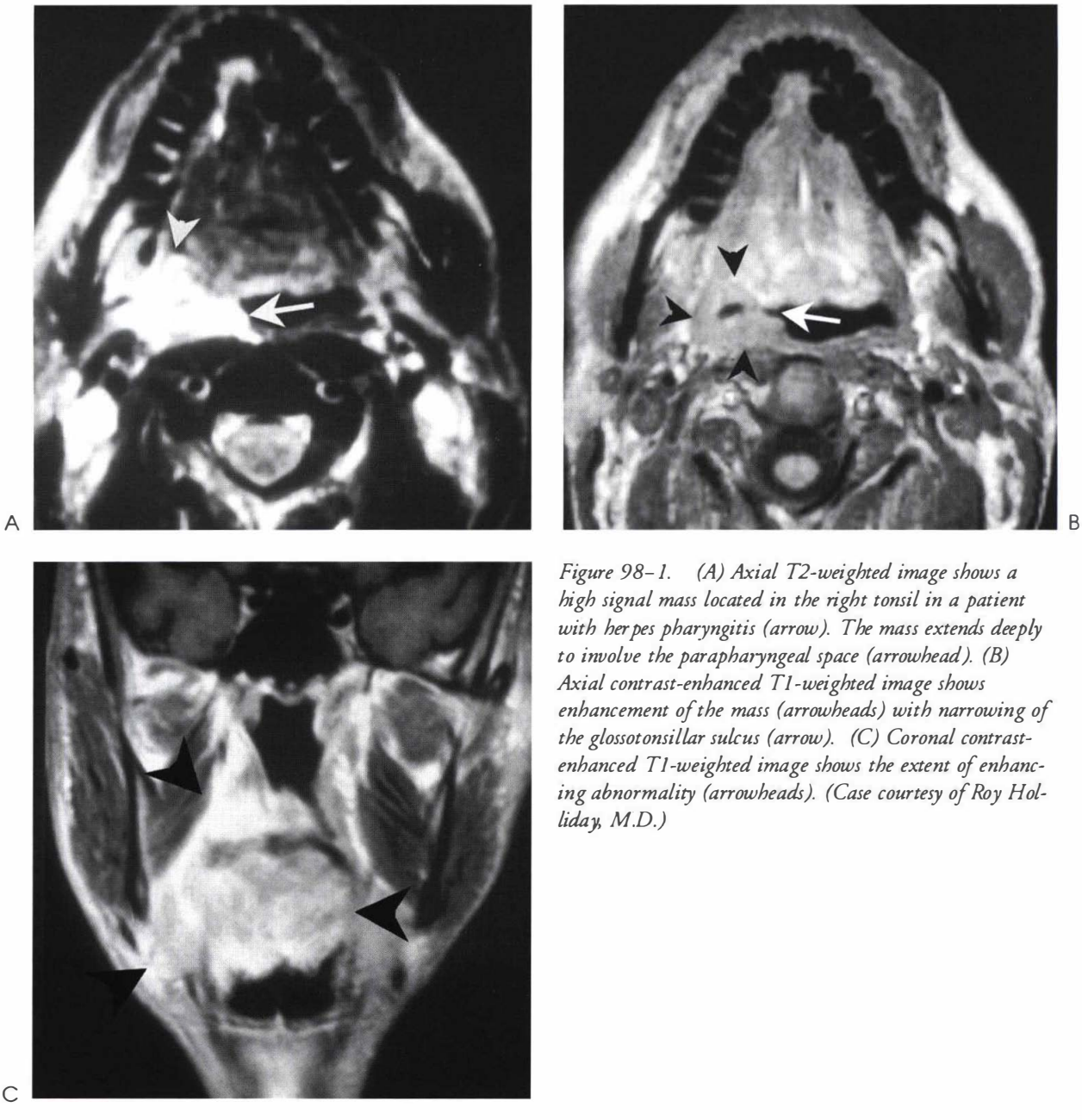

Figure 98–1. (A) Axial T2-weighted image shows a high signal mass located in the right tonsil in a patient with herpes pharyngitis (arrow). The mass extends deeply to involve the parapharyngeal space (arrowhead). (B) Axial contrast-enhanced T1-weighted image shows enhancement of the mass (arrowheads) with narrowing of the glossotonsillar sulcus (arrow). (C) Coronal contrast-enhanced T1-weighted image shows the extent of enhancing abnormality (arrowheads). (Case courtesy of Roy Holliday, M.D.)

Imaging Pearls

- The imaging findings of herpes pharyngitis are nonspecific.
- MR is the study of choice due to its increased ability to detect mucosal and submucosal involvement and adjacent phlegmon.

Suggested Readings

1. Mukherji SK, Holliday RA, Weissman JL. Pharynx. In: Som PM, Curtin HD, eds. *Head and Neck Imaging*, Vol 1. 3rd ed. St. Louis: Mosby; 1996:468–469.
2. Holliday RA. Manifestations of AIDS in the oromaxillofacial region: the role of imaging. *Radiol Clin North Am* 1993;31:4560.

Chapter 99

Laryngeal Tuberculosis

Epidemiology

There is an increasing incidence of tuberculosis in the United States since 1986. This trend is attributed to the increased incidence of acquired immune deficiency syndrome. This increase involves both pulmonary and extrapulmonary disease but involvement of the larynx remains rare. Laryngeal tuberculosis is usually secondary to active pulmonary tuberculosis. In the past, laryngeal tuberculosis typically affected patients between the ages of 20 and 40. In recent times patients in the older age group are more commonly seen.

Clinical Findings

Patients may present with any of the following symptoms: fever, weight loss, neck pain, dysphagia, hoarseness, and voice weakness. Clinical examination may reveal laryngeal edema, ulcerations, and associated cervical lymphadenopathy. Lung signs such as consolidation or collapse may also be evident.

Pathology

Expectoration or the pooling of infected sputum brings infected material into contact with the larynx. Infection may subsequently spread via the lymphatics to the regional lymph nodes. Tuberculosis typically produces granulomas where *Mycobacterium tuberculosis* is scanty. In contrast, the acid-fast bacilli appear in abundance in patients with tuberculous abscesses.

Treatment

The treatment of pulmonary, laryngeal, or nodal tuberculosis is anti-tuberculous therapy using various combinations of ethambutol, ethionamide, isoniazid, rifampicin, and streptomycin. In general head and neck tuberculosis responds well to standard chemotherapeutic agents. However, any abscess that forms during the course of the disease should be drained. Surgery may be required for extensive disease or nodes not responding to antibiotics.

Imaging Findings

CT

CT shows diffuse swelling, thickening, and ulceration of the larynx with or without a focal mass. There is no specific pattern of involvement and the following sites are commonly involved: vocal cords, epiglottis, and paralaryngeal tissues. The thyroid cartilage however is rarely involved and calcifications are seldom seen. Cervical nodal enlargement may also be demonstrated with or without nodal necrosis. Scans farther inferior usually show active pulmonary infiltrates, pleural effusion, or lobar collapse (Fig. 99–1).

MR

Thoracic tuberculosis should be assessed by CT. Patients with pulmonary and laryngeal disease often have respiratory difficulties making them poor candidates for a successful MR study. On MR imaging, tuberculosis shows nonspecific enhancement following injection or contrast and high signals on T2-weighted images.

Imaging Pearls

- The differential diagnosis of laryngeal tuberculosis includes laryngeal carcinoma, sarcoidosis, syphilis, leprosy, fungal infection, and lethal midline granuloma.

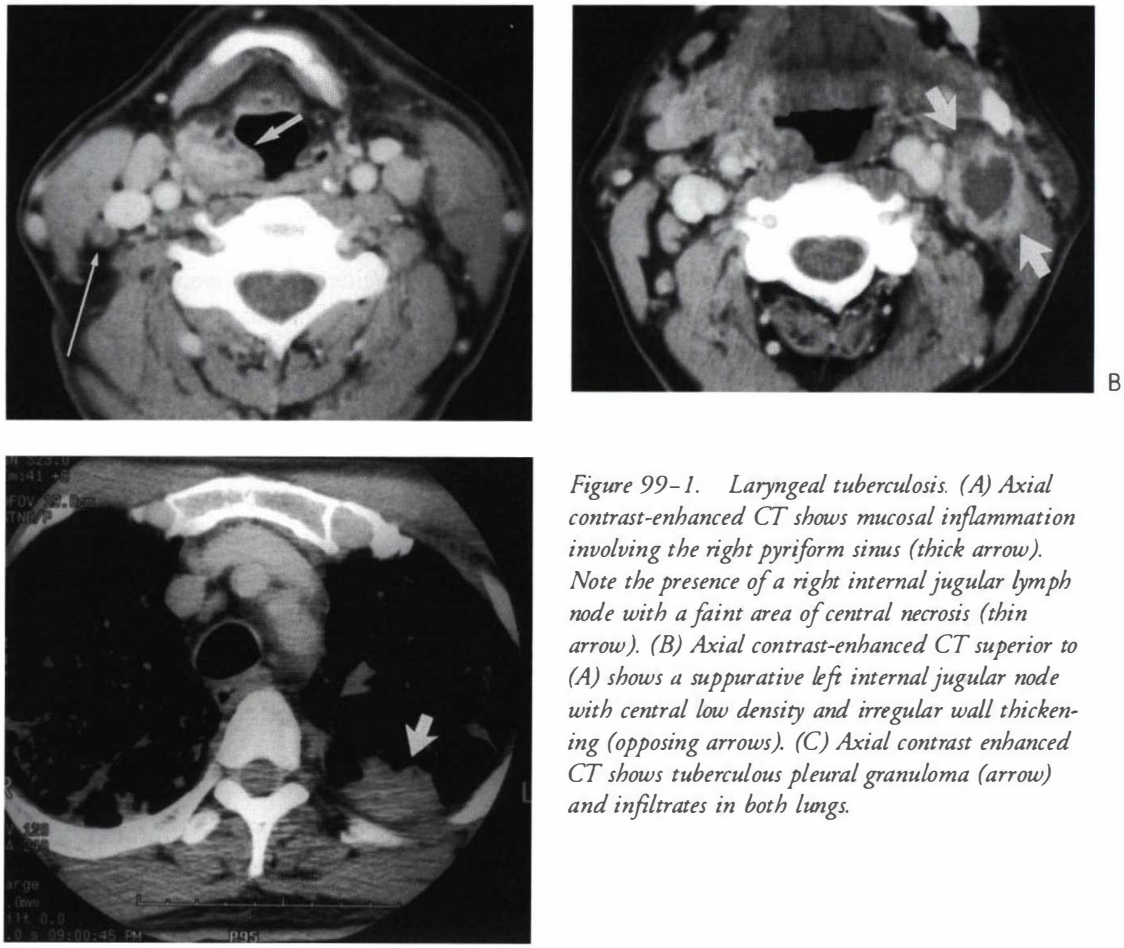

Figure 99-1. Laryngeal tuberculosis. (A) Axial contrast-enhanced CT shows mucosal inflammation involving the right pyriform sinus (thick arrow). Note the presence of a right internal jugular lymph node with a faint area of central necrosis (thin arrow). (B) Axial contrast-enhanced CT superior to (A) shows a suppurative left internal jugular node with central low density and irregular wall thickening (opposing arrows). (C) Axial contrast enhanced CT shows tuberculous pleural granuloma (arrow) and infiltrates in both lungs.

- Laryngeal tuberculosis is the most common laryngeal granulomatous disease and this entity should be suspected if active lung disease is present.
- The presence of tuberculosis should always raise the possibility of an underlying human immunodeficiency virus (HIV) disease. Conversely, patients with known HIV infection and laryngeal disease should raise the possibility of tuberculous infection.

Suggested Readings

1. Lindell MM, Jing BS, Wallace S. Laryngeal tuberculosis. *AJR Am J Roentgenol* 1977;129:677–680.
2. Swallow CE, McAdams HP, Colon CE. Tuberculosis manifested by a large mass on CT scans. *AJR Am J Roentgenol* 1994;163:179–180.
3. Moon WK, Han MH, Chang KH, et al. CT and MR imaging of head and neck tuberculosis. *Radiographics* 1997;17:391–402.

Chapter 100

Wegener's Granulomatosis of the Larynx

Epidemiology

Wegener's granulomatosis is a granulomatous vasculitis. The etiology is unknown but may be immunologically mediated. It is characterized by three specific criteria: necrotizing granulomas with vasculitis of the upper and lower respiratory tracts, systemic vasculitis, and focal necrotizing glomerulitis. There is a limited form of this disease that involves the upper respiratory tract, lower respiratory tract, or both. However, the limited form does not involve the kidneys, or the respiratory involvement precedes the renal involvement by a long interval. Laryngeal involvement usually occurs as subglottic narrowing or stenosis. Of 158 patients treated at the National Institutes of Health, over 90% had otolaryngologic abnormalities and 16% had subglottic stenosis. The incidence of subglottic stenosis appears to be increased in patients under the age of 20.

Clinical Findings

Patients with laryngeal involvement usually present with sore throat and laryngitis. Occasionally, the subglottic stenosis may progress and require tracheostomy. Because Wegener's is a systemic disease, other symptoms are common and include fever, arthralgia, sinusitis, otitis media, and saddle-nose deformity. Patients with laryngeal involvement typically have or will soon develop widespread pulmonary involvement (Fig. 100–1).

Pathology

The pathological hallmark of the disease is necrotizing granulomas, inflammation of the upper and lower respiratory tracts, focal necrotizing vasculitis, and necrotizing glomerulitis.

Treatment

The disease is rapidly progressive in its classic form and is associated with a 2-year 90% mortality if untreated. Death is usually due to renal failure. Early forms of the disease can be successfully treated with cytotoxic drugs such as cyclophosphamide.

Imaging Findings

CT

The usual finding is concentric subglottic narrowing due to enhancing soft tissue. This disease should not invade the cartilage (Fig. 100–2).

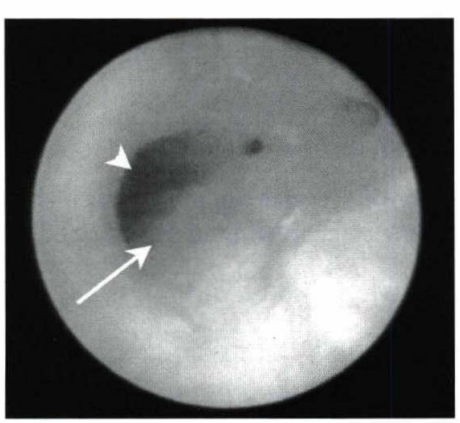

Figure 100–1. Endoscopic view of Wegener's granulomatosis shows a submucosal mass (arrow) narrowing the subglottis (arrowhead).

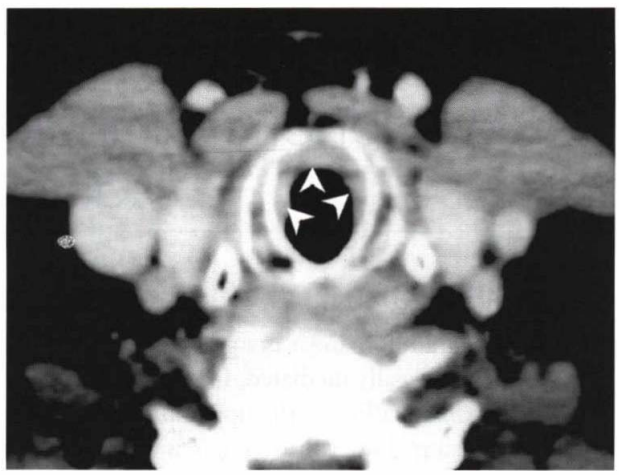

Figure 100–2. CT findings of Wegener's granulomatosis. Axial contrast-enhanced CT shows an eccentric soft tissue mass involving the anterior portion of the subglottis (arrowheads). There is mild enhancement detected on CT.

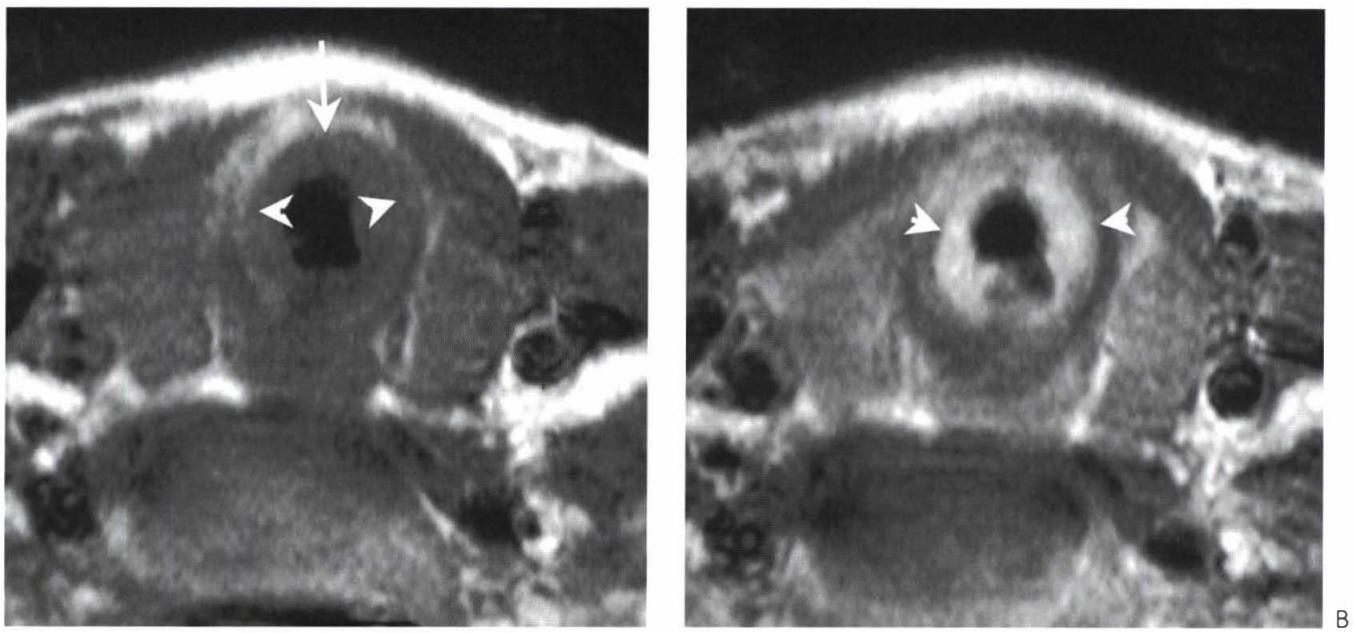

A B

Figure 100–3. MR findings of Wegener's granulomatosis. (A) Noncontrast T1-weighted image shows an intermediate signal mass involving the periphery of the subglottis. (arrow). There is some inhomogeneity of the high signal in the expected location of the cricoid cartilage that may be due to fat replacement within the cartilage by the inflammatory process (arrowheads). (B) The mass densely enhances after administration of intravenous contrast (arrowheads).

MR

The MR findings have not been well-described. In our experience, the lesion is intermediate on T1-weighted images and diffusely enhances following contrast administration. The T2 signal is variable and may be iso- to hyperintense compared with surrounding mucosa (Fig. 100–3).

Imaging Pearls

- The imaging findings are nonspecific.
- The diagnosis of Wegener's granulomatosis should be considered in patients presenting with subglottic stenosis without a history of prior intubation or other relevant clinical history.

Suggested Readings

1. Talerman A, Wright D. Laryngeal obstruction due to Wegener's granulomatosis. *Arch Otolaryngol* 1972;96:376–379.
2. Scully RE, Mark EJ, McNeely BU. Case records of the Massachusetts General Hospital. *N Engl J Med* 1986;315:378–387.
3. Lebovics RS, Hoffman GS, Leavitt RY, et al. The management of subglottic stenosis in patients with Wegener's granulomatosis. *Laryngoscope* 1992;102:1341–1345.

Chapter 101

Tornwaldt's Cyst

Epidemiology

Tornwaldt cyst (TC) is a benign developmental lesion of the nasopharynx that arises from anomalous embryogenesis of the notochord. The incidence of TC in autopsy series is 4%. The peak age of incidence is 15 to 30 years of age. There is no reported gender predilection for TC.

Clinical Findings

TCs are usually asymptomatic lesions that are often incidental findings on imaging studies. Occasionally, the internal pressure within the cyst may increase and overcome the relative stenosis at the cyst orifice causing the release of anaerobic secretions into the nasopharynx. As a result, patients may complain of periodic halitosis, foul taste, or persistent nasal discharge. On endoscopic examination, these lesions are usually submucosal and are not tender to palpation. TCs may become infected and subsequently lead to formation of an abscess in the retropharyngeal space.

Embryology

During development, the notochord descends into the primitive pharynx and comes into contact with the overlying endoderm. A small outpouching of the pharyngeal mucosa develops that is directed toward the brain. This is known as Seessel's pouch and contributes to the formation of the preoral gut. TC appears to occur when a focal adherence develops between the notochord and the mucosal covering of the primitive pharynx. As a result of the adherence, a small portion of the nasopharyngeal mucosa is carried along with the notochord as it ascends into the developing skull base. This results in the creation of a midline cyst or tract that is located between the longus coli muscles and deep to the nasopharyngeal mucosa.

Pathology

Because they are remnants of a developmental midline diverticulum, TC are lined by squamous epithelium. It is thought the orifice swells and closes when the patient develops a pharyngitis. This results in a cyst that may become infected with anaerobic bacteria and have high protein content. This may account for T1 and T2 shortening that may be seen on MR imaging studies.

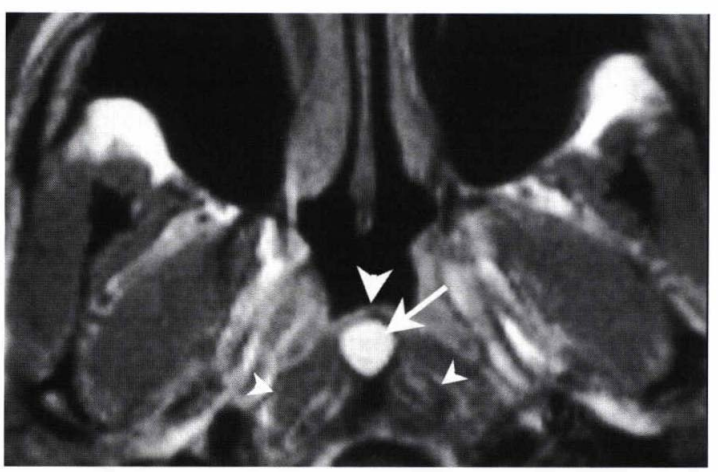

Figure 101-1. Axial noncontrast T1-weighted image obtained through the nasopharynx demonstrates a round mass that contains high T1 signal (arrow) located in the pharyngeal bursa between the paired longus coli muscles (small arrowheads). Note how the mass is below the mucosa (large arrowhead) of the nasopharynx ("submucosal").

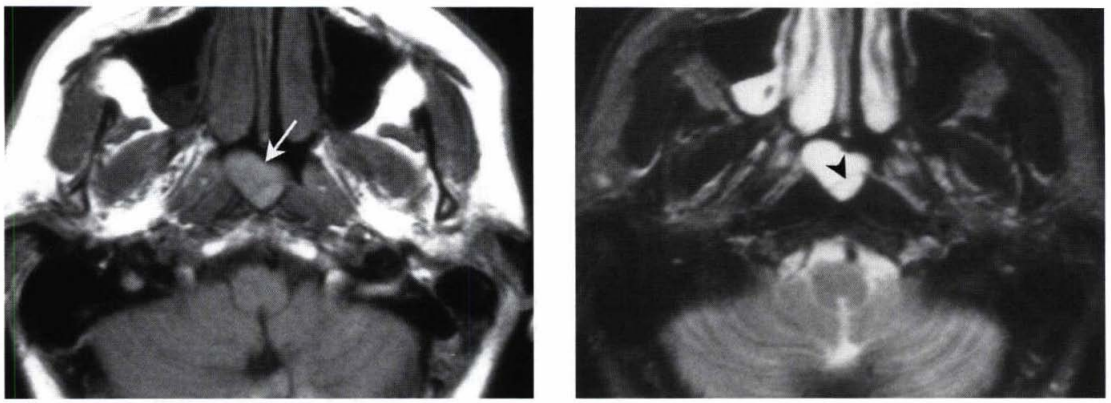

Figure 101-2. (A) Axial noncontrast T1-weighted image shows a high signal mass located in the pharyngeal bursa (arrow). (B) T2-weighted image demonstrates that the Tornwaldt's cyst is high signal. The arrowhead indicates a septum within the cyst.

Treatment

Asymptomatic TC require no treatment. Infected cysts or cysts that are symptomatic may require drainage. The drainage procedure is usually performed through a transoral approach.

Imaging Findings

CT

The CT appearance of a TC is a midline mass located along the posterior wall of the nasopharynx. The high protein content of the cyst increases its internal attenuation and may make it difficult to separate from the nasopharyngeal adenoidal tissue. This may result in TC resembling prominent adenoid tissue or mimicking a soft tissue mass on CT.

MR

The MR imaging findings are a cystic mass that is situated between the longus coli muscles at the level of the nasopharynx (pharyngeal bursa). The size usually varies between 2 and 10 mm in diameter. TC may be high signal on T1-weighted sequences and low signal on T2-weighted sequences. This is felt to be due to the high protein content that may be present in some cysts. The wall is typically very thin and does not enhance with contrast (Figs. 101-1 and 101-2).

Imaging Pearls

- We prefer to use MR imaging for evaluating patients suspected of having TC. The intrinsic signal characteristics allow the cyst to be easily separated from the surrounding nasopharyngeal adenoid tissue.

Suggested Readings

1. Dillon WP. The pharynx and oral cavity. In: Som PM, Bergeron RT, eds. *Head and Neck Imaging.* 2nd ed. St. Louis: Mosby Year Book; 1991:431.

Chapter 102

Nasopharyngeal Infiltrative Ectopic Pituitary Adenoma

Epidemiology

Ectopic pituitary adenomas are uncommon. In 73% of patients, the ectopic adenomas are located in an extracranial site, most frequent location being in the sphenoid sinus. Other extracranial sites include the nasal cavity, nasopharynx, petrous temporal bone, and clivus. The presence of ectopic pituitary tissue in the skull base is a common phenomenon, but a pituitary adenoma arising from these ectopic sites without sellar involvement is extremely rare. It is believed that the ectopic pituitary tissues represent remnants of the craniopharyngeal duct along the ingrowth of Rathke's pouch.

Clinical Findings

Headache is a common symptom but the clinical manifestations of ectopic pituitary adenomas vary and they are mainly related to local mass effects. Fifty-eight percent of patients have functional activity at presentation. They include Cushing's syndrome, acromegaly, hyperparathyroidism, amenorrhea, and multiple endocrine neoplasia.

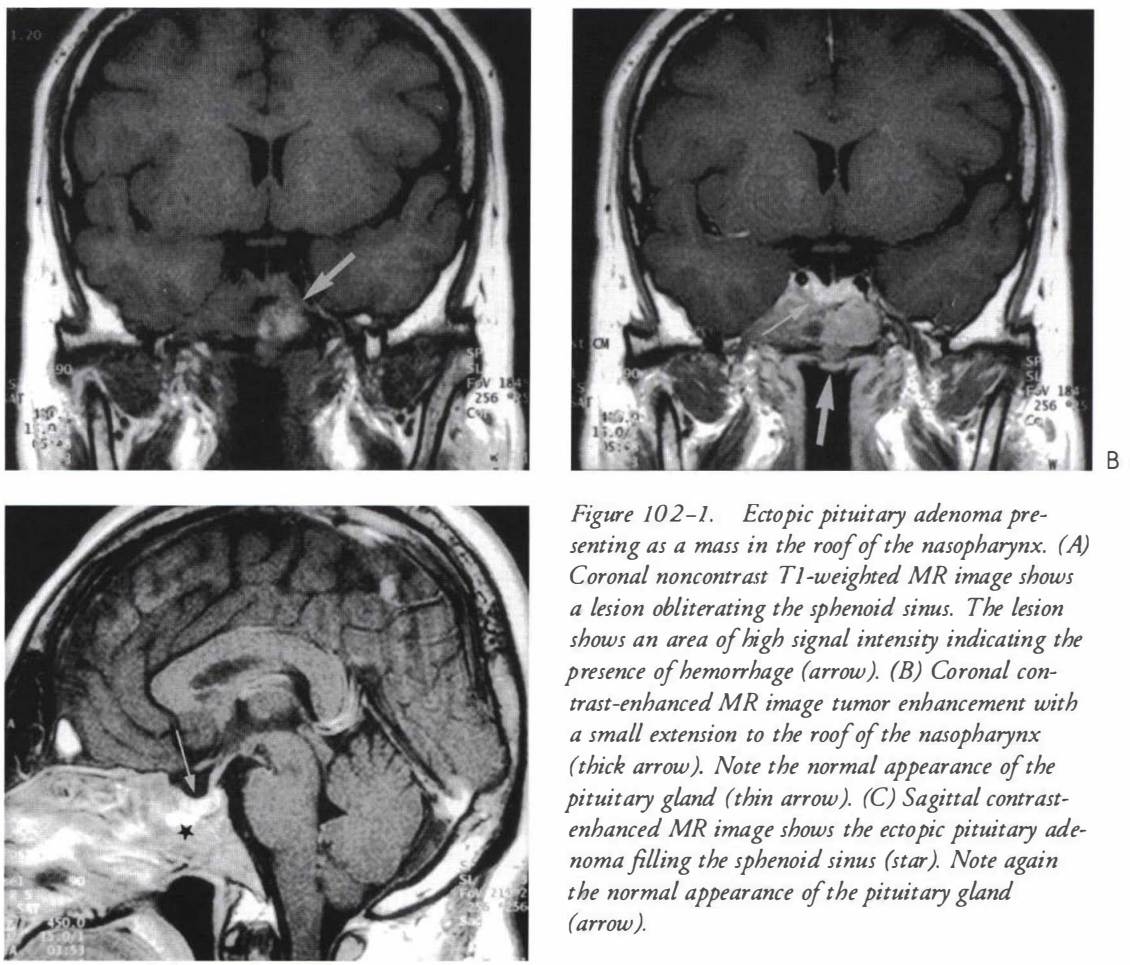

Figure 102–1. Ectopic pituitary adenoma presenting as a mass in the roof of the nasopharynx. (A) Coronal noncontrast T1-weighted MR image shows a lesion obliterating the sphenoid sinus. The lesion shows an area of high signal intensity indicating the presence of hemorrhage (arrow). (B) Coronal contrast-enhanced MR image tumor enhancement with a small extension to the roof of the nasopharynx (thick arrow). Note the normal appearance of the pituitary gland (thin arrow). (C) Sagittal contrast-enhanced MR image shows the ectopic pituitary adenoma filling the sphenoid sinus (star). Note again the normal appearance of the pituitary gland (arrow).

Pathology

The histology of ectopic pituitary adenomas also varies; 58% of cases are chromophobic and 16% eosinophilic. Immunohistochemical staining is required for the characterization of the functional activity of these tumors.

Treatment

Surgery is the mainstay of treatment. When surgical resection is incomplete, postoperative radiation therapy is indicated. In addition, pharmacotherapy may benefit some patients.

Imaging Findings

CT

Ectopic pituitary adenomas show moderate to intense contrast enhancement on CT. The extent of bone erosion can be clearly delineated in the skull base. Tumor invasion of the cavernous sinus can also be delineated but the intracranial component, if present, is best assessed on coronal MR images.

MR

On T1-weighted images, the ectopic pituitary adenoma shows intermediate signal intensity and enhances moderately following the injection of contrast. The pituitary gland may be entirely normal. The tumor may have both nasopharyngeal and sphenoid sinus components (Fig. 102-1).

Imaging Pearls

- The diagnosis of ectopic pituitary adenoma is based on a combination of histologic diagnosis and imaging evaluation. Biopsy will confirm the diagnosis of pituitary adenoma but cannot suggest an ectopic tumor. The presence of a skull base lesion, a radiologically normal pituitary gland, and a histologic diagnosis of a pituitary tumor will establish the correct diagnosis.

Suggested Readings

1. Anand VK, Osborne M, Harkey HL. Infiltrative clival pituitary of ectopic origin. *Otolaryngol Head Neck Surg* 1993;108:178-183.
2. Melchionna RH, Moore RA. The pharyngeal pituitary gland. *Am J Pathol* 1938;14:763-761.
3. Chong VFH, Fan YF, Lau DPC, Chee LWJ, TM Nguyen TM, Sethi DS. Imaging the sphenoid sinus. *Australas Radiol* 2000;44:143-154.

Chapter 103

Congenital Tracheal Stenosis

Epidemiology

Congenital tracheal stenosis (CTS) is a rare congenital tracheal anomaly that often presents within the first few months of life. Males and females are equally affected. CTS is often associated with other systemic anomalies, including tracheoesophageal fistula, pulmonary hypoplasia, and anomalous vasculature of the great vessels, including vascular slings.

Clinical Findings

CTS has been classified into three main categories: (1) generalized hypoplasia, (2) funnel-shaped narrowing, and (3) segmental stenosis. In the generalized hypoplastic form, the trachea is diffusely narrowed to just above the carina with the main bronchi being of normal diameter. The diameter of the narrowed tracheal lumen in the newborn is 1 to 3 mm. In the funnel-shaped form, the trachea progressively narrows from a normal proximal diameter to a tight stenosis just above the carina (Fig. 103–1). The main bronchi may be of normal caliber. With segmental stenosis, the narrowed segment may occur anywhere along the trachea.

The presenting symptoms of CTS are multiple and include cough, persistent wheezing, stridor, and intermittent cyanosis. Advanced forms of CTS present at birth. Some patients with mild forms of tracheal stenosis may be asymptomatic. Symptoms are thought to result when the oxygen demand exceeds the amount that can be delivered through a compromised airway. Symptoms may be exacerbated by agitation. Definitive diagnosis is made at endoscopy. In most cases, the diameter of the affected segment is < than 3 mm. The walls of the trachea are typically rigid and non-distensible.

Pathology

CTS is believed to be due to abnormal cartilage that completely encircles the involved tracheal region. The normal horseshoe-shaped rings that are present in the normal trachea are replaced by complete or near-complete cartilaginous rings. This results in the absence of the normally present posterior membranous wall, which is typically soft and pliable. The result is a nondistensible trachea with a narrowed lumen.

Treatment

The prognosis of patients with CTS is generally poor. About half of patients with CTS die either of this condition or of some other associated major anomaly. Patients with respiratory distress occurring within the first 24 hours of life, as well those with other major anomalies, have a very grim prognosis. Surgical resection of the stenosed segment may be helpful in selected cases, however, it is very rarely felt to be feasible.

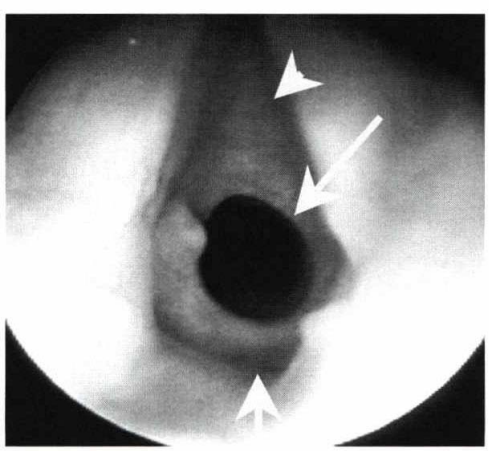

Figure 103–1. Endoscopic view of congenital tracheal stenosis shows narrowing of the junction of the upper trachea and subglottis (long arrow) caused by abnormal fibrous tissue located both anterior (arrowhead) and posterior to the airway (short arrow).

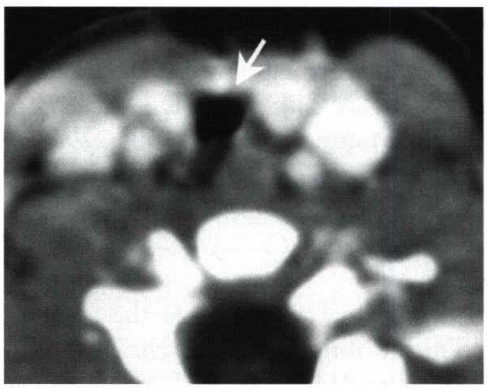

Figure 103–2. Axial contrast-enhanced CT performed in an infant shows the characteristic imaging findings of congenital tracheal stenosis. The wall of the trachea does not have its typical round shape and the airway is narrowed (arrow).

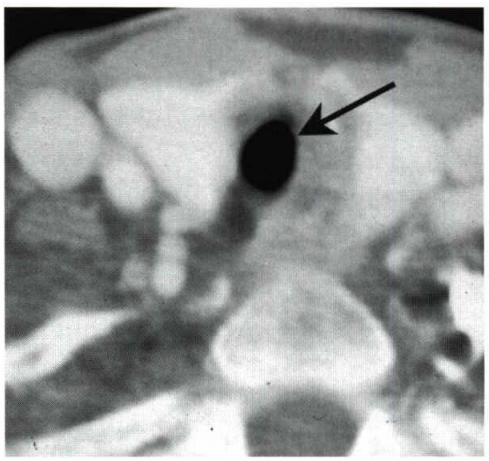

A

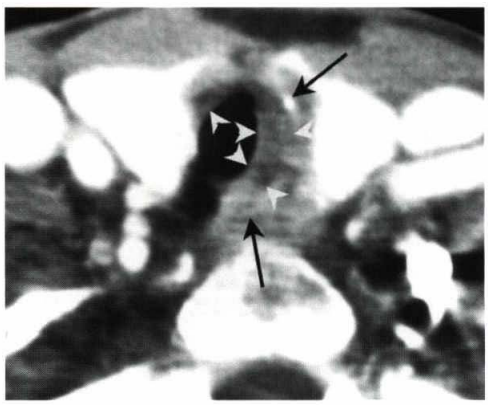

B

Figure 103–3. (A) CT performed in a 2-year-old reconstructed at wide windows demonstrates a narrow tracheal airway (arrow). (B) Soft tissue windows show the narrowing is due to increased abnormal soft tissue (arrowheads) between the tracheal airway and the tracheal ring (black arrows).

Imaging Findings

Plain Films

These studies demonstrate a narrowed tracheal lumen. However the extent of the narrowing may be underestimated.

CT

The normal-appearing trachea with its flattened posterior margin is replaced by a completely round tracheal air column. The caliber of the trachea is narrowed and often measures < 3 mm in affected neonates. The cartilages are not visualized because they are not calcified in the age group normally evaluated for CTS (Figs. 103–2 and 103–3).

Imaging Pearls

- Helical CT is the preferred cross-sectional modality for evaluating patients who are stable enough to undergo imaging and are suitable candidates for surgical intervention.
- Three-dimensional reconstruction is helpful for evaluating the extent of the stenotic segment.
- Patients with CTS should also be evaluated for associated anomalies that are known to occur with CTS.

Suggested Readings

1. Benjamin B. Congenital disorders of the trachea. In: Cummings CW, Frerickson JM, Harker LA, Krause CJ, Schuller DE, eds. *Otolaryngology and Head and Neck Surgery*, Vol 3. St. Louis: Mosby Year Book; 1993:2294–2296.
2. Myer CM, Cotton RT. Congenital abnormalities of the larynx and trachea and management of congenital malformations. In: Paparella MM, Shumrick DA, Gluckman JL, Meyeroff WL, eds. *Otolaryngology*, Vol 3. 3rd ed. Philadelphia: WB Saunders; 1973:2225.
3. Stark P. Congenital anomalies of the trachea. In: *Radiology of the Trachea*. Stuttgart: Georg Thieme Verlag; 1991:12–13.
4. Loeff DS, Filler RM, Vinograd I, et al. Congenital tracheal stenosis: a review of 22 patients from 1965 to 1987. *J Ped Surg* 1988;23:744–748.

Chapter 104

Laryngomalacia (Congenital Flaccid Larynx)

Epidemiology

Laryngomalacia (LM) is the most common congenital laryngeal abnormality and accounts for 60% of laryngeal problems in the newborn. It is the most common cause of stridor in infants. The condition usually presents within the first few weeks of life. LM is frequently associated with other coexistent abnormalities of the larynx. There is no reported gender predeliction for LM.

Clinical Findings

Patients with LM present with inspiratory stridor. Stridor is seldom present at birth but usually starts within the first few days to weeks of life. The stridor is of variable intensity and is aggravated with crying, feeding, or other periods of excitement or activity. Stridor is also worse when patients lie on their back with their head flexed. Patients are acyanotic with a normal cry. LM is rarely associated with dyspnea or difficulty swallowing.

Pathology

LM appears to be related to flaccidity and incoordination of the soft tissue and cartilages of the supraglottic larynx. The exact cause of LM is currently under debate. Some authors feel certain anatomic abnormalities predispose patients to develop LM, including (1) an elongated epiglottis that curls upon itself (omega-shaped epiglottis), (2) fore-shortened aryepiglottic folds, and (3) bulky arytenoids, which tend to prolapse into the airway with inspiration. Other investigators feel that LM is caused by poor neuromuscular control resulting in inadequate muscular support of the cartilaginous framework of the epiglottis with increased compliance of the supraglottic tissues. This may be due to delayed development of the neuromuscular pathways controlling the airway in affected patients.

Clinical Findings

Definitive diagnosis is made by direct endoscopic examination. A flexible laryngoscope is suitable for examination. The characteristic findings are a narrow elongated epiglottis, which may curve upon itself (omega-shaped epiglottis) with long floppy redundant aryepiglottic folds, prominent arytenoids, and a deep interarytenoid cleft. During inspiration, the supraglottic structures collapse into the lumen of the airway around a vertical axis and leave a slit-like opening.

Treatment

LM is a benign and self-limited condition that usually resolves within 6 months to 2 years of age. The symptoms are often improved by placing the child in the prone position with the head hyperextended. Surgical intervention is only necessary in patients who fail to spontaneously improve or have persistent symptoms of sleep apnea, cor pulmonale, feeding difficulties, or failure to thrive.

Imaging Findings

Plain Films

Anteroposterior and lateral plain films are the imaging modality of choice for patients suspected of having LM. The characteristic plain film findings consistent with a diagnosis of LM are anterior bowing and inferior displacement of the aryepiglottic folds. The epiglottis and hyoid bone may also be positioned lower than normally expected due to the imbalance between the suprahyoid and infrahyoid strap muscles. The hypopharynx and vallecula may also be dilated due to intermittent airway obstruction (Fig. 104–1).

Imaging Pearls

- Currently, CT and MR play very little role for diagnosing patients with LM. CT may be helpful for detecting the presence of associated congenital anomalies of the larynx, including subglottic or tracheal stenosis (Figs. 104–2 and 104–3).

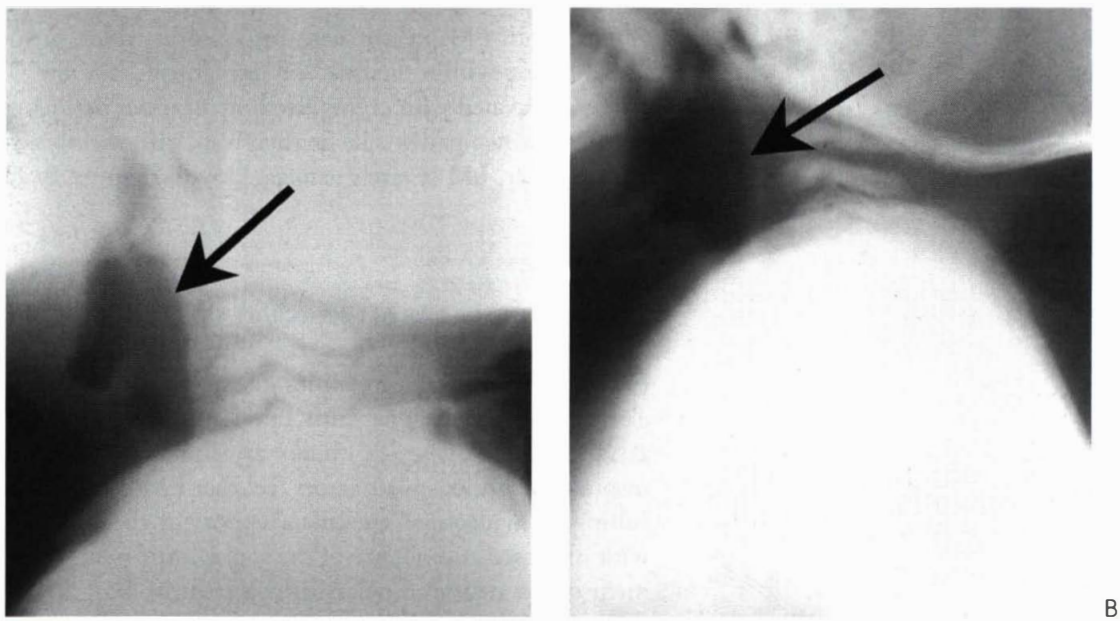

Figure 104–1. Plain film findings of laryngomalacia. (A) Lateral view performed on inspiration shows normal expansion of the oropharyngeal airway (arrow). (B) Lateral view performed in expiration shows abnormal persistent dilation of the oropharyngeal airway (arrow), which is indicative of laryngomalacia. The size of the airway should normally decrease in size on expiration.

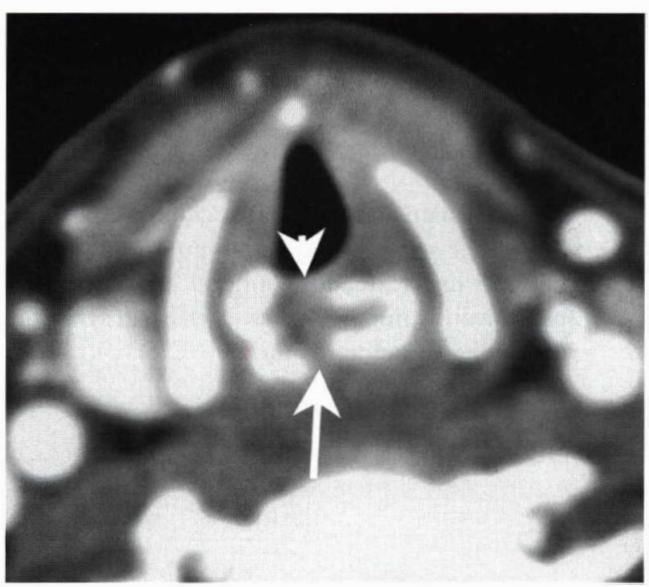

Figure 104–2. Axial contrast-enhanced CT obtained at the level of the true vocal cords in a child with laryngomalacia demonstrates abnormal increased soft tissue in the posterior commissure (arrowhead), which likely represents redundant tissue in this region. There is a cleft in the cricoid cartilage that is indicative of chondromalacia of the cricoid cartilage (arrow).

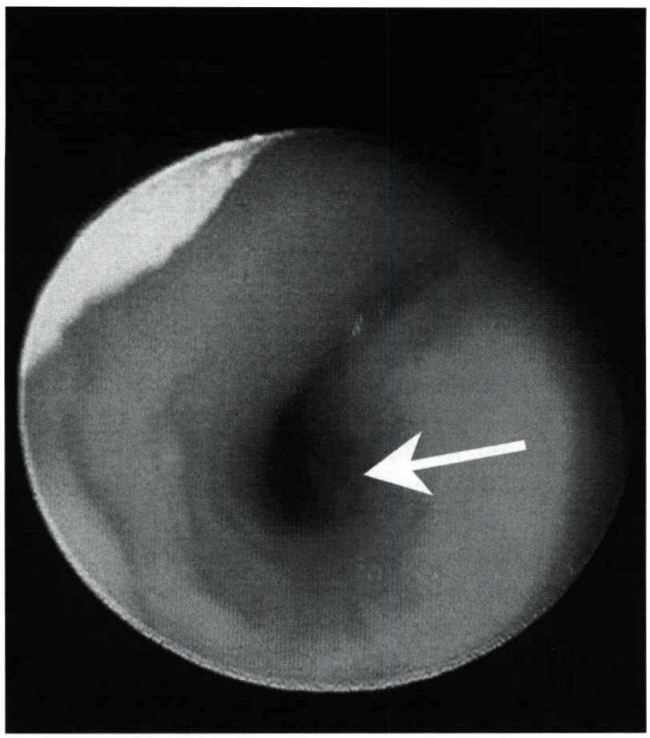

Figure 104-3. Endoscopic view of laryngomalacia shows narrowing of the laryngeal airway (arrow).

Suggested Readings

1. Benjamin B. Congenital disorders of the larynx. In: Cummings CW, Frerickson JM, Harker LA, Krause CJ, Schuller DE, eds. *Otolaryngology and Head and Neck Surgery.* Vol 3. St. Louis: Mosby Year Book; 1993:1840–1842.
2. Myer CM, Cotton RT. Congenital abnormalities of the larynx and trachea and management of congenital malformations. In: Paparella MM, Shumrick DA, Gluckman JL, Meyeroff WL, eds. *Otolaryngology,* Vol 3. 3rd ed. Philadelphia: WB Saunders; 1991:2217–2219.
3. Cotton RT, Reilly JS. Congenital malformations of the larynx. In: Bluestone CD, Stool SE, Scheetz MD, eds. *Pediatric Otolaryngology,* Vol 2. Philadelphia: WB Saunders; 1990:1122.

Chapter 105

Tracheoesophageal Fistula and Esophageal Atresia

Epidemiology

Tracheoesophageal fistula (TEF) and esophageal atresia (EA) are part of a complex of congenital malformations characterized by abnormal communication between the esophagus and trachea. The incidence is 1 in 3000 to 4000 births. Thirty percent of patients are born prematurely. There is no reported gender predilection. Coexisting anomalies are present in up to 50% of patients with these congenital anomalies. The best known pattern of anomalies is referred to as VATER (*v*ertebral defects, imperforate *a*nus, *t*racheo*e*sophageal fistula, *r*adial and *r*enal dysplasia) and VACTERL (*v*ertebral, *a*nal, *c*ardiac, *t*racheal, *e*sophageal, *r*enal, and *l*imb deformities). Other coexisting anomalies include Down syndrome and atresias of the gastrointestinal tract, including duodenal atresia. Cardiovascular anomalies include patent ductus arteriosus, ventricular septal defect, and right-sided aortic arch. Patients with TEF have an increased incidence of tracheomalacia, with the latter being an important cause of postoperative respiratory complications. Rarely, TEF may be acquired by erosion from a granulomatous inflammatory process, tumor, or foreign body.

Embryology

This group of anomalies is believed to result from a disorder in the separation of the primitive foregut into the trachea and esophagus. The most likely cause is thought to be a failure of complete formation of the tracheoesophageal septum that separates the respiratory and digestive systems. The developmental error is thought to most likely occur between the fourth to fifth weeks of gestation.

TEF has been classified into five separate types: type I—isolated EA (5–10%); type II (proximal fistula; 1–3%)—EA with an upper fistula connecting the proximal blind-ending esophageal pouch with the trachea (there is no communication with the distal esophageal segment); type III (distal fistula; 80–90%)—EA with a blind ending upper pouch and a fistula connecting the trachea with the distal pouch; type IV (proximal and distal fistulas; 1–3%)—EA with separate fistulas from the trachea communicating with both the proximal and the distal segments; type V (H-type; 5–8%)—direct communication between the esophagus and trachea. Type V TEF is the only type without EA.

Clinical Findings

Eighty-five percent of affected patients present with symptoms 24 hours after birth; the most common symptom being difficulty during feeding. Symptoms exacerbated during feeding include drooling, coughing, respiratory distress, and choking. Other symptoms include recurrent pneumonias, gaseous abdominal distention, and failure to thrive. Inability to pass a nasogastric (NG) tube into the stomach is characteristic of TEF, although a tube may be passed into the stomach in the H-type fistula (Fig. 105-1).

Treatment

The treatment of TEF is surgical repair. The exact type of repair depends on the type of fistula and the distance between the proximal and distal ends of the esophagus in cases of atresia.

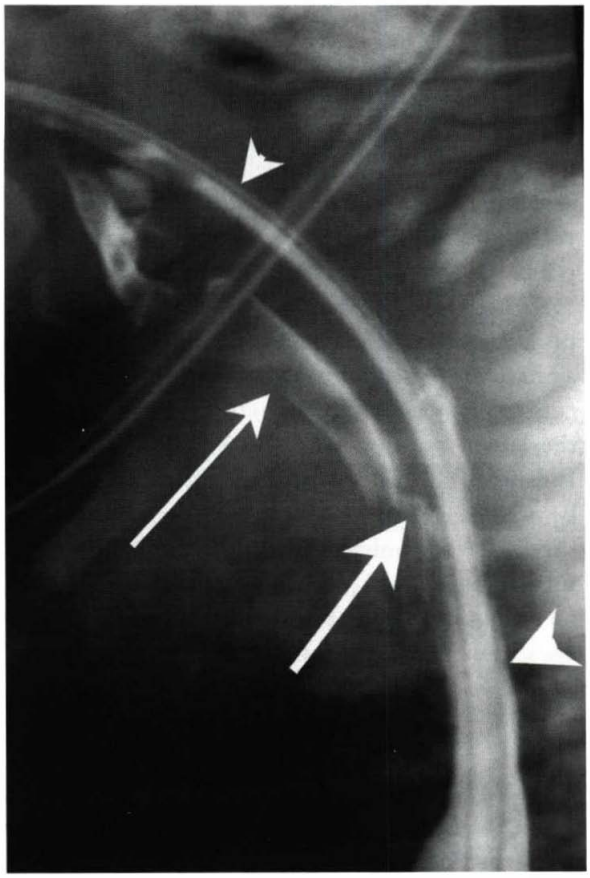

Figure 105-1. "H-type" fistula. Sagittal view demonstrates contrast material instilled via a feeding tube (small arrowhead) The large arrowhead shows contrast in the esophagus. The small arrow shows contrast in the airway. The large arrow identifies the fistulous communication between the esophagus and the airway. (Case courtesy of Peter Strouse, M.D.)

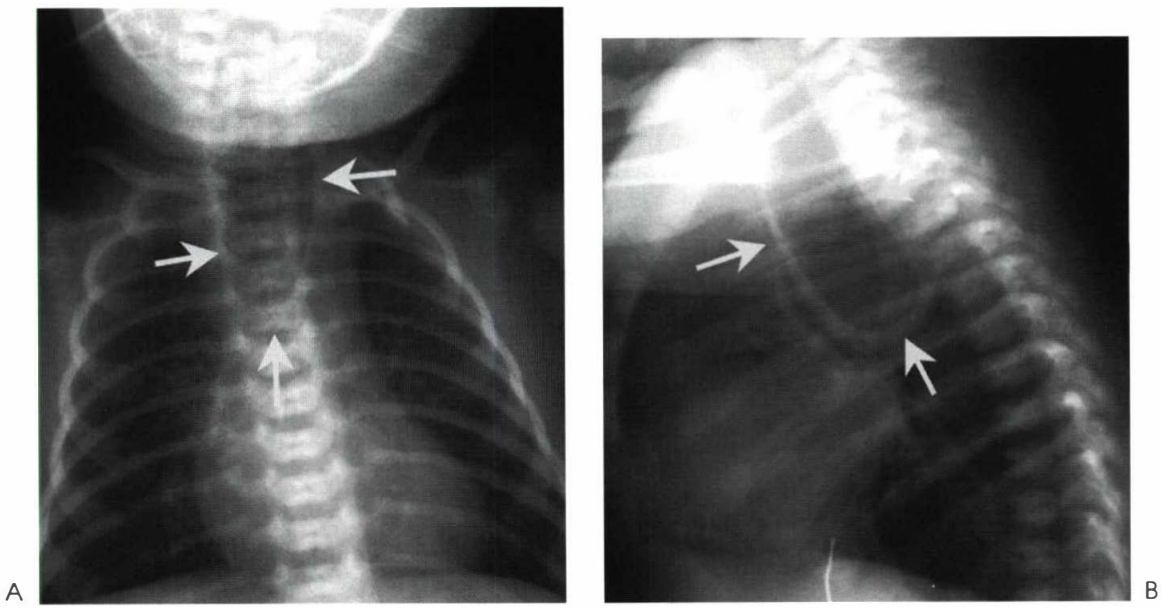

A B

Figure 105-2. Esophageal atresia with a distal fistula. (A) Frontal view of the chest demonstrates an air-filled midline pouch overlying the mediastinum (arrows). Bowel gas was present on a plain of the abdomen (not shown). (B) Lateral view of the chest shows the dilated proximal esophagus (arrows). (Case courtesy of Peter Strouse, M.D.)

Imaging Findings

Plain Films

These typically demonstrate lack of a stomach bubble in patients with complete EA. The presence of a gaseous abdomen with air in the stomach in patients with EA is indicative of a communication between the trachea and the distal pouch (Fig. 105-2).

Fluoroscopy

If EA or TEF is suspected clinically, a pediatric feeding tube (8F) should attempt to be passed through the nose into the stomach. A coiled NG tube in the proximal pouch is indicative of underlying EA. Air may be injected into the NG tube to better visualize the proximal pouch. Care must be taken not to perforate the proximal pouch or advance the tube into the bronchial tree as could occur in TEF with a proximal fistula. If EA is associated with air in the stomach, there must be a communication between the trachea and the distal pouch.

Contrast may be injected into the proximal pouch to confirm the diagnosis and identify a proximal fistula, aid in determining the side of the aortic arch, and exclude the possibility of a pharyngeal pseudodiverticulum. Only 0.5 to 1.0 mL of aqueous barium should be used if contrast material is elected to be administered via the feeding tube. The patient should be in the lateral position with the head slightly elevated prior to administration of contrast. Isolated TEF (H-type) may be difficult to diagnose and visualize. The examination should be performed by passing an 8F polyethylene feeding tube into the distal esophagus. Barium should be administered under pressure while slowly withdrawing the tip of the feeding tube. This study should be performed with the patient in the prone position with horizontal beam fluoroscopy because this allows the barium to opacify the ventral wall of the esophagus, thus maximizing the ability to visualize the fistula.

Imaging Pearls

- There is no role for cross-sectional imaging in the initial diagnosis of TEF. CT and MR may be helpful for identifying and evaluating the multitude of associated abnormalities that are known to occur with EA and TEF. CT may at times be helpful in identifying patients with oblique fistulas.

Suggested Readings

1. Kirks DR, Caron KH. Gastrointestinal tract. In: Kirks DR, ed. *Practical Pediatric Imaging: Diagnostic Radiology of Infants and Children*. 2nd ed. Boston: Little, Brown; 1991 pp. 744–750.
2. Stark P. Congenital anomalies of the trachea. In: *Radiology of the Trachea*. Stuttgart: Thieme; 1991:13–15.
3. Swischuck LE. Alimentary tract. In: *Imaging of the Newborn and Young Infant*. Baltimore: Williams and Wilkins; 1989:371–375.

Chapter 106

Laryngeal Cysts

Epidemiology

Laryngeal cysts (*LCs*) is a term used to identify a variety of air-containing or fluid-filled cysts that include laryngoceles and saccular cysts. Laryngoceles and saccular cysts both result from dilatation of the laryngeal saccule. Laryngoceles have a persistent communication with the laryngeal ventricle, whereas a saccular cyst is isolated from the ventricle. Laryngoceles and saccular cysts may be seen in all ages. LCs may be seen in infants and children and are a known cause of stridor in newborn and young children. There is no reported gender predilection for LCs.

Laryngocele

A laryngocele is an abnormal dilatation or diverticulum of the ventricle that communicates with the laryngeal ventricle. These lesions may be filled with air or mucus, and have been classified as internal, external, or mixed. A laryngocele is termed an internal laryngocele when the mass is confined to the interior of the larynx and limited to the endolaryngeal structures of the larynx. An external laryngocele extends laterally through the thyrohyoid membrane into the soft tissues of the neck. This extension usually occurs through the natural opening in the membrane for the superior laryngeal artery. A laryngocele with both internal and external components is termed a mixed laryngocele.

Laryngoceles may be unilateral or bilateral. These lesions may become infected during periods of upper respiratory tract infections. Laryngoceles may be congenital or acquired. In children, these masses are felt to be congenital in origin. In adults, there is an increased association of laryngoceles with glottic tumors. Two to six percent of glottic squamous cell carcinomas are associated with laryngocele formation; therefore, malignancy must be excluded in any adult who presents with a laryngocele.

Saccular Cysts

A saccular cyst (congenital cyst) is a fluid-filled dilatation of the saccule, that does not communicate with the laryngeal lumen. These cysts may be congenital or acquired. Congenital forms are believed to result from a simple atresia of the saccular orifice and are thought to be the etiology for saccular cysts seen in children. The exact embryogenesis of saccular cysts is controversial. Acquired saccular cysts are believed to occur from complete occlusion and isolation of the cysts due to inflammation, tumor, or trauma.

There are two forms of saccular cysts. The lateral saccular cyst extends posterosuperiorly into the false vocal cord and aryepiglottic fold. The anterior saccular cyst extends medially and posteriorly between the true and false vocal cords into the laryngeal lumen.

Other Cysts

A laryngopyocele is an infected laryngocele, which may contain pus. Some authors extend the definition to include any infected form of saccular cyst. A ductal cyst (mucus retention cyst) results from retention of mucus within the mucous glands located within the submucosa of the larynx. These cysts may occur anywhere in the larynx and may involve the vallecula. These cysts are typically smaller than laryngoceles or saccular cysts and are usually < 1 cm in diameter, although, at times, they may be large enough to obstruct the airway.

Clinical Findings

Clinically, the presenting signs are dependent on the size and extent of the lesion. Children may present with signs of respiratory distress such as inspiratory stridor, intercostal retractions, and episodes of cyanosis. Patients may have intermittent hoarseness or aphonia or a muffled cry. Associated anomalies include laryngomalacia and vocal cord paresis.

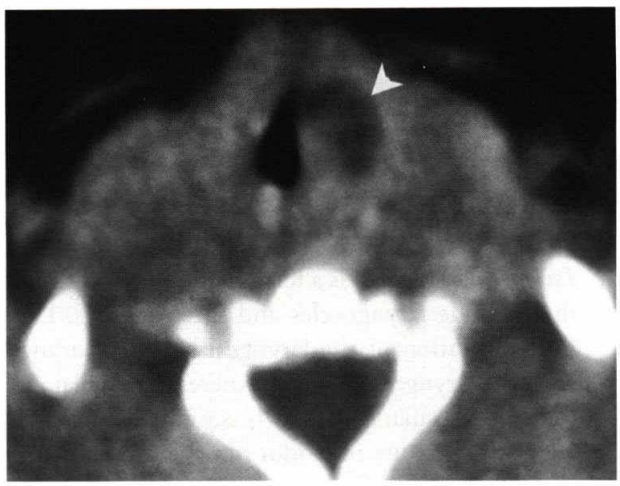

Figure 106-1. Noncontrast CT obtained at the level of the true vocal cords in a newborn shows a cystic mass (arrowhead) indicative of a congenital laryngeal cyst.

At endoscopy, saccular cysts and laryngoceles appear as soft, rounded, submucosal soft tissue masses, which may involve the pyriform sinus, aryepiglottic fold, pyriform sinus, glottis, and hypopharynx. These lesions are mucosally covered and have a characteristic bluish hue. Large lesions may extend into and obstruct the laryngeal lumen. The diagnosis of laryngocele is confirmed if the lesion is seen to inflate and deflate at endoscopy.

The treatment of saccular cysts in children is usually by needle aspiration. Unroofing of the cysts may be necessary in cases of recurrent cysts. The treatment of laryngoceles is surgical. The exact approach is based on the size of the lesion and whether the laryngocele has an extralaryngeal component. The region of the orifice of laryngoceles and saccular cysts should be biopsied to exclude the presence of an underlying neoplasm.

Imaging Findings

Both CT (Fig. 106-1) and MR may be used to evaluate patients with laryngeal cysts. CT is the preferred modality in children due to reduced imaging time resulting in reduced need for sedation. Spiral CT may be especially helpful in studies that are initially limited by motion artifact.

It may be difficult to separate a laryngocele from a saccular cyst by imaging alone. On plain films, laryngeal cysts present as soft tissue masses within the glottic and supraglottic region. The presence of air within the lesion suggests that the mass communicates with the airway and is therefore a laryngocele. Conventional tomography may domonstrate a communication between the larynx and the mass. On CT and MR, these lesions present as smoothly marginated soft tissue masses. The internal characteristics of a laryngeal cyst are those of a fluid-filled mass. The internal attenuation and signal charcteristics may vary depending on the protein content of the lesion. Highly proteinaceous fluid will result in increased attenuation on CT and increased signal on T1-weighted images.

Laryngoceles typically extend along the paraglottic fat planes and may extend superiorly into the preepiglottic fat. Extension of the mass through the thyrohyoid membrane is suggestive of an extermal component of the laryngocele. Uninfected laryngeal cysts do not characteristically enhance with contrast. An enhancing lesion, especially located at the base of a laryngeal cyst, is suggestive of an underlying neoplasm.

Suggested Readings

1. Hollinger LD, Rarnes DR, Smid LJ, Holinger PH. Laryngocele and saccular cysts. *Arch Otol* 1978;87:675-684.
2. Doengan JO, Strife JL, Seid AB, Cotton RT, Dunbar JS. Internal laryngocele and saccular cysts in children. *Ann Otol* 1980;89:408-423.
3. Curtin HC. The larynx. In: Som PM, Bergeron RT, ed. *Head and Neck Imaging.* 2nd ed. St. Louis: Mosby Year Book; 1991:667-669.

Chapter 107

Laryngocele

Epidemiology

A laryngocele is an abnormal cystic dilatation of the laryngeal ventricle with a persistent the communication between the cyst and the laryngeal ventricle. These lesions may be filled with air or fluid. Laryngoceles are classified as internal, external, or mixed. Internal laryngoceles are confined to the endolarynx, whereas an external laryngocele extends through the thyrohyoid membrane into the soft tissues of the neck. This extension usually occurs through the natural opening in the thyrohyoid membrane for the superior laryngeal artery. A laryngocele with both internal and external components is termed a mixed laryngocele.

Laryngoceles may be congenital or acquired and are seen in all ages. In children, laryngoceles are thought to be congenital and are a cause of stridor in newborn and young children. Laryngoceles may be unilateral or bilateral. There is no reported gender predilection. In adults, laryngoceles may be idiopathic in origin. In the past they have been associated in adults who are trumpet players or glass blowers. However, in our experience, the most common association in adults is squamous cell carcinoma involving the true vocal cords. Two to six percent of glottic squamous cell carcinomas are associated with laryngocele formation.

Clinical Findings

The clinical findings often depend on the size and extent of the lesion. Children may present with signs of respiratory distress such as inspiratory stridor, intercostal retractions, and episodes of cyanosis. Patients may have intermittent hoarseness or aphonia or a muffled cry. Associated anomalies include laryngomalacia and vocal cord paresis.

At endoscopy, laryngoceles appear as soft rounded submucosal soft tissue masses that may involve the pyriform sinus, aryepiglottic fold, pyriform sinus, glottis, and hypopharynx (Fig. 107–1). These lesions are mucosally covered and have a characteristic bluish hue. Large lesions may extend into and obstruct the laryngeal lumen. The diagnosis of laryngocele is confirmed if the lesion is seen to inflate and deflate at endoscopy.

Laryngoceles may become infected and contain pus. An infected laryngopyocele is termed a laryngopyocele.

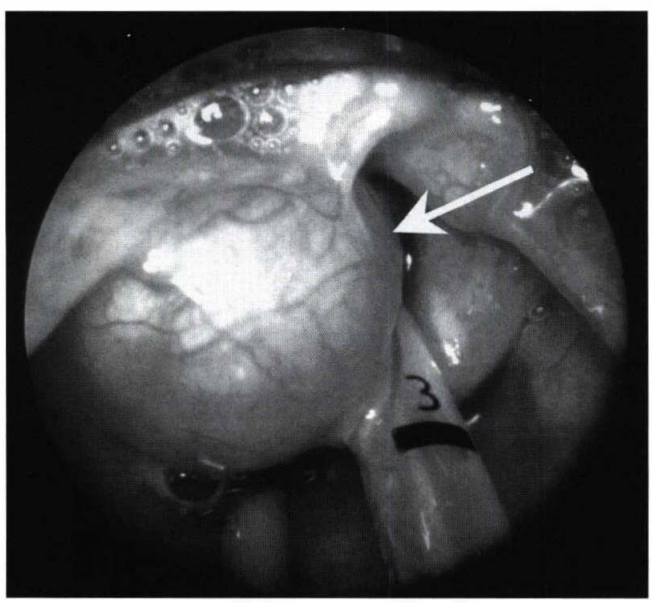

Figure 107–1. Endoscopic image demonstrates the otolaryngologist's view of a laryngocele (arrow).

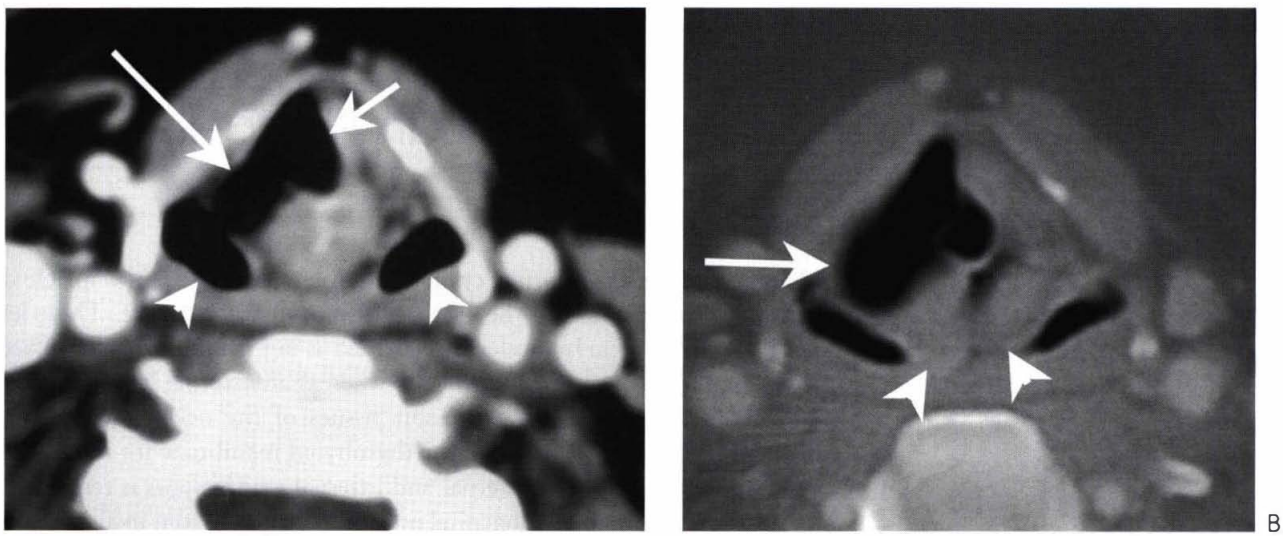

Figure 107–2. (A) Axial contrast-enhanced CT shows air in the paralaryngeal fat (long arrow) that appears to communicate with the laryngeal airway (short arrow). Arrowheads indicate air in the pyriform sinus. (B) Bone algorithm image demonstrates that the air-filled laryngocele (arrow) does not extend through the thyrohyoid membrane and is therefore classified as an "internal" laryngocele. Arrowheads indicate the aryepiglottic folds.

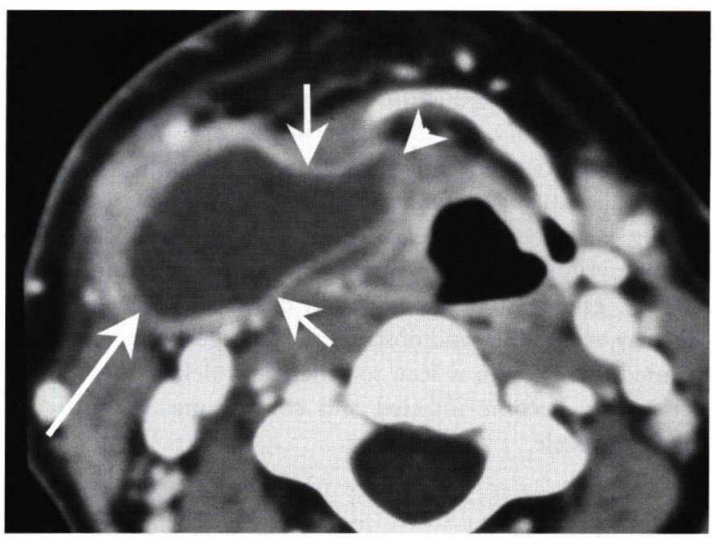

Figure 107–3. Axial contrast-enhanced CT shows a cystic mass that involves the paralaryngeal fat (arrowhead) that extends laterally through the thyrohyoid membrane into the soft tissues of the neck (long arrow). There is enhancement of the wall of the laryngocele that suggests prior infection (short arrows). This would be classified as a mixed laryngocele.

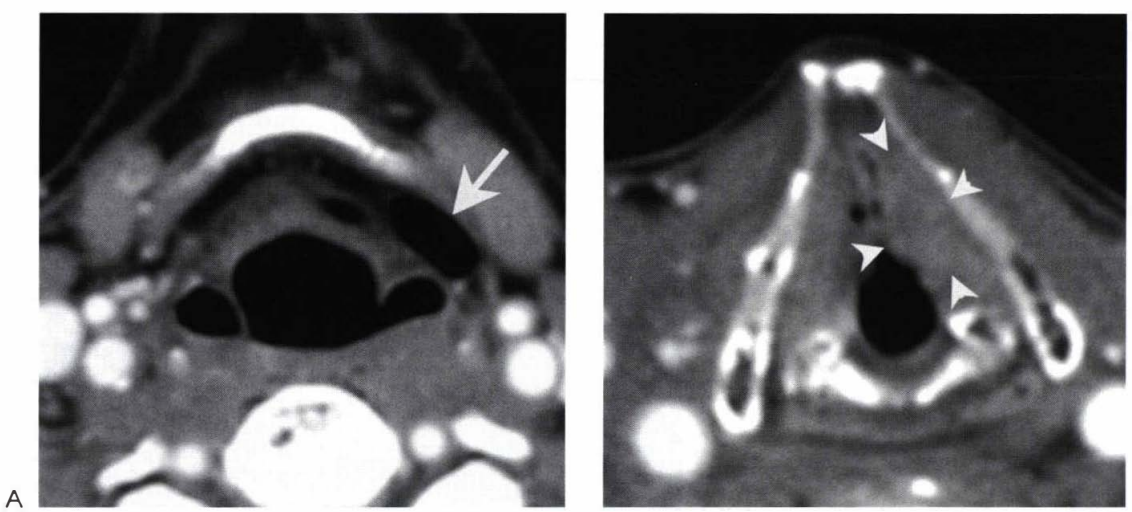

Figure 107–4. (A) Axial contrast-enhanced CT demonstrates an air-filled laryngocele in the left paralaryngeal space (arrow). (B) Image obtained at the level of the true vocal cord demonstrates that the laryngocele is caused by obstruction of the laryngeal ventricle due to an early stage true vocal cord carcinoma (arrowheads).

Treatment

The treatment of laryngoceles is surgical resection. The exact approach is based on the size and extent of the lesion. Internal laryngoceles can be treated endoscopically. External and mixed laryngoceles require a cervical approach. The region of the laryngeal ventricle should be biopsied to exclude the presence of an underlying neoplasm.

Imaging Findings

CT

The typical appearance is a fluid- or air-filled, smoothly marginated mass located in the paraglottic (paralaryngeal) space. The cyst may extend to the level of the hyoid bone. The internal characteristics may vary depending on the protein content of the fluid. The cyst wall does not usually enhance with contrast. An enhancing wall with high fluid attenuation is suggestive of ongoing or recent infection. Laryngoceles that are located with the endolarynx are internal laryngoceles. Lesions that have an endolaryngeal and exolaryngeal component are termed mixed laryngoceles (Figs. 107–2 to 107–4).

MR

The typical appearance is a cystic mass that is low signal on T1-weighted sequences and high signal on T2-weighted sequences. However, the MR signal can vary depending on the protein content. Highly proteinaceous lesions can demonstrate T1 and T2 shortening.

Imaging Pearls

- Pure external laryngoceles are very unusual lesions. A thyroglossal duct cyst is a more likely diagnosis than a purely external laryngocele when evaluating an exolaryngeal cystic paramedian mass located at the level of the thyrohyoid membrane.
- The true and false vocal cords must be closely evaluated to exclude the presence of an occult squamous cell carcinoma.
- Vallecular cysts result from obstruction of a mucous gland and may be confused with an internal laryngocele. These cysts are centered within the vallecula and usually do not involve the paralaryngeal space.

Suggested Readings

1. Hollinger LD, Rarnes DR, Smid LJ, Holinger PH. Laryngocele and saccular cysts. *Arch Otol* 1978;87:675–684.
2. Doengan JO, Strife JL, Seid AB, Cotton RT, Dunbar JS. Internal laryngocele and saccular cysts in children. *Ann Otol* 1980;89:408–423.
3. Curtin HC. The larynx. In: Som PM, Bergeron RT, eds. *Head and Neck Imaging*. 2nd ed. St. Louis: Mosby Year Book; 1991:667–669.

Chapter 108

Laryngeal Webs

Epidemiology

Laryngeal webs (LWs) are rare lesions that result from incomplete recanalization of the embryonic larynx during the seventh to eighth week of gestation. LWs are part of a continuum of congenital laryngeal abnormalities that include laryngeal atresia and congenital subglottic stenosis, which result from varying degrees of resorption of the epithelium of the fetal larynx. LWs are associated with other congenital anomalies. One third of patients will have an associated abnormality of the respiratory tract, the most common of which is subglottic stenosis.

Clinical Findings

Seventy-five percent of LWs are located at the level of the true vocal cords. These lesions are most often located in the region of the anterior commissure. LWs may also occur in the region of the posterior commissure resulting in interarytenoid fixation. LWs have also been described to involve the supraglottic and subglottic larynx. The cricoid cartilage may be involved in patients with LWs occurring within the subglottic region.

Patients with LWs are usually symptomatic at birth and present with signs of airway obstruction. Characteristic clinical features include weak cry, aphonia, respiratory distress, and cyanosis. Stridor is an unusual presentation. Some patients may present later with symptoms believed to represent recurrent or atypical croup.

Pathology

LWs appear as a soft tissue membrane that extends across the airway. The thickness of the web varies greatly and may range from a thin membrane to a thick fibrous band (Fig. 108–1). The peripheral portion of the web is generally thicker than the free margin, which is typically concave and sharply outlined. Larger lesions are associated with greater degrees of airway obstruction.

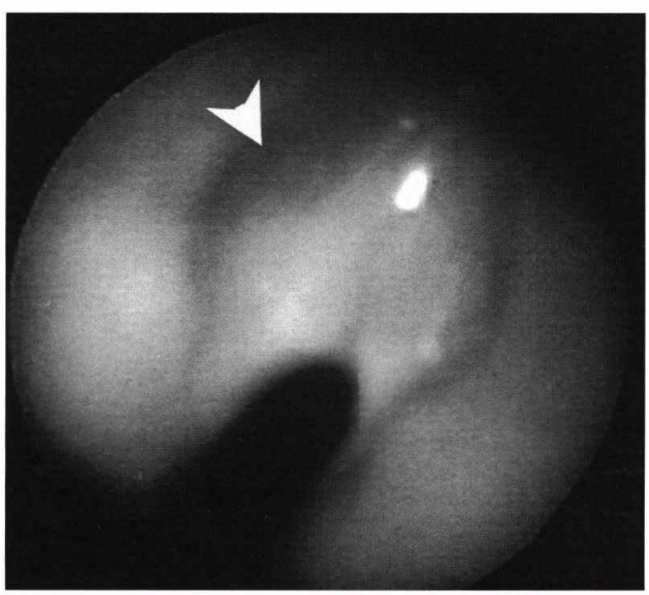

Figure 108–1. Endoscopic view of a laryngeal web in an infant shows a fibrotic mass involving the anterior aspect of the true vocal cords (arrowhead).

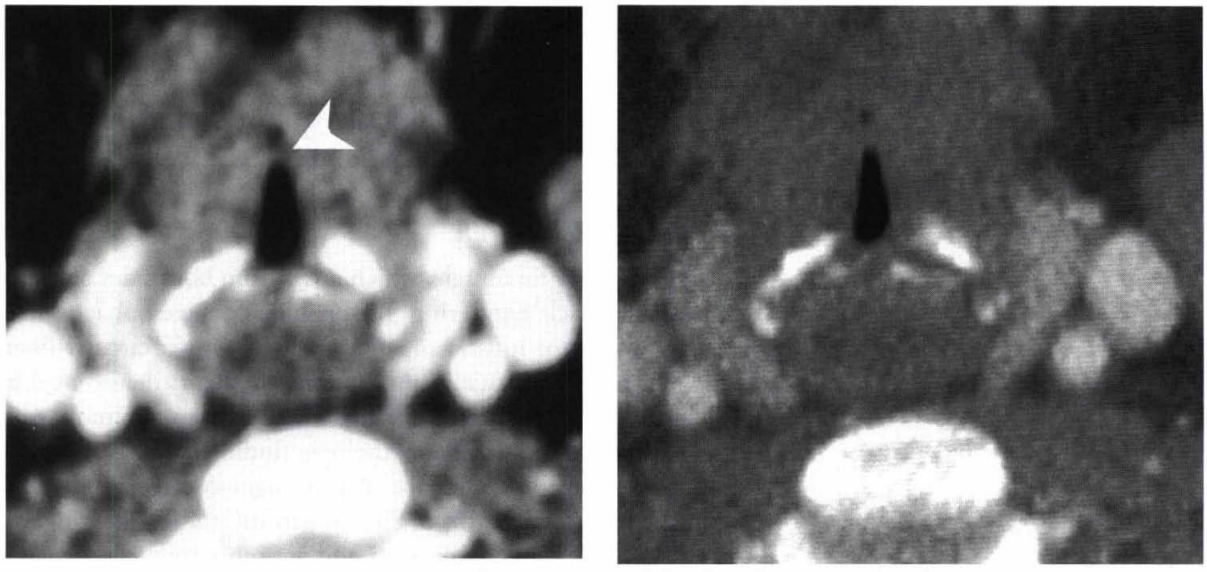

Figure 108–2. (A) Axial contrast-enhanced CT obtained at the level of the true vocal cords shows narrowing of the laryngeal lumen due to a laryngeal web located at the level of the anterior commissure (arrowhead). (B) Bone algorithm better demonstrates the degree of narrowing of the laryngeal airway.

Treatment

The treament of LW is dependent on the thickness of the web. Thin webs may be treated with endoscopic lysis using a carbon dioxide laser or knife. Patients with severe respiratory distress due to larger webs may require emergent intubation or tracheostomy. Thick webs may require tracheotomy in addition to an open laryngeal procedure. Laryngeal dilation may be required to prevent recurrence after the initial procedure.

Imaging Findings

Plain Films

Lateral radiographs may provide valuable information regarding the thickness of the web.

CT

Small laryngeal webs may not be detected by CT. More advanced lesions may demonstrate narrowing of the airway at the expected level of the true vocal cords (Fig. 108–2).

Imaging Pearls

- The diagnosis is usually made at endoscopy. However, LW may prevent passage of the endoscope thereby preventing adequate examination of the larynx distal to the web. Sagittal reformations may help detect the presence and extent of associated laryngeal abnormalities such as subglottic stenosis.
- Spiral CT is the cross-sectional modality of choice due to the short imaging time

Suggested Readings

1. Myer CM, Cotton RT. Congenital abnormalities of the larynx and trachea and management of congenital malformations. In: Paparella MM, Shumrick DA, Gluckman JL, Meyeroff WL, eds. *Otolaryngology*, Vol 3. 3rd ed. Philadelphia: WB Saunders; 1991:2220–2222.
2. Benjamin B. Congenital disorders of the larynx. In: Cummings CW, Fredrickson JM, Harker LA, Krause CJ, Schuller DE, eds. *Otolaryngology and Head and Neck Surgery*, Vol. 3. St. Louis: Mosby Year Book; 1993:1846–1848.

Chapter 109

Zenker's Diverticulum

Epidemiology

The cricopharyngeal muscle, which arises from both sides of the cricoid cartilage to form a continuous muscle band, rings the opening of the esophagus. These fibers blend with the inferior constrictor muscle superiorly and the inner circular fibers of the esophagus inferiorly. There is a potential gap posteriorly (Killian's dehiscence) between the cricopharyngeal and inferior constrictor muscles where a diverticulum may originate. In 1878 Zenker described the classical clinicopathologic findings of 34 patients with pharyngoesophageal diverticula. The true incidence of pharyngoesophageal diverticula is unknown but they have been reported in 0.1% of 20,000 barium studies. Pharyngoesophageal diverticula typically affect elderly white patients and are more frequently encountered in females.

Clinical Findings

Patients usually present with dysphagia and this may be associated with regurgitation of food and drink. At a later stage, when the diverticula are large enough to produce obstruction, chronic aspiration and lung infection complicate the clinical picture. In neglected patients, there is resultant weight loss and emaciation. Clinical diagnosis is based on history and barium swallow and are further assessed with manometric recordings. Endoscopy is usually difficult and potentially dangerous owing to obstruction of the true lumen by a large diverticulum and the attendant risk of diverticular perforation.

Pathology

Zenker's diverticulum is thought to be a motility disorder associated with spasm of the cricopharyngeal muscle. Mucosal herniation initially begins in the midline posteriorly through Killian's dehiscence. The diverticulum progressively enlarges posteriorly but is soon deflected to one side (usually the left) because of the prevertebral fascia. As the diverticulum enlarges, it pushes the esophagus aside and may come into a position directly in line with the pharynx. Most food then passes into the pouch.

Treatment

Cricopharyngeal myotomy is performed to relieve the motility. Diverticulotomy is indicated when pressure symptoms are present.

Imaging Findings

CT and MR imaging are seldom performed to evaluate pharyngoesophageal diverticula. A barium examination will serve the purpose of confirming the diagnosis (Fig. 109–1).

Imaging Pearls

- The diagnosis of a pharyngoesophageal diverticulum during a barium examination is usually straightforward. Because chronic aspiration is a known complication, fluoroscopic examination of the lungs should be performed at the same time as the barium examination. A chest radiograph should be obtained if there is fluoroscopic evidence of chronic aspiration.

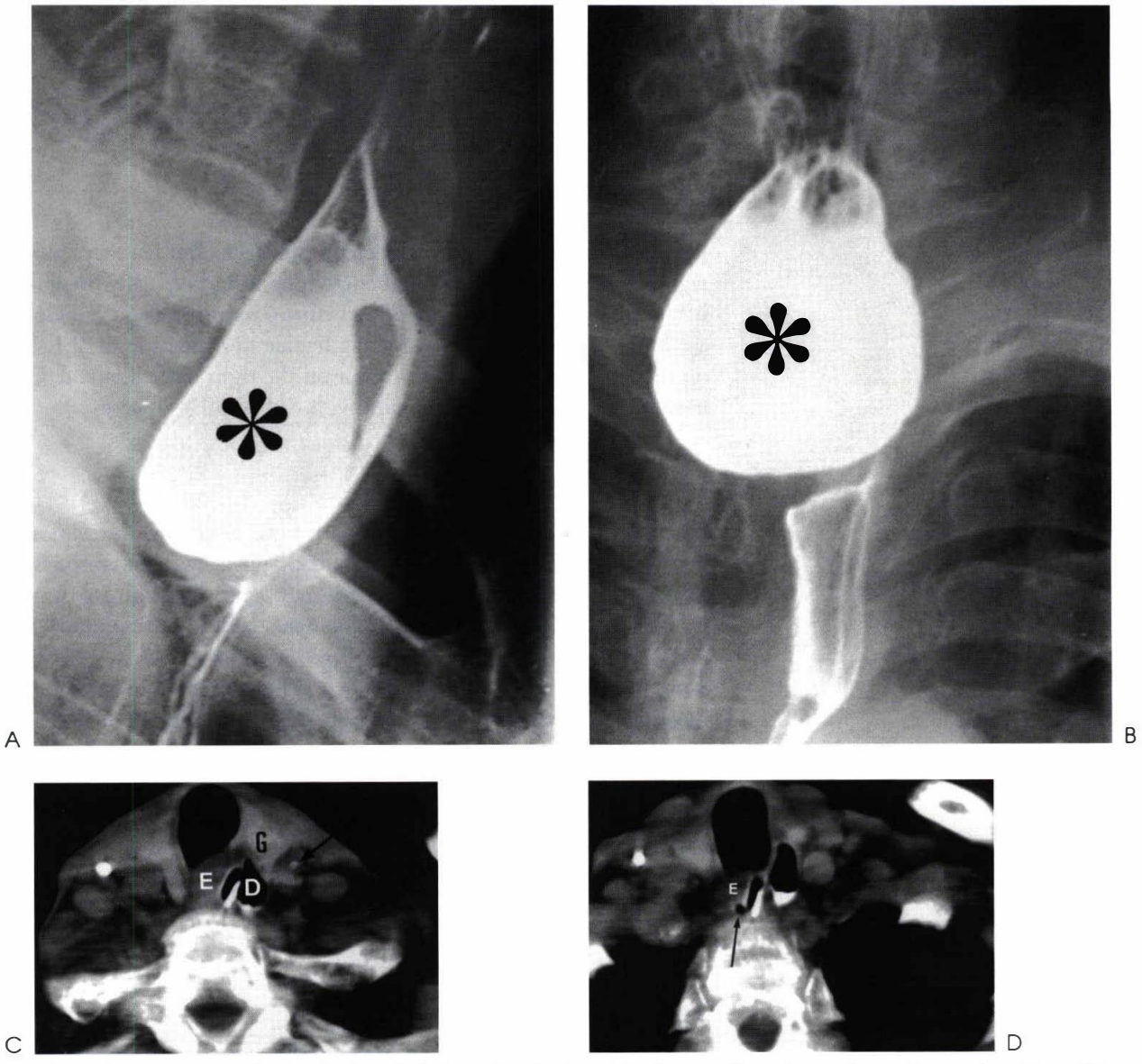

Figure 109–1. Zenker's diverticulum. (A) Lateral projection of barium swallow shows a large diverticulum (asterisk) originating from the upper esophagus. (B) Frontal projection shows the diverticulum (asterisk) to be in line with the pharynx thus receiving the swallowed barium directly. (C) Axial CT shows the diverticulum (D) deflected to the left. Note the relationship of the diverticulum with the esophagus (E), left lobe of the thyroid gland (G), and left carotid artery (arrow). (D) Axial CT, inferior to (C) shows the origin of the diverticulum (arrow) posterior to the esophagus (E) and subsequent deflection of the diverticulum to the left. (Courtesy of SH Ng, MD, Chang Gung Memorial Hospital, Tao Yuan, Taiwan)

Suggested Readings

1. Peters JH, Demeester TR. Esophagus and diaphragmatic hernia. In: Schwartz SI, Shires GT, Spencer TC, eds. *Principles of Surgery.* 6th ed. New York: McGraw-Hill; 1994:1043–1122.
2. Mukherji SK, Weissmann, Holliday RA. In: Som PM, Curtin HD, eds. *Head and Neck Imaging.* 3rd ed. St. Louis: Mosby; 1996:437–487.
3. Graney DO, Marsh B. Trachea/esophagus: anatomy. In: Cummings CW, Fredrickson JM, Harker LA, et al. *Otolaryngology: Head and Neck Surgery.* St. Louis: Mosby Year Book; 1993:2207–2216.

Chapter 110

Subglottic Hemangioma

Epidemiology

Hemangiomas may occur anywhere in the larynx but have a predilection for the subglottic region. They are slow-growing benign lesions and typically present within the first year of life, with 85% of masses presenting before 6 months of age. Subglottic hemangiomas (SHs) are more common in females with a female to male ratio of 2:1. They are more common on the left; however, they may occur on the right or be bilateral. Cutaneous hemangiomas have been reported in association with SH in 50% of cases.

Clinical Findings

Patients with SH typically present with signs or airway obstruction with inspiratory or biphasic stridor. Other symptoms include dyspnea, cyanotic episodes, hoarseness, cough, and difficulty feeding. Continued growth may cause significant airway obstruction. The symptoms are often exacerbated by excitement, crying, or respiratory tract infection. Occasionally, symptoms may progress to acute respiratory distress. The typical endoscopic appearance is that of a red or blue submucosal mass situated in the subglottis. The mass is compressible and may extend into the posterior commissure or upper trachea.

Pathology

Histologically, these are considered true hemangiomas according to the classification of Mulliken and Glowacki. SHs are vascular neoplasms that consist of proliferating endothelial cells. This is in contrast to hemangiomas that occur in adults which are more commonly the cavernous form.

Treatment

The majority of SHs will spontaneously involute after 12 to 18 months, although some lesions may enlarge. Tracheostomy may be necessary for maintaining airway control in patients with respiratory obstruction. A variety of treatments have been used to treat SH. Carbon dioxide laser excision is a generally accepted mode of treatment. Steroids may be beneficial, although the specific indications may not have been defined. Radiation therapy has been used in the past; however, this is no longer felt to be appropriate given the potential risk of malignant degeneration.

Imaging Findings

Plain Films

SHs may be detected on anteroposterior and lateral plain films of the neck and present as a soft tissue mass extending into and narrowing the tracheal air column (Fig. 110-1).

CT

These lesions present as enhancing endolaryngeal polypoid soft tissue masses, which partially obstruct the airway. These lesions are most commonly located just below the true vocal cords in the subglottic region. Occasionally, SHs may present as a concentric narrowing rather than an endophytic mass. Phleboliths may occasionally be present in larger lesions.

MR

SHs are intermediate signal on T1-weighted sequences and increased signal on T2-weighted sequences. These lesions usually enhance following contrast administration. Exolaryngeal extension is unusal (Fig. 110-2).

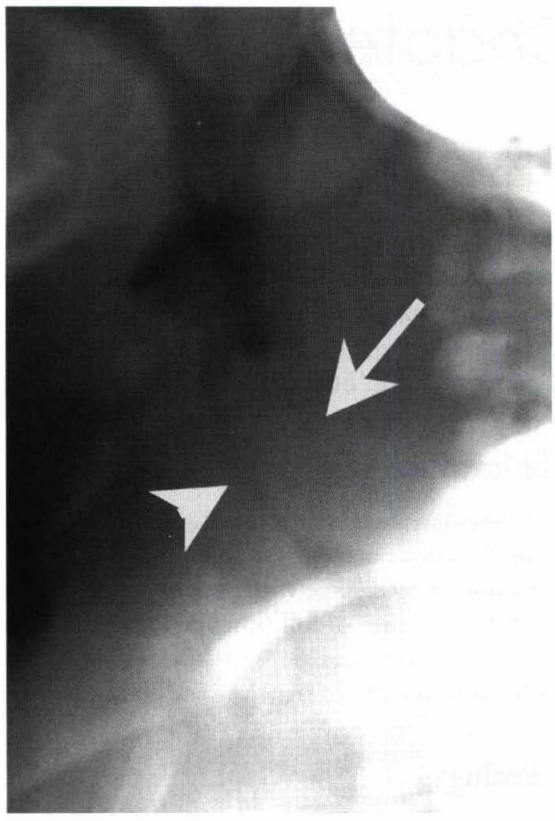

Figure 110–1. Lateral plain film shows a soft tissue mass (arrow) due to a subglottic hemangioma located in the subglottis extending inferiorly that is narrowing the airway (arrowhead).

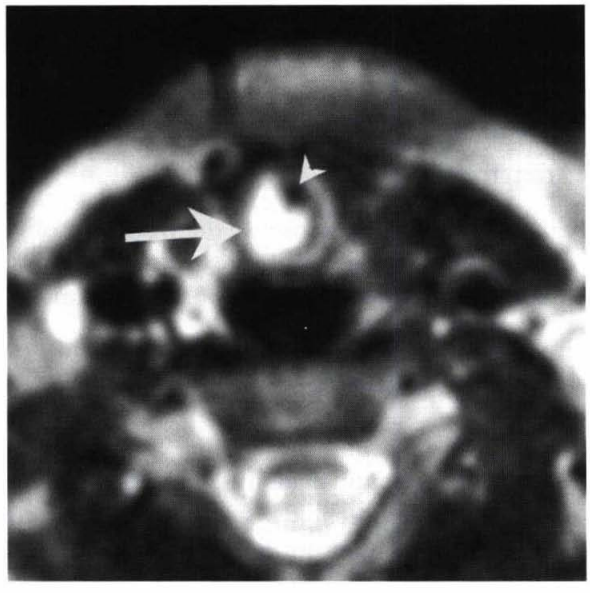

Figure 110–2. Axial T2-weighted image of a subglottic hemangioma demonstrates a high signal intraluminal mass located in the subglottis (arrow) causing marked narrowing of the airway (arrowhead).

Imaging Pearls

- The diagnosis of SH is usually made at endoscopy. If necessary, the role of CT and MR is to define the full extent of the mass. Special care must be taken prior to performing such imaging studies in infants with airway compromise because CT and MR may require the child to be sedated. Helical technique should be performed if CT is thought to be necessary in the work-up of a patient with SH.

Suggested Readings

1. Pransky SM, Seid AB. Tumors of the larynx, trachea and bronchi. In: Bluestone CD, Stool SE, Scheetz MD, eds. *Pediatric Otolaryngology*. Vol. 2. Philadelphia: WB Saunders; 1990:1218–1220.
2. Curtin HC. The larynx. In: Som PM, Curtin H, eds. *Head and Neck Imaging*. 3rd ed. Mosby New York: Mosby; 1996:612–707.

Chapter 111

Venous Malformations

Epidemiology

Venous malformations are categorized as a type of vascular malformation using the classification system of Mulliken and Glowacki. Most authors now classify what were once termed cavernous hemangiomas in children as venous malformations. These lesions are believed to be present at birth but are usually detected in late childhood or early adulthood.

Clinical Findings

Small lesions may present as an asymptomatic bluish mass that is easily compressible. More advanced lesions may be painful and may result in functional impairment or hemorrhage. The lesions may enlarge with patient position or crying. The lesions may also enlarge with Valsalva's maneuver or following placement of a tourniquet to obstruct the venous outflow. The most common locations in the extracranial head and neck include subcutaneous tissues of the face, muscles of mastication, periorbital region, and deep neck spaces.

Pathology

These lesions arise from anomalous venous development. The absence of valves results in stagnant flow and variable communication with the surrounding normal venous system. Enlargement of the lesion over time is due to growth of the patient rather than endothelial proliferation.

Treatment

Complete surgical resection is the treatment of choice for localized lesions with well-defined margins. Because these are low-flow venous lesions, percutaneous sclerotherapy is becoming an accepted treatment option for patients with advanced infiltrative lesions.

Imaging Findings

Ultrasound

Gray-scale ultrasound demonstrates variable internal echogenicity with margins that are often irregular. Hypoechoic cystic spaces that are compressible are often present. Echogenic phleboliths may result in distal acoustic shadowing. Doppler analysis shows slow venous flow with normal arterial flow in the surrounding vessels.

CT

These lesions are usually seen when they arise in the subcutaneous tissues but are difficult to detect when they are intramuscular. Phleboliths are a hallmark of the diagnosis.

MR

Venous malformations have intermediate signal on T1-weighted sequences and are slightly more intense than adjacent muscle. There may be mild enhancement following contrast administration. They have increased signal on T2-weighted sequences. Flow-sensitive sequences show slightly increased signal. Flow voids are not typically identified (Fig. 111-1).

Angiography

These lesions may not be detected at angiography because they are located at the postcapillary level. Normal arterial and capillary phases are expected. Arteriovenous shunting should not be seen. Visualization of the entire extent of the venous anomaly may require direct puncture.

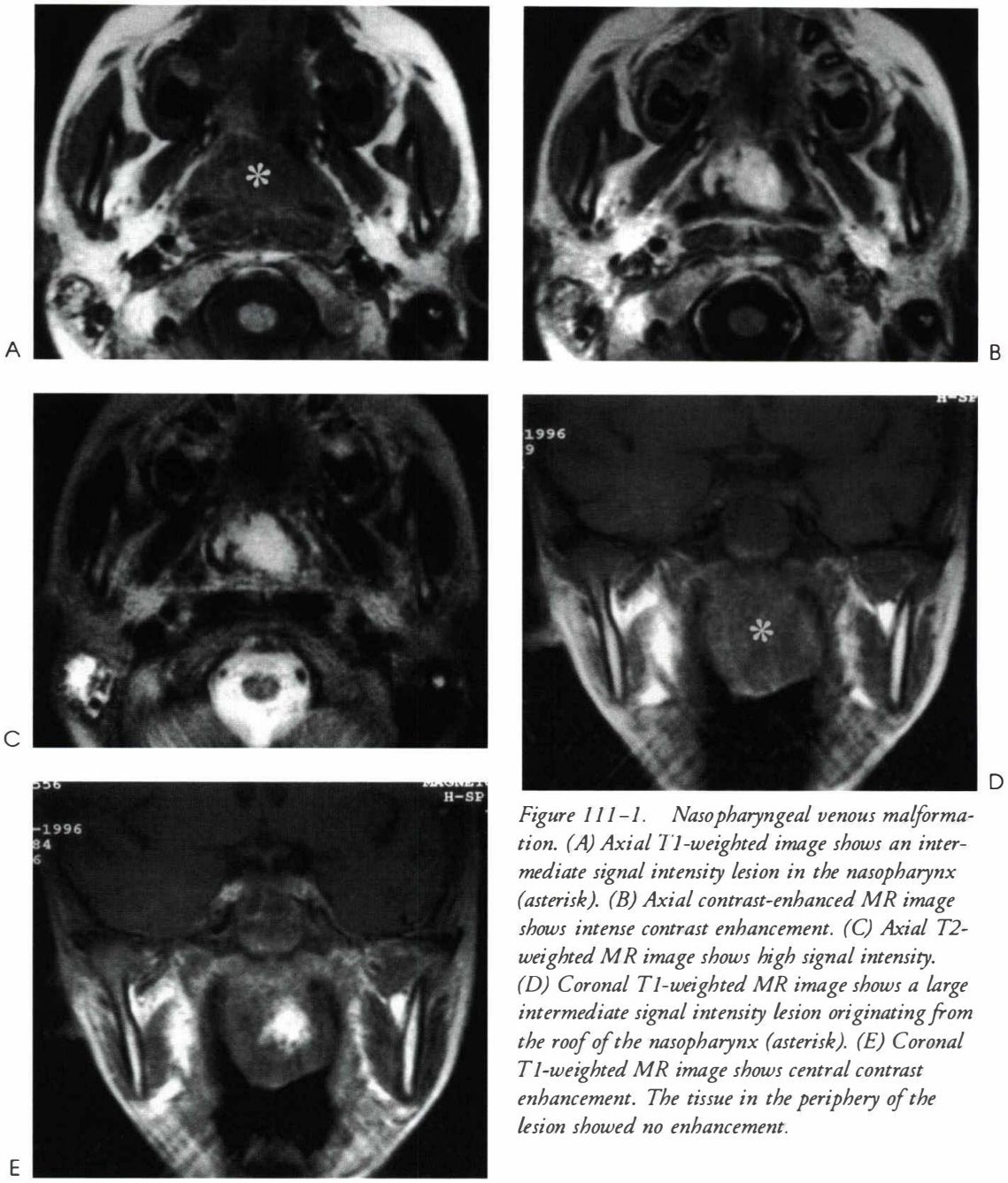

Figure 111–1. Nasopharyngeal venous malformation. (A) Axial T1-weighted image shows an intermediate signal intensity lesion in the nasopharynx (asterisk). (B) Axial contrast-enhanced MR image shows intense contrast enhancement. (C) Axial T2-weighted MR image shows high signal intensity. (D) Coronal T1-weighted MR image shows a large intermediate signal intensity lesion originating from the roof of the nasopharynx (asterisk). (E) Coronal T1-weighted MR image shows central contrast enhancement. The tissue in the periphery of the lesion showed no enhancement.

Imaging Pearls

- The imaging findings are crucial to the treatment of these lesions. Identification of internal venous flow without arterial flow using ultrasound and the absences of flow voids on MR confirm the diagnosis of a low-flow lesion. This precludes the need for angiography prior to surgical resection.
- The absence of flow voids helps distinguish these from high-flow lesions such as arteriovenous malformations and hemangiomas in the proliferative phase.
- MR imaging is the best cross-sectional modality for defining the extent of the lesions and may detect intramuscular malformations that cannot be seen on CT.
- Localized lesions, as determined by cross-sectional imaging, are often treated with surgery, whereas extensive lesions that are not completely resectable may be treated with percutaneous sclerotherapy.

Suggested Readings

1. Mulliken JB, Glowacki J. Hemangiomas and vascular malformations in infants and children: a classification based on endothelial characteristics. *Plast Reconstr Surg* 1982;69:412–422.
2. Meyer JS, Hoffer FA, Barnes PD, Mulliken JB. Biological classification of soft-tissue vascular anomalies: MR correlation. *AJR Am J Roentgol* 1991;157:559–564.
3. Waner M, Suen JY. A classification of congenital vascular malformations. In: Warner M, Suen JY, eds. *Hemangiomas and Vascular Malformations of the Head and Neck*. New York: Wiley-Liss; 1999:1–12.
4. James CA. Diagnostic imaging of congenital vascular lesions. In: Warner M, Suen JY, eds. *Hemangiomas and Vascular Malformations of the Head and Neck*. New York: Wiley-Liss; 1999:171–215.

Chapter 112

Thyroid Adenoma

Epidemiology

Thyroid adenomas are classified based on their histology as papillary, follicular, and Hürthle cell. The most common benign thyroid neoplasm is the follicular adenoma. Thyroid adenomas also tend to be divided based on their hormonal activity. Most adenomas (90–95%) do not produce significant quantities of thyroid hormones. Solitary tumors are estimated to occur in 1 to 3% of the adult population. The incidence is more common in females (2:1). The incidence of thyroid nodules is approximately 0.1%/yr. In general, it is estimated that between 3 and 4% of patients who develop a solitary nodule have thyroid carcinoma.

Clinical Findings

Patients with nonhormonally active adenomas usually present with asymptomatic masses that are initially discovered on routine physical exam. Tumors typically become palpable when they reach 1 cm, but on occasion may reach 5 to 10 cm without being noticed.

Most functioning adenomas are quiescent and are incidentally found on clinical examination. Functioning adenomas that are $>$ 3 cm tend to result in thyrotoxicity.

Pathology

True adenomas are encapsulated and compress adjacent tissue. Follicular adenoma varies in size from microscopic to 8 to 10 cm. These are composed of normal-appearing thyroid epithelium arranged in a follicular structure. The follicles may be very small with little colloid (fetal adenoma or microfollicular adenoma) to large distended structures (macrofollicular adenoma). An embryonal adenoma is a more primitive-appearing structure possessing very little colloid. Hürthle cell adenomas (oxyphil adenomas) are tumors composed of oxyphils. Hypercellular adenomas are difficult to differentiate from follicular carcinomas on needle biopsy.

Treatment

The presence of an autonomously functioning nodule virtually precludes the diagnosis of thyroid carcinoma. The treatment of these lesions is based on the thyroid status. Annual follow-up is indicated for euthyroid patients, whereas surgery or I-131 treatment may be necessary for hyperthyroid patients. The treatment for a solitary cold nodule is beyond the scope of this text and we refer you to one of the excellent references under "Suggested Readings."

Imaging Findings

CT

Benign thyroid adenomas have protean CT findings and are nonspecific. These masses most commonly appear as enhancing masses but enhance less than the surrounding thyroid gland. Occasionally, they may appear as low attenuation masses with a surrounding rim of enhancement that may represent a capsule or compressed surrounding thyroid parenchyma (Figs. 112–1 to 112–3).

MR

Thyroid adenomas are typically intermediate signal on T1-weighted images and enhance with contrast. Occasionally, they may have increased T1-weighted images compared with the adjacent thyroid gland. Thyroid adenomas are usually higher signal on T2-weighted images.

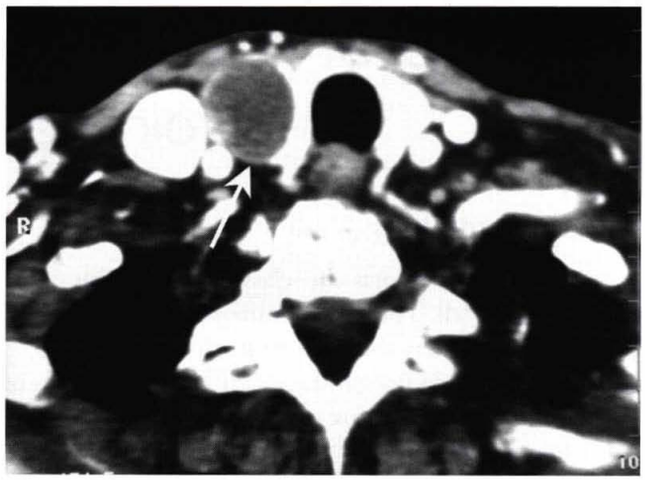

Figure 112–1. Axial contrast-enhanced CT demonstrates a low attenuation thyroid adenoma involving the right lobe of the thyroid gland (arrow).

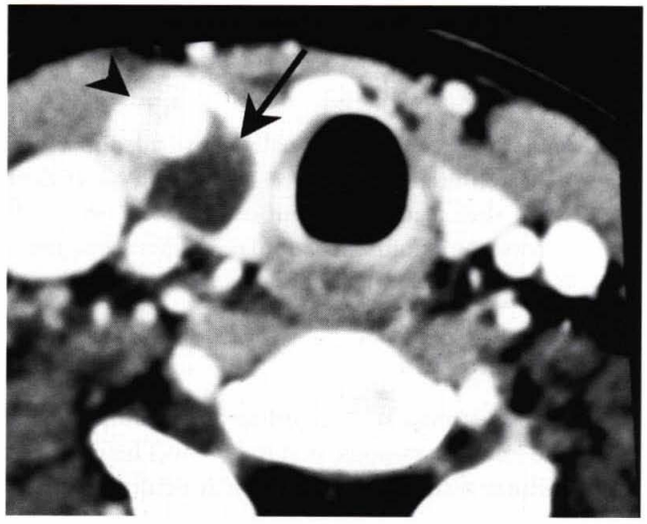

Figure 112–2. Axial contrast-enhanced CT shows a thyroid adenoma with both a low attenuation (arrow) and an enhancing component (arrowhead).

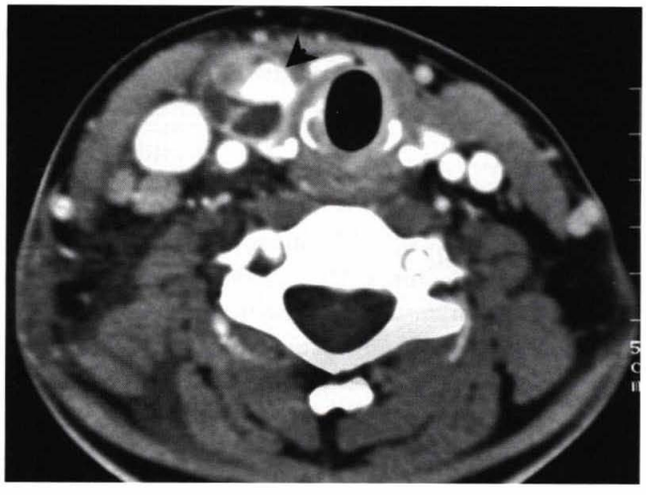

Figure 112–3. Conrast-enhanced CT illustrates a heterogeneous thyroid adenoma that contains calcification (arrowhead).

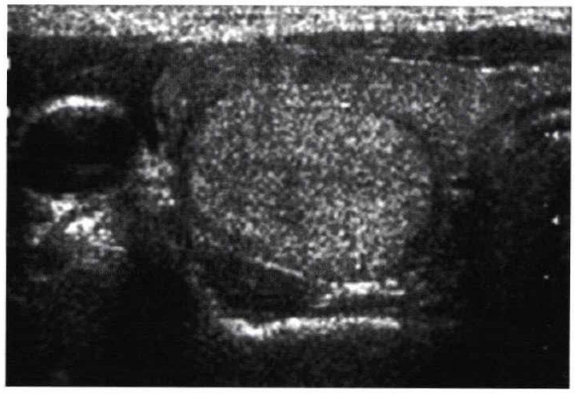

Figure 112–4. Transverse sonogram showing a well-defined, haloed, isoechoic, homogeneous, noncalcified, solid, thyroid nodule. The appearance is commonly seen in follicular lesions. (Case courtesy of Anil Ahuja, M.D.)

Imaging Pearls

- The US (Fig. 112-4), CT, and MR findings are nonspecific and rarely help in differentiating between the various benign types of thyroid adenomas.
- A thyroid malignancy should be considered in the presence of a solitary mass that is present in a patient with a previous exposure to therapeutic thyroid irradiation in childhood, family history of thyroid cancer, enlargement of cervical lymph nodes, development of recurrent laryngeal palsy, or continuing enlargement of a nodule in an otherwise stable gland.
- The diagnosis is based on histologic evaluation of the entire specimen and usually cannot be made on fine needle aspiration. This has led some authors to use the term *follicular lesions* to include both the benign and malignant counterparts.

Suggested Readings

1. Larsen PR. The thyroid. In: Wyngaarden JB, Smith LH, eds. *Cecil Textbook of Medicine*. 17th ed. Philadelphia: WB Saunders; 1985:1294-1295.
2. Wartofsky L, Ingbar SH. Diseases of the thyroid gland. In: Wilson JD, Braunwald E, Isselbacher KJ, Petersdorf RG, Martin JB, Fauci AS, Root RK, eds. *Harrison's Textbook of Internal Medicine*. 12th ed. New York: McGraw-Hill; 1991;1709-1710.
3. Noma S, Kanaoka M, Minami S, et al. Thyroid masses: MR imaging and pathologic correlation. *Radiology* 1988;168:759-764.

Chapter 113

Goiter

Epidemiology

There are different types of goiter. *Sporadic goiter* refers to enlargement of the thyroid gland that occurs in a relatively small portion of the population. The etiology varies from patient to patient. *Endemic goiter* refers to a generalized or localized thyroid enlargement that occurs in > 10% of the population. The etiology is similar in the population being studied and may be due to one or several environmental influences, the most common being iodine deficiency. Although the causes of sporadic and endemic goiters differ, the pathology and pathophysiology are similar. Thyroid enlargement is thought to be due to hypersecretion of thyroid stimulating hormone (TSH) in response to decreased production of thyroid hormones, especially T4. In cases of sporaid goiter, the reduction of T4 is thought to be due to an intrinsic abnormality of thyroid hormone synthesis. In cases of endemic goiter T4 reduction is thought to result from the lack of adequate quantities of iodine in the diet or the presence of goitrogen in the environment. As a result of the elevated TSH secretion, the T3 level may be normal and the patient may be clinically euthyroid at the expense of elevated TSH concentration and an enlarged thyroid gland.

Coexistent thyroid carcinoma and multinodular goiter are rare. The suspicion will be higher in patients with previous exposure to therapeutic thyroid irradiation in childhood, family history of thyroid cancer, enlargement of cervical lymph nodes, development of recurrent laryngeal palsy, or continuing enlargement of a cold nodule in an otherwise stable gland.

Clinical Findings

Goiters are most commonly found on routine physical examination in asymptomatic patients. Patients with large goiters may present with respiratory obstruction or dysphagia. The goiter may extend retrosternally. Large substernal goiters may result in jugular venous distension and suffusion of the face (Pemberton's sign). The most significant clinical aspect of multinodular goiter is the tendency to develop hyperthyroidism late in life (Plummer's disease).

Pathology

In the early phases, the gland is diffusely enlarged due to cellular hyperplasia characterized by uniform hypertrophy, hyperplasia, and hypervascularity due to TSH stimulation. As the disease progresses, the thyroid is characterized by large follicles with low epithelium. Some follicles are stimulated whereas other follicles become atrophic and fibrotic. Areas of hemorrhage and irregular calcification may be seen.

Treatment

The purpose of the treatment is to reduce the size of the goiter. The proper treatment depends on the etiologic factors in each patient. Small doses of iodide may be helpful in disorders due to iodine deficiency or impairment of the thyroid iodide-concentrating mechanism. Surgical resection should be reserved to relieve obstructive symptoms especially after failure of medical therapy. Surgical exploration may also be necessary in some patients where there is the suggestion of a coexistent carcinoma.

Imaging Findings

US

The enlarged thyroid parenchyma is characterized by isoechoic solid nodules with well-defined nodules. The nodules may contain cystic components that are due to hemorrhage or colloid. Fibrous septa that separate nodules may appear as linear areas of increased echotexture.

Areas of calcification are characterized by focal areas of increased echotexture with distal shadowing. Doppler imaging demonstrates a predominantly perinodular vascularity. The debris and septa within the nodule appear avascular. A "comet tail" artifact may be seen within colloid nodules (Fig. 113-1).

CT

The thyroid gland may be focally or diffusely enlarged. The contours are lobular. Internal irregular calcifications may be present. Goiters typically heterogeneously enhance after contrast. The nodular meshwork of the goiter is better visualized following contrast administration (Figs. 113-2 and 113-3).

MR

Goiters have heterogeneous signal on T1-weighted and T2-weighted images. Areas of T1-weighted shortening may be due to prior areas of hemorrhage or colloid. Goiters typically heterogeneously enhance following contrast. Large goiters may extend retrosternally or may extend superiorly behind the hypopharynx in the retropharyngeal space (Fig. 113-4).

Imaging Pearls

- To diagnose a goiter the thyroid gland must be enlarged. A goiter should not be considered if the gland is not enlarged.

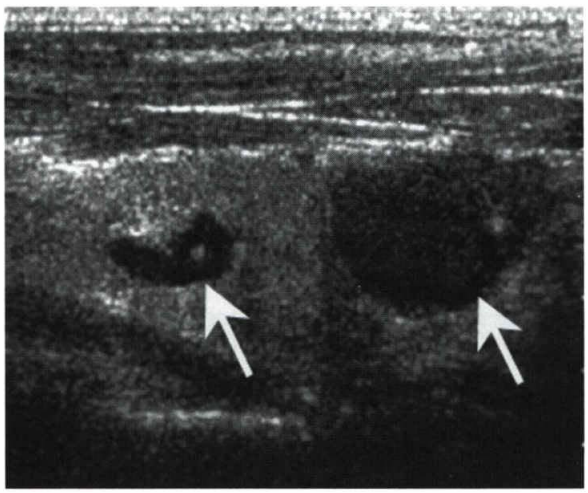

Figure 113-1. Longitudinal sonogram showing multiple, heterogeneous, predominantly cystic thyroid nodules (arrows) with small solid component. On Doppler the 'solid' portion is usually avascular and represents previous intranodular hemorrhage. (Case Courtesy of Anil Ahuja, M.D.)

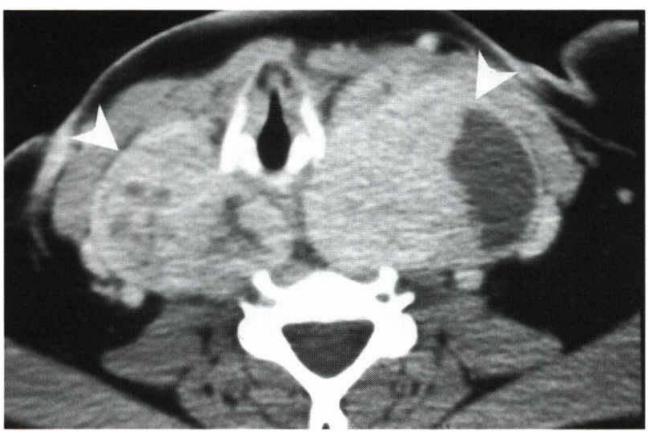

Figure 113-2. Axial contrast-enhanced CT demonstrates a large multinodular goiter that has enlarged both lobes of the thyroid gland (arrowheads). There is heterogeneous enhancement with focal areas of decreased attenuation present in both lobes.

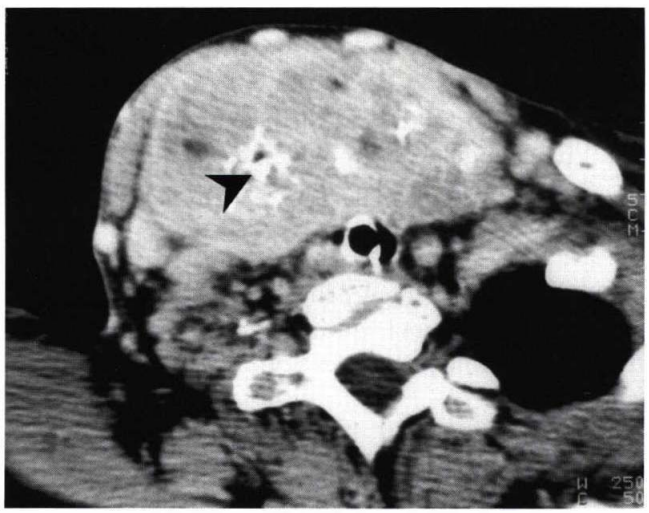

Figure 113–3. Axial contrast-enhanced CT shows a multinodular goiter involving a heterogeneously enhancing thyroid gland. The arrowhead identifies a focal area of calcification within the thyroid gland.

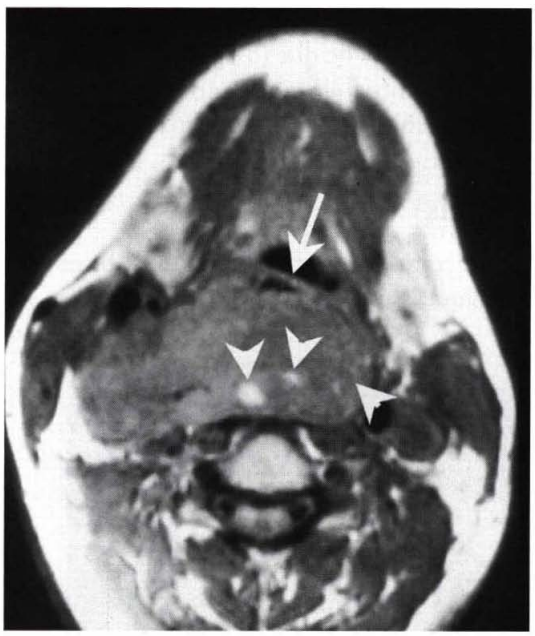

A

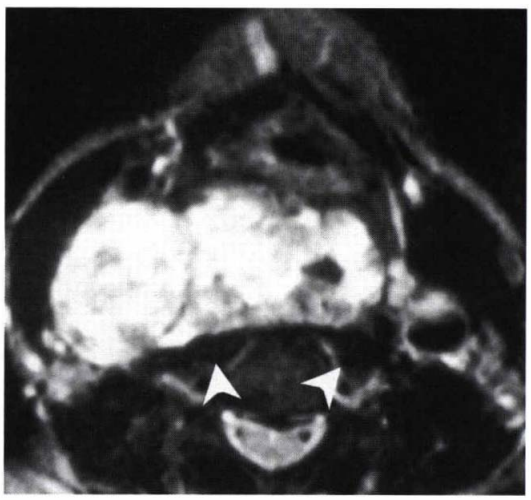

B

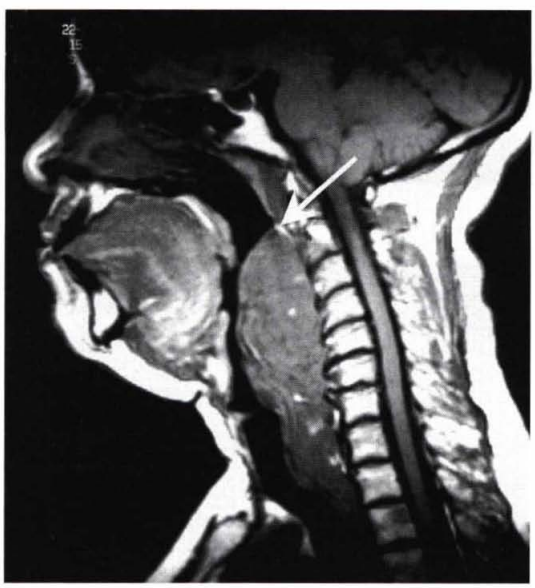

C

Figure 113–4. (A) Axial non-contrast T1-weighted image obtained at the level of the free margin of the epiglottis (arrow) shows a heterogeneous mass in the retropharyngeal space. The mass contains focal areas of increased T1-weighted signal (arrowheads). (B) Axial T2-weighted images demonstrate that the mass is primarily high signal with focal areas of decreased signal. The arrowheads show that the longus coli muscles are intact indicating that the mass is not involving the prevertebral space. Pathology revealed multinodular goiter. (C) Sagittal noncontrast T1-weighted image demonstrates the heterogeneous goiter posterior to the posterior pharyngeal wall in the retropharyngeal space. The goiter narrows the pharyngeal airway. The extensive mass extends superiorly to the level of the oropharynx (arrow).

- The presence of an enlarged thyroid gland that contains irregular calcification is indicative of a goiter.
- The presence of a coexistent thyroid carcinoma and multinodular goiter is rare. It is difficult to make this distinction on CT or MR. The presence of an enlarging nodule in an otherwise stable gland raises a suspicion, especially in the presence of proper history.

Suggested Readings

1. Larsen PR. The thyroid. In: Wyngaarden JB, Smith LH, eds. *Cecil Textbook of Medicine*. 17th ed. Philadelphia: WB Saunders; 1985:1298–1299.
2. Wartofsky L, Ingbar SH. Diseases of the thyroid gland. In: Wilson JD, Braunwald E, Isselbacher KJ, et al., eds. In: *Harrison's Textbook of Internal Medicine*. 12th ed. New York: McGraw-Hill; 1991:1699–1700.
3. Noma S, Kanaoka M, Minami S, et al. Thyroid masses: MR imaging and pathologic correlation. *Radiology* 1988;168:759–764.

Chapter 114

Thyroid Cyst

Epidemiology

Thyroid cysts are common lesions of the thyroid gland. These may be simple cysts, or they may arise due to cystic degeneration of a thyroid adenoma or nodule. True epithelial cysts are rare and the latter are more common. They occur in all age groups and show no sex predilection.

Clinical Findings

Simple thyroid cysts are usually asymptomatic. Infrequently, large cysts may produce slight fullness in the lower neck.

Pathology

Simple thyroid cysts are generally < 2 to 3 cm. They consist of mucinous, clear secretion lined by thyroid epithelium. Cysts that arise due to degeneration of a thyroid adenoma or nodule are often filled with brown, turbid fluid containing blood and cell debris.

Treatment

Asymptomatic thyroid cysts do not require any specific treatment. Ultrasonography-guided aspiration of the cyst may be performed in cases of high clinical suspicion for a malignancy.

Imaging Findings

US

Ultrasonography reveals a well-defined cystic mass within the thyroid gland. Internal echoes may be seen in cases of degenerated nodules.

CT

Most of the thyroid cysts are incidentally detected on the CT studies. They appear as well-defined masses of low attenuation on the unenhanced CT study. They do not demonstrate enhancement following administration of intravenous contrast (Fig. 114–1).

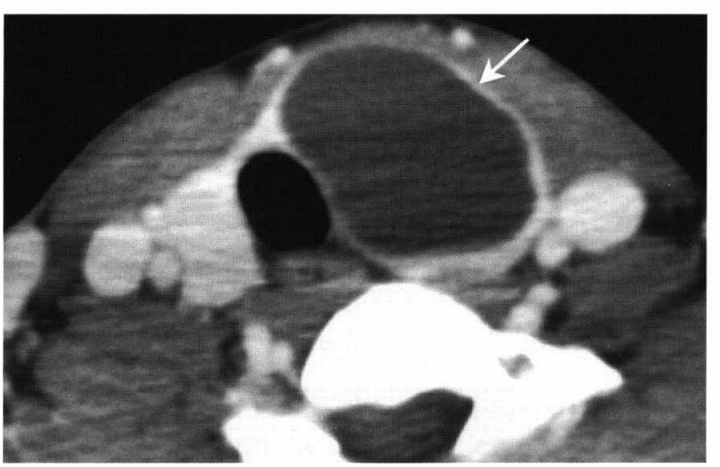

Figure 114–1. Axial contrast-enhanced CT shows a well-defined low attenuation mass replacing the left lobe of the thyroid (arrow). No solid enhancing component is associated with the mass. These findings are strongly indicative of a benign thyroid cyst.

MR

Thyroid cysts appear as well-defined masses within the thyroid gland that are hypointense on the T1-weighted sequences and hyperintense on the T2-weighted sequences. They may sometimes appear bright on the T1-weighted images due to blood products or proteinaceous material within.

Suggested Readings

1. James EM, Charboneau JW, Hay ID. The thyroid. In: Rumack CM, Wilson SR, Charboneau JW, eds. *Diagnostic Ultrasound*. Vol. 2. St. Louis: Mosby Year Book; 1991:507–523.
2. Yousem DM, Scheff AM. Thyroid and parathyroid. In: Som PM, Curtin H, eds. *Head and Neck Imaging*. 3rd ed. New York: Mosby; 1996:952–974.
3. Rumack CM, Wilson SR, Charboneau JW. The thyroid. In: *Diagnostic Ultrasound*. Vol. 2. 2nd ed. Mosby Year Book; 1998:509–516.
4. Ahuja AT. The thyroid and parathyroids. In: Ahuja A, Evans R, eds. *Practical Head and Neck Ultrasound*. London: Greenwich Medical Media Limited; 2000:37–66.

Chapter 115

Medullary Thyroid Carcinoma

Epidemiology

Medullary carcinoma of the thyroid gland (MTC) is an uncommon malignancy and accounts for 5 to 10% of thyroid neoplasms. It occurs in either a sporadic or a familial form. The sporadic form accounts for 70% of cases and is primarily a tumor of middle-aged adults with a female to male ratio of 1.3:1. The familial form is inherited in an autosomal dominant pattern and expressed clinically as multiple endocrine neoplasia (MEN), types IIa and IIb, or as familial MTC alone (10–20%). The tumor is slightly more common in females and is seen in children as well as adults.

Clinical Findings

Patients generally present with a lower neck mass. Sipple's syndrome (MEN IIa) is the association of medullary carcinoma with pheochromocytoma and parathyroid adenomas/hyperplasia. MEN IIb is said to be present when mucosal neuromas and marfanoid facies coexist with medullary thyroid carcinoma.

Pathology

MTC arises from the parafollicular C cells of the thyroid gland. MTC cells secrete the polypeptide hormone calcitonin that serves as a tumor marker. The *'ret'* protooncogene is consistently expressed in cases of MEN IIa. On gross examination, the tumor is soft to firm and well circumscribed but not encapsulated. Familial and sporadic variants are indistinguishable histologically. Individual tumor cells may be round, polygonal, or spindle-shaped and show eccentric nuclei with eosinophilic cytoplasm. Foci of necrosis and hemorrhage may be seen. Amyloid deposits are present in almost 50% of cases.

Treatment

Surgery is the treatment of choice. The development of calcitonin radioimmunoassay and the screening of patients at risk for the familial forms of MTC allow the diagnosis of the neoplasm at an early stage when total thyroidectomy results in virtually 100% cure. MTC has a more aggressive course in patients with MEN IIb, whereas it is more indolent in MEN IIa.

Imaging Findings

US

The tumor is generally seen as a hypoechoic (77%) or isoechoic (14%) mass with heterogeneous echotexture on ultrasonography. This may be associated with foci of calcifications or amyloids that are seen as hyperechoic areas with posterior acoustic shadowing. These tumors have a chaotic vascular pattern on Doppler imaging (Fig. 115–1).

Nuclear Medicine Study

The agents used for thyroid imaging include iodine 123, iodine 131, technetium 99m pertechnetate, and thallium 201.The risk of cancer in a cold nodule is 15 to 25%; in a hot nodule, 1 to 4%; and in a warm nodule, 8 to 10%.

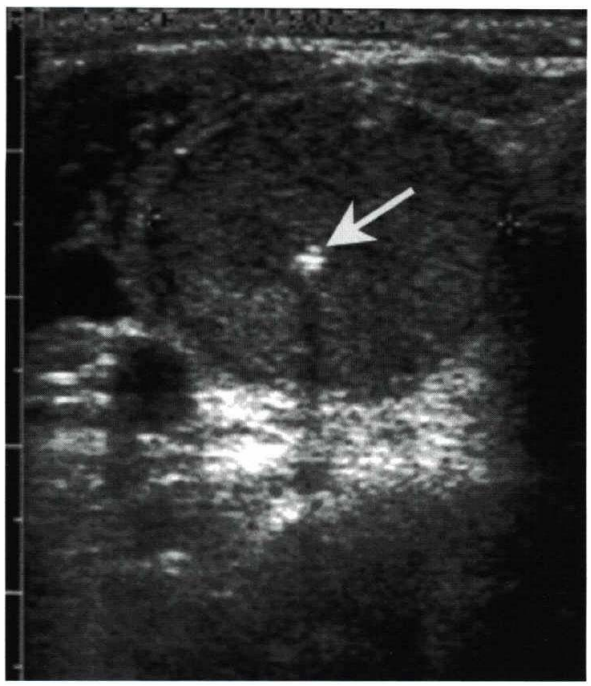

Figure 115–1. Transverse sonogram showing a solid, hypoechoic, fairly well-defined thyroid nodule. Note the focal area of calcification within the mass that probably represents a combination of amyloid and calcification (arrow). Malignant lesions may sometimes demonstrate sharp borders; the hypoechogenicity of the lesion suggests its suspicious nature. (Case courtesy of Anil Ahuja, M.D.)

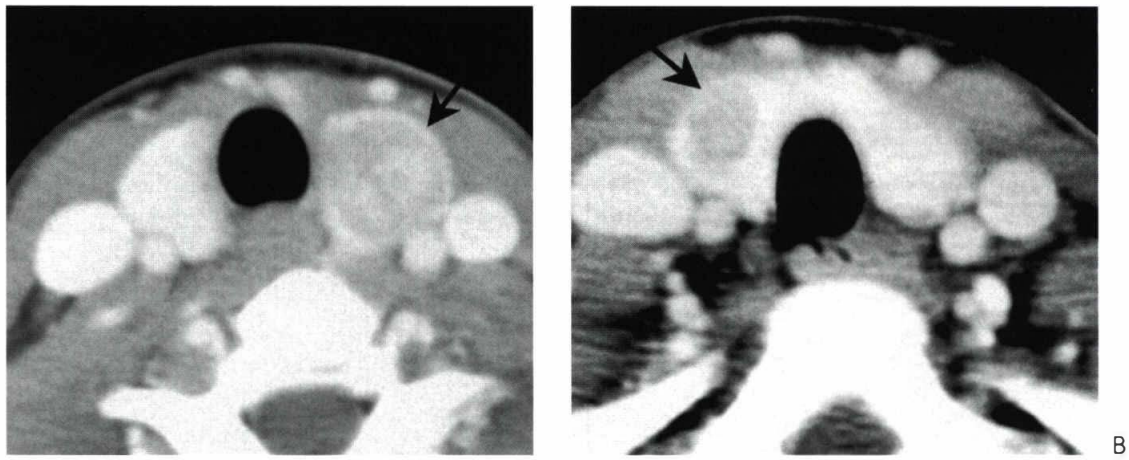

A B

Figure 115–2. Medullary thyroid carcinoma. (A) Axial contrast-enhanced CT shows a mass (arrow) involving the right lobe of the thyroid gland. (B) Contrast-enhanced CT shows a mass arising from the right lobe of the thyroid gland (arrow).

CT

The typical appearance is an intrathyroidal mass with infiltrating margins, which may show calcification and cystic components. Sporadic cases are usually unilateral, whereas familial tumors are found to be multicentric. MTC has a propensity for bone and nodal metastases. Bone metastases are seen as focal areas of bone lysis or destruction. Nodal metastases often show calcification and enhance homogeneously following administration of contrast (Fig. 115–2).

MRI

The mass appears to be hypointense on T1-weighted images and hyperintense on T2-weighted images. The increased signal on T2-weighted images has been attributed to amyloid deposition and high tumor cellularity. These tumors typically enhance following contrast. MRI is very good in delineating the extracapsular spread of the disease.

Imaging Pearls

- The imaging appearance is nonspecific. The diagnosis can be suggested if the mass is located in the upper third of the gland in the proper clinical setting.
- The diagnosis may be suggested if the patient has evidence of the systemic signs of an MEN syndrome.
- The imaging information that will directly impact the surgical management is determining where the disease is localized to one lobe or involves both lobes, describing the inferior extent of the tumor, determining the presence of tracheal or esophageal invasion. MR is probably better than CT for determining this information.

Suggested Readings

1. Lairmore TC, Wells SA Jr. Medullary carcinoma of the thyroid: current diagnosis and management. *Semin Surg Oncol* 1991;7:92–99.
2. Pombo F, Rodriguez E, Cao JI, et al. Cervical lymph node metastases of medullary thyroid carcinoma: CT findings. *Eur Radiol* 1997;7:99–101.
3. Som PM, Curtin HD. Thyroid and parathyroid. In: *Head and Neck Imaging*. 3rd ed. New York: Mosby; 1996:952–975.

Chapter 116

Follicular Thyroid Carcinoma

Epidemiology

Follicular carcinoma is a relatively uncommon thyroid malignancy that accounts for 2 to 4% of thyroid cancers. The incidence is increased in regions where iodine deficiency is endemic. When the diet is supplemented with iodine, the incidence of papillary carcinoma increases. It is believed that the majority of follicular carcinomas develop from a preexisting adenoma. Follicular carcinoma often coexists with papillary thyroid carcinoma. This tumor is more common in elderly females. Children are rarely affected.

Clinical Findings

These tumors usually present as fullness or swelling in the region of the thyroid gland. Clinical examination reveals a palpable solitary nodule. This may be associated with dysphagia or dyspnea due to pressure on the esophagus or trachea, respectively. The tumor spreads hematogeneously and metastases may occur in the bone, lungs, brain, and liver. Cervical nodal metastases disease is relatively uncommon (2–10%).

Pathology

A pure follicular carcinoma is very rare. Follicular carcinomas frequently coexist with the papillary forms. According to the Armed Forces Institute of Pathology (AFIP), a tumor is classified as a follicular carcinoma when more than 50% of the thyroid mass is composed of follicles. Capsular and vascular invasion are the features that distinguish a follicular carcinoma from its benign counterpart, a follicular adenoma. There are three histological types: encapsulated, minimally invasive, and widely invasive. The encapsulated tumor shows minimal capsular invasion without capsular penetration or vascular invasion. The minimally invasive tumor shows capsular invasion and penetration without vascular invasion. The widely invasive form shows obvious vascular invasion.

Treatment

The minimally invasive and the encapsulated subtypes are treated with lobectomy or subtotal thyroidectomy with suppression of thyroid stimulating hormone (TSH). These tumors rarely metastasize. The widely invasive type is treated with total thyroidectomy followed by radioactive iodine. It has a greater likelihood for metastatic spread (50–80%) and a high fatality rate (50%).

Imaging Findings

US

Follicular carcinoma is predominantly solid and rarely becomes cystic or necrotic. It appears homogeneous and is isoechoic to hyperechoic in half of all cases and hypoechoic in the other half. A capsular halo has been reported in 80% of cases. Doppler imaging shows that the majority of benign lesions show a perinodular vascularity, and malignant lesions demonstrate chaotic intranodular vascularity (Fig. 116-1).

Nuclear Medicine Study

The agents used for thyroid imaging include iodine 123, iodine 131, technetium 99m pertechnetate, and thallium 201. These tumors usually present as a cold nodule. The risk of malignancy in a cold nodule is 15 to 25%; in a hot nodule, 1 to 4%; and in a warm nodule, 8 to 10%.

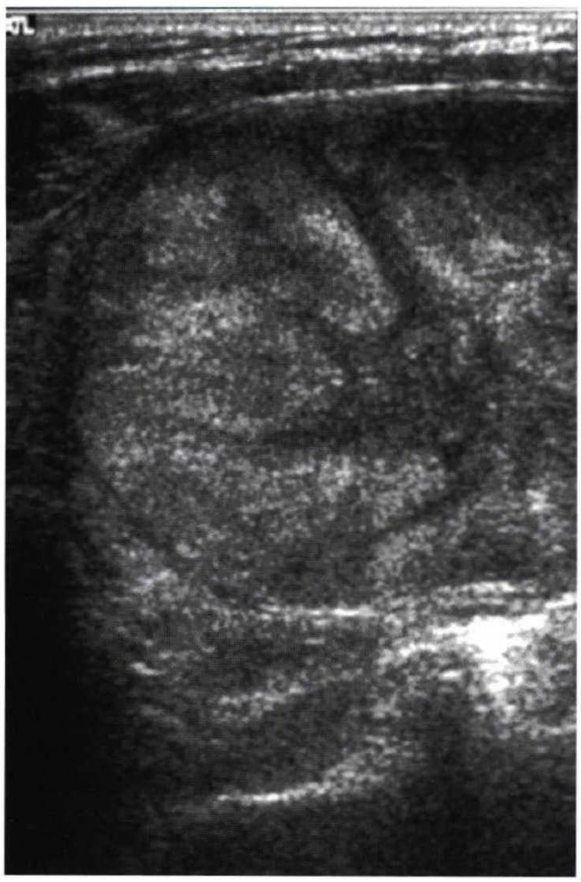

Figure 116–1. Transverse sonogram, showing a solid, heterogeneous, isoechoic, noncalcified thyroid nodule. This patient presented with skeletal metastases of thyroid origin. The nodule was confirmed to be a follicular carcinoma. (Case courtesy of Anil Ahuja, M.D.)

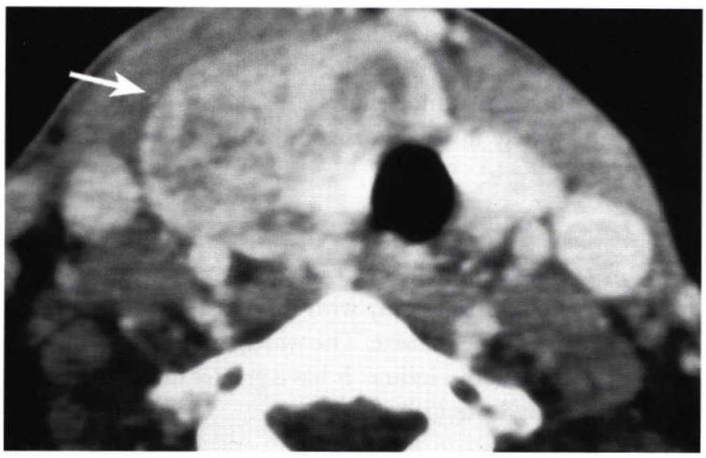

Figure 116–2. Axial contrast-enhanced CT shows a heterogeneously enhancing mass located in the right lobe of the thyroid gland (arrow). The mass extends to the midline but does not appear to involve the left lobe. Pathology revealed follicular cell carcinoma.

CT

The imaging features are nonspecific. The tumor is typically seen as a solitary, ill-defined intrathyroidal mass that is low attenuation on noncontrast CT. The nodule usually mildly enhances following contrast administration. Cystic or necrotic areas are unusual. Calcification within the tumor may be present. Advanced tumors may spread outside the thyroid gland to involve the adjacent soft tissues and great vessels (Fig. 116–2).

MRI

These tumors often present as an ill-defined mass that is hypointense on T1-weighted images and high signal on T2-weighted scans. It rarely shows necrotic or calcific areas. The tumors enhance following contrast administration.

Imaging Pearls

- The diagnosis is based on histologic evaluation of the entire specimen and usually cannot be made on fine needle aspiration. This has led some authors to use the term *follicular lesions* to include both the benign and the malignant counterparts.
- The diagnosis of a malignant lesion can be suggested on ultrasound if the lesion is ill defined, hypoechoic with heterogeneous internal echoes. Other signs suggesting malignancy include adjacent vascular invasion, extracapsular spread, and a thick irregular capsule.
- MR is the study of choice in advanced lesions for evaluation of extraglandular spread and invasion of adjacent structures.

Suggested Readings

1. Yousem DM, Scheff AM. Thyroid and parathyroid. In: Som PM, Curtin H, eds. *Head and Neck Imaging*. 3rd ed. New York: Mosby; 1996:952–974.
2. Rumack CM, Wilson SR, Charboneau JW. The thyroid. In: Rumack CM, Wilson SR, Charboneau JW. eds. *Diagnostic Ultrasound*. Vol. 1. New York: Mosby; 1991:509–516.
3. Ahuja AT. The thyroid and parathyroids. In: Ahuja A, Evans R, eds. *Practical Head and Neck Ultrasound*. London: Greenwich Medical Media Limited; 2000:37–66.

Chapter 117

Papillary Thyroid Carcinoma

Epidemiology

Papillary thyroid carcinoma is the most common thyroid neoplasm and accounts for 55 to 80% of all thyroid malignancies. Females are generally more commonly affected than males (2.5:1). The most common age at presentation is most often between 20 and 40 years. Papillary thyroid carcinoma has the highest incidence of cervical metastases among the thyroid malignancies. Almost 50% of cases have cervical nodal metastases at the time of presentation. It has been suggested that there is an increased incidence of papillary carcinoma in patients with Graves' disease but this has not been proven definitively.

Clinical Findings

Patients generally present with an indolent, slowly growing, lower neck mass. Large masses can cause breathing or swallowing problems due to tracheal or esophageal compression. Pressure on the recurrent laryngeal nerve may cause hoarseness and aspiration secondary to vocal cord malfunction.

Pathology

On gross examination, the tumor may have a varied appearance and be solid or cystic. It can be encapsulated and well defined or infiltrative. Histological examination shows psammoma bodies, ground glass nuclei, and a branching pattern with a fibrovascular papillary stroma. When present, psammoma bodies are considered pathognomonic of papillary carcinoma of the thyroid. Histologically, they are seen as calcific concretions with well-defined concentric laminations that develop around a nidus of a necrotic cell. Follicular growth patterns may coexist with papillary thyroid carcinoma.

Treatment

Total thyroidectomy followed by iodine 131 radiotherapy is generally the treatment of choice. Lobectomy or subtotal thyroidectomy followed by suppression with thyroid stimulating hormone therapy is another accepted treatment option. Papillary carcinoma has the best prognosis among the cell types of thyroid malignancies.

Imaging

US

These are predominantly hypoechoic, ill-defined lesions with irregular borders. The majority are mostly solid, however 20 to 30% may have a cystic component. The presence of punctate calcification is highly specific for papillary carcinoma and likely represents psammoma bodies. Doppler imaging suggests that the majority of tumors show chaotically arranged vessels within the mass (Fig. 117-1).

Nuclear Medicine Study

The agents used for thyroid imaging include iodine 123, iodine 131, technetium 99m pertechnetate, and thallium 201.The risk of cancer in a cold nodule is 15 to 25%; in a hot nodule, 1 to 4%; and in a warm nodule, 8 to 10%. Distant metastases in the lungs and liver may be assessed with scintigraphic studies.

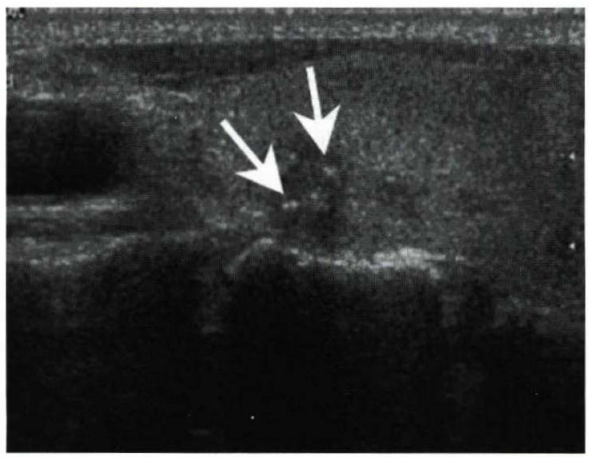

Figure 117-1. Longitudinal sonogram, showing an ill-defined, solid, hypoechoic nodule with multiple echogenic foci of punctate calcification (arrows), which represent psammoma bodies, and are suggstive of papillary carcinoma. (Case courtesy of Anil Ahuja, M.D.)

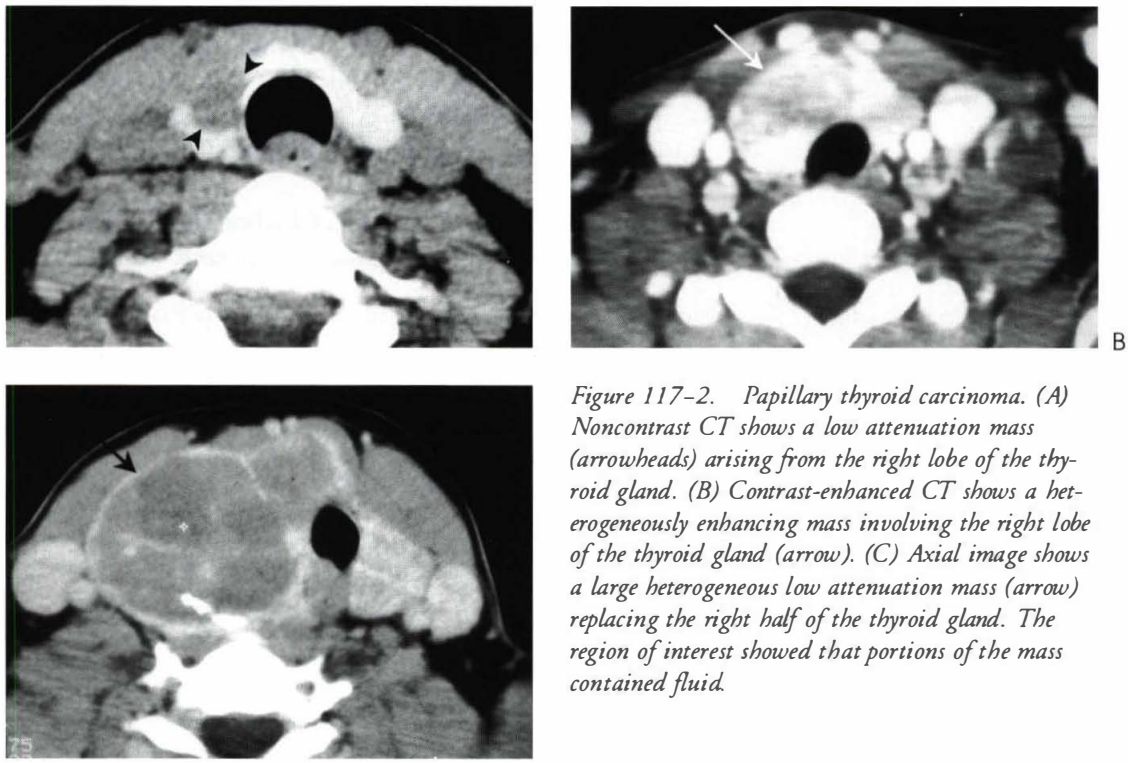

Figure 117-2. Papillary thyroid carcinoma. (A) Noncontrast CT shows a low attenuation mass (arrowheads) arising from the right lobe of the thyroid gland. (B) Contrast-enhanced CT shows a heterogeneously enhancing mass involving the right lobe of the thyroid gland (arrow). (C) Axial image shows a large heterogeneous low attenuation mass (arrow) replacing the right half of the thyroid gland. The region of interest showed that portions of the mass contained fluid.

CT

On CT the tumor is seen as an intrathyroidal mass with infiltrating margins, which may show calcification and cystic components. A mass with well-defined margins does not necessarily exclude a thyroid malignancy. Papillary carcinoma may be multicentric in 20% of cases. When present, associated cervical adenopathy favors the diagnosis of a malignant thyroid mass. The nodal metastases may show multiple discrete calcifications or may even appear as cystic lesions. The nodal metastases may also be hypervascular or have areas of high attenuation due to intranodal hemorrhage or high concentration of thyroglobulin (Fig. 117-2).

MRI

The mass appears to be hypointense on T1-weighted images and turns bright on T2-weighted images. The nodal metastases have a varied appearance and may range from densely enhancing masses to cystic lesions on T2-weighted sequences. A high concentration of thyroglobulin in the nodes may increase the signal on T1-weighted images.

Imaging Pearls

- Contrast-enhanced CT is not recommended in the evaluation of thyroid malignancy because iodine can take months to clear from the patient's system and thereby postpone iodine-131 therapy. Thus it is helpful to integrate preoperative imaging studies with potential treatment options.
- The appearance of cervical nodal metastases of papillary thyroid carcinoma is very variable. The suggestion of a primary papillary thyroid carcinoma should be considered in patients with densely enhancing enlarged or cystic lymph nodes in whom a primary tumor has not been identified.
- The imaging information that will directly impact surgical management is determining whether the disease is localized to one lobe or involves both lobes, describing the inferior extent of the tumor, and determining the presence of tracheal or esophageal invasion. MR is probably better than CT for determining this information.

Suggested Readings

1. Yousem DM, Scheff AM. Thyroid and parathyroid. In: Som PM, Curtin HD, eds. *Head and Neck Imaging*. 3rd ed. New York: Mosby; 1996:952–974.
2. Som PM, Brandwein M, Lidov M, et al. The varied presentations of papillary thyroid carcinoma cervical nodal disease: CT and MR findings. *AJNR Am J Neuroradiol* 1994;15:1123–1128.
3. Rumack CM, Wilson SR, Charboneau JW. The thyroid. In: Rumack CM, Wilson SR, Charboneau JW. *Diagnostic Ultrasound*. Vol. 1. Chicago: Mosby; 1991:509–516.

Chapter 118

Anaplastic Thyroid Carcinoma

Epidemiology

Anaplastic thyroid cancer is one of the most aggressive malignancies of the head and neck. It constitutes almost 10% of all thyroid cancers. It occurs in older adults and is more common in females than in males. About 50% of anaplastic thyroid carcinomas are believed to arise in goiters and often coexist with other forms of thyroid cancer.

Clinical Features

Patients usually present with a rapidly enlarging thyroid mass. Other commonly associated symptoms include dyspnea, dysphagia, and hoarseness of voice due to pressure or invasion of the recurrent laryngeal nerve. Nodal or distant metastases occur in 80% of patients.

Pathology

Grossly, the tumor appears as a large firm mass with necrotic and hemorrhagic areas. It frequently replaces the entire thyroid gland and invades the surrounding soft tissues. Histologically, three morphological patterns are seen. These include the spindle cell, giant cell, and squamoid patterns. These patterns may often coexist. Cellular pleomorphism, high mitotic activity, necrosis, and pronounced invasiveness are typical histological findings.

Treatment

Total thyroidectomy followed by radiotherapy and chemotherapy is the most accepted form of treatment.

Imaging

US

The tumor is predominantly a large hypoechoic mass that replaces the involved lobe. The mass is often heterogeneous and frequently shows calcification (58%) and necrosis (78%) within.

Nuclear Medicine Study

The agents used for thyroid imaging include iodine 123, iodine 131, technetium 99m pertechnetate, and thallium 201. The mass usually presents as a cold nodule. The risk of malignancy in a cold nodule is 15 to 25%; in a hot nodule, 1 to 4%; and in a warm nodule, 8 to 10%.

CT

The typical appearance is a very aggressive mass that often replaces the thyroid gland and extends into the adjacent soft tissue. Involvement of the adjacent soft tissue structures is present in 30 to 50% of cases. These tumors are typically heterogeneous and contain both solid and cystic components. The solid components typically enhance following contrast administration. About 50% of cases may contain dystrophic calcification. Associated metastatic cervical adenopathy is fairly common. Fifty percent of the metastatic nodes show necrotic areas (Figs. 118–1 and 118–2).

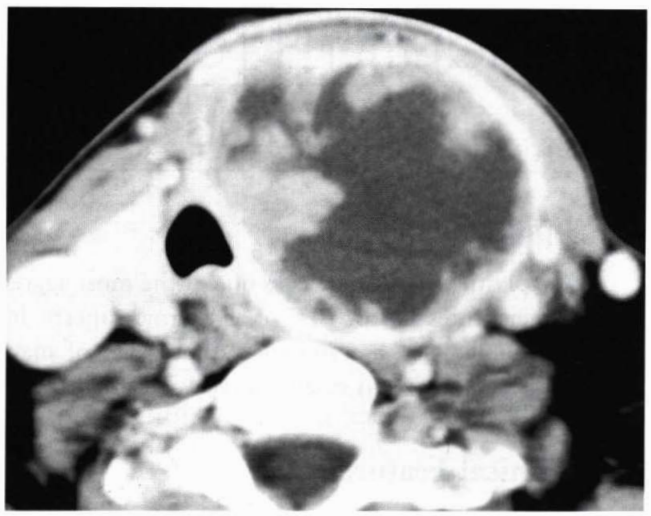

Figure 118–1. Axial contrast CT reveals a very necrotic anaplastic thyroid carcinoma replacing the left lobe of the thyroid gland.

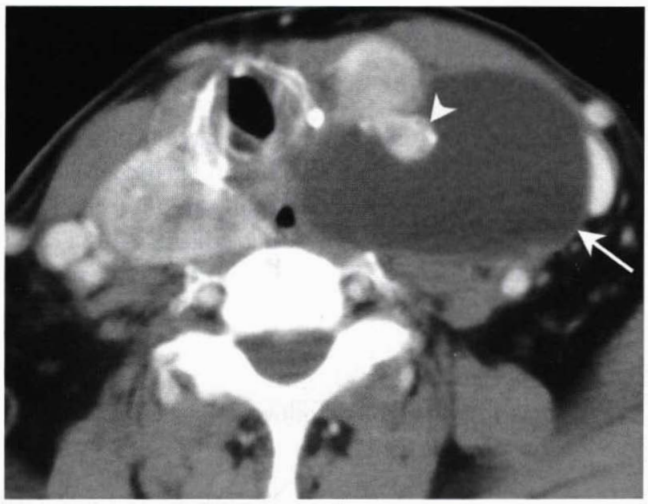

Figure 118–2. Contrast-enhanced CT shows a cystic mass (arrow) with a peripheral enhancing nodule (arrowhead) arising from the left lobe of the thyroid gland. Pathology revealed anaplastic thyroid carcinoma.

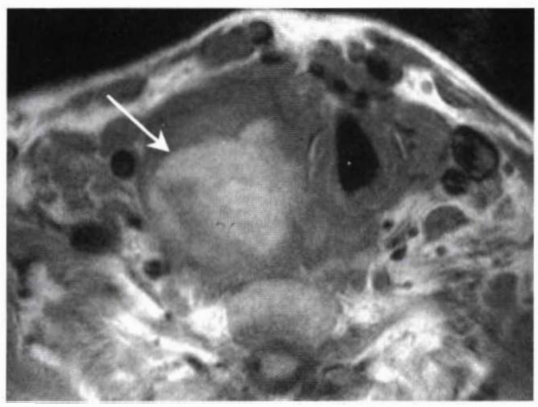

A

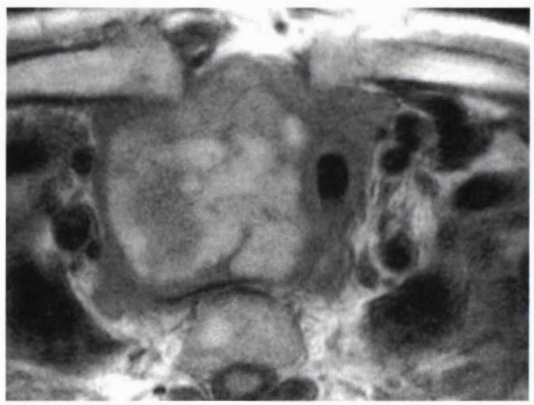

B

Figure 118–3. (A) Axial noncontrast T1-weighted sequence obtained at the base of the cricoid cartilage shows a large mass that contains high signal (arrow). (B) The mass extends inferiorly to the thoracic inlet. Pathology revealed anaplastic thyroid carcinoma.

MR

MR shows an aggressive mass with irregular and ill-defined margins that is hypointense on the T1-weighted images and high signal T2-weighted sequences. The solid components of the tumors densely enhance following intravenous contrast. The tumors are typically heterogeneous. The heterogeneity is attributed to calcification, hemorrhage, and necrosis (Fig. 118–3).

Imaging Pearls

- The diagnosis can be suggested by the presence of an aggressive heterogeneous mass at the level of the thyroid gland in a patient with a rapidly enlarging neck mass.
- These tumors often completely replace the thyroid gland.
- It is essential to determine if there is invasion of the trachea, esophagus, or carotid artery and to identify the inferior extent of disease. MR is the study of choice for evaluating these specific areas.

Suggested Readings

1. Yousem DM, Scheff AM. Thyroid and parathyroid. In: Som PM, Curtin HD, eds. *Head and Neck Imaging*. 3rd ed. New York: Mosby; 1996:952–974.
2. Rumack CM, Wilson SR, Charboneau JW. The thyroid. In: Rumack CM, Wilson SR, Charboneau JW, eds. *Diagnostic Ultrasound*, Vol 1. St. Louis: Mosby; 1991:509–516.
3. Ahuja AT. The thyroid and parathyroids. In: Ahuja A, Evans R, eds. *Practical Head and Neck Ultrasound*. London: Greenwich Medical Media Limited; 2000:37–66.

Chapter 119

Thyroid Metastasis

Epidemiology

Metastasis to the thyroid gland is rare but well documented. The thyroid gland is the second most richly vascularized organ, with a blood flow of 560 mL/100 g of tissue/minute. Compared with other organs, it is relatively immune to secondary deposits. The most common sites of origin are the kidney, breast, lung, and skin (melanoma), which account for 70% of reported cases. Colonic, prostate, or nasopharyngeal carcinoma metastases in the thyroid gland have also been documented.

Clinical Findings

Thyroid metastasis may present as a mass; difficulty in breathing, swallowing, or talking; or stridor. Clinical examination may reveal a thyroid mass whereas endoscopic examination may show tumor within the larynx as a result of extrathyroid spread.

Pathology

The incidence of metastasis documented at autopsy is much higher than that suggested by clinical findings. Approximately 10% of patients who died of malignancy have secondary lesions in the thyroid gland. These lesions were mainly microscopic but 42% were evident macroscopically. Renal and malignant melanoma tend to produce discrete nodules; carcinoma of the bronchus, a solitary nodule; and breast carcinoma, a diffuse pattern. However, the pattern of involvement appears to be more closely related to the stage of the disease than to the site of the primary neoplasm.

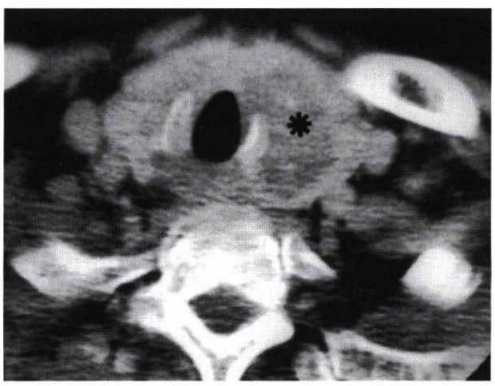

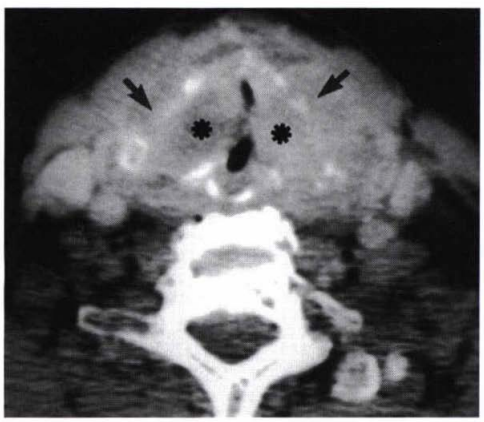

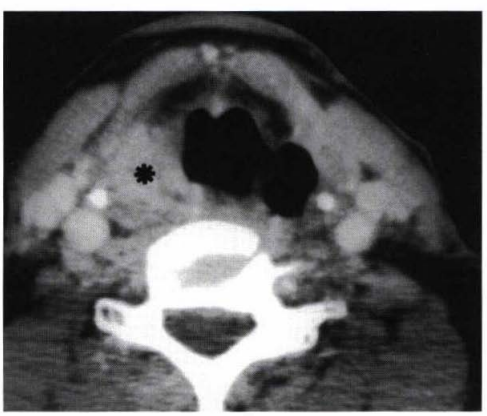

Figure 119-1. Rectal carcinoma with thyroid and laryngeal metastasis. (A) Axial contrast-enhanced CT shows diffuse infiltration of the thyroid gland (asterisk) from rectal carcinoma. (B) Axial contrast-enhanced CT superior to (A) shows diffuse infiltrates eroding the thyroid cartilage (arrows) and thickening of the glottis bilaterally (asterisks). (C) Axial contrast-enhanced CT superior to (B) shows mass in the right pyriform sinus mimicking a primary tumor (asterisk).

Color Plates

Color Plate I-1. Schematic illustration of the masticator space (see Fig. I-1). (Figure reproduced with permission from Mukherji SK, Castillo M. A simplified approach to the spaces of the suprahyoid neck. Rad. Clin N Am *1998;36:761-780.)*

Masticator

Color Plate II-1. Schematic illustration shows the location of the parotid gland (see Fig. II-1). (Figure reproduced with permission from Mukherji SK, Castillo M. A simplified approach to the spaces of the suprahyoid neck. Rad. Clin N Am *1998;36:761-780.)*

Parotid

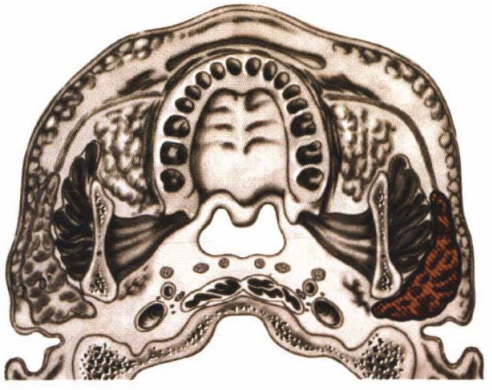

Color Plate III-1. (A) Schematic illustration of the visceral space (arrows) (see Fig. III-1A) along with (B) correlative CT and (C) MR images. (Figure reproduced with permission from Mukherji SK, Castillo M. A simplified approach to the spaces of the suprahyoid neck. Rad. Clin N Am *1998;36:761-780.)*

Visceral

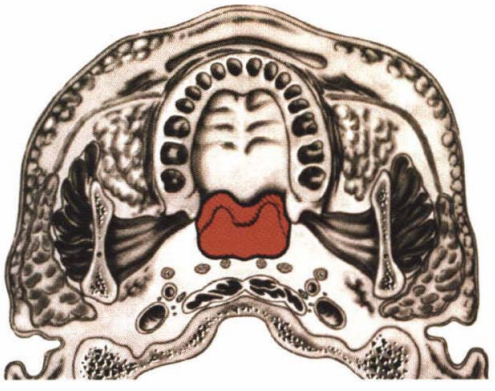

Color Plate IV-1. Schematic illustration shows the normal location of the retropharyngeal space. Solid line = visceral fascia, long-dash line = alar fascia, short-dash line = prevertebral fascia (see Fig. IV-1).
(Figure reproduced with permission from Mukherji SK, Castillo M. A simplified approach to the spaces of the suprahyoid neck. Rad. Clin N Am *1998;36:761-780.)*

Retropharyngeal

Pre-vertebral (Perivertebral Space)

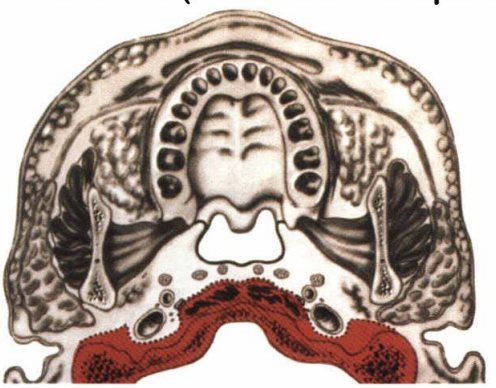

Color Plate V-1. Schematic illustration demonstrates the location of the pre-vertebral space (see Fig. V-1). (Figure reproduced with permission from Mukherji SK, Castillo M. A simplified approach to the spaces of the suprahyoid neck. Rad. Clin N Am *1998;36:761-780.)*

Parapharyngeal
(Pre-styloid Parapharyngeal)

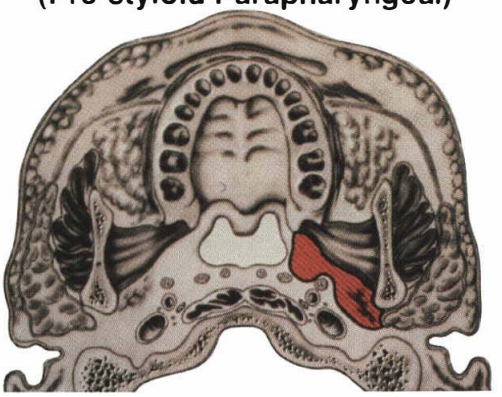

Color Plate VI-1. Schematic illustration demonstrates the location of the parapharyngeal space (see Fig. VI-1). (Figure reproduced with permission from Mukherji SK, Castillo M. A simplified approach to the spaces of the suprahyoid neck. Rad. Clin N Am *1998;36:761-780.)*

Carotid Sheath
(Carotid, Post-styloid Parapharyngeal)

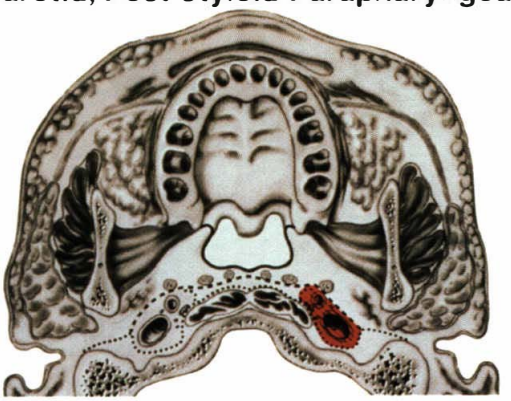

Color Plate VII-1. Schematic illustration deomonstrates the location of the "carotid space" ("carotid sheath", "poststyloid parapharyngeal space") (see Fig. VII-1) (Figure reproduced with permission from Mukherji SK, Castillo M. A simplified approach to the spaces of the suprahyoid neck. Rad. Clin N Am *1998;36:761-780.)*

Buccal

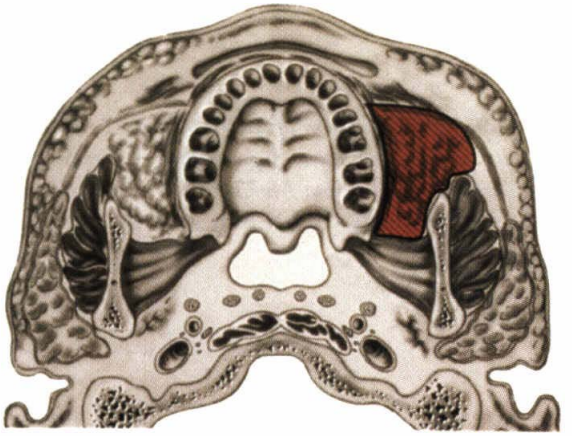

Color Plate VIII-1. Schematic illustration of the buccal space (see Fig. VIII-1) (Figure reproduced with permission from Mukherji SK, Castillo M. A simplified approach to the spaces of the suprahyoid neck. Rad Clin N Am *1998;36:761-780.)*

Color Plate 205-1. Schematic illustration of the cervical lymph nodes. The level I lymph nodes are shaded (see Fig. 205-1). (Reproduced with permission from Mukherji SK, Armao DM, Joshi VM. Cervical nodal metastases in squamous cell carcinoma of the head and neck: what to expect. Head Neck. *2001;23:995-1005.)*

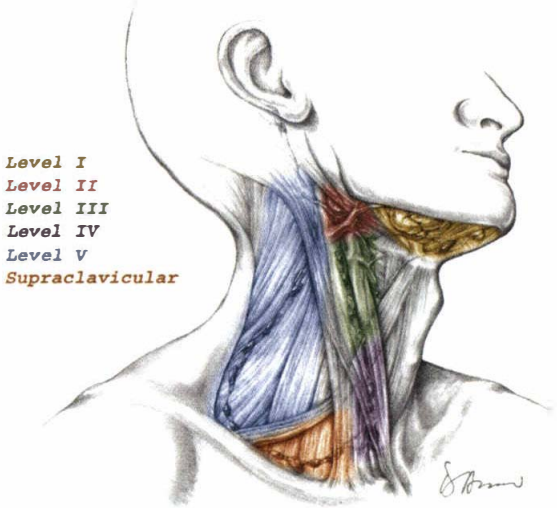

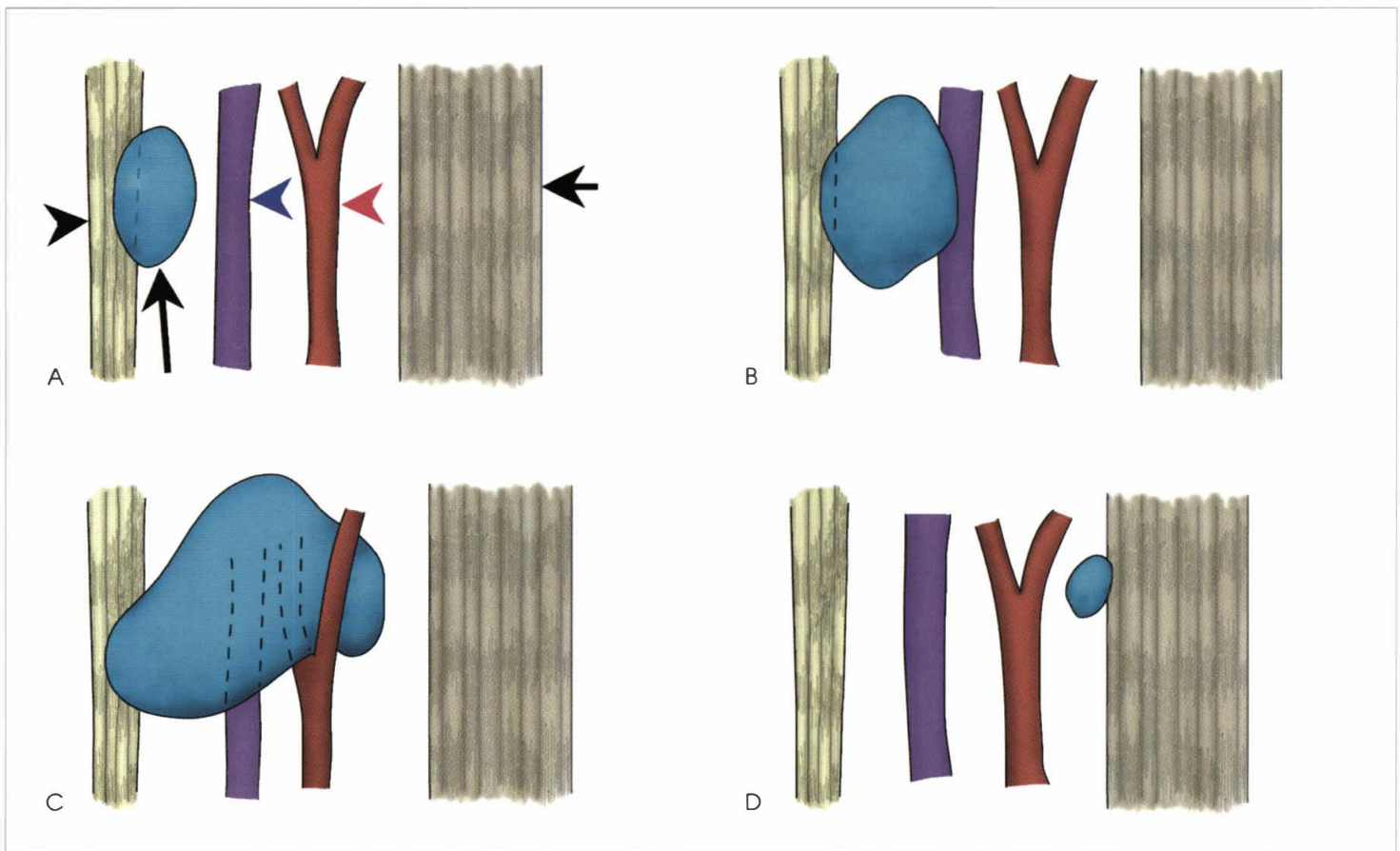

Color Plate 209-1. Schematic illustrations of the subclassification of second branchial cleft cysts as proposed by Bailey. Black arrowhead, platysma muscle; long black arrow, cyst; short black arrow, viscera; blue arrow, jugular vein; red arrowhead, carotid artery. (A) Type 1. (B) Type 2. (C) Type 3. (D) Type 4 (see Fig. 209-1). (Reproduced with permission from Mukherji SK, Fatterpekar G, Castillo M, Stone JA, Chung CJ. Imaging of the congenital anomalies of the brachial apparatus. Neuroimaging Clin N Am. *2000;10:75-93.)*

Treatment

A mass appearing in the thyroid gland in a patient with a known malignancy elsewhere is more likely a secondary lesion than a primary neoplasm. Clinical awareness is important because unnecessary thyroidectomy can be avoided and early appropriate therapy instituted. Thyroid metastasis may be treated with chemotherapy, radiation therapy, or both depending on the site of the primary lesion.

Imaging Findings

CT

Imaging cannot distinguish between a primary thyroid neoplasm from a metastatic mass. Contrast-enhanced CT may show discrete nodular lesions or diffusely infiltrating disease. The metastatic lesions may spread to involve the thyroid cartilage and soft tissues of the larynx. Involvement of the trachea may also be demonstrated (Fig. 119-1).

MR

The MR imaging features of metastatic disease in the thyroid gland show intermediate signal intensity on T1-weighted images, good contrast enhancement, and high signals on T2-weighted images. Vascular metastasis such as renal secondaries or melanomas may show high signals on both T1- and T2-weighted images.

Imaging Pearls

- Metastasis involving the thyroid gland and the larynx is unusual. However, metastasis should be considered in patients with a known history of malignancy presenting with a thyroid mass.

Suggested Readings

1. Czech JM, Lichtor TR, Carney JA, van Heerden JA. Neoplasms metastatic to the thyroid gland. *Surg Gynecol Obstet* 1982;155:503-505.
2. Watts NB. Carcinoma metastatic to the thyroid: prevalence and diagnosis by fine-needle aspiration cytology. *Am J Med Sci* 1987;293:13-17.
3. Brady LW, O'Neill EA, Farber SH. Unusual sites of metastases. *Semin Oncol* 1977;4:59-64.
4. Chong VF, ChanYM, Sng I. Metastasis to the thyroid gland with laryngeal involvement. *AJR Am J Radiol* 1996;167:1071-1072.

Chapter 120

Thyroid Lymphoma

Epidemiology

Thyroid lymphoma constitutes 4% of all thyroid malignancies. It may arise primarily from the thyroid or involve the gland as part of a systemic disease. It is much more common in elderly women. The majority of patients with thyroid lymphoma have a history of Hashimoto's thyroiditis.

Clinical Features

Patients generally present with a rapidly enlarging mass in the lower neck. Large masses can cause breathing or swallowing problems due to tracheal or esophageal compression. Pressure on the recurrent laryngeal nerve may cause hoarseness or aspiration secondary to vocal cord malfunction.

Pathology

The tumor is usually a B cell non-Hodgkin's lymphoma. Lymphomatous involvement of the thyroid may be focal or diffuse. Grossly, the tumor appears as a firm, lobulated mass. Extension into the surrounding tissues occurs in 50 to 60% of cases. On histologic examination, the tumor is usually a diffuse large cell type. Low-grade lymphomas are less frequent and are usually the small cell type variant.

Treatment

Radiation therapy with or without chemotherapy is the most accepted form of treatment. Surgical resection is not recommended.

Imaging

US

On ultrasonography, the tumor may present as a focal mass or diffuse replacement of the thyroid gland. The tumor is typically diffusely hypoechoic. Calcific foci or necrotic areas are rare.

Nuclear Medicine Study

The agents used for thyroid imaging include iodine 123, iodine 131, technetium 99m pertechnetate, and thallium 201. Lymphoma is cold on technetium and iodine scans. However gallium scans may show increased activity.

CT

Thyroid lymphoma may be seen as a focal solitary mass, multiple thyroid nodules, or diffuse enlargement of the thyroid gland. The tumor appears as low attenuation on noncontrast CT. These tumors moderately enhance following contrast administration. Calcification and necrosis are unusual and are seen in $< 10\%$ of cases. Vascular invasion may be present in up to 25% of cases. There is usually associated cervical lymphadenopathy. The involved nodes are typically homogeneously enlarged without necrosis or calcification (Fig. 120–1).

MR

Thyroid lymphoma is usually isointense on T1-weighted images and turns homogeneously bright on T2-weighted scans. These lesions enhance following contrast administration. Necrotic or calcific areas are rarely seen within the tumor. Associated cervical adenopathy also shows homogeneously bright signal on T2-weighted scans.

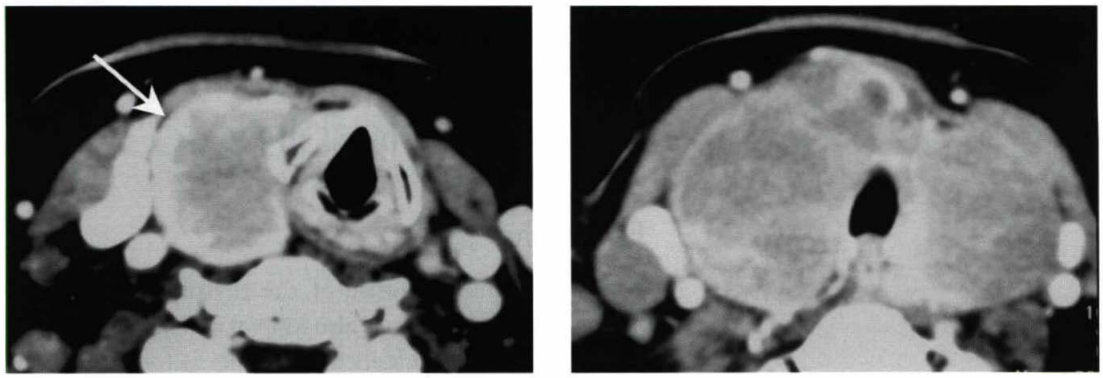

Figure 120–1. (A) Axial contrast-enhanced CT obtained in a patient with Hashimoto's thyroiditis shows a large mass involving the right lobe of the thyroid gland (arrow). (B) Images obtained at a lower level in the same patient show diffuse enlargement of the thyroid gland by the relatively homogeneous mass. Biopsy of the mass revealed lymphoma.

Imaging Pearls

- The diagnosis should be considered if the thyroid gland is diffusely enlarged without evidence of focal masses. However, this appearance may be indistinguishable from diffuse enlargement caused by a homogeneous thyroid goiter.
- The presence of enlarged lymph nodes supports the diagnosis of thyroid lymphoma.
- MRI is the study of choice for evaluating spread outside the thyroid gland and invasion of adjacent structures.

Suggested Readings

1. Takashima S, Nomura N, Noguchi Y, et al. Primary thyroid lymphoma: evaluation with US, CT and MRI. *J Comput Assist Tomogr* 1995;19:282–288.
2. Shibata T, Noma S, Nakano Y, et al. Primary thyroid lymphoma: MR appearance. *J Comput Assist Tomogr* 1991;15:629–633.
3. Yousem DM, Scheff AM. Thyroid and parathyroid. In: *Head and Neck Imaging*. Vol. 2 :952–974.

Chapter 121

Hashimoto's Thyroiditis

Epidemiology

This autoimmune disease of the thyroid gland is the most common form of chronic thyroiditis. The disease is also known as "chronic lymphocytic thyroiditis" and "lymphadenoid goiter." The incidence in females is four to five times more common than in males. The disease is most common in the fifth and sixth decades of life and increases in incidence with increasing age. There is a strong association between Hashimoto's disease and primary thyroid lymphoma. The majority of patients with thyroid lymphoma have coexistent Hashimoto's thyroiditis, and a small proportion of patients with Hashimoto's thyroiditis develop primary thyroid lymphoma. Other disorders that may be associated with Hashimoto's disease include Sjögren's syndrome, chronic active hepatitis, systemic lupus erythematosus, rheumatoid arthritis, adrenal insufficiency (Schmidt's syndrome), diabetes mellitus, opathic thrombocytopenia, pernicious anemia, and Graves' disease.

Clinical Findings

There are two clinical forms of the disease. In one type ("atrophic form"), the gland is normal or reduced in size and the patients are hypothyroid. This may be the same syndrome as idiopathic myxedema.

The second form is characterized by variable degrees of thyroid enlargement and patients complain of signs and symptoms associated with a goiter. The gland is symmetrically enlarged and firm on palpation. Patients are typically hypothyroid and may have a family history of Graves' or Hashimoto's disease.

Pathology

The sera of affected patients contain antibodies to one or more thyroid antigens, which include thyroid microsomes, thyroglobulin, or other colloid antigens. Microscopic examination reveals varying degrees of fibrosis and infiltration by lymphocytes. It may be difficult to differentiate Hashimoto's disease from thyroid lymphoma.

Treatment

The treatment is based on the degree of hypothyroidism. Occasionally, patients with Hashimoto's disease may present with hyperthyroidism ("hashitoxicosis") and are treated as Graves' disease.

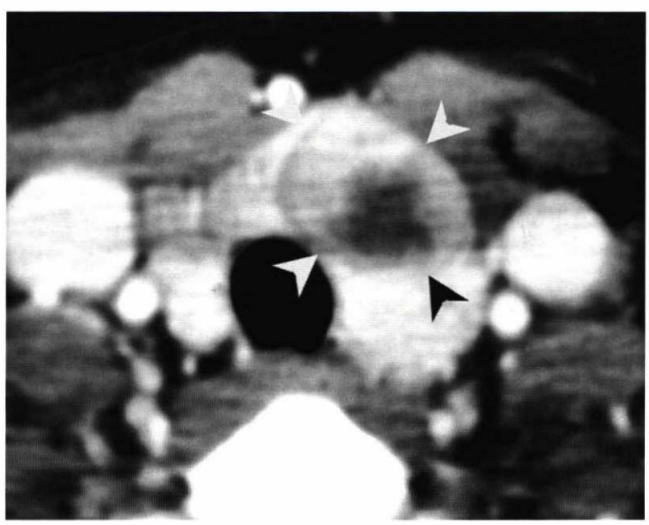

Figure 121–1. Axial contrast-enhanced CT demonstrates a focal heterogeneous mass (arrowheads) involving the left lobe of the thyroid gland and extending to the midline. Biopsy revealed Hashimoto's disease.

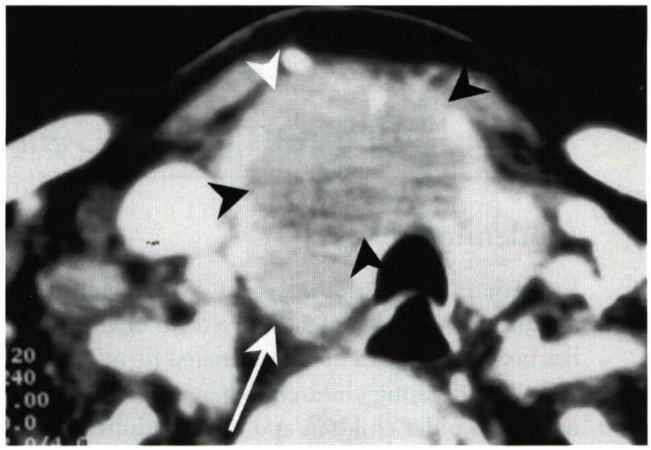

Figure 121-2. Contrast-enhanced CT shows diffuse enlargement of the right lobe of the thyroid gland. (arrow) Within the right lobe, there is mass that does not enhance to the same degree as the remainder of the thyroid gland (arrowheads). Pathology demonstrated Hashimoto's disease with coexistent lymphoma.

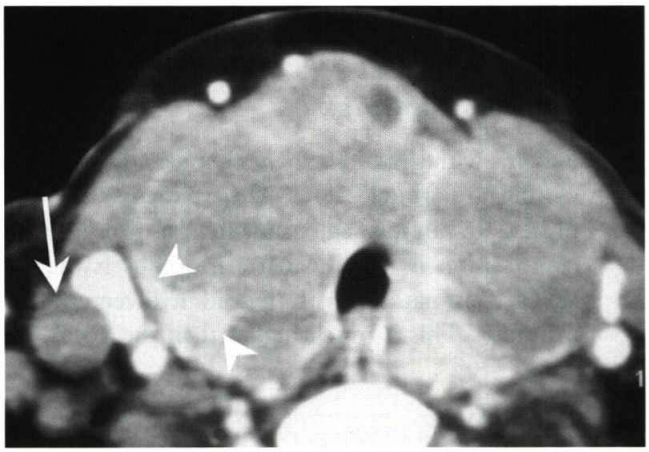

Figure 121-3. Axial CT performed after intravenous contrast demonstrates replacement of the normal thyroid gland (arrowheads) by a large, relatively homogeneously enhancing mass. Surgery revealed Hashimoto's disease with coexistent thyroid lymphoma. The arrow indicates an enlarged cervical lymph node due to lymphomatous involvement.

Imaging Findings

CT

The gland is typically symmetrically enlarged, and homogeneously enhances with contrast. However, focal areas of Hashimoto's disease can mimic a thyroid adenoma or carcinoma. Advanced cases may result in narrowing of the trachea (Figs. 121-1 to 121-3).

MR

The enlarged gland is usually intermediate signal on T1-weighted images and homogeneously enhances with contrast. The gland is typically increased signal on T2-weighted images.

Imaging Pearls

- The diagnosis of Hashimoto's disease can be suggested in patients with a diffusely enlarged thyroid gland that homogeneously enhances with contrast.
- It is difficult to differentiate coexistent thyroid lymphoma occurring in a patient with Hashimoto's disease unless one identifies a focal mass within the thyroid gland. Takashima et al suggest that MR signal intensity ratios may help make this differentiation.

Suggested Readings

1. Larsen PR. The thyroid. In: Wyngaarden JB, Smith LH, eds. *Cecil Textbook of Medicine.* 17th ed. Philadelphia: WB Saunders; 1985:1293–1294.
2. Takashima S, Fukuda H, Tomiyama N, Fujita N, Iwatani Y, Nakamura H. Hashimoto thyroiditis: correlation of MR imaging signal intensity with histopathologic findings and thyroid function test results. *Radiology* 1995;197:213–219.
3. Higgins CB, McNamara MT, Fisher MR, Clark OH. MR imaging of the thyroid. *AJR Am J Roentgol* 1986;147:1255–1261.

Chapter 122

Langerhans Cell Histiocytosis

Epidemiology

Langerhans cell histiocytosis (LCH), previously known as histiocytosis X, is believed to be an autoimmune disorder. There is no obvious sex predilection although familial incidence has been reported. The disseminated form of this disease (Letterer-Siwe disease) is found in infants and young children, whereas the localized form (eosinophilic granuloma) is found mainly in older children and young adults. Between these forms is an intermediate group called Hand-Schüller-Christian disease. LCH with involvement of the thyroid gland is uncommon. Until 1991, there were only 10 such patients reported in the English literature. An English literature search through 1995 revealed a further six reports.

Clinical Findings

Patients with thyroid involvement usually have associated multiple organ involvement such as lung and orbital lesions. These patients may also have severe seborrhea or maculopapular rashes. Respiratory embarrassment as a result of thyroid gland enlargement and tracheal compression is rare. Diabetes insipidus is the most common endocrine abnormality in LCH. Most patients with thyroid involvement (80%) appear to have concomitant diabetes insipidus. This is much higher than the 20 to 50% generally reported in LCH.

Pathology

LCH is characterized by the proliferation of Langerhans cells of marrow origin. These cells have abundant vacuolated cytoplasm with vesicular oval or indented nuclei. These cells show HX bodies (Birbeck granules) in the cytoplasm and they are variably admixed with eosinophils, lymphocytes, plasma cells, and neutrophils. The eosinophil component ranges from a few scattered cells to masslike sheets.

Treatment

Localized LCH (usually involving bone) has an excellent prognosis, and treatment consists of curettage. The prognosis of the disseminated form depends on age, organ dysfunction, and the response to treatment. Chemotherapy, radiation therapy, or both can be used to treat the chronic disseminated form. Patients with disseminated lesions confined to bone have a good prognosis, whereas more than half the patients with multiple system involvement have long-term sequelae such as diabetes insipidus, neurological deficits, and chronic lung disease. Acute disseminated disease responds poorly to treatment and often shows a rapid fatal outcome.

Imaging Findings

CT

CT findings of thyroid involvement are nonspecific. The thyroid gland shows diffuse enlargement and enhances well following the administration of contrast. The trachea may show deviation or compression. CT features in the lungs include nodules, cysts, pneumothorax, and hazy ground-glass opacities (Fig. 122–1).

MR

MR findings in the thyroid have not been well described largely because of the rarity of this entity. However, lesions in the hypothalamus have been well documented on both CT and MR imaging. Thickening of the pituitary stalk and enhancing hypothalamic mass bulging into the basal cistern may be seen in association with thyroid disease.

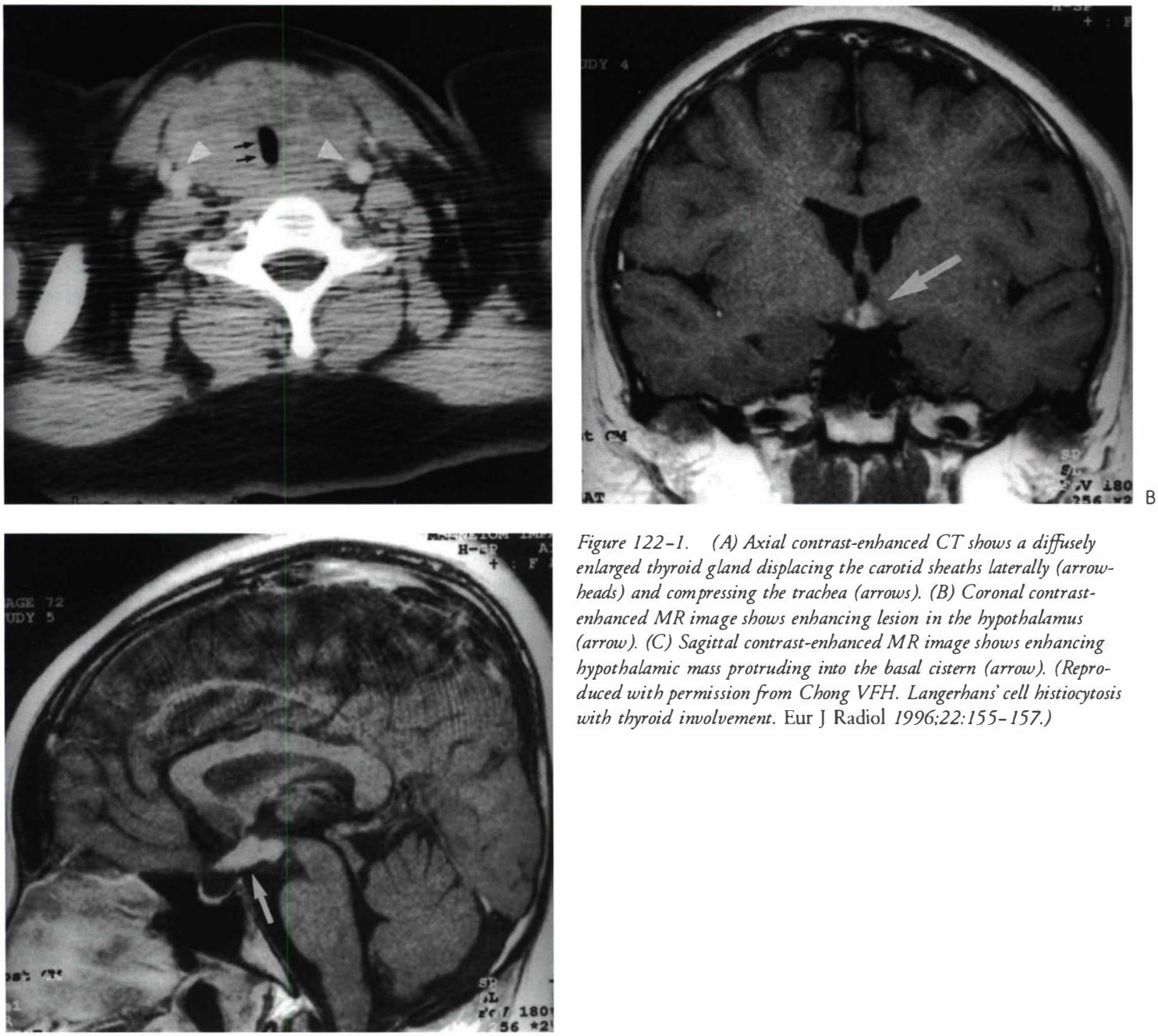

Figure 122-1. (A) Axial contrast-enhanced CT shows a diffusely enlarged thyroid gland displacing the carotid sheaths laterally (arrowheads) and compressing the trachea (arrows). (B) Coronal contrast-enhanced MR image shows enhancing lesion in the hypothalamus (arrow). (C) Sagittal contrast-enhanced MR image shows enhancing hypothalamic mass protruding into the basal cistern (arrow). (Reproduced with permission from Chong VFH. Langerhans' cell histiocytosis with thyroid involvement. Eur J Radiol *1996;22:155-157.)*

Imaging Pearls

- The imaging features of thyroid involvement in LCH are nonspecific. However, the thyroid gland in conjunction with diabetes insipidus should suggest the diagnosis of LCH. Eighty percent of patients with thyroid involvement have diabetes insipidus.

Suggested Readings

1. Gaines P, Chan JCN, Cockram CS. Histiocytosis X involving the thyroid and hypothalamus. *Postgrad Med J* 1991;67:680-682.
2. Tien RD, Newton TH, McDermott MW. Thickened pituitary stalk on MR images in patients with diabetes insipidus and Langerhans' cell histiocytosis. *AJNR Am J Neuroradiol* 1991;11:703-708.
3. Marcus RB, Post J, Mancuso AA. Pediatric tumors of the head and neck. In: Million RR, Cassisi NJ, eds. *Management of Head and Neck Cancer.* Philadelphia: JB Lippincott; 1994:811-839.
4. Chong VFH. Langerhans' cell histiocytosis with thyroid involvement. *Eur J Radiol* 1996;22:155-157.

Chapter 123

Thyroglossal Duct Cyst

Epidemiology

Thyroglossal duct cyst is a congenital lesion that arises from anomalous development and migration of the thyroid gland. Thyroglossal duct cyst is the most common midline neck mass in children. The majority of cases present in children < 10 years of age. These lesions may be seen in young adults. Less than 2% of cases arise in patients > 60 years of age. No gender predilection has been reported.

Clinical Findings

Thyroglossal duct cysts usually present as nontender, gradually increasing midline neck masses. The average size at presentation is 2 to 4 cm. Recent enlargement may occur as a result of an associated upper respiratory tract infection. Because thyroglossal duct cysts are often attached to the tongue or hyoid bone, these lesions characteristically move when the tongue is protruded. Thyroglossal duct cyst may arise anywhere along the course of migration of the embryonic thyroglossal duct and thyroid gland. The most common location is below the level of the hyoid bone (65%). Twenty percent of thyroglossal duct cysts are suprahyoid in location, whereas 15% of lesions are located at the level of the hyoid bone. Seventy-five percent of thyroglossal duct cysts are midline or slightly off the midline.

Embryology

The thyroid gland is the first endocrine gland to appear in the developing fetus and begins its embryogenesis around the 24th day of gestation. The gland arises from an endodermal thickening in the midline of the developing tongue base. This area is known as the foramen cecum and is located posterior to the apex of the circumvallate papilla. The thyroid gland descends as a result of elongation of the embryo and growth of the tongue. The developing gland migrates as a bilobed diverticulum and forms an epithelial lined cord during descent. Normal involution of the thyroglossal duct occurs between the eighth and tenth weeks of gestation. Failure of involution of the epithelial cord predisposes the patient to formation of a thyroglossal duct cyst. Cyst formation is believed to be due to either inflammatory changes that stimulate secretion of fluids within the ductal remnants or trapping of fluids produced from residual secretory epithelium located in the epithelial cord remnant.

During descent, the developing cartilage of the second branchial arch that gives rise to the hyoid bone comes in close proximity to the descending thyroglossal duct. The thyroid gland may descend superficial to, through, or deep to the hyoid bone. As a result, the location of thyroglossal duct cysts with the hyoid bone is variable. The duct then continues its downward course and lies anterior to the thyrohyoid membrane. The duct terminates at the superior border of the thyroid gland. Migration of the thyroid gland is completed by the eighth week of gestation.

Pathology

The vast majority of thyroglossal duct cysts are benign lesions. Histologically, these cysts have a squamous lining. Thyroid tissue is an uncommon finding in the cyst wall. Occasionally, inflammatory changes may obliterate the epithelial mucosal lining causing the diagnosis to be based on characteristic clinical and radiographic findings. Fistulas may result from infection, cyst rupture, or complication of prior surgery. The following types of fistulas may occur: internal, with an opening into the pharynx; external, with an opening to the skin surface; or complete, with direct communications between the skin and pharynx.

Coexistent malignancy may exist in < 1% of thyroglossal duct cysts. This is often an incidental finding. The most common associated malignancy is papillary carcinoma. This is thought to arise from rests of ectopic thyroid tissue located within the thyroglossal duct cyst.

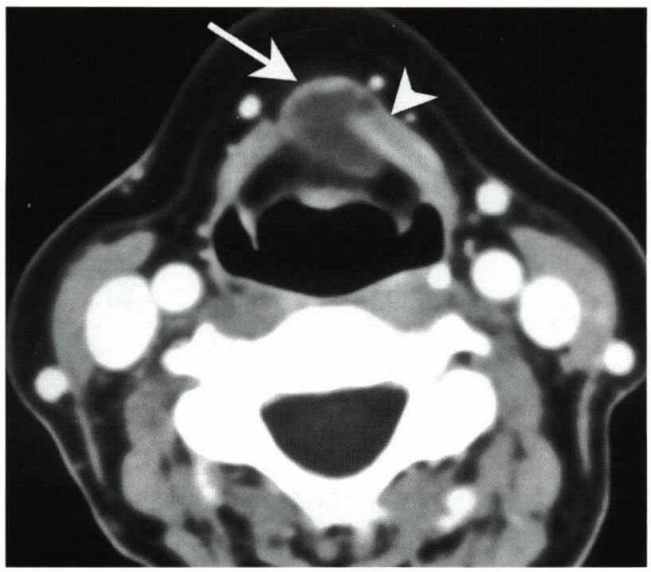

Figure 123-1. Axial contrast-enhanced CT shows a characteristic appearance of a thyroglossal duct cyst (arrow). The mass is a cystic midline mass with a mildly enhancing rim. Note how the mass is embedded with the strap muscle (arrowhead). This combination of findings is indicative of a thyroglossal duct cyst.

Treatment

The treatment of choice for thyroglossal duct cyst is complete surgical resection. The Sistrunk procedure is the method of choice and involves complete removal of the entire cyst tract from the tongue base to the superior border of the thyroid gland. The central portion of the hyoid bone and cuff of the tongue base are included in the resection. Complete resection utilizing the Sistrunk procedure is associated with a 3% recurrence rate, whereas the recurrence rate is significantly increased if thyroglossal duct cysts are locally excised.

Imaging Findings

The CT findings are that of a unilocular or multilocular cystic mass with peripheral enhancement. Recurrent infection may increase the attenuation of the cystic component and cause thickening of the enhancing rim. The lesion may extend anywhere from the tongue base to the superior portion of the thyroid gland. The relationship of a thyroglossal duct cyst to the hyoid bone is variable. Thyroglossal duct cysts may be located superficial or deep to or directly involve the hyoid bone (Figs. 123-1 to 123-3).

On MR imaging, a thyroglossal duct cyst appears as a cystic lesion that is low to intermediate signal on T1-weighted and increased signal on T2-weighted images. Sagittal or coronal images may be useful for identifying the extent of the lesion prior to resection (Fig. 123-4).

Imaging Pearls

- The presence of a cystic mass that is embedded within the infrahyoid strap muscle is useful for arriving at a diagnosis of atypical-appearing thyroglossal duct cysts.
- The superior and inferior margins of the thyroglossal duct cyst need to be closely evaluated. Occasionally, a subtle enhancing tract may be seen arising from the superior or inferior margin of the cyst. This information will help confirm the diagnosis and inform the surgeon of a tract that may be clinically occult.
- Scintigraphy may be more sensitive than MR or CT for localizing rests of ectopic thyroid tissue. However, we do not usually perform this study because a properly executed Sistrunk procedure routinely removes tissue along the normal path of migration of the thyroid gland.
- Normally, there should be no solid enhancing component of a thyroglossal duct cyst. The presence of an intracystic solid enhancing mass may represent residual thyroid tissue. This finding, however, is also suspicious of a coexisting papillary carcinoma and needs to be conveyed to the referring physician.

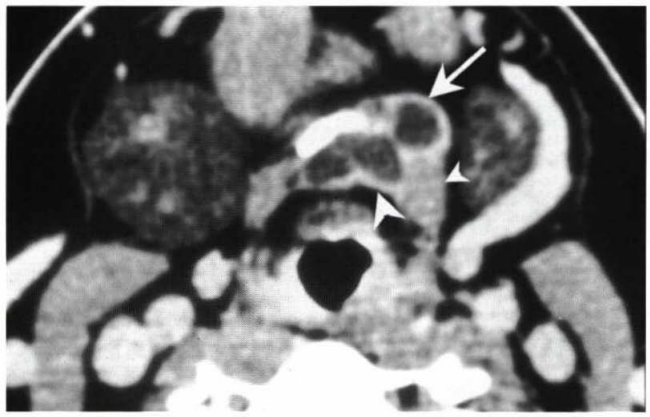

Figure 123-2. Contrast-enhanced CT shows a multicystic mass located at the level of the thyrohyoid membrane. One component of the mass is superficial to the thyrohyoid membrane (arrow), and a second component is deep to the membrane and is located in the preepiglottic space (large arrowhead). Note how the mass is embedded in the left strap muscle (small arrowhead).

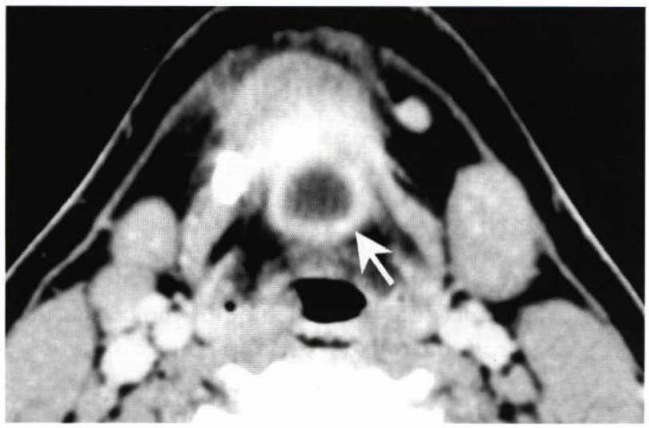

Figure 123-3. Axial image shows an atypical appearance of a thyroglossal duct cyst. The mass is located in the preepiglottic space (arrow). The thick enhancing rim likely represents prior infection.

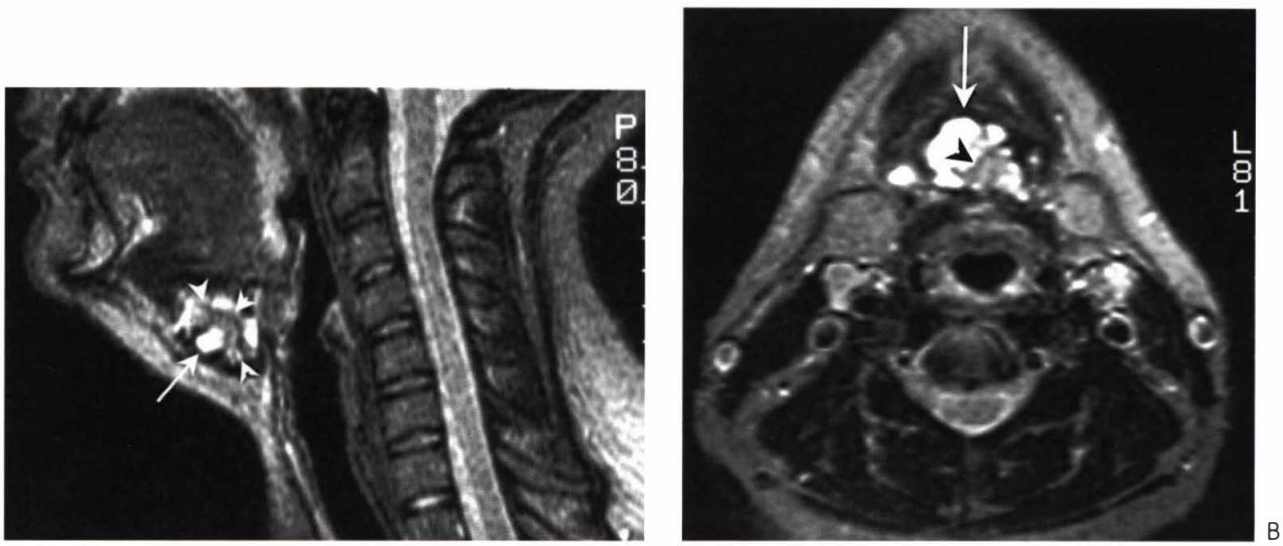

A B

Figure 123-4. (A) Sagittal T2-weighted image shows a thyroglossal duct cyst located in the submandibular space (arrow). The mass has a solid component, which is unusual for a typical thyroglossal duct cyst (arrowheads). (B) Axial T2-weighted image confirms the presence of a solid component (black arrowhead) within the mass (arrow). These findings are suspicious for concurrent thyroid malignancy. Pathology revealed a thyroglossal duct cyst along with papillary carcinoma.

Suggested Readings

1. Moore KL. The branchial apparatus and the head and neck. In: Moore KL, ed. *The Developing Human: Clinically Oriented Embryology*. 4th ed. Philadelphia: WB Saunders; 1988:184–186.
2. Batsakis JG. Parenchymal cysts of the neck. In: Batsakis JG, ed. *Tumors of the Head and Neck*. Baltimore: Williams and Wilkins; 1979:233–252.
3. Hudgins PA, Jacobs IN, Castillo M. Pediatric airway disease. In: Som PM, Curtin H, eds. *Head and Neck Imaging*. 3rd ed. New York: Mosby; 1996:545–611.
4. Karmody CS. Developmental abnormalities of the neck. In: Bluestone CD, Stool SE, Scheetz MD, eds. *Pediatric Otolaryngology*. Vol. 2. Philadelphia: WB Saunders; 1990:1313–1314.
5. Drake AF, Hulka GF. Congenital neck masses. In: Shockley WM, Pillsbury HC, eds. *The Neck: Diagnosis and Surgery*. New York: Mosby; 1994:93–107.

Chapter 124

Lingual Thyroid

Epidemiology

The thyroid anlage is located in the foramen cecum. This region corresponds to the junction of the anterior two thirds and the posterior one third of the tongue. During embryogenesis, the primordial thyroid gland descends anterior to the hyoid bone, larynx, and trachea. The hollow thyroglossal duct connects the foramen cecum to the descending thyroid during embryogenesis. Arrest in the migration of the thyroid gland may be partial or complete. A complete arrest results in a lingual thyroid gland. This phenomenon is more commonly seen in women and occurs in 1 in 3000 patients with thyroid disease. Incomplete arrest may be seen and small amounts of thyroid tissues can also be found along the thyroglossal duct or within thyroglossal cysts.

Clinical Findings

The lingual thyroid is easily detected as a midline mass at the junction between the anterior two thirds and posterior one third of the tongue. Although this is a congenital anomaly patients often present at puberty when the thyroid gland rapidly increases in size. Ectopic thyroid tissues usually present as nodular lesions close to the midline in the upper neck.

Pathology

The cause of thyroid maldescent is unknown. These ectopic thyroid tissues have normal histological appearances and they may represent the only normal-functioning thyroid tissues in the body. They may undergo malignant changes similar to the thyroid gland in the normal site. Malignant changes in the lingual thyroid have been reported to be more frequent than carcinomas in thyroglossal cysts.

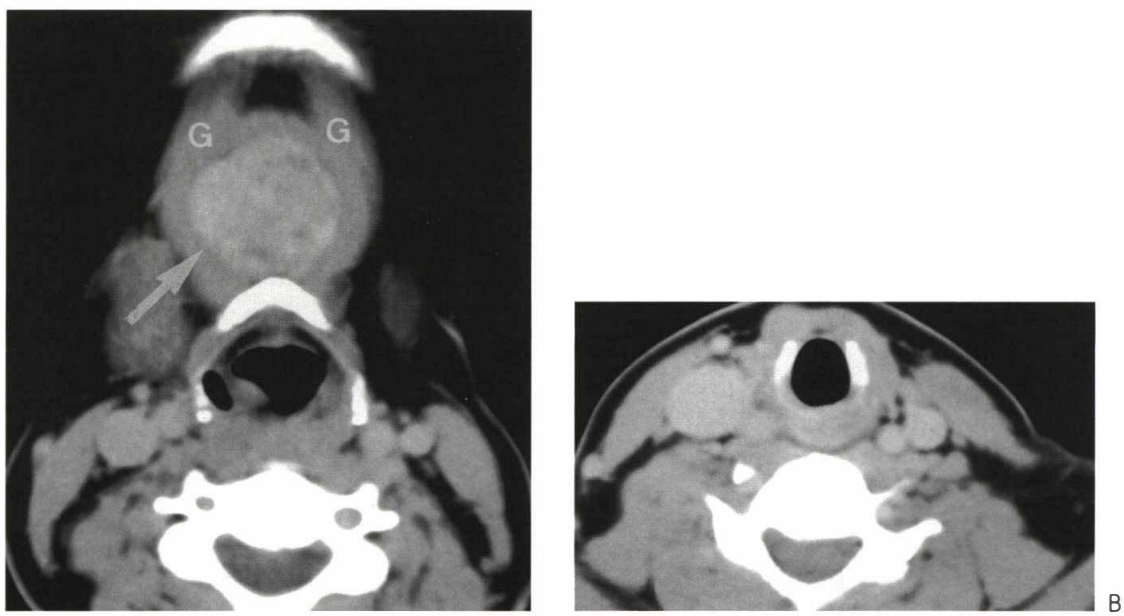

Figure 124–1. Lingual thyroid gland. (A) Axial contrast-enhanced CT shows enhancing thyroid tissues in the tongue base (arrow) splaying the geniohyoid muscles (G). (B) Axial contrast-enhanced CT through the thyroid bed shows the absence of a thyroid gland. (Courtesy of SH Ng, M.D., Chang Gung Memorial Hospital, Taoyuan, Taiwan.)

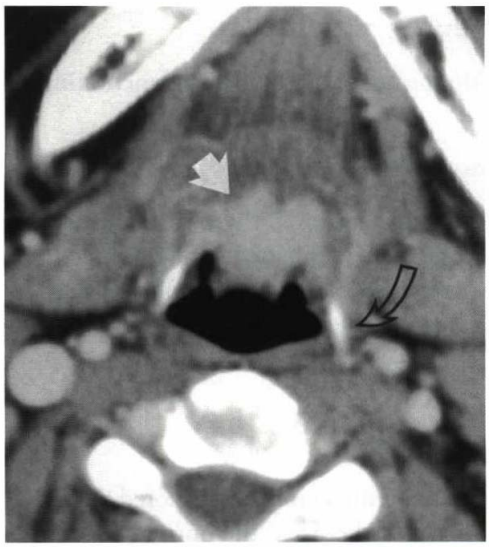

Figure 124–2. Ectopic thyroid gland. Axial contrast-enhanced CT shows enhancing thyroid tissue (white arrow) at the level of the hyoid bone (hollow arrow). (Courtesy of SH Ng, M.D., Chang Gung Memorial Hospital, Taoyuan, Taiwan.)

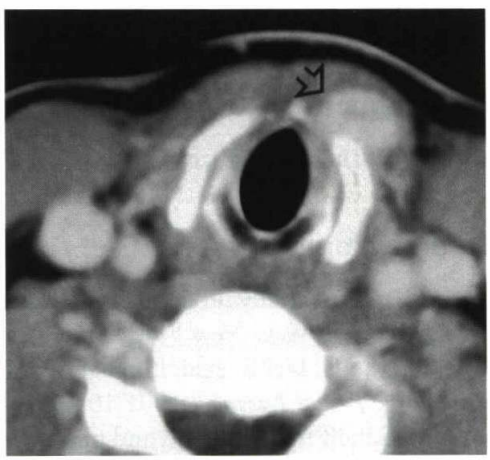

Figure 124–3. Axial contrast-enhanced CT shows ectopic thyroid tissue embedded in the left strap muscles (arrow). (Courtesy of SH Ng, M.D., Chang Gung Memorial Hospital, Taoyuan, Taiwan)

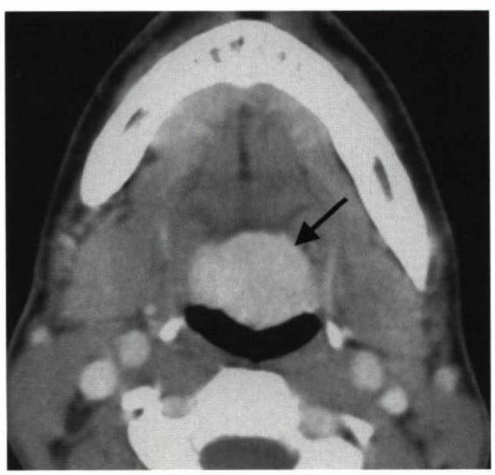

A

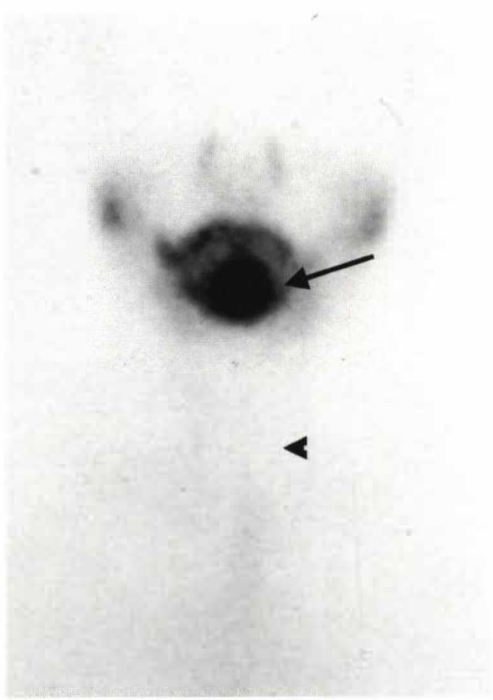

B

Figure 124-4. (A) Contrast-enhanced CT shows an enhancing mass situated at the tongue base (arrow) which was suspicious for a lingual thyroid. (B) Frontal view of a Tc-99m pertechnetate study shows abnormal uptake in the region of the tongue base (arrow) corresponding to the mass seen on the CT. These findings are indicative of a lingual thyroid. There is no uptake in the lower neck in the region of the thyroid bed (arrowhead) indicating that the thyroid gland has not migrated to its normal location. (Case Courtesy Mitchell T. Pace, D.O.)

Treatment

Ectopic thyroid tissues are normal-functioning tissues and they require no treatment.

Imaging Findings

Lingual thyroid or ectopic thyroid tissues have similar CT attenuation characteristics of thyroid gland. They enhance strongly after the injection of iodinated contrast. Nuclear medicine scans are excellent in demonstrating thyroid tissue activity. Small collections of ectopic tissues, not evident on CT, may be readily identified on nuclear medicine scans (Figs. 124-1 to 124-4).

Imaging Pearls

When a strongly enhancing mass is noted on CT in the region of the tongue base or along the anterior aspect of the neck, the normal position of the thyroid gland should be examined. Lingual thyroid glands are associated with the absence of a normal thyroid gland in the neck in 70 to 80% of patients. A nuclear medicine scan should be done to determine the number of ectopic sites or the functional status of these thyroid tissues. On MR imaging, the signal characteristics of a lingual thyroid is similar to normal thyroid tissues in the neck.

Acknowledgement

Case courtesy of Mitchell T. Pace, D.O.

Suggested Readings

1. Weissmann JL. The infrahyoid neck. In: Valvassori GE, Mafee MF, Carter BL eds. *Imaging of the Head and Neck*. New York: Thieme; 1995:424-444.
2. Guneri A, Ceryan K, Igci E, et al. Lingual thyroid: the diagnostic value of magnetic resonance imaging. *J Otol Laryngol* 1991;105:493-495.
3. Yousem DM, Scheff AM. Thyroid and parathyroid. In: Som PM, Curtin HD eds. *Head and Neck Imaging*. 3rd ed. St. Louis: Mosby; 1996:952-975.

Chapter 125

Thyroid Amyloidosis

Epidemiology

Amyloid is an extracellular proteinaceous substance consisting of 95% amyloid fibril protein and 5% P component (a glycoprotein). Of the 15 biochemically distinct proteins, the primary components are amyloid light chain (derived from plasma cells) and amyloid-association protein (a unique nonimmunoglobulin synthesized by the liver). Amyloid deposits can be seen in almost all organs and are associated with a diverse number of clinical settings. Amyloidosis may present as a localized lesion or a systemic disease. Systemic amyloidosis may be further classified into primary (associated with immunocyte dyscrasia) and secondary amyloidosis (complication of an underlying chronic disease). Microscopic amyloid deposits in the thyroid gland are not uncommonly seen in systemic disease but localized amyloid goiter is unusual.

Clinical Findings

Thyroid amyloidosis usually presents with a history of painless neck swelling for several months. Clinically, the diffusely enlarged thyroid feels firm, nodular, and nontender. There are usually no associated signs of hyperfunction or hypothyroidism.

Pathology

When amyloid is stained with iodine followed by sulfuric acid it turns blue, a characteristic shared by starch. This observation led Virchow to suggest the term *amyloid*. Amyloid is most reliably demonstrated by Congo red stain followed by examination with polarized light. Amyloid characteristically shows red-green birefringence. The predominant histologic appearance is one of diffuse amyloid deposit surrounding thyroid follicles. Typically, multinuclear giant cells and foreign body–like reaction can be seen. In the thyroid gland, a nodular pattern of amyloid deposition with compression and distortion of follicular architecture may also be seen. Furthermore, amyloid deposits are often accompanied by mature adipose tissues. These features may account for the nodular appearance simulating adenomatous goiter on both CT and MR imaging.

Treatment

Amyloid rarely regresses and causes its pathological effects by progressive accumulation that leads to atrophy of tissues. Localized thyroid amyloidosis has a good prognosis and is usually not associated with endocrine dysfunction. The amyloidoma may be excised. However, the prognosis of primary generalized amyloidosis is poor, with most patients succumbing within 2 years of diagnosis. Secondary amyloidosis has a better prognosis and depends on the nature and control of the primary disease.

Imaging Findings

CT

There is a wide range of CT findings in amyloidosis. CT may show diffuse enlargement of both lobes with or without evidence of calcification. Cystic changes may be a prominent feature in amyloid goiter. A nodular enhancement pattern may be noted following the injection of contrast material. Striking fatty infiltration of the thyroid gland may be noted. Such an appearance is highly suggestive of amyloidosis (Fig. 125–1).

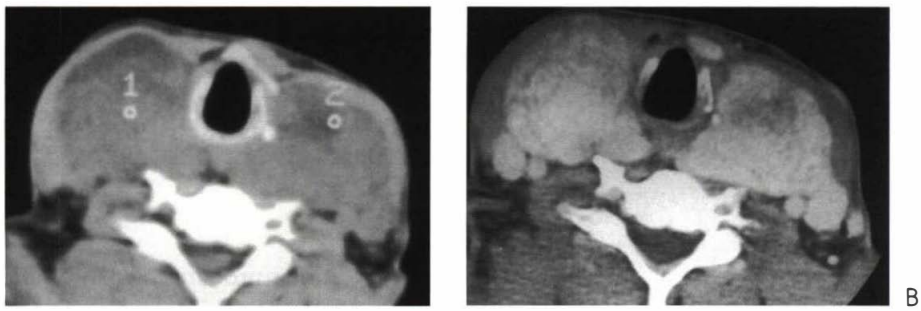

Figure 125-1. Amyloidosis involving thyroid gland. (A) Axial CT shows a diffusely enlarged thyroid gland with relatively low attenuation values (#cursor 1 shows 46 HU and #cursor 2 shows 22 HU) (B) Axial contrast-enhanced CT shows a nodular enhancing pattern in both thyroid lobes.

MR

MR imaging features of amyloid infiltration of the thyroid appear variable. Fontan reported low signals on T2-weighted images in solid areas of the amyloid goiter. In addition, they observed low signals in the T1-weighted images as well.

Imaging Pearls

- Amyloid goiter may present nonspecific imaging findings. However, the presence of fatty deposits should suggest the presence of amyloidosis.
- On both T1- and T2-weighted images, amyloid deposits may show low signal intensity.

Suggested Readings

1. Miyake H, Maeda H, Isomoto I, et al. Computed tomography in amyloid goiter. *J Comput Assist Tomogr* 1988;12:621-623.
2. Hatabu H, Iida Y, Kasagi K, et al. Amyloid goiter: radiologic findings. *AJR Am J Radiol* 1990;155:193-194.
3. Fontan FJP, Cordido F, Mosquera J, et al. Amyloid goiter: CT and MR findings. *Clin Radiol* 1995;50:409-411.
4. Chong VFH, Fan YF. Amyloidosis of the thyroid gland. *AJR Am J Radiol* 1997;168:845-846.

Chapter 126

Parathyroid Adenoma

Epidemiology

Parathyroid adenoma is the most common cause of primary hyperparathyroidism, accounting for almost 80 to 85% of the cases. Parathyroid adenoma is generally a solitary lesion and affects a single parathyroid gland, however multiple adenomas may be seen in 2 to 3% of cases. They show no sex predilection and may occur at any age, although the middle-aged adults are most commonly affected. The typical sites for a parathyroid adenoma are behind the thyroid gland, behind the strap muscles, or 1 to 2 cm away from the lower pole of the thyroid within the thyrothymic ligament. Infrathyroid lesions are generally spherical. Intrathyroid parathyroid adenomas occur in 1 to 2% of the cases.

Clinical Features

Most patients are asymptomatic. Symptoms include fatigue, weakness, and mental disturbances. Patients with significant hypercalcemia may present with confusion, lethargy, and hyporeflexia.

Pathology

Grossly, parathyroid adenomas are well-encapsulated, soft, yellowish tumors. On histological examination, they are composed principally of chief cells, but many transitional and oxyphil cells are often present. The cells are arranged in large islands or broad bands. A rim of normal or atrophic parathyroid tissue with scattered fat cells can be seen external to the capsule, helping to differentiate an adenoma from diffuse hyperplasia.

Treatment

Surgical parathyroidectomy is the only definitive treatment for primary hyperparathyroidism. Oral phosphates may be given to lower serum calcium temporarily.

Imaging Findings

US

Parathyroid adenomas are usually hypoechoic and well-defined masses with a very sharp edge between the adenoma and the adjacent thyroid parenchyma.

Nuclear Medicine Study

The radionuclide agents used for scanning include thallium and Tc 99m sestamibi. Neither of these radioisotopes is taken up exclusively by the parathyroid adenoma as uptake is also the thyroid gland. Thus visualization of abnormal parathyroid adenoma uptake requires some form of subtraction technique using Tc 99m pertechnetate. However, Tc 99m sestamibi is concentrated for a longer time in the parathyroid adenoma than in the thyroid gland. The agent washes out of the thyroid gland rapidly but is retained in the parathyroid for a longer time. Thus delayed images following administration of Tc 99m sestamibi localize the adenoma thereby obviating the need for subtraction (Fig. 126–1).

CT

Parathyroid adenomas appear as spherical or oval lesions of low attenuation on the noncontrast CT. Following administration of intravenous contrast, only 25% of adenomas enhance. They rarely show calcification. However, when present in the tracheoesophageal groove, the presence of calcification may help differentiate a parathyroid adenoma from a tracheoesophageal lymph node. Apart from the typical locations previously mentioned, adenomas may also occur in ectopic sites which include posterior to the trachea, and anterior mediastinum (Figs. 126–2 and 126–3).

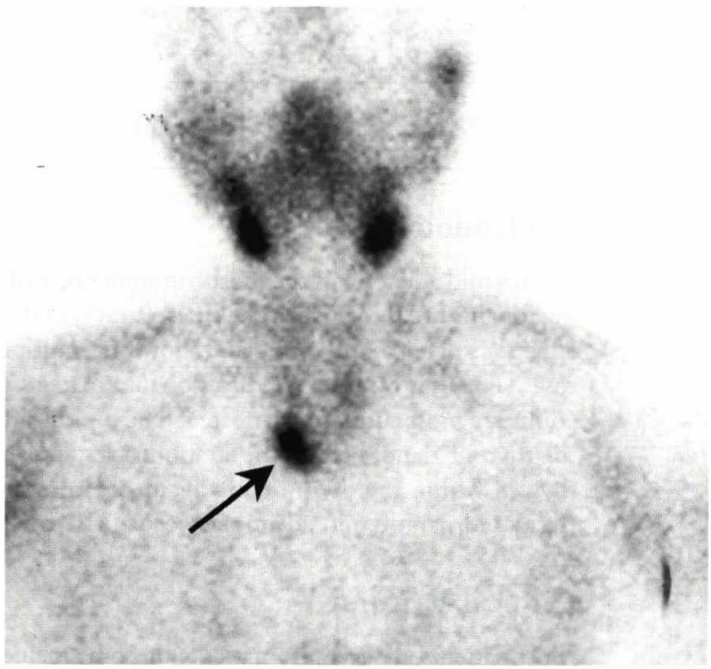

Figure 126–1. Planar image from a sestamibi study shows focal uptake inferior to the right lobe of the thyroid gland, which was suspicious for parathyroid adenoma (arrow). This was confirmed at surgery.

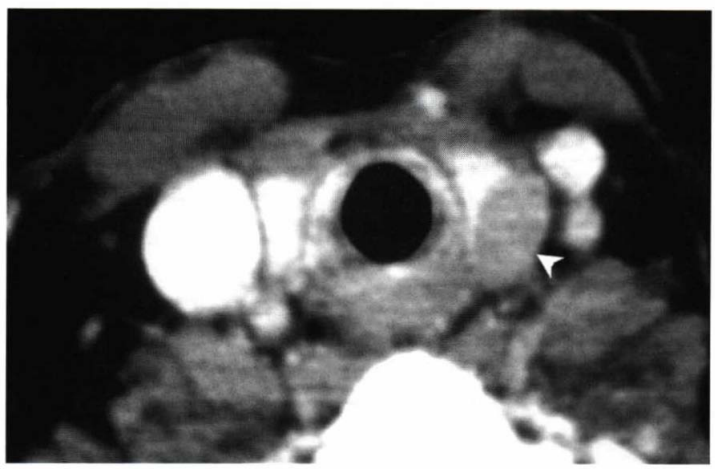

Figure 126–2. Axial contrast-enhanced CT shows a round homogeneous mass (arrowhead) medially displacing the lower pole of the left lobe of the thyroid gland. Pathology revealed parathyroid adenoma.

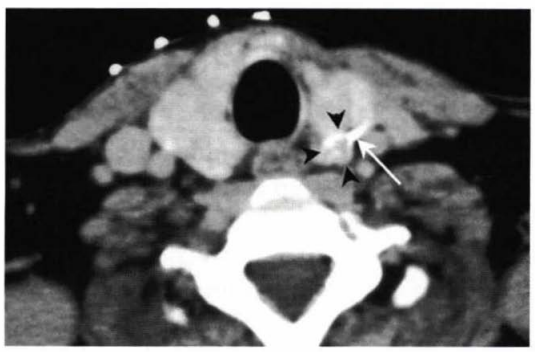

A

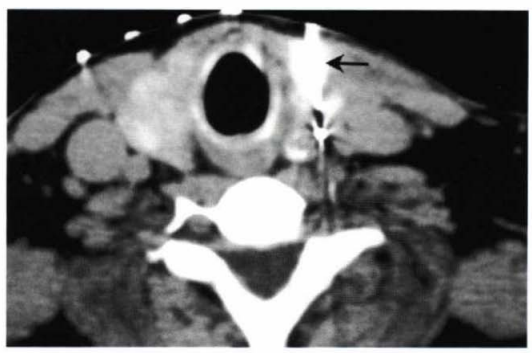

B

Figure 126–3. (A) Contrast-enhanced CT shows a round mass deep to the left lobe of the thyroid gland in the left tracheoesophageal groove (arrowheads). The mass contains some eccentric calcification (arrow). (B) A CT-guided needle biopsy (arrow) of the mass revealed parathyroid adenoma.

MR

Parathyroid adenomas are seen as well-defined oval or spherical lesions that are hypointense on T1-weighted images and hyperintense on T2-weighted images. Most of them enhance following administration of gadolinium and are bright on postgadolinium T1-weighted images. Fat-suppressed scans following administration of gadolinium are useful in the demonstration of these adenomas against a dark background.

Imaging Pearls

- In our experience, Tc 99m sestamibi is the most consistent technique for identifying parathyroid adenomas. CT and MRI may be used; however, the imaging appearance is often indistinguishable from a paratracheal lymph node.
- There is no consensus as to whether all patients with primary hyperparathyroidism should undergo imaging prior to exploration or whether imaging should be reserved for patients with persistent hyperparathyroidism following initial surgery.

Suggested Readings

1. Siegel AM. The parathyroid glands, hypercalcemia and hypocalcemia. In: Wyngaarden JB, Smith LH, eds. *Cecil Textbbook of Medicine*. 17th ed. Philadelphia: WB Saunders; 1985:1412–1419.
2. DeLillis RA. The endocrine system. In: Cotran RS, Kumar V, Robbins SL, eds. *Robbins Pathologic Basis of Disease*. Philadelphia: WB Saunders; 1989:1244–1245.
3. Yousem DM, Scheff AM. Thyroid and parathyroid. In: Som PM, Curtin H, eds. *Head and Neck Imaging*. 3rd ed. New York: Mosby; 1996:952–975.

Section IV

Retropharyngeal Space

The retropharyngeal space (RPS) is the space located directly behind the pharynx (visceral space); thus the name *"retropharyngeal"* (Fig. IV–1). What we commonly refer to as the RPS is a potential space that is bordered anteriorly by the visceral fascia and posteriorly by the prevertebral fascia (Fig. IV–2). In actuality, however, there is a very thin fascial layer (alar fascia) that divides the RPS into anterior and posterior compartments. The alar fascia may occasionally be identified in patients who develop edema of the retropharyngeal space following radiation therapy (Fig. 128–1).

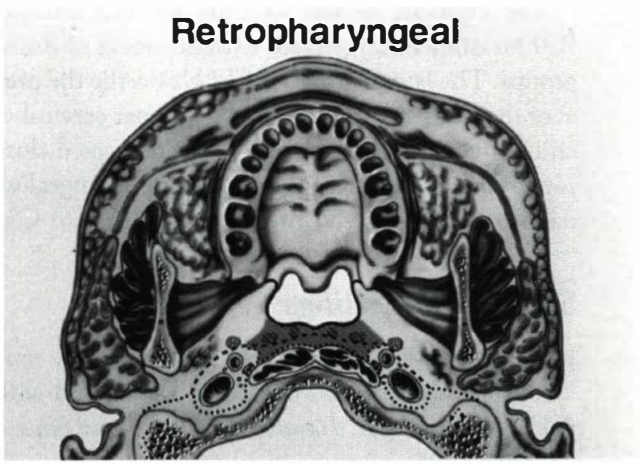

Figure IV–1. Schematic illustration shows the normal location of the retropharyngeal space. Solid line = visceral fascia, long-dash line = alar fascia, short-dash line = prevertebral fascia. (Figure reproduced with permission from Mukherji SK, Castillo M. A simplified approach to the spaces of the suprahyoid neck. Rad. Clin N Am *1998;36:761–780.)*

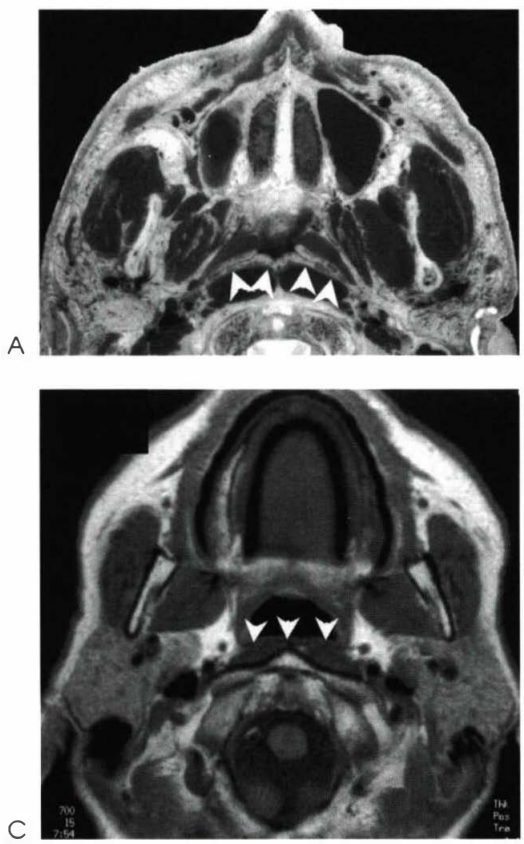

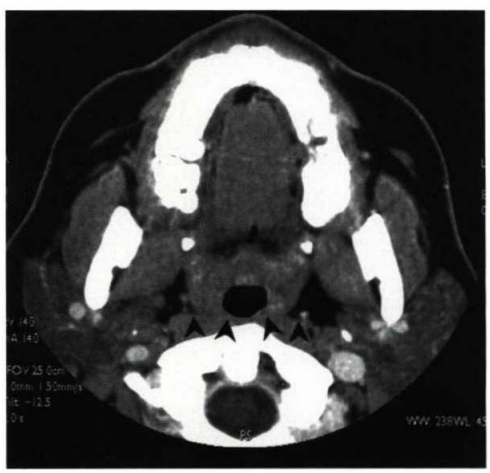

Figure IV–2. The arrowheads denote the location of the retropharyngeal space, which is a potential space on (A) the anatomic section, (B) CT, and (C) MR.

The anterior compartment, which is located between the visceral fascia and the alar fascia, is the "true" retropharyngeal space. This space extends from the skull base to the location where the alar fascia fuses with the visceral fascia. This level varies between C6 and T4. The posterior compartment, which is bordered anteriorly by the alar fascia and posteriorly by the prevertebral fascia, is referred to as the "danger space." This space extends from the skull base to the diaphragm and provides a direct pathway for head and neck infections to spread into the posterior mediastinum. Because the alar fascia is not an effective barrier and is commonly eroded by infection, many authors combine the "true" retropharyngeal space proper and the danger space into the "RPS."

The contents of the RPS are fat and retropharyngeal lymph nodes (RPLNs). The RPLNs, sometimes referred to as the nodes of Rouvière, are divided into lateral and median groups. The lateral group of RPLNs overlie the prevertebral fascia at approximately the level of the transverse processes of the upper cervical vertebra. The median RPLNs are smaller and not consistently present. They are located close to the midline and adjacent to the retropharyngeal surface of the posterior pharyngeal wall. Both the lateral and the median nodal groups may extend from the skull base to C3.

Suggested Readings

1. Davis WL, Harnsberger HR, Smoker WR, et al. Retropharyngeal space: evaluation of normal anatomy and diseases with CT and MR imaging. *Radiology* 1990;174:59–64.
2. Harnsberger HR. *Handbook of Head and Neck Imaging*. 2nd ed. St. Louis: Mosby Year Book; 1995.
3. Grodinsky M, Holyoke EA. The fasciae and fascial spaces of the head, neck and adjacent regions. *Am J Anat* 1938;63:367–408.
4. Mukherji SK, Castillo M. A simplified approach to the spaces of the extracranial head and neck. *Radiol Clin North Am* 1998;36:761–780.
5. Rouvière H. Lymphatic system of the head and neck. In: *Anatomy of the Human Lymphatic System*. Ann Arbor: Edward Brothers; 1938.

Chapter 127

Tortuous Carotid Artery

Epidemiology

The retropharyngeal space may be widened by a variety of pathological processes such as abscesses, hematoma, and edema. Medially deviated carotid arteries may also widen the retropharyngeal space but this phenomenon is rare and is usually found in the elderly.

Clinical Findings

Tortuous carotid arteries with medial deviation are usually detected as incidental findings. However, in patients with suspected cervical spine trauma, widening of the retropharyngeal space on a lateral cervical radiograph is often worrying. In such patients further evaluation is usually required to rule out cervical spinal injury.

Pathology

The cause of medial deviation of the carotid arteries is unknown. It may be congenital but is likely to be related to arteriosclerosis. In the elderly, arteriosclerosis results in elongation and migration of the affected artery. In the neck, this elongation leads to migration of the artery into adjacent spaces such as the retropharyngeal space.

Treatment

No treatment is required. However, surgeons performing operative procedures in the neck should be aware of the unusual location of these affected arteries.

Imaging Findings

CT

Recognition of medially deviated carotid arteries is apparent on contrast enhanced CT (Fig. 127-1). The opacified artery can be seen migrating medially between the pharyngeal mucosal space anteriorly and the cervical spine posteriorly.

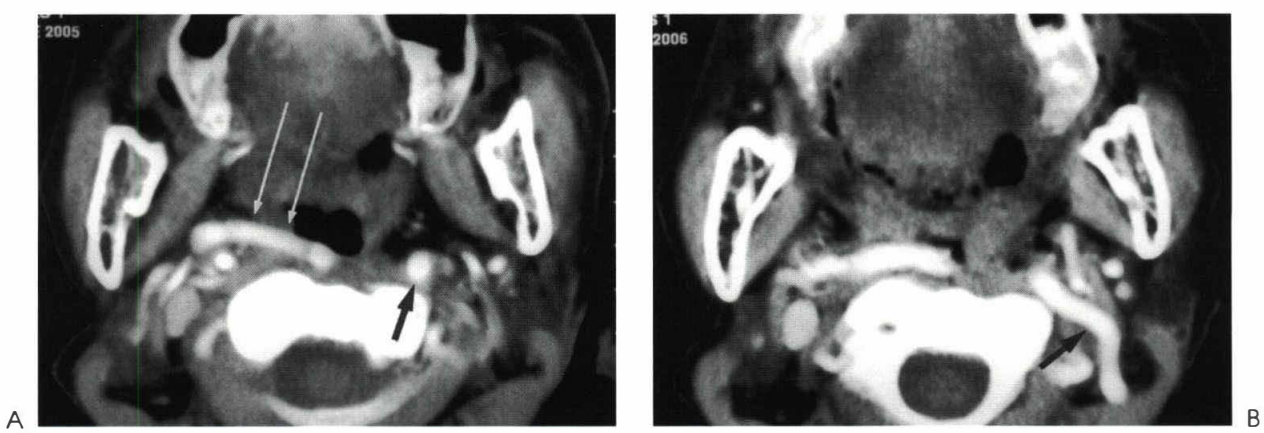

Figure 127-1. Tortuous internal carotid arteries. (A) Axial contrast-enhanced CT shows a normally placed left internal carotid artery (single arrow). Note the tortuous right internal carotid artery deviating medially to occupy a retropharyngeal position (double arrows). (B) Axial contrast-enhanced CT inferior to (A) shows the retropharyngeal position of the right internal carotid artery. The left internal carotid artery is tortuous with deviation into the left posterior triangle (arrow).

MR

On T1- and T2-weighted images, the affected arteries appear as flow voids. Contrast-enhanced images may show variable enhancement depending on the tortuosity of the vessels. These arteries are often better seen on gradient echo sequences.

Imaging Pearls

- Retropharyngeal carotid arteries are incidental findings but can be clinically significant. The presence of a retropharyngeal artery and any mass effect of the adjacent pharyngeal wall should be reported, especially in patients with metastatic lymph nodes without an obvious primary tumor ("unknown primary"). Patients with an initial diagnosis of an unknown primary tumor usually undergo endoscopy and biopsy of suspicious submucosal masses. Identification of a retropharyngeal carotid artery that is causing mass effect on the pharynx can help prevent a disaster.
- Medially deviated carotid arteries are usually affected by arteriosclerosis. When widening of the retropharyngeal space is noted on a lateral cervical radiograph, the presence of a deviated carotid artery may be suspected if arterial calcifications can be demonstrated. If no calcifications can be detected, contrast-enhanced CT will be required to confirm the diagnosis.

Suggested Readings

1. Fix TJ, Daffner RH, Deeb ZL. Carotid transposition: another cause of wide retropharyngeal soft tissues. *AJR Am J Roentgenol* 1996;167:1305–1307.
2. Chong VFH, Fan YF. Radiology of the retropharyngeal space. *Clin Radiol* 2000;55:740–748.

Chapter 128

Retropharyngeal Edema Following Radiation Therapy

Epidemiology

Radiation therapy is effectively used to treat a variety of head and neck malignancies. Following irradiation, fluid may accumulate in the retropharyngeal space (RPS) in up to 50% of patients irradiated for laryngeal malignancy. These fluid collections typically appear 4 to 6 weeks following irradiation and usually persist for up to 3 months. RPS edema may also be present in patients with suppurative retropharyngeal adenitis, usually due to tonsillitis, and prevertebral cellulitis.

Clinical Findings

RPS fluid collection following radiation therapy is asymptomatic. RPS edema associated with infections of the oropharynx result in neck stiffness and pain. Patients are usually febrile and have difficulty swallowing.

Pathology

Following irradiation, connective tissues show an acute inflammatory response. This is associated with detachment of the endothelial lining of vessels leading to increased permeability. Exudates may therefore be seen in the subcutaneous tissues, and fluid may also accumulate in potential spaces such as the RPS.

Treatment

No treatment is required if the etiology of the edema is due to prior radiation therapy. RPS edema will resolve following appropriate antibiotic therapy. Surgical exploration or drainage is not indicated for RPS edema.

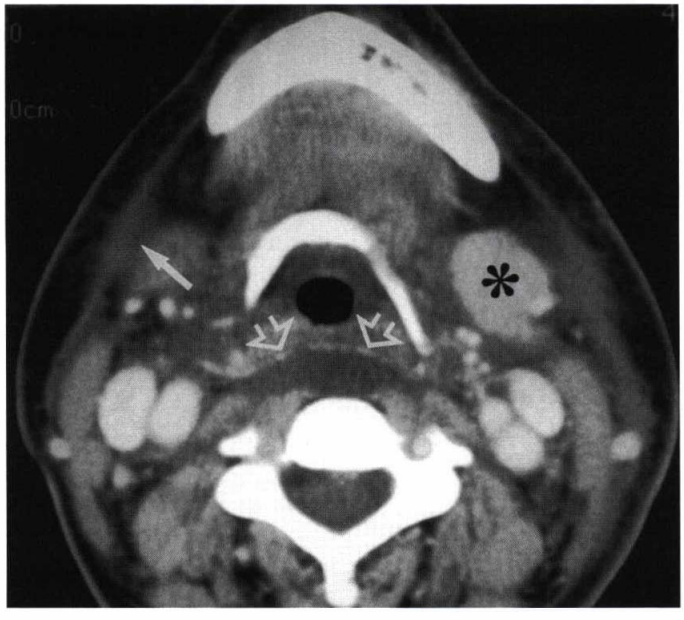

Figure 128–1. Radiation-induced retropharyngeal effusion. Axial contrast-enhanced CT shows low attenuation fluid in the retropharyngeal space (open arrows). There are associated radiation-induced subcutaneous streaking and platysma muscle thickening (solid arrow). Note the prominent submandibular enhancement following radiation therapy (asterisk). It is unusual to have a retropharyngeal space abscess following treatment with radiation therapy.

Imaging Findings

CT

RPS edema can be identified by diffusely symmetric low in attenuation in the RPS. There is symmetric expansion of the RPS without a focal fluid collection. There is no peripheral enhancing rim (Fig. 128-1).

MR

On T1-weighted images, the fluid shows intermediate and high signal on T2-weighted images. There may be enhancement of the posterior pharyngeal wall and prevertebral fascia.

Imaging Pearls

- RPS edema may be confused with RPS abscess, especially in RPS edema and especially in patients with oropharyngeal infections.
- RPS edema is characterized by low attenuation that expands the retropharyngeal space in a symmetric manner. RPS abscess is identified by tense expansion of the RPS by an asymmetric fuid collection.

Suggested Readings

1. Mukherji SK, Mancuso AA, Kotzur IM, et al. Radiologic appearance of the irradiated larynx, I: Expected changes. *Radiology* 1994;193:141-148.
2. Chong VFH, Fan YF. Radiology of the retropharyngeal space. *Clin Radiol* 2000;740-748.
3. Pameijer FA, Mukherji SK, Balm AJM, van der Laan BFAM. Imaging of squamous cell carcinoma of the hypopharynx. *Semin Ultrasound CT MRI* 1998;19:476-491.

Chapter 129

Retropharyngeal Infections: Cellulitis, Suppurative Adenitis, Abscess

Epidemiology

Acute pharyngitis is common in childhood and most often affects children < 3 years of age. The most likely causal organism is *Haemophilus influenzae*. Retropharyngeal cellulitis or abscess in children is usually secondary to acute pharyngitis. In adults, infection is usually due to penetrating injury, and gram-positive cocci are the most common pathogen.

Clinical Findings

Patients often present with fever with the sensation of a lump in the throat. Patients may also complain of a choking feeling and difficulty in swallowing. Inspection of the pharynx will reveal edema and redness.

Pathology

From the pharynx, microorganisms can spread to the retropharyngeal nodes resulting in suppurative adenitis. If treatment is delayed, suppurated lymph nodes may rupture and result in formation of a retropharyngeal abscess.

Treatment

Acute pharyngitis and lymphadenitis can be readily controlled with antibiotics. Retropharyngeal abscess should be surgically managed expediently because rapid enlargement may lead to airway compromise.

Imaging Findings

Plain Films

This demonstrates thickening of the soft tissues in the prevertebral space. This is a nonspecific finding and may be seen in retropharyngeal cellulitis, retropharyngeal suppurative adenitis, and retropharyngeal abscess formation.

CT

Retropharyngeal cellulitis is identified by symmetric low attenuation in the retropharyngeal space. There is some anterior displacement of the posterior wall of the pharynx from the prevertebral muscles. However, the symmetric displacement does not exceed a few millimeters. Retropharyngeal suppurative adenitis is identified by enlarged paramedian retropharyngeal lymph nodes that contain a low attenuation center. A retropharyngeal abscess is identified by a low attenuation fluid collection that causes substantial anterior displacement of the posterior wall of the pharynx from the prevertebral muscles. This collection may be asymmetric. Retropharyngeal abscesses usually do not have a thick enhancing wall (Figs. 129–1 and 129–2).

MR

Enlarged retropharyngeal nodes show intermediate signal intensity on T1-weighted images and strong contrast enhancement. Rim enhancement indicates the presence of suppurative lymphadenitis. On T2-weighted images, the inflamed nodes show high signal intensity. Soft tissue thickening as a result of cellulitis also shows strong contrast enhancement and high signals onT2-weighted images.

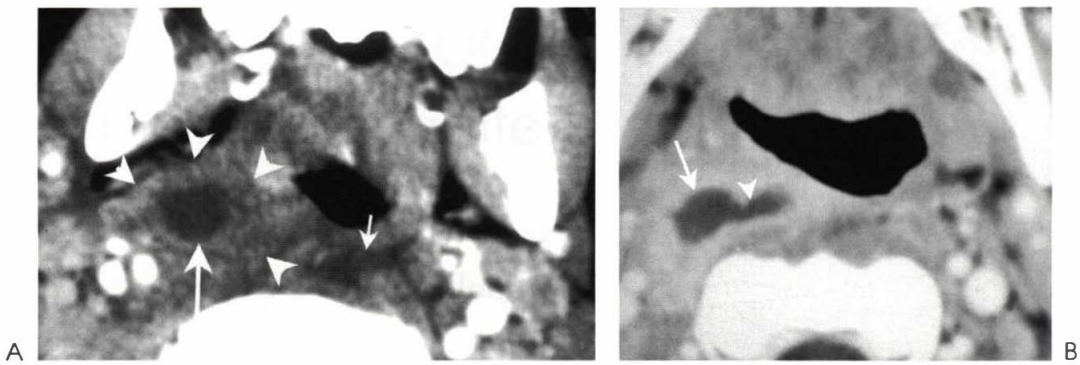

Figure 129–1. Suppurative adenitis. (A) Axial contrast-enhanced CT shows a suppurative retropharyngeal lymph node (large arrow) with surrounding phlegmon (arrowheads). The low attenuation in the retropharyngeal space (small arrow) is edema and is not a retropharyngeal space abscess. (B) This image shows another example of a suppurative retropharyngeal lymph node (arrow). The pus appears to have ruptured through the capsule of the node and is extending medially (arrowhead).

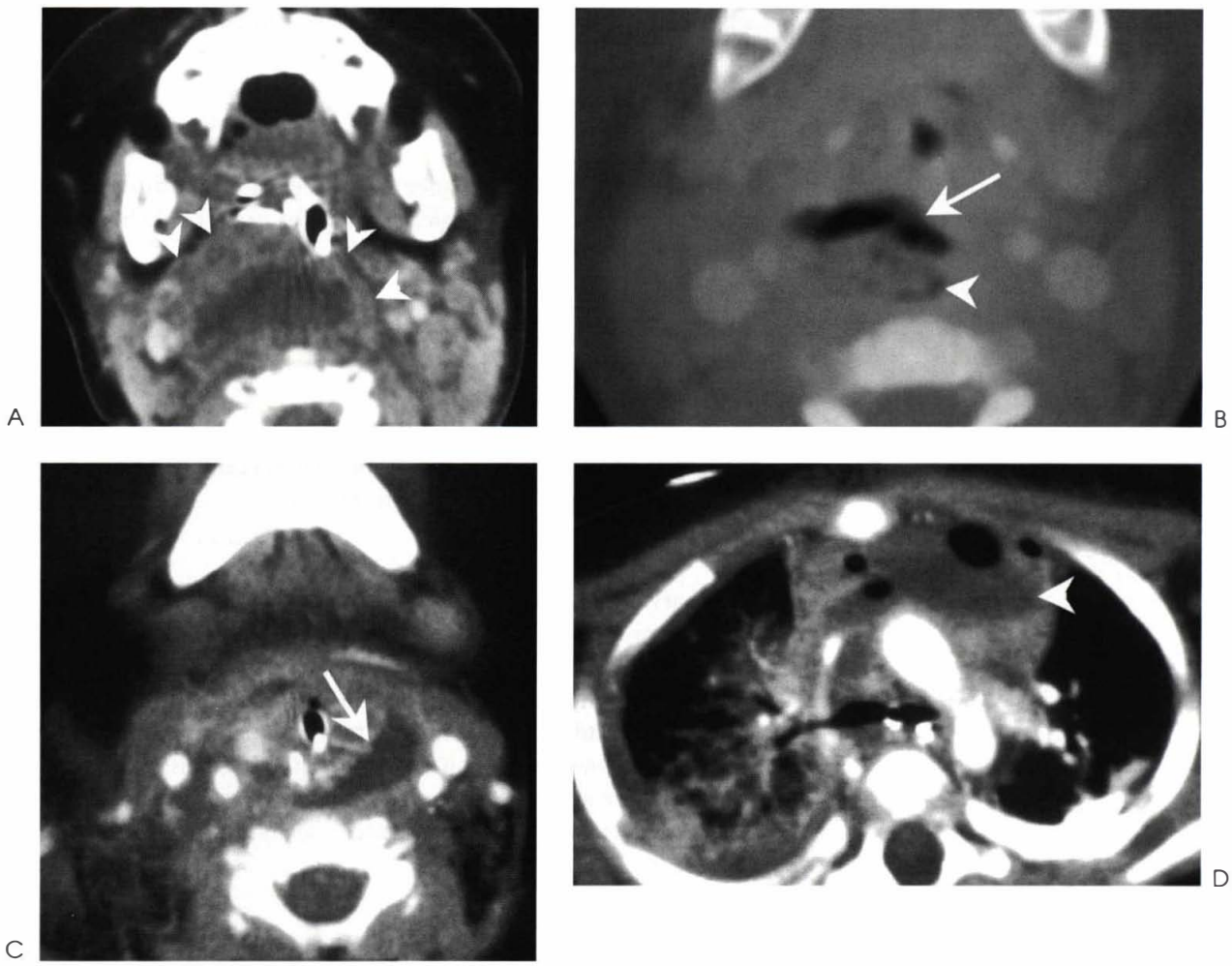

Figure 129–2. Retropharyngeal space abscess. (A) Axial contrast-enhanced CT shows a large fluid mass centered within the retropharyngeal space (arrowheads). Note the phlegmon surrounding the mass. (B) Axial CT filmed at bone windows shows an abscess that contains air (arrow) and fluid (arrowhead). (C,D) Abscess involving the left side of the retropharyngeal space (arrow). (D) Image obtained through the mediastinum shows fluid and air in the anterior mediastinum indicative of mediastinitis (arrowhead). This likely resulted from inferior spread of the infection illustrated in (C) via the retropharyngeal and danger spaces.

Imaging Pearls

- The retropharyngeal space stretches from the skull base to approximately T4. It is therefore important to visualize the superior and inferior extent of inflammation.
- The retropharyngeal space is located anterior to the prevertebral muscles. If the inflammatory process extends posterior to the prevertebral muscles, the prevertebral space is also affected.
- Cross-sectional imaging should only be performed on patients with a stable or controlled airway. CT is usually the cross-sectional study of choice.
- Some authors have recommended ultrasound for initial evaluaion of patients with retropharyngeal infections.

Suggested Readings

1. Davis WL, Harnsberger HR, Smoker WRK, Watanabe AS. Retropharyngeal space: evaluation of the normal anatomy and diseases with CT and MR imaging. *Radiology* 1990;174:59–64.
2. Harnsberger HR. *Handbook of Head and Neck Imaging*. 2nd ed. St Louis: Mosby; 1995;89–104.
3. Chong VFH, Fan YF. Radiology of the retropharyngeal space. *Clin Radiol* 2000;55:740–748.

Chapter 130

Retropharyngeal Cellulitis

Epidemiology

Acute pharyngitis is common in childhood and most often affects children <of three 3 years of age. The most likely causal organism is *Haemophilus influenzae*. Retropharyngeal cellulitis or abscess in children is usually secondary to acute pharyngitis. In adults, infection is usually due to penetrating injury, and gram-positive cocci are the most common pathogen.

Clinical Findings

Patients often present with fever with the sensation of a lump in the throat. Patients also complain of a choking feeling and difficulty in swallowing. Inspection of the pharynx will reveal edema and redness.

Pathology

From the pharynx, microorganisms can spread to the retropharyngeal nodes resulting in suppurative lymphadenitis. If treatment is delayed, lymphadenitis can lead to retropharyngeal cellulitis and abscess formation.

Treatment

Acute pharyngitis and lymphadenitis can be readily controlled with antibiotics. Retropharyngeal abscess should be surgically managed expediently because rapid enlargement may lead to airway compromise.

Imaging Findings

CT

A lateral plain film of the neck (Fig. 130–1) may show prevertebral soft tissue thickening but suppurative lymphadenitis, retropharyngeal cellulitis, or abscess is better delineated on CT. Contrast-enhanced CT may show enlarged retropharyngeal nodes with low central areas indicating suppuration (Fig. 130–2).

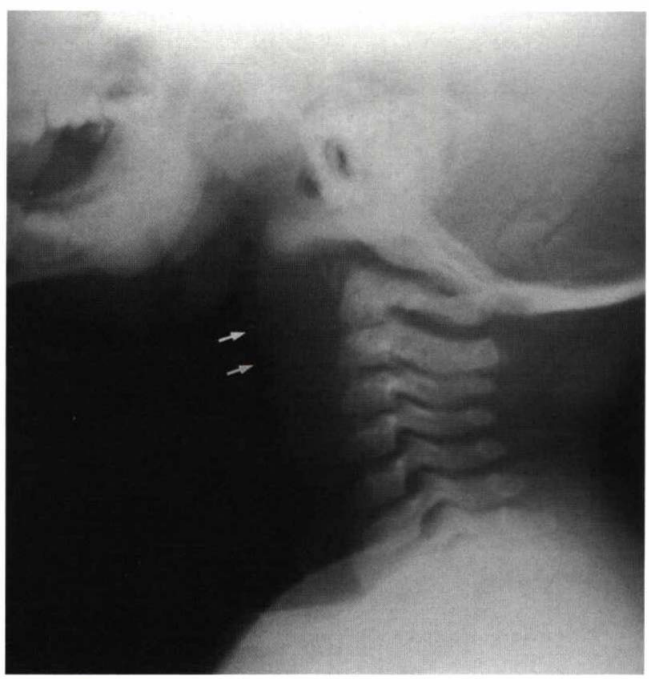

Figure 130–1. Retropharyngeal cellulitis. Lateral radiograph shows widening of the retropharyngeal space (arrows).

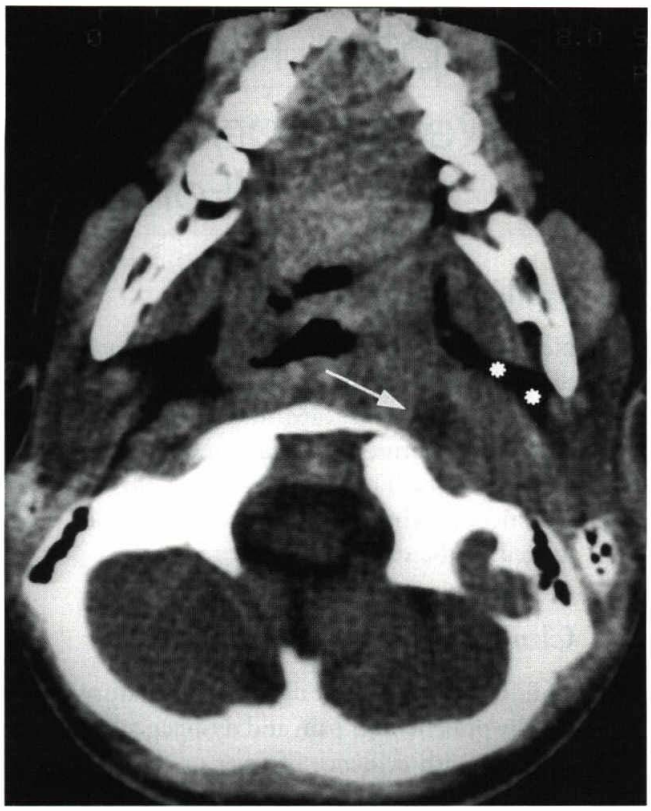

Figure 130–2. Retropharyngeal cellulitis. Axial contrast-enhanced CT shows a left retropharyngeal lymph node with central low density suggesting suppuration (arrow). Note the associated retropharyngeal soft tissue swelling and displacement of the left parapharyngeal space anteriorly (asterisks).

MR

Enlarged retropharyngeal nodes show intermediate signal intensity on T1-weighted images and strong contrast enhancement. Rim enhancement indicates the presence of suppurative lymphadenitis. On T2-weighted images, the inflamed nodes show high signal intensity. Soft tissue thickening as a result of cellulitis also shows strong contrast enhancement and high signals on T2-weighted images.

Imaging Pearls

- The retropharyngeal space stretches from the skull base to approximately T4. It is therefore important to visualize the superior and inferior extent of inflammation.
- The retropharyngeal space is located anterior to the prevertebral muscles. If the inflammatory process extends posterior to the prevertebral muscles, the prevertebral space is also affected.

Suggested Readings

1. Davis WL, Harnsberger HR, Smoker WRK, Watanabe AS. Retropharyngeal space: evaluation of the normal anatomy and diseases with CT and MR imaging. *Radiology* 1990;174:59–64.
2. Hudgins PA, Dorey JH, Jacobs IN. Internal carotid artery narrowing in children with retropharyngeal lymphadenitis and abscess *AJNR Am J Neuroradiol* 1998;19:1841–1843.
3. Chong VFH, Fan YF. Radiology of the retropharyngeal space. *Clin Radiol* 2000; 55:740–748.

Chapter 131

Retropharyngeal Space Abscess (Foreign Body)

Epidemiology

Nearly 80% of all cases of swallowed pharyngeal and esophageal foreign bodies are seen in the pediatric population. Children and psychiatric patients may swallow a variety of foreign bodies such as coins, caps, and small toys. Senile and stuporous patients may inhale dental bridges or dentures. In adults, the most commonly swallowed foreign bodies are fish and chicken bones. These objects are usually lodged in areas of normal anatomic narrowing in the cricopharyngeal area, the aortic arch, or the distal esophagus. Most animal bones are lodged in the cricopharyngeal region.

Clinical Findings

Children present clinically with respiratory distress, drooling, or regurgitation but adults usually present with pain and dysphagia. Senile, psychiatric, or stuporous patients may present late with evidence of fever or sepsis.

Pathology

Sharp objects may perforate the pharynx or esophagus and migrate along tissue planes and compartments. This may result in abscess formation in the adjacent spaces such as the retropharyngeal space.

Treatment

Surgical removal under antibiotic cover should be performed soon after radiological localization of the foreign body. If the history is short and if there are no complications, the foreign body can be removed endoscopically.

Imaging Findings

CT

Plain CT of the neck may be performed to confirm the presence or absence of an ingested foreign body. Contrast-enhanced CT (Fig. 131–1)will demonstrate the site and level of the resultant inflammation or abscess. Frequently, gas translucencies are detected within the retropharyngeal space.

MR

MR imaging is seldom indicated in the management of an ingested foreign body. This modality cannot define reliably the presence of foreign body or gas collections.

Imaging Pearls

- The posterior cricoid lamina may mimic a swallowed foreign body on a lateral neck radiograph (Fig. 131–2) as well as on CT. The clue to recognizing this normal variant is first an awareness of this entity and second, the presence of normal soft tissue planes around the posterior cricoid lamina.
- It is important to determine the lower limit of the retropharyngeal abscess, which may extend down to the mediastinum.

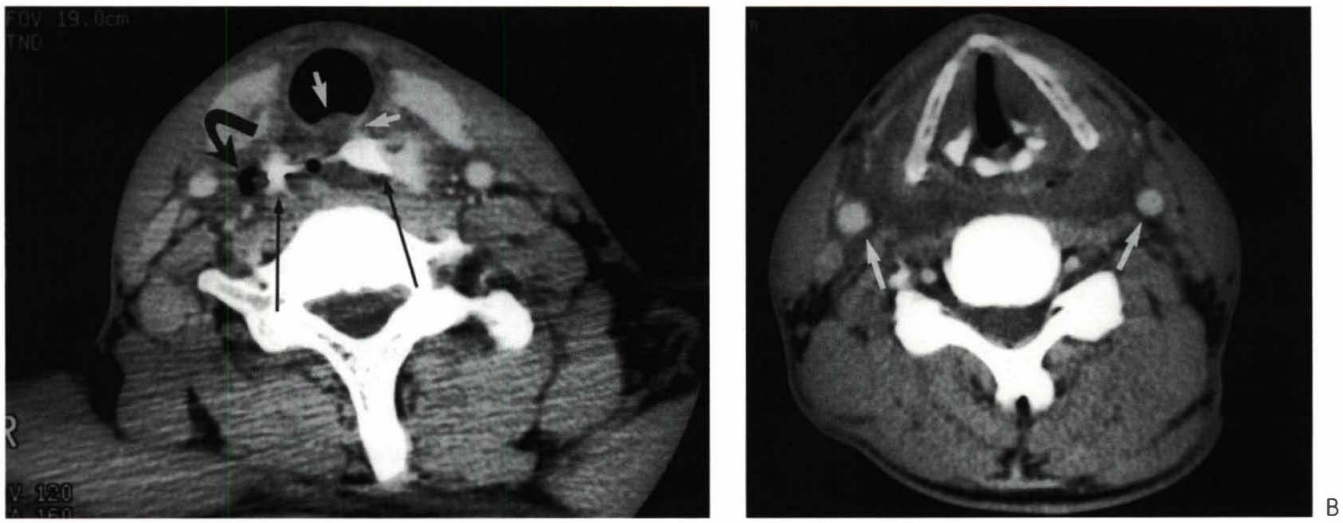

Figure 131-1. Swallowed denture with perforation into the retropharyngeal space. (A) Contrast-enhanced CT shows a denture lodged in the retropharyngeal space (long arrows). Note the anteriorly located esophagus (white arrows) and gas within the retropharyngeal space (curved arrow). (B) Contrast-enhanced CT (at glottic level) shows low attenuation in the retropharyngeal space, indicating edema. There is loss of the normal fat planes and displacement of the carotid sheaths bilaterally (arrows).

Figure 131-2. Normal cricoid lamina calcification, which may mimic swallowed foreign body. (A) Lateral neck radiograph shows a linear laryngeal calcific density at level C5/C6 (arrow). Axial CTs, (B) bone window and (C) soft tissue show isolated calcification in the cricoid lamina (white arrow) located anterior to the esophagus (black arrow).

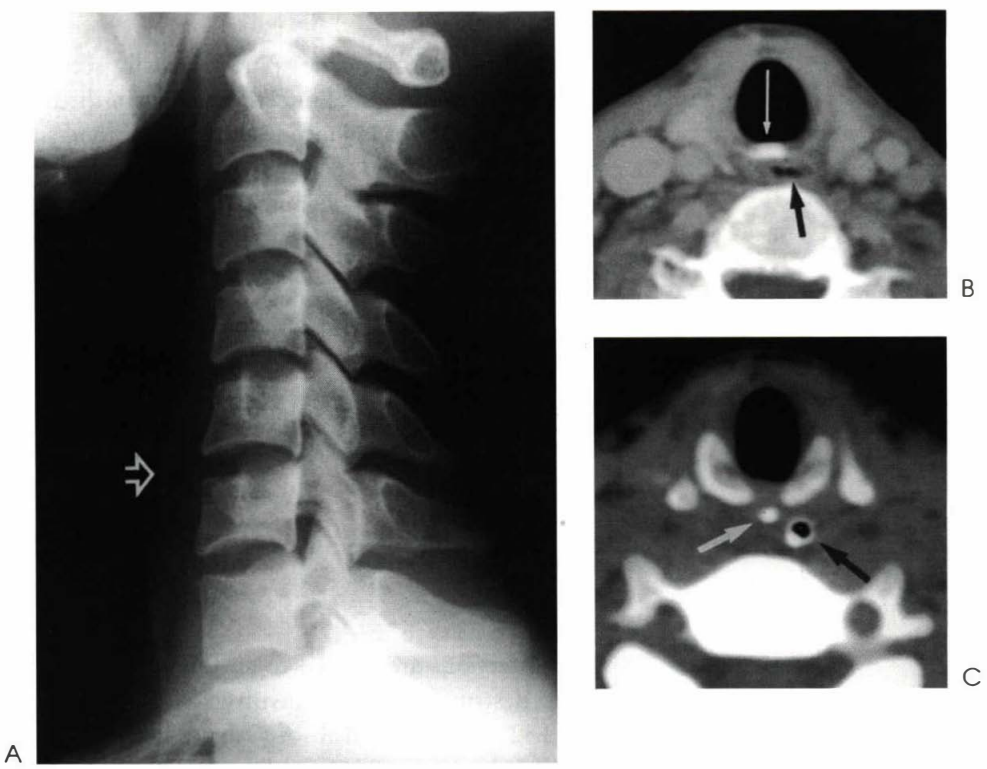

Suggested Readings

1. Levine MS. Miscellaneous abnormalities. In: Gore RM, Levine MS, Laufer I, eds. *Textbook of Gastroenterology Radiology.* Philadelphia: Saunders; 1994:512–530.
2. Keats TE. *Atlas of Normal Variants That May Simulate Disease.* 4th ed. Chicago: Year Book Medical Publishers; 1988.
3. Chong VFH, Fan YF. Radiology of the retropharyngeal space. *Clin Radiol* 2000; 55:740–748.

Chapter 132

Tuberculous Retropharyngeal Space Abscess

Epidemiology

The most common cause of vertebral body infection throughout the world is tuberculosis. This is particularly evident in developing countries but with the current acquired immune deficiency syndrome (AIDS) epidemic, there is a recrudescence of spinal tuberculosis in Western countries. Approximately 75% of cases of spinal tuberculosis occur before the age of 20 years.

Clinical Findings

Patients may present with fever, weight loss, neck pain, or dysphagia. Patients with destruction of the vertebral bodies may show deformity of the spine. Epidural spread produces neurological deficit in 10 to 20% of patients.

Pathology

Tuberculosis involving the spine is usually secondary to hematogenous spread from the lungs. In children, spinal infection begins in the richly vascularized end plates and discs. In adults, as a result of involution of the rich blood supply to the end plates, infection usually starts in the metaphyseal area adjacent to the anterior longitudinal ligament. Infection may subsequently spread subligamentously or to the intervertebral disc. Extension through the anterior longitudinal ligament leads to the formation of prevertebral or retropharyngeal abscess. Destruction of the vertebral body results in acute angulation of the spine.

Treatment

Following the initiation of appropriate antituberculosis therapy, the tuberculous abscess should be drained. Destruction of the vertebral bodies may require spinal stabilization procedures.

Imaging Findings

CT

Most infections are limited to an intervertebral disc and the adjacent vertebral body. CT shows destruction of the involved vertebral body and associated paravertebral abscess. (Fig. 132-1). The "cold abscess" may extend over several vertebral body levels and show the typical appearance of central liquefaction with peripheral enhancement. The prevertebral abscess may subsequently decompress into the retropharyngeal space. Chronic tuberculous abscess may also show calcification.

MR

Sagittal T1-weighted MR image shows a decrease in the height of the intervertebral disc with associated loss of the normal high signal vertebral body marrow. T2-weighted images show increased signals in the vertebral bodies and paraspinal abscess. Contrast-enhanced MR images show enhancement in the intervertebral disc, vertebral bodies, and abscess rim.

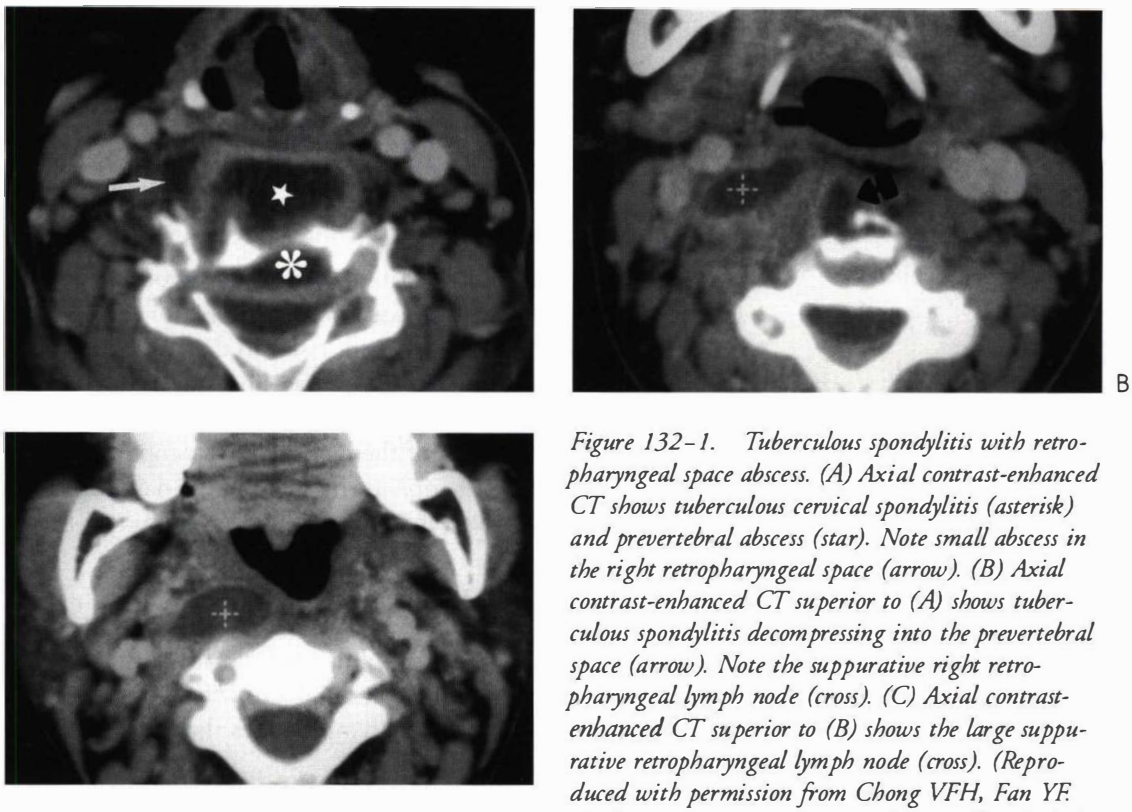

Figure 132–1. Tuberculous spondylitis with retropharyngeal space abscess. (A) Axial contrast-enhanced CT shows tuberculous cervical spondylitis (asterisk) and prevertebral abscess (star). Note small abscess in the right retropharyngeal space (arrow). (B) Axial contrast-enhanced CT superior to (A) shows tuberculous spondylitis decompressing into the prevertebral space (arrow). Note the suppurative right retropharyngeal lymph node (cross). (C) Axial contrast-enhanced CT superior to (B) shows the large suppurative retropharyngeal lymph node (cross). (Reproduced with permission from Chong VFH, Fan YF. Radiology of the retropharyngeal space. Clin Radiol *2000;55:740–748.)*

Imaging Pearls

- The diagnosis of a retropharyngeal space abscess should be considered if there is multilevel involvement of the cervical spine associated with a kyphosis.
- Paraspinal abscess calcifications are highly suggestive of tuberculosis.
- Compared with pyogenic infection, subligamentous spread with involvement of the anterior vertebral bodies with direct spread into the adjacent soft tissue is more frequently encountered in tuberculosis.

Suggested Readings

1. Mark SA. Infectious and inflammatory diseases of the spine. In: Atlas SW, ed. *Magnetic Resonance Imaging of the Brain and Spine*. 2nd ed. Philadelphia: Lippincott-Raven; 1996:1207–1264.
2. Smith AS, Weinstein MA, Mizushima A, et al. MR imaging characteristics of tuberculous spondylitis vs vertebral osteomyelitis. *AJNR Am J Neuroradiol* 1989;10:619–625.
3. Ruiz A, Post MJD, Ganz WI, et al. Inflammatory and infectious processes of the cervical spine. *Neuroimaging Clin N Am* 1995;5:401–425.
4. Smith AS, Weinstein MA, Mizushima A, et al. MR imaging characteristics of tuberculous spondylitis vs vertebral osteomyelitis. *AJR Am J Roentgenol* 1989;153:399–405.

Chapter 133

Retropharyngeal Lymphadenopathy

Epidemiology

Rouvière described a lateral and medial group of retropharyngeal lymph nodes (RPLNs) (Fig. 133–1). Primary squamous cell carcinoma arising from the nasopharynx, oropharynx, and hypopharynx may metastasize to the RPLNs. The most common primary malignancy that spreads to the RPLNs is nasopharyngeal carcinoma. More than 51% of patients with nasopharyngeal carcinoma will show RPLN involvement at presentation. The RPLNs are first echelon nodes of the nasopharynx, oropharynx, and hypopharynx. However, in one third of patients lymphatic drainage of the nasopharynx bypasses the first echelon nodes to drain directly into the internal jugular chain.

Clinical Findings

Enlargement of the RPLNs is a radiological diagnosis because these nodes cannot be palpated. Patients with malignant nodes usually do not have symptoms referable to the metastatic nodes. Retropharyngeal lymph nodes should be considered as cervical lymph nodes when staging the neck.

Pathology

Hasegawa and Matsuura reported nodal size with histopathological proof in 24 patients with advanced carcinoma of the oropharynx and hypopharynx. The average size of 12 positive nodes was 15 mm (range 5–22 mm). The average size of 17 negative nodes was 11 mm (range 3–25 mm). The authors also reported that in 11 nodes $>$ 15 mm, eight (73%) were positive, whereas in 18 nodes $<$ 15 mm, only four (22%) were positive. There was clearly a large overlap of positive and negative nodes.

Treatment

Retropharyngeal metastasis is of no prognostic significance in nasopharyngeal carcinoma. However, RPLN metastasis directly affects the treatment and indicates a worse prognosis in patients with primary lesions arising from outside the nasopharynx. RPLNs are not usually treated in standard neck dissections and may not be included in standard radiation ports for oropharyngeal or hypopharyngeal tumors. Proper assessment will directly alter the treatment of most patients with oropharyngeal or hypopharyngeal tumors. The presence of metastases to the RPLNs is associated with decreased neck control, increased distant metastasis, and decreased survival.

Figure 133–1. Schematic illustration demonstrates the location of the lateral (arrows) and medial (arrowheads) retropharyngeal lymph nodes.

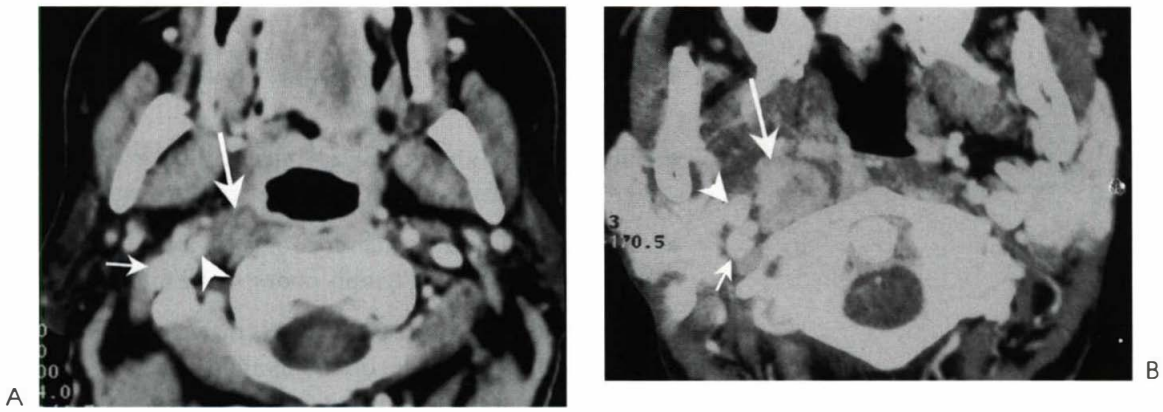

Figure 133–2. (A,B) Axial contrast-enhanced CT shows two examples of enlarged metastatic retropharyngeal lymph nodes. The large arrows identify the enlarged lymph nodes. The arrowhead and small arrow show lateral displacement of the carotid artery and jugular vein, respectively.

Figure 133–3. Axial contrast-enhanced T2-weighted image shows an enlarged retropharyngeal lymph node from nasopharyngeal carcinoma (arrow).

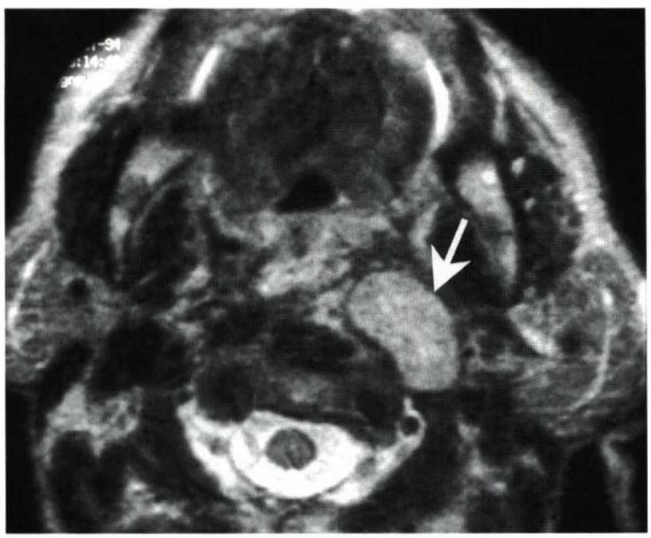

Imaging Findings

CT

Almost all RPLNs are located at levels C1 and C2. The lateral group is more likely to be identified than the medial group. These nodes are located just anterior to the longus colli muscle in the retropharyngeal space. Normal RPLNs are usually not seen on CT. When visible, normal RPLNs measure between 3 and 5 mm. Metastases to the RPLNs are characterized by mild to moderate contrast enhancement. A central low density surrounded by a rim of enhancement indicates nodal necrosis (Fig. 133–2).

MR

Normal RPLNs may be identified on axial T2-weighted MR images (Fig. 133–3). The margins of the enlarged nodes are usually well defined in metastatic disease. An irregular outline indicating extracapsular spread is uncommon. Involved nodes show good contrast enhancement and high signals on T2-weighted images. Ring enhancement may also be encountered.

Imaging Pearls

- Normal RPLNs can be very large in children. Thus large RPLNs in children should not be considered pathological.
- The criteria for abnormally enlarged RPLNs in adults is debatable. The maximum diameter for suspicious lymph nodes varies between 7 and 10 mm.
- The presence of a central area of decreased attenuation is the most accurate sign for RPLN metastases for lymph nodes < 10 mm.
- Nodal necrosis in metastatic RPLNs may be confused with abscess or suppurative lymphadenitis. Necrotic nodes often maintain a clear nodal margin with no signs of surrounding inflammation. Patients with retropharyngeal abscess, on the other hand, are usually septic. Imaging shows associated inflammatory changes in the surrounded spaces such as the parapharyngeal or carotid spaces.
- A mass in the nasopharynx may consist of a primary nasopharyngeal tumor and enlarged RPLNs. MR imaging can clearly separate the primary tumor from nodes. On T2-weighted images the nodes show higher signal intensities.

Suggested Readings

1. Rouvière H. *Anatomy of the Human Lymphatic System*. Ann Arbor: Edward Brothers; 1938.
2. Chong VFH, Fan YF, Khoo JBK. Retropharyngeal lymphadenopathy in nasopharyngeal carcinoma. *Eur J Radiol* 1995;21:100–105.
3. McLaughlin MP, Mendenhall WM, Mancuso AA, et al. Retropharyngeal adenopathy as a predictor of outcome in squamous cell carcinoma of the head and neck. *Head Neck* 1995;17:190–198.
4. Chua DTT, Sham JST, Kwong DLW, Au GKH, Choy DTK. Retropharyngeal lymphadenopathy in patients with nasopharyngeal carcinoma. *Cancer* 1997;79:869–877.
5. Mancusco AA, Hansberger HR, Muraki AS, Stevens MH. Computed tomography of cervical and retropharyngeal lymph nodes: normal anatomy, variants of normal, and applications in staging head and neck cancer, II: Pathology. *Radiology* 1983;148:715–723.
6. Hasegawa Y, Matsuura H. Retropharyngeal node dissection in cancer of the oropharynx and hypopharynx. *Head and Neck* 1994;16:173–180.

Chapter 134

Tumor Spread into the Retropharyngeal Space

Epidemiology

Compared with benign lesions, the retropharyngeal space (RPS) is much more commonly affected by malignancy either by direct invasion or through metastasis to the retropharyngeal nodes. Squamous cell carcinoma of the upper aerodigestive tract may extend into the RPS. However, progressive extension through the prevertebral fascia and into the prevertebral space is unusual.

Clinical Findings

Invasion of the RPS is often overshadowed by symptoms related to the primary tumor in the upper aerodigestive tract. Superior extension with subsequent erosion of the skull base may be associated with deep pain. The pharyngeal mucosa may be displaced anteriorly by the retropharyngeal mass. However, retropharyngeal tumor spread is usually a radiological diagnosis made during tumor mapping.

Pathology

Tumors can spread both inferiorly and superiorly along the RPS. Tumors spreading superiorly are impeded by the attachment of the fascia defining the RPS to the skull base. This may result in extensive erosion of the clivus. It is possible that tumor spread along the RPS originates from metastatic retropharyngeal lymphadenopathy with extracapsular extension.

Treatment

The primary lesion (depending on histology) is treated with radiation therapy or surgery or both. Tumors affecting the skull base are deemed nonresectable at most institutions and are treated with radiation therapy with or without chemotherapy.

Imaging Findings

CT

The primary tumor can be easily defined by contrast-enhanced CT. RPS infiltration can be recognized by RPS soft tissue thickening in contiguity with the primary tumor. Superior extension with skull base erosion can be demonstrated on both CT and MR imaging (Figs. 134–1 and 134–2).

MR

RPS infiltration shows diffuse contrast enhancement on T1-weighted images and high signals on T2-weighted images. The tumor extent is adequately seen on axial sections, but sagittal images can provide in a single image the craniocaudal extent of the disease.

Imaging Pearls

- Nasopharyngeal carcinoma can spread inferiorly along the RPS to the hypopharynx. Such tumors are designated T4 disease.

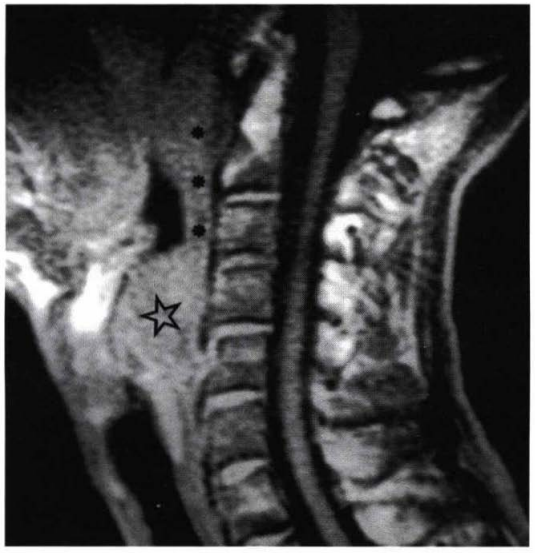

A

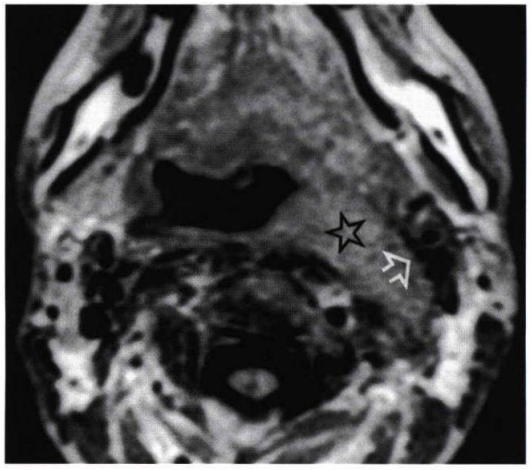

B

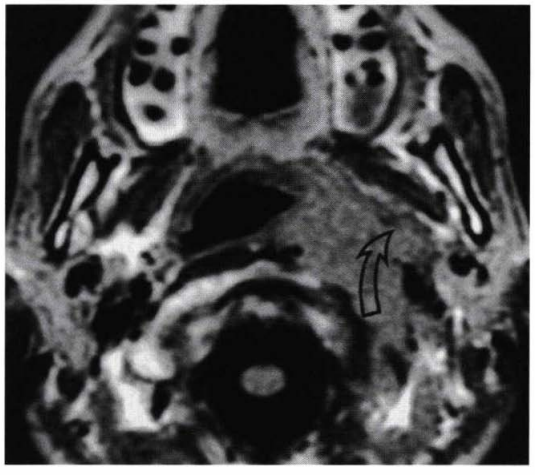

C

Figure 134–1. Recurrent supraglottic carcinoma with superior spread. (A) Sagittal T1-weighted MR image shows the large supraglottic tumor (star) with superior extension and thickening of the retropharyngeal tissue (asterisks). (B) Axial contrast-enhanced MR image (oropharyngeal level) shows tumor occupying the left retropharyngeal space (star) and displacement of the carotid space (arrow). (C) Axial contrast MR image superior to (B) shows tumor infiltration in the retropharyngeal spaces with involvement of the adjacent parapharyngeal space (arrow).

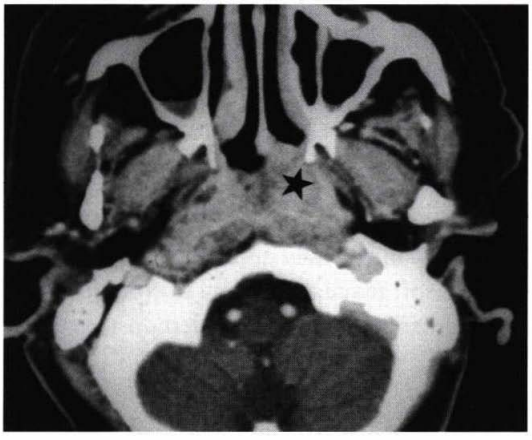

A

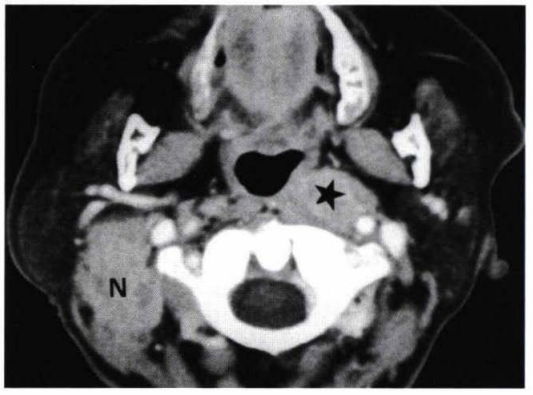

B

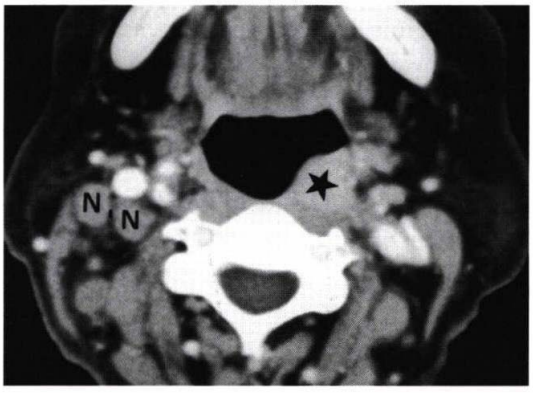

C

Figure 134–2. Nasopharyngeal carcinoma with inferior retropharyngeal space spread. (A) Axial contrast-enhanced CT shows a large enhancing tumor in the nasopharynx (star). (B) Axial contrast-enhanced CT shows a large tumor-infiltrated left retropharyngeal lymph node (star). Note also the enlarged right cervical nodes (N). (C) Axial contrast-enhanced CT (oropharyngeal level) shows tumor in left retropharyngeal space (star). Note again the involved right internal jugular nodes (N).

Suggested Readings

1. Harnsberger HR. *Handbook of Head and Neck Imaging*. 2nd ed. St. Louis: Mosby; 1995:199–223.
2. Chong VFH, Fan YF. Radiology of the retropharyngeal space. *Clin Radiol* 2000;55:740–748.
3. Som PM, Curtin HD. Fasciae and spaces. In: Som PM, Curtin HD, eds. *Head and Neck Imaging*. St Louis: Mosby; 1996.

Chapter 135

Chordoma

Epidemiology

Chordomas are thought to arise from the remnants of the notochord, the embryonic precursor of the axial skeleton. Chordomas are usually seen in the fifth and sixth decades but they may be found in all age groups. There is no sex predilection. Spheno-occipital chordomas account for 35% of cases and are more commonly encountered in children and the younger age group. Fifty percent of chordomas are located in the sacrococcygeal area; these tumors usually occur in the fifth and sixth decades.

Clinical Findings

Clinical signs and symptoms depend on the size and location of the tumor. Encroachment of the neural or jugular foramen may produce cranial nerve palsy. Intracranial extension may produce signs related to brainstem compression. If the tumor extends into the nasopharynx or nasal cavity, breathing difficulty and nasal stuffiness may be the presenting symptoms.

Pathology

Grossly, they are locally invasive, soft or firm lobulated masses. There are two histologic varieties of chordomas. The regular type closely resembles normal notochord tissue in different stages of development. In typical chordomas, vacuolated physaliphorous cells with variable amounts of intracytoplasmic mucin are embedded in pools of extracellular mucin. The second variety is the chondroid type that is associated with a cartilaginous matrix.

Treatment

Chordomas are relatively radioresistant and they do not respond to chemotherapy. Treatment therefore depends on surgical excision. However, in recent years high energy particles (proton beams) and advanced cranial base surgical techniques have offered better control of this disease. The chondroid variety has a better prognosis and these patients may live for another 20 to 30 years following diagnosis. The regular type shows a 5-year survival of 30 to 50%. Local recurrences are common and distant metastasis may be seen in 10% of patients.

Imaging Findings

CT

The tumor shows gross destruction of the clivus. There is moderate tumor enhancement and 50% of these tumors may show calcifications. The tumor typically shows a large soft tissue component relative to the area of bony destruction.

MR

This tumor shows intermediate signal on T1-weighted sequences and high signal on T2-weighted sequences. Contrast enhancement is variable and heterogeneous. Tumor may extend into the retropharyngeal space and spread inferiorly within this fascial compartment. This is best seen on axial contiguous sections (Fig. 135–1).

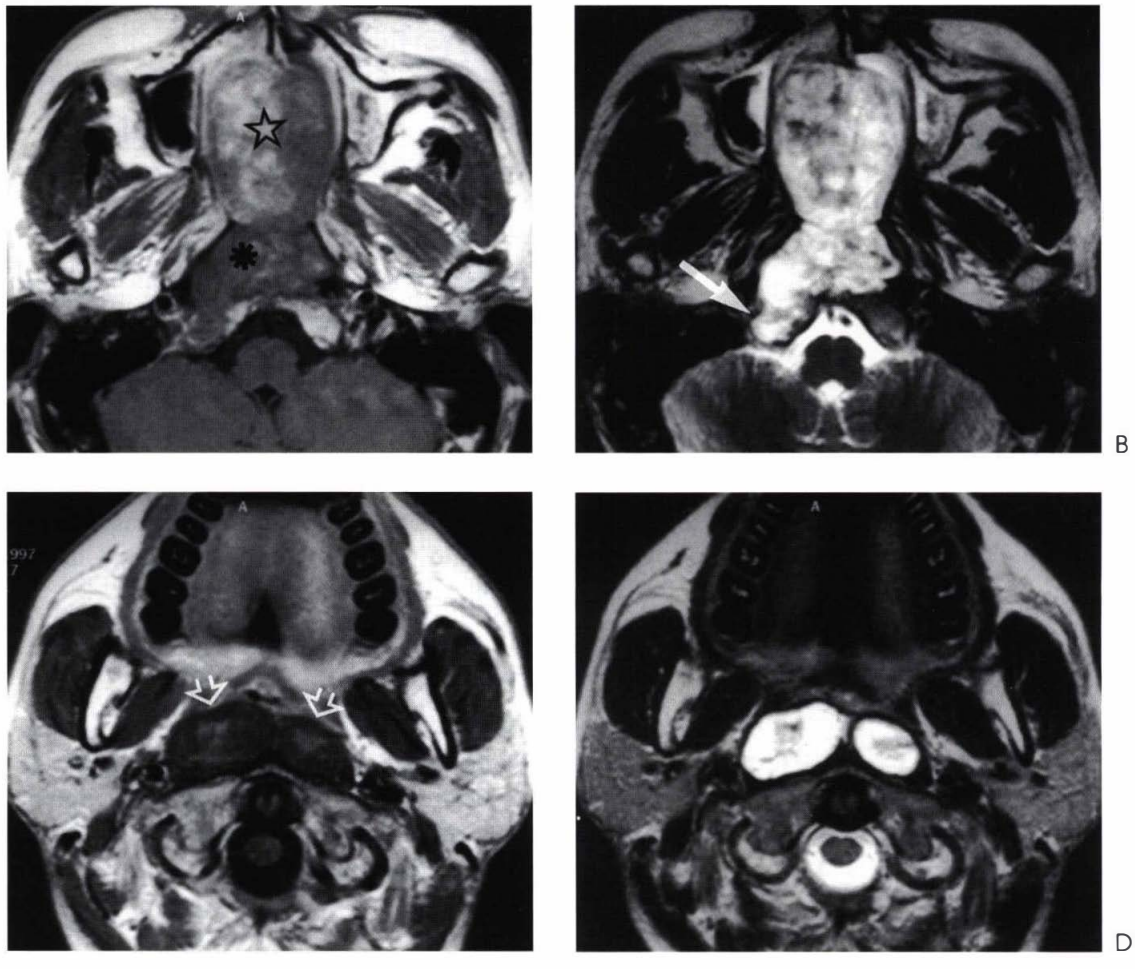

Figure 135-1. Chordoma with retropharyngeal space involvement. (A) Axial contrast-enhanced MR image shows a large chordoma filling almost entirely the nasopharyngeal space (asterisk) and the nasal fossa (star). The tumor shows only slight patchy enhancement. (B) Axial T2-weighted MR image shows high signals in the tumor. Note the involvement of the clivus (arrow). (C) Axial contrast-enhanced MR image inferior to (A) shows apparent enlargement of the prevertebral muscles (arrows). Note the slight patchy contrast enhancement. (D) Axial T2-weighted MR image shows high signal intensity tumor extending inferiorly along the retropharyngeal space.

Imaging Pearls

- Chordomas are typically located medial to the petroclival fissure. Any midline or paramedian lesion in this region associated with bone destruction or calcifications is likely to be a chordoma.
- The presence of increased T2-weighted signal in a skull base mass medial to the petroclival fissure is suggestive of chordoma.
- Chordomas are gelatinous and tend to creep into various spaces. They may spread along tissue planes such as the retropharyngeal space.

Suggested Readings

1. Rosai J. Bones and joints. In: Rosai J, ed. *Ackerman's Surgical Pathology*. 8th ed. St. Louis: Mosby; 1996:1917–2020.
2. Nuss DW, Janecka IP. Cranial base tumors. In: Myers EN, Suen JY, eds. *Cancer of Head and Neck*. 3rd ed. Philadelphia: WB Saunders; 1996:234–275.
3. Chong VFH, Fan YF. Radiology of the retropharyngeal space. *Clin Radiol* 2000;55:740–748.

Chapter 136

Lipoma

Epidemiology

Primary neoplasms originating in the retropharyngeal space (RPS) are extremely uncommon. Primary lesions of the RPS are usually related to the contents, which are lymph nodes and fatty tissues. As a result, lipomas may be seen in the RPS. These are unusual lesions, so gender and age predilections have not been thoroughly described.

Clinical Findings

Small RPS lipoma may be an incidental finding. However, large lesions may displace adjacent structures and produce vague symptoms. Clinical examination may show displacement of the pharyngeal mucosa.

Pathology

Lipomas are yellow, lobulated, and very well encapsulated tumors. They consist of normal adult adipose tissue. Lipomas are classified histologically according to the kind of other tissues that may be present (e.g., fibrolipoma, angiolipoma, and myxolipoma). These tumors very rarely undergo malignant degeneration. Liposarcomas originate from lipoblasts within fascia rather than ordinary lipocytes.

Treatment

Lipomas are benign lesions. If they are asymptomatic they can be left alone. Surgical excision is indicated if the lesions are large and compressing adjacent structures.

Imaging Findings

CT

The CT appearance of lipomas is distinctive. Lipomas have smooth margins and they register typically low attenuation values. An irregular margin or foci of intermediate attenuation within the lesion should raise the possibility of a liposarcoma. In the RPS, lipomas maintain an elliptical configuration conforming to the shape of a distended RPS. The pharyngeal airspace is displaced anteriorly (Fig. 136-1).

MR

The MR imaging features of RPS lipoma are also distinctive. The signal intensity of lipoma parallels that of normal fat. Lipomas show high signal intensity on both T1-weighted images and fast spin-echo (FSE) T2-weighted images. With fat suppression, lipomas reveal a low signal intensity pattern, which may render it inconspicuous.

Imaging Pearls

- The low attenuation value of a lipoma adjacent to or bulging into the pharyngeal air space may be confused with an air-containing structure. This potential pitfall can be avoided by viewing images with appropriate window levels and measuring the attenuation value of the suspected abnormality.
- A lipoma can be diagnosed with a high degree of certainty if the tumor is homogeneous low attenuation. However, a liposarcoma cannot be excluded if the lesion contains areas of intermediate attentuation.

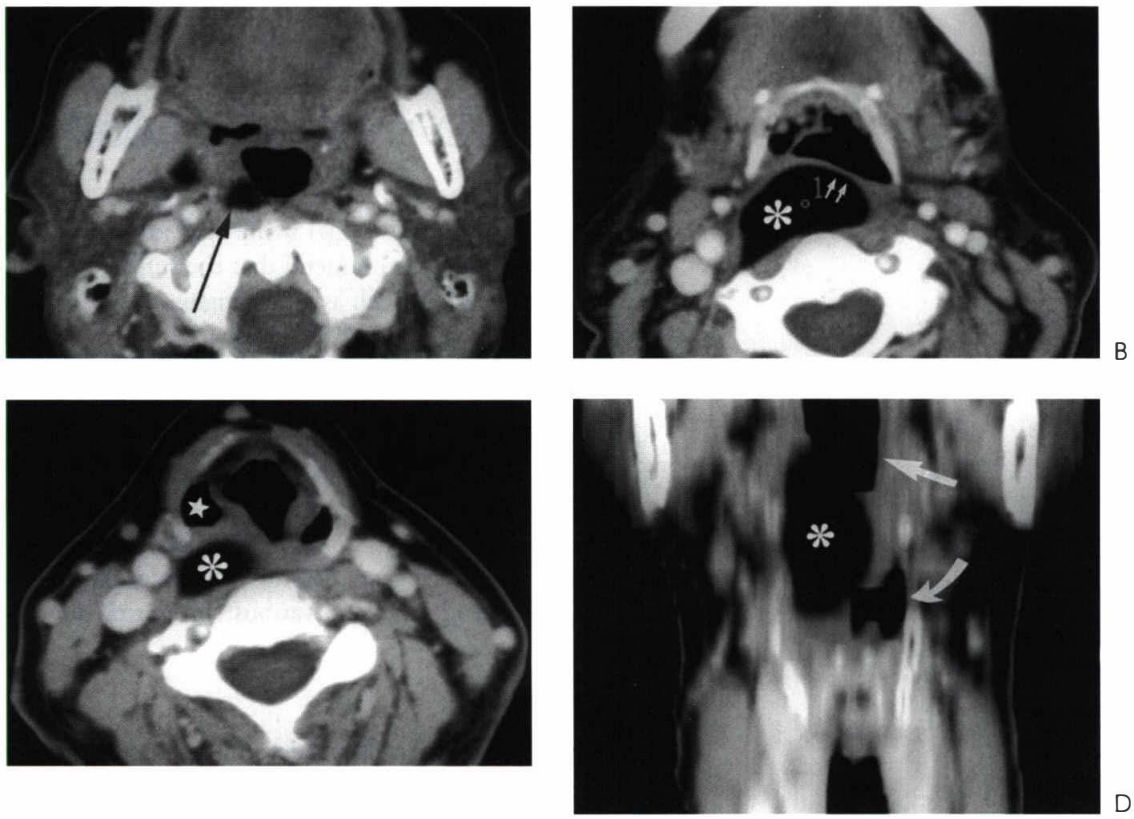

Figure 136–1. Retropharyngeal lipoma. (A) Axial contrast-enhanced CT shows the superior end of a retropharyngeal lipoma (arrow) at level C1/C2. (B) Axial contrast-enhanced CT shows lipoma (asterisk) at the level of the hyoid bone. Density measurement confirmed fat attenuation characteristics. Note the anteriorly displaced posterior pharyngeal wall (arrows). (C) Axial contrast-enhanced CT shows retropharyngeal lipoma (asterisk) at the level of the thyroid cartilage displacing the pyriform sinus (star) anteriorly. (D) Coronal reconstruction shows the lipoma (asterisk) adjacent to the pharyngeal air space (solid arrow) and the laryngeal air space (curve arrow).

Suggested Readings

1. Harnsberger HR. *Handbook of Head and Neck Imaging.* 2nd ed. St Louis: Mosby; 1995:199–223.
2. Smoker RK. Oral cavity. In: Som PM, Curtin HD, eds. *Head and Neck Imaging.* 2nd ed. St. Louis: Mosby; 1996:488–544.
3. Chong VFH, Fan YF. Radiology of the retropharyngeal space *Clin Radiol* 2000;55:740–748.

Chapter 137

Lymphatic Malformations

Lymphatic malformation (*LM*) is the current term used to describe lymphangiomas. Mulliken and Glowacki recommend that the suffix *"-oma"* only be used in lesions that exhibit cellular proliferation, such as a hemangioma. LM is a congenital lesion that results from a defect in embryogenesis of the lymphatic system. They occur in equal frequency in males and females. They most commonly present in newborn children, with 65% of lesions noted at birth, 80% present at 1 year, and 90% present by 2 years of age. Ten percent of LMs may initially present in adulthood. LMs may be localized or associated with a generalized malformation of the lymphatic system. Advanced malformations may be seen as diffuse lymphangiectasis in utero and are incompatible with life. LMs have been associated with a number of syndromes, the most common being Turner's syndrome. Other syndromes include Noonan's syndrome, fetal alcohol syndrome, familial pterygium syndrome, distichiasis-lymphedema syndrome, and various chromosomal aneuploidies.

Embryology

LM is thought to occur from a defect in the normal drainage of the lymphatic channels into the venous system. The result is a progressive enlargement of the isolated lymphatic spaces due to the continued secretion of lymph. There are several proposed explanations for this malformation. The malformation may be due to a portion of the lymphatic network that fails to reestablish a communication with the venous system and is sequestered early in embryogenesis. Early malformations involving the more primitive jugular, subclavian, and axillary sac are thought to result in the formation of the larger cystic hygromas. These lesions occur in soft areolar tissues in areas with wide fascial planes, with the result being sharply demarcated round or oval lesions. Lesions that have smaller cystic spaces and are more diffuse and infiltrative are believed to occur later in embryogenesis. These malformations have time to grow distally along narrower facial planes and insinuate themselves along vessels and nerve trunks. This probably results in the mixed malformations described by Mulliken and Glowacki such as lymphaticovenous and lymphaticocapillary malformations. Thus, LMs that occur in the cheeks, lips, and tongue tend to contain more of an angiomatous component.

Pathology

Pathologically, LMs have been categorized in the past based on the size of the anomalous lymphatic space. It should be noted that *lymphatic malformation* is the current term used to describe these malformation and that the terms *cavernous lymphangioma* and *capillary lymphangioma* probably refer to the mixed lymphatic malformations described by Mulliken and Glowacki. We present the older terminology in the following text for historical consistency.

Cystic hygroma is the most common form and consists of a honeycomb of very large dilated lymphatic spaces lined by a single layer of flat endothelium. These lesions are often solitary and occur in the presence of an otherwise normal lymphatic system. Seventy-five percent of these lesions occur in the neck, with a predilection for the posterior compartment of the neck.

A cavernous lymphangioma is composed of mild to moderately dilated lymphatic spaces, the size of which is between the cystic spaces seen in cystic hygromas and capillary hemangiomas. These lesions tend to be situated in the oral cavity or salivary glands. Cavernous lymphangiomas tend to be subcutaneous lesions, which tend to penetrate adjacent muscular and neurovascular structures without destroying them. The peripheral location and subcutaneous spread are suggestive of a defect in embryogenesis during a later phase of lymphatic development (9–10 weeks) as compared with a cystic hygroma.

Capillary hemangioma (simple, lymphangioma simplex) is composed of a network of small lymph, thin-walled channels that are the size of capillaries and is the least common form of lymphangioma. These lesions are located predominantly within the epidermis and

can occur anywhere throughout the body. Because of their superficial location, capillary hemangiomas are believed to form the latest in development.

Clinical Findings

The extracranial head and neck is the most common site of LMs (75%). When they occur in the retropharyngeal space, they typically present as a painless submucosal neck mass. Patients with large masses may present with difficulty swallowing. LMs tend to enlarge commensurate with the growth of the child and not by endothelial proliferation. Potential complications include disfigurement, respiratory compromise, and recurrent infections. Rapid enlargement may be due to infection or spontaneous hemorrhage within the lesion.

Treatment

Surgical resection is the treatment of choice for lymphangiomas with distinct margins. However, distal lesions that extend over several anatomical areas are difficult to resect completely and are prone to recurrence. Such patients need close follow-up and may require multiple surgical procedures. Percutaneous sclerotherapy is gaining wider acceptance for more advanced lesions that infiltrate the deep fascial planes. Some authors advocate angiography and embolization for lymphaticocapillary lesions that involve the oral cavity and tongue. The role of interferon therapy for very advanced and infiltrative lesions is currently under investigation.

Imaging Findings

CT

The classic appearance of an LM in the retropharyngeal space is a sharply demarcated, low attenuation mass that does not contain a visible wall. Lesions that have been partially resected or have been repeatedly infected may demonstrate an enhancing wall or contain internal septations. Mixed LMs are heterogeneous and infiltrative. These lesions extend along fascial planes and often involve multiple spaces ("transspatial"). Because of the angiomatous components, mixed lesions may enhance with contrast.

MR

A pure LM is low signal on T1-weighted sequences and high signal on T2-weighted sequences. There is no perceptible wall or enhancement following contrast administration. Pure LMs are low-flow lesions and lack flow voids. Mixed malformations are infiltrative heterogeneous lesions that enhance following contrast. The degree of the enhancement is likely due to the angiomatous component of the mixed lesion (Figs. 137-1 and 137-2).

US

Pure LMs are hypoechoic masses that may occasionally contain internal septations or debris. Doppler analysis may be helpful in identifying and characterizing mixed LMs by identifying and characterizing the presence of intralesional blood flow.

Angiography

Pure LMs are avascular low-flow lesions. However, mixed LMs that have a substantial angiomatous component are hypervascular and have enlarged feeding vessels. Arteriovenous shunting is rare.

Imaging Pearls

- It may be difficult to differentiate a lymphatic malformation from a large retropharyngeal space abscess based on imaging alone. Patients with lymphatic malformations are usually afebrile, whereas patients with a retropharyngeal abscess are febrile and have difficulty holding down secretions.
- A predominantly cystic mass that is transspatial is the characteristic imaging of an LM.

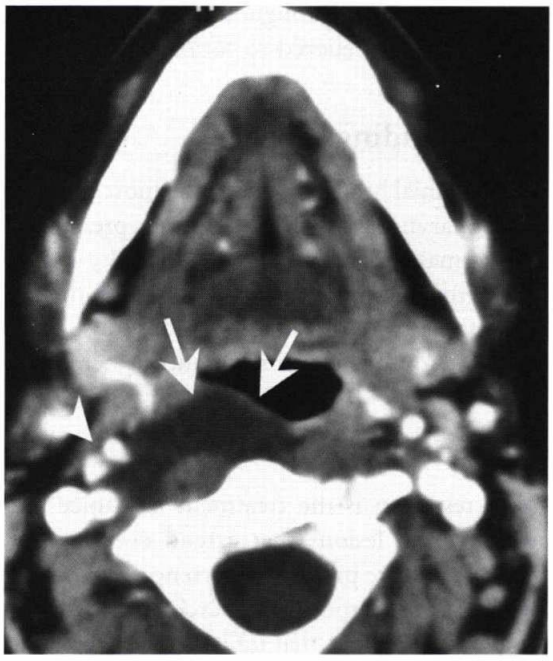

Figure 137-1. Axial contrast-enhanced CT shows a lymphatic malformation involving the retropharyngeal space (arrows). The lesion extends laterally and displaces the contents of the carotid space (arrowhead).

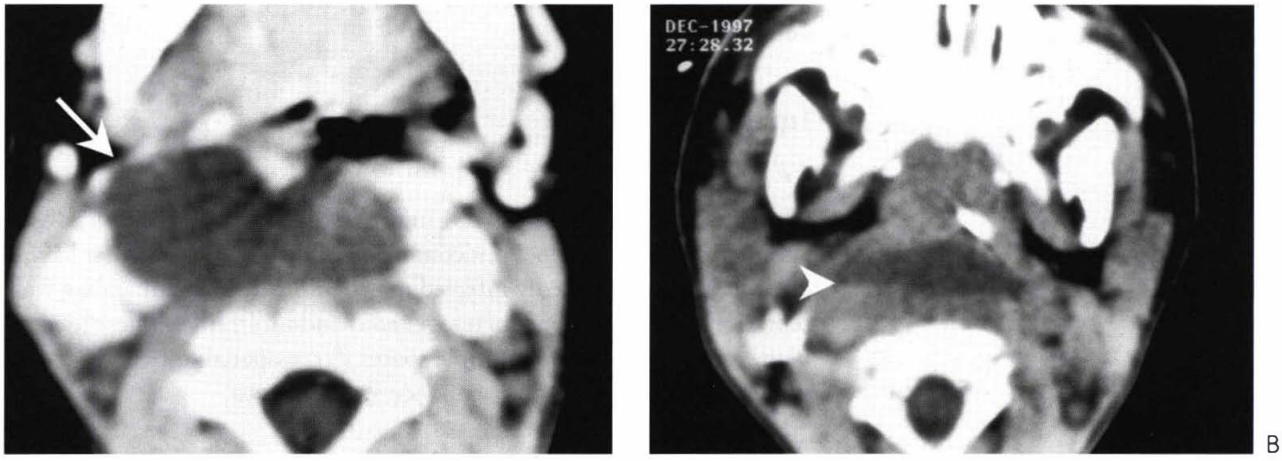

A B

Figure 137-2. (A) Axial contrast-enhanced CT shows a well-defined low attenuation mass that is expanding the retropharyngeal space. Similar to Figure 137-1, the mass is displacing the contents of the carotid space (arrow). The fat planes surrounding this mass are intact. This was interpreted by the surgeons (films never seen by a radiologist) as an abscess in this afebrile patient. The patient underwent needle aspiration that revealed pink straw-colored fluid. (B) CT following needle aspiration demonstrates a fluid-fluid level (arrowhead) likely indicating interval hemorrhage into the retropharyngeal space lymphatic malformation.

Suggested Readings

1. Zadvinski DP, Benson MT, Kerr HH, et al. Congenital malformations of the cervicothoracic lymphatic system: embryology and pathogenesis. *Radiographics* 1992;1175–1189.
2. Batsakis JG. Vasoformative tumors. In: *Tumors of the Head and Neck*. 2nd ed. Baltimore: Williams and Wilkins; 1979:518–520.
3. Mulliken JB, Glowacki J. Hemangiomas and vascular malformations in infants and children: a classification based on endothelial characteristics. *Plast Reconstr Surg* 1982;69:412–422.
4. Mulliken JB. Vascular malformations of the head and neck. In: Mulliken JB, Young AE, eds. *Vascular Birthmarks: Hemangiomas and Malformations*. Philadelphia: WB Saunders; 1988:301–307.

Section V

Prevertebral Space

The prevertebral fascia encloses the prevertebral space. The prevertebral space (PVS) is directly posterior to the retropharyngeal space (RPS). Recently, some authors have suggested renaming the PVS the perivertebral space. We prefer the term *prevertebral space* because this is the original name, and more importantly, it is the designation most often used by the otolaryngologist–head and neck surgeon.

There are certain imaging features that allow one to determine that a mass is involving the PVS. Vertebral body involvement is the most conclusive sign. Primary PVS masses typically displace the RPS and the posterior wall of the visceral space anteriorly, and the contents of the carotid sheath laterally.

An anatomically based differential diagnosis can be generated by knowing anatomic components of the PVS. The contents of the PVS in the suprahyoid neck are the "prevertebral" muscles (longus coli), vertebral body, cervical disc, spinal canal, vertebral artery, and phrenic nerve.

Masses that arise from the prevertebral muscles are most likely of mesenchymal origin. In children, the most common PVS malignancy is rhabdomyosarcoma. However, this lesion may be difficult to differentiate from a neuroblastoma. In the suprahyoid neck, neuroblastomas arise from the sympathetic chain, which is located in the adjacent carotid sheath. Advanced stages of both lesions may erode the vertebral body. Erosion of the adjacent anterior portion of the vertebral body favors a malignant mesenchymal tumor arising from the PVS, whereas erosion along the lateral aspect of the vertebra favors neuroblastoma. Involvement of the PVS may also result from direct extension of a nasopharyngeal carcinoma.

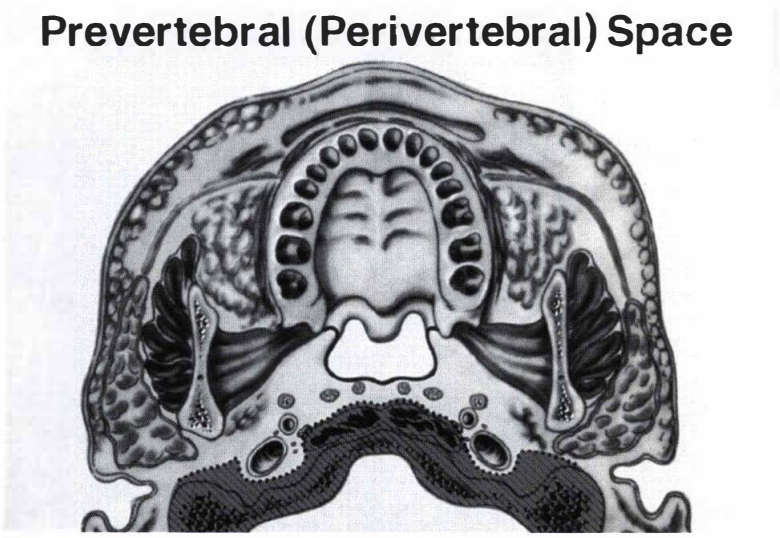

Figure V–1. Schematic illustration demonstrates the location of the prevertebral space (see Color Plate V–1). (Figure reproduced with permission from Mukherji SK, Castillo M. A simplified approach to the spaces of the suprahyoid neck. Rad. Clin N Am *1998;36:761–780.)*

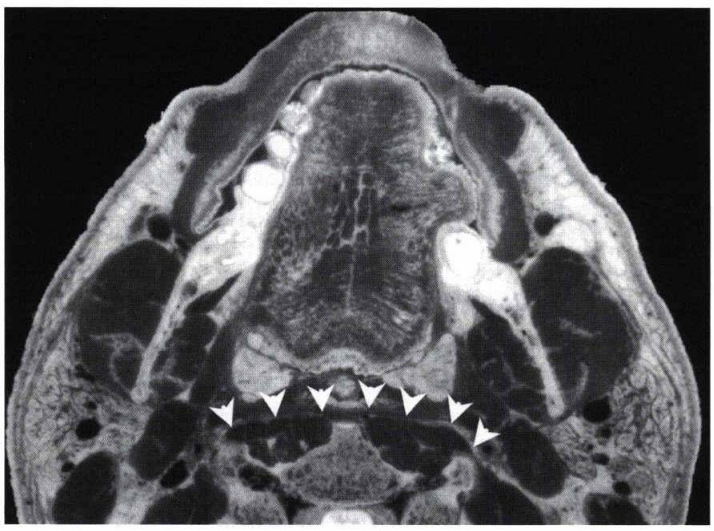

Figure V–2. The arrowheads contour the anterior margin of the prevertebral space.

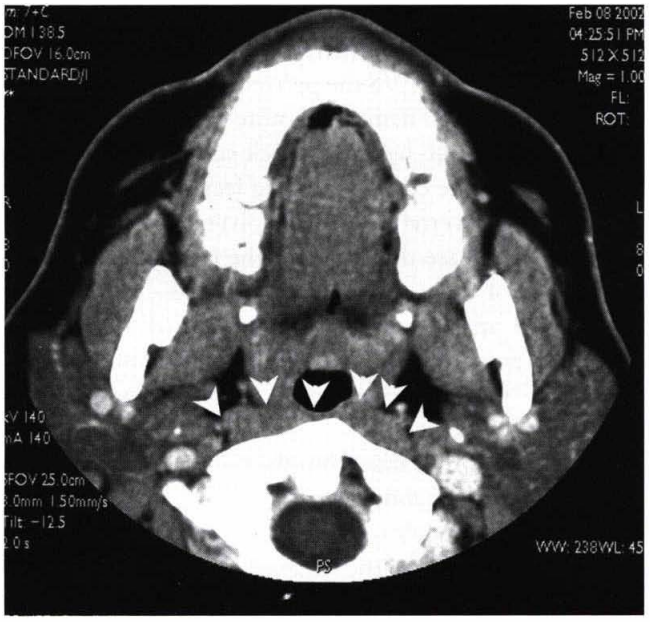

Figure V–3. The anterior margin of the prevertebral space is outlined by the arrowheads.

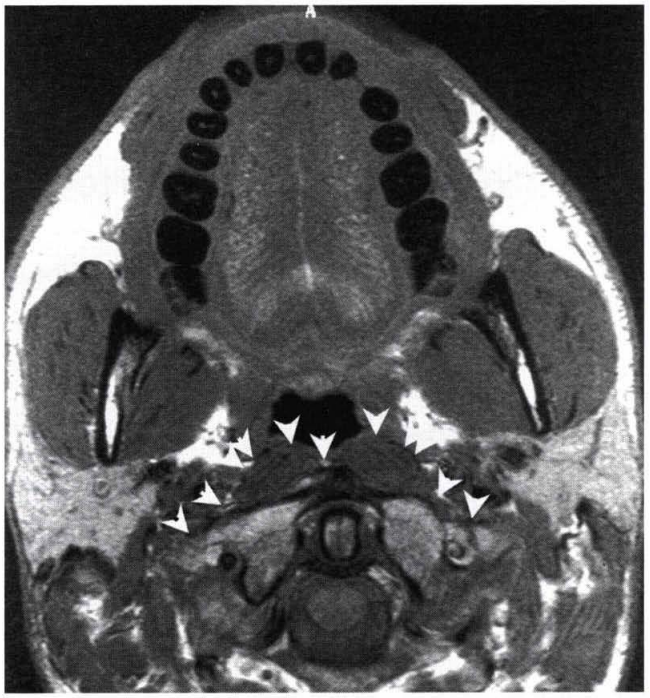

Figure V–4. The anterior limit of the prevertebral space is outlined by the arrowheads on this noncontrast T1-weighted image.

A variety of pathologies may arise from the vertebral body. The most common vertebral body masses are degenerative anterior spondylosis, osteomyelitis, bone metastases, and primary bone tumors. The most frequent cervical disc pathologies are either discitis or anterior disc herniation. A soft tissue mass that extends into the spinal canal and expands a neural foramen is suggestive of a neurogenic tumor. Rarely, an aneurysm or pseudoaneurysm associated with a vertebral artery dissection may present as a PVS mass. Tumors that arise from the phrenic nerve are very unusual.

Suggested Readings

1. Grodinsky M, Holyoke EA. The fasciae and fascial spaces of the head, neck and adjacent regions. *Am J Anat* 1938;63:367–408.
2. Harnsberger HR. *Handbook of Head and Neck Imaging*. 2nd ed. St. Louis: Mosby Year Book; 1995.
3. Mukherji SK, Castillo M. A simplified approach to the spaces of the extracranial head and neck. *Radiol Clin North Am* 1998;36:761–780.

Chapter 138

Anterior Osteophyte

Epidemiology

Spinal osteophytosis (spondylosis deformans) is very common. Approximately 60% of women and 80% of men demonstrate osteophyte formation by the age of 50 years. The disease is more frequent in patients engaged in occupations that require heavy physical labor. Any segment of the vertebral column may be affected. Osteophytes frequently occur in the anterior and anterolateral portions of the vertebral bodies.

Clinical Findings

The presenting symptoms depend on the size and location of the anterior osteophytes and their relationship to adjacent soft tissue and neurological structures. Common symptoms that may be associated with large anterior osteophytes include neck stiffness, restricted motion, and dysphagia. Lateral osteophytes may impinge on the exiting nerve roots and cause radiculopathy.

Pathology

Osteophytes are bony outgrowths that develop in response to disc degeneration. The annulus fibrosus is attached to the vertebral rim by calcified cartilage and to the anterior vertebral surface by Sharpey's fibers. Abnormalities and breakdown in the attachment of the outer annular fibers to the vertebral body rim cause displacement of disc material anteriorly and anterolaterally. This leads to stress at the site of attachment of the Sharpey's fibers. Osteophytes develop at these areas of maximal stress, several millimeters from the actual edge of the vertebra, where the vertebral body and cartilaginous rim unite. They initially extend in a horizontal direction and then in a vertical direction and may eventually bridge the intervertebral disc space.

Treatment

Conservative management, consisting of analgesics and a cervical collar, is usually elected in most patients with anterior osteophytes. Surgical removal may be performed in patients with severe dysphagia or odynophagia due to impingement on the cervical esophagus. Lateral extension into the foramina resulting in radiculopathy may require surgical resection.

Imaging

CT

Anterior osteophytes are seen as focal bony outgrowths from the vertebral body extending into the prevertebral space. The prevertebral muscle is often displaced anteriorly. Anterior osteophytes may be associated with a diffuse disc bulge (Fig. 138-1).

MRI

Anterior osteophytes are seen as hypointense masses in the prevertebral space. They are usually decreased signal on all pulse sequences. Anterior osteophytes are usually associated with degenerative disc disease.

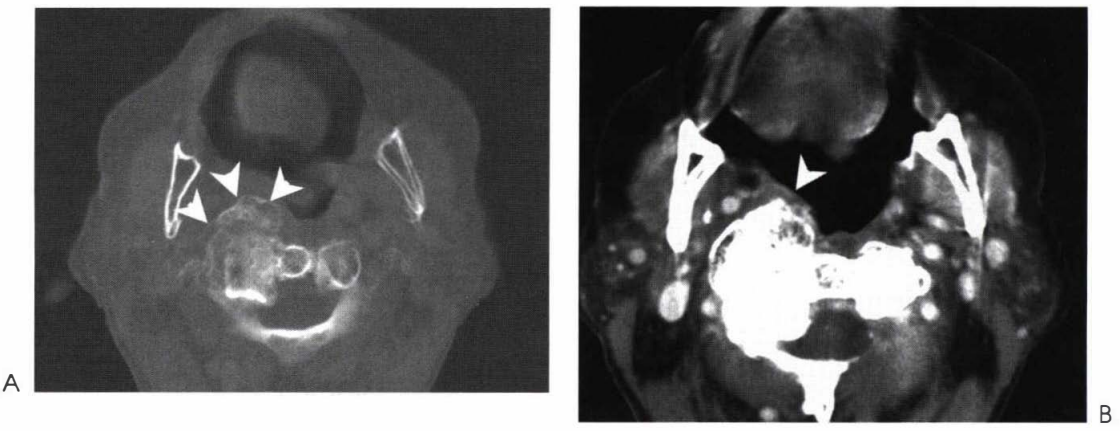

Figure 138-1. (A) Axial CT reconstructed with bone algorithms shows a large osteophyte extending into the prevertebral space (arrowheads). (B) Soft tissue algorithm at a different level demonstrates anterior displacement of the posterior pharyngeal wall by the large osteophyte (arrowhead).

Imaging Pearls

- The diagnosis of anterior osteophytes is usually very straightforward. Sagittal MR or sagittal reformations are helpful in the occasional case where the diagnosis may be uncertain.

Suggested Readings

1. Resnick D, Niwayama G. Degenerative diseases of the cervical spine. In: Resnick D. *Diagnosis of Bone and Joint Disorders*, Vol. 3. 3rd ed. Philadelphia: WB Saunders; 2002:1372-1462.
2. Russell EJ. Computed tomography and myelography in the evaluation of cervical degenerative disease. *Neuroimaging Clin N Am* 1995;5:329-348.

Chapter 139

Vertebral Metastases

Epidemiology

Metastatic disease is the most common extradural malignant spine tumor in adults. The most common age at presentation is between 50 and 60 years, but may occur earlier. There is no gender predilection. In adults, the majority of the spinal metastases arise from multiple myeloma (77%); breast (61%), lung (55%), and prostate cancer (51%); and lymphoma (40%). Spinal metastases in children are most often caused by Ewing's sarcoma and neuroblastoma followed by osteogenic sarcoma, rhabdomyosarcoma, and lymphoma. The site of metastatic disease is thoracic in approximately 68%, lumbar or sacral in 16%, and cervical in 15% of cases.

Clinical Features

The most frequent symptoms of cervical spinal metastatic disease are pain and progressive neurological deficits. The pain may be local or radicular. Metastatic lesions of C1 and C2 most frequently present with severe pain and only rarely with neurological involvement, probably due to the size of the spinal canal at these levels.

Pathology

Metastatic disease spreads to the spine hematogenously. The metastatic lesions develop in a distribution that correlates with the blood supply to the vertebra and the distribution of red marrow. The vertebral body constitutes the major part of the vertebra and is abundant in red marrow. In adults, the vertebral body is supplied by many short secondary intraosseus arteries that arise from the periosteal arterial network surrounding the anterolateral and posterior surfaces. The posterolateral corners of the body have the highest concentration of intraosseus arteries and are likely to be affected the earliest and have the highest frequency of hematogenous metastases. Also, the posteriorly located basivertebral vein serves as an entrance site. The pedicles arise from the upper part of the posterolateral corner and are invaded by tumor by local extension from the vertebral body. Epidural spread of the disease usually occurs through direct extension through the posterior longitudinal ligament. In children, the posterior part of the vertebral body adjacent to the pedicles is remarkably deficient in arteries. Pediatric metastatic tumors typically invade the spinal canal via the neural foramen.

Treatment

Radiation therapy accompanied by the administration of steroids is the treatment of choice for most patients with extradural spinal cord compression associated with vertebral metastases. Decompressive laminectomy may be useful in patients who do not respond to radiation. Patients with spinal metastases confined to the vertebral bodies without extradural or paravertebral extension may be treated with chemotherapy.

Imaging

Plain Films

Pedicle destruction is the most common plain film finding. Loss of trabecular bone is difficult to visualize on plain films; 50 to 70% of the trabecular bone must be destroyed before lysis is visible on plain films. This may explain why loss of visibility of the pedicle has been interpreted as an early sign of lytic metastases. Most metastases are osteolytic, although breast and prostate cancer and lymphoma can cause osteoblastic lesions.

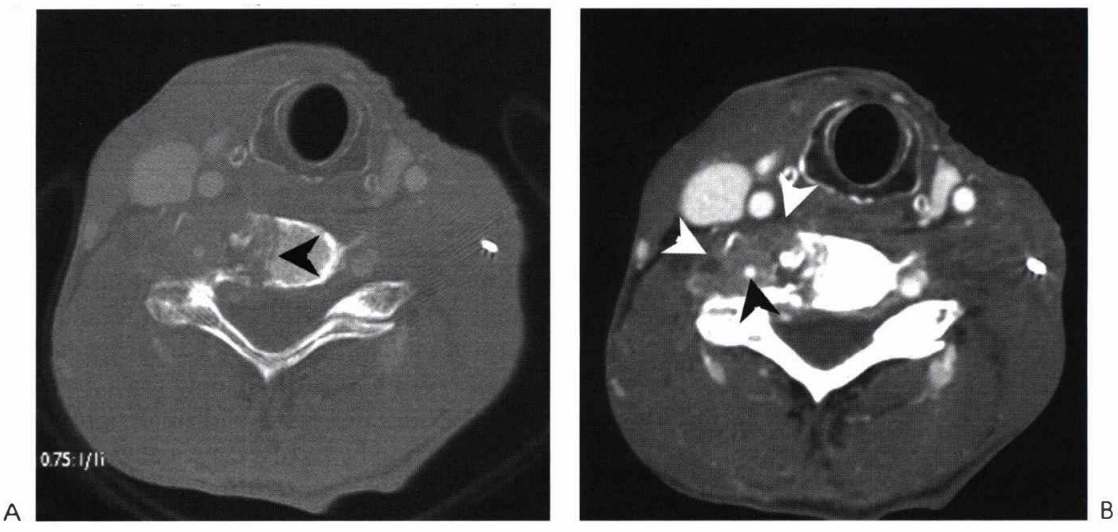

Figure 139-1. (A) Axial CT obtained with bone algorithm shows a destructive mass involving the right side of the vertebral body (arrowhead). (B) Soft tissue algorithm obtained for a contrast-enhanced CT shows a soft tissue mass extending into the prevertebral mass (white arrowheads). The mass also encases the vertebral artery (black arrowhead).

CT

The CT findings of vertebral metastases are cortical irregularity and erosions, or frank osteolytic or sclerotic lesions within the vertebrae. Associated prevertebral and/or epidural soft tissue mass may be seen (Fig. 139-1).

MRI

MRI is the most sensitive modality for depiction of vertebral metastases. MR also delineates the epidural and paraspinous soft tissue involvement. Cord compression is easily evaluated. Four patterns of vertebral metastatic disease are seen: focal lytic, focal sclerotic, diffuse inhomogeneous, and diffuse homogeneous. The most common pattern is multifocal lytic lesions that are low signal on T1-weighted and high signal on T2-weighted images. Sclerotic lesions are hypointense in both T1- and T2-weighted images. The multiplicity of lesions is strong evidence for a metastatic origin. Contrast is required to delineate the epidural component of the disease.

Imaging Pearls

- Noncontrast T1-weighted sequences are the most reliable sequences for detecting vertebral metastases.
- Vertebral metastases may be masked if only postcontrast T1-weighted sequences are obtained.

Suggested Readings

1. Algra PR, Heimans JJ, Valk J, et al. Do metastases in vertebrae begin in the body or pedicles? Imaging study in 45 patients. *AJR Am J Roentgenol* 1992;158:1275–1279.
2. Osborne AG. Cysts, Tumors and tumor-like lesions of the spine and spinal cord. In: *Diagnostic Neuroradiology*. St. Louis: Mosby Year Book; 1994:893–895.
3. Ratcliffe JF. Metastases and arteries of the vertebral body. *AJR Am J Roentgenol* 1992;161:450.

Chapter 140

Vertebral Osteomyelitis/Discitis

Epidemiology

The incidence of bacterial vertebral osteomyelitis/discitis typically affects adults, with a slight male predominance. Immunocompromised patients, drug abusers, and patients with head and neck infections are at greatest risk. The incidence of postoperative discitis ranges from 0.2 to 0.3%.

Clinical Features

The most common clinical presentation is neck pain followed by fever. However, up to 40% of patients may be afebrile. The onset is usually acute. Paresthesias may occur if there is periradicular inflammatory extension of the infection. Neurological deficit may occur in advanced cases that are associated with epidural phlegmon or abscess.

Pathology

Staphylococcus aureus is the most common pyogenic organism in adults. The infection is believed to reach the spine by hematogenous spread rather than by direct extension from adjacent soft tissue infection. The dominant cell is the polymorphonuclear leukocyte.

In children, the disc is richly vascularized and is the initial site of infection. Hematogenous spread to anastomosing arteries located at the metaphyseal end plates and intermetaphyseal anastomoses with arteries of the adjacent vertebrae predispose children to an initial discitis. The infections then extend to the adjacent vertebral end plates.

In adults, the blood supply to the intervertebral disc regresses and the primary blood supply is to end arteries to the metaphyses. As a result, the primary site of infection in adults is thought to arise in the end plates and then spread to the adjacent disc.

Treatment

Aggressive treatment with specific drugs is the first line of treatment in patients with inflammatory phlegmon. Surgical drainage is required in cases of symptomatic epidural abscess.

Imaging

Plain Films

Plain radiographs of the cervical spine are not sensitive in detecting early stages of cervical vertebral osteomyelitis/discitis. Abnormalities such as disc space narrowing and end plate erosions are subtle and may not be detected until late in the course.

CT

Vertebral end plate irregularity and cortical bone destruction are the characteristic findings on CT studies. The disc space is narrowed early in the course of the pyogenic infections. Contrast-enhanced CT may also depict associated paraspinous soft tissue abscesses.

MRI

MRI is the study of choice for the evaluation of inflammatory and infectious processes of the spine. T1-weighted images typically show a narrowed disc space and irregularity and erosions of the vertebral body end plates. Low signal intensity in the adjacent vertebral bodies reflects marrow edema. T2-weighted images show high signal in the affected discs. Disc enhancement is the hallmark of discitis. Contrast is essential and is useful in defining the extent of prevertebral and epidural phlegmon and for identifying an abscess (Figs. 140–1 and 140–2).

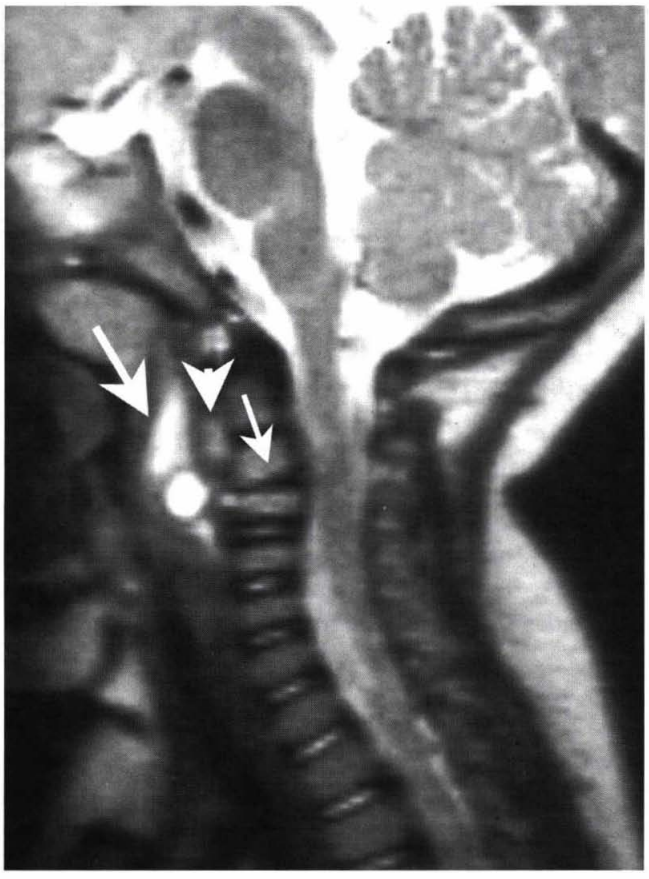

Figure 140–1. Sagittal T2-weighted image shows loss of height of the C2–3 disc due to bacterial osteomyelitis (small arrow). This is associated with a prevertebral soft mass located in the prevertebral space (arrowhead). There is focal mass surrounded by edema that is likely within the retropharyngeal space (large arrow).

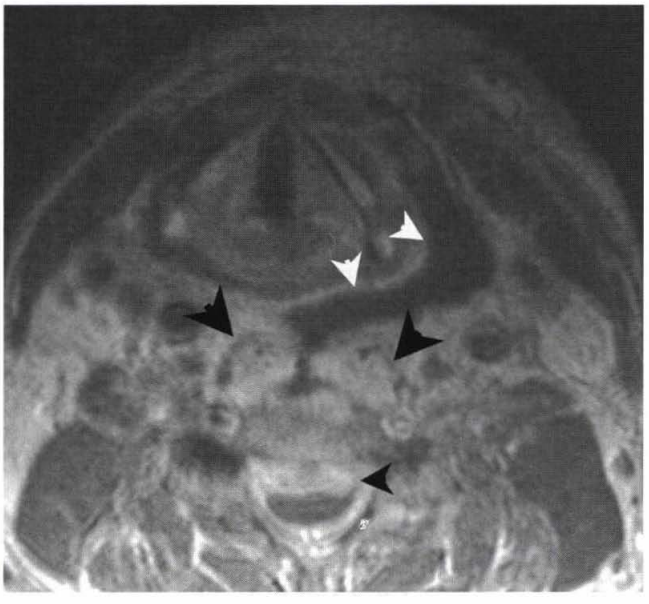

Figure 140–2. There is a diffuse osteomyelitis with enhancement of the longus coli muscles (large black arrowheads). There appears to be epidural phlegmon extending into the spinal canal (small black arrowhead). This osteomyelitis is communicating with a large retropharyngeal abscess (white arrowheads).

Imaging Pearls

- Contrast-enhanced MR is the study of choice for evaluating osteomyelitis and discitis.
- Sagittal CT reformations may be useful for evaluating subtle end plate erosions.
- Osteomyelitis/discitis may be associated with phlegmon or abscess in the prevertebral or retropharyngeal space.

Suggested Readings

1. Ruiz A, Post MJD, Ganz WI, et al. Inflammatory and infectious processes of the cervical spine. *Neuroimaging Clin N Am* 1995;5:401–425.
2. Smith AS, Weinstein MA, Mizushima A, et al. MR imaging characteristics of tuberculous spondylitis vs vertebral osteomyelitis. *AJR Am J Roentgenol* 1989;153:399–405.
3. Whelan MA, Naidich DP, Post JD, Chase NE. Computed tomography of spinal tuberculosis. *J Comput Assist Tomogr* 1983;7:25–30.

Chapter 141

Granulomatous Spondylitis

Epidemiology

Granulomatous infection, especially tuberculous spondylitis, is a disease of children in developing countries, but occurs occasionally in adults. Debilitation, immunosuppression, alcoholism, and drug addiction are predisposing conditions. There is no gender predilection. The cervical spine is a relatively uncommon site.

Clinical Features

The onset is insidious and the course more indolent. Low-grade fever and malaise are the common systemic manifestations.

Pathology

Granulomatous infection is most commonly caused by *Mycobacterium tuberculosis*. Other organisms include brucella and actinomycetes. The spread of infection is hematogenous. The hallmark is mononuclear phagocytic cells, some of which fuse to form multinucleated giant cells around the lesion. The bacilli lodge in the anterior or subchondral portions of the vertebral body. The infection spreads in a subligamentous fashion to involve the adjacent vertebral body. Because the tubercle bacilli do not produce proteolytic enzymes, there is relative preservation of the disc. The transverse processes and the posterior elements are less frequently involved.

Treatment

Antituberculous drugs are prescribed for a period of 9 to 12 months. Surgical debridement and stabilization are required in cases of significant mass effect causing airway/cord compression.

Imaging

Plain Films

Cortical destruction is evident late in the course of the disease. Widening of the prevertebral stripe may be seen in cases of large prevertebral abscess.

CT

This shows bony erosion and large paraspinous abscesses. The size of soft tissue abscesses is often disproportionate to the amount of bone destruction. The presence of calcification and thick rim-enhancing multiloculated paraspinal abscesses strongly points to the diagnosis of tuberculous infection. Untreated patients develop progressive vertebral collapse with anterior wedging and a gibbus deformity.

MRI

The typical cases demonstrate anterior cortical erosion. The disc height is maintained for a long time as opposed to pyogenic infection where the discs are involved very early. Subligamentous spread to involve the adjacent vertebral bodies is better appreciated on MR. Contrast-enhanced studies may also identify enhancement of the meninges and intramedullary tuberculomas. Multilevel involvement is very common in tuberculous spondylitis and is best identified on MR imaging (Figs. 141–1 and 141–2).

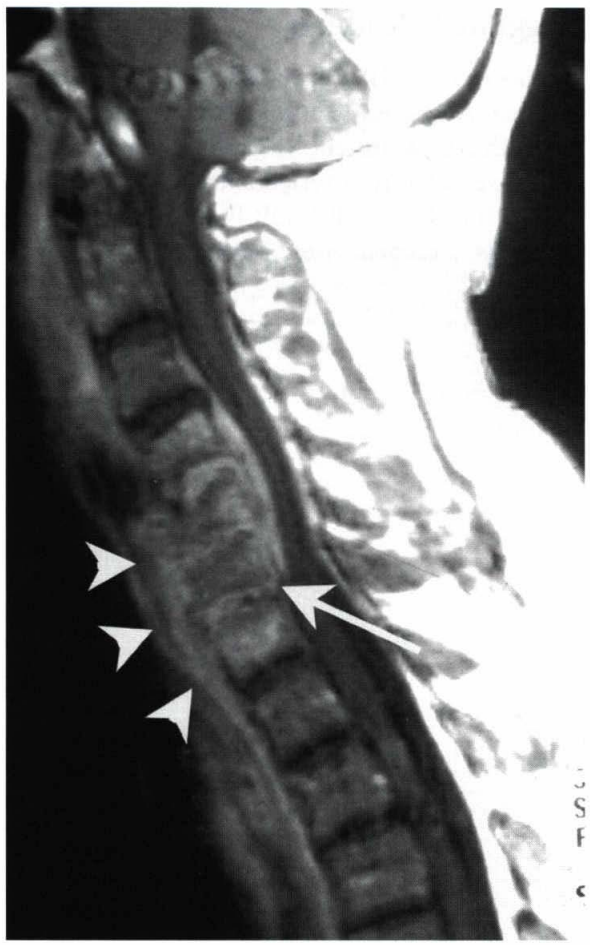

Figure 141-1. Sagittal contrast-enhanced T1-weighted image shows diffuse enhancement of C4-C7 with destruction of the end plates (arrow). There is extension of the phlegmon of the granulomatous spondylitis into the epidural space and anterior extension into the prevertebral space (arrowheads).

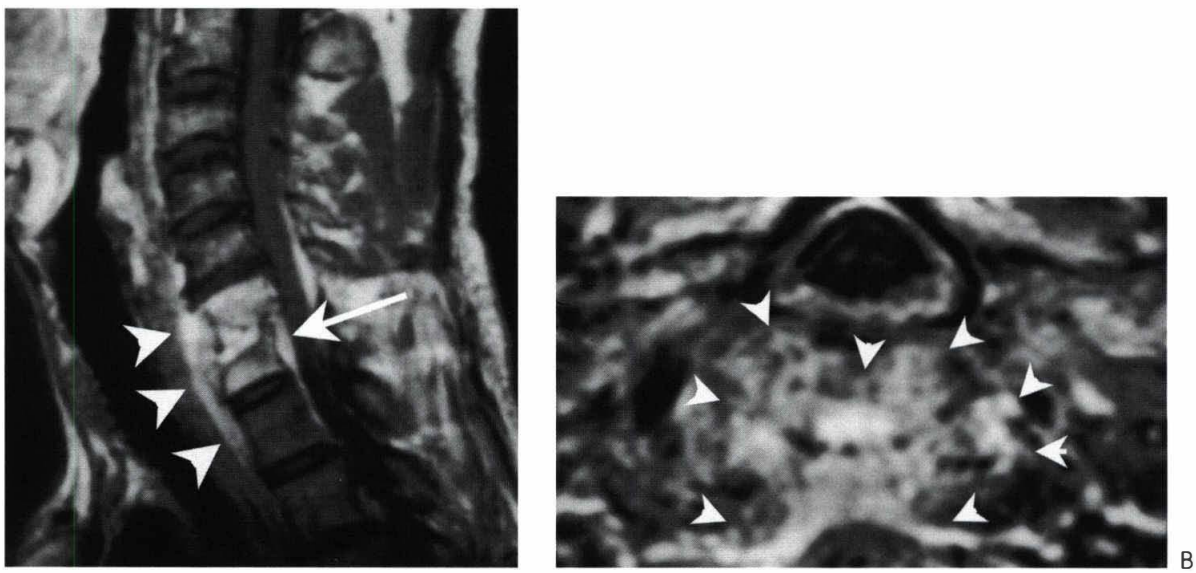

Figure 141-2. (A) Contrast enhanced sagittal T1-weighted image shows granulomatous spondylitis of C6-C7. The arrow demonstrates the epidural involvement and the arrowheads demonstrate the extension into the prevertebral space. (B) Axial contrast-enhanced T1-weighted image shows diffuse enhancement of phlegmon into the prevertebral space (arrowheads). (Courtesy of Dr. Ravi Ramakantra)

Imaging Pearls

- The diagnosis of tuberculous osteomyelitis can be suggested by multilevel osteomyelitis/discitis and predominance of anterior vertebral body erosion with relative preservation of the disc space.
- Advanced disease will result in gibbus deformity and spine instability.

Suggested Readings

1. Ruiz A, Post MJD, Ganz WI, et al. Inflammatory and infectious processes of the cervical spine. *Neuroimaging Clin N Am* 1995;5:401–425.
2. Smith AS, Weinstein MA, Mizushima A, et al. MR imaging characteristics of tuberculous spondylitis vs vertebral osteomyelitis. *AJR Am J Roentgenol* 1989;153:399–405.
3. Whelan MA, Naidich DP, Post JD, Chase NE. Computed tomography of spinal tuberculosis. *J Comput Assist Tomogr* 1983;7:25–30.

Chapter 142

Chordoma

Epidemiology

Chordomas are rare tumors that account for 3 to 4% of primary malignant bone tumors and are the most common primary sacral neoplasm. Chordomas can occur at any age, but the peak incidence is in the sixth decade. There is a 2:1 male predominance. These tumors can occur anywhere along the skull base and spine: 50% arise in the sacrum, 35% in the clivus, and 15% in the vertebrae. In the spine, the areas most commonly involved are the cervical, lumbar, and thoracic spine, in descending order of frequency. Chordomas are locally invasive tumors with no propensity for metastatic spread. However, chordomas arising in the vertebral bodies have a greater likelihood for distant metastases than their counterparts in the sacrum or the clivus. Although metastases have been reported in 10 to 15% of all cases, metastases occur in 80% of chordomas arising in the vertebral bodies.

Clinical Features

Pain is the most common symptom and is usually localized to the site of origin. Vertebral chordomas may result in cord compression as they enlarge.

Pathology

Chordomas arise from the remnants of the embryonic notochord found throughout the axial skeleton. Grossly, they are locally invasive, soft or firm lobulated masses. They are separated into two pathologic subsets: typical chordomas and chondroid chordomas. In typical chordomas, vacuolated physaliphorous cells with variable amounts of intracytoplasmic mucin are embedded in pools of extracellular mucin. In chondroid chordomas, this watery gelatinous matrix is replaced by cartilaginous foci. They may extend anteriorly to involve the prevertebral space. Extraosseus notochordal rests known as ecchondroses are found anterior to the pons and also in the retropharyngeal space and may be the cause of primary extraosseus chordomas that may occur in these locations.

Treatment

Surgical resection followed by radiation therapy is generally the treatment of choice.

Imaging

Plain Films

Plain films typically show a destructive skull base or vertebral lesion involving multiple levels. Calcification occurs in 30 to 70% of cases. An associated soft tissue mass is often present.

CT

Non-contrast CT scans commonly show a lytic, destructive mass with solid and cystic components. The soft tissue component of the neoplasm usually demonstrates intratumoral dystrophic calcification. The posterior elements are typically spared (Fig. 142–1).

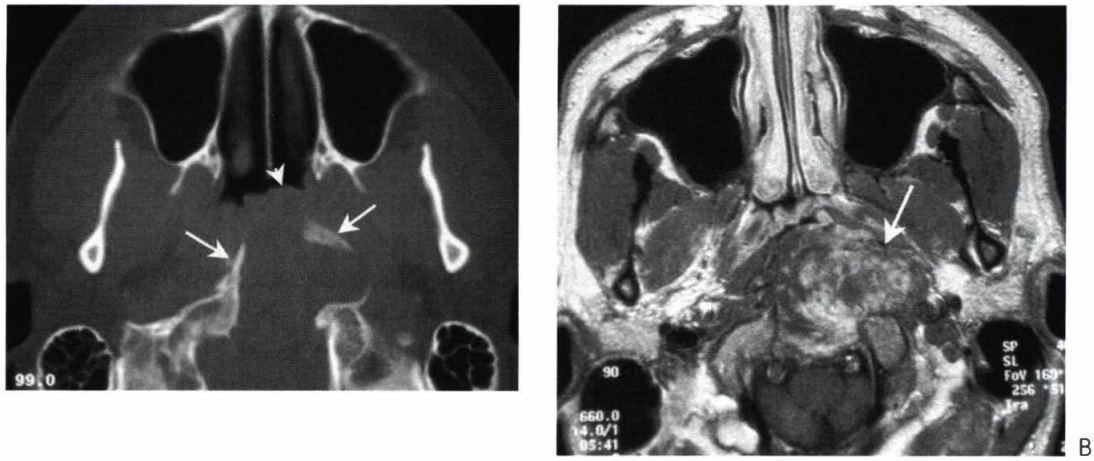

Figure 142–1. (A) Bone algorithms from a CT show a chordoma arising from the vertebral body and extending into the prevertebral space. There is remodeling and anterior displacement of the bony skull base (arrows), which is displacing the posterior wall of the nasopharynx (arrowhead). (B) Axial contrast-enhanced T1-weighted image shows the heterogeneous enhancement of the chordoma that is illustrated in (A) (arrow).

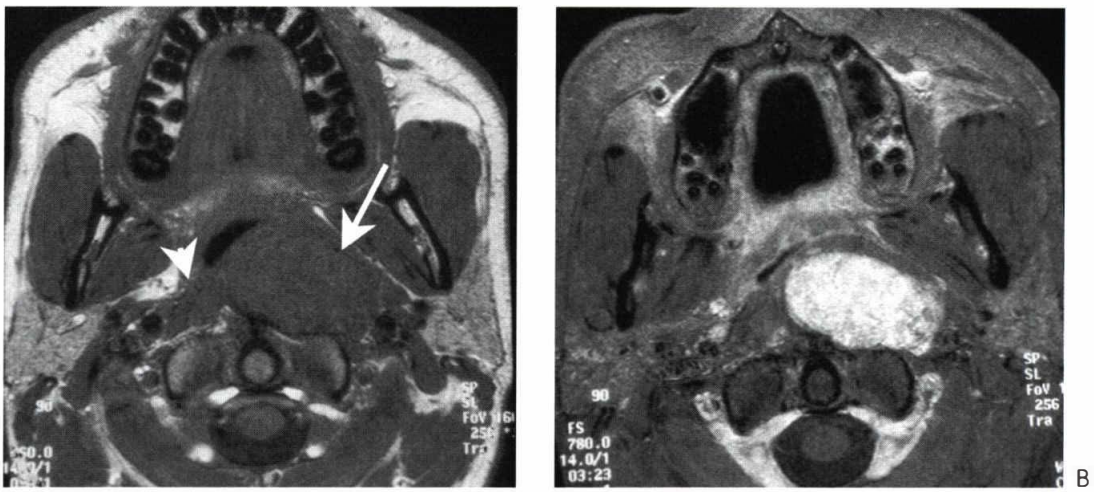

Figure 142–2. (A) Axial noncontrast T1-weighted image shows an extraosseous chordoma centered in the left longus coli muscle (arrow). The arrowhead indicates the right longus coli muscle. (B) This tumor demonstrates diffuse homogeneous contrast enhancement on fat-suppressed T1-weighted images.

MRI

Typical chordomas have inhomogeneous, predominantly low signal intensity on T1-weighted images and are hyperintense on T2-weighted images. Chondroid chordomas are low signal on T1-weighted images and iso- to hypointense on T2-weighted images. The tumor enhances on the postgadolinium study. MRI is inferior to CT in showing bony destruction or calcification. MRI, however, is better able to show epidural disease and the true extent of disease involving the bone. Areas of hemorrhage and cystic change are readily demonstrated if present (Figs. 142–2 and 142–3).

Imaging Pearls

- Chordomas should be considered for all tumors arising at the craniocervical junction and skull base.
- The presence of intratumoral increased T2-weighted signal in tumors arising at the skull base is highly suggestive of chordomas.
- Chordomas usually arise medial to the petroclival fissure whereas chondrosarcomas are typically located lateral to the fissure.

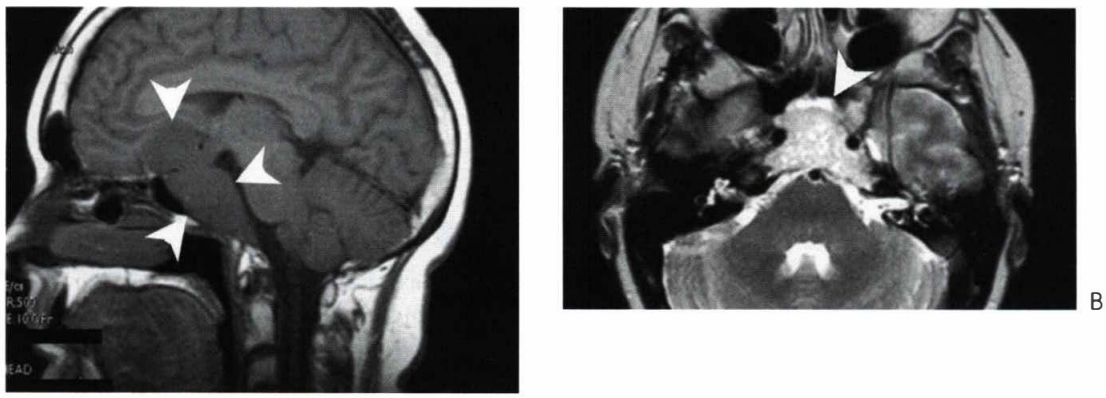

A B

Figure 142–3. (A) Sagittal noncontrast T1-weighted image shows the intermediate signal of a clival chordoma (arrowheads). (B) Axial T2-weighted image shows the characteristic high signal within the mass (arrowhead).

Suggested Readings

1. Osborne AG. Cysts, tumors and tumor-like lesions of the spine and spinal cord. In: *Diagnostic Neuroradiology*. St. Louis: Mosby Year Book; 1994:886–890.
2. Wippold FJ, Koeller KK, Smirniotopoulos JG. Clinical and imaging features of cervical chordoma. *AJR Am J Roentgenol* 1999;172:1423–1426.

Chapter 143

Vertebral Artery Aneurysm

Epidemiology

Aneurysms of the extracranial vertebral artery are rare. They usually result from penetrating gunshot or stab wounds. Cervical spinal surgery, birth trauma, cervical fractures, and dislocations have also been implicated. These commonly occur in the terminal cervical portion from the C2 level to the skull base or where the artery curves to enter the foramen transversarium of the sixth cervical vertebra. Atraumatic aneurysms are even less frequent. They may be secondary to the vasculopathy as in Ehlers-Danlos syndrome, neurofibromatosis, and fibromuscular dysplasia. Degenerative aneurysms due to atherosclerotic disease usually occur in older age groups with no gender predilection.

Clinical Features

Small aneurysms may be asymptomatic. Very large aneurysms may present as pulsatile neck masses. When dissection occurs, the patient has severe neck pain and associated vertigo and dizziness. Dissections may also result in a cerebellar infarct.

Pathology

Vertebral artery aneurysms are broadly categorized as true and false types. True aneurysms are generally fusiform in shape and are exaggerated arterial ectasias due to severe atherosclerosis. Intraluminal clots are common. Saccular aneurysms of the vertebral artery are very rare. False aneurysms are sequelae to dissection that may be subintimal or subadventitial, depending on the location of the hematoma. If the intima ruptures, a communication between the hematoma and the vessel lumen is created producing a vessel dissection. A complete vessel wall laceration may result in a perivascular hematoma. A pseudoaneurysm (false aneurysm) is formed when the perivascular hematoma cavitates and communicates with the vessel lumen. Mycotic aneurysms are caused by an infectious arteritis that results in weakening of the vessel wall.

Treatment

Historically, surgety has been the most common treatment for vertebral artery aneurysms. Proximal and distal ligation with excision of the aneurysm and subsequent bypass grafting may be performed. An 8% risk of ischemia has been reported after ligation of the vertebral artery. Recently, endovascular therapies have gained acceptance for treatment of vertebral aneurysms with excellent results.

Imaging

US

A fusiform aneurysm is seen as a dilated anechoic segment of the vertebral artery. An intraluminal thrombus is seen as an iso- to hyperechoic mass within the aneurysm. Vertebral artery dissection can also be detected and monitored by duplex Doppler. This is seen as an area of a high resistance signal. The abnormality is not specific but reflects an impediment to normal arterial flow that could also exist in atherosclerotic or embolic occlusion of the distal vertebral artery. Other findings include a localized increase in diameter with decreased pulsatility.

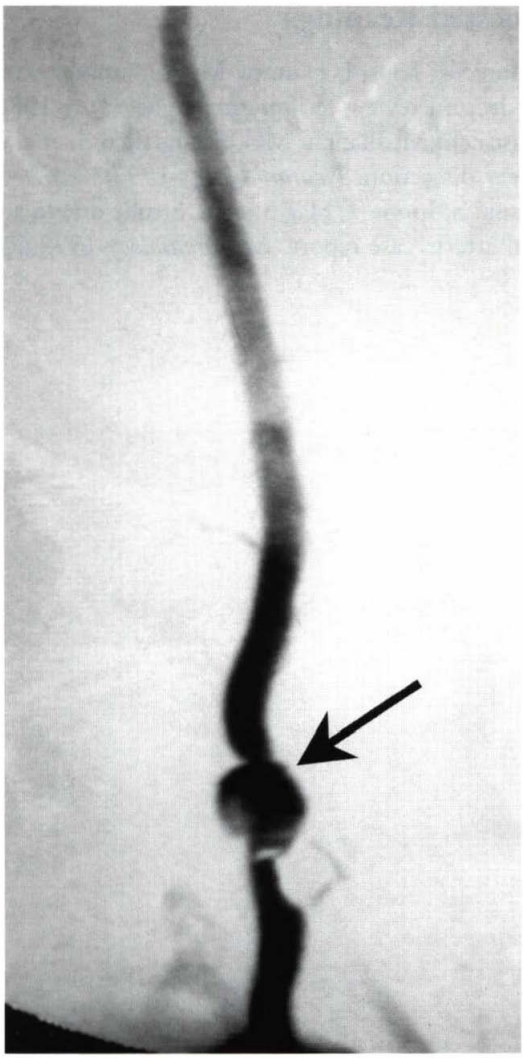

Figure 143–1. Digital subtraction angiogram shows a vertebral artery aneurysm (arrow).

CT

Vertebral artery aneurysm may present as a hyperdense mass in the prevertebral space on noncontrast CT. A nonthrombosed aneurysm enhances intensely following administration of intravenous contrast. The residual lumen of a partially thrombosed aneurysm will enhance strongly following contrast administration. Completely thrombosed aneurysm is variably hyperdense on noncontrast studies and may not enhance following contrast administration. Vertebral artery aneurysms may cause widening of the foramen transversarium or pressure erosion of the adjacent vertebral body.

MRI

Vertebral artery aneurysms are seen as dilated segments of flow void on the T1- and T2-weighted sequences. Turbulent flow may give a heterogeneous signal. Partially thrombosed aneurysms have a complex signal on MR. The thrombus may appear multilaminated due to the blood products in different stages. Subacute thrombus is predominantly hyperintense on T1- and T2-weighted studies. Two-dimensional time-of-flight MR angiography sequence also depicts the aneurysms in multiple projections (Fig. 143–1). A crescentic or rounded rim of high signal on T1-weighted images is considered characteristic for mural hematoma in dissection.

Imaging Pearls

- The presence of a round mass that is hyperdense on CT or has increased T1-weighted signal on MR imaging in the prevertebral space should raise the possibility of an aneurysm.
- MRA is helpful for diagnosing vertebral artery aneurysms. However, MRA may miss vertebral artery dissections. Axial noncontrast T1-weighted images are necessary to detect the crescentic subintimal hematoma.

Suggested Readings

1. Mann SR, Laub J, Haimov M. Atraumatic extracranial vertebral artery aneurysm: case report and review of literature. *J Vasc Surg* 1986;4:288–293.
2. Mascalchi M, Bianchi MC, Mangiafico S, et al. MRI and MR angiography of vertebral artery dissection. *Neuroradiology* 1997;39:329–340.
3. Suzuki S, Inoue T, Hag S, et al. Stroke due to a fusiform aneurysm of the cervical vertebral artery: case report. *Neuroradiology* 1998;40:19–22.

Section VI

Parapharyngeal Space

The parapharyngeal space (PPS) is, as its name suggests, next to the pharynx (Fig. VI-1). The PPS is delimited superiorly by the skull base and is continuous inferiorly with the submandibular space (Fig. VI-2).

This space is also referred to as the prestyloid parapharyngeal space. If one elects to use the latter term, then the adjacent space posterior to the styloid process should be termed the poststyloid parapharyngeal space. If one prefers the term *parapharyngeal space*, then the space posterior to the styloid process should be referred to as the carotid sheath or carotid space.

The parapharyngeal space consists primarily of fat (Fig. VI-3), vascular structures, and small branches of the mandibular division of the fifth cranial nerve. The vascular components include the internal maxillary artery, ascending pharyngeal artery, and pharyngeal venous plexus. Other less commonly recognized components of the PPS are lymph nodes and ectopic rests of minor salivary gland tissue (Fig. VI-4).

Localizing a mass to the PPS may, at first, be difficult. Primary PPS masses typically displace the lateral wall of the visceral space medially, the deep lobe of the parotid gland laterally, and the contents of the carotid sheath posteriorly (Fig. VI-5).

It is important not to confuse a primary PPS mass with a mass arising from the deep lobe of the parotid gland. Nonvascular masses localized to the PPS may be resected transorally, whereas deep parotid lobe masses require a total parotidectomy. PPS masses usually displace the deep lobe of the parotid gland laterally, whereas deep lobe masses may be surrounded medially by a thin rim of parotid tissue. Primary PPS masses usually do not extend into the superficial lobe of the parotid gland. Therefore, a mass that extends into the superficial lobe is likely to be a primary parotid space lesion rather than a PPS mass. PPS masses are usually unifocal, whereas parotid space masses may be multifocal. Thus a mass is likely in the deep lobe of the parotid gland if it is associated with ipsilateral or contralateral parotid lesions.

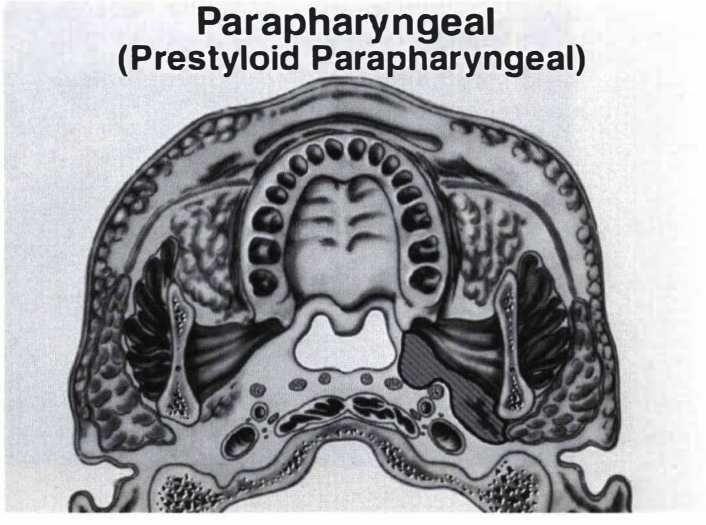

Figure VI-1. Schematic illustration demonstrates the location of the parapharyngeal space (see Color Plate VI-1). (Figure reproduced with permission from Mukherji SK, Castillo M. A simplified approach to the spaces of the suprahyoid neck. Rad. Clin N Am *1998;36:761-780.)*

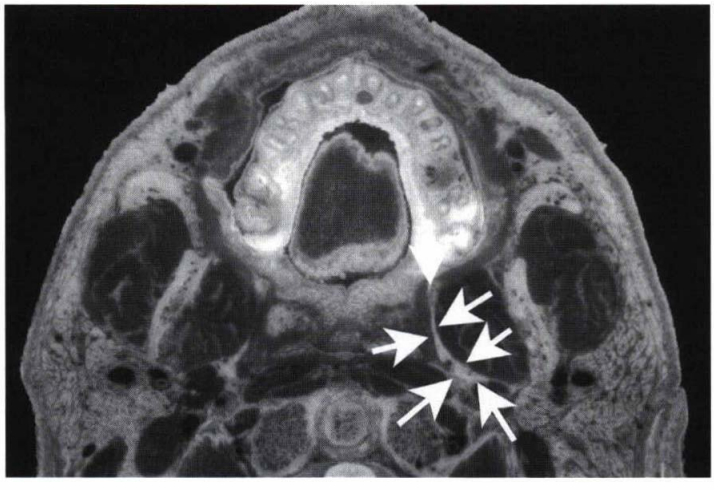

Figure VI-2. The extent of the parapharyngeal space is delineated by the arrows on this axial anatomic section.

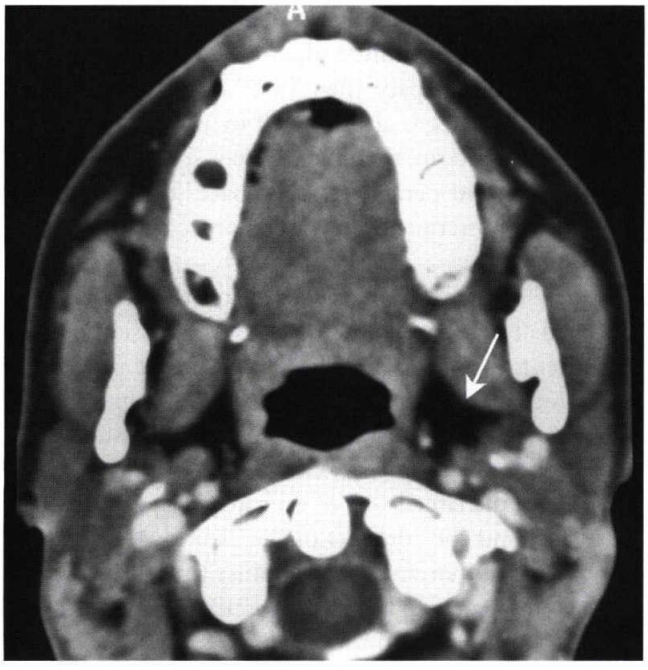

Figure VI–3. Axial contrast-enhanced CT shows the triangular configuration of the fat in the parapharyngeal space (arrow).

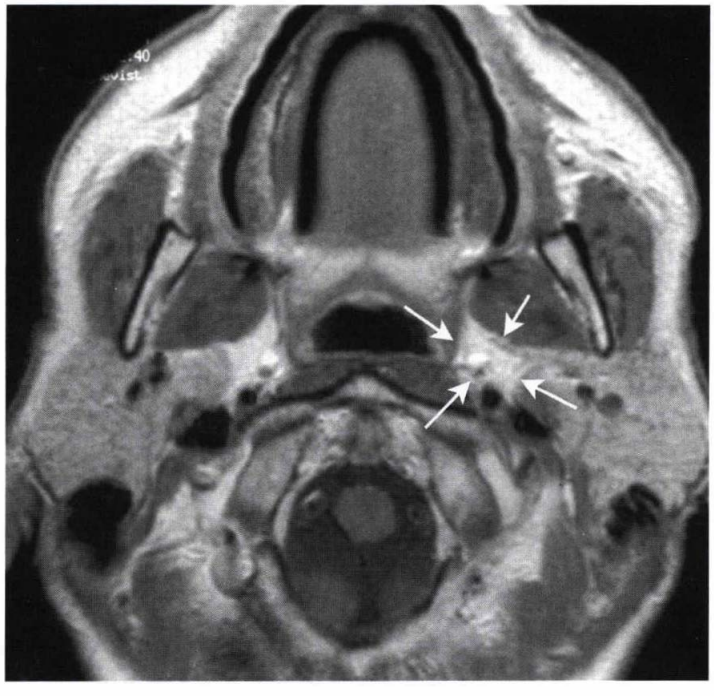

Figure VI–4. Axial noncontrast T1-weighted image shows the normal left parapharyngeal space (arrows).

PPS masses may also be difficult to separate from deep extension of a primary masticator space lesion. Proper spatial localization is important because the anatomically based differential diagnoses of masses within these spaces is very different. A primary PPS mass arises medial to medial pterygoid muscle. A large mass may displace the medial pterygoid muscle laterally but usually does not invade this muscle. A mass that involves both the medial pterygoid muscle and the PPS is likely to be a masticator space mass which has extended secondarily into the PPS.

The most common lesions in the PPS result from secondary extension of pathological processes arising from adjacent spaces. The most common pathology is deep extension of squamous cell carcinoma (SCCA) arising in the tonsillar region (visceral space, oropharynx). Spread into the PPS is important information to convey to the otolaryngologist because it contraindicates resection of a tonsillar carcinoma with wide local excision through an intraoral approach. Abscesses of the parapharyngeal space may result from lateral spread of an advanced tonsillar infection or from medial extension of an odontogenic infection arising in the masticator space.

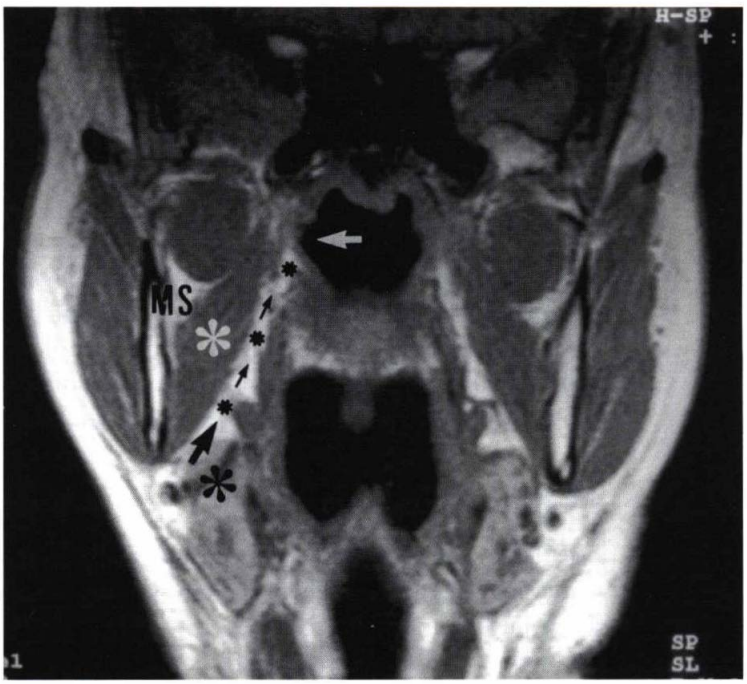

Figure VI-5. Normal relationships between submandibular space, parapharyngeal space, and nasopharyngeal wall. Coronal T1-weighted MR image shows the submandibular gland (black asterisk) at the inferior end of the parapharyngeal space (small asterisks). Note how pus can track up (arrows) the parapharyngeal space with involvement of the medial pterygoid muscle (white asterisk) in the masticator space (MS) and the nasopharyngeal wall (arrow).

Primary PPS masses are unusual. However, knowing that there are ectopic rests of salivary tissue within the PPS helps us remember that the most common primary lesion of the PPS is a minor salivary gland tumor (usually a pleomorphic adenoma). Very rarely, an adenoid cystic carcinoma, mucoepidermoid carcinoma, or other malignant minor salivary gland lesion may arise in the PPS.

Suggested Readings

1. Mukherji SK, Castillo M. A simplified approach to the spaces of the extracranial head and neck. *Radiol Clin North Am* 1998;36:761–780.
2. Harnsberger HR. *Handbook of Head and Neck Imaging*. 2nd ed. St. Louis: Mosby Year Book; 1995.
3. Grodinsky M, Holyoke EA. The fasciae and fascial spaces of the head, neck and adjacent regions. *Am J Anat* 1938;63:367–408.
4. Babbel RW, Harnsberger HR. The parapharygeal space: the key to unlocking the suprahyoid neck. *Sem Ultrasound CT MR* 1990;11:444–459.

Chapter 144

Infection

Epidemiology

Parapharyngeal cellulitis or abscesses are usually caused by infection originating in adjacent structures such as tonsillar, submandibular, and parotid gland abscesses. The most common site of the primary infection is an infected tonsil. An odontogenic abscess may also spread to the parapharyngeal space after involving the masticator space. Abscess may occur at any age but is more frequent in adolescents and adults.

Clinical Findings

Patients with parapharyngeal abscess usually present with fever, painful throat, and trismus that may be marked. There is often swelling of the neck, and the pharyngeal mucosa is often pushed medially.

Pathology

A variety of organisms may infect the parapharyngeal space such as *Streptococcus, Staphylococcus, Pseudomonas,* and *Haemophilus.* The initial pathological process is spreading cellulitis. If treatment is delayed, frank pus formation may ensue. Acute laryngeal edema or internal jugular thrombophlebitis that may result in subsequent septicemia may complicate the infection.

Treatment

Parapharyngeal cellulitis is treated with systemic antibiotics. The treatment of a parapharyngeal space abscess is drainage through a cervical approach. Care must be taken to use efficient suction to prevent the inhalation of blood and pus.

Imaging Findings

CT

Cellulitis results in the obliteration of the low attenuation parapharyngeal fat with little mass effect on the surrounding structures. Abscess formation is indicated by a well-defined low attenuation mass that may have an enhancing rim. Abscess formation often results in medial displacement of the pharyngeal wall or lateral displacement of the medial pterygoid muscle. The presence of gas as a result of infection by gas forming organism is easily recognized with CT (Fig. 144–1).

MR

Cellulitis effaces the high-signal-intensity fat on T1-weighted MR images. Fat-suppressed contrast-enhanced MR images show good contrast enhancement in inflamed tissues. Abscesses are easily identified as nonenhancing areas within a mass. Inflamed tissues on T2-weighted MR images show high signal intensity. The presence of a small amount of gas is difficult to detect on MR imaging (Fig. 144–2).

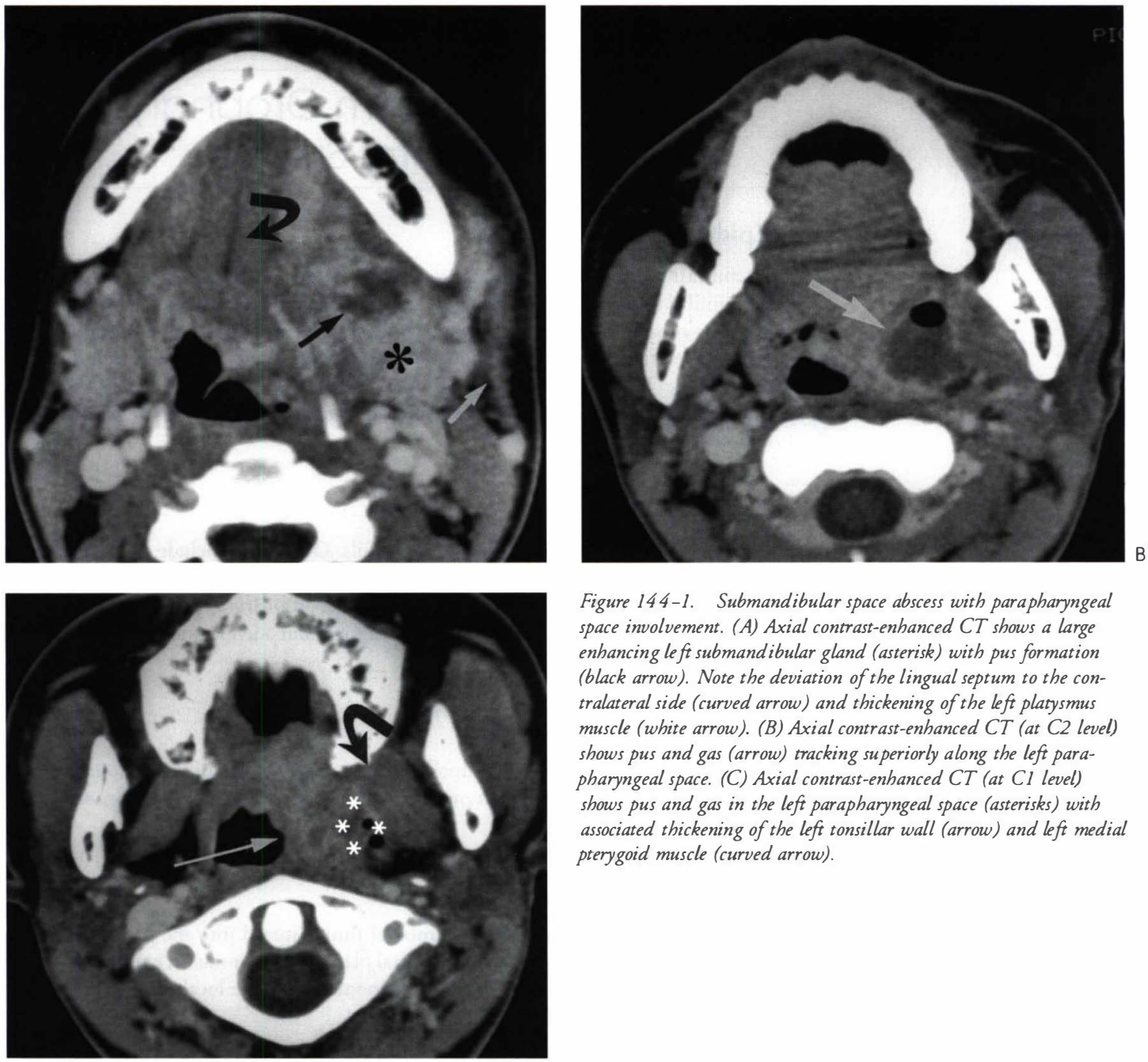

Figure 144-1. Submandibular space abscess with parapharyngeal space involvement. (A) Axial contrast-enhanced CT shows a large enhancing left submandibular gland (asterisk) with pus formation (black arrow). Note the deviation of the lingual septum to the contralateral side (curved arrow) and thickening of the left platysmus muscle (white arrow). (B) Axial contrast-enhanced CT (at C2 level) shows pus and gas (arrow) tracking superiorly along the left parapharyngeal space. (C) Axial contrast-enhanced CT (at C1 level) shows pus and gas in the left parapharyngeal space (asterisks) with associated thickening of the left tonsillar wall (arrow) and left medial pterygoid muscle (curved arrow).

Imaging Pearls

- The treatment of infections in the parapharyngeal region is determined by the imaging findings. The interpreting radiologist must be able to differentiate parapharyngeal space cellulitis from a parapharyngeal space abscess or from a tonsillar abscess (visceral space).
- Parapharyngeal cellulitis (phlegmon) is treated with systemic antibiotics.
- A true parapharyngeal space abscess is drained by a cervical approach.
- A tonsillar abscess is drained via an intraoral approach.

Suggested Readings

1. Paonessa DF, Goldstein JC. Anatomy and physiology of head and neck infections with emphasis on the fascia of the face and neck. *Otolaryngol Clin North Am* 1976;9:561-580.
2. Som PM, Curtin HD. Fascia and spaces. In: Som PM, Curtin HD, eds. *Head and Neck Imaging*. 3rd ed. St. Louis: Mosby; 1996;738-746.

Chapter 145

Tumor Spread from Oropharyngeal Visceral Space

Epidemiology

In contrast to the rarity of primary tumors in the parapharyngeal space, secondary malignant infiltration of the parapharyngeal space is frequently encountered. Oropharyngeal carcinomas commonly extend into the parapharyngeal space, and some tumors may extend into the masticator space. Traditionally, oropharyngeal carcinomas are seen in men > 60 years of age. However, there are now more patients presenting in their third through fifth decade. In addition, more females are affected given their increasing use of tobacco and alcohol.

Pathology

Most oropharyngeal tumors arise in the tonsils. Other sites include the anterior tonsillar pillar and the soft palate. Although the retromolar trigone is anatomically located in the oral cavity, retromolar trigone malignancies behave like oropharyngeal carcinoma. The vast majority of these lesions are squamous cell carcinomas but adenocystic carcinoma and lymphomas may also be encountered.

Clinical Findings

There are no specific signs and symptoms that suggest invasion of the parapharyngeal space. The involvement of the parapharyngeal space is readily diagnosed radiologically during tumor mapping and staging.

Treatment

The otolaryngologist should be informed of tumor spread into the parapharyngeal space because this information is crucial in surgical planning. For instance, parapharyngeal spread contraindicates resection of a tonsillar carcinoma with wide local excision through an intraoral approach.

Imaging Findings

CT

Malignant infiltration is recognized by the encroachment of intermediate attenuation tumor in the low attenuation, fat-filled parapharyngeal space. The parapharyngeal fat may be completely effaced by an oropharyngeal tumor extending across the parapharyngeal space into the masticator space (Fig. 145–1).

MR

T1-weighted images are excellent for identifying intermediate signal intensity tumor infiltrating the high-signal-intensity fat within the parapharyngeal space. Following contrast enhancement, the tumor interface with the medial or lateral pterygoid muscles is clearly defined. However, the interface with fat may be less conspicuous because of the enhancement of the parapharyngeal venous plexus (Fig. 145–2).

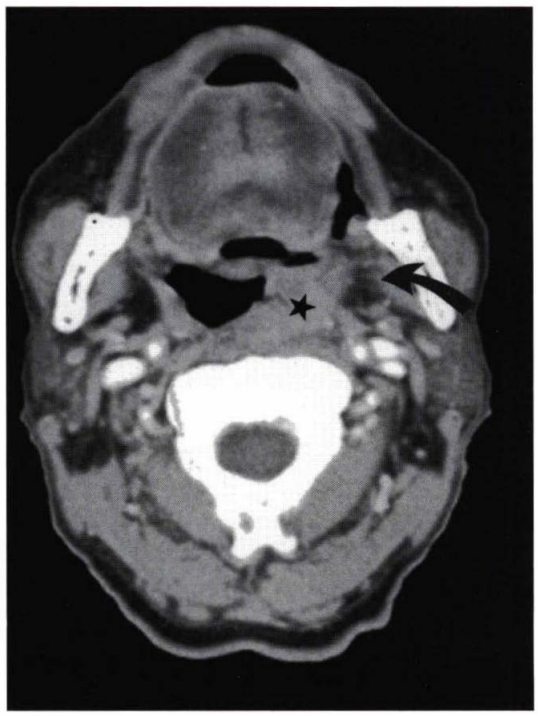

Figure 145–1. Oropharyngeal carcinoma with early parapharyngeal spread. Axial contrast-enhanced CT shows a left oropharyngeal carcinoma (star). Note the reticulation of the parapharyngeal space fat which is suspicious for early spread (arrow).

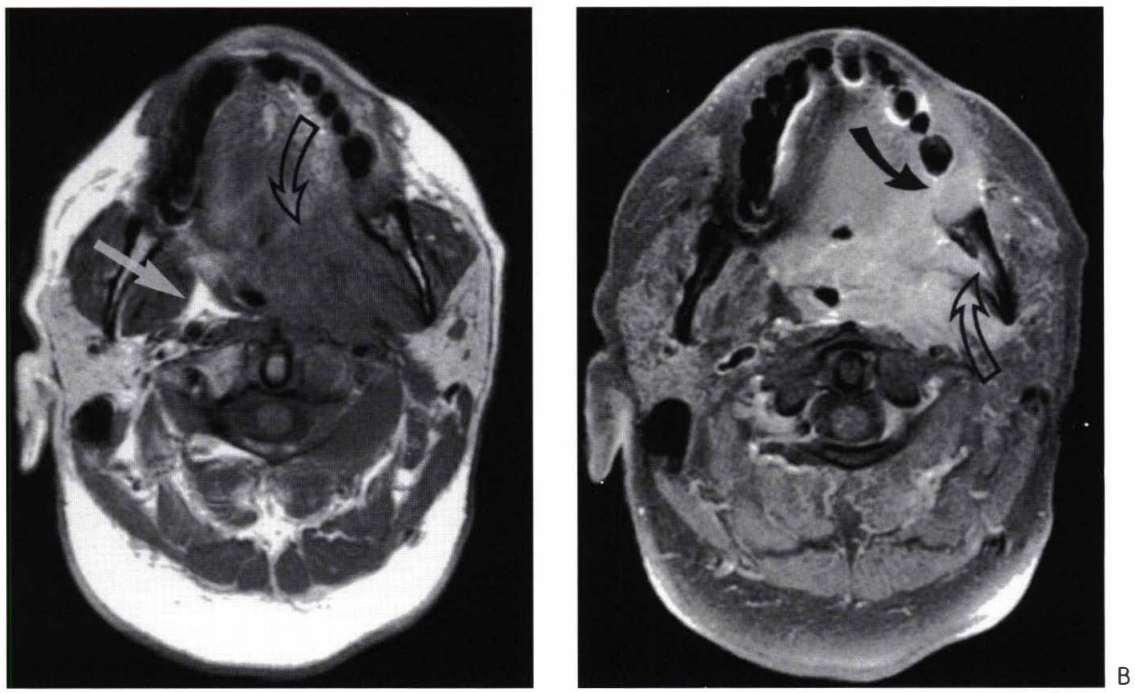

A B

Figure 145–2. Oropharyngeal carcinoma with spread to parapharyngeal and buccal spaces. (A) Axial non-contrast T1-weighted MR image shows an intermediate signal intensity left oropharyngeal tumor (curved arrow) effacing the ipsilateral parapharyngeal space with involvement of the medial pterygoid muscle. Note the normal right parapharyngeal space (straight arrow). (B) Axial contrast-enhanced MR image shows tumor extension into the buccal space (solid arrow). Note the marrow enhancement (hollow arrow) in the ipsilateral mandible suggesting the presence of tumor infiltration.

Imaging Pearls

- Apart from spread to the parapharyngeal space, tongue base, and hypopharynx, oropharyngeal carcinoma commonly spreads posteriorly to involve the retropharyngeal space. The superior and inferior extent of this tumor must be established during tumor mapping.

Suggested Readings

1. Mukherji SK, Holliday RA. Nasopharynx-oropharynx. In: Som PM, Curtin HD, eds. *Head and Neck Imaging*. 2nd ed. St Louis: Mosby; 1996:438–472.
2. Gluckman GL, Thompson RT. Cancer of the oropharynx. In: Myers EN, Suen JY, eds. *Cancers of the Head and Neck*. 2nd ed. New York: Churchill Livingston; 1989:465–494.

Chapter 146

Tumor Spread from Nasopharyngeal Visceral Space

Epidemiology

The most common lesion in the parapharyngeal space at the level of the nasopharynx is direct tumor extension from a nasopharyngeal carcinoma. Nasopharyngeal carcinomas spread along well-defined routes, with parapharyngeal extension being the most frequent direction of spread. This finding may be seen in > 40% of patients.

Pathology

Histologically, 98% of nasopharyngeal carcinomas are of the undifferentiated variety. They often have heavy lymphocytic infiltration, which explains why they were previously called lymphoepitheliomas. The tumor is intimately related to the Epstein-Barr virus because almost all patients have significantly raised antibody titer against the virus. Nasopharyngeal carcinomas show aggressive local spread, skull base erosion, and intracranial extension. There is nodal metastasis in 80% of patients at presentation.

Clinical Findings

There are no specific signs and symptoms that suggest invasion of the parapharyngeal space. The involvement of the parapharyngeal space is a radiological diagnosis made usually during tumor staging.

Treatment

The mainstay of treatment is radiation therapy. Identifying parapharyngeal invasion is important because this finding is reported to be an independent prognostic factor in local tumor recurrence and distant metastasis. Parapharyngeal spread is classified as T2b disease. These tumors are associated with an increased rate of local treatment failure and higher frequency of distant metastasis. Hence, tumors with parapharyngeal extension is frequently treated more aggresively.

Imaging Findings

CT

Nasopharyngeal carcinoma shows moderate contrast enhancement. Malignant encroachment into the parapharyngeal space is easily recognized by deformity of the parapharyngeal fat.

MR

Involvement of the parapharyngeal space is best demonstrated on T1-weighted images. Tumor shows an intermediate signal intensity against a background of high-signal-intensity fat. The tumor–fat interface is not always clearly defined after contrast administration even when a fat suppression pulse is added. This is due to the opacification of the rich parapharyngeal venous plexus (Fig. 146–1).

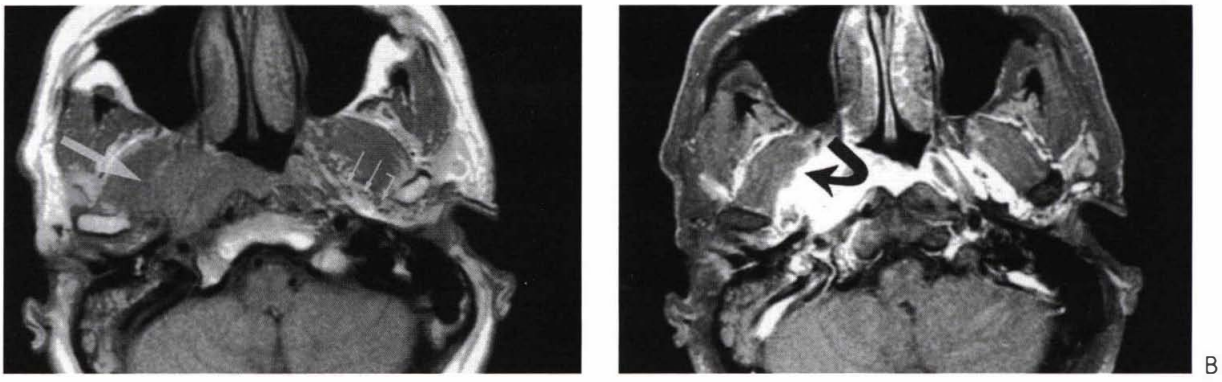

Figure 146-1. Nasopharyngeal carcinoma with parapharyngeal space (PPS) spread. (A) Axial T1-weighted MR image shows an intermediate signal intensity lesion involving the right side of the nasopharynx (arrow) and extending deeply into the right PPS. Note the normal fat-filled left PPS (small arrows). (B) Axial fat-suppressed T1-weighted contrast-enhanced MR shows intense tumor enhancement. There is early tumor infiltration and displacement of the right lateral pterygoid muscle (curved arrow).

Imaging Pearls

- The pharyngobasilar fascia separates the nasopharyngeal visceral space from the fat-filled parapharyngeal space. To locate the position of the pharyngobasilar fascia, draw a line joining the tip of the medial pterygoid plate and the lateral margin of the carotid artery. (The pharyngobasilar fascia is the cranial extension of the superior constrictor muscle from the level of the soft palate to the skull base. From the pharyngeal tubercle, this fascia passes laterally over the prevertebral muscles, along the back of the foramen lacerum to the petrous apex just anterior to the carotid foramen. It continues anteriorly and attaches to the posterior border of the medial pterygoid plate.)
- Tumor extending beyond the above line is deemed to have spread beyond the pharyngobasilar fascia into the parapharyngeal space.
- The pharyngobasilar fascia is a tough barrier, and tumor pressing against it often produces a smooth bulge. Imaging cannot reliably determine whether the fascia has been breached or just displaced under such circumstances.

Suggested Readings

1. Sham JST, Cheung YK, Choy D, Chan FL, Leong L. Nasopharyngeal carcinoma: CT evaluation of patterns of tumor spread. *AJNR Am J Neuroradiol* 1990;12:265–270.
2. Chong VFH, Fan YF, Mukherji SK. Nasopharyngeal carcinoma. *Semin Ultrasound CT MR* 1998;19:449–462.
3. Chong VFH, Mukherji SK, Ng SH, et al. Nasopharyngeal carcinoma: review of how imaging affects staging. *J Comput Assist Tomogr* 1999;23:984–993.

Chapter 147

Tumor Spread from Temporal Bone

Epidemiology

Carcinoma of the temporal bone is uncommon and represents < 1% of all head and neck neoplasms. Most of these tumors arise in the external auditory canal (EAC), whereas tumors originating in the middle ear cavity are very rare. These tumors occur in middle- and older-age groups. The etiology is unknown but appears to be related to chronic ear infection and exposure to ionizing radiation.

Pathology

The histological appearance of squamous cell carcinoma of the EAC and the middle ear is similar to lesions of squamous cell carcinoma elsewhere. Early lesions are confined within the EAC. Neglected lesions cause massive temporal bone destruction with intracranial extension and spread to the skull base. Skull base extension may lead to parapharyngeal extension.

Clinical Findings

Squamous cell carcinoma of the EAC typically presents as a soft tissue mass in the EAC. Bleeding is common and there may be concomitant signs of infection. The presence of other signs such as hearing loss, vertigo, or CN VII palsy depends on tumor extent.

Treatment

The treatment of choice is surgical resection. Postoperative radiation therapy may be given depending on tumor size and resectibility.

Imaging Findings

CT

In general, CT is better for delineating the extent of bony involvement. CT can demonstrate the extent of the soft tissue mass in the EAC, anterior erosion through the tympanic plate, and inferior extension into masticator or parapharyngeal spaces. However, CT cannot differentiate the soft tissue tumor from obstructed secretions.

MR

MR imaging is better for identifying intracranial spread into the middle and posterior cranial fossa. The tumor shows intermediate signal intensity and enhances well following contrast administration. Coronal imaging is helpful at demonstrating direct extension superiorly through the skull base and inferiorly into the parapharyngeal space (Fig. 147-1).

Imaging Pearls

- The parapharyngeal space extends from the skull base to the level of the submandibular glands. It is important to examine the parapharyngeal space because temporal bone resection must take into account the degree of parapharyngeal space involvement.

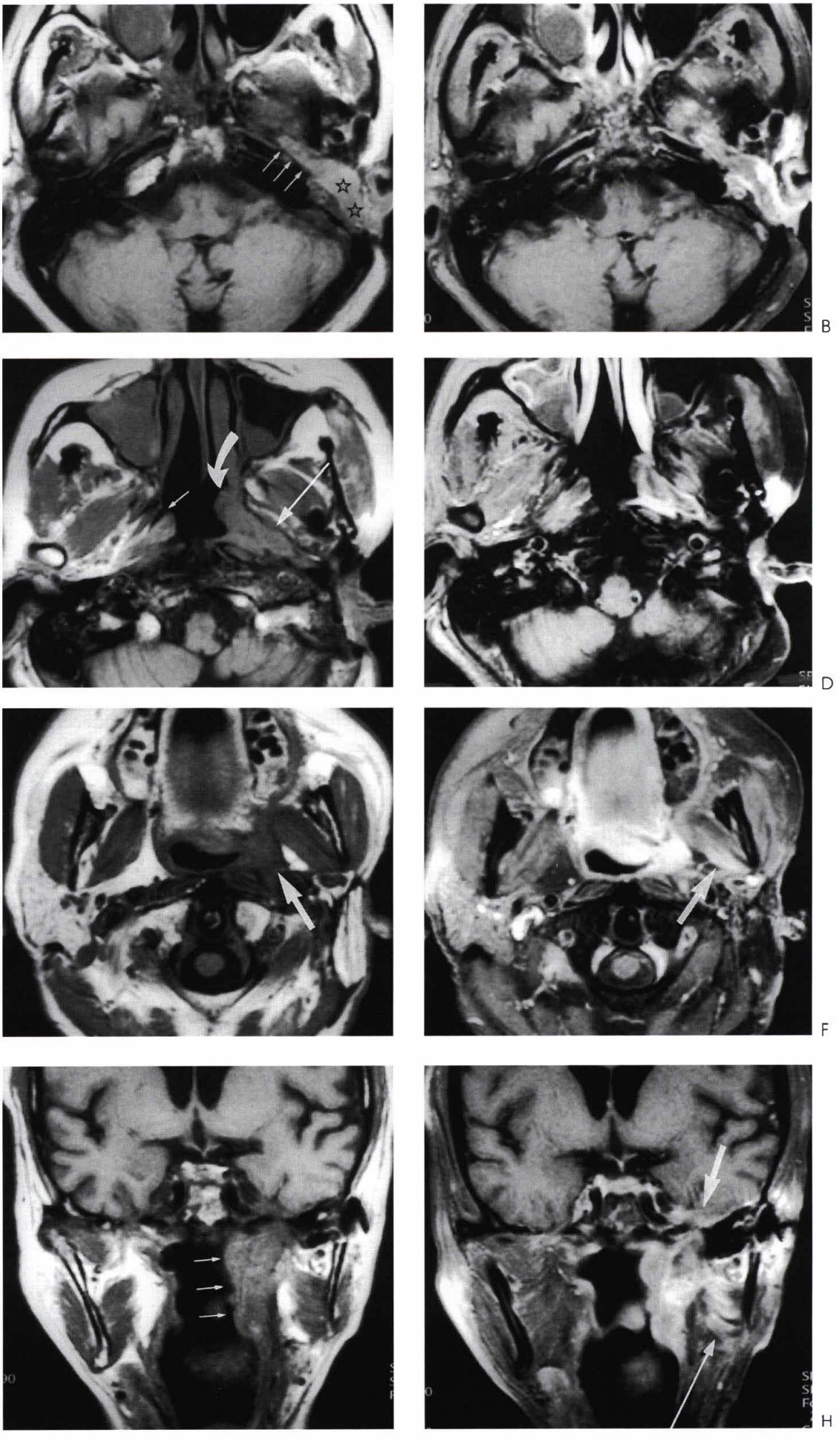
A
B
C
D
E
F
G
H

◁ *Figure 147-1. Recurrent squamous cell carcinoma of the left external acoustic canal with spreadthrough the eustachian tube and along the parapharyngeal space. (A) Axial T1-weighted MR image shows tumor in the left temporal bone (stars) extending along the left eustachian tube (arrows). (B) Axial contrast-enhanced MR image shows heterogeneous enhancement of the tumor tissue. (C) Axial T1-weighted MR image inferior to (A) shows replacement of fat in the left parapharyngeal space (straight arrow), and obliteration of the opening of the eustachian tube (curved arrow). Compare with the normal eustachian tube opening on the right (small arrow). (D) Axial contrast-enhanced MR image shows enhancing tumor tissue around the left torus tubarius and obliteration of the left parapharyngeal space. (E) Axial T1-weighted MR image inferior to (C) shows tumor in the left parapharyngeal space adjacent to the pharyngeal wall (arrow). (F) Axial contrast-enhanced MR image shows tumor enhancement in the left parapharyngeal space. Note contrast enhancement in the left pterygoid muscle (arrow) suggesting denervation due to V_3 perineural infiltration. (G) Coronal T1-weighted MR image shows tumor extending down the left parapharyngeal space and displacement of the pharyngeal wall medially (arrows). (H) Coronal contrast-enhanced MR image shows enhancement in the tumor tissue and the left medial pterygoid muscle (thin arrow). Note tumor extension through the left foramen ovale (thick arrow).*

Suggested Readings

1. Crabtree JA, Britton BH, Pierce MK. Carcinoma of the external auditory canal. *Laryngoscope* 1976;86:405-415.
2. Goh YH, Chong VFH, Low WK. Temporal bone tumours in patients irradiated for nasopharyngeal neoplasms. *J Laryngol Otol* 1999;113:222-228.
3. Harnsberger HR. *Handbook of Head and Neck Imaging*. 2nd ed. St. Louis: Mosby; 1995:29-45.

Chapter 148

Tumor Spread from Nasal Fossa

Epidemiology

Cancers in the nasal cavity and paranasal sinuses are uncommon. Taken as a group, nasal cancers account for 24% of malignancies, whereas paranasal sinus cancers make up 76%. Together these tumors account for < 1 per 100,000 population or < 5% of all body tumors. These tumors are more common in men and are found mainly in patients > 40 years of age.

Pathology

Squamous cell carcinoma accounts for > 80% of all malignant tumors of the nasal cavity and paranasal sinuses. The others include undifferentiated carcinoma, lymphoma, and tumors of salivary gland origin such as adenocystic carcinoma and mucoepidermoid carcinoma. Adenoid cystic carcinoma originating in the nasal cavity is rare. Most nasal tumors present late and the exact site of origin is often difficult to determine.

Clinical Findings

Tumors usually present late with symptoms of nasal obstruction. The tumor may be seen extending through the nostrils or the hard palate. Tumor extension through the sphenopalatine foramen may result in perineural infiltration of CN V_2 resulting in paresthesia over the cheek.

Treatment

The treatment of choice is surgical resection with postoperative radiation therapy.

Imaging Findings

CT

Adenocystic carcinoma shows moderate contrast enhancement with no distinctive features to separate it from the more common squamous cell carcinoma. Depending on the stage of diagnosis, the tumor may extend superiorly into the ethmoid sinus or intracranial cavity; laterally into the maxillary sinus; inferiorly through the hard palate; and posteriorly into the nasopharynx. Extension into the parapharyngeal space is recognized by obliteration of the parapharyngeal fat.

MR

On T1-weighted MR images, the tumor shows intermediate signal intensity and enhances with contrast. T2-weighted images contain high signals. Tumor extending posteriorly to involve the parapharyngeal space is well demonstrated on contrast-enhanced MR imaging (Fig. 148–1).

Imaging Pearls

- The pharyngobasilar fascia, attached anteriorly to the medial pterygoid plate, separates the visceral space from the parapharyngeal space. A tumor in the nasal cavity can spread posteriorly between the medial and lateral pterygoid plates to gain access to the parapharyngeal space.

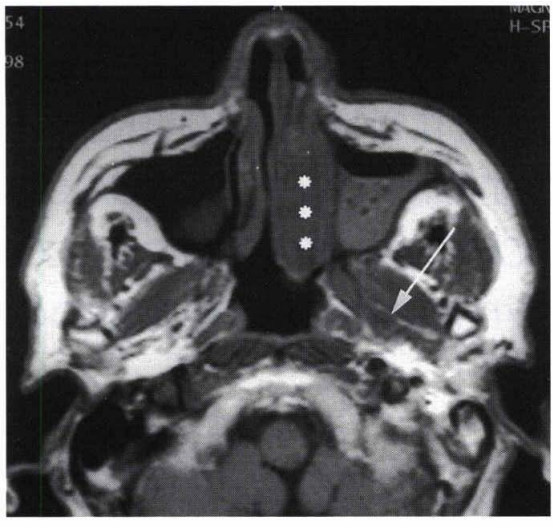

A

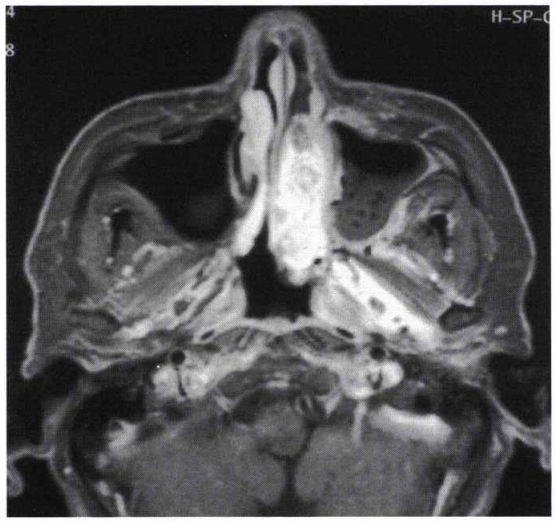

B

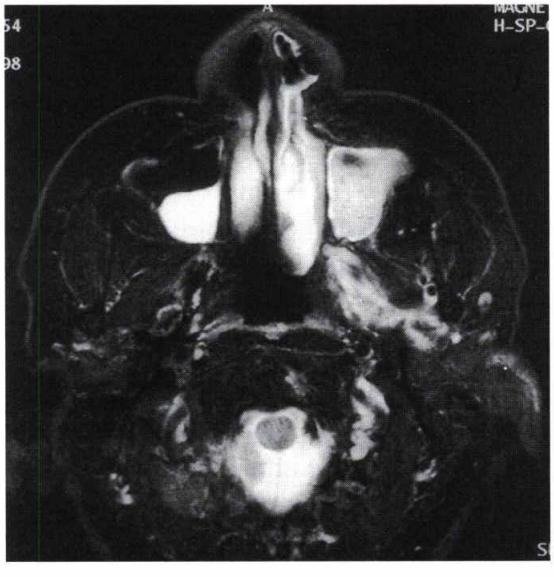

C

Figure 148–1. Adenocystic carcinoma of the nasal cavity with parapharyngeal space spread. (A) Axial T1-weighted MR image shows intermediate signal intensity tumor in the left nasal cavity (asterisks) and in the ipsilateral parapharyngeal space (arrow). Note fluid in the left maxillary sinus due to tumor obstruction. (B) Axial contrast-enhanced MR image shows intense tumor enhancement in the left nasal cavity and left parapharyngeal space. (C) Axial T2-weighted MR image shows high signal intensities corresponding to the abnormalities seen on T1-weighted and contrast-enhanced images.

Suggested Readings

1. Harnsberger HR. *Handbook of Head and Neck Imaging.* 2nd ed. St. Louis: Mosby; 1995:29–45.
2. Sisson G, Snyderman NL, Becker S. Cancer of the nasal cavity and paranasal sinuses. In: Myers EN, Suen JY, eds. *Cancers of the Head and Neck.* 2nd ed. New York: Churchill Livingstone; 1989:311–336.

Chapter 149

Malignant Minor Salivary Gland Tumors (Adenoid cystic, Mucoepidermoid, Adenocarcinoma, Low-Grade Polymorphous Adenocarcinoma)

Epidemiology

The same malignancies that arise in the major salivary glands occur in the minor salivary glands. Depending on the series, approximately half of all tumors of minor salivary gland origin are malignant. The most common location is the palate. An interesting paradox is that the smaller the salivary gland, the greater the likelihood that a tumor originating from that gland will be malignant. The incidence of a salivary gland tumor being malignant is substantially greater in the palate than in the parotid.

Clinical Findings

Patients often present with asymptomatic masses that have been present for several months. Pain and ulceration may be present; however, these are not consistent findings.

Pathology

There are an estimated 500 to 1000 minor salivary glands located throughout the oral cavity and oropharynx. They may be found within the hard and soft palate, uvula, lips, retromolar trigone, tongue base, floor of mouth, and tonsil. The malignancies that constitute minor malignant salivary gland tumors include adenoid cystic carcinoma, mucoepidermoid carcinoma, and adenocarcinoma. Many investigators now include low-grade polymorphous adenocarcinoma as a tumor of minor salivary gland origin. The most common malignancy of the minor salivary glands is adenoid cystic carcinoma.

Treatment

The treatment of malignant salivary gland tumors depends on the exact histologic type. In general, complete surgical resection offers the best chance for cure. Postoperative radiation therapy is required in the majority of cases. The role of neutron beam therapy for unresectable adenoid cystic carcinomas is currently being evaluated.

Imaging Findings

CT

The CT findings are nonspecific. These are usually soft tissue masses that enhance following contrast. The presence of aggressive bone erosion is suggestive of a high-grade malignancy (Fig 149–1).

MR

These tumors are usually intermediate signal on T1-weighted sequences and enhance following contrast administration. The T2-weighted signal is variable (Fig 149–2).

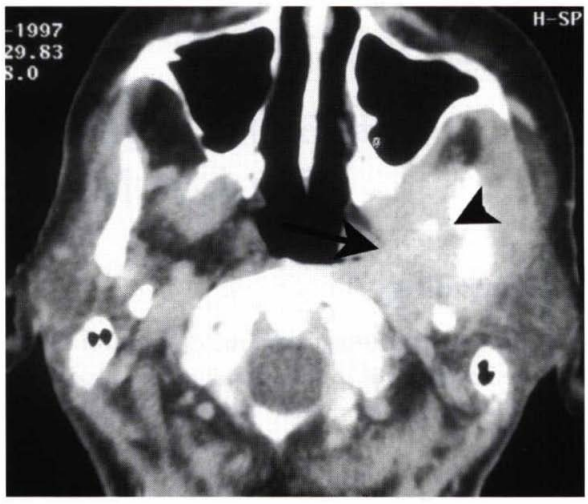

Figure 149–1. Axial contrast-enhanced CT demonstrates an aggressive tumor involving both the parapharyngeal space (arrow) and masticator (arrowhead) spaces. Pathology revealed mucoepidermoid carcinoma.

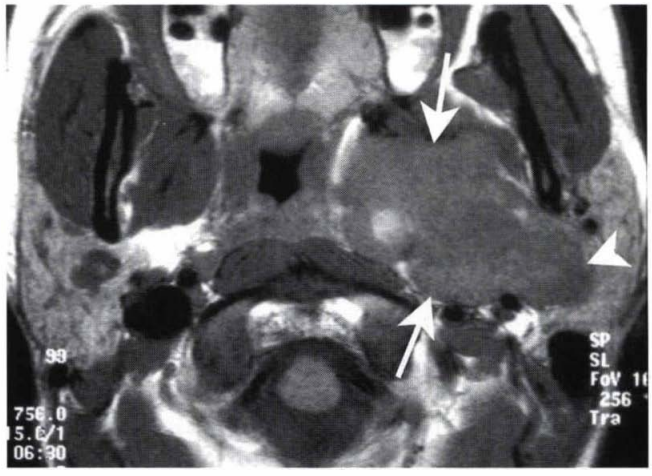

Figure 149–2. Axial T1-weighted MR shows a heterogeneous mass centered in the left parapharyngeal space (arrows). The lateral portion of the mass extends into the deep lobe of the parotid gland (arrowhead). Adenoid cystic carcinoma was found at surgery.

Imaging Pearls

- For adenoid cystic carcinoma involving the hard palate, CT should be performed to evaluate for bone erosion in the regions of the incisive canal and greater and lesser palatine foramen. MR should be performed to evaluate for extension into the pterygopalatine fossa and possible retrograde perineural spread along the maxillary division of cranial nerve V or along the nerve of the vidian canal. These are potential pathways of spread in the cavernous sinus.
- These potential spread patterns should be evaluated in all patients because this may preclude primary surgical resection at many institutions.
- Patients who present with infraorbital numbness and paresthesias should undergo a high resolution MR of the palate and trigeminal nerve to evaluate for the presence of clinically occult adenoid cystic carcinoma of the hard or soft palate that has invaded the infraorbital nerve.
- We recommend performing MR imaging in patients with polymorphous adenocarcinoma arising in the oral cavity because, based on our experience, it appears this tumor has a propensity for marrow invasion.

Suggested Readings

1. Batsakis JG. Neoplasms of the minor and lesser major salivary glands. In: Batsakis JG, ed. *Tumors of the Head and Neck*. Baltimore: Williams and Wilkins; 1979:76–99.
2. Smoker WRK. Oral cavity. In: Som PM, Curtin HD, eds. *Head and Neck Imaging*. 3rd ed. New York: Mosby; 1996:488–544.
3. Shockley WM. Parotid tumors. In: Shockley WM, Pillsbury HC, eds. *The Neck: Diagnosis and Surgery*. New York: Mosby; 1994:265–294.

Chapter 150

Pleomorphic Adenoma (Benign Mixed Tumor)

Epidemiology

Pleomorphic adenoma is the most common (80–90%) of all primary minor salivary gland tumors to arise within the parapharyngeal space. These tumors may occur in any age group, but they most often present between 40 and 50 years of age. Males and females are equally affected.

Clinical Findings

Patients usually present with a painless submucosal tonsillar mass. On physical examination, the mass is nonpulsatile and firm to palpation.

Pathology

Parapharyngeal space pleomorphic adenomas are thought to arise from rests of minor salivary gland tissue located in the fat of the parapharyngeal space. On gross pathological examination, these tumors are encapsulated smooth round or oval masses. The terms *pleomorphic* and *benign mixed* refer to the histologic appearance of this neoplasm. The tumor consists of both epithelial and mesenchymal elements. The epithelial component consists of an inner layer of epithelial cells, whereas the outer layer consists of myoepithelial cells that constitute the mesenchymal component. Both elements must be present for the diagnosis of pleomorphic adenoma to be made. These tissue elements may be arranged in a variety of patterns and associated with a variable amount of stroma. The stroma can consist of variable amounts of mucoid, fibroid, chondroid, vascular, or myxochondroid elements. The mucoid stroma is thought to be responsible for the signal characteristics present on T2-weighted imaging.

There are several malignancies associated with pleomorphic adenomas, including carcinoma–expleomorphic adenoma, carcinosarcoma, and benign mixed tumor. These tumors will be discussed in detail in separate chapters. The incidence of an associated malignancy is believed to be related to long-standing tumors and those that have had multiple recurrences.

Treatment

The treatment of parapharyngeal space pleomorphic adenomas is resection. The surgical approach is determined by the extent of the disease identified on imaging. The full extent of disease cannot be determined by clinical examination. Low-volume lesions may be resected through a transoral approach. However, advanced lesions require a cervical approach. Most cases of recurrence are felt to be due to incomplete tumor removal or disruption of the surrounding capsule with subsequent tumor spillage into the surgical bed.

Imaging Findings

CT

The typical CT appearance of a pleomorphic adenoma is a smoothly marginated low attenuation mass. Larger masses may contain areas of higher attenuation that represent areas of hemorrhage or calcification which arise within the stromal matrix (Fig. 150–1).

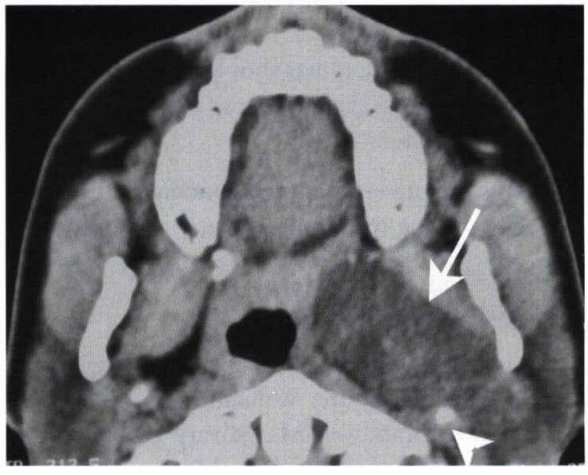

Figure 150–1. Axial contrast-enhanced CT shows a pleomorphic adenoma in the left parapharyngeal space (arrow). The mass is lower attenuation than the adjacent muscle. The posterior displacement of the internal carotid artery (arrowhead) helps localize the mass to the parapharyngeal space.

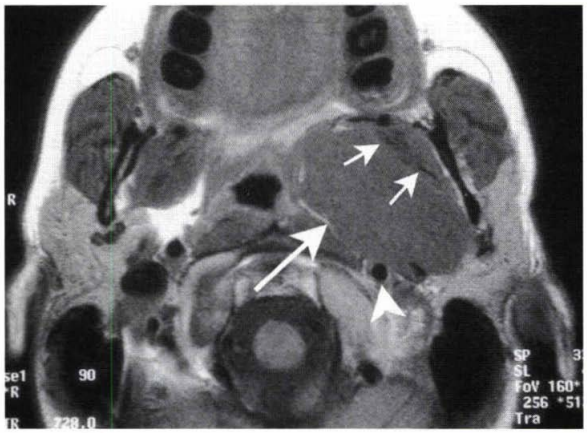

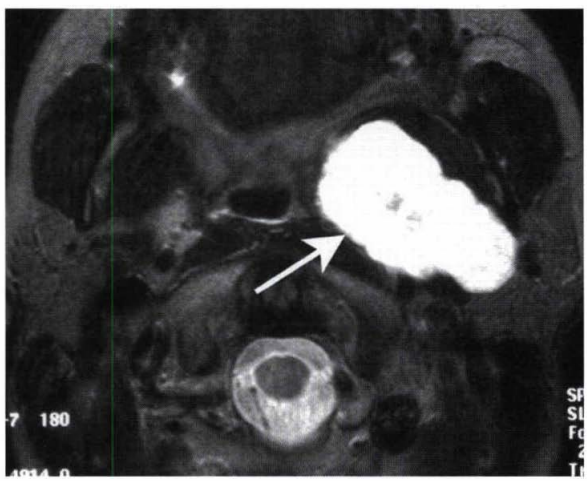

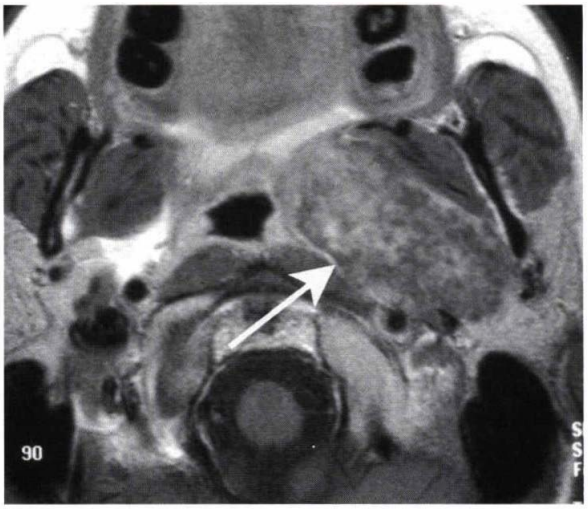

Figure 150–2. MR findings of pleomorphic adenoma. (A) Axial noncontrast T1-weighted image shows an intermediate signal mass located in the left parapharyngeal space (large arrow). Note the posterior displacement of the carotid artery (arrowhead) and the lateral displacement of the medial pterygoid muscle (small arrows). These findings help localize the mass to the parapharyngeal space. (B) There is heterogeneous enhancement of the mass following contrast administration (arrow). This enhancement pattern is not specific for pleomorphic adenoma. (C) Axial T2-weighted image shows the mass has increased signal. This homogeneously increased T2-weighted signal within a mass centered in the parapharyngeal space or within the parotid gland is strongly suggestive of pleomorphic adenoma (arrow).

MR

On MR imaging, these lesions are lobulated, low signal masses on T1-weighted imaging. They mildly enhance with contrast. These tumors are usually high signal on T2-weighted sequences (Fig. 150–2).

Imaging Pearls

- Pleomorphic adenomas should be considered in the differential diagnosis for all primary parapharyngeal space masses. The characteristic imaging findings should help confirm the diagnosis.
- MR is the preferred imaging modality for evaluating parapharyngeal space pleomorphic adenoma due to the multiplanar capabilities and superior soft tissue characterization.

Suggested Readings

1. Batsakis JG. Tumors of the major salivary glands. In: Batsakis JG, ed. *Tumors of the Head and Neck*. Baltimore: Williams and Wilkins; 1979:1–76.
2. Som PM, Brandwen M. Salivary glands. In: Som PM, Curtin H, eds. *Head and Neck Imaging*. 3rd ed. New York: Mosby; 1996:823–914.
3. Ikeda K, Katoh T, Ha-Kawa SK, Iwai H, Yamashita T, Tanaka Y. The usefulness of MR in establishing the diagnosis of parotid pleomorphic adenoma. *AJNR Am J Neuroradiol* 1996;17:555–559.

Chapter 151

Neurofibroma

Epidemiology

Plexiform neurofibromas may involve the parapharyngeal space (PPS). PPS neurofibromas typically occur in patients with neurofibromatosis type 1 (NF type 1).

Clinical Findings

Patients with nerofibromas of the PPS typically have known neurofibromatosis and have associated findings. The involvement of the PPS is due to involvement of branches of small nerves that traverse the PPS. Rarely do patients present with findings associated with PPS masses as the only symptoms.

Pathology

Neurofibromas are composed of enlarged neurofibrils, whereas schwannomas are composed of enlarged Schwann's cells. Schwannomas are encapsulated tumors and are easier to resect from the involved nerve. Neurofibromas are difficult to resect because they arise from intrinsic components of the nerve.

Treatment

Because NF type 1 may involve multiple sites and structures and neurofibromas are difficult to resect, surgery is warranted only if there are symptoms and significant compression of vital structures or if there is a suspicion of malignant degeneration.

Imaging Findings (Fig. 151–1)

CT

These are predominantly low attenuation masses with well-defined margins located in the PPS. These lesions have a variable enhancement pattern.

MR

On T1-weighted images, neurofibromas are isointense with skeletal muscles. They homogeneously enhance following contrast and are high signal on T2-weighted sequences. Early lesions have well-defined margins; however, advanced lesions can spread along the involved nerve to include adjacent spaces.

Imaging Pearls

- The diagnosis of a neurofibroma or schwannoma should be considered for a well-defined enhancing mass situated in the PPS in a patient with neurofibromatosis.
- It is difficult to distinguish a single neurofibroma from a schwannoma.
- Neurofibroma or schwannoma cannot be distinguished from its malignant counterpart on a single study. Development of an enhancing and enlarging mass is suggestive of malignant transformation.

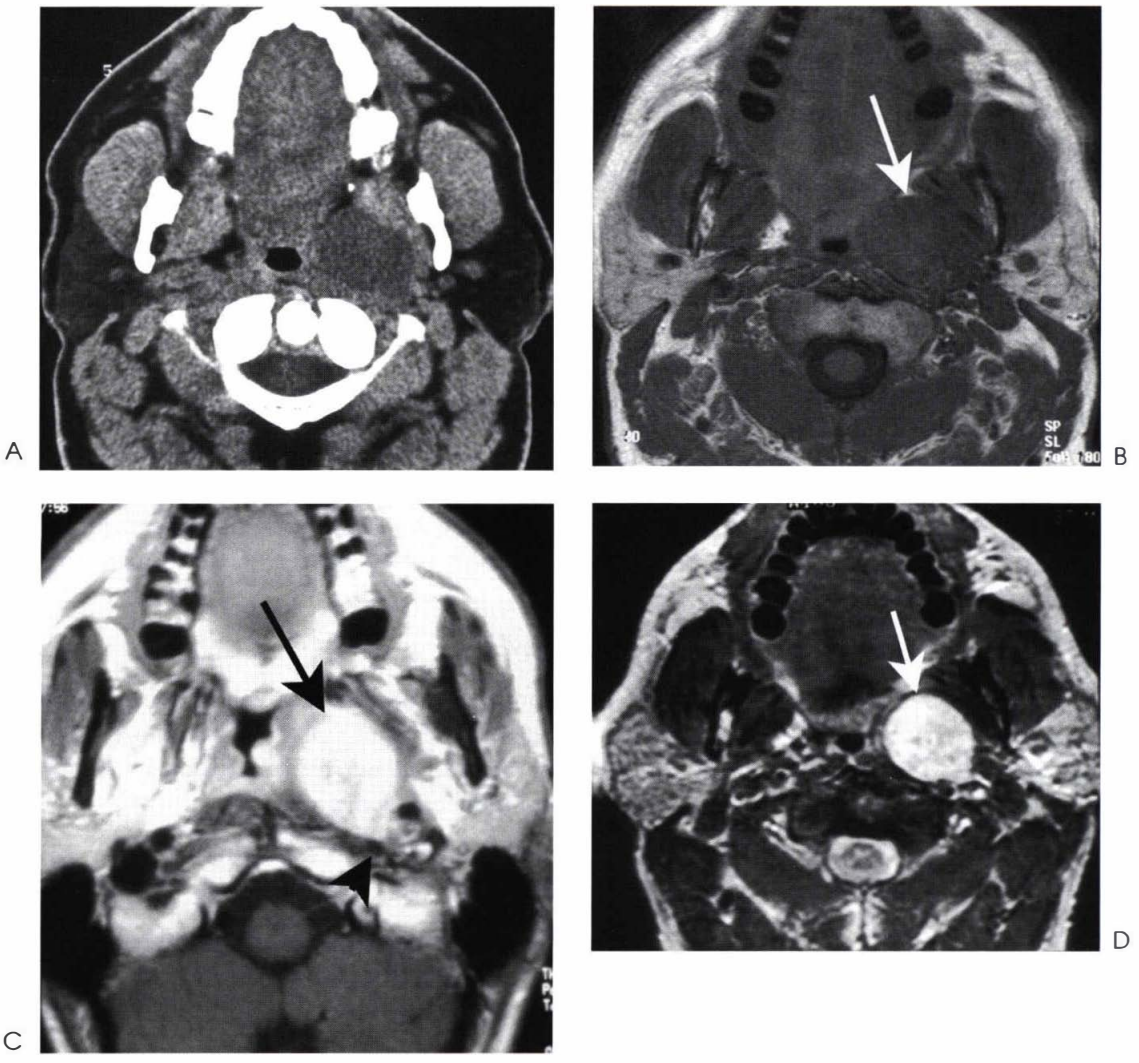

Figure 151-1. Neurofibroma of the parapharyngeal space. (A) Axial noncontrast CT demonstrates a well-defined mass in the left parapharyngeal space (arrow). The lateral displacement of the medial pterygoid muscle (large arrowheads) and posterior displacement of the prevertebral muscle (small arrowhead) isolate the mass to the parapharyngeal space. (B) Axial noncontrast T1-weighted image shows the mass to be intermediate signal (arrow). (C) There is dense enhancement of the mass following contrast administration (arrow). Note the posterior displacement of the carotid artery (arrowhead) which isolates the mass to the parapharyngeal space. (D) Axial T2-weighted image shows homogeneously increased signal within the mass (arrow). Similar findings can be seen in pleomorphic adenoma or schwannoma. Neurofibroma and schwannoma should be the primary considerations for masses with this appearance in this location identified in patients with a history of neurofibromatosis.

Suggested Readings

1. Smirniotopoulos JG, Murphy FM. Central nervous system manifestations of the phakomatoses and other inherited syndromes. In: Atlas SW, ed. *Magnetic Resonance Imaging of the Brain and Spine*. 2nd ed. Philadelphia: Lippincott-Raven; 1996:773–802.
2. Kyriakos M, El-Mofty S. Pathology of selected soft tissue of head and neck. In: Thawley SE, Panje WR, Batsakis JG, Lindberg RD, eds. *Comprehensive Management of Head and Neck Tumors*. 2nd ed. Philadelphia: WB Saunders; 1999:1322–1394.
3. Weber AL, Montandon C, Robson CD. Neurogenic tumors of the neck. *Radiol Cin North Am* 2000;38:1077–1090.

Chapter 152

Adenoidcystic Carcinoma

Epidemiology

Primary tumors of the parapharyngeal space are rare and they usually arise from minor salivary glands. The hard palate has the highest concentration of minor salivary glands in the upper aerodigestive tract, and it is the most common site for benign and malignant minor salivary gland tumors. Minor salivary glands are also found in the tongue, hard palate, lips, and cheeks, but occasionally these tumors are seen in the parapharyngeal space. About half of all minor salivary gland tumors are malignant and two thirds of them are adenoid cystic carcinoma.

Clinical Findings

The parapharyngeal space is large and deep-seated. Most tumors present when they have reached a large size. These tumors produce pain when they erode other structures such as bone. Adenoid cystic carcinoma with perineural spread may also present with pain.

Pathology

Adenoid cystic carcinomas most commonly arise submucosally and often presents as advanced disease. Histologically, adenoid cystic carcinomas are low-grade malignancies but their biological behavior resembles that of high-grade malignancies. There is a high tendency for recurrence and a 50% chance of distal metastasis. These tumors have a high propensity for perineural infiltration and this mode of spread may be seen in 50% of patients.

Treatment

The treatment of choice is surgical excision followed by postoperative radiation therapy. It is important to differentiate an adenoid cystic carcinoma arising in the parapharyngeal space or in the deep lobe of the parotid gland. A primary lesion in the parapharyngeal space is reached from a cervical approach, whereas a deep parotid lobe lesion requires a parotid dissection to preserve the facial nerve.

Imaging Findings

CT

Adenoid cystic carcinomas are of soft tissue attenuation and demonstrate moderate contrast enhancement. These tumors are usually large and may have smooth margins despite their malignant nature.

MR

On T1-weighted images, adenoid cystic carcinoma may show a heterogeneous pattern of intermediate signal intensity. T2-weighted images demonstrate variable signal intensity. Following the injection of contrast, the degree of contrast enhancement may vary in different parts of the tumor (Fig. 152–1).

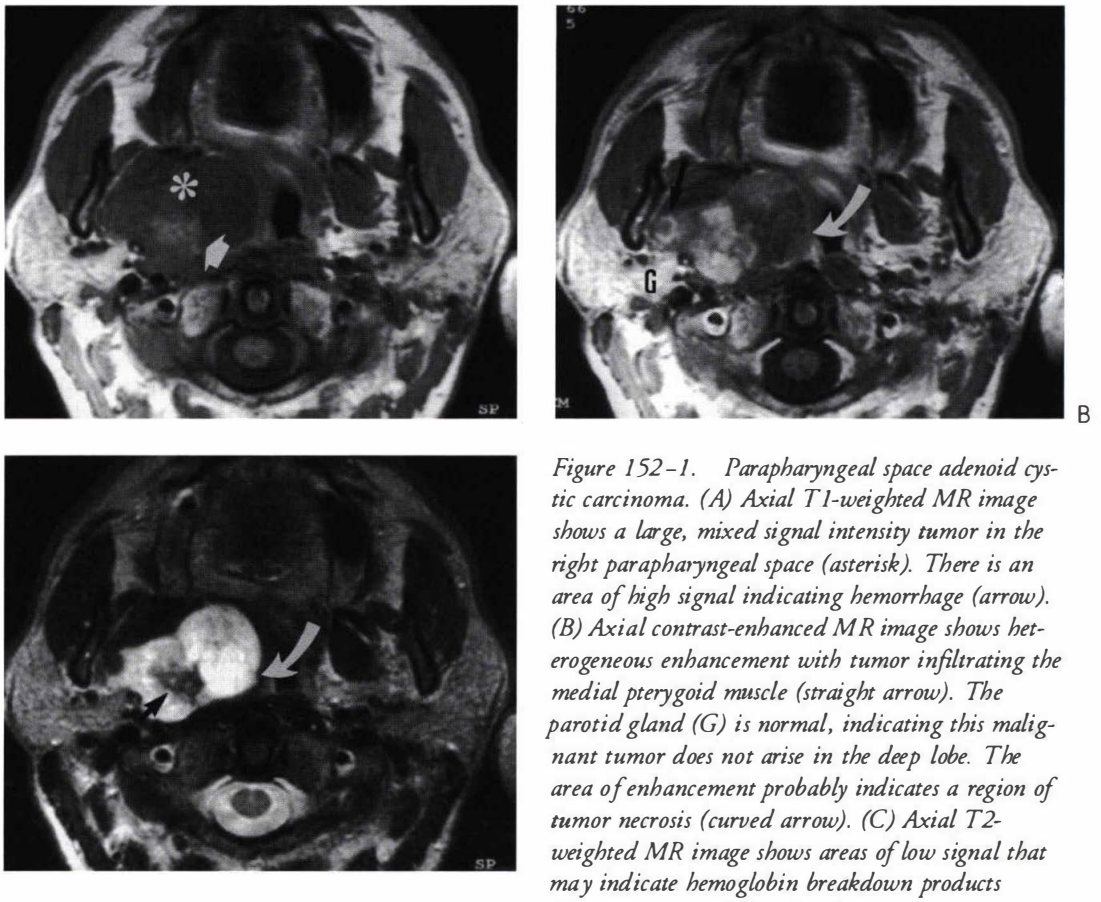

Figure 152-1. Parapharyngeal space adenoid cystic carcinoma. (A) Axial T1-weighted MR image shows a large, mixed signal intensity tumor in the right parapharyngeal space (asterisk). There is an area of high signal indicating hemorrhage (arrow). (B) Axial contrast-enhanced MR image shows heterogeneous enhancement with tumor infiltrating the medial pterygoid muscle (straight arrow). The parotid gland (G) is normal, indicating this malignant tumor does not arise in the deep lobe. The area of enhancement probably indicates a region of tumor necrosis (curved arrow). (C) Axial T2-weighted MR image shows areas of low signal that may indicate hemoglobin breakdown products (short arrow) and high signal suggesting necrosis (curved arrow).

Imaging Pearls

- On CT, adenoid cystic carcinomas are soft tissue attenuation and enhance, whereas pleomorphic adenomas of the parapharyngeal space are low attenuation and show mild enhancement.
- Pleomorphic adenomas of the parapharyngeal space characteristically have lobulated margins and have increased signal on T2-weighted sequences. The margins and the T2-weighted signal characteristics are variable.

Suggested Readings

1. Million RR, Cassisi NJ. Minor salivary gland tumors. In: Million RR, Cassisi NJ, eds. *Management of Head and Neck Cancer*. Philadelphia: JB Lippincott; 1994:737–750.
2. Mukherji SK, Castillo M. A simplified approach to spaces of the suprahyoid neck. *Radiol Clin North Am* 1998;36:761–780.
3. Chong VFH, Mukherji SK, Goh CHK. The suprahyoid neck: normal and pathological anatomy. *J Laryngol Otol* 1999;113:501–508.

Chapter 153

Lipoma

Epidemiology

The parapharyngeal space is predominantly fat-filled, and primary tumors in this space are uncommon. The most common primary tumor is a pleomorphic adenoma. Occasionally, a lipoma may be seen in this space. Most of the lipomas found in the head and neck are located in the triangle.

Clinical Findings

Lipomas are more common in overweight individuals. They may show rapid increase in size during periods of weight gain. They often present as incidental findings on imaging but patients may also complain of vague neck discomfort. When these tumors are large enough, they may encroach on the adjacent spaces and present as mass lesions.

Pathology

Lipomas are yellow, lobulated, and very well encapsulated tumors. They consist of normal adult adipose tissue. Lipomas are classified histologically according to the kind of other tissues that may be present (e.g., fibrolipoma, angiolipoma, and myxolipoma). These tumors very rarely undergo malignant degeneration. Liposarcomas originate from lipoblasts within fascia rather than ordinary lipocytes.

Treatment

Lipomas are benign lesions. If they are asymptomatic, no treatment is required. Surgical excision of lipomas is only considered if they are symptomatic. Pain may be related to the compression of normal structures, and the possibility of malignant degeneration should always be entertained. Because lipomas are well encapsulated, they can be easily enucleated.

Imaging Findings

CT

The appearance of lipoma in the parapharyngeal space is similar in appearance to lipomas that occur elsewhere in the body. Lipomas are low attenuation. However, the margin of the lesion may not be distinctly visible against the background of normal parapharyngeal fat. When the mass abuts adjacent muscles or tissues of intermediate attenuation, the tumor outline is usually smooth. An irregular margin or foci of intermediate attenuation within the lesion should raise the possibility of a liposarcoma (Fig. 153–1).

MR

The signal intensity of a lipoma parallels that of normal fat. On T1-weighted images, lipomas show high signal intensity. On T2-weighted MR images, the fat shows relatively lower signals. However, on fast spin echo (FSE) T2-weighted images, the signal intensity lipomas remain high. With fat suppression lipomas reveal a low signal intensity pattern. Lipomas show no significant enhancement following the injection of contrast.

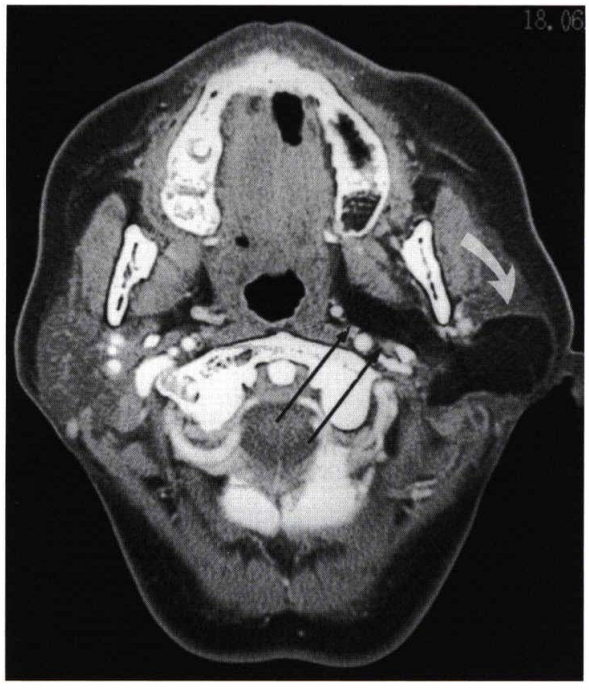

Figure 153-1. Parapharyngeal space lipoma. Axial contrast-enhanced CT shows a lipoma involving the left parapharyngeal space (straight arrows) and the parotid gland (curved arrow).

Imaging Pearls

- The imaging features of lipomas on CT and MR imaging are characteristic. The attenuation or signal intensity of lipomas parallels that of subcutaneous fat.
- A liposarcoma cannot be excluded if what is thought to be a lipoma contains linear areas of soft tissue on CT or MR.

Suggested Readings

1. Harnsberger HR. *Handbook of Head and Neck Imaging.* 2nd ed. St. Louis: Mosby; 1995:199-223.
2. Smoker RK. Oral cavity. In: Som PM, Curtin HD, eds. *Head and Neck Imaging.* 2nd ed. St. Louis: Mosby; 1996:488-544.

Chapter 154

Arteriovenous Malformation

Epidemiology

Arteriovenous malformations (AVMs) are developmental malformations of the vascular system that result in abnormal communication between arteries and veins. The primary abnormality appears to be at the level of the capillary bed. AVMs are classified as a type of vascular malformation using the classification system of Mulliken and Glowacki. AVMs also include arterial malformations and arteriovenous fistulae and are characterized as high-flow lesions. AVMs of the parapharyngeal space are not isolated and usually involve adjacent spaces.

Clinical Findings

The clinical findings can be variable depending on the extent of the lesion. The neck and craniofacial region are common sites of occurrence. On clinical examination, AVMs present as a soft tissue fullness that is compressible. Superficial AVMs may be associated with a palpable thrill or audible bruit. The overlying skin may be discolored due to dilated superficial veins. Patients with more advanced lesions may present with facial deformity, skin ulceration, or functional compromise. Patients may also present with hemorrhage that may be spontaneous or follow minor trauma such as tooth extraction. AVMs may enlarge with pregnancy. It is unclear as to whether the growth is due to direct hormonal stimulation or results secondarily from an increase in the circulating blood volume.

Pathology

AVMs result from abnormal development of the arterial, capillary, and venous components of the vascular system. The lesions grow commensurately with the individual and show no evidence of endothelial proliferation. The vascular channels are lined by mature endothelium with normal mitotic activity.

Treatment

The treatment of choice is combined therapy consisting of embolization followed by surgical excision. Complete resection of the nidus is necessary to prevent recurrence.

Imaging Findings

CT

AVMs are characterized by a tangle of enhancing serpiginous vessels that are not associated with a surrounding soft tissue mass. Lesions adjacent to facial bones may be associated with enlargement and overgrowth of the adjacent bone (Fig. 154-1).

MR

The MR findings of an AVM are multiple flow voids without an associated soft tissue mass. Increased vascular flow is seen on flow sensitive sequences.

US

Doppler analysis will demonstrate arterial and venous components and may show arterialized waveforms of a draining vein due to arteriovenous shunting.

Angiography

AVMs have enlarged tortuous feeding arteries that supply a nidus. Arteriovenous shunting into enlarged draining veins is a characteristic finding. The primary blood supply is from various branches of the external carotid artery.

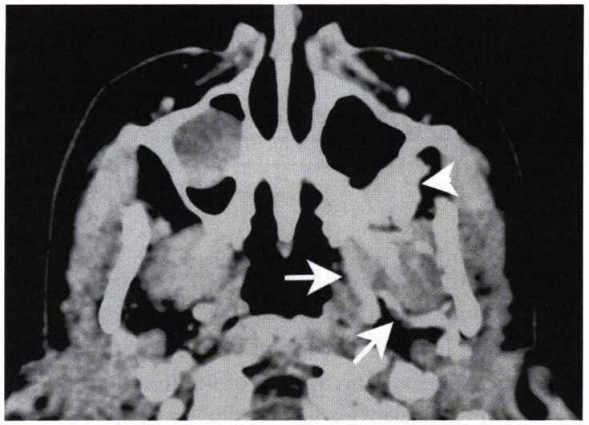

A

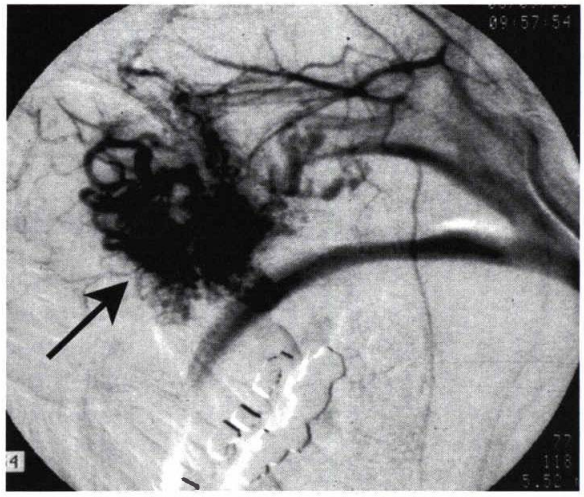

B

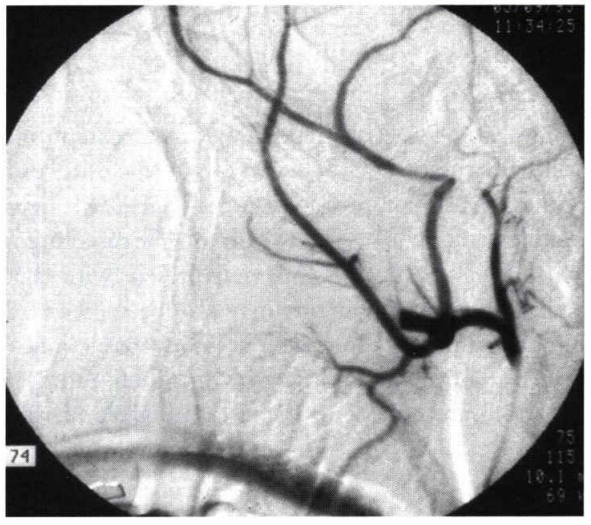

C

Figure 154–1. (A) Axial contrast-enhanced CT demonstrates an enhancing lesion located in the left parapharyngeal space (arrows). There is also a component in the left buccal space (arrowhead). (B) Selective external carotid angiogram demonstrates a large arteriovenous malformation (arrow). (C) There is complete obliteration of the arteriovenous malformation following embolization.

Imaging Pearls

- The treatment of AVMs is directly affected by the imaging findings. Identification of a high-flow vascular malformation with arteriovenous shunting contraindicates treatment with percutaneous sclerotherapy.
- The presence of potential collateral formation between branches of the external carotid artery and the vertebral artery or between branches of the internal carotid artery needs to be closely evaluated for during embolization procedures.
- Craniofacial AVMs should not be treated with a particle size < 200 μm due to the possibility of inciting overlying skin necrosis, direct shunting of particles into the pulmonary bed, or intracranial circulation.

Suggested Readings

1. Mulliken JB, Glowacki J. Hemangiomas and vascular malformations in infants and children: a classification based on endothelial characteristics. *Plast Reconstr Surg* 1982;69:412–422.
2. Meyer JS, Hoffer FA, Barnes PD, Mulliken JB. Biological classification of soft-tissue vascular anomalies: MR correlation. *AJR Am J Roentgenol* 1991;157:559–564.
3. Smoker WRK. Oral cavity. In: Som PM, Curtin H, eds. *Head and Neck Imaging*. 3rd ed. New York: Mosby; 1996:488–544.
4. James CA. Diagnostic imaging of congenital vascular lesions. In: Warner M, Suen JY, eds. *Hemangiomas and Vascular Malformations of the Head and Neck*. New York: Wiley-Liss; 1999:171–215.

Chapter 155

Lymphatic Malformations

Introduction

Lymphatic malformation (*LM*) is the current term used to describe lymphangiomas. Mulliken and Glowacki recommend that the suffix *-oma* only be used in lesions that exhibit cellular proliferation such as a hemangioma. LM is a congenital lesion that results from a defect in embryogenesis of the lymphatic system. Such lesions occur in equal frequency in males and females. They most commonly present in newborn children, with 65% of lesions noted at birth, 80% present at 1 year, and 90% present by 2 years of age. Ten percent of LMs may initially present in adulthood. LMs may be localized or associated with a generalized malformation of the lymphatic system. Advanced generalized disorders may be seen as diffuse lymphangiectasis in utero and are incompatible with life. LM has been associated with a number of syndromes, the most common being Turner's syndrome. Other syndromes include Noonan's syndrome, fetal alcohol syndrome, familial pterygium syndrome, distichiasis–lymphedema syndrome, and various chromosomal aneuploidies.

Embryology

LM is thought to occur from a defect in the normal drainage of the lymphatic channels into the venous system. The result is a progressive enlargement of the isolated lymphatic spaces due to the continued secretion of lymph. There are several proposed explanations of this malformation. The malformation may be due to a portion of the lymphatic network that fails to reestablish a communication with the venous system and is sequestered early in embryogenesis. Early malformations involving the more primitive jugular, subclavian, and axillary sac are felt to result in the formation of the larger cystic hygromas. These lesions occur in soft areolar tissues in areas with wide fascial planes with the result being sharply demarcated round or oval lesions. Lesions that have smaller cystic spaces and are more diffuse and infiltrative are felt to occur later in embryogenesis. These malformations have time to grow distally along narrower fascial planes and insinuate themselves along vessels and nerve trunks. This probably results in the mixed malformations described by Mulliken and Glowacki such as lymphaticovenous and lymphaticocapillary malformations. Thus, LMs that occur in the cheeks, lips, and tongue tend to contain more of an angiomatous component.

Pathology

Pathologically, LMs have been categorized in the past based on the size of the anomalous lymphatic space. It should be noted that *lymphatic malformation* is the current term used to describe these malformations and that terms such as *cavernous lymphangioma* and *capillary lymphangioma* probably refer to the mixed lymphatic malformations described by Mulliken and Glowacki. We present the older terminology for historical consistency.

Cystic hygroma is the most common form and consists of a honeycomb of very large dilated lymphatic spaces lined by a single layer of flat endothelium. These lesions are often solitary and occur in the presence of an otherwise normal lymphatic system. Seventy-five percent of these lesions occur in the neck. These lesions have a predilection for the posterior compartment of the neck.

A cavernous lymphangioma is composed of mild to moderately dilated lymphatic spaces, the size of which is between the cystic spaces seen in cystic hygromas and capillary hemangiomas. These lesions tend to be situated in the oral cavity or salivary glands. Cavernous LA tend to be subcutaneous lesions which have penetrated adjacent muscular and neurovascular structures without destroying them. The peripheral location and subcutaneous spread are suggestive of a defect in embryogenesis during a later phase of lymphatic development (9–10 weeks) as compared with a cystic hygroma.

Capillary hemangioma (simple, lymphangioma simplex) is composed of a network of small lymph, thin-walled channels that are the size of capillaries. This is the least common form of lymphangioma. These lesions are located predominantly within the epidermis and can occur anywhere throughout the body. Because of their superficial location, capillary hemangiomas are believed to form the latest in development.

Clinical Findings

The extracranial head and neck is the most common site of LMs (75%). They typically present as a painless neck mass. Lesions that occur in the face are more likely to be mixed LMs. LAs tend to enlarge commensurate with the growth of the child and not by endothelial proliferation. Potential complications include disfigurement, respiratory compromise, and recurrent infections. Rapid enlargement may be due to infection or spontaneous hemorrhage within the lesion.

Treatment

Surgical resection is the treatment of choice for LMs with distinct margins. However, distal lesions that extend over several anatomical areas are difficult to completely resect and are prone to recurrence. Such patients need close follow-up and may require multiple surgical procedures. Percutaneous sclerotherapy is gaining wider acceptance for more advanced lesions that infiltrate the deep fascial planes. Some authors advocate angiography and embolization for lymphaticocapillary lesions that involve the oral cavity and tongue. The role of interferon therapy for very advanced and infiltrative lesions is currently under investigation.

Imaging Findings

CT

The classic appearance of an LM is a sharply demarcated, low attenuation mass that does not contain a visible wall. Large lesions may be multilobular and have considerable mass effect and may displace the structures of the carotid sheath and adjacent sternocleidomastoid muscle. Lesions that have been partially resected or have been repeatedly infected may demonstrate an enhancing wall or contain internal septations. Mixed LMs are heterogeneous and infiltrative. These lesions extend along fascial planes and often involve multiple spaces (transspatial). Because of the angiomatous components, mixed lesions may enhance with contrast (Figs. 155–1 and 155–2).

MR

A pure LM is low signal on T1-weighted sequences and high signal on T2-weighted sequences. There is no perceptible wall or enhancement following contrast administration. The best sequences to identify the full extent of the lesion are noncontrast T1- and T2-weighted. Pure LMs are low-flow lesions and lack flow voids. Mixed malformations are infiltrative heterogeneous lesions that enhance following contrast. The degree of the enhancement is likely due to the angiomatous component of the mixed lesion (Fig. 155–3).

US

Pure LMs are hypoechoic masses that may occasionally contain internal septations or debris. Doppler analysis may be helpful in identifying and characterizing mixed LMs by identifying and characterizing the presence of intralesional blood flow.

Angiography

Pure LMs are avascular low-flow lesions. However, mixed LMs that have a substantial angiomatous component are hypervascular and have enlarged feeding vessels. Arteriovenous shunting is rare.

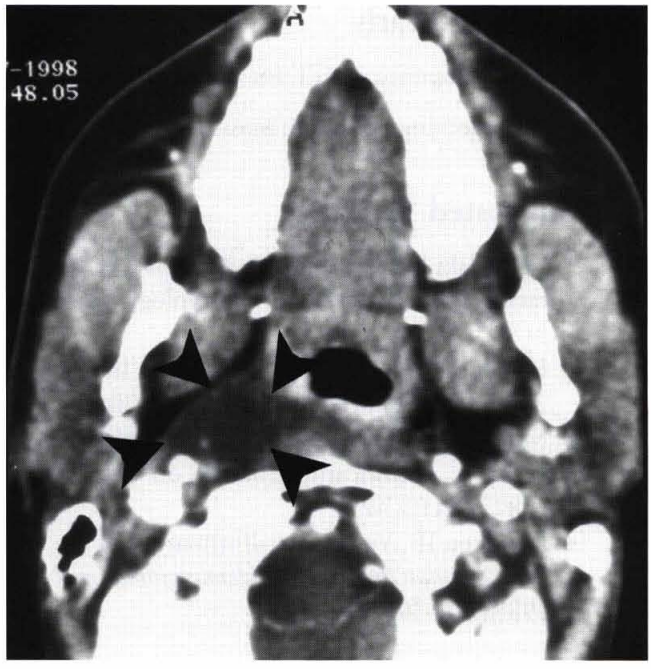

Figure 155–1. Axial contrast-enhanced CT shows a low attenuation lymphatic malformation centered in the right parapharyngeal space (arrowheads).

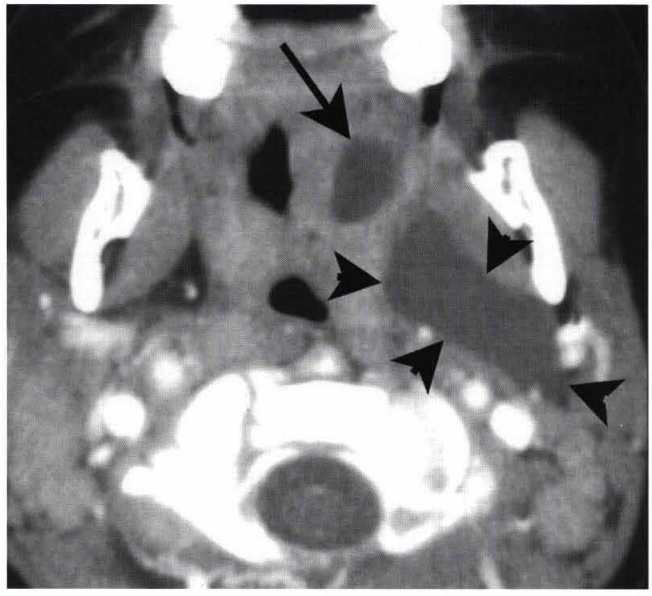

Figure 155–2. Contrast-enhanced CT in a child shows a lymphatic malformation in the left parapharyngeal space (arrowheads). There appears to be a second component identified anterior to the left portion of the soft palate (arrow).

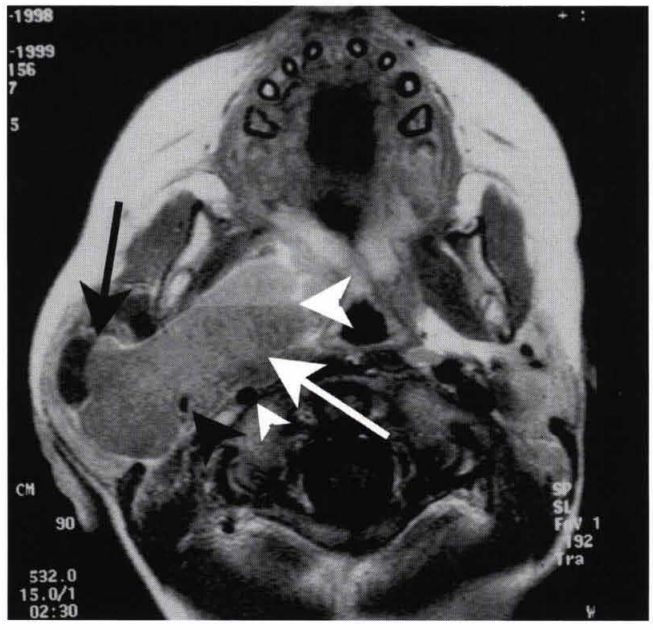

Figure 155–3. Axial T1-weighted image of a lymphatic malformation (white arrow) demonstrates several characteristic features. The lesion extends into several spaces (transspatial). The mass is centered in the right parapharyngeal space and extends laterally into the parotid space (black arrow). The mass distorts the jugular vein and separates it from the carotid artery (small white arrowhead), which indicates the lesion involves the carotid space. The mass contains a "fluid–fluid" level (large white arrowhead) that may represent prior hemorrhage within the lesion. The above MR findings are characteristic of a lymphatic malformation of the parapharyngeal space.

Imaging Pearls

- MR is superior to CT for defining the full extent of the lesion.
- A predominantly cystic mass that is transspatial is the characteristic imaging on an LM.

Suggested Readings

1. Zadvinski DP, Benson MT, Kerr HH, et al. Congenital malformations of the cervicothoracic lymphatic system: embryology and pathogenesis. *Radiographics* 1992;12:1175–1189.
2. Batsakis JG. Vasoformative tumors. In: Batsakis JG, ed. *Tumors of the Head and Neck.* 2nd ed. Baltimore: Williams and Wilkins; 1979:518–520.
3. Mulliken JB, Glowacki J. Hemangiomas and vascular malformations in infants and children: a classification based on endothelial characteristics. *Plast Reconstr Surg* 1982;69:412–422.
4. Mulliken JB. Vascular malformations of the head and neck. In: Mulliken JB, Young AE, eds. *Vascular Birthmarks: Hemangiomas and Malformations.* Philadelphia: WB Saunders; 1988:301–307.

Section VII

Carotid Space

The carotid space (CS) is an enclosed fascial space located posterior to the styloid process and lateral to the retropharyngeal space (RPS) and prevertebral space (PVS). A slip of alar fascia contributes to the medial wall of the CS and helps separate the retropharyngeal space and prevertebral space from the CS (Figs. VII-1 through VII-3).

In the suprahyoid neck, the CS is bordered anteriorly by the styloid process and the parapharyngeal space, laterally by the anterior belly of the digastric muscle and the parotid space, and medially by the lateral margin of the RPS. As a result, the nomenclature for this space is confusing. The carotid space is also known as the poststyloid parapharyngeal space or the carotid sheath. Any of these terms are acceptable with the following caveats: *carotid space* or *carotid sheath* is preferred when it is used in conjunction with the term *parapharyngeal space*. However, *poststyloid parapharyngeal space* must be used with *prestyloid parapharyngeal space*. Adhering to the proper use of this nomenclature will prevent further confusion regarding this terminology.

The CS contains the internal carotid artery, internal jugular vein, cranial nerves IX through XII, and lymph nodes. The actual location of the sympathetic chain is controversial. Some authors suggest that a portion of the course is located within the carotid space. The CS extends superiorly to the jugular foramen and inferiorly to the aortic arch. A mass may be localized to the CS if it is centered within the area of the carotid artery and jugular vein.

The majority of masses that involve the CS are lesions that originate primarily within this space. Masses that involve the carotid artery or jugular vein can be easily identified on con-

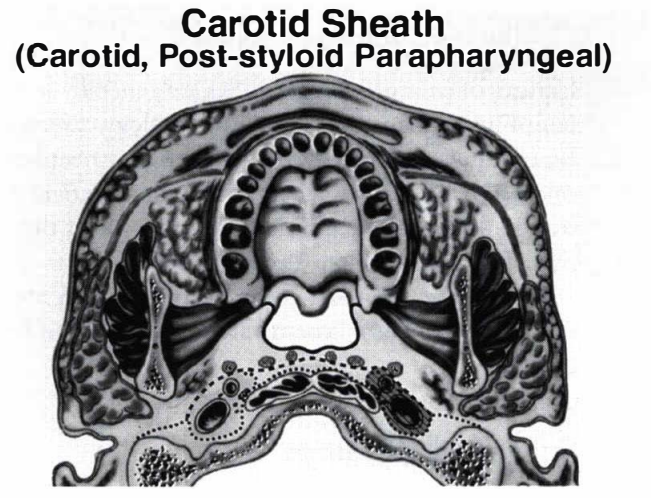

Figure VII-1. Schematic illustration deomonstrates the location of the "carotid space" ("carotid sheath", "poststyloid parapharyngeal space") (see Color Plate VII-1) (Figure reproduced with permission from Mukherji SK, Castillo M. A simplified approach to the spaces of the suprahyoid neck. Rad. Clin N Am *1998;36:761-780.)*

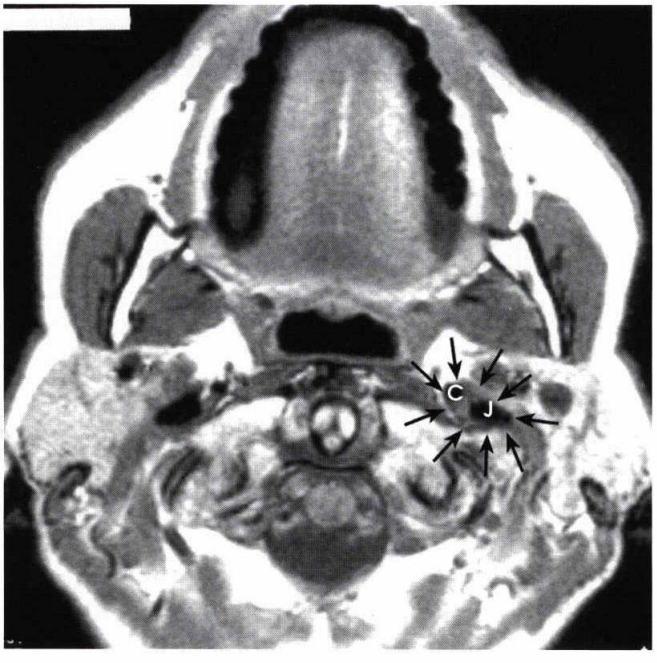

Figure VII-2. Axial noncontrast T1-weighted image demonstrates the location of the carotid space (small arrows). C, carotid artery; J, jugular vein.

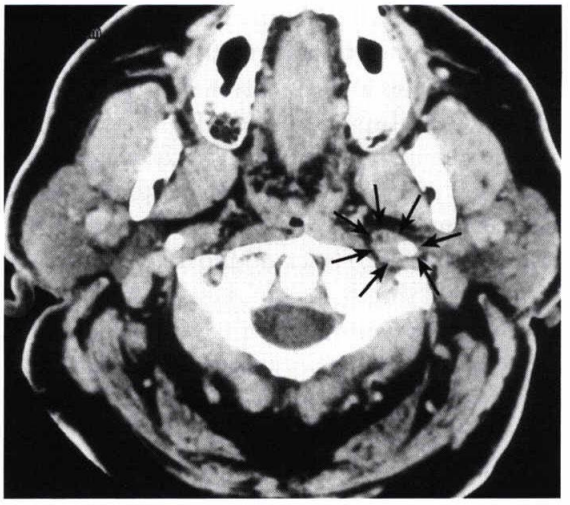

Figure VII-3. The arrows outline the margins of the carotid space on the axial contrast-enhanced CT.

trast-enhanced CT. Paragangliomas and neurogenic tumors may arise in similar locations. The presence of internal flow voids on MR imaging in a mass that is > 2 cm is suggestive of a paraganglioma rather than a schwannoma. Flow voids are not helpful in distinguishing between these two lesions when their mean diameter is < 2 cm.

Enlarged lymph nodes are the most common pathology of the CS. However, the imaging features of enlarged lymph nodes are generally nonspecific and are usually not helpful in attempting to identify the inciting etiology. Enlarged lymph nodes with areas of decreased central attenuation may be due to either neoplastic or inflammatory causes. Peripherally calcified lymph nodes may indicate that a patient has been exposed to silicosis or previously treated for lymphoma. Enlarged lymph nodes that appear very vascular or cystic are suggestive of metastases from thyroid carcinoma.

In children, the most common primary CS malignancy is neuroblastoma. The imaging findings of a neuroblastoma are nonspecific, and differentiating it from a sarcoma may be difficult.

Suggested Readings

1. Grodinsky M, Holyoke EA. The fasciae and fascial spaces of the head, neck and adjacent regions. *Am J Anat* 1938;63:367–408.
2. Harnsberger HR. *Handbook of Head and Neck Imaging*. 2nd ed. Chicago: Mosby; 1995.
3. Chong VFH, Fan YF. Radiology of the carotid space. *Clin Radiol* 1996;51:762–768.

Chapter 156

Normal Variants That May Mimic Disease

"Enlarged" Internal Jugular Veins

Asymmetry of the internal jugular vein is not uncommon. One vein may be considerably larger than the other but this finding is of no clinical significance (Fig. 156–1). It is usually detected incidentally but patients may present clinically as having a vague neck mass. The clinician may also feel a soft mass in the neck.

Contrast Layering in the Internal Jugular Vein

Occasionally, contrast may be seen layering in the dependent portion of the internal jugular vein (Fig. 156–1). This observation is of no clinical significance. It is not clear why layering should be present in an otherwise normal vein. Examination of the internal jugular vein fails to identify venous obstruction or possible causes of slow venous drainage.

Unopacified Facial Vein Mimicking Lymphadenopathy

Rapid image acquisition using spiral CT often takes place before the various vascular structures show contrast opacification. The unopacified facial vein may mimic cervical nodes in the segment just before draining into the internal jugular vein (Fig. 156–2). Awareness of this potential pitfall should prevent a misdiagnosis. The unopacified facial vein can be traced to the internal jugular vein.

Filling Defect in Internal Jugular Vein

Sometimes a filling defect may be encountered in the internal jugular vein mimicking a propagating thrombus or tumor invasion. The defect is due to unopacified or relatively unopacified blood from the facial vein flowing into the internal jugular vein (Fig. 156–2). The clue to the nature of the filling defect is identifying the facial vein. This can be done by tracing the retromandibular vein inferiorly. The retromandibular vein will join the facial vein and eventually drain into the internal jugular vein.

Medially Deviated Carotid Artery

Not infrequently, a tortuous carotid artery deviates medially and presents as a pulsatile submucosal lesion in the pyriform sinus (Fig. 156–3) or posterior pharyngeal wall. This is usually an incidental finding. However, patients may present with a vague history of throat discomfort. This normal variation is easily recognized on contrast-enhanced CT and is of no clinical significance. However, it should be recognized for what it is because a biopsy may result in catastrophic consequences.

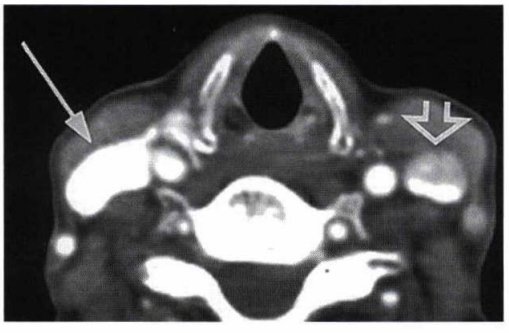

Figure 156–1. Axial contrast-enhanced CT shows asymmetry of the internal jugular veins. There is "enlargement" of the right internal jugular vein (straight arrow). Note the layering of contrast in the left internal jugular vein (hollow arrow).

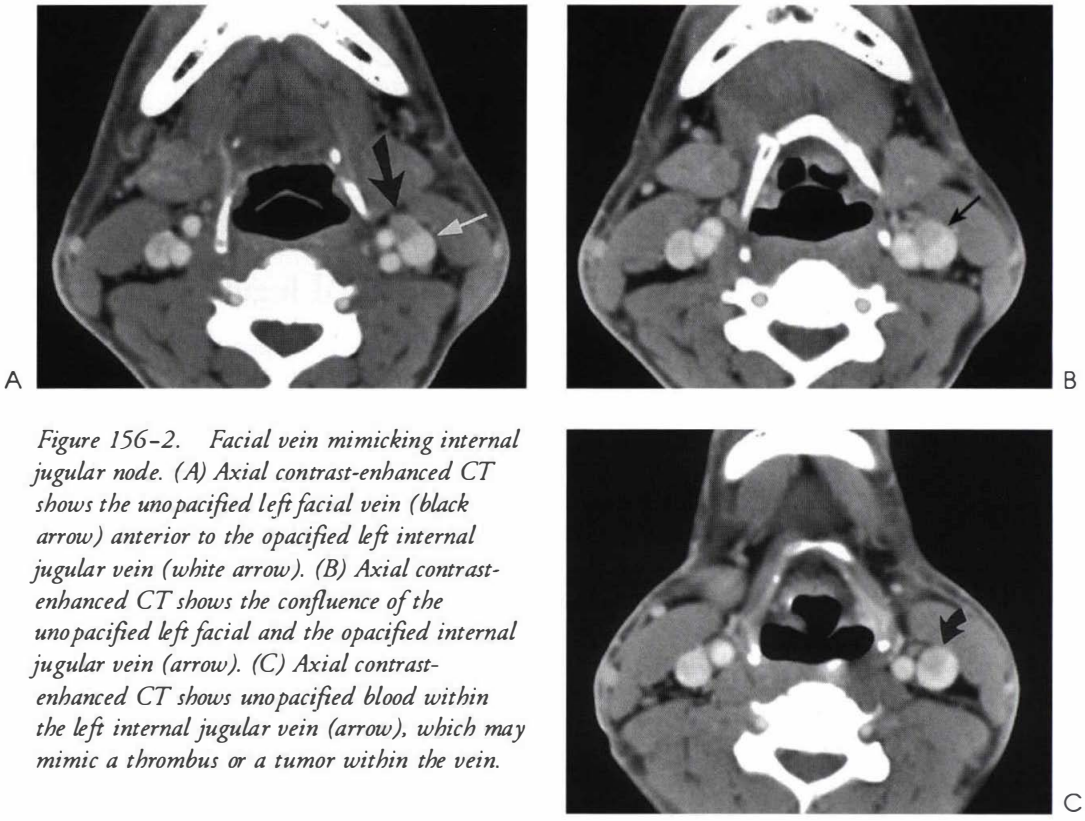

Figure 156–2. Facial vein mimicking internal jugular node. (A) Axial contrast-enhanced CT shows the unopacified left facial vein (black arrow) anterior to the opacified left internal jugular vein (white arrow). (B) Axial contrast-enhanced CT shows the confluence of the unopacified left facial and the opacified internal jugular vein (arrow). (C) Axial contrast-enhanced CT shows unopacified blood within the left internal jugular vein (arrow), which may mimic a thrombus or a tumor within the vein.

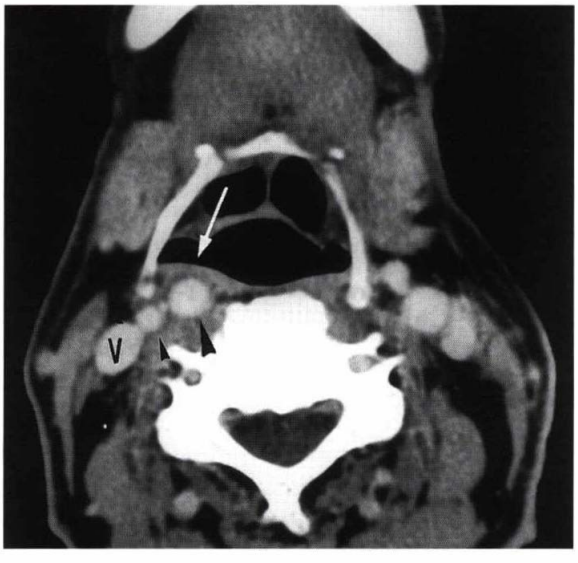

Figure 156–3. Medially deviated carotid artery. Axial contrast-enhanced CT shows the internal jugular vein (V) and internal (large arrowhead) and external (small arrowhead) carotid arteries (arrowheads) deforming the right pyriform sinus (white arrow).

Suggested Readings

1. Suprahyoid muscles. In: Banister RH et al, eds. *Gray's Anatomy.* 38th ed. Edinburgh: Churchill Livingstone; 1995:806–807.
2. Harnsberger HR. *Handbook of Head and Neck Imaging.* 2nd ed. St. Louis: Mosby; 1995:75–88.
3. Chong VFH, Fan YF. Radiology of the carotid space. *Clin Radiol* 1996; 51:762–768.

Chapter 157

Carotid Artery Dissection

Epidemiology

A dissection is hemorrhage into the arterial wall. The etiology may be either traumatic or spontaneous. Traumatic dissections result from either blunt or penetrating trauma. Spontaneous, or atraumatic, dissections typically result from prolonged or rapid head turning, flexion, or extension or after physical exertion or strenuous activity. The cervical segment just distal to the carotid bifurcation is the most common site of an internal carotid dissection. The most common intracranial site of a carotid artery dissection is the supraclinoid carotid artery. There is an increased association between systemic disorders that cause dysplasia of the vessel wall (such as fibromuscular dysplasia) and spontaneous carotid dissection.

Clinical Features

The most common symptoms are headache or neck pain. These complaints occur in about 75% of affected patients. Other symptoms include retroorbital headache and Horner's syndrome. Dissection is believed to cause between 2 and 3% of strokes in the general population and 5 to 20% of strokes in young patients.

Pathology

Bleeding into the arterial wall may be due to direct hemorrhage into the media from the vasa vasorum or secondary to an intimal tear. Hemorrhage into the media results in lumen narrowing whereas extension into the subadventitial plane may result in formation of a dissecting aneurysm. Intracranial dissection may result in subarachnoid hemorrhage.

Treatment

The treatment is usually conservative and consists of anticoagulation therapy. Resolution or significant improvement of stenosis is reported in about 80% patients who undergo follow-up angiography. Some authors suggest that traumatic dissections have a worse outcome.

Imaging Findings

Angiography

The most common finding is a smooth or mildly irregular tapered narrowing. This finding is present in about 65% of cases. The extent of luminal narrowing can range from mild to sever stenosis ("string sign"), to total occlusion. Other findings associated with dissection include pseudoaneurysm indicating a contained extravasation and identification of a double lumen. This latter finding is unusual in the carotid arteries (Fig. 157-1).

CT

There is an eccentric rim of low attenuation mural thickening that represents the hematoma. There may be an enhancing rim surrounding the hematoma that represents the enhancing vasa vasorum.

MR

Cross-sectional imaging demonstrates an eccentric periarterial rim of hemorrhage that narrows the luminal flow void. This rim of hematoma typically has increased T1 signal indicating the presence of methemoglobin. The T2 signal is also usually increased. MRA shows narrowing of the vessel lumen (Fig. 157-2).

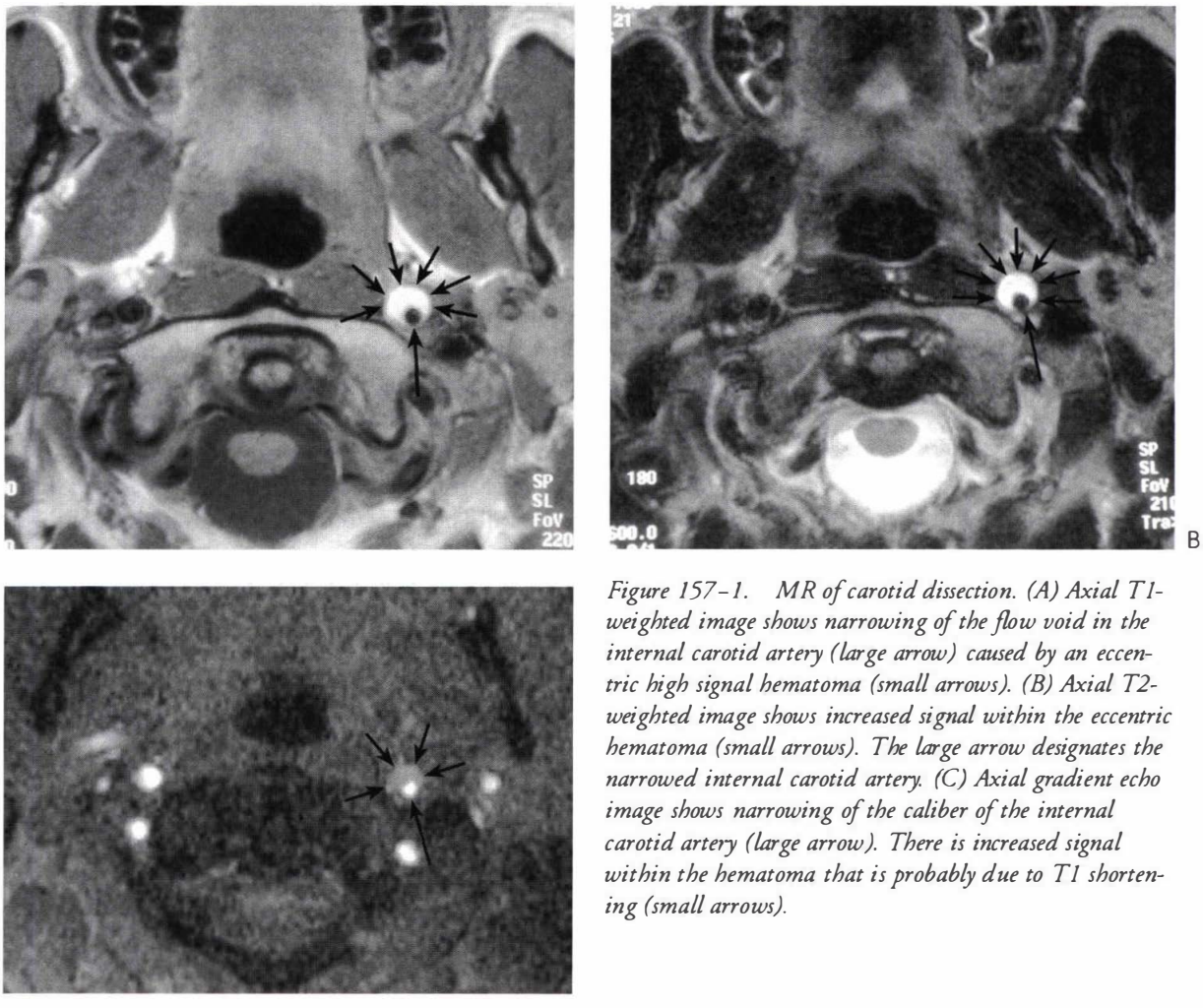

Figure 157–1. MR of carotid dissection. (A) Axial T1-weighted image shows narrowing of the flow void in the internal carotid artery (large arrow) caused by an eccentric high signal hematoma (small arrows). (B) Axial T2-weighted image shows increased signal within the eccentric hematoma (small arrows). The large arrow designates the narrowed internal carotid artery. (C) Axial gradient echo image shows narrowing of the caliber of the internal carotid artery (large arrow). There is increased signal within the hematoma that is probably due to T1 shortening (small arrows).

Figure 157–2. Selective injection of the internal carotid artery performed in the same patient illustrated in Figure 157–1 shows narrowing of the carotid artery (small arrows) due to the eccentric hematoma and an associated pseudoaneurysm (large arrow). No intimal flap is identified, which is common for internal carotid dissections.

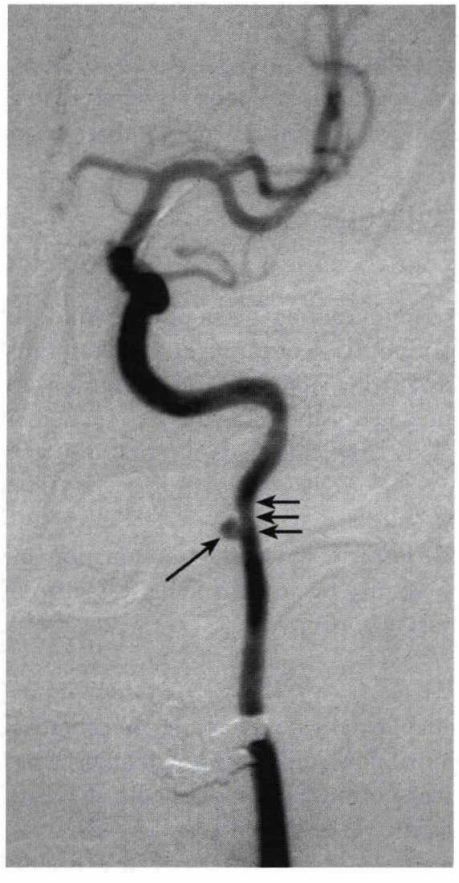

US

The most specific sign is identification of an echogenic flap. However, this is present in a minority of cases. Other findings include echogenic thrombus, smooth tapering of the arterial wall, and visualization of both the true and the false lumen.

Imaging Pearl

- Identification of the "double-lumen" sign in carotid dissection is unusual for dissections in the extracranial carotid artery. The most common finding on MRA is narrowing of the internal carotid artery that may be nonspecific. Noncontrast axial T1- and T2-weighted images confirm the diagnosis of carotid dissection by identifying the periarterial hemorrhage.

Suggested Readings

1. Provenzale JM. Dissection of the internal carotid and vertebral arteries: imaging features. *AJR Am J Roentgenol* 1995;165:1099–1104.
2. Hart RG, Esaton JD. Dissections of cervical and cerebral arteries. *Neurol Clin North Am* 1983;1:255–282.
3. Bui LN, Brandt-Zawadzki MN, Verghese P, Gillan G. Magnetic resonance angiography of cervicocranial dissection. *Stroke* 1993;24:126–131.

Chapter 158

Thrombosed Internal Jugular Vein

Epidemiology

In contrast to venous thrombosis in the lower limbs, thrombosis of the internal jugular vein is uncommon. This entity is usually seen in patients with a history of central venous line insertion, drug abuse, neck infection, previous neck irradiation, and systemic disease such as sepsis or malignancy.

Clinical Findings

Patients usually have an underlying disease. They may be asymptomatic or have neck swelling. The thrombus may become infected and result in a thrombophlebitis. These patients present with pain, tenderness, erythema, and sometimes fever. On palpation, the thrombosed vein resembles a thick tubular structure. In the chronic phase, the thrombosed vein resembles a hard cord.

Pathology

In the neck, an indwelling catheter may cause damage to the vessel wall thus inducing platelet aggregation. Strands of fibrin are deposited trapping both red and white blood cells. Thrombosis may proceed to total internal jugular vein thrombosis. The thrombus thus formed is usually very adherent to the inflamed vessel wall. There is therefore a very low risk of thromboembolism. However, thrombosis induced by bacterial infection is prone to disintegrate, resulting in septic thromboembolism

Treatment

Treatment is directed at removing the underlying cause of the thrombosis. Sepsis should be treated and the indwelling catheter, if present, removed. Anticoagulation therapy may also be started depending on the cause of thrombosis.

Imaging Findings

US

Duplex Doppler will demonstrate loss of the normal venous waveform of the internal jugular vein. Color flow Doppler demonstrates absence of the normal venous flow.

CT

A normal contrast-filled internal jugular vein cannot be identified. There is instead, an enlarged internal jugular vein with a filling defect. A rim of enhancing vessel wall is frequently demonstrated (Figs. 158–1 and 158–2).

MR

On T1-weighted images, a thrombus replaces the normal flow void. The signal intensity depends on the age of the lesion and is often composed of both low and high signal intensities. Following contrast injection, there is a rim of enhancement along the vessel wall. T2-weighted images will show heterogeneous high and low signals.

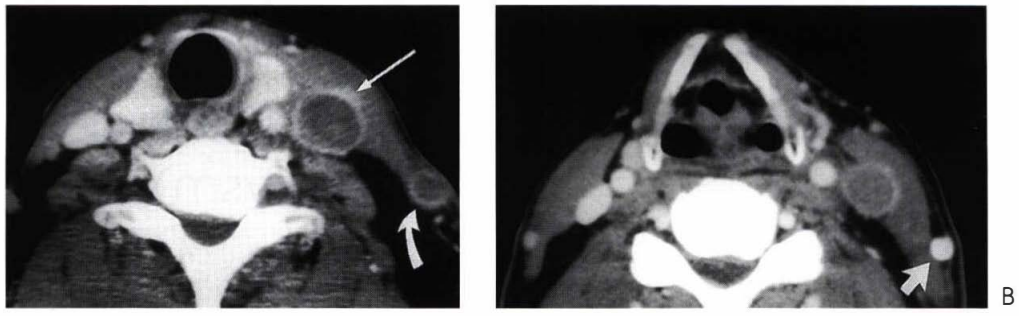

Figure 158-1. Thrombosis of the infrahyoid internal and external jugular veins. (A) Axial contrast-enhanced CT shows a distended left internal jugular vein with a nonopacified thrombus-filled lumen and vessel wall enhancement (straight arrow). Note also the thrombosed external jugular vein (curved arrow). (B) Axial contrast-enhanced CT [superior to (A)] shows a distended but densely contrast-filled external jugular vein (arrow).

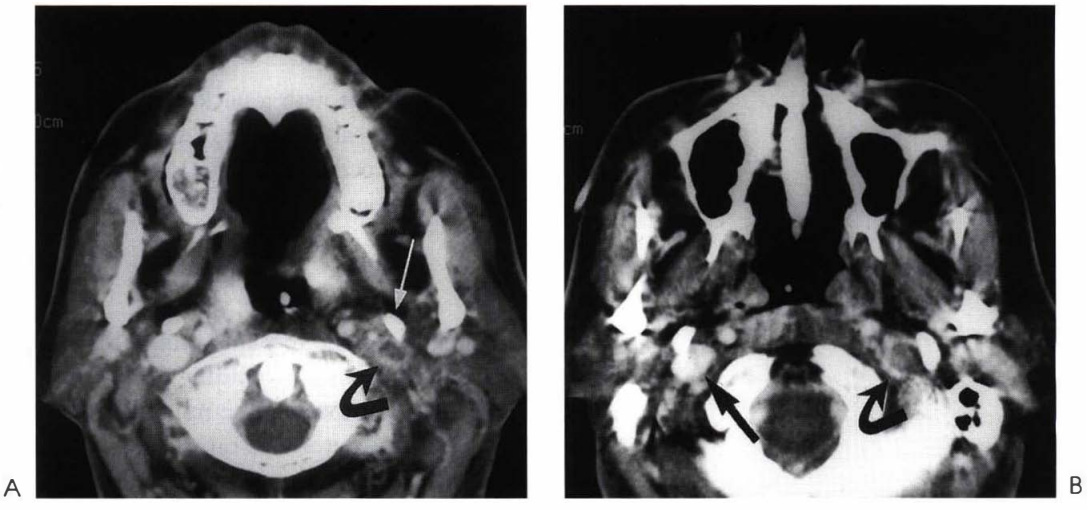

Figure 158-2. Thrombosis of suprahyoid internal jugular vein. (A) Axial contrast-enhanced CT shows a thrombosed left internal jugular vein (curve arrow) posterior to the styloid process (straight arrow). (B) Axial contrast-enhanced CT shows internal jugular vein thrombosis at the level of the skull base (curve arrow). Compare with the normal right internal jugular vein (straight arrow).

Imaging Pearls

- On CT, a thrombosed jugular vein may be confused with a necrotic lymph node or an abscess. The key to differentiating features is obtained by examining contiguous sections. Thrombosis is evident when contiguous sections show the lesion to be tubular.
- The jugular vein may not be seen in patients with nodal metastases. Often the lack of visualization is due to compression of the adjacent vein rather than thrombosis.
- A thin rim of enhancement around the jugular vein strongly suggests thrombosis.
- Turbulent or slow flow in the jugular vein at the jugular bulb or in the neck can be confused with thrombosis on MR imaging. The presence of blood products or marked enhancement following contrast indicates thrombosis. Magnetic resonance venography can help differentiate turbulent flow from thrombosis.

Suggested Readings

1. Walter JB, Israel MS. Thrombosis and its occurrence in the venous system. In: *General Pathology.* Edinburgh: Churchill Livingstone; 1988;522–529.
2. Chong VFH, Mukherji SK, Goh CHK. The suprahyoid neck: normal and pathological anatomy. *J Laryngol Otol* 1999;113:501–508.
3. Harnsberger HR. *Handbook of Head and Neck Imaging.* 2nd ed. St. Louis: Mosby; 1995:75–88.

Chapter 159

Trauma (Pseudoaneurysm (Dissecting Aneurysm) and Hematoma)

Epidemiology

False aneurysm of the carotid artery may be due to penetrating trauma. However, the most common cause is related to previous carotid artery surgery; for instance, following endarterectomy for atherosclerosis. Rarely, needle biopsies of neck masses may result in the formation of false aneurysms.

Clinical Findings

Patients usually present with a neck mass following prior neck surgery or biopsy. Physical examination may reveal evidence of surgical scars or skin changes due to biopsy. Pseudoaneurysms may also occur as a complication of peritonsillar abscess, cervical adenitis, or infection of the adjacent soft tissues. The mass may be pulsatile.

Pathology

Pseudoaneurysms are due to penetrating or surgical injury to the arterial wall resulting in leakage of blood into the surrounding neck tissues. False aneurysms can expand, spontaneously thrombose, or rupture. The resultant hematoma associated with the false aneurysm can surround and compress the carotid artery or internal jugular vein. Injury to the vagus nerve is unusual and distal embolization is rare.

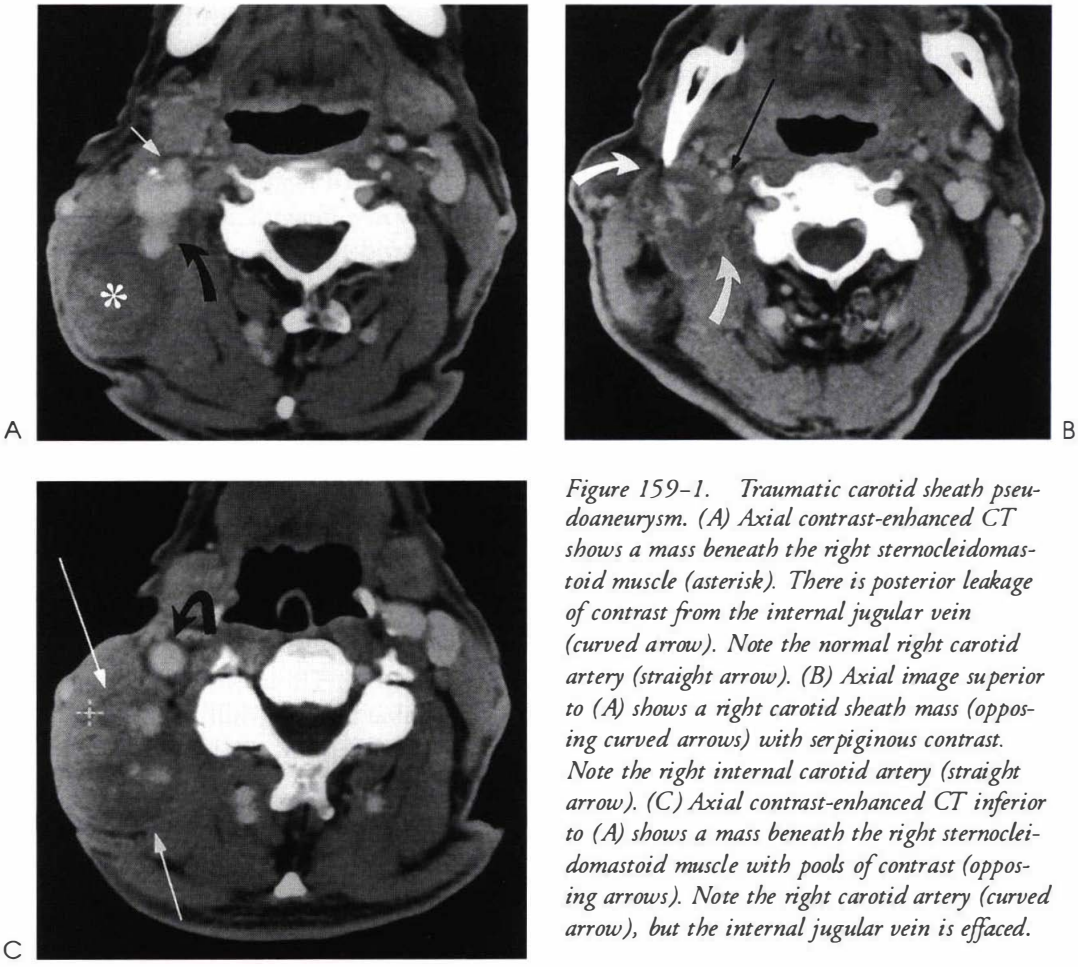

Figure 159–1. Traumatic carotid sheath pseudoaneurysm. (A) Axial contrast-enhanced CT shows a mass beneath the right sternocleidomastoid muscle (asterisk). There is posterior leakage of contrast from the internal jugular vein (curved arrow). Note the normal right carotid artery (straight arrow). (B) Axial image superior to (A) shows a right carotid sheath mass (opposing curved arrows) with serpiginous contrast. Note the right internal carotid artery (straight arrow). (C) Axial contrast-enhanced CT inferior to (A) shows a mass beneath the right sternocleidomastoid muscle with pools of contrast (opposing arrows). Note the right carotid artery (curved arrow), but the internal jugular vein is effaced.

Treatment

Treatment depends on the size of the pseudoaneurysm or degree of arterial leakage. For instance, very small pseudoaneurysms can be managed conservatively. In contrast, an enlarging pseudoaneurysm or a symptomatic mass should be treated surgically. Endovascular stenting is becoming a more accepted method of treatment.

Imaging Findings

CT

A mass corresponding to the site of previous surgery or penetrating injury is evident. This lesion usually shows a mixed pattern of both high and intermediate attenuation reflecting the evolving age of the hematoma or thrombus on noncontrast CT. Peripheral calcification may be present in some lesions. There is intense enhancement of the lumen following contrast administration. The internal jugular vein may be effaced as a result of the pressure effect of the expanding mass lesion (Fig. 159–1).

MR

The MR appearance of a false aneurysm is similar to a combination of subacute and chronic hematoma. The mass shows a mixture of high and low signals reflecting the various stages of hemoglobin breakdown. Flow sensitive sequences or magnetic resonance angiography can be helpful in confirming the diagnosis.

Imaging Pearl

- In the presence of an appropriate history, the diagnosis of a pseudoaneurysm poses little difficulty. The issue to be settled is whether there is an arteriovenous fistula (AVF). An AVF is readily diagnosed clinically by the presence of a bruise. The internal jugular vein will show dilatation or increased flow both clinically and radiologically. In contrast, a pseudoaneurysm, if large enough, typically effaces the internal jugular vein.

Suggested Readings

1. More WS, William JQB. Carotid artery. In: More WS, ed. *Vascular Surgery.* 3rd ed. Philadelphia: Saunders; 199:434–472.
2. Harnsberger HR. *Handbook of Head and Neck Imaging.* 2nd ed. St. Louis: Mosby; 1995:75–88.

Chapter 160

Enlarged Cervical Lymph Nodes in Patients with Acquired Immunodeficiency Syndrome

Epidemiology

Acquired immunodeficiency syndrome (AIDS) is associated with a defect in cell-mediated immunity. AIDS appears to result in a decline in helper-inducer CD4 T lymphocytes. Reduced CD4 counts are associated with progressive symptoms. AIDS is associated with an increase in number and size of cervical lymph nodes. This is one of the most common head and neck manifestations and has been reported to be an initial finding in up to 75% of symptomatic patients. The cervical lymph nodes are often the first group of lymph nodes involved in what has been termed progressive generalized lymphadenopathy. Cervical adenopathy in patients positive for human immunodeficiency virus (HIV+ patients) is associated with lower CD4 counts compared with HIV+ patients without cervical lymphadenopathy.

Clinical Features

There are a variety of clinical findings in the extracranial head and neck with which HIV+ patients may present. These include multiple enlarged cervical lymph nodes, parotid masses, and upper respiratory complaints.

Pathology

The histologic findings of tissue biopsies of enlarged lymph nodes are nonspecific. These findings include follicular hyperplasia and an increased number of lymph follicles. In more advanced disease, the findings are more suggestive of HIV infection and include follicular

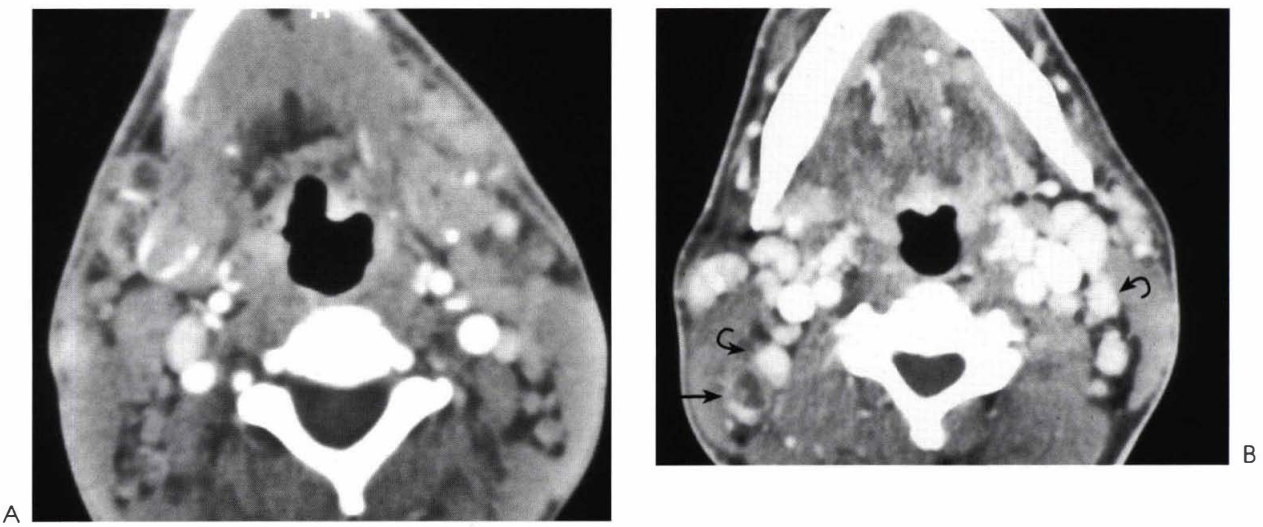

Figure 160-1. (A) Axial contrast-enhanced CT shows multiple lymph nodes, some of which are enlarged, situated at levels I and II in two HIV+ patients. There are some level I nodes that are low attenuation. Note the variable enhancement of the lymph nodes. Some nodes are hypervascular (curved arrows) and some have decreased attenuation (straight arrow). (B) These findings are nonspecific and could be due to a variety of systemic disorders that cause an increase in the number and size of cervical lymph nodes.

involution and lymphocyte depletion.

Treatment

There is no specific treatment directed toward the cervical nodal enlargement in HIV+ patients. The treatment is aimed at controlling or curing the disease itself.

Imaging Findings

CT

Cervical nodal involvement in HIV+ patients is characterized by an increase in both the number and the size of the lymph nodes. The majority of the cervical lymph nodes are typically < 2 cm in greatest axial dimension. The nodes are homogeneous and lack low attenuation centers or extracapsular penetration. Associated findings that suggest HIV disease include enlarged nasopharyngeal adenoidal tissue and parotid cysts (Fig. 160-1).

MR

The imaging findings of the lymphadenopathy are nonspecific. The nodes have intermediate T1 signal and moderately increased T2 signal. These nodes homogeneously enhance following contrast administration.

Imaging Pearls

- The imaging findings of persistent generalized lymphadenopathy in the neck are nonspecific. Other disorders that have an increased risk of involving the cervical nodes in HIV+ patients include infections (bacterial, mycobacterial, fungal) and various neoplasms (lymphoma, squamous cell carcinoma, and Kaposi's and other sarcomas). However, routine biopsy of enlarged lymph nodes in AIDS patients is not recommended because only between 3 and 15% of patients have significant findings that indicate an opportunistic infection or neoplasm.
- The diagnosis of persistent generalized lymphadenopathy can be suggested by identifying multiple homogeneous lymph nodes < 2 cm diameter without central areas of decreased attenuation or extracapsular penetration.
- Very large homogeneous cervical lymph nodes should suggest the diagnosis of lymphoma.
- The "triad" of head and neck abnormalities that suggest HIV+ disease includes cervical lymphadenopathy, enlarged adenoidal tissue, and lymphoepithelial cysts in the parotid glands.

Suggested Readings

1. Chakeres DW, Zawodniak LJ, Bornstein RA, McGhee RB, Whitacre CC. MR of head and neck adenopathy in asymptomatic HIV-seropositive men. *AJNR Am J Neuroradiol* 1993;14:1367-1371.
2. Rosenberg RA, Schneider KL, Cohen NL. Head and neck presentations of acquired immunodeficiency syndrome. *Otolaryngol Head Neck Surg* 1985;93:700-704.
3. Olsen WL, Jeffrey RB, Sooy CD, Lynch MA, Dillon WP. Lesions of the head and neck in patients with AIDS: CT and MR findings. *AJR Am J Roentgenol* 1988;151:785-790.

Chapter 161

Cat Scratch Disease

Epidemiology

Cat scratch disease is a benign, self-limited disease caused by the bacterium *Bartonella henselae*. This organism is typically present in the saliva of a normally healthy kitten and may be transferred by a lick, scratch, or bite. It is important to note that a history of a cat scratch is not necessary to make the diagnosis. The disease is most common in children and is most prevalent in regions with a warm and humid climate.

Clinical Features

The initial symptoms usually develop 6 to 8 weeks after initial exposure. The disease often initially presents as a reddish-brown papule at the site of contact. The patients typically develop fever, fatigue, malaise, and myalgias accompanied by characteristic tender regional lymphadenopathy (Fig. 161-1). The lymph nodes gradually enlarge and reach a maximal size over 2 to 3 weeks. Approximately 10% of patients develop overlying erythema and fluctuant lymph nodes that require drainage.

Pathology

Bartonella henselae is a gram-negative, agyophilic, non-acid fast, pleomorphic bacilli. The diagnosis is confirmed using immunofluorescent antibody, PCR or ELISA serology. Pathologic findings from biopsied lymph nodes reveal granulomatous changes.

Treatment

This is typically a self-limited disease in most patients and no antiobiotic treatment is required. Infection appears to confer lifetime immunity because reports of recurrences are rare. Antibiotics such as erythromycin, azithromycin, and gentamicin may be required in more serious cases.

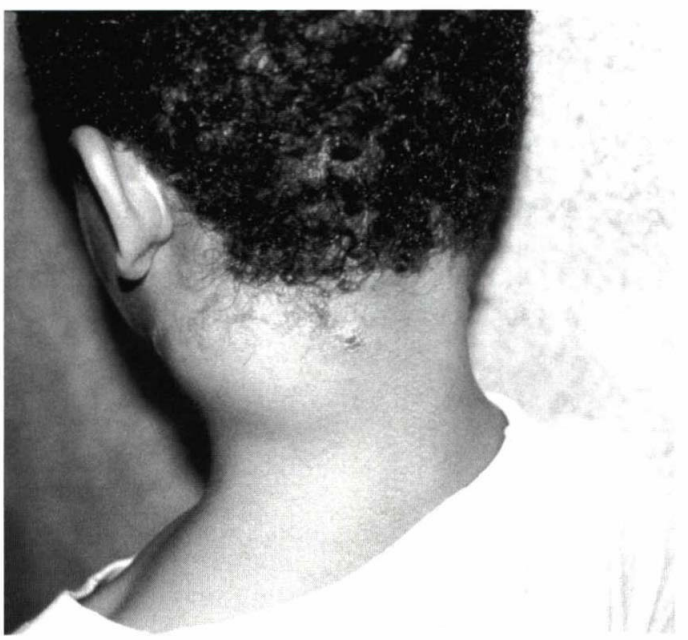

Figure 161-1. Clinical example of a patient with cat scratch disease.

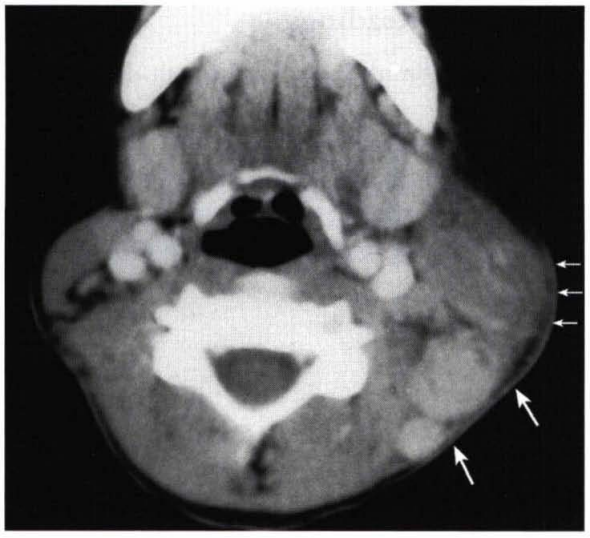

Figure 161–2. Axial contrast-enhanced CT shows enlarged level II and V lymph nodes in a patient with pathologically proven cat scratch disease (large arrows). Note the reticulation of the subcutaneous fat suggestive of an inflammatory process (small arrows).

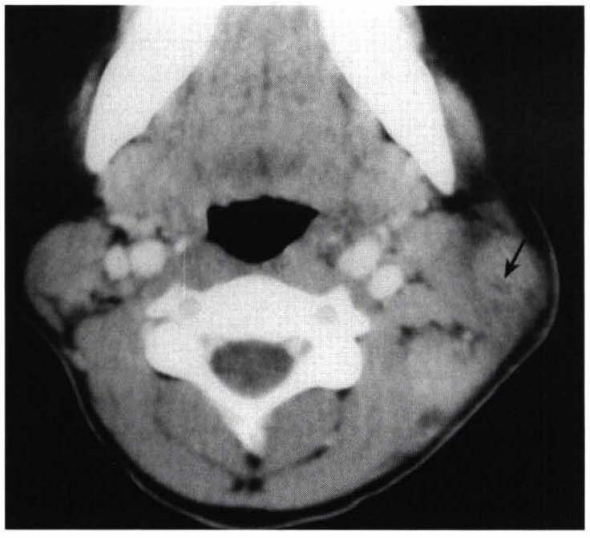

Figure 161–3. Axial contrast-enhanced CT shows multiple enlarged nodes. Note the small area of decreased attenuation in the enlarged level II node (arrow).

Imaging Findings

CT

The typical findings are a unilateral clumped group of enlarged lymph nodes clustered in the primary echelon drainage of the site of contact (Fig. 161–2). Central areas of decreased attenuation within the lymph nodes are rare. There may be some subtle reticulation of the fat surrounding the lymph nodes (Fig. 161–3); however, gross findings of extracapsular extension are rare.

MR

The signal characteristics are nonspecific and can be seen in a variety of disorders. The nodes typically enhance with contrast and contain high T2 signal.

Imaging Pearls

- The imaging findings are nonspecific. The differential diagnosis includes viral adenitis and lymphoma.
- The diagnosis of cat scratch disease can be suggested by the presence of a unilateral group of clustered enlarged lymph nodes in a child who has a cat in the house.

Suggested Readings

1. Spires JR, Smith RJH. Cat scratch disease. *Otolaryngol Head Neck Surg* 1986;94:622–627.
2. Bass JW, Vincent JM, Person DA. The expanding spectrum of bartonella infections, II: Cat scratch disease. *Pediat Infect Dis J* 1997;16:163–179.
3. Adal KA, Cockerell CJ, Petri WA. Cat scratch disease, bacillary angiomatosis and other infections due to rochalimes. *N Engl J Med* 1994;330:1509–1515.

Chapter 162

Tuberculous Lymphadenitis

Epidemiology

There is a dramatic rise in the prevalence of tuberculosis in industrialized countries due to the acquired immunodeficiency syndrome (AIDS) epidemic, drug abuse, and increased migration. The most common form of head and neck tuberculosis is lymphadenitis. This form of tuberculosis represents 15% of cases of extrapulmonary disease and 1 to 2% of all new cases of tuberculosis.

Clinical Findings

Cervical lymphadenopathy is usually painless. Involvement is commonly bilateral and most frequently involves the internal jugular, posterior triangle, and supraclavicular nodes. In advanced stages, the overlying skin may be inflamed and sinus tracts may appear. Systemic symptoms are not common in tuberculosis confined to cervical nodes. When tuberculosis is suspected, a chest radiograph should be obtained because 40 to 70% of patients have signs of active or healed pulmonary tuberculosis. Skin tests and sputum examination should also be performed. Nodal biopsy may be necessary to confirm diagnosis if these tests appear equivocal.

Pathology

Tuberculosis typically shows tubercles with marked fibroplastic response. These tubercles show characteristic amorphous caseating necrosis surrounded by epithelioid and Langerhans' giant cells. Caseating lymph nodes may rupture into surrounding structures such as the airway and bloodstream causing endobronchial or hematogenous dissemination.

Treatment

Tuberculosis is treated with specific antituberculosis chemotherapy (using various combinations of ethambutol, ethionamide, isoniazid, rifampicin, and streptomycin). In general, head and neck tuberculosis responds well to standard chemotherapeutic agents and heals without leaving behind much residual changes. Large lesions, however, show areas of fibrosis. These areas may in due course show dystrophic calcifications.

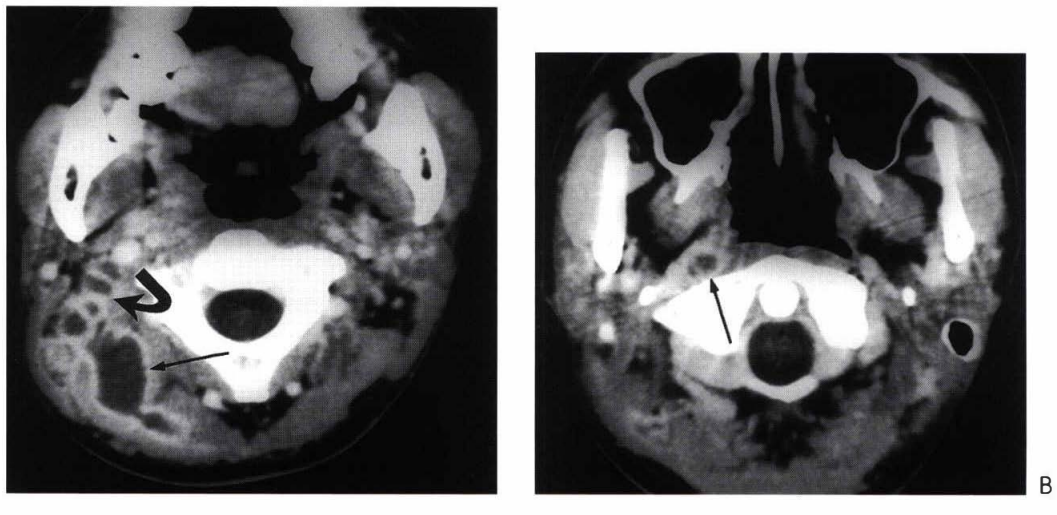

Figure 162-1. Tuberculous lymphadenitis. (A) Axial contrast-enhanced CT shows multiple necrotic right cervical lymphadenopathy (curved arrow). There is also extranodal tuberculous extension with abscess formation demonstrates rim enhancement (arrow). (B) Axial enhanced CT shows necrotic right retropharyngeal lymphadenopathy (arrow).

Imaging Findings

CT

In the early stages of tuberculous lymphadenitis, the nodes show homogeneous contrast enhancement. As the disease evolves, central necrosis can be detected as foci of low density associated with rim enhancement (Fig. 162–1). Healed lesions and nodes undergoing chemotherapy may show calcifications.

MR

MR imaging shows nonspecific homogeneous enhancement on T1-weighted images and high signals on T2-weighted images. In nodes undergoing necrosis contrast-enhanced MR imaging shows rim enhancement with a central area of no enhancement representing caseating necrosis. These nodes typically show high signal intensity on T2-weighted images. MR imaging, though helpful in demonstrating lymphadenitis, cannot detect nodal calcifications.

Imaging Pearls

- The diagnosis of tuberculous lymphadenitis calls for a high index of clinical suspicion in patients belonging to high-risk groups such as patients with AIDS or recent immigrants from regions showing high disease prevalence.
- Cervical tuberculous lymphadenitis is frequently associated with pulmonary tuberculosis. Hence patients with pulmonary disease and cervical lymphadenopathy should give rise to a suspicion of tuberculosis.

Suggested Readings

1. Moon WK, Han MH, Chang KH, et al. CT and MR imaging of head and neck tuberculosis. *Radiographics* 1997;17:391–402.
2. Lee Y, Park KS, Chung SY. Cervical tuberculous lymphadenitis: CT findings. *J Comput Assist Tomogr* 1994;18:370–375.
3. Hopewell PC. A clinical review of tuberculosis. *Radiol Clin North Am* 1995;33:641–653.

Chapter 163

Carotidynia

Epidemiology

Carotidynia is an idiopathic syndrome consisting of neck pain associated with tenderness to palpation over the region of the carotid bifurcation. There is no reported incidence or gender predilection, given that the mere existence of this "disease" is controversial. However, the trend is to consider carotidynia a diagnosis of exclusion that represents an idiopathic "organic" disease of the carotid artery. In general, the disease appears to involve patients between the third and sixth decade of life. To make the diagnosis in a patient with characteristic symptoms and findings, one must exclude other disorders that can give a similar presentation, including metastatic squamous cell carcinoma, lymphoma, giant cell arteritis, atherosclerosis, thrombosis, intraluminal hemorrhage, fibromuscular dysplasia, aneurysm, and dissection.

Pathology

No pathological studies of carotidynia have been performed due to the benign course of the disease and the risks associated with biopsy of the carotid. Carotidynia is thought to be inflammatory in nature and may involve the adventitial layer of the wall of the carotid artery.

Clinical Findings

The clinical diagnosis based on the International Headache Society (1988) criteria includes the following points:

1. At least one of the following overlying the carotid artery
   a. Tenderness
   b. Swelling
   c. Increased pulsations
2. Appropriate investigations not revealing structural abnormality
3. Pain over the affected side of the neck; may project to the ipsilateral side of the head
4. A self-limiting syndrome of < 2 weeks' duration

Treatment

This is a self-limited disease that characteristically lasts for < 2 weeks. The pain associated with carotidynia typically responds promptly to nonsteroidal antiinflammatory medications or a short course of corticosteroids.

Imaging Findings

CT

There is intermediate soft tissue thickening of the wall of the carotid artery which does not narrow the lumen (Figs. 163-1 and 163-2). The most common location is at the level of the carotid bifurcation. There is minimal contrast enhancement.

MR

There is increased soft tissue surrounding the carotid artery that is indistinguishable from the wall of the artery (Fig. 163-3). The soft tissue is intermediate signal on T1-weighted images and densely enhances following contrast administration. The tissue may be slightly increased signal on T2-weighted images.

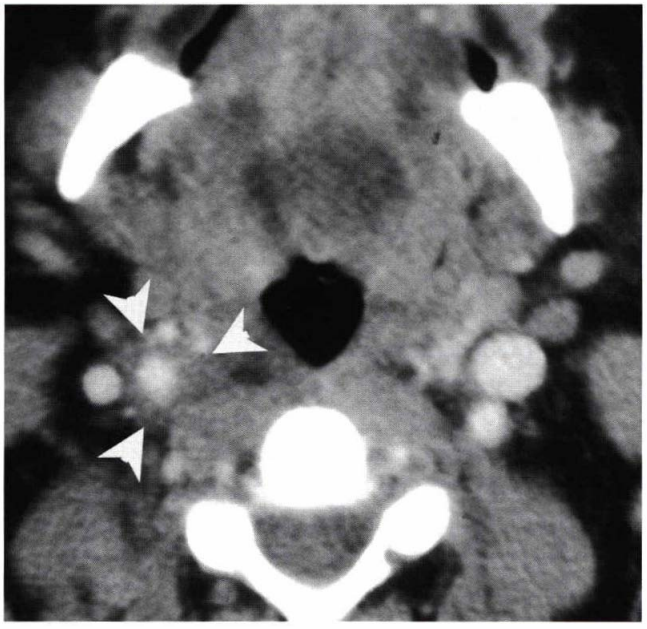

Figure 163–1. Axial contrast-enhanced CT performed in a patient with palpable right neck pain demonstrates a ring of intermediate soft tissue surrounding the internal carotid artery (arrowheads). A thorough investigation revealed no evidence of neoplasm of systemic disease. The findings were believed to be due to carotidynia.

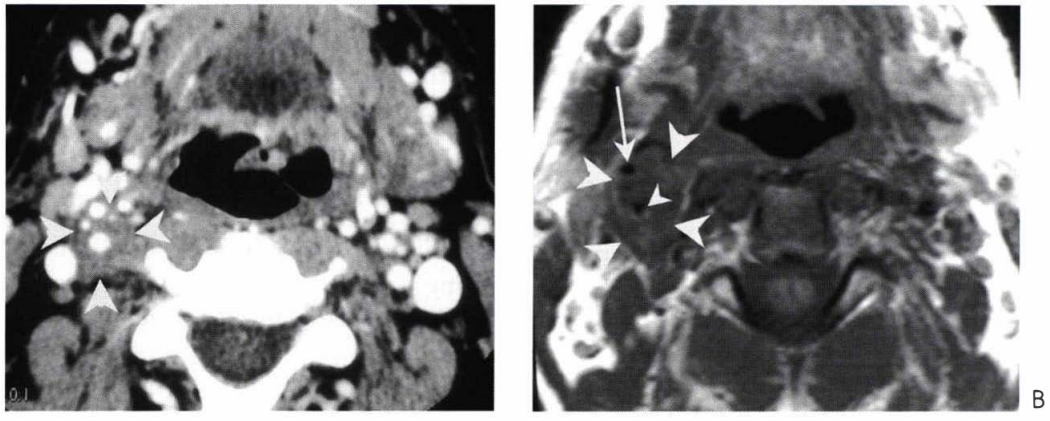

Figure 163–2. (A) Axial contrast-enhanced CT performed in another patient with presumed carotidynia demonstrates circumferential soft tissue surrounding both the internal and external carotid artery (arrowheads). (B) Axial noncontrast T1-weighted image obtained in the same patient shows the mass to contain intermediate signal (large arrowheads). Note the flow voids of the internal (small arrowhead) and external (arrow) carotid arteries.

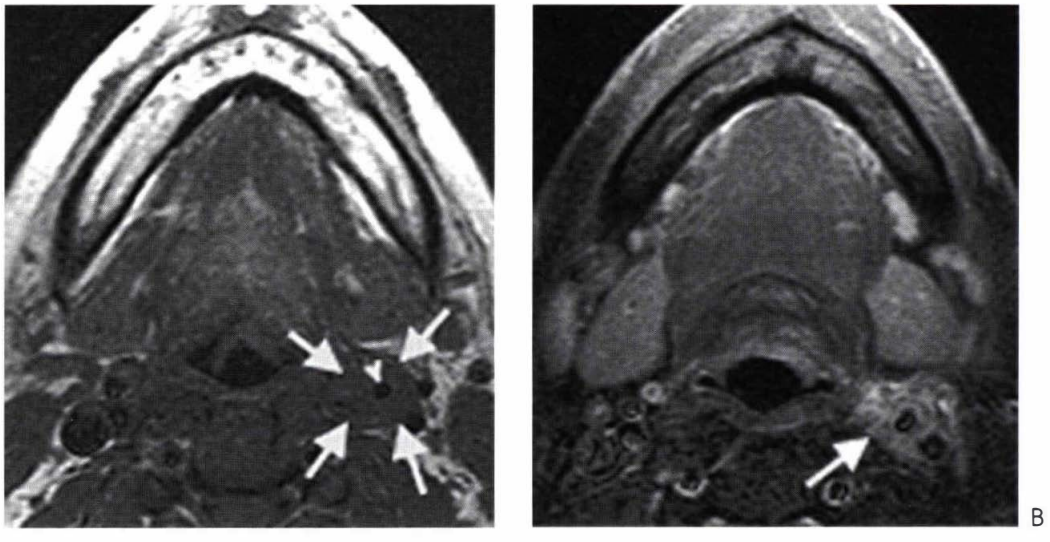

Figure 163–3. (A) Axial noncontrast-enhanced T1-weighted MR demonstrates an intermediate signal mass (arrows) surrounding the left internal carotid artery (arrowhead). (B) Axial fat-suppressed, contrast-enhanced T1-weighted image demonstrates diffuse enhancement of the mass (arrow). The patient had no primary tumor and had a classic presentation of carotidynia. Based on the clinical presentation and characteristic imaging findings, the patient was treated with antiinflammatory medications and improved.

Imaging Pearl

- The diagnosis can be suggested by the presence of a diffusely thickened carotid wall at the level of the carotid bifurcation. However, other disorders that can mimic these findings must be excluded.

Suggested Readings

1. Burton BS, Syms MJ, Petermann GW, Burgess LPA. MR imaging of patients with carotidynia. *AJNR Am J Neuoradiol* 2000;21:766–769.
2. Headache Classification Committee of the International Headache Society. Classification and diagnosis criteria for headache disorders, cranial neuralgias, and facial pain. *Cephalgia* 1988;8(suppl 7):48–49.
3. Emmanuelli JL, Gutierrez JR, Chiossone JA, Chiossone E. Carotidynia: a frequently overlooked or misdiagnosed syndrome. *Ear Nose Throat J* 1998;77:462–469.

Chapter 164

Metastatic Cervical Lymphadenopathy

Epidemiology

Cervical nodal metastasis is extremely common. Most head and neck tumors spread to the neck nodes as part of their natural history. For instance, depending on the primary site, up to 80% of patients with upper aerodigestive mucosal malignancy will have cervical nodal metastasis at presentation. The presence of cervical lymphadenopathy is noted to reduce the long-term survival rate by 50%.

Classification of Cervical Nodes

The traditional terminology of cervical nodes is based on the description by the French anatomist, Rouvière. This system refers to the classical surface triangles of the neck. The orientation of these triangles makes them rather unsuitable for description in axial images. In recent years, the simpler numerical system (Table 164–1; Fig. 164–4) became the dominant nomenclature. The retropharyngeal, parotid, and facial groups are not included in this classification. Under this system, a radiologist can assign a numerical level for nodal involvement and when the retropharyngeal, parotid, or facial nodes are involved they should be reported as such. In 1997 the International Union against Cancer and the American Joint Committee on Cancer (AJCC) introduced a new group of nodes to specifically address the importance of supraclavicular nodal metastasis in nasopharyngeal carcinoma. These nodes represent the lower level IV and V nodes.

Pathology

Carcinomas show a high tendency to infiltrate local lymphatics at an early stage. Groups of tumor cells within the infiltrated lymphatics may embolize to the regional lymph nodes (Figs. 164–1 and 164–2). It takes about 1 billion malignant cells to form a mass of 1 mm^3. Such lesions are difficult to see with the naked eye, let alone on CT or MR imaging (Fig. 164–3). The embolized malignant cells initially lodge in the subcapsular sinuses. If they survive they will eventually replace the lymph node. This may lead to extracapsular spread or further extension to the next group of lymph nodes via the efferent lymphatics.

Clinical Findings

Patients with cervical lymphadenopathy may present in several ways. First, the initial presentation is that of the primary disease wherein cervical lymphadenopathy is detected during physical or radiological assessment. Second, patients may present with hard neck masses and the primary malignant lesion is found during further evaluation. Third, in 2 to 3% of all patients with head and neck cancer who present with cervical lymphadenopathy, the primary tumor was never found.

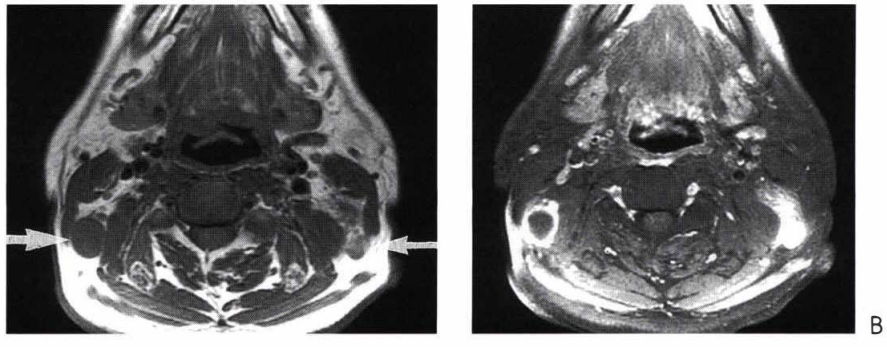

Figure 164–1. Cervical lymphadenopathy with nodal necrosis. (A) Axial T1-weighted MR image shows a well demarcated right cervical node (large arrow). There are also nodes on the contralateral side (small arrow). (B) Axial contrast-enhanced MR image shows right cervical node demonstrating rim enhancement and necrotic center. Note the intense enhancement on the contralateral side.

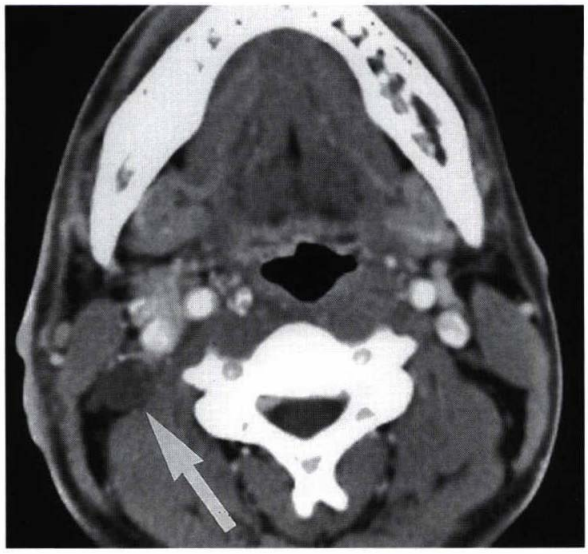

Figure 164–2. Cystic metastasis from thyroid carcinoma. Axial contrast-enhanced CT shows an almost entirely cystic right level II node (arrow).

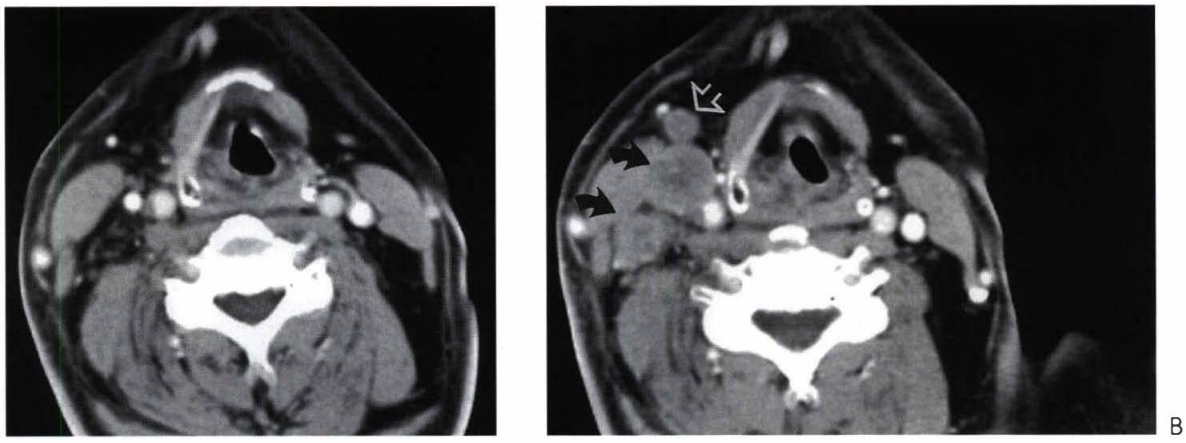

A B

Figure 164–3. Occult nodal metastasis. (A) Axial contrast-enhanced CT shows no evidence of nodal enlargement. (B) Axial contrast-enhanced CT 8 months later showed enlarged right external jugular node (hollow arrow) and level III nodes (solid arrows). These involved nodes appear unremarkable in the initial scan highlighting the dilemma in managing N0 necks.

Table 164–1
Simplified Numerical Classification System

Level	Location
IA	Submental lymph nodes
IB	Submandibular lymph nodes
II	Internal jugular (deep cervical) chain from the base of the skull to the inferior border of the hyoid bone
III	Internal jugular (deep cervical) chain from the hyoid bone to the inferior border of the cricoid arch
IV	Internal jugular (deep cervical) chain between the inferior border of the cricoid arch and the supraclavicular fossa
V	Posterior triangle or spinal accessory nodes
VI	Central compartment nodes from the hyoid bone to the suprasternal notch
VII	Nodes inferior to the suprasternal notch in the upper mediastinum

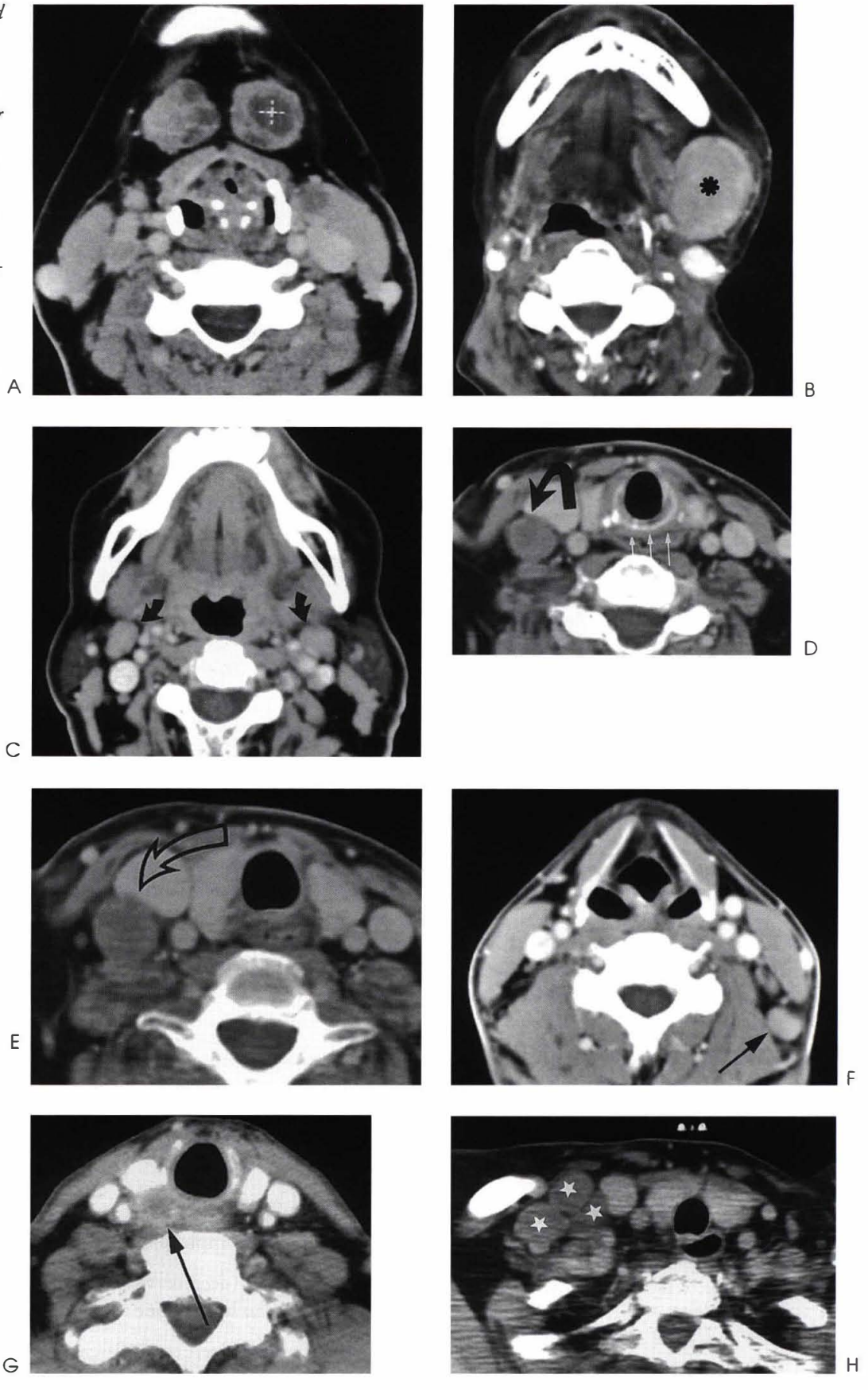

Figure 164-4. Axial contrast-enhanced CT showing nodal levels I to VI. (A) Level IA submental nodes (cross). Note the low densities indicating nodal necrosis. (B) Level IB enlarged submandibular nodes (asterisk). (C) Level II normal jugulodigastric nodes (arrows). (D) Level III metastatic node (curved arrow). The level III nodes are superior to the cricoid cartilage (straight arrow) whereas level IV nodes are inferior. (E) Level IV metastatic node (arrow). (F) Level V metastatic node (arrow) in the posterior triangle. (G) Level VI metastatic tracheoesophageal or paratracheal node (arrow). (H) Supraclavicular metastatic nodes (stars).

Treatment

The treatment for cervical lymphadenopathy depends on several factors: (1) the primary disease, (2) the presence of extracapsular spread, and (3) nodal recurrence. In most upper aerodigestive tract malignancies, cervical lymphadenopathy is treated with neck dissection. This may be supplemented with radiation therapy or chemotherapy depending on the pres-

ence of extracapsular spread or whether the nodes could be totally resected. In contrast, in patients with nasopharyngeal carcinoma, nodal metastasis is best treated with radiation therapy because both primary and nodal diseases are very radiosensitive. However, nodal recurrence in nasopharyngeal carcinoma is best treated with radical neck dissection.

Imaging Findings

CT

Cervical lymphadenopathy shows variable contrast enhancement. Enhancement depends on the volume and rate of contrast delivery as well as histology. Thyroid carcinoma, for instance, shows strong contrast uptake. Lymph nodes along the cervical chain are intimately related to the internal jugular vein and the carotid sheath. In general, nodes > 10 mm should be considered abnormal. However, the diagnostic accuracy of imaging varies directly with the size. The presence of nodal necrosis irrespective of size indicates metastatic involvement. Extracapsular spread is diagnosed when the nodes appear matted or the nodal outline appears streaky.

MR

On T1-weighted MR images, nodes show intermediate signal intensity. T2-weighted images typically show high signals. Following contrast enhancement, nodes show good enhancement and this may decrease their conspicuity if no fat suppression is instituted. MR imaging is likely less sensitive than CT in identifying nodal necrosis and extracapsular spread. Carotid artery involvement may be presumed if the artery is encased by greater than 270° by malignant nodes.

Imaging Pearls

- Nodal necrosis may be confused in two conditions. First, fat deposition may produce a low attenuation focus in the suspected node on CT. Density measurements are of limited value in small lesions because of partial volume averaging. The location of the low attenuation focus is of help because necrosis is generally situated centrally whereas fat is usually deposited around the hilum. Second, nodes with suppuration also show central areas of low attenuation in association with irregular and ill-defined margins. Inflammatory lymphadenitis is usually evident clinically and radiologically. The presence of cellulitis may help to separate these conditions. As the posterior belly of the digastric muscle crosses the carotid sheath, the muscle may be mistaken as an enlarged jugulodigastric node. This potential pitfall can be avoided by comparing with the opposite side. Furthermore, the digastric muscle can be easily traced from the origin in the mastoid process to the floor of the mouth.
- For a detailed analysis of the effect of lymph node on the diagnostic accuracy of CT and MR see Curtin HD, Iswaran H, Mancusco AA, Dalley RW, Candy DT, McNeil BJ. Comparison of CT and MR imaging in staging of neck metastasis. *Radiology* 1998;207:123–130.

Suggested Readings

1. Harnsberger HR. *Handbook of Head and Neck Imaging.* 2nd ed. St. Louis: Mosby; 1995:283–298.
2. Curtin HD, Iswaran H, Mancuso AA, Dalley RW, Caudy DJ, McNeil BJ. Comparison of CT and MR imaging in staging of neck metastasis. *Radiology* 1998;207:123–130.
3. Chong VFH, Fan YF, Khoo JBK. MRI features of cervical nodal necrosis in metastatic disease. *Clin Radiol* 1996;51:103–109.
4. Som PM, Curtin HD, Mancuso AA. An imaging-based classification for the cervical nodes designed as an adjunct to recent clinically based nodal classifications. *Arch Otolaryngol Head Neck Surg* 1999;125:388–396.

Chapter 165

Tumor Spread to the Carotid Sheath

Epidemiology

The arrangement of the cervical fascia can readily explain how tumors tend to spread in a predictable manner. The retropharyngeal, parapharyngeal, and prevertebral spaces are well-recognized routes for the spread of infection and malignancy. Malignant infiltration can take place along the parapharyngeal space or the carotid space (Fig. 165-1).

Clinical Findings

Patients usually present with symptoms related to the primary neoplasm. The primary lesion is usually a mucosal malignancy located in the nasopharynx, oropharynx, or hypopharynx. Involvement of the CS may produce cranial nerve palsies such as hoarseness and vocal cord paralysis. Late signs include denervation atrophy of the latissimus dorsi and the sternocleidomastoid muscles.

Pathology

The fascia that encloses the carotid sheath is a substantive fascia formed by all three layers of the deep cervical fascia and is particularly evident between the carotid bifurcation and the clavicle. This fascia prevents disease from entering the CS or disease within the CS from spreading into adjacent spaces. Grodinsky and Holyoke found in their experimental studies that injecting the CS showed no significant spread either cranially or caudally and concluded that this space is of limited importance as a pathway for the spread of infection. Above the carotid bifurcation, the fascia is often incomplete and may even be absent. This is why some authors feel that the CS is not a true fascia-bound space above the level of the carotid bifurcation and hence should more appropriately be considered as the posterior portion of the parapharyngeal space. Unlike the section between the carotid bifurcation and the clavicle, tumor can spread with relative ease above the carotid bifurcation to the skull base. Malignant tissue may reach the CS by direct tumor extension or through nodal metastasis. Metastatic deposits after extracapsular spread can infiltrate along the CS in cranial, caudal, or both directions.

Treatment

Tumor infiltration along the CS usually renders the patient a nonsurgical candidate at most institutions. The patient can be offered palliative treatment, which may consist of radiation therapy, chemotherapy, or both.

Imaging Findings

CT

Tumors involving the CS show moderate to good contrast enhancement. Malignant infiltration produces soft tissue thickening around and along the CS. This involvement may extend over several vertebral segments.

MR

Malignant tissues exhibit increased signals on T1-weighted images following contrast injection. On T2-weighted images they show high signal intensity. The flow void in the carotid artery is usually evident but the jugular vein may be completely effaced by the space-occupying effect of the malignant tissues.

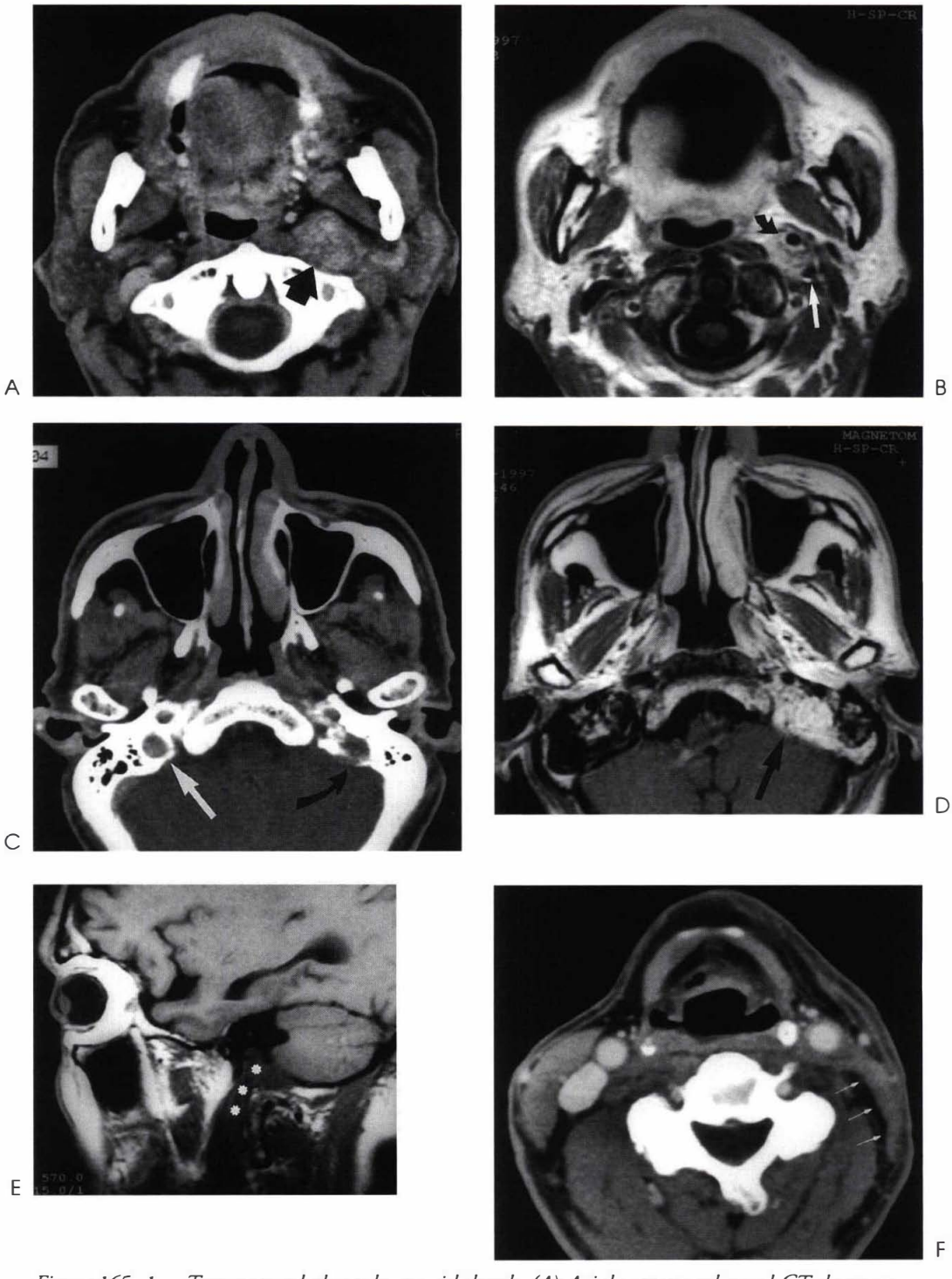

Figure 165–1. Tumor spread along the carotid sheath. (A) Axial contrast-enhanced CT shows an enhancing mass distending the left carotid sheath (arrow). The patient had recurrent left tonsillar carcinoma. (B) Axial contrast-enhanced MR image shows left internal carotid artery (black arrow) and jugular vein flow (white arrow) voids. (C) Axial contrast-enhanced CT shows irregularity of the left jugular foramen (black arrow). Compare with the normal right jugular foramen (white arrow). (D) Axial contrast-enhanced MR image shows tumor spread into the left jugular foramen (arrow). (E) Sagittal T1-weighted MR image shows intermediate signal intensity tumor spreading superiorly through the jugular foramen (asterisks). (F) Axial contrast-enhanced CT shows atrophy of the left sternocleidomastoid muscle (arrows) indicating accessory nerve palsy.

Imaging Pearls

- The CS should be traced to the skull base. Malignancies originating from the oropharynx and hypopharynx may spread as high as the jugular foramen.
- A tumor that directly abuts the carotid artery may be focally adherent. Encasement of the carotid artery is diagnosed if at least 270 degrees of the carotid wall is involved by tumor.
- Retropharyngeal lymphadenopathy should be differentiated from malignant infiltration along the CS. These lymph nodes are located between the CS and the nasopharyngeal air space and typically do not enlarge to encase the CS.

Suggested Readings

1. Grodinsky M, Holyoke EA. The fasciae and fascial spaces of the head, neck and adjacent regions. *Am J Anat* 1938;63:367–408.
2. Harnsberger HR. *Handbook of Head and Neck Imaging*. 2nd ed. Chicago: Mosby; 1995.
3. Som PM, Curtin HD. Fasciae and spaces. In: Som PM, Curtin HD, eds. *Head and Neck Imaging*. St Louis: Mosby; 1996.

Chapter 166

Encasement of the Carotid Sheath

Epidemiology

Cervical nodal enlargement is frequently encountered in patients with head and neck cancers. Nodal involvement is an important determinant of prognosis. The presence of lymphadenopathy reduces the prognosis by half. The carotid artery can be involved following advanced nodal metastasis with extracapsular spread (Fig. 166-1). Encasement of the carotid artery at the skull base may be due to perineural invasion along CN X.

Clinical Findings

Apart from the primary disease, carotid invasion may be silent. However, patients may have hoarseness of voice or Horner's syndrome indicating tumor involvement of the carotid sheath.

Pathology

Carotid encasement may be due to direct extension of the primary tumor or advanced nodal metastases. The presence of carotid encasement should also be evaluated in patients with neck recurrence.

Treatment

Most surgeons consider encasement of the carotid artery a contraindication for nodal resection. However, others would resect the carotid artery and repair the defect with an end-to-end anastomosis or using a vein or synthetic graft. Ligation of the internal carotid artery carries significant risks of neurological complications, including death. Malignant infiltration of the adventitia may potentially be resected by dissection along the plane below the adventia.

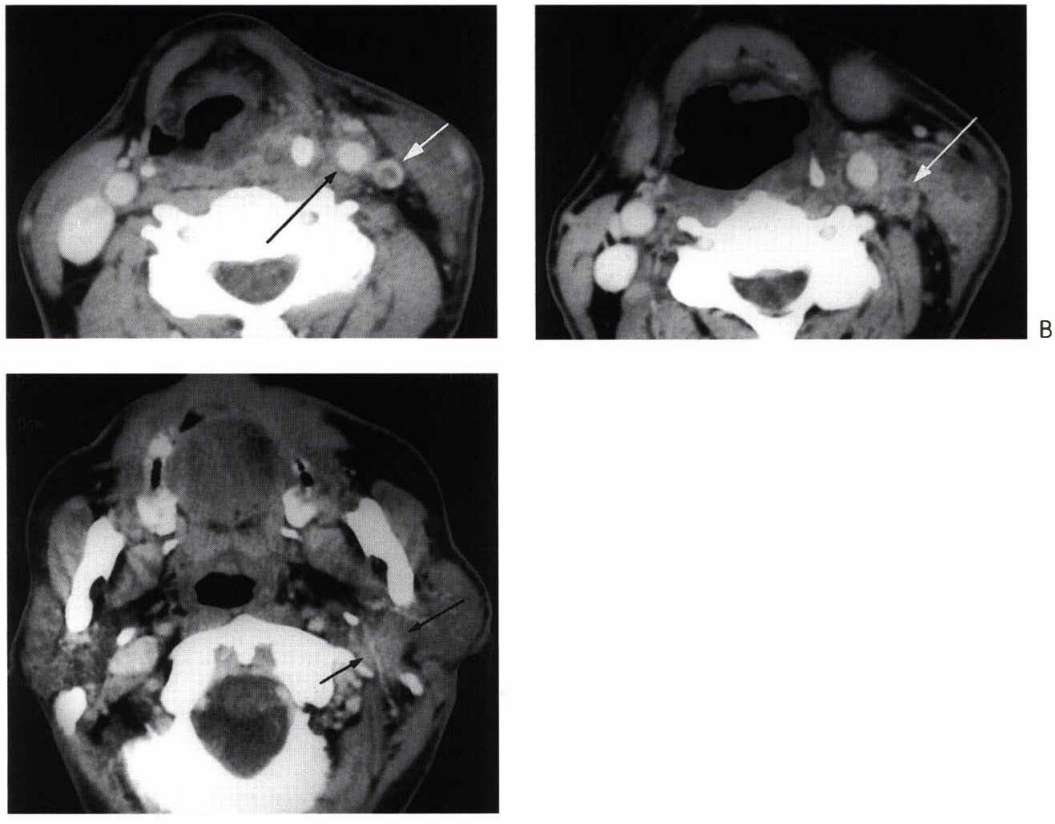

Figure 166-1. Hypopharyngeal carcinoma with carotid sheath invasion. (A) Axial contrast-enhanced CT shows hypopharyngeal carcinoma with tumor encircling the left carotid artery (black arrow). Note the tumor thrombus within the left internal jugular vein (white arrow). (B) Axial contrast-enhanced CT [superior to (A)] shows tumor encasing the left carotid sheath. Note the thrombosed left internal jugular vein (arrow). (C) Axial contrast-enhanced CT shows tumor thrombosis involving the left jugular vein up to C2 level (opposing arrows).

Imaging Findings

CT

Encasement of the carotid artery is diagnosed if at least 270 degrees of the carotid wall is involved by tumor. A tumor may be focally fixed if a tumor directly abuts the carotid artery but does not meet the criteria of encasement.

MR

The criteria of MR for encasement of the carotid artery by tumor is similar to the CT criteria.

Imaging Pearls

- Encasement of the carotid artery by tumor substantially reduces prognosis and makes patients unresectable at most institutions.
- The carotid artery should be evaluated to the level of the skull base in all patients with recurrent tumors.
- Encasement of the carotid artery is often clinically occult and places the patient at greater risk for a sentinel bleed.

Suggested Readings

1. Suen SY, Stern SJ. Cancer of the neck. In: Myers EN, Suen JY, eds. *Cancer of the Head and Neck*. 2nd ed. Philadelphia: WB Saunders; 1996:462–484.
2. Myers NM, Fagan JF. Treatment of N+ neck in squamous cell carcinoma of the upper aerodigestive tract. *Otolaryngol Clin North Am* 1998;31: 671–686.
3. Yousem DM. Suprahyoid spaces of the head and neck. *Semin Roentgenol* 2000;35:63–71.

Chapter 167

Hodgkin's Disease

Epidemiology

The incidence of lymphomas has been increasing over the last 4 decades. In the United States, it is now the fifth leading cause of death in men and the seventh in woman. Hodgkin's disease (HD) has a bimodal distribution, with the first peak in teenagers and young adults and the second peak in middle age (50 to 60 years old). This malignancy is more common in men.

Clinical Findings

HD is principally a disease involving lymph nodes, and the involvement of extranodal sites is uncommon. Patients usually present with painless neck masses. These nodes may be painful if there is rapid growth resulting in nodal necrosis. This phenomenon is present in high-grade lymphomas. Systemic symptoms such as fever and night sweats are uncommon in HD of the head and neck.

Pathology

The diagnosis of HD is based on the presence of Reed-Sternberg cells. There are four main histologic types: nodular sclerosing, mixed cellularity, lymphocytic predominant, and lymphocytic depletion.

Treatment

Treatment of HD depends on staging and grading. The most widely used system is that of the Ann Arbor classification into four stages:

I: Involvement of a single lymph node or a single extralymphatic organ
II: Involvement of two or more nodes on the same side of the diaphragm or localized involvement of a single extralymphatic site (IIE)
III: Involvement of nodes on both sides of the diaphragm (III) or localized involvement of an extralymphatic site (IIIE) or spleen (IIIS)
IV: Involvement of disseminated disease

The majority of HDs of the head and neck are classified in the staging categories I or II and are usually of intermediate grade. They are most commonly treated with chemotherapy. In the presence of large nodal disease, radiation therapy may be added following chemotherapy.

Imaging Findings

CT

Contrast-enhanced CT may show slight to moderate enhancement. These enlarged nodes do not usually show invasion of adjacent structures (Fig. 167–1). Central nodal necrosis may be detected but this finding is relatively uncommon compared with metastatic lymphadenopathy. Calcification is not a feature of HD but nodes may calcify following radiation therapy.

MR

MR imaging of nodal enlargement in HD is nonspecific. The nodes show intermediate signals on T1-weighted images and enhance well following contrast injection (Fig. 167–2). On T2-weighted images they show high signals.

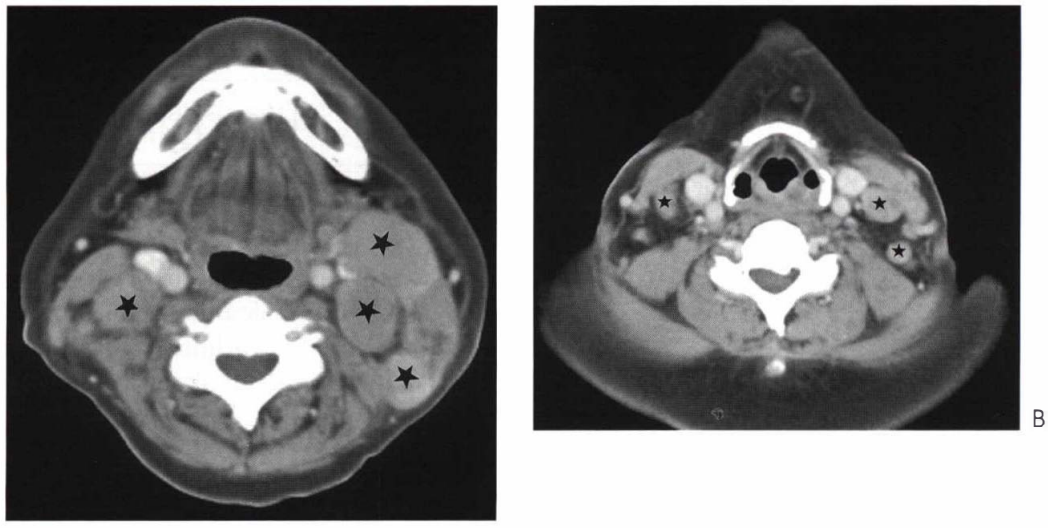

Figure 167–1. Hodgkin's disease. (A) Axial contrast-enhanced CT shows bilateral enlarged level II cervical nodes (stars). (B) Axial contrast-enhanced CT shows bilateral level III nodal involvement (stars).

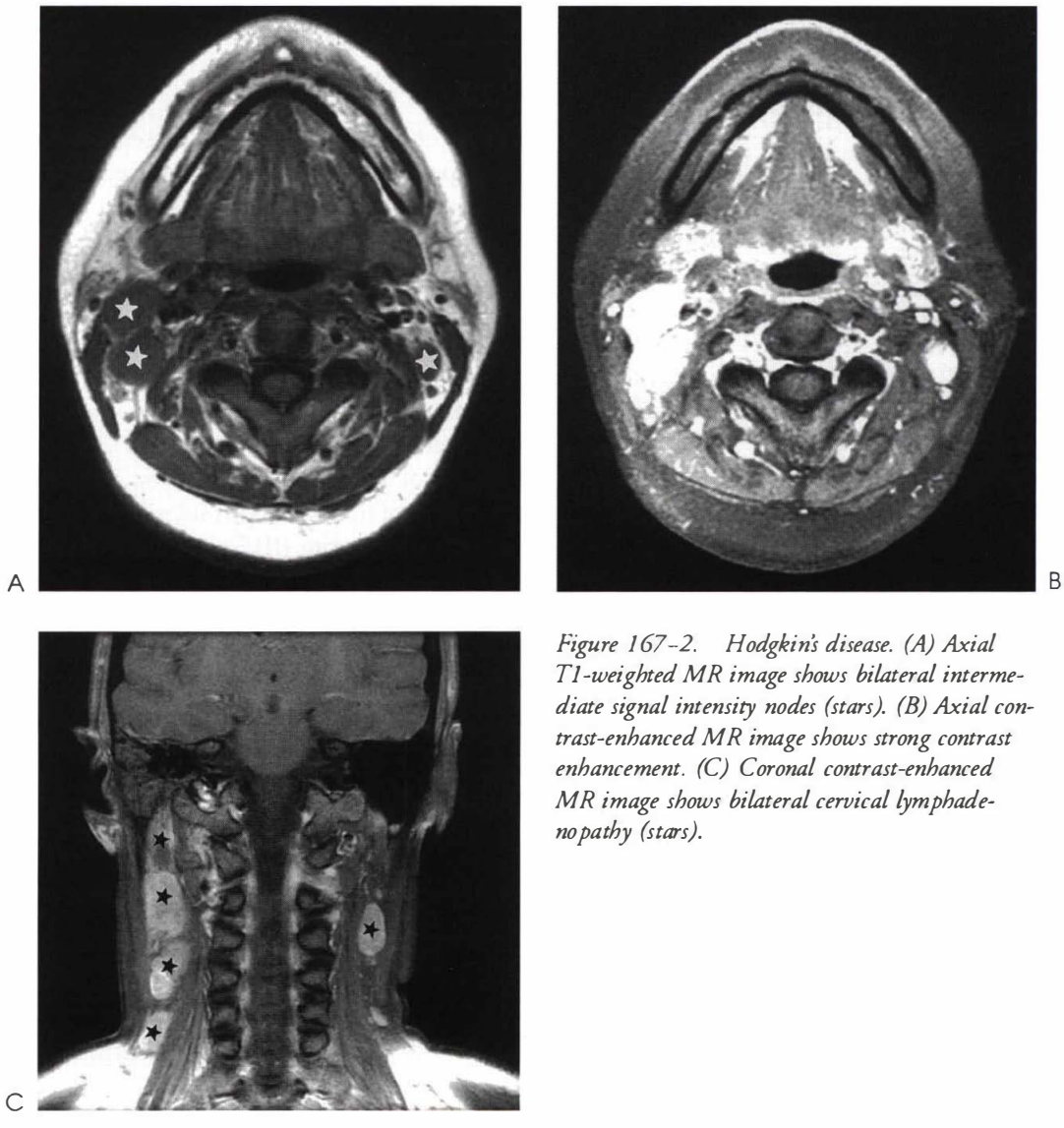

Figure 167–2. Hodgkin's disease. (A) Axial T1-weighted MR image shows bilateral intermediate signal intensity nodes (stars). (B) Axial contrast-enhanced MR image shows strong contrast enhancement. (C) Coronal contrast-enhanced MR image shows bilateral cervical lymphadenopathy (stars).

Imaging Pearls

- HD may be suspected if there is bilateral lymphadenopathy involving several nodal groups especially the supraclaulcular region in a young patient. This finding is unusual in metastatic disease with perhaps the exception of nasopharyngeal carcinoma.
- In an older patient, isolated involvement of the supraclaulcular nodes raises the possibility of esophageal or brachogeric carcinoma in addition to lymphoma.

Suggested Readings

1. Mendenhall NP. Lymphomas and related diseases presenting in the head and neck. In: Million RR, Cassisi NJ, eds. *Management of Head and Neck Cancer*. Philadelphia: JB Lippincott; 1994:857–878.
2. Rodriguez MA, Hong WK. Diagnosis and management of lymphomas in the head and neck. In: Myers EN, Suen JY, eds. *Cancer of the Head and Neck*. 2nd ed. Philadelphia: WB Saunders; 1996:462–484.
3. Som PM. Lymph nodes. In: Som PM, Curtin HD, eds. *Head and Neck Imaging*. St. Louis: Mosby; 1996:772–793.

Chapter 168

Castleman's Disease

Epidemiology

Castleman's disease (also known as localized nodular hyperplasia, angiofollicular lymph node hyperplasia, angiomatous lymphoid hamartoma, and giant lymph node hyperplasia) is a rare benign lymphoproliferative disorder that is characterized by lymph node hyperplasia. The mediastinum is most commonly involved, with the extracranial head and neck being the second most common site of involvement. The disease does not appear to have a sex or age predilection; however, isolated involvement of the neck is often reported in adolescents and young adults. The etiology is unknown and may be due to a hamartomatous, infectious, or inflammatory process. There are two distinct types of Castleman's disease based on histology: hyaline vascular (90%) and plasma cell variant (10%).

Clinical Features

Patients with the hyaline vascular type of Castleman's disease present with a neck mass but are otherwise asymptomatic. In addition to the palpable neck mass, approximately 50% of patients with the plasma cell variant will have systemic anomalies that include fever, elevated sedimentation rate, and hypergammaglobulinemia.

Pathology

The hyaline vascular type of Castleman's disease consists of large fibrous masses in the perivascular area with interspersed areas of plasma cells. The capillaries are hyalinized and surrounded by lymphocytes. The plasma cell variant has sheets of mature plasma cells in the interfollicular tissue with small areas of hyaline.

Treatment

The treatment for the hyaline vascular form is local resection. Because the plasma cell form is often associated with systemic disease, the treatment requires local resection, close follow-up, and in some instances, chemotherapy.

Imaging Findings

CT

The affected lymph nodes are enlarged and typically densely enhance following contrast administration. The margins of the involved nodes are well-defined without evidence of extracapsular penetration (Fig. 168–1).

MR

The involved nodes are enlarged and are hypointense to muscle on T1-weighted sequences and increased signal on T2-weighted sequences. The lymph nodes usually densely enhance following contrast administration. However, mildly enhancing variants of the hyaline type that contain a central stellate area of low T2 signal have been described.

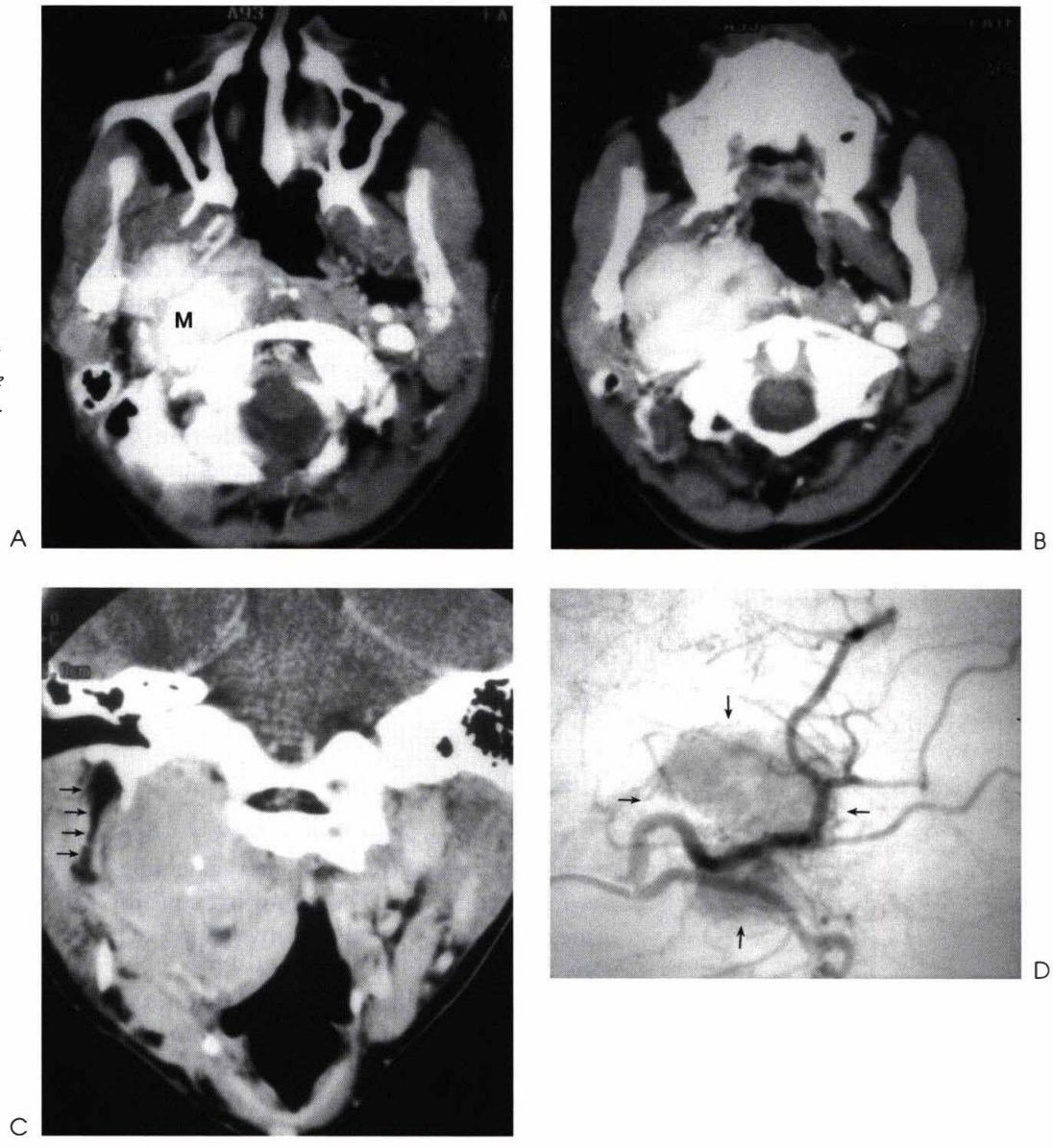

Figure 168-1. Castleman's disease. (A) Axial contrast-enhanced CT shows a densely enhancing mass (M), which appears to involve both the carotid and parapharyngeal spaces. (B) This mass extends inferior to the level of the soft palate. (C) Coronal CT shows lateral displacement of the fat within the parapharyngeal space (arrows) by the mass. This lateral displacement of the parapharyngeal space fat suggests the mass is arising from the carotid space. (D) Selective external carotid angiogram shows the vascular blush (small arrows) characteristic of Castleman's disease. (Courtesy Doug Phillips, M.D.)

Imaging Pearls

- The imaging findings of the involved cervical lymph nodes are nonspecific. However, the enhancement of the nodes is typically much greater than that seen in lymphoma.
- The diagnosis may be suggested by the presence of unilateral densely enhancing homogeneous lymph nodes in a young adult without a known primary tumor or thyroid mass.

Suggested Readings

1. Glazer M, Rao VM, Reiter D, McCue P. Isolated castleman disease of the neck: MR findings. *AJNR Am J Neuroradiol* 1995;16:669–671.
2. Davis BT, Bagg A, Milmoe GJ. CT and MR appearance of Castleman's disease of the neck. *AJR Am J Roentgenol* 1999;173:861–862.
3. Yi AY, deTar M, Becker TS, Rice DH. Giant lymph node hyperplasia of the head and neck (Castleman's disease): a report of five cases. *Otolaryngol Head Neck Surg* 1995;113:462–466.

Chapter 169

Neuroblastoma

Epidemiology

Neuroblastoma is the most common solid tumor of infancy and childhood, outside the central nervous system. Children < 5 years of age are most commonly affected. It usually arises from the adrenal medulla (40%), but tends to involve the spine and paraspinal regions in 25% of cases. Paraspinal involvement occurs most frequently in the thoracic and lumbar regions and is rare in the cervical area. Only 2 to 4% of lesions arise primarily in the neck. There is a slight male predilection. Ganglioneuroma and ganglioneuroblastoma present later than neuroblastomas and are most often seen in the 5- to 8-year age group

Clinical Features

For neuroblastomas that involve the extracranial head and neck, the common presentation is a palpable mass that may be mildly painful. The most common presenting symptoms for paraspinal masses that extend into the spinal canal include local pain and spinal cord dysfunction.

Pathology

Neuroblastoma arises from primitive cells called neuroblasts, which are of neural crest origin. These neural crest cells embryologically form the adrenal medulla and the paravertebral sympathetic chain. The tumor is frequently hemorrhagic. Histologically, neuroblastomas are composed of small primitive round cells with hyperchromatic dense nuclei. Calcifications are seen in 10% of cases.

Ganglioneuroblastoma is a mixture of immature neuroblastoma and more mature elements, whereas ganglioneuroma is composed primarily of mature cells. The nuclei are large, and there is more cytoplasm present within the cells than in neuroblastoma. Calcifications are seen in 20% of cases.

Treatment

Surgery is the initial treatment of choice followed by radiotherapy and chemotherapy. Factors consistent with a favorable outcome include younger age at diagnosis, extra-adrenal location, more differentiated histology, and more localized disease.

Imaging Findings

Plain Films

Plain radiographs reveal a paraspinal soft tissue mass associated with vertebral body destruction. Calcification may be seen in 10% of cases.

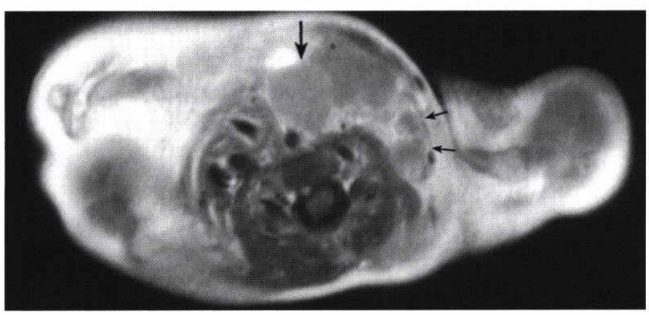

Figure 169-1. Axial contrast-enhanced T1-weighted image shows a primary neuroblastoma thought to be arising from the sympathetic chain (large arrow). There are multiple enlarged lymph nodes in the adjacent cervical chain (small arrows). (Courtesy of Bernadette Koch, M.D., Cinncinnati Children's Hospital)

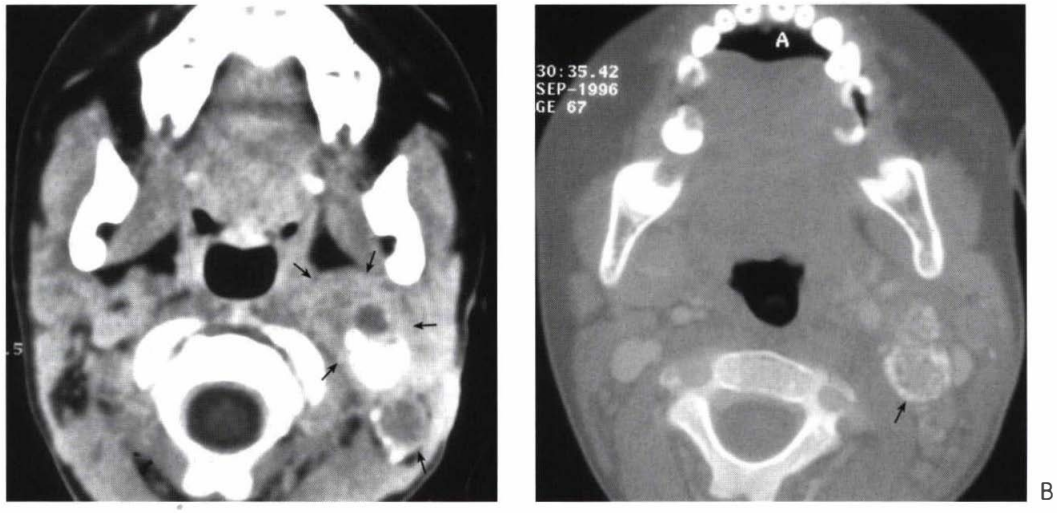

Figure 169-2. (A) Axial contrast-enhanced CT shows multiple metastatic cervical lymph nodes from neuroblastoma (arrows). (B) Bone algorithm shows that a portion of the nodal mass is partially calcified (arrow).

CT

CT shows a soft tissue mass in the carotid space that may extend into the pre-vertebral space and through the neural foramen. Advanced tumors may spread in the epidural space and displace and compress the thecal sac. Calcification may be present in 10% of cases. The vertebral body shows lytic or sclerotic destruction and expansion of the neural foramina. The mass shows mild to moderate enhancement on the postcontrast study. The slow-growing ganglioneuroblastomas and ganglioneuromas show calcification in approximately 20% of cases. They generally cause scalloping of the posterior vertebral bodies and widening of the neural foramina and the spinal canal (Figs. 169-1 and 169-2).

MRI

The mass is hypointense to isointense on T1-weighted images. The T2-weighted signal characteristics are variable. MRI accurately demonstrates the intraspinal extension of tumor. Areas of nonhemorrhagic necrosis have low signal intensity on T1-weighted images and increased signal intensity on T2-weighted images. Focal areas of hemorrhage may be seen. Large areas of calcification may be visualized as areas of signal void. Finally, with contrast administration these tumors tend to enhance. Advanced disease may result in diffuse bony metastases.

Imaging Pearls

- The majority of neuroblastomas that involve the neck will be due to nodal metastases rather than the primary site or origin.
- Calcification of cervical neuroblastomas usually occurs following treatment and is unusual at initial presentation.

Suggested Readings

1. Vazquez E, Enriquez G, Castellote A, et al. US, CT and MR imaging of neck lesions in children. *Radiographics* 1995;15:105.
2. Castillo M, Mukherji SK. *Imaging of Pediatric Head, Neck and Spine*. Philadelphia: Lippincott-Raven; 1996:606-607.
3. Barkovich AJ. *Pediatric Neuroimaging*. 2nd ed. New York: Raven Press; 1995:564-565.

Chapter 170

Meningioma

Epidemiology

Intracranial meningiomas are the most common nonglial tumor. Extracranial meningiomas are uncommon and may be found in relation to the optic nerve. Rarely, meningiomas originating in the posterior cranial fossa may extend into the jugular foramen and beyond into the neck along the carotid sheath. These tumors are most commonly seen in middle age and show a predilection for females. Meningiomas may be multiple in 1 to 8% of patients and are associated with neurofibromatosis (NF-2).

Clinical Findings

Small meningiomas involving the jugular foramen may be asymptomatic. Larger legions typically present with multiple lower cranial nerve palsies. The most common complaint is hoarseness of voice and signs of vocal cord palsy. In addition, lesions that track down the carotid sheath may be sufficiently low to become palpable.

Pathology

The histologic patterns of meningiomas are variable and can be divided into three classic types: meningotheliomatous, fibroblastic, or transitional. The majority of reported jugular foramen meningiomas are classified as meningotheliomatous. Meningiomas may also be classified into four grades: benign, atypical, anaplastic, and sarcomatous. Six percent of jugular foramen lesions are meningosarcomas. In addition, meningiomas are classified according to morphological appearances: globular (most common), en plaque, and multicentric (least common).

Treatment

Meningiomas are slow-growing, benign tumors. Tumors that are detected incidentally may be followed up. Rapidly growing tumors should be surgically removed because they may be meningiosarcomas. Tumors in the jugular foramen with signs of cranial nerve compromise should be surgically treated to prevent further progression of cranial nerve deficits. Excision of the jugular or carotid sheath component can be carried out without removing the intracranial component.

Imaging Findings

CT

Unenhanced CT may detect a variable amount of calcification. The tumor typically enhances strongly with contrast. Meningiomas may cause florid hyperostosis of the jugular foramen or the adjacent temporal bone (Fig. 170–1).

MR

Gross calcifications in meningiomas may be visible on MR imaging as foci of signal void. On T1-weighted images meningiomas usually show an intermediate signal intensity. On T2-weighted images, meningiomas appear heterogeneous and are typically hyperintense. Following the injection of contrast, these lesions enhance intensely. The status of the carotid artery can be inferred by the presence or absence of flow void or with MR angiography.

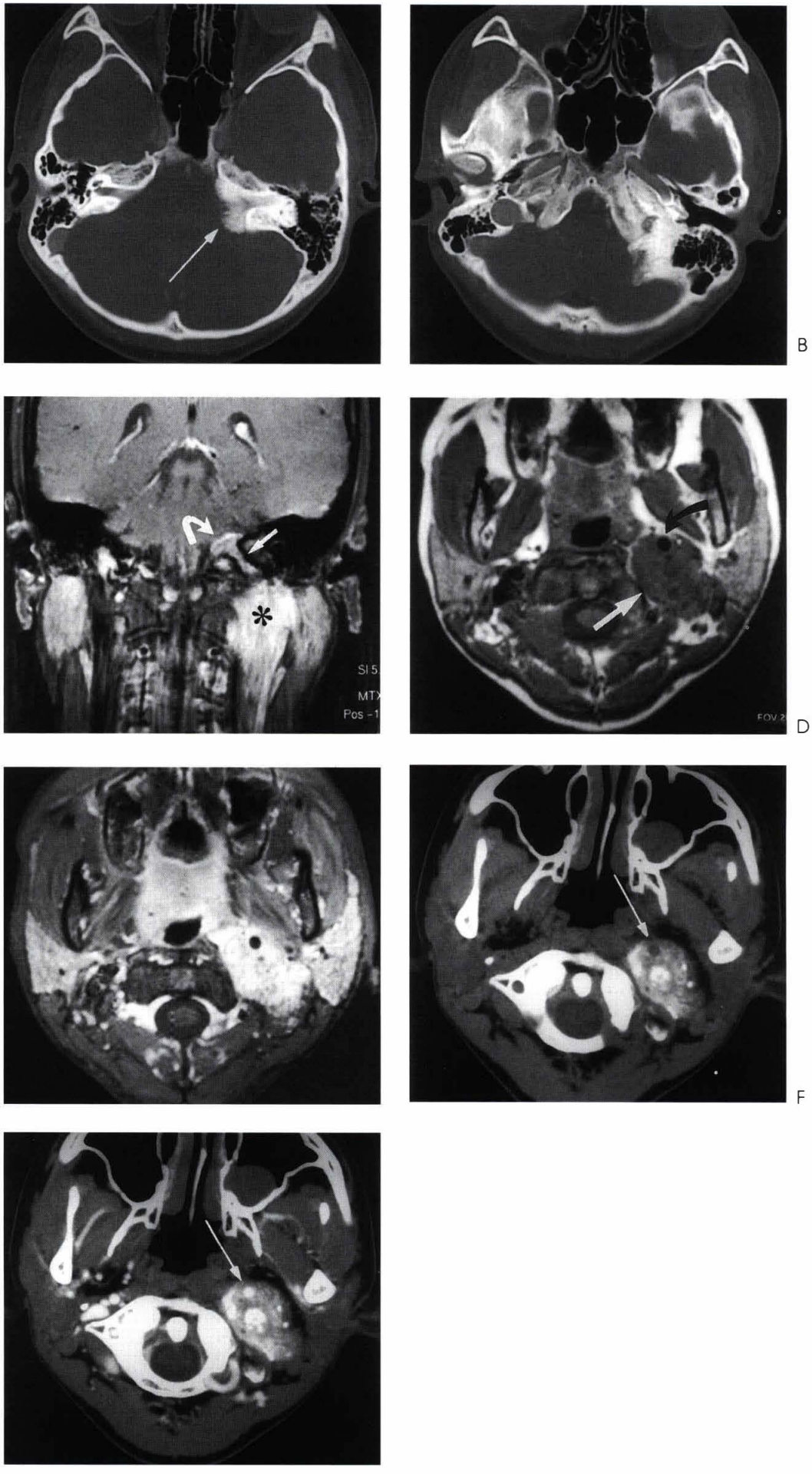

Figure 170–1. Posterior cranial fossa meningioma with extracranial extension into the carotid space. (A) Axial CT shows florid hyperostosis involving the left temporal bone due to en plaque meningioma (arrow). (B) Axial CT shows gross hyperostosis of the left temporal bone and narrowing of the jugular foramen. (C) Coronal contrast-enhanced MR image shows intracranial en plaque meningioma (curved arrow), tumor within the jugular foramen (straight arrow), and a large extracranial meningioma (asterisk). (D) Axial T1-weighted MR image shows an intermediate signal intensity left carotid space mass (arrow). Note the carotid artery flow void (curved arrow) is anteriorly displaced. The internal jugular vein is effaced. (E) Axial contrast-enhanced fat-saturation MR image shows strong contrast enhancement in the tumor. (F) Axial CT shows dense patchy psammomatous calcifications in the tumor. Note the unenhanced left carotid artery (arrow). (G) Axial contrast-enhanced CT shows opacification of the left carotid artery (arrow). The tumor itself is relatively unchanged in density.

Imaging Pearls

- The main differential diagnosis of a jugular foramen meningioma with carotid sheath extension is a glomus jugulare tumor or vagal schwannoma. Glomus jugulare tumors typically cause permeative erosion of the jugular foramen, whereas meningiomas and schwannomas result in smooth expansion.
- Signal loss due to dephasing from intratumoral calcification may be confused with flow voids. CT is helpful in identifying the presence of intratumoral calcification, thereby strongly suggesting the diagnosis of meningioma.
- En plaque spread (dural-tail) along the skull base favors the diagnosis of meningioma.

Suggested Readings

1. Tekkok IH, Ozcan OE, Turan E, Onol B. Jugular foramen meningioma: report of a case and review of the literature. *J Neurosurg Sci* 1997; 41:283–292.
2. Molony TB, Brackmann DE, Lo WW. Meningiomas of the jugular foramen. *Otolaryngol Head Neck Surg* 1992;106:128–136.

Chapter 171

Jugular Foramen Hemangiopericytoma

Epidemiology

Hemangiopericytomas are vascular tumors that occur mainly in adults. In the pediatric age group, these tumors are almost exclusively seen below the age of 1 year. Hemangiopericytomas represent 1% of all vasoformative tumors and most of them occur in the extremities and retroperitoneum whereas 20% occur in the head and neck region. They may be found in the sinonasal area, orbit, lacrimal sac, or jugular foramen. About 50% of cases are malignant, and distant metastasis, although rare, may occur, especially to the lungs.

Clinical Findings

Patients with sinonasal tumors usually present with a history of epistaxis, nasal obstruction, or discharge. Facial pain may be related to associated paranasal sinusitis secondary to tumor obstructing the drainage pathways. Patients with a jugular foramen lesion may present with pain or cranial nerve palsies.

Pathology

Hemangiopericytomas can be either benign or malignant. It is often difficult to separate these varieties based on histology. Electron microscopy and immunohistochemical techniques may be necessary to differentiate hemangiopericytomas from other sarcomatous tumors. Hemangiopericytomas are composed of irregular pericytes surrounding normal endothelial lined capillaries. The tumors are hypercelluar and the malignant variety tends to show necrosis and increased mitosis. A histologic diagnosis of hemangiopericytoma is based on a characteristic immunostaining pattern.

Treatment

Hemangiopericytomas in children < 1 year old can be treated by surgery alone. These tumors rarely recur or show metastasis. In older children, tumors tend to behave like the adult variety where local recurrence is common and metastatic disease can be seen frequently. The treatment of choice is wide surgical excision with radiation therapy or added chemotherapy. Because hemangiopericytomas show high recurrence rates, careful follow-up is important with these patients.

Imaging Findings

CT

On contrast-enhanced CT, hemangiopericytomas appear as bulky or lobulated tumors showing moderate to marked enhancement. They may show associated bone erosion.

MR

These tumors show intermediate signal intensity on T1-weighted images and may enhance intensely following the injection of contrast material. These tumors are hyperintense on T2-weighted images (Fig. 171–1).

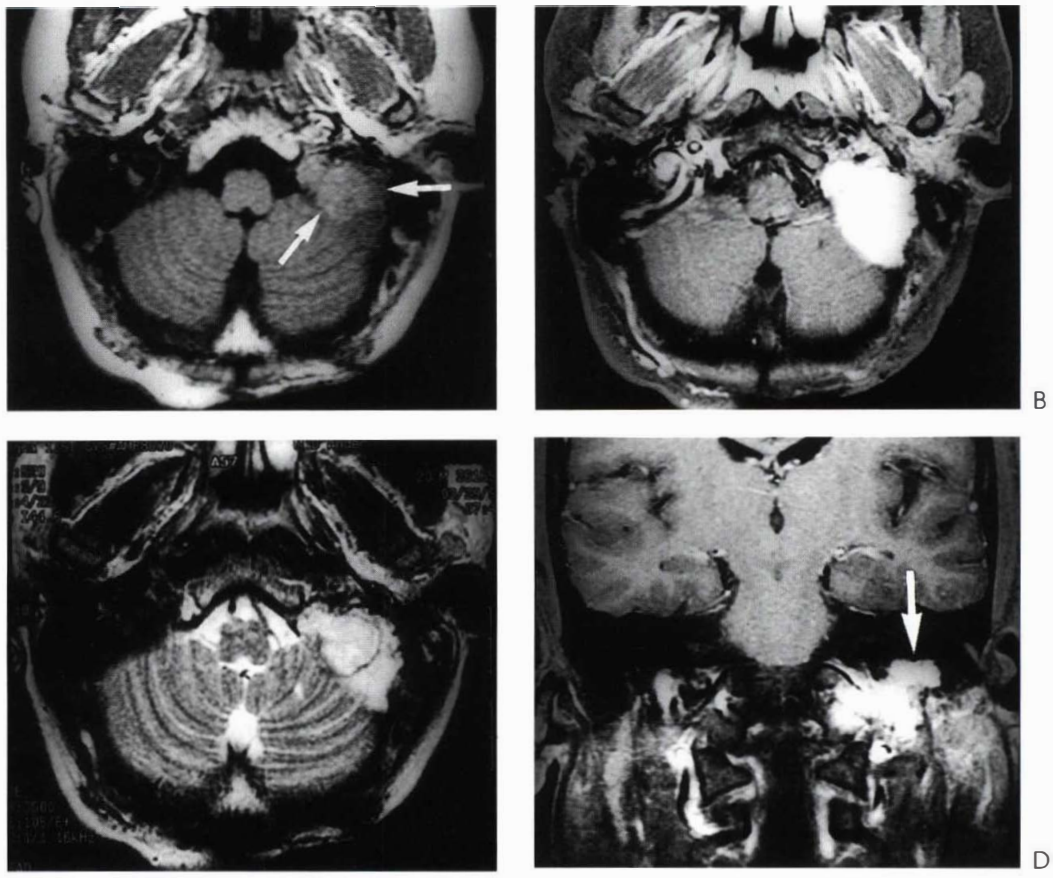

Figure 171-1. Jugular foramen hemangiopericytoma. (A) Axial T1-weighted MR image shows an intermediate signal intensity lesion involving the left jugular foramen (arrows). (B) Axial contrast-enhanced MR image shows intense tumor enhancement. (C) Axial T2-weighted MR image shows high signal intensity hemangiopericytoma. (D) Coronal contrast-enhanced MR image shows intense tumor enhancement in the left jugular foramen. Note the erosion of the mastoid portion of the temporal bone (arrow).

Imaging Pearl

- The CT and MR imaging findings of hemangiopericytomas are nonspecific. This entity should be included in the list of differential diagnosis in vascular lesions seen in the jugular foramen.

Suggested Readings

1. Volpe A, Sullivan J, Chong F. Aggressive malignant hemangiopericytoma in the neck. J Sur Oncol 1991;47:136–138.
2. Robb P, Singh S, Hartley RB, Shaheen OH. Malignant hemangiopericytoma of the parapharyngeal space. *Head Neck Surg* 1987;9:179–183.
3. Eichhorn JH, Dickersin GR, Bhan AK, Goodman ML. Sinonasal hemangiopericytoma: a reassessment with electron microscopy, immunohistochemistry and long-term follow-up. *Am J Surg Pathol* 1990;14:856–866.

Chapter 172

Paraganglioma

Epidemiology

Paragangliomas are slow-growing tumors arising from paraganglion cells of neural crest origin. They may be found along the superior cervical ganglion of the vagus nerve situated in the jugular foramen (glomus jugulare), around Arnold's or Jacobson's nerves in the middle ear (glomus tympanicum), along the nodose ganglion of the vagus nerve (glomus vagale) and the carotid bifurcation (carotid body tumor). These lesions show a female preponderance and are most commonly seen in middle age. Paragangliomas are multiple in 3 to 5% of patients but the incidence rises to 20 to 30% in patients with a positive family history.

Clinical Findings

Clinical presentation depends on the site of origin. Although all these tumors contain norepinephrine and epinephrine precursors, secretion of significance is very rare. This is related to the relative sparsity of secretory granules in these tumors. Carotid body tumors usually present as painless pulsatile neck masses. Similarly, glomus vagale may present as a painless lump but may show signs of vagus nerve dysfunction. Glomus jugulare usually presents with symptoms of nerve compression involving cranial nerves IX through XI. Pulsatile tinnitus is also common.

Pathology

The tumor consists of clumps of neoplastic cells separated by numerous slitlike vascular channels in a matrix of fibrous tissue. These tumors are histologically benign but may exhibit malignant behavior in less than 5% of cases. A diagnosis of malignancy is based on clinical behavior rather than on histological features. Regional nodal metastasis is present in 50% with malignant paragangliomas. Most cells stain positive for chromogranin.

Treatment

The preferred management is surgical resection. Small tumors can be resected without significant blood loss or nerve injury. Large vascular lesions may be embolized prior to resection. Tumors that are surgically inaccessible may be treated with radiation therapy.

Imaging Findings

CT

Paragangliomas are hypervascular lesions that show intense enhancement. Carotid body tumors typically splay the carotid bifurcation. Glomus vagale tumors are seen in relation to the carotid sheath displacing the internal carotid artery anteriorly. Glomus jugulare often show permeative erosion of the margin of the jugular foramen and commonly descend alongside the jugular vein (Fig 172–1).

MR

These tumors show intermediate signal intensity on T1-weighted images and enhance intensely after contrast injection. On T2-weighted images paragangliomas show moderately high signals and may exhibit the typical "salt and pepper" appearance. The low signals are thought to be flow voids whereas high signal foci are due to slow flow (Fig. 172–2 through 172–5).

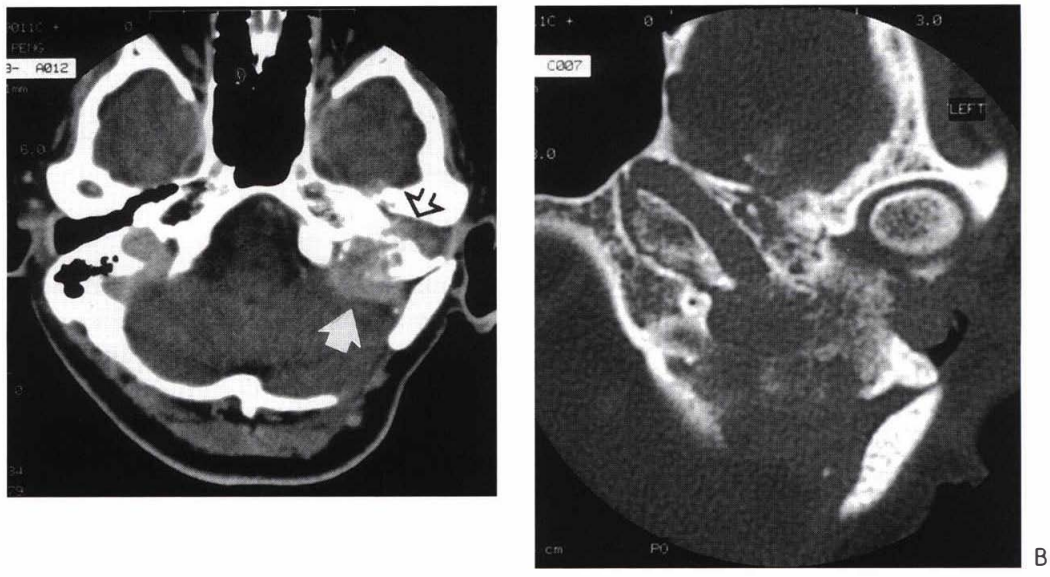

Figure 172–1. Recurrent jugular foramen paraganglioma. (A) Axial contrast-enhanced CT shows an enhancing recurrent paraganglioma in the left jugular foramen (solid arrow) with erosion into the external auditory canal (open arrow). (B) Axial CT (bone window) shows permeative destruction of the jugular foramen.

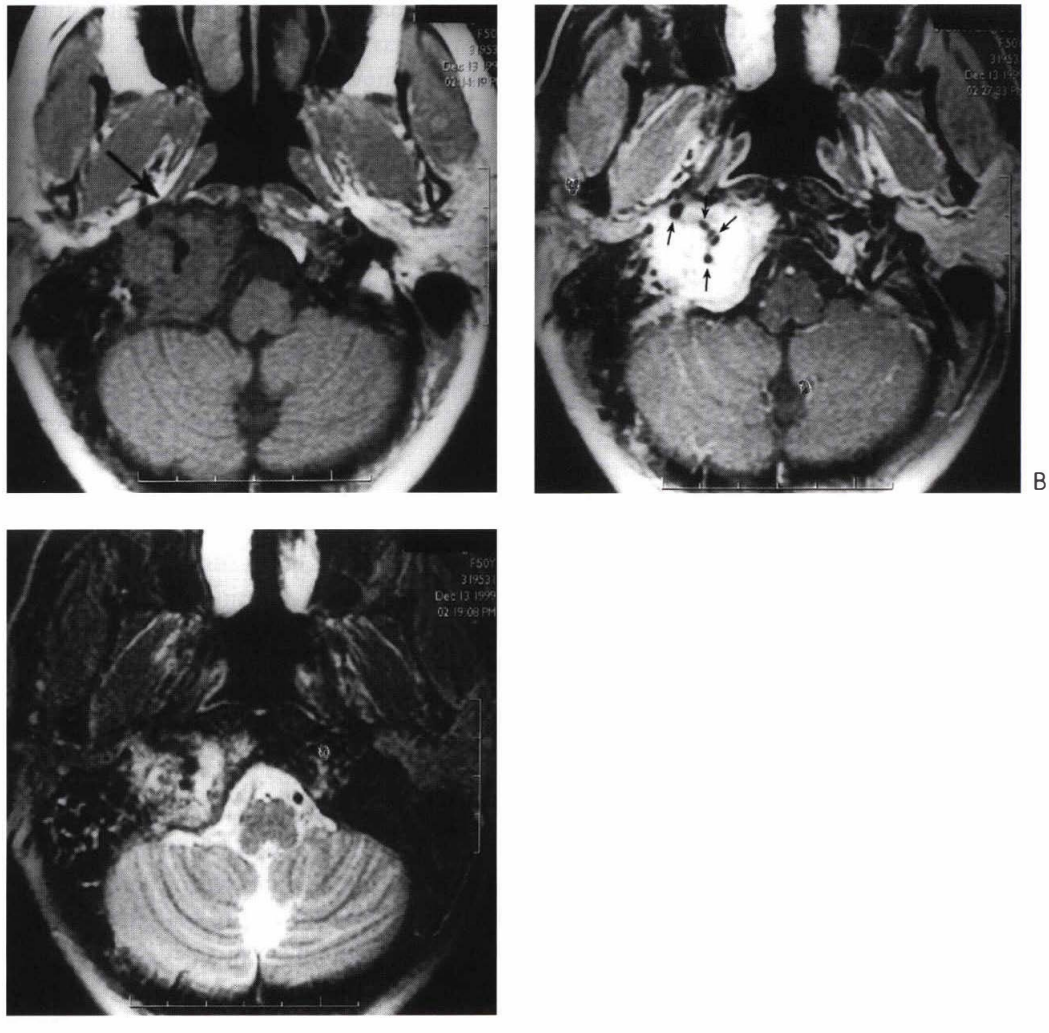

Figure 172–2. Jugular foramen paraganglioma. (A) Axial T1-weighted MR image show a large intermediate signal intensity lesion involving the right jugular foramen (arrow). (B) Axial contrast-enhanced MR image shows intense contrast enhancement. Note the signal void vessels within the mass (arrows). (C) Axial T2-weighted MR image shows scattered foci of signal void within a matrix of high signal intensity ("salt and pepper" appearance).

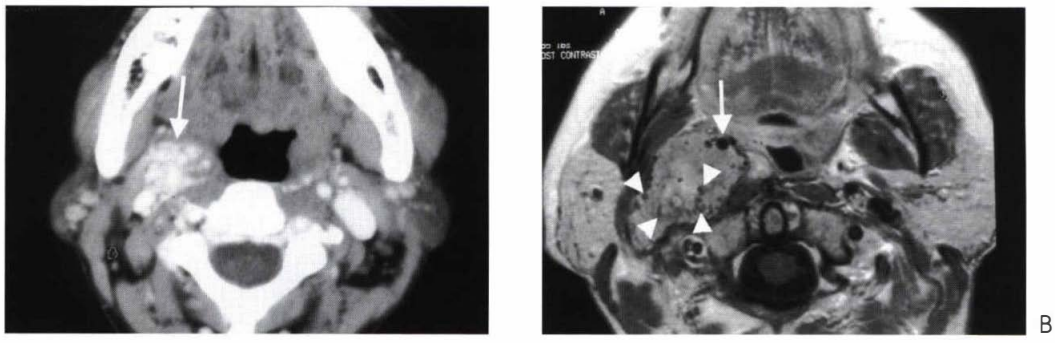

Figure 172-3. (A) Axial contrast-enhanced demonstrates a densely enhancing mass located in the carotid space (arrow). It is difficult to distinguish between a carotid body tumor and a glomus vagale on the current study. (B) Axial contrast-enhanced T1-weighted image in a different patient shows an enhancing mass with multiple flow voids (arrowheads). The carotid artery is anteriorly displaced (arrow) indicating that the mass is in the carotid space. These findings are characteristic of a carotid body tumor or a glomus vagale. The anterior displacement of the carotid artery is suggestive of a glomus vagale tumor.

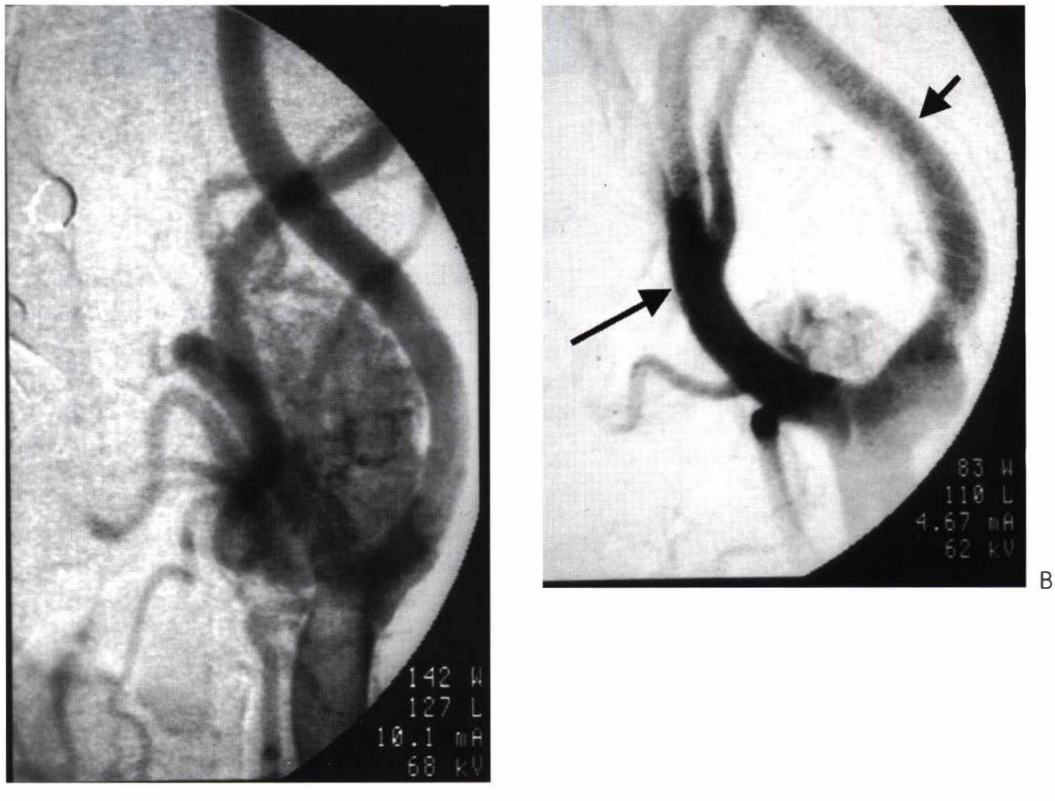

Figure 172-4. Carotid Body Tumor. (A) Common carotid angiogram show a hypervascular mass located at the carotid bifurcation. (B) There is significant devascularization of the tumor following embolization. The splaying of the internal (small arrow) and external (large arrow) carotid arteries indicates this is a carotid body tumor.

Imaging Pearl

- Glomus tumors often show features that may be used to distinguish them from neurogenic tumors. Glomus jugulare typically produces a permeative pattern of destruction of the jugular foramen in contrast to neurogenic lesions, which characteristically cause a smooth scalloped appearance. Glomus tumors intensely enhance on CT and they may appear inseparable from the adjacent vessels with rapid image acquisition using multidetector CT. This feature is less commonly seen in hypervascular neurogenic tumors.

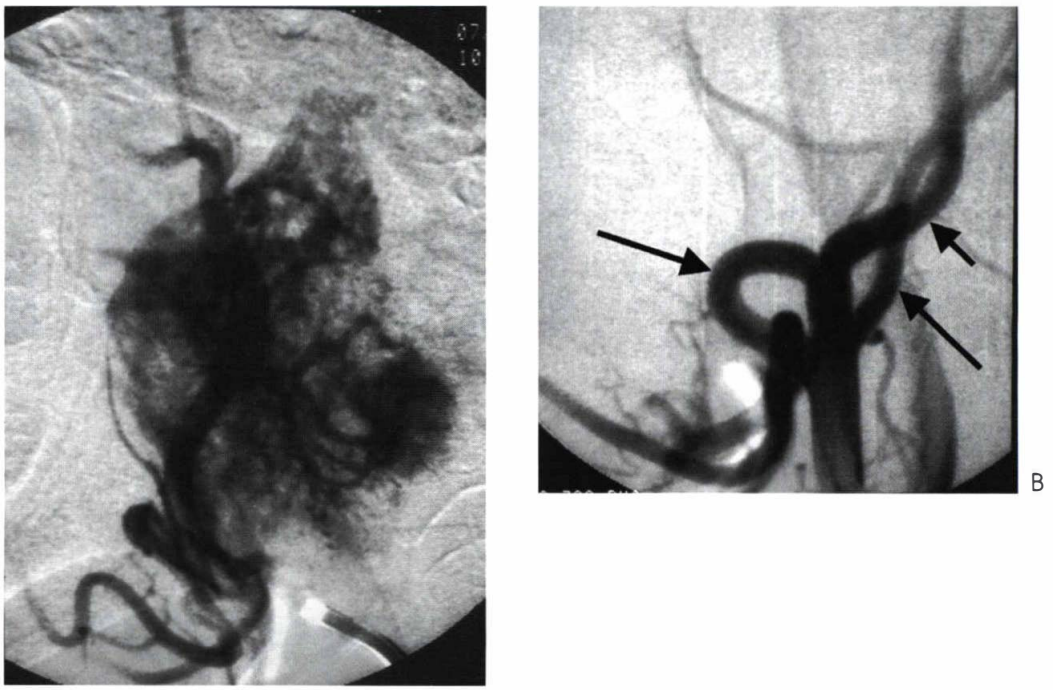

Figure 172-5. Glomus Vagale. (A) External carotid angiogram shows a hypervascular mass located just distal to the carotid bifurcation. (B) Common carotid angiogram demonstrates complete devascularization of the tumor following embolization. The close proximity of the internal (short arrow) and external (long arrows) carotid arteries indicates this is a glomus vagale tumor.

Suggested Readings

1. Olsen WL, Dillon WP, Kelly WM, Norman D, Brandt-Zawadski M, Newton TH. MR imaging of paragangliomas. *AJR Am J Roentgenol* 1987;148:210–204.
2. Mukherji SK, Kasper ME, Tart RP, Mancuso AA. Irradiated paragangliomas of the head and neck: CT and MR appearances. *AJNR Am J Neuroradiol* 1994;15:357–363.
3. Lewin JS. Imaging the suprahyoid neck. In: Valvassori GE, Mafee MF, Carter BL, eds. *Imaging of the Head and Neck*. New York: Thieme; 1995.

Chapter 173

Schwannoma

Epidemiology

Schwannomas most commonly affect cranial nerve VIII. In the neck, they usually involve the vagus nerve but may also originate in other cranial nerves and the sympathetic trunk. Schwannomas are more common neurofibromas. They usually present in the fourth decade of life.

Clinical Presentation

Schwannomas in the neck may present as a painless mass. Deeply seated tumors in the region of the jugular foramen may cause nerve compression resulting in single or multiple cranial nerve palsies.

Pathology

Schwannomas, unlike neurofibromas, are encapsulated tumors. Histology shows Schwann's cells organized in compact interlacing groups associated with fibrous strands. Schwannomas may show two histological patterns. Antoni type A shows compact palisading cells whereas Antoni type B shows a less cellular pattern consisting of cells with cytoplasmic lipids. Cystic degeneration is common. These tumors arise from a single focus and they grow by projecting from one side of the nerve.

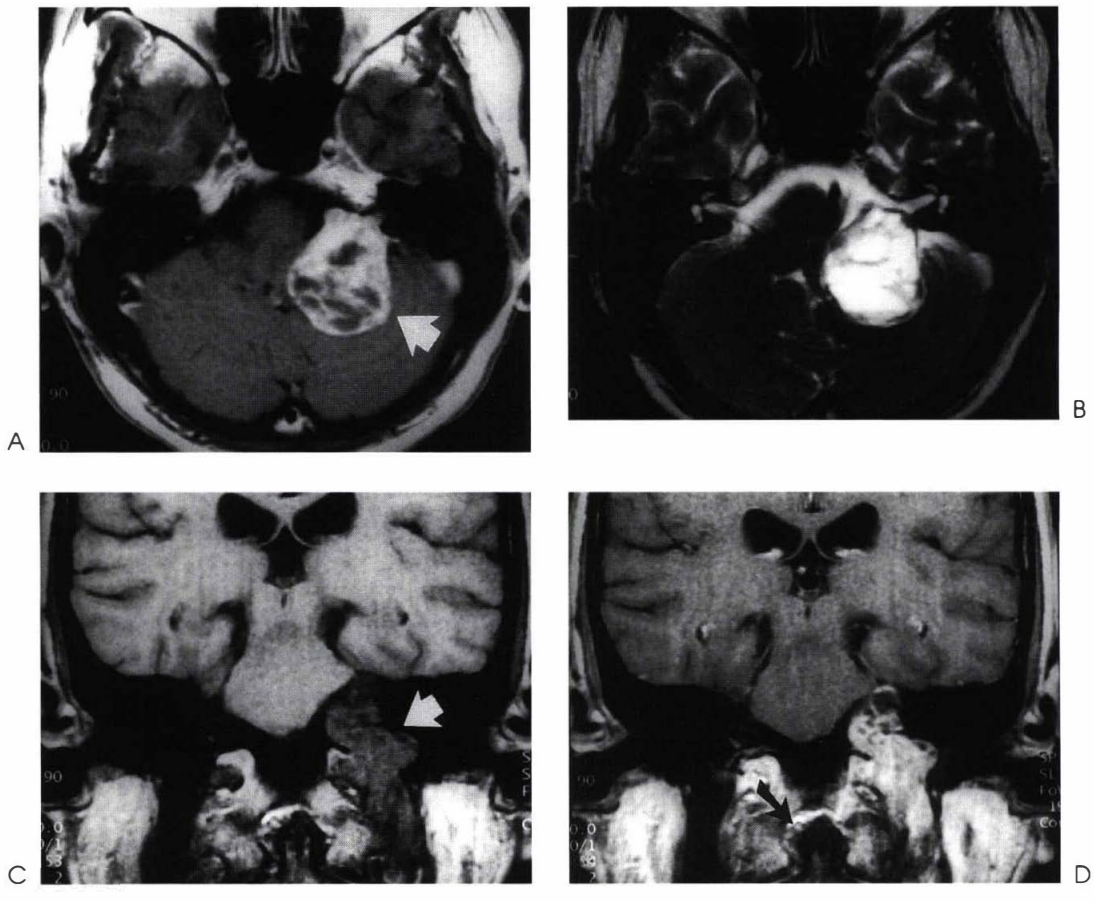

Figure 173–1. Vagal schwannoma with transjugular extension. (A) Axial contrast-enhanced MR image shows a heterogeneously enhancing mass in the left cerebellopontine angle (arrow). (B) Axial T2-weighted MR image shows the high signal intensity mass is not associated with a mass in the internal acoustic meatus. (C) Coronal T1-weighted MR image shows an intermediate signal intensity mass straddling the left jugular foramen (arrow). (D) Coronal contrast-enhanced MR image shows good contrast enhancement. Note that the odontoid process (arrow) is a good landmark to locate the jugular foramen on coronal MR images. (continues)

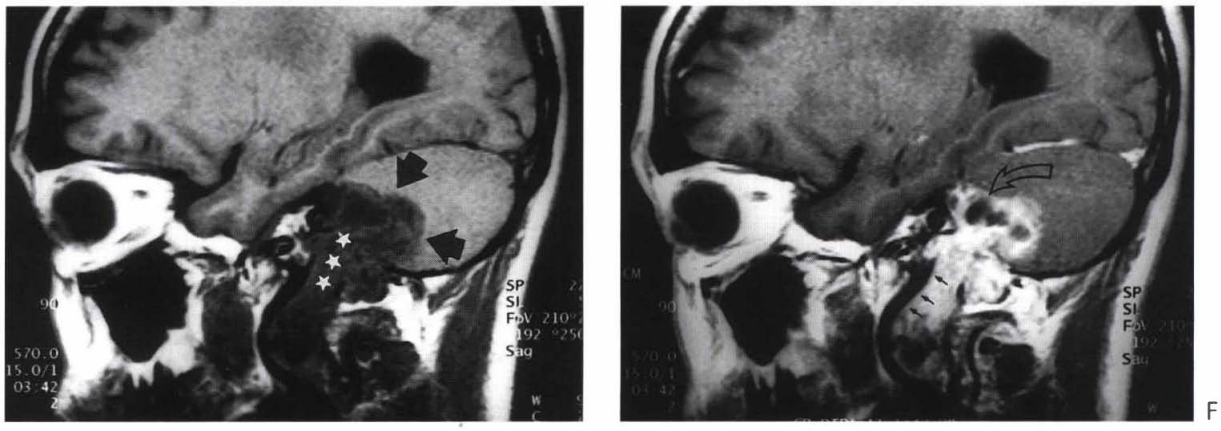

E F

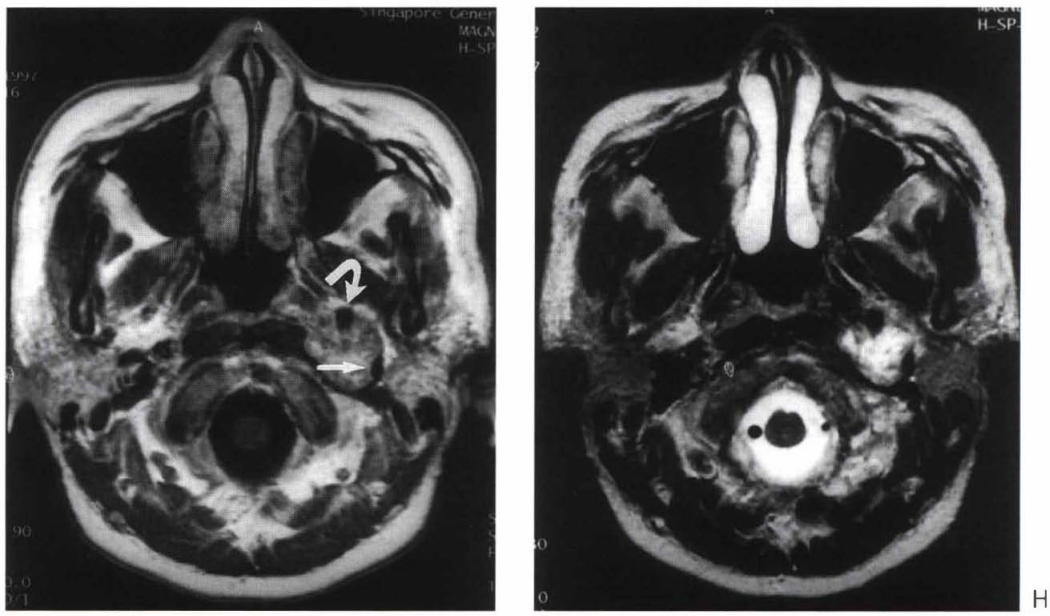

G H

Figure 173–1. (continued) (E) Sagittal T1-weighted MR image shows a heterogeneous intermediate mass in the posterior cranial fossa (arrows) extending through the jugular foramen (stars). (F) Sagittal contrast-enhanced MR image shows tumor enhancement but also areas of cystic degeneration (curved arrow). Note the anterior displacement of the carotid artery (arrows). (G) Axial contrast-enhanced MR image shows enhanced tumor in the left carotid sheath displacing the carotid artery anteriorly (curved arrow) and the internal jugular vein posterolaterally (arrow). (H) Axial T2-weighted MR image shows a high signal intensity carotid sheath mass splaying the left carotid artery and the internal jugular vein.

Treatment

Schwannomas are treated with surgical excision. As the tumor enlarges, it pushes away the parent nerve. These tumors may be removed without transecting the nerve.

Imaging Findings

CT

Schwannomas typically displace the internal carotid artery anteriorly and the jugular vein posterolaterally. Tumors originating high in the carotid sheath can cause scalloped erosion of the jugular foramen. These lesions show intermediate attenuation and good contrast enhancement. CT may also detect signs of vocal cord palsy or wasting of the sternocleidomastoid muscle.

MR

On T1-weighted images, schwannomas demonstrate intermediate signal intensity. These tumors show high signal intensity onT2-weighted images and also exhibit enhancement following contrast administration (Figs. 173–1 and 173–2).

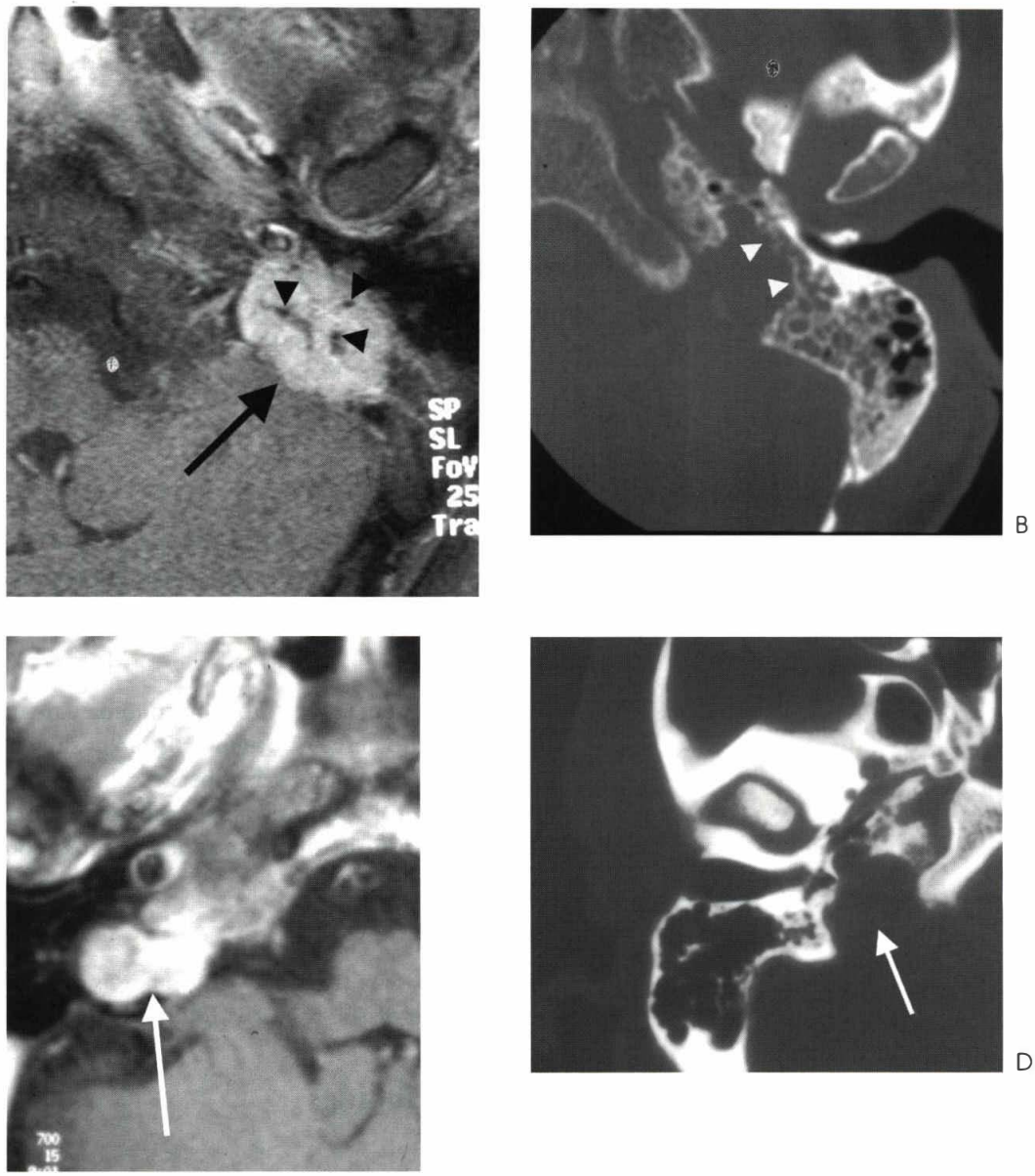

Figure 173-2. Skull Base Schwannoma versus Glomus Jugulare. (A) Axial contrast-enhanced MR shows a hypervascular mass (arrow) with multiple flow voids (arrowheads) which is characteristic of a glomus jugulare. (B) Corresponding CT through the jugular foramen shows enlargement and erosion of the inner cortex (arrowheads) which is characteristic of a glomus jugulare. (C) Axial contrast-enhanced MR in a different patient demonstrates an enhancing mass without internal flow voids located in the jugular foramen (arrow). These findings may be seen in a jugular foramen meningioma, or in this case, a schwannoma. (D) CT performed through the skull base in a patient with a jugular foramen schwannoma shows smooth expansion of the foramen (arrow) without bone erosion.

Imaging Pearls

- Schwannomas can be differentiated from glomus tumors by the lack of flow voids in larger lesions (> 2.5 cm diameter)
- A solitary schwannoma is indistinguishable from a neurofibroma.
- Vagal schwannomas can be separated from a sympathetic chain schwannoma. Sympathetic chain schwannomas typically displace the carotid artery laterally whereas vagal schwannomas displace the carotid artery anteriorly.
- Glomus jugulare lesions typically produce a permeative pattern of destruction of the jugular foramen in contrast to neurogenic tumors or meningiomas that characteristically cause scalloped enlargement of the jugular foramen.

Suggested Readings

1. Lewin JS. Imaging the suprahyoid neck. In: Valvassori GE, Mafee MF, Carter BL, eds. *Imaging of the Head and Neck*. New York: Thieme, 1995.
2. Caldemeyer KS, Mathews VP, Azzarelli B, Smith RR. The jugular foramen: a review of anatomy, masses, and imaging characteristics. *Radiographics* 1997;17:1123–1139.
3. Chong VFH, Fan YF. Radiology of the jugular foramen. *Clin Radiol* 1998;53:405–416.

Chapter 174

Neurofibroma

Epidemiology

Neurofibromas can arise from cranial as well as spinal nerves. These tumors may occur in isolation or as part of syndromes such as neurofibromatosis. Only 10% of patients with neurofibromas have neurofibromatosis. Neurofibromas usually present in the fourth or fifth decade of life. Neurofibroma in the neck typically involves the vagus nerve but may also arise from other cranial nerves and the sympathetic chain.

Clinical Findings

The usual presentation is that of a painless neck mass. However, associated cranial nerve symptoms may be evident such as paresthesia or cranial nerve palsy.

Pathology

Neurofibromas, in contrast to schwannomas, are nonencapsulated tumors. They contain all elements of the nerve of origin. Histology shows a mixture of Schwann's cells and fibroblasts dispersed among nerve fibers resulting in a fusiform dilation of the involved nerve. The matrix consists of mucopolysaccharides and an abundance of tissue fluid. The risk of malignant transformation into a neurofibrosarcoma is $< 5\%$.

Treatment

Neurofibromas are treated by surgical excision. As the fusiform tumor arises from the nerve itself, excision of the tumor is followed by nerve repair.

Imaging Findings

CT

The typical appearance of neurofibromas is a low attenuation fusiform mass on CT. This appearance may be due to a rich lipid or mucopolysaccharide content. These tumors may not show appreciable contrast enhancement. The low density (near water) on CT is characteristic (Fig. 174-1).

MR

The MR imaging appearance depends on the mucopolysaccharide or lipid constituent of the tumor. On T1-weighted images, the tumor usually shows intermediate signal intensity but in some patients may reveal high signals. These lesions usually enhance following contrast administration. On T2-weighted MR images, they have high signals reflecting the abundance of cellular fluid (Fig. 174-2).

Imaging Pearls

- Vagal neurofibromas originate within the carotid sheath. They cause displacement and separation of the carotid artery and internal jugular vein. They can be distinguished from glomus vagale because neurofibromas seldom show the degree of contrast enhancement demonstrated in glomus tumors, and they lack flow voids.
- A solitary neurofibroma has the same imaging characteristics and is indistinguishable from a solitary schwannoma.

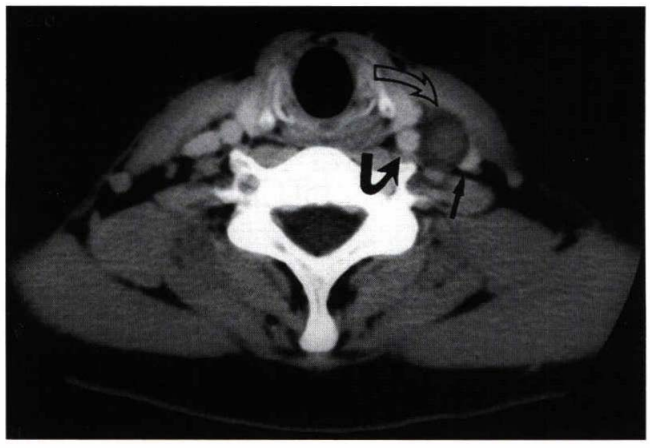

Figure 174–1. Vagal nerve neurofibroma. Axial contrast-enhanced CT shows a well-defined, low-density neurofibroma (hollow arrow) in the left carotid sheath. Note the medially displaced internal carotid artery (curved arrow) and the laterally displaced internal jugular vein (straight arrow).

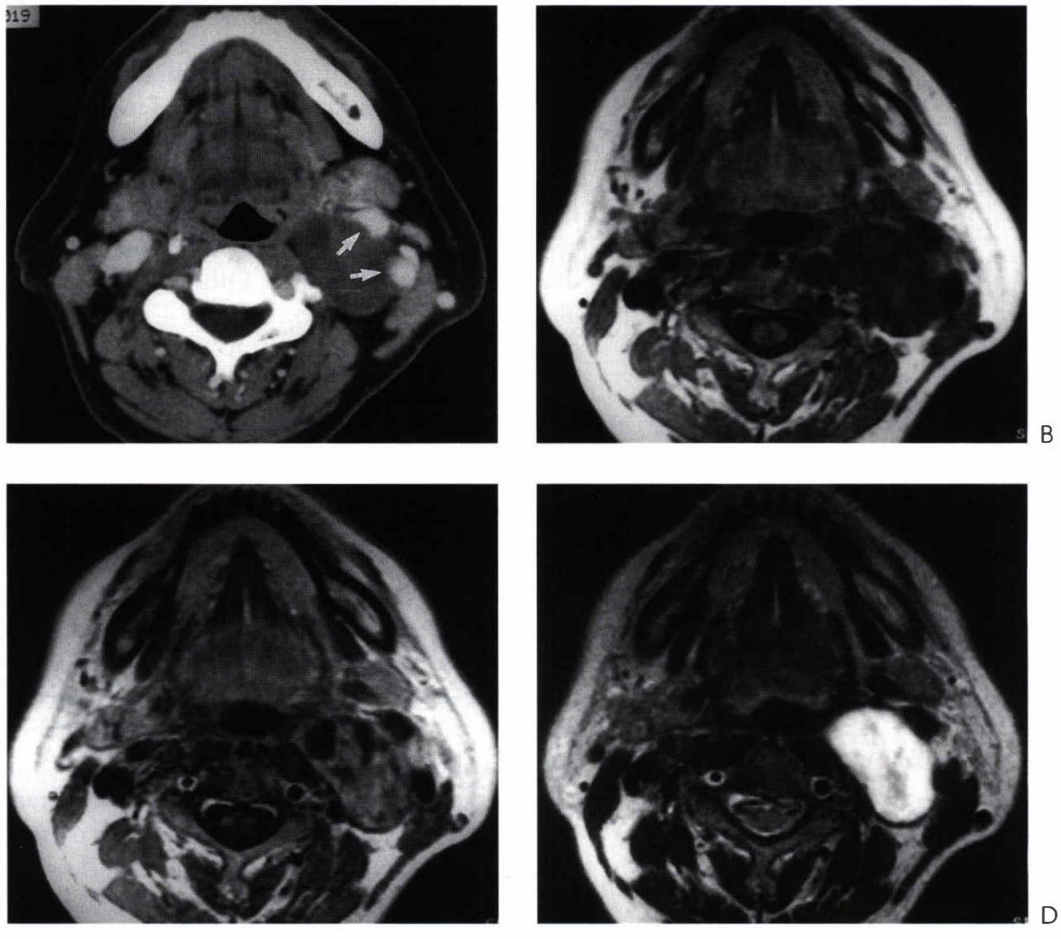

Figure 174–2. Sympathetic nerve neurofibroma. (A) Axial contrast-enhanced CT shows large, low-density carotid space mass displacing and splaying the internal and external carotid arteries (arrows). (B) Axial T1-weighted MR image shows an intermediate signal intensity sympathetic neurofibroma. (C) Axial contrast-enhanced MR image shows heterogeneous enhancement reminiscent of a schwannoma (lesion pathologically proven neurofibroma). (D) Axial T2-weighted MR image shows a well-circumscribed high signal intensity lesion.

- The presence of enhancement on a single imaging study cannot be used to distinguish between a neurofibroma and a neurofibrosarcoma. An enlarging lesion or a lesion that demonstrates increasing enhancement on serial studies is suspicious for sarcomatous degeneration in a patient with neurofibromatosis.

Suggested Readings

1. Kumar AJ, Kuhadja FP, Martinez CR, et al. Computed tomography of extracranial nerve sheath tumors with pathological correlation. *J Comput Assist Tomogr* 1983;7:857–865.
2. Harnsberger HR. *Handbook of Head and Neck Imaging.* Chicago: Mosby; 1995.
3. Chong VFH, Fan YF. Radiology of the carotid space. *Clin Radiol* 1996;51:762–768.

Chapter 175

Congenital Anomalies of the Third Branchial Apparatus

Epidemiology

Congenital anomalies of the third branchial complex are unusual lesions that can either consist of fistulas, sinuses, or cysts. There is no reported gender predilection. Because the third branchial pouch gives rise to a portion of the parathyroid glands and thymus, anomalous embryogenesis may result in a multisystem disease (DiGeorge's syndrome) rather than an isolated anomaly.

Embryology

The cartilage of the third branchial arch forms the lower body and greater horns of the hyoid bone. The musculature derived from the third branchial arch is limited to the stylopharyngeus muscle, which is supplied by the glossopharyngeal nerve. The mucosa covering the posterior third of the tongue base is also a derivative of the third arch. Some authors claim that the palatopharyngeus muscle and a portion of the skin over the carotid artery are also third arch derivatives. The third branchial cleft is normally obliterated by overgrowth of the second branchial arch. Other derivatives include the inferior parathyroid and thymus glands.

Clinical Features

The course of a third branchial apparatus fistula can be predicted based on the embryogenesis of the branchial arches and is illustrated in Figure 175–1. The skin opening of a third branchial apparatus fistula is in a similar location to that of a second branchial fistula along the anterior border of the sternocleidomastoid muscle. The tract ascends posterior to the common carotid or internal carotid arteries and anterior to the vagus nerve. During its ascent, the tract is located lateral to CN XII. However, near the angle of the mandible, the tract courses medially and passes over the hypoglossal nerve and below the glossopharyngeal nerve. Because the glossopharyngeal nerve innervates the third arch, the path of the fistula would be expected to course caudal to this nerve. The tract enters the posterolateral thyrohyoid membrane and communicates with the pyriform sinus.

Some authors have described isolated third branchial cysts. The cysts may be very extensive and extend inferiorly to the level of the thyroid gland. There is no significant enhancement of the cyst wall. The overlying sternocleidomastoid mastoid muscle is displaced laterally by the cyst. On initial evaluation, a third branchial cyst may be difficult to differentiate from a lymphatic malformation (lymphangioma). However, based on the embryology, some authors have suggested that a well-defined cystic mass located posterior to the carotid artery and jugular vein is indicative of a cyst of third branchial origin. The presence of a sinus opening confirms the diagnosis.

Pathology

Third branchial cleft cysts are epithelial-lined cysts that are located in the lateral compartment of the neck.

Treatment

The treatment is surgical resection with complete eradication of the fistulous tract.

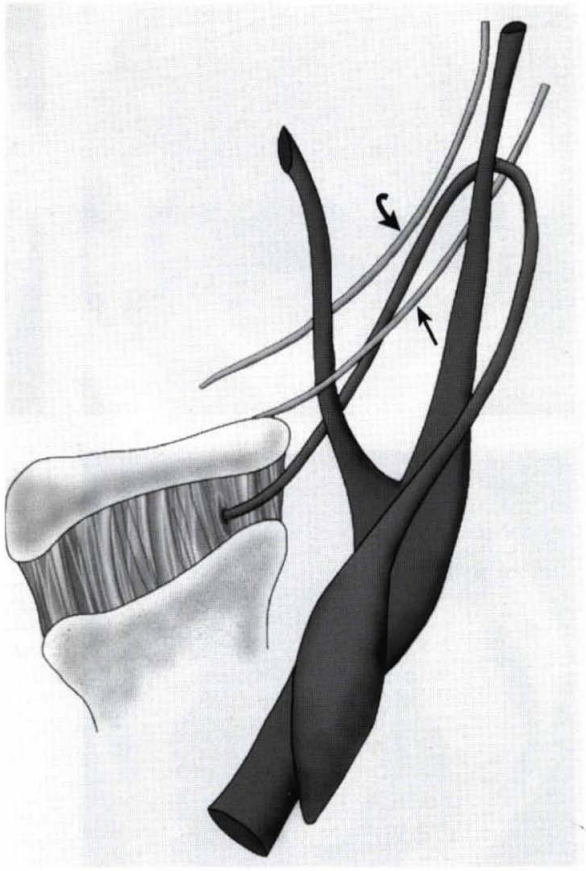

Figure 175–1. Schematic illustration of the third branchial cleft cyst. The tract ascends posterior to the carotid. Near the angle of the mandible, the tract courses medially and passes superior to the hypoglossal nerve (straight arrow) and below the glossopharyngeal nerve (curved arrow). The tract enters the posterolateral thyrohyoid membrane and communicates with the pyriform sinus. (Figure reproduced with permission from Mukherji SK, Fatterpekar G, Castillo M, Stone JA, Chung CJ. Imaging of congenital anomalies of the branchial apparatus. Neuroimaging Clin N Am *2000;10:75–93.)*

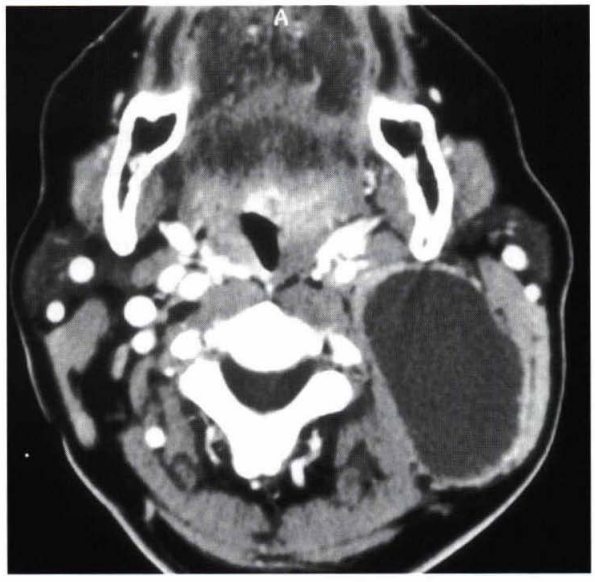

Figure 175–2. Axial contrast-enhanced CT shows the typical appearance of a pathologically proven third branchial cleft cyst. The mass is cystic with a very thin enhancing wall. The mass is posterior to the carotid space.

Imaging Findings

CT

Third branchial cleft cysts are well-defined, low attenuation cysts situated posterior to the carotid artery and jugular vein in the lateral compartment of the neck (Fig. 175–2). They may extend inferiorly to the level of the thyroid gland. There is no significant enhancement of the cyst wall.

MR

These lesions are low signal on T1-weighted sequences and high signal on T2-weighted sequences. There is a thin cyst wall that does not enhance with contrast (Fig. 175–3).

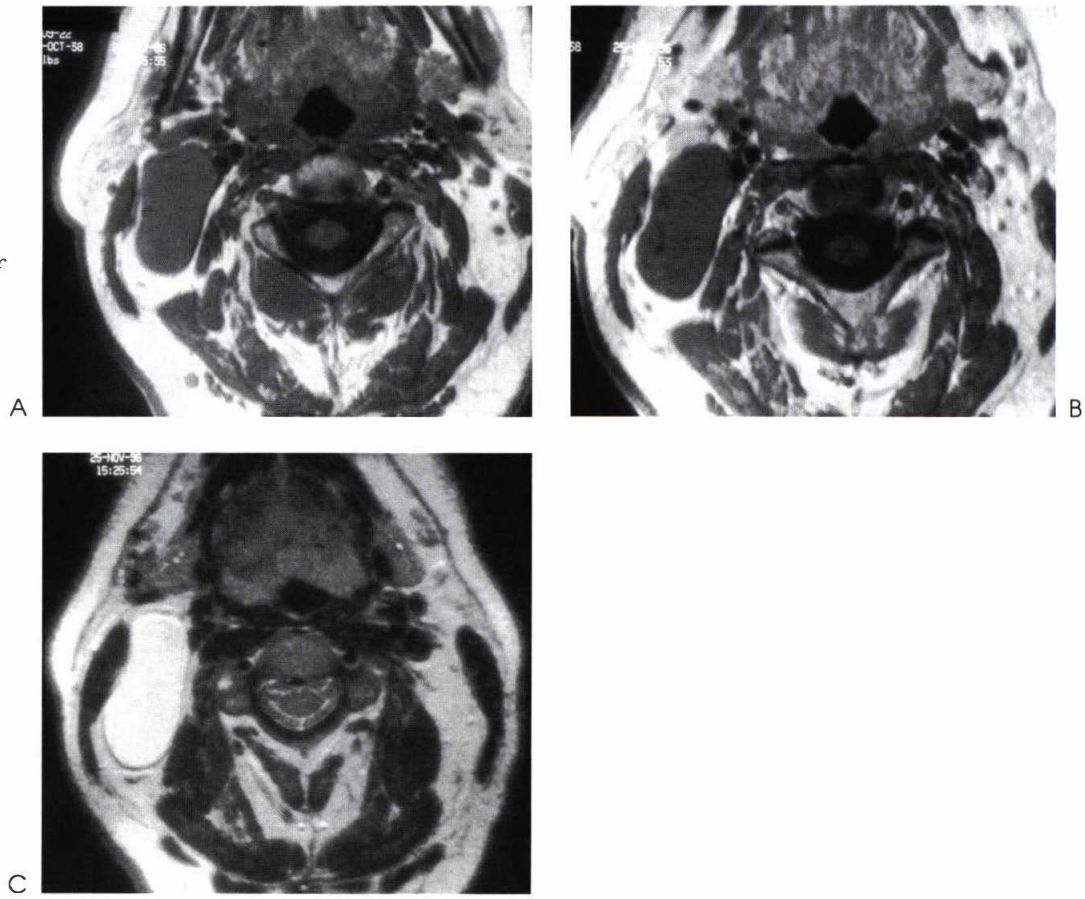

Figure 175-3. MR imaging of pathologically proven third branchial cleft cyst. (A) Axial noncontrast T1-weighted image shows an intermediate signal mass situated posterior to the carotid space. (B) There is minimal enhancement of the wall of the cyst following contrast administration. (C) Axial T2-weighted study shows increased signal indicative of the fluid within the cyst. (Figure reproduced with permission from Mukherji SK, Fatterpekar G, Castillo M, Stone JA, Chung CJ. Imaging of congenital anomalies of the branchial apparatus. Neuroimaging Clin N Am *2000;10:75-93.)*

Imaging Pearls

- Third branchial fistulas with a visible opening into the pyriform sinus may not be detected on cross-sectional imaging. A fistulogram may be necessary to identify the entire length of the tract.
- Third branchial cleft cysts may be difficult to differentiate from a lymphatic malformation (lymphangioma). The diagnosis of a third branchial cleft cyst should be suggested based on the characteristic location in the lateral compartment of the neck.

Suggested Readings

1. Himalstein MR. Branchial cysts and fistulas. *Ear Nose Throat J* 1980;59:47-53.
2. Zadvinskis DP, Benson MT, Som PM, Smoker WRK. Embryology and congenital cystic lesions. In: Som PM, Curtin H, eds. *Head and Neck Imaging.* 3rd ed. New York: Mosby; 1996:747-769.
3. Benson MT, Dalen K, Mancuso AA, Kerr HH, Cacciarelli AA, Mafee MF. Congenital anomalies of the branchial apparatus: embryology and pathologic anatomy. *Radiographics* 1992;12:943-960.

Chapter 176

Congenital Anomalies of the Fourth Branchial Apparatus

Epidemiology

Congenital anomalies of the fourth branchial complex are very rare lesions. Although both have been reported, fistulous tracts are more common than cysts. Occasionally, branchial cleft cysts have been described in the mediastinum. These cysts may represent either fourth or sixth branchial vestiges. If the cyst is located under the aorta, it represents a fourth branchial anomaly. However, a cyst situated below the pulmonary artery is believed to represent vestigial remnants of the sixth branchial apparatus. Congenital anomalies of the fourth branchial apparatus are more frequently found on the right than on the left (9:1). There is no reported gender predilection.

Embryology

The fourth pharyngeal pouch has dorsal and ventral components. The dorsal portion develops into the superior parathyroid glands. These migrate caudally and come to rest along the dorsal surface of the thyroid gland. The ventral portion of the fourth branchial pouch forms the ultimobranchial body, which gives rise to the calcitonin-producing parafollicular cells (C cells). The fifth pharyngeal pouch is incorporated into the fourth pouch and may, in part, contribute to the formation of the ultimobranchial body.

Clinical Findings

The course of a fourth branchial fistula is illustrated in Fig. 176–1 and is based on its embryology. The opening of the fistulous tract is located along the anterior border of the sternocleidomastoid muscle in a similar location to fistulas of second and third branchial origins. The tract penetrates the platysma muscle and initially descends anterior to the carotid sheath into the thoracic inlet. The tract then hooks inferiorly around the adjacent vascular structures derived from the fourth arch (left = aortic arch, right = subclavian artery) in a manner similar to the recurrent laryngeal nerve. It then ascends posterior to the common and internal carotid arteries in close association with the recurrent laryngeal nerve. The tract loops over the hypoglossal nerve and passes deep to the internal carotid artery. Because the superior laryngeal nerve is associated with the fourth arch, the tract remains inferior to this nerve. The tract penetrates the thyrohyoid membrane and communicates with the hypopharynx near the apex of a pyriform sinus.

Remnants of the fourth branchial arch may present with recurrent infections. Recurrent abscesses may be located in the neck or be associated with the thyroid gland. These cases will often have a fistulous opening at the base of the pyriform sinus. The presence of an internal fistula should be evaluated preoperatively because resection of the entire fistulous tract is necessary for a successful surgical treatment.

Pathology

Fourth branchial cleft cysts are characterized by a nonkeratinized stratified squamous epithelial lined wall surrounded by reactive lymphoid tissue.

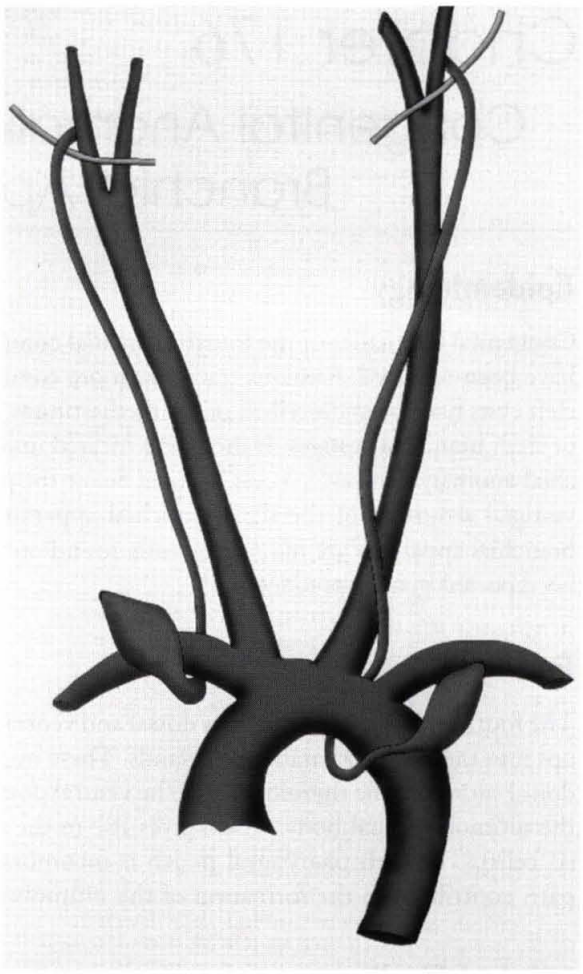

Figure 176-1. Schematic illustration of fourth branchial anomalies. The course of the tract mirrors the course of the recurrent laryngeal nerve and runs beneath the aortic arch on the left and the subclavian artery on the right. (Figure reproduced with permission from Mukherji SK, Fatterpekar G, Castillo M, Stone JA, Chung CJ. Imaging of congenital anomalies of the branchial apparatus. Neuroimaging Clin N Am *2000;10:75-93.)*

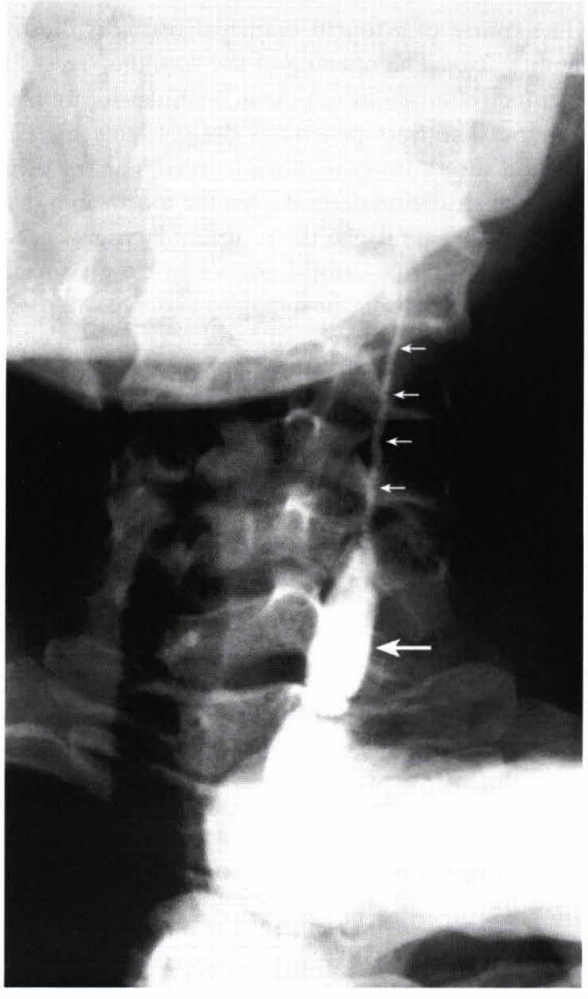

Figure 176-2. Fistulogram of a fourth branchial anomaly demonstrates both a cystic (large arrow) and a "tract" (small arrows) component of the anomaly. (Figure reproduced with permission from Castillo M, Mukherji SK. Imaging of the Pediatric Head, Neck and Spine. *Philadelphia; Lippincott-Raven;1996:576.)*

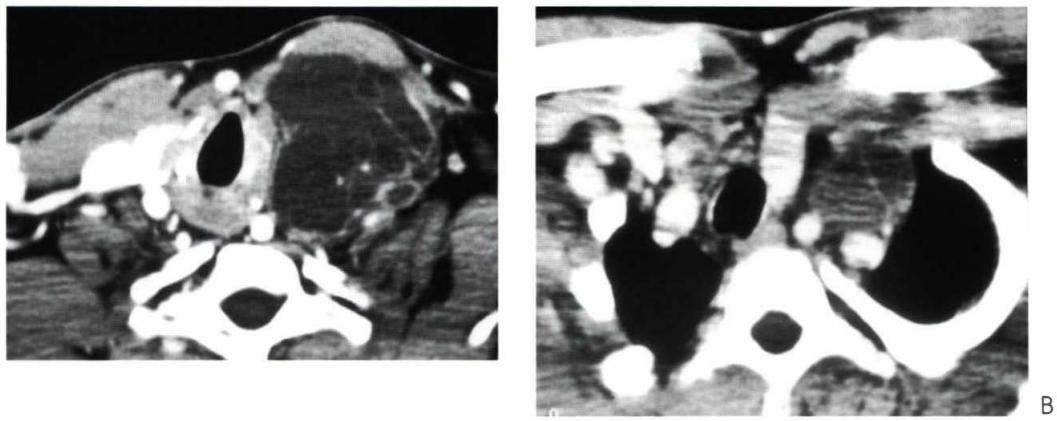

Figure 176–3. Pathologically proven branchial anomaly. (A) Axial contrast-enhanced CT shows a cystic mass with multiple internal septations located deep to the sternocleidomastoid muscle. (B) The mass extends inferiorly into the thoracic inlet. Pathology revealed branchial anomaly. Given the location and the course of the lesion, this was believed to represent a fourth branchial anomaly.

Imaging Findings

Fistulogram

A fistulogram performed with water soluble iodinated contrast material is the study of choice for evaluating patients suspected of having a fistula arising from the fourth branchial apparatus. Cross-sectional imaging is of limited value because a small fistulous tract may not be detected (Fig. 176–2).

CT

CT performed after opacification of the tract may be beneficial; however, because these lesions are so rare the true utility of this technique is not yet determined (Fig. 176–3).

Imaging Pearls

- A fourth branchial pouch cyst in the larynx adjacent to the pyriform sinus needs to be differentiated from a laryngocele.
- A sinus opening associated with a fistulous tract that descends into the mediastinum is suggestive of a fourth branchial anomaly.
- Children with recurrent infections of the soft tissues of the neck or thyroid gland should be evaluated for having an underlying congenital anomaly of the fourth branchial apparatus.

Suggested Readings

1. Al-Ghamdi S, Freedman A, Just N, Rochon, L, Frenkel S. Fourth branchial cleft cyst. *J Otolaryngol* 1992;21:447–449.
2. Whitworth IH, Suvarna SK, Wight RG, Walsh-Warning GP. Fourth branchial arch anomaly: a rare incidental finding in an adult. *J Laryngol Otol* 1993;107:238–239.
3. Benson MT, Dalen K, Mancuso AA, Kerr HH, Cacciarelli AA, Mafee MF. Congenital anomalies of the branchial apparatus: embryology and pathologic anatomy. *Radiographics* 1992;12:943–960.

Section VIII

Buccal Space

The location and name of the buccal space (BS) can be easily remembered if one realizes that the buccal space is bordered medially by the buccinator muscle that attaches to the outer cortex of the maxillary alveolar ridge. The BS is tucked away between the maxillary alveolar ridge medially, the masticator space posteriorly, and the parotid space laterally. Anteriorly, the BS is separated from the subcutaneous tissues of the face by the plane formed by the superficial muscles of facial expression (greater and lesser zygomatic muscles, risorius) and the investing fascia (Figs. VIII–1 through VIII–4A,B).

The BS does not have a complete fascial covering that separates it from the adjacent spaces. The lack of defined boundaries allows extension of clinically overt and occult infections through the BS. Inferiorly, the BS blends with the submandibular space. The deep fat of the BS also blends into the fat of the posterolateral portion of the MS (suprazygomatic MS, infratemporal fossa). This extension passes deep to the zygomatic arch and ascends superiorly and laterally to surround the coronoid process of the mandible and the insertion of the temporalis muscles, which are part of the MS.

The BS consists mostly of adipose tissue. The other contents of the BS are minor salivary gland tissue and the parotid duct, lymph nodes, facial vein, facial (angular) and buccal artery, buccal branch of the facial nerve, and buccal division of the mandibular division of CN V. The facial artery and vein lie just anterior to the buccal segment of the parotid duct. These structures separate the buccal space into anterior and posterior compartments. The adipose tissue of the deep BS is distinct from the fat within the anterior BS and subcutaneous tissue. The fat of the deep BS is a special form of adipose tissue known as syssarcosis. This is likely the remnant of the succatory fat pad of infants that aids the muscular motion needed to open and close the mouth. This unique tissue can be identified on CT by its consistently lower attenuation compared with the fat of the anterior BS and subcutaneous tissue of the face.

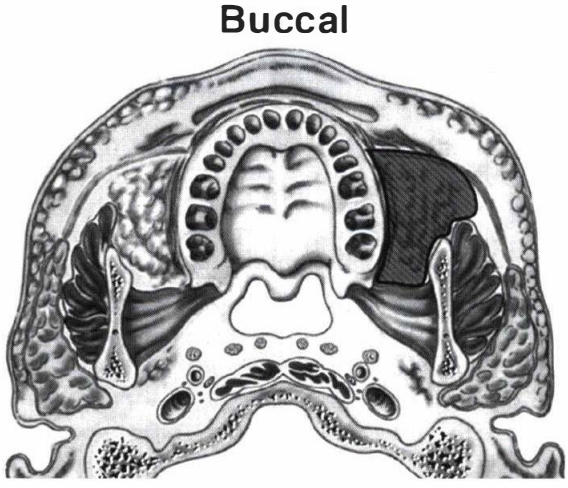

Figure VIII–1. Schematic illustration of the buccal space (see Color Plate VIII–1) (Figure reproduced with permission from Mukherji SK, Castillo M. A simplified approach to the spaces of the suprahyoid neck. Rad Clin N Am *1998;36:761–780.)*

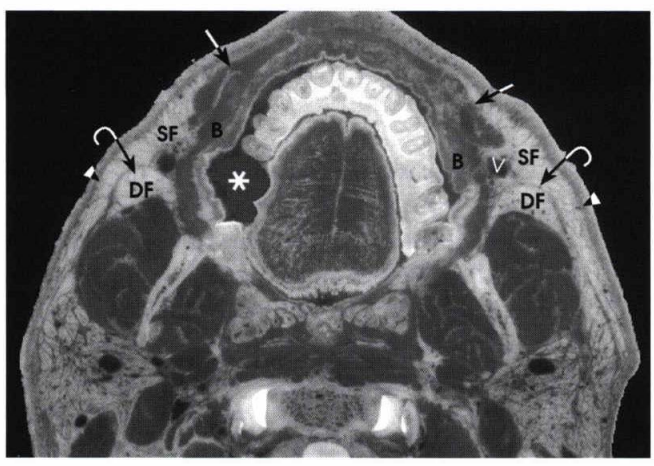

*Figure VIII–2. Anatomic image of the buccal space demonstrates the normal antomy of the buccal space. V, facial vein; DF, deep fat of the buccal space; arrowheads, lateral extent of the fat of the buccal space; curved arrow, parotid duct; * alveolar recess of the alveolar ridge; small arrows, superficial muscles of facial expressions; B, buccinator muscles). Note the difference in the appearance of the deep fat of the buccal space compared with the fat of the anterior BS (SF) and subcutaneous tissue of the face on the various images.*

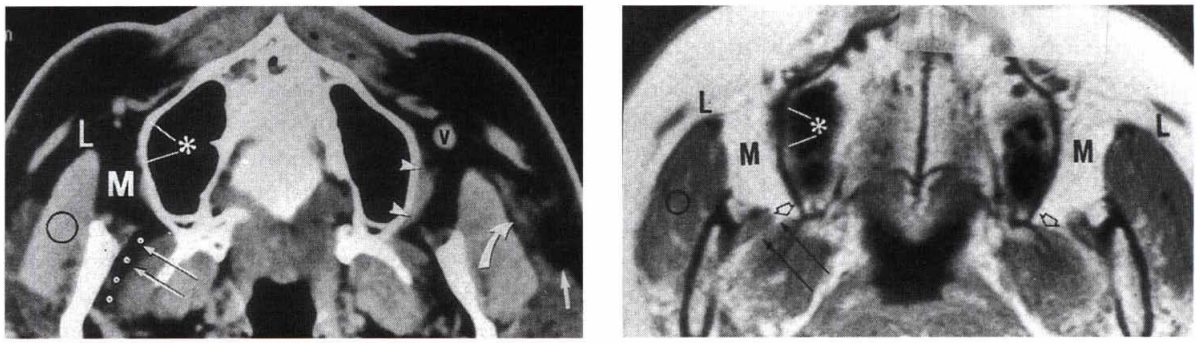

A B

Figure VIII-3. Normal anatomy of the upper buccal space depicted by (A) a contrast material-enhanced CT scan and (B) an unenhanced T1-weighted MR image of different patients. At this level, the lateral projection of buccal fat (L) extends to the anterior margin of the parotid gland [short straight arrow in (A)] and envelops an accessory parotid gland on the left [curved arrow in (A)] within the left buccal space. The medial projection of buccal fat (M) is seen between the masseter muscle (o) and the maxilla (•). The posterior extent of the medial buccal fat pad (M) is limited by the pterygoid muscle and the overlying fascia [open arrows in (B)]. This investing fascia is incomplete, so there is often a direct communication between the medial buccal fat pad and the fat within the masticator space [dots in (A)] between the pterygoid muscles (long thin arrows). The origin of the buccinator muscle [arrowheads in (A)] is seen on the left side. The facial vein [v in (A)] is seen within the buccal space on the left side. (Figures and captions reproduced with permission from Tart RP, Kotzur IM, Mancuso AA, et al. CT and MR imaging of the buccal space and buccal space masses. Radiographics *1995;15:531-550.)*

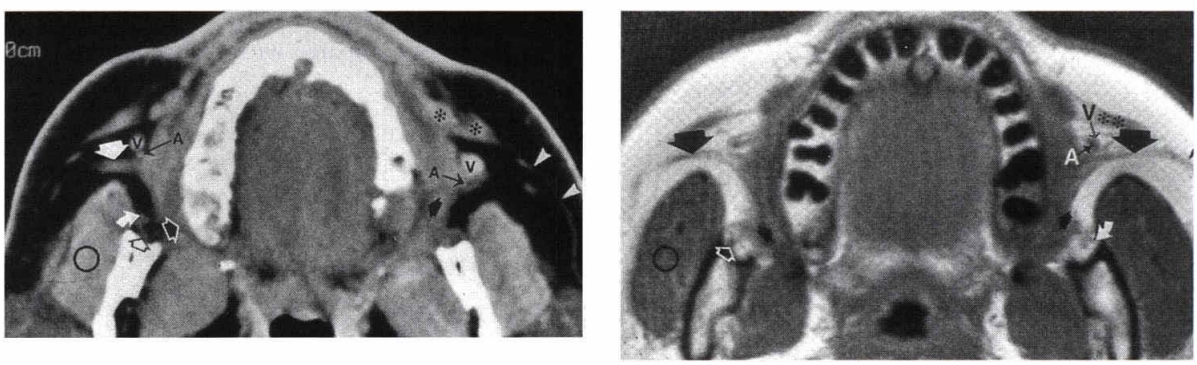

A B

Figure VIII-4. Normal anatomy of the middle buccal space depicted by a contrast-enhanced CT scan (A) and unenhanced T1-weighted MR image (B) of different patients. This level is demarcated by the parotid duct coursing through the buccal space (large arrows). Anterior to the duct lies the angular portion of the facial vein (V) and artery (A), which are typically found close to each other. Note that the posterior extension of the submucosal fat pad (small straight solid arrows) is more distinctly seen on MRI than on CT images. Generally, in our series, this fat pad was seen inconsistently with CT and MR imaging, and its absence did not reliably represent infiltration by a neoplasm. It is more important to look for asymmetry between the left and right sides in each individual patient. Note the decreased attenuation and increased signal intensity, relative to subcutaneous fat, of the buccal fat pad, which is separated by the superficial muscles of facial expression (*) and investing fascia (arrowheads). This difference in attenuation is more distinctly and reliably seen on the CT scan. The buccal artery (curved arrow) was consistently seen at this level along the medial margin of the masseter muscle (○), just anterior to the tendon of the temporal muscle (open arrow). (Figures and captions reproduced with permission from Tart RP, Kotzur IM, Mancuso AA, et al. CT and MR imaging of the buccal space and buccal space masses. Radiographics *15:531-550, 1995.).*

The most common mass involving the BS is squamous cell carcinoma. The tumor may extend into the BS from deep extension of a buccal carcinoma arising from the oral or nasal cavity or as metastatic involvement of a buccal lymph node. The most common primary lesion of the BS of uncertain cause is a minor salivary gland tumor. Other mesenchymal lesions arising in the buccal space include hemangiomas, lipomas, and soft tissue sarcomas. BS cellulitis or abscess may arise from an infection of the MS or oral cavity. BS lymphoma may either arise within the buccal lymph node or be extranodal. A dilated parotid duct, most commonly due to an obstructed calculi located at the orifice of Stensen's duct, or accessory parotid tissue may also present as a BS mass.

Suggested Readings

1. Grodinsky M, Holyoke EA. The fasciae and fascial spaces of the head, neck and adjacent regions. *Am J Anat* 1938;63:367–408.
2. Mukherji SK, Castillo M. A simplified approach to the spaces of the extracranial head and neck. *Radiol Clin North Am* 1998;36:761–780.
3. Harnsberger HR. In: *Handbook of Head and Neck Imaging*. 2nd ed. St. Louis: Mosby Year Book; 1995.
4. Kostrubula JG. Potential anatomic spaces in the face. *Am J Surg* 1945;68:28–37.
5. Tart RP, Kotzur IM, Mancuso AA, et al. CT and MR imaging of the buccal space and buccal space masses. *Radiographics* 1995;15:531–550.

Chapter 177

Accessory Salivary Tissue

Epidemiology

In the embryo, the parotid gland appears as an elongation developing from the buccal epithelium. The main portion of this elongation persists as the parotid duct; the proximal end becomes the opening of the parotid duct whereas the distal end branches repeatedly to form the parotid gland. The accessory parotid gland is separate from the main parotid gland and develops superior to the main parotid duct. Minor salivary glands can also be seen along the parotid duct and in the buccal space.

Clinical Findings

Small lesions are asymptomatic and are detected incidentally on scans performed for unrelated reasons. The most common presentation is a painless cheek mass. The lesion feels soft and nontender. However, tumors and infections may involve the minor salivary glands and present clinically as a cheek mass.

Pathology

Biopsy shows normal salivary gland tissues.

Treatment

No treatment is required if the lesion is small and asymptomatic. Large lesions may be considered for surgery based on cosmetic reasons.

Imaging Findings

CT

Contrast-enhanced CT shows a mass in the buccal space superficial to the parotid duct with imaging characteristics that are similar to a normal adjacent parotid gland (Figs. 177-1 and 177-2).

MR

The signal intensity of the mass in the buccal space parallels that of normal parotid gland tissues in all MR imaging sequences.

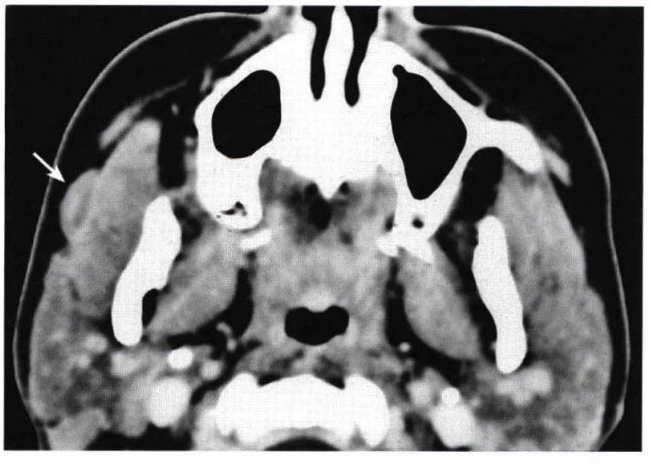

Figure 177-1. Axial contrast-enhanced CT demonstrates a well-circumscribed, low attenuation mass located anterior to the parotid gland in the posterolateral aspect of the buccal space (arrow). This is the typical appearance of accessory salivary tissue.

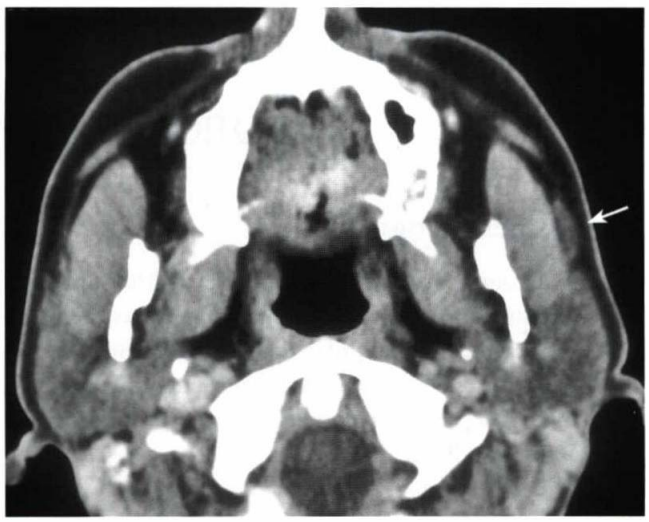

Figure 177–2. Axial contrast-enhanced CT demonstrates another typical appearance of accessory salivary tissue in the posterolateral aspect of the buccal space (arrow).

Imaging Pearl

- Accessory parotid tissue has a characteristic appearance and location. It should not be confused with a neoplasm.

Suggested Readings

1. Mukherji SK, Castillo M. A simplified approach to spaces of the suprahyoid neck. *Radiol Clin North Am* 1998;36:761–780.
2. Bannister LH, Berry MM, Collins P, et al. *Gray's Anatomy*. 38th ed. Edinburgh: Churchill Livingstone; 1995:174–181.

Chapter 178

Parotid Duct Calculus

Epidemiology

The main parotid (Stensen's) duct courses anteriorly over the masseter muscle, turns medially into the buccal space, and penetrates the buccinator muscle. The duct opens opposite the second upper molar tooth. Most stones in the parotid gland are solitary but multiple stones or calcifications are often encountered in patients with chronic infection. Chronic infection may be secondary to recurrent bacterial infection or granulomatous disease such as tuberculosis.

Clinical Findings

Patients usually present with a history of repeated episodes of acute sialadenitis. There are intervening asymptomatic periods associated with a decrease in the size of the parotid gland. Some patients may, however, present with a slowly enlarging gland with episodes of acute infection. Physical examination reveals an enlarged parotid gland, which may be tender. A dilated parotid duct, which is usually due to a stone in the orifice of Stensen's duct or accessory parotid tissue, may rarely appear as a mass in the buccal space.

Pathology

Chronic recurrent sialadenitis is usually secondary to incomplete ductal obstruction as a result of sialolithiasis or strictures from previous suppuration. Repeated episodes of infection often lead to destruction of the glandular acini and multiple small abscesses.

Treatment

It is important to differentiate between chronic infection caused by obstructive versus nonobstructive disease because management is often different. Local excision or removal through an endoluminal approach may be used to treat small stones located at the opening of Stensen's duct. Parotidectomy may be required for patients with recurrent, severe infection and extensive acinar destruction.

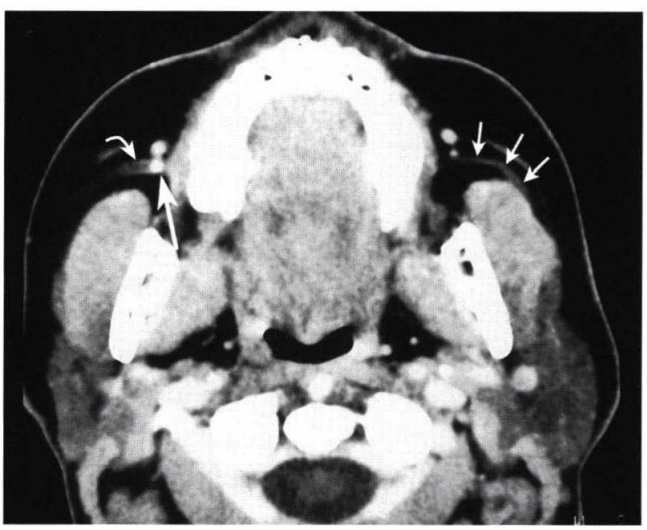

Figure 178–1. Axial contrast-enhanced CT demonstrates a small calculus located in the distal aspect of the parotid duct (large arrow). There is dilatation of the duct just proximal to the stone (curved arrow). Note the normal appearance of the parotid duct on the opposite side (small arrows).

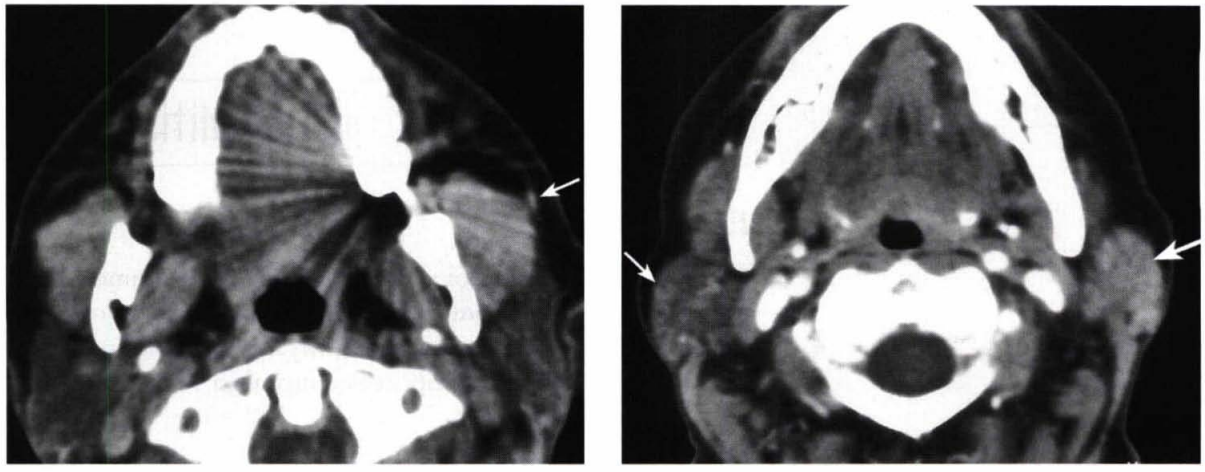

Figure 178–2. (A) Noncontrast CT demonstrates a small calculus located in the proximal parotid duct as it exits the parotid gland (arrow). (B) Contrast-enhanced CT performed in the same patient illustrated in (A) demonstrates increased enhancement of the parotid gland due to an obstructive sialadenitis caused by the obstructing calculus (large arrow). Note the appearance of normal gland on the opposite side (small arrow).

Imaging Findings

CT

Noncontrast CT should be performed to identify the calculus. The dilated parotid duct can be seen either on noncontrast or contrast-enhanced studies. Contrast-enhanced CT shows diffuse enlargement and increased density of the affected gland. There may be scattered calcified stones in the main parotid duct or within the glandular parenchyma (Figs. 178–1 and 178–2).

MR

On T1-weighted MR images, the gland shows low to intermediate signal intensity. On T2-weighted and contrast-enhanced images, there are heterogeneous high signal intensity areas reflecting regions of inflammation and fibrosis.

Imaging Pearls

- Parotid sialography is still a useful technique in separating obstructive from nonobstructive causes of recurrent parotid infection. This modality is, however, contraindicated in patients during episodes of acute infection.
- CT is the imaging modality of choice because calcified stones often escape detection by MR imaging.

Suggested Readings

1. Som PM, Brandwen M. Salivary glands. In: Som PM, Curtin H, eds. *Head and Neck Imaging*. 3rd ed. New York: Mosby; 1996:823–914.
2. Batsakis JG. Nonneoplastic diseases of the salivary glands. In: Batsakis JG, ed. *Tumors of the Head and Neck*. 2nd ed. Baltimore: Williams and Wilkins; 1979:100–120.

Chapter 179

Cellulitis

Epidemiology

Infection originating from the buccal space is uncommon. However, cellulitis spreading into the buccal space from adjoining spaces or structures can frequently be detected. Infection usually originates in the face, buccal cavity, and masticator space and mandible or odontogenic structures. Other causes include a variety of traumatic injuries.

Clinical Findings

Cellulitis involving the buccal space is, as a rule, overshadowed by infection in the space or structure of origin. Clinically, inflammation is detected in the cheek anterior to the masseter muscle.

Pathology

The buccal space can be involved in patients with mandibular osteomyelitis or odontogenic or masticator space abscess. These patients are typically adolescents or adults with poor oral hygiene. Other underlying causes include previous irradiation for head and neck malignancy and diabetes mellitus. *Staphylococcus* is the most commonly implicated organism but a wide variety of anaerobes may also be found.

Treatment

Treatment is directed at the underlying cause. Cellulitis can be controlled with antibiotics but abscesses require surgical drainage.

Imaging Findings

CT

Contrast-enhanced CT shows enhancement in the buccal space. This is easy to identify on CT, as the buccal space is normally filled with fat, which provides an excellent natural contrast (Figs. 179–1 through 179–4).

MR

T1 MR imaging can easily identify the buccal space component of an inflammatory process. Inflammation shows intermediate signal intensity in contrast to the normal high signal intensity fat. The signal is increased on T2-weighted sequences. There is diffuse enhancement on contrast-enhanced T1-weighted images. Differentiation between cellulitis and adjacent normal fat on postcontrast T1-weighted images depends on the quality of fat suppression.

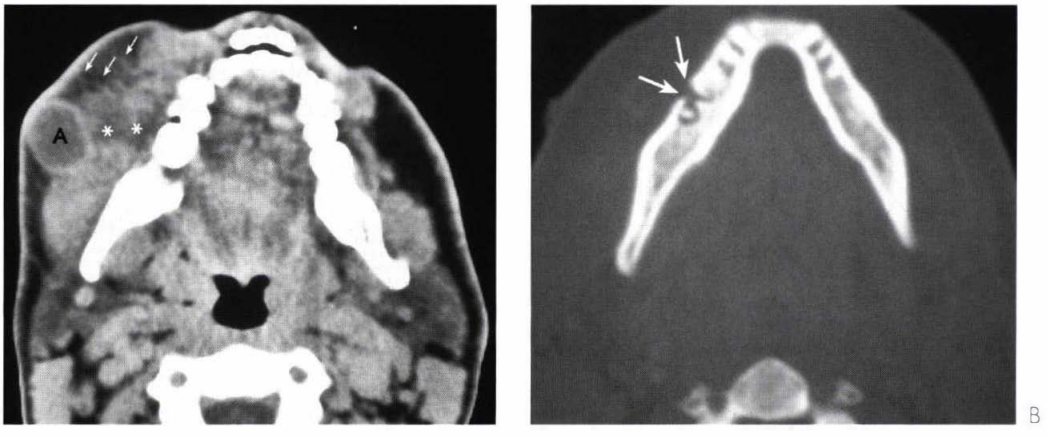

Figure 179–1. (A) Axial contrast-enhanced study obtained through buccal space demonstrates reticulation of the subcutaneous fat (small arrows), edema in the buccal space (*), and an abscess (A). (B) Bone algorithm demonstrates a focal cortical erosion of the buccal cortex overlying a molar consistent with severe odontogenic infection with associated osteomyelitis (arrows). This process was believed to be the cause of the cellulitis and abscess illustrated in (A).

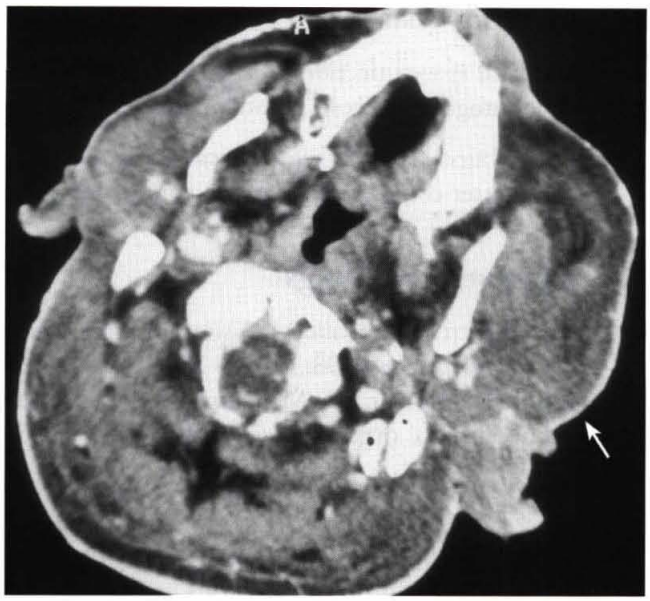

Figure 179–2. There is diffuse swelling and edema of the left buccal space (arrow) in a patient who was severely burned.

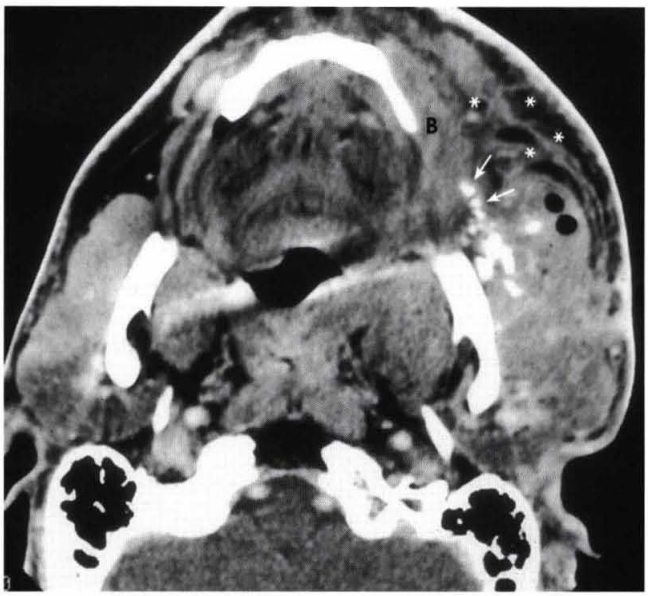

Figure 179–3. Axial image obtained in a patient following a gunshot injury demonstrates multiple metallic fragments involving the masticator space, which extend into the buccal space (arrows). Note the edema and reticulation of the subcutaneous fat (*) and thickening of the buccinator muscle (B).

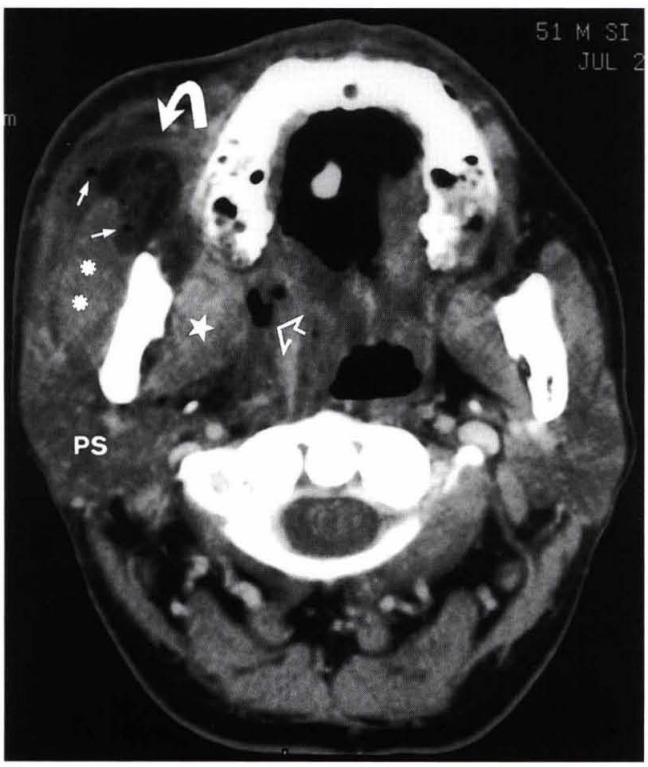

Figure 179–4. Axial contrast-enhanced CT shows spreading inflammation involving the right parotid space (PS), masticator space [medial pterygoid muscle (star), masseter muscle (asterisks)], and buccal space (curved arrow). The small gas bubbles in the right buccal space (arrows) and gas (hollow arrow) in the right parapharyngeal space may represent abscess formation or necrotizing fasciitis.

Imaging Pearls

- Buccal space infection is usually due to inflammation elsewhere. A search may reveal an odontogenic abscess, mandibular osteomyelitis or parotid abscess.
- The buccal space is symmetrical. Early disease in the buccal space may be easier to identify after comparison with the contralateral side.

Suggested Readings

1. Mukherji SK, Castillo M. A simplified approach to spaces of the suprahyoid neck. *Radiol Clin North Am* 1998;36:761–780.
2. Tart RP, Kotzur IM, Mancuso AA, et al. CT and MR imaging of the buccal space and buccal space masses. *Radiographics* 1995;15:531–550.

Chapter 180

(Buccinator) Lymph Nodes

Epidemiology

The "facial" nodes belong to one of the most inconsistently demonstrated groups of nodes. Most of the afferent drainage of these nodes is from the skin and mucous membranes of the face. The efferent drainage is via the submandibular nodes. The facial nodes are usually divided into five groups: mandibular, buccinator, infraorbital, malar, and retrozygomatic nodes (Fig. 180-1). The buccinator nodes are located in the buccal space. Lymphoma and metastatic lymphadenopathy affect these nodes infrequently. A review of the literature showed 44 cases, of which imaging studies were available in 25.

Clinical Findings

Buccal space lymphadenopathy presents as a mass in the cheek. The primary lesion is usually already evident.

Pathology

The reported primary malignancies include squamous cell or adenocarcinoma of the maxillary sinus, tongue, lip, buccal mucosa, preauricular skin, salivary glands, retromolar trigone, and nasopharynx. Metastases to facial lymph nodes from squamous cell carcinoma usually occur in patients with multiple recurrences (Figs. 180-2 through 180-4). The prognosis tends to be poor because this represents metastases from dermal lymphatic metastases. Lymphomas also form a major group responsible for facial lymphadenopathy. Others include metastatic disease from ocular melanoma and distant sites such as bladder carcinoma.

Treatment

The lymph nodes with metastasis should be excised along with the primary lesion. Postoperative radiation therapy may be combined with surgery. In patients with lymphoma, the recommended treatment is chemotherapy or radiation therapy depending on tumor staging and histologic type.

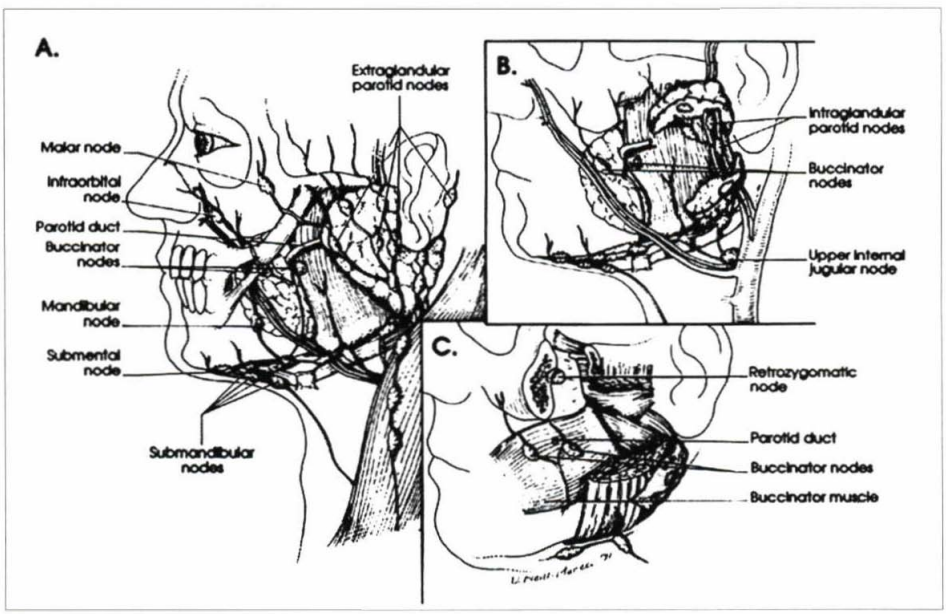

Figure 180-1. Schematic illustration of the facial lymph nodes including the buccal (buccinator) group of lymph nodes. (Figure reproduced with permission from Tart RP, Mukherji SK, Avino AJ, Stringer SP, Mancuso AA. Facial lymph nodes: normal and abnormal CT appearances. Radiology *1993;188:695-700.)*

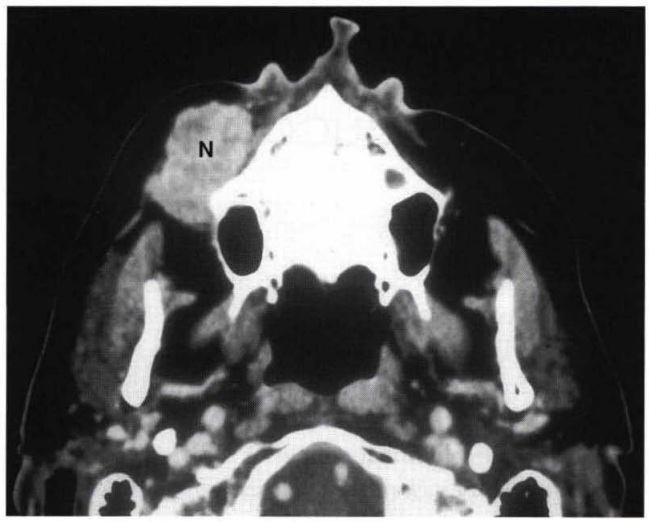

Figure 180–2. Axial contrast-enhanced CT demonstrates an enlarged right buccal lymph node (N) located in the inferior portion of the buccal space. This patient had a history of multiple recurrent squamous cell carcinomas of the oral cavity and presented with a right "cheek" mass.

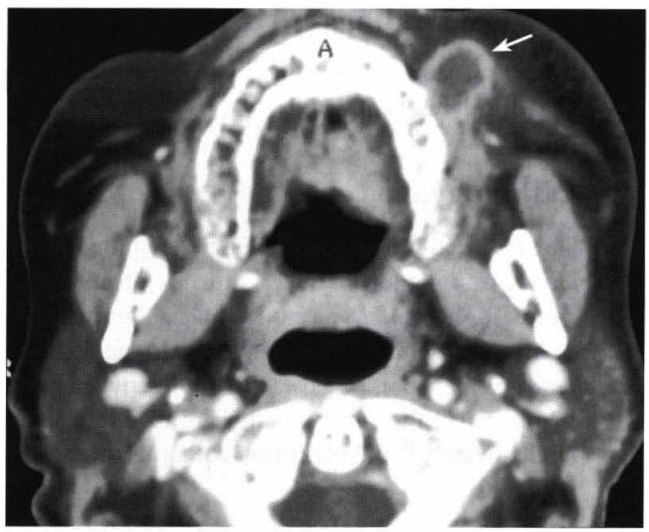

Figure 180–3. Contrast-enhanced CT shows a necrotic left buccal space lymph node (arrow). Pathology revealed squamous cell carcinoma.

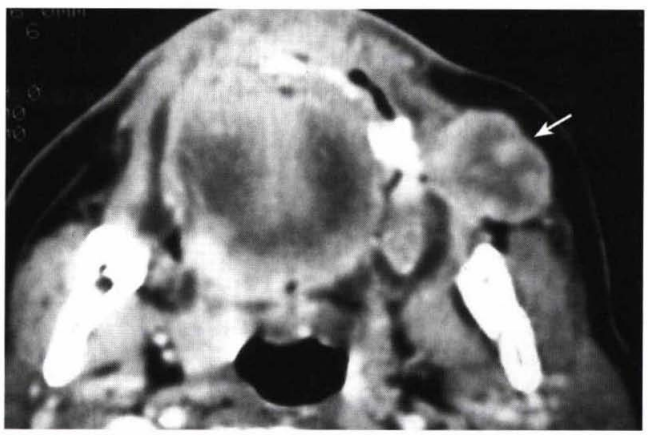

Figure 180–4. This illustration demonstrates another characteristic example of an enlarged metastatic buccal lymph node (arrow). The central areas of decreased attenuation are either metastatic deposits or necrosis.

Imaging Findings

CT

Facial nodes are found along the course of the facial vessels. Normal facial lymph nodes are seen on cross-sectional imaging. Hence all identifiable facial nodes should be considered abnormal. Buccal nodes may show central necrosis with rim enhancement.

MR

Buccal space nodes show intermediate signal intensity on T1-weighted images but some of them may show high signal intensities indicating the presence of hemorrhage. These nodes typically show high signal on T2-weighted images and following the injection of contrast medium.

Imaging Pearls

- The normal lymphatic drainage pattern is frequently disrupted following radiation therapy. This places the facial nodes at risk.
- The mandibular group of facial nodes are often confused clinically with submandibular lymph nodes.

Suggested Readings

1. Tart RP, Mukherji SK, Avino AJ, Stringer SP, Mancuso AA. Facial lymph nodes: normal and abnormal CT appearances. *Radiology* 1993;188:695–700.
2. Robins JP, Slaughter FH, Constable WC. Involvement of the buccinator node in facial malignancy. *Arch Otolaryngol* 1971;94:356–358.
3. Chong VFH, Fan YF. Facial lymphadenopathy in nasopharyngeal carcinoma. *Clin Radiol* 2000;55:363–367.

Chapter 181

Squamous Cell Carcinoma

Epidemiology

The most common mass in the buccal space is due to a squamous cell carcinoma (SCCA) involving the buccal mucosa. Buccal SCCA constitutes 10% of all oral mucosa carcinomas in the United States but more than 40% in India. This disparity is related to betel nut chewing. SCCA of the buccal mucosa is related to tobacco and alcohol consumption. Although the tumor is more commonly seen in males, there is an increasing incidence in females due to increasing use of tobacco and alcohol. Other risk factors include ill-fitting dentures, leukoplakia, and the consumption of smokeless tobacco (especially in the southeastern United States).

Clinical Findings

More than half of patients with buccal space tumors present with advanced stage lesions (stage III and IV). Buccal mucosal tumors are usually exophytic, and deep invasion or ulcerations are relatively uncommon. Involvement of the pterygoid muscles gives rise to trismus.

Pathology

Buccal SCCA may extend into the buccal space from deep extension through the buccinator muscle. Posterior spread behind the pterygomandibular raphe leads to pterygoid muscle infiltration (Fig. 181–1). Late lesions may erode the mandible, hard palate, or maxillary sinus. Occult metastasis is present in 10% of patients, and 50% of patients have lymph node involvement at presentation.

Treatment

Early lesions can be treated by either surgery or radiation therapy. Late lesions are treated with combined surgery and postoperative radiation therapy. Because the incidence of occult metastasis is relatively low there is usually no need for neck dissection.

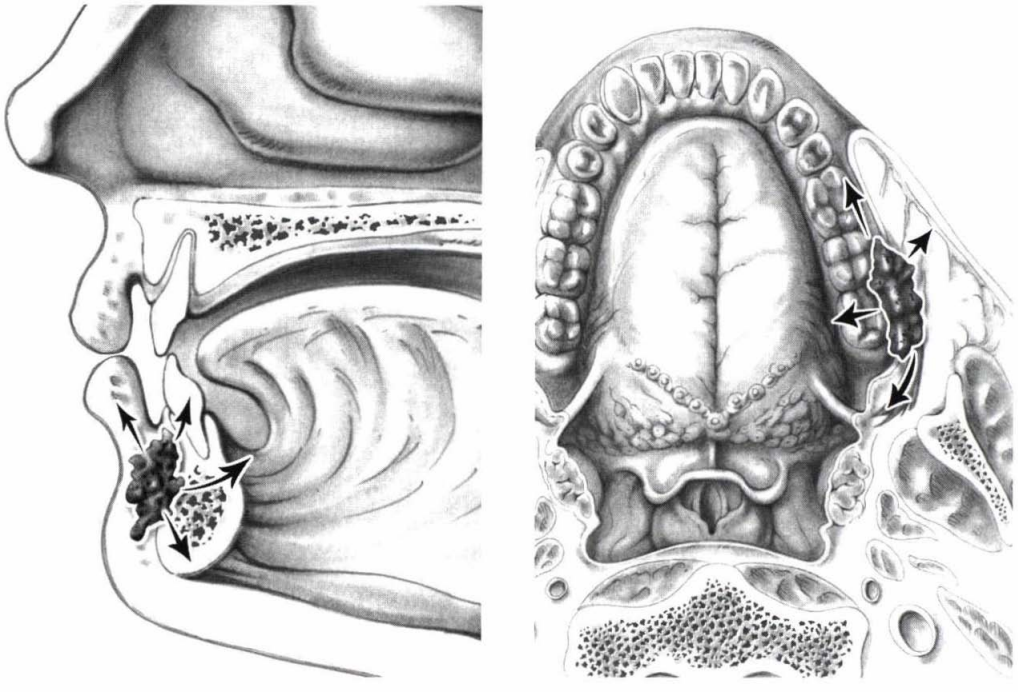

Figure 181-1. Sagittal (A) and axial (B) schematic illustrations demonstrate the potential spread patterns of buccal carcinomas. (Figures reproduced with permission from Mukherji SK, Pillsbury H, Castillo M. Imaging squamous cell carcinomas of the upper aerodigestive tract: what the clinicians need to know. Radiology *1997;205:629-646.)*

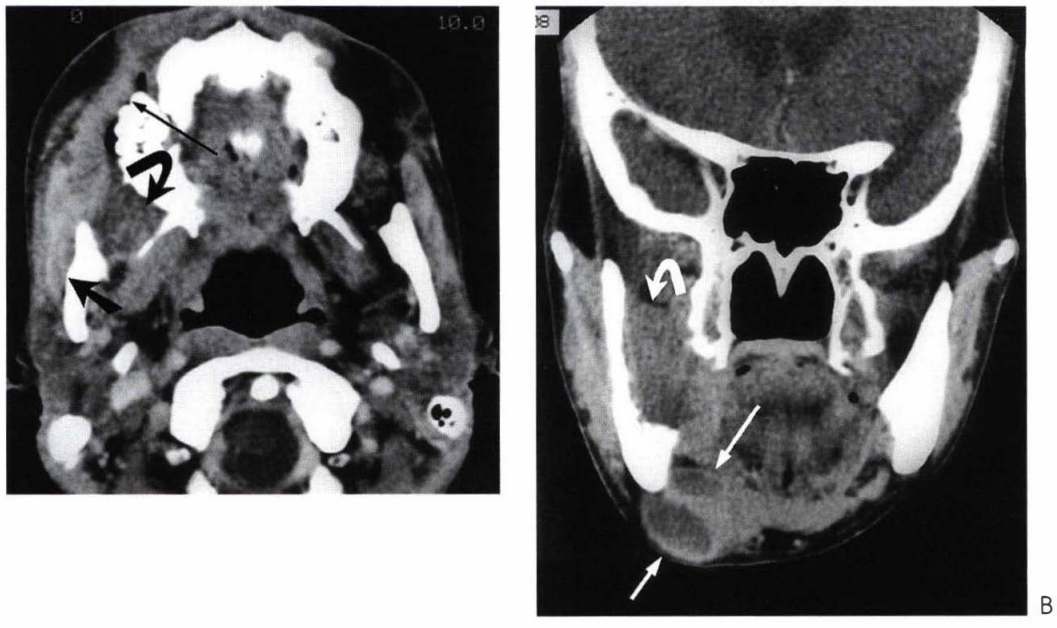

Figure 181–2. Buccal squamous cell carcinoma with buccal space extension (A) Axial contrast-enhanced CT shows extensive buccal mucosal thickening (thin arrow) with invasion of right masseter muscle (thick arrow) and buccal space (curved arrow). (B) Coronal contrast-enhanced CT shows obliteration of right buccal fat (curved arrow) and a necrotic right submandibular lymph node (opposing arrows).

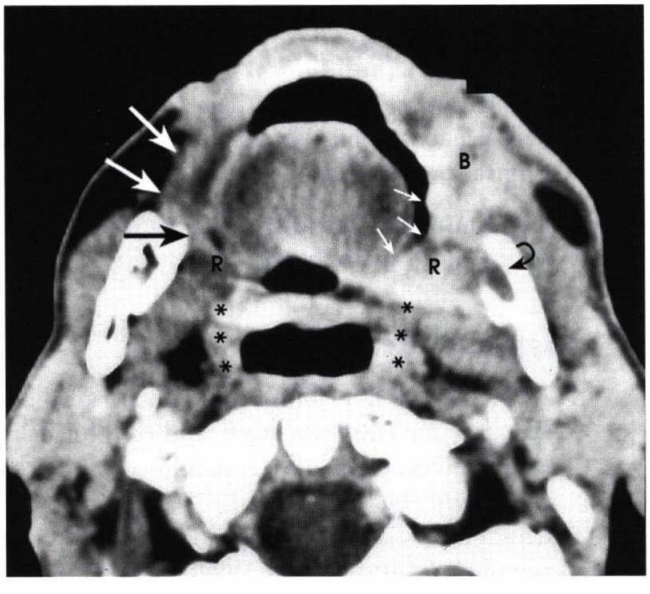

Figure 181–3. Axial contrast-enhanced CT shows a left buccal carcinoma (B) that is extending posteriorly along the buccinator muscle (small arrows) to the pterygomandibular raphe (R). The pterygomandibular raphe is formed by the interdigitation of the muscular fibers of the buccinator muscle (large arrows) with the superior constrictor muscle (*). The tumor erodes the anterior portion of the ramus of the mandible (curved arrow).

Imaging Findings

CT

Early tumors are often not identified on CT. More advanced lesions present as an aggressive soft tissue mass extending along the buccinator muscle. Deep extension may result in erosion of the maxillary or mandibular alveolar ridge, hard palate, or maxillary (Figs. 181–2 through 181–4).

MR

High signal intensity buccal space fat provides a good natural contrast against intermediate signal intensity tumor on T1-weighted images. These lesions are intermediate signal on T2-weighted sequences. Some lesions appear less conspicuous in contrast-enhanced, fat-suppressed images or T2-weighted images with fat suppression. Similarly, mandibular marrow infiltration is easily recognized on T1-weighted images.

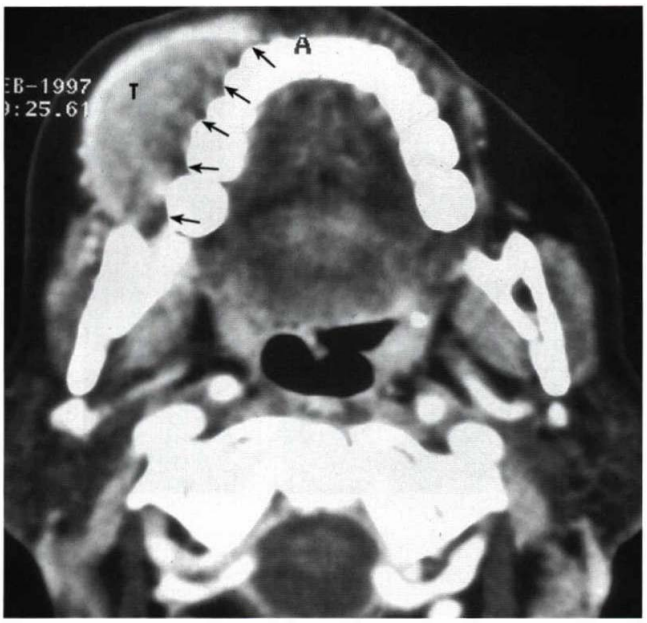

Figure 181-4. Axial contrast-enhanced CT demonstrates an aggressive tumor (T) involving the right buccal space that abuts the buccal cortex of the maxillary alveolar ridge (arrows).

Imaging Pearls

- CT is usually more useful than MR imaging because cortical erosions of the mandible, hard palate, and maxillary sinus are more readily appreciated. These findings have direct surgical implications.
- The conspicuity of early lesions may be improved if CT studies are acquired while patients "puff" their cheeks.

Suggested Readings

1. Alvi A, Myers EN, Johnson JT. Cancer of the oral cavity. In: Myers EN, Suen JY, eds. *Cancer of the Head and Neck.* 2nd ed. Philadelphia: WB Saunders; 1996:321-360.
2. Mukherji SK, Castillo M. A simplified approach to spaces of the suprahyoid neck. *Radiol Clin North Am* 1998;36:761-780.
3. Chong VFH, Mukherji SK, Goh CHK. The suprahyoid neck: normal and pathological anatomy. *J Laryngol Otol* 1999;113:501-508.
4. Weissman JL, Carrau RL. "Puffed-cheek" CT improves evaluation of the oral cavity. *AJNR Am J Neuroradiol* 2001;22:741-744.

Chapter 182

Benign Minor Salivary Gland Tumors (Pleomorphic Adenoma, Monomorphic Adenoma, Warthin's Tumor)

Epidemiology

A minor salivary gland consists of cellular constituents of the major salivary glands (parotid, submandibular, sublingual) that are located within the mucosa of the upper aerodigestive tract. It has been estimated that there are between 500 and 1000 minor salivary glands located throughout the oral cavity and oropharynx. They may be found within the hard and soft palate, uvula, lips, retromolar trigone, tongue base, floor of mouth, and tonsil. The same malignancies that arise in the major salivary glands occur in the minor salivary glands. Depending on the series, approximately 50% of minor salivary gland tumors are benign, whereas approximately 70 to 80% of parotid tumors are benign.

Clinical Findings

Patients often present with asymptomatic masses that have been present for several months. Pain and ulceration may be present; however, these are not consistent findings.

Pathology

The benign tumors that constitute minor salivary gland tumors include pleomorphic adenoma, monomorphic adenoma, and Warthin's tumor. The pathology of these lesions has been reviewed in other sections of this textbook.

Treatment

The exact treatment depends on the pathology. For most benign tumors complete local resection is adequate.

Imaging Findings

CT

The CT findings are not specific. The presence of regressive remodeling of the surrounding bone for lesions that arise in the hard palate is suggestive of a benign minor salivary gland tumor (Figs. 182-1 through 182-3).

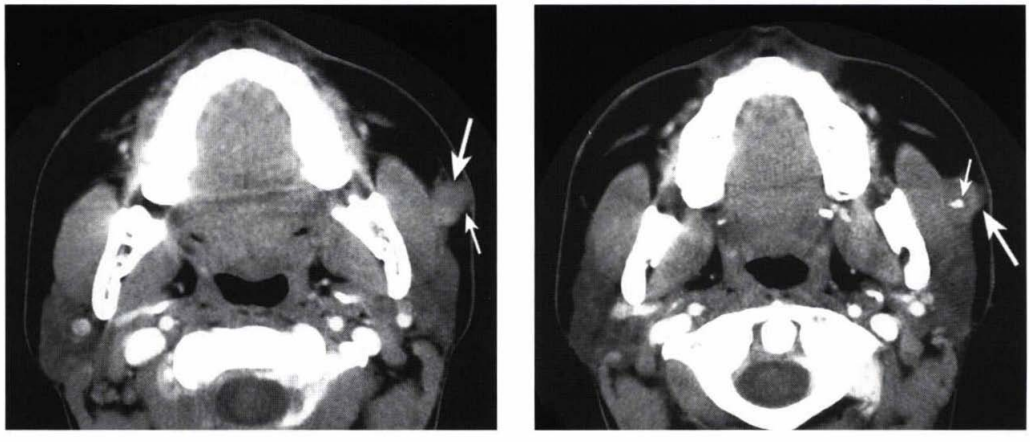

Figure 182-1. Pleomorphic adenoma. (A) Axial contrast-enhanced CT demonstrates a mildly enhancing soft tissue mass located in the far lateral portion of the buccal space (large arrow). The mass extends superficially into the subcutaneous fat (small arrow). (B) Axial CT performed 5 mm below (A) shows a central area of increased attenuation (small arrow) that may represent focal central enhancement (large arrow), or, more likely, central calcification. A noncontrast study was not performed.

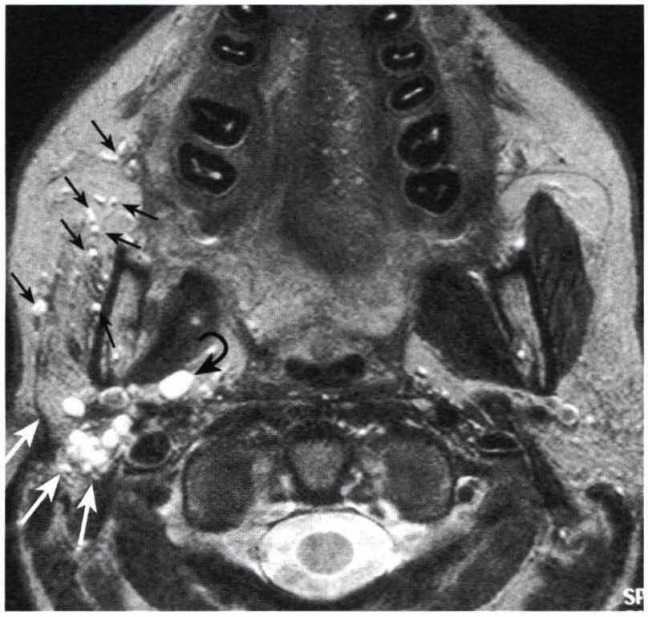

Figure 182-2. Axial T2-weighted image in a patient who has undergone prior resection of a parotid pleomorphic adenoma demonstrates multiple foci of increased signal indicative of recurrent or residual disease. There are multiple foci in the parotid (large arrows), parapharyngeal (curved arrow), and buccal spaces (small arrows).

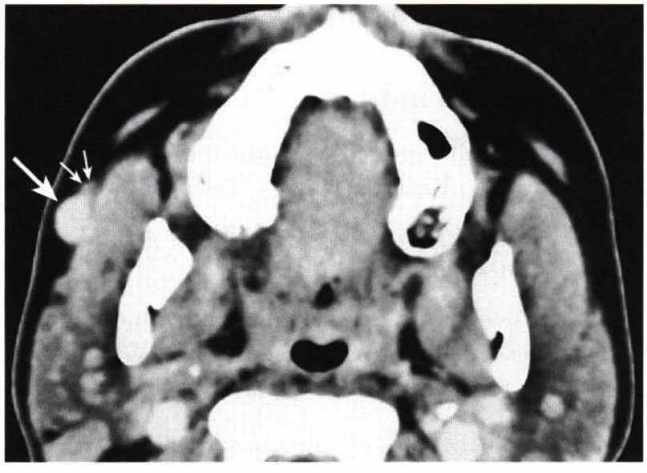

Figure 182-3. Axial contrast-enhanced CT shows a mass arising in accessory salivary tissue situated in the lateral buccal space. Pathology revealed pleomorphic adenoma (large arrow-pleomorphic adenoma, small arrows-accessory salivary tissue).

MR

In general, the imaging findings are nonspecific. However, oral cavity or oropharyngeal lesions that are low to intermediate signal on T1-weighted and increased signal on T2-weighted sequences are suggestive of pleomorphic adenoma.

Imaging Pearl

- In general, these are uncommon lesions with the diagnosis being made following biopsy. The intent of imaging is to provide information that cannot be detected on clinical examination. CT is helpful to evaluate the extent of bone erosion. MR should be performed to determine the presence of submucosal spread and deep invasion.

Suggested Readings

1. Batsakis JG. Neoplasms of the minor and lesser major salivary glands. In: Batsakis JG, ed. *Tumors of the Head and Neck*. Baltimore: Williams and Wilkins; 1979:76-99.
2. Smoker WRK. Oral cavity. In: Som PM, Curtin H, eds. *Head and Neck Imaging*. 3rd ed. New York: Mosby; 1996:488-544.
3. Shockley WM. Parotid tumors. In: Shockley WM, Pillsbury HC. *The Neck: Diagnosis and Surgery*. New York: Mosby ; 1994:265-294.

Chapter 183

Malignant Minor Salivary Gland Tumors (Adenoidcystic, Mucoepidermoid, Adenocarcinoma, Low Grade Polymorphous Adenocarcinoma)

Epidemiology

The same malignancies that arise in the major salivary glands occur in the minor salivary glands. Depending on the series, approximately half of all tumors of minor salivary gland origin are malignant. The most common location is the palate. An interesting paradox is that the smaller the salivary gland, the greater the likelihood that a tumor originating from that gland will be malignant. The incidence of a salivary gland tumor being malignant is substantially greater in the palate than in the parotid.

Clinical Findings

Patients often present with asymptomatic masses that have been present for several months. Pain and ulceration may be present; however, these are not consistent findings.

Pathology

It has been estimated that there are between 500 and 1000 minor salivary glands located throughout the oral cavity and oropharynx. They may be found within the hard and soft palate, uvula, lips, retromolar trigone, tongue base, floor of mouth, and tonsil. The malignancies that constitute minor salivary gland tumors include adenoid cystic carcinoma, mucoepidermoid carcinoma, and adenocarcinoma. Many investigators now include low grade polymorphous adenocarcinoma as a tumor of minor salivary gland origin. The most common malignancy of the minor salivary glands is adenoid cystic carcinoma.

Treatment

The treatment of malignant salivary gland tumors depends on the exact histologic type. In general, complete surgical resection offers the best chance for cure. Postoperative radiation therapy is required in the majority of cases. The role of neutron beam therapy for unresectable adenoid cystic carcinomas is currently being evaluated.

Imaging Findings

CT

The CT findings are nonspecific. These are usually soft tissue masses that enhance following contrast. The presence of aggressive bone erosion is suggestive of a high grade malignancy (Figs. 183–1 through 183–5).

MR

These tumors are usually intermediate signal on T1-weighted sequences and enhance following contrast administration. The T2-weighted signal is variable.

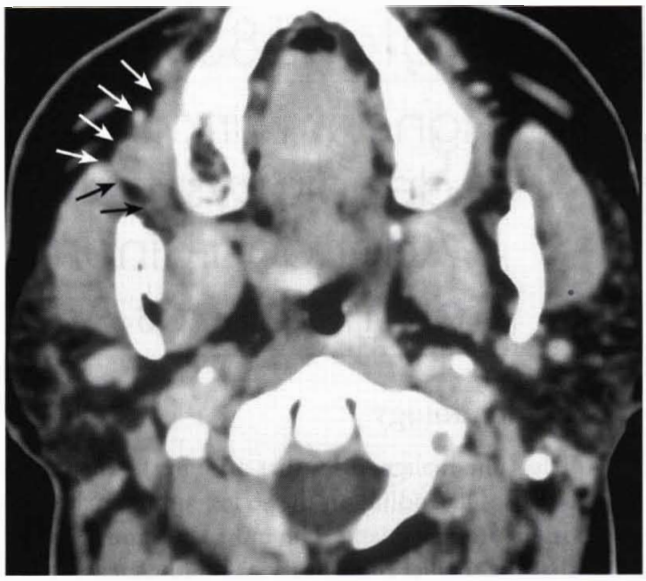

Figure 183–1. Axial contrast-enhanced CT demonstrates a soft tissue mass located in the right buccal space (arrows). Biopsy revealed adenoid cystic carcinoma.

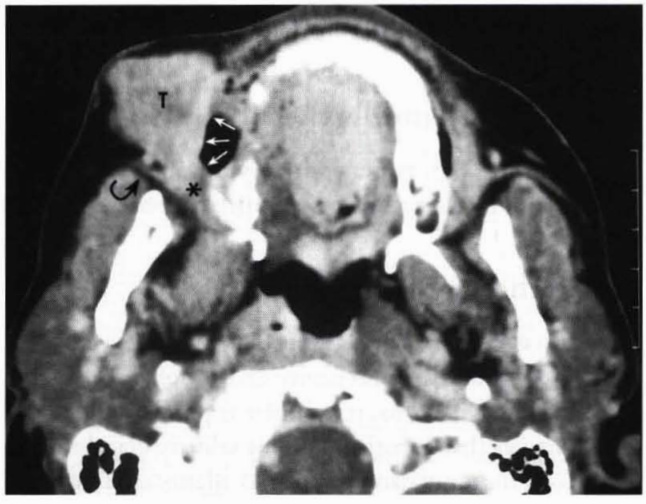

Figure 183–2. Axial contrast-enhanced CT shows an aggressive tumor (T) arising from the buccal space. The lesion extends deeply to invade the buccinator muscle (small arrows) and the area where the parotid duct (curved arrow) pierces the buccinator muscle (*). Biopsy revealed low grade adenocarcinoma.

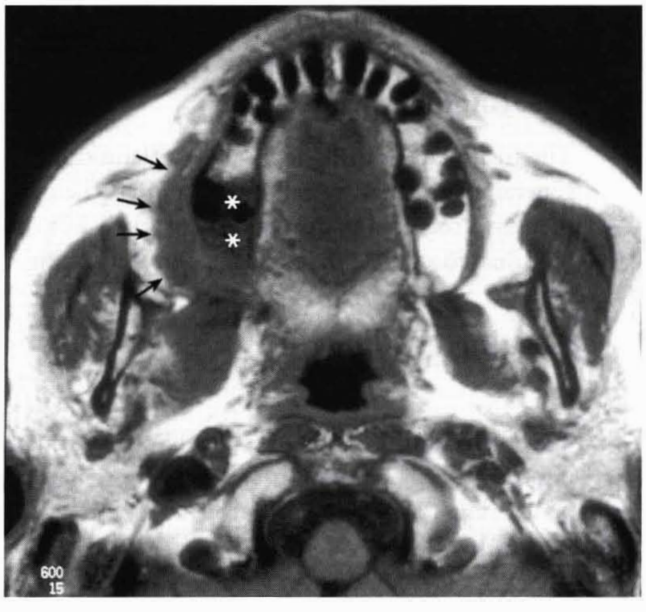

Figure 183–3. Noncontrast T1-weighted image shows an adenoid cystic carcinoma that involves both the superficial and the deep portions of the buccal space (arrows). There is erosion of the maxillary tuberosity as shown by replacement of the normal high T1-weighted signal (*). Compare this with the normal appearance on the contralateral side.

Imaging Pearls

- For adenoid cystic carcinoma involving the hard palate, CT should be performed to evaluate for bone erosion in the regions of the incisive canal and greater and lesser palatine foramen. MR should be performed to evaluate for extension into the pterygopalatine

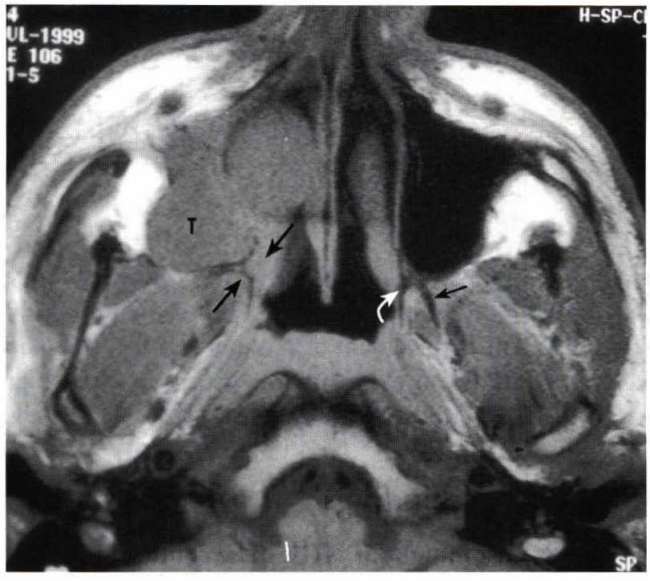

Figure 183-4. Noncontrast T1-weighted image shows an adenoid cystic carcinoma (T) involving the deep portion of the buccal space, which extends deeply into the pterygopalantine fossa. There is erosion of the lateral and medial pterygoid plates (large arrows), which is indicative of perineural spread along the greater and lesser palatine nerves. The small arrow indicates the lateral pterygoid plate, and the curved arrow the medial pterygoid plate.

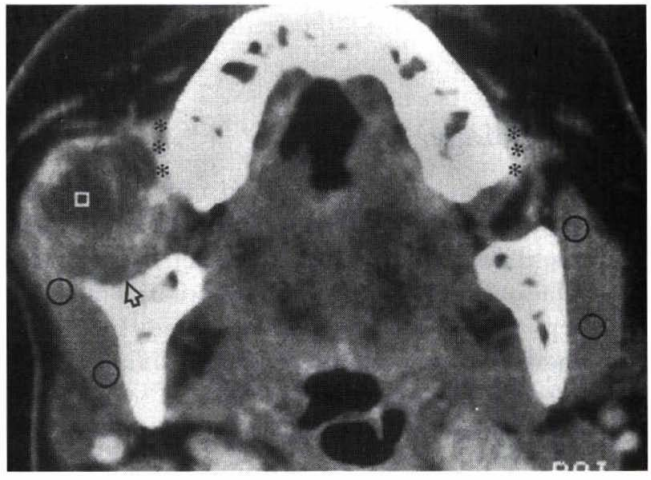

Figure 183-5. Contrast-enhanced CT scan shows a mass in the right posterior buccal space with a low-attenuation center (square cursor) suggestive of necrosis and infiltrating margins with mandibular cortical remodeling (arrows). The bone remodeling suggests the characteristic slow growth of most minor salivary gland tumors. Note also the infiltration of the masseter muscle (o) and of the buccinator muscle origin (•). This case, as in all of those of buccal masses with infiltrating margins, proved to be an aggressive malignancy. The diagnosis at surgery was mucoepidermoid carcinoma. (Figures and captions reproduced with permission from Tart RP, Kotzur IM, Mancuso AA, et al. CT and MR imaging of the buccal space and buccal space masses. Radiographics *1995;15:531-550.)*

fossa and possible retrograde perineural spread along the maxillary division of cranial nerve V or along the nerve of the vidian canal. These are potential pathways of spread in the cavernous sinus. These potential spread patterns should be evaluated in all patients because this may preclude primary surgical resection at many institutions.

- Patients who present with infraorbital numbness and paresthesias should undergo a high-resolution MR of the palate and trigeminal nerve to evaluate for the presence of clinically occult adenoid cystic carcinoma of the hard or soft palate that has invaded the infraorbital nerve.
- We recommend performing MR imaging in patients with polymorphous adenocarcinoma arising in the oral cavity because, based on our experience, it appears this tumor has a propensity for marrow invasion.

Suggested Readings

1. Batsakis JG. Neoplasms of the minor and lesser major salivary glands. In: Batsakis JG, ed. *Tumors of the Head and Neck.* Baltimore: Williams and Wilkins; 1979:76-99.
2. Smoker WRK. Oral cavity. In: Som PM, Curtin H, eds. *Head and Neck Imaging.* 3rd ed. New York: Mosby; 1996:488-544.
3. Shockley WM. Parotid tumors. In: Shockley WM, Pillsbury HC. *The Neck: Diagnosis and Surgery.* New York: Mosby; 1994:265-294

Chapter 184

Non-Hodgkin's Lymphoma

Epidemiology

Lymphomas account for 4% of all cancer diagnoses and deaths in the United States. Non-Hodgkin's lymphoma (NHL) is more common than Hodgkin's disease (HD) by a ratio of 5:1. The involvement of extranodal soft tissues and nodes in the buccal space is usually due to NHL because this entity is associated with a high incidence of extranodal involvement in the head and neck. In contrast, HD is almost always confined to nodal disease.

Clinical Findings

It is uncommon for NHL to be confined to the buccal space. Buccal space involvement is almost always part of a larger-scale disease process. NHL involving the buccal space is therefore overshadowed by cervical nodal enlargement or large extranodal masses elsewhere in the head and neck. NHL usually has a shorter history and the lesions enlarge faster than in HD.

Pathology

Histologic classification of NHL is notoriously difficult but newer techniques for classification such as immunologic phenotyping, nucleic acid analysis with flow cytometry, and molecular genetics may help explain the apparent diversity of morphological appearances. One of the most popular classifications is the Rappaport system, which is based on the pattern of involvement and cellular appearance. In general, nodular lymphomas have a more indolent course compared with the diffuse variety. Although Kaposi's sarcoma is by far the most common tumor associated with acquired immune deficiency syndrome, there is now a recognized higher incidence of NHL as well.

Treatment

For treatment purposes, NHL is divided into favorable and nonfavorable treatment outcome categories. The favorable group comprises patients with nodular lymphocytic and well-differentiated lymphocytic subtypes. The rest of the subtypes belong to the unfavorable outcome group. They include four histologic patterns: diffuse poorly differentiated lymphocytic, diffuse histiocytic, diffuse undifferentiated, and nodular histiocytic. Patients with stage I favorable group can be treated with radiation therapy alone whereas higher stages of the favorable group and all nonfavorable histologic subtypes are treated with a combination of radiation therapy and chemotherapy.

Imaging Findings

CT

Extranodular NHL appears as nodular masses in the head and neck. Involvement of the buccal space may be unilateral or bilateral. There is often associated involvement of other sites such as the parotid glands, Waldeyer's ring, and neck nodes (Figs. 184–1 and 184–2). These lesions show moderate contrast enhancement.

MR

NHL shows moderately high signal intensities following the injection of contrast and on T2-weighted images. Nodal necrosis, though less common than squamous cell carcinoma metastasis, may also be seen.

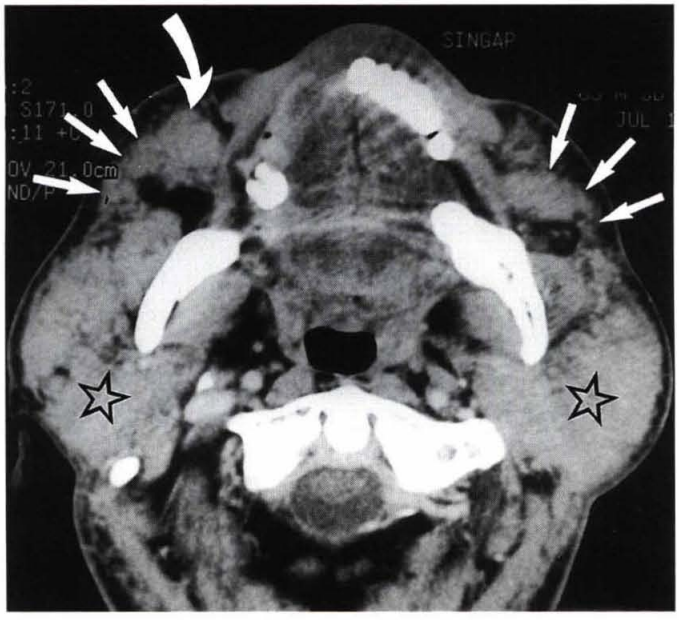

Figure 184–1. Axial contrast-enhanced CT shows bilateral diffuse infiltration of the parotid ducts (straight arrows) by non-Hodgkin's lymphoma. There is also diffuse infiltration of the parotid glands (stars). The focal mass (curved arrow) may represent an enlarged buccal lymph node.

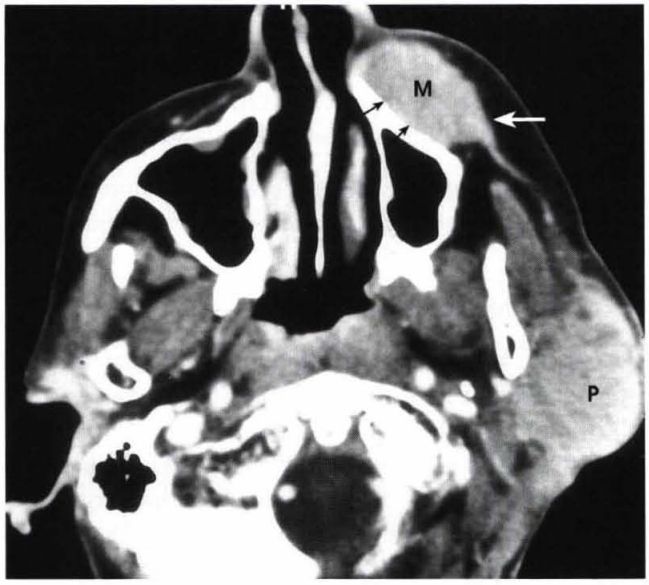

Figure 184–2. Axial contrast-enhanced CT shows a mass (M) in the medial aspect of the buccal space (large arrow) that extends medially into the superior aspect of the canine fossa (small arrows). Biopsy revealed non-Hodgkin's lymphoma. Given the associated involvement of the parotid gland (P) and the medial aspect of the buccal space and canine fossa, the mass could represent lymphomatous involvement of an infraorbital facial lymph node.

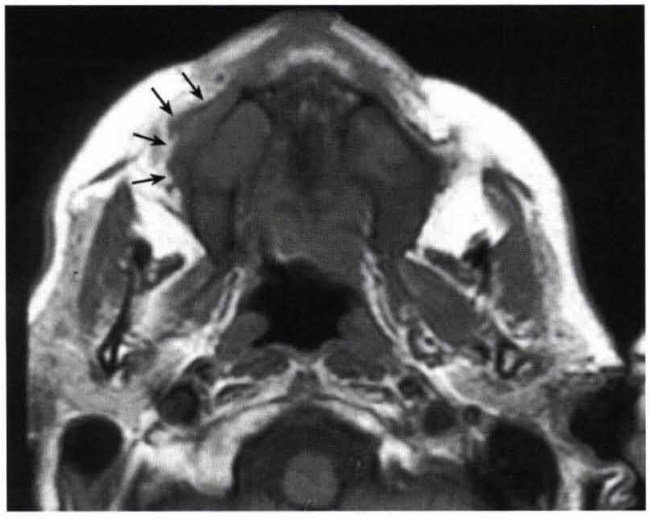

Figure 184–3. Axial noncontrast T1-weighted image shows an intermediate signal mass involving the right buccal space (arrows). Biopsy revealed non-Hodgkin's lymphoma.

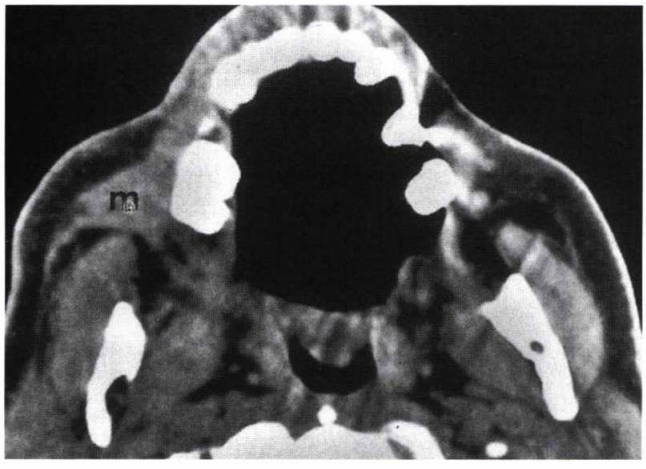

Figure 184-4. Contrast-enhanced CT scan reveals an intermediate signal mass (m) in the right anterior buccal space. The mass was felt to represent extranodal lymphoma of the buccal space. (With permission from Tart RP, Kotzur IM, Mancuso AA, et al. CT and MR imaging of the buccal space and buccal space masses. Radiographics *1995;15:531-550.)*

Imaging Pearls

- NHL tends to be generalized at the time of presentation whereas HD is usually confined to the lymph nodes.
- Buccal space involvement by NHL probably occurs from spread from initial involvement of buccal lymph nodes (Figs. 184-3 and 184-4).
- NHL involves the marrow much more frequently than HD. MR imaging may detect marrow changes in addition to extranodal and nodal lesions.

Suggested Readings

1. Mendenhall NP. Lymphomas and related diseases presenting in the head and neck. In: Million RR, Cassisi NJ, eds. *Management of Head and Neck Cancer.* Philadelphia: Lippincott; 1994:841-856.
2. Linberg RD, Paris KJ, Fletcher GH. Radiation therapy of tumors of the neck. In: Thawley SE, Panje WR, Batsakis JG, Lindberg RD, eds. *Comprehensive Management of Head and Neck Tumors.* 2nd ed. Philadelphia: WB Saunders; 1999:1450-1477.
3. Tart RP, Mukherji SK, Avino AJ, Stringer SP, Mancuso AA. Facial lymph nodes: normal and abnormal CT appearances. *Radiology* 1993;188:695-700.

Chapter 185

Ameloblastoma

Epidemiology

Ameloblastoma (also known as adamantinoma, adamantinoblastoma, basiloma, and epithelioma ameloblastoides) is the most common odontogenic tumor and accounts for 11% of all odontogenic neoplasms. However, it remains an uncommon lesion accounting for about 1% of all tumors and cysts arising in the jaw. Two thirds of all patients are found in the 20- to 49-year age group with a mean age of 39 years. There is no known sex or ethnic predilection.

Clinical Findings

Ameloblastomas are slow growing tumors and most patients complain of slow painless facial deformity. Seventy-five percent of patients have swelling as the main complaint whereas 25% present with pain. Other manifestations include mobile teeth, ill-fitting dentures, ulcerations, draining sinuses, and nasal obstruction.

Pathology

The majority of ameloblastomas are benign, with < 1% showing malignant behavior such as rapid growth, bone destruction, and distant metastases. Ameloblastomas infiltrate between bone trabeculae but involvement of cortical bone is limited only to superficial erosion. They can be divided into several gross morphological types. The tumor may be intraosseous solid, well-circumscribed unicystic, multicystic, and peripheral (extraosseous). Well-circumscribed unicystic lesions mimic dentigerous cysts in appearance and show less aggressive behavior compared with the other gross morphological types.

Treatment

Treatment is by surgical resection. Partial mandibulectomy or maxillectomy is the treatment of choice. Radiation therapy is usually not required following surgery. Curettage or enucleation (which may be sufficient for small unicystic lesions) is not recommended because it is associated with a high recurrence rate of up to 59%.

Imaging Findings

CT

There is a spectrum of changes demonstrable on CT. At one end is a small unilocular cyst, with or without an associated tooth, and at the other end is an expansile multilocular lesion with compartmentalization. Small unilocular cysts cannot be distinguished from dentigerous cysts. Both cystic and solid components can be readily identified on CT. The cysts show nonenhancing, low attenuation values whereas solid components show moderate enhancement (Fig. 185-1).

MR

The MR imaging feature depends on the relative size and the relationship between the cystic and solid tumor components. On T1-weighted images, the lesion shows intermediate signal intensity but cysts with high protein content may demonstrate high signals. The cystic and solid areas show typical high signal intensities on T2-weighted images. The solid regions demonstrate good contrast enhancement.

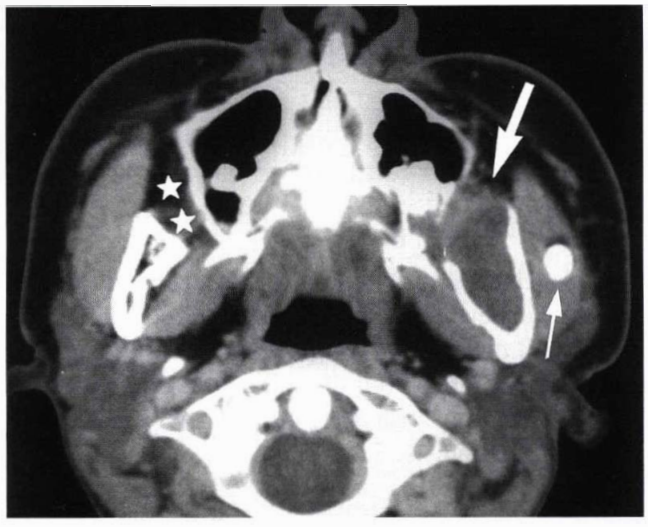

Figure 185–1. Ameloblastoma. Axial contrast-enhanced CT shows a low attenuation tumor in the left mandibular ramus (masticator space). Note the extension into the left buccal space (large arrow) and compare with the normal right side (stars). Curiously, a tooth was displaced into the masseter muscle (small arrow).

Imaging Pearl

- CT is recommended for the demonstration of the typical bone expansion and the typical thin rim of remaining cortical bone. The dental crown is easily recognized on both CT and MR imaging.

Suggested Readings

1. McDaniel RK. Odontogenic cysts and tumors. In: Thawley SE, Panje WR, Batsakis JG, Lindberg RD, eds. *Comprehensive Management of Head and Neck Tumors.* 2nd ed. Philadelphia: WB Saunders; 1999:1566–1610.
2. Stewart JCB, Betts JB, Barber HD, Ellis E, Fonseca RJ. In: Thawley SE, Panje WR, Batsakis JG, Lindberg RD, eds. *Comprehensive Management of Head and Neck Tumors.* 2nd ed. Philadelphia: WB Saunders; 1999:1611–1636.
3. Delbalso AM. An approach to the diagnostic imaging of jaw lesions, dental implants, and the temporomandibular joint. *Radiol Clin North Am* 1998;855–890.

Chapter 186

Lipoma

Epidemiology

The predominant tissue in the buccal space is adipose tissue. Lipoma is a common benign tumor arising in the buccal space, usually in adults. There is no reported gender predilection.

Clinical Findings

Patients with lipomas typically present with a long history of a slowly enlarging facial mass. The lesion is soft and nontender. It may enlarge in parallel to body weight gain.

Pathology

Lipomas are well-encapsulated tumors that consist of normal adult lipocytes. They may be mistaken for normal fatty tissue but there is always a fibrous capsule separating the lesion from the surrounding normal tissue. These tumors rarely undergo malignant transformation. Liposarcomas originate from lipoblasts within fascia rather than ordinary lipocytes.

Treatment

Surgical excision is performed for cosmetic reasons or to exclude the possibility of a liposarcoma in enlarging lesions.

Imaging Findings

CT

Classic buccal space lipomas are homogeneously low attenuation and have Housefield units that are characteristic of fat (Fig. 186–1). They do not enhance following contrast administration. Large lipomas extend along planes of least resistance and do not erode the adjacent bony structures. Occasionally lipomas will contain linear areas of intermediate attenuation. However, in such cases, the diagnosis of a liposarcoma cannot be excluded.

MR

Lipomas display characteristic high signal intensity on T1-weighted images. The lesion does not show an increase in signal intensity following contrast injection. In fat suppressed sequences, lipomas show parallel decrease in signal compared with subcutaneous fat.

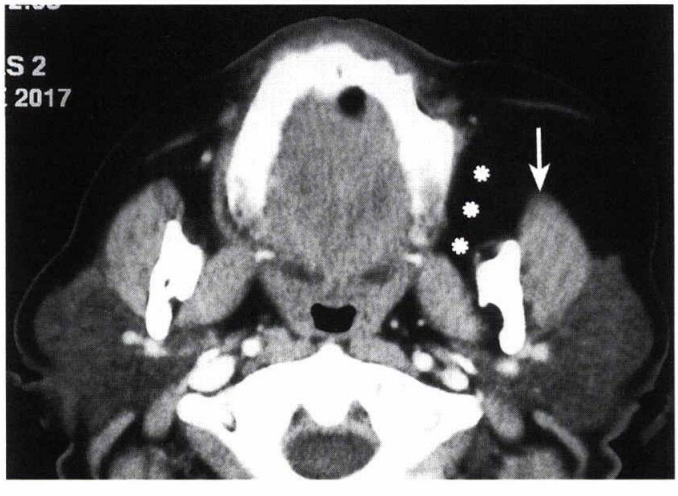

Figure 186–1. Buccal space lipoma. Axial contrast-enhanced CT shows a lipoma involving the left buccal space. Note the distended left buccal space (asterisks) and laterally displaced masseter muscle (arrow).

Imaging Pearls

- The diagnosis of a lipoma should be considered for a clinically palpable mass that is not obvious on imaging. The only imaging findings may be asymmetry of the superficial muscles of facial expression or the parotid duct.
- The diagnosis of a liposarcoma cannot be excluded if a presumed lipoma contains internal areas of soft tissue.

Suggested Readings

1. Mukherji SK, Castillo M. A simplified approach to spaces of the suprahyoid neck. *Radiol Clin North Am* 1998;36:761–780.
2. Tart RP, Kotzur IM, Mancuso AA, et al. CT and MR imaging of the buccal space and buccal space masses. *Radiographics* 1995;15:531–550.

Chapter 187

Capillary Malformations

Epidemiology

Capillary malformations are categorized as a type of vascular malformation using the classification system of Mulliken and Glowacki. Capillary malformations constitute what were once termed port-wine stains. There is no gender predilection for vascular malformations. These lesions are usually present at birth and grow along with the child.

Capillary malformations are commonly associated with the neurocutaneous Sturge-Weber syndrome (encephalotrigeminal angiomatosis), which also involves a vascular anomaly of the choroid plexus and leptomeninges. Other syndromes that have been associated with capillary malformations include ataxia telangiectasia (Louis-Bar's) and Rendu-Osler-Weber (hereditary hemorrhagic telangiectasia).

Clinical Findings

The craniofacial findings consist of cutaneous abnormality that consists of a bluish smooth macular lesion that is located along the sensory distribution of V_2. Commonly affected areas include the cheek, lip, and gingiva. As the patient matures, these dermal lesions often become more coarsened and papular. The color often darkens to a purplish or dark crimson hue. Occasionally, gingival hypertrophy and chronic hemorrhage may occur. Sturge-Weber syndrome is likely to be associated with a port-wine stain if the distribution of the cutaneous abnormality is more extensive and involves V_1.

Pathology

These malformations are thought to be due to abnormal embryogenesis of the capillary system. These lesions consist of flat, normal appearing endothelial cells with abnormally formed capillary channels. There is normal endothelial cell turnover and a normal rate of mitosis.

Treatment

The treatment depends on the location and the extent of the lesion. Supportive therapy is commonly chosen. Laser surgery has become an accepted method for treatment of these dermal lesions. Two of the most commonly used lasers are argon and neodymium:yttrium-aluminum-garnet (Nd:YAG). Argon lasers are often used to treat small macular lesions, whereas, Nd:YAG lasers have been utilized for more advanced and deeper lesions.

Imaging Findings

CT

These superficial lesions may only be seen as skin thickening overlying the face and cheek. Despite extensive disease, the imaging findings are often minimal.

MR

The MR findings include skin thickening with replacement of the subcutaneous tissue by intermediate tissue. These lesions usually enhance after contrast. There are no flow voids (Fig. 187–1).

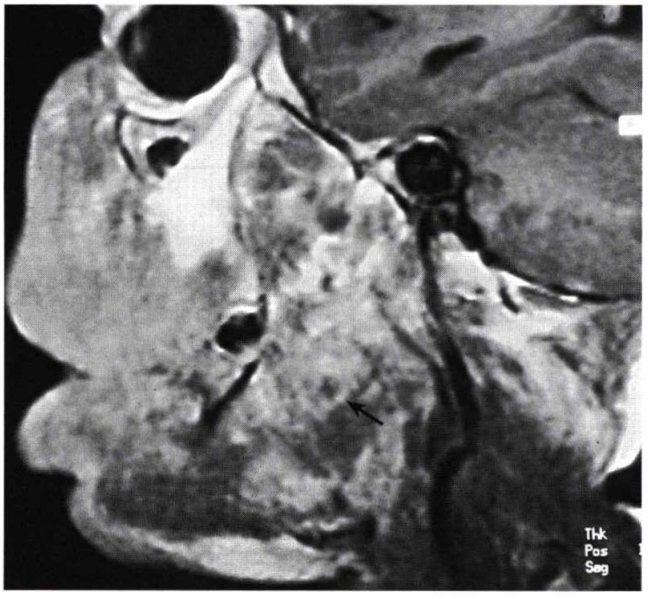

Figure 187-1. Sagittal postcontrast T1-weighted image demonstrates an extensive capillary malformation involving the face. The heterogeneous lesion involves the lips and gingiva and extends deeply to involve the buccal space (arrow).

Imaging Pearls

- This is a clinical diagnosis with very little role for imaging
- Despite being classified as a vascular malformation, these are "low flow" lesions and are not associated with enlarged feeding arteries or draining veins.

Suggested Readings

1. Mulliken JB, Glowacki J. Hemangiomas and vascular malformations in infants and children: a classification based on endothelial characteristics. *Plast Reconstr Surg* 1982;69:412–422.
2. Meyer JS, Hoffer FA, Barnes PD, Mulliken JB. Biological classification of soft-tissue vascular anomalies: MR correlation. *AJR Am J Roentgenol* 1991;157:559–564.
3. Smoker WRK. Oral cavity. In: Som PM, Curtin H, eds. *Head and Neck Imaging*. 3rd ed. New York: Mosby; 1996:488–544.
4. James CA. Diagnostic imaging of congenital vascular lesions. In: Warner M, Suen JY, eds. *Hemangiomas and Vascular Malformations of the Head and Neck*. New York: Wiley-Liss; 1999:171–215.

Chapter 188

Venous Malformations

Epidemiology

Venous malformations are categorized as a type of vascular malformation using the classification system of Mulliken and Glowacki. Most authors now classify what were once termed cavernous hemangiomas as venous malformations. These lesions are felt to be present at birth but are usually detected in late childhood or early adulthood.

Clinical Findings

Small lesions may present as an asymptomatic bluish mass that is easily compressible. More advanced lesions may be painful, may result in functional impairment, or hemorrhage. The lesions may enlarge with patient position or with crying. The lesions may also enlarge with Valsalva's maneuver or following a placement of a tourniquet to obstruct the venous outflow. The most common locations in the extracranial head and neck include subcutaneous tissues of the face, muscles of mastication, periorbital region and deep neck spaces.

Pathology

These lesions arise from anomalous venous development. The absence of valves result in stagnant flow and variable communication with the surrounding normal venous system. Enlargement of the lesion over time is due to growth of the patient rather than to endothelial proliferation.

Treatment

Complete surgical resection is the treatment of choice for localized lesions with well-defined margins. Because these are low flow venous lesions, percutaneous sclerotherapy is becoming an accepted treatment option for patients with advanced infiltrative lesions.

Imaging Findings

US

Gray scale ultrasound demonstrates variable internal echogenicity with margins that are often irregular. Hypoechoic cystic spaces that are compressible are often present. Echogenic phleboliths may result in distal acoustic shadowing. Doppler analysis shows slow venous flow with normal arterial flow in the surrounding vessels.

CT

These lesions are usually seen when they arise in the subcutaneous tissues but are difficult to detect when they are intramuscular (Fig. 188-1). Phleboliths are a hallmark of the diagnosis.

MR

Venous malformations have intermediate signal on T1-weighted sequences and are slightly more intense than adjacent muscle. There may be mild enhancement following contrast administration. They have increased signal on T2-weighted sequences. Flow sensitive sequences show slightly increased signal. Flow voids are not typically identified.

Angiography

Venous malformations may not be detected at angiography because these lesions are located at the postcapillary level. Normal arterial and capillary phases are expected. Arteriovenous shunting should not be seen. Visualization of the entire extent of the venous anomaly may require direct puncture.

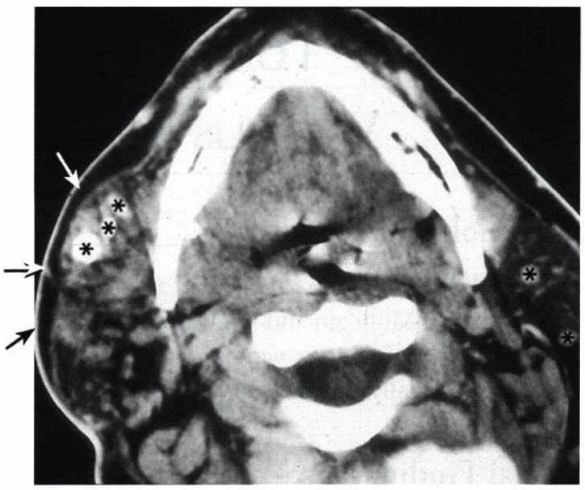

Figure 188-1. Axial contrast enhanced CT shows a heterogeneously enhancing mass (arrows) in the inferior portion of the right buccal space. Note the multiple focal internal calcifications (*) which suggest the diagnosis of venous malformations.

Imaging Pearls

- The imaging findings are crucial to the treatment of these lesions. Identification of internal venous flow without arterial flow using ultrasound, and the absence of flow voids on MR confirms the diagnosis of a low flow lesion. This precludes the need for angiography prior to surgical resection.
- The absence of flow voids helps distinguish these from high flow lesions such as arteriovenous malformations and hemangiomas in the proliferative phase.
- MR imaging is the best cross-sectional modality for defining the extent of the lesions and may detect intramuscular malformations that cannot be seen on CT.
- Localized lesions, as determined by cross-sectional imaging, are often treated with surgery, whereas extensive lesions that are not completely resectable may be treated with percutaneous sclerotherapy.

Suggested Readings

1. Mulliken JB, Glowacki J. Hemangiomas and vascular malformations in infants and children: a classification based on endothelial characteristics. *Plast Reconstr Surg* 1982;69:412–422
2. Meyer JS, Hoffer FA, Barnes PD, Mulliken JB. Biological classification of soft-tissue vascular anomalies: MR correlation. *AJR Am J Roentgenol* 1991;157:559–564.
3. Waner M, Suen JY. A classification of congenital vascular malformations. In: Warner M, Suen JY, eds. *Hemangiomas and Vascular Malformations of the Head and Neck*. New York: Wiley-Liss; 1999:1–12.
4. James CA. Diagnostic imaging of congenital vascular lesions. In: Warner M, Suen JY, eds. *Hemangiomas and Vascular Malformations of the Head and Neck*. New York: Wiley-Liss; 1999:171–215.

Chapter 189

Arteriovenous Malformations

Epidemiology

Arteriovenous malformations (AVMs) are developmental malformations of the vascular system that result in abnormal communication between arteries and veins. The primary abnormality appears to be at the level of the capillary bed. AVMs are classified as a type of vascular malformation using the classification system of Mulliken and Glowacki. AVMs also include arterial malformations and arteriovenous fistulae and are characterized as high flow lesions.

Clinical Findings

The clinical presentation can be variable depending on the extent of the lesion. The neck and craniofacial region are common sites of occurrence. On clinical examination, AVMs present as a soft tissue fullness that is compressible. Superficial AVMs may be associated with a palpable thrill or audible bruit. The overlying skin may be discolored due to dilated superficial veins. Other presentations in more advanced lesions include facial deformity, skin ulceration, or functional compromise. Patients may also present with hemorrhage that may be spontaneous or may follow minor trauma such as tooth extraction. AVMs may enlarge with pregnancy. It is unclear as to whether the growth is due to direct hormonal stimulation or whether it results secondarily from an increase in the circulating blood volume.

Pathology

AVMs result from abnormal development of the arterial, capillary, and venous components of the vascular system. The lesions grow commensurately with the individual and show no evidence of endothelial proliferation. The vascular channels are lined by mature endothelium with normal mitotic activity.

Treatment

The treatment of choice is combined therapy consisting of embolization followed by surgical excision. Complete resection of the nidus is necessary to prevent recurrence.

Imaging Findings

CT

Contrast-enhanced CT demonstrates densely enhancing lobulated serpiginous lesions in the buccal space. Prominent draining veins are evident and they can be seen to communicate with the pterygoid plexus, parapharyngeal, retromandibular or facial veins (Figs. 189–1 and 189–2).

MR

The typical appearance is multiple flow voids indicating enlarged vessels with high flow without an associated soft tissue mass. Increased vascular flow is seen on flow-sensitive sequences.

US

Doppler analysis will demonstrate arterial and venous components and may show arterialized waveforms of a draining vein due to arteriovenous shunting.

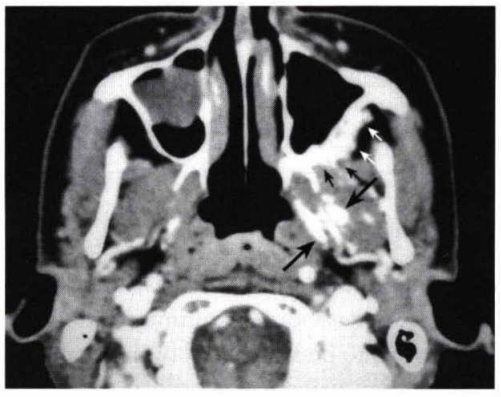

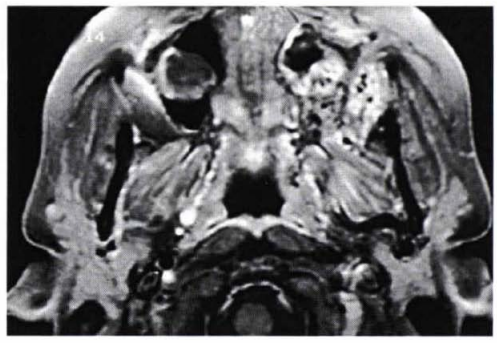

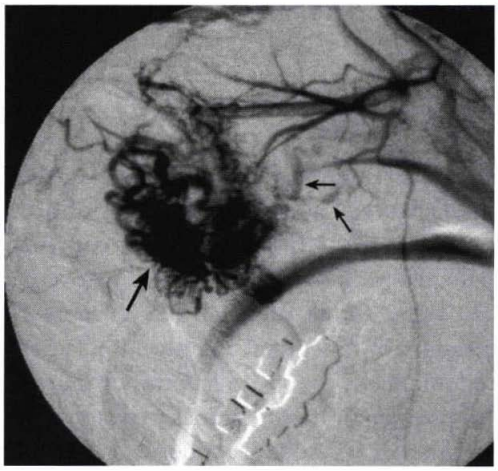

Figure 189–1. (A) Axial contrast-enhanced CT demonstrates diffuse abnormal enhancement situated in the left buccal space (small arrows) that is not associated with a soft tissue mass. There is also abnormal enhancement present in the masticator space along the lateral pterygoid muscle (large arrows). (B) Contrast-enhanced T1-weighted image performed following fat saturation obtained in the same patient illustrated in (A) shows multiple flow voids in the left buccal space consistent with a vascular lesion. (C) Selective angiogram of the left internal maxillary artery demonstrates a densely enhancing tangle of vessels (large arrow) with early draining veins indicative of an arteriovenous malformation (small arrows).

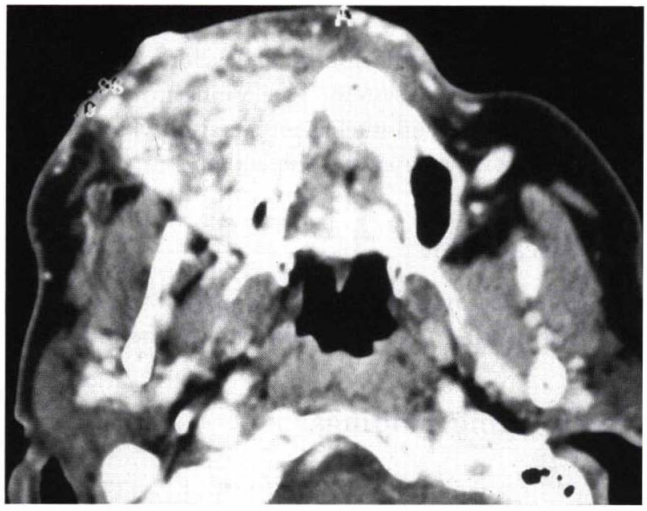

Figure 189–2. Axial contrast-enhanced CT shows a large densely enhancing lesion with multiple dilated vascular structures consistent with a buccal space arteriovenous malformation.

Angiography

AVMs have enlarged tortuous feeding arteries that supply a nidus. Arteriovenous shunting into enlarged draining veins is a characteristic finding. The primary blood supply is from various branches of the external carotid artery.

Imaging Pearls

- The treatment of AVMs is directly affected by the imaging findings. Identification of a high flow vascular malformation with arteriovenous shunting contraindicates treatment with percutaneous sclerotherapy.
- The presence of potential collateral formation between branches of the external carotid artery and the vertebral artery or branches of the internal carotid artery needs ro be evaluated during endovascular procedures.

- Craniofacial AVMs should not be treated with a particle size < 200 μm due to the possibility of overlying skin necrosis or direct shunting of particles into the pulmonary bed or intracranial circulation.

Suggested Readings

1. Calcattera T, Wang MB, Sercarz JA. Unusual tumors. In: Myers EN, Suen JY, eds. *Cancer of the Head and Neck.* 2nd ed. Philadelphia: WB Saunders; 1996:644–669.
2. Mulliken JB, Glowacki J. Hemangiomas and vascular malformations in infants and children: a classification based on endothelial characteristics. *Plast Reconstr Surg* 1982;69:412–422.
3. Smoker WRK. Oral cavity. In: Som PM, Curtin H, eds. *Head and Neck Imaging.* 3rd ed. New York: Mosby; 1996:488–544.

Chapter 190

Hemangiomas

Epidemiology

Hemangiomas are proliferative endothelial vascular lesions that are identified by their characteristic clinical appearance and course. These lesions may arise in the buccal space. Forty percent of hemangiomas are present at birth and 60% appear within the first few months of life. Hemangiomas are more common in females than in males (5:1). Common sites of occurrence include skin, face, orbits, larynx, nasal cavity, and deep neck spaces.

Clinical Findings

Superficial hemangiomas are bright red papular lesions. Subcutaneous hemangiomas often present as a bluish mass that may be difficult to differentiate from a venous malformation or arteriovenous malformation.

Hemangiomas rapidly grow during the first 12 to 18 months of life (proliferative phase). This is followed by gradual regression (involuting phase) over the next 6 to 10 years. Approximately half of all lesions will completely involute whereas the remainder will partially involute. Incomplete involution may result in residual telangiectasias, hypoplastic patches, or scarring. The majority of hemangiomas have an uneventful course, with spontaneous and complete involution. More advanced lesions may cause severe facial disfigurement.

Pathology

The proliferative phase consists of proliferating plump endothelial cells with frequent mitoses. The end of the proliferative phase is characterized by a reduction in the mitotic activity, progressive flattening of the cells, and an abundance of mast cells. Apoptosis and progressive endothelial cells encompassed by large ectatic vascular channels in a matrix of fibrofatty tissue characterize the involutional phase.

Treatment

Because most hemangiomas undergo complete or near-complete spontaneous involution, the treatment is conservative and consists of observation and parental reassurance. More aggressive options such as steroid therapy and compression therapy are reserved for enlarging lesions that result in functional compromise. Surgery is reserved as a secondary procedure following initial therapy or incomplete involution. The role of antiangiogenesis agents is currently under investigation.

Imaging Findings

CT

Hemangiomas show a lobulated appearance on contrast-enhanced CT. There is moderate to good enhancement following the injection of contrast media. True hemangiomas should not contain phleboliths. The presence of phleboliths is suggestive of a venous malformation using the classification proposed by Mulliken and Glowacki. These lesions may also be seen in the adjacent masseter muscle, the parotid gland, and the nasopharyngeal masticator space.

MR

The lesions are intermediate signal, focal soft tissue masses seen on noncontrast T1-weighted images. These lesions enhance following the injection of contrast. They are increased signal on T2-weighted sequences. Flow voids may be present in the proliferative phase and are typically not present in the involuting phase (Figs. 190–1 and 190–2).

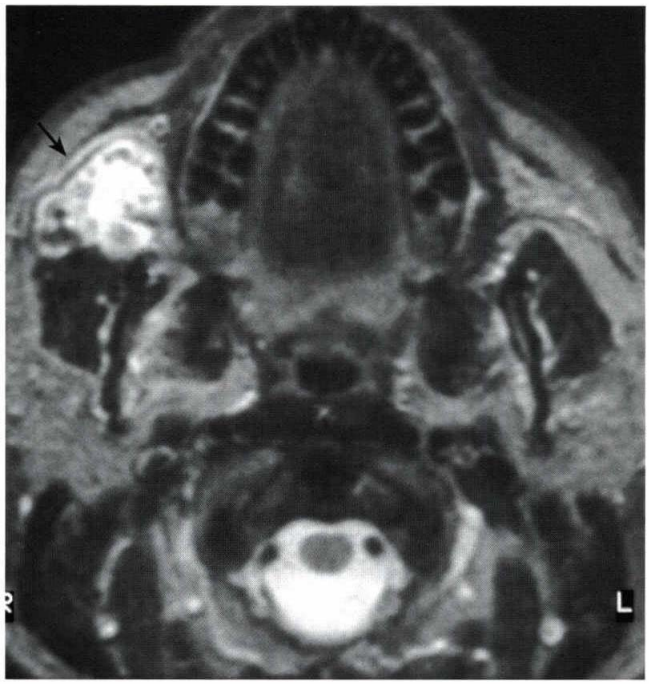

Figure 190–1. Axial T2-weighted image demonstrates a predominantly increased signal mass isolated to the buccal space (arrow). The focal areas of decreased signal may represent blood products, flow voids, or calcifications.

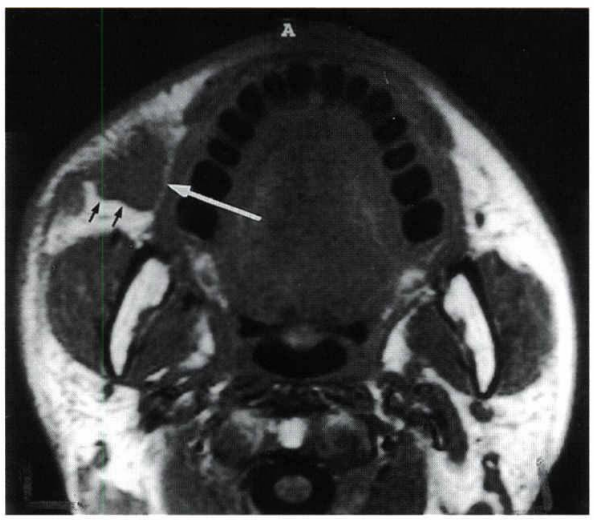

A

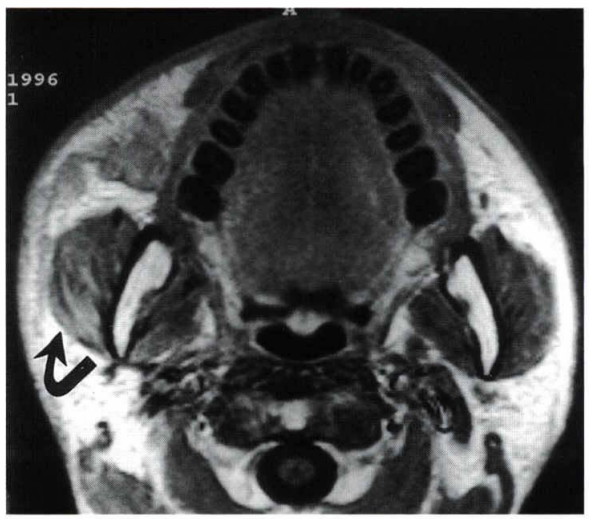

B

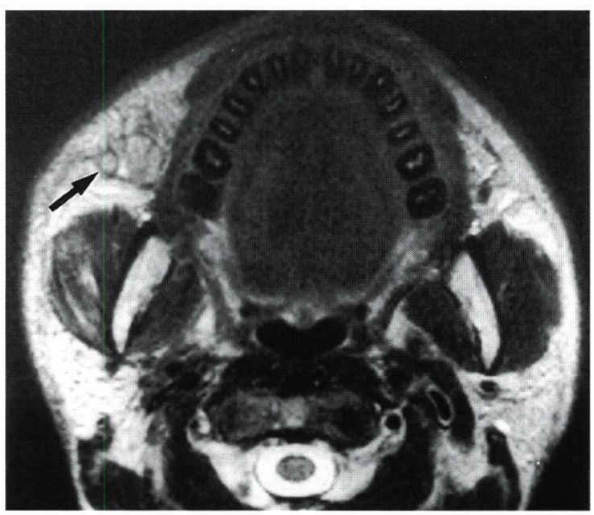

C

Figure 190–2. (A) Axial T1-weighted MR image shows an intermediate signal intensity hemangioma (large arrow) indenting the right buccal fat pad (small arrows). (B) Axial contrast-enhanced MR image shows contrast enhancement in the buccal space lesion. There is enhancement in the right masseter muscle indicating similar involvement (arrow). Note the mild streaks in the adjacent subcutaneous fat, but no skin thickening is present. (C) Axial T2-weighted MR image shows high signals in the buccal space and masseter muscle lesion (arrow). There is a loss of lesion conspicuity in the buccal space without fat suppression.

Imaging Pearls

- The diagnosis of a true hemangioma is very narrow using the classification proposed by Mulliken and Glowacki. This classification should be limited to children with vascular malformations.
- A focal soft and pliable enhancing soft tissue buccal space mass in an adult that is not accessory parotid tissue is usually categorized as a hemangioma. However, this would not be considered a hemangioma using the classification proposed by Mulliken and Glowacki.

Suggested Readings

1. Calcattera T, Wang MB, Sercarz JA. Unusual tumors. In: Myers EN, Suen JY, eds. *Cancer of the Head and Neck*. 2nd ed. Philadelphia: WB Saunders; 1996:644–669.
2. Mukherji SK, Castillo M. A simplified approach to spaces of the suprahyoid neck. *Radiol Clin North Am* 1998;36:761–780.
3. Mulliken JB, Glowacki J. Hemangiomas and vascular malformations in infants and children: a classification based on endothelial characteristics. *Plast Reconstr Surg* 1982;69:412–422.
4. Meyer JS, Hoffer FA, Barnes PD, Mulliken JB. Biological classification of soft-tissue vascular anomalies: MR correlation. *AJR Am J Roentgenol* 1991;157:559–564.

Chapter 191

Lymphatic Malformations

Epidemiology

Lymphatic malformation (*LM*) is the current term used to describe lymphangiomas. Mulliken and Glowacki recommend that the suffix *-oma* only be used in lesions that exhibit cellular proliferation such as a hemangioma. LMs are congenital lesions that result from a defect in embryogenesis of the lymphatic system. They occur in equal frequency in males and females. They most commonly present in newborn children, with 65% of lesions noted at birth, 80% present at 1 year, and 90% present by 2 years of age. Ten percent of LMs may initially present in adulthood. LMs may be localized or associated with a generalized malformation of the lymphatic system. Advanced generalized disorders may be seen as diffuse lymphangiectasis in utero, which is incompatible with life. Lymphangiectasis has been associated with a number of syndromes, the most common being Turner's syndrome. Other syndromes include Noonan's syndrome, fetal alcohol syndrome, familial pterygium syndrome, distichiasis–lymphedema syndrome, and various chromosomal aneuploidies.

Embryology

LM is thought to occur from a defect in the normal drainage of the lymphatic channels into the venous system. The result is a progressive enlargement of the isolated lymphatic spaces due to the continued secretion of lymph. There are several proposed explanations of this malformation. The malformation may be due to a portion of the lymphatic network that fails to reestablish a communication with the venous system and is sequestered early in embryogenesis. Early malformations involving the more primitive jugular, subclavian, and axillary sac are felt to result in the formation of the larger cystic hygromas. These lesions occur in soft areolar tissues in areas with wide fascial planes, with the result being sharply demarcated round or oval lesions. Lesions that have smaller cystic spaces and are more diffuse and infiltrative are believed to occur later in embryogenesis. These malformations have time to grow distally along narrower facial planes and insinuate themselves along vessels and nerve trunks. This probably results in the mixed malformations described by Mulliken and Glowacki such as lymphaticovenous and lymphaticocapillary malformations. Thus, LMs that occur in the cheeks, lips, and tongue tend to contain more of an angiomatous component.

Pathology

Pathologically, LMs have been categorized in the past based on the size of the anomalous lymphatic space. As already noted, *lymphatic malformation* is the current term used to describe these malformations and that terms such as *cavernous lymphangioma* and *capillary lymphangioma* probably refer to the "mixed" lymphatic malformations described by Mulliken and Glowacki. We use the older terminology following here for historical consistency.

Cystic hygroma is the most common form and consists of a honeycomb of very large dilated lymphatic spaces lined by a single layer of flat endothelium. These lesions are often solitary and occur in the presence of an otherwise normal lymphatic system. Seventy-five percent of these lesions occur in the neck, with a predilection for the posterior compartment of the neck.

A cavernous lymphangioma is composed of mild to moderately dilated lymphatic spaces, the size of which is between the cystic spaces seen in cystic hygromas and capillary hemangiomas. These lesions tend to be situated in the oral cavity or salivary glands. Cavernous lymphangiectasis tend to be subcutaneous lesions that have a propensity to penetrate adjacent muscular and neurovascular structures without destroying them. The peripheral location and subcutaneous spread are suggestive of a defect in embryogenesis during a later phase of lymphatic development (9–10 weeks) than that of a cystic hygroma.

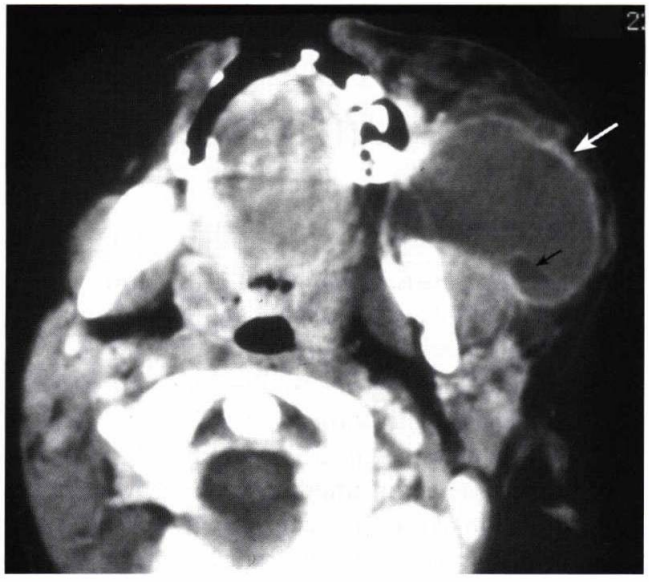

Figure 191-1. CT findings of lymphatic malformations. Axial contrast-enhanced CT shows a low attenuation mass that contains internal septations situated in the left buccal space (large arrow). Note the fluid-fluid level that could represent recent hemorrhage (small arrow).

Capillary hemangioma (simple, lymphangioma simplex) is composed of a network of small lymph, thin-walled channels that are the size of capillaries and is the least common form of lymphangioma. These lesions are located predominantly within the epidermis and can occur anywhere throughout the body. Because of their superficial location, capillary hemangiomas are believed to form the latest in development.

Clinical Findings

Most (75%) LMs occur in the extracranial head and neck. They typically present as a pliable painless cheek mass. Lesions that occur in the face are more likely to be mixed LMs. LMs tend to enlarge commensurate with the growth of the child and not by endothelial proliferation. Potential complications include disfigurement and recurrent infections. Rapid enlargement may be due to infection or spontaneous hemorrhage within the lesion.

Treatment

Surgical resection is the treatment of choice for LMs with distinct margins. However, distal lesions that extend over several anatomical areas are difficult to completely resect and are prone to recurrence. Such patients need close follow-up and may require multiple surgical procedures. Percutaneous sclerotherapy is gaining wider acceptance for more advanced lesions that infiltrate the deep fascial planes. The role of interferon therapy for very advanced and infiltrative lesions is currently under investigation.

Imaging Findings

CT

The classic appearance of an LM is a sharply demarcated, low attenuation mass that does not contain a visible wall. Lesions that have been partially resected or have been repeatedly infected may demonstrate an enhancing wall or contain internal septations. Mixed LMs are heterogeneous and infiltrative. These lesions extend along fascial planes and often involve multiple spaces ("transspatial"). Because of the angiomatous components, mixed lesions may enhance with contrast (Fig. 191-1).

MR

A pure LM is low signal on T1-weighted sequences and high signal on T2-weighted sequences. There is no perceptible wall or enhancement following contrast administration. Pure LMs are low flow lesions and lack flow voids. Mixed malformations are infiltrative heterogenous lesions that enhance following contrast. The degree of the enhancement is likely due to the angiomatous component of the mixed lesion (Fig. 191-2).

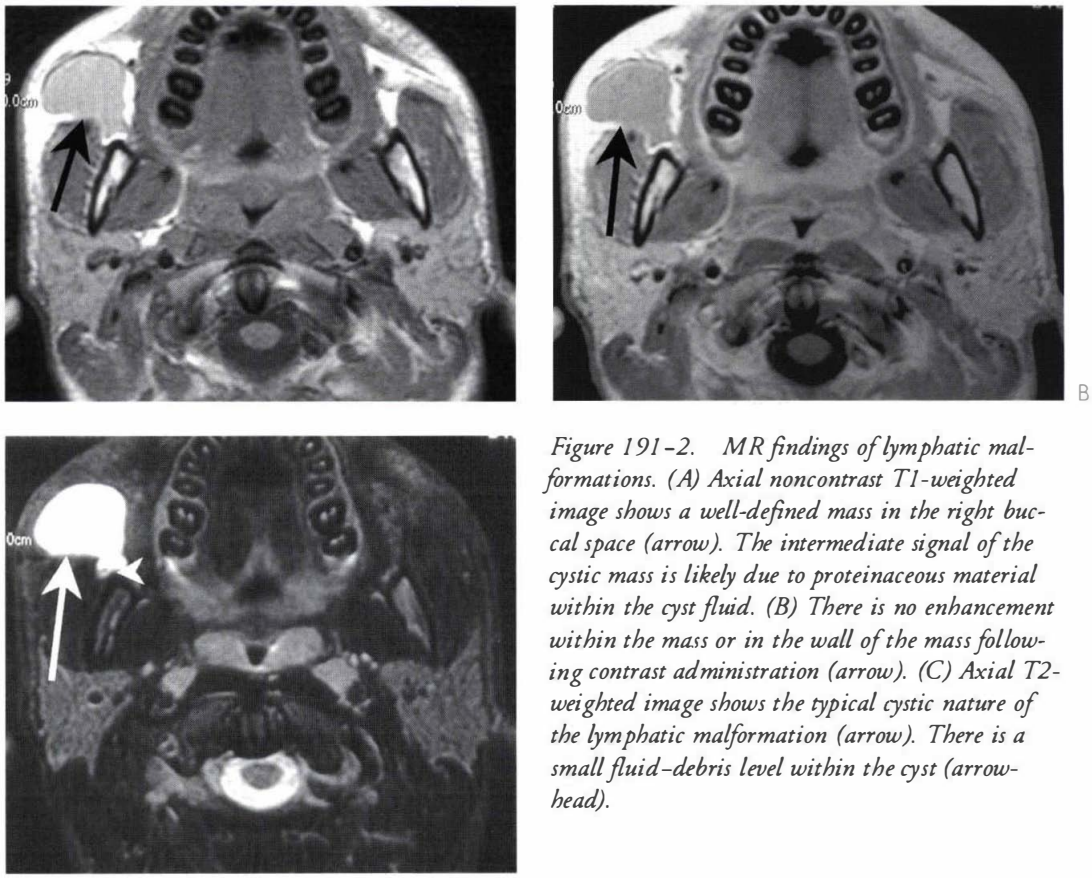

Figure 191-2. MR findings of lymphatic malformations. (A) Axial noncontrast T1-weighted image shows a well-defined mass in the right buccal space (arrow). The intermediate signal of the cystic mass is likely due to proteinaceous material within the cyst fluid. (B) There is no enhancement within the mass or in the wall of the mass following contrast administration (arrow). (C) Axial T2-weighted image shows the typical cystic nature of the lymphatic malformation (arrow). There is a small fluid-debris level within the cyst (arrowhead).

US

Pure LMs are hypoechoic masses that may occasionally contain internal septations or debris. Doppler analysis may be helpful in identifying and characterizing mixed LMs by identifying and characterizing the presence of intralesional blood flow.

Angiography

Pure LMs are low flow lesions. However, mixed LMs that have a substantial angiomatous component are hypervascular and have enlarged feeding vessels. Arteriovenous shunting is rare.

Imaging Pearls

- MR is superior to CT for defining the complete extent of the lymphatic malformation.
- A predominantly cystic mass that is transspatial is the characteristic imaging of an LM.

Suggested Readings

1. Zadvinski DP, Benson MT, Kerr HH, et al. Congenital malformations of the cervicothoracic lymphatic system: embryology and pathogenesis. *Radiographics* 1992;1175–1189.
2. Batsakis JG. Vasoformative tumors. In: *Tumors of the Head and Neck.* 2nd ed. Wilkens Baltimore: Williams and Wilkins; 1979:518–520.
3. Mulliken JB, Glowacki J. Hemangiomas and vascular malformations in infants and children: a classification based on endothelial characteristics. *Plast Reconstr Surg* 1982;69:412–422.
4. Mulliken JB. Vascular malformations of the head and neck. In: Mulliken JB, Young AE, eds. *Vascular Birthmarks: Hemangiomas and Malformations.* Philadelphia: WB Saunders; 1988:301–307.

Section IX

Sublingual Space

The sublingual space (SLS) is easy to identify if one realizes that *lingua* is Latin for *tongue*. Thus, the sublingual space is the space located below the tongue. Another name for the sublingual space often used by otolaryngologists is *floor of mouth*.

The SLS is a teacup-shaped space that is situated within the confines of the mylohyoid muscle. This appearance is best appreciated on coronal imaging. The mylohyoid muscle attaches to the lingual surface of the mandible at the mylohyoid line. Thus, the mylohyoid muscle forms a muscular "sling," which is analogous to the muscles that make up the pelvic sling musculature. Whereas the pelvis sling musculature contains the contents of the pelvis, the mylohyoid muscle contains the contents of the SLS (Figs. IX–1 and IX–2).

The contents of the SLS are muscles (anterior extension of the hyoglossus muscle) and the hypoglossal nerve, lingual nerve, lingual artery and vein, sublingual gland and ducts, hilum of the submandibular gland and duct, and lymph nodes. Some authors separate the SLS into right and left halves by the midline genioglossus–geniohyoid complex. However, for practical purposes, one can consider the sublingual space as one large compartment.

The most common lesion of the sublingual space is a squamous cell carcinoma arising from the epithelial covering of the sublingual space followed by spread from an odontogenic infection and developmental masses.

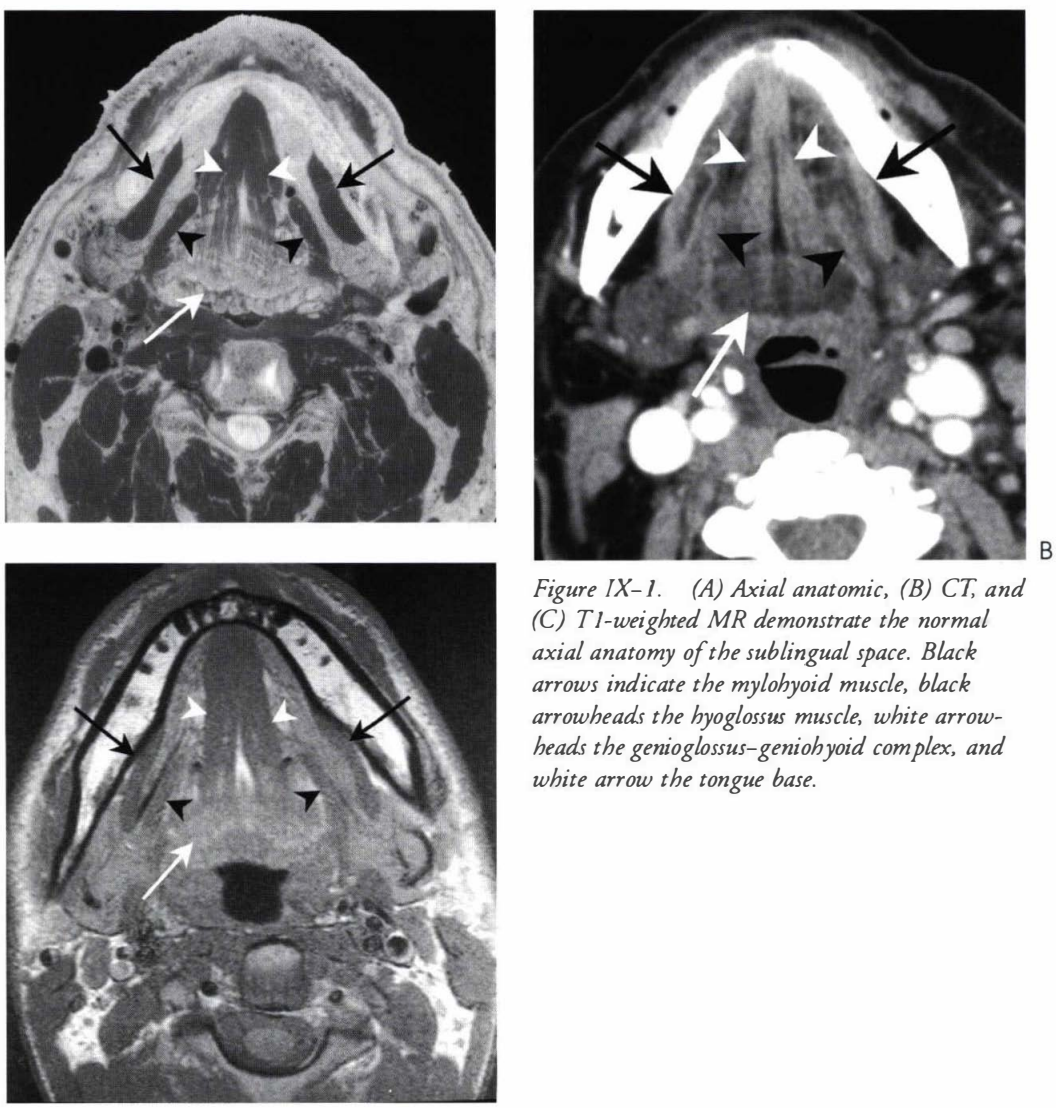

Figure IX–1. (A) Axial anatomic, (B) CT, and (C) T1-weighted MR demonstrate the normal axial anatomy of the sublingual space. Black arrows indicate the mylohyoid muscle, black arrowheads the hyoglossus muscle, white arrowheads the genioglossus–geniohyoid complex, and white arrow the tongue base.

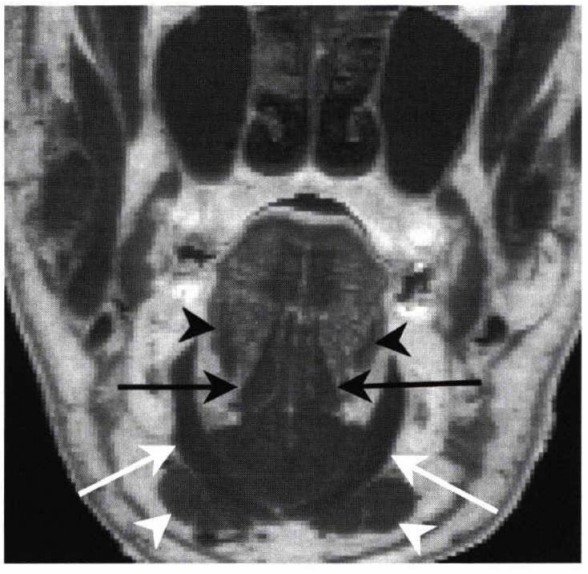

Figure IX-2. Coronal anatomic image shows the mylohyoid muscle (white arrows) separate the sublingual space (above) from the submandibular space (below). Small white arrowheads indicate the anterior belly of the digastric muscle, black arrows the geniohyoid–genioglossus complex, black arrowheads the hyoglossus muscles.

Suggested Readings

1. Harnsberger HR. *Handbook of Head and Neck Imaging*. 2nd ed. St. Louis: Mosby Year Book;1995.
2. Grodinsky M, Holyoke EA. The fasciae and fascial spaces of the head, neck and adjacent regions. *Am J Anat* 1938;63:367–408.
3. Mukherji SK, Castillo M. A simplified approach to the spaces of the extracranial head and neck. *Radiol Clin North Am* 1998;36:761–780.

Chapter 192

Abscess

Epidemiology

The sublingual space (SLS) is located inferior to intrinsic muscles of the oral tongue, medial to the mandible, and superomedial to the mylohyoid muscle. Posteriorly, the SLS communicates with the submandibular space (SMS) with no fascia separating these spaces. Abscesses originating in this space may be due to sublingual or submandibular duct stenosis or calculus disease. Dental infection or mandibular osteomyelitis may also extend into the SLS.

Clinical Findings

Patients with SLS abscess usually present with pain, tenderness, and swelling in the anterior floor of the mouth. This may be associated with trismus when inflammation involves the medial pterygoid muscle. There may be a history of salivary colic, recent dental disease, or dental manipulation.

Pathology

An enlarging SLS abscess, like a plunging ranula, decompresses posteriorly into the SMS. Because the SMS is more commodious, the submandibular component of the lesion frequently overshadows that of the SLS. As in SMS infection, the most commonly encountered organisms are *Staphylococcus aureus* and *Streptococcus viridans*.

Treatment

Treatment of an SLS abscess should commence with antibiotic therapy followed by surgical drainage. Any stone within the submandibular duct (which is located in the SMS) should be removed at the same time. An underlying dental infection or osteomyelitis should also be treated accordingly.

Imaging Findings

CT

CT shows an enhancing mass involving the SLS associated with subcutaneous streaking and thickening of the platysmus muscle. The genioglossus–geniohyoid complex is often displaced medially or across the midline. If an SMS component is present, this abscess may track into parapharyngeal space where further spread can take place in a craniocaudal axis. Infection may also spread to the medial pterygoid or masseter muscles (Fig. 192-1).

MR

MR imaging is rarely used for inflammatory diseases involving the SLS. An SLS abscess shows the typical enhancing mass on T1-weighted images and high signal intensity on T2-weighted images. In contrast-enhanced images, a central area of no enhancement indicating pus collection can readily be demonstrated. Mandibular marrow edema is more readily demonstrated on MR because intermediate signal tissues replace high signal intensity fat on T1-weighted images.

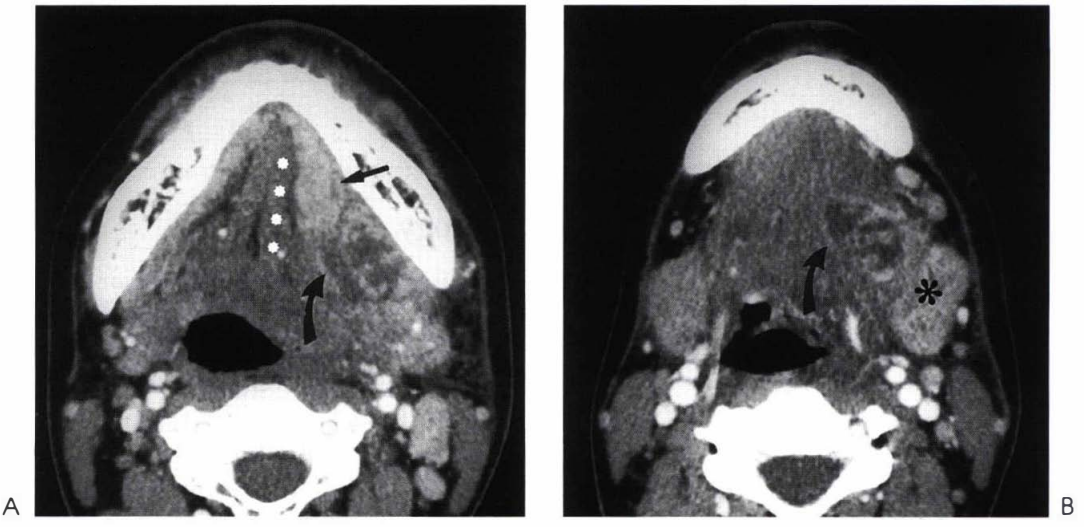

Figure 192-1. Sublingual space abscess. (A) Axial contrast-enhanced CT shows a mixed attenuation abscess in the left sublingual space (curved arrow). Note the enlargement of the left sublingual gland (straight arrow) and displacement of the left genioglossus (asterisks) to the contralateral side. (B) Axial contrast-enhanced CT shows abscess extends inferiorly into the left submandibular space (curved arrow) abutting and slightly displacing the left submandibular gland (asterisk).

Imaging Pearls

- Inflammation involving the SLS should be evaluated with CT. Calculus disease, gas pockets, or cortical erosion of the mandible are much easier to identify on CT when compared with MR imaging.
- When an SMS abscess is identified, the telltale sign of a sublingual component should be also be sought. This can be accomplished by looking for the characteristic tail extending anteriorly between the mylohyoid muscle laterally and the genioglossus-geniohyoid complex. This sign is especially important because, on rare occasions, the lesion is due to an infected ranula. For a complete cure the sublingual component must be excised.

Suggested Readings

1. Harnsberger HR. *Handbook of Head and Neck Imaging.* 2nd ed. Chicago: Mosby; 1995:129-134.
2. Carter BL. Salivary glands. In: Valvassori GE, Mafee MF, Carter BL, eds. *Imaging of the Head and Neck.* New York: Thieme; 1995:475-509.
3. Mukherji SK, Castillo M. A simplified approach to spaces of the suprahyoid neck. *Radiol Clin North Am* 1998;36:761-780.

Chapter 193

Ludwig's Angina

Epidemiology

The term *Ludwig's angina* refers to cellulitis involving the SLS. In 1939 Grodinsky put forward the diagnostic criteria for this clinical entity: (1) involvement of both submandibular and sublingual spaces either unilaterally or bilaterally; (2) the formation of serosanguinous phlegmon or gangrene but without the formation of abscess; (3) involvement of connective tissues, fascia, and muscles but not the submandibular or sublingual glands; and (4) disease propagation by direct extension (without the involvement of lymphatics). The presence of an odontogenic infection is common and should be evaluated in all cases. Because the SLS is an enclosed space, one can consider the progressive inflammation and phlegman a "compartment syndrome" of the SLS. Advanced cases will result in airway obstruction.

Clinical Findings

Patients usually present with pain, tenderness, and swelling of the floor of mouth. Progression of disease will result in laryngeal edema and resultant airway obstruction. In neglected cases, Ludwig's angina may spread inferiorly through fascial planes into the mediastinum. Hence, some patients may present with chest pain.

Pathology

Cellulitis of the floor of mouth is usually secondary to infection of the mandibular molars in as high as 90% of the cases. This infection is usually due to *Streptococcus* or *Staphylococcus*.

Treatment

Treatment should start with the institution of appropriate intravenous antibiotics. The underlying dental disease should also be treated. Surgical drainage of all abscess collections needs to be performed, especially those involving the sublingual space. Because the airway may be compromised, securing a patent airway is an important aspect of the management of this entity.

Imaging Findings

CT

Contrast-enhanced CT shows swelling of the floor of mouth. This finding is frequently associated with streaky changes in the adjacent subcutaneous fat and thickening of the overlying platysmus muscle. Enlargement of the submental or submandibular lymph nodes may also be seen. In late cases, pus or gas formation may take place and the airway may be compressed (Figs. 193–1 and 193–2).

MR

MR imaging is usually not performed for inflammatory disease involving the submandibular space because stone disease, cortical erosion of the mandible, and gas formation may remain undetected. Contrast-enhanced MR images show a thickened floor of mouth with strong enhancement. On T2-weighted images, diffuse high signals are evident in the floor of mouth and adjacent soft tissues.

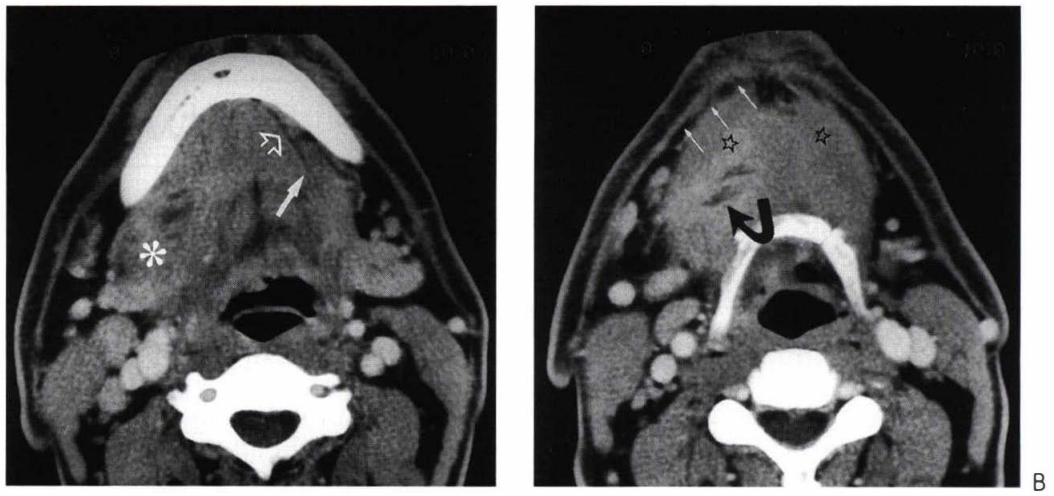

Figure 193–1. (A) Axial contrast-enhanced CT shows soft tissue thickening involving the right submandibular space (asterisk). Note the associated loss of tissue planes around the right floor of mouth. Compare with the normal left mylohyoid muscle tissue plane (solid arrow) and sublingual space (hollow arrow). (B) Axial contrast-enhanced CT shows diffuse swelling involving the anterior bellies of the digastric muscles bilaterally (stars). Note the presence of low densities indicating gas formation (curved arrow). There is also thickening of the platysmus muscle (small arrows).

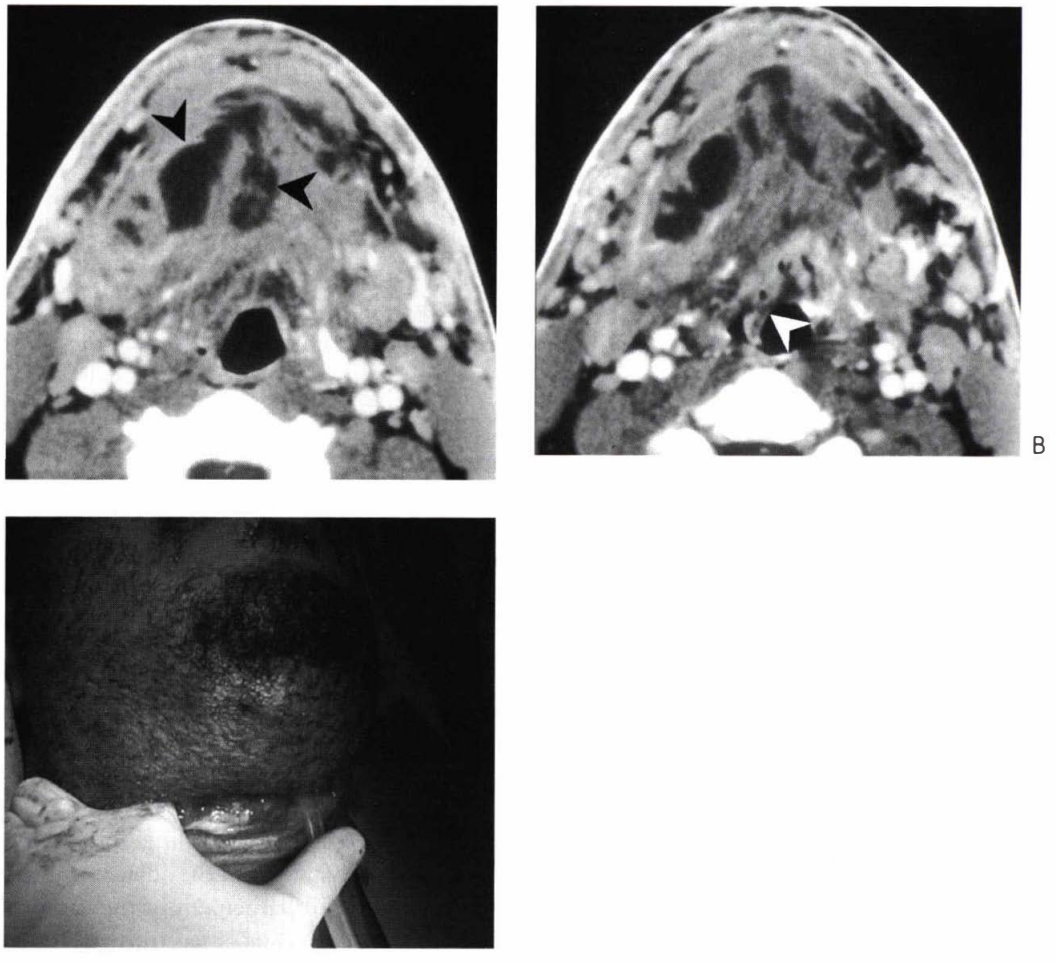

Figure 193–2. (A) Axial contrast-enhanced CT shows mutiple abcesses layering within the sublingual space (arrowheads). (B) Axial image obtained 6 mm inferior to (A) shows edema of the suprahyoid epiglottis (arrowhead). (C) An intraoperative photograph demonstrates that this patient was treated with a cervical excision with drainage of the multiple abscesses.

Imaging Pearls

- Inflammation of the floor of mouth can extend posteriorly to the hyoid bone and down the visceral space into the mediastinum. It is therefore important to trace the margins of the inflammatory process.
- The majority of cases of Ludwig's angina are due to mandibular osteomyelitis or dental abscess. A search for mandibular osteolysis should be made and CT studies should be reconstructed using bone algorithm. On MR, the T2-weighted images should be evaluated for focal areas on increased signal on T2-weighted images originating from tooth sockets or the mandibular marrow space.

Suggested Readings

1. Smoker WRK. Oral cavity. In: Som PM, Curtin HD, eds. *Head and Neck Imaging*. St. Louis: Mosby; 1996:488–544.
2. Nguyen VD, Potter JL, Hersh-Schick MR. Ludwig angina: an uncommon and potentially lethal neck infection. *AJNR Am J Neuroradiol* 1992;13:215–219.
3. Grodinsky MD. Ludwig's angina: an anatomical and clinical study with review of the literature. *Surgery* 1939;5:678–696.

Chapter 194

Squamous Cell Carcinoma of the Floor of Mouth

Epidemiology

Squamous cell carcinoma (SCCA) of the floor of mouth (FOM) is the second common site of SCCA of the oral cavity and accounts for approximately 10 to 15% of all oral cavity carcinomas. The disease is more common in men between the ages of 40 and 60 (Fig. 194–1). Risk factors include smoking, alcohol abuse, and chewing betel nut. There does not appear to be an increased risk of FOM SCCA in patients with human immunodeficiency virus (HIV) disease. However, FOM SCCA appears to be more aggressive when it does occur in these patients.

Clinical Features

The most frequent location is the anterior floor of mouth. Table 194–1 lists the American Joint Committee on Cancer staging classification of the oral cavity. Early lesions appear as a slightly elevated, reddish area with ill-defined borders with minimal induration. Advanced lesions may extend along the periosteum, erode the mandible, or invade the tongue base. Early lesions are usually asymptomatic and may be detected on a routine dental checkup.

About 30% of patients will have positive nodes at initial presentation. The lymphatic drainage of the FOM is supplied by an anterior and a posterior complex. The anterior complex drains the anterior half of the FOM and anterior portion of the sublingual gland. These lymphatic vessels terminate in the Level I nodes. The posterior group drains the posterior two thirds of the FOM. The primary drainage is to the ipsilateral Level II lymph nodes. However, there is occasionally a direct lymphatic drainage to the Level III nodes that bypasses the Level II nodes. Anatomic studies have shown significant cross-over of the lymphatic drainage of superficial lymphatic capillaries. As a result, both sides of the neck are at risk for metastases arising from FOM malignancies.

Pathology

Histologically, SCCA is classified as well, moderately, and poorly differentiated. On microscopic examination, SCCA appears as anaplastic-appearing cells found below the basement membrane with a variable degree of keratin production and intracellular bridges. FOM SCCA tend to be well differentiated.

Table 194–1
Sixth American Joint Committee on Cancer Staging Classification of the Oral Cavity

TX	Primary tumor cannot be assessed
T0	No evidence of primary tumor
Tis	Carcinoma in situ
T1	Tumor ≤ 2 cm in greatest dimension
T2	Tumor more than 2 ≥ 4 cm in greatest diameter
T3	Tumor ≥ 4 cm
T4 (lip)	Tumor invades through cortical bone, inferior alveolar nerve, floor of mouth, or skin of face (i.e., chin or nose)
T4a (oral cavity)	Tumor invades adjacent structures [e.g., through cortical bone, into deep (extrinsic) muscle of tongue (genioglossus, hyoglossus, palatoglossus, and styloglossus), maxillary sinus, skin of face]
T4b	Tumor invades masticator space, pterygoid plates, or skull base and/or encases internal carotid artery

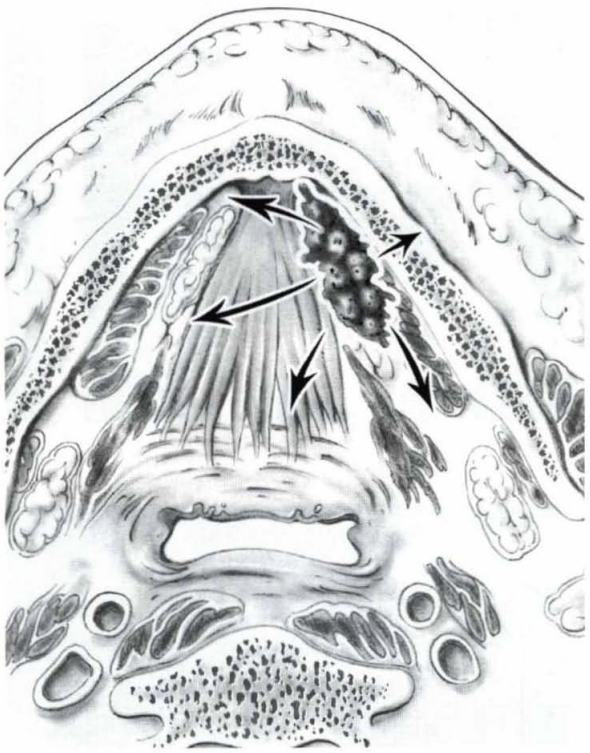

Figure 194-1. Schematic illustration of a floor of mouth cancer. The arrows denote potential spread patterns. (Figure reproduced with permission from Mukherij, SK, Pillsbury H, Castillo M. Imaging squamous cell carcinomas of the upper aerodigestive tract: what the clinicans need to know. Radiology *1997;205:629-646.)*

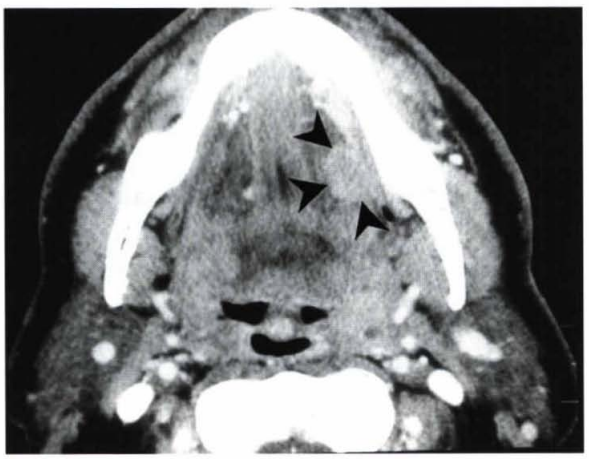

Figure 194-2. Axial contrast-enhanced CT shows an enhancing SCCA in the left side of the floor of mouth (arrowheads).

Treatment

The most common treatment for SCCA is surgical resection. Wide local excision is performed for superficial lesions. A marginal mandibulectomy is performed for tumors that are fixed to but do not invade the mandible. A segmental mandibulectomy is performed for tumors that erode the mandible. Combined chemotherapy and radiation therapy is gaining acceptance for advanced tumors that cross the midline or invade the tongue base.

Imaging Findings

CT

These tumors present as enhancing masses located in the sublingual space (Figs. 194-2 through 194-4). Early lesions may present as a subtle asymmetry, whereas advanced lesions are aggressive enhancing lesions. FOM tumors may extend inferiorly along the hyoglossus muscle or posteriorly to involve the tongue base. Occasionally, advanced tumors may extend over the free margin of the mylohyoid muscle into the soft tissues of the neck.

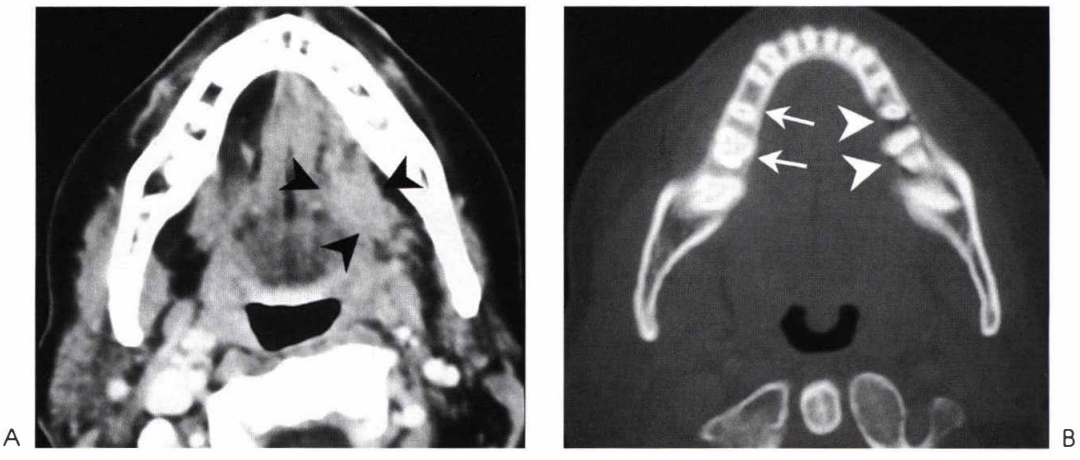

Figure 194-3. (A) Axial contrast-enhanced CT shows a left-sided floor of mouth cancer (arrowheads). (B) Bone algorithm shows absence of the lingual cortex adjacent to the tumor (arrowheads). Compare this to the appearance of the normal cortex on the uninvolved side (arrows).

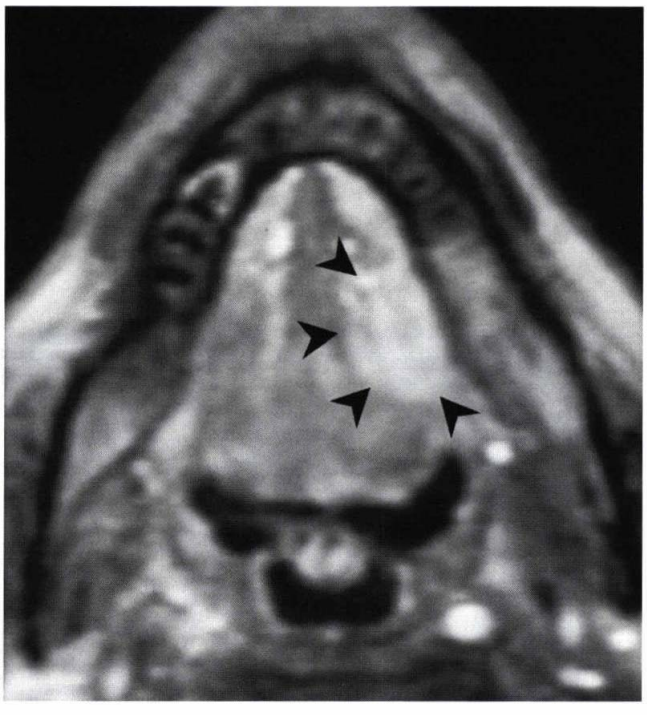

Figure 194-4. Contrast-enhanced gradient echo image shows a densely enhancing mass located in the left floor of mouth (SLS) (arrowheads).

MR

SCCA is usually intermediate signal on T1-weighted and slightly increased signal on T2-weighted images. The lesions usually enhance following contrast administration. Mandibular involvement may be suspected if there is replacement of the normal high signal of the marrow by intermediate signal.

Imaging Pearls

- In our experience, the sequences that best identify the extent of disease at the primary site on MR are noncontrast T1-weighted and dynamic enhanced two-dimensional gradient echo sequences with fat saturation.
- The following specific information must be described in the reports and will directly affect the treatment and management of patients with floor of mouth carcinoma:
  - Presence and extent of bone erosion
  - Deep invasion along the mylohyoid and hyoglossus muscles
  - Relationship to ipsilateral lingual neurovascular bundle
  - Extension across the midline and relationship to the contralateral neurovascular bundle
  - Tongue base invasion
  - Extension into the soft tissues of the neck

Suggested Readings

1. Mukherji SK, Pillsbury H, Castillo M. Imaging squamous cell carcinomas of the upper aerodigestive tract: what the clinicians need to know. *Radiology* 1997;205:629–646.
2. Million RR, Cassisi NJ, Mancuso AA. Oral cavity. In: Million RR, Cassisi NJ, eds. *Management of Head and Neck Cancer: A Multidisciplinary Approach.* Philadelphia: JB Lippincott; 1994:321–400.
3. Batsakis JG. Squamous cell carcinoma of the oral cavity and oropharynx. In: Batsakis JG, ed. *Tumors of the Head and Neck.* Baltimore: Williams and Wilkins; 1979:144–176.

Chapter 195

Malignant Minor Salivary Gland Tumors (Adenoidcystic, Mucoepidermoid, Adenocarcinoma, Low Grade Polymorphous Adenocarcinoma)

Epidemiology

The same malignancies that arise in the major salivary glands occur in the minor salivary glands. Depending on the series, approximately half of all tumors of minor salivary gland origin are malignant. The most common location is the palate. An interesting paradox is that the smaller the salivary gland, the greater the likelihood that a tumor originating from that gland will be malignant. The incidence of a salivary gland tumor being malignant is substantially greater in the palate than in the parotid.

Clinical Findings

Patients often present with asymptomatic masses that have been present for several months. Pain and ulceration may be present; however, these are not consistent findings.

Pathology

It has been estimated that there are between 500 and 1000 minor salivary glands located throughout the oral cavity and oropharynx. They may be found within the hard and soft palate, uvula, lips, retromolar trigone, tongue base, floor of mouth, and tonsil. The malignancies that constitute minor salivary gland tumors include adenoid cystic carcinoma, mucoepidermoid carcinoma, and adenocarcinoma. Many investigators now include low grade polymorphous adenocarcinoma as a tumor of minor salivary gland origin. The most common malignancy of the minor salivary glands is adenoid cystic carcinoma.

Treatment

The treatment of malignant salivary gland tumors depends on the exact histologic type. In general, complete surgical resection offers the best chance for cure. Postoperative radiation therapy is required in the majority of cases. The role of neutron beam therapy for unresectable adenoid cystic carcinomas is currently being evaluated.

Imaging Findings

CT

The CT findings are nonspecific. These are usually soft tissue masses that enhance following contrast. The presence of aggressive bone erosion is suggestive of a high-grade malignancy (Fig. 195–1).

MR

These tumors are usually intermediate signal on T1-weighted sequences and enhance following contrast administration. The T2-weighted signal is variable (Fig. 195–2).

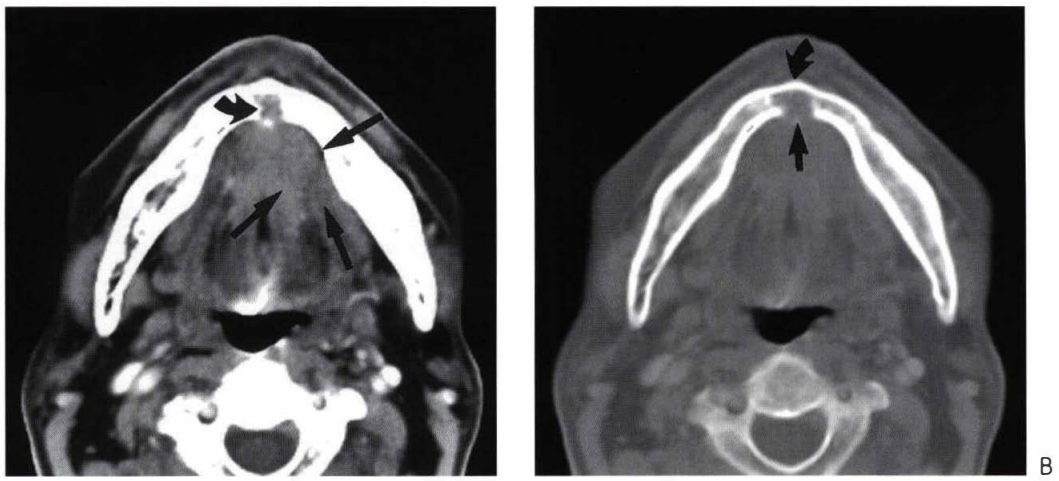

Figure 195–1. CT of adenoid cystic carcinoma. (A) Axial contrast-enhanced CT shows an aggressive mass involving the anterior left side of the sublingual space (floor of mouth) (straight arrows). The mass extends to the midline and erodes the lingual cortex of the mandible at the level of the genial tubercle (curved arrow). (B) Bone algorithm confirms the bone erosion along the lingual cortex of the mandible (short arrow) with sparing of the buccal cortex (curved arrow).

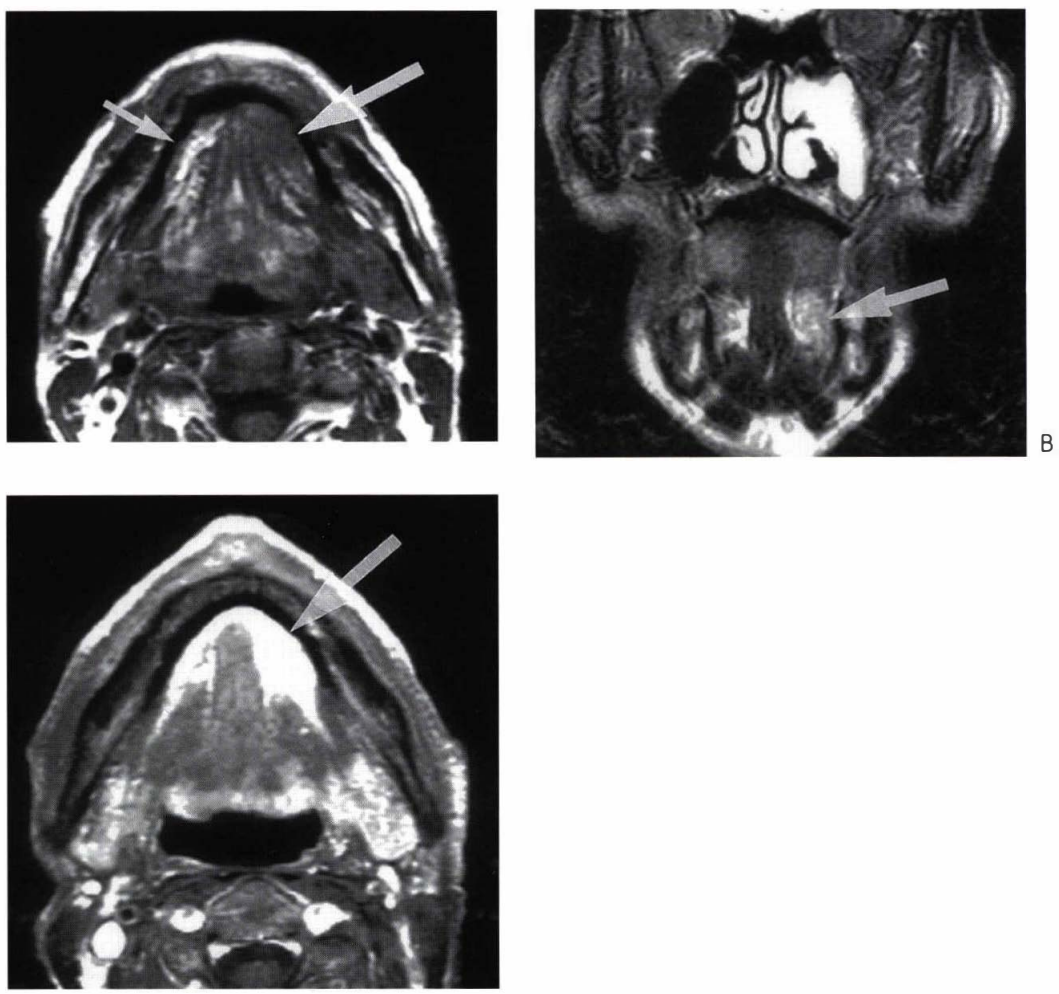

Figure 195–2. MR of adenoid cystic carcinoma. (A) Axial noncontrast T1-weighted image shows a mass in the left sublingual space (large arrow). Compare this with the appearance in the normal contralateral side (small arrow). (B) Coronal T2-weighted image shows the mass contains intermediate T2-weighted signal (arrow). This finding suggests that the mass is not a pleomorphic adenoma. (C) Fat-suppressed contrast-enhanced T1-weighted image shows the mass diffusely enhances with contrast (arrow). Pathology revealed adenoid cystic carcinoma.

Imaging Pearls

- For adenoid cystic carcinoma involving the hard palate, CT should be performed to evaluate for bone erosion in the regions of the incisive canal and greater and lesser palatine foramen. MR should be performed to evaluate for extension into the pterygopalatine fossa and possible retrograde perineural spread along the maxillary division of the fifth cranial nerve or along the nerve of the vidian canal. These are potential pathways of spread in the cavernous sinus. These potential spread patterns should be evaluated in all patients as this may preclude primary surgical resection at many institutions.

- Patients who present with infraorbital numbness and paresthesias should undergo a high resolution MR of the palate and trigeminal nerve to evaluate for the presence of clinically occult adenoid cystic carcinoma of the hard or soft palate that has invaded the infraorbital nerve.
- We recommend performing MR imaging in patients with polymorphous adenocarcinoma arising in the oral cavity because, based on our experience, it appears this tumor has a propensity for marrow invasion.

Suggested Readings

1. Batsakis JG. Neoplasms of the minor and lesser major salivary glands. In: Batsakis JG, ed. *Tumors of the Head and Neck*. Baltimore: Williams and Wilkins; 1979:76–99.
2. Smoker WRK. Oral cavity. In: Som PM, Curtin H, eds. *Head and Neck Imaging*. 3rd ed. New York: Mosby; 1996:488–544.
3. Shockley WM. Parotid tumors. In: Shockley WM, Pillsbury HC. *The Neck: Diagnosis and Surgery*. New York: Mosby; 1994:265–294.

Chapter 196

Benign Minor Salivary Gland Tumors (Pleomorphic Adenoma, Monomorphic Adenoma, Warthin's Tumor

Epidemiology

A minor salivary gland consists of cellular constituents of the major salivary glands (parotid, submandibular, sublingual) that are located within the mucosa of the upper aerodigestive tract. It has been estimated that there are between 500 and 1000 minor salivary glands located throughout the oral cavity and oropharynx. They may be found within the hard and soft palate, uvula, lips, retromolar trigone, tongue base, floor of mouth, and tonsil. The same malignancies that arise in the major salivary glands occur in the minor salivary glands. Depending on the series, approximately 50% of minor salivary gland tumors are benign compared with approximately 70 to 80% of parotid tumors that are benign.

Clinical Findings

Patients often present with an uncomfortable mass under the tongue. There is typically a delay in the initial medical observation and onset of symptoms.

Pathology

The benign tumors that constitute minor salivary gland tumors include pleomorphic adenoma, monomorphic adenoma, and Warthin's tumor. The pathology of these lesions has been reviewed in other sections of this textbook.

Treatment

The exact treatment depends on the pathology. For most benign tumors complete local resection is adequate.

Imaging Findings

CT

The CT findings are nonspecific. The presence of regressive remodeling of the surrounding bone for lesions that arise in the hard palate is suggestive of a benign minor salivary gland tumor (Fig. 196–1).

MR

In general, the imaging findings are nonspecific. However, oral cavity or oropharyngeal lesions that are low to intermediate signal on T1-weighted and increased signal on T2-weighted sequences is suggestive of pleomorphic adenoma.

Imaging Pearl

- In general, these are uncommon lesions with diagnosis usually at histology following initial biopsy. The intent of imaging is to provide information that cannot be detected on clinical examination. CT is helpful to evaluate the extent of bone erosion. MR should be performed to determine the presence of submucosal spread and deep invasion.

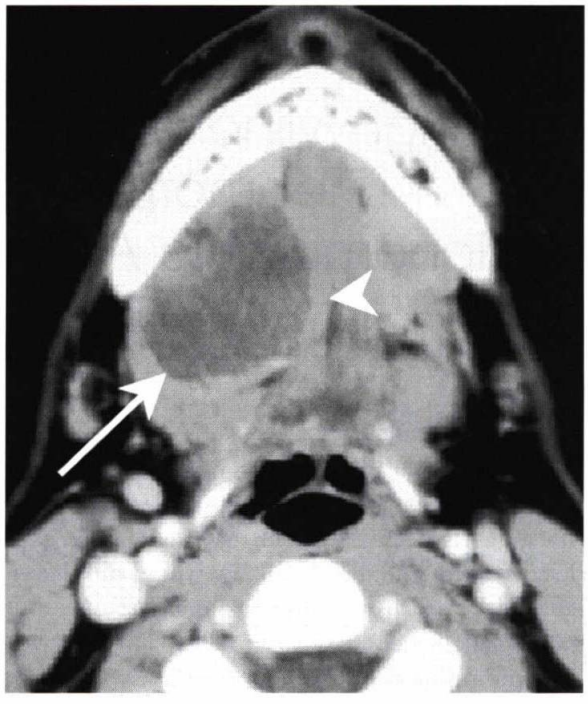

Figure 196-1. Axial contrast-enhanced CT shows a heterogeneous mass that is a predominantly low attenuation mass situated in the right sublingual space (arrow). The mas medially displaced the geniohyoid muscle (arrowhead). Pathology revealed a pleomorphic adenoma. (Courtesy of Dr. Wendy Smooker, M.D.)

Suggested Readings

1. Batsakis JG. Neoplasms of the minor and lesser major salivary glands. In: Batsakis JG, ed. *Tumors of the Head and Neck.* Baltimore: Williams and Wilkins; 1979:76–99.
2. Smoker WRK. Oral cavity. In: Som PM, Curtin H, eds. *Head and Neck Imaging.* 3rd ed. New York: Mosby; 1996:488–544.
3. Shockley WM. Parotid tumors. In: Shockley WM, Pillsbury HC. *The Neck: Diagnosis and Surgery.* New York: Mosby; 1994:265–294.

Chapter 197

Simple Ranula

Epidemiology

A ranula is a cystic lesion arising in the floor of mouth that is believed to result from obstruction of the sublingual or minor salivary gland. The obstruction is most commonly thought to be congenital or posttraumatic in origin. The cysts develop from continued secretion of the mucous glands into an obstructed duct. Ranulas have also been referred to as mucoceles or pseudocysts in the floor of mouth. Although ranulas have been reported in all age groups, they are most common in children and young adults. There is no reported gender predilection.

Clinical Findings

There are two types of ranulas, simple and complex. A simple ranula is the most common form. By definition, simple ranulas are above the mylohyoid muscle and are confined to the sublingual space. They are usually paramedian and are situated in the vicinity of the sublingual gland. Simple ranulas present as submucosal SLS masses. They are typically pliable palpation on and exhibit a characteristic translucent, bluish hue ("frog belly" appearance). Ranulas may occasionally rupture, causing expulsion of viscid fluid into the oral cavity.

The diving ranula (plunging, complex) is believed by some to arise from rupture of a simple ranula. These lesions extend inferiorly below the level of the mylohyoid muscle either by extending over the free margin of the mylohyoid muscle or by passing directly through it. Diving ranulas present as a painless, fluctuant, soft tissue neck mass. The majority of diving ranulas are above the hyoid bone, although large lesions may extend into the thoracic inlet or mediastinum.

Pathology

Simple ranulas are epithelial-lined cysts. Because diving ranulas are thought to result from cyst rupture, these lesions do not contain an epithelial lining. Instead, they tend to resemble pseudocysts that are lined by dense connective or granulation tissue. Histologically, the fluid component consists of mucin and histiocytes.

Treatment

The treatment of ranulas is dependent on the type of ranula. The type of ranula is determined by the extent of the lesion seen on imaging. Simple ranulas confined to the floor of mouth may be treated by marsupialization through a transoral approach. Removal of the ipsilateral sublingual gland at the time of surgery is associated with a lower rate of recurrence. Diving ranulas require a more aggressive approach. Adequate resection requires a wider exposure that can only be obtained through a combined transoral and cervical approach. Attempted marsupialization of a diving ranula with its nonepithelial-lined capsule is associated with a high likelihood of recurrence.

Imaging Findings

CT

The CT appearance of a simple ranula is a well-defined unilocular cystic lesion confined to the floor of mouth. Calcifications are very unusual. The cyst wall is typically very thin unless there has been a history of previous surgery or infection. Ranulas that have been repeatedly infected or have undergone prior surgery may have an enhancing wall or contain internal septations. By definition, these masses are above the mylohyoid muscle and contained in the sublingual space. Simple ranulas conform to the fascial boundaries of the sub-

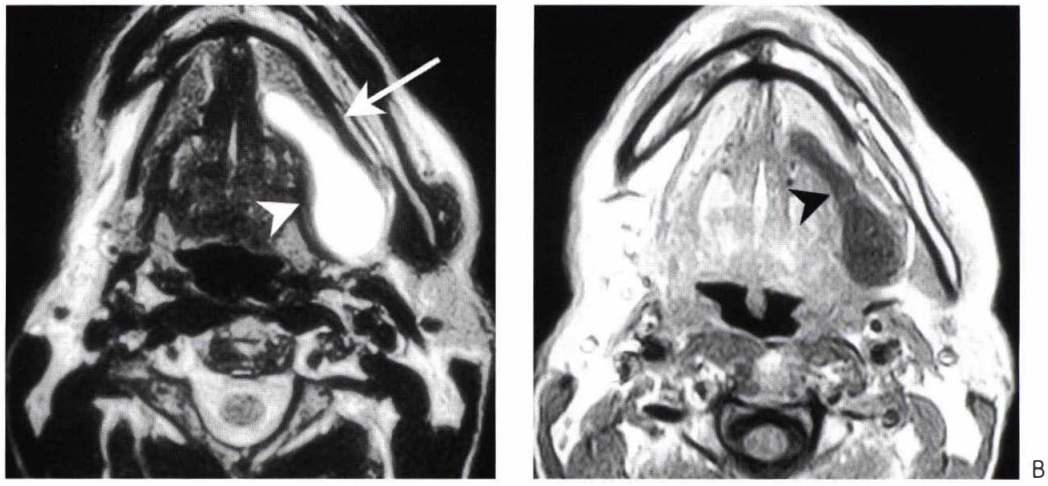

Figure 197-1. Ranula. (A) Axial T2-weighted image shows a paramedian high signal mass situated between the mylohyoid (arrow) and the hyoglossus (arrowhead) muscles. (B) Axial contrast-enhanced T1-weighted image shows no significant internal enhancement of the mass (arrowhead). A ranula located only in the sublingual space is referred to as a simple ranule. (Case courtesy of Robin Stacy-Humphries, M.D.)

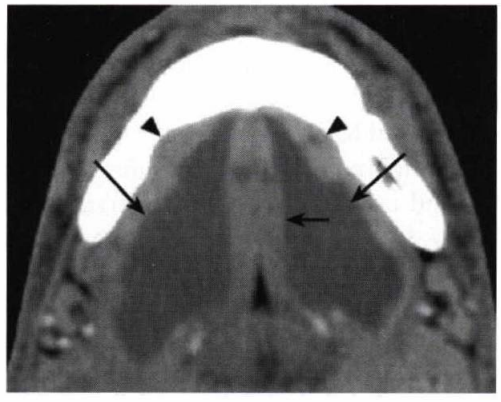

Figure 197-2. Axial contrast-enhanced CT shows bilateral paramedian non-enhancing cystic masses (black arrows) that are medial to the mylohyoid muscles (arrowheads) and lateral to the geniohyoid-genioglossus complexes (white arrow). These findings are characteristic for bilateral simple ranulas.

lingual spaces and are bordered laterally by the mylohyoid muscle and medially by the genioglossus and geniohyoid muscles. By definition, complex ranulas extend into the submandibular or parapharyngeal space.

MR

The MR appearance of ranulas is that of a cystic lesion with low to intermediate signal on T1-weighted and increased signal on T2-weighted sequences. The T1-weighted signal may at times vary depending on the protein content of the lesion (Fig. 197-1).

Imaging Pearls

- The diagnosis of a ranula is suggested if a cystic sublingual space mass has a "sausage-shaped" appearance.
- In the sublingual space, ranulas are easily differentiated from thyroglossal duct cysts because ranulas are paramedian, whereas thyroglossal duct cysts are midline.
- Very large ranulas may distort or replace the normal anatomy of the floor of mouth. These atypical ranulas are difficult to separate from large epidermoids.

Suggested Readings

1. Batsakis JG. Parenchymal cysts of the neck. In: Batsakis JG, ed. *Nonneoplastic Diseases of the Salivary Glands.* Baltimore: Williams and Wilkins; 1979:100–139.
2. Smoker WRK. Oral cavity. In: Som PM, Curtin H, eds. *Head and Neck Imaging.* 3rd ed. New York: Mosby; 1996:488–544.
3. Batsakis JG, McClathchy KD. Cervical ranulas. *Ann Otol Rhinol Laryngol* 1988;97:561–562.
4. Coit WE, Harnsberger HR, Osborn AG, Smoker WRK, Stevens MH, Lufkin RB. Ranulas and their mimcks: CT evaluation. *Radiology* 1987;163:211–216.

Chapter 198

Epidermoid/Dermoid (Dermoid Cyst)

Epidemiology

The term *"dermoid cyst"* (*DC*) encompasses various benign germ cell masses. These lesions include epidermoid, dermoid, and teratoid cysts, of which epidermoids and dermoids are most common. Teratoid tumors are very rare. About 7% of DCs occur in the head and neck region. The majority of these lesions (65%) occur in orbital and nasal regions, whereas 24% arise in the oral cavity. There is no reported sex predominance for DCs.

Clinical Findings

The epidermoid variety usually presents at birth, whereas dermoids most commonly present in the second or third decade of life. Oral cavity DCs typically arise in the sublingual space. Other sites include the dorsum of the tongue, hard or soft palate, lips, and buccal mucosa. DCs are usually midline lesions.

The clinical presentation usually depends on the location with respect to the mylohyoid muscle. On physical examination, these lesions tend to have a doughy texture and may demonstrate pitting after palpation. Floor of mouth DCs often present as submucosal masses. These masses may be confused clinically with a ranula. Because these lesions may elevate the tongue, patients may present with difficulty swallowing. Submandibular DCs are located below the mylohyoid muscle. These lesions may present as an anterior neck mass. Because these lesions are not fixed to the tongue or hyoid bone, these lesions do not move when the tongue is protruded. This finding may be used to differentiate DCs from thyroglossal duct cysts.

Embryology

DCs are thought to arise as a result of anomalous embryogenesis between the third and fifth weeks of gestation. There are two main theories used to explain the embryogenesis of DCs. One theory states that these lesions arise from epithelial rests that were trapped during midline closure of developing components of the first and second branchial arches. Trapping of ectodermal elements during formation of the tongue and floor of mouth during fusion of the lateral processes of the mandible and tuberculum impar would account for the predilection of epidermoids to occur in the floor of mouth. A second theory suggests that DCs occur when the surface ectoderm fails to completely separate from the underlying neural tube.

Pathology

The various lesions classified as "dermoid cysts" are histologically distinct. A fibrous capsule lined by simple squamous epithelium encloses epidermoids. There are no adnexal structures present within the wall. A dermoid is an epithelial-lined cavity that contains a variety of structures derived from both ectoderm and mesoderm. The contents of dermoids include hair, sebaceous glands, fat, smooth and striated muscle, cartilage, bone, minor salivary glands, nerves, and lymph nodes. Teratoid tumors are composed of poorly differentiated cell types originating from all three germ layers. The lining of a teratoid cyst varies from simple stratified squamous epithelium to a ciliated type of respiratory epithelium. The cystic portion of these lesions contains a proteinaceous cheesy keratinaceous material that results from desquamation of the squamous epithelial lining.

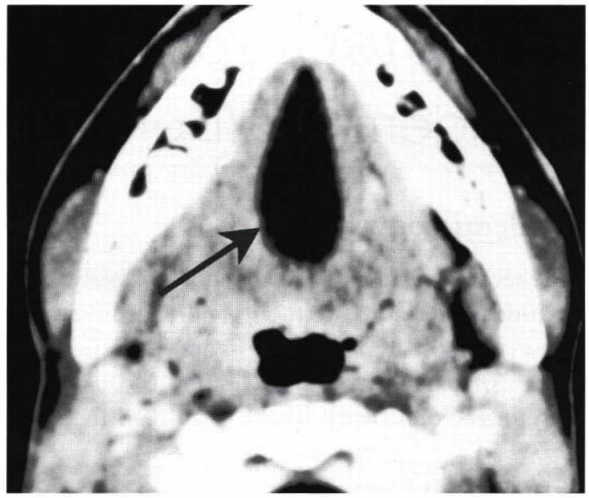

Figure 198–1. Axial contrast CT shows a low attenuation oval mass situated in the midline of the floor of mouth (arrow). Pathology revealed epidermoid.

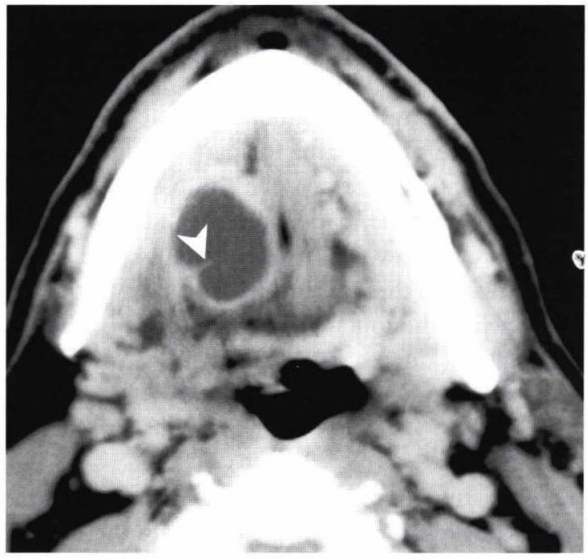

Figure 198–2. Contrast-enhanced CT demonstrates a low attenuation paramidline floor of mouth mass with a small internal septation (arrowhead). Pathology revealed dermoid.

Treatment

The treatment of DCs is surgical excision. However, the exact procedure is based on the relationship to the mylohyoid. This relationship is best evaluated on imaging. Lesions situated above the mylohyoid may be best resected through a transoral approach. Lesions situated inferior to the mylohyoid require a cervical approach.

Imaging Findings

CT

The most common CT appearance of epidermoids is a cystic, unilocular midline lesion located in the sublingual space. These lesions are usually sharply demarcated and may contain a thin enhancing rim. The presence of fat within the lesion is strongly suggestive of a dermoid. In the absence of fat, dermoids are indistinguishable from epidermoids. Bone erosion or remodeling is a very unusual finding in DCs (Figs. 198–1 and 198–2).

MR

Epidermoids are usually low signal on T1-weighted sequences and high signal on T2-weighted sequences. Occasionally, DCs may be composed of highly proteinaceous fluid resulting in higher T1-weighted signal. The high signal fat on T1-weighted images is very helpful in distinguishing dermoids from epidermoids.

Imaging Pearls

- Coronal images are useful for presurgical planning of sublingual space DCs to determine the relationship of the lesion to the mylohyoid muscle.
- Oral cavity dermoids and teratomas are associated with other midline anomalies including medial cleft syndrome and duplicated pituitary gland.
- Occasionally, dermoids may show lipid material floating on top of the heavier keratinaceous debris rather than the focal fatty masses that are often seen in teratomas.

Suggested Readings

1. Batsakis JG. Teratomas of the head and neck. In: Batsakis JG, ed. *Tumors of the Head and Neck*. 2nd ed. Baltimore: Williams and Wilkins; 1979:226–229.
2. Smoker WRK. Oral cavity. In: Som PM, Curtin H, eds. *Head and Neck Imaging*. 3rd ed. New York: Mosby; 1996:488–544.
3. Vogl TJ, Steger W, Ihrler S, Ferrera P, Grevers G. Cystic masses in the floor of the mouth: value of MR imaging in planning surgery. *AJR Am J Roentgenol* 1993;161:183–186.
4. Smirniotopoulos JG, Chiechi MV. Teratomas, dermoids, and epidermoids of the head and neck. *Radiographics* 1995;15:1437–1455.

Chapter 199

Thyroglossal Duct Remnant

Epidemiology

Thyroglossal duct remnants are congenital lesions that arise from anomalous development and migration of the thyroid gland. These remnants may accumulate fluid and be referred to as thyroglossal duct cysts. Thyroglossal duct cysts are the most common midline neck mass in children. The majority of cases present in children < 10 years of age. These lesions may be seen in young adults. Less than 2% of cases arise in patients > 60 years of age. No gender predilection has been reported.

Clinical Findings

Thyroglossal duct cysts usually present as nontender, gradually increasing, midline neck masses. The average size at presentation is 2 to 4 cm. Recent enlargement may occur as a result of an associated upper respiratory tract infection. Because thyroglossal duct cysts are often attached to the tongue or hyoid bone, these lesions characteristically move when the tongue is protruded.

Embryology

The thyroid gland is the first endocrine gland to appear in the developing fetus and begins its embryogenesis around day 24 of gestation. The gland arises from an endodermal thickening in the midline of the developing tongue base. This area is known as the foramen cecum and is located posterior to the apex of the circumvallate papilla. The thyroid gland descends as a result of elongation of the embryo and growth of the tongue. The developing gland migrates as a bilobed diverticulum and forms an epithelial lined cord during descent. Normal involution of the thyroglossal duct occurs between the eighth and tenth weeks of gestation. Failure of involution of the epithelial cord results in thyroid remnants and may result in the formation of a thyroglossal duct cyst. Cyst formation is believed to occur from inflammatory changes that stimulate secretion of fluids within the ductal remnants or to trapping of fluids produced from residual secretory epithelium located in the epithelial cord remnant.

Based on the embryology, thyroid remnants may be found in the foramen cecum or in the sublingual space. A thyroid gland that does not descend and is located at the foramen cecum is referred to as a lingual thyroid.

Pathology

The vast majority of thyroglossal duct cysts are benign lesions. Histologically, these cysts have a squamous lining. Thyroid tissue is an uncommon finding in the cyst wall. Occasionally, inflammatory changes may obliterate the epithelial mucosal lining causing the diagnosis to be based on characteristic clinical and radiographic findings. Fistulas may result from infection, cyst rupture, or complication of prior surgery. Several types of fistulas may occur: internal, with an opening into the pharynx; external, with an opening to the skin surface; or complete, with direct communications between the skin and pharynx.

Coexistent malignancy may exist in < 1% of thyroglossal duct cysts. This is often an incidental finding. The most common associated malignancy is papillary carcinoma. This is thought to arise from rests of ectopic thyroid tissue located within the thyroglossal duct cyst.

Treatment

The treatment of choice for a thyroglossal duct cyst is complete surgical resection. The Sistrunk procedure is the method of choice and involves complete removal of the entire cyst tract from the tongue base to the superior border of the thyroid gland. The central portion

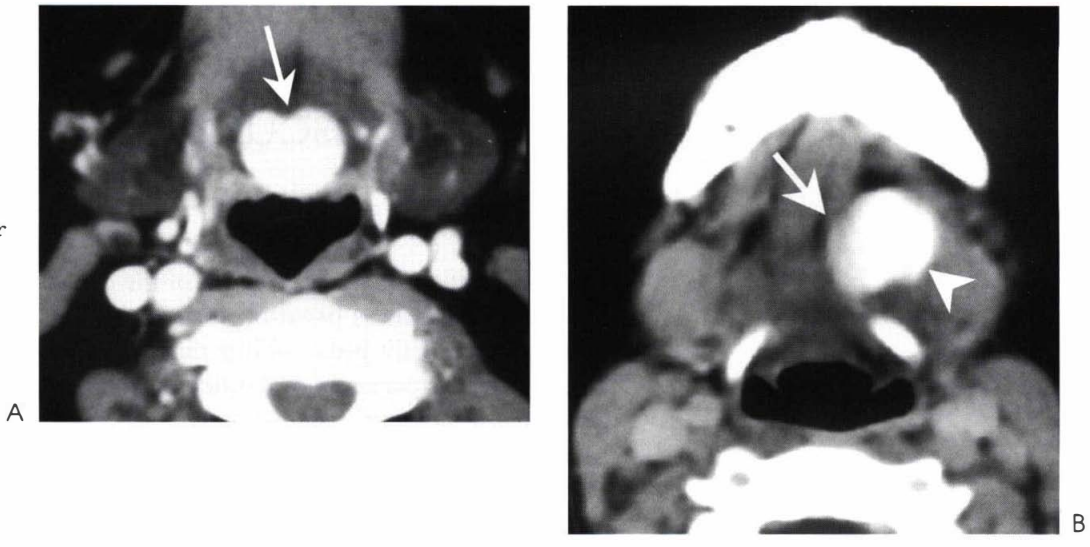

Figure 199-1. Thyroglossal duct remnant. (A) Contrast-enhanced CT shows a homogeneous, high attenuation mass located in the tongue base (lingual thyroid) (arrow). (B) Axial image obtained in the floor of mouth revealed a separate mass with a similar appearance to the lesion illustrated in (A) that is located off midline in the floor of mouth (arrowhead). Note the medial deviation of the genioglossus muscle (arrow).

of the hyoid bone and a portion of the tongue base are included in the resection. Complete resection utilizing the Sistrunk procedure is associated with a 3% recurrence rate, whereas the recurrence rate is significantly increased if thyroglossal duct cysts are locally excised.

Imaging Findings

CT

The CT findings are that of a thyroglossal duct remnant is a solid mass that is high attenuation that enhances following contrast administration. A thyroglossal duct cyst is a unilocular or multilocular cystic mass with peripheral enhancement. Thyroglossal duct remnants are solid masses that are often high attenuation which may be found in the tongue base or sublingual space (Fig. 199-1).

MR

On MR imaging, thyroglossal duct cysts appear as a cystic lesion that is low to intermediate signal on T1-weighted and increased signal on T2-weighted images. Sagittal or coronal images may be useful for identifying the extent of the lesion prior to resection.

Imaging Pearls

- Scintigraphy may be more sensitive than MR or CT for localizing rests of ectopic thyroid tissue and will confirm the presence of a lingual thyroid.
- Normally, there should be no solid enhancing component of a thyroglossal duct cyst. The presence of an intracystic solid enhancing mass may represent residual thyroid tissue. This finding, however, is also suspicious of a coexisting papillary carcinoma and must be conveyed to the referring physician.

Suggested Readings

1. Moore KL. The branchial apparatus and the head and neck. In: Moore KL, ed. *The Developing Human: Clinically Oriented Embryology*. 4th ed. Philadelphia: WB Saunders; 1988:184-186.
2. Batsakis JG. Parenchymal cysts of the neck. In: Batsakis JG, ed. *Tumors of the Head and Neck*. Baltimore: Williams and Wilkins; 1979:233-252.
3. Hudgins PA, Jacobs IN, Castillo M. Pediatric airway disease. In: Som PM, Curtin H, eds. *Head and Neck Imaging*. 3rd ed. New York: Mosby; 1996:545-611.
4. Karmody CS. Developmental abnormalities of the neck. In: Bluestone CD, Stool SE, Scheetz MD, eds. *Pediatric Otolaryngology*. Vol 2. Philadelphia: WB Saunders; 1990:1313-1314.
5. Drake AF, Hulka GF. Congenital neck masses. In: Shockley WM, Pillsbury HC, eds. *The Neck: Diagnosis and Surgery*. New York: Mosby; 1994:93-107.

Chapter 200

Vascular Malformations

Epidemiology

The classification of vascular lesions of the extracranial head and neck developed by Mulliken and Glowacki is based on their biological and clinical characteristics. In the past, different terms have been used by different specialties to describe the same lesions. This classification system attempts to unify the nomenclature and improve the understanding of these complex lesions. Vascular lesions are classified as malformations and hemangiomas. Malformations are further divided based on their histology and include capillary, venous, arteriovenous (fistulae), lymphatic, and mixed. Hemangiomas are further subdivided based on their growth phase, which consists of a proliferating and an involuting phase.

Clinical Findings

Vascular malformations are always present a birth. Enlargement of these lesions is due to growth of the child rather than proliferation of the endothelial cells that make up the lesion. These lesions do not undergo spontaneous involution. The incidence in males is equal to that in females.

Hemangiomas typically present in neonates or in early infancy. These lesions enlarge by endothelial proliferation and begin to undergo spontaneous involution after the first year of life. Hemangiomas are more common in females (5:1)

Pathology

All vascular lesions are composed of endothelial cells. Vascular malformations consist of flat endothelial cells that have a normal rate of mitosis and cell growth. The types of malformed endothelial cells that may be seen include venule, veins, capillaries, and lymphatic vessels. The histology determines the specific type of vascular malformation. Mixed vascular malformations such as venous–lymphatic malformations may occur due to close association in the embryogenesis of the lymphatic and venous systems.

The histologic features of hemangiomas are based on the growth phase. Plump, proliferating endothelial cells characterize the proliferating phase. Apoptosis and progressive flattening of endothelial cells characterize the involutional phase. There is a progressive reduction in vascular channels and an increase in the surrounding fibrofatty matrix.

Treatment

Because of their spontaneous regression, most hemangiomas are observed. More aggressive therapy is reserved for lesions that result in functional impairment. The treatment of vascular malformations is based on the specific type of malformation.

Imaging Findings

The specific CT and MR imaging findings are discussed in detail in the appropriate sections of this text.

Imaging Pearl

- Imaging is used to (1) identify the specific type of vascular lesion, (2) determine the extent of the lesion, and (3) characterize the lesion as high flow or low flow (Figs. 200–1 through 200–3). On MR imaging, the presence of flow voids or enhanced signal on flow-sensitive sequences within the lesion is indicative of a high flow state. On Doppler ultrasound, high flow lesions show arterial waveforms.

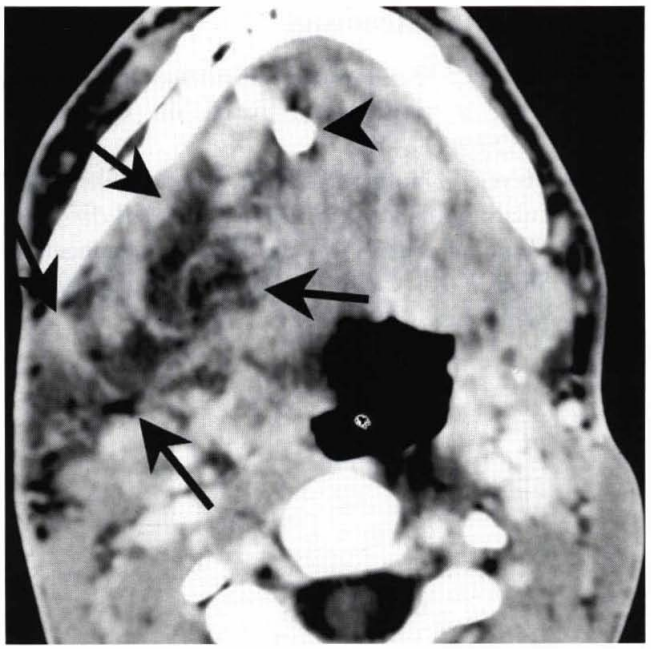

Figure 200–1. Contrast-enhanced CT demonstrates a mixed vascular malformation in the floor of mouth (arrows). The mass is heterogeneous and transspatial. The focal area of calcification (arrowhead) within the lesion suggests that this vascular malformation has a venous component. The lack of enhancement combined with the calcification indicates that this is a low flow vascular malformation.

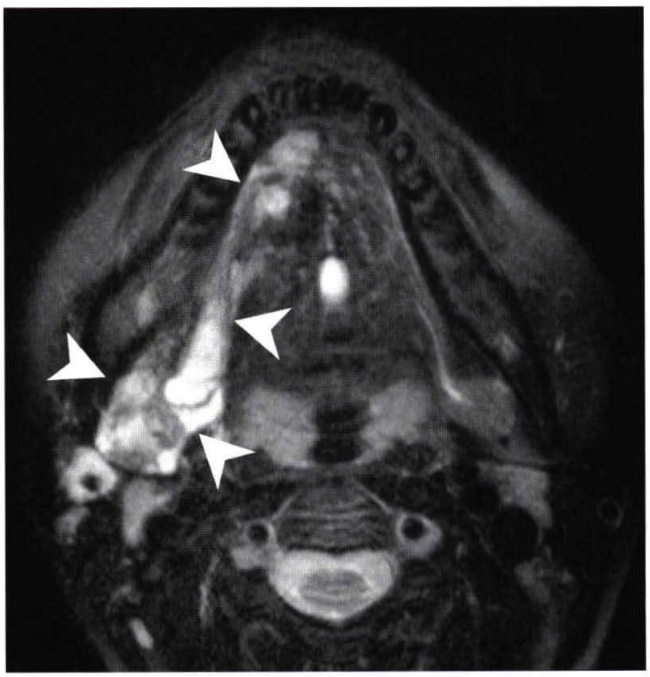

Figure 200–2. Axial T2-weighted image shows a heterogeneous mass that is predominantly high signal and lacks flow voids (arrowheads). The lack of flow voids indicates that this is again a low flow vascular malformation.

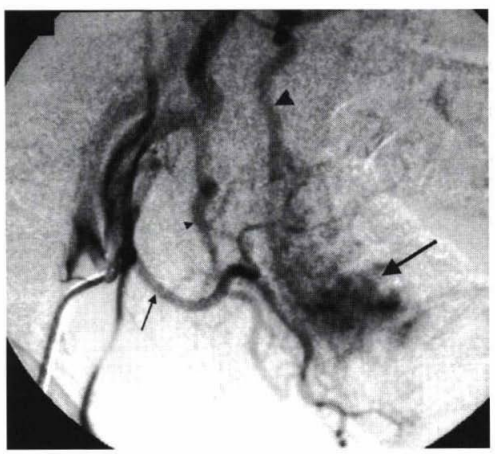

A

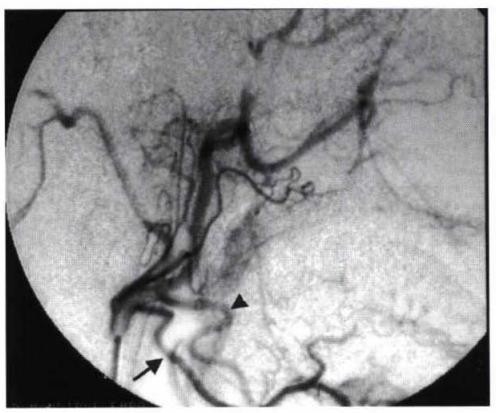

B

Figure 200-3. (A) Lateral view from a selective external carotid angiogram performed in a 37-week pregnant patient who presented with spontaneous hemorrhage in her mouth shows a large hypervascular blush (large arrow). The primary supply appears to be arising from the inferior alveolar branch of the internal maxillary artery (large arrowhead). Delayed images demonstrated early draining veins confirming the diagnosis of an arteriovenous malformation (small arrowhead = facial artery), (small arrow = lingual artery). (B) The patient underwent emergent embolization with complete devascularization of the lesion (lateral view). The patient delivered a healthy child the next day by cesarean section (arrowhead = facial artery), (arrow = lingual artery).

Suggested Readings

1. Mulliken JB, Glowacki J. Hemangiomas and vascular malformations in infants and children: a classification based on endothelial characteristics. *Plast Reconstr Surg* 1982;69:412–422.
2. Meyer JS, Hoffer FA, Barnes PD, Mulliken JB. Biological classification of soft-tissue vascular anomalies: MR correlation. *AJR Am J Roentgenol* 1991;157:559–564.
3. Waner M, Suen JY. A classification of congenital vascular malformations. In: Warner M, Suen JY, eds. *Hemangiomas and Vascular Malformations of the Head and Neck*. New York: Wiley-Liss; 1999:1–12.

Section X

Submandibular Space

Simply stated, the submandibular space (SMS) is located below the mandible (Figs. X-1 through X-3). Specifically, the SMS is situated inferior to the mylohyoid muscle in contrast to the SLS, which is located above the mylohyoid muscle. Because the posterior aspect of the mylohyoid muscle is not attached to a bony structure and is free (often referred to as the free margin of the mylohyoid muscle), the posterior portion of the SMS is in direct communication with the posterior aspect of the SLS and the inferior extension of the parapharyngeal space. The inferior margin of the SMS is the hyoid bone.

The contents of the SMS are the anterior belly of the digastric muscle, superficial portion of the submandibular gland, submandibular and submental (level I) lymph nodes, facial artery and vein, fat, and inferior loop of the hypoglossal nerve.

In adults, the most common pathology of the submandibular space consists of metastatic lymph nodes from squamous cell carcinoma of the oral tongue and floor of mouth. In children, the most common lesions are second branchial cleft cysts.

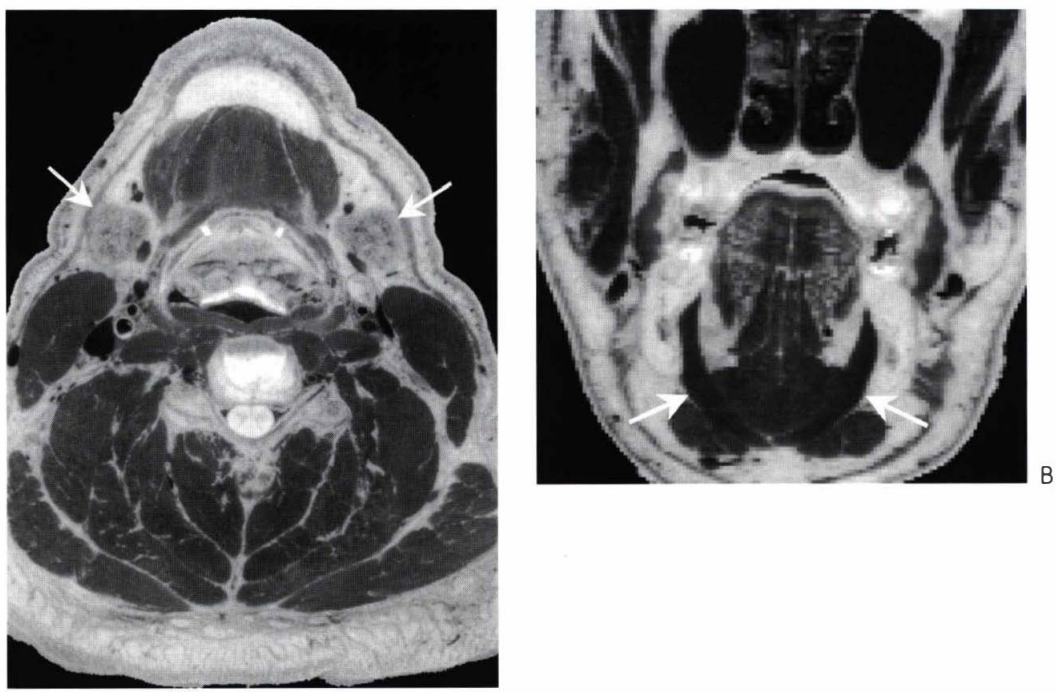

Figure X-1. (A) Axial anatomic section shows the location of the submandibular space. The arrows identify the submandibular glands. (B) The arrows identify the mylohyoid muscle on this coronal image. The submandibular gland is below the mylohyoid muscle whereas the sublingual gland is above the mylohyoid muscle.

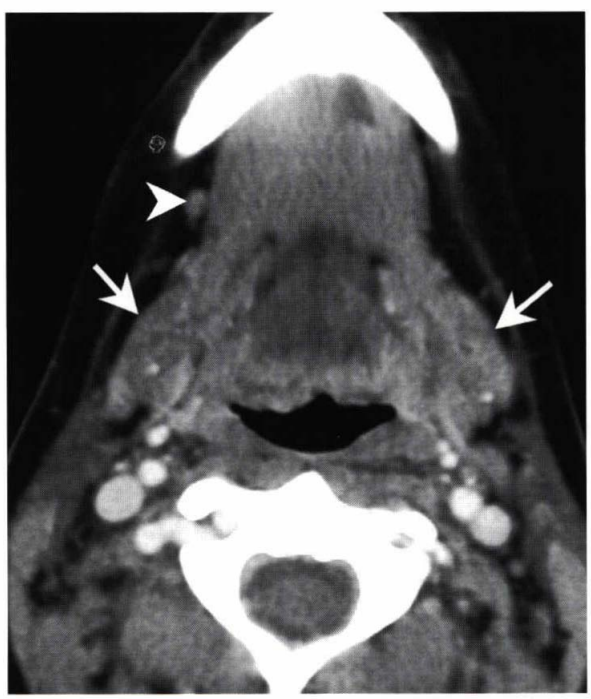

Figure X-2. Axial contrast-enhanced CT shows the normal appearance of the submandibular space. The arrows denote the submandibular glands, and the arrowhead identifies a small, level I lymph node.

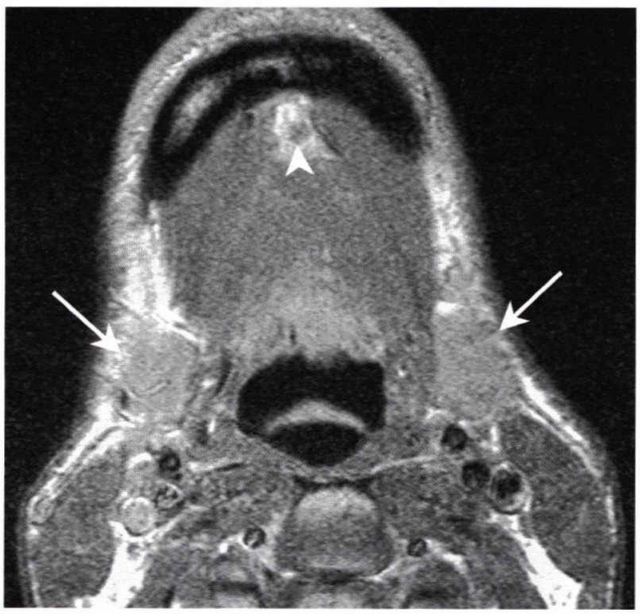

Figure X–3. Axial noncontrast T1-weighted image shows the normal appearance of the submandibular space. The arrows denote the submandibular glands, and the arrowhead identifies a small, level I lymph node.

Suggested Readings

1. Harnsberger HR. *Handbook of Head and Neck Imaging.* 2nd ed. St. Louis: Mosby Year Book; 1995.
2. Grodinsky M, Holyoke EA. The fasciae and fascial spaces of the head, neck and adjacent regions. *Am J Anat* 1938;63:367–408.
3. Mukherji SK, Castillo M. A simplified approach to the spaces of the extracranial head and neck. *Radiol Clin North Am* 1998;36:761–780.

Chapter 201

Submandibular Sialolithiasis

Epidemiology

Submandibular sialoliths usually occur between 30 and 50 years of age and are slightly more common in men. Salivary gland calculi are rare in children and when present usually involve the submandibular gland. Submandibular gland stones constitute between 80 and 90% of all salivary gland stones. The majority of submandibular stones are single (> 70%). Multiple stones are more commonly seen in patients with chronic sialadenitis.

Pathology

Submandibular sialoliths are composed of calcium phosphate in the form hydroxyapatite with small amounts of magnesium, carbonate, and ammonium. The matrix consists of carbohydrates and amino acids.

Several explanations have been proposed for the higher incidence of stones in the submandibular gland compared with the parotid gland. These include thicker and more mucous secretions, a narrow orifice, an uphill course of Wharton's duct in the standing position, a more alkaline pH that facilitates precipitation of salts, and a higher concentration of hydroxyapatite and phosphatase.

Clinical Findings

Patients often present with recurrent episodes of pain and swelling of the parotid region, most often associated with eating. The symptoms usually last between 2 and 3 hours and gradually subside. Larger stones may completely obstruct the gland and result in chronic atrophy if left untreated. Associated symptoms include unilateral sore throat or swelling, expression of purulent exudate, or a palpable enlarged gland due to chronic inflammation (Kuttner's tumor).

The majority of submandibular stones are detected in Wharton's duct, with < 20% occurring in the hilum or within the substance of the gland. Common sites of occurrence include the ostial opening, the midportion, and at a bend in the duct as it crosses over the free margin of the mylohyoid muscle. Strictures may result from calculi, with or without an underlying infection.

Treatment

Small stones located at the opening of Wharton's duct may be treated with local excision or removal through an endoluminal approach. Resection of the submandibular gland may be required for patients with severe painful swelling or recurrent infections.

Imaging Findings

Plain Films

Plain films are still the initial study of choice for evaluating patients with submandibular sialolithiasis. Eighty percent of submandibular stones are radiopaque on plain films.

Sialography

Sialography is still commonly performed for detection of intraductal stones. These are identified by intraluminal filling defects following installation of contrast into the cannulated duct.

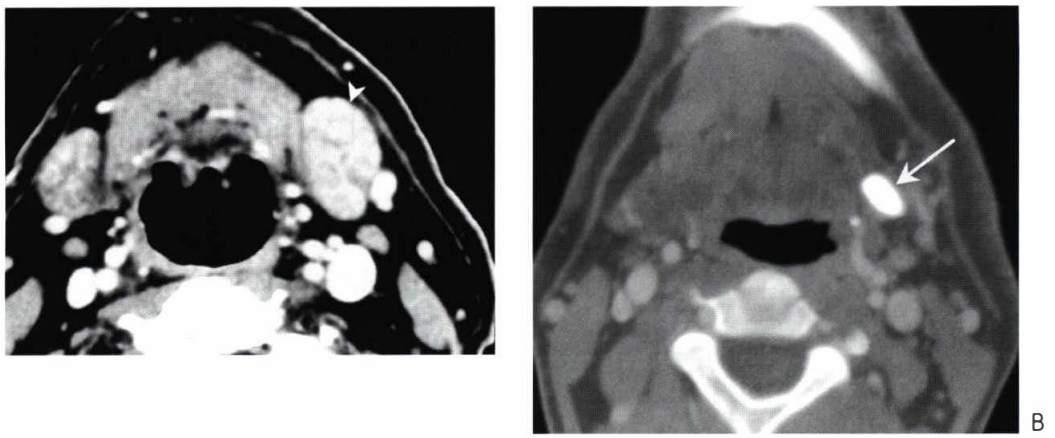

Figure 201-1. (A) Axial contrast-enhanced CT demonstrates an enlarged and asymmetrically enhancing left submandibular gland (arrowhead) indicative of an obstructive sialadenitis. (B) Bone algorithm shows a sialolith (arrow) obstructing the left submandibular duct.

CT

CT has a tenfold increase over plain films in the ability to detect stones and is able to detect most stones that cannot be seen with plain films. A recently obstructed gland is enlarged and has intense contrast enhancement (Fig. 201-1). A chronically obstructed gland is atrophic with only mild contrast enhancement.

Imaging Pearls

- Either sialography or CT can be used to detect nonradiopaque stones.
- Noncontrast CT is required for detection of intraparotid stones. The contrast-enhanced study will identify an obstructed submandibular gland.
- MR sialography is an excellent technique for identifying extraglandular and intraglandular ductal dilation. However, this technique may miss small intraductal calculi.

Suggested Readings

1. Batsakis JG. Nonneoplastic diseases of the salivary glands. In: Batsakis JG, ed. *Tumors of the Head and Neck*. 2nd ed. Baltimore: Williams and Wilkins; 1979:100–120.
2. Som PM, Brandwen M. Salivary glands. In: Som PM, Curtin H, eds. *Head and Neck Imaging*. 3rd ed. New York: Mosby; 1996:823–914.
3. Rabinov K, Weber AL. *Radiology of the Salivary Glands*. Boston: GK Hall; 1985:1–221.
4. Varghese JC, Thornton F, Lucey BC, Walsh M, Farrel MA, Lee MJ. A prospective comparative study of MR sialography and conventional sialography of salivary duct disease. *AJR Am J Roentgenol* 1999;173:1497–1503.

Chapter 202

Infection

Epidemiology

Submandibular space (SMS) abscess, or cellulitis, is usually secondary to infections involving the submandibular nodes, submandibular gland, teeth, or mandible. Submandibular gland abscesses are frequently associated with ductal stenosis or calculi (Fig. 202–1). Submandibular duct calculi are relatively common and account for 85% of all salivary gland stones. Odontogenic infections occur in patients with poor oral hygiene. There is no known sex predilection for SMS infection, and this condition is seen mainly in the adult population.

Clinical Findings

Patients usually present with unilateral pain and tenderness in the SMS. In patients with underlying calculus disease, a history of salivary colic or submandibular gland swelling following meals may be elicited. SMS abscess arising from dental infection may produce trismus if the adjacent medial pterygoid muscle is also involved.

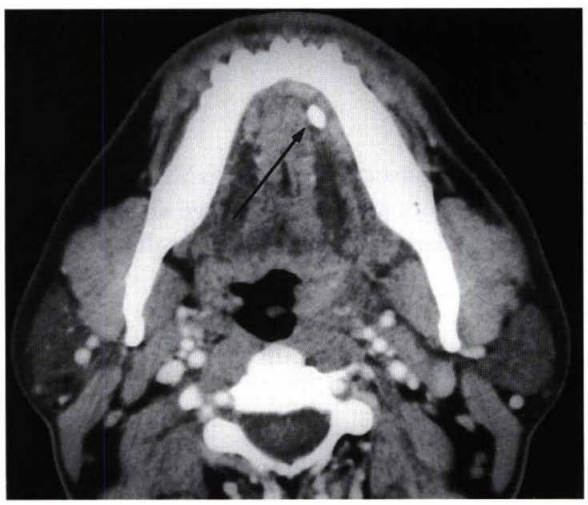

A

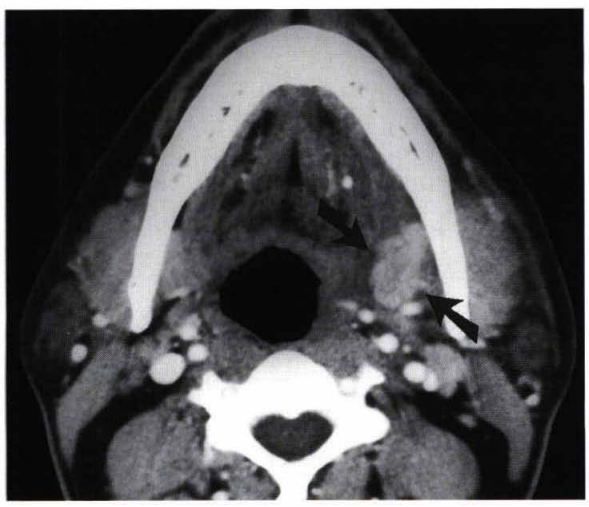

B

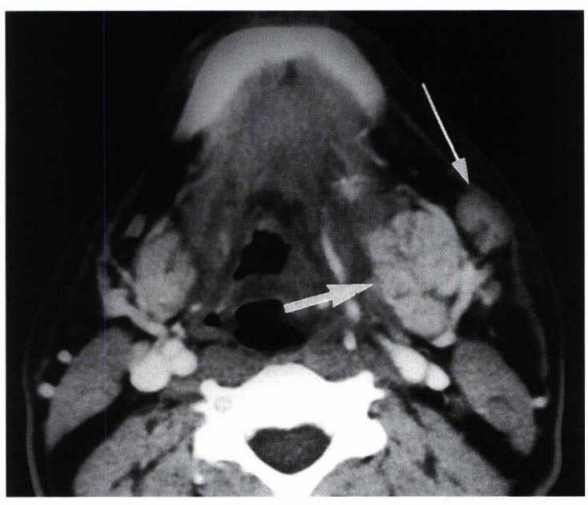

C

Figure 202–1. Submandibular inflammation secondary to calculus. (A) Axial contrast-enhanced CT shows a stone in the left submandibular duct (arrow). (B) Axial contrast-enhanced CT shows enlarged left submandibular gland (opposing arrows). (C) Axial contrast-enhanced CT shows enlarged left submandibular gland (thick arrow). Note the associated enlarged submandibular lymph node (thin arrow).

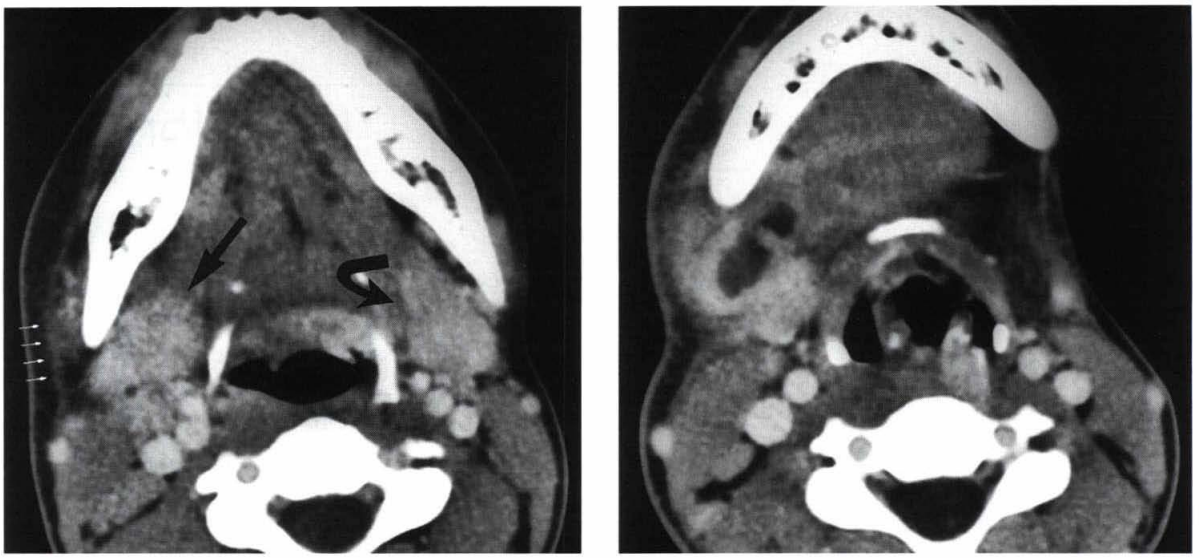

Figure 202–2. Submandibular space abscess. (A) Axial contrast-enhanced CT shows a swollen right submandibular gland with ill-defined margins (large arrow). Compare with the smooth outline of the normal left submandibular gland (curved arrow). Note the adjacent thickened platysmus muscle (small arrows). (B) Axial contrast-enhanced CT shows abscess formation in the right submandibular gland.

Pathology

Acute bacterial infection of the submandibular gland is often the result of dehydration, retrograde infection from the oral cavity, or ductal obstruction. The most common organisms are *Staphylococcus aureus* and *Streptococcus viridans*. There are usually three submandibular lymph nodes and they drain a wide region including the external nose, cheeks, upper lips, gingiva, and teeth. These nodes may undergo suppuration as a result of afferent lymphatics draining the infected areas.

Treatment

Antibiotic therapy should be instituted as soon as SMS infection is diagnosed. This will suffice if infection (cellulitis) does not reach the stage of abscess formation. All pus should be drained surgically. The underlying etiology such as ductal stones or dental abscess should also be addressed.

Imaging Findings

CT

CT shows a mass in the SMS with or without pus collection. Inflammation often produces a "dirty" appearance in the subcutaneous fat, and thickening of the platysma muscle (Fig. 202–2). CT is the modality of choice because radiopaque calculi, mandibular cortical erosions, and gas pockets are well demonstrated.

MR

MR imaging is seldom used to assess SMS infection because it may not recognize the presence of a calculus, gas collections, or cortical bone erosion. However, marrow edema is well delineated on MR imaging. The inflammation typically shows high signal intensity on T2-weighted images and enhances strongly on T1-weighted images following contrast injection.

Imaging Pearl

- It may be possible to demonstrate on CT a low attenuation tubular structure representing a dilated submandibular duct. If no radiopaque stone is noted, the dilatation may be due to ductal stenosis or secondary to a radiolucent stone.

Suggested Readings

1. Harnsberger HR. *Handbook of Head and Neck Imaging.* 2nd ed. Chicago: Mosby; 1995:134–149.
2. Som PM, Brandwein M. Salivary glands. In: Som PM, Curtin HD, eds. *Head and Neck Imaging.* St. Louis: Mosby; 1996:823–877.
3. Silvers AR, Som PM. Salivary glands. *Radiol Clin North Am* 1998;36:941–966.

Chapter 203

Necrotizing Fasciitis

Epidemiology

Necrotizing fasciitis describes a severe and potentially life-threatening soft tissue infection usually caused by *Streptococcus* (beta-hemolytic *Streptococcus*) or mixed bacterial flora. There are several types of bacterial soft tissue infections. Erysipelas involves the more superficial layers of the skin and cutaneous lymphatic vessels. A cellulitis is a bacterial infection that extends more deeply into the subcutaneous tissue but spares the fascia. Necrotizing fasciitis indicates destruction of the fascia or fat with or without skin or muscle necrosis. Myositis/myonecrosis describes bacterial involvement of the underlying muscle.

In the past, different aspects of the disease spectrum have been described by different terms. These terms include nonclostridial gangrene, synergistic necrotizing cellulitis, and acute hemolytic streptococcal gangrene.

Necrotizing fasciitis is uncommon and typically affects elderly or immunocompromised patients. However the incidence appears to be increasing in young, healthy patients with an intact immune response. Common sites of origin include odontogenic, tonsillar, or pharyngeal infections or a prior history of surgery or radiation therapy.

Clinical Features

The initial findings are nonspecific and consist of fever, regional neck swelling, and erythema. The disease course is then characterized by the rapid onset of sepsis and associated complications that include septic shock and multisystem organ failure. The disease may extend inferiorly and result in a mediastinitis. The reported mortality rate is up to 75% of affected individuals.

Pathology

The disease is characterized by infiltration of the deep dermis, fascia, and muscular planes by bacterial and polymorphonuclear cells. There is necrosis of fat, fascia, and muscular tissue, with fragmentation and secondary degeneration of muscle fibers. Vasculitis, thrombosis, and liquefactive thrombosis are also frequent findings.

Treatment

This disease requires prompt and aggressive surgical exploration and debridement. Antibiotic therapy alone is insufficient. Supportive medical management also includes fluid management and blood pressure support with vasopressors.

Imaging Findings

CT

There is diffuse increased reticulation of the subcutaneous fat, and thickening and enhancement of the platysma (Figs. 203-1 through 203-3). This is often associated with myositis with thickening and enhancement of the underlying muscles. There are often multiple areas of abscess formation extending along the fascial planes of the neck (Fig. 203-2). The presence of gas in the soft tissues in the absence of trauma or surgical intervention is characteristic of the disease. Involvement of the mediastinum may be present in advanced disease.

MR

There is reticulation of the subcutaneous fat and thickening and enhancement of the underlying fascia. Multiple pockets of abscess formation are often present along the fascial planes. Diffuse thickening and enhancement of the underlying muscles indicative of a myositis.

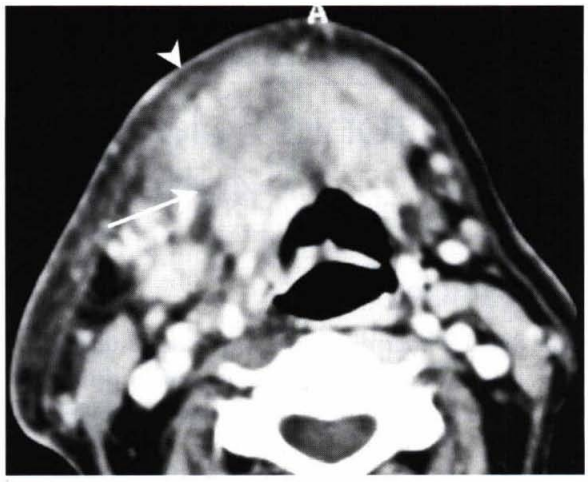

Figure 203–1. Axial contrast-enhanced CT shows diffuse enhancement of the soft tissues (arrow) and reticulation of the subcutaneous fat consistent with a cellulitis (arrowhead).

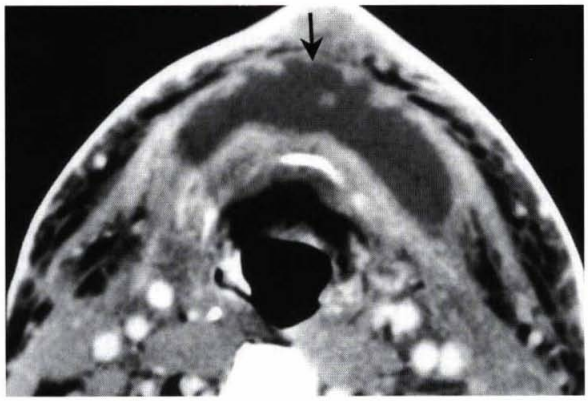

Figure 203–2. Axial contrast-enhanced CT shows a fluid collection in the submandibular space consistent with an abscess (arrow).

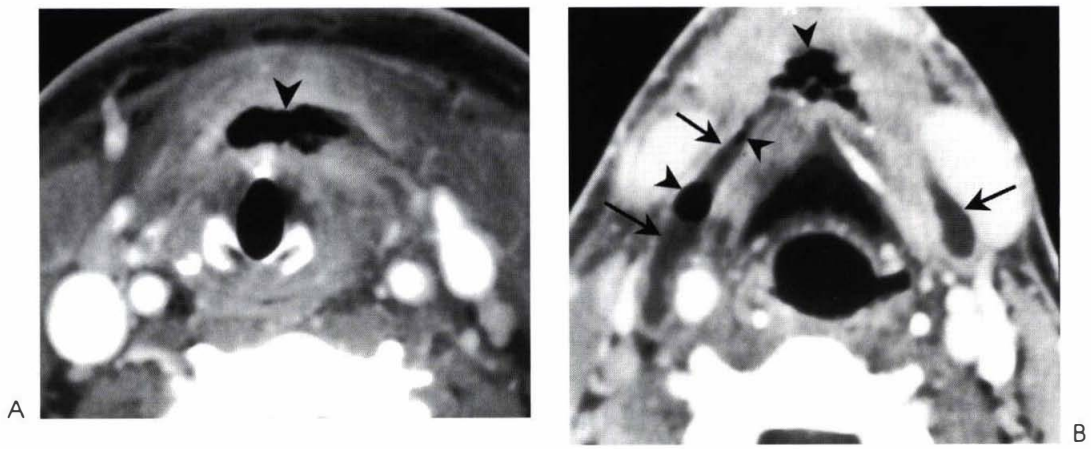

Figure 203–3. (A,B) Examples of air (arrowheads) and fluid, which represents pus (arrows), dissecting along the fascial planes. These findings are characteristic of necrotizing fasciitis.

Imaging Pearls

- Necrotizing fasciitis is usually a clinical diagnosis. The diagnosis can be suggested by the presence of gas in the soft tissues in the absence of previous trauma or surgical manipulation. CT is probably superior to MR for identifying subcutaneous gas.
- MR is superior to CT for identifying the full extent of the subcutaneous and fascial disease and muscular involvement.

Suggested Readings

1. Becker M, Zbaren P, Hermans R, et al. Necrotizing fasciitis of the head and neck: role of CT in diagnosis and management. *Radiology* 1997;202:471–476.
2. Tovi F, Fliss DM, Zirkim HJ. Necrotizing soft tissue infections in the head and neck: a clinicopathologic study. *Laryngoscope* 1991;101:619–625.
3. Maisel RH, Karlen R. cervical necrotizing fasciitis. *Laryngoscope* 1994;104:795–798.
4. Grodinsky MD. Retropharyngeal and lateral pharyngeal abscesses: an anatomic and clinical study. *Ann Surg* 1939;110:177–199.

Chapter 204

Chronic Sclerosing Sialadenitis—"Kuttner's Tumor"

Epidemiology

In 1896 Kuttner described a disease resulting in swelling and hardening of the submandibular glands. This lesion represents a primary obstructive electrolyte sialadenitis caused by a secretory disorder. The disease is progressive and leads to immunologic destruction.

Clinical Findings

This disorder is characterized by progressive enlargement with hardening of the submandibular gland. It is usually unilateral but may also be bilateral. Chronic sclerosing sialadenitis is more common in females and affects patients in the middle and older age groups.

Pathology

Kuttner's tumor is a term applied to chronic sclerosing sialadenitis involving the submandibular gland. It can be divided into four stages. Stage 1 shows focal chronic inflammation characterized by lymphocytic infiltration around the salivary ducts. The ducts are moderately dilated and contain inspissated secretions. Stage 2 is characterized by diffuse lymphocytic infiltration with severe periductal fibrosis. Stage 3 shows marked lymphocytic infiltration with hyalinization around ducts and the formation of lymphoid follicles. Stage 4 shows marked fibrosis with lobular architecture resembling liver cirrhosis, and normal glandular parenchyma is seldom found.

Treatment

The majority of patients with chronic sialadenitis will experience varying degrees of decreased flow of saliva. These patients are usually adequately managed conservatively by massage and the use of sialagogues. Any superimposed infection can be controlled with antibiotics. However, in severe cases involving xerostomia pain or infection, surgical excision is indicated.

Imaging Findings

CT

CT shows markedly enlarged submandibular glands with intense enhancement. In advanced stages, the submandibular glands show a lobulated architecture (Fig. 204–1). Calcifications may also be demonstrated in 50% of the affected glands.

MR

MR findings in chronic sialadenitis are nonspecific. The affected glands show intermediate signals on T1-weighted and high signals on T2-weighted images. Strong enhancement can be seen following the injection of contrast.

Imaging Pearl

- The imaging findings of Kuttner's tumor are nonspecific. This diagnosis may be suggested in patients with progressive submandibular gland swelling accompanied by calcifications, diffuse glandular enlargement, and contrast enhancement.

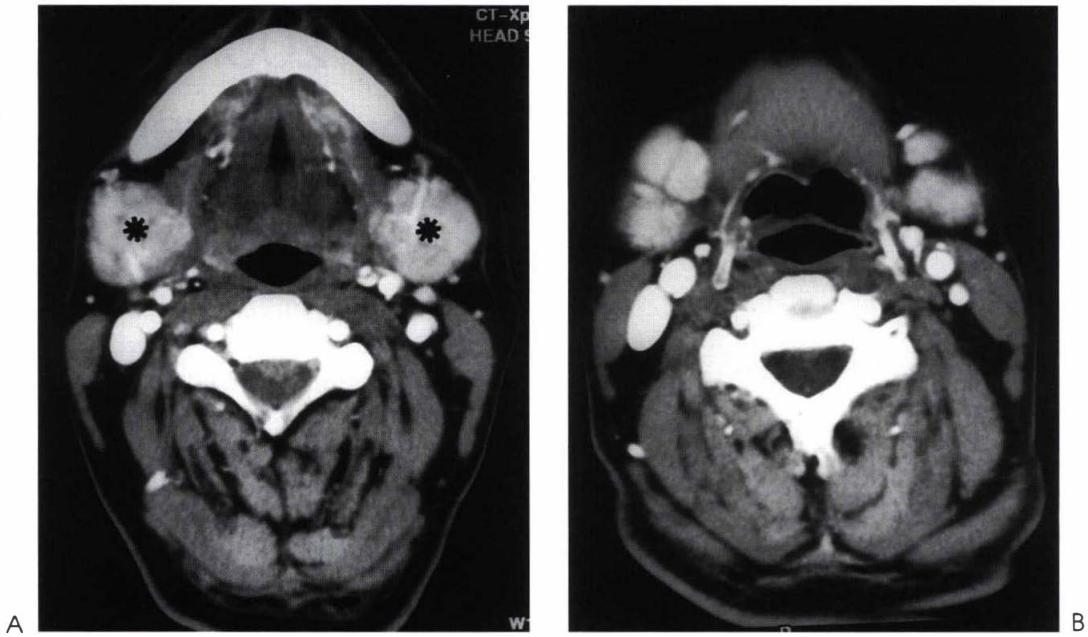

Figure 204–1. Chronic sclerosing sialadenitis. (A) Axial contrast-enhanced CT shows bilateral grossly enlarged submandibular glands (asterisks) with dense contrast enhancement. (B) Axial contrast-enhanced CT inferior to (A) shows a lobulated outline in both submandibular glands.

Suggested Readings

1. Siefert G, Donath K. Zurpathogenes des Kuttner Tumours der Submandibularis: analysis von 349 Fallen mit. *HNO* 1981; 25:81–85.
2. Spiro RH. Salivary gland neoplasms: overview of a 35-year experience with 2807 patients. *Head Neck Surg* 1986;177–182.
3. Luna MA. Pathology of tumors of the salivary glands. In: Thawley SE, Panje WR, Batsakis JG, Lindberg RD, eds. *Comprehensive Management of Head and Neck Tumors.* 2nd ed. Philadelphia: WB Saunders; 1999:1106–1146.
4. Som PM, Brandwein M. In: Som PM, Curtin HD, eds. *Head and Neck Imaging.* St. Louis: Mosby; 1996:846–877.

Chapter 205

Group (Level) I Lymph Nodes (Submandibular–Submental)

Epidemiology

The group (level) I lymph nodes are situated above the hyoid bone, superficial to the mylohyoid muscles and anterior to a transverse line drawn on each axial image through the posterior edge of the submandibular gland (Fig. 205–1). Nodes are considered level I if the majority of the cross-sectional area of the node lies anterior to a line drawn tangential along the posterior edge of the submandibular gland. A node is considered level II if the majority of the cross-sectional area of the gland is located posterior to this line.

Level I nodes can be subclassified into levels IA and IB. Level IA (submental) are situated between the medial margins of the anterior bellies of the digastric muscle, below the mylohyoid muscle and above the hyoid bone. Level IB (submandibular) are located posterior and lateral to the medial edge of the anterior belly of the digastric muscle, below the mylohyoid muscle, above the hyoid bone, and anterior to a transverse line drawn tangential to the posterior surface of the submandibular gland.

Clinical Features

The afferent drainage is from the oral cavity, sinonasal cavity, and facial nodes.

Pathology

Normal level I nodes can be routinely seen on imaging. Level I nodes are longitudinally oriented, whereas levels II through V are vertically oriented. Thus, it is possible to visualize an eccentric fatty hilum on transverse imaging. This should not be confused with a peripheral metastasis or an area of necrosis.

Level I nodes can be enlarged by a variety of pathological processes (Figs. 205–2 and 205–3). The diseases most commonly involving the level I nodes are nodal metastases from oral cavity carcinomas and inflammation from oral cavity infections.

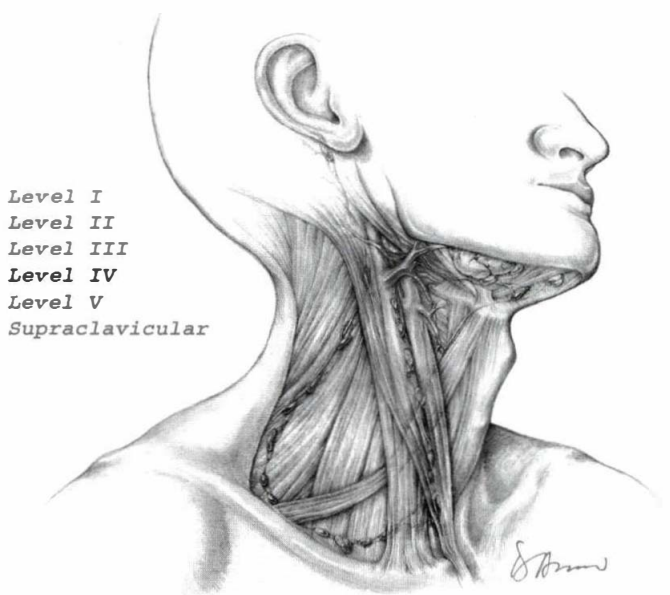

Figure 205–1. Schematic illustration of the cervical lymph nodes. The level I lymph nodes are shaded (see Color Plate 205–1).

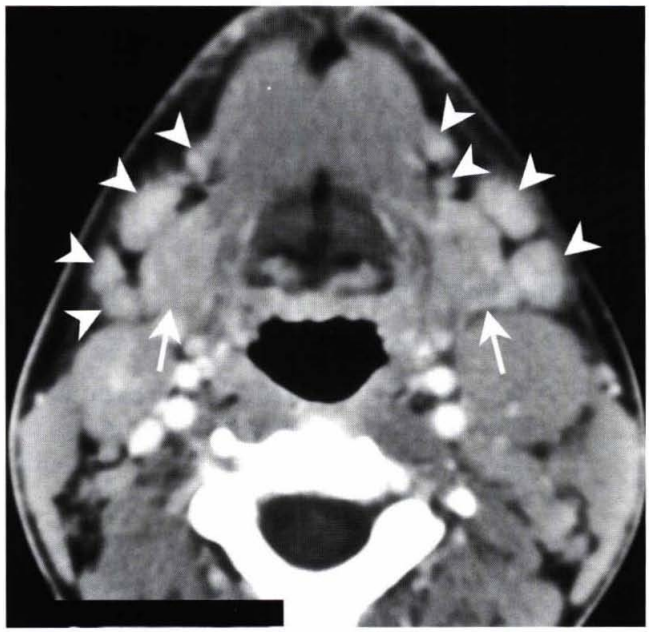

Figure 205–2. Axial contrast-enhanced CT shows multiple enlarged level I lymph nodes in a patient with Hodgkin's disease (arrowheads). The arrows identify the submandibular glands.

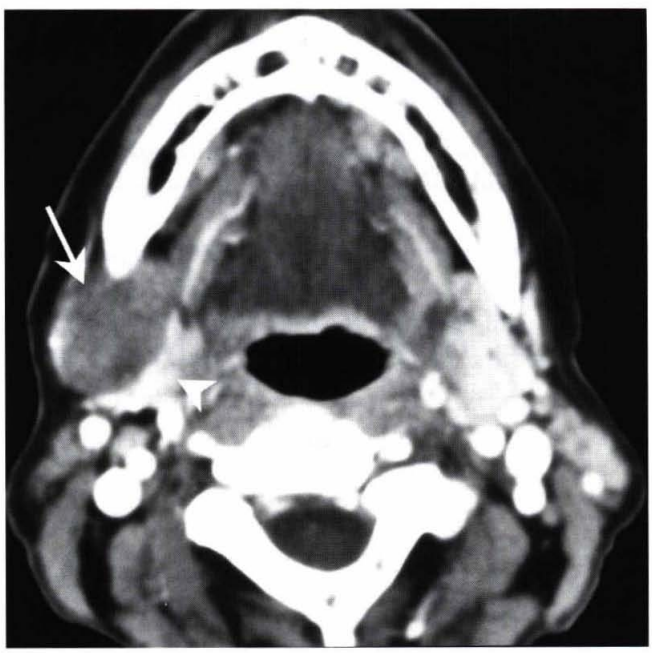

Figure 205–3. Contrast-enhanced CT shows an enlarged level I lymph node (arrow), which is displacing the submandibular gland posteriorly (arrowhead).

Treatment

The nodes are important to recognize, especially for oncological purposes. The level I nodes are routinely treated for tumors arising from the oral cavity and are resected during a supraomohyoid neck dissection. For early-stage tumors of the oral cavity, the level I nodes may be "watched" if the clinical exam and imaging are negative.

Imaging Findings

CT

Level I nodes are all located anterior to a line drawn tangential to the posterior margin of the submandibular gland. Level IA (submental) nodes are situated between the medial margins of the anterior bellies of the digastric muscle, below the mylohyoid muscle and above the hyoid bone. Level IB (submandibular) nodes are located posterior and lateral to the medial edge of the anterior belly of the digastric muscle, below the mylohyoid muscle and above the hyoid bone.

MR

The level I lymph nodes are ovoid masses that are typically intermediate signal on T1-weighted and slightly increased signal on T2-weighted images. The nodes usually diffusely enhance following contrast administration. Noncontrast T1-weighted images may be helpful in identifying a high-signal fatty hilum, which is suggestive of a nonmetastatic lymph node.

Imaging Pearls

- Most authors do not separate level IA and level IB nodes, but rather consider all as level I.
- There are various criteria that have been proposed for differentiating between involved and uninvolved level I nodes in patients with oral cavity carcinoma. It is important to remember that the level I nodes lie in a longitudinal orientation as opposed to the vertical orientation of levels II through V.
- We tend to use the following criteria for suggesting level I node metastases: maximal transverse diameter $>$ 10 mm, or a central area of decreased attenuation that is not a fatty hilum, or asymmetric clumping of lymph nodes in an area that is in a primary echelon drainage of the primary site. However, many other centers use different criteria and it is important to discuss the criteria you elect to use with your referring physicians.

Suggested Readings

1. Dinardo LJ. Lymphatics of the submandibular space: an anatomic, clinical and pathologic study with applications to floor-of-mouth carcinoma. *Laryngoscope* 1998;108:206–214.
2. Rouvièrre H. *Anatomie des Lymphatiques de l'Homme.* Paris: Masson et Cie; 1932.
3. Som PM, Curtin HD, Mancuso AA. An imaging-based classification for the cervical nodes designed as an adjunct to recent clinically based nodal classifications. *Arch Otolaryngol Head Neck Surg.* 1999;125:388–396.

Chapter 206

Facial Lymph Nodes: Mandibular Group

Epidemiology

The facial lymph nodes were first described by Rouvière. They are an inconsistent group of lymph nodes that are located in the subcutaneous tissue along the branches of the facial vessels and lymphatic channels that drain the face (Fig. 206–1). Five groups have been described: buccinator, malar, infraorbital, retrozygomatic, and mandibular. This section describes the mandibular nodes; the buccal group is described in the buccal space section.

The mandibular nodes (supramaxillary, supramandibular, inframandibular) are deep to the superficial muscles of facial expression and are situated along the external surface of the mandible adjacent to the facial artery and anterior to the masseter muscle. There may be an additional node within this group (inferior maxillary, inframaxillary node) that is located in the subcutaneous tissue near the inferior margin of the mandible.

Clinical Features

The afferent drainage is from the skin and subcutaneous tissues of the cheek, lower lip, and gingiva, along with the efferent drainage of the infraorbital and buccinator facial nodes. The efferent drainage is to the submandibular (group I) lymph nodes. Two groups of patients are at greatest risk for developing facial adenopathy. The most likely group are patients with advanced or recurrent squamous cell carcinoma that has spread extensively into the soft tissues of the face or sinonasal region. The second group is patients who are locally controlled but fail in the facial nodes. Involvement may also be seen in patients with lymphoma or melanoma.

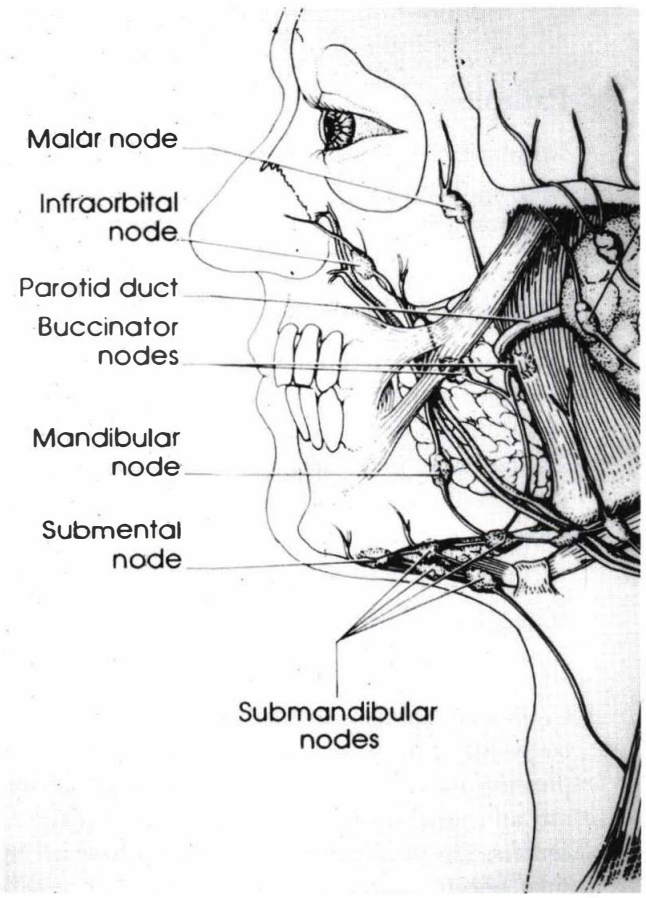

Figure 206–1. Schematic illustration of the facial lymph nodes. (With permission from Tart RR, Mukherji SK, Avino AJ, Stringer SP, Mancuso AA. Facial lymph nodes: normal and abnormal CT appearance. Radiology *1993;188:695–700.)*

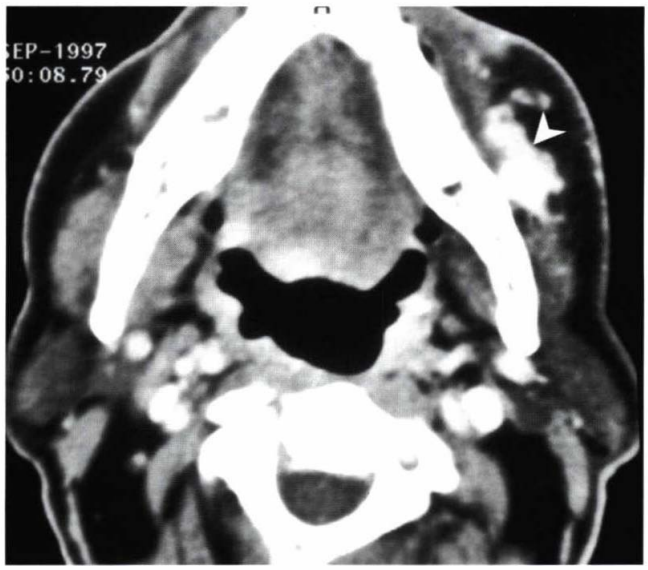

Figure 206–2. Contrast-enhanced CT demonstrates an enlarged and enhancing left mandibular facial lymph node (arrowhead).

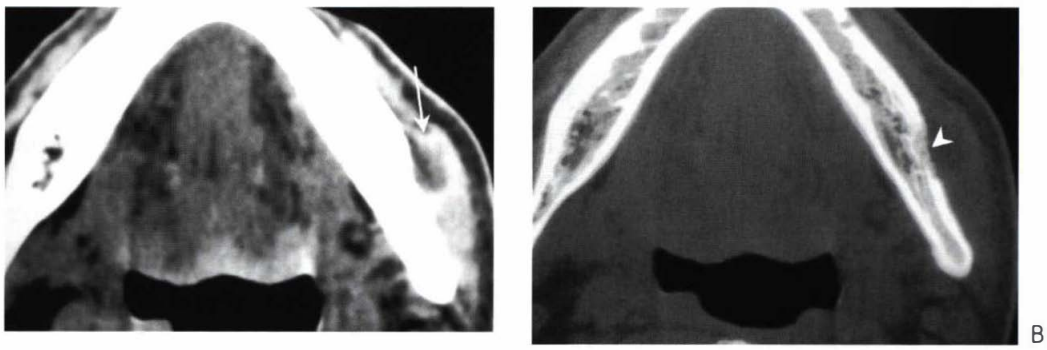

Figure 206–3. (A) Axial image shows an enlarged left mandibular facial lymph node with a low attenuation center (arrow). (B) Bone algorithm demonstrates that the lymph is eroding the buccal cortex of the mandible (arrowhead). (With permission from Tart RR, Mukherji SK, Avino AJ, Stringer SP, Mancuso AA. Facial lymph nodes: normal and abnormal CT appearance. Radiology *1993;188:695–700.)*

Pathology

Normal facial nodes cannot be identified. Only pathological nodes can be visualized by imaging. Involvement by recurrent squamous cell carcinoma of the facial area is the most common cause for enlargement of the mandibular nodes (Figs. 206–2 and 206–3).

Treatment

The nodes are important to recognize for oncological purposes. These nodes need to be identified when located at a distance from the primary cancer because the planned surgical resection or high-dose radiation therapy ports may not include these nodes. Enlarged mandibular nodes may become clinically fixed to the mandible and, in advanced cases, erode the mandibular cortex. This would require performing some form of mandibulectomy for adequate resection.

Imaging Findings

CT

Cross-sectional imaging does not routinely identify normal mandibular lymph nodes. Enlarged mandibular nodes are oval masses that are deep to the superficial muscles of facial expression and are situated along the external surface of the mandible adjacent to the facial artery and anterior to the masseter muscle. Enlarged nodes will often contain low attenuation centers. The solid lymph nodes usually have irregular margins that may be due to extracapsular penetration.

MR

The facial lymph nodes are ovoid masses that are typically intermediate signal on T1-weighted and slightly increased signal on T2-weighted images. The nodes usually diffusely enhance following contrast administration.

Imaging Pearls

- In our experience, mandibular nodes are usually identified in patients with recurrent carcinoma of the anterior oral cavity.
- It is important to remember that normal facial lymph nodes are not routinely identified on imaging. The presence of a clearly identifiable mandibular node in a patient with an advanced or recurrent cancer should be considered abnormal.
- Due to the fact that mandibular nodes may be fixed to the mandible and erode the mandibular cortex, thin-section axial and coronal CT or MR imaging may be helpful to evaluate for mandibular erosion in patients with mandibular nodes that are clinically fixed to the mandible.

Suggested Readings

1. Tart RR, Mukherji SK, Avino AJ, Stringer SP, Mancuso AA. Facial lymph nodes: normal and abnormal CT appearance. *Radiology* 1993;188:695–700.
2. Rouvière H. *Anatomie des Lymphatiques de l'Homme*. Paris: Masson et Cie; 1932.
3. Robbins JP, Slaughter FH, Constable WC. Involvement of the buccinator node in facial malignance. *Arch Otolaryngol* 1971;94:356–358.

Chapter 207

Benign Minor Salivary Gland Tumors

Epidemiology

The same neoplasms that arise in the parotid gland may arise in the submandibular gland. Only 10% of all salivary gland neoplasms occur in the submandibular gland. However, a larger percentage of tumors are malignant (50%) when compared with the parotid gland. This observation is more abundantly true for the sublingual and minor salivary gland tumors. Primary salivary gland tumors of the submandibular gland are rare. Approximately 40% of all tumors of the submandibular gland are benign mixed tumors. These tumors occur more often in females (2:1).

Clinical Findings

Patients often present with asymptomatic masses that have been present for several months. Pain and ulceration may be present; however, these are not consistent findings.

Pathology

The benign tumors that constitute minor salivary gland tumors include pleomorphic adenoma, monomorphic adenoma, and Warthin's tumor. The pathology of these lesions has been reviewed in other sections of this text.

Treatment

The exact treatment depends on the pathology. For most benign tumors complete local resection is adequate.

Imaging Findings

CT

Benign lesions are typically slightly low attenuation and diffusely enhance following contrast administration (Figs. 207–1 through 207–3).

MR

In general, the imaging findings are nonspecific. Pleomorphic adenomas are usually low attenuation on T1-weighted images and high signal on T2-weighted sequences. These lesions typically diffusely enhance following contrast administration.

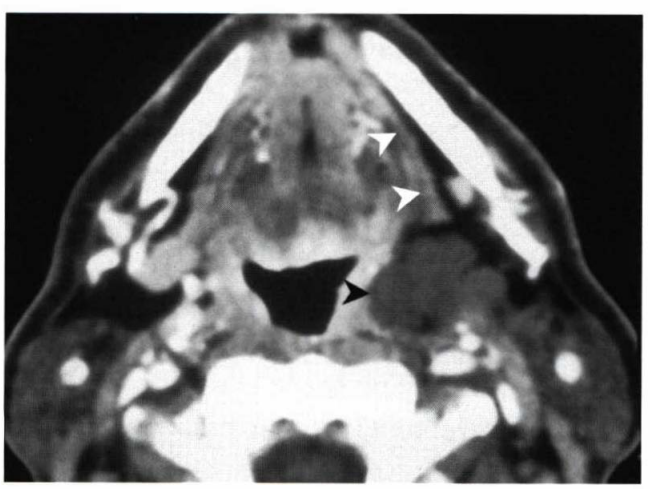

Figure 207–1. Contrast-enhanced CT shows a low attenuation mass located in the inferior aspect of the parapharyngeal space in the location where the parapharyngeal space becomes continuous with the submandibular space (black arrowhead). This occurs at the free margin of the mylohyoid muscle. White arrowheads indicate the mylohyoid muscle. Pathology revealed pleomorphic adenoma.

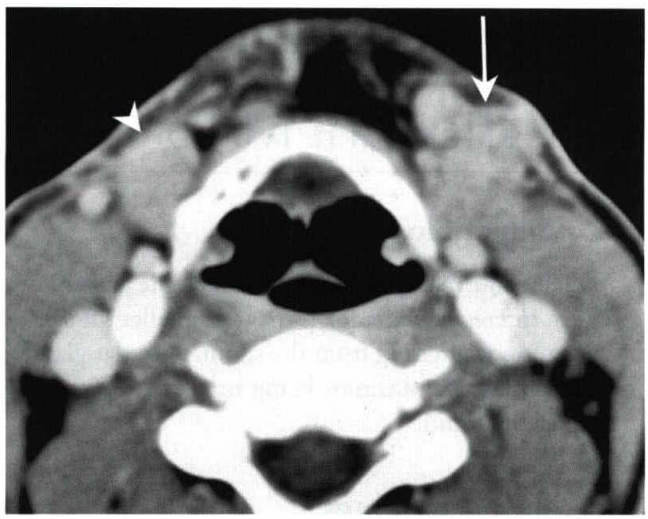

Figure 207–2. Contrast-enhanced CT shows a lobulated mass in the left submandibular space (arrow). The patient had undergone prior resection of a left submandibular gland pleomorphic adenoma. Pathology revealed recurrent pleomorphic adenoma. The arrowhead indicates a normal submandibular gland.

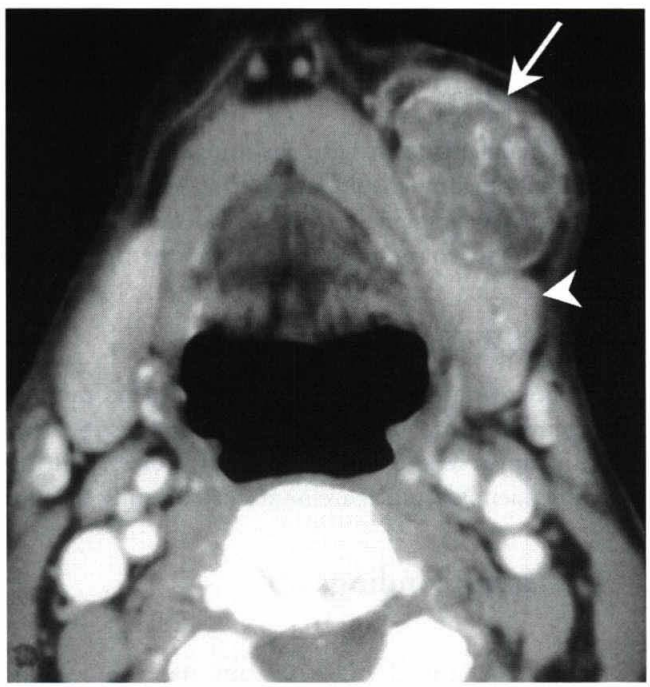

Figure 207–3. Axial contrast-enhanced CT shows a heterogeneously enhancing mass involving the left submandibular space (arrow). The submandibular gland is displaced posterior (arrowhead). At surgery, the mass was found to be arising from the submandibular gland. Pathology revealed pleomorphic adenoma.

Imaging Pearl

- It might be difficult to differentiate a mass arising from the submandibular gland from an enlarged nodal mass. Imaging is used to determine the relationship of the mass with the submandibular gland and to evaluate for enlarged lymph nodes.

Suggested Readings

1. Batsakis JG. Neoplasms of the minor and lesser major salivary glands. In: Batsakis JG, ed. *Tumors of the Head and Neck.* Baltimore: Williams and Wilkins; 1979:76–99.
2. Smoker WRK. Oral cavity. In: Som PM, Curtin H, eds. *Head and Neck Imaging.* 3rd ed. New York: Mosby; 1996:488–544.
3. Shockley WM. Parotid tumors. In: Shockley WM, Pillsbury HC. *The Neck: Diagnosis and Surgery.* New York: Mosby; 1994:265–294.

Chapter 208

Malignant Minor Salivary Gland Tumors

Epidemiology

The same malignancies that arise in the parotid gland can arise in the submandibular gland. An interesting paradox is that the smaller the salivary gland, the greater the likelihood that a tumor originating from the submandibular gland will be malignant. Thus the incidence of a salivary gland tumor being malignant in the submandibular gland is higher than in the parotid gland.

Clinical Findings

Patients often present with asymptomatic masses that have been present for several months. Advanced lesions may result in facial numbness or facial nerve palsy.

Pathology

The malignancies that constitute malignant salivary gland tumors include adenoid cystic carcinoma, mucoepidermoid carcinoma, and adenocarcinoma. Many investigators now include low grade polymorphous adenocarcinoma as a tumor of minor salivary gland origin. The most common malignancy of the minor salivary glands is adenoid cystic carcinoma.

Treatment

The treatment of malignant salivary gland tumors depends on the exact histologic type. In general, complete surgical resection offers the best chance for cure. Postoperative radiation therapy is required in the majority of cases. The role of neutron beam therapy for unresectable adenoid cystic carcinomas is currently being evaluated.

Imaging Findings

CT

The CT findings are nonspecific. These are usually soft tissue masses that involve the submandibular gland and enhance following contrast. These tumors rarely invade the adjacent mandible (Fig. 208–1).

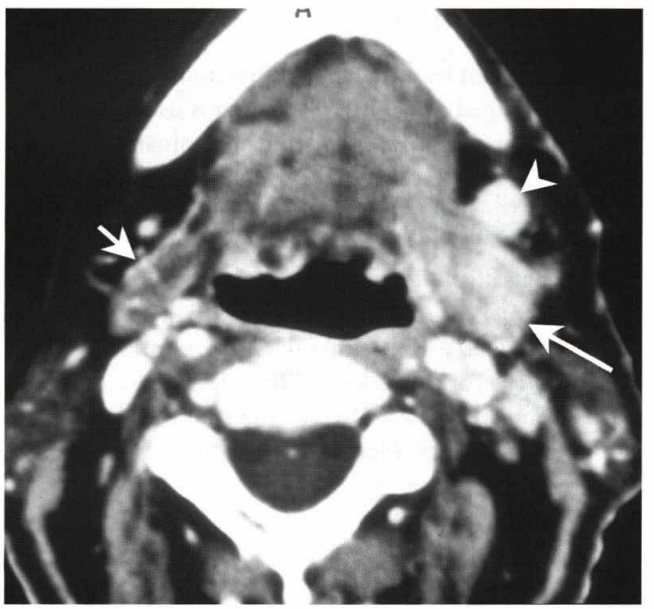

Figure 208–1. Axial contrast-enhanced CT demonstrates a densely enhancing mass replacing the left submandibular gland (long arrow). There is an abnormal level I lymph node adjacent to the mass (arrowhead). Compare this to normal appearance of the submandibular gland on the contralateral side (short arrow). Pathology revealed a primary mucoepidermoid carcinoma of the submandibular gland with a metastatic level I lymph node.

MR

These tumors are usually intermediate signal on T1-weighted sequences and enhance following contrast administration. The T2-weighted signal is variable.

Imaging Pearl

- The imaging findings are nonspecific. However, a malignant salivary gland tumor should be considered for a mass that involves the submandibular gland associated with a cranial nerve palsy.

Suggested Readings

1. Batsakis JG. Neoplasms of the minor and lesser major salivary glands. In: Batsakis JG, ed. *Tumors of the Head and Neck*. Baltimore: Williams and Wilkins; 1979:76–99.
2. Smoker WRK. Oral cavity. In: Som PM, Curtin H, eds. *Head and Neck Imaging*. 3rd ed. New York: Mosby; 1996:488–544.
3. Shockley WM. Parotid tumors. In: Shockley WM, Pillsbury HC. *The Neck: Diagnosis and Surgery*. New York: Mosby; 1994:265–294.

Chapter 209

Congenital Anomalies of the Second Branchial Apparatus

Epidemiology

Congenital anomalies of the second branchial apparatus arise from anomalous embryogenesis of a component of the second branchial complex. These are the most common branchiogenic anomalies and constitute 95% of all branchial abnormalities. Cysts are the most common malformation and usually present at between 10 and 40 years of age. Other malformations consist of sinuses and fistulas. There is no consistently reported gender predilection for these lesions.

Embryology

Cysts

Branchial cleft cysts (BCC) are thought by most authors to result from incomplete obliteration of the epithelial-lined cervical sinus. BCC may occur anywhere along the developmental path of the second branchial complex from the tonsillar fossa to the level of the hyoid bone. The typical location is along the anterior border of the sternocleidomastoid muscle, lateral to the jugular vein at the level of the carotid bifurcation.

BCC are classified by Bailey into four types (Fig. 209–1). Type 1 are superficial lesions located along the anterior border of the sternocleidomastoid muscle just beneath the superficial cervical fascia. Type 2 BC are the most common form and represent deeper lesions that abut the carotid sheath. Type 3 lesions are cysts that pass medially between the internal and external carotid arteries and extend inward toward the lateral wall of the pharynx. Occasionally, type 3 cysts have been noted to extend cranially as far as the skull base. Type 4 is a BCC that is lined by columnar epithelium.

Sinus

A sinus arising from the second branchial apparatus is felt to occur from a communication connecting an incompletely obliterated cervical sinus and the skin.

Fistula

Second branchial groove fistulas are thought to develop if the second branchial groove communicates with the second branchial pouch. The result is a fistula with an internal opening within the tonsillar fossa, often adjacent to the posterior tonsillar pillar, and an external opening along the anterior border of the sternocleidomastoid muscle. The fistulous tract is situated lateral to the ninth and twelfth cranial nerves. The tract may pass between the internal and external carotid arteries and pierce the platysma muscle just prior to its external communication.

Clinical Findings

BCC often present as a fluctuant cystic mass located at the angle of the mandible deep to the anterior border of the sternocleidomastoid muscle. These lesions are usually painless and moveable and not adherent to adjacent structures. Patients may present with symptoms if the cysts become infected.

Sinuses and fistulae may present as an asymptomatic dimple or pigmented spot along the anterior border of the sternocleidomastoid muscle. The fistulous opening is usually present at the level of the hyoid bone or lower. These lesions often present with discharge of clear yellow mucoid secretion. The fistulous tract is prone to recurrent infection.

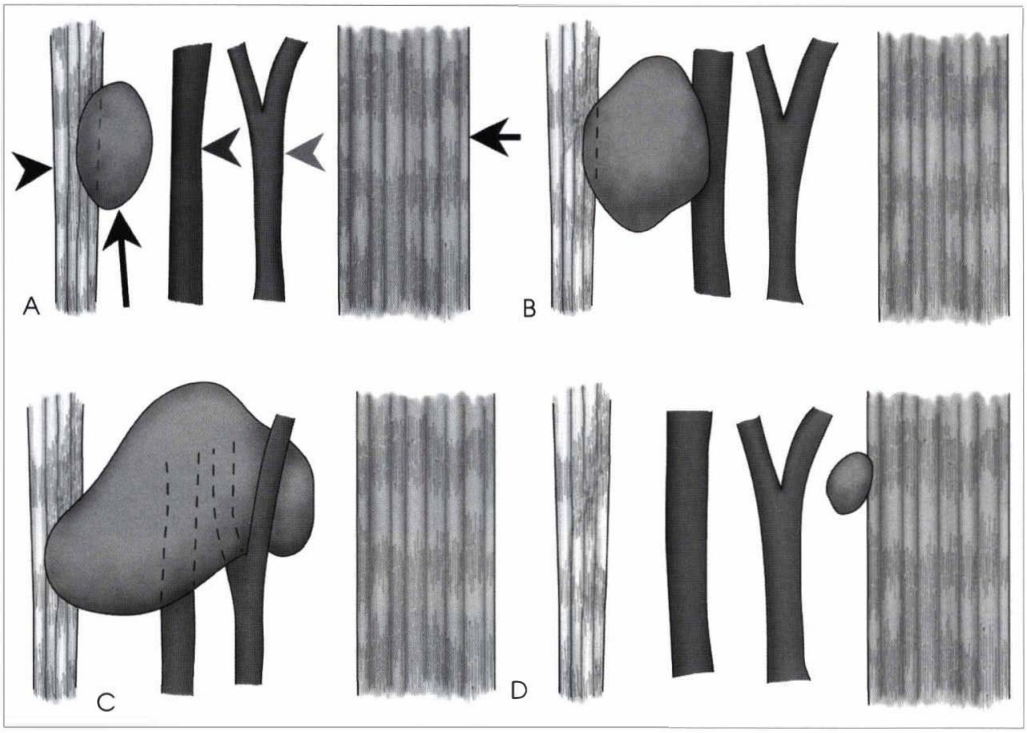

Figure 209-1. Schematic illustrations of the subclassification of second branchial cleft cysts as proposed by Bailey. Black arrowhead, platysma muscle; long black arrow, cyst; short black arrow, viscera; blue arrow, jugular vein; red arrowhead, carotid artery. (A) Type 1. (B) Type 2. (C) Type 3. (D) Type 4 (see Color Plate 209-1).

Pathology

Histologically, BCC are thin-walled lesions lined by stratified squamous epithelium with lymphoid tissue deep to the lining membrane. Respiratory columnar epithelium may be present in approximately 4% of cases. Changes of chronic inflammation may occasionally be found. BCC contain turbid, yellowish fluid that may contain cholesterol crystals. Carcinomas arising within a BCC is extremely rare.

The lining of the fistulous tract, typically stratified epithelium along the external portion and columnar epithelium along its internal course, reflects its embryonic origin.

Treatment

BCC is usually treated with surgical excision. The likelihood of adherence to surrounding structures is increased if the cyst has been chronically infected. Preoperative antibiotics should be administered if the cyst is acutely infected on initial presentation.

Sinuses and fistulae are usually treated by surgical excision. Sinus tracts follow the course of the second branchial complex and tend to course between the carotid bifurcation. Surgical dissection is often aided by filling the sinus tract with methylene blue at the time of surgery.

Imaging Findings

CT

The typical presentation of BC is a thin-walled, low attenuation cystic mass that is located along the anterior aspect of the sternocleidomastoid muscle (Figs. 209-2 and 209-3). The sternocleidomastoid muscle is typically displaced posteriorly or posterolaterally. There is minimal peripheral enhancement of the wall. The presence of an enhancing wall, increased attenuation, or internal septations is suggestive of prior infection (Fig. 209-4).

MR

BCC is usually low signal on T1-weighted images and high signal on T2-weighted sequences. However, the MR signal often may vary depending on the protein content of the cyst fluid. Highly proteinaceous fluid may contain increased T1-weighted signal and exhibit dephasing on T2-weighted sequences. The enhancement and thickening of the cyst wall may vary depending on the degree of prior infection.

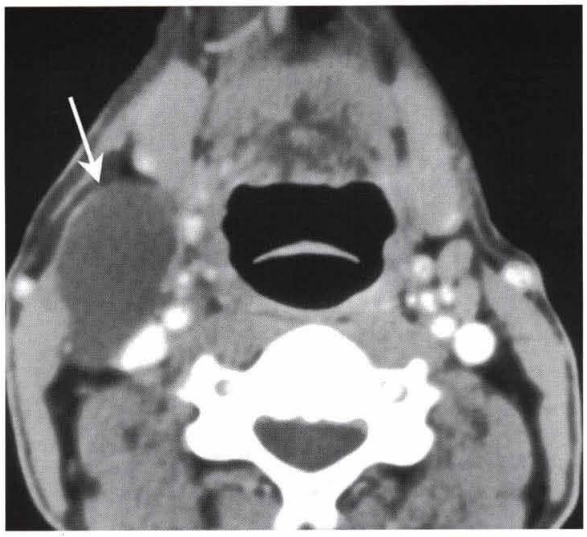

Figure 209–2. Axial contrast-enhanced CT shows the classic appearance of a branchial cleft cyst (arrow). The mass is low attenuation surrounded by a very thin rim.

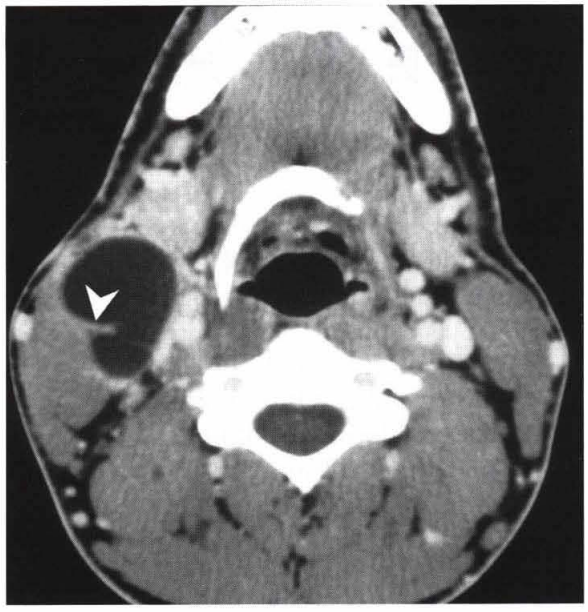

Figure 209–3. Axial contrast-enhanced CT shows a branchial cleft cyst with a small internal septation (arrowhead).

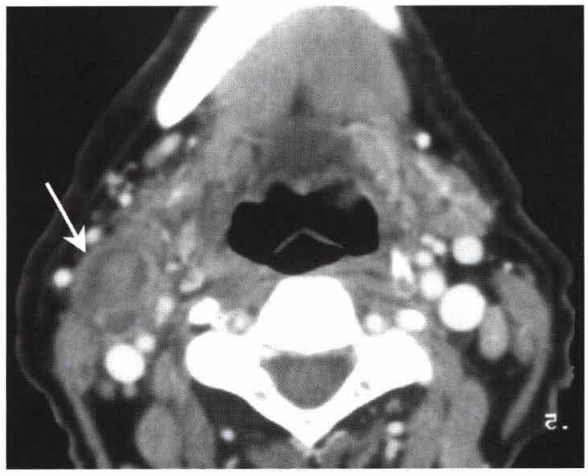

Figure 209–4. This illustration demonstrates the atypical appearance of a branchial cleft cyst. The mass has a very heterogeneous appearance and lacks the homogeneous cystic appearance (arrow). This appearance has likely resulted from prior hemorrhage or infection within the mass. The diagnosis of a second branchial cleft cyst may be considered in the differential diagnosis; however, one must also consider a nodal mass in an adult.

US

BCC are usually cystic lesions with enhanced through transmission. Proteinaceous debris may occasionally be seen within the cyst.

Imaging Pearls

- Uninfected BC usually have a characteristic appearance.
- One must be very careful when evaluating a cystic mass with an enhancing wall located in the expected location of a second branchial cleft cyst (BCC) in adults. This appearance may be due to either an infected second BCC or a metastatic lymph node from squamous cell carcinoma or papillary thyroid carcinoma.
- Cross-sectional imaging may not detect a sinus or fistula, thereby, necessitating a sinogram or fistulogram to identify the full extent of these lesions.

Suggested Readings

1. Karmody CS. Developmental abnormalities of the neck. In: Bluestone CD, Stool SE, Scheetz MD, eds. *Pediatric Otolaryngology.* Vol. 2. Philadelphia: WB Saunders; 1990:1308– 1315.
2. Batsakis JG. Cysts, sinuses and "coeles." In: Batsakis JG, ed. *Tumors of the Head and Neck.* 2nd ed. Baltimore: Williams and Wilkins; 1979:518–520.
3. Bailey H. *Branchial Cysts and Other Essays on Surgical Subjects in the Facio–Cervical Region.* London: HK Lewis; 1929.

Chapter 210

Arteriovenous Malformation

Epidemiology

Arteriovenous malformations (AVMs) are developmental malformations of the vascular system that result in abnormal communication between arteries and veins. The primary abnormality appears to be at the level of the capillary bed. AVMs are classified as a type of vascular malformation using the classification system of Mulliken and Glowacki.

Clinical Presentation

The clinical presentation can be variable depending on the extent of the lesion. The neck and craniofacial region are common sites of occurrence. On clinical examination, AVMs present as a soft tissue fullness that is compressible. Superficial AVMs may be associated with a palpable thrill or audible bruit. The overlying skin may be discolored due to dilated superficial veins. Other presentations in more advanced lesions include facial deformity, skin ulceration, or functional compromise. Patients may also present with hemorrhage that may be spontaneous or may follow minor trauma such as tooth extraction. AVMs may enlarge with pregnancy. It is unclear as to whether the growth is due to direct hormonal stimulation or results secondarily from an increase in the circulating blood volume.

Pathology

AVMs result from abnormal development of the arterial, capillary, and venous components of the vascular system. The lesions grow commensurately with the individual and show no evidence of endothelial proliferation. The vascular channels are lined by mature endothelium with normal mitotic activity (Fig. 210–1).

Treatment

The treatment of choice is combined therapy consisting of embolization followed by surgical excision. Complete resection of the nidus is necessary to prevent recurrence

Imaging Findings

CT

AVMs are characterized by a tangle of enhancing serpiginous vessels that are not associated with a surrounding soft tissue mass. Lesions adjacent to facial bones may be associated with enlargement and overgrowth of the adjacent bone.

MR

The MR findings of an AVM are multiple flow voids without an associated soft tissue mass. Increased vascular flow is seen on flow sensitive sequences.

US

Doppler analysis will demonstrate arterial and venous components and may show arterialized waveforms of a draining vein due to arteriovenous shunting.

Angiography

AVMs have enlarged tortuous feeding arteries that supply a nidus. Arteriovenous shunting into enlarged draining veins is a characteristic finding. The primary blood supply is from various branches of the external carotid artery.

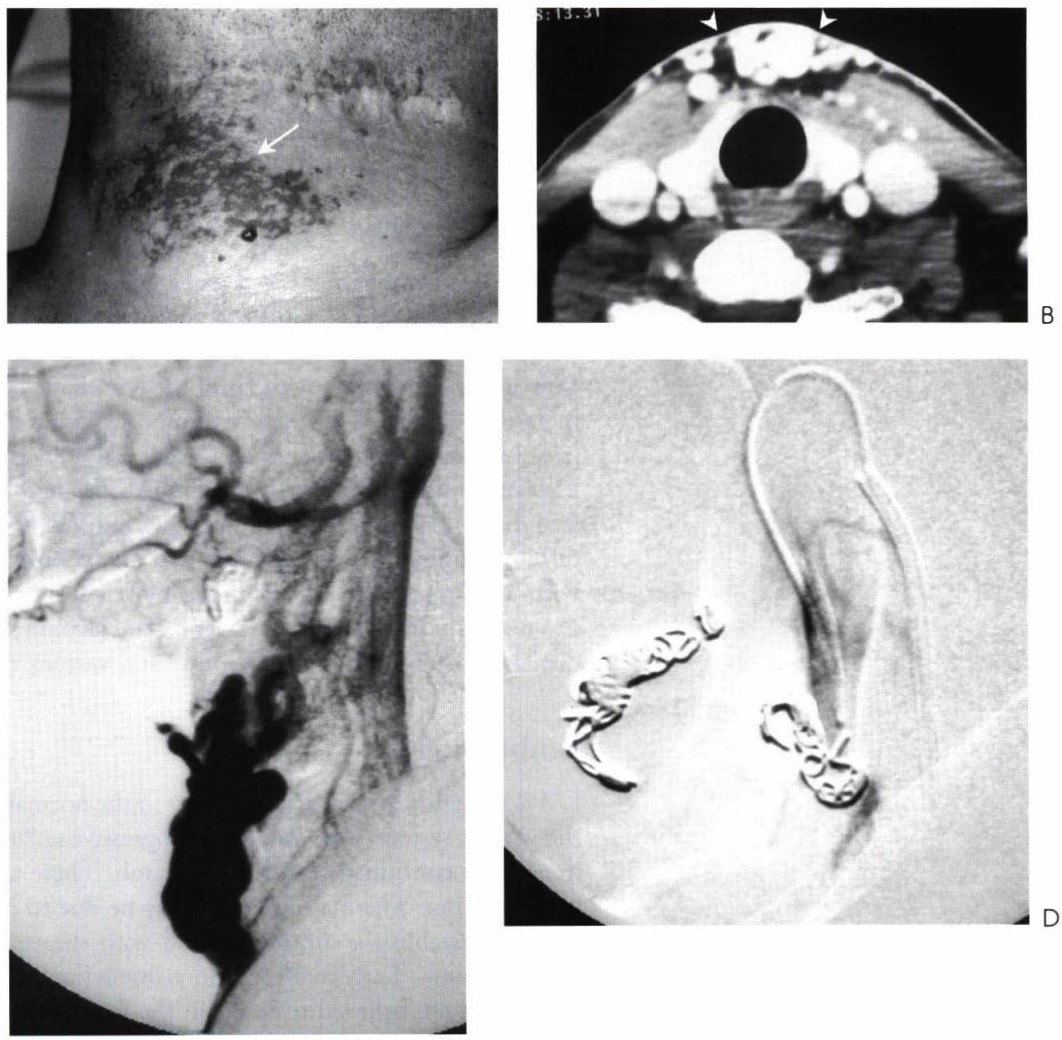

Figure 210–1. Arteriovenous malformation. (A) Photograph shows the reddish skin discoloration of a patient with the superficial AVM of the submandibular space (arrow). (B) Contrast-enhanced CT shows multiple dilated vessels in the subcutaneous fat (arrowheads). (C) Selective external carotid angiogram shows multiple abnormal, enlarged vessels confirming the diagnosis of an AVM. (D) There is markedly reduced flow within the AVM following embolization.

Imaging Pearls

- The treatment of AVMs is directly affected by the imaging findings. Identification of a high-flow vascular malformation with arteriovenous shunting contraindicates treatment with percutaneous sclerotherapy.
- The presence of potential collateral formation between branches of the external carotid artery and the vertebral artery or branches of the internal carotid artery need to be closely evaluated for during endovascular procedures.
- Craniofacial AVMs should not be treated with a particle size < 200 μm due to the possibility of overlying skin necrosis or direct shunting of particles into the pulmonary bed or intracranial circulation.

Suggested Readings

1. Mulliken JB, Glowacki J. Hemangiomas and vascular malformations in infants and children: a classification based on endothelial characteristics. *Plast Reconstr Surg* 1982;69:412–422.
2. Meyer JS, Hoffer FA, Barnes PD, Mulliken JB. Biological classification of soft-tissue vascular anomalies: MR correlation. *AJR Am J Roentgenol* 1991;157:559–564.
3. Smoker WRK. Oral cavity. In: Som PM, Curtin H, eds. *Head and Neck Imaging*. 3rd ed. New York: Mosby; 1996:488–544.
4. James CA. Diagnostic imaging of congenital vascular lesions. In: Warner M, Suen JY, eds. *Hemangiomas and Vascular Malformations of the Head and Neck*. New York: Wiley-Liss; 1999:171–215.

Chapter 211

Lymphatic Malformations

Epidemiology

Lymphatic malformation (*LM*) is the current term used to describe lymphangiomas. Mulliken and Glowacki recommend that the suffix *-oma* only be used in lesions that exhibit cellular proliferation, such as does a hemangioma. LMs are congenital lesions that result from a defect in embryogenesis of the lymphatic system. They occur in equal frequency in males and females. They most commonly present in newborn children, with 65% of lesions noted at birth, 80% present at 1 year, and 90% present by 2 years of age. Ten percent of LMs may initially present in adulthood. LMs may be localized or associated with a generalized malformation of the lymphatic system. Advanced generalized disorders may be seen as diffuse lymphangiectasis in utero and are incompatible with life. LM has been associated with a number of syndromes, the most common being Turner's syndrome. Other syndromes include Noonan's syndrome, fetal alcohol syndrome, familial pterygium syndrome, distichiasis–lymphedema syndrome, and various chromosomal aneuploidies.

Embryology

LM is thought to occur from a defect in the normal drainage of the lymphatic channels into the venous system. The result is a progressive enlargement of the isolated lymphatic spaces due to the continued secretion of lymph. There are several proposed explanations of this malformation. The malformation may be due to a portion of the lymphatic network that fails to reestablish a communication with the venous system and is sequestered early in embryogenesis. Early malformations involving the more primitive jugular, subclavian, and axillary sac are believed to result in the formation of the larger cystic hygromas. These lesions occur in soft areolar tissues with wide fascial planes. The results in the lesions being round or oval lesions with well-defined borders. Lesions that have smaller cystic spaces and are more diffuse and infiltrative are believed to occur later in embryogenesis. These malformations have time to grow distally along narrower facial planes and insinuate themselves along vessels and nerve trunks. This probably results in the mixed malformations described by Mulliken and Glowacki, such as lymphaticovenous and lymphaticocapillary malformations. Thus, LMs that occur in the cheeks, lips, and tongue tend to contain more of an angiomatous component.

Pathology

Pathologically, LMs have been categorized in the past based on the size of the anomalous lymphatic space. It should be noted that *lymphatic malformation* is the current term used to describe these malformation and that terms such as *cavernous lymphangioma* and *capillary lymphangioma* probably refer to the "mixed" lymphatic malformations described by Mulliken and Glowacki. We define the older terminology following here for historical consistency.

Cystic hygroma is the most common form and consists of a honeycomb of very large dilated lymphatic spaces lined by a single layer of flat endothelium. These lesions are often solitary and occur in the presence of an otherwise normal lymphatic system. Seventy-five percent of these lesions occur in the neck, with a predilection for the posterior compartment of the neck.

A cavernous lymphangioma is composed of mild to moderately dilated lymphatic spaces, the size of which is between the cystic spaces seen in cystic hygromas and capillary hemangiomas. These lesions tend to be situated in the oral cavity or salivary glands. Cavernous LAs tend to be subcutaneous lesions which tend to penetrate adjacent muscular and neurovascular structures without destroying them. The peripheral location and subcutaneous spread are suggestive of defect in embryogenesis during a later phase of lymphatic development (9–10 weeks) than the classic cystic hygroma.

Capillary hemangioma (simple, lymphangioma simplex) is composed of a network of small lymph, thin-walled channels that are the size of capillaries, and is the least common form of lymphangioma. These lesions are located predominantly within the epidermis and can occur anywhere throughout the body. Because of their superficial location, capillary hemangiomas are believed to form the latest in development.

Clinical Findings

The extracranial head and neck is the most common site of LMs (75%). They typically present as a painless neck mass. Cystic hygromas present as soft, doughy, compressible masses situated in the posterior triangle of the neck. Lesions that occur in the face are more likely to be mixed LMs. LMs tend to enlarge commensurate with the growth of the child and not by endothelial proliferation. Potential complications include disfigurement, respiratory compromise, and recurrent infections. Rapid enlargement may be due to infection or spontaneous hemorrhage within the lesion.

Treatment

Surgical resection is the treatment of choice for LMs with distinct margins. However, distal lesions that extend over several anatomic areas are difficult to completely resect and are prone to recurrence. Such patients need close follow-up and may require multiple surgical procedures. Percutaneous sclerotherapy is gaining wider acceptance for more advanced lesions that infiltrate the deep fascial planes. Some authors advocate angiography and embolization for lymphaticocapillary lesions that involve the oral cavity and tongue. The role of interferon therapy for very advanced and infiltrative lesions is currently under investigation.

Imaging Findings

CT

The classic appearance of an LM is a sharply demarcated low attenuation mass that does not contain a visible wall. These lesions have a tendency to occur in the posterior compartment of the neck. Large lesions may be multilobular and have considerable mass effect and may displace the structures of the carotid sheath and adjacent sternocleidomastoid muscle. Lesions that have been partially resected or have been repeatedly infected may demonstrate an enhancing wall or contain internal septations. Mixed LMs are heterogeneous and infiltrative. These lesions extend along fascial planes and often involve multiple spaces (transspatial). Because of the angiomatous components, mixed lesions may enhance with contrast (Fig. 211-1).

MR

A pure LM is low signal on T1-weighted sequences and high signal on T2-weighted sequences. There is no perceptible wall or enhancement following contrast administration. Pure LMs are low flow lesions and lack flow voids. Mixed malformations are infiltrative heterogenous lesions that enhance following contrast. The degree of the enhancement is likely due to the angiomatous component of the mixed lesion (Fig. 211-2).

US

Pure LMs are hypoechoic masses that may occasionally contain internal septations or debris. Doppler analysis may be helpful for evaluating LMs by identifying and characterizing the presence of intralesional blood flow.

Angiography

Pure LMs are avascular, low flow lesions. However, mixed LMs that have a substantial angiomatous component are hypervascular and have enlarged feeding vessels. Arteriovenous shunting is rare.

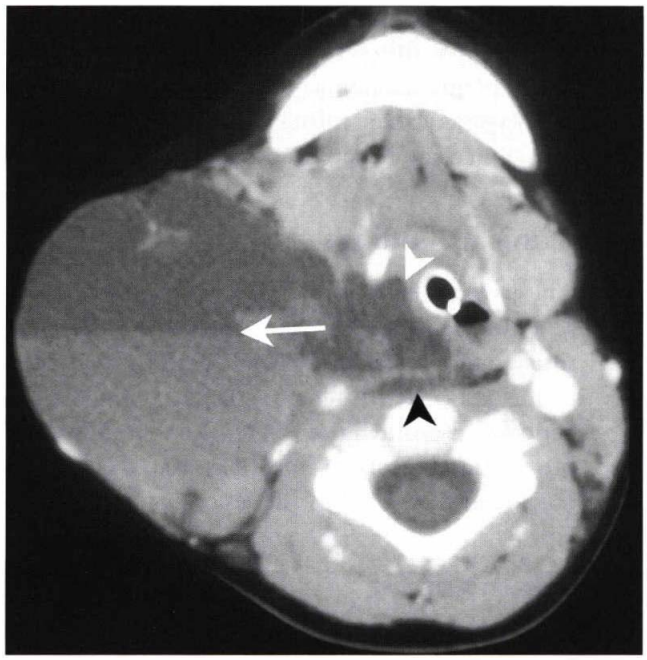

Figure 211–1. Contrast-enhanced CT shows a large lymphatic malformation involving the right submandibular space. The fluid–fluid level likely represents recent hemorrhage (white arrow). A component of the LM extends into the visceral space (white arrowhead). The low attenuation within the retropharyngeal space (black arrowhead) could be due to involvement by the LM or edema.

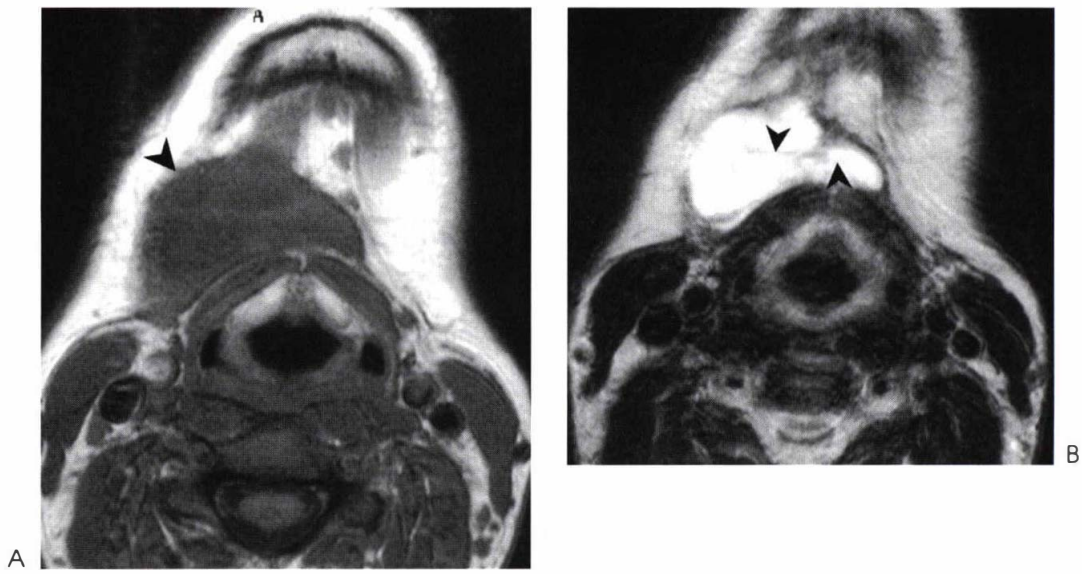

Figure 211–2. MR of lymphatic malformation. (A) Axial noncontrast T1-weighted image shows an intermediate signal mass in the right submandibular space (arrowhead). (B) Axial T2-weighted image shows the mass to be high signal and contain internal septations (arrowheads).

Imaging Pearls

- It may be difficult to differentiate a pure LM located in the posterior triangle of the neck from a third branchial cleft cyst.
- A predominantly cystic mass that is transspatial is the characteristic imaging of an LM.

Suggested Readings

1. Zadvinski DP, Benson MT, Kerr HH, et al. Congenital malformations of the cervicothoracic lymphatic system: embryology and pathogenesis. *Radiographics* 1992;1175–1189.
2. Batsakis JG. Vasoformative tumors. In: Batsakis JG, ed. *Tumors of the Head and Neck.* 2nd ed. Baltimore: Williams and Wilkins; 1979:518–520.
3. Mulliken JB, Glowacki J. Hemangiomas and vascular malformations in infants and children: a classification based on endothelial characteristics. *Plast Reconstr Surg* 1982;69:412–422.
4. Mulliken JB. Vascular malformations of the head and neck. In: Mulliken JB, Young AE, eds. *Vascular birthmarks: hemangiomas and malformations.* Philadelphia: WB Saunders; 1988:301–307.

Chapter 212

Madelung's Disease

Epidemiology

Madelung's disease (benign symmetrical lipomatosis) is a rare disorder initially described by Brodie in 1846. The disease is characterized by massive deposition of fat in the neck, shoulders, and upper thorax. The disease is most common in men living in the Mediterranean region. The reported incidence is approximately 1 in 25,000 Italian men. The exact cause of the disease is unknown. Possible causes include a defect in adrenergic-stimulated lipolysis or a response to "functional sympathetic denervation." Madelung's disease appears to be sporadic, although some familial cases have been reported. There appears to be a strong association with excessive alcohol intake. Other associated conditions include reduced glucose intolerance, gout, liver disease, polyneuropathy, diabetes mellitus, peripheral insulin resistance, renal tubular acidosis, hypertension, hypothyroidism, hyperlipidemia, and increased lipoprotein lipase activity.

Clinical Features

These patients often have a characteristic appearance. Patients may have a "hamster" or "pseudoathletic" appearance due to symmetric fat deposition in the neck, upper thorax, lower face, and shoulders. Involvement of the visceral space may result in tracheal or laryngeal compression. Patients may also have a peripheral or sensory motor neuropathy. Malignant degeneration has been reported but is very rare.

Pathology

The lipomatous changes in Madelung's disease consists of normal, unencapsulated adipose tissue that infiltrates adjacent structures.

Treatment

The standard treatment is intermittent surgical debulking. It is often difficult to completely resect the infiltrative fatty depositions. Therefore, surgery is often regarded as palliative. Liposuction has been attempted with varying degrees of success.

Imaging Findings

CT

The disease is characterized by massive fatty deposition throughout the neck (Figs. 212–1 and 212–2). The fatty deposition has a tendency to be more posterior and often displaces the adjacent musculature. Involved sites include the anterior and posterior subcutaneous tissues surrounding the sternocleidomastoid, trapezius muscles, and paraspinal muscles. The lipomatous changes may extend inferiorly into the supraclavicular fossa. The fat may also infiltrate into the deep fascial spaces to involve the retropharyngeal and carotid spaces. It may also extend into the larynx to enlarge the paraglottic fat.

MR

The signal characteristics of the fat in Madelung's disease are similar to those seen in routine benign lipomas. There are linear areas of stranding present within the lipoma. Thus, one cannot completely exclude the possibility of a low-grade liposarcoma. However, this is unlikely given the very low reported incidence of liposarcoma in Madelung's disease.

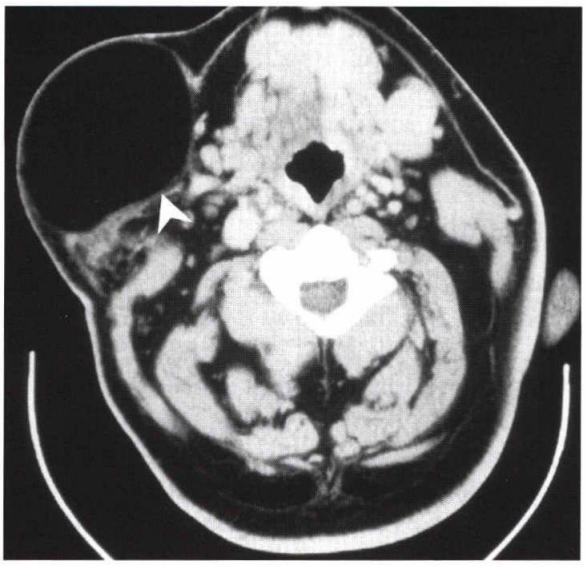

Figure 212–1. Axial contrast-enhanced CT shows a large lipoma in the right submandibular space (arrowhead).

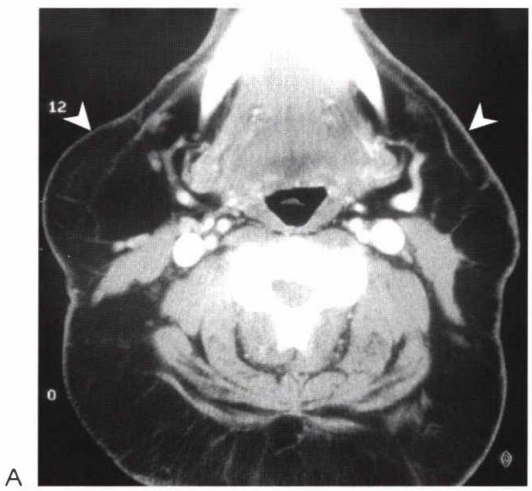

A

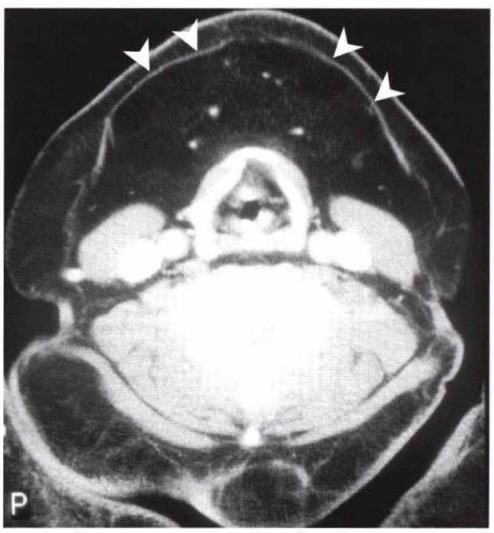

B

Figure 212–2. (A) Contrast-enhanced CT performed in a patient with Madelung's disease shows copious amounts of fat in the subcutaneous tissue. This fat extends anteriorly into the submandibular space (arrowheads). (B) Axial image obtained inferior to (A) shows diffusely increased amount of fat in the submandibular space deep to the platysma muscle. Arrowheads indicate the platysma muscle.

Imaging Pearls

- Madelung's disease is usually diagnosed clinically.
- The preponderance of fat is nonspecific and may be present in obese patients or patients on steroids.
- The diagnosis can be suggested on imaging by deep infiltration of fat into the fascial spaces (retropharyngeal space) or into the paraglottic fat.

Suggested Readings

1. Williams DW, Ginsberg LE, Moody DM, McCain BL. Madelung disease: MR findings. *AJNR Am J Neruoradiol* 1993;14:1070–1073.
2. Ahuja AT, King AD, Chan ESY, et al. Madelung disease: distribution of cervical fat and preoperative findings at sonography, MR, and CT. *AJNR Am J Neruoradiol* 1998;19:707–710.
3. Luscher NJ, Prein J, Speiss B. Lipomatosis of the neck (Madelung's disease). *Ann Plast Surg* 1986;16:502–508.

Chapter 213

Hemangiomas

Epidemiology

Hemangiomas are proliferative endothelial vascular lesions that are identified by their characteristic clinical appearance and course. Forty percent of hemangiomas are present at birth and 60% appear within the first few months of life. Hemangiomas are more common in females than males (5:1). Common sites of occurrence include skin, face, orbits, larynx, nasal cavity, and deep neck spaces.

The classification proposed by Mulliken and Glowacki distinctly separates hemangiomas from vascular malformations based on biological and clinical characteristics. Previous descriptive terms such as *strawberry, capillary, juvenile,* or *cellular* are not currently used to describe hemangiomas. These older names are now encompassed by the term *hemangioma.* Most authors now feel that "cavernous" hemangiomas are venous malformations. "Port-wine" hemangiomas are now considered capillary malformations.

Clinical Findings

Superficial hemangiomas are bright red papular lesions. Subcutaneous hemangiomas often present as a bluish mass that may be difficult to differentiate from a venous malformation or an arteriovenous malformation.

Hemangiomas rapidly grow during the first 12 to 18 months of life (proliferative phase). This is followed by gradual regression (involuting phase) over the next 6 to 10 years. Approximately half of all lesions will completely involute, whereas the remainder will partially involute. Incomplete involution may result in residual telangiectasias, hypoplastic patches, or scarring.

Hemangiomas usually arise in the superficial layers of the skin and mucosa. The majority of hemangiomas have an uneventful course with spontaneous and complete involution. More advanced lesions, depending on their location, may cause severe facial disfigurement, impaired vision, or respiratory stridor.

In the past, hemangiomas have been associated with a variety of syndromes that include Dandy-Walker, Klippel-Trénaunay, Sturge-Weber, Beckwith-Wiedemann, Hippel-Lindau, and Rendu-Osler-Weber. There is also an association with Kasabach-Merritt syndrome; a consumptive coagulopathy complicated by platelet trapping, hemorrhage, or high-output congestive heart failure that may occur with large hemangiomas. These associations were identified prior to the Mulliken and Glowacki classification system. Further investigations will be needed to determine whether these associations are still valid using the currently accepted classification scheme.

Pathology

The proliferative phase consists of proliferating plump endothelial cells with frequent mitoses. The end of the proliferative phase is characterized by a reduction in the mitotic activity, progressive flattening of the cells, and an abundance of mast cells. Apoptosis and the presence of endothelial cells encompassed by large ectatic vascular channels in a matrix of fibro-fatty tissue characterize the involuting phase.

Treatment

Because most hemangiomas undergo complete or near-complete spontaneous involution, the treatment is conservative and consists of observation and parental reassurance. More aggressive options such as steroid therapy and compression therapy are reserved for enlarging lesions that result in functional compromise. Surgery is reserved as a secondary procedure following initial therapy or incomplete involution. The role of antiangiogenesis agents is currently under investigation.

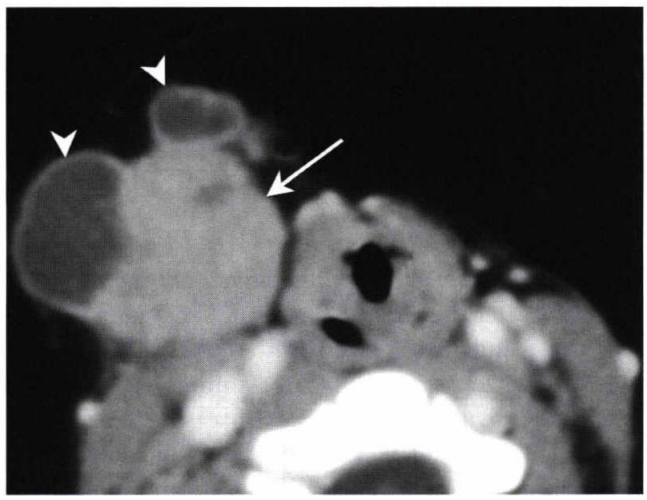

Figure 213–1. Contrast CT performed in an infant shows an enhancing hemangioma located in the right submandibular space (arrow). The cystic components (arrowheads) of the hemangioma are atypical.

Imaging Findings

CT

These are densely enhancing soft tissue masses that may be localized or extend deeply along the fascial planes (Fig. 213–1). Phleboliths are uncommon in true hemangiomas.

MR

These lesions are soft tissue masses that are intermediate signal on T1-weighted sequences and bright on T2-weighted sequences. These lesions densely enhance following contrast administration. The presence of internal flow voids suggests hemangiomas in the proliferative phase. These are characterized as high flow lesions. The absence of flow voids suggests that the tumor is involuting and is a low flow lesion.

Angiography

There is an organized pattern of arterial supply from the enlarged feeding arteries in high flow lesions. Hemangiomas show an intense parenchymal enhancement with pooling of contrast material. Arteriovenous shunting is uncommon.

Doppler US

This technique may be useful in attempting to differentiate between high flow and low flow lesions. High flow hemangiomas in the proliferative phase will demonstrate an arterial waveform, whereas involuting low flow lesions will have a venous waveform.

Imaging Pearls

- Flow-sensitive MR sequences may be helpful to confirm that a mass is a high flow lesion.
- The role of endovascular therapy for hemangiomas is currently under investigation. This approach may be best suited for extensive high flow hemangiomas in the proliferative phase.
- High flow hemangiomas can be differentiated from high flow arteriovenous malformations based on the findings that hemangiomas are associated with a soft tissue mass, whereas there is no parenchymal component associated with an arteriovenous malformation.
- Late involuting (low flow) hemangiomas may be difficult to differentiate from low flow venous malformations.

Suggested Readings

1. Mulliken JB, Glowacki J. Hemangiomas and vascular malformations in infants and children: a classification based on endothelial characteristics. *Plast Reconstr Surg* 1982;69:412–422.
2. Meyer JS, Hoffer FA, Barnes PD, Mulliken JB. Biological classification of soft-tissue vascular anomalies: MR correlation. *AJR Am J Roentgenol* 1991;157:559–564.
3. Waner M, Suen JY. A classification of congenital vascular malformations. In: Warner M, Suen JY, eds. *Hemangiomas and Vascular Malformations of the Head and Neck*. New York: Wiley-Liss; 1999:1–12.
4. James CA. Diagnostic imaging of congenital vascular lesions. In: Warner M, Suen JY, eds. *Hemangiomas and Vascular Malformations of the Head and Neck*. New York: Wiley-Liss; 1999:171–215.

Chapter 214

Thyroglossal Duct Cyst

Epidemiology

Thyroglossal duct cyst is a congenital lesion that arises from anomalous development and migration of the thyroid gland. This results in remnants of residual thyroid tissue along the migrational route. Thyroglossal duct cyst is the most common midline neck mass in children. The majority of cases present in children < 10 years of age. These lesions may be seen in young adults. Less than 2% of cases arise in patients > 60 years of age. No gender predilection has been reported.

Clinical Findings

Thyroglossal duct cysts may arise anywhere along the course of migration of the embryonic thyroglossal duct and thyroid gland. The most common location is below the level of the hyoid bone (65%). Seventy-five percent of thyroglossal duct cysts are midline masses. A thyroglossal duct cyst usually present as nontender, gradually increasing midline neck masses. The average size at presentation is 2 to 4 cm. Recent enlargement may occur as a result of an associated upper respiratory tract infection. In the submandibular space, thyroglossal duct cysts are often attached to the hyoid bone. As a result, these lesions may be suspected clinically because these masses usually move when the patient swallows ("deglutination").

Embryology

The thyroid gland is the first endocrine gland to appear in the developing fetus and begins its embryogenesis around day 24 of gestation. The gland arises from an endodermal thickening in the midline of the developing tongue base. This area is known as the foramen cecum and is located posterior to the apex of the circumvallate papilla. The thyroid gland descends as a result of elongation of the embryo and growth of the tongue. The developing gland migrates as a bilobed diverticulum and forms an epithelial-lined cord during descent. Normal involution of the thyroglossal duct occurs between the eighth and tenth weeks of gestation. Failed involution of the epithelial cord predisposes the patient to formation of a thyroglossal duct cyst. Cyst formation is believed to be caused either by inflammatory changes that stimulate secretion of fluids within the ductal remnants or by the trapping of fluids produced from residual secretory epithelium located in the epithelial cord remnant.

During descent, the developing cartilage of the second branchial arch that gives rise to the hyoid bone comes in close proximity to the descending thyroglossal duct. The thyroid gland may descend superficial to, through, or deep to the hyoid bone. As a result, the location of thyroglossal duct cysts with the hyoid bone is variable. The duct then continues its downward course and lies anterior to the thyrohyoid membrane. The duct terminates at the superior border of the thyroid gland. Migration of the thyroid gland is completed by the eighth week of gestation.

Pathology

The vast majority of thyroglossal duct cysts are benign lesions. Histologically, these cysts have a squamous lining. Thyroid tissue is an uncommon finding in the cyst wall. Occasionally, inflammatory changes may obliterate the epithelial mucosal lining, causing the diagnosis to be based on characteristic clinical and radiographic findings. Fistulas may result from infection, cyst rupture, or complication of prior surgery. Several types of fistulas may occur: internal, with an opening into the pharynx; external, with an opening to the skin surface; or complete, with direct communication between the skin and the pharynx.

Malignancy may coexist in < 1% of thyroglossal duct cysts. This is often an incidental finding. The most common associated malignancy is papillary carcinoma, which is thought to arise from rests of ectopic thyroid tissue located within the thyroglossal duct cyst.

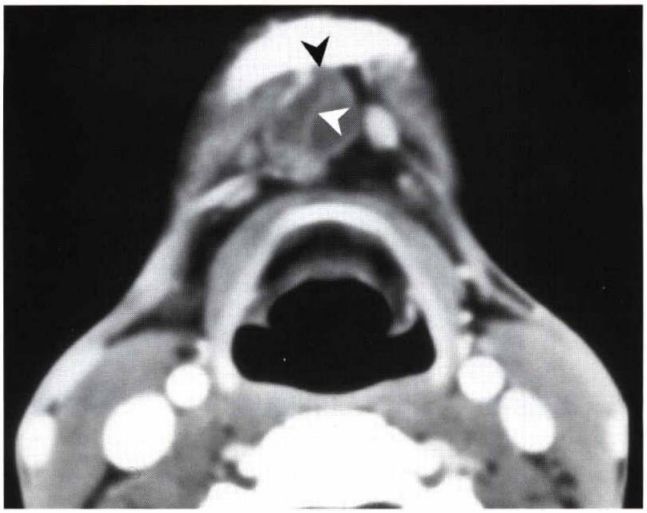

Figure 214-1. Contrast-enhanced CT shows a thyroglossal duct cyst located in the submandibular gland (black arrowhead) There are multiple septations seen within the cyst (white arrowhead).

Treatment

The treatment of choice for thyroglossal duct cyst is complete surgical resection. The Sistrunk procedure is the method of choice and involves complete removal of the entire cyst tract from the tongue base to the superior border of the thyroid gland. The central portion of the hyoid bone and a cuff of the tongue base are included in the resection. Complete resection utilizing the Sistrunk procedure is associated with a 3% recurrence rate, whereas the recurrence rate is significantly increased if thyroglossal duct cysts are locally excised.

Imaging Findings

CT

The findings are that of a unilocular or multilocular cystic mass with peripheral enhancement (Fig. 214-1). Recurrent infection may increase the attenuation of the cystic component and cause thickening of the enhancing rim. The lesion may extend anywhere from the tongue base to the superior portion of the thyroid gland. The relationship of a thyroglossal duct cyst to the hyoid bone is variable. Thyroglossal duct cysts may be located superficial or deep to, or may directly involve, the hyoid bone.

MR

The thyroglossal duct cyst appears as a cystic lesion that is low to intermediate signal on T1-weighted and increased signal on T2-weighted images. Sagittal or coronal images may be useful for identifying the extent of the lesion prior to resection (Fig. 214-2).

Imaging Pearls

- The presence of a cystic mass that is embedded within the infrahyoid strap muscle is useful for arriving at a diagnosis of atypical-appearing thyroglossal duct cysts.
- The superior and inferior margins of the thyroglossal duct cyst must be closely evaluated. Occasionally, a subtle enhancing tract may be seen arising from the superior or inferior margin of the cyst. This information will help confirm the diagnosis and inform the surgeon of a tract that may be clinically occult.
- Scintigraphy may be more sensitive than MR or CT for localizing rests of ectopic thyroid tissue. However, we do not usually perform this study because a properly executed Sistrunk procedure routinely removes tissue along the normal path of migration of the thyroid gland.
- Normally, there should be no solid enhancing component of a thyroglossal duct cyst. The presence of an intracystic solid enhancing mass may represent residual thyroid tissue. This finding, however, is also suspicious of a coexisting papillary carcinoma and needs to be conveyed to the referring physician (Fig. 214-2A,B).

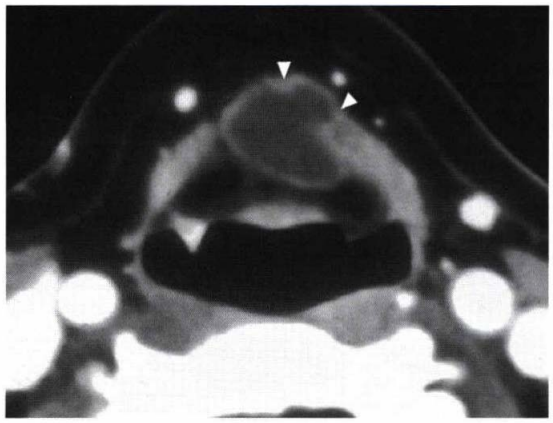

Figure 214-2. Axial contrast-enhanced CT obtained at the level of the thyrohyoid membrane shows a cystic midline extending into the pre-epiglottic space (arrows). Note that the lateral portion of the mass is embedded in the stap muscle (arrowhead). This finding confirms the diagnosis of a thyroglossal duct cyst.

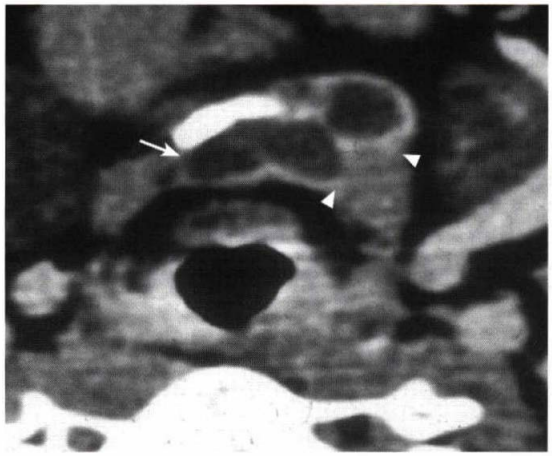

Figure 214-3. Axial contrast-enhanced CT shows a lobulated thyroglossal duct cyst encircling the hyoid bone. Note that a portion of the mass is superficial to the hyoid bone (small arrow) while a different component is deep to the hyoid bone and extends into the pre-epiglottic space (large arrow). The arrowheads indicate that the thyroglossal duct cyst is embedded within the strap muscles.

Suggested Readings

1. Moore KL. The branchial apparatus and the head and neck. In: Moore KL, ed. *The Developing Human: Clinically Oriented Embryology*. 4th ed. Philadelphia: WB Saunders; 1988:184–186.
2. Batsakis JG. Parenchymal cysts of the neck. In: Batsakis JG, ed. *Tumors of the Head and Neck*. Baltimore: Williams and Wilkins; 1979:233–252.
3. Hudgins PA, Jacobs IN, Castillo M. Pediatric airway disease. In: Som PM, Curtin H, eds. *Head and Neck Imaging*. 3rd ed. New York: Mosby; 1996:545–611.
4. Karmody CS. Developmental abnormalities of the neck. In: Bluestone CD, Stool SE, Scheetz MD. *Pediatric Otolaryngology*. Vol. 2. Philadelphia: WB Saunders; 1990:1313–1314.
5. Drake AF, Hulka GF. Congenital neck masses. In: Shockley WM, Pillsbury HC, eds. *The Neck: Diagnosis and Surgery*. New York: Mosby; 1994:93–107.

Chapter 215

Complex (Diving, Plunging) Ranula

Epidemiology

Ranulas are cystic lesions arising in the sublingual space (floor of mouth) that are believed to result from obstruction of the sublingual or minor salivary gland. The obstruction is most commonly thought to be congenital or posttraumatic in origin. The cysts develop from continued secretion of the mucous glands into an obstructed duct. Ranulas have also been referred to as mucoceles or pseudocysts in the floor of mouth. Although ranulas have been reported in all age groups, they are most common in children and young adults. There is no reported gender predilection.

Clinical Findings

There are two types of ranulas. A simple ranula is the most common form. By definition, simple ranulas are above the mylohyoid muscle and are confined to the sublingual space. They are usually paramedian and are situated in the vicinity of the sublingual gland. Simple ranulas present as mucosal covered masses within the floor of mouth. These masses are typically cystic in nature and exhibit a characteristic translucent, bluish hue ("frog belly" appearance). Ranulas may occasionally rupture, causing expulsion of viscid fluid into the oral cavity.

The diving ranula (plunging, complex) is believed by some to arise from rupture of a simple ranula. However, in our experience we have seen ranulas that extend into the submandibular space that are intact. These lesions extend inferiorly below the level of the mylohyoid muscle either by extending over the free margin of the mylohyoid muscle or by extending directly through it. Diving ranulas present as a painless, fluctuant soft tissue neck mass. The majority of diving ranulas are above the hyoid bone, although large lesions may extend into the thoracic inlet or mediastinum.

Pathology

The cyst wall of a diving ranula resembles a pseudocyst that is lined by dense connective or granulation tissue. Histologically, the fluid component consists of mucin and histiocytes.

Treatment

The treatment of ranulas is dependent on the type of ranula. The type of ranula is determined by the extent of the lesion seen on imaging. Simple ranulas confined to the floor of mouth may be treated by marsupialization through a transoral approach. Removal of the ipsilateral sublingual gland at the time of surgery is associated with a lower rate of recurrence. Diving ranulas require a more aggressive approach. Adequate resection requires a wider exposure that can be obtained only through a combined transoral and cervical approach. Attempted marsupialization of a diving ranula with its nonepithelial-lined capsule is associated with a high likelihood of recurrence.

Imaging Findings

CT

The CT appearance of a complex (diving) ranula is a well-defined cystic lesion that extends into the submandibular or parapharyngeal space (Fig. 215–1).

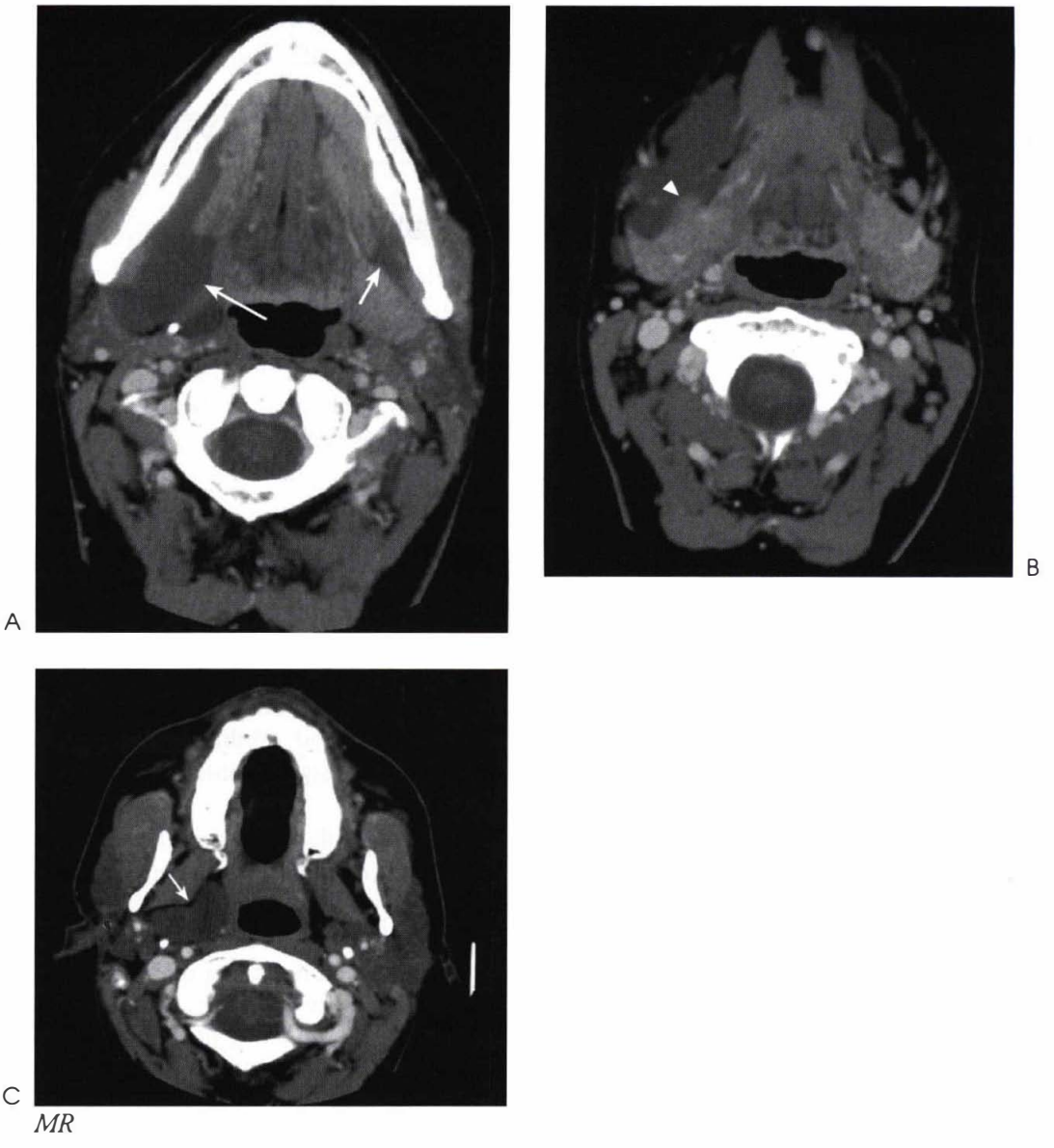

Figure 215-1. (A) Axial contrast-enhanced CT shows a large ranula involving the right SLS (white arrow) and extending to the posterior limit of this space. A smaller ranula is seen on the left (small arrow). (B) Axial image obtained in the submandibular space shows the ranula to have extended below the mylohyoid muscle into the right submandibular space. This is the characteristic finding of a complex (diving) ranula. The small arrow shows the patient also has a smaller complex ranula on the left. (C) Axial image obtained at the level of the oral cavity shows that the same ranula has extended superiorly into the parapharyngeal space (arrow).

MR

The MR appearance of ranulas is that of a cystic lesion with low to intermediate signal on T1-weighted and increased signal on T2-weighted sequences. The T1-weighted signal may at times vary depending on the protein content of the lesion.

Imaging Pearls

- Complex or diving ranulas are typically paramedian lesions situated in the submandibular space that are usually more lateral than thyroglossal duct cysts or epidermoids. These lesions are usually more superior and anterior than branchial cleft cysts.
- Radiologic evidence that a ranula is involving the submandibular space and is not isolated to the sublingual space (simple) changes the surgical approach from a transoral resection to a combined transoral and cervical resection.

Suggested Readings

1. Batsakis JG. Parenchymal cysts of the neck. In: Batsakis JG, ed. *Nonneoplastic Diseases of the Salivary Glands.* Baltimore: Williams and Wilkins; 1979:100–139.
2. Smoker WRK. Oral cavity. In: Som PM, Curtin H, eds. *Head and Neck Imaging.* 3rd ed. New York: Mosby; 1996:488–544.
3. Batsakis JG, McClathchy KD. Cervical ranulas. *Ann Otol Rhinol Laryngol* 1988; 97:561–562.
4. Coit WE, Harnsberger HR, Osborn AG, Smoker WRK, Stevens MH, Lufkin RB. Ranulas and their mimicks: CT evlauation. *Radiology* 1987;163:211–216.

Index

A

F

G

R

S